

HANDBUCH DER ASTROPHYSIK

HERAUSGEGEBEN VON

G EBERHARD · A KOHLSCHUTTER
H LUDENDORFF

BAND V / ZWEITE HALFTE

DAS STERNSYSTEM

ERSTER TEIL



BERLIN
VERLAG VON JULIUS SPRINGER
1933

DAS STERNSYSTEM

ERSTER TEIL

II

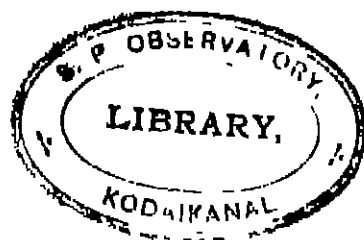
BEARBEITET VON

HEBER D. CURTIS · B. LINDBLAD

K. LUNDMARK · H. SHAPLEY

MIT 118 ABBILDUNGEN

UND 2 TAFELN



BERLIN
VERLAG VON JULIUS SPRINGER
1933



HANDBUCH DER ASTROPHYSIK

HIERAUSGEGEBEN VON

G. EBERHARD · A. KOHLSCHUTTER
H. LUDENDORFF

BAND V / ZWEITE HALFTE

DAS STERNSYSTEM

ERSTER TEIL



BERLIN
VERLAG VON JULIUS SPRINGER
1933

Inhaltsverzeichnis.

Chapter 4

Luminosities, Colours, Diameters, Densities, Masses of the Stars.

By Prof Dr KNUT LUNDMARK, Lund

(Continued.)

(With 12 illustrations)

	Seite
d) The Diameters of the Stars	575
190. The Diameters of the Stars Earlier Conceptions Pioneer Work	575
191. WILSON's Investigations	578
192. RUSSELL's Method	582
193. Diameters from a_p/T	584
194. Diameters from Radiometric Measurements	585
195. KALMÄR's Investigation	586
196. Interferometer Measurements at Mount Wilson	587
197. Varying Stellar Diameters	590
198. The Theoretical Investigations of M HAMV	591
199. DAWSON's Interferometer-Method	596
200. The Companion of Sirius (Sirius B)	596
201. Diameters from Scintillation-Observations	599
202. The Fallacy in S POKROWSKY's Method	599
e) The Densities of the Stars	600
203. Densities of the Stars Pioneer Work	600
204. Densities of Visual Binary Stars	600
205. The Ratio of Densities in Double Stars	603
206. Densities of Eclipsing Binaries. Methodical	604
207. SHAPLEY's Work	605
208. Parallaxes and Absolute Magnitudes of Eclipsing Binaries	606
209. Recent Statistics of the Eclipsing Binaries	607
f) The Masses of the Stars	608
210. Methods of Deriving Stellar Masses	608
211. Are Derived Mass-Values Representative?	610
212. Historical Notes Observational Evidences	611
213. Equipartition of Stellar Energy	617
214. SCHLESINGER's and BAKER's Study on Spectroscopic Binaries	619
215. LUDENDORFF's Researches on the Masses of Spectroscopic Binaries	619
216. Frequency of Stellar Masses for Different Spectral Classes	622
217. Spatial Determinations of Masses	626
218. FIRMAN's Investigation	627
219. Statistics of accurately Determined Stellar Masses	629
220. Real and Apparent Masses	630
221. SHAPLEY's Researches	631
222. Stellar Masses from Spectrographic Parallaxes	637
223. Masses of P-K Stars	638
224. Colour-Mass-Density Relation	641
225. VON ZEIPPEL's Method	641
226. The Method of FREUNDLICH and HEISKANEN	645

227	MARTINS's Method	646
228	Recent Work Concerning Masses of Spectroscopic Binaries	653
229	Preferential Values of Stellar Masses	656
230	Dwarf Nature of Spectroscopic Binaries	658
231	Discovery of Mass-Luminosity Relation	658
232	EDDINGTON's Mass-Luminosity Law and Cosmogonic Time-Scale	662
233	Discrepancies between SEARIS's and EDDINGTON's Results	666
234	JEANS's Theory	667
235	The Cosmogonic Time-Scale by JEANS and SMART	672
236	BRILL's Theory and Parallax-Method for Binaries	673
237	Mass-Reduction by Annihilation of Protons and Electrons	676
238	The Theory of RABE	678
239	Convergence of Mass-Ratios with Increasing Age	682
240	VOGT's Extension of EDDINGTON's Theory	682
241	Statistical Investigations Concerning the Mass-Ratio in Binaries	683
242	Theoretical Derivation of the Mass-Ratio in Double Stars	684
243	LUNDMARK's and LUYTEN's Differential Method	685
244	The Masses and Luminosities of the Eclipsing Binaries	686
245	The Upper Limit for the Stellar Masses	687
246	Relation between Stellar Mass and Proper Motion	689
247	Relation between Stellar Mass and Form of Orbits of Binary Stars	690
248	The Mass of the Orion Nebula	691
249	Planetary Nebulae	692
250	Mass of the Stellar System	693
251	The Masses and Mass-Ratios of Stellar Systems	694
252	The Angular Moments of Visual Binaries	695
253	The Origin of Binary Stars	695
254	Concluding Remarks	696
Appendix I. Catalogue of Stars Brighter than 5 ^m .00		1077
Appendix II. Catalogue of Stellar Diameters		1135

Chapter 5

Stellar Clusters.

By Prof II SHAPLEY, Cambridge (Mass.)

(With 21 illustrations)

a)	Introductory Survey	698
1	The Significance of Clusters	698
2	Historical Notes on Clusters	698
b)	Classification, Number and Distribution	700
3	A Comparison of Galactic and Globular Clusters	700
4	The Number of Clusters	700
5	Classification of Galactic Clusters	704
6	Classification of Globular Clusters	705
7	Clusters in or near Obstructing Nebulosity	706
8	The Apparent Distribution of Globular Clusters	708
9	The Apparent Distribution of Galactic Clusters	710
10	Peculiarities in the Distribution of Galactic Clusters	710
c)	On the Spectral Composition of Clusters	711
11	Integrated Spectra of Globular Clusters	711
12	Stellar Types in Globular Clusters	712
13	On the Masses of Giant Stars	714
14	Spectra in Individual Galactic Clusters	715
d)	Variable Stars in Star Clusters	717
15	The Frequency and General Properties of Variable Stars in Clusters	717
16	A Summary of Known Variables	718
e)	The Distribution of Stars in Globular Clusters	720
17	Are Cluster Stars Arranged Spirally?	720
18	On the Laws of Distribution	720
19	Luminosity Curves for Stars in Clusters	722

f) The Forms of Clusters	Seite 724
20 Definition and Difficulties	724
21 The Elongation of Messier 13	725
22 Ellipticity and Orientation of Globular Clusters	726
23 Some Peculiar Clusters	728
24 The Structure of Galactic Clusters	730
g) The Transparency of Space	733
25 Early Investigations of Light Scattering	733
26 Blue Stars in Messier 13	733
27 Faint Blue Stars in the Milky Way	734
28 Colors in Other Distant Objects	735
29 Messier 5 and the Relative Speeds of Blue and Yellow Light	735
h) The Distances and Dimensions of Clusters	737
30. The Photographic Period-Luminosity Curve	737
31 Distances of Globular Clusters Obtained from Cepheids and Bright Stars	740
32. Distances of Globular Clusters Obtained from Diameters and Integrated Magnitudes	744
33 A Working Catalogue of Galactic Clusters (Appendix B)	746
34 Parallaxes of Galactic Clusters	747
35 Radial Velocities of Globular Clusters	748
36. Dimensions and Star Densities of Clusters	749
i) Star Clusters in the Magellanic Clouds	750
37. Types of Clusters and Nebulae	750
38 The Globular Star Clusters	751
39. Distances of the Clouds	752
40. On the Relation of the Clusters to the Magellanic Clouds	753
j) Dimensions of the Galaxy	754
41 Membership in the Galaxy	754
42. The System of Galactic Clusters	755
43. The Higher Systems of Globular Clusters	755
44 The Distance to the Galactic Center	758
45 On the Size and Structure of the Galaxy	759
Appendix A. Catalogue of Globular Clusters	761
Appendix B. Catalogue of Galactic Clusters	766

Chapter 6.

The Nebulae.

By Prof. HERBER D. CURTIS, Ann Arbor (Mich.).

(With 58 illustrations in the text and on a plate.)

a) Introduction	774
1 Definition of Nebulae	774
2 Historical Notes	774
3. Bibliographical Notes	776
4 Classification and Units	777
b) The Diffuse Nebulae	779
5. Definition	779
6 Number and Distribution	779
7 Physical Characteristics of Diffuse Nebulae	781
8. Dark Nebulae	784
9. Cosmic Clouds	787
10. Distances and Dimensions of Diffuse Nebulae	792
11 Luminous Diffuse Nebulae	793
12 Proper Motions and Internal Motions (Visual)	795
13 Radial Velocities of Diffuse Nebulae	797
14. Turbulence Effects in Diffuse Nebulae	797
15. Luminosity of the Diffuse Nebulae: Gaseous Spectra	799

	Seite
16 Emission Variations	801
17 Luminosity of the Diffuse Nebulae Reflection or Resonance Effects	802
18 Variable Diffuse Nebulae	803
19 Evolutionary Status of the Diffuse Nebulae	805
c) The Planetary Nebulae	806
20 Definition of the Planetary Type	806
21 Number and Distribution of the Planetary Nebulae	807
22 Forms Assumed by the Planetary Nebulae	808
23 Proper Motions of the Planetary Nebulae	809
24 Distances and Dimensions of the Planetary Nebulae	810
25 Planetary Spectra, Spectrum of the Nebulous Matter	813
26 Planetary Spectra, Spectrum of Planetary Nuclei	815
27 Radial Velocities of Planetary Nebulae, Rotation	817
28 Spectroscopic Distribution Effects	817
29 Turbulence Effects in the Planetary Nebulae	819
30 Mechanical Theories of Planetary Structure	823
31 Quantum Theory and Planetary Structure	824
32 The Theories of ZANSTRA, BOWEN, CARROLL and BERMAN	825
33 Evolutionary Status of the Planetary Nebulae	831
d) The Spirals	833
34 Historical Note on the Spirals	833
35 Apparent Distribution of the Spirals, Super-Galaxies	838
36 The Number of the Spirals	839
37 Conspectus of Forms Assumed	840
38 True Spirals	842
39 Barred Spirals	842
40 Elliptical Spirals, the Provenance of the "Minute" Spirals	843
41 Irregular and Magellanic Type Spirals	844
42 Occulting Matter in the Spirals, and its Bearing on Observed Distribution	844
43 Proper Motions of the Spirals	847
44 The Spirals as a System of Reference	850
45 Internal Motions of the Spirals, Visual Determinations	850
46 Rotation of the Spirals, Spectrographic	851
47 Spectra of the Spirals, Stellar Type	852
48 Spectra of the Spirals, Emission Lines	853
49 Color Indices of the Spirals, the Results of SLARLS	854
50 The Radial Velocities of the Spirals	855
51 Distances of the Spirals Parallaxes	858
52 Distances of the Spirals from Novae	858
53 Distances of the Spirals from Cepheids	861
54 Distances of the Spirals from a Distance-Velocity Correlation	863
55 Distances of the Spirals Photometric, the "Average" Galaxy	868
56 Distances and Dimensions of the Spirals	873
57 Masses of the Spirals	876
58 TEN BRUGGENCAAT's Theory of Elliptical Spirals	877
59 Theories of Spiral Structure Introductory	878
60 Agreement of Spiral Arms with Mathematical Spirals	879
61 WILCZYNSKI's Gravitational Spiral	881
62 JEANS's Theory of Spiral Structure	882
63 BROWN's Theory of Spiral Structure	882
64 LINDBLAD's Theory of Spiral Structure	884
65 Theories of Spiral Structure Summary	886
66 Evolutionary Status of the Spirals	887
67 Cosmogonical Deductions Introduction	887
68 The CHARLIER Infinite Universe	888
69 The Spirals and Relativity Universes Introduction	891
70 TOLMAN's Critique of the DE SITTER Relativity Universe	894
71 An Expanding Relativity Universe the Work of LEMAITRE, EDDINGTON, MCCREA, and MCVITTIE	898
72 The Size of the Universe According to SILBERSTEIN	902
73 Various Determinations of the "Radius" of Space-Time	903
74 Summary the Dilemma of Choice between an Expanding Relativity Universe and Distance-Velocity Correlation	903
75 Other Cosmogonical Deductions an Aberration Effect	904

76 Further Considerations on the Apparent Recession of the Spirals	905
77 Earlier Values of the Motion of our Galaxy in Space	906
78 MOUSSARD'S Modification of the DOPPLER Formula	907
79. Conclusion	907
a) Appendices	908
1 Finding List for Names frequently Used in the Older Literature	908
2 Finding Lists for Sir W HERSCHEL'S Classes and Numbers	910
3 Finding List for General Catalogue Numbers	918
4 Finding List for Sir J HERSCHEL'S Numbers	919
5 Systems of Nebular Classification	919
6 Published Reproductions of Nebulae	922
7 Abridged Nebular Bibliographical Apparatus	931
8. A Test of the MOUSSARD Modification of the DOPPLER Formula in a Universe of the CHARLIER Type	932

Kapitel 7

Die Milchstraße.

Von Prof. Dr B LINDBLAD, Stockholm

(Mit 28 Abbildungen und 1 Tafel)

a) Einleitung	937
1 Die Milchstraße als Objekt der Forschung	937
2 Übersichtliche Darstellungen und Monographien	937
b) Das visuelle Milchstraßenbild	938
3 Die Beschreibung und zeichnerische Darstellung der Milchstraße	938
4. Photometrische Eichung der Isophoten	947
5 Die absolute Helligkeit des Himmelsgrundes	948
c) Die Photographie der Milchstraße	952
6. Die prinzipiellen Versuchsbedingungen der visuellen und photographischen Beobachtungen	952
7. Die photographischen Arbeiten einzelner Forscher	953
8. Milchstraßenzeichnungen auf Grund photographischer Aufnahmen Photographische Photometrie der Milchstraße	960
d) Das allgemeine Bild der Milchstraße nach den visuellen und photographischen Beobachtungen	962
9 Der Verlauf der Milchstraße am Himmel in großen Zügen	962
10. Die MAGELLANschen Wolken	965
11 Die Lage der Milchstraße	967
12. Galaktische Koordinaten	972
e) Der Einfluß der diffusen Nebel auf das Milchstraßenbild	975
13 Die galaktischen Nebelfelder	975
14. Dunkle, wohl markierte Flecke im Sternstratum	979
15. HAZENs dunkle Nebel	979
f) Die astrophysikalisch-statistischen Ergebnisse über die Natur der Milchstraße	981
16. Die galaktische Konzentration der Sterne und die effektive Sterngröße des Milchstraßenlichtes	981
17. Das Integralspektrum der Milchstraße. Effektive Entfernung der Milchstraßensterne	985
18 Übersicht der allgemeinen statistischen Untersuchungen über die Verteilung der Sterne im Raum	987
19. Die Verteilungsgesetze verschiedener Spektraltypen	999
20. Die galaktische Verteilung spezieller Objekte von großer absoluter Leuchtkraft	1003
21 Die Entfernung der Sonne von der Symmetrieebene der Milchstraße	1009
22. Spezielle Untersuchungen der Sternhaaren und Sternwolken der Milchstraße	1010
23 Spezielle Untersuchungen über die Natur der MAGELLANschen Wolken	1022
24 Die Absorption des Lichts im interstellaren Raum	1024
25 Die Kaliumwolken in der Milchstraße	1027

	Seite
g) Die Dynamik der Milchstraße	1033
26 Milchstraße und Gastheorie Rotation der Milchstraße	1033
27 Allgemeine statistische Mechanik des Sternsystems	1034
28 Theorie der Sternströmung im typischen Sternsystem	1039
29 Einheitliche Theorie des Milchstraßensystems	1042
30 Die asymmetrische Geschwindigkeitsverteilung in ihrer Beziehung zur Rotation	1048
31 Differentielle Rotationseffekte in den beobachteten Geschwindigkeiten	1056
32 Die Beziehung zwischen dem Geschwindigkeitsellipsoid und der Rotation	1065
33 Die Dimensionen, die Masse und die Rotationszeit der Milchstraße	1067
34 Übersicht verschiedener Anschauungen über die Natur des Milchstraßensystems	1069
Sachverzeichnis	1151

Inhalt der ersten Hälfte.

Chapter 1	Classification and Description of Stellar Spectra	By Prof R H CURTISS †, Ann Arbor
Kapitel 2	Zur Statistik der Spektraltypen	Von Dr FR BECKLER, Bonn
Kapitel 3	Die Temperaturen der Fixsterne	Von Prof Dr A BRILL, Neubabelsberg
Chapter 4	Luminosities, Colours, Diameters, Densities, Masses of the Stars	By Prof. Dr K LUNDMARK, Lund

Ergänzungen und Berichtigungen zu Band V.

Seite 51,	Labelle, dritte Zeile der ersten Kolumne lies $K/H\delta$ statt $K/H\gamma$
Seite 53,	Fig 9 lies OII 4076 statt OII 4016
Seite 177,	G1 (62) unter dem Integral lies T_s statt T_{s_1} , wo T_s die schwarze Temperatur der Sternstrahlung für die Wellenlänge λ bedeutet
Seite 342,	Zeile 10 von oben lies at which statt of which
Seite 433,	Zeile 10 von unten lies working statt to work
Seite 436,	Zeile 1 von unten, except ist zu streichen
Seite 454,	Zeile 17 von unten lies systems statt system
Seite 482,	Zeile 13 von unten lies and with spectrographically statt and spectrographically
Seite 497,	Fig 129 links lies Absolute Magnitude statt Apparent Magnitude Die Figur rührt nicht von LÖNNQUIST, sondern von TEN BRUGGENCATE (Die Sternhaufen, Berlin 1927) her
Seite 513,	2 Gleichung lies $\Sigma' = \Sigma'$ statt $\Sigma' - \Sigma'$
Seite 530,	2 Tabelle, vorletzte Zeile lies F8 statt F0
Seite 535,	Fig 140, letztes Wort der Unterschrift lies magnitudes statt magnitude
Seite 570,	Zeile 10 von oben lies 20 th statt 19 th
Seite 572,	Zeile 17 von oben lies anagalactic statt galactic
Seite 641	Hinter der ersten Labelle ist einzuschalten WALLENIQUIST divided the stars into four groups according to bolometric magnitude, while VON ZEIPPEL and LINDEREN had divided them into four colour-groups, called g-giants, b- and a-type stars, f-dwarfs, and g-dwarfs Their results are given in the second part of the table together with the mean absolute bolometric magnitudes computed by WALLENIQUIST for the different colour-groups used In both cases the mass of the stars in the second group has been selected as unity

Chapter 4.

Luminosities, Colours, Diameters, Densities, Masses of the Stars.

By

KNUT LUNDMARK-Lund
(Continued.)

With 12 illustrations.

d) The Diameters of the Stars.

190. The Diameters of the Stars. Earlier Conceptions. Pioneer Work. The underestimation of the distance and the dimensions of the Sun that was a dominating feature of Greek astronomy, was adopted by the astronomers of the Occident and believed until the end of the 17th century. Practically nothing was known about the physical nature of the stars until that time. The distances of the stars also were underestimated and that fact may explain why many observers thought that the stars displayed measurable diameters. It is clear that it was the irradiation and diffraction that deceived the pioneers. In order to illustrate the kind of rôle these phenomena sometimes play we quote some measurements of the "diameters" of different magnitudes

Apparent magnitude	CARDANUS ¹	TYCHO BRAHE ²	MAGINUS ³	LANDSBERGII ⁴	VAN DER HOVE ⁵	HOOKE ⁶	HAWKES ⁷
1 ^m	480''	120''	600''	60''		13'', 7-16'', 7	5'', 1-6'', 6
2	360	90	330	40	6''	7, 9-12, 3	4, 5
3	240	65	240	30	5	7, 0	3, 8
4	180	45	180	20	4	6, 2	3, 2
5	120	30	120	10	3	5, 3	2, 5
6	60	20	60	5	2	4, 4	2, 0

KEPLER⁸ who must have had a poor eyesight, although not so poor as MAGINUS and CARDANUS, thought at first that the brightest stars displayed diameters of 240'' (Sirius), but, after the invention of the telescope, he states⁹ that when a larger magnification is used the diameters become smaller. He was con-

¹ Libelli duo, unus de supplemento almannach etc Norimbergae (1543)

² Opera omnia 2, p 429 (1925); Astronomiae instauratae progymnasmatia. Pragae (1602)

³ Novae coelestium orbium theoricar. Moguntiaci (1608)

⁴ Uranometria. Middelburgi (1631).

⁵ HORRENSIIUS, Landsbergii commentationes in motum terrae Middelburgi (1630)

⁶ Almagestum novum I, p. 424, 716 (1651).

⁷ Mercurius in Sole visus, p. 92. Godani (1662)

⁸ Opera II, p 676, 689 (1859) ⁹ Opera VI, p 335 (1866)

vinced that the stars had no appreciable diameters, but were "puncta mea" J HORROCKS¹ also was of the same opinion. A little later A KIRCH² called attention to the optical phenomena tending to increase the size of small discs (e.g. diffraction) and concluded that the estimates of stellar diameters are illusory.

The thought that the stars displayed such appreciable diameters and the fact that no parallaxes could be derived from his observations convinced TYCHO BRAHE³ that the heliocentric system was not tenable and seem to have made him start his short-lived compromise-system.

The experiences of the telescope made it gradually clear that the diameters of the stars must be very small. HOOKE⁴ concluded that the dimensions of the stars were below 1" and later E HALLEY⁵ reached the same conclusion.

It was clear to J MICHELL⁶ that even in the case of SIRS the apparent angular diameter must be less than 0",01. He pointed out that if the "native brightness" was in accordance with colour the white stars would have the largest dimensions.

The different conceptions regarding the diameter of SIRS since the middle ages are illustrated from the following summary.

Authority	Diameter of SIRS	Authority	Diameter of SIRS
ALBATEGNIUS	45"	HEWELKE	6",57
KEPLER	(240)	J. CASSINI	5
GALILEI	5,3	MICHELL	0,01
VAN DER HOOVE	10	W. HERSCHEL	<0,01
RICCIOLI	18	Actual value	0,0053

W. HERSCHEL⁷ examined a number of bright stars and used extremely high magnifying power in order to determine whether the stars have sensible dimensions. He found that the telescopic discs appeared smaller with increasing telescopic power and accordingly he considered spurious the discs of light seen in telescopes. He also used this phenomenon as a ready criterion for determining whether a small bright body has an appreciable size or only impresses the sense of sight by virtue of its intrinsic brightness.

In 1835, F. M. SCHWED⁸ suggested a method for determining the diameters of the stars which is based on measurements with two different telescopes in order to eliminate the influence of the diffraction and concluded that the diameter of Altair is 0",104.

The method applied by S. STAMPFER⁹ in 1852 is of much interest. The image of the Sun observed through a telescope was reduced through a globe of Mercury until it matched the image of a star seen in the same telescope. STAMPFER concluded that the diameter of the first magnitude stars is 0",00491, which is a little too low, but of the right order of magnitude (0",0085).

¹ Venus in Sole visa anno 1639, p. 139, edited by HEVELIUS, see Note 7, p. 575, De magnitudine fixarum Opera, p. 61 (1672-78), ed. by WALLIS, London.

² Ars magna lucis et umbrae, p. 119. Romae (1646).

³ Opera omnia 2, p. 429 (1925), Astronomiae instauratae progymnasmatia Pragae (1602).

⁴ An Attempt to prove the Motion of the Earth, p. 26. London (1674).

⁵ London Phil. Trans. p. 853 (1718), p. 3 (1720).

⁶ London Phil. Trans. p. 234 (1767).

⁷ Collected Works II, p. 297 (1912).

⁸ Die Beugungserscheinungen aus der Undulationstheorie analytisch entwickelt. Mannheim (1835).

⁹ Wien Denkschr. Akad. Wiss. II. Cl. 5, p. 91 (1852).

In 1868 FIZEAU¹ suggested a method for the direct measurement of the stellar diameters. When interference is produced by the apparatus of THOMAS YOUNG², the mirrors of FRÉSNEL³, or a biprism the apparent diameter of the light source must be very small, if the fringes are to be pure. If the diameter of the light source is varied, the sharpness of the fringes decreases as the diameter increases, and for a certain value of the diameter the fringes disappear. Proportionality exists between the separation of the fringes and the limiting diameter of the source. The complete theory of this phenomenon has been given by A. MICHELSON in 1890-92⁴. He derived the condition that the fringes become invisible when the angular diameter D of the source is a little greater than the interval l that separates one fringe from the next. Thus:

$$D = 1,22 l$$

The reason why the fringes disappear if the source has an extension is the following. Each separate point gives a system of pure fringes. The systems corresponding to different points will trespass upon each other's ground and mutually blend together. The condition for disappearance of the fringes is that a uniform intensity should be produced, which happens when the law of MICHELSON is fulfilled.

The method of FIZEAU was applied by STEPHAN⁵ at the Observatory of Marseilles in 1873. The objective of the 80 cm telescope was covered with an opaque screen that had two apertures placed symmetrically with regard to the centre. The two pencils converged at the focal plane and the image was examined under high magnification. The apparatus could not distinguish angular diameters less than $0'',2$. Since all the stars investigated gave very clear-cut fringes, it was possible to conclude that none of them had a diameter of $0'',2$, but that probably even the largest were far beneath this value.

The interferometer method was later independently applied by MICHELSON⁶ and HAMY⁷ for the measurement of the satellites of Jupiter.

In a paper of 1880 E. C. PICKERING⁸ gave a masterly treatment of the problem of determining the diameters of stars. He first derived the expression:

$$\log d_* = \log d_{\odot} + 0,2 m_{\odot} - 0,2 m_* - 0,5 \log j,$$

d being the diameters expressed in seconds of arc and j the intrinsic brightness of the star (or in other words the ratio borne by the quantity of light emitted by the star to that emitted by the Sun from the same superficial area), m_* and m_{\odot} the magnitude of the star and the Sun respectively.

Substituting the numerical values then at his disposal the formula read:

$$\log d_* = 8,184 - 0,2 m_* - 0,5 \log j.$$

PICKERING suggested the following way of determining the approximate value of j . An electric current heats a platinum-iridium wire to incandescence and the brightness of a short portion of it is compared with an artificial star, while the current is varied by a known amount. As the current increases the colour changes. The ratio of the blue light to red light may be determined by

¹ CR 66, p 932 (1868) FIZEAU also pointed out the possibility of using the phenomena of scintillation for the determination of stellar diameters.

² London Phil Trans (1802), A Course of Lectures on Natural Philosophy, London (1807)

³ Ann Chim Phys I (1816); XI (1819), Paris Mém de l'Acad V (1826)

⁴ Phil Mag (5) 30, p 1 (1890), (5) 31, p 338 (1891); (5) 34, p 280 (1892); Amer J of Science (3) 39, p 115 (1890).

⁵ CR 78, p 1008 (1874)

⁶ Publ ASP 3, p 274 (1891)

⁷ B A 16, p 257 (1899)

⁸ Proc Amer Academy of Arts and Sciences 16, p 1 (1880)

inserting a double-image prism in the collimator of a spectroscope, and viewing the wire through it. The relative brightness of the two images is varied by a Nicol in the eye-piece, which can be turned a known amount.

PICKERING also pointed out that only an approximate value of the comparative light emitted by equal areas of the two bodies can be obtained. The effect of absorption is not allowed for, and thus a difference of temperature is assumed to be the only cause of the observed difference in colour.

As far as the author is aware this scheme was not put into practice before it was applied in the Potsdam determination of stellar temperatures.

The term equivalent diameter, the diameter of the stars if they all had the same temperature as the Sun, was introduced by E. C. PICKERING by taking $\gamma = 1$. The following table gives this diameter for different magnitudes and represents very closely the means of the modern determinations where the temperature has been taken into account.

Apparent magnitude	Equivalent diameter	Apparent magnitude	Equivalent diameter	Apparent magnitude	Equivalent diameter
0 ^m	0'',0153	5 ^m	0'',0015	10 ^m	0'',00015
1	0,0096	6	0,0010	11	0'',00010
2	0,0061	7	0,0006	12	0,00006
3	0,0038	8	0,0004	13	0,00004
4	0,0024	9	0,0002	14	0,00002

NORDMANN¹ has claimed that he should have priority for being the first who derived a formula how to compute the diameter of a star. In 1911 he derived the formula

$$\log \frac{R_*}{R_\odot} = \log \frac{\pi_\odot}{\pi_*} - \left\{ 0,2 (m_* - m_\odot) + \frac{1}{2} \log \frac{E_*}{E_\odot} \right\},$$

where R are the diameters and E the "éclats intrinsèques effectives" or the surface brightnesses. The quantities $\frac{R_*}{R_\odot}$ were computed for 10 stars from their effective temperatures.

This attempt is certainly one of the first, but NORDMANN cannot be given the priority, because HERTZSPRUNG had already in 1906 advised essentially the same method².

Somewhat earlier than NORDMANN wrote his paper also B. V. ILARKANYI³ had investigated the effective temperatures T of the stars and had derived formulae for computing the diameter of a star from T and m_{vis} or m_{ph} .

191. WILSON's Investigations⁴. When estimating stellar colours several observers have remarked that the stars do not exhibit any other colours than those represented in the radiation from cooling metals. The spectral-photometric work at Potsdam confirmed this view. It was found that the energy distribution in stellar spectra corresponded to that of a black-body radiator. If such is the case the colour or rather the effective temperature will be determined by a comparison with the energy distribution at the same temperature as the celestial body. But the temperatures of terrestrial sources cannot be raised above 3000°. It will then be necessary to transform the stellar radiation into radiation of a lower temperature. This can be done by using mirrors that selectively reflect the incident light or by using absorbing media.

¹ C. R. 152, p. 73 (1911)

² Z. f. wiss. Photogr. 4, p. 43 (1906)

³ A. N. 185, p. 33 (1910), 186, p. 161 (1910)

⁴ Potsd. Publ. No. 76 (1920)

If a mirror is used with a reflection coefficient of $\alpha e^{-b/\lambda}$, then the reflected radiation is:

$$E = c_1 \alpha \int_{\lambda_1}^{\lambda_2} \lambda^{-5} e^{-(\alpha_1/T + b)\lambda^{-1}} d\lambda,$$

and thus the reflected radiation corresponds to the temperature T_1 which is determined by the formula $c_1/T_1 = c_1/T + b$. The only mirrors suitable for the purpose are those of gold. It was found by the aid of two parallel mirrors that after five reflections the effective temperature of the B and A stars could be brought to equality with that of an electric lamp. It was also confirmed that the spectral distribution did not change appreciably by the repeated reflexions. During the course of the work it was found that the use of a red-filter yields still better results than the reflection-method, and thus a red-wedge from SCHOTT in Jena was taken into use which has the property that its transmission is closely represented by means of the expression $-(\beta_0 + \beta_1/\lambda)d \log e$, where d is the thickness of the wedge. The red filter has been used in connection with a ZÖLLNER photometer.

The intensity of radiation of wave length λ outside our atmosphere is expressed by means of $c_1 \lambda^{-5} e^{-\gamma_0 - \gamma_1 (\frac{\alpha_1}{T} + \kappa) \lambda^{-1}}$, where γ_0 and γ_1 are defined by the expression:

$$\gamma_0 \log e = \log (1 - e^{-\alpha_1/T}) - \frac{\gamma_1 \log e}{\lambda}, \quad \gamma_1 \log e = 0.0075 \cdot 10^{-8} (T - 3000).$$

When the radiation has passed the atmosphere, its intensity is equal to

$$c_1 \lambda^{-5} e^{-\gamma_0 - \alpha_1 l - \gamma_1 (\frac{\alpha_1}{T} + \kappa + \alpha_1 l) \lambda^{-1}},$$

where l is the relative path through the atmosphere at a certain distance from the zenith. This expression has further to be multiplied by the factor $e^{-(\beta_0 + \beta_1/\lambda)d}$, corresponding to the scale reading $d = d' - \delta$, where δ is the scale-reading for the zero-point. The values for the photometer-lamp corresponding to T and α_1 are T' and α_1' . By integrating the energy between λ 4500 and λ 6800 it is found that the equation can be divided into the two expressions:

$$\begin{aligned} c_1/T + \gamma_1 + \alpha_1 l + \beta_1 d' &= c_1'/T', \\ c_1 e^{-\gamma_0 - \alpha_1 l - \gamma_1 (\frac{\alpha_1}{T} + \kappa + \alpha_1 l) \lambda^{-1}} &= c_1' \sin^2 \varphi. \end{aligned}$$

The reading of the intensity-circle gives the value φ . The first of the expressions gives the effective temperature in terms of T' , d' ; the constants are $\alpha_1 = +0.338$; $\beta_1 = +0.214$. The ratio of the energy of two stars within the defined interval is given by the equation:

$$\log \frac{s_2}{s_1} = -2.5(n_2 - n_1) = 2(\log \sin \varphi_2 - \log \sin \varphi_1) - 0.138(l_2 - l_1) - 0.1420(d_2 - d_1) + \log \varphi(s_2) - \log \varphi(s_1).$$

$\varphi(s)$ is the definite integral of the modified equation of PLANCK, viz.:

$$\begin{aligned} E &= c_1 \int_{\lambda_{4500}}^{\lambda_{6800}} \frac{\lambda^{-5} e^{-\frac{\alpha_1}{T} \lambda^{-1}}}{1 - e^{-\frac{\alpha_1}{T} \lambda^{-1}}} d\lambda = c_1' \sin^2 \varphi e^{\alpha_1 l + \beta_1 d'} \int_{\lambda_{4500}}^{\lambda_{6800}} \lambda^{-5} e^{-\frac{1}{\lambda} (\frac{\alpha_1}{T} + \kappa)} d\lambda \\ &= c_1' \sin^2 \varphi e^{\alpha_1 l + \beta_1 d'} \int_{\lambda_{4500}}^{\lambda_{6800}} \lambda^{-5} e^{-s/\lambda} d\lambda = c_1' \sin^2 \varphi e^{\alpha_1 l + \beta_1 d'} \varphi(s), \end{aligned}$$

$$\text{or } \varphi(s) = \left[\frac{-\frac{1}{s}}{\frac{1}{s} \lambda^4} \left(1 + 3 \frac{\lambda}{s} + 6 \left(\frac{\lambda}{s} \right)^2 + 6 \left(\frac{\lambda}{s} \right)^3 \right) \right]_{\lambda_{4500}}^{\lambda_{6800}},$$

where $s = \frac{\alpha_1}{T} + \gamma_1$.

A comparison between colorimetrically measured c_2/T and those derived from spectral-photometric values at Potsdam showed good agreement. The mean error for a three-day determination was in the former case in the mean ± 0.11 , whereas the second method gave ± 0.12 .

Next a comparison was made between the colorimetric magnitudes and the visual magnitudes in the Potsdam Durchmusterung. A somewhat unexpected result was found, namely that there was good agreement between the two different magnitudes. This agreement involves not only the possibility of the radiation in the whole spectral interval under consideration being represented by means of the radiation law, but it also involves proportionality between the radiated energy and the relative sensibility of the observer's eye to light of the different colours.

The results of H. E. IVES¹, H. BENDER², P. G. NUTTING³, and W. W. COBLENTZ⁴ concerning the visibility of radiation on the normal curve of the sensibility of the eye for different colours were collected and discussed. The physiological intensity

$$\varphi_s(\epsilon) = \int_{\lambda 4500}^{\lambda 6800} s_\lambda \lambda^{-5} e^{-\epsilon/\lambda} d\lambda$$

was determined by WILSING, and it was found that $\log[\varphi_s(\epsilon)/\varphi_s(\epsilon)]$ was remarkably constant. The limits for the wave lengths in the photographic region are 3600 Å and 4850 Å. The energy of this spectral region is then $c_1 e^{-\epsilon_p} \varphi_p(\epsilon_p)$, where

$$\varphi_p(\epsilon_p) = \int_{\lambda 3600}^{\lambda 4850} \lambda^{-5} e^{-\epsilon_p/\lambda} d\lambda.$$

The following small table gives the values of this integral.

ϵ	$\log \varphi(\epsilon_p)$	ϵ	$\log \varphi(\epsilon_p)$
0.9	0.06	3.0	7.88
1.0	9.95	4.0	6.86
2.0	8.91	4.5	6.36

The difference $\log \varphi_p(\epsilon_p + 1) - \log \varphi_p(\epsilon_p)$ is of sufficient constancy and thus

$$\varphi_{ps}(\epsilon_p) = \int_{\lambda 3600}^{\lambda 4850} s_p e^{-\epsilon_p/\lambda} d\lambda = a_p e^{-b_p \epsilon_p},$$

if $s_p(\lambda)$ is the curve of sensibility of the plate.

It is found that the proportionality between the radiation and the physiological intensity is not dependent on a symmetrical form for $\varphi_s(\epsilon)$. Nor are the limits selected for the integration of much importance. In the case of the sodium cell the deviations from proportionality between the radiation and the intensity curve of the cell are considerable on account of the wider range in wave length ($\lambda 3650$ to $\lambda 5780$).

The equations given above permit the establishment of a relation between the constants of the selective atmospheric extinction α_0 and the mean coefficient of transmission ϕ . The result of G. MÜLLER that the influence of a selective absorption is negligible in the magnitude determinations of the stars was confirmed by WILSING.

¹ Phil Mag 24, p. 352 (1912).

² Dissert. Breslau (1913).

³ Phil Mag 29, p. 301 (1915), Amer Illum Engin Soc Trans 9, p. 633 (1915).

⁴ Scientific Pap Bureau Stand No 303 (1917).

With regard to the question of the physical meaning of the effective temperatures the measurements of the intensity in the solar spectrum are of much importance. It was found that the measured intensities could be very satisfactorily represented by means of the law of PLANCK, if the temperature was taken at 6070° abs. By applying the radiation law of WIEN certain systematic deviations were found. It was concluded that the solar radiation has the same properties as the black-body radiation if the deviations are neglected that are produced from the mixture of different temperatures that give rise to the solar spectrum.

The presence of the absorption-bands in the K and M stars is found to influence the temperature to an amount of some 200°.

It can thus be concluded that the effective and the real temperature of a star do not differ considerably. The diameters of the stars can then be approximated from the radiation law. The radiation in the visual and the photographic part of the stellar spectra can be represented by.

$$-0,4m_p = \log g \left(\frac{d}{\Delta} \right)^2 \sigma^{-r_p} \int_{14500}^{16500} \lambda^{-5} e^{-c_2/\lambda} d\lambda + h_p$$

$$-0,4m_p = \log g \left(\frac{d}{\Delta} \right)^2 \sigma^{-r_p} \int_{13600}^{14850} \lambda^{-5} e^{-c_2/\lambda} d\lambda + h_p,$$

where d and Δ are the diameter and distance of a star and g depends on the constant σ in the STEFAN radiation law and the radiation constant c_2 . Further

$$\frac{1}{\Delta} = 2 \frac{\pi}{\varrho_{\odot}} \sin \frac{1}{2} \varrho'_{\odot}$$

is introduced, where π is the parallax, ϱ_{\odot} the linear diameter, and ϱ'_{\odot} the apparent diameter of the Sun; then the equation is obtained:

$$\log \left(\frac{\varrho}{\varrho_{\odot}} \right)^2 = -0,4m_p + 0,4m_{\odot} + \gamma_{sp}(s_p) \log s - \gamma_{sp}(\varrho_{\odot}) \log s + \log \varphi_p(\varrho_{\odot}) - \log \varphi_p(s_p) - \log \pi^2$$

which is simplified to:

$$\log \left(\frac{\varrho}{\varrho_{\odot}} \right)^2 = -0,4m_p + \gamma_{sp}(s_p) \log s - \log \varphi_p(s_p) - 2 \log \pi - 1,35,$$

putting $m_{\odot} = -25^m,93$ and expressing π in seconds of arc.

The diameters corresponding to the visual magnitudes in P D are computed according to the formula:

$$\log \left(\frac{\varrho}{\varrho_{\odot}} \right)^2 = -0,4m_v + \gamma_{sv}(s_v) \log s - \log \varphi_v(s_v) - 2 \log \pi - 1,16.$$

The first formula was applied to 104 bright stars that had been measured for photographic magnitude by E. S. KING¹ using the out of focus method.

The following mean diameters for different spectral classes were found.

s_v/T	Spectral class	Diameter	n	s_p/T	Spectral class	Diameter	n
0,5-1,0	B	8,6 \odot	12	3,0-3,5	G, K	16,7 \odot	21
1,0-1,5	B, A	5,9	4	3,5-4,0	G, K	32,1	12
1,5-2,0	A, F	2,1	8	4,0-4,5	K	50,6	10
2,0-2,5	F, G	5,0	12	4,5-5,0	K, M	61,0	9
2,5-3,0	F, G	8,9	14				

¹ Harv Ann 59, Nr 6 (1912).

WILSING computed a diameter value of α Orionis of $0''.0395$ which is of a certain interest as being very close to the value $0''.045$, actually measured a year after WILSING's prediction

It would certainly be of much interest to apply WILSING's formula to the material in PD and Göttinger Aktinometrie, New DRAPER Catalogue, and other sources, and to derive the diameters from a consideration of existing values of

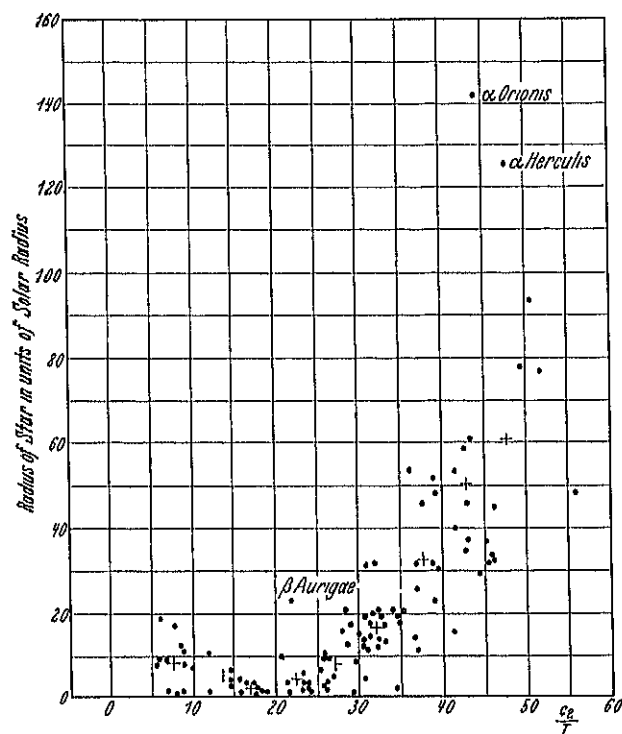


Fig 148 The radii of stars as a function of the inverse value of their effective temperature according to WILSING's investigations. Dots denote individual values and crosses mean values. The minimum value of the radii around $c_2/T = 20$, corresponding to A stars, is no doubt caused by the selection in data because the main bulk of the investigated stars are giants. Compare the following figure

magnitude and J the surface brightness of a star, it follows from elementary considerations that:

$$d = \text{const} \cdot 10^{-0.2m} J^{-1/2}$$

By inserting the data for the Sun the constant is found to be $0''.0087$, provided that the Sun's surface brightness is taken as unity. Further $j = -2.5 \log J$ is introduced. The above equation may then be written

$$d = 0.0087 (0.631)^{m-j}.$$

The following method for a determination of j was used. The difference

parallaxes or substitutes of parallaxes. In this way some 10000 star diameters of tolerable accuracy could be derived.

J. HOPMANN¹ has used the red-wedge colorimeter according to the construction of WILSING for measuring stars of spectral type N and red variable stars. His observations of twenty objects, mainly N stars, give for the temperature of the Na stars 2440° and for the Nb stars 2370° . HOPMANN has derived the diameter of 19 Piscium as $0''.017$. PERTTILÄ and NICHOLSON² have computed the value $0''.018$. Thus the star might be measurable with the aid of the interferometer.

192. RUSSELL'S Method. H. N. RUSSELL³ discussed in 1920 the determination of the diameters of the stars. If d is the apparent diameter, m the visual

¹ A N 222, p 237, 226, p 1 (1925); 226, p 225 (1926).

² Mt Wilson Contr No 369 (1928), Ap J 68, p 279

³ Publ A S F 32, p 307 (1920)

in surface brightness of two stars expressed in magnitudes is proportional to the difference in colour indices C . Thus for two stars

$$i_2 - i_1 = k(C_2 - C_1)$$

The constant k depends on the wave lengths used in measuring the surface brightness and colour index, but is the same for all stars. As long as WIEN's formula can be applied, $k = \lambda_{phot}/(\lambda_{vis} - \lambda_{phot})$, and at higher temperatures, when PLANCK's formula has to be used, the value of k gradually increases, since for an infinite temperature this formula gives infinite surface brightness, but finite colour index.

The Sun permits a direct observational test of this law. The work of SCHWARZSCHILD, ABBOTT, and LINDBLAD makes it very probable that different parts of the Sun's disc differ in colour and brightness, because at the centre we see down further and into hotter layers than near the limb where the line of vision is more oblique. It can therefore be assumed that on passing from the centre to the limb of the Sun we meet successively with conditions very similar to those met with in the photospheres of cooler stars. ABBOT's observations of 1913 have been used for a determination of k . In some cases the values closely agree with those predicted, but in others the discordances are considerable, probably on account of a departure from black-body conditions.

The different scales of C have to be standardized on account of the fact that some of the scales are more open than the others. The standardization is made by deriving the ratios C/C_{stars} in one and the same system. The colour index (C_{stars}) for K stars is then called the colour equation of the given system. A system for which C_{stars} is exactly 1.00 was suggested by PICKERING as a standard. Let K be the value of k , referred to such a system. For any other system of C , with a colour equation E , we have $k = K/E$. This new constant K is equal to $i_{\text{stars}} - i_{\text{stars}}$. In the case of PARKHURST's colour indices λ_{vis} is 5410 and $\lambda_{ph} = 4280$ and thus $k = 3.8$. In order to correct for the systematic difference between his spectra and those of Harvard RUSSELL takes $E = 1.27$ and hence $K = 4.8$. An independent system of colour indices has been derived by ROSENBERG from photographic spectra and gives the intensity at $\lambda 4000$ relative to that at $\lambda 5000$. Arranging his data according to the Harvard spectral classification RUSSELL finds $C_K - C_A = 1.83 - 0.10$ and $K = 6.7$ for $\lambda 5200 \text{ \AA}$.

Then the stellar temperatures determined by WILSON and SCHERER were used. By applying PLANCK's formula RUSSELL has found $K = 4.0$ for $\lambda 5200 \text{ \AA}$.

Also other astronomical data could be used, e.g. eclipsing binaries, or a comparison of densities of eclipsing binaries with the relation between density and surface brightness derived from visual double stars. RUSSELL derived in his address of 1914 the relation¹.

Spectral class	C	i	Spectral class	C	i
B	-0.3	-1.2	G	+0.7	+2.0
A	0.0	0.0	M	+1.6	>4.5
F	+0.3	+0.9			

Also the concomitant variations in magnitude and colour index of the Cepheids can be used, provided that the observed variation is due to changes of temperature in a radiating surface of constant area. This assumption is very dubious, as has been pointed out by RUSSELL.

¹ Pop Astr 22, p. 339 (1914).

Collecting the results we have

Method	K
PARKHURST, colour indices	4,8
ROSENBERG, colour indices	6,7
WILSING and SCHNEIDER, temperatures	4,0
U Cephei (direct observations)	3,2
Eclipsing variables (colour indices)	3,1
Comparison of eclipsing variables and binary stars	3,5
Colour change of Cepheids	2,3
	Mean $3,9 \pm 0,4$
	Adopted 4,0

Then the colour indices of KING, SCHWARZSCHILD, PARKHURST, and Harvard are expressed in units of $C_K - C_A$ so that they all have $C = 1,00$ for K0 stars. The values of j are derived. The small table given here will facilitate considerably the computation of d . When the parallax is known the linear diameter D is found by $D = 9,22 (0,631)^{M-j}$, the Sun's absolute magnitude being 4,83

Spectral class	$-j$	Spectral class	$-j$	$\frac{m-j}{M-j}$	d	D
B0	+3 ^m ,2	F8	+0 ^m ,1	0,10	0'',0087	9,2 \odot
B2	+3,0	G0	0,0	0,5	69	7,3
B5	+2,7	G5	-0,9	1,0	55	5,8
B8	+2,5	K0	-1,9	1,5	43	4,6
A0	+2,1	K2	-2,9	2,0	34	3,7
A2	+1,7	K5	-3,3	2,5	27	2,9
A5	+1,3	Ma	-3,7	3,0	22	2,3
F0	+1,0	Mb	-4,0	3,5	17	1,8
F5	+0,6	N	-6,3	4,0	14	1,5
				4,5	11	1,2
				5,0	0'',0009	0,9

A number of diameter-values were computed by RUSSELL, and among these were values of β Andromedae, Betelgeuze, and Antares. Betelgeuze was measured about a year later with the interferometer, it was found then a very good agreement between the diameters actually measured and those computed by RUSSELL, WILSING, and others.

193 Diameters from c_2/T . As has been described in the chapter on stellar colours, E. HERTZSPRUNG¹ has reduced the principal determinations of colours or colour equivalents of the brighter stars to a homogeneous system from which c_2/T is derived. These values have been used for a derivation of the angular diameter d of 734 stars according to the formula

$$5 \log \sin \frac{d}{2} = -43,44 + 2,3 (c_2/T)^{0,93} - m$$

All the available trigonometric parallaxes of these stars as well as all available spectrographic data have been collected by me and the values of the linear diameters computed in terms of that of the Sun. Also $\pi_{8\mu}$ has been used. It is evident that in many cases already a knowledge of the colour and proper motion will give the linear diameter of a star with fair accuracy.

K. F. BOTTLINGER² has derived the following linear diameter formula:

$$\log D/2 = 0,2(m_{\odot} - m_*) - \log \pi + (\log c_2/T_* - \log c_2/T_{\odot}) + 5,3144$$

where D is the linear diameter in units of the diameter of the Sun; the magnitudes are reduced to the bolometric scale. The diameters were first computed

¹ Leiden Ann. XIV. 1 (1922)

² Berlin-Babelsberg Veröff. 3. H. 4 (1923)

for 104 stars for which the colour index had been measured photo-electrically. In a subsequent paper¹ the diameters have been computed for some 400 stars. The diagram connecting diameter and spectral class shows a certain resemblance with the RUSSELL diagram. The dispersion in diameter on the giant branch is considerable and it does not seem quite impossible that we have, in fact, two branches, a giant and a supergiant branch. The fact that the diameter values computed on the basis of data of eclipsing binaries do not deviate systematically from the values computed from the temperatures is of a certain importance.

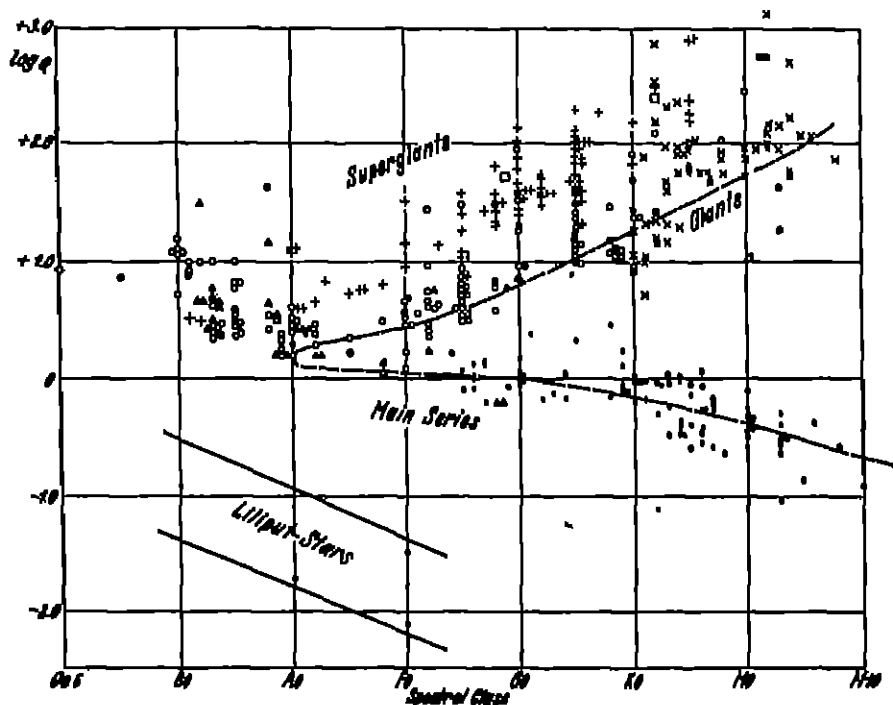


Fig. 149. Distribution of the logarithms of the diameters of stars within different spectral classes according to BORTLINGER. The triangles denote eclipsing binaries, dots trigonometric parallaxes or dynamical parallaxes of high weight, open circles theoretical parallaxes (moving clusters, companions). Further denote \times spectrographic parallaxes and $+$ parallaxes of Cepheids. The two squares give the mean values of $\log d$ for the O stars.

BORTLINGER suggests the name lilliputian stars for the white dwarfs. The spectra should according to his proposal be denoted e.g. B_9 .

194. Diameters from Radiometric Measurements. PETTIT and NICHOLSON² have derived the following expression:

$$\log T = 2.638 - 0.1 (m_r - \Delta m_r) - 0.5 \log d$$

where d is the apparent diameter of the star in seconds of arc and T is the temperature, m_r the apparent radiometric magnitude of a star, and Δm_r the correction to no atmosphere including atmospheric absorption and losses in the telescope. The following table contains the diameters measured directly by PEARSE, and the diameters computed from the above formula with temperatures

¹ Seeliger-Festschr. p. 338 (1924).

² Mt. Wilson Contr. No. 369, Ap. J. 68, p. 279 (1928).

derived from water-cell absorptions and from heat indices, it further contains the temperatures computed from measured d , water-cell absorptions, and heat indices (comp ciph 187)

Object	Diameter			Absolute temperature		
	Measured by interferometer	Computed from m_0	Computed from C_H	From measured d and m_r	From m_0	From C_H
Arcturus	0'',020	0'',031	0'',028	4300°	3440°	3580°
Aldebaran	0,020	0,033	0,031	3890	3080	3170
Betelgeuze	0,047	0,071	0,076	3270	2700	2600
Antares	0,040	0,062	0,065	3270	2680	2620
β Pegasi	0,021	0,029	0,028	3140	2730	2730
α Hercules A	0,030	0,065	0,090	3320	2340	2030
α Ceti A (max)	0,056	0,038	0,073	2210	2610	1970

195 KALMÁR'S Investigation¹ The author starts from the following formula which is easily derived

$$\log \varrho = 0,5 \log J_O / J_* - 2,6243$$

where J_* is determined from the equation of PLANCK

$$J_* = C \int_{\lambda_1}^{\lambda_2} \lambda^{-5} \left(e^{\frac{c_2}{\lambda T}} - 1 \right)^{-1} d\lambda.$$

C is equal to $590\mu^2 \text{ ergsec}^{-1}$, $c_2 = 14600^\circ \mu$ degree Celsius. As limits for the integral $\lambda_1 = 0,40\mu$, $\lambda_2 = 0,76\mu$ have been taken. The following substitution is made

$$a = \frac{c_2}{\lambda_1 T}, \quad b = \frac{c_2}{\lambda_2 T}, \quad x = \frac{\frac{c_2}{\lambda T} - a}{b - a},$$

$$J_* = C(a - b) \left(\frac{c_2}{T} \right)^{-4} \int_0^1 \frac{[a - x(a - b)]^3}{[e^{a - x(a - b)} - 1]^3} dx$$

The integral is then evaluated by means of mechanical quadrature. If r and R are the radius and distance of the star and ϱ the apparent radius

$$r = R \operatorname{tg} \varrho$$

Introducing the parallax π and measuring R in light-years we have

$$\log \pi_0 = \log \pi + 0,2 m, \text{ and } R = \frac{3,228}{\pi}$$

where $\log \pi_0$ is the parallax reduced to apparent magnitude $m = 0$.

From the derivation of stellar temperatures by BRILL² the following values have been taken

Spectral class	B	A	F	G	K	M
c_2/T	1,22	1,51	2,06	2,81	3,74	4,17

$$\text{For the Sun } c_2/T = 2,35, \quad J_O = 52,75 \text{ ergsec}^{-1} \mu^{-2}.$$

A number of the existing parallaxes had to be excluded on account of uncertainty. The author has selected 260 parallaxes, from which the following values of π_0 have resulted

¹ A N 233, p 93 (1928). Also thesis in Budapest (Hungarian).

² A N 219, p 21 (1923).

	B	α	A	α	F	α	G	α	K	α	M	α
Giants	0",170	21	0",138	13	0",140	7	0",132	14	0",128	15	0",122	7
Dwarfs	—	—	0,284	26	0,796	43	1,263	56	4,031	54	6,158	2

From the data at hand the following results have been found by KALMAR.

Spectral class	Absolute temperature	Surface brightness J_s	Mean app. radius	Mean rad. dist. R_s	Linear radius
Giants	M 3500°	2,38	0",0198	26,5	34,8 \odot
	K 3900	4,53	0,0144	26,0	24,8
	G 5200	23,46	0,0063	24,6	10,3
	F 7100	87,00	0,0031	23,0	4,7
	A 9700	266,73	0,0019	20,9	2,7
	B 12000	475,23	0,0014	18,1	1,8
Dwarfs	A 9700	266,73	0,0019	10,3	1,3
	F 7100	87,00	0,0031	5,3	1,1
	G 5200	23,46	0,0063	2,2	0,9
	K 3900	4,53	0,0144	0,8	0,8
	M 3500	2,38	0,0198	0,6	0,7

196. Interferometer Measurements at Mount Wilson. The reason why the interferometer method was not applied earlier to diameter measurements of stars must have been because astronomers have thought that atmospheric disturbances are a too serious source of error. As a matter of fact observations have proved to be feasible even when visibility is poor. According to A. A. MICHELSON and F. G. PEASE¹ the explanation is that the atmospheric disturbances, being irregularly distributed over the surfaces, simply blur the diffraction pattern. In the case of two isolated pencils, too small to be affected by such an integrated disturbance, the resulting interference fringes, though in motion, are quite distinct unless the period of the disturbances is too rapid for the eye to follow them².

As the diameter of the 100 inch reflector was not sufficiently large for the fringes to vanish, an interferometer with movable outer mirrors was constructed. The maximum separation was 20 feet.

Four mirrors, M_1 , M_2 , M_3 , and M_4 , about 150 mm in diameter, inclined at 45° to the base, are mounted on slides. M_2 and M_3 are adjusted by three screws at the back, and M_1 and M_4 can be adjusted about two horizontal axes by means of fine screws at the ends of lever arms. The mirrors M_2 and M_3 are kept fixed at a constant separation of 114,2 cm, except that M_2 has a motion of several millimetres along its slide and parallel to the beam.

The fringe pattern has a spacing equal to 0,02 mm and is easily visible with a magnification of 1600.

The observations are made at the CASSEGRAIN focus, corresponding to an equivalent focal length of 40,84 m. Two pencils from the star are reflected from the outer mirrors, M_1 and M_4 , to M_2 and M_3 , and from there along the ordinary optical way to the large mirror, the convex mirror, the Coudé flat, and finally to the focus. The coincidence of the pencils at the focus is obtained by adjusting

¹ Mt Wilson Contr No 184, 185 (1920) and No. 203 (1921), Ap J 51, p. 257, 263; 53, p. 249

² Recent work by W. A. CALDER at Harvard College Observatory [Harv Bull 885 (1931)] using the Harvard 15 inch refractor and a stellar interferometer in front of the objective, emphasises the importance of good seeing at interferometer measures. CALDER concludes: "... that the statements frequently found to the effect that, in contrast to what might be expected, the interferometer does not require excellent seeing conditions, are unduly optimistic. Atmospheric conditions appear to be the controlling factor, and seriously restrict the possibilities of the interference method."

the outer mirrors M_1 and M_4 and then tilting a plane parallel glass plate of 15 mm thickness in the path of one of the pencils. The equality of the paths of the pencils is obtained by setting the outer mirrors as nearly symmetrically as possible on the beam, and then by adjusting a double wedge of glass in the path of one of the pencils, the relative motion of the wedges alters the paths slowly and continuously.

In order to obtain "zero" fringes for purposes of reference the end of the telescope tube is entirely covered, except for two apertures in the beam 152 mm in diameter. The pencils entering these apertures pass through the wedges and the compensating plate, and produce an image of the star in the field of vision; when they have been adjusted for coincidence and equality of path, these pencils interfere and produce the zero fringes which cross the reference images.

The interferometer images are next brought into the field of the eyepiece and made to coincide at a short distance from the zero star, thus forming a second star in the field. The parallel plate compensator is used only for differential deflection of the steel beam. When the wedge is moved in order to equalize the difference in the path of the interferometer pencils, the zero fringes disappear, and the number of turns of the rod are determined which are required to bring the first fringes into view. The mirror M_3 is then moved a small amount in order to compensate for this difference. After several trials both sets of fringes are seen in the field of vision crossing their respective images.

The distribution of light in the disc to be measured is represented by the formula:

$$I = I_0 (R^2 - r^2)^n$$

where r is the distance from the centre, R the radius of the star, and n the exponent expressing the amount of darkening at the limb. The visibility V of the interference bands is defined by

$$V = \frac{1}{P} \sqrt{C^2 + S^2}$$

where $C = \int F(x) \cos kx dx$, $S = \int F(x) \sin kx dx$,

$$P = \int F(x) dx, \quad k = \frac{2\pi b}{\lambda_{\text{eff}} d},$$

in which b is the distance between the two pencils entering the interferometer, λ_{eff} the mean effective wave length of the light-source, d its distance, and $F(x) dx$ is the total intensity of a strip of the source having a width of dx in a coordinate system where x, y are the coordinates of a luminous point in the disc of the star. The star disc must be symmetrical and thus.

$$V = \frac{C}{P}$$

Assuming the illumination to be a function of the distance from the centre in the way indicated above we have, when substituting $r^2 = x^2 + y^2$

$$F(x) = \int_0^{\sqrt{R^2 - x^2}} (R^2 - x^2 - y^2)^n dy$$

Expanding in series and substituting in V MICHELSON and PEASE¹ find:

$$V = \frac{\int_0^R (R^2 - x^2)^{\frac{2n+1}{2}} \cos kx dx}{\int_0^R (R^2 - x^2)^{\frac{2n+1}{2}} dx}$$

¹ Mt Wilson Contr No 203, Ap J 53, p 249 (1921)

The following table computed under the direction of F. R. MOULTON gives the values of the integral.

$$F(h, n) = \int_0^1 (1 - x^2)^{\frac{2n+1}{2}} \cos h\pi x dx.$$

n=0		n=0.5		n=1		n=2	
<i>h</i>	<i>F</i> (<i>h</i> , <i>n</i>)	<i>h</i>	<i>F</i> (<i>h</i> , <i>n</i>)	<i>h</i>	<i>F</i> (<i>h</i> , <i>n</i>)	<i>h</i>	<i>F</i> (<i>h</i> , <i>n</i>)
0°	+0.785	0°	+0.785	0°	+0.785	0°	+0.785
100	+0.507	30	+0.765	40	+0.746	40	+0.761
130	+0.378	60	+0.702	80	+0.663	80	+0.694
160	+0.243	90	+0.607	120	+0.536	120	+0.590
200	+0.065	120	+0.490	160	+0.383	160	+0.468
230	-0.024	150	+0.363	200	+0.237	200	+0.342
240	-0.050	180	+0.238	240	+0.112	240	+0.221
280	-0.100	210	+0.127	280	+0.024	280	+0.123
320	-0.095	240	+0.038	320	-0.029	320	+0.054
360	-0.053	257.45	+0.000	360	-0.045	360	+0.003
400	-0.007	270	-0.024	400	-0.039	400	-0.019
440	+0.036	300	-0.057	440	-0.020	440	-0.024
520	+0.042	330	-0.068	480	-0.001	480	-0.018
600	-0.011	360	-0.059	520	+0.012	520	-0.006
		390	-0.040	600	+0.013	600	0.000
		420	-0.016	640	+0.005	640	+0.005
		450	+0.005	680	-0.004	680	+0.005
		480	+0.019			720	+0.002
		510	+0.028				
		540	+0.026				
		570	+0.019				
		600	+0.009				
		630	-0.002				

The authors point out the theoretical possibility of deriving the actual distribution of light in the source from observations of the visibility curve itself. Even if the present means are not able to give such a result, it does not seem impossible that future observations will do so.

If b_1 and b_2 are the distances for which the fringes vanish the first and second times, the following formula gives a fair approximation to the value of n :

$$n = -1 + 75 \left(\frac{b_1}{b_2} - \frac{1}{2} \right)^2.$$

Denoting the visibility of the first negative maximum by V_{\max} we have:

$$n = 0.22 \left(\frac{1}{V_{\max}} - 7.8 \right)^{0.7}.$$

The value sought by the measurements is $F(h, n) = 0$ or the separation between the outer minors M_1 and M_2 for which the fringes vanish. P. MERRILL, when using the ANDERSON interferometer used for the investigation of the orbit of Capella, found that the visibility of the fringes of α Orionis decreased, for the maximum separation of 100 inches, in that apparatus. As the decrease was independent of the position angle of the interferometer the star was certainly not a binary.

On December 13, 1920, after the adjustment of the instrument had been checked by means of settings on other stars, α Orionis was investigated. A separation of 121 inches did not give any fringes for that star, although the zero fringes were quite visible. The disappearance of the interferometer fringes evidently could not be caused by any disturbances of an instrumental nature. The instrument was not provided at that time with means for continuously altering the distance between the movable mirrors.

The effective wave length was assumed to be λ 5750 for α Orionis, and the angular diameter was thus found to be

$$d = 0''.047.$$

Somewhat later J A ANDERSON made an investigation of the effective wave length¹ and found the value λ_{eff} 5520, from which it follows that:

$$d = 0''.045 \pm 0''.0045.$$

The stars for which a value of the diameter has been found by direct measurements are the following:

Star	Diameter	Parallax				Diameter in linear measure
		Trigo nometric	Spectro graphic	Spectral proper motion	Concluded value	
α Orionis	0'',047	0'',011	0'',010	0'',012	0'',011	460 ☉
α Bootis	0,022	0,085	0,131	0,158	0,090	26
α Scorpii	0,040	0,026	0,013	0,010	0,026	160
α Ceti	0,056	0,011	—	0,020	0,010	600
α Herculis	0,021	0,030	0,002?	0,008	0,007	320
α Tauri	0,020	0,057	0,083	0,096	0,060	36
β Pegasi	0,021	0,019	0,023	0,028	0,020	110
γ Andromedae	(0,014)	0,010	0,007	0,024	0,010	(150)
α Arietis	(0,011)	0,037	0,053	0,046	0,040	(30)

The values within parentheses depend on extrapolation of the visibility-curves and on a correction for seeing, and are hence uncertain and subject to changes when a larger separation can be used, so that the actual disappearance of the fringes will be estimated

The value for α Orionis is given above as 0'',045 and the mean value of 8 determinations is 0'',042. I have preferred to use the original value from 1920. The value for α Scorpii has been checked at different epochs.

The linear diameter D is found from the formula $D = 107,5 d''/\pi''$. On account of the importance of knowing the linear dimensions the existing values of the parallaxes have been discussed with great care, as an example, we give in some detail the discussion for α Orionis.

α Orionis. Six trigonometric values of the parallax are known $+0''.031 \pm 0''.024$ (Yale), $+0''.018 \pm 0''.007$ (SCHLESINGER), $+0''.022 \pm 0''.007$ (LEE); $+0''.013 \pm 0''.006$ (MITCHELL), $+0''.011 \pm 0''.006$ (VAN MAANEN), and $-0''.005 \pm 0''.007$ (ALDEN). Spectrographic determinations are 0'',012 (Mount Wilson), 0'',014 (Norman Lockyer Observatory), 0'',009 (Victoria). The spectral proper motion method gives $\pi_{\theta\mu} = 0'',012$.

A weighted mean of the trigonometric values gives 0'',011 and of the spectrographic values 0'',010. The high luminosity of α Orionis makes it probable that its mass is high. Thus a systematic difference ought to be present between π_{tr} and π_s . But if a mass factor is present the luminosity would be too small in the second case and the parallax too large. It thus seems that either the parallaxes available do not suggest such an effect or the mass is small.

Anyhow it seems that the best parallax value to be derived from the material is 0'',011.

197. Varying Stellar Diameters. The most sensational discovery concerning the diameters of the stars is without doubt that of PEASE² that the dimensions of α Orionis vary between certain limits. Numerous tests have shown that the

¹ Mt Wilson Contr No 222 (1922), Ap J 55, p 48

² Publ ASP 34, p 346 (1922), Mt Wilson Reports 1920—1928

variation must be real. Thus it is proved that pulsations occur among the stars. The data are too few to admit the establishment of correlations between the apparent magnitude, the radial velocity, and the diameter. There seems to be some relation, but the observations are too few. Besides, the estimates of magnitudes are liable to considerable uncertainty on account of the lack of comparison stars and the rather exceptional colour of the star. The following determinations have been obtained by PEASE:

Epoch	Apparent diameter	Epoch	Apparent diameter
December 1920	0",047	December 1924 . . .	0",044
September-November 1921	0,054	December 1925 . . .	0,034
October 1922 . . .	0,034	December 1926 . . .	0,041
December 1923 . . .	0,041	February 1928 . . .	0,037

Adopting the parallax above the following values of the linear diameter are found: 460 \odot , 540 \odot , 330 \odot , 400 \odot , 430 \odot , 330 \odot , 400 \odot , and 360 \odot respectively. This gives a mean value of 400 \odot and a dispersion of $\pm 71\odot$ around the mean.

It is possible that the dimension of Mira Ceti also varies, but the observations available cannot decide this question.

The new interferometer with a maximum base of 50 feet was taken into use at the end of 1930, with this magnificent instrument the number of measurable stars will be increased to forty or more. In the Mt Wilson Report for 1931 it is stated that the adjustment and operation of the 50 feet interferometer have been continued by PEASE, who has observed fringes with mirror-separations up to 44 feet. Measurements of α Orionis give an angular diameter of about 0",040 and of β Andromedae 0",016.

198. The Theoretical Investigations of M. HAMY. M. HAMY¹ has proved that the light E of a point in a circular star can be expressed by the convergent series:

$$E = A_0 + A_1(1 - q^2)^{\frac{1}{2}} + A_2(1 - q^2) + A_3(1 - q^2)^{\frac{3}{2}} + \dots$$

where q is the ratio between the angular distance of the point considered from the centre and the angular diameter, and A_0, A_1, A_2, \dots are constants depending on the constitution of the stellar atmosphere.

For the Sun and $\lambda_{\text{eff}} = 5062 \text{ \AA}$ we have:

q	E_{obs}	E_{comp}	q	E_{obs}	E_{comp}
0,00	1,0000	1,0000	0,825	0,7196	0,7195
,20	0,9891	0,9882	0,875	0,6605	0,6607
,40	0,9510	0,9503	0,92	0,5909	0,5911
,53	0,8998	0,9003	0,95	0,5289	0,5285
,65	0,8516	0,8521	0,97	0,4719	0,4721
,75	0,7871	0,7865			

The values E_{comp} are formed from the following values of the constants derived by the aid of a least square solution:

$$\begin{aligned} A_0 &= 0,257379 & A_1 &= 0,941025 & A_2 &= -0,255333 \\ A_3 &= 0,076874 & A_4 &= -0,019945 \end{aligned}$$

The formula for E has an interesting application to the measurements of the diameters of the stars.

¹ C R 174, p 342 (1922); Journal de Mathématiques pures et appliquées 1917 and 1920; B A Mém et Var I, p. 198 (1920).

When two apertures are used the fringes of YOUNG will disappear as soon as the well-known relation

$$\varepsilon = 1,22 \frac{\lambda_{\text{eff}}}{l}$$

is fulfilled, ε is the angular diameter of the star and l the distance between the apertures. The relation presumes the star disc to be uniform.

It is also possible to determine the value of ε and the variation in the surface brightness of the star in cases where an absorbing atmosphere gives a non-uniform distribution of light over the disc, if the ratios of the intensities of the maxima and minima of the fringes have been observed.

If l is the value for which the fringes disappear, K_i the ratio of the intensities when the distance is l_i , and $\alpha_i = l_i/l$, and if further $m = \pi_0 \frac{l_\varepsilon}{\lambda_{\text{eff}}}$ and $m_i = \pi_0 \frac{l_i \varepsilon}{\lambda_{\text{eff}}}$ and thus $m_i = m \alpha_i$, we obtain, by using the expression above for E , the following equation

$$A_0 [I_0(m_i) - K_i F_0(m_i)] + A_1 [I_1(m_i) - K_i F_1(m_i)] + \dots = 0$$

The value of the n constants is determined from n equations, that is, from n determinations of the K_i . The functions I and F are known and depend on the evaluation of an integral of the form

$$\int_0^1 (1-x^2)^{p-\frac{1}{2}} \cos qx dx,$$

where p is a whole positive number or zero and q has not a high value.

In a subsequent note¹ HAMMY makes use of the following designations:

$$U_0 = \sum_{n=0}^{\infty} (-1)^n \frac{m^{2n}}{(1 \cdot 2 \dots n)^2} \frac{1}{n+1} = \frac{4}{\pi} \int_0^1 (1-u^2)^{\frac{1}{2}} \cos 2mu du,$$

$$U_1 = \sum_{n=0}^{\infty} (-1)^n \frac{m^{2n}}{(1 \cdot 2 \dots n)^2} \frac{1}{(n+1)(n+2)} = \frac{8}{3\pi} \int_0^1 (1-u^2)^{\frac{1}{2}} \cos 2mu du,$$

$$B = \frac{A_0}{2} + \frac{A_1}{2} + \frac{A_2}{4} + \frac{A_3}{5} + \frac{A_4}{6},$$

$$C = A_0 \frac{U_0}{2} + A_1 \frac{1}{4m^2} \left(\frac{\sin 2m}{2m} - \cos 2m \right) + A_2 \frac{U_1}{2} \\ + A_3 \frac{9}{4m^2} \left[\frac{1}{4m^2} \left(\frac{\sin 2m}{2m} - \cos 2m \right) - \frac{1}{3} \frac{\sin 2m}{2m} \right] \\ + A_4 \frac{1}{m^2} (2U_1 - U_0)$$

The coefficients A_0, A_1, A_2, A_3, A_4 in the expression for C are tabulated in the table on p 593.

HAMMY shows that the maxima of intensity are proportional to $B + C$ and the minima to $B - C$.

If l_0 is used as a designation for the value for which the fringes disappear, the ratio K then equals unity. If $\alpha_i = l_i/l$ and $\mu = m_i/\alpha_i$ we have the following system

$$\begin{array}{ll} 2C = 0 & \text{For } l = l_0, m = \mu \\ (B+C)_1 - K_1 (B-C)_1 = 0 & \dots = l_1 = \alpha_1 \mu \\ (B+C)_2 - K_2 (B-C)_2 = 0 & \dots = l_2 = \alpha_2 \mu \\ (B+C)_3 - K_3 (B-C)_3 = 0 & \dots = l_3 = \alpha_3 \mu \\ (B+C)_4 - K_4 (B-C)_4 = 0 & \dots = l_4 = \alpha_4 \mu \end{array}$$

¹ CR 174, p 904 (1922)

These equations determine the quantities:

$$\mu, \frac{A_1}{A_0}, \frac{A_2}{A_0}, \frac{A_3}{A_0}, \frac{A_4}{A_0}$$

The diameter ε is found from:

$$\mu = \pi_0 \frac{l_0 \varepsilon}{\lambda_{\text{eff}}}$$

In the case of the Sun the application is simple because the law of distribution of the intensity is known. If the diameter is ε when consideration is taken of the variation in intensity on the solar disc, and ε' when no variation in intensity is supposed, the following relation is found.

$$\varepsilon' = 0,91 \varepsilon.$$

In the case of super-giants and ordinary giants the correction is certainly much larger on account of the extended atmosphere and the rapid falling off in intensity towards the limbs

Later on HAMV¹ considered the case where the dimension of the apertures could not

be considered as negligible in comparison with the distance between them. In his earlier work he had reached an approximative solution².

If we denote the common width of the apertures by a , the distance between them by l , by Θ the angular distance from the centre of a point in the focal image of the star taken parallel with the line joining the centres of the apertures, by w another angle in the same direction as Θ , then the intensity I in the direction Θ is proportional to the integral:

$$\int_{-\pi/2}^{\pi/2} \left(\frac{a^2}{4} - w^2 \right)^{1/2} \left[\frac{\sin \frac{\pi_0 a}{\lambda_{\text{eff}}} (w - \Theta)}{\frac{\pi_0 a}{\lambda_{\text{eff}}} (w - \Theta)} \right]^2 \cos^2 \pi_0 \frac{l}{\lambda_{\text{eff}}} (w - \Theta) dw.$$

Putting:

$$w = \frac{a}{2} u; \quad \Theta = \frac{a}{2} \tau; \quad \frac{a}{l} = \alpha; \quad m = \frac{\pi_0 l}{2 \lambda_{\text{eff}}}.$$

¹ C R 175, p. 1123 (1922).

² B A 16, p 257 (1899)

M	A ₀	A ₁	A ₂	A ₃	A ₄
0,0	+0,5000	+0,3333	+0,2500	+0,2000	+0,1667
0,1	,4975	,3320	,2492	,1994	,1663
0,2	,4901	,3280	,2467	,1977	,1650
0,3	,4779	,3215	,2426	,1949	,1630
0,4	,4611	,3125	,2369	,1910	,1601
0,5	,4401	,3012	,2298	,1861	,1565
0,6	,4153	,2877	,2213	,1802	,1522
0,7	,3871	,2724	,2116	,1735	,1472
0,8	,3562	,2554	,2008	,1659	,1417
0,9	,3231	,2371	,1890	,1577	,1355
1,0	,2884	,2177	,1764	,1489	,1290
1,1	,2527	,1975	,1632	,1395	,1220
1,2	,2168	,1769	,1496	,1298	,1147
1,3	,1811	,1561	,1308	,1198	,1071
1,4	,1464	,1354	,1219	,1097	,0993
1,5	,1131	,1152	,1080	,0996	,0916
1,6	,0817	,0957	,0944	,0895	,0838
1,7	,0527	,0771	,0813	,0796	,0760
1,8	,0265	,0597	,0686	,0699	,0684
1,9	+0,0034	,0436	,0567	,0606	,0610
2,0	-0,0165	,0290	,0455	,0518	,0538
2,1	,0330	,0160	,0352	,0435	,0469
2,2	,0461	+0,0047	,0258	,0357	,0404
2,3	,0558	-0,0049	,0174	,0285	,0343
2,4	,0622	,0128	,0101	,0220	,0286
2,5	,0655	,0190	+0,0037	,0162	,0233
2,6	,0660	,0236	-0,0016	,0110	,0186
2,7	,0640	,0267	,0059	,0065	,0143
2,8	,0597	,0283	,0004	+0,0027	,0105
2,9	,0537	,0287	,0119	-0,0005	,0071
3,0	,0461	,0280	,0135	,0031	,0043
3,1	,0376	,0263	,0144	,0051	+0,0018
3,2	,0284	,0238	,0147	,0066	-0,0002
3,3	,0190	,0207	,0143	,0075	,0018
3,4	,0096	,0172	,0135	,0081	,0030
3,5	-0,0007	,0135	,0123	,0082	,0039
3,6	+0,0076	,0096	,0109	,0080	,0045
3,7	,0148	,0058	,0091	,0076	,0048
3,8	,0210	-0,0021	,0073	,0069	,0049
3,9	,0238	+0,0012	,0054	,0061	,0048
4,0	+0,0294	+0,0042	-0,0035	-0,0052	-0,0046

one can write

$$I = 2 \int_{-1}^{+1} (1 - u^2)^{\frac{1}{2}} \left[\frac{\sin m \alpha (u - \tau)}{m \alpha (u - \tau)} \right]^2 \cos^2 m(u - \tau) d\tau$$

Further we put

$$2m\tau = x,$$

$$S(m) = \frac{4}{\pi_0} \int_0^1 (1 - u^2)^{\frac{1}{2}} \cos 2mu du,$$

$$T(m) = \frac{4}{3\pi_0} \int_0^1 (1 - u^2)^{\frac{1}{2}} \sin 2mu du$$

Then one can easily derive.

$$\frac{4}{\pi_0} \int_0^1 u^2 (1 - u^2)^{\frac{1}{2}} \cos 2mu du = S(m) - 3T(m),$$

$$\frac{4}{\pi_0} \int_0^1 u (1 - u^2)^{\frac{1}{2}} \sin 2mu du = 2mT(m)$$

The numerical values of $S(m)$ and $T(m)$ have been computed by HAMM as follows:

m	$S(m)$	$T(m)$	m	$S(m)$	$T(m)$
0,0	1,0000	0,2500	1,0	0,5767	0,1764
0,1	0,9950	0,2492	1,1	0,5054	0,1632
0,2	0,9801	0,2467	1,2	0,4335	0,1496
0,3	0,9557	0,2426	1,3	0,3622	0,1308
0,4	0,9221	0,2369	1,4	0,2927	0,1219
0,5	0,8801	0,2298	1,5	0,2261	0,1080
0,6	0,8305	0,2213	1,6	0,1633	0,0944
0,7	0,7742	0,2116	1,7	0,1054	0,0813
0,8	0,7124	0,2008	1,8	0,0530	0,0686
0,9	0,6461	0,1890	1,9	0,0067	0,0567
1,0	0,5767	0,1764	2,0	-0,0330	0,0455
			2,1	-0,0660	0,0352

Supposing α to be small and including terms of the third order we can derive the following formula, taking $2m\tau = x$

$$\frac{2}{\pi_0} I = 1 + S(m) \cos x - \frac{\alpha^2}{6} \left\{ \frac{x^2}{2} + \frac{m^2}{2} + \left[\frac{S(m)}{2} x^2 + 2m^2 S(m) - 6m^2 T(m) \right] \cos x - 4m^2 T(m) x \sin x \right\}$$

$S(m)$ is zero for $m = m_1 = 1,916$. The intensity has maxima when $x = 2K\pi_0$ and minima when $x = (2K + 1)\pi_0$, where K is an integral number. The fringes disappear when

$$m_1 = \frac{\pi_0 \lambda \varepsilon}{2\lambda_{\text{eff}}} = 1,916,$$

or

$$\varepsilon = 1,22 \frac{\lambda_{\text{eff}}}{\lambda}$$

This is the formula derived by MICHELSON

When α is small, but not zero, we get from the above formula

$$\frac{2}{\pi_0} \frac{\partial I}{\partial x} = -S(m) \sin x - \frac{\alpha^2}{6} \left[x + [S(m) - 4m^2 T(m)] x \cos x - \left\{ \frac{S(m)}{2} x^2 + [S(m) - T(m)] 2m^2 \right\} \sin x \right]$$

It is known that if m is smaller than m_1 , the equation $\frac{\partial I}{\partial x} = 0$ has real roots near $x = K\pi$. Only the root $x = 0$ remains fixed when α and m vary. In the neighbourhood of $x = 0$ we have:

$$\frac{2}{\pi} \frac{\partial I}{\partial x} = -x \left\{ S(m) + \frac{\alpha^2}{6} [1 + (1 - 2m^2) S(m) - 2m^2 T(m)] \right\} + \frac{\pi^2}{6} \left\{ S(m) - \frac{\alpha^2}{3} [(m^2 - 3) S(m) + 5m^2 T(m)] \right\} + x^3 (\dots) + \text{higher terms.}$$

When $m = 0$ the coefficient of x is negative. It remains negative as long as m is below the smallest positive value μ that makes the coefficient disappear. The root $x = 0$ then corresponds to a maximum of I .

The coefficient of x cannot disappear more than for a value of m that makes $S(m)$ of the same order of magnitude as α^2 .

The equation

$$S(\mu) + \frac{\alpha^2}{6} [1 - 2m_1^2 T(m_1)] = 0,$$

determines μ . Developing $S(\mu)$ in terms following powers of $\mu - m_1$ and dropping $(\mu - m_1)^2$, which is of the order α^4 , one finds the equation:

$$\mu = \frac{\pi_2 l s}{2 \lambda_{\text{eff}}} = 1.916 + 0.236 \alpha^2$$

or:

$$s = \frac{\lambda_{\text{eff}}}{l} (1.22 + 0.15 \alpha^2).$$

This formula is not strictly applicable when α is not very small. When α is a considerable fraction of the unit, μ cannot be derived without a laborious numerical discussion.

HAMY has derived the values of μ for the following cases:

In another paper¹ HAMY has made further studies of the problem. The study of variation in the intensity of the central maximum does not permit any conclusion concerning the value of the diameter of the light source.

The disappearance of the two minima encompassing the central maximum ought, on the other hand, to be able to give a value of s if the relation is known between s and l when such a disappearance occurs.

α	μ	$\frac{\lambda_{\text{eff}}}{l} s$
$\frac{1}{2}$	1.992	1.268
$\frac{1}{3}$	1.960	1.248
$\frac{1}{4}$	1.945	1.238
$\frac{1}{5}$	1.932	1.230
$\frac{1}{6}$	1.922	1.224
$\frac{1}{8}$	1.918	1.221
0	1.916	1.220

One can write the expression for the intensity:

$$I = \int_{-1}^{+1} (1 - u^2)^2 \frac{2 - \cos 2\pi s(\alpha + 1)(u - v) - \cos 2\pi s(\alpha - 1)(u - v) + 2 \cos 2\pi s(u - v) - 2 \cos 2\pi s \alpha(u - v)}{m^2 \alpha^2 (u - v)^2} du.$$

From this can be deduced:

$$\frac{I}{\pi} = 0 = \sum_{p=0}^{p=\infty} (-1)^p \frac{2 - (\alpha + 1)^{2p+4} - (\alpha - 1)^{2p+4} - 2\alpha^{2p+4}}{(2p+3)(2p+4)\alpha^2} m^{2p} \sum_{q=1}^{q=p+1} \frac{(2\pi)^{2p-2}}{\Gamma(2q)\Gamma(p+q+2)\Gamma(p-q+3)},$$

$$\frac{I}{\pi} = 0 = \sum_{p=0}^{p=\infty} (-1)^p \frac{2 - (\alpha + 1)^{2p+4} - (\alpha - 1)^{2p+4} - 2\alpha^{2p+4}}{(2p+3)(2p+4)\alpha^2} m^{2p} \sum_{q=1}^{q=p+1} \frac{(2\pi)^{2p-2}}{\Gamma(2q-1)\Gamma(p-q+2)\Gamma(p-q+3)}.$$

¹ CR 176, p 1849 (1923).

The problem to be solved is to find the smallest positive value of m and the smallest value of τ that simultaneously satisfy the equations. When α is very small the following solution is found,

$$m = \mu_1 = 1.916 - 1.15\alpha^2,$$

$$2\tau = 2.911$$

By taking "small" values of α , for instance $\alpha = \frac{1}{10}$, and substituting neighbouring values, the unknowns are found by a process of interpolation.

199. DANJON'S Interferometer-Method¹. The apparatus used in applying this method is of the same type as the interferometer of JAMIN, where the interference is caused by a system of thick glass plates. When observing through this instrument, the star to be measured is seen moving upon a field of bright and dark fringes. If the star has no sensible dimension it disappears completely when its light passes through the centre of the dark fringes. But if the star has an appreciable disc, not all the points of this disc will disappear. The extinction will only be complete along a chord coinciding with the centre of the dark fringe. On each side of this chord there are illuminated parts. When the star is circular and has its light uniformly distributed over the disc, the ratio γ between the maximum and minimum brightness is defined by

$$\gamma = \frac{1-J}{1+J},$$

where

$$J = 1 - \frac{1}{2} \frac{n}{2^2} + \frac{1}{3} \frac{n^2}{(2 \cdot 4)^2} - \dots$$

and n is equal to $\pi_0 \rho$, where ρ is the ratio between the angular diameter of the star and the distance between the fringes. The determination of the apparent radius is thus dependent on actual photometric measurements of the quantity γ . No results of the experiments at Strassburg have been published as yet.

200. The Companion of Sirius (Sirius B). In his paper on the relation between the masses and luminosities of stars EDDINGTON² pointed out the possibility that Sirius B had a density of 53 000 that of the water, on account of the electrons being in the capture zone of two or more nuclei simultaneously. The question whether such density really exists could be settled if the EINSTEIN shift $+0.62 \frac{v}{R}$ km/sec, amounting to 20 km/sec, could be measured. The possibility of testing the general theory of relativity as well as the theory of extremely dense matter was independently pointed out by BOTTLINGER and by WEBER³.

In 1925 W. S. ADAMS⁴ communicated the results of measuring spectrograms of Sirius B. Direct measurements are difficult on account of the diffuse character of the lines, and the large registering photometer was accordingly used. Several observers have checked the measurements. The difference in velocity between Sirius A and Sirius B varies between 2 and 37 km for different spectral lines, but outstanding features of the results are the definite character of the positive displacement and its change with the amount of the wave length. The greater relative intensity of the spectrum of scattered light of Sirius A towards violet and the increasing influence of the superposition of the lines in its spectrum upon those of Sirius B will tend to reduce the amount of measured displacement. An approximate correction was derived from photometric measurements

¹ C R 174, p 1408 (1922)

² M N 84, p 308 (1924)

³ Berlin-Babelsberg Veröff 3, No 4 (1923), A N 220, p 189 (1924)

⁴ Wash Nat Acad Proc 11, p 382 (1925)

of the relative intensities of the continuous spectrum of Sirius A and Sirius AB. The correction factor d is found from.

$$d = 1 + \frac{h_A}{h_B}$$

where h_A is the density of the spectrum of scattered light of Sirius A, and h_B that of the companion. By applying the correction factors the mean values were found

$H\beta$.. .	+26 km/sec
$H\gamma$.. .	+21 "
Additional lines	.. .	+22 "

The relative orbital velocity at the epoch is +1.7 km/sec. The remaining displacement of 21 km is interpreted as a relativity displacement. The following elements for Sirius B were derived by using STRASS's values for surface brightness, on the alternatives of F0 or A5 for the spectral class.

	F0	A5
Surface brightness	-0 ^m .88	-1 ^m .45
Radius	24 000 km	18 000 km
Density (Water = 1)	30 000	64 000
Relativity displacement .	+0.23 A	0.32 A

The radial velocity of Sirius B also was determined at the Lick Observatory in 1928. J. H MOORE¹ found the following values on the basis of 4 spectrograms:

Hel. disp	Number of lines	Relative density at $H\gamma$, companion/scattered light
1928 Febr. 13 +22 km/sec	7	3.7
20 (+10)	4	1.2
27 +29	6	10.0 (Underexposed)
March 20 +21	4.9	2.8 (Mean of two)
Mean 24		

The result of ADAMS is thus confirmed

Although the idea that Sirius B is an enormously dense body seems to be accepted generally, it seems fair to consider some other explanation. ANDING² and others suggested that the light of the companion is reflected from a dark body. The fact that the spectrum is not identically the same as that of the primary does not make this theory impossible. Because of its general importance for stellar photometry we give a short review of ANDING's paper.

A luminous surface element d with intensity I emits light at an angle of emanation s to an element d' at the distance r , and at an angle of incidence s' . The light received by d' is:

$$dL = I d / \cos s \frac{d' \cos s'}{r^2}.$$

The element d' not emitting light itself reflects the light dL at an angle of emanation s'' to another element d'' :

$$dL' = I d / \cos s \frac{1}{r^2} \frac{A}{\pi} d' \cos s' \cos s'' \frac{1}{r^2} d'' \cos s''',$$

where A is the albedo according to the definition of LAMBERT, s''' the angle of incidence of this element and r' its distance.

Applying this to Sirius we have the integral J (extended over an hemisphere).

$$J = \int I d / \cos s,$$

¹ Publ A S P 40, p. 229 (1928).

² A N 229, p. 69 (1926).

as the expression for the luminosity of the star. If D_s is the distance of SIRIUS A from the Earth, the density of its light rays as observed by us is

$$H_s = \frac{J}{D_s^2}.$$

Further we introduce

$$d\sigma' = R_c^2 d\sigma'$$

where $d\sigma'$ is the surface element of a sphere of unit radius and R_c the radius of SIRIUS B. The angle between the radius vector SIRIUS-Companion and the radius vector Earth-SIRIUS is called $\pi_0 - \alpha$. Then we have

$$\int \cos i' \cos e' d\sigma' = \frac{2}{3} [(\pi_0 - \alpha) \cos \alpha + \sin \alpha]$$

Further in the formula for dL' above r' stands for D_0 (the distance of the companion from the Earth), and the value of the light H_c from the companion is.

$$H_c = J \frac{R_c^3}{r^2} A \frac{2}{3\pi_0} \{(\pi_0 - \alpha) \cos \alpha + \sin \alpha\} \cdot \frac{1}{D_s^2}.$$

The distance of SIRIUS A is equal to that of SIRIUS B, or $D_0 = D_s$. We then get the expression for the ratio of the light of the two objects

$$\frac{H_c}{H_s} = A \frac{R_c^3}{r^2} \frac{2}{3\pi_0} \{(\pi_0 - \alpha) \cos \alpha + \sin \alpha\}$$

For simplifying purposes we assume $A = 1$, r equal to the mean distance a between SIRIUS A and B, and $\alpha = \frac{\pi_0}{2}$.

Then

$$\frac{H_c}{H_s} = \frac{2}{3\pi_0} \left(\frac{R_c}{a} \right)^2$$

or expressed in magnitudes

$$m_c = m_s + 1,7 - 5 \log \frac{R_c}{a}$$

The value of a is 20 astronomical units and the mass of the companion equals the mass of the Sun. If R_c is supposed to be equal to the Sun the following value is found

$$m_c = 18^m,5.$$

Thus SIRIUS B should be ten magnitudes fainter than is the actual case. If R_c is computed from the value $m_c = 8,5$ it is found that $R_c = 100 \odot$ and the density would be 1/955 000 of that of the Sun! The observations show the contrary to be the case, but it might be possible to explain the facts in favour of the reflection theory if the companion is surrounded by a swarm of dark bodies having the character of a dust-cloud.

A detailed investigation does not make the existence of such a dust-cloud very probable. Another hypothesis is that the companion of SIRIUS is a close binary system where one of the components is dark and has the same mass as the Sun. If the distance between the dark companion and SIRIUS B is equal to one planetary unit, the magnitude of the dark companion will be $21^m,8$ on account of the light reflected from SIRIUS B, if the same distance is 0,4, the magnitude of the dark companion will be $16^m,8$.

In order to test the theory it will be necessary to observe the radial velocity of SIRIUS B at different epochs, because in the case of an orbital motion the radial velocity of SIRIUS B will show corresponding variations.

201. **Diameters from Scintillation-Observations.** G. TICHOV¹ has used the colour changes caused by the scintillation of the stars for computing the apparent diameters. From 77 stars he finds the simple relation.

$$d = \frac{5.5036}{S} - 0.0607$$

where d is the diameter in seconds of arc, and S the number of changes in the colour in a second of time

The theory of scintillation shows that the blinking is related in a simple way to the apparent diameter of the stars. DUFOUR² has found that the red stars do not undergo such rapid changes as the white stars. MONTIGNY³ has published a series of papers concerning the scintillation and he has given, in a catalogue, observations of the number of colour changes for 120 stars. I have used his data and tried to establish a relation analogous to that of TICHOV, but so far without success. It seems that so many variables enter into the determination of the number of changes that the diameter is a very complicated function of S . Anyhow, it is clear that the diameters cannot be determined from the material of MONTIGNY with such an accuracy as when they are derived from observations of colour and magnitude. The details of TICHOV's investigation have not been accessible to me and it is possible that his data are more accurate than those of MONTIGNY.

202. **The Fallacy in S. Pokrowsky's Method.** This method was based on the use of elliptically polarised light and was published at first in the year 1912⁴ and later on in 1915⁵. As plans have been made to apply the method in practice, EDDINGTON⁶ took up the "ungrateful and ungracious" task of showing the breakdown of the method. The essential principle is the bringing into superposition of two widely separated beams that have been previously polarised in perpendicular planes. If the phase-difference is zero or $\frac{1}{2}\lambda$, plane polarized light is obtained, and circularly polarized light for phase differences of $\frac{1}{4}\lambda$ or $\frac{3}{4}\lambda$. For intermediate values elliptically polarised light is obtained, which cannot be completely extinguished by a Nicol prism as is the case with plane polarised light. With point-source light the phase difference can be made zero and the image completely extinguished, but with a finite disc the difference will not be zero for all points of the disc simultaneously and the image will not wholly disappear. The angular diameter should result from the intensity of the residual image. The fallacy in the method arises according to EDDINGTON from the fact that the intensity that is calculated by POKROWSKY is not that of the whole star-image, but the intensity at a certain point in the focal plane. If the star is slowly displaced with regard to the instrumental axis, its image does not pop in and out, but bright and dark interference bands pass across the point considered.

The inadequacy of the treatment in the paper of POKROWSKY arises on account of the assumption that for a point-source plane waves emerge from the two apertures and travel in a particular direction. Owing to the diffraction, the waves travel in various directions inclined at angles that are not small compared to the angles, such as $0''.003$, occurring in the investigation.

¹ Mitteilungen Lehafts Inst Leningrad (Russian) 2, p. 126 (1921).

² Recueil Inaugural de l'Université de Lausanne (1892). La scintillation des étoiles.

³ Bull de l'Acad Roy Belg Ser. II, 25, p. 631 (1868); 29, p. 80 (1870), 29, p. 455 (1870); 37, p. 165 (1874); 38, p. 300 (1874) (Catalogue), 42, p. 255 (1876); 44, p. 694 (1877); 43, p. 391 (1878); 46, p. 17 (1878), 46, p. 328 (1878), 46, p. 598 (1878), 47, p. 753 (1879); 48, p. 22 (1879) Ser. III, 1, p. 231 (1881), 6, p. 426 (1883), 9, p. 85 (1883); 16, p. 160, 553 (1888); Ann de l'Obs Bruxelles 1878, p. 245.

⁴ Ap J 36, p. 156 (1912); A N 192, p. 21 (1912); B A 29, p. 305 (1912).

⁵ Ap J 41, p. 147 (1915).

⁶ M N 87, p. 34 (1926).

e) The Densities of the Stars.

203. Densities of the Stars. Pioneer Work. The densities of the stars can, of course, be derived as soon as their masses and dimensions have been computed. A determination of the density itself is only possible in cases of visual binaries and eclipsing variables and involves a knowledge of the mass ratio.

E C. PICKERING¹ and later on W H S MONCK² have separately derived an equation for binary stars with known orbital elements which renders it possible to determine the relation between brightness and mass of these stars quite independently of their distance. It is easy to show that the formula does not distinguish between the extent of the surface and the temperature. The difference in mass-brightness may be due to variety in mean density (diameter) or to variety in surface brilliancy or temperature. The effects observed will be quite the same. PICKERING realized that if the temperatures were considered as not varying from star to star the mean densities of binary stars could be easily derived.

In a paper of 1891 E. W. MAUNDER³ drew attention to several circumstances that indicate that the spectral class marks a difference in constitution rather than a difference in the stage of development. In this paper the author computed the densities of 51 double stars assuming that the intrinsic brightness per unit of surface is the same for all the stars, which is far from truth. He found for the Sirius stars the mean density $\bar{\rho} = 0.0211 \odot$ and for the solar stars $\bar{\rho} = 0.3026 \odot$. He also determined the ratio of the absolute brightness of the two groups of stars as 45.6/70.5, corresponding to a difference in absolute magnitude of $1.0^M, 15$, whereas it should be $-3^M, 3$. The author also points out the possibility of using the double stars for studying the differences in absolute magnitude of different spectral groups.

204. Densities of Visual Binary Stars. The densities of visual binary stars have recently been computed by E. ÖPIK⁴, who derived a relation giving the mean densities ρ , expressed in terms of the elements of the orbit and of the masses M_A and M_B (Solar mass is taken as unit). If R is the radius of the primary star in linear measure and I_A the surface brightness of the primary expressed in that of the Sun as unit, ι_A the apparent brightness, and π the parallax, the relation:

$$\frac{\iota_A}{I_A} = R^2 \pi^2 \sin^2 i''$$

is immediately derived. Further we have the well-known equation:

$$\text{Further} \quad M_A + M_B = a^3 \pi^{-3} P^{-2}$$

$$\text{And} \quad M_A = \rho_A R^3, \quad M_A + M_B = \rho_A R^3 \left(1 + \frac{M_B}{M_A}\right)$$

$$\log \rho_A = \log \frac{a^3}{P^2} + \frac{3}{2} (\log I_A - \log \iota_A) - \log \left(1 + \frac{M_B}{M_A}\right) - 3 \log 206265$$

Taking the stellar magnitude of the Sun to be $-26^m, 60$, we have:

$$m_A + 26,60 = -2,5 \log \iota_A,$$

Expressing the surface brightness in stellar magnitudes and taking the Sun as unit:

$$\iota_A = -2,5 \log I_A$$

¹ Proc Amer Acad of Arts and Sciences 16, p 1 (1880) ² Obs 10, p. 96 (1887)

³ J B A A 2, p 35 (1891); Astronomy and Astrophysics 11, p 145 (1892).

⁴ Ap J 44, p 293 (1916).

and after substitution, the following formulas

$$\log q_A = \log \frac{\sigma^3}{P_A^3} + 0,6(m_A - 1_A) + 0,02 - \log \left(1 + \frac{M_B}{M_A}\right),$$

$$\log q_B = \log \frac{\sigma^3}{P_B^3} + 0,6(m_B - 1_B) + 0,02 - \log \left(1 + \frac{M_A}{M_B}\right),$$

give the densities of the two components.

The surface temperature depends on the absolute temperature and thus, also, on the spectral type. This dependence can be derived from the colour index, but ÖRIK preferred to use the effective temperatures of 109 stars, as determined by WILSING and SCHEINER. If λ_* and λ_\odot denote the wave lengths of maximum spectral energy of the two sources, PLANCK's formula gives for the spectral region λ :

$$\frac{I_\lambda}{I_\odot} = \frac{\frac{4,965 \lambda_\odot}{\lambda} - 1}{\frac{4,965 \lambda_*}{\lambda} - 1}.$$

For visual light we have $\lambda = 0,56 \mu$, $\frac{4,965}{\lambda} = 8,87 = c$, and the difference (in magnitudes) of the visual surface brightnesses of a star and the Sun becomes

$$j = 2,5 \log \frac{\sigma^3 \lambda_*^{-1}}{\sigma^3 \lambda_\odot^{-1}}.$$

From WIEN's formula, $\lambda_* T = 2940$, λ_* can be computed if T is known.

The effective temperatures determined by WILSING and SCHEINER are probably systematically too low. The temperature of the Sun, 5130° , corresponds to a value, $1,16 \text{ cal/cm}^2$ of the solar constant, which is much smaller than the value observed, $1,6-1,7 \text{ cal/cm}^2$. The value for T_\odot , 6250° , as derived by ABBOT and FOWLE, was therefore assumed as a zero-point, and the Potsdam temperatures were differentially corrected.

ÖRIK finds from the table giving the means of T for various spectral subdivisions and the mean reduced wave length of the spectral energy-maximum that the temperature varies somewhat irregularly with spectral class. The fact that the spectral scale is qualitative makes it possible that the abrupt changes in T between some stellar classes may be real.

The mass-ratio must also be known for a computation of the densities. There are few cases where such a determination has been possible, and it is necessary to assume that the relation between $M_B - M_A$ and M_B/M_A is known. Eleven cases were available, and from them the following table was derived.

The results as to the densities are not reviewed here because the following investigation by BERNEWITZ contained a more extensive material than that at disposal in 1916.

In 1921 E. BERNEWITZ¹ published an investigation concerning the densities of binary stars. The formula giving q_A was adopted in the form:

$$\log q_A = \log \frac{\sigma^3}{P_A^3} + 0,6(m_A - 1_A) - \log \left(1 + \frac{M_B}{M_A}\right) + 0,089.$$

$M_B - M_A$	M_B/M_A	$M_B - M_A$	M_B/M_A
0 ^m ,0	1,00	3 ^m ,0	0,76
0 ,8	1,00	5 ,0	0,60
1 ,0	0,93	10 ,0	0,30
2 ,0	0,88		

¹ A N 213, p 1 (1921).

The determination of the surface magnitude j is based on the equation of PLANCK¹

$$\frac{I_*$$

The quantity j_A has to be defined in the same way as the apparent magnitude m and thus account must be taken of the visibility curve $g(\lambda)$ of the human eye. We can assume

$$-0,4 \log \int_0^\infty \left[\frac{c_2 \lambda^{-5}}{e^{\frac{c_2}{\lambda T_*}} - 1} \right] g(\lambda) d\lambda = m$$

The function $g(\lambda)$ is taken in accordance with HENNING's result¹ as

$$g(\lambda) = \left[\frac{5520}{\lambda} e^{1 - \frac{5520}{\lambda}} \right]^{140} + 0,1 \left[\frac{4600}{\lambda} e^{1 - \frac{4600}{\lambda}} \right]^{1000} - 0,07 \left[\frac{6600}{\lambda} e^{1 - \frac{6600}{\lambda}} \right]^{1000}$$

The values of the integral are computed by means of numerical integration. The following corrections have to be applied to the visual magnitudes

Spectral class	Correction Δm	λ_{eff}	Spectral class	Correction Δm	λ_{eff}
A0	+0 ^m ,049	5420	K0	-0 ^m ,035	5580
G0	0 ,000	5490	K5	-0 ,041	5630
G5	-0 ,022	5540	Mc	-0 ,039	5680

The effective temperatures were used as determined by WILSING. The following values of j were found

Spectral class (ADAMS)	$\frac{c_2}{T}$	j	Spectral class (ADAMS)	$\frac{c_2}{T}$	j
B0	1,45	-1 ^m ,93	G0	2,64	+0 ^m ,45
B5	1,45	-1 ,93	G3	2,85	+0 ,86
B8	1,48	-1 ,87	G5	3,00	+1 ,15
A0	1,53	-1 ,76	G8	3,28	+1 ,70
A2	1,62	-1 ,58	K0	3,52	+2 ,16
A5	1,72	-1 ,37	K3	3,92	+2 ,94
A8	1,87	-1 ,07	K5	4,18	+3 ,45
F0	1,99	-0 ,83	K8	4,48	+4 ,03
F3	2,16	-0 ,49	Ma	4,62	+4 ,30
F5	2,29	-0 ,24	Mb	4,76	+4 ,51
F8	2,50	+0 ,18	Mc	4,87	+4 ,78

For the determination of the mass-ratio 10 pairs were used and the following relation resulted:

Δm	$\frac{M_B}{M_A}$	Δm	$\frac{M_B}{M_A}$	Δm	$\frac{M_A}{M_B}$
0 ^M ,0	1,00	2 ^M ,0	0,81	4 ^M ,0	0,68
1 ,0	0,90	3 ,0	0,74	5 ,0	0,62

For 31 out of 63 pairs, only the mean density of both components could be computed. An attempt was made to find a relation between absolute magnitude and density. The results are given in the following table.

¹ Jahrb d Radioakt u Elektronik 1919, H 1.

The data under the heading II refer to the remaining material when 5 spectroscopic pairs and α Centauri were excluded. By forming the part I of the table σ^4 Eridani, Sirius B and σ Hydrae were excluded. We see from the table that there is a steady

M	I		II		Limits of spectral class
	\bar{q}	n	\bar{q}	n	
0 ^M ,8	0,08 \odot	4	0,08 \odot	4	A0—F3
1 ,5	0,20	6	0,14	4	A0—F2 (F1)
2 ,6	0,26	10	0,23	9	A0 (A2)—G0
3 ,5	0,24	9	0,24	9	A2—K2
4 ,6	0,58	12	0,45	11	F1 (F4)—G5
5 ,6	0,43	12	0,40	11	F5—K0
6 ,2	0,45	9	0,50	8	F2—K5
7 ,9	0,47	5	0,47	5	K2—K5
10 ,8	2,81	2	2,81	2	Mb

increase in the mean density from 0,08 \odot to about 0,5 \odot . Between 5^M and 10^M \bar{q} is sensibly constant, but seems to increase for $M > 10^M,0$. There also seems to be a certain increase in \bar{q} with spectral class from A2 to Mb, but the evidence is rather uncertain.

A. R. THOMPSON¹ has recently derived the formulae for computing the density of binary stars, evidently without any knowledge of earlier work. In several cases the agreement with earlier results is not very good. The principal cause of such deviations is to be sought in different assumptions concerning the temperature. The uncertainties arising from uncertain mass-ratios and uncertain orbital elements are not of nearly such importance as those arising from differences in the scale of effective temperatures.

I have derived the absolute magnitudes of most of the objects in THOMPSON's list and have found the following dependence between M and \bar{q} :

M	\bar{q}	n	M	\bar{q}	n
Brightest—0 ^M ,0	0,33 \odot	2	6 ^M ,0—7 ^M ,9	2,43 \odot	16
0 ^M ,0—0 ,9	0,14	3	8 ,0—10 ,9	3,50	3
1 ,0—1 ,9	0,36	16	Krö 60 A	62	1
2 ,0—2 ,9	0,94	17	σ^4 Erid C	48	1
3 ,0—3 ,9	0,54	17	Krö. 60 B	9,6	1
4 ,0—4 ,9	1,40	15	σ^4 Erid. B	16600	1
5 ,0—5 ,9	0,99	15	Sirius B	46000	1

There seems to be a general relation between the absolute magnitude and the density, but the dispersion is considerable. In spite of all the uncertainty that is undoubtedly connected with the derivation of \bar{q} , it is difficult to avoid the impression obtained from a close scrutiny of the material that the actual relation between M and \bar{q} is not a one to one correspondence. This question has undoubtedly some bearing on the question of the character of the mass-luminosity law.

205. The Ratio of Densities in Double Stars. From the formula quoted earlier it follows immediately that

$$\log q_A - \log q_B = 0,6 (m_A - m_B) - 0,6 (j_A - j_B) + \log \frac{R_A}{R_B}.$$

If both the spectra are known and the mass-ratio can be approximated, the ratio of the densities can thus be computed without any knowledge of the elements of the orbit. The mass-ratio can be computed from the formula: $\frac{R_B}{R_A} = -0,61 + 0,36 (M_B - M_A)$ derived from a least square solution using existing material.

If both spectra have been observed the above formula will give us the change in logarithm of density $\Delta \log q$ for different groups. We can also form the

¹ J B A A 39, p. 247, 253 (1929).

mean values of $d \log \varrho / dS$, where dS gives the change in spectral index. Putting

$$\frac{d \log \varrho}{dS} = \varphi(S)$$

it will be possible, by applying a process of graphical integration, to find the curve

$$\log \varrho = \psi(S)$$

which gives the relation between density and spectral class. An attempt has been made to derive this curve but it seems that the present material is rather scanty and that we should wait for a more extensive material. A practical difficulty arises on account of the selection in the material which favours small dS (equal spectra). This part of the material can be used for a derivation of the dispersion in $\log \varrho$ for the different spectral classes. The following small table gives the results hitherto obtained

Spectral class	$d \log \varrho$	$\sigma d \log \varrho$	Mean spectral index (B=1.0, M=5.0) and its dispersion	n
B	0.68	± 0.50	0.4 ± 0.3	19
A	0.47	± 0.38	1.4 ± 0.3	11
F	0.23	± 0.35	2.5 ± 0.2	11
G	-0.07	± 0.41	3.3 ± 0.2	7
K	+0.13	± 0.11	4.7 ± 0.4	5

206 Densities of Eclipsing Binaries. Methodical. The possibility of deriving the mean density of an eclipsing binary system was first pointed out by MÉRIAU¹ in 1896. We have

$$P^2 = \frac{k a^3}{\mathfrak{M}_A + \mathfrak{M}_B} = \frac{3 k a^3}{4 \pi_* (r_A^3 \varrho_A + r_B^3 \varrho_B)}$$

where k is a constant, P the period, a the semi-axis major of the orbit, ϱ_A and ϱ_B the densities of the two components, r_A and r_B their radii. Putting $r_A = a n_A$, $r_B = a n_B$, and $3k/\pi_* = k_1$, we have

$$P^2 = \frac{k_1}{4 (n_A^3 \varrho_A + n_B^3 \varrho_B)},$$

$$\bar{\varrho} = \frac{n_A^3 \varrho_A + n_B^3 \varrho_B}{n_A^3 + n_B^3},$$

when $\bar{\varrho}$ is the mean density of the two components

In the case of a circular orbit the duration of the eclipse is $2\pi_* t/P$ where t is the duration of the light variation. Further let i be the inclination of the orbital plane. Then

$$n_A + n_B = \left(1 - \cos^2 \frac{\pi_* t}{P} \cos^2 i\right)^{\frac{1}{2}}$$

and thus

$$\bar{\varrho} = \frac{(n_A + n_B)^3}{4 (n_A^3 + n_B^3)} \frac{k_1}{P^2 \left(1 - \cos^2 \frac{\pi_* t}{P} \cos^2 i\right)^{\frac{3}{2}}}.$$

The term $(n_A + n_B)^3$ is $\leq 4(n_A^3 + n_B^3)$. If $r_A = r_B$, the limiting value of the first factor of the expression for $\bar{\varrho}$ is 1, and if $r_B = 0$ (no eclipse then takes place), the same factor has the value $\frac{1}{4}$. n_A , n_B , P , t , and i can be derived from the light-curve and the value of k_1 is taken from solar data:

$$k_1 = 5.56 \sin^3 16' 2''.$$

Thus $\bar{\varrho}$ can be computed

¹ C R 122, p 1254 (1896).

In the case of an elliptical orbit the formulae become very complicated.

A. W. ROBERTS discussed in 1899 the densities of four Algol stars¹ and derived the following expressions for the densities

$$\varrho_A = \frac{(0.0092)^3}{p^3 P^3} \left(\frac{M_A}{M_A + M_B} \right),$$

$$\varrho_B = \frac{(0.0092)^3}{q^3 P^3} \left(\frac{M_B}{M_A + M_B} \right),$$

where P is the period (in years), p and q the diameters of the components, expressed in terms of the semi-axis major of the system.

As the two mass terms must always be less than unity or rather as only one of them can ever approach unity, a limit is given in one direction by the expressions

$$\lim \varrho_A = \frac{(0.0092)^3}{p^3 P^3}, \quad \lim \varrho_B = \frac{(0.0092)^3}{q^3 P^3}.$$

The following results were obtained:

	$\lim \varrho_A$	$\lim \varrho_B$
X Carinae	0.25	0.25
S Velorum	0.61	0.03
RR Centauri	0.27	0.27
RS Sagittarii	0.16	0.21

At the same time H. N. RUSSELL² made a derivation of a limiting value for the mean density of 17 variable stars of the Algol type and found,

$$\bar{\varrho}_{AB} \leq \frac{M_A + M_B}{\frac{4}{3} \pi_* (r_A^3 + r_B^3)}.$$

Now

$$r_A^3 + r_B^3 \geq \frac{1}{4} (r_A + r_B)^3,$$

the sign of equality only holding good when $r_A = r_B$

At the first and fourth contacts we have the projection of the distance between the centres of the two stars upon a plane perpendicular to the line of sight = $r_A + r_B$. The arc described during the time from the beginning to the middle of the eclipse is $\pi_* t/P$, where t is the duration of the light variation, and the projected displacement is $a \sin \pi_* t/P$, where a is the radius of the orbit. Then we have the condition:

$$r_A + r_B \geq a \sin \frac{\pi_* t}{P}.$$

The sign of equality only holds good when the transit is central. Besides there is the relation:

$$M_A + M_B = h \frac{a^3}{P^3}$$

and thus:

$$\bar{\varrho}_{AB} \leq \frac{3h}{\pi_* P^3 \sin^3 \frac{\pi_* t}{P}}.$$

Taking the Earth density as 5.53 RUSSELL found $3h/\pi_* = 44.1$ (the unit of the time being 1^h and the unit of density that of water), and derived the densities for 17 stars.

207. SHAPLEY's Work. In 1915 H SHAPLEY published his extensive research concerning the orbital elements of 90 eclipsing binaries based on nearly 10000 magnitudes obtained with the polarizing photometer of the observatory at

¹ Ap J 10, p. 308 (1899)

² Ap J 10, p. 315 (1899)

PRINCETON¹ The memoir discusses the theory of the orbital determination, and then all existing observational data were used for deriving the elements. The total number of observations used is 27094. A general experience in the discussion of this extensive material is that the light curves of eclipsing binaries are, in general, symmetrical, smooth, and regular. The irregularities and anomalies that are often reported in the older literature do not gain any support from accurate photometric work. The investigations of SHAPLEY also disposed of the supposition so prominent in earlier days that one component of the ordinary Algol star is non-luminous. The disparity in brightness of the eclipsing binaries is even smaller than in the case of visual binaries. In all cases except for five or six eclipsing binaries there is positive evidence that the fainter star is itself luminous.

The existence of a darkening toward the limb of the same order of magnitude as in the Sun seems to be well established. It was also found that there is general agreement between the actual gravitational elongation of eclipsing binary stars and the theoretical ellipticity of homogeneous fluid bodies according to G. H. DARWIN'S investigations.

By assuming that the components of each binary are equal to the Sun in mass the "equal mass densities" were computed according to the formulas

$$\varrho_A = (5.29 P^{\frac{2}{3}} r_A)^{-3}, \quad \varrho_B = (5.29 P^{\frac{2}{3}} r_B)^{-3},$$

where P is the period in days, r_A and r_B the radii, the radius of the relative orbit being taken as unit, and ϱ_A and ϱ_B the densities. These were corrected for polar flattening and for the mass-ratio. The mean density is independent of the total mass of the system relative to the Sun, but a knowledge of the mass-ratio is essential for a derivation of the mean densities of the components. At that time the spectroscopic data for eclipsing binaries were very scanty.

The corrected densities for "darkened" solutions were compared with the spectral classes and the following distribution, which is still of interest, was found:

Spectral class log ϱ	B	A	F	G	K	Spectral class log ϱ	B	A	F	G	K
+0.5 to 0.0					2	-2.0 to -3.0	1				
0.0 " -0.5			11	7	1	-3.0 " -4.0	1			2	1
-0.5 " -1.0	8	24	3	1		-4.0 " -5.0					
-1.0 " -1.5	5	13				-5.0 " -6.0			1	1	
-1.5 " -2.0	3	6	1	1							

208. **Parallaxes and Absolute Magnitudes of Eclipsing Binaries.** The parallaxes of eclipsing binaries have been derived by H. N. RUSSELL and H. SHAPLEY² on basis of the following considerations. If the radius and the surface brightness of a certain star are R and J , expressed in units of the solar radius and surface brightness, respectively, we have

$$M = 4.75 - 5 \log R - 2.5 \log J$$

The elements of the eclipsing systems give us the value of r , that is the radius of the brighter component expressed in units of the mean distance a of the components. The mass is assumed to be $2M_{\odot}$ times the Sun's mass. Taking the radius of the Sun as unit and expressing the period, P , in days the mean distance will be

$$a = 5.29 P^{\frac{1}{3}} M^{\frac{1}{3}}$$

¹ Princeton Obs Contr, No 3 (1915)

² Ap J 40, p 417 (1914)

Hence

$$R = ar = 5,29rP^{\frac{1}{3}}\mathfrak{M}^{\frac{1}{3}}.$$

Setting for brevity $5,29rP^{\frac{1}{3}} = A$

we find.

$$M = 4,75 - 5 \log A - \frac{1}{3} \log \mathfrak{M} - \frac{1}{3} \log J$$

A may be derived from the known elements of the eclipsing system. The parallax π is then found from the formula:

$$M = m + 5 + 5 \log \pi$$

For computing M and π two assumptions have thus to be made, viz. the value of \mathfrak{M} and of J . When the spectral class is known, both the quantities can be fairly approximated and thus also a tolerable value of M or π computed. In this way the parallaxes of some 100 eclipsing binaries have been computed¹. In the cases where the masses are known the individual densities of eclipsing binaries can be derived with a considerable degree of accuracy.

800. Recent Statistics of the Eclipsing Binaries. These stars give valuable contributions to our knowledge of several of the physical properties of the stars. Also in those cases where no orbits have been calculated but the eclipsing nature of the pair is known, the maximum possible mean density can be derived.

DEAN McLAUGHLIN² has discussed the data of eclipsing binaries. Altogether photometric orbits have been derived for 116 stars. The densities of the brighter components of each binary are tabulated against spectra as follows.

Relation between spectrum and density.

Density \ Spectral class	O-B3	B8-A3	A3-F3	F8-G5	K-M	Sum
<0,001		1	1	2		4
0,001-0,01	2	2		2		6
0,01-0,05	6	7	1	1		15
0,05-0,10	4	15	1			20
0,10-0,30	3	31	4			38
0,30-0,70		16	7	1		24
0,70-1,0		2	1			3
>1,0				3	1	4
Sum	15	74	15	9	1	114

Mean values of the radii r_A were derived for certain period intervals as is shown in the next table.

Periods	Mean period (η)	Radius of orbit in km. (a)	Radius of brighter star		n
			in parts of a	in km	
< 1 ^d ,0	0 ^d ,6	4,2·10 ⁸	0,37	1,6·10 ⁸	16
1 ^d ,0 - 2,2	1,6	8,0	0,30	2,4	24
2,2 - 3,2	2,7	11,4	0,23	2,6	21
3,2 - 4,25	3,7	14,0	0,21	3,0	17
4,25 - 5,3	4,7	16,4	0,19	3,2	13
5,3 - 7,0	6,0	19,3	0,19	3,5	9
7,0 - 10,0	8,5	24,3	0,10	2,4	4
10 - 100	25	50	0,14	7,1	9

The radii of the orbits have been calculated from the formula $80 = \frac{4}{10^{10}} \cdot \frac{a^3}{P^2}$. The average mass of eclipsing binaries is, in fact lower than that value but

¹ RUSSELL and SHAFLEY, Ap J 40, p. 417 (1914) and subsequent papers by numerous workers within this field.

² A J 38, p. 45 (1927).

even if we take the value of $M_A + M_B$ equal to $4.5\odot$ as suggested from spectroscopic eclipsing binaries, the computed radii will be diminished by only 16 percent.

The radii of the stars are more nearly constant than the radii of their orbits.

The stars of the period group $< 1^d, 0$ days are probably smaller than has been calculated, since they are dwarfs which are less massive than has been assumed.

It seems likely that the discovery-chance has resulted in an unduly large radius for stars of periods $1^d, 0 - 10^d, 0$ since the greater radii will mean longer duration of eclipse. Then it is quite possible that the average radius will be nearly constant.

f) The Masses of the Stars.

210. Methods of Deriving Stellar Masses. The laws of gravitation furnish a method of deriving the masses of heavenly bodies. As soon as a gravitational effect exercised by one body on another can be measured the mass is easily determined. Inasmuch as the motions of the stars are not known to such an extent and accuracy that we can determine any curvature of the orbits it is not possible to derive any masses. The only cases for which it has been possible to determine individual masses is when the absolute orbit of a visual double star has been derived with accuracy or when the DOPPLER displacements in both spectra of an eclipsing binary star have been measured. When both spectra in an ordinary spectroscopic binary are exhibited and their displacements measured the mass-ratio can be accurately determined. When the relative orbit of one component of a visual binary is known the sum of the masses of the component can be determined. In the case of spectroscopic binaries showing one spectrum a rather complicated function of the mass can be derived, which treated statistically can yield results of value concerning the mean mass of groups of stars.

For groups of visual binaries for which the orbital motion has been observed but the orbital elements are unknown, the mean value of the masses can be derived if the distances are accurately known.

Finally there seems to be some gravitational effect in the upper layers of the atmosphere of the stars affecting the intensity of certain lines in spectra. The problem cannot be said to be solved as yet, but some mass-effect seems to be present in the spectrographic parallaxes, which fact will probably lead to methods of determining the stellar mass from certain spectral characteristics.

In the case of clusters or agglomerations of stars of cluster structure it is possible to determine the mass-ratios of such groups of members as have a different spatial distribution and hence a different distribution when projected on a photographic plate. The differences in the space densities are effects of the gravitation (e. g. heavy bodies will be more concentrated towards the centre of the agglomeration than less massive ones) and when the distribution in space of the separate groups is known the mass-ratios can be derived. This, of course, involves accurate determinations of the distance of the agglomeration.

The cases mentioned are the only ones where a direct determination of the masses or the mean masses of groups can be performed. In order to extend our knowledge to ordinary stars we have to search for simple relations between the masses and other characteristics of the stars.

Such a relation is known to exist between mass and spectral class; there is also a relation between mass and luminosity, which was first found empirically but later on derived from the theory of radiative equilibrium. The establishment of the mass-luminosity relation is of fundamental importance and too many efforts can scarcely be made with regard to the accurate derivation of this relation from empirical data and theoretical deductions. It is possible that the mass-luminosity

relation only represents a first approximation and that the actual relation should include a second variable, the effective temperature.

The mass can also be related to the reduced proper motion, which is sometimes of advantage. There probably exists a relation between the density and the mass, but it cannot at present be established with any accuracy. There seems to be a relation between the mean mass of a group of stars and the mean squared space- (or radial) velocities of the same group (equipartition of energy).

The sum of the masses of the two components in a binary system is found applying the third law of KEPLER ("the harmonic law"). We have:

$$M_A + M_B = \frac{a^3}{\pi^2 P^2},$$

if we select as units the year and the solar mass. The major axis a is taken in seconds of arc as well as the parallax π .

In the case of spectroscopic binaries this equation can be written:

$$M_A + M_B = \frac{4\pi^3}{h^3} \frac{(a_A + a_B)^3}{P^2}$$

(h is the Gaussian constant, $\log h = 8,23558 - 10$) or:

$$M_A + M_B = K \frac{a^3}{P^2}$$

where P is the period expressed in days, a the major axis expressed in km, and K a numerical constant. We do not know a or $a_A + a_B$ but only its projection $a \sin i$ and thence we have to multiply both members with $\sin^3 i$ where i is the inclination of the orbit.

Thus:

$$(M_A + M_B) \sin^3 i = K (a_A \sin i + a_B \sin i)^3 P^{-2}.$$

From the theory of the determination of orbits of spectroscopic binaries we have:

$$a_A \sin i + a_B \sin i = K' (K_A + K_B) P \sqrt{1 - e^2}$$

where K_A and K_B are the semi-amplitudes of the radial velocities of the two components, expressed in km/sec, and K' is a constant, hence.

$$(M_A + M_B) \sin^3 i = k_1 (K_A + K_B)^3 P (1 - e^2)^{\frac{3}{2}}.$$

The numerical value of $\log k_1$ is 3,01642 - 10.

If both spectra have been measured we have:

$$M_A \sin^3 i = k_1 (K_A + K_B)^3 K_B P (1 - e^2)^{\frac{3}{2}},$$

$$M_B \sin^3 i = k_1 (K_A + K_B)^3 K_A P (1 - e^2)^{\frac{3}{2}}$$

In fact,

$$\frac{M_A}{M_B} = \frac{K_B}{K_A}.$$

When only one spectrum (of component A) is visible another formula has to be used:

$$\frac{M_B^2 \sin^3 i}{(M_A + M_B)^2} = k_1 K_A^3 P (1 - e^2)^{\frac{3}{2}}.$$

At any rate it is necessary to assume a mean value for $\sin^3 i$. We have.

$$\overline{\sin^3 i} = \frac{\int_0^{\pi/2} \sin^4 i \, di}{\int_0^{\pi/2} \sin i \, di} = \frac{3}{16} \pi = 0,59.$$

Because of the preference for high values of i , it is better to adopt a somewhat higher value for $\sin^2 i$ than 0.59, for instance 0.66. Sometimes even as high a value as 0.93 has been adopted¹.

We have seen above how the mass-ratio can be determined in case of spectroscopic binaries. If such a system also is observed as an eclipsing binary the value of i can be found when deriving the orbit and thus the masses of the pair can also be computed. In case of visual binaries the mass-ratio can be determined in the following way.

Let A and B denote the two components of a binary and C be a star that does not take part in the motion of the system AB , or in other words does not belong to the system.

Let

ϱ_{AC} = the angular distance between A and C

θ_{CA} = position angle of C with respect to A

x_A, y_A = the rectangular coordinates of A with C as origin, the x -axis being directed toward the North Pole

x_0, y_0 = the rectangular coordinates of the centre of gravity O of the system AB with C as origin

ξ_0, η_0 = the coordinates of O with A as origin

ϱ_{AB} = the distance between A and B

θ_{BA} = the position angle of B with respect to A .

$$k = \frac{m_A}{m_A + m_B}$$

The coordinates of the centre of gravity of AB are

$$x_0 = x_A + \xi_0,$$

$$y_0 = y_A + \eta_0,$$

which may be written in the form

$$x_0 = +k \varrho_{AB} \cos \theta_{BA} - \varrho_{AC} \cos \theta_{CA},$$

$$y_0 = +k \varrho_{AB} \sin \theta_{BA} - \varrho_{AC} \sin \theta_{CA}.$$

The motion of the centre of gravity O with respect to C is rectilinear and thus we can write

$$x_0 = a + b(t - t_0),$$

$$y_0 = a' + b'(t - t_0),$$

where a, a', b , and b' are constants, t a certain epoch of observation, and t_0 an initial epoch.

$$\begin{aligned} \text{Thus} \quad a + b(t - t_0) - k \varrho_{AB} \cos \theta_{BA} &= -\varrho_{AC} \cos \theta_{CA}, \\ a' + b'(t - t_0) - k \varrho_{AB} \sin \theta_{BA} &= -\varrho_{AC} \sin \theta_{CA}. \end{aligned}$$

The problem is, in fact, nearly identical with the problem of determining the trigonometric parallax of a star, only that the period is much longer than a year, and the same methods can be applied with advantage in practice. It seems that observers have not always appreciated the great advantage of connecting visual doubles with a sufficient number of stars being independent of the system. The student is advised to consult the two observing lists for the determinations of mass-ratios as given by AIRKEN [Lick Bull 7, p 3 (1912)] and by VAN BIESBROECK [A J 29, p 173 (1916)].

211 Are Derived Mass-Values Representative? It will certainly be asked whether we have any right to extend our knowledge concerning the masses or the densities of the double stars to ordinary stars. The following facts may be

¹ KREIKEN, MN 89, p 589 (1929)

mentioned which show that the double stars do not form an exceptional group among the stars of the stellar system

The distribution of double stars on the sky is the same as the distribution of ordinary stars. Our knowledge concerning the special distribution of the former is scanty, but the evidence so far shows the general agreement in the distribution in space of the two groups (LEWIS¹, KREIKEN²).

The motions of the double stars do not differ from the motions of the single stars in any known respect. The present writer has investigated the proper motions and radial velocities of some 150 binaries without finding any peculiar behaviour. C. LUTLAU-JANSSEN³ has determined

the apex of double stars and found the values $A = 265^\circ$, $D = +26^\circ$, $V = 17.1$ km/sec. J. OORT⁴ has found the adjoined mean residual radial velocities of binary stars.

Mean residual velocity \bar{v} .

Spectral class	Spectroscopic binaries	n	Single stars (CANNON ⁵) ⁶	n
B0—B9	6.6 km/sec	43	6.5 km/sec	225
A0—A9	12.0	30	11.0	177
F0—F9	12.4	20	14.1	184
G0—K9	16.0	18	13.6	492

He derives the ratio $V_{\text{single stars}}/V_{\text{binaries}} = 1.03 \pm 0.05$ and concludes that the average mass of the brighter component of a visual binary is about equal to that of a single star of the same spectrum and absolute brightness.

The double stars exhibit typical stellar spectra (MISS CANNON⁵, LEONARD⁷, and others). No such spectral peculiarities are found among double stars as to place them among the special groups of stars. The RUSSELL diagram of the binary stars as first constructed by F. C. LEONARD⁷ has the same form as that of single stars. Applying a different method the present writer and W. J. LUYTEN⁸ later on derived a typical RUSSELL diagram on the basis of some 300 double stars.

As far as all the evidence goes it is only the fact that two or more bodies are moving within the activity-spheres of each other's gravitation that places the double or multiple stars in a certain class. With regard to motion, space distribution, physical properties, absolute magnitudes, temperatures, densities, general chemical and physical constitution the double stars are typical citizens of the stellar realm.

Thus it seems justifiable to conclude that the masses or densities of binaries should not differ systematically from the masses or densities of the ordinary stars.

212. Historical Notes. Observational Evidences. The first star for which it was possible to obtain accurate knowledge of its dimensions, mass, and density was our Sun. When the first trigonometric parallaxes of stars had been secured, and orbital elements of double stars had been computed, the third law of KEPLER ("the harmonic law") was applied and it was evident that the masses of neighbouring stars did not differ systematically from that of the Sun. Already in Madras⁹ about 1850 JACOB found the mass of the α Centauri system to be $\frac{1}{2} \odot$ and interpreted this result as showing that the mass of the system is of the same order of magnitude as the mass of the Sun. On account of the slow progress of the determinations of stellar parallax our knowledge of the masses of the stars also advanced slowly. A table in AGNES M. CLERKE's well-known work "The System of the Stars" (1905) is, I think, representative of the knowledge possessed of the stellar masses at that time. The sums of the masses

¹ Mem R A S 56 (1906).

² M N 89, p. 647 (1929).

³ A N 203, p. 9 (1916); København K Acad Forhandl Overagt 1916, No. 1.

⁴ A J 35, p. 141 (1924).

⁵ Lick Bull 6, p. 125 (1911).

⁶ Harv Ann 56, No. 7 (1912).

⁷ Lick Bull 10, p. 169 (1923).

⁸ A J 35, p. 93 (1923).

⁹ M N 10, p. 170 (1850).

in twelve binary systems are given in that table. The values range between 0,67 \odot and 12,66 \odot . It is of a certain interest that Capella is included with a minimum value of 2,14 \odot derived on the strength of the observations at Greenwich in 1905, when the separation was estimated as 0",05. These observations could not be confirmed at Lick and the Greenwich results were not generally accepted. A comparison by J. HAAS¹ of the positions derived on basis of the orbital elements from the Mount Wilson interferometer measurements with the Greenwich estimates in 1905 has made it very probable that Capella actually was seen as oblong by the Greenwich observers—a very remarkable observation!

The astronomers of the 19th century certainly took a keen interest in the development of methods to determine physical characteristics of the stars. In 1844 BESSEL noticed that the proper motions of Sirius and of Procyon were variable. This led him to investigate in a masterly written paper the possible causes of changes in proper motions of the stars². He found it most probable that the changes in Sirius and in Procyon were caused by the gravitation of a possible dark companion to the brilliant star. It is well known how after many disappointments on account of presumed, but not confirmed, discoveries this theoretical investigation finally led to ALVAN CLARK's discovery of the companion of Sirius in 1862. It is also well known how the investigations of BESSEL and the later work of AUWERS³ led to the discovery by J. M. SCHABERLE of the companion of Procyon in 1896. The point that concerns us here is that these investigations have developed the methods of determining the mass-ratio in double stars in such a definite way that at present we have no reason to change or modify the classical formulae.

This method depends on accurate determinations of periodic changes of small amplitude in the proper motions. It is very difficult to obtain reliable results. When T. LEWIS⁴ published in 1906 his large catalogue of the Σ double stars, he collected the results then existing concerning the value⁵ of M_A/M_B . On the basis of the material he arrived at the wrong conclusion that the fainter component in a binary system is generally the more massive one. The evidence accumulated later shows that this conclusion is not tenable. The mass-ratios known hitherto are still affected by considerable uncertainty in the case of visual binaries but their general accuracy has much increased since 1905. We also have nowadays the possibility of deriving accurate mass-ratios from spectroscopic binaries giving impressions of both spectra on photographic plates.

Of the different computations of the mean masses of the binary stars we mention here only a few. In 1910 R. G. AITKEN⁶ used the material in the parallax catalogue of KAPTEYN and WEERSMA⁷ and found the masses to vary between 0,002 \odot and 371 \odot , most of the variation being attributable to the uncertainty of the parallax measurements. It could be assumed that the real variation in the size of stellar masses is very small.

In the following table the results of some computations of the total mass of stellar systems, generally not specially mentioned or reviewed in the text, are collected. No completeness is aimed at. The sole purpose is to illustrate the general development during the last decades of our knowledge of stellar masses.

¹ Obs 47, p 376 (1924).

² A N 22, p 145 (1844), Abhandlungen von FRIEDRICH WILHELM BESSEL, herausg von R ENGELMANN II, p 306 (1875).

³ A N 58, p 33 (1862).

⁴ Mem R A S 56 (1906).

⁵ LEWIS did not care to derive $M_A + M_B$ from his material, but pointed out the possibility of doing so [Mem R A S 56, p. XXI (1906)].

⁶ Pop Astr 18, p 483 (1910).

⁷ Groningen Publ, No 24 (1910).

Authority	Mean value	Range	n	Epoch	Source
AUWERS	1,6 ⊙	1,04 — 2,20 ⊙	2	1892	A N 129, p 232.
YOUNG	1,6	0,33 — 3,1	4	1899	General Astronomy.
GORE	5	1,9 — 15	5	1907	Astronomical Essays
DOBERCK	1 ¹ / ₂	—	few cases	1908	A N 178, p. 381
NEWCOMB-ENGELMANN	1,4	0,1 — 3,5	7	1911	Populäre Astronomie, IV. Aufl
	1,4	0,3 — 3,2	9	1921	Populäre Astronomie, VI Aufl
DOBERCK	2,46	0,43 — 372	11	1912	A N 191, p. 425
AITKEN	2,5—3,0	0,002—371	24	1910	Pop Astr 18, p 483
CAMPBELL	1,9	1,0 — 5,0	6	1913	Stellar Motions
FOUCHÉ	2,0	0,3 — 7,8	13	1916	B S A F 30, p 90.
AITKEN	1,76	0,45 — 3,3	14	1918	The Binary Stars.
VAN MAANEN	4,2	0,18 — 45,7	39	1919	Publ ASP 31, p. 231
MITCHELL	10	0,38 — 71,3	19	1920	McCormick Publ III
MILLER and PITMAN	5,44	0,11 — 134,5	68	1922	A J 34, p 127.
LUNDMARK	1,7	0,2 — 150	250	1929	Card Catalogue.

In 1916 R. T. A. INNES¹ discussed the size of the stellar masses. For 50 stars fairly reliable orbits had been computed. Because of the lack of data concerning the parallaxes of those stars the author assumed that the absolute magnitudes were constant and equal to the absolute magnitude of the Sun. INNES prefers the term "gravitative power" instead of mass, as the last term suggests a body of matter and it is an assumption to consider mass as equivalent to gravitative power. Among the many interesting conclusions in INNES's paper we quote the one that few of the double stars have a gravitative power equal to that of the Sun. In general the mass must be considerably smaller than the solar mass. It seems probable that the spectrum varies with the mass. On account of his assumption the masses of the B stars in INNES's list came out too low and the masses of red dwarfs too high. Some of the conclusions are naturally influenced by this fact. Only a few years later the situation with regard to our knowledge of stellar parallaxes had changed in such a favourable way that the order of magnitude of the mean masses of different spectral classes could be determined with fair accuracy.

In 1919 A. VAN MAANEN² derived the masses of 55 binaries, of which the parallaxes of 39 could be accepted as fairly well determined. The dispersion in the values is very small; indeed, it only amounts to 2,1 ⊙. Two stars which had a mass larger than 10 ⊙ were excluded and the lowest of the values was 0,18 ⊙. When the masses were plotted against the absolute magnitudes a quite definite relation was found, which was in good agreement with later theoretical derivations of the mass-luminosity relation. Also a relation between mass and velocity was sought for, but no definite result was found.

In 1922 B. MEYERMAN³ computed the masses of the components of 59 pairs. The mean values are $M_1 = 1,4 ⊙$ and $M_2 = 1,2 ⊙$, and the dispersion is very small indeed. In a subsequent paper⁴ the relation between mass and proper motion (reduced to km/sec by means of the known parallaxes) was investigated and gave as a main result:

Mass	V	n
3,7 ⊙	19,8 km/sec	19
1,2 ⊙	25,4 "	39

¹ South African Journal of Science, 1916 June.

² Publ A S P 31, p. 231 (1919).

³ A N 216, p. 301 (1922).

⁴ A N 216, p. 385 (1922).

Mass-ratios Visual Binaries,

System	α 1900	δ 1900	ΔM (visual)	M_1/M_2	Authority	M_1/M_2 (adopt)	Period (years)
Σ 3062	0 ^h 1 ^m .0	+57° 53'	1.0	1.0	BOSS	1.0	106
13 Ceti	0 30.1	- 4 9	0.8	1.32	PARASKEVOPOULOS	1.0	6.88
γ Cassiopeiae	0 43.0	+57 17	3.6	0.92 0.27 0.5 0.76 0.34	POGO STRUVE LEWIS BOSS MITCHELL		
α^2 Eridani BC	4 10.7	- 7 49	2.0	0.27 1.08 1.0 0.47 0.42 0.64	VAN BIESBROECK LEWIS MITCHELL VAN DEN BOS AIDUN ABETTI	0.38	346
80 Tauri	4 24.4	+15 25	3.3	0.39	VAN DEN BOS	0.45	248
α Aurigae	5 9.3	+45 54	0.5	0.79	MERRILL	0.39	150.2
Sirius	6 40.7	-16 35	10.0	0.47 0.5 0.39	AUWILRS SEC BOSS	0.79	0.28
Castor	7 28.2	+32 6	0.86	20 1.0 0.81	FURNER MITCHELL RABE	0.44	50.2
Procyon	7 34.1	+ 5 29	13.0	0.60 0.2 0.33 0.31	RABE SEC BOSS BOSS	0.80	306
γ Argus	7 47.1	-13 38	0.6	0.315 0.37 0.4	JONES MITCHELL O STRUVE	0.31	40.3
ζ Canceri	8 6.5	+17 57	0.24	1.0	SEELIGER	0.30	23.1
ϵ Hydrae	8 41.5	+ 6 47	1.5	6 0.9 1.0	LEWIS SEELIGER MITCHELL	1.0	57.89
ξ Urs Majoris	11 12.9	+32 6	0.5	1.5 1.0 0.72	BOWYER BOSS ABETTI	0.95	15.3
γ Virginis	12 36.6	- 0 54	0.0	1.0 1.0 1.0	HERTZSPRUNG LEWIS BOSS	0.9	59.8
α Centauri	13 33.0 14 32.8	+36 48 -60 25	1.9 1.37	2.0 1.0 1.05 0.96 0.85	FURNER ELKIN GILL ROBERTS BOSS	2.0	220
ξ Bootis	14 46.8	+19 31	2.0	1.2 0.87	BOWYER BOSS	0.97	80.09
ξ Scorpii	15 58.9	-11 6	0.3	1.3	S HERR	0.87	151.4
σ Cor Borealis	16 10.9	+34 7	0.9	4 1.1 0.47 2.6	LEWIS HADLEY BOSS ABETTI	1.0	44.7
λ Ophiuchi	16 25.9	+ 2 12	2.1	4.3	LEWIS	1.5	500
ζ Herculis	16 37.5	+31 47	3.5	1.0 0.43 0.88 4.0	LEWIS BOSS CHANG PREY	4.3	110
70 Ophiuchi	18 0.4	+ 2 31	1.70	0.79 0.5 0.82	COMSTOCK LAU BOSS	0.7	34.46

Mass-ratios. Visual Binaries. (Continued)

System	α 1900	δ 1900	ΔM (visual)	M_2/M_1	Authority	M_2/M_1 (adopt.)	Period (years)
70 Ophiuchi . .	18 ^h 0 ^m .4	+ 2° 31'		0.56 0.79 0.89	PAVEL MITCHELL VAN BIESBROECK	0.8	87.7
β Delphini . .	20 32.9	+14 15	1.0	1.13 (0.15)	CHANG HADLEY	1.1	26.8
τ Cygni . .	21 10.8	+37 37	4.2	0.89 0.89 0.77	HADLEY VAN BIESBROECK ABETTI	0.9	49.2
π Pegasi . . .	21 40.1	+23 11	0.5	0.40	HEWOTRAU	0.40	11.6
Kruiger 60 . .	22 24.5	+57 12	1.5	1.14 0.83 0.45 0.91 0.83	RUSSELL MITCHELL RUSSELL ALDEN PAVEL and BERNEWITZ	0.8	44.27
85 Pegasi . . .	23 36.9	+26 33	5.15	4 3 1.0 1.7 1.78	FURNER LEWIS BOSS COMSTOCK VAN BIESBROECK	1.7	25.42

Computing the total space motions on the basis of data for 15 objects MEYERMAN found

$\overline{M_{\text{sun}}}$	\overline{V}	n
4.0 \odot	23.5 km/sec	8
1.4 \odot	33.7 "	7

The masses that are derived on the basis of double star data are dependent on the amount of the gravitation between the components. Thus the total mass of the binary system is obtained, i. e. not only the mass of the two stars, but also of planets and other dark bodies that may be present. There are 10 typical Sun stars for which the mass has been determined with a fair degree of accuracy. The mean value of the masses is $1.05 \odot \pm 0.11 \odot$ and the mean value of the absolute magnitudes $M = 4.76$. It seems that these systems cannot be of a structure radically different from that of our solar system.

A remarkable event was the discovery of J. S. PLASKETT¹ in 1922 that the O star BD + 6° 1309 was a very massive system. The two components had the mass values.

$$M_A = \frac{75.6}{\sin^2 i} \odot, \quad M_B = \frac{63.3}{\sin^2 i} \odot.$$

The system has later been carefully watched for changes in the magnitudes, but so far without positive results. PLASKETT's star does not seem to be an eclipsing binary system and therefore it is justifiable to conclude that the sum of the masses is at least 160 \odot .

In EDDINGTON's first theory of stellar evolution 40 \odot was determined as the upper limit for the mass of a star. H. VON ZIEPEL has pointed out several times in his lectures that this was not a necessary consequence; if there is an upper limit it has a very high value. In the final theory of EDDINGTON there seems to be no low limit for the possible size of stellar masses; on the other hand it seems that a limit exists, and it must be a quite exceptional case if a stellar mass is much above 100 \odot .

The tables on p. 614 to 616 summarize the results hitherto found for the mass-ratios in visual binaries and eclipsing variables. There exist also some 100 well

¹ M.N. 82, p. 447 (1922).

determined mass-ratios of spectroscopic binaries where both spectra have been observed. These have been excluded because of the lack of data for the magnitude of the components. The student interested in these stars should consult the catalogues by J. H. MOORE [Lick Bull 11, p 141 (1924)] and A. BILLER [Beih. Bab. Veroeff 5, H 6 (1927)]

Eclipsing Binaries.

Object	α 1900	AM	M_B/M_A	Radius	Density	Parallax	M	Sp
				of brighter comp				
HD 1337	0 ^h 12 ^m .5	1.2	0.93	23.8	0.0027	0",002	-6.0 -4.8	O8,5n O8,5n
TV Cassiopeiæ	0 13 .9	1.82	0.59	2.54	0.112	0 ,0047	+0.8 +2.6	A0n A0
γ Tauri	3 55 .1	1.49	0.33	5.35	0.024	0 ,0095	-1.1 +0.4	B3
β Aurigæ	5 52 .2	0.00	0.98	2.83	0.11	0 ,030	+0.6 +0.6	A0n A0n
WW Aurigæ	6 25 .9	—	0.86	1.9	0.32	0 ,010	+2.2	A7
Castor C	7 28 .2	0.21	0.90	0.76	1.4	0 ,074	+9.6 +9.8	M1e
V Puppis	7 55 .4	0.45	0.77	7.5	0.050	0 ,004	-2.0 -1.5	B1n B3n
S Antliae	9 27 .9	0.74	0.56	1.34	0.31	0 ,007	+2.9 +3.6	A8n A8n
W Ursæ Majoris	9 36 .7	0.04	0.72	0.72	1.92	0 ,013	+5.4 +5.4	F8n F8n
RS Can Venaticorum	13 6 .0	0.92	1.00	7.1	0.004	0 ,0022	-0.0 +0.9	F3n K0
δ Bootis	15 0 .5	0.0	1.00	0.6	2.2	0 ,152(?)	+6.3 +6.3	G2
U Cor Borealis	15 14 .1	2.96	0.38	2.94	0.19	0 ,0037	+0.4 +3.4	B3n B3n
U Ophiuchi	17 11 .5	0.18	0.88	3.23	0.18	0 ,0059	+0.2 +0.4	B3n B5n
α Herculis	17 13 .6	0.88	0.40	4.64	0.094	0 ,0071	-0.8 +0.1	B3n B3n
TX Herculis	17 15 .4	0.68	0.87	1.57	0.53	0 ,0053	+2.3 +3.0	A2s A2s
Z Herculis	17 53 .6	0.35	0.87	1.77	0.28	0 ,013	+3.3 +3.6	F2s F2
RX Herculis	18 26 .0	0.12	0.95	1.95	0.280	0 ,0064	+1.8 +1.9	B9n B9n
β Lyrae	18 46 .4	—	0.41	13.6	0.0012	0 ,005	-3.1 -2.6	B2ep cB8
RS Vulpeculae	19 13 .4	2.35	0.31	4.22	0.06	0 ,0045	-0.4 +2.0	B8n B9
Z Vulpeculae	19 17 .5	1.45	0.45	4.54	0.052	0 ,0018	-0.7 +0.7	B3n B3
σ Aquilæ	19 34 .3	0.36	0.82	3.48	0.15	0 ,0060	-0.2 +0.2	B8n B8n
Y Cygni	20 48 .1	0.38	0.92	4.60	0.17	0 ,0022	-0.8 -0.4	B2n B2n

I think that the first table will show how imperfect our knowledge of the mass-ratios of visual binaries still is. The length of the periods makes it difficult in most cases to cover even one period by observations. The values in the second table are by far more accurate than those in the first table.

The mass-ratios when plotted against differences in magnitudes show certain deviations from the curve computed in accordance with the mass-luminosity relation. There seems to be some systematic difference between the mass-ratios

of visual and eclipsing binaries. The considerable dispersion in the mass-ratios does not seem to be dependent on the errors in the individual determinations alone.

218. Equipartition of Stellar Energy. J. HALM¹ was one of the first to apply the law of equipartition of the energy to the derivation of the average mass of the stars. According to the Maxwellian law the number of molecules of mass M with velocities between u, v, w and $u + du, v + dv, w + dw$ is,

$$A e^{-h^2 M (u^2 + v^2 + w^2)} du dv dw,$$

where A and h are constants.

The kinetic energy of a single molecule of mass M is:

$$\frac{1}{2} M (u^2 + v^2 + w^2).$$

Hence the total energy of all the molecules.

$$E = \frac{1}{2} A M \int_{-\infty}^{+\infty} \int_{-\infty}^{+\infty} \int_{-\infty}^{+\infty} e^{-h^2 M (u^2 + v^2 + w^2)} (u^2 + v^2 + w^2) du dv dw,$$

or:

$$E = \frac{1}{8} \frac{A}{h^3} \sqrt{\frac{\pi_0}{h^3 M}} \times \left[\int_{-\infty}^{+\infty} \int_{-\infty}^{+\infty} e^{-h^2 M (v^2 + w^2)} dv dw + \int_{-\infty}^{+\infty} \int_{-\infty}^{+\infty} e^{-h^2 M (u^2 + w^2)} du dw + \int_{-\infty}^{+\infty} \int_{-\infty}^{+\infty} e^{-h^2 M (u^2 + v^2)} du dv \right],$$

or, the three integrals in the brackets being identical,

$$E = \frac{3}{8} \frac{A}{h^3} \sqrt{\frac{\pi_0}{h^3 M}} \int_{-\infty}^{+\infty} \int_{-\infty}^{+\infty} e^{-h^2 M (v^2 + w^2)} dv dw.$$

The total number of molecules is:

$$N = A \int_{-\infty}^{+\infty} \int_{-\infty}^{+\infty} \int_{-\infty}^{+\infty} e^{-h^2 M (u^2 + v^2 + w^2)} du dv dw = \frac{1}{2} A \sqrt{\frac{\pi_0}{h^3 M}} \int_{-\infty}^{+\infty} \int_{-\infty}^{+\infty} e^{-h^2 M (v^2 + w^2)} dv dw.$$

Hence.

$$\bar{E} = \frac{E}{N} = \frac{3}{4} h^2,$$

i. e. the average kinetic energy is independent of the mass. If Q denotes the average speed we thus find:

$$M Q^2 = \text{const.},$$

i. e. the average speed is inversely proportional to the square root of the mass.

HALM says that it is certainly not illogical to associate the rate of development from earlier to later types with the mass of a star. If stars of different masses started their development at the same time, it would be expected a priori that the lighter stars would cool down more quickly, and hence arrive at the more advanced spectral stages sooner than the heavy stars. The average mass of the "earlier" spectral classes will be larger than that of the more "advanced" spectral classes. In this way the lesser average speed of the earlier stars could be explained.

¹ M N 71, p. 610 (1911).

HALM quotes the results of KAPTEYN

Spectral class	Mean radial velocity	"	Spectral class	Mean radial velocity	"
B—B9	6,0 km/sec	64	G—G5	12,6 km/sec	26
A—A5	11,2 "	18	K—K5	15,4 "	55
F—F8	14,5 "	17	Ma	19,3 "	6

HALM points out that the ratio $\mathcal{M}_B/\mathcal{M}_A$ is probably independent of spectral class and quotes the following results

Group	$\mathcal{M}_B/\mathcal{M}_A$
Spectroscopic binaries	$\begin{cases} 0,77 & \text{"Orion type"} \\ 0,83 & \text{Other classes} \end{cases}$
Visual binaries	0,81

Thus it is admissible to assume that the ratios of the average values of the mass-function

$$\frac{\mathcal{M}_B^3 \sin^3 i}{(\mathcal{M}_A + \mathcal{M}_B)^2}$$

for different types are practically identical with the ratio of their combined masses

From spectroscopic binaries showing both the spectra HALM derived.

$$\begin{aligned} \text{Orion type } (\mathcal{M}_A + \mathcal{M}_B) \sin^3 i &= 16,4 \pm 3,4 \odot \\ \text{Classes A—G} &1,9 \pm 0,3 \odot \end{aligned}$$

Ratio of average mass Orion stars/other classes = 8,6

Using the binaries where only one component was seen, i.e. where only the mass-function is determined, it was found

Period	Mass ratio Orion stars/other classes	"
$< 5^d$	8,6 \odot	29
5^d-30	4,6	24
> 30	6,2	20
All	6,5 \odot	

The square roots of the two values of the mean ratio of Orion stars/other classes are 2,9 and 2,5. Thus it is justifiable to assume that the Orion stars are on the average more massive than the stars of more advanced type.

From the above table of KAPTEYN the ratio of average speed of Orion stars/average speed of other classes is 0,42, whereas the inverse square root of the mass-ratio of the two groups is 0,34 or 0,40. Thus the agreement is good, a fact that seems to support the equipartition of energy

HALM has used the average parallaxes according to KAPTEYN's formula and found (see close by)

H. N. RUSSELL¹ had found (see close by)

Combining his results with the preceding conclusion concerning the heavier mass of the earlier stars, HALM makes the remarkable statement that, "we may also say that intrinsic brightness and mass are in direct relationship"

This is the first time, as far as the present writer knows, that a mass-luminosity relation has been thought to exist among the stars

Group	Apparent magnitude	$\bar{\pi}$	M
Orion stars	5,0	0'',0066	-0 ⁿ ,9
A stars	5,0	0,0098	0,0
F—K stars	5,0	0,0224	+1,8

Spectral class	Apparent magnitude	$\bar{\pi}$	M
F8	7,0	0'',044	5 ⁿ ,2
G—G2	7,8	0,029	5,1
G5	8,6	0,064	7,6
K	7,4	0,119	7,8
K5	8,2	0,254	10,2
M	8,3	0,221	10,0

¹ A J 26, p 147 (1910)

HALM's investigation does not tell us anything concerning the size of the dispersion in stellar mass. It is not possible to determine this element without making complicated investigations. The method is of much value in any case, because of its possibilities for determining the average mass of the stars that do not belong to such selected groups as double stars or stellar clusters.

The relation between the mean speed and \overline{M} is perhaps not applicable to all classes of stars. The O stars and the planetary nebulae are undoubtedly heavy bodies, but do not move as slowly as the B stars. When reviewing SEARLES's results we will see how the law of equipartition in general fits modern data concerning the space motion of the stars.

214. SCHLESINGER's and BAKER's Study on Spectroscopic Binaries. An early contribution to this subject was made by SCHLESINGER and BAKER¹, who analysed data derived from spectroscopic binaries. Considering first the systems in which spectra of both components have been observed they found without exception that the brighter component of a spectroscopic binary is always the more massive of the two. The close correspondence between mass and relative brightness (one could also say absolute brightness) is shown from the following summary where I stands for the (absolute) intensity

M_B/M_A	I_B/I_A	n	M_B/M_A	I_B/I_A	n
0.99	1.00	2	0.74	0.53	3
0.91	0.73	3	0.66	0.40	4

The authors assumed that the discovery-chance of spectroscopic binaries is $\propto \sin^3 i$. Thus $\overline{\sin^3 i}$ will be equal to 0.68, a value which is considered somewhat too low nowadays. They concluded that in fifteen pairs showing both spectra the average mass was between 4 \odot and 5 \odot . They also concluded that this statement could not be extended to other spectroscopic binaries. The difficulties arising from the use of the mass-function were pointed out. From 44 pairs showing only one of the spectra it was concluded that the masses of spectroscopic binaries are of very different orders, some being much greater than that of our sun, while others are doubtless insignificant in comparison.

The peculiar law of distribution of the values $\frac{M_B^3 \sin^3 i}{(M_A + M_B)^3}$ for Copeland variables was also commented upon. Reasons were also given for the considerable uncertainty affecting several of the data for M_B/M_A collected or derived by LEWIS, which were not in agreement with the conclusions of the authors.

215. LUDENDORFF's Researches on the Masses of Spectroscopic Binaries. As a rule only the "mass-function", f , is determinable for a spectroscopic binary, viz

$$f = \frac{M_B^3 \sin^3 i}{(M_A + M_B)^3} = +0.03993 \frac{(\alpha \sin i)^3}{P^3}.$$

LUDENDORFF² puts $M_B/M_A = \alpha$.

Hence:

$$f = \frac{\alpha^3}{(1 + \alpha)^3} M_A^3 \sin^3 i$$

There is a wide disparity in the values of f . The numbers do not give much guidance for forming conclusions concerning the size of stellar mass. The situation turns out more favourably when the dependence between $\alpha \sin i$ and P is used. If the spectroscopic binaries are divided into groups according to the size of the period, and means are formed, a regular increase with \overline{P} is found in $\overline{\alpha \sin i}$, in such a way that f or $0.03993 \frac{(\alpha \sin i)^3}{(\overline{P})^3}$ is rather constant.

¹ Publ. Allegheny Obs. 4, No. 21 (1910)

² A N 189, p. 145 (1911).

The stars were divided into two groups containing the stars of the spectral classes Oe5-B8 and A-K. The mean numbers are given below, being still of interest.

When \bar{P} is plotted against $\alpha \sin i$ the points of the two groups define a smooth curve. The smoothed values are given under the heading $A \sin J$. The constant C is defined from the equation.

B stars.				
\bar{P}	$\alpha \sin i$	n	$A \sin J$	$\alpha \sin i - A \sin J$
0 ^d .22	0.040	2	0.74	-0.70
2.58	3.30	5	3.84	-0.54
4.16	5.37	4	5.28	+0.09
6.23	5.17	4	6.92	-1.75
9.75	6.82	3	9.32	-2.50
28.15	26.47	2	18.90	+7.57
121.62	54.10	2	50.13	+3.97
137.64	51.46	3	54.44	-2.98

$$A \sin J = \left(\frac{C \bar{P}^3}{0.03993} \right)^{\frac{1}{3}},$$

and has the following values.

$C = 0.34 \odot$ for the B stars

$C = 0.11 \odot$ for the A-K stars.

A-K stars				
\bar{P}	$\alpha \sin i$	n	$A \sin J$	$\alpha \sin i - A \sin J$
1 ^d .35	1.04	2	1.71	-0.67
2.60	1.42	4	2.65	-1.23
4.39	3.87	4	3.76	+0.11
11.38	6.11	4	7.09	-0.98
18.89	8.51	4	9.94	-1.43
39.34	16.43	3	16.21	+0.22
71.80	25.12	2	24.22	+0.90
102.56	31.51	3	30.72	+0.79

For 8 stars of such a period that they could not be included in the graphs the agreement with the A-K curve was still good.

Next LUDENDORFF inquires concerning the significance of the relations.

$$\text{B stars } \frac{\alpha^3}{(1+\alpha)^2} \mathcal{M}_A \sin^3 i = 0.34 \odot,$$

$$\text{A-K stars } \frac{\alpha^3}{(1+\alpha)^2} \mathcal{M}_A \sin^3 i = 0.11 \odot$$

The difference in C can be explained in different ways. The inclination for B stars might be systematically higher than for other stars on account of a preference of the former to move in orbits parallel with the galactic plane. This explanation does not seem very likely, because no dependence can be found between $\alpha \sin i$ and the galactic latitude, but the material available was meagre.

Another explanation is that the mass-ratio should be systematically larger for the helium stars than for other systems. As soon as α deviates from unity small changes in α give rise to considerable changes in $\frac{\alpha^3}{(1+\alpha)^2}$. A means of testing the possibility of the hypothesis is found in the cases where both spectra have been observed. LUDENDORFF finds

$(\mathcal{M}_A + \mathcal{M}_B) \sin^3 i$	α	n	Group
8.5 \odot	0.70	9	B stars
2.6 \odot	0.80	7	A-K stars

The scanty material rather suggests that the differences in mass-ratio work in the opposite direction, as regards the values of C , to that found above. LUDENDORFF therefore thinks that the difference in C is best explained by an actual difference in mass, as is also indicated from the numbers given above for $(\mathcal{M}_A + \mathcal{M}_B) \sin^3 i$.

LUDENDORFF pointed out that the results concerning the higher mass of the B stars in comparison with the other stars are preliminary, and that the difference may be explained partly by other causes. On account of the higher accuracy attainable when measuring spectra of later types, smaller changes will be more easily discovered than in the case of B stars. Thus small amplitude B stars will not, as a rule, be discovered, which makes the mean value of the masses for

the later types apparently too low. A closer study of the material available showed that no such dangerous effect had crept in among the numbers used.

The stars with the c and ac character in their spectra were not used, because of their peculiar position as regards the value of f . This constant which is on an average 0,0034, suggests that α is of the order 0,1 for these stars.

In general no conclusions can be made from the value of f concerning the size of the sum of the masses. If we have an infinite number of stars, $\overline{\sin^2 i}$ is 0,59. Because of the preference of high values of i , the value will be higher. LUDENDORFF assumes the value to be 0,75. Thus the mean masses are

$$M_A = 0,45 \frac{(1+\alpha)^2}{\alpha^3} \odot \quad (\text{B stars}), \quad M_A = 0,15 \frac{(1+\alpha)^2}{\alpha^3} \odot \quad (\text{A-K stars}).$$

For different values of α the following table gives the values of M_A and M_B .

Mean value α	$\frac{(1+\alpha)^2}{\alpha^3}$	B stars			A-K stars		
		M_A	M_B	$M_A + M_B$	M_A	M_B	$M_A + M_B$
0,1	1210	544 \odot	54 \odot	598 \odot	181 \odot	18 \odot	199 \odot
0,2	180	81	16	97	27	5	32
0,3	63	28	8	36	9	3	12
0,4	31	14	6	20	4,6	1,8	6,4
0,5	18	8	4	12	2,7	1,4	4,1
0,6	11,8	5,3	3,2	8,5	1,8	1,1	2,9
0,7	8,4	3,8	2,7	6,5	1,3	0,9	2,2
0,8	6,3	2,8	2,2	5,0	0,9	0,7	1,6
0,9	5,0	2,3	2,1	4,4	0,8	0,7	1,5
1,0	4,0	1,8	1,8	3,6	0,6	0,6	1,2

LUDENDORFF¹ returned to the subject in a later paper. A considerably increased material was at his disposal owing to the energy of the American astronomers who went in for the determination of orbits of spectroscopic binaries.

The following groups were excluded as before: the c and ac stars, some stars whose orbits were dependant on the displacements of the H and K lines, some stars where the orbital motion is not very well established (e. g. α Orionis), ν Sagittarii, stars with variable amplitude such as 12 Lacertae and β Cephei, Boss 1275, where the period used is probably much too large, and, lastly, five stars with periods $> 1000^d$. The following mean values were found, the f being computed from

$$f = 0,03993 \frac{\overline{\sin^2 i}}{\overline{P^3}} :$$

P	$\overline{\sin^2 i}$	n	f	P	$\overline{\sin^2 i}$	n	f
Oe—Oe5				A			
15 ^d ,66	21,60	3	1,6	1 ^d ,49	1,57	4	0,07
Bo—B5				2,57	1,60	5	0,02
1,18	1,55	4	0,11	3,62	2,43	4	0,04
2,54	3,12	5	0,19	4,02	4,09	4	0,17
3,81	4,94	5	0,33	6,82	4,72	4	0,09
5,12	6,02	4	0,33	10,21	5,92	5	0,08
7,60	6,92	5	0,23	17,37	9,67	5	0,12
20,24	11,18	4	0,14	47,47	23,50	4	0,23
123,54	53,36	5	0,40	114,79	31,71	3	0,10
B8 and B9				F			
1,82	2,68	4	0,23	1,38	0,51	5	0,003
4,41	3,75	4	0,11	4,52	2,97	5	0,05
47,54	17,13	3	0,09	10,87	6,88	5	0,11
				49,89	16,94	3	0,08

¹ A N 211, p 105 (1920)

If α and ι are on an average the same for the different spectral classes, then $M_B/M_{B8} = 1.7$, $M_B/M_A = 2.5$, $M_B/M_1 = 4$, where M_B , M_{B8} , M_A , M_1 are the mean masses of stars of the spectral classes B0—B5, B8—B9, A, and F respectively. The stars of the Oe class seem to have a very large mass.

There are only few binaries with known orbits in the G and K class, and there is a lack of short periods among the former stars. Four K stars give $\bar{\iota} = 0.02$, which suggests even a lower mass for these stars than for the F stars.

LUDENDORFF then made investigations as to whether the stars of the same class give a constant value for $\bar{\iota}$. He remarks that this quantity seems to increase with increasing period. At first it might, therefore, seem natural to think that systems of long period also have large masses, but a closer inquiry will show that this is not the case.

216 Frequency of Stellar Masses for Different Spectral Classes. The important problem concerning the frequency of stars of different mass has been investigated by E VON DER PAHLEN¹. For that purpose he makes use of the number of stars of different spectral classes and the relation between stellar mass and spectrum. Besides this the relation between spectral class and mean velocity is also used as an indicator of the mean mass for different classes, or in other words the equipartition of energy is supposed to hold also within the stellar system.

It is not enough to use these two series of data. It is also necessary to possess knowledge of the cosmogonic time scale or the time for each stage of development from the stage when a star starts more or less as a giant until it becomes more and more dwarfish. Before the theory of EDDINGTON was worked out there was no possibility whatever of overcoming the difficulty. By the aid of a hypothetical assumption explained later on, V D PAHLEN computed the frequency. Other assumptions involved in his investigation are that the visible stellar system is in a stationary stage, in such a way that the number of visible stars in each spectral subdivision is constant with respect to the time. Putting the assumption in another form it means that for each interval of time just as many stars of each mass enter as giants as there are stars of the same mass developing into dwarfs through cooling, and thus becoming invisible.

The following notation is used

- N_B, N_A, \dots, N_M , Number of stars within each spectral class
 V_B, V_A, \dots, V_M , Mean radial velocities for each spectral class
 M_B, M_A, \dots, M_M , Masses of the stars which at the top of their evolution reach the spectral classes given as subscripts
 n_B, n_A, \dots, n_M , Frequency of stars of masses M_B, M_A , etc.
 v_B, v_A, \dots, v_M , Mean radial velocities of stars of masses M_B, M_A , etc.
 $T^{(B)}, T^{(A)}, \dots, T^{(M)}$, The lengths of time or periods during which stars of masses M_B, M_A , etc are visible.
 $t_B^{(B)}, t_A^{(B)}, \dots, t_M^{(B)}$, The periods for a star of mass M_B to pass the spectral classes B, A, ..., M
 $t_A^{(A)}, t_F^{(A)}, \dots, t_M^{(A)}$, The same quantities for a star of mass M_A .
 $t_F^{(F)}, \dots, t_M^{(F)}$, The same quantities for a star of mass M_F .
 $t_M^{(M)}$, The same quantity for a star of mass M_M .

¹ A N 216, p 309 (1922)

Instead of the absolute periods t and T of time the following ratios are used

$$\begin{aligned} \tau_B^{(B)} &= \frac{t_B^{(B)}}{T^{(B)}}; & \tau_A^{(B)} &= \frac{t_A^{(B)}}{T^{(B)}}; & \tau_F^{(B)} &= \frac{t_F^{(B)}}{T^{(B)}}; & \tau_G^{(B)} &= \frac{t_G^{(B)}}{T^{(B)}}; & \tau_K^{(B)} &= \frac{t_K^{(B)}}{T^{(B)}}; & \tau_M^{(B)} &= \frac{t_M^{(B)}}{T^{(B)}}; \\ \tau_A^{(A)} &= \frac{t_A^{(A)}}{T^{(A)}}; & \tau_F^{(A)} &= \frac{t_F^{(A)}}{T^{(A)}}; & \tau_G^{(A)} &= \frac{t_G^{(A)}}{T^{(A)}}; & \tau_K^{(A)} &= \frac{t_K^{(A)}}{T^{(A)}}; & \tau_M^{(A)} &= \frac{t_M^{(A)}}{T^{(A)}}; \\ \tau_F^{(F)} &= \frac{t_F^{(F)}}{T^{(F)}}; & \tau_G^{(F)} &= \frac{t_G^{(F)}}{T^{(F)}}; & \tau_K^{(F)} &= \frac{t_K^{(F)}}{T^{(F)}}; & \tau_M^{(F)} &= \frac{t_M^{(F)}}{T^{(F)}}; \\ \tau_G^{(G)} &= \frac{t_G^{(G)}}{T^{(G)}}; & \tau_K^{(G)} &= \frac{t_K^{(G)}}{T^{(G)}}; & \tau_M^{(G)} &= \frac{t_M^{(G)}}{T^{(G)}}; \\ \tau_K^{(K)} &= \frac{t_K^{(K)}}{T^{(K)}}; & \tau_M^{(K)} &= \frac{t_M^{(K)}}{T^{(K)}}; \\ \tau_M^{(M)} &= \frac{t_M^{(M)}}{T^{(M)}}. \end{aligned}$$

Of these 21 quantities the last one is known and has a value = 1 because a star, having the mass \mathfrak{M}_M , belongs during all the time it is visible to spectral class M.

Then we have the equations:

$$N_B = n_B \tau_B^{(B)}$$

$$N_A = n_B \tau_A^{(B)} + n_A \tau_A^{(A)}$$

$$\dots \dots \dots$$

$$N_M = n_B \tau_M^{(B)} + n_A \tau_M^{(A)} + n_F \tau_M^{(F)} + n_G \tau_M^{(G)} + n_K \tau_M^{(K)} + n_M \tau_M^{(M)}$$

and:

$$V_B = v_B$$

$$V_A = \frac{v_B n_B \tau_A^{(B)} + v_A n_A \tau_A^{(A)}}{n_B \tau_A^{(B)} + n_A \tau_A^{(A)}}$$

$$\dots \dots \dots$$

$$V_M = \frac{v_B n_B \tau_M^{(B)} + v_A n_A \tau_M^{(A)} + v_F n_F \tau_M^{(F)} + v_G n_G \tau_M^{(G)} + v_K n_K \tau_M^{(K)} + v_M n_M \tau_M^{(M)}}{n_B \tau_M^{(B)} + n_A \tau_M^{(A)} + n_F \tau_M^{(F)} + n_G \tau_M^{(G)} + n_K \tau_M^{(K)} + n_M \tau_M^{(M)}}.$$

The unknown v 's can be eliminated by using the equipartition of energy in the following form:

$$\mathfrak{M}_B v_B^2 = \mathfrak{M}_A v_A^2 = \mathfrak{M}_F v_F^2 = \mathfrak{M}_G v_G^2 = \mathfrak{M}_K v_K^2 = \mathfrak{M}_M v_M^2 = \text{Const.}$$

The second equation then becomes:

$$n_B \tau_A^{(B)} (V_A - V_B) + n_A \tau_A^{(A)} \left\{ V_A - \left(\frac{\mathfrak{M}_B}{\mathfrak{M}_A} \right)^{\frac{1}{2}} V_B \right\} = 0.$$

Further notation introduced is as follows:

$$\begin{aligned} n_B \tau_B^{(B)} &= p_B; & n_A \tau_A^{(A)} &= p_A; & n_F \tau_F^{(F)} &= p_F; & n_G \tau_G^{(G)} &= p_G; \\ n_K \tau_K^{(K)} &= p_K; & n_M \tau_M^{(M)} &= p_M; & V_A - V_B &= C_A^B, & V_A - \left(\frac{\mathfrak{M}_B}{\mathfrak{M}_A} \right)^{\frac{1}{2}} V_B &= C_A^A; \dots \end{aligned}$$

and in general:

$$C_B^B = V_B - \left(\frac{\mathfrak{M}_B}{\mathfrak{M}_B} \right)^{\frac{1}{2}} V_B.$$

(p_B is the number of stars of spectral class S).

The equations then take the form

$$N_B = \phi_B$$

$$N_A = \phi_B \frac{\tau_1^{(B)}}{\tau_B^{(B)}} + \phi_A$$

$$N_F = \phi_B \frac{\tau_F^{(B)}}{\tau_B^{(B)}} + \phi_A \frac{\tau_F^{(A)}}{\tau_A^{(A)}} + \phi_F$$

$$C_A^B \phi_B \frac{\tau_A^{(B)}}{\tau_B^{(B)}} + C_A^A \phi_A = 0$$

$$C_F^B \phi_B \frac{\tau_F^{(B)}}{\tau_B^{(B)}} + C_F^A \phi_A \frac{\tau_F^{(A)}}{\tau_A^{(A)}} + C_F^F \phi_F = 0$$

The system of equations is indeterminate on account of the appearance of the quantities $\tau_s^{(n)}$, of which we do not know much, if anything at all. If we represent the development of a star passing through the spectral classes by means of a curve that is some function of the time, then the mass is the parameter that will determine the form of this curve. It seems plausible that a continuous change in mass corresponds to a continuous change in this curve, and that when the masses do not vary within too wide limits, the different curves show some general resemblance. This will be the same as if the ratios of the periods expressing the times it takes for a star to pass through the spectral classes, will oscillate around some values valid for a star of mean mass. Approximately the ratios of periods for corresponding spectral stages (counting from the highest stage attainable for a star of given mass) will be equal for all stars.

In this way we reach the necessary number of conditions to enable us to solve the above system. V. D. PAHLEN is aware that the assumption is rather bold. According to the theory of EDDINGTON the difference between two stars of which one can reach the B stage and the other the A stage is some $3 \odot$. On the other hand the same difference for two stars of classes K and M is only some $\frac{1}{20} \odot$. If the idea of V. D. PAHLEN were to be worked out strictly it would be necessary to make a new spectral division fulfilling the condition that the masses increase in arithmetical proportion from class to class.

According to the assumption made above we have:

$$\frac{\tau_A^{(B)}}{\tau_B^{(B)}} = \frac{\tau_A^{(A)}}{\tau_1^{(A)}} = \frac{\tau_G^{(F)}}{\tau_F^{(F)}} = \frac{\tau_K^{(G)}}{\tau_G^{(G)}} = \frac{\tau_M^{(K)}}{\tau_K^{(K)}} = \sigma_A$$

$$\frac{\tau_F^{(B)}}{\tau_B^{(B)}} = \frac{\tau_G^{(A)}}{\tau_1^{(A)}} = \frac{\tau_K^{(F)}}{\tau_F^{(F)}} = \frac{\tau_M^{(G)}}{\tau_G^{(G)}} = \sigma_F$$

$$\frac{\tau_G^{(B)}}{\tau_B^{(B)}} = \frac{\tau_K^{(A)}}{\tau_A^{(A)}} = \frac{\tau_M^{(F)}}{\tau_F^{(F)}} = \sigma_G$$

$$\frac{\tau_K^{(B)}}{\tau_B^{(B)}} = \frac{\tau_M^{(A)}}{\tau_A^{(A)}} = \sigma_K$$

$$\frac{\tau_M^{(B)}}{\tau_B^{(B)}} = \sigma_M.$$

Hence:

$$N_B = p_B$$

$$N_A = p_B \sigma_A + p_A$$

$$N_F = p_B \sigma_F + p_A \sigma_A + p_F$$

$$N_G = p_B \sigma_G + p_A \sigma_F + p_F \sigma_A + p_G$$

$$N_K = p_B \sigma_K + p_A \sigma_G + p_F \sigma_F + p_G \sigma_A + p_K$$

$$N_M = p_B \sigma_M + p_A \sigma_K + p_F \sigma_G + p_G \sigma_F + p_K \sigma_A + p_M$$

and:

$$C_A^B p_B \sigma_A + C_A^A p_A = 0$$

$$C_F^B p_B \sigma_F + C_F^A p_A \sigma_A + C_F^F p_F = 0$$

$$C_G^B p_B \sigma_G + C_G^A p_A \sigma_F + C_G^F p_F \sigma_A + C_G^G p_G = 0$$

$$C_K^B p_B \sigma_K + C_K^A p_A \sigma_G + C_K^F p_F \sigma_F + C_K^G p_G \sigma_A + C_K^K p_K = 0$$

$$C_M^B p_B \sigma_M + C_M^A p_A \sigma_K + C_M^F p_F \sigma_G + C_M^G p_G \sigma_F + C_M^K p_K \sigma_A + C_M^M p_M = 0.$$

From these all p 's and σ 's can be determined.

The following data were used:

Spectral class	N	V	Temperature	\mathcal{R}
B	3196	6,8 km/sec	17000°	4,27 ☉
A	8852	11,5 "	10000	1,23
F	7950	14,5 "	6750	0,59
G	7400	15,4 "	4750	0,32
K	9090	16,4 "	3700	0,20
M	684	17,2 "	3100	0,15

The numbers in the second vertical row give the numbers of stars brighter than $8^m,0$ per 10000 square degrees according to Tab. 11 in Groningen Publ No. 30.

In the computations it was necessary to include the M stars in the K group.

The results are:

	In percent	
$n_K = 1582$	4,3	$\tau_B^{(B)} = 0,337$
$n_G = 2802$	7,5	$\tau_A^{(B)} = 0,177$
$n_F = 6033$	16,3	$\tau_F^{(B)} = 0,080$
$n_A = 17266$	46,5	$\tau_G^{(B)} = 0,217$
$n_B = 9486$	25,5	$\tau_K^{(B)} = 0,189$

According to the author these numbers are to be taken only as a first rough approximation.

It is also of importance to know the frequency function of masses for stars in a certain volume of space. This problem can be solved by reducing the number of stars $n_B, n_A \dots$ in the above equations to equal volumes. Because of the lack of parallaxes EDDINGTON's theory is used in such a way that the absolute (bolometric) magnitudes, M , are used which are computed from the supposition of constant space-density

The space unit is a sphere with such a radius that the stars of mass \mathcal{R}_B in stage B which are situated on its surface are of apparent magnitude $+8^m,0$. Thus:

$$M_B + C_B = 8^m,0,$$

where M_B is the bolometric magnitude of a star of mass \mathcal{R}_B and C_B the reduction to be applied to M_B to give it the absolute visual magnitude of spectral

class B The ratio of the distances r_1 and r_2 of two stars of equal apparent magnitude having the absolute magnitudes M_1 and M_2 is

$$r_1/r_2 = 10^{-0.2(M_1 - M_2)}$$

and the ratio of the two volumes v_1 and v_2 with radii r_1 and r_2 is.

$$v_1/v_2 = 10^{-0.6(M_1 - M_2)}.$$

A star of mass M_B in spectral stage A has a visual magnitude $M_B + C_A$ and thus n_B in the equations related to stage A has to be multiplied by the factor

$$10^{-0.6(C_A - C_B)}.$$

In the equations corresponding to stages F, G, etc n_B appears multiplied by the factors $10^{-0.6(C_F - C_B)}$, $10^{-0.6(C_G - C_B)}$ etc

In the same way we find for n_A in the equation for the A stage the factor

$$10^{-0.6(M_A + C_A - M_B - C_B)} = 10^{-0.6(M_A - M_B)} \cdot 10^{-0.6(C_A - C_B)}$$

We introduce

$$\overline{n_A} = n_A 10^{-0.6(M_A - M_B)}$$

$$\overline{n_F} = n_F 10^{-0.6(M_F - M_B)}$$

$$\overline{n_K} = n_K 10^{-0.6(M_K - M_B)}$$

The following values were used in the calculation

$M_B = -2^m.3$	$C_B = +1^m.8$
$M_1 = +0.2$	$C_A = +0.3$
$M_F = +2.2$	$C_F = 0.0$
$M_G = +4.0$	$C_G = +0.2$
$M_K = +5.0$	$C_K = +0.8$

from which it was found that

			In percent
$\overline{n_A} = 850$	$n_A = 20389000$	88.92	$\tau_B^{(n)} = 0.589$
$\overline{n_G} = 376$	$n_G = 2268000$	9.89	$\tau_A^{(n)} = 0.039$
$\overline{n_F} = 464$	$n_F = 232000$	1.01	$\tau_K^{(n)} = 0.035$
$\overline{n_A} = 1123$	$n_A = 35500$	0.15]	$\tau_G^{(n)} = 0.070$
$\overline{n_B} = 5424$	$n_B = 5500$	0.02	$\tau_K^{(n)} = 0.267$

Another computation was undertaken of the frequency function of the masses of stars brighter than $8^m.0$, in which attention was paid to the change in the visual magnitude with the colour. The following results were found

Spectral class	M_B	M_A	M_F	M_G	M_K	Sum	Mean masses
B	3196	0	0	0	0	3196	$\overline{M_B} = 4.27 \odot$
A	1679	7176	0	0	0	8855	$\overline{M_A} = 1.81$
F	2008	1248	4698	0	0	7954	$\overline{M_F} = 1.62$
G	3210	748	410	3028	0	7396	$\overline{M_G} = 2.14$
K	5525	680	141	152	3267	9773	$\overline{M_K} = 2.56$
Sum	15618	9860	5249	3180	3267	37174	

217. Sproul Determinations of Masses In 1922 J A MILLER and J H. PITMAN¹ made use of the material available for computing the masses of the visual binary stars. The original parallax programme of the Sproul Observatory was outlined with a view to determine the masses of these stars. All the visual binaries

¹ A J 34, p 127 (1922)

with well-determined orbits have been included, together with objects for which tolerable elements will be known in the near future. Most of these objects have also been included in the other parallax observatories, so in most cases determinations of several modern parallax values are available.

Most of the pairs in question are so close together that the combined images on the plates at Sproul are sensibly round. The question then arises whether the orbital motion will not change the shape of the photographic image and vitiate the determination of the parallaxes. PITMAN and Miss POWELL have made an investigation with regard to this question using the equation

$$C + i\mu + i\pi + \frac{e}{2} \sin \theta = d,$$

in which d is the total displacement, and the fourth term on the left side takes into account the apparent orbital motion, q and θ being the radius vector and the position angle of the star in its orbit. For the stars with Δm smaller than 2^m it was found that there were the following changes in the parallaxes:

According to the opinion of the present writer the errors in the trigonometric parallaxes, other things being equal, are alighty larger in the case of double than in the case of single stars. As the orbital motion contributes so little to the error, the discrepancy is certainly caused by other factors, which are mainly dependent on the nearness of the images

$\Delta \pi$	n
0",000—0",001	11
0 ,002	1
0 ,004	1
0 ,009	1

The average sums of the masses within the different spectral classes are as follows according to MILLER and PITMAN:

Spectral class	B	A	F	G	K	M
$M_A + M_B$ %	(14,91) ⊙ 8	3,49 ⊙ 8	3,92 ⊙ 11	1,77 ⊙ 6	1,57 ⊙ 3	0,65 ⊙ 2

The mass of the B stars was taken from other sources

218. PITMAN's Investigation. An extensive presentation of the existing material for deriving the masses of the binary stars was given by J. H. PITMAN in 1929¹. The orbits of the binaries are generally those given by VAN DEN BOS² together with a few orbits, new or revised, published since the latter's paper appeared. The parallaxes are taken from the manuscript catalogue of the Sproul Observatory. In general only modern determinations are used. These are corrected for systematic errors and weighted according to the method given in Pop Astr 34, p. 244. The corrections reduced the determinations of trigonometric parallaxes to the same system as ADAMS's spectroscopic results; in this sense the parallaxes tabulated are absolute.

The objects are divided into three groups, which are given in separate tables. Table I contains 33 stars for which the probable error of the parallax does not exceed fifteen per cent of the parallax itself. Table II contains 20 stars for which the probable error lies between fifteen and thirty per cent of the parallax, while Table III contains 54 cases in which the probable error exceeds thirty per cent and those for which only one trigonometric determination has been made. In each case the trigonometric parallax has been made the basis of classification.

The results are summarized in the following table, where the absolute magnitudes are visual values. The second lines in the table give the average masses and absolute magnitudes for the single components. The numbers n

¹ A J 39, p. 57 (1929). ² B A N 3, p. 149 (1926).

75 such systems and compared the minimum values of \overline{M} with the mass-luminosity law. The comparisons of PITMAN show that there is a correlation between M and $\log \overline{M}$. The value of the coefficient of correlation can be estimated as having a value of about 0.7. Another question is whether such a correlation has a physical meaning such as that expressed in the mass-luminosity law. For the present it hardly seems possible to answer this question even if the material available seems to suggest a revision of the constants in EDDINGTON's formula.

§19. Statistics of accurately Determined Stellar Masses. E. B. WILSON and W. J. LUYTEN¹ made an investigation with a view to discuss the material concerning stellar masses as a set of precise astronomical measurements.

To begin with they quote the 8 cases of stellar mass determinations given by EDDINGTON in his well-known book, "Stellar Movements". The figures expressed in terms of the mass of our Sun are in order of size 0.7, 1.0, 1.0, 1.3, 1.8, 1.9, 2.5, 3.4, from which $\overline{M} = 1.7 \pm 0.2$. As no masses may be negative and there is no restriction, except through disintegration by internal light-pressure or dynamical fission upon the upper side, it is natural to discuss the distribution, not of the mass itself, but of its logarithm. The 8 results are $-0.155, 0.000, 0.000, 0.114, 0.255, 0.279, 0.398, 0.532$, from which $\log \overline{M} = 0.178 \pm 0.05$. The dispersion σ is 0.21 ± 0.035 and the probable error $\rho = \frac{1}{2} \sigma = 0.14$. The geometric mean mass is 1.5 and coincides with the median. If the distribution is normal a departure of $9 \rho = 1.26$ in the logarithm from its mean 0.18 could not occur; because there is only one chance in a billion and a half that $\log \overline{M}$ should exceed 1.44 and an equal chance that it should be less than $8.92-10$, and there are probably less than one billion stars nearer than 2000 parsecs, which makes it certain that no such numbers could possibly be registered on the best photographic plate. There are at least three known binaries the mass of which exceeds $10^{1.44} = 27.5 \odot$. It is clear, therefore, that a normal distribution as determined from these data has no correspondence in the stellar world.

Then the authors use the following 15 systems² as having reasonably well-determined masses:

α Aurigae	7.50 \odot	$= 4.18 \odot + 3.32 \odot$	η Cassiopeiae	1.13 \odot	$= 0.89 \odot + 0.24 \odot$
β Aurigae	4.72	$= 2.38 + 2.34$	ϵ Bootis	1.09	$= 0.58 + 0.51$
α Can Maj	3.41	$= 2.45 + 0.96$	Sun	1.00	
80 Tauri	2.57	$= 1.85 + 0.72$	85 Pegasi	0.93	$= 0.60 + 0.33$
α Centauri	2.11	$= 1.14 + 0.97$	μ Horologii BC	0.88	$= 0.44 + 0.44$
70 Ophiuchi	1.82	$= 0.96 + 0.86$	Kruiger 60	0.43	$= 0.30 + 0.13$
ζ Herculis	1.60	$= 1.12 + 0.48$	σ^3 Iridani BC	0.41	$= 0.21 + 0.20$
α Can. Min.	1.50	$= 1.13 + 0.37$			

The mean $\overline{M} = 1.97 \pm 0.28$, the median is still 1.50, $\log \overline{M}$ is 0.18 ± 0.06 , and $\sigma_{\log} = 0.34 \pm 0.04$. The mean deviation θ is 0.27 and the test $\sigma_{\theta} = 1.25 \theta$ for normality is perfect. A study of the distribution of the $\log \overline{M}$'s with regard to the size of the probable error, $\rho = 0.23$, also gives evidence of the satisfactory normality of the frequency function. The \overline{M} is $1.5 \odot$. The larger material in this second case has increased the size of the error by a fifth. The authors say that even considering the small size of samples 8 and 15 it is difficult to reconcile the relative magnitudes of the standard deviation and their probable errors; the difficulty would have been even greater if the additional 7 had been treated as a second sample. The fact is that the two sets probably do not belong to the same statistical universe—one at least of the samples is not fair.

¹ Wash Nat Ac Proc 10, p. 394 (1924)

² From HERTZSPRUNG's paper in B A N 2, p. 15 (1923).

If charmed with the excellence of the normal distribution of the 15 cases one would derive the probability of a binary with $\log \mathcal{M}$ as great as $0,18 \pm 9\sigma = 2,21$ it is found that the chance will be one in a billion and a half for a star of mass $162 \odot$. The authors point out that we have PLASKETT's star with such a mass, and that 27 Canis Majoris probably has a still larger mass.

Of course, considerable uncertainty is involved on account of imperfect parallax data. The figures may be inaccurate by 30 percent, which means a variation of some 0,12 in the individual logarithms. If there is nothing systematic in such errors the error in the mean will be about 0,03. As far as the accidental errors go, the mean will be reasonably well-established although the error is liable to increase when a more extensive material is at hand.

A similar discussion is given for the 29 stars of HERZSPRUNG's list when each component of a binary is counted separately. The $\overline{\mathcal{M}}$ is then $1,07 \pm 0,12$ and the median mass 0,86 and the distribution is skew. The $\log \mathcal{M}$ is $9,984 - 10 \pm 0,044$, the median $9,934 - 10$, and $\overline{\mathcal{M}} = 0,965$. The dispersion is $0,357 \pm 0,030$, and checks perfectly with σ . Its value is not greater for 29 stars than for 15 systems. The mean is better determined statistically in the first sample than could be expected before when one remembers that the scanty material has only been doubled.

220. Real and Apparent Masses If the mass of a star undergoes a steady decrease from spectral class B to M, as is indicated by the work of STARRS¹, various suggestions present themselves as an explanation of this phenomenon. B. A. KOSTITZIN² has applied the results of MAJORANA³ with regard to a possible absorption of the gravitation. The real mass of a star is designated by \mathcal{M}_r and the apparent mass by \mathcal{M}_a . Let further r be the radius, $\bar{\rho}$ the mean density, and α the coefficient of absorption $= 7,59 \cdot 10^{-12}$ for the Sun. Then the attractive force will be diminished in accordance with the "law of progressive absorption" and in the case of a homogeneous liquid mass, where $\bar{\rho}$ is equal to the true density, the following equations hold good:

$$\mathcal{M}_a = \frac{\pi \rho r^3}{\alpha} \left[1 + \frac{e^{-2\alpha \bar{\rho} r}}{\alpha \bar{\rho} r} + \frac{e^{-2\alpha \bar{\rho} r}}{2\alpha^2 \bar{\rho}^2 r^2} - \frac{1}{2\alpha^2 \bar{\rho}^2 r^2} \right], \quad \mathcal{M}_r = \frac{4}{3} \pi \bar{\rho} r^3.$$

Introducing a new variable $2\alpha \bar{\rho} r = v$ and putting

$$\varphi(v) = [(1+v)e^{-v} + 0,5v^2 - 1] \frac{3}{2} v^{-3}$$

KOSTITZIN finds the relation:

$$\mathcal{M}_a = \mathcal{M}_r \varphi(v)$$

Accordingly $\varphi(v)$ is the ratio between the apparent density and the true density. If the above value of α and $\mathcal{M}_r = 5,3$ times the apparent mass of the Sun are accepted for the Sun, it is found that for a star with the same real mass as the Sun and $r = 9 r_\odot$ the apparent mass \mathcal{M}_a is nearly equal to its real mass, viz 5,3 times the apparent mass of the Sun. If $r = 3 r_\odot$ the apparent mass is four times the apparent mass of the Sun. The diameters thus derived for different spectral classes are of the same order of magnitude as the computed ones.

H. N. RUSSELL⁴ has pointed out that if the absorption of gravitation is accepted there are a number of important astronomical consequences. The true masses of the planets have been computed according to this theory and it is found that the inertial masses cannot be equal to the true masses. If they are assumed

¹ Mt Wilson Contr 226 (1922)

² Publ Obs Astrophys Centr Russ Moscou 2, p 289, 303 (1923)

³ Phil Mag 39, p 488 (1920)

⁴ Ap J 54, p 334 (1921), Mt Wilson Contr 216.

to be equal to the apparent gravitational masses we are led to such discrepancies in the case of the tides that the conclusion is unavoidable that the coefficient of absorption cannot exceed $1/5000$ of the value assigned to it by MAJORANA.

221. SEARES's Researches. In an extensive paper of 1921 F. II. SEARES¹ has made an interesting study of the masses and densities of the stars partly along new lines. The salient point in his method is a comparison between the absolute magnitude M_d as derived from the dynamical parallax π_d and the spectrographic magnitude M as derived from π . The well-known relation

$$\mathfrak{M} = \mathfrak{M}_A + \mathfrak{M}_B = \frac{a^3}{\pi^3 P^4}$$

gives.

$$\log \mathfrak{M} = h - 0,6 M,$$

where

$$M = m + 5 + 5 \log \pi$$

and

$$h = 3 \log a - 2 \log P + 0,6 m + 3.$$

The assumption used in the computation of π_d is $\mathfrak{M} = 2 \odot$.

Thus if the orbital elements are known:

$$0,30 = h - 0,6 M_d,$$

and:

$$\log \mathfrak{M} = 0,30 - 0,6 (M - M_d) = 0,30 - 0,6 \Delta M$$

and for a group of stars:

$$\overline{\log \mathfrak{M}} = \log \mathfrak{M} = 0,30 - 0,6 (\overline{M} - \overline{M}_d) = 0,30 - 0,6 \Delta \overline{M}$$

The next last equation only holds good for individual stars in the case of binaries where the elements are known, because the mean inclination of the orbital planes is involved in the dynamical parallaxes. The last equation holds good for any group of stars.

At that time, in the case of the binaries investigated, only M_d was known, and thus an indirect process was necessary. SEARES used M_s from single stars of known parallax, whose selection with respect to the stars as a whole presented the same characteristics as those of the binaries themselves.

If \overline{M}_s represents the mean absolute magnitude of a certain spectral type of single stars of known parallax, and \overline{M}_b the corresponding value for binaries of the same type, we have:

$$\overline{M}_b = \overline{M}_s + \delta M.$$

Thus δM expresses the influence of difference in selection. We may write:

$$\overline{M}_b - \overline{M}_s = \Delta \overline{M} = \overline{M}_b - \overline{M}_s + \delta M = \Delta \overline{M}_s + \delta M.$$

SEARES has derived δM from the some hundred binaries of measured parallax and calculated $\Delta \overline{M}_s$ for each spectral type by comparing the 550 stars in the lists of JACKSON and FURNER with the homogeneously selected single stars of known parallax. Then $\Delta \overline{M}$ was formed and \mathfrak{M} computed. The underlying assumption is that the mass-luminosity relation is the same for both binaries and ordinary stars.

The binaries and single stars of known parallax were grouped according to apparent magnitude and spectral class. The comparison between 505 binaries and 1152 parallax stars from ADAMS's catalogue in Mt Wilson Contr 199 and from

¹ Mt Wilson Contr, No. 226 (1922), Ap J 55, p. 165 (1922).

KAPTEYN's investigation of the parallaxes of the helium stars¹ gave the following table

Median apparent magnitude	B			A			Γ			G5—K5		G	K
	B S	J & F P ₁	K & A P ₁	B S	J & F P ₁	K & A P ₁	B S	J & F P ₁	K & A P ₁	B S	J & F P ₁	K & A P ₁	K & A P ₁
3,5	0,1			0,1			0,4			1			
4,5	0,2	7	34	0,2	3	17	0,3	3	12	3	3	3	0,4
5,5	0,2	2	13	0,6	2	4	0,3	2	6	0,8	2	4	1,5
6,5	1,0	1,0	1,0	1,0	1,0	1,0	1,0	1,0	1,0	1,0	1,0	1,0	1,0
7,5	∞	0,52	0,00	1,6	0,29	0,18	1,5	0,38	0,25	2,2	0,80	0,33	0,46
8,5	∞	0,08	0,00	1,5	0,04	0,03	1,8	0,10	0,05	3,5	0,54	0,08	0,34
9,5	—	0,00	0,00	0,2	0,00	0,02	0,7	0,01	0,01	0,5	0,02	0,02	0,12

$$\frac{B}{S} = \frac{\text{binaries}}{\text{single stars}}; \quad \frac{J \& F}{P_1} = \frac{\text{JACKSON \& FURNER}}{\text{PICKERING}}, \quad \frac{K \& A}{P_1} = \frac{\text{KAPTEYN \& ADAMS}}{\text{PICKERING}}$$

If the selection for the two lists were the same, the ratios of the corresponding numbers would not vary with magnitude, and if the selection were homogeneous the ratios for the different classes would show the same change.

The number of A stars in the spectrographic list then available was small, and in order to obtain a test SEARES used the star counts of W. H. PICKERING².

The degree of homogeneity is satisfactory and the only deviations of a serious nature are those of the faint G5—K5 stars and the faint B stars. The absence of pronounced irregularities in the curve $M_d = f(\text{Sp. Class})$ shows that the error in the corresponding $\Delta \bar{M}_s$ must be small. The limitation in this value for earlier B stars, on account of the fact that KAPTEYN's investigations do not include stars fainter than 6^m.0, will not be of much consequence.

The increment δM determines the zero-point, which can easily be proved. SEARES has used the spectrographic parallaxes alone, since they are based on a homogeneous system.

A diagram given in fig. 150 was constructed giving \bar{M}_s and \bar{M}_d as functions of the spectral class. The table shows the value of the zero-point for different spectral classes, the two lists of JACKSON and FURNER being treated separately:

Spectral class	$\bar{M}_b - \bar{M}_d$	$\Delta \bar{M}_s$	δM	n	Spectral class	$\bar{M}_b - \bar{M}_d$	$\Delta \bar{M}_s$	δM	n
A7	-0 ^m .7	-0 ^m .5	-0 ^m .2	3	A9	-0 ^m .8	-0 ^m .4	-0 ^m .4	11
F2	-0 .6	-0 .2	-0 .4	14	F5	0 .0	0 .0	0 .0	7
F5	-0 .1	0 .0	-0 .1	13	G0	+0 .3	+0 .4	-0 .1	9
G0	0 .0	+0 .4	-0 .4	18	K3	+0 .3	+0 .8	-0 .5	9
G4	+0 .4	+0 .6	-0 .2	10					
K2	+0 .4	+0 .7	-0 .3	7					
K8	+0 .5	+0 .8	-0 .3	4					
Mean			-0 .29	69				-0 .27	36

From 69 and 36 stars respectively mean values of $\delta M = -0^m.29$ and $-0^m.27$ were found, thus as a mean

$$\Delta \bar{M} = \Delta \bar{M}_s - 0^m.3$$

was adopted. The fact that there is no marked progression in the values of δM with spectral class confirms the conclusion concerning the homogeneity of the selection.

In the determination of the zero-point a certain systematic difference was found between the results of JACKSON and FURNER with regard to π_d as determined

¹ Mt. Wilson Contr. No. 82, 147, Ap. J. 40, p. 43 (1914), 47, p. 146, 255 (1918)

² Publ. A. S. P. 33, p. 140 (1921)

from known elements or from arcs of relative motion. In the former case the agreement between π_1 and π_2 was excellent. In the second case the following systematic difference was found:

$$\pi_1 = \pi_2 - 0''.010$$

The stars occurring in both lists give

$$\pi_1 = \pi_2 - 0''.007.$$

The value ΔM , determines the rate $\Delta M / \Delta S$, where ΔS is the change in spectral index S , while the constant δM determines the zero-point. For the determination of δM only spectrographic parallaxes have been used. In computing $M_s - M_d$ it has to be borne in mind that the M_s correspond to the most probable values of the parallaxes and thus are not the most probable values of the magnitudes themselves. Thus a small correction of $+0^m.08$ to the tabular values was adopted.

The following geometrical mean masses were derived:

Spectral class	$\overline{M_s}$	$\overline{M_d}$	Visual binarism \overline{BR}	Single stars \overline{A}
B0	-1.60	(-0.25)	18.0	10.0
B5	-0.20	+1.00	14	8.3
A0	+0.70	1.65	10.5	6.0
F0	2.40	2.70	4.4	2.5
F5	3.32	3.27	2.7	1.5
G0	4.35	3.95	1.7	1.0
G5	5.20	4.60	1.3	0.76
K0	5.90	5.20	1.2	0.68
K5	7.10	6.30	1.1	0.62
M0	+9.80	8.95	1.0	0.59

In order to test the influence of selection on the values of \overline{BR} on account of the lack of more distant stars the following comparison was made:

π	Sp	$\Delta \log \overline{BR}$	n	π	Sp	$\Delta \log \overline{BR}$	n
0''.018	F2	-0.08	10	0''.061	G3	-0.04	10
0.026	F6	-0.12	10	0.102	G1	+0.04	10
0.032	G1	-0.08	10	0.270	G8	+0.12	9
0.046	F7	+0.03	10				

The slight systematization of the numbers shows that the mean masses of more distant stars have been computed too large. This suggests that the variation of \overline{BR} with spectral class has been influenced by selection, and in order to make the data fully representative a constant correction to the $\log \overline{BR}$ of -0.08 has to be applied. The values given above contain this correction.

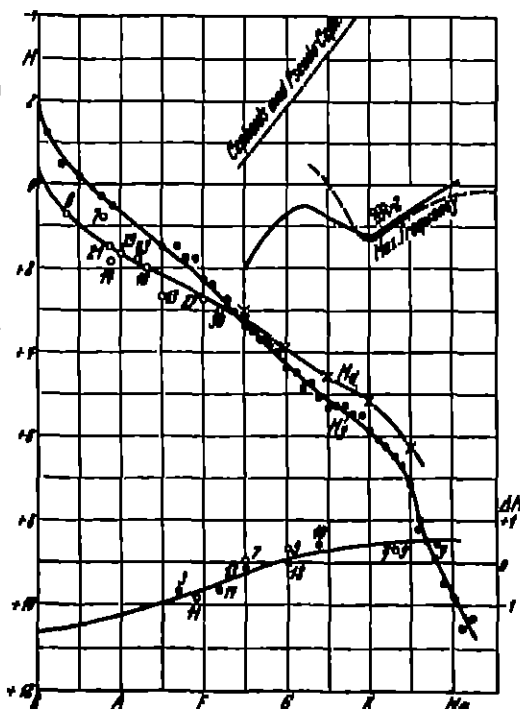


Fig. 150. SEAR'S determination of the masses of the stars from the different slants of the stars in the RUSSELL diagram. The curve M_s is the line of maximum frequency of M for the B stars of KAPTEYN and the dwarfs from the list of spectroscopic parallaxes. M_d is the similar curve for the absolute magnitudes as based upon the dynamical parallaxes derived by JACKSON and TURNER. The differences in the ordinates, corrected for zero point, are shown by the curve below (ΔM). The straight line "Cepheids and Pseudo-Ceph." is the absolute magnitude spectral relation according to LUNDQVIST. The dotted curve to the right is the line of maximum frequency for giants and the full drawn curve the mass line $\overline{BR} = 2$.

In deriving the geometrical mean masses \mathcal{M} of single stars a constant value of $\mathcal{M}_B/\mathcal{M}_A = 0.75$ was assumed.

The probable dispersion in the mass for dwarfs of F0 to M was determined as:

$$\sigma_{\log \mathcal{M}} = \pm 0.22.$$

This is not the true dispersion, but includes the errors in M and M_d as well. The dispersion in M is not well known and thus only the following dependence can be indicated:

σ_M	$\sigma_{\log \mathcal{M}}$	Limits for probable error	σ_M	$\sigma_{\log \mathcal{M}}$	Limits for probable error
$\pm 0^m.35$	± 0.07	$(0.85-1.18) \mathcal{M}$	$\pm 0^m.20$	± 0.18	$(0.66-1.51) \mathcal{M}$
0 .30	0.13	$(0.74-1.35) \mathcal{M}$	0 .15	0.20	$(0.63-1.58) \mathcal{M}$
0 .25	0.16	$(0.69-1.45) \mathcal{M}$			

If the kinetic theory of gases can be applied to the stars, this implies the equipartition of energy of translation so that:

$$\mathcal{M}_n \bar{V}_n^2 = \text{const.}$$

The theory for a collection of stars is much simpler than for a gas, because encounters and collisions occur so seldom that they may be neglected. The effective agency for the transfer of energy is only that which arises from the attraction of the bulk of stars upon individual members of the system. The effect of this simplification is an enormous increase in the time of relaxation and for that reason several theorists have rejected the analogy between the stellar system and a collection of gases. On the other hand, JEANS concurs with the application of the theory of gases to the stellar universe.

Several objections are considered by SEARES, who finds that equipartition has not been obtained within the stellar system, but that there may be an approach to that state.

The distribution of the logarithms of the space velocities can be represented by means of a normal (Gaussian) distribution. By applying the mean value theory to the frequency function it is found that

$$\log \bar{V}^2 = 2 \log \bar{V} + 0.148 = 2 \log \underline{V} + 0.296.$$

Further, as has been shown by CAMPBELL, the mean space velocity is equal to twice the mean radial velocity. On determining $\log (\mathcal{M} \bar{V}^2)$ for different spectral

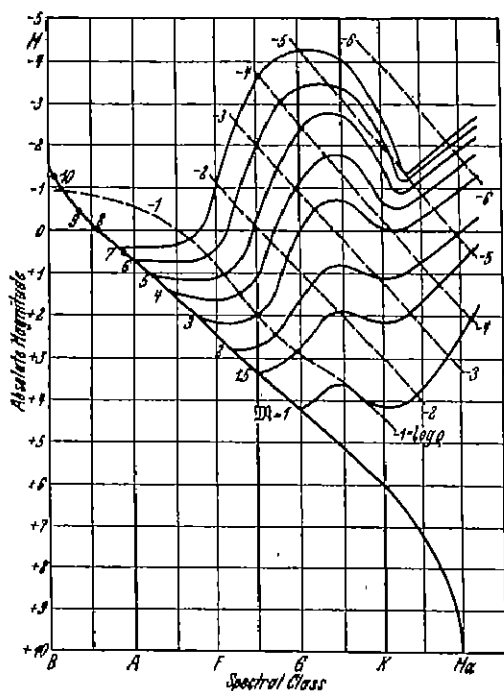


Fig. 151. Nomogram showing distribution of mass (full curves) and mean density (broken curves) of stars derived by SEARES from the principle of equipartition. The full-drawn curve running downward to the right is the line of the maximum frequency of the dwarfs or the main series.

classes remarkable constancy was found. The total range of the values is only from 3.21 to 3.66 and most values are very close to the mean, 3.57. It thus seems justifiable to evaluate the masses. For spectral classes F5, G5, K3, and Ma a mass-luminosity relation was found as follows:

The surface brightness was derived by the aid of STEFAN's law. The following expression was derived for the surface brightness

$$j = M_{vis} - M_{bol} - 10 \log T_e + \text{const.}$$

This formula was tested by comparison with the one derived by HERTZSPRUNG in 1906 which was based on PLANCK's law and the measurements of visual sensibility by LANGLEY,

ABNEY, and others. The formulae involve quadratures. The excellent agreement is illustrated here:

Spectral class	MR			
	F5	G5	K3	Ma
-3		5.5 ⊙		9.5 ⊙
-2	6.0 ⊙	4.2		4.4
-1	5.5	3.2	5.3 ⊙	2.6
0	4.8	2.4	2.8	1.7
+1	4.2	1.9	1.9	1.2
2	3.2	1.5	1.5	
3	2.0	1.1	1.2	
4	1.0	0.9	1.0	
5	0.6	0.8	0.9	
6		0.6	0.8	
7			0.7	
8			0.6	
10				0.5

T	M _{vis} -M _{bol}	f _{SEARES}	f _{HERTZSPRUNG}	T	M _{vis} -M _{bol}	f _{SEARES}	f _{HERTZSPRUNG}
2540°	+2 ^m .59	+6 ^m .32	+6 ^m .32	7500°	+0 ^m .02	-0 ^m .95	-0 ^m .93
3000	+1 .71	+4 .72	+4 .68	9000	+0 .12	-1 .64	-1 .62
3600	+0 .93	+3 .17	+3 .16	10500	+0 .31	-2 .12	-2 .09
4500	+0 .35	+1 .60	+1 .58	12000	+0 .53	-2 .48	-2 .45
6000	0 .00	0 .00	0 .00				

The connection of these results with the spectral classes was obtained by the aid of the spectral-photometric measurements of WILSON¹ giving c_d/T of 199 stars, mainly giants. In order to include dwarfs use was made of the un-

Spectral class	Giants, M=0		Dwarfs		
	c_d/T	f	c_d/T	f	M
B0	1.36	-2 ^m .28			
B5	1.43	-2 .14			
A0	1.55	-1 .89			
A5	1.76	-1 .45			
F0	2.04	-0 .88			
F5	2.35	-0 .26	2.35	-0 ^m .26	+3 ^m .3
G0	2.70	+0 .44	2.48	0 .00	+4 .4
G5	3.10	+1 .24	2.60	+0 .25	+5 .2
K0	3.70	+2 .41	2.93	+0 .90	+5 .9
K5	4.37	+3 .71	3.47	+1 .96	+7 .1
Ma	4.65	+4 .25	4.30	+3 .58	+9 .8
Mb	4.82	+4 .58			
Mo	4.94	+4 .81			

This difference must be considered in any discussion of the surface brightness of stars of "late" spectral classes.

The change $\Delta j/\Delta M$ could not be determined with accuracy and some extrapolation was necessary. A partial con-

Object	α Orionis	α Bootis	α Scorpis
Spectral class	Ma	K0	Ma
M	-2 ^m .6	+0 ^m .1	-4 ^m .2
f observed	+4 .6	+2 .2	+4 .5
f calculated	+4 .4	+2 .4	+4 .5
Diam. observed	252 ⊙	25 ⊙	506 ⊙
Diam. calculated	235 ⊙	27 ⊙	513 ⊙
MR (appr.)	8 ⊙	3 ⊙	15 ⊙

¹ Publ. No. 74 (1919)

² Mt. Wilson Comm. 59, Wash. Nat. Ac. Proc. 5, p. 232 (1919)

trol of j was afforded by measurements of the diameter of three stars as performed by PEASE

The following formulæ given by SEARES connect the angular diameter d , the linear diameter D , the mass \mathcal{M} , the density ϱ , the surface brightness j , and the apparent and absolute magnitudes

$$\log d = 0,2 (j - m) - 2,061$$

$$\log D = 0,2 (j - m) - \log \pi - 0,030$$

$$\log D = 0,2 (j - M) + 0,970$$

$$D = 107,4 d/\pi$$

$$j = 5 \log d + m + 10,30$$

$$\log \varrho = \log \mathcal{M} - 3 \log R + 0,14$$

$$\log \varrho = \log \mathcal{M} + 0,6 (M - j) - 2,77$$

The values of the masses and densities were also revised by means of Cepheids. If the pulsation theory is correct the mean density will vary inversely as the square of the period

$$\log \varrho = -2 \log P + \text{const.}$$

Further the period-luminosity relation taken as $M = a + b \log P$, where a and b are constants, determines the absolute magnitude. Thus the next last equation can be written

$$\log \mathcal{M} = -2 \log P - 0,6 (M - j) + \text{const.}$$

Only small corrections to the data gained from other evidence were obtained from the 28 Cepheids for which the mass could be computed.

The decrease in mass may be partly or perhaps wholly accounted for by selection, but the possibility that mass may decrease with loss of energy by radiation is also suggested, a possibility which agrees with the theory of relativity and is not necessarily in conflict with NEWTON's mechanical principles.

Immediately after the work of SEARES was published H. N. RUSSELL¹ pointed out that the spectrographic parallaxes ought to be dependent on the mass, and that thus by their very nature they are not very suitable for a determination of the dispersion in stellar mass. The

spectrographic magnitude M_s is a function of the temperature T and the density ϱ . The equation giving the density is easily transformed into

$$\log \mathcal{M}_s = \log \varrho + 0,6 j - 0,6 / (j, \varrho) + \text{const.}$$

The masses \mathcal{M}_s are identical for stars with the same density and the same surface brightness, but the real masses may differ. Thus the masses computed by SEARES should not be adopted in order to obtain the real dispersion in \mathcal{M} and RUSSELL suggests the use of trigonometric parallaxes for such a determination.

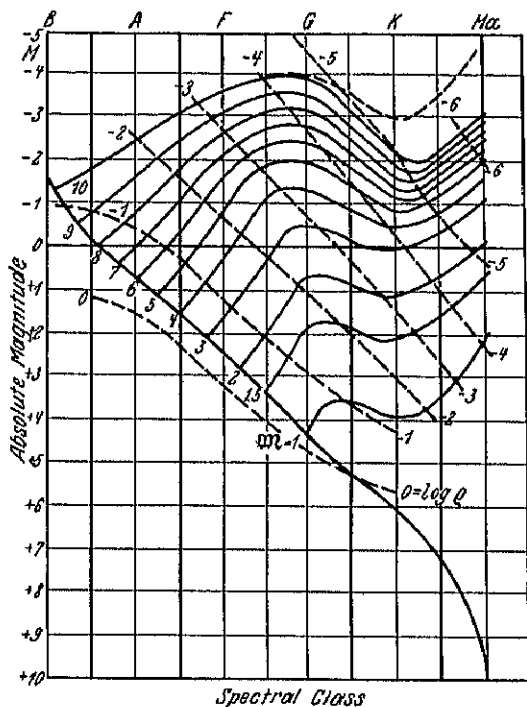


Fig 152 Nomogram according to SEARES showing distribution of mass and mean density revised with the aid of Cepheids. The dotted curve at the top indicates the reduction to bolometric absolute magnitude for stars of spectral class F8—Ma of $\mathcal{M} = 10 \odot$

¹ Ap J 55, p. 238 (1922), Mt Wilson Contr 226

The present writer found in 1924 the following results, which remain to-day (1929) substantially unchanged.

	Dispersion
Trigonometric parallaxes	$\pm 3.4 \odot$
Spectrographic parallaxes	$\pm 3.0 \odot$
Spectral proper-motion parallaxes	$\pm 4.0 \odot$

222. Stellar Masses from Spectrographic Parallaxes. In an extensive paper dealing with the ionization in stellar atmospheres A ПАННЕКОЕ¹ took up the question of a possible dependence between the intensities of the absolute magnitude lines and the masses. The Mount Wilson spectrographic determinations of parallaxes are founded on the relative intensity of some enhanced lines and some arc lines of the stars. The relative intensities of arc lines and enhanced lines of a certain element are wholly determined as far as their dependency on the degree of ionization is concerned by the relative position in the pressure-temperature-diagram of the ionization curve and the atmospheric curve, defined by

$$\log p = -10^{\tau-r} + 2.5\tau - 6.49,$$

$$\tau - \tau_1 = /(\log p - \log \frac{g}{h})$$

where p is the pressure of the ionized gas, τ the logarithm of the absolute temperature, and r a parameter depending on the ionization potential of the element.

The position of the atmospheric curve depends on the effective temperature T and the factor g/h . Stars of the same effective temperature, i. e. of the same spectral class, will show differences depending on the factor g/h . On account of the lack of data the coefficient of mass-absorption h has to be assumed to be constant. Further $g = / M/R^3$ and $L = 4\pi\sigma R^2$, where σ is the surface brightness of a star. Then:

$$g \propto \sigma M/L.$$

The reduction curves used at Mount Wilson have been adjusted by means of directly measured parallaxes for each separate spectral class. The real quantity measured at Mount Wilson is not L but $L M_0/M$, if M_0 is the mean mass for the spectral interval considered.

In order to test the theory use was made of dynamical parallaxes. We then have the relations.

$$M_{dyn} = 2 \left(\frac{\pi_d}{\pi_{tr}} \right)^3; \quad M_{sp} = \left(\frac{\pi_{sp}}{\pi_{tr}} \right)^3 M_0.$$

As is evident from the following summary there seems to be a correlation between the two sets of masses.

$\log \pi_d - \log \pi_{tr}$	$\log \frac{M_{sp}}{M_0}$	$\log M_{dyn}$	$\log M_{sp}$	n
+0.53	+0.53	+1.59	+1.06	5
+0.14	+0.16	+0.42	+0.32	6
+0.06	+0.13	+0.18	+0.26	9
-0.04	+0.06	-0.12	+0.12	8
-0.09	-0.05	-0.27	-0.10	7
-0.17	-0.12	-0.51	-0.24	7
-0.23	-0.23	-0.69	-0.50	4
-0.44	-0.47	-1.29	-0.94	4

From the double stars the following table was obtained:

$M_A - M_B$	$\log \frac{M_A}{M_B}$	n	$M_A - M_B$	$\log \frac{M_A}{M_B}$	n
-0 ^m .3	0.09	10	-1 ^m .3	0.26	10
-0 .8	0.18	9	-2 .9	0.36	9

¹ B A N 1, p. 107 (1922), Obs. 46, p. 304 (1923).

Predictions of the masses were made for a number of stars. The result, namely that the Cepheids should have small masses, and that the companions of the three pairs, α Herculis ($3^m.5$; $5^m.4$; Mb, F9), Bu 8114 (6.5, 8.6, K2, F0), and γ Delphin ($4^m.5$, $5^m.5$; K1, F6), have a greater mass (13, 3 and 5 times greater) than the absolutely much brighter principal star of redder colour is of general interest.

Later on P. DOIG¹ compared the theory of PANNEKOEK with the evidence from binary stars. The following fourfold table in which π_{spectral} denotes the parallax derived on basis of the mean value \bar{M} of the absolute magnitude of different spectral classes is of interest.

	$\pi_{\text{spectral}} > \pi_{\text{tr}}$	$\pi_{\text{spectral}} < \pi_{\text{tr}}$
$\pi_{\text{spectrographic}} > \pi_{\text{tr}}$	18	0
$\pi_{\text{spectrographic}} < \pi_{\text{tr}}$	2	14

This indicates the existence of a pronounced positive correlation between $\pi_{\text{spectrographic}}$ and π_{spectral} . When this happens the stars in question are more luminous than the normal star of their class and thus also more massive.

The masses of 19 stars derived directly when compared with those computed according to PANNEKOEK's formula did show rather good agreement. On the other hand, the present writer² found at the same time that there were no such systematic differences between the masses computed on the basis of trigonometric, spectrographic and spectral proper-motion parallaxes as were demanded by the theory of PANNEKOEK but it has to be added that we have to wait for more extensive data before any safe statements can be presented.

Further investigations, which cannot be reviewed in detail here, have convinced me that there are no such deviations between masses derived from trigonometric and spectrographic and proper-motion parallaxes as make it possible to determine even mean mass values from an analysis of different parallaxes. This does not exclude, of course, the possibility that there is a mass effect in the spectrographic parallaxes. It is only to be regretted that this effect is evidently so small that it will require much work on the refinement of the trigonometric and spectrographic methods of determining the absolute magnitude before we can derive masses for single stars.

Another way of showing the smallness of the mass-factor in spectrographic parallaxes is to use the relation

$$\Delta M = \Delta m$$

This relation does only hold good when no errors in m and M are present. In case of each quantity having mean errors of ε_M and ε_m , respectively, we can write

$$\Delta M \pm \varepsilon_M = \Delta m \pm \varepsilon_m$$

Even reasonable treatment of the data concerning spectroscopic binaries in the Mount Wilson material will lead to errors in M of the same size as those derived from single stars. If we had a mass-factor the equation would be

$$\Delta M + a' \pm \varepsilon_M + f(bM + cM^2) = \Delta m \pm \varepsilon_m,$$

if $\log M$ is supposed to be $= a + bM + cM^2$. Although the material is small it seems that no appreciable mass-factor can be derived.

223. Masses of F—K Stars. GERASIMOVICH³ has determined the masses of the stars of spectral classes F—K, starting from the following assumptions: 1. the reversing layer of a star is in radiative and hydrostatic equilibrium. The absorp-

¹ J B A A 34, p 144 (1924)

² V J S 59, p 203 (1924)

³ A N 227, p 145 (1926), Charkov Obs Publ, No 1, p 12 (1927)

tion lines that determine M are not of a chromospheric character, i. e. they arise in the level where the selective radiation pressure is small in comparison to the gas pressure, 2 each line arises at the same optical depths in the reversing layers of all stars of the same spectral type. If these hypotheses are correct the intensity of a given spectral line is a function of the effective temperature and the gravity at the surface only. The chief cause of a variation in an intensity-ratio must be a change in the gravity. The following equation can be established:

$$M - 2,5 \log \mathfrak{R} J = \varphi(M_s, T_s) = M_s + f(M_s, T_s)$$

where J is the surface brightness and T_s the effective temperature and the subscript s stands for spectrographic data. It follows from the above equation that:

$$f(M_s, T_s) = -2,5 \log \mathfrak{R} J.$$

On account of the lack of data the direct method cannot be applied and we must proceed by successive approximations. At first it is supposed that

$$\log \mathfrak{R} = 0,4 [M - M_s] - \log J + \overline{\log \mathfrak{R} J}.$$

From an analysis of the Victoria list of spectrographic parallaxes the following abbreviated results were found when the differences between the spectrographic and trigonometric magnitudes were grouped according to the magnitude:

These values are only approximate on account of my condensation of the data.

The systematic course of $M_s - M_{tr}$ is very striking and according to GERASI-

Absolute magnitude	F stars		G stars		K stars	
	$M_s - M_{tr}$	n	$M_s - M_{tr}$	n	$M_s - M_{tr}$	n
<0,0-0,9	+1 ^M ,4	6	+1 ^M ,0	30	+0 ^M ,7	26
1,0-2,9	+0 ,2	26	-0 ,6	29	0 ,0	18
3,0-3,9	+0 ,1	40	-0 ,3	19	-1 ,1	13
4,0-4,9	-0 ,3	28	1 0 ,1	28	-1 ,1	10
5,0-5,9	-1 ,1	13	-0 ,6	20	-0 ,3	14

MOVIČ cannot be explained as a consequence of some systematic error in the trigonometric parallaxes. The same phenomenon as is illustrated above has been noted by VAN RIJN¹, who made a comparison between the Mount Wilson M_s and M_{tr} based on the Groningen determinations of π as a function of proper motion and apparent magnitude. VAN RIJN explains the phenomenon by the lack of sensitiveness of the spectrographic criteria for luminous stars. From the fact that the systematization in question also exists among the dwarfs GERASIMOVIČ concludes that we cannot neglect the influence of stellar masses on the spectrographic parallaxes.

The largest uncertainty involved in the method is the determination of T_s . The author made use of the values of the surface intensity given by SEARES² which are based on the data of Potsdam and Mount Wilson observers. In this way the following results were found:

π	G stars			K stars		
	$\log \mathfrak{R}$	M	n	$\log \mathfrak{R}$	M	n
0'',010-0'',020	+0,558	+0 ^M ,3	20	+0,424	+0 ^M ,4	26
0 ,021-0 ,030	+0,034	+1 ,6	24	-0,023	+1 ,3	14
0 ,031-0 ,060	-0,101	+3 ,0	43	-0,421	+1 ,9	17
0 ,061-0 ,100	-0,230	+4 ,3	24	-0,476	+4 ,9	10
>0 ,100	-0,383	+5 ,3	18	-0,377	+6 ,5	14

$\log \mathfrak{R}$ clearly depends on the value of π and the same dependence also exists in the F stars. The dependence is partly caused by the well-known selection of

¹ Gron Publ. No. 34, p. 60 (1923).

² Ap J 55, p. 198 (1922)

stars in all parallax-programms and partly by a general dependence between M and \mathfrak{M} . A special investigation of the F stars proved that there is no dependence between π and \mathfrak{M} inside this spectral class.

Using 15 stars with known masses among the Victoria objects GERASIMOVICH found the following relation

$$\mathfrak{M}_{\text{calc}} = 0,80 \mathfrak{M}_{\text{obs}}$$

The author points out that the conclusion of PANNEKOEK that the Cepheids probably have a very small mass cannot be maintained because the method it depends upon only gives the effective gravity, i.e. the gravity diminished by radiation pressure.

Further on an examination is made with regard to whether the principle of the equipartition of the energy holds good. $\overline{\mathfrak{M}V^2}$ was computed as follows. At first the space velocity V_1 of a star relatively to the Sun was computed. If V_0 is the velocity of the Sun relatively to the centroid of the stars and K expresses the systematic correction in the radial velocities to be applied to stars of a given spectral class, then

$$\overline{\mathfrak{M}V^2} = \overline{\mathfrak{M}V_1^2} - \overline{\mathfrak{M}(V_0^2 + K)}.$$

For V_0 the value of W. W. CAMPBELL (20 km/sec) was adopted. From his earlier work GERASIMOVICH adopted $K = +3,4$ km/sec and $+3,0$ km/sec for F dwarfs and G giants respectively. For other groups $K = 0$ was assumed. The following results are found

	$\log \overline{\mathfrak{M}V^2}$	n
F stars . . .	$3,474 \pm 0,596$	88
G stars . . .	$3,446 \pm 0,756$	73
K stars . . .	$3,595 \pm 0,705$	43

The weighted mean is 3,50, which may be compared with SEARIS's value 3,57. The good agreement is a fact that speaks strongly in favour of the correctness of the method. The considerable dispersion in $\log \overline{\mathfrak{M}V^2}$ prevents that quantity being treated as constant for each star.

A detailed investigation of the probable errors of the calculated masses was next undertaken. The following orders of magnitude of the probable error were found:

π	Prob. error
$0'',010$	$\pm 2,5 \mathfrak{M}$
$0,050$	$\pm 0,52 \mathfrak{M}$
$0,100$	$\pm 0,29 \mathfrak{M}$
$0,200$	$\pm 0,19 \mathfrak{M}$

Thus the mass of a giant star cannot claim individual accuracy, but when the parallax exceeds $0'',070$ the mass will possess some degree of individual accuracy. The masses computed by the aid of the Victoria parallaxes were also compared with the values that resulted from the Mount Wilson and Norman Lockyer parallaxes. The agreement of the data for small and moderate masses appears to be very satisfactory. It is not so good for the larger masses, and values of masses larger than $20 \odot$ are probably illusory. The mean masses were computed according to the following summary

	$M < 3M_{\odot}$	n	$M \geq 3M_{\odot}$	n
F stars . . .	$3,3 \odot$	33	$1,5 \odot$	82
G stars . . .	$3,6$	55	$0,9$	70
K stars . . .	$4,3$	54	$1,0$	26

Next the mass-luminosity relation was investigated. The curves for the different spectral classes are somewhat different from the theoretical curve of EDDINGTON¹.

¹ M N 84, p. 308 (1924)

This difference cannot be explained by the variation of $\log R/J$, but it can be explained by the assumption of a slight variation of the molecular weight during the evolution of the star.

Also the luminosity-density curve was derived on the basis of BOTTLINGER's photoelectric determinations of the colour indices. A linear relation between log density and absolute magnitude M_B was found for each spectral class:

$$\begin{array}{lcl} \text{GERASIMOVICH} & \log \rho = 0.63 M_B - 2.17 & \log \rho = 0.54 M_B - 2.52 \\ \text{SEARES} & \log \rho = 0.57 M_B - 1.33 & \log \rho = 0.57 M_B - 2.55 \end{array}$$

A catalogue of the masses of 71 stars, for which $\pi > 0''.070$, is appended to the paper. The mass of Arcturus comes out as 1.6 \odot and that of 61 Cygni as 2.2 \odot and 3.5 \odot respectively.

224. Colour-Mass-Density Relation. G. ABETTT¹ investigated in 1922 the masses and densities as derived from the data of double stars. The parallax-data were mainly based on Mount Wilson parallaxes or proper motion parallaxes according to KAPTEYN's and VAN RIJN's formula. The table summarizes the most important of the results:

	Spectral class		M_A	Differences in colour index	ΔM	Mass	Density	n
	A	B						
Giants . .	K2	F0	-0 ^m .5	+0 ^m .80 \pm 0 ^m .10	+2 ^m .2 \pm 0 ^m .2	15 \odot	<0.1 \odot	9
	G3	F7	-0 .1	+0 .22 \pm 0 .13	+1 .7 \pm 0 .4	14	<0.1	7
Intermediate	A2	A4	+0 .9	-0 .06 \pm 0 .04	+0 .8 \pm 0 .2	9	0.2	14
	F3	F8	+2 .5	-0 .14 \pm 0 .07	+1 .1 \pm 0 .4	4.4	0.3	10
	F7	G4	+3 .9	-0 .24 \pm 0 .09	+1 .3 \pm 0 .4	2.2	0.4	12
Dwarfs . .	G3	G5	+4 .8	-0 .07 \pm 0 .04	+0 .4 \pm 0 .2	1.5	0.5	7
	G7	K1	+5 .7	-0 .18 \pm 0 .05	+1 .0 \pm 0 .3	1.2	0.6	7
	K4	K6	+7 .7	-0 .06 \pm 0 .03	+0 .8 \pm 0 .3	1.1	0.8	9

Later on ABETTT² has determined the colour indices of the components of 35 double star systems.

ABETTT³ has also applied the theory of PANNEKOEK for the derivation of stellar masses.

225. Von Zeipel's Method. Up to 1921 the stars in the clusters were considered to have equal masses. This year H. VON ZEIPPEL published his interesting method which is derived from considerations concerning the distribution of molecules of a gaseous mass enclosed in a spherical space. The method can be applied to star clusters where a concentration of massive members has taken place around the centre and to star clouds in the Milky Way and it can certainly also be applied to clusters of anagalactic nebulae (galaxies). The problem of deriving the spatial distribution of stars within stellar clusters was at first attacked by E. C. PICKERING⁴, who studied the globulars 47 Tucanae, ω Centauri and M 13. He proved that the law of apparent distribution of stars, derived from the projected images of the clusters upon photographic plates, was the same for the three objects investigated. He tried to express the law analytically by the formula $(1 - r)^n$, where r is the distance from centre and n a constant. Some years later the problem of finding the spatial distribution from the projected distribution was solved by H. VON ZEIPPEL⁵ and next year⁶ a successful attempt was made by him to apply the results obtained from the dynamical theory of gases to the law of distribution of stars in globular cluster systems.

¹ Acc del Lincei Rend 31, 1^o Sem, p 359; 2^o Sem, p 93 (1922).

² Arcetri Pubbl Fasc No 40 (1923)

³ Harv Ann 26, p 213 (1897).

⁴ C.R. 144, p. 361 (1907)

⁵ Acc del Lincei Rend 33, p. 554 (1924).

⁶ Ann Obs Paris, Mémo 23, 1^{re} (1906).

The idea of treating the distribution of astronomical masses as the distribution of the molecules of a mass of gas can be traced back to Lord KELVIN's and G. H. DARWIN's¹ part in the discussion concerning the meteoric hypothesis by Sir N. LOCKYER. Later on² Lord KELVIN also discussed from the point of view of dynamical theory of gas the distribution of stars in our stellar system in relation to its age. POINCARÉ³ suggested in 1906 investigations based on the analogies between stellar systems and masses of gases and emphasized the great possibilities for extending our knowledge as to the construction of the Milky Way system. He also pointed out the difference between stellar systems and masses of gas. In the second case the mean free path is small when compared with the dimensions of the molecules but in the first case the mean free path is large in comparison with the dimensions of the stars. In the stellar system a very long time must elapse before a stage of equilibrium is reached and POINCARÉ assumed the Milky Way system to have not reached this stage as yet. In the globular clusters the influence of one star on the other is more pronounced and POINCARÉ suggested that the distribution of stars in clusters obeys the same law as that expressing the distribution of molecules in a mass of gas only subject to its own gravitational force.

The first step in the development of the theory is to compute a spherical distribution from knowledge of a circular one⁴. The photographs give us the number of stars $\Delta(r)$ per unit of area at the distance r from the centre. These apparent densities must be transformed into space densities $D(r)$. If r is the projected distance, ϱ the radius vector, and $l = \sqrt{\varrho^2 - r^2}$, VON ZEIPPEL⁵ derives the equation:

$$\Delta(r) = 2 \int_0^{\sqrt{R^2 - r^2}} D(\varrho) d\varrho,$$

where R is the limiting distance from the centre of the cluster.

In order to eliminate $d\varrho$ this relation can also be written:

$$\Delta(r) = 2 \int_r^R \frac{D(\varrho) \varrho d\varrho}{\sqrt{\varrho^2 - r^2}}.$$

Integrating by parts we have:

$$\Delta(r) = 2D(R) \sqrt{R^2 - r^2} - 2 \int_r^R \sqrt{\varrho^2 - r^2} D'(\varrho) d\varrho.$$

This equation is differentiated:

$$\Delta'(r) = -2D(R) \frac{r}{\sqrt{R^2 - r^2}} + 2r \int_r^R \frac{D'(\varrho) d\varrho}{\sqrt{\varrho^2 - r^2}}.$$

Further we multiply with $\frac{dr}{\sqrt{r^2 - r_1^2}}$, where $r_1 < R$, and then the integration between r_1 and R is performed. Then we obtain:

$$\int_{r_1}^R \frac{\Delta'(r) dr}{\sqrt{r^2 - r_1^2}} = -D(R) \int_{r_1}^R \frac{2r dr}{\sqrt{(R^2 - r^2)(r^2 - r_1^2)}} + 2 \int_{r_1}^R \frac{r dr}{\sqrt{r^2 - r_1^2}} \int_r^R \frac{D'(\varrho) d\varrho}{\sqrt{\varrho^2 - r^2}}.$$

¹ London Phil Trans 180 A, p. 1 (1889).

² Phil Mag 6th Ser. 2, p. 161 (1901).

³ B S A F 25, p. 153 (1906).

⁴ Ann Obs Paris, Mém 25, F (1906).

⁵ K Svenska Vet Akad Handl 61, No. 15, p. 109 (1921).

The order of integration is changed in the second integral

$$2 \int_0^R D'(q) dq \int_0^q \frac{r dr}{\sqrt{(q^2 - r^2)(r^2 - r_1^2)}}$$

Further it is found that

$$\int_0^{\theta} \frac{2r dr}{V(q^2 - r^2)(r^2 - r_1^2)} = \pi_0.$$

Нерсе,

$$\int_a^R \frac{D'(r) dr}{\sqrt{r^2 - 1}} = -\pi_0 D(r) + \pi_1 \int_a^R D'(q) dq = -\pi_0 D(r_1).$$

Instead of r_1 , r is used and instead of r, ρ Then:

$$D(r) = -\pi_0^{-1} \int_0^R \frac{A'(p) dp}{\sqrt{p^2 - r^2}} = -\pi_0^{-1} \int_0^{\sqrt{R^2 - r^2}} \frac{A'(\sqrt{p^2 + r^2})}{\sqrt{p^2 + r^2}} dp.$$

Next, VON ZEIPPEL makes the substitution:

$$p(r) = -\frac{1}{r} \frac{d\Delta(r)}{dr}$$

which gives:

$$D(r) = \pi_0^{-1} \int_0^{\sqrt{R^2 - r^2}} p(\sqrt{l^2 + r^2}) dl.$$

The star counts give $\Delta(r) + \Delta_0$, where Δ_0 can be presumed to be a constant value due to the foreground and background stars. As can easily be shown, this effect will be eliminated.

The value of $\phi(r)$ could be computed by the formulae for numerical differentiation, but as according to the above definition of $\phi(r)$ it is not valid for small values of r , the following expansion into series will be used:

$$p(r) = \frac{1}{\pi} \left\{ \frac{1}{288} (28 n_1 - 11 n_2 + n_3) - \frac{r^2}{1920} (10 n_1 - 5 n_2 + n_3) \right\},$$

where n is the number of stars in the region in question. Finally:

$$D(r) = \frac{\omega}{\pi} \left\{ \Sigma p(\sqrt{a^2 \omega^2 + r^2}) - \frac{1}{2} p(r) \right\},$$

where ω is an interval of t taken sufficiently small and $i = 0, 1, 2, \dots$ in succession. [The problem of deriving a spherical distribution from a (projected) circular distribution on a plate has been solved more recently from a somewhat different point of view by S. D. WICKERLY¹.]

The dynamical stage of a certain stellar agglomeration at the moment t is expressed by the correlation surface of the 7th order;

$$\varphi(x, y, z, t, \dot{x}, \dot{y}, \dot{z}, \ddot{x}, \ddot{y}, \ddot{z}, t) dx dy dz d\dot{x} d\dot{y} d\dot{z} d\ddot{x} d\ddot{y} d\ddot{z} dt,$$

where x, y, z are the coordinates and $\dot{x}, \dot{y}, \dot{z}$ the velocities. By applying a method of GIBBS it can be shown that the most probable state is expressed by:

$$\varphi = f(\mathbb{R}) e^{-h \mathbb{R} (x^2 + y^2 + z^2 - 2V(r))},$$

¹ Lund Medd Ser I, No 104 (1924).

where $V(r)$ is the potential of the group and r the distance from the centre. Further $f(r, \mathcal{M}) dx dy dz d\mathcal{M}$ is the frequency of stars of mass \mathcal{M} and of co-ordinates x, y, z . Then

$$f(r, \mathcal{M}) = \int_{-\infty}^{+\infty} \int \int \rho dx dy dz$$

and according to the last equation but one which expresses the Maxwellian distribution

$$f(r, \mathcal{M}) = \beta(\mathcal{M}) e^{2h\mathcal{M}V(r)} = \gamma(\mathcal{M}) [f(r, 1)]^{\mathcal{M}}$$

The function $\gamma(\mathcal{M})$ is independent of r and the equation can be written

$$-\log f_i(r) = C_i + \mathcal{M}_i [-\log f(r)], \quad i = 1, 2, 3$$

where the subscript i refers to a certain subgroup, C_i is a constant independent of r , and \mathcal{M}_i is the mass of a certain group or the mass-ratio of the group if one of these is selected as unit. The method thus gives the relative masses and not the absolute ones. The theorem of VON ZEIPPEL thus says that for two sub-groups of stars in a stellar agglomeration there is proportionality between the mass-ratios and the logarithms of the spatial densities. The method cannot, of course, be employed when the objects are too few to permit a decent determination of the spatial densities.

VON ZEIPPEL and LINDGREN¹ applied the method to the determination of the mass-ratios in Messier 37.

As photographic magnitudes were used in VON ZEIPPEL's and LINDGREN's work a reduction to bolometric magnitudes proved necessary. Such a reduction was made by Å WALLENQUIST², who obtained the following results.

WALLENQUIST			VON ZEIPPEL & LINDGREN		
\bar{M}_{bol}	$\mathcal{M}_i/\mathcal{M}_1$	n	\bar{M}_{bol}	$\mathcal{M}_i/\mathcal{M}_1$	n
1 ^M ,0	1.60 ± 0.09	231	1 ^M ,1	1.76	57
2 ,2	1.00	312	2 ,6	1.00	795
3 ,2	1.23 ± 0.05	556	4 ,2	0.673	682
4 ,1	(0.85 ± 0.06)	757	4 ,4	(0.360)	1203

The values of the last group are uncertain, as the colour indices have not been observed directly.

Å WALLENQUIST³ has measured the magnitudes of the open clusters M36 by applying the same method as VON ZEIPPEL and has also computed the mass-ratios.

\bar{M}_{bol}	$\mathcal{M}_i/\mathcal{M}_1$	n
-0 ^M ,8	1.57 ± 0.09	46
+1 ,8	1.00	130
+3 ,4	0.67	297

These results cannot be considered as accurate as those in the case of Messier 37, on account of the paucity of the stars that build up Messier 36, which makes the derivation of the spatial densities uncertain.

Å WALLENQUIST¹ has recently applied the method of VON ZEIPPEL to the determination of the mass-ratios of special star-groups in Messier 3. The material

¹ K Svenska Vet Akad Handl 61, No 15 (1924)

² Ark Mat Astr Fys 20 A, No 26 (1928), Upsala Medd 36

³ K Svenska Vet Akad Handl (3) 4, No. 8 (1928), Upsala Medd 32

⁴ B A N 5, p 67 (1929)

consisted of 848 stars in SHAPLEY's and Miss DAVIS's Catalogue¹ The stars were divided into four groups, for which the following results were found

Group	$\overline{M}_{\text{red}}$	$\overline{M}/\overline{M}_0$	n	von Zeipel's theory	Konstorum's formula	$\overline{M}_{\text{red}}$
Red "hypergiants"	14 ^m .69	1,297 \pm 0.031	268	3.88 \odot	3.90 \odot	-0 ^m .31
White "hypergiants"	15 .65	1,000	267	2.99 \odot	2.98 \odot	+0 .65
Ordinary red giants . .	16 .66	0.898 \pm 0.117	197	2.69 \odot	2.10 \odot	+1 .66
White stars	17 .09	0.620 \pm 0.123	122	1.86 \odot	1.86 \odot	+2 .09

\overline{M}_0 , the mass of the white "hypergiants", has been selected as unit

In order to reduce the determined mass-ratios into absolute masses the parallax of the cluster must be known. As the most probable value of the parallax $\pi = 0''.00010$ is accepted. This leads to the numbers in the last columns. If SHAPLEY's value for the \overline{M} of the cluster type variables had been used the four values of \overline{M} would have been 5.48 \odot , 4.22 \odot , 3.79 \odot , and 2.62 \odot respectively.

226. The Method of FREUNDLICH and HEISKANEN. Independently of VON ZEIPPEL, E. FREUNDLICH and W. HEISKANEN² have developed an analogous method. According to SHAPLEY there seems to exist a "galactic" plane in the globular clusters in the sense that only the brightest stars have a spherical distribution, whereas the fainter stars show an elliptical distribution. Let $\overline{M}_e/\overline{M}_s$ be the ratio of the total mass of the elliptically distributed stars to the total mass of the spherically distributed stars, and let a and b be the axes of the ellipsoidally distributed stars and e' a measure of the ellipticity of the equipotential surfaces, then³

$$e' \left[1 + \frac{\overline{M}_e}{\overline{M}_s} \left(1 + \frac{3}{5} \frac{b^2 \lambda^2}{a^2} \right) \right] = \frac{3}{10} \frac{\overline{M}_e}{\overline{M}_s} \frac{b^2 \lambda^2}{a^2}, \quad \text{where} \quad \lambda = \frac{a^2 - b^2}{b^2}.$$

If the equipotential surfaces cut the equator at the distance a and the polar axis at the distance r , then $e' = \frac{a}{r} - 1$

According to H. C. PLUMMER⁴ and VON ZEIPPEL⁴ the density in the cluster increases $\propto r^{\frac{1}{2}}$. Applying the slightly modified formula to SHAPLEY's material in M13 gives $\overline{M}_e/\overline{M}_s \approx 0.5$. This means that the mass of the spherically distributed stars, which amount to only 0.01 of the total number, should be at least two thirds of the total mass of the cluster. This will make the mean mass of the spherically distributed K and M giants 500 \odot , which seems incredible. The authors then repented SHAPLEY's star counts on the basis of his star catalogue⁵ and that of LUDENDORFF⁶. It was found that there were such individual deviations in the distribution of the different classes of stars that the authors think it is doubtful whether the above formula can be applied. They therefore turned their attention to investigating the relative concentration towards the centre of the different classes and to applying the theory of gases. If q_i is the number of molecules in unit space of a gas of atomic weight μ_i , V the gravitational potential, and h and q_0 certain parameters depending on the temperature and density at the centre, we have the equation⁷

$$q_i = q_0 e^{-2\frac{1}{2}\mu_i V}.$$

¹ Mt Wilson Contr No. 176 (1920).

² Z f Phys 14, p. 226 (1923).

³ M N 71, p. 460 (1914), 76, p. 107 (1915).

⁴ K Svenska Vet Akad Handl 51, No. 5 (1913).

⁵ Mt Wilson Contr No. 116 (1915).

⁶ Potsdam Publ 15, No. 50 (1905).

The theory has been applied to the clusters M3 and M13. The colour indices corresponding to the A and F stars have been taken together to form one group, those corresponding to G, K, and M stars to form another. Consider two spectral elements at distances r_1 and r_2 from the centre and attribute the subscripts A and K to the two spectral groups. Then

$$\frac{M_A}{M_K} = \frac{\log e_1^A - \log e_1^K}{\log e_2^A - \log e_2^K},$$

where

$$e_A^1 = e_0^{(A)1} \cdot e^{-2hM_A V_1}, \quad e_K^1 = e_0^{(K)1} \cdot e^{-2hM_K V_1},$$

$$e_A^2 = e_0^{(A)2} \cdot e^{-2hM_A V_2}, \quad e_K^2 = e_0^{(K)2} \cdot e^{-2hM_K V_2}.$$

From the observed number of stars on the plates the numbers in space were derived according to VON ZEPPEL's formula. The following results were derived

Distance from centre	M13 M_A/M_K	M3 M_A/M_K	Distance from centre	M13 M_A/M_K	M1 M_A/M_K
2'	1,420	1,761	5'	1,215	1,326
3'	1,135	1,865	6'	1,190	
4'	1,240	1,518			

227. MARTENS's Method¹. In order to obtain a handy expression of the exhaustion of the potential energy of a stellar cluster MARTENS assumes that the effects of collisions and passages are negligible when compared with the effect of the gravitation from the cluster. Further it is assumed that the mean values of kinetic energy per degree of freedom are constant for all degrees of freedom and independent of the coordinates of position. These two assumptions mean in other words the assumption of dynamical equilibrium and equipartition of energy.

MARTENS then performs a closer examination on basis of JEANS's work "The Dynamical Theory of Gases", in order to find out if the two assumptions are concordant.

The stellar system under consideration consists of n stars having $3n$ coordinates q_1, q_2, \dots, q_{3n} . Instead of the velocities dq_i/dt , the variables p_i are introduced.

The life history of the stellar system is represented by a certain curve in the $6n$ -dimensional space determined by the rectangular coordinates of position and velocities.

Next a great number of stellar systems is considered, so selected that the initial values of the $6n$ quantities q_i and p_i are so near each other that the representative points can be treated as forming a continuous medium. The number of points per unit of $6n$ -dimensional volume or the density of this medium is τ . If t is the time, the equation of continuity takes the form

$$\frac{\partial \tau}{\partial t} + \sum_{i=1}^{3n} \left\{ \frac{\partial}{\partial p_i} \left(\tau \frac{dp_i}{dt} \right) + \frac{\partial}{\partial q_i} \left(\tau \frac{dq_i}{dt} \right) \right\} = 0.$$

Combining this equation with the equations of motion and taking $D\tau/Dt$ as representing the increase in τ as we follow the group of points in its motion JEANS² has shown that

$$\frac{D\tau}{Dt} = \tau \sum_{i=1}^{3n} \frac{\partial^2 I_i}{\partial q_i \partial p_i},$$

¹ A Research on the Spherical Dynamical Equilibrium-Distribution of Stars of Unequal Masses Göteborg 1928

² The Dynamical Theory of Gases Fourth Edition Cambridge 1925

where $\frac{dE}{dt} = -2F$, E being the total kinetic energy of the system and $2F$ being a quadratic function of the velocities and giving the rate of dissipation of energy. JEANS has shown that the right member of this equation is always ≥ 0 , and only $= 0$ if $F = 0$. It then follows as a consequence of collisions between stars that mechanical energy is transformed into heat and that the points representing different initial configurations of the stellar systems are crowded together and that, independently of the initial states, the final states of the stellar systems are the same.

It can be shown on basis of J. OHLSSON's¹ investigations that the effect of collisions and passages can be fully neglected. OHLSSON thus estimates the time of relaxation measuring the rate at which the Galaxy as an effect of collisions approaches to equilibrium to be of the order of 10^{21} years. The corresponding time as an effect of passages is found to be of the order of 10^{18} years. These quantities are certainly much smaller in globular and open clusters but still the passages and then a fortiori the collisions have been neglected in MARTENS's work.

Then: $F = 0$ and $D\tau/Dt = 0$ (LIOUVILLE's theorem)

A part of the stellar system consisting of N stars is then considered. The stars have not equal masses but can be ordered into ν groups. The stars N_j in each group have the same mass M_j . Hence,

$$\sum_{j=1}^{\nu} N_j = N.$$

The stars are assumed to be material points. Every star then possesses three degrees of freedom and its state is determined by 6 quantities:

$$\varphi_1, \varphi_2, \varphi_3, \varphi_4, \varphi_5, \varphi_6.$$

The space containing the N points is divided into n equal elements of volume. The state of the stars is then statistically determined by certain quantities a_{ij} , giving the number of stars of mass M_j contained in the i th element of volume. We have then:

$$\sum_i a_{ij} = N_j, \quad (j = 1, 2, \dots, \nu)$$

Similarly to this distribution, called A by JEANS, there exists another distribution B , determined by the numbers b_{ij} , and so on. The task is to determine the a_{ij} in such a way that distribution A becomes the most probably one.

By variation of the last equations above the following ν conditions are found:

$$\sum_i \delta a_{ij} = 0, \quad (j = 1, \dots, \nu) \quad (a)$$

The N_j stars can be permuted in $\frac{N_j!}{a_{1j}! a_{2j}! \dots a_{nj}!}$ ways without changing the distribution A . The most probable distribution is the one that makes the volume containing the points of distribution A a maximum. This leads to the equations of condition:

$$\sum_{j=1}^{\nu} \sum_{i=1}^n \left[\log \frac{n_{ij}}{N_j} + 1 + \frac{1}{2a_{ij}} \right] \delta a_{ij} = 0. \quad (b)$$

Finally using the equation $E = \text{constant}$ and taking:

$$\frac{\partial E}{\partial a_{ij}} = s_{ij},$$

¹ Lund Medd Ser. II, No. 48 (1927).

and disregarding terms of higher order of δa_{ij} it is found by variation from the energy equation

$$\sum_{j=1}^i \sum_{i=1}^n \varepsilon_{ij} \delta a_{ij} = 0 \quad (c)$$

The set of variation-equations (a) is multiplied by the arbitrary factors l_j and the last one (c) by a factor m . The expressions are then added to the equation (b). It is then found that the a_{ij} have to satisfy the equations

$$\log \frac{na_{ij}}{N_j} + 1 + \frac{1}{2a_{ij}} + l_j + m\varepsilon_{ij} = 0$$

The a_{ij} are supposed to be so great that $\frac{1}{2a_{ij}}$ can be neglected. Further it is assumed that ε_{i1} is independent of a_{i1} , although dependent of the other a_{ij} . The equation is then solved into,

$$a_{i1} = \frac{N_i}{n} e^{-(1+l_i)-m\varepsilon_{i1}}$$

Introduce a function τ_j so that $\tau_j d\varphi_{j1} d\varphi_{j2} d\varphi_{j3} d\varphi_{j4} d\varphi_{j5} d\varphi_{j6}$ gives the number of stars within the limits $d\varphi_{jk}$, where $k=1, \dots, 6$, and whose masses are \mathfrak{M}_j .

Then τ_1 is proportional to a_{i1} and we can write

$$\tau_1 = C_1 e^{-m\varepsilon_1},$$

where C_1 is a constant and ε_1 a smooth function of the values ε_{i1} . ε_1 is assumed to have the form

$$\varepsilon_1 = \frac{1}{2} \beta_{11} \varphi_{11}^2 + \frac{1}{2} \beta_{12} \varphi_{12}^2 + \frac{1}{2} \beta_{13} \varphi_{13}^2 + f_1(\varphi_{11}, \varphi_{15}, \varphi_{16})$$

Then

$$\tau_1 d\varphi_{11} d\varphi_{12} d\varphi_{13} d\varphi_{14} d\varphi_{15} d\varphi_{16} = C_1 (e^{-\frac{1}{2}m\beta_{11}\varphi_{11}^2} d\varphi_{11}) \dots (e^{-m\beta_{1i}\varphi_{1i}^2} d\varphi_{1i}) \dots$$

This shows that the distributions of the coordinates are independent of one another.

The mean value of the contribution of φ_{11} to the energy is

$$\overline{\frac{1}{2} \beta_{11} \varphi_{11}^2} = \frac{1}{2m}, \quad \text{and also} \quad \overline{\frac{1}{2} \beta_{12} \varphi_{12}^2} = \overline{\frac{1}{2} \beta_{13} \varphi_{13}^2} = \dots = \frac{1}{2m}$$

It can also be shown that

$$\overline{\frac{1}{2} \mathfrak{M}_j \left(\frac{dq_{jk}}{dt} \right)^2} = \frac{1}{2m} \quad (k=1, 2, 3, j=1, \dots, n)$$

which expresses the law of equipartition of energy.

The assumption that the ε_{ij} are independent of a_{ij} is then made subject to a special examination on basis of CHARLIER'S¹, JEANS'S² and OHLSSON'S³ work and it is found that the assumption is justified when dealing with stellar systems and that equipartition of energy exists in a state of dynamical equilibrium. The author emphasizes the extreme difficulties presenting themselves when a search is made for the mechanism resulting in the equipartition of energy when collisions and passages are neglected. He quotes a postulate formulated by CHARLIER¹: "Each population of individuals approaches asymptotically that state which can be proved to possess the greatest probability."

¹ Lund Medd Ser II, No 16 (1917)

² M.N. 76, p. 70, 555 (1915-16), Problems of Cosmogony and Stellar Dynamics Cambridge 1919

³ Lund Medd Ser II, No 48 (1927) Also Dissertation Lund

⁴ Publ. A.S.P. 37, p. 125 (1925)

MARTENS finds that if the equations which determine the most probable distribution of the positional coordinates are solved, the a_i will be found to be independent of i , which means that the stars would be uniformly distributed over the whole space. But the task is not to seek for the most probable distribution among all possible ones but for the most probable distribution among those having a certain value of their potential energy. This is proved by applying the theorem of the virial¹.

If q_k are the rectilinear coordinates of N stars and Q_k the components of the acting forces in the same direction the equations of motion will be

$$M_k \frac{d^2 q_k}{dt^2} = Q_k. \quad (k = 1, \dots, N)$$

We designate by S the summation over all three directions of coordinates, then $S \sum_{k=1}^N M_k q_k^2$ is the moment of inertia of the system, and, as we are seeking stationary distributions, we write

$$\frac{d^2}{dt^2} S \sum_{k=1}^N M_k q_k^2 = S \sum_{k=1}^N M_k \frac{d^2}{dt^2} q_k^2 = 0,$$

the bar over an expression denoting an average over a long time.

The virial \bar{V} of CLAUSIUS is then found to be:

$$\bar{V} = -\frac{1}{2} S \sum_{k=1}^N q_k Q_k.$$

The following deductions are made on the assumption that the system is spherically distributed. The radius of the sphere is called R . It follows from the assumption of a limiting radius that the total gravitational force of all stars outside this sphere is zero. Thus only the forces due to the stars inside the sphere shall be taken into account. On another hand a number of stars will escape from the sphere at a certain moment, but these losses are counterbalanced by outside stars passing into the sphere and as it is assumed that the distribution is stationary, both outside and inside the limiting sphere, the counterbalancing effect appears to be more or less the same as if the outgoing stars met an elastic wall and were reflected by it. Of course, the identity is not kept after the imaginary reflection; it is another star that pursues the broken orbit. The expression of potential energy is not changed except in the immediate neighbourhood of the limiting sphere and this applies also to the law of distribution which is a function of the potential energy. These circumstances overcome the principal difficulties presented by the escaping and invading stars.

If N stars move under the sole influence of their gravitational interactions it follows that a simple relation exists between the virial \bar{V} and the exhaustion Ω of potential energy of the forces, which has the form:

$$\Omega = \frac{1}{2} \sum_{k=1}^N \sum_{l=1}^{N'} * M_k M_l \frac{1}{[S(q_l - q_k)^2]^{\frac{1}{2}}}.$$

The apostrophe by the second \sum sign means that during the summation $k \neq l$ must be excluded. $*$ is a numerical constant depending on the units used.

¹ The virial is the sum of the attractions between all the pairs of particles of a system, each multiplied by the distance between the pair.

Comparing the expressions for V and Ω it is found in accordance with EDDINGTON¹

$$V = -\frac{1}{2} S \sum_{k=1}^N q_k \sum_{l=1}^{N'} Q_{kl} = \frac{1}{4} \sum_{k=1}^N \sum_{l=1}^{N'} \kappa \mathfrak{M}_k \mathfrak{M}_l \frac{1}{[S(q_l - q_k)^2]^{\frac{1}{2}}} = \frac{1}{2} \Omega$$

Applying the virial-theorem earlier quoted it follows that

$$T - \frac{1}{2} \Omega = 0$$

The equations of motion possess the wellknown integral

$$-\frac{1}{2} h = T - \Omega,$$

where h is an arbitrary constant. Thus

$$\Omega = h \quad (d)$$

Next Ω will be expressed as a function of the quantities a_{ij} . The expression for the exhaustion of potential energy can be written:

$$\Omega = \sum_{k=1}^N \sum_{l=1}^{k-1} \kappa \mathfrak{M}_k \mathfrak{M}_l \frac{1}{[S(q_l - q_k)^2]^{\frac{1}{2}}}$$

if the indices k are chosen in such a manner that $Sq_k^2 < Sq_{l+1}^2$. The neglect of irregular forces permits to substitute for the attraction of a number of discrete stars the attraction of a homogeneous sphere having the same mass as the sum of the masses of the discrete stars. The terms expressing the exhaustion of potential energy of attraction on the mass \mathfrak{M}_s , $\kappa \mathfrak{M}_s \sum_{i=1}^{s-1} \mathfrak{M}_i [S(q_i - q_s)^2]^{-\frac{1}{2}}$ are thus substituted by the expression $\kappa \mathfrak{M}_s [Sq_s^2]^{-\frac{1}{2}} \sum_{i=1}^{s-1} \mathfrak{M}_i$.

In the distribution A determined by the numbers a_{ij} the stars having the same index i are situated within a spherical shell. The harmonic mean distance of these stars from the centre is r_i . The stars in the element s contribute to the exhaustion of potential energy by a quantity

$$\kappa \frac{\sum_{j=1}^r a_{sj} \mathfrak{M}_j}{r_i} \sum_{i=1}^{s-1} \sum_{j=1}^r a_{ij} \mathfrak{M}_j$$

and observing (d) we obtain:

$$\Omega = \kappa \sum_{s=1}^n \frac{\sum_{j=1}^r a_{sj} \mathfrak{M}_j}{r_s} \sum_{i=1}^{s-1} \sum_{j=1}^r a_{ij} \mathfrak{M}_j = h. \quad (e)$$

The variations δa_{sj} are to be connected by the condition

$$\kappa \sum_{s=1}^n \sum_{j=1}^r \delta a_{sj} \left\{ \frac{\mathfrak{M}_j}{r_s} \sum_{i=1}^{s-1} \sum_{j=1}^r a_{ij} \mathfrak{M}_j + \mathfrak{M}_j \sum_{i=s+1}^{n-1} \frac{\sum_{j=1}^r a_{ij} \mathfrak{M}_j}{r_i} \right\} = 0.$$

Further is

$$\sum_{j=1}^r \sum_{s=1}^n \delta a_{sj} \left\{ \log \frac{n a_{sj}}{N_j} + 1 + \frac{1}{2 a_{sj}} \right\} = 0$$

and

$$\sum_{s=1}^n \delta a_{sj} = 0$$

¹ M N 76, p 525 (1916)

The a_{sj} are then found by using the method of indetermined multipliers. Neglecting the term $1/2a_{sj}$ the following set of equations is found.

$$\log \frac{a_{sj}}{N_j} + 1 + l_j + m\pi \mathfrak{M}_j \left(\frac{1}{r_s} \sum_{i=1}^{s-1} \sum_{j=1}^r a_{ij} \mathfrak{M}_j + \sum_{i=s+1}^{s-1} \frac{\sum_{j=1}^r a_{ij} \mathfrak{M}_j}{r_i} \right) = 0, \quad (f)$$

where l_j and m are arbitrary factors. To these $s \cdot j$ equations are joined the j equations $\sum_{i=1}^s a_{ij} = N_j$ and equation (e) above. We have thus $s \cdot j + j + 1$ equations to determine the $s \cdot j + j + 1$ unknown quantities a_{sj} , l_j and m .

The radius of the sphere enclosing the stars in the system considered is R . If W is the volume then the volume of each cell is W/n and $\pi a_{sj}/W$ gives the density of stars of mass \mathfrak{M}_j at the distance r_s from the centre. Further is introduced:

$$f_j(r_s) = \frac{\pi a_{sj}}{W}.$$

If $r_{s+1/2}$ is the radius of the spherical surface separating the cell s from the cell $s+1$ we have.

$$\frac{W}{n} = \int_{r_{s-1/2}}^{r_{s+1/2}} 4\pi_s r^2 dr \quad \text{and} \quad a_{sj} = f_j(r_j) \int_{r_{s-1/2}}^{r_{s+1/2}} 4\pi_s r^2 dr$$

On considering the quantities $f_j(r_s)$ as being continuous functions of r and assuming the cells to be thin we may put:

$$a_{sj} = \int_{r_{s-1/2}}^{r_{s+1/2}} 4\pi_s r^2 f_j(r) dr$$

Then the equations (f) are transformed following the same assumption. Applying the Laplacian operator ∇^2 to the expressions (f) and dropping the index s it is finally found:

$$\nabla^2 \left[-\frac{1}{m\pi \mathfrak{M}_j} \log \left(\frac{W}{N_j} e^{1+l_j} f_j(r) \right) \right] = -4\pi_s \sum_{j=1}^r \mathfrak{M}_j f_j(r). \quad (j = 1, \dots, r)$$

This gives the equation

$$\frac{\partial^2 \log f_j(r)}{\partial r^2} + \frac{2}{r} \frac{\partial \log f_j(r)}{\partial r} = 4\pi_s m\pi \sum_{j=1}^r \mathfrak{M}_j f_j(r) \quad (j = 1, \dots, r) \quad (g)$$

Each one of these equations contains in its left member one of the unknown functions but in its right member all the unknown functions. By considering the equations for the potentials of gravitation it is found that:

$$\frac{1}{m\pi \mathfrak{M}_j} \left(\log \frac{W}{N_j} e^{1+l_j} f_j(r) \right) = \frac{1}{m\pi \mathfrak{M}_j} \left(\log \frac{W}{N_j} e^{1+l_j} f_j(r) \right) \quad (h)$$

or:

$$\left(\frac{W}{N_j} e^{1+l_j} f_j(r) \right)^{1/\mathfrak{M}_j} = \left(\frac{W}{N_j} e^{1+l_j} f_j(r) \right)^{1/\mathfrak{M}_j},$$

which are the relations used by VON ZIEPEL and LINDGREN.

Introducing

$$C_{ij} = \frac{N_i}{W} \left(\frac{W}{N_i} \right)^{\frac{\mathfrak{M}_i}{\mathfrak{M}_j}} e^{-(1+l_i) + \frac{\mathfrak{M}_i}{\mathfrak{M}_j}(1+l_j)}$$

we have.

$$f_i(r) = C_{ij} [f_j(r)]^{\mathfrak{M}_i/\mathfrak{M}_j}.$$

$\log r^2$	p		Δ	q		Δ	u		Δ	w		Δ
	$\log f_1 \text{ obs}$	$\log f_1 \text{ calc}$		$\log f_2 \text{ obs}$	$\log f_2 \text{ calc}$		$\log f_2 \text{ obs}$	$\log f_2 \text{ calc}$		$\log f_3 \text{ obs}$	$\log f_3 \text{ calc}$	
$-\infty$	9.233-10	9.154-10	+0.079	9.604-10	9.613-10	-0.009	8.901-10	8.888-10	+0.013	8.313-10	8.306-10	+0.007
0.000	9.182	9.082	+0.100	9.581	9.572	+0.009	8.882	8.861	+0.021			+0.009
0.602	8.972	8.893	+0.079	9.505	9.465	+0.040	8.802	8.789	+0.013			+0.011
0.954	8.556	8.640	-0.084	9.367	9.321	+0.046	8.693	8.692	+0.001			+0.038
1.398	7.927	8.095	-0.168	8.993	9.012	-0.019	8.476	8.484	-0.008			
1.800	7.350	7.383	-0.033	8.526	8.608	-0.082	8.161	8.212	-0.051			

and the differential equation then becomes

$$\frac{d^2 \log f_j(r)}{dr^2} + \frac{2}{r} \frac{d \log f_j(r)}{dr} = 4\pi_0 \kappa m \mathfrak{M}_j \sum_{i=1}^v \mathfrak{M}_i C_{ij} [f_j(r)]^{p_i/q_i},$$

where both the membra only contain one of the unknown functions. In order to find all functions of distribution we need only to solve one of the v equations. The other $v-1$ functions are then found by aid of the relations (h).

For the application of this theory to a cluster there are required observations on functions of distribution of different groups of stars, classified according to attributes correlated to the masses of the stars. As such observations of globular clusters were not accessible MARTENS compared the results of his theory with the distributions in the open cluster M 37 (NGC 2099) observed by VON ZIEPPEL and LINDGREN. These authors divided the stars of M 37 according to their magnitudes and colour indices into four groups, p, q, u, w . The p -stars were interpreted as g -giants, the q -stars as b - and a -stars, the u -stars as f -dwarfs and the w -stars as g -dwarfs. From their observations VON ZIEPPEL and LINDGREN have calculated the distributions $f_1 \text{ obs}$, $f_2 \text{ obs}$ in space of the four types of stars given in the adjoining table. MARTENS compared these observed distributions with those calculated ($f_1 \text{ calc}$, $f_2 \text{ calc}$) on the supposition that the cluster is in its most probable state.

It is obvious from the distribution of the differences $\Delta = \text{obs} - \text{calc}$ that the value of m determined for different groups would be about the same. This is an indication of equipartition of energy on the different masses. Further the differences show that the stars are more concentrated to the centre of the cluster than is required by the calculated distribution. This phenomenon, well-known for distributions in globular clusters, disregarding unequalities of masses of the stars, is usually interpreted as displaying that the clusters are built up in adiabatic equilibrium instead of in isothermic. According to the theory here developed there is, however, another possible explanation. Doubtless there are within the cluster stars that are not luminous enough to be observed. These stars do not influence the observed distributions, but as they contribute to the potential of the cluster they are able to affect the calculated distributions, as has been shown on the preceding pages, in a direction to diminish and perhaps abolish the differences of the table.

Among other results found by MARTENS the fact may be mentioned that if equipartition has taken place in a stellar cluster then the most probable state of distribution is expressed by the Maxwellian law. Such a system has no limitation in space or, in other words, its radius is infinite. If the mass-ratios exceed $3/2$ within such a system, the number of the smaller masses must be infinite, whereas the number of the greater masses is finite. It seems that

the adiabatic distribution in globular clusters can be explained by the assumption that within these objects the mass-distribution is the most probable one

228. Recent Work Concerning Masses of Spectroscopic Binaries. It is only four and a half decades since the first discovery of a spectroscopic binary was announced. At present orbital elements are known for some 250 systems. When both spectra have been observed and also the system is an eclipsing binary, we obtain complete and, in most cases, very accurate knowledge of the components. When the system is not an eclipsing binary, but both spectra are known, we get the minimum values of the masses, because the orbital determination gives the quantities $M_A \sin^3 i$ and $M_B \sin^3 i$. Reasonable assumptions concerning the value of $\sin^3 i$ can also be made and thus our knowledge of the mean value of M for certain groups of binaries can be considerably advanced

The third case, i. e. when only the spectrum of one of the components is registered, presents several difficulties as far as the determination of the mass is concerned. This case is certainly the most common one. As soon as the components in a double star system differ two magnitudes or more, the chances are very small that both spectra will appear on the plates. The observations of a spectroscopic binary give in the case of one spectrum the so-called mass-function, $f = M_B^3 \sin^3 i (M_A + M_B)^{-2}$, which can be written

$$(M_A + M_B) \sin^3 i = [3.01642 - 10] K_A^2 \left(1 + \frac{M_A}{M_B}\right)^2 P (1 - e^2)^{\frac{1}{2}},$$

where K_A is the semi-amplitude of the velocity variation for M_A and P the period in days

R. G. ATKIN has expressed doubts in his book "The Binary Stars", with regard to whether the mass-function can give any information concerning the masses of the stars. Generally the value K_A or a corresponding expression has been used and then, of course, the range is considerable. It is fair to use K_A in order to get a quantity that is proportional to the cube root of the mass, because in direct determinations of stellar masses we cannot get more than a fair knowledge of $(M_A + M_B)^{\frac{1}{3}}$ from our best determinations of stellar parallaxes. The use of K_A has also been recommended by OTTO STRUVE¹ and others.

STRUVE has assumed:

$$K_A = C P^{-\frac{1}{2}},$$

which is justifiable for certain groups of stars. The curve combining P and K corresponds very nearly to the equation $K = C P^{-\frac{1}{2}}$ for $P = 9$ years to $P = 2.45$ days, ($\log C = 2.0695$). LUDENDORFF has reached a number of important conclusions which are given already in ciph. 215 of this chapter.

Extensive use of STRUVE's formula has been made by BIER in his paper, "Zur Charakterisierung der spektroskopischen Doppelsterne"². This extensive and valuable monograph cannot be reviewed here excepting from the point of view of determination of stellar masses

From 434 objects BIER finds the value $K P^{\frac{1}{2}} = 125.1$. He makes use of the above relation for a discussion of the probability of a certain group of stars exhibiting variable radial velocities being binaries (e. g. the Cepheids) and classifies the real binaries according to the characteristics of the P, K -curves.

¹ Ap J 60, p. 167 (1924)

² Berlin-Babelsberg Veröffentlich. V, H 6 (1927)

BEER has collected 88 pairs showing both spectra, and finds the following frequencies of the values $(M_A + M_B) \sin^3 i$

$(M_A + M_B) \sin^3 i$	<i>n</i>	$(M_A + M_B) \sin^3 i$	<i>n</i>	$(M_A + M_B) \sin^3 i$	<i>n</i>
> 100 ○	2	8 — 9 ○	—	3,0—3,5 ○	3
50—100	1	7 — 8	2	2,5—3,0	13
40—50	—	6 — 7	—	2,0—2,5	11
30—40	3	5 — 6	5	1,5—2,0	11
20—30	5	4,5—5,0	—	1,0—1,5	8
10—20	4	4,0—4,5	4	0,5—1,0	6
9—10	6	3,5—4,0	3	< 0,5	1

This table seems to lend some support to the theory of HERTZ RICH¹ assuming the existence of preferential mass values (cf ciph 229)

The relation between mass and spectral class is illustrated in the following summary:

Spectral class	$M_A \sin^3 i$	$M_B \sin^3 i$	Range for $(M_A + M_B) \sin^3 i$	<i>n</i>
O6—B4	13,18 ○	10,50 ○	139 — 2,60 ○	21
B5—A4	2,71	1,73	26,4 — 0,21	30
A5—F4	1,80	1,24	13,4 — 0,52	18
F5—G4	1,01	0,89	3,37—0,87	15
G5—K4	0,87	0,68	2,10—1,05	3

In 33 cases the individual masses were known. By assuming $\sin^3 i = 0,667$ the following mean values were found

Spectral class	$M_A + M_B$	<i>n</i>	$[M_A + M_B]$	<i>n</i>	Adopted mean
O6—B4	17,17 ○	9	20,28 ○	10	18,8
B5—B9	10,15	4	10,64	5	10,4
A0—A4	4,47	7	3,53	14	3,8
A5—F4	2,70	4	3,00	12	2,9
F5—G4	1,42	7	3,54	8	2,6
G5—K4	1,94	2	2,25	1	2,0

The values $M_A + M_B$ are the mean values derived directly from known inclinations (eclipsing binaries), whereas $[M_A + M_B]$ are the means derived from the above assumption as to the mean value of $\sin^3 i$.

The group of stars later than F0 consists of 12 giants and 17 dwarfs. No systematic difference with regard to the mean masses can be found which is contrary to what is the case when the masses of visual binaries are derived:

Spectral class	Giants			Dwarfs		
	$(M_A + M_B) \sin^3 i$	$M_A + M_B$	<i>n</i>	$(M_A + M_B) \sin^3 i$	$M_A + M_B$	<i>n</i>
F0—F4	1,90 ○	2,85 ○	7	2,34 ○	3,51 ○	4
F5—G4	2,38	3,57	5	1,69	2,53	10
G5—K4				1,55	2,32	3

The mass-ratios M_B/M_A have a mean value of 0,75. The distribution with regard to spectral class is as follows

¹ A N 220, p 249 (1924)

Spectral class	Mass-ratios					Mean mass-ratio
	0,11—0,30	0,31—0,50	0,51—0,70	0,71—0,90	0,91—1,00	
O6—B4	—	3	4	7	4	0,74
B5—A4	4	4	6	9	7	0,68
A5—F5	1	1	2	7	8	0,81
F5—G4	—	2	—	5	6	0,83
G5—K4	—	—	1	2	—	0,76
Sum	5	10	13	30	25	

A tendency of M_B/M_A to increase in the course of evolution seems to be present, but is not very pronounced.

There seems to be some relation between M_B/M_A and $(M_A + M_B) \sin^3 i$ as follows:

M_B/M_A	$(M_A + M_B) \sin^3 i$	n	M_B/M_A	$(M_A + M_B) \sin^3 i$	n
0,32	7,15	10	0,86	5,09	10
0,52	4,37	10	0,89	6,53	10
0,69	7,54	10	0,95	4,38	10
0,79	3,68	10	0,99	5,01	10

The dispersion within the individual groups is considerable and the general relation cannot be established at present.

BERR uses the quantity $f = M_B(M_B + M_A)^{-1} \sin^3 i$ and divides the material into binaries showing one spectrum ($n = 151$) and two spectra ($n = 93$). Periods of 1000^d or more have to be excluded, as has been pointed out by LUDENDORFF, as they are not comparable with short periodic systems on account of the very nature of the function f . The following correlation surface is found for the remaining 233 systems.

Spectral class	f											Sum
	>1,00	1,00 to 0,90	0,90 to 0,80	0,80 to 0,70	0,70 to 0,60	0,60 to 0,50	0,50 to 0,40	0,40 to 0,30	0,30 to 0,20	0,20 to 0,10	to <0,10	
O6—B4 one	4	1	3	3	2	1	3	3	4	3	5	32
two	8	4	—	2	2	2	—	—	—	—	—	19
B5—A4 one	2	—	—	2	2	3	4	10	8	7	—	38
two	2	—	2	2	4	12	4	1	8	—	—	34
A5—F4 one	—	—	1	—	—	4	3	4	2	5	2	21
two	1	—	—	2	9	8	—	2	—	—	—	19
F5—G4 one	—	—	1	—	3	2	4	4	9	3	1	27
two	—	—	—	2	4	5	2	—	2	—	—	18
G5—K4 one	—	—	1	—	3	6	4	6	1	—	1	22
two	—	—	—	—	—	2	—	1	—	—	—	8
K5—M7 one	—	—	—	—	—	1	1	—	1	—	—	3
two	—	—	—	—	—	—	—	—	—	—	—	—
Sum one	6	1	6	5	10	17	19	27	25	16	9	143
two	11	4	2	9	19	27	6	4	7	—	—	98

BERR has investigated the mean errors in the mean values of f and confirms the conclusion of LUDENDORFF that within each spectral class the mean value of f is practically constant and thus very suitable for a derivation of the mean value of the mass.

The ratio of the masses of B stars and A stars (including A stars and the following classes) is found to be 3,42 and 5,80 for stars showing one and two spectra respectively. A direct computation from the direct data which avoids using f gives 5,48 for the second group.

The material concerning the spectroscopic binaries is given in J II MOORE'S "Third Catalogue of Spectroscopic Binary Stars" (which includes the material to July 1st, 1924) in LICK BULL No 355 (1924) and in BEER'S paper (which includes the material to March 1927). On pages 122—124 BEER gives corrections and additions to the Third Catalogue. The student of spectroscopic binaries is recommended to consult these two sources, which give a complete collection of the material up to 1927, whenever investigations of a general nature concerning these objects are to be undertaken.

The correlation between the frequencies of one and two spectra is comparatively low. An analysis of the two frequencies has not yet been undertaken, but would undoubtedly reveal several points of interest.

BEER forms the equation

$$\left(\frac{\mathcal{M}_B}{\mathcal{M}_A}\right)_I = \frac{f_I^{\frac{1}{2}} f_{II}^{-\frac{1}{2}} [\mathcal{M}_B/(\mathcal{M}_A + \mathcal{M}_B)]_{II}}{1 - f_I^{\frac{1}{2}} f_{II}^{-\frac{1}{2}} [\mathcal{M}_B/(\mathcal{M}_I + \mathcal{M}_B)]_{II}}$$

where the subscripts I and II refer to the groups with one and two spectra respectively. HE finds from his material

Spectral class	$(\mathcal{M}_B/\mathcal{M}_I)_{II}$	"	$(\mathcal{M}_B/\mathcal{M}_I)_I$	"	"
A	0.683	30	0.415	36	32
F	0.806	19	0.466	21	18
G	0.826	13	0.508	27	15

229. Preferential Values of Stellar Masses. In order to determine the masses and the mass-ratios of spectroscopic binaries J HELLERICH has investigated 173 pairs, of which 61 exhibited the spectra of both components. The Cepheids, stars of the same type as β Canis Majoris, and stars with periods larger than 1000^d were excluded. HELLERICH¹ found that stars of the classes A to G did not have very different mean masses.

Spectral class	$(\mathcal{M}_A + \mathcal{M}_B) \sin^3 i$	"
A	2.72 \odot	22
F	2.08 \odot	13
G	2.07 \odot	3

Within the classes Oc—B9 the range in the mass value is from 1 \odot to 139 \odot . On account of this dispersion no mean values were formed for these spectral classes. Besides, the material suggested that the masses were grouped around certain maxima of frequency, viz 32 \odot , 22 \odot , 16 \odot , 10 \odot , and 2.5—3.0 \odot . Although the material is small, it nevertheless seems difficult to explain the preferential values as due to chance. The frequency of large masses decreases very rapidly with the increase in the value of the mass.

The adjoining distribution of the values $\mathcal{M}_B/\mathcal{M}_A$ was found

The mean values are

$\mathcal{M}_B/\mathcal{M}_A$	Oc—B9	A—G	$\mathcal{M}_B/\mathcal{M}_A$	Oc—B9	A—G
0.1—0.2		1	0.6—0.7	3	5
0.2—0.3		1	0.7—0.8	3	5
0.3—0.4	3		0.8—0.9	4	10
0.4—0.5	1	1	0.9—1.0	7	13
0.5—0.6		2			

Spectral class	$\mathcal{M}_B/\mathcal{M}_I$	"	Spectral class	$\mathcal{M}_B/\mathcal{M}_I$	"
B0—B5	0.64	13	F	0.88	13
B8—B9	0.76	4	G	0.86	3
A	0.79	22			

No relation was found between the mass-ratio and $(\mathcal{M}_A + \mathcal{M}_B) \sin^3 i$

¹ A N 220, p 249 (1924)

HELLERICH recommends the use of the quantity f/t and investigates the frequency of this quantity in his material. A decided difference with regard to the distribution of the f/t values is found between the systems for which one spectrum has been observed and those for which both spectra have been observed. In the first case these values are considerably lower than in the second case.

This remarkable difference may arise from a number of causes. It does not seem likely that a systematically different orientation in space of the orbits

of the two groups can be present. Nor can any systematic difference be assumed in the mass values themselves or in the mean eccentricities. An inspection of the material shows that the mean periods of the two groups are not very different. The only possible explanation seems to be to assume that the mass-ratios of the binaries with double spectra really are systematically larger than the mass-ratios of the binaries with a single spectrum, which means that the dispersion in the single masses in the former case should be smaller than the dispersion in the latter.

Comparing the values of f/t with the corresponding values of M_B/M_A and excluding stars for which M_B/M_A is smaller than 0.80 HELLERICH finds for group I the following values for the mean mass-ratio:

Spectral class	M_B/M_A	n
A stars .	0.37	27
F stars .	0.29	20

In those cases where the companion has a considerably lower brightness than the principal star the mass of the companion will also be very small in comparison with that of the more massive star. The theory implies that the dispersion in stellar mass is larger than has generally been assumed but it scarcely gains support from an investigation of visual binaries. Mass-ratios as low as 0.3 seem to be rather exceptional among the 50 pairs so far investigated. The enormous difference in luminosity of 150000 between Procyon and its companion corresponds to a difference in the masses of only 0.9 \odot .

In a subsequent paper HELLERICH¹ returns to the question, if preferential values of stellar mass exist. He points out that the results at the Cape Observatory by HALM² concerning the preferential values of colour indices also pointed in the direction that there are six maxima in the frequencies of masses computed from the absolute magnitude and temperature. HALM's maxima are

11.6 \odot , 5.8 \odot , 2.8 \odot , 1.32 \odot , 0.66 \odot , 0.32 \odot .

From the material at hand of spectroscopic binaries HELLERICH found five maxima, viz

33 \odot , 22 \odot , 16 \odot , 10 \odot and 2.5–3.5 \odot

The values 2.8 \odot and 10 \odot are common to both series, the value 1.3 \odot is weakly indicated in the spectroscopic material. The small values 0.66 \odot and 0.32 \odot are wanting in the spectroscopic material as they correspond to very small amplitudes in the curves of radial velocity. On the other hand, the large mass values 16 \odot , 22 \odot , 33 \odot are not extant in HALM's series, for the stars used by him are of classes F to K and, therefore, cannot have large masses, as is known from other investigations.

HALM's series of the frequency-maxima of stellar masses nearly forms a geometrical progression with the proportion $1/2$. Extrapolating this series to large masses, one obtains 23 \odot , 46 \odot , 92 \odot , 184 \odot . The comparison with the

¹ A N 221, p. 49 (1924)

² Report of H. M. Astronomer at the Cape of Good Hope 1922, p. 4.

second series shows that the value $23\odot$ is extant. Further, we know two spectroscopic binaries with masses not too far from $92\odot$ and $184\odot$ respectively.

Testing HALM's series with the material offered by visual binaries HERTZSPRUNG finds indications of a frequency maximum between $0.9\odot$ and $1.5\odot$.

230. Dwarf Nature of Spectroscopic Binaries. E A KREIKEN¹ has advanced the idea that spectroscopic binaries are generally dwarf stars. From the catalogues of J MOORE and A BEER 97 systems with two spectra were collected. The value of $\sin i$ was found to be much larger than has been assumed earlier. When the log's of the values $M_A \sin^3 i$ and $M_B \sin^3 i$ were plotted against spectral class a rather definite curve was found. As there is no reason why the mean value of $M \sin^3 i$ should systematically depend on spectral class, the actual relation between M and spectrum will be found when the plotted curve is shifted over an interval corresponding to the logarithm of $\sin^3 i$. The masses of the giants were computed according to EDDINGTON's theory and the masses of the dwarfs according to BRILL's investigation². The following table shows the result.

Spectral class	$\log M$		$\log M \sin^3 i$	$\log M - \log M \sin^3 i$	
	Giants	Dwarfs		Giants	Dwarfs
O5	—	2.00	1.90	—	+0.10
B0	0.87	1.00	1.10	-0.23	-0.10
B5	0.65	0.65	0.44	+0.21	+0.21
A0	0.56	0.44	0.22	+0.34	+0.22
A5	0.54	0.30	0.11	+0.43	+0.19
F0	0.52	0.18	0.05	+0.47	+0.13
F5	0.45	0.08	0.00	+0.46	+0.09
G0	0.44	0.00	0.00	+0.49	+0.05
G5	0.43	-0.08	0.00	+0.53	+0.02
K0	—	-0.16	0.00	—	-0.02

Although in the case of the dwarf hypothesis the residuals exhibit a systematic run there is no doubt that they should not be preferred. Uncertainty is involved in the computation of the mean masses because the frequencies in the RUSSELL diagram used have not been reduced to equal space. Anyhow it is evident that the dwarf hypothesis might be worth a serious consideration. KREIKEN found for dwarf stars the value $\log \sin^3 i = 9.905 - 10$ and thus $\sin i = 0.927$ and for giant stars $\log \sin^3 i = 9.525 - 10$ and $\sin i = 0.695$ which is very near the value 0.667 generally adopted.

In order to test the result the hypothetical distances were derived from the masses computed by multiplying $M \sin^3 i$ by the two values 0.927³ and 0.695³ corresponding to the dwarf and giant hypotheses. The masses were converted into distances by means of EDDINGTON's mass-luminosity formula. A comparison between the distances thus obtained and the distances derived from trigonometric parallaxes or spectrographic determinations of the absolute magnitude decides in favour of the value $\sin i = 0.927$.

231. Discovery of Mass-Luminosity Relation. The relation between stellar mass and luminosity was at first indicated in EDDINGTON's work³ concerning the radiative equilibrium of the stars. It was concluded that the luminosities of giants vary approximately as M^2 and of the dwarf stars as M^3 . The first time a mass-luminosity relation was established in an empirical way was, as far as I am aware, in a paper by HERTZSPRUNG⁴ in 1919 in which he derived the formula:

$$\log M = -0.06 M = -0.06 (m + 5 + 5 \log \pi)$$

Somewhat later C LUPAU-JANSSEN⁵ went over HERTZSPRUNG's material again, but preferred to leave the coefficient M/M unchanged. At the same

¹ M N 89, p 589 (1929)

² M N 77, p 596 (1917)

³ Undersøgelser over Doppelstjerner III (1919)

⁴ Berlin-Babelsberg Veröff VII, Heft 1 (1927)

⁵ A N 208, p 96 (1919)

time independently of HERTZSPRUNG A VAN MAANEN¹ derived a mass-luminosity relation of practically the same form. From VAN MAANEN's paper the following table has been prepared giving the mean values of M , M and $\log M$ together with the corresponding dispersions around the means

$M \pm \sigma_M$	$M \pm \sigma_M$	$\log M \pm \sigma_{\log M}$	n
0.42 ± 0.33	15.84 ± 17.4	0.94 ± 0.46	4
1.63 ± 0.44	7.99 ± 8.2	0.75 ± 0.33	6
3.00 ± 0.35	3.42 ± 2.04	0.46 ± 0.25	6
4.63 ± 0.27	1.72 ± 1.47	0.13 ± 0.33	12
5.77 ± 0.40	1.24 ± 0.29	0.08 ± 0.11	8
10.7 ± 0.81	0.58 ± 0.22	-0.21 ± 0.14	3

The curvature of the line connecting the mean values of M and M and the small dispersion in the values below $M = 4.5$ are notable results in this investigation. The mean values of the mass compare favourably with later investigations when more extensive material has been available.

Of the subsequent treatments of the mass-luminosity relation we shall only mention those of F. H. SEARES² and W. J. LUYTEN³. The latter derived the expression

$$\log M = -0.09 (M - 4.8).$$

In 1923 HERTZSPRUNG⁴ returned to the question. From a list of 15 first-class determinations, which included our Sun, he determined the diagram reproduced in fig. 153. The general decrease of mass with luminosity is clearly shown. The faint companion of Sirius is extraordinarily massive in comparison with its small intrinsic brightness.

HERTZSPRUNG assumed the following linear relation:

$$\log M = -0.084 (m + 5 \log \pi)$$

but remarked that the quadratic expression

$$m + 5 \log \pi = -11 \log M + 2 (\log M)^2$$

would represent stars of great mass somewhat better.

He introduces the conception of angular mass being

$$(M_A + M_B) \cdot \pi^2 = \frac{a^3}{P^3}$$

Knowing M_A/M_B and a^3/P^3 we find the absolute magnitudes of each component reduced to the mass of the Sun to be:

$$m_A + 5 \log \pi + \frac{1}{2} \log M_A,$$

$$m_B + 5 \log \pi + \frac{1}{2} \log M_B.$$

From the relation between mass and absolute magnitude it is possible to compute the parallax of a double star from m_A , m_B , and a^3/P^3 . The formula will be

$$0.86 \log \pi = \log \pi - \frac{1}{2} \log [1 + 10^{-0.084(m_B - m_A)}] + 0.028 m_A.$$

The dynamical parallax $\pi_d = \frac{a}{P}$ is computed in this case by assuming the mass-sum to be equal to the mass of the Sun.

If the above quadratic formula holds good the computation of π will be more complicated. HERTZSPRUNG has given a table in his paper from which

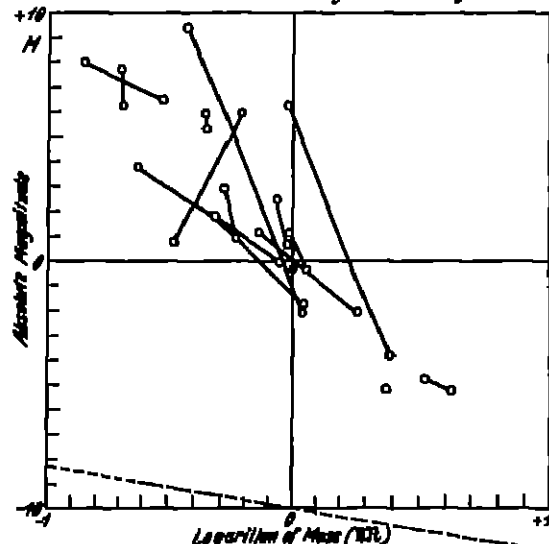


Fig 153 Mass-luminosity diagram according to HERTZSPRUNG. The full-drawn lines join the components of double stars. The single circle near the origin indicates the position of our Sun.

¹ Publ A S P 34, p 231 (1919)

² Harv Ann 85, No 5 (1923).

³ Mt Wilson Contr 226, Ap J 55, p. 165 (1922)

⁴ BAN 2, p. 15 (1923).

the value of $\log M_A$ is found by double interpolation, using $m_B - m_A$ and $5 + m_A + 5 \log \pi_d$ as arguments. In accordance with the above quadratic formula, M_A is found and from the difference $M_{\text{lig}} - M_{\text{dyn}}$ the ratio π_d/π_l , from which $M_A + M_B$ is found.

HERTZSPRUNG's Table of values of $m_A + 5 \log \pi_d + 5$ (for $M_A + M_B = 1$)

$\log M_A$	$m_B - m_A$								$m_A + 5 + 5 \log \pi_d$
	0m	1m	2m	3m	4m	5m	10m	∞	
-1.0	16.84	16.78	16.73	16.69	16.65	16.62	16.49	16.33	18.00
0.9	15.52	15.46	15.42	15.37	15.34	15.30	15.17	15.02	16.52
0.8	14.25	14.19	14.14	14.10	14.06	14.02	13.89	13.75	15.08
0.7	13.02	12.96	12.91	12.86	12.82	12.78	12.66	12.51	13.68
0.6	11.82	11.77	11.71	11.66	11.62	11.59	11.46	11.32	12.32
0.5	10.67	10.61	10.55	10.51	10.47	10.43	10.30	10.17	11.00
0.4	9.56	9.49	9.44	9.39	9.35	9.31	9.18	9.05	9.72
0.3	8.48	8.42	8.36	8.31	8.27	8.23	8.10	7.98	8.48
0.2	7.45	7.38	7.33	7.28	7.23	7.19	7.06	6.95	7.28
-0.1	6.46	6.38	6.33	6.28	6.23	6.19	6.07	5.95	6.12
0.0	5.50	5.43	5.37	5.32	5.27	5.23	5.11	5.00	5.00
+0.1	4.59	4.52	4.45	4.40	4.35	4.31	4.19	4.09	3.92
0.2	3.72	3.64	3.57	3.52	3.47	3.43	3.31	3.21	2.88
0.3	2.88	2.80	2.74	2.68	2.63	2.59	2.47	2.38	1.88
0.4	2.09	2.01	1.94	1.88	1.83	1.79	1.67	1.59	0.92
0.5	1.34	1.25	1.18	1.12	1.07	1.03	0.92	0.83	0.00
0.6	0.62	0.54	0.46	0.40	0.35	0.31	0.20	0.12	0.88
0.7	-0.05	-0.14	-0.22	-0.28	-0.33	-0.37	-0.48	-0.55	-1.72
0.8	0.68	0.78	0.86	0.92	0.97	1.01	1.12	1.19	2.52
0.9	1.28	1.38	1.46	1.52	1.57	1.61	1.72	1.78	3.28
1.0	1.83	1.94	2.02	2.09	2.13	2.17	2.28	2.33	4.00
1.1	2.34	2.45	2.54	2.60	2.66	2.70	2.79	2.85	4.68
1.2	2.82	2.93	3.02	3.09	3.14	3.18	3.27	3.32	5.32
1.3	3.25	3.37	3.46	3.53	3.58	3.62	3.71	3.75	5.92
1.4	3.64	3.77	3.87	3.94	3.99	4.02	4.11	4.15	6.48
+1.5	-4.00	-4.14	-4.23	-4.30	-4.35	-4.39	-4.47	-4.50	-7.00

In joint work with W S ADAMS and A H JOY, H. N. RUSSELL¹ has compared dynamical and spectrographic parallaxes in order to derive the masses of the stars. The number of stars for which such a comparison could be made was 327, including giants and dwarfs of spectral classes from O8 to M6. The stars were grouped in the following way.

Spectral class	ΔM	$M_d - M_l$	π_d/π_l	Residual	M	n
O8-B2	-1.2	+1.31	0.54	-0.02	6.2 ☉	10
B3-B8	+0.5	+1.24	0.56	-0.07	5.6	8
B9-A1	+1.2	+0.61	0.75	+0.09	2.4	35
G9-gM6	+1.2	+0.67	0.73	+0.07	2.5	28
G6-gG8	+1.6	+0.96	0.64	-0.04	3.8	31
A2-A4	+2.0	+0.55	0.78	+0.07	2.1	29
A5-A9	+2.5	+0.50	0.80	+0.06	2.0	35
F0-F3	+3.2	+0.69	0.73	-0.02	2.6	17
F4-F5	+3.3	+0.40	0.83	+0.07	1.7	24
dF6-dF8	+4.4	+0.68	0.73	-0.08	2.5	28
dF9-dG0	+4.3	+0.39	0.84	+0.03	1.7	25
dG1-dG5	+5.2	+0.63	0.75	-0.09	2.4	24
dG6-dK1	+5.6	+0.56	0.77	-0.09	2.2	25
dK2-dK6	+6.5	+0.25	0.89	-0.01	1.4	21
dK7-dM6	+9.2	+0.01	1.00	-0.02	1.0	7
dA-dF	+10.8	-0.32	1.16	+0.07	0.6	2
O8-B1	-1.4	+1.64	0.47	-0.08	9.7	9
B2-B9	+0.6	+1.39	0.53	-0.07	6.8	22

¹ Publ A S P 35, p 189 (1923)

The values in the two last rows are derived from KAPTEYN's cluster parallaxes M_d is the absolute magnitude corresponding to the combined light of the pair and is based on the assumption that the sum of the masses of the components is $\approx \odot$ M_s is the absolute magnitude based on the spectrographic parallax. The mass M corresponds to the geometrical mean mass, from the ratio π_d/π_s which in its turn is the value corresponding to $M_d - M_s$.

The authors remark that the mean mass is by no means a simple function of the spectral class. But if the masses are plotted against the absolute magnitudes all the stars fall into a straight line. The white dwarfs are no longer outstanding exceptions, their mass is small in the proportion to be expected from their low luminosity.

As a first approximation the relationship can be taken as linear and the straight line:

$$\pi_d/\pi_s = 0.62 + 0.045 M_d$$

as the relation curve. The residuals are given in the above table.

The values for the masses of B and A stars found by these authors did not amount to much more than 50 per cent of those found by SEARES. The discrepancy arises from the following cause: SEARES's material consisted of the stars known to be in relative motion, and for more distant pairs this involves a selection in the sense that distant pairs of slow apparent motion are not included. The result of this is too high an estimate of the mean rate of motion, and of the mean mass. A correction was applied by SEARES for the effect in question, but the later results show that the value has evidently been too small. In the investigation now under review all well observed pairs were included, even if the apparent motion was very small. Also, on account of the more extensive material, the values in the above table are certainly entitled to more weight as far as the early spectral classes are concerned.

In this paper the necessity of improving the dynamical parallaxes by means of correction factors depending on the size of the mass was also pointed out.

The dynamical parallaxes ordinarily given, π_d , should be multiplied by the factor $(M_d + M_s)^{\frac{1}{2}}$ in order to be comparable with the parallaxes used in the above formula.

The dependance between mass and luminosity is really to be expected as follows from easy calculations. Combining the equation giving the

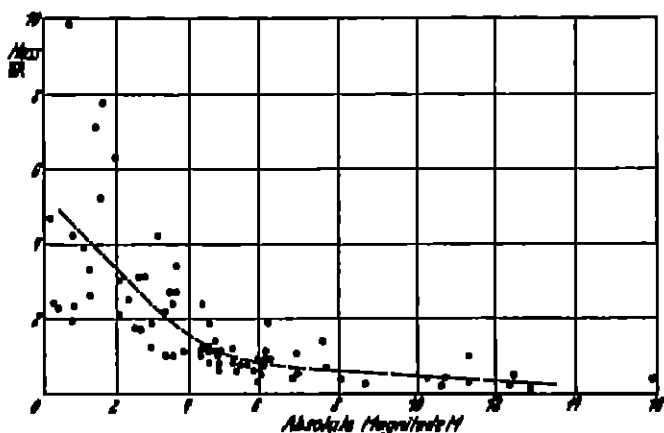


Fig 154. Relation between absolute magnitude M and mass M according to LUNDMARK. For this diagram the masses of double stars were derived using all available determinations of orbits and trigonometric parallaxes up till 1924. The dotted line represents the course of the mean values of various groups with regard to M .

mass-sum in visual binaries with the equation of definition for M obtain

$$M_A + M_B = 10^{3(\log a + 1) - 2 \log P} 10^{0.6(m - M)}$$

The empirical data show that there is some slight dependence between M and the expression $10^{3(\log a + 1) - 2 \log P}$, but a more obvious dependence between expression and the absolute magnitude. We can write

$$M_A + M_B = 10^{p(m, M)} \cdot 10^{0.6M}$$

There is, using the actually determined masses, no dependence shown between m and M and there are no reasons that such a dependence should exist. The principal point of the mass-luminosity relation thus can be derived without theoretical deductions provided that $\log M$ can be expressed as a power of M . The higher terms in the expression

$$\log M = \sum_{i=1}^n a_i M^i$$

are derived on the basis of theoretical work, be it along the lines in Eddington or in JEANS's theory of radiative equilibrium.

Although the former in connection with his original theory of the evolution of the stars showed that there is a general relation between mass and absolute magnitude it is not within the scope of this paper to present a long historical count of earlier theoretical work. The student interested in this problem is advised to consult Vol III/1 of this Handbook.

232. EDDINGTON's Mass-Luminosity Law¹ and Cosmogonic Time

A theory concerning the stellar absorption coefficient ought to lead to a method of determining the absolute magnitude of the giant stars for which the mass and effective temperature are known. In order to avoid a determination of the absolute values of the constants the observational data of Capella are used. From these the absolute magnitudes of ordinary stars are computed on the basis of the theory, regardless of whether they are giants or dwarfs. According to the giant and dwarf theory the absolute magnitude is a double-valued function of mass and effective temperature. A star of mass 1 and temperature 5800° has two possible magnitudes, viz that of the Sun at present and that of the Sun when it passed through the same temperature on the up grade with a larger surface area than now.

The suggestion underlying the theory is that the dense stars like the Sun are in the condition of a perfect gas and will rise in temperature if they contract. All ordinary stars are "giants". Theoretical reasons are given in the paper of EDDINGTON which assert that the stellar matter should be able to contract to an enormously high density before deviation from the laws of a perfect gas becomes appreciable.

The results of HERTZSPRUNG and of RUSSELL, ADAMS, and JOY, which have been reviewed earlier, indicated that M plotted against M resulted in a continuous line, a conclusion which is difficult to reconcile with the giant and dwarf theory.

According to the theory of radiation we have

$$1 - \beta = 0.00309 M^2 \mu^4 \beta^4$$

where μ is the average molecular weight and $1 - \beta$ is the ratio of gas pressure to the whole pressure. The total radiation L of a star is proportional to $M(1 - \beta)/k$, where k is the coefficient of absorption. In EDDINGTON's earlier work k was believed to be approximately independent of temperature.

¹ M N 84, p 308 (1924)

density ρ . The theory of nuclear capture and KRAMERS'S theory, as well as other evidence suggest the form $h \propto \rho/\mu T^{\frac{1}{2}}$. By the aid of this proportionality the following expression for the total radiation is found

$$L = \text{const. } M^{\frac{1}{2}} (1 - \beta)^{\frac{1}{2}} \mu^{\frac{1}{2}} T_e^{\frac{1}{2}}.$$

The value of μ is likely to be about 2.2 for Capella and EDDINGTON adopted $\mu=2.11$.

The following values computed from his formula show the general course of the mass-luminosity relation

$1-\beta$	Mass	M_{bol}	M_{vis}	T_e	Spectral class
0.80	90.63 \odot	- 6.71	—	26200*	O
0.75	56.15	- 5.88	—	—	—
0.70	37.67	- 5.16	—	22500	O ₆
0.65	26.66	- 4.52	(-2.2)	—	—
0.60	19.62	- 3.92	(-1.1)	—	—
0.55	14.84	- 3.35	—	—	—
0.50	11.46	- 2.81	(-1.1)	17460	B2
0.45	8.98	- 2.26	—	—	—
0.40	7.12	- 1.72	—	—	—
0.35	5.67	- 1.16	—	—	—
0.30	4.53	- 0.56	0.00	13260	B7
0.20	2.83	+ 0.81	0.87	10520	A0
0.10	1.58	+ 2.82	2.88	8250	A3
0.05	1.00	+ 4.64	4.55	6290	F8
0.030	0.75	+ 5.93	6.17	5160	G4
0.025	0.67	+ 6.38	—	—	—
0.015	0.51	+ 7.63	8.03	4540	K0
0.010	0.41	+ 8.61	—	—	—
0.004	0.26	+10.82	11.9	3210	K9
0.0025	0.20	+11.95	—	—	—
0.0015	0.16	+13.17	—	—	—
0.0010	0.13	+14.14	17.0	2550	Md

In this table have also been inserted the absolute visual magnitude and the corresponding effective temperature and mean spectral class.

In this table as in the corresponding fig. 1 in EDDINGTON'S paper, the same effective temperature as that of Capella, 5200°, is assumed. For other temperatures the correction $-2 \log (T_e/5200)$ has to be added to M_{bol} . The whole range from 3000° to 12000° only introduces a correction of 1^m.2.

The following table gives the correction to the magnitudes arising from the temperature term as well as the correction for reducing visual magnitude to bolometric magnitude as derived by EDDINGTON in his earlier work¹

T_e	$-2 \log T_e/5200$	$M_{\text{vis}} - M_{\text{bol}}$	T_e	$-2 \log T_e/5200$	$M_{\text{vis}} - M_{\text{bol}}$	T_e	$-2 \log T_e/5200$	$M_{\text{vis}} - M_{\text{bol}}$
2000°	+0 ^m .82	—	6000°	-0 ^m .14	0.00	18000°	-1 ^m .10	—
2500	+0 .62	+2.65	7000	-0 .28	+0.02	20000	-1 .19	—
3000	+0 .46	+1.71	8000	-0 .39	+0.05	25000	-1 .38	—
3500	+0 .32	+1.04	9000	-0 .49	+0.12	30000	-1 .54	—
4000	+0 .20	+0.80	10000	-0 .59	+0.23	35000	-1 .68	—
4500	+0 .10	+0.35	12000	-0 .74	+0.53	40000	-1 .79	—
5000	+0 .02	+0.14	14000	-0 .88	—			
5500	-0 .07	+0.05	16000	-1 .00	—			

The theoretical curve was compared by EDDINGTON with the following observational data: 8 first-class determinations of masses of binary stars together with the mass of the Sun; 21 second class determinations of masses of binary stars. To these are added 6 double stars in the Hyades, 5 Cepheids, and 13 eclipsing binaries. The agreement between the 54 used mass-values derived

¹ MN 77, p. 605 (1917).

from the best observational data and the curve computed according to the theory is good, indeed. The average of the residuals is $\pm 0^m.56$, most of which might fairly be attributed to errors in the observational data, and the maximum discordance is $1^m.7$. Certain refinements of the nature of a second approximation are suggested by EDDINGTON, who derives the following relation between a change in the molecular weight and a change in the absolute magnitude¹

$$- \Delta M = \frac{9\beta + 8}{4 - 3\beta} \log e \frac{\Delta \mu}{\mu}$$

At the time this investigation was carried out the first approximation certainly sufficed. The accumulation of further data since then may invite us to make a second approximation.

The masses of the Cepheids were computed on the basis of the pulsation theory. The method is that of successive approximations. A value of M is assumed. From T_e (spectral class) the radius is deduced and then the mean density. The central density ρ_c is 54.25 times the mean density. The period P is then obtained from the expression

$$P \rho_c^{\frac{1}{2}} = 0.29 (\gamma\alpha)^{-\frac{1}{2}}$$

where $(\gamma\alpha)^{\frac{1}{2}}$ is taken from MN 79, p. 15, table V with $1 - \beta$ as argument. The process is repeated until P stands. The highest value is $26.2 \odot$ for γ Ophiuchi and the lowest $4.14 \odot$ for RR Lyrae.

EDDINGTON inquires if, assuming that the gas-laws hold good for ordinary stars, we then should expect that each star will have the precise luminosity deducible from its mass and effective temperature or, in other words, whether the theory is accurate individually or only statistically. The sources of residual differences are principally abnormal composition and abnormal rotation. With regard to the first source an unduly large proportion of hydrogen would make the star fainter. With regard to rotation it has been shown by L. A. MITCHELL that a rapid rotation makes the star slightly fainter, but that the effect is very small until the speed is sufficient to deform the star considerably. What is to be feared, concludes EDDINGTON, is that the observed spectrum misleads us concerning the true value of T_e . An unsuspected binary ought to betray itself by having a magnitude fainter than that predicted from a knowledge of its combined mass.

The very interesting theoretical considerations as to whether it is physically likely that a dense star such as our Sun can obey the laws of a perfect gas cannot be given here. The student is referred to § 9 in EDDINGTON's paper.

The high density of the white dwarfs is not absurd. At a very low effective temperature smaller than that of a dwarf of spectral class M the star Sirius B is probably able to produce in some way "an imitation of leading features of the F spectrum sufficiently close to satisfy the expert observer". The deviation of this star from the mass-luminosity curve is not surprising if the density is $53\,000 \odot$; new considerations enter into the calculation of k , since the electrons are in the capture zone of two or more nuclei simultaneously. Also the deviation from the gas-laws may be considerable. On the other hand the star ρ^2 Eridani B agrees quite well with the mass-luminosity relation.

In KRAMERS's theory the absorption coefficient k contains² an additional factor $\propto (1 + h\nu_1/RT)$. The effect of this factor was calculated and found to vary between $+0.2$ and -1.6 . There are general reasons for accepting a correction factor of this form, which represents the ratio of the energy given up on capture

¹ MN 84, p. 323 (1924)

² MN 84, p. 325 (1924)

at the mean ionization level to the mean free energy before capture. If the mass is supposed to be constant during the course of stellar evolution, then the mass-luminosity law is in disagreement with the views on stellar evolution accepted on the basis of HERTZSPRUNG'S and RUSSELL'S work. EDDINGTON points out that the giant and dwarf theory definitely held the view that the influence of mass on luminosity was small and unimportant. It was thought that the stars along the main series had in the mean a lesser mass than the stars along the giant branch. The most generally advocated view was that the stars with smaller mass traversed their course more quickly than the heavier stars, although the theoretical arguments tend to show that the latter would reach the end-stage first. The results of EDDINGTON show that the systematic difference in mass is not a minor detail, and that the correction to be applied before the RUSSELL diagram can give the evolutionary course of individual stars is considerable.

Another possibility is that a star gradually diminishes its mass during its evolution. This would happen if the star is "burning itself away", i. e. if it obtains its energy of radiation by annihilating electrons and protons. A star burning itself up may increase continuously in density and internal temperature, although the effective temperature first rises, but then falls.

If the theory of annihilation of matter holds good the relative number of stars of different spectral classes can be computed, because the frequency of a certain evolutionary stage will be proportional to the duration.

The abundance of any stage should be proportional to the duration δt of the stage. If δM is the amount of mass carried off as radiant energy during the stage then

$$\delta t \propto \int_{M-\delta M}^M \frac{\delta M}{L}.$$

Approximately L is proportional to $M(1-\beta)^3/\beta$ if the factor T^{-1} in k is neglected. Then

$$\delta t \propto \frac{\beta}{(1-\beta)^3} \frac{\delta M}{M}, \quad \text{or} \quad \propto \frac{4-3\beta}{(1-\beta)^3} d\beta.$$

Integrating we find

$$\delta t \propto \delta \left\{ \frac{1+3(1-\beta)}{(1-\beta)^3} \right\}.$$

The following table¹ gives the cosmogonical time-scale according to EDDINGTON. Under the duration of stage is given the time it takes to develop between successive values of mass or M_{bol} given as arguments.

However large the initial mass, there cannot be more than $2\odot$ left at the end of a billion years. If a cluster contains stars $> 2\odot$, the age of the agglomeration cannot exceed 10^{11} years. Now since most of the clusters contain absolutely faint and bright stars mixed

Mass M	M_{bol}	Duration of stage
∞ to $35\odot$	$< -5^M$	$0.038 \cdot 10^{11}$ years
35 " 10	-5^M to $-2^M.5$	0.065
10 " 3.7	-2.5 " 0	0.214
3.7 " 1.73	0 " 2.5	0.93
1.73 " 0.92	2.5 " 5	5.21
0.92 " 0.53	5 " 7.5	36.3
0.53 " 0.31	7.5 " 10	281
0.31 " 0.18	10 " 12.5	2190

together the faint stars cannot have evolved appreciably. But, asks EDDINGTON, if we have to deny the evolution of dwarf stars in clusters is there any point in assuming the evolution of dwarf stars in general?

¹ Nature 117, Suppl. p. 25 (1926)

The numbers under the heading "duration of stage" should be proportional to the frequency of the absolute magnitudes or $\varphi(M)$. The theoretical luminosity-curve also agrees fairly well with the one found from observational evidence. This fact seems to the present writer to be the strongest support we have, at present, in favour of the theory of evolution by the loss of mass.

The frequencies of stellar masses among different absolute magnitudes have been derived by LUYTEN¹ on the basis of the mass-luminosity relation found by him, $M = L^{0.225}$, and the luminosity law of KAPTEYN. Similar calculations have been made by J. OHLSSON², who has derived the distribution of stellar masses within ten parsecs on the basis of the material of the present writer and the mass-luminosity law of EDDINGTON and of JEANS.

ΔM	$\varphi(M_e)$	M	$\psi(M)$
1^M to 0^M	5	3.16—4.00	2
1 " 2	13	1.99—2.50	5
3 " 4	39	1.26—1.60	17
5 " 8	42	0.79—1.00	53
7 " 8	62	0.50—0.63	57
9 " 10	30	0.32—0.40	45
11 " 12	12	0.20—0.25	19
13 " 14	3	0.13—0.16	8
15	1	0.10	1

EDDINGTON has also given a discussion of the fundamental quartic equation of the theory of radiative equilibrium in which the gradual increase in μ from the centre to the boundary of the star is taken into account.

For several practical purposes it has been thought to be convenient to express the mass-luminosity

law in a quadratic form of $\log M$. A least square solution of EDDINGTON'S material has given

$$M = 10^{+0.6144 - 0.1576 M + 0.00112 M^2}$$

This curve represents the material available with a sufficient degree of accuracy.

233 Discrepancies between SEARES'S and EDDINGTON'S Results. G. SHAJN³ has compared the masses as computed according to the theory of SEARES⁴ and according to that of EDDINGTON. The agreement is unsatisfactory for the giant stars, and the divergence is of a systematic character. EDDINGTON'S masses of very high luminosity for late spectral classes are greater than the corresponding values of SEARES, and the difference increases with increasing luminosity. For giants of early classes SEARES'S values are greater than EDDINGTON'S, while for late spectral classes the reverse is the case.

Observational data of double stars, part of which have been obtained by SHAJN at Pulkowa, lead to the following paradoxical result

Spectral class		A_m (bolom.)	M_{bol}		M/M_A		n
Primary	Secondary		Primary	Secondary	EDDINGTON	SEARES	
K1	A8	2 ^m .19	+0 ^m .3	+2 ^m .5	0.43	1.37	28
G2	A5	1.26	+0.6	+1.9	0.60	1.42	36
F2	A5	0.90	+1.0	+1.9	0.74	1.13	75

The result derived on the basis of SEARES'S theory is in conflict with other evidence concerning the mass-ratios in binaries and it does not seem very probable that so many systems like those of δ Pegasi and β Lyrae should exist. It seems that a revision of the data used by SEARES would be of much interest.

¹ Harv Ann 85, No 5 (1923)

² A.N. 225, p 305 (1925)

³ Lund Medd Ser II, No 48 (1927).

⁴ Ap J 55, p 179; Mt Wilson Contr 226 (1922)

234. JEANS's Theory. Sir JAMES JEANS has brought rather severe criticism against EDDINGTON's researches on the mass-luminosity relation¹. It is not possible to give a full account here of the contents of JEANS's papers or to declare which method is to be preferred. It seems that the results reached by both the eminent authors by means of analysis do not differ very much as regards a good representation of the observational material.

JEANS claims that, when the problem is treated in a sufficiently general way, the supposed mass-luminosity law disappears entirely as a theoretical law, so that a star of given mass can always adjust itself so as to radiate energy at whatever rate may happen to be required by the generation of energy in its interior. A general relation is found to exist between the mass, luminosity and surface-temperature so that the said adjustment can be made in only one way. The whole interior constitution of a star is uniquely determined by its mass and its rate of generation of energy.

The main point of difference between JEANS's work and that of EDDINGTON is that the former considers the ratio λ , gas-pressure over radiation-pressure, or $\beta/(1-\beta)$ to vary within one and the same star, whereas EDDINGTON assumes this quantity to be constant throughout a star. JEANS is of opinion that in those cases most favourable for constancy λ varies $\sim T^{\frac{1}{2}}$ and that a variation of 1000 between different regions in the same star can hardly be dismissed as impossible.

The gas-pressure, p , and radiation-pressure, q , are defined as follows.

$$p = \frac{\Re}{m\mu} \rho T; \quad q = \frac{1}{3} a T^4,$$

where m is the mass of the hydrogen atom, a the radiation constant, μ the mean molecular weight, \Re the universal gas-constant, and ρ the density.

The dynamical equation of equilibrium is then

$$\frac{d}{dr}(p+q) = -\frac{\gamma \rho}{r^2} \int_0^r 4\pi s \rho r^2 dr, \quad (1)$$

where $\gamma = 6.66 \cdot 10^{-8}$ (gravitation constant).

If H is the outward flux of radiant energy per unit area, then the equation of transfer of radiation is.

$$H = -\frac{16\sigma T^3}{3c\kappa} \frac{\partial T}{\partial r} \quad (2)$$

where σ is STEFAN's constant of radiation $= \frac{1}{4} a C$ and c the opacity of the star at the point considered. The energy is generated at a rate of $4\pi s$ per unit volume and the average value of s inside a sphere of radius r is denoted by \bar{s} . The flux of energy across a sphere of radius r surrounding the centre of the star must be equal to the total generation of energy inside this sphere so that

$$4\pi r^2 H = 4\pi \int_0^r s \rho r^2 dr$$

The second of the above equations then takes the form

$$\frac{4aCT^3}{3\kappa} \frac{dT}{dr} = -\frac{\gamma \rho}{r^2} \int_0^r 4\pi s \rho r^2 dr$$

¹ M N 85, p 196 (1925).

All theories agree that the main part of c is $\propto \rho/\mu T^3$ EDDINGTON assumes an additional factor T^{-1} and JEANS puts $c = \frac{\kappa_0}{\mu T^3} T^{-n}$, where κ is a constant. The integral, that is common to the equilibrium-equation and the radiation-transfer-equation can be eliminated and then the following is obtained

$$\frac{d}{dr} (p + q) = \frac{3C\mathfrak{M}\gamma}{a\kappa m} \frac{T^n}{\bar{\epsilon}} \frac{q}{p} \frac{dq}{dr}$$

Further it is assumed that $\bar{\epsilon} = \bar{\epsilon}_0 T^l$ (l being a small and positive constant and $\bar{\epsilon}_0$ another constant) This expresses the tendency of $\bar{\epsilon}$, the average generation of energy, to decrease from the centre as we pass out to the cooler external regions

We can now put

$$\frac{T^{n-1}}{\bar{\epsilon}_0} = \zeta q^s \quad (3)$$

where, since $q = \frac{1}{2} a T^4$, we have $4s = n - l$ Putting $p = \lambda q$ and denoting $K = \frac{3C\mathfrak{M}\gamma\zeta}{a\kappa m}$ the equation (3) becomes

$$q \frac{\partial \lambda}{\partial q} = \frac{K q^s}{\lambda} - (\lambda + 1)$$

or taking $K q^s = \lambda^2$,

$$\frac{1}{2} s \lambda \frac{\partial \lambda}{\partial v} = v^2 - \lambda (\lambda + 1)$$

The most general solution of this equation is obtained by assuming for λ^2 an expression of the form

$$\lambda^2 = x^2 (A + Bx^{-1} + Cx^{-2} + Dx^{-3} + \dots) + x^{-1/2} (\alpha + \beta x^{-1} + \gamma x^{-2} + \delta x^{-3} + \dots + v^{-3/2} (\dots))$$

The method of equating coefficients of equal powers leads to

$$\lambda^2 = \frac{2}{s+2} v^2 \pm \frac{4}{s+4} \left(\frac{2}{s+2} \right)^{\frac{1}{2}} x + \frac{2}{s+4} \pm \frac{4(s+2)}{(4-s)(s+4)^2} \left(\frac{2}{s+2} \right)^{-\frac{1}{2}} v^{-1} + \dots$$

$$+ \dots + \alpha v^{-1/2} \left[1 \mp \frac{2(s+2)^{\frac{1}{2}}}{s} v^{-1} \dots \right]$$

The first part of this equation is the standard solution for λ^2 . In the interior of a star, in regions where x is large in comparison with its value at the boundary, the actual solution may be supposed to coincide with the standard solution. The series in which the standard solution is expressed is convergent in the special case of $s = 0$ as long as $4v^2 > \frac{1}{2}$ or $\lambda > 0.207$ or $1 - \beta < 0.828$, which corresponds to a mass less than $124\odot$. When s is $\neq 0$ the limits of convergence will be different but as the value of s will be small the series can be assumed to converge for all reasonable mass-values

Further it is shown that $p + q$ can be taken equal to $S\rho^n$, where $n = k\rho$ and $\rho \propto \mu q^r$

The mass of a star is found from the equilibrium-equation to be

$$\mathfrak{M} = -\frac{r^2}{\gamma \rho} \frac{d}{dr} (p + q) = -\frac{r^2 S n}{\gamma} \rho^{n-2} \frac{d\rho}{dr}$$

The equilibrium-equation is transferred to the standard form discussed by EMDEN¹, viz

$$\frac{1}{R^2} \frac{d}{dR} \left(R^2 \frac{d\sigma}{dR} \right) + \sigma^{n-1} = 0,$$

¹ Gaskugeln p 61 (1907)

where $r^2 = \frac{\pi S}{(n-1)4\pi\sigma} R^2$ and $\rho^{n-1} = \sigma$. The only solutions of astrophysical interest are those for which $d\sigma/dR$ vanishes when $R=0$. The most general solution will be

$$\sigma = f\sigma_1, \quad R = \frac{n-2}{2s-2}R_1,$$

where f is a constant and R_1 and σ_1 refer to the particular solution tabulated by EMDEN. When λ is large the expression for \mathfrak{M} becomes:

$$\log \mathfrak{M} = \frac{3}{4(2s+3)} \log \bar{s}_0 + \frac{3n-4}{2n-2} \log f + \text{const.},$$

where the constant term contains only absolute constants of nature.

For very small values of λ

$$\log \mathfrak{M} = \frac{6}{4s+3} \log \bar{s}_0 + \frac{3n-4}{2n-2} \log f + \text{const.} \quad (4)$$

The consideration is restricted to the simple case $l=0$, which corresponds to uniform generation of energy. Then the emission E is equal to $4\pi\bar{s}_0\mathfrak{M}$ or,

$$\log \bar{s}_0 = \log E - \log \mathfrak{M} + \text{const.}$$

The two equation (3) and (4) then take the form

$$(2s+3.75)\log \mathfrak{M} = \frac{3}{4} \log E + (2s+3) \left(\frac{3n-4}{2n-2} \right) \log f,$$

$$(4s+9)\log \mathfrak{M} = 6 \log E + (4s+3) \left(\frac{3n-4}{2n-2} \right) \log f$$

At the surface of the star the following equations are valid

$$\frac{1}{3} \alpha T^4 = \frac{E}{8\pi_0 C r^2} = \frac{(n-1) \cdot 7}{2C\pi S R^2} E / \frac{n-2}{n-1}.$$

Hence,

$$4 \log T = \log E - \log S - \left(\frac{n-2}{n-1} \right) \log f + \text{const.}$$

and from the dynamical equation of equilibrium combined with the equation by EMDEN

$$\log \mathfrak{M} = \frac{3}{2} \log S + \left(\frac{3n-4}{2n-2} \right) \log f + \text{const.}$$

If S is eliminated from these last two equations we have

$$4 \log T + \frac{2}{3} \log \mathfrak{M} = \log E + \frac{2}{3(n-1)} \log f + \text{const.}$$

By eliminating f from this equation and (4) and introducing absolute magnitude and temperature the resulting equation becomes:

$$c_1 \log T + c_2 \log \mathfrak{M} + c_3 M = \text{const.},$$

where:

$$c_1 = 36(\varphi-1) + 18(\varphi-24)s,$$

$$c_2 = -(2s+3.75) + 6(\varphi-1) + (3\varphi-4)s,$$

$$c_3 = 0.3[-1 + 12(\varphi-1) + (6\varphi-8)s].$$

If the values of T , M and \mathfrak{M} were known for at least three stars with very high accuracy, it would be possible to use the data to evaluate the ratio of $c_1:c_2:c_3$ and so to determine the values of φ and s . Instead an average solution of six stars (Sun, Capella A and B, α Centauri A and B, and Sirius A) was carried out. The best fit is obtained from the approximate expression:

$$\frac{1}{4} \log T + 8.75 \log \mathfrak{M} + M = 11.17$$

The computation of the values of s and φ led to impossible results and then the equation was adjusted to

$$M + 2 \log T + 11.92 \log \mathfrak{M} = \text{const} \quad (\lambda \text{ large})$$

For stars of small λ 's the following equation was derived

$$M + 4 \log T + 3.25 \log \mathfrak{M} = \text{const}$$

JEANS points out that these results are in some respects in very good agreement with those obtained by EDDINGTON. For small masses (λ large) the equation of JEANS shows that for $T = \text{const}$ the total rate of energy-emission ε is $\propto \mathfrak{M}^{1.7}$, whereas in EDDINGTON's theory it is $\propto \mathfrak{M}^{1.1}$. For stars of very great mass JEANS finds $\varepsilon \propto \mathfrak{M}^{1.3}$, while EDDINGTON has $\varepsilon \propto \mathfrak{M}^{1.1}$.

EDDINGTON's theory, which was based on the assumption $s = 0$, predicted a hard-and-fast relation between the rate of emission of radiation and the mass \mathfrak{M} . This relation will be represented by a single curve in a diagram in which ε and \mathfrak{M} are taken as coordinates. According to JEANS's theory there is an infinite number of such curves in the ε and \mathfrak{M} plane as soon as s differs even infinitesimally from zero. The only part of the plane that is ruled out is that in which the star would not be in a gaseous state.

The two equations for \mathfrak{M} , T , and M give the limiting forms of the curves in regions where \mathfrak{M} is small and large respectively, and from these the assembly of curves can be constructed as in JEANS's fig 2. EDDINGTON's curve would be approximately represented by any one of the curves for which $T = \text{const}$. According to JEANS there seems to be no reason why a star should keep its surface temperature constant during its evolution, so that evolution along a mass-luminosity curve would seem to be entirely improbable.

One of the curves in the diagram will correspond to the temperature T_1 which divides dark stars from visible ones. The observed values will, of course, all fall above that curve. A surface temperature T_2 may also be imagined such that when the surface of a star has temperature in excess of T_2 it radiates energy with such extreme rapidity that its surface temperature falls almost immediately below T_2 . The observed stars will fall below that upper-limit curve. This seems to agree approximately with the observed facts as for instance shown in EDDINGTON's diagram.

In a subsequent paper¹ JEANS assumes a solution in ascending powers of s of the differential equation treated above as follows

$$\lambda = A_0 + s A_1 + s^2 A_2 + \dots$$

and finds:

$$\lambda = \left[\left(x^2 + \frac{1}{4} \right)^{\frac{1}{2}} - \frac{1}{2} \right] + \left\{ - \frac{x^2}{4x^2 + 1} \right\} A_0 s - \left[\frac{x^4 + x^2}{(4x^2 + 1)^2} + \frac{x^4 - x^2}{2(4x^2 + 1)} \right] A_0 s^2 + \dots,$$

where $A_0 = (x^2 + \frac{1}{4})^{\frac{1}{2}} - \frac{1}{2}$.

The solution is rapidly convergent for small values of s . It is found from the data that the closest fit is for s around $1/18$. For such values the terms containing s^2 can be omitted. A table in the paper gives A_0 , $\psi_0 = \frac{A_0}{\lambda}$, $1 - \frac{s x^2}{4x^2 + 1}$, λ , $1 - \beta$ and \mathfrak{M} with x as argument.

By using the new expression of the mass-luminosity law the following is derived, viz

$$(2s + 2.5) \log \mathfrak{M} + 4s \log T - (s + 0.5) \log E + (2s + 4) \log \mu + (4s + 7) \log \psi = \text{const}$$

¹ M N 85, p 394 (1925)

In this formula $\psi = \lambda/x$ and $\log E = -0.4M + \text{const}$. Introducing M we obtain

$$(2s + 2.5)\log M + 4s\log T + 0.2(2s + 1)M + (4s + 7)\log \psi = \text{const.}$$

From the six stars used before the value $s = 1/18$ is derived and hence

$$m + \log T_s + 11.75 \log M + 32.5 \log \psi_0 = 8.332$$

A comparison has been made between this formula and EDDINGTON's material by J. ÖHLSSON¹. The agreement is just as good as between EDDINGTON's formula and his material.

In a reply to JEANS's criticism EDDINGTON² states that the principal point at issue is the dependance of M on T_s . He writes the fundamental equation of the theory in the form:

$$d\left(p + \frac{1}{3} a T^4\right) = \frac{4\pi c G M}{L \bar{\kappa}_s} d\left(\frac{1}{3} a T^4\right),$$

$$d\left(p + \frac{1}{3} a T^4\right) = -g Q dr,$$

where p is the gas-pressure, $\frac{1}{3} a T^4$ the radiation-pressure, M the mass, L the energy radiated per second, κ the absorption coefficient, c the velocity of light, G the constant of gravitation; $\bar{\kappa}$ is unity at the boundary and varies inwards in a way determined by the distribution of the source of the star's energy. As long as the mass is unaltered the solutions of these equations are homologous. If, keeping the mass of every element fixed, we multiply its linear dimensions by R , the following factors must be introduced: T is multiplied by R^{-1} , Q by R^{-3} , p and $\frac{1}{3} a T^4$ by R^{-4} , g by R^{-2} , κ by R^{+2} , L by R^{-2} , s is unaltered. The equation then continues to be satisfied. Hence

$$L \propto R^{-2}$$

Further:

$$L = 4\pi R^2 \frac{1}{4} a c T_s^4.$$

By eliminating R and converting into absolute magnitude:

$$-dM = \frac{10\pi}{2+\pi} d(\log T_s).$$

For EDDINGTON's law of absorption $\kappa = \frac{1}{4}$, and the same correction is obtained as was given in his paper of 1924. To make κ differ greatly from $\frac{1}{4}$ would, as EDDINGTON states, "be to reject altogether the law of absorption on which I have based my conclusions; but, of course, I do not suppose the law to be exact, and I have nothing against values of κ reasonably near to 1, say, between 0 and 1".

EDDINGTON points out that if a given rate of generation of energy is greater than the rate of radiation L , fixed by the formula, then the energy of the stars is increasing, and the star is expanding indefinitely. By the above formula L varies as R^{-2} and therefore diminishes.

An analysis of JEANS's paper has convinced EDDINGTON that there is nothing singular about his value $\kappa = \frac{1}{4}$ and that the exponent 4 does not affect the magnitude-mass-temperature relation in the two cases considered. Furthermore the mass-luminosity relation is not reached by treating λ as a variable quantity. JEANS's generalisation of the problem consists in limiting λ between the two values 0 and ∞ .

¹ Lund Medd Ser II, No 48. Also thesis Lund (1927).

² M N 85, p 403 (1925).

235. The Cosmogonic Time-Scale by JEANS and SMART. The results reached by VON DER PAULEN (cf ciph 216) could certainly be improved if the cosmogonic time-scale established by JEANS or EDDINGTON (see ciph 232) were used. The procedure according to JEANS was taken into account that possibly positive and negative electric charges fall together and annihilate one another, their energy being transformed into radiation. The discovery of the mass-luminosity relation increased the probability of this conjecture enormously.

JEANS has derived the relation¹

$$\frac{dM}{dt} = -\alpha M^3,$$

where $\alpha = 5,2 \cdot 10^{-88}$ is found by taking the values for the solar system $M = 2 \cdot 10^{33}$, $-\frac{dM}{dt} = 4,2 \cdot 10^{12}$. Solving the equation he finds the time required for a star to pass from mass M_A to mass M_B to be given by

$$t = \frac{1}{2\alpha} \left(\frac{1}{M_B^2} - \frac{1}{M_A^2} \right)$$

JEANS has also given in this connection the following interesting theorem concerning the relation between mass and size of orbit of a star.

From the motion of a particle under a central force M/r^2 the equation

$$\frac{d}{dt} \left[\frac{1}{2} \left(\left(\frac{dr}{dt} \right)^2 + r^2 \left(\frac{d\theta}{dt} \right)^2 \right) - \frac{M}{r} \right] = -\frac{1}{r} \frac{dM}{dt}$$

is readily deduced¹, which becomes

$$\frac{d}{dt} \left(\frac{M}{2a} \right) = \frac{1}{r} \frac{dM}{dt}$$

when a is the major axis of the orbit.

Averaging over a complete revolution, JEANS finds

$$\frac{d}{dt} \left(\frac{M}{2a} \right) = \frac{1}{a} \frac{dM}{dt},$$

from which follows

$$Ma = \text{const}$$

If our Sun ever was a B star or if its mass ever was $4 \odot$ the time elapsed since this epoch must be about $7,1 \cdot 10^{12}$ years.

SMART², who has connected the above differential equation with the theory of EDDINGTON, finds a scale in substantial agreement with that of JEANS. By three different procedures he has derived the following values of t necessary for a star to pass from different values of M_A to $M_B = 1 \odot$.

$M_A =$		$8,981 \odot$		$4,137 \odot$		$1,582 \odot$
Method	1	$7,6 \cdot 10^{12}$ years		$7,2 \cdot 10^{12}$ years		$4,6 \cdot 10^{12}$ years
	2	$5,1 \cdot 10^{12}$ "		$4,9 \cdot 10^{12}$ "		$3,7 \cdot 10^{12}$ "
	3	$9,1 \cdot 10^{12}$ "		$9,0 \cdot 10^{12}$ "		$5,9 \cdot 10^{12}$ "

The scale must be still longer, because no account is taken of the increase in mass necessary on account of the meteor frequency. The investigations of the frequency of meteors show that they are not restricted to our solar system but are universal phenomena. Taking into account the frequency of meteors we find that the mass of the Sun will be doubled during a period of 10^{13} years. Thus the increase of the stellar mass due to encountering meteors will partly counterbalance the secular decrease of the mass.

¹ M N 85, p 2 (1924)

² M N 85, p 423 (1925)

236. BRILL'S Theory and Parallax-Method for Binaries¹ According to the theory of radiative equilibrium $ks^{\frac{1}{2}}$ should be constant within a certain star (k is the mean absorption coefficient of the total radiation) but should vary from star to star with the size of the mass. If we assume the relation,

$$1 - \beta = 7.83 \cdot 10^{-10} \mathfrak{M}^2 \mu^4 \beta^4$$

to hold good, it follows from statistical considerations of data concerning magnitudes, parallaxes, and masses that the relation,

$$ks^{\frac{1}{2}} = \text{const}$$

holds good for nearly all stars. In order to see the reason for this we must transform the expression. If a is the constant in STEFAN'S law and \mathfrak{R} is the gas constant, we have the equations:

$$Q = \frac{\mu a \beta}{3 \mathfrak{R} (1 - \beta)} T^3,$$

$$k = 3.28 \cdot 10^{27} \cdot \frac{a}{3 \mathfrak{R}} \frac{\beta}{1 - \beta} T^{-\frac{1}{2}}.$$

Further the central temperature $T_0 = 1.7 T$ is introduced and the radius R Then:

$$T_0 = \frac{6.9011 \mathfrak{R}}{\mu \beta R} \left(\frac{3(1 - \beta)}{\pi_0 a G} \right)^{\frac{1}{2}}.$$

According to the definition-equation

$$1 - \beta = \frac{ks}{4\pi_0 a G}$$

and thus,

$$s = \frac{12\pi_0 a G \mathfrak{R}}{a 3.28 \cdot 10^{27}} \frac{(1 - \beta)^2}{\beta} \left(\frac{T_0}{1.7} \right)^{\frac{1}{2}}$$

and,

$$k \sqrt{s} \propto \beta^{\frac{1}{2}} / T_0^{-\frac{1}{2}}$$

The central temperature is rather constant, varying as it does between $35 \cdot 10^6$ and $40 \cdot 10^6$ degrees. The constancy of $ks^{\frac{1}{2}}$ is mainly determined by the quantity $\beta^{\frac{1}{2}}$. If \mathfrak{M} varies between $10 \odot$ and $0.16 \odot$, the corresponding variation in $\beta^{\frac{1}{2}}$ is from 0.73 to 1.00.

Independently of the theory of the stellar absorption coefficient the quantity $ks^{\frac{1}{2}}$ can be expressed in quantities furnished by observational work. If the stars are in radiative equilibrium, the radiated energy is equal to the energy produced in the interior of the star:

$$\pi_0 a c R^2 T_0^4 = s \mathfrak{M},$$

where T_0 is the radiation temperature

If the value of $ks^{\frac{1}{2}}$ from the above definition-equation is substituted in the present expression, k becomes equal to $4G(1 - \beta) \mathfrak{R} (\pi_0 R^2 T_0^4)^{-1}$ and thus:

$$k \sqrt{s} = 4G(\pi_0 a)^{\frac{1}{2}} s^{-\frac{1}{2}} (1 - \beta) \mathfrak{R}^{-1} R^{-1} T_0^{-2}.$$

Introducing the numerical values of the constants and selecting solar units we obtain as the final equation:

$$\log k \sqrt{s} = 3.459 + 2 \log \frac{a}{T_0} - \log \frac{R}{R_{\odot}} + \log (1 - \beta) + \frac{1}{2} \log \frac{\mathfrak{M}}{\mathfrak{M}_{\odot}}.$$

¹ Berlin-Habelsberg Veröff 7, H 1 (1927)

In order to determine the numerical value of $k\sqrt{F}$ the material of RAME¹ (38 pairs $\pi < 0''.040$) and that of BOTTLINGER² (17 eclipsing variables) together with data for the Sun and Capella were used. The value 2.85 for $\log k\sqrt{F}$ resulted from 68 stars

BRILL discusses at length the derivation of T_0 , the radiation temperature corresponding to the radiation temperature of the bolometric magnitude of the central part of the star disc. The colour temperature of a star refers to the course of the energy curve in a certain part of the star spectrum and corresponds to the

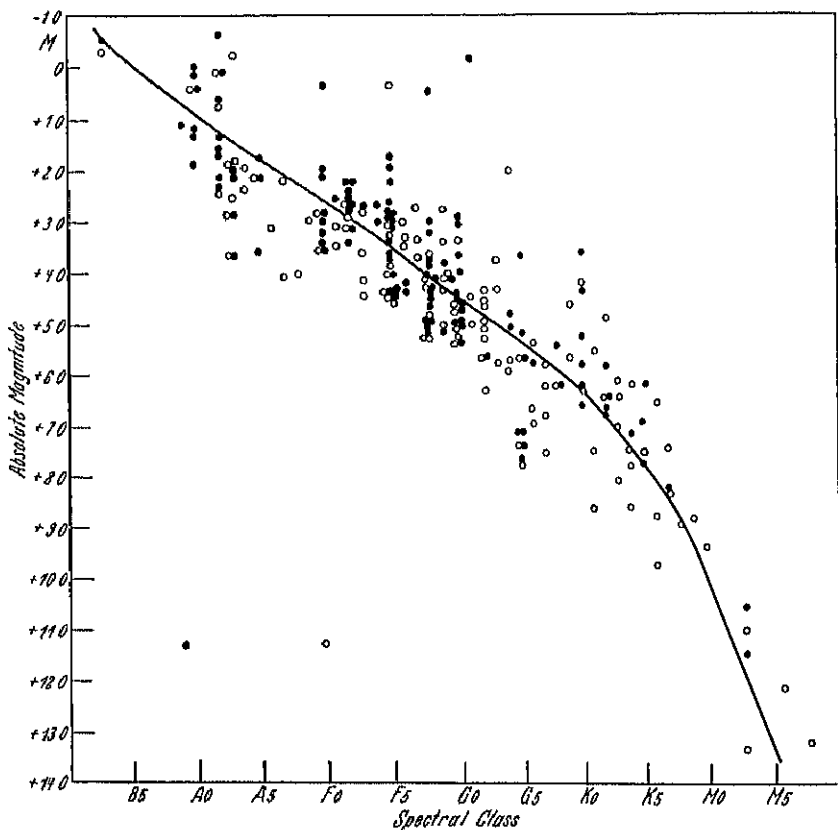


Fig 155 The RUSSELL diagram as derived by BRILL on basis of parallaxes of binaries using the theoretical relation $ke\lambda = \text{const}$. Full circles refer to primaries and open circles to secondaries of binary stars

temperature of a black body radiator whose energy curve in the same part has the same form as that of the star. The radiation temperature refers to the intensity of the emitted radiation and corresponds to a black body radiator that emits radiation in equal intensity to that of the star. If the conception of effective temperature is to be preserved it ought to be defined as the temperature of a star for which the total emission of a black body radiator equals that of the star.

In order to obtain accurate values of the colour temperature it is necessary to supplement the visual and photographic measurements with bolometric,

¹ A N 225, p 217 (1925).

² Atti della Pontificia Accad (1924).

radiometric, and thermoelectric measurements in the ultra-red. The radiation temperature cannot be determined without a knowledge of the stellar diameter. Only a few stars have been measured as yet with interferometric methods; thus our knowledge of the radiation temperature is very restricted. For the Sun the following values of the radiation temperature are derived

Radiation temp. of the Sun from	Bolom. data	Visual data	Photogr. data
Mean solar radiation .	5775°	6075°	5835°
Central solar radiation	6075°	6435°	6190°

The following are the results from the stars:

Object	Spectral class	Radius	Apparent magnitude	Rad temp. of the vis. ray.	Colour temperature
Sun	G0	961",2	-26 ^m ,90	$c_0/T = 2,36$	$c_0/T = 2,05$
Arcturus	K0	0,0100	+ 0,24	3,44	3,50
Aldebaran . . .	K8	0,0100	+ 1,06	3,82	4,39
Betelgeuze . . .	M1	0,0235	+ 0,92	4,69	4,65
Antares	M2	0,0200	+ 1,22	4,66	4,77
β Pegasus . . .	M3	0,0105	+ 2,61	4,66	4,61

At present we can do no better than assume equality between the radiation and the colour temperature.

The following temperature scale was assumed.

Spectral class	T	c_0/T
O5	28000°	0,51
B0	20800	0,69
B5	16900	0,85
A0	13000	1,10
A5	10200	1,40
F0	8300	1,72
gF5	7200	2,00
dF5	7200	2,00
gG0	6050	2,37
dG0	6240	2,30
gG5	4880	2,96
dG5	5560	2,58
gK0	4310	3,33
dK0	4910	2,92
gK5	3380	4,24
dK5	3910	3,67
gM0	3200	4,49
dM0	3420	4,20

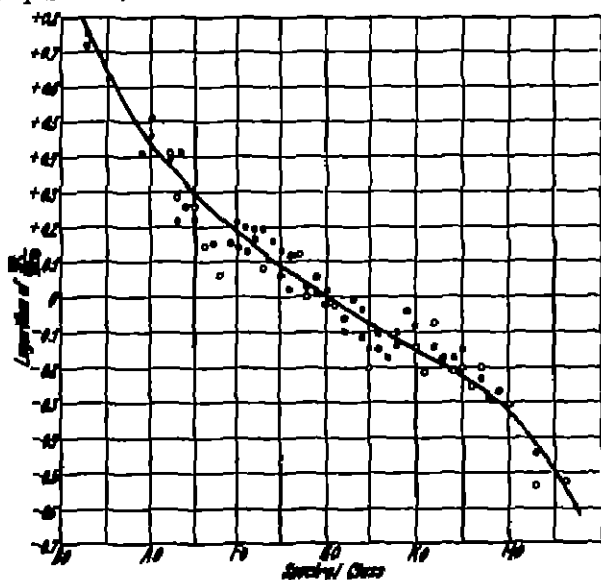


Fig 156. Relation between logarithm of stellar mass and spectral class according to BRILL. Full circles refer to primaries in binary stars and open circles to secondaries.

For 123 visual pairs with known orbital elements BRILL has computed the radiation-energy parallaxes π_m , which enter into the expression $\log R/R_\odot$ owing to the relation:

$$\log R/R_\odot = 0,2(M - m - \Delta m) - \log \pi_m + 4,946$$

where M is the surface-intensity magnitude, m the apparent visual magnitude and Δm the correction to bolometric magnitude. The computation of π_m has to be performed by means of successive approximations. For this purpose an extensive table is given in BRILL's paper with $1 - \beta$ as argument, $\log(1 - \beta)$, $\log R/R_\odot$, and $\Delta \log(1 - \beta)$; $\Delta \log R/R_\odot$ as functions. Further the expressions $\frac{1}{2} \log R/R_\odot + \log(1 - \beta)$ and $\Delta \log R/R_\odot \cdot \Delta [\frac{1}{2} \log R/R_\odot + \log(1 - \beta)]$ are given in order to facilitate the necessary interpolations.

The agreement between π_{r0} and π_{tr} or π_* is very good indeed. The masses, mass-ratios, dimensions, densities, and central temperatures are also determined and entered in the catalogue.

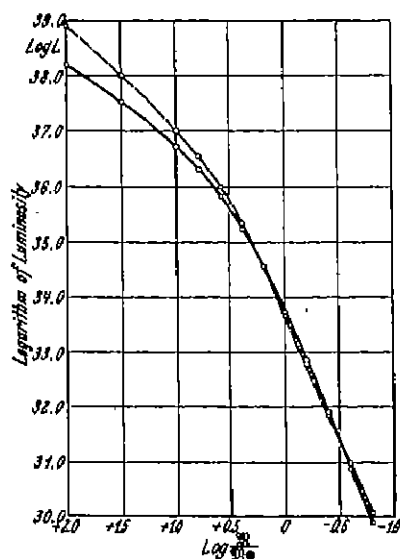


Fig. 157. Relation between logarithm of stellar luminosity and mass. The full-drawn curve is the relation derived by BRILL on the assumption that $k\epsilon^1 = \text{const.}$ and the dotted curve is the relation according to EDDINGTON.

The agreement of the derived RUSSELL diagram with the observed one shows that the relation between the mass and the product $k\epsilon^1$ as derived by EDDINGTON is in agreement with the observations. Furthermore it also proves the probable reality within a wide range of the formula of BRILL ($k\epsilon^1 = \text{const.}$), which is partly based on the theory of radiative equilibrium and partly on an empirical foundation.

The agreement between the mass-luminosity relation according to EDDINGTON and according to BRILL is very good. There are practically no deviations for the luminosity range $\log L = 30.0-36.5$ (M8 to B0 stars roughly) or for the entire main series.

237. Mass-Reduction by Annihilation of Protons and Electrons. C. LÖNNQUIST¹ has examined various hypotheses concerning the evolution on the basis of EDDINGTON's theory by using the empirical RUSSELL diagram as guidance and test.

The investigations of EDDINGTON in 1924 showed that it is the difference in mass and not in intensity that causes the considerable difference in the luminosity

of the giants and dwarfs. Although it is still possible that the stars develop from the giant stage to the dwarf stage in the traditional way there is no longer any explanation why they should develop in just that way. But if such an evolution takes place, then the mass reduction must be investigated. Such a reduction is not only dependent on a possible throwing off of matter into space. The stars also radiate away enormous quantities of energy, and as energy is equivalent to mass the stellar masses must be diminished in the course of time, if no compensating factors exist.

It has been shown by EDDINGTON that the energy lost by radiation cannot be fully compensated by the energy liberated by contraction since the time-scale thus obtained is altogether too short. If the mass $11.5 \odot$ is taken, such a contraction-development from the giant M to the giant F stage would take only 30000 years, and for the Sun itself $1.5 \cdot 10^7$ years. From geological evidence it is found that the age of the Earth must be 10^9 years at least and the minimum age of the Sun ought to be at least 10^{10} years.

The investigations of F. W. ASTON in 1920 gave rise to the hypothesis of EDDINGTON² that the helium in the stars is built up of hydrogen. This process involves a change of 0.008 of the mass into energy. It seems also that something

¹ Ark Mat Astr Fys 20 A, No. 21. Also thesis Upsala (1927).

² Brit. Assoc. Report 1920, p. 45. This theory seems also to have been presented independently by J. PERREIN: Annales de Physique 2, p. 89 (1919), and Revue du Mois 21 p. 113 (1920).

similar can be postulated concerning the composition of other light atoms, but the effects in these cases might be considerably smaller. It seems hardly possible to reach an amount exceeding 0.010 of the mass. The time the Sun would require for such a mass-reduction is $1.5 \cdot 10^{11}$ years, which is sufficient for geological demands if the Sun has from the beginning an abundance of hydrogen of 10 per cent. But if this hypothesis is accepted the evolution will principally follow a mass line, as has been pointed out by LÖNNQUIST, and the RUSSELL diagram cannot mark the evolution-course of the stars, but only the loci of the most stable equilibrium points of the stars.

EDDINGTON points out that helium must have been produced somewhere. The doubts of some physicist that the interior of the stars may not have a sufficient temperature are met with the advice "to seek a hotter place". EDDINGTON seems to assume that the processes of building up the atoms already occur in the nebulae so that they have taken place to a great extent while the stars are in an early stage of evolution. The stars can hardly contain hydrogen any longer. EDDINGTON's arguments against the occurrence of hydrogen in the stars are based on the following views.

A large percentage of hydrogen would decrease the molecular weight μ so much that the radiation pressure would become insignificant in comparison with the gas pressure even in case of the most massive stars known. The radiation pressure would lose most of the importance ascribed to it as an explanation of the fact that the stellar masses are situated within comparatively narrow limits.

On account of the change in the value of μ , entering in the luminosity formula with the expression μ^3 , a considerable amount of hydrogen would alter the mass-luminosity relations. Besides, if the abundance of hydrogen differed for stars of the same mass, the stars would not lie along a mass-luminosity line, but would exhibit greater or smaller deviations from it. LÖNNQUIST finds from a lengthy discussion that the assumption of the importance of the radiation pressure for the size of the star-masses is untenable, and that it does not form any valid argument against the presence of hydrogen in the stars. While a not inconsiderable proportion of hydrogen appears necessary for Capella in order to obtain agreement between the theoretical and observed luminosity, varying proportions of hydrogen in stars of the same mass appear to lead to not inconsiderable deviations from the luminosity as computed from EDDINGTON's luminosity law. The testing of that law by means of stars of known masses and luminosities cannot be made with such accuracy as to allow a decision concerning the nature of the individual deviations. The theory requires special revision as regards the abundance of hydrogen.

The radioactive hypothesis cannot explain, in its original form, a considerable mass reduction. The radioactive processes have, as far as is known, the property of being independent of temperature and density. In order to have an important mass reduction one would have to imagine, with JEANS, another kind of radioactivity. He has suggested an annihilation of matter within the atom nuclei together with a liberation of energy. To describe this as radioactive would then be an accentuation of these processes—just like the radioactive—being independent of density and temperature.

JEANS's theory introduces a third hypothesis, the boldest of them all, namely the annihilation of protons and electrons with transformation of the mass into energy. This idea is not new and it arose even before the question of the evolution of the stars had advanced any considerable way. EDDINGTON mentions J. LARMOR as one of the precursors of this theory and as early as in 1904 JEANS expressed

himself in favour of this line of thought, while EDDINGTON suggested the hypothesis for the first time in 1917. MACMILLAN also supposes the contrary process to take place, i.e. a transformation in space of the radiations of the stars into matter, into protons and electrons from which the nebulae arise. In this way a circulation is obtained between mass and energy, which is certainly of much importance for cosmology.

The annihilation of protons and electrons may be supposed to be a nucleus process analogous to the radioactive ones or the result of a collision between a free electron and a nucleus proton. EDDINGTON conceives both possibilities. In the former case the process evades every calculation regarding dependence on the outer physical conditions. The process might possibly depend on the very constitution of the atom nucleus. In the second case the density and temperature may be thought of as deciding the rate of the process.

LÖNNQVIST's paper is partly devoted to an examination in detail of the second of the above-mentioned cases, which the author calls the hydrogen hypothesis. He finds that the known facts concerning the components of the double stars seem on the whole to agree with the hydrogen hypothesis. For the development of the widely separated binaries from close pairs an evolution with mass reduction seems necessary. The long time-scale associated with such an evolution is of extreme importance for cosmogonic problems. The evidence of the clusters has also been investigated. The facts scarcely decide in favour of one or the other theory of evolution, but they do not seem to confirm RUSSELL's evolution scheme. Stars are probably formed with very different masses. Only the larger ones are checked in the giant stage, while the smaller ones go directly into the main series.

238. The Theory of RABE. The aim of this investigation¹ was to establish the relation between the absolute magnitude, the temperature, and the mass of dwarf stars. It has to be assumed that there exists a one to one relation between $M = T$, and M , which is also in agreement with the empirical and theoretical results. On account of the comparatively high density of the dwarfs it is comparatively easy to define the conception of the stellar surface that is necessary for the theory developed. It is sufficient to start from the surface conditions of our Sun and to assume that the thickness of the layer from which the visible radiation has its origin is small in comparison with the radius of the star. But on the other hand, it has to be assumed that the layer in question has such radial extension that the surface radiation can be considered to be emitted by a black-body radiator. Above such a surface a cooler atmosphere may be situated, which, of course, would absorb part of the radiation. The results of spectral analysis show that the amount of this absorption is comparatively small for classes earlier than F, but becomes appreciable in that class, and increases continuously to the end of the main series. The absorption is certainly selective so that the coefficient of transmission is a (unknown) function of the wave length. It is then necessary to use a mean value of the coefficient which is a function of the surface temperature and the mass, as the gravitative power exerts an influence on the general atmospheric condition of a star. The stars have to be assumed to be perfect spheres and the size of the surface is thus determined by means of the mass and the mean density. This quantity can be considered, at least at a first approximation to be a function of the surface temperature and mass. Although BERNEWITZ² could not establish a definite relation between the mean density and the mass still the probability that such a relation exists is very great³.

¹ A N 225, p. 217 (1925). ² A N 213, p. 1 (1921).

³ In fact, such a relation was established by ABETTI in 1922.

Let i_0 be the intensity of radiation of a surface element, ϕ the mean value of the coefficient of transmission, T the effective surface temperature, and c a factor of proportionality, then the observable radiation i of a surface element is:

$$i = \phi i_0 = c\phi (c_0/T)^{-4}.$$

Let further ρ be the mean density and C another factor of proportionality. Then the total radiation of the star is

$$I = C(R/\rho)^{\frac{1}{2}} \phi (c_0/T)^{-4}$$

If this quantity is transformed into magnitudes we have:

$$M + \Delta M = \Phi + 10 \log c_0/T - \frac{1}{2} \log R + \frac{1}{2} \log \rho - \frac{1}{2} \log \phi. \quad (1)$$

ΔM is the correction of the visual absolute magnitude M to bolometric magnitude and Φ a constant.

As a result of numerous trials RAHE selected the following expression for ρ and ϕ .

$$\rho = c(c_0/T)^{\frac{1}{2}} R^{\frac{1}{2}},$$

$$\phi = (T/T_0)^{\nu} R^{\mu} \leq 1.$$

T_0 is the limiting temperature for which at unit mass an appreciable atmosphere sets in. The second equation does not seem very plausible from a theoretical point of view but RAHE gives a reason for its use. If we pass over to solar units the above equation takes the form $\rho = (T_{\odot}/T)^{\frac{1}{2}} R^{\frac{1}{2}}$.

Then the equation (1) takes the form:

$$M + \Delta M = (10 + \frac{1}{2}\kappa + \frac{1}{2}\nu) \log c_0/T - [\frac{1}{2}(1 - \lambda) + \frac{1}{2}\mu] \log R + \Phi - \frac{1}{2}\kappa \log c_0/T_{\odot} - \frac{1}{2}\nu \log c_0/T_0. \quad (2)$$

The unknowns κ , λ , ν , μ , and T_0 can be determined from the observational data. If ϕ should be larger than one, the terms containing ν and μ must be dropped. The masses were determined from 38 dwarf binaries with a parallax equal to or larger than 0''.040. The values of ΔM were derived from the radiation law of PLANCK and the spectrophotometric measurements of WILSON. Further $M_{\odot} = 4.79$, the observed value of c_0/T for the Sun = 2,40, $\phi_{\odot} = 0.71$, and hence $c^{\frac{1}{2}}/T_{\odot} = 2,40 \cdot \phi_{\odot}^{\frac{1}{2}} = 2,20$, and $\Phi = 1^m.42$ were used.

Next the value of λ is determined. For stars earlier than F5 it has very nearly the value 1 and thus the density-ratio of such stars can be determined without any knowledge of ϕ . The author finds $\lambda = 0,293 \pm 0,012$. The value of κ is situated between 2,5 and 3 and the last value is adopted. The coefficient of $\log R$ in the above equation, $b = -[\frac{1}{2}(1 - \lambda) + \frac{1}{2}\mu]$, is determined from binaries of equal spectra and varies with the spectral class:

Spectral class	b	κ	Spectral class	b	κ
G0	-1,98	9	K0	-2,28	7
G4	-2,35	11	K4	-2,23	6

This, if real, suggests a complicated form for the functions ρ and ϕ . At present it does not seem possible to decide whether the variation is real or not. If b is taken as -2,71, μ is found to be $\frac{1}{2}$.

It is unavoidable that the determination of the different constants must be affected with some uncertainty owing to the paucity and in several cases the uncertainty of the data. RAHE finds the following two formulae:

Stars without atmosphere ($\phi = 1$): $M_{\text{bol}} = 15 \log c_0/T - \frac{1}{2} \log R - 0,29$.

Stars with atmosphere ($\phi < 1$): $M_{\text{bol}} = 20 \log c_0/T - \frac{1}{2} \log R - 1,63$.

In order to have one formula the following expression is adopted

$$M_{bol} = 1.5 \log \frac{c_2}{T'} - 2.5 \log M + 0.90.$$

Here c_2/T' has to be selected in such a way that both the formulae are represented

The essential point in the theory of RABE is that M is considered to depend on the temperature much more than is the case in the theory of EDDINGTON. The theory is of considerable interest and ought to be compared with the empirical data as soon as more observations have been collected.

The c_2/T -value in the above formulae corresponds to the surface temperature and is related to the effective temperature T_e in the following way

$$\log(c_2/T_e) = \frac{3}{2} \log \frac{c_2}{T} - \frac{1}{2} \log M - 0.134$$

The effective temperatures that result from the material of RABE are in very good agreement with those computed according to the methods of SPARRE and of BRILL. If the c_2/T -values are diminished by ten per cent they are in very good agreement with the corresponding values derived by M. N. SAHA¹ on the basis of his theory of ionization. It is certainly very interesting that the theory of RABE is able to explain most of the differences between the results of BRILL and SAHA.

Using the temperature-scale thus established RABE has computed the absolute magnitudes and the masses and derived the following mean errors

Spectral class	Mean errors		
	in M	in $\log M$	n
A0—F9	$\pm 0.11, 34$	± 0.19	22
G0—G9	± 0.148	± 0.17	23
K0—Mdp	± 0.132	± 0.11	20

RABE then makes a revision of his system and finds from a discussion of the values of m_0 and c_2/T_0 a correction that should be added to the constants in his equation. He finds

$$\log \frac{c_2}{T} = \frac{1}{2} \log Q - \frac{1}{2} \log M + 0.342$$

For the application to binaries the equations giving the mass-luminosity relation are changed into the following forms:

Stars without atmosphere:

$$\log \pi = 9 \log \frac{c_2}{T} - \frac{2}{3} \log \frac{M_A}{M_A + M_B} - 2 \log a + \frac{4}{3} \log P - \frac{3}{5} (m + 5 + \Delta m_{bol}) - 0.288.$$

Stars with atmosphere

$$\log \pi = -6 \log \frac{c_2}{T} + \frac{5}{6} \log \frac{M_A}{M_A + M_B} + \frac{5}{2} \log a - \frac{5}{3} \log P + \frac{3}{10} (m + 5 + \Delta m_{bol}) + 0.546.$$

Computing the parallaxes and comparing with those actually determined RABE has found the mean error of one value to be $\pm 0.295\pi$.

The mass-ratio of stars where both the spectra have been observed but no orbital elements are known can be computed from the formula

$$\log \left(\frac{M_B}{M_A} \right) = \frac{9}{25} \left[20 \left(\log \frac{c_2}{T_B} - \log \frac{c_2}{T_A} \right) - (m_B - m_A) - (\Delta m_B - \Delta m_A) \right]$$

¹ Zf Phys 6, p 40 (1921), Ap J 50, p 220 (1919), Phil Mag (6) 40, p 809 (1920), 41, p 267 (1921), London RS Proc (A) 99, p 135 (1921)

The following table summarises the results of RABE

Spectral class	Temperature T	M	q	d	n
A 2,3	9400°	2,29 ☉	0,43 ☉	1,74 ☉	3
F 3,4	7900	2,78	0,77	1,42	11
F 8,0	6600	1,07	0,98	1,02	8
G 1,0	6400	0,92	0,98	0,96	12
G 6,0	6100	0,88	1,22	0,88	10
K 1,7	5600	0,61	1,27	0,78	9
K 5,0	5000	0,69	1,96	0,70	8
M 2,5	3800	0,36	3,58	0,45	4

The diameters d are accurately represented by means of the linear relation

$$d = 1,03 + 0,00023 (T - 6500^\circ).$$

In a subsequent paper RABE¹ has taken up a remark by BRILL that the mass and the surface temperature cannot be considered to be independent of each other. In order to decide between the influence of the temperature and the mass upon the absolute magnitude it is appropriate to consider stars of unequal mass but of the same spectral class. RABE used a number of new data, but could not find that his general conclusions ought to be changed. In order to show that the correlation between mass and luminosity is not as high as is generally believed he quotes the following well-determined cases where the absolute magnitude has been computed from EDDINGTON's mass-luminosity law

Object	Spectral class	M	M_V	M_{bol}	M_{calc}	$M_{obs} - M_{calc}$
α Pegasus A	F3	8,60 ☉	1 ^M ,79	1 ^M ,78	-2 ^M ,42	+4 ^M ,20
γ Virginis A	F0	4,48	2 ,39	2 ,37	-0 ,85	+3 ,22
α Pegasus B	(F5)	4,00	2 ,29	2 ,29	-0 ,45	+2 ,74
ϵ Cygni A	F1	2,48	2 ,14	2 ,12	0 ,96	+1 ,16
Procyon A	F3	1,13	2 ,92	2 ,92	3 ,92	-1 ,00
δ Scorpis A	F2	1,02	3 ,04	3 ,03	4 ,29	-1 ,26
θ Argus A	G0	10,96	3 ,46	3 ,43	-2 ,79	+6 ,22
B	(G2)	4,38	4 ,06	3 ,98	-0 ,41	+4 ,39
Sun	G0	1,00	4 ,90	4 ,89	4 ,56	+0 ,33
δ Urs Majoris A . .	F9	0,68	5 ,26	5 ,25	6 ,28	-1 ,03

The difference $M_{obs} - M_{calc}$ shows such a definite dependence on M that it seems to indicate that M does not depend on M in such a high degree as was predicted in the theory of EDDINGTON.

The author gives the following mass-luminosity-temperature relation.

Spectral class	Absolute magnitude	Temperature T	M	q/T
B0	-3 ^M ,0	20400°	15,7 ☉	0,70
B5	-0 ,4	12400	7,2	1,15
A0	+1 ,1	9800	3,8	1,45
A5	1 ,9	8900	2,2	1,60
F0	2 ,5	8200	1,8	1,74
F5	3 ,3	7300	1,4	1,95
G0	4 ,5	6500	1,10	2,20
G5	5 ,2	6100	0,94	2,33
K0	6 ,0	5800	0,75	2,47
K5	7 ,6	5000	0,63	2,85
M0	10 ,0	4200	0,43	3,43

¹ A N 231, p 79 (1927).

239. Convergence of Mass-Ratios with Increasing Age. One of the important consequences of the theory of EDDINGTON was pointed out by VOGT¹. It follows from the theory that M_A/M_B varies in direct proportion to M . In the case of double stars the mass-ratio M_A/M_B must thus become smaller and more nearly equal to one the "older" the pair is. VOGT mainly made use of 85 double stars in LEONARD's dissertation². The mass-ratios were not known and had to be computed from EDDINGTON's mass-luminosity relation. In the table giving the results S_A denotes the spectral class of the principal star.

S_A	M_A/M_B	n	S_A	M_A/M_B	n
gM	18,4	2	A	1,6	9
gK	2,7	6	dF	1,3	23
gG	1,9	9	dG	1,25	18
gF	3,0	5	dK	1,23	11
B	4,6	8	dM	1,19	2

In order to investigate the possibility that the mass becomes smaller with the age of the star, one can also make use of the relation:

$$\frac{dM_A}{dM_B} \sim \frac{L_A}{L_B},$$

where L is the luminosity. VOGT computes the values $[M_A/M_B]$ for a double star whose principal component is of spectral class A with a mass of $2,5 \odot$ and $M_A/M_B = 1,6$ and whose components undergo in the course of evolution a mass-reduction in proportion to their luminosities. These values compare with the mass-ratios actually derived in the following way:

S_A	M_A	$[M_A/M_B]_{\text{obs}}$	$[M_A/M_B]_{\text{calc}}$
A	2,5	1,6	1,6
F	1,5	1,3	1,2
G	1,0	1,25	1,10
K	0,7	1,23	1,06
M	0,4	1,19	1,04

According to VOGT the probability is thus comparatively great in favour of the opinion that the RUSSELL diagram gives the general course of stellar evolution.

240. Vogt's Extension of EDDINGTON's Theory. The theory of EDDINGTON is based on the assumption that the product kQ is constant, where k is the coefficient of mass-absorption and Q the mean value of the energy produced per unit mass and time within a sphere with the radius r . H. VOGT³ has derived the mass-luminosity relation in the case when kQ is not constant, but varies in some general way with r . The two fundamental equations give:

$$L = \frac{4\pi c a c g r^3}{3k} \frac{dT^4}{dr} = \frac{4\pi c c G}{k} M(1-\beta) \left[1 + \frac{P}{1-\beta} \frac{d(1-\beta)}{dr} \right],$$

where $dP = -g \rho dr$, $P = M g T / \mu + \frac{1}{2} a T^4$ or the sum of the gas-pressure and light-pressure, and $g = G M / r^2$, μ is the molecular weight, g the gravitational force, ρ the density, T temperature, M the universal gas constant $= 8,26 \cdot 10^7$, and a STEFAN's constant $= 7,63 \cdot 10^{-15}$. L and M correspond to the values within a certain radius r , but their total values may be introduced if P , $1-\beta$, and k are referred to the layers near the surface. The equation can be transferred by applying the relations:

$$T^4/T_1^4 = (1-\beta)/(1-\beta_1) M^2/R^4 \quad \text{and} \quad T/T_1 = \beta/\beta_1 M \mu/R$$

existing between $1-\beta$, M , and μ in the case of homologous stars. In these equations the subscript one refers to a homologous star of unit mass, the

¹ Z f Phys 26, p. 139 (1924).

² A N 226, p. 302 (1926).

³ Lick Bull 10, p. 169 (1923).

radius and mean molecular weight of which are equal to one. By eliminating T between the above equations we get:

$$\frac{(1-\beta)}{\beta^4} = \frac{1-\beta_1}{\beta_1^4} \mathfrak{M}^3 \mu^4 = \varphi(r) \mathfrak{M}^3 \mu^4,$$

where $\varphi(r)$ is a function of the distance r from the centre of the star expressed in units of the radius r . It follows from the last equation that:

$$\frac{1}{1-\beta} \frac{d(1-\beta)}{dr} = \frac{\beta}{4-3\beta} \frac{1}{\varphi(r)} \frac{d\varphi(r)}{dr}.$$

Further:

$$\frac{1}{a} = \frac{1}{P} \frac{\frac{dP}{dr}}{\frac{1}{\varphi(r)} \frac{d\varphi(r)}{dr}}$$

is introduced. The luminosity-mass equation then becomes:

$$L = \frac{4\pi a G}{h} \mathfrak{M} (1-\beta) \left[1 + a \frac{\beta}{4-3\beta} \right].$$

The coefficient of absorption h corresponds to the homologous niveau-surfaces, and its dependence upon \mathfrak{M} and R can be taken $\propto \rho^\lambda T^\nu$ where λ and ν are arbitrary powers of the density and of the temperature, h is then brought into the form:

$$h = \text{const } (1-\beta)^{\nu\lambda} \mathfrak{M}^{1+\nu\lambda} / R^{3\lambda+\nu}.$$

Further $L = 4\pi R^2 \frac{1}{4} a \sigma T_e^4$ and R can thus be eliminated and the effective temperature substituted.

In reality hQ is not such a function of P , T and q that the stars are homologous systems.

Because of that, a and $\varphi(r)$ will vary with \mathfrak{M} just as the density-distribution varies from star to star with the total mass.

241. Statistical Investigations Concerning the Mass-Ratio in Binaries. E. B. WILSON and W. J. LUYTEN¹ have used accurate mass-ratios for 69 spectroscopic binaries for a statistical investigation. By taking $x = \log \mathfrak{M}_B / \mathfrak{M}_A$ and by taking the mass-ratios $\frac{\mathfrak{M}_A}{\mathfrak{M}_B}$ and $\frac{\mathfrak{M}_B}{\mathfrak{M}_A}$ both ways in each pair a symmetrical distribution was necessarily obtained of the 138 values of x . The dispersion σ_x is $\pm 0.26 \pm 0.02$ and the ratio of the fourth moment about the mean to the square of the second moment about the mean is 4.3 ± 0.4 , whereas a normal error curve gives 3.0. In a previous note the authors have found for 14 binaries and the Sun the value of the dispersion of $\log \mathfrak{M}$ to be 0.36 ± 0.03 . The value of σ for the logarithm of the mass-ratios of these 14 systems is 0.30 ± 0.04 .

If r is the coefficient of correlation between the logarithmic masses of the components in binaries we have:

$$r = 1 - \sigma_x^2 / 2\sigma^2.$$

By using the above data r is found to be 0.74 and thus there appears to be a high degree of correlation between the masses in the pairs or a great tendency for the masses to be equal, which is also a very general assumption. It should not be overlooked, however, that there is probably a strong observational selection at work. The authors inquire what would be the standard deviation of x for the statistical distribution of the 406 hypothetical binaries that could be constructed by pairing in all possible ways the 29 stars used in a previous note (see ciph. 219)

¹ Wash Nat Ac Proc 10, p. 433 (1924).

with $\sigma = \pm 0.36$. They find $\sigma'_w = 0.50$ or nearly double the value of σ_x . In the material of 69 actual binaries that was investigated there is not one with a mass-ratio greater than 5, whereas in the 406 hypothetical binaries there are 79. Assuming that these high mass-ratios, if they existed, would not be observed and measured the authors find for the remaining 327 pairs a dispersion of 0.34, which is not far from the value of 0.26 that is actually found.

The following table is computed on the basis of the material available:

M_B/M_A	Discovery-chance	Luminosity ratio	M_B/M_A	Discovery-chance	Luminosity ratio
1/20	1/9000	1/100 000 000	1/2	1/1.6	1/70
1/10	1/220	1/400 000	1/1.5	1/1.2	1/11
1/5	1/14	1/250 00	1	1	1
1/3	1/3.7	1/600			

In view of the very great luminosity ratios it might appear reasonable to believe that the discovery-chances have been overestimated, and that when the discovery-chance is considered the observed mass-ratios are more scattered than would be the case if the two components were selected at random. It seems that there is considerable probability that the apparent clustering of the mass-ratios about unity is due to observational selection.

242. Theoretical Derivation of the Mass-Ratio in Double Stars. The question whether the RUSSELL-diagram represents loci of equilibrium during the evolution course or an actual course of evolution ought, as has been pointed out by G. SHAJN¹, to benefit from an examination of double stars. Because of the equation $\Delta m = \Delta M$ we can write, applying EDDINGTON's theory and denoting the secondary by the subscript *A* and the primary by *B*,

$$-0.4 \Delta m = \frac{7}{5} (\log M_A - \log M_B) + \frac{3}{5} [\log (1 - \beta_A) - \log (1 - \beta_B)] + \frac{1}{5} (\log T_A - \log T_B).$$

The mass-ratio cannot be determined without a knowledge of the temperature and of $\frac{1 - \beta_A}{1 - \beta_B}$ as a function of $\frac{M_A}{M_B}$. The observational material was augmented by using systems for which the absolute magnitude is known only by indirect or statistical methods. Thus computations were made for 342 systems, most of which are certainly physical pairs. The results are summarised as follows:

Giants			Dwarfs		
Spectral index	M_A/M_B	n	Spectral index	M_A/M_B	n
0.0—0.4	0.88	78	0.0—0.4	0.88	65
0.5—0.9	0.72	12	0.5—0.9	0.85	16
1.0—1.4	0.66	33	1.0—1.4	0.70	15
1.5—1.9	0.62	20	1.5—1.9	0.63	12
2.0—2.4	0.45	18	2.0—4.5	0.35	4
2.5—2.9	0.56	9			
3.0—4.5	0.37	9			

For systems with components of B stars the values of M_A/M_B for the first three spectral intervals are: 0.68, 0.41, and 0.34 respectively. The fact that the spectral index increases with Δm and the result of LEONARD² that in giant systems the spectrum of

the companion belongs to an earlier class than that of the primary, whereas in the dwarf systems the spectrum of the secondary is of a later class, lead to the conclusion that these relations indicate the course of the stellar evolution, which will be that indicated by RUSSELL.

¹ M N 85, p. 245 (1925).

² Lick Bull 10, p. 169 (1922).

AITKEN¹ has shown that the mass-ratios of spectroscopic binaries increase with advancing spectral class from B to G. The same relation results from SHAJN's material

SHAJN			AITKEN		
Spectral class	$\mathfrak{M}_A/\mathfrak{M}_B$	n	Spectral class	$\mathfrak{M}_A/\mathfrak{M}_B$	n
B0—B9	0.60	50	B0—B8	0.70	11
A0—A9	0.77	69	B9—A5	0.75	16
F0—F9	0.78	109	F	0.92	3

SHAJN does not think that these facts can be taken as proving that a gradual decrease of mass takes place during the lifetime of a star. The existence a priori of systems of very unequal masses can be expected. Further, the two spectra are not independent of each other. When the primary is M or K, the companion may exhibit a spectrum of gm—A, but very seldom of a late spectral class. In a dwarf system of, say, class K the spectrum of the secondary is dK or dM. Thus it is natural to expect an average decrease of ΔSp with increasing $\mathfrak{M}_A/\mathfrak{M}_B$ as is actually found.

248. LUNDMARK's and LUYTEN's Differential Method². The statistical relationship between the two forms of energy in the stars, the radiant energy, expressed as absolute magnitude, and the inert energy, expressed as mass, was derived from differential data of spectroscopic binaries. When both spectra of a spectroscopic binary have been observed an accurate value for the mass-ratio or $\Delta \log \mathfrak{M}$ is found from the amplitudes K_1 and K_2 by means of the relation:

$$-\Delta \log \mathfrak{M} = \log K_1 - \log K_2 = a.$$

In many cases there are estimates of the relative brightness of the two spectra and thus also the difference in absolute magnitude ΔM can be determined. If the spectroscopic binary is an Algol variable the value of $\Delta \mathfrak{M}$ can be determined comparatively accurately from the determination of the orbit.

Suppose we have the relation.

$$M_A = f(\log \mathfrak{M}_A),$$

$$M_B = f(\log \mathfrak{M}_B),$$

and

$$M_A = \varphi(M_B).$$

The problem is then to solve the equation:

$$f(\log \mathfrak{M}_A) = \varphi[f(\log \mathfrak{M}_A + a)]$$

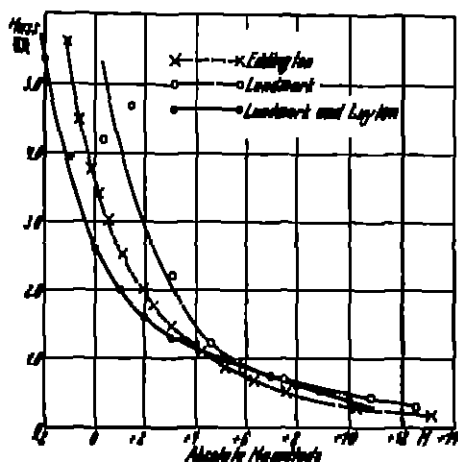


Fig. 158 The relation between absolute magnitude and mass as integrated from mass-ratios and differences in luminosity in spectroscopic binaries. For comparison purposes EDLING's curve [M N 84, p. 308 (1924)] has been inserted and the curve derived on basis of double stars for which the orbital elements and the parallax are known (Compare fig. 154.)

¹ The Binary Stars, p. 207. New York (1918)

² Ark. Mat. Astr. Fys. 20A, No. 18 (1927); Upsala Medd. No. 34.

or to determine the form of f when φ and a are given. In practice it will be sufficient to use a graphical method and to construct the curve $M = f(\log \mathfrak{M})$ from values of $\frac{d \log \mathfrak{M}}{dM} = \frac{d \log \mathfrak{M}}{dM}$ for given values of M . The following mean values for the differential quotient were obtained:

M_{AB}	$\frac{d \log \mathfrak{M}}{dM}$	n	M_{AB}	$\frac{d \log \mathfrak{M}}{dM}$	n
Brightest to $-2^m,0$	$-0,168$	4	$+2^m,0$ to $+4^m,0$	$-0,060$	6
$-2^m,0$ „ $0,0$	$-0,221$	16	$4,0$ „ $6,0$	$-0,060$	9
$0,0$ „ $+2,0$	$-0,102$	17	$6,0$ „ faintest	$-0,073$	3

As constant of integration the value $\mathfrak{M} = 1 \odot$ for $M = 5,0$ was selected. The following relation resulted:

M	$\log \mathfrak{M}$	\mathfrak{M}	M	$\log \mathfrak{M}$	\mathfrak{M}
$-2^m,0$	0,780	$6,0 \odot$	$+5^m,0$	0,000	1,0
$-1,0$	0,595	3,9	$6,0$	$-0,060$	0,87
$0,0$	0,410	2,6	$7,0$	$-0,130$	0,74
$+1,0$	0,295	2,0	$8,0$	$-0,200$	0,63
$2,0$	0,195	1,6	$9,0$	$-0,275$	0,53
$3,0$	0,130	1,3	$10,0$	$-0,350$	0,45
$4,0$	0,065	1,2			

The agreement between this curve and that derived by EDDINGTON is comparatively good. The values dM were not reduced to bolometric magnitudes, but an inquiry has shown that such a reduction will not materially change the results. The same applies to the inclusion of new material available.

244. The Masses and Luminosities of the Eclipsing Binaries. DEAN McLAUGHLIN¹ has discussed the contribution of the eclipsing variables to stellar luminosities and masses. Altogether 48 eclipsing stars have been observed for radial velocities. In 28 cases the two spectra have been measured and in 3 others the rotation effect has been observed. In 21 cases the mass-ratio is known from the amplitude-ratio K_1/K_2 . The mass-ratio has been plotted against L_A , the luminosity of the brighter star, and a smooth curve has been drawn. From this curve the value of the mass-ratio corresponding to any value of L_A could be read. It was then possible to calculate the hypothetical mass of each component. Altogether the masses have been calculated in 41 systems, and in 38 of these linear dimensions and densities are known. Hence absolute magnitudes and hypothetical parallaxes may be calculated. By using SEARES's values for surface brightness J_A the formula:

$$M_A = J_A - 5 \log r_A + 4,75,$$

where r_A is the geometrical mean of the major and minor axes of the star, gives the absolute magnitude. The apparent magnitude m_A of the bright component alone is obtained from:

$$m_{AB} - m_A = 2,5 \log (1 - L_A),$$

where m_{AB} is the apparent magnitude of the system at maximum brightness. Then:

$$\log \pi = 0,2 (M_A - m_A) - 1$$

gives the hypothetical parallax. Further:

$$\Delta M = m_n - m_A = 2,5 \log [L_A / (1 - L_A)].$$

¹ A J 38, p. 21 (1927).

² Ap J 55, p. 198 (1922).

The bolometric magnitudes have been calculated from the formula given by EDDINGTON.

$$M_{bol} = 4.75 - 5.0 \log r_A - 10 \log T_A / 5860^\circ$$

The bolometric magnitudes have been reduced to EDDINGTON's standard curve for $T_A = 5200^\circ$ by applying the temperature correction term:

$$2 \log \frac{T_A}{5200^\circ}.$$

The RUSSELL diagram shows that the dwarf sequence is well determined by the eclipsing binaries. Yellow and red giants are almost totally lacking. The relation of mass to spectral class is shown in the following synopsis.

Spectral class	M	Stars	Palms
O8.5	35.0	2	1
B0—B2	16.6	6	4
B3—B5	5.2	12	8
B8—A0	3.1	18	14
A2—A8	2.7	8	5
F0—F5	0.7	5	3
F8—G5	1.1	10	5
M1	0.6	2	1

Then the mass-luminosity diagram was formed. The scattering around the relation curve was found to be comparatively large. The sources of appreciable errors must be limited to the radii and the effective temperatures. It does not seem likely that in any case errors of the radii could affect the result by as much as one magnitude, which would correspond to an error of roughly 30%.

in the radius. The effective temperature should not introduce an error greater than half a magnitude. Thus a deviation of $1^{M.5}$ ought to be relatively infrequent, but at least five well-determined stars equal or exceed that limit, and several others of less certain mass so far exceed it that no reasonable adjustment of temperature will bring them within $1^{M.5}$ of the relation curve. The author is of the opinion, which is also shared by me, that we are not justified in saying that the mass and effective temperature of a star determine a unique value of the luminosity.

MCLAUGHLIN has pointed out that if there is a strict one-to-one correspondence between mass and luminosity within a group of stars with the same effective temperature but with different masses, the density of each star would be uniquely determined. The curves of constant dimensions and temperatures have been calculated from EDDINGTON's mass-luminosity relation. The figure provides a check on the calculated density, since the point for any given star will fall in a position corresponding to the assumed radius, regardless of whether the star satisfies the theory or not.

Few of the stars show such great deviations from the theoretical densities that the calculated ones would have to be multiplied or divided by 8 or a greater factor. It is very doubtful whether as great a change of radius as 30 per cent would be permissible in any of these cases. Considerable deviations are also shown in other cases. Nor would an adjustment of the scale of effective temperatures remove the disagreement between observation and theory.

245. The Upper Limit for the Stellar Masses. H. VOGT has discussed this important question¹. The observations suggest that an upper limit exists and the theory concerning the interior of the stars indicates that unstable conditions must arise as soon as the radiation pressure equals the amount of the gas pressure. VOGT assumed an arbitrary law of density distribution within a star ($\rho = F(r)$) possessing spherical symmetry. The amount of energy L_r passing in unit time through the niveau-surface at a distance r from the centre is

$$L_r = - \frac{4\pi c r^2}{3k\rho} \cdot \frac{dT}{dr},$$

¹ A. N. 230, p. 241 (1927)

which can be transformed into:

$$L_r = \frac{4\pi c G}{k} \mathfrak{M}_r (1 - \beta) \left[1 + \frac{P}{1 - \beta} \frac{d(1 - \beta)}{dP} \right],$$

where \mathfrak{M}_r is the mass within the distance r . If a star is compared with a homologous star with $\mathfrak{M} = 1$, $R = 1$, and the mean molecular weight $m = 1$, the following relations exist:

$$T^4/T_1^4 = (1 - \beta)/(1 - \beta_1) \mathfrak{M}^2/R^4,$$

$$T/T_1 = \beta/\beta_1 \mathfrak{M} m/R.$$

Putting:

$$\varphi(v) = (1 - \beta_1)/\beta_1,$$

we have:

$$(1 - \beta)/\beta^4 = \varphi(v) \mathfrak{M}^2 m^4,$$

from which we obtain:

$$\frac{1}{1 - \beta} \cdot \frac{d(1 - \beta)}{dv} = \frac{\beta}{4 - 3\beta} \cdot \frac{1}{\varphi(v)} \cdot \frac{d\varphi(v)}{dv};$$

combining with the equation for L_r we obtain:

$$L_r = \frac{4\pi c G}{k} \mathfrak{M}_r (1 - \beta) \left[1 + \psi(v) \frac{\beta}{4 - 3\beta} \right]$$

where:

$$\psi(v) = \frac{1/\varphi(v) \cdot d\varphi(v)/dv}{1/P \cdot dP/dv} = \frac{1/\varphi(v) \cdot d\varphi(v)/dv}{1/P_1 \cdot dP_1/dv}.$$

Denoting by $Q = L_r/\mathfrak{M}_r$ the mean energy produced we have:

$$kQ = 4\pi c G (1 - \beta) [1 + \psi(v) \cdot \beta/(4 - 3\beta)].$$

The equation says that within homologous stars the quantity kQ varies comparatively little as the mass becomes larger. It is also clear that when we are considering very heavy stars, a small change in the function kQ will correspond to a change in $\psi(v)$ that is as much larger as is the value of the mass. If the mass approaches an infinite value, the formation of a star is only possible if kQ is independent of v and has a constant value equal to $4\pi c G$.

If kQ is not a constant, but proportional to a function of v , it can be shown that $1 - \beta$ reaches, either in the central parts or in the shells near the surface, the value 1 according as kQ increases as we proceed to or from the centre. Then the upper limit for the value of the mass is reached, as every further contribution of matter to the star will be driven away by the radiation pressure. — In reality the condition $kQ = \text{const.}$ will not be fulfilled in the interior parts of a star, because it is very unlikely that the quantity kQ is such a function of temperature, density, and pressure that it would have a constant value for such a distribution as corresponds to the condition $kQ = \text{const.}$ Already for that reason the masses of the stars must have an upper limit.

In the preceding lines it is assumed that the stars do not rotate. If rotation is taken into account the conclusions will remain principally unchanged.

The question whether an upper limit exists for the stellar masses has also been discussed by W. ANDERSON¹ and later by G. I. POKROWSKI². The former starts from the energy formula:

$$E = \frac{3k\mathfrak{M}^2}{5r},$$

where k is the constant of gravitation, E the potential energy, and r the radius. The formula is valid if infinitely scattered matter is united into a homogeneous sphere (star) of radius r . In the cosmical cloud from which the sphere is formed

¹ A N 218, p. 205 (1923); Z f Phys 53, p. 597 (1929).

² Z f Phys 49, p. 587 (1928).

the potential energy E is assumed to have been uniformly distributed. If the material mass of this cloud is M_1 , the mass corresponding to E is M_2 , the mass of other energy present M_3 , and the total mass M so that

$$M = M_1 + M_2 + M_3 = M_1 + M_2,$$

we have $M_2 = E/c^2$, where c is the velocity of light. The above equation can then be transformed into

$$E^2 - \left(\frac{5\pi c^4}{3k} - 2M_1 c^2 \right) E + M_1^2 c^4 = 0,$$

which when solved gives

$$E = \frac{5\pi c^4}{6k} - M_1 c^2 + \left[\frac{25\pi^2 c^8}{36k^2} - \frac{5\pi c^4 M_1}{3k} \right]^{1/2}$$

E has thus real values only when

$$M_1 \leq \frac{5\pi c^4}{12k}$$

Thus the mass of a star has an upper limit. A maximal value of M is derived from the above inequality and this gives a maximal value for the total mass of the cosmical cloud

$$M = \frac{5\pi c^4}{6k} = \left(\frac{5}{6} \right)^{1/2} \frac{c^4}{2} \left(\frac{3}{\pi \rho k^2} \right)^{1/2},$$

where ρ is the density of the star.

In an analogous way POKROWSKI has derived a maximum value that only differs from that of ANDERSON in the respect that the numerical factor $(\frac{5}{6})^{1/2}$ is not present.

The upper limit corresponds to a value of $\log M = 35$ and thus enormous masses could exist.

246. Relation between Stellar Mass and Proper Motion. When the masses of visual double stars are being derived the great difficulty is the determination of the parallax. The data must necessarily be selected. The systems for which orbits have been determined must either be exceptionally massive or the linear separation must be relatively small. It seems very reasonable to suppose that the latter provides the greater part of the explanation.

J. JACKSON¹ has tried to use the proper motion instead of the parallaxes in order to test the masses independently. The proper motions were divided by the dynamical parallaxes π_d and the resulting linear motions analyzed by AIRY's method. The following results were found:

Stars with known orbits.

Spectral class	Coordinates of apex	Velocity ratio units per year	M	n
A2	258°.5 32°.0	2.18	13.4 (C)	21
F5	267°.5 29°.1	3.07	4.81	52
G2	290°.6 41°.6	4.79	1.27	30
K2	269°.3 10°.2	8.17	0.26	12

Stars with short arcs only

Spectral class	Coordinates of apex	Velocity ratio units per year	M	n
B6	278°. 32°.	2.07	12.6 (C)	24
A2	267°.2 15°.8	2.16	11.02	83
F4	261°.0 24°.2	3.91	1.87	102
G3	293°.6 41°.7	6.63	0.38	74
K1	269°.3 25°.6	4.87	0.96	42

¹ M N 83, p. 444 (1923)

A comparison was made with the mass values of SEARES. The agreement is good when the fact is taken into account that SEARES's results refer to geometrical mean masses and JACKSON's to $[\overline{M}]^3$. Owing to the small dispersion in \overline{M} the two values do not differ much.

The present writer has derived a mass-proper-motion relation. The derivation of the masses on the basis of spectral proper-motion parallaxes has convinced me that it will be possible to find a rather definite relation between \overline{M} and $H = m + 5 + 5 \log \mu$. Such a relation will be of use for deriving the frequency of stellar masses from the frequency of absolute proper-motion magnitudes.

Using 62 cases of well-determined individual masses the following relation has been found by a least-squares solution:

$$\log \overline{M} = 0,9750 - 0,1021 H + 0,00131 H^2.$$

Using the relation between mass and absolute magnitude as derived in ciph. 232 (p. 666) and making the assumption that $M = H - 5,6$ the following formula was found:

$$\log \overline{M} = 1,6262 - 0,2037 H + 0,00412 H^2.$$

247. Relation between Stellar Mass and Form of Orbits of Binary Stars.

Already in the early material it seemed suggested that there is a relation between the total absolute magnitude and excentricity of binaries. As the difference in mass ΔM is directly dependent upon the difference in M the existence of the thought relation would prove a relation between stellar mass and form of the orbit of double stars. It seems obvious that no definite relation can be established. Using different determinations of trigonometric and spectrographic parallaxes of stars the absolute magnitudes of 347 binaries have been approximated by me¹. The coefficient of correlation between excentricity, e , and absolute magnitude M was found to be:

$$r = +0,388 \pm 0,048$$

and the regression lines:

$$M = 0,360 e + 1,586,$$

$$e = 0,032 M + 0,273.$$

The correlation found is not very high but should probably be taken as real. This result has been doubted by H. SIEDENTOPF² who finds when treating the spectroscopic and the visual binaries separately no correlation between M and e and thinks that the correlation above is spurious and a result of selection in the material³.

Earlier C. D. PERRINE⁴ has discussed the question of a dependence of orbital excentricity upon the absolute magnitude of the components of binary stars. He used the difference ΔM and compared with e and found the following relation:

Limits of e	\bar{e}	$\overline{\Delta M}$	n
0,00 to 0,29	0,19	0,60	7
0,30 „ 0,44	0,37	1,29	16
0,30 „ 0,44	(0,37) ⁵	(0,95)	(15)
0,45 „ 0,58	0,50	1,32	18
0,59 and larger	0,71	2,04	16
0,59 „ „	(0,71) ⁶	(1,47)	(15)

¹ Ark Mat Astr Fys 20 A, No. 12 (1927); Upsala Medd No. 20.

² Göttingen, Univ Sternw Veröff H. 3 (1928).

³ If so the conclusions concerning stellar masses and their relation to luminosity will also be affected to a certain extent.

⁴ A J 33, p. 180 (1921).

⁵ Excluding 85 Pegasi.

⁶ Excluding Sirius.

This seems to be a pretty well established relation but on another hand a similar grouping made by me on basis of 116 pairs and represented graphically in Fig 159 does not seem to reveal any correlation between e and M . It thus seems that we have here one of the many problems where our present material is insufficient to give a definite answer upon the inquiry

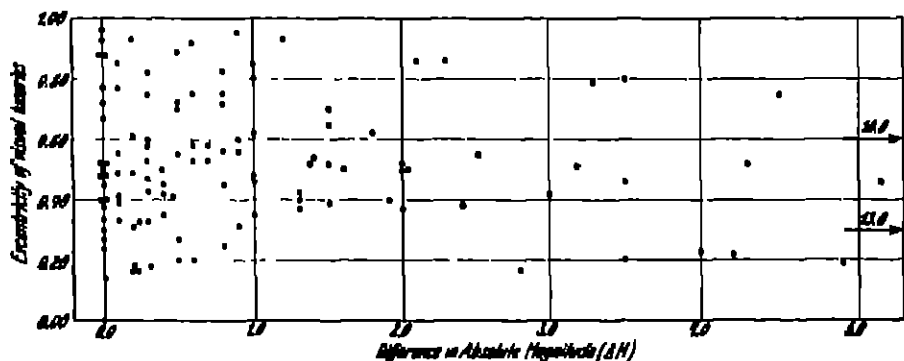


Fig. 159 Test for a supposed relationship between eccentricity of visual binaries and the difference in absolute magnitude ΔM between the components

248 The Mass of the Orion Nebula. The method of determining stellar masses is not restricted to the binary stars. It applies to every cases of a rotating body where the period of revolution can be determined for a particle at a certain distance. Thus the mass of the solar system could be approximated when an outside observer had observed the difference in velocity between the Sun and Neptune as soon as he had a knowledge of the linear distance between the two bodies

It was found by FAIRY, BUISSON, and BOURGET when they were applying the interferometer method, that internal motions existed within the Orion nebula and that the character of the motion was that of rotation. Later on CAMPBELL and MOORE¹ determined the radial velocities of 96 points near the Trapezium. The motion is of rotational character, although considerable individual deviations occur. In order to determine the amount of rotation it has been assumed that the nebula rotates as a rigid body within a distance of $2'$ from the centre. With the aid of a least square solution the plane was found that gives the closest representation of the velocities. This corresponds to a rotational component in the radial velocity amounting to 5 km/sec at a distance of $2'$

If M is the central mass and m the (infinitely) small mass of a particle at the distance r , v the linear velocity, and k the gravitation constant, we have

$$M + m = v^2 r k^{-1},$$

or

$$M + m = 0.001129 \frac{a''}{r} v^2,$$

where a'' is the distance of the point considered in seconds of arc, v is the linear circular velocity at this point measured in km/sec. Next the parallax has to be derived. In a paper of mine still unpublished it has been found that the value:

$$\pi_{\text{Orion}} = 0''.0030,$$

¹ Lick Publ 13, p 96 (1918).

derived from a discussion of absolute magnitudes, proper motions, motions of binaries etc., and the distribution of stars in front of the dark nebula accompanying the bright one is the best that can be derived from the existing data.

Thus the minimum mass of the nebula is found to be $48 \odot$, which is not astonishing when one remembers that the trapezium-stars alone are certainly very massive¹.

The value thus derived is the minimum mass of the nebula; on account of that we cannot locate the axis of rotation and the observed rotation is thus a component of the actual rotation.

The method can also be applied to the anagalactic objects.

249. Planetary Nebulae. The central stars of planetary nebulae are O stars that evidently do not differ from the ordinary O stars in any other way except that they are surrounded by nebulosity. W. H. WRIGHT has said that the disparity among the central stars in planetaries is no larger than the disparity among non-nebulous O stars.

The extensive survey of the spectra of 125 bright-line nebulae at Lick Observatory has revealed the important fact that several planetaries show internal motions that are most likely interpreted in terms of rotational motions. The internal motions are in several cases of a very complicated nature and there are certainly other phenomena present that change the spectral lines, such as a possible extension or outward motion of the gaseous envelope, differential effects of radiation pressure, ZEEMAN or STARK effects, etc. Still, it seems to be justifiable to try to find a general rotational component.

In 23 cases it seems possible to derive a rotation component. The uncertainty is considerable, but still there seems no doubt that the planetaries are very massive and bodies of a low temperature.

Object	Distance from centre	Rotation component in km/sec	Parallax π	Mass of star and nebula	Density of central star	Temperature of central star
NGC 1535	4",4	4,0	0",0017	46 \odot	4390 \odot	$38 \cdot 10^3$
J 320	3 ,1	6,6	0 ,00062	240	22400	$34 \cdot 10^3$
IC 2165	4 ,2	2,8	0 ,00025	149	9320	$51 \cdot 10^3$
NGC 2392	15 ,0	16,0	0 ,0015	2900(?)	4470	$27 \cdot 10^3$
2452	10 ,0	14,0	0 ,00019	11500(?)	100000000(?)	$85 \cdot 10^3$
3242	{ 13 ,0	4,4	0 ,0018	156	40900	$58 \cdot 10^3$
	{ 5 ,5	6,2				
IC 4593	2 ,05	2,15	0 ,00095	13,3	480	$22 \cdot 10^3$
NGC 6210	{ 3 ,5	6,4	0 ,0014	113	7270	$36 \cdot 10^3$
	{ 4 ,5	4,0		57	3650	
6543	3 ,5	5,0	0 ,0023	43,5	5600	$40 \cdot 10^3$
6565	3 ,0	7,0	—	—	—	—
6572	4 ,0	2,8	0 ,0019	19,4	540	$31 \cdot 10^3$
6567	1 ,8	7,5	0 ,0005	220	58000	$45 \cdot 10^3$
6720	25 ,0	2,0	0 ,0012	94	415000	$72 \cdot 10^3$
6741	4 ,1	2,4	0 ,00025	107	128000	$58 \cdot 10^3$
6807	1 ,0	4,3	0 ,00019	1100	2860000	$66 \cdot 10^3$
6818	9 ,0	2,4	0 ,0011	54	2090000	$70 \cdot 10^3$
6826	10 ,4	4,0	0 ,0020	94	4820	$34 \cdot 10^3$
6886	2 ,8	5,0	0 ,00032	250	156000	$52 \cdot 10^3$
IC 4997	2 ,4	5,7	0 ,00019	460	26800	$35 \cdot 10^3$
NGC 7009	{ 4 ,5	4,5	0 ,0029	36	178000	$50 \cdot 10^3$
	{ 9 ,0	6,1		132	650000	
7026	3 ,7	18,4	0 ,00045	3100	8140000	$45 \cdot 10^3$
7027	5 ,5	10,0	0 ,00044	1420	18000000	$86 \cdot 10^3$
7662	5 ,6	8,0	0 ,0018	230	151000	$52 \cdot 10^3$

¹ Lund Obs Circ 3, p. 64 (1931).

To this table should be added the remark that the densities have been computed on the assumption that all the mass is concentrated into the central star. This seems reasonable when one considers recent work concerning the formation of gaseous nebula.

The parallaxes are generally the ones derived by H ZANSTRA¹. In some cases parallaxes have been derived by me according to the same method. The same applies to the temperatures of the central stars.

Although the dispersion in the density values is considerable there seems to be a rather definite relation between the temperature and density. Thus

T	ϱ
32000°	3800
17000	38000
75000	6000000

This may be due to a systematic error in the temperatures but it might also be a real phenomenon. It is interesting to see that the densities, although high in many cases, still are not above the upper limit assigned to the density of matter. Thus E. C. STONER² has on basis of LUNNINGTON's theory on stellar evolution computed an upper limit for the central densities of the stars on reasonable assumptions, he finds this limit to be $5 \cdot 10^8 \odot$.

250. Mass of the Stellar System. The total mass of the stars in the Milky Way System is given by

$$\mathfrak{M}_{\text{tot}} = N \iiint D(\alpha, \delta, r) \mathfrak{M}(M, \alpha, \delta, r) d\alpha d\delta dr dM,$$

in which $\mathfrak{M}(M, \alpha, \delta, r)$ is the mass of an individual star of absolute magnitude M at the point α, δ, r , and N the number of stars per cubic parsec in the vicinity of the Sun.

At present we cannot suppose anything else than that the mean mass of a certain number of stars is the same everywhere, that is, that $\mathfrak{M}(M, \alpha, \delta, r)$ is independent of position. LUYTEN³ has adopted the density law of KAPTEYN. The above formula simplifies to

$$\mathfrak{M}_{\text{tot}} = \bar{\mathfrak{M}} \cdot N_{\infty},$$

where N_{∞} is the total number of stars in the universe and is obtained by means of the relation

$$N_{\infty} = 0,0451 \int_0^{\infty} 4\pi_0 (5,102)^3 \varrho^3 \Delta(\varrho) d\varrho,$$

ϱ being the polar semi-diameter of the homologous ellipsoids around the Sun and $\Delta(\varrho)$ the density of stars in space. Further according to KAPTEYN

$$\log \Delta(\varrho) = -5,356 + 4,890 \log \varrho - 1,200 \log^2 \varrho$$

LUYTEN finds:

$$N_{\infty} = 1,5 \cdot 10^8.$$

For $\bar{\mathfrak{M}}$ he adopts $0,945 \odot$ and thus

$$\mathfrak{M}_{\text{tot}} = 1,42 \cdot 10^8 \odot.$$

¹ Z f Astrophys 2, p. 329 (1931)

² M N 92, p. 662 (1932)

³ Harv Ann 85, No. 5 (1923)

The value of N_{∞} is perhaps six times too small, as is suggested if we adopt the results of SEARES¹. On the other hand LUYTEN's value of \overline{M} seems to be too large. I have adopted $\overline{M} = 0,6 \odot$. Thus the total mass should be:

$$M_{\text{tot}} = 5,4 \cdot 10^9 \odot.$$

251. The Masses and Mass-Ratios of Stellar Systems. In 1916 V. M. SLIPNER² announced that the spiral nebula NGC 4594 rotates in its own plane approximately as a rigid body. This conclusion was confirmed by the subsequent work of F. G. PEASE³ at Mount Wilson. Later on the rotational motion of the Andromeda nebula was also established by means of the measurements of PEASE and ADAMS⁴. Already in 1914 M. WOLF⁵ had found a rotational component in the motion in Messier 81, but details were not published until later on. The results given below for Messier 33 and Messier 51 are poor, as the rotational motion is based on the difference in motion between the centre and one outside object in each case, NGC 598 and NGC 5194, respectively.

The method of computing the mass is the same as in the case of double stars⁶. Uncertainties are involved principally on account of the uncertainties in the parallax adopted and the inaccuracy in assuming that the inclination of an anagalactic object is derived from its ellipticity.

Object	M_{tot}	M_{tot}
Andromeda Nebula . . .	$1,8 \cdot 10^9$	—17,8
Messier 81	$7,6 \cdot 10^{11}$	—24,2
NGC 4594	$3 \cdot 10^{10}$	—17,0
Messier 33	$1,5 \cdot 10^{10}$	—15,1
Messier 51	$1 \cdot 10^{10}$	—16,6
Our Milky Way System .	$1 \cdot 10^{11}$	—16

The mass derived from values for the spectrographic rotation is dependent on the immediate effect of the gravitation. The gravitational mass thus also includes the dark matter within the anagalactic objects, such as extinct stars, dark nebulae, and meteors. On the other hand an approximation of the mass of an anagalactic object can be derived from the total absolute magnitude. This involves the assumption that the mass-luminosity relation is the same in different parts of the universe. On account of the fact that the proportions of different spectral classes within different galaxies do not vary considerably, and that hence the luminosity curve seems to be rather equal, it seems justifiable to assume as a first approximation the universality of the mass-luminosity relation. The luminous mass so derived does not include the dark matter and thus it will be possible to obtain an approximation of the ratio, Dark matter/Bright matter, in the cases where both the mass-values have been estimated.

Ratio: $\frac{\text{Dark + bright matter}}{\text{Bright matter}}$

Object	Ratio	Object	Ratio
Messier 81	100:1	Messier 51	10:1
NGC 4594	30:1	Messier 33	6:1
Andromeda Nebula . . .	20:1	Milky Way System . .	10:1

¹ Mt Wilson Contr No. 301 (1925); Ap J 62, p. 320.

² Lowell Obs Bull No. 62 (1914).

³ Wash Nat Ac Proc 2, p. 517 (1916).

⁴ Wash Nat Ac Proc 4, p. 21 (1918).

⁵ V J S 49, p. 162 (1914).

⁶ Upsala Medd No. 40; Ark Mat Astr Fys 21, No. 10 (1928); Populär Astronomisk Tidskrift 10, p. 19 (1929).

In the case of double nebulae the mass-ratio of the components can be determined from measurements of the spectrographic rotation. Let two particles, in each of the two components, be at the same angular distance α'' from the centre, then their linear distances are equal and the mass-ratio will be

$$\mathfrak{M}_B/\mathfrak{M}_A = V_B^2/V_A^2$$

where V_A and V_B are the circular velocities at the said distance. The application of the method will involve much observational work, but it does not seem to be impossible to find cases where one ought to be able to photograph both the spectra of regions at such distances from the nucleus that decent values of $\mathfrak{M}_B/\mathfrak{M}_A$ can be derived.

Assuming that the mass-luminosity law holds good we can take the ratio $E = I/\mathfrak{M}$, where I is the luminosity and \mathfrak{M} the mass within unit space. Then

$$\pi_{AB} = \frac{i_A}{L_A d_A} \left(\frac{V_0}{V_A} \right)^2 = \frac{i_B}{L_B d_B} \left(\frac{V_0}{V_B} \right)^2$$

where V_0 is the velocity of the Earth, α'' the angular distance from the centre, i the apparent intensity. Determinations of V_A and V_B can make a contribution to the value of E in both systems or test the binary character of the pair.

252. The Angular Moments of Visual Binaries. SHINZO SUINJO and YOSHIKATSU WATKINAI¹ derived in 1918 the masses and the angular moments of visual double stars. If H denotes the angular momentum of a system we have

$$H = 2\pi a^2 P^{-1} \pi^{-1} (1 - e^2)^{\frac{1}{2}} \mathfrak{M}_A \mathfrak{M}_B (\mathfrak{M}_A + \mathfrak{M}_B)^{-1}$$

if the terms caused by the rotation of the components are neglected.

The authors conclude that the masses and angular moments of star systems are, on the whole, of the same order of magnitude. The multiple systems have somewhat greater angular moments, the masses on the other hand remaining about the same. For spectroscopic binaries the angular moments are comparatively less than for visual binaries, the masses, however, being considerably greater. Our solar system has an angular momentum over hundred times less.

It is really very remarkable that the values of H are of the same order of magnitude, when one remembers that the fifth power of the parallaxes enters into the determination of the moments. It is difficult to avoid the conclusion that this result has a certain cosmogonic bearing. The authors compute the angular momentum of a primordial swarm of meteorites, which possesses spherical symmetry and is isolated from other external influences, and also suggest a theory for the explanation of the celestial rotation, perhaps the most enigmatic problem in cosmogony.

253. The Origin of Binary Stars. H. N. RUSSELL² has pointed out that the problem whether the binaries are the result of fission or condensation in a nebula can be advanced by means of studies of the triple and multiple systems. Systems originating from independent nuclei should not show any definite relations between masses or relative distances. An analysis of the problem shows that if a gaseous mass divides by fission without external disturbance into two parts the distance of the centres at the time of division is greater and the density

¹ Mem Coll of Sc Kyoto Imp Univ 3, No 7, p 199 (1918).

² Ap J 31, p. 185 (1910)

less the more unequal the parts (components) are. The ratio in which the initial distance can be increased by tidal action increases as the components become more unequal. The smaller component has the greater density immediately after the separation. The contraction necessary for a second fission is less for the more massive component. The ratio of the dimensions of the separate masses in the case of the second fission to that in the case of the first is always small. The increase in density between the fissions is very great.

The distribution of masses that is found among binaries makes the fission theory very probable. As the orbital elements are known only to a small extent, it is necessary to investigate the distribution of the (projected) distances, S_2 and S_1 . Only pairs with common proper motion were used; of 800 such pairs 74 are triple or multiple. It seems that the fission theory accounts for existing peculiarities of arrangement and gives a simple and fairly detailed account of their origin. The stars for which the separation is 1000 astronomical units exhibit two maxima of frequency, of which one, $S_2/S_1 = 0,15$, can be accounted for by fission theory, but the second, $S_2/S_1 = 0,40$, cannot. The theory that multiple stars have developed from nebulae that originally had well defined nuclei corresponding to the members of the system must in any case be called on in order to account for such wide groups as the Trapezium in Orion. In the case of the binary stars it seems reasonable to adopt the fission theory.

254. Concluding Remarks. Whereas the magnitude of the stars can be measured directly and their colour estimated or their colour equivalents derived in terms of magnitudes, the dimensions and the masses of the stars cannot be measured by any direct method except in the case of the apparently brightest stars, the diameters of which can be measured by the aid of interferometer methods.

The important elements, stellar dimensions and stellar masses, are thus derived or inferred quantities that are therefore not only affected by the errors in the observed quantities, but also by the uncertainty concerning the constants in the equations connecting the given quantities and those required for. The dimensions can be derived for all stars for which we possess tolerable knowledge of the quantities M and c_2/T . It cannot be said that we have a reliable temperature-scale as yet, in spite of all the varied research work carried out within this branch. As regards the masses our knowledge must be restricted for a long, long time to binary stars, and the application of the results to ordinary stars will certainly be justifiable, but will, no doubt, increase the uncertainty of the conclusions.

The third element considered here, the density of the stars, can be determined from observations of binary stars. The parallax does not enter and thus the density will be determined with fair accuracy as soon as the temperature is known.

The present situation with regard to the possibilities of deriving stellar dimensions and stellar masses seems rather satisfactory. The standardization of the temperatures (colours) inaugurated by HERTZSPRUNG could easily be extended to embrace several thousand intermediate stars. The parallaxes available will give linear dimensions of fair accuracy for at least a thousand stars. The new interferometer at Mount Wilson will furnish a means of measuring the dimensions of perhaps fifty stars or more, thus making it possible in the near future to standardize the system of computed diameters.

It might at first seem that the further extension of our knowledge of stellar masses will advance very slowly. But the discovery of new eclipsing binaries or the orbital determination of pairs that have been previously insufficiently

observed will add many good cases within a short time to our previous stock. The discovery by ATKIN of a number of visual binaries of short period makes it possible for us to obtain within the next ten or twenty years orbital elements of a number of binaries. Many of these ATKIN pairs are very imperfectly known as regards their parallax, proper motion, spectral class, and other attributes, but they can easily be entered on current programmes. It also seems likely that the publication of ATKIN's extension of the BURNHAM General Catalogue of double stars will considerably increase the number of new binary star orbits. It does not seem to be too optimistic to expect to have gained a knowledge of 500 individual stellar masses ten years from now. A necessary condition for the proper increase in data concerning the masses is intimate co-operation between the astrophysicist and the representatives of astronomy of position.

The approximations to the spectral-mass relation, mass-luminosity relation, and mass-temperature-luminosity relation hitherto reached will no doubt be more accurately established within a short time from now. The results of EDDINGTON, JEANS, and others concerning the theoretical mass-luminosity relation will certainly be improved upon by the aid of new observational data in the near future.

An application of the interferometer methods to the method of determining the mass-ratios seems to be of interest. If stars that take no part in the motion of the components of binaries, but that are not too far from them, are measured interferometrically, the results concerning the mass-ratios should be obtained in a much shorter time than when the derivations are based on meridian observations.

The general attitude of astronomers towards the problems we have dealt with in this paper sometimes seems to involve a certain overestimation of the bearing of certain theoretical results. It sometimes happens that the reasoning goes round in a circle, e.g. if the mass of a star does not agree with EDDINGTON's curve this does not prove anything concerning the correctness or incorrectness of the result. This is a commonplace, but still it seems to me that it should be pointed out. It has often happened that when new results have been presented it has been asked "How does that result compare with EDDINGTON's, JEANS's or RUSSELL's formula?" Of course, such comparisons should be made, but if there is only poor agreement it is not necessary for the observers to apologise and to regret that the observations do not fit the theoretical demands.

I am so far from denying the value of investigations of theoretical problems within astronomy that I wish to say that many efforts must be made on the part of the theorists in order to advance a number of questions on the basis of the now available material. We really should feel under much obligation to the theoretical astronomers for their splendid contributions. Theories give us the best guidance with regard to the requirements of future work and, what is most important, theories discover and formulate the general laws of Nature. Without any theories the astronomical observations would be a quite worthless collection of dead figures and descriptions.

But the theoretical interpretations of astronomical facts are always changing. Theories do good service and are dismissed. New theories are advanced and serve for a longer or shorter time. The solid construction on which astronomical theories are embroidered consists of the vast accumulation of recorded facts that has been going on from antique times up to recent days.

Chapter 5.

Stellar Clusters.

By

H. SHAPLEY-Cambridge, Mass.

With 21 illustrations.

a) Introductory Survey¹.

1. The Significance of Clusters. We designate as star clusters those groupings of stars in which the members are known to be gravitationally associated or may be assumed from their apparent positions relative to each other to constitute distinct physical organizations. Such a category includes both the typical globular systems and the more numerous and less well defined open clusters which range, for instance, from the Hyades to the fairly compact system of Messier 11.

There are also, in all parts of the sky, among the faint stars thousands of less obvious groupings. The studies of star distribution on the astrographic charts by TURNER², and by ÖRIK and LUKK³, indicate that the distribution is not at random. Working on this problem with Harvard plates⁴, I have shown that the clusterings and vacancies are real and are not to be attributed to occultation by nebulosity. The observed irregularities in the star counts, beyond those allowed by the law of chance, are to be attributed in general to the very prevalent stellar associations, which are not commonly recognized by casual inspection, and cannot be separated from surrounding stars except through laborious investigations.

The typical star clusters, however, are in themselves numerous and widely distributed, and their many problems are intimately interwoven with some of the most significant questions of stellar organization and galactic evolution. The general study of clusters deals with a wide variety of subjects. It involves, for instance, the problems of super-giant stars, stellar luminosity curves, irregularities in stellar distribution, star streaming, island universes, and the genesis of galactic systems; it considers primarily, however, the composition, structure, distribution, and cosmic position of the easily recognizable galactic and globular clusters, and in the following sections these groups will receive almost exclusive attention.

2. Historical Notes on Clusters. The history of the scientific study of star clusters is neither extensive nor very significant. Several clusters of naked eye

¹ Since the manuscript for this chapter was submitted to the publisher in May 1930, several important studies of star clusters have appeared. Only a few of these could be considered in the course of proof reading. November 1932.

² Obs 48, p. 173 (1925).

³ Publ Obs Astr Univ Tartu (Dorpat) 26, No. 2 (1924).

⁴ Harv Circ 281 (1925).

stars—for example, the Pleiades, Praesepe, Coma Berenices—have of course always been known, though their definite assignment to the cluster category came with the work on proper motions in the last fifty years. In a few constellations the majority of the brighter stars are now known to lie near together in space, and to form physical systems. Among such constellation groups are Taurus, Orion, Ursa Major, Perseus, Scorpio, Sagittarius, and Vela. But no close physical connection exists for the bright stars of Cassiopeia, Lyra, Aquila, Canis Major, and many others.

A score of the brighter galactic clusters and half a dozen of the globular clusters can be seen with the naked eye under good conditions. These objects were probably all known, therefore, to the ancients, but only a few appeared in our permanent records before the second half of the eighteenth century.

The records of HIPPARCATUS contain references to the double cluster in Perseus and to Praesepe, although neither was recognized as a group of distinct stars until the invention of the telescope. Both were first resolved by GALILEO, who described "the nebula called Praesepe", "not one star, only, but a mass of more than forty small stars".

Messier 22, the first globular cluster to be recorded as such, was discovered by LILLIE¹ in 1665, ω Centauri was noted as a lucid spot in the sky by HALLEY in 1677, and had previously been known to BAYER as a hazy star, and to PROLEMUS as a star in the cloud on the HORSE's back; in 1702 KIRCH discovered Messier 5, and the famous Messier 13 (the Hercules cluster), the brightest in the northern sky, was accidentally found by HALLEY in 1714.

The open cluster Messier 41 had already been recorded by KIRCH in 1681, but the majority of bright galactic clusters, except the Pleiades and the Hyades, were first recorded as such by MESSIER² in 1771. The conspicuous groups of stars around γ Carinae and the cluster near α Crucis were discovered by Sir JOHN HERSCHTEL.

For both open and globular clusters, as well as for bright nebulae of all kinds, the systematic listing by MESSIER in 1784 marked an epoch in the recording of observations of star groups. The HERSCHTELS advanced the work materially. Especially significant were the General Catalogue published by Sir JOHN HERSCHTEL in 1834³, and its important sequels by DREYER in the New General Catalogue and the Index Catalogues.

SCHULTZ and BARNARD were among the pioneers in determining visually the positions of the individual stars in globular clusters. The powerful photographic method of charting positions was first used by the HENRYS and GOULD for galactic clusters, and by SCHMINER, LUDKENDORFF, and von ZIEPEL for globular systems.

The Pleiades, the Hyades, Praesepe, δ and χ Persei, and some of the other bright galactic groups have, for the past fifty years or more, been the subject of frequent investigations of positions and proper motions. It is not unfair to say, however, that, except for studies of these nearby objects, the work done on individual clusters before the present century is now of little value. The development of photographic methods, the modern large telescope with its rapid spectroscope, and the standardizing of magnitude sequences have all tended to make the earlier work obsolete. The present views of the nature, dimensions, and significance of the globular clusters are less than twenty years old⁴.

¹ GALILEO, *Siderius Nuncius*, 1610, AILEN, *Star Names and their Meanings*, p. 113 (1899); see SHAPLEY and HOWARTH, *A Source Book in Astronomy*, p. 49 (1929).

² R. WOLF, *Geschichte der Astronomie*, p. 420 (1877).

³ *Hist. de l'Acad. R. des Sci.*, Paris 1771, p. 423.

⁴ *Phil. Trans.* 154, p. 1 (1864).

A very full bibliography of the work done on clusters is to be found in Appendix C of *Star Clusters*, Harv. Obs. Monograph No. 2 (1930).

In striking contrast to the present conception of a hundred globular clusters and hundreds of thousands of extra-galactic nebulae spread throughout measured millions of light years, with diameters of hundreds of light years for the clusters, and thousands of light years for the star clouds and nebulae, is the picture suggested by HALLEY's comment on his discovery of the Hercules cluster:

"But a little patch—and similar to the lucid spot around Theta Orionis (Orion Nebula), Andromeda (Andromeda Nebula), and in the Centaur (ω Centauri)—most of them but a few minutes in diameter; yet since they are among the fixed stars \therefore they cannot fail to occupy spaces immensely great, and perhaps not less than our whole solar system."

b) Classification, Number, and Distribution.

3. A Comparison of Galactic and Globular Clusters. It is proposed to adopt in the present treatment only two main divisions—globular clusters and galactic clusters¹. The principal characteristics of globular clusters are strong central concentration and richness in faint stars (fig. 1 and 2). The galactic clusters (fig. 3), looser and much less populous, are extremely varied; for example, Messier 11 is relatively rich, Messier 35 is irregular, the Pleiades and Messier 16 are nebulous, and Messier 103 and N.G.C. 1981 may be but accidental groupings. The so-called moving clusters are merely the brighter and nearer of the galactic types in which radial or transverse motions have been measured.

In future studies, especially in the Magellanic Clouds, we may find examples of clusters in a transitional stage between the richer galactic groups and the most open globular clusters. At present, however, there seems to be a rather sharp division which distinguishes the globular clusters as a special group of sidereal organizations—a group limited to about one hundred objects. The galactic clusters grade indefinitely into multiple stars in one direction, and in another into the condensed systems like Messier 11 and N.G.C. 2477 which closely simulate loose globular clusters.

Clear discrimination between galactic and globular clusters is also possible on the basis of distribution in the sky. The most conspicuous feature of the distribution is that galactic clusters are almost exclusively in the Milky Way and distributed irregularly throughout all galactic longitudes, while the globular clusters are rather widely scattered in latitude, but quite restricted in longitude. The globular clusters are, in fact, mostly in one half of the sky, as will be shown in subsequent diagrams.

4. The Number of Clusters. Thousands of new nebulae and millions of stars have been disclosed by modern telescopes and photographic plates, but the essentially complete listing of globular clusters antedated photography. Every recognized globular cluster except one bears a number from the New General Catalogue of DREYER, and all but a few were catalogued more than ninety years ago in the earlier Herschel lists. This early completion of the discovery of the globular clusters led BAILEY² to suggest that the limit of the region occupied by these systems had been reached, a suggestion that appears to be supported by subsequent work³.

There is, however, a vast difference between cataloguing an object and

¹ The term galactic cluster, suggested by TRUMPLER [Publ A S P 37, p. 307 (1925)] and others, is a natural name for the non-globular cluster, which is almost without exception near the galactic plane. It replaces the term "open cluster" which has caused some confusion because of the open type of globular cluster.

² A special study now in progress at Harvard, of the environs of the Large Magellanic Cloud adds several new globular clusters to the list; some of them may not be outlying members of the Cloud, and two or three are not N.G.C. or I.C. objects. In A N 246, p. 171 (1932) LAMPLAND and TOMBAUGH report that N.G.C. 5694 is a typical globular cluster.

recognizing its true character. Many of the entries given in the New General Catalogue (N G C) as globular clusters have proved to be something else, generally galactic groups or extra-galactic nebulae, and thirty-four of the globular clusters now recognized were not described as such in the New General Catalogue.

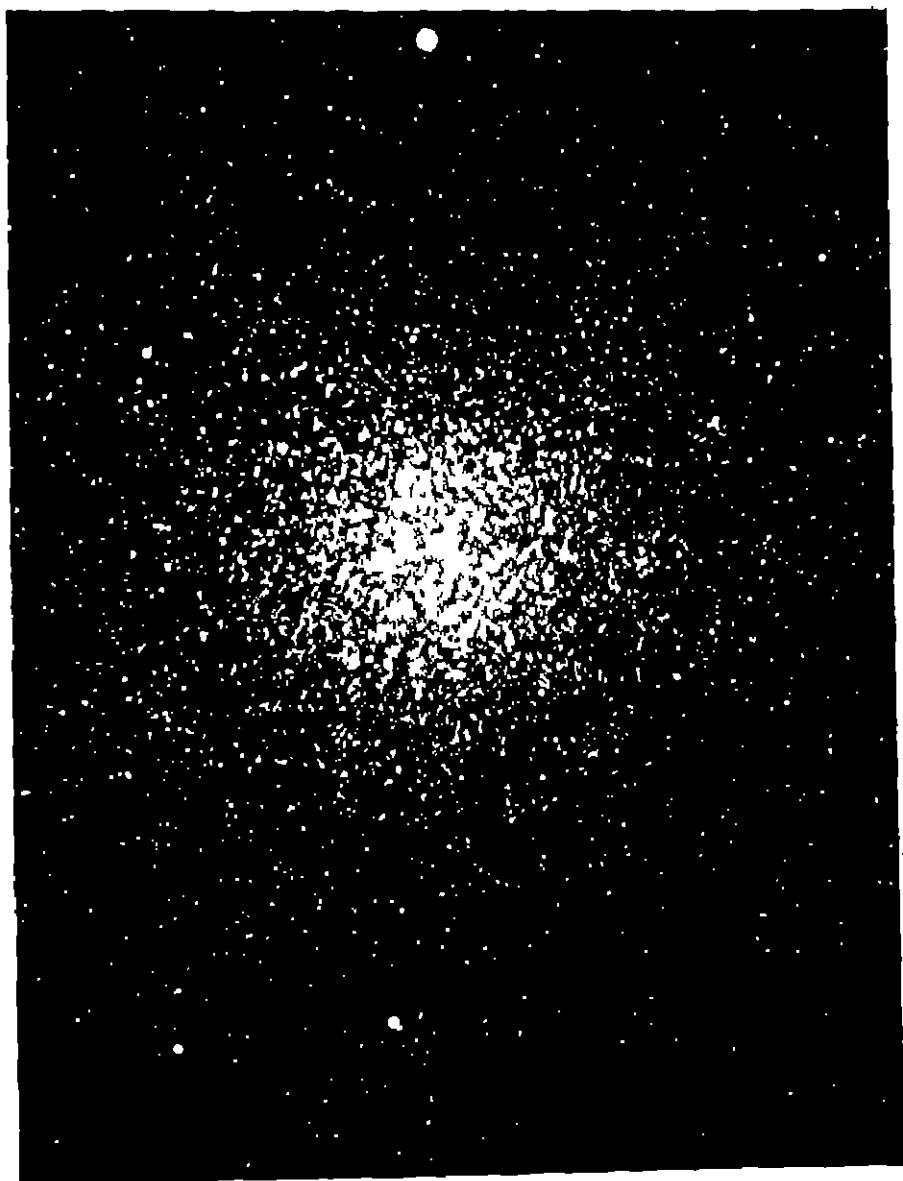


Fig. 4 Globular cluster ω Centauri, taken with 13-inch Boyden telescope at the Harvard Observatory

The large photographic telescopes have been of service in recent years in examining many faint and doubtful N G C objects, and an occasional addition to the list of globular clusters has resulted. A number of remote groups are still

questioned, however, even after some of them have been tested with large reflectors. The most doubtful globular clusters, which are marked with daggers in Appendix A, are the following¹:

N.G.C.	Radec ²	Galactio	Distance ³	Notes
1651	0438-71	249-36	—	Rejected; see Harv Circ 271 (1925).
5946	1528-50	295+04	32.2	A small, poor, loose cluster in a rich region.
6352	1718-48	308-07	19.7	A comparatively large cluster of very faint stars, on the edge of the Milky Way.
6535	1759-00	354+10	26.7	A small cluster on the edge of a rich region, with few stars.
6539	1759-08	348+06	38.7	A very faint cluster in a large observed area

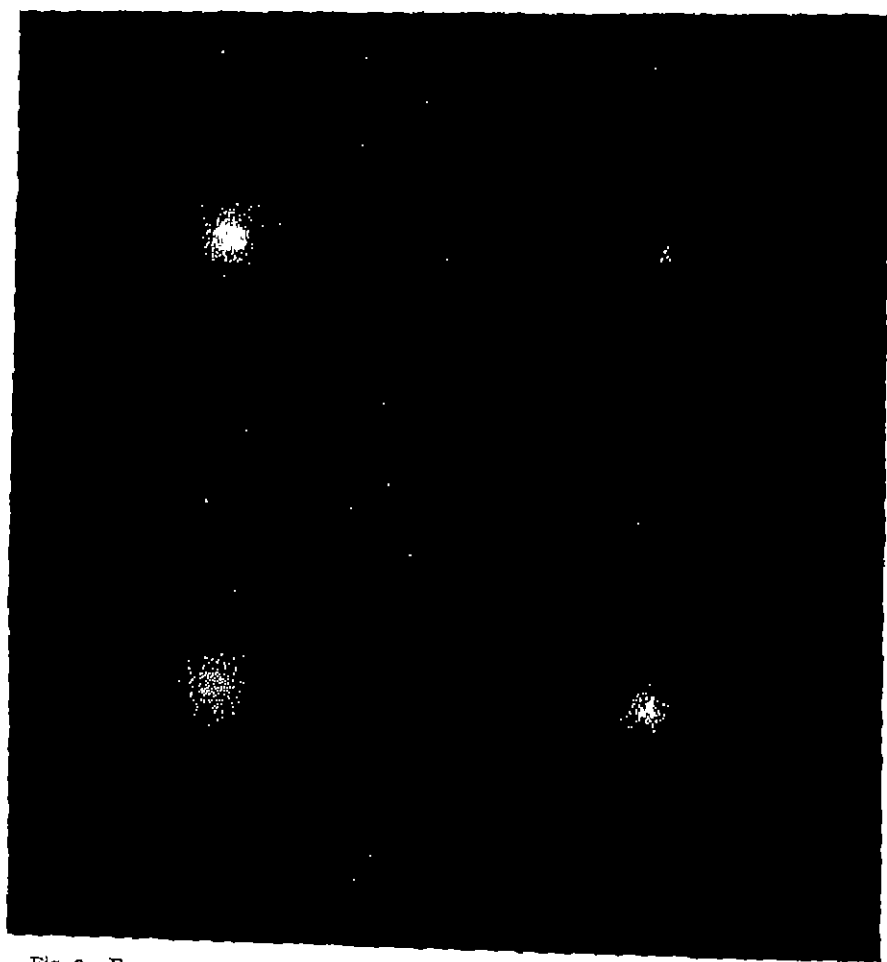


Fig. 2. Four exposures of the globular cluster Messier 13 taken at Mount Wilson.

¹ SAWYER and SHAPLEY, Harv Bull 848 (1927).

² The approximate positions for 1900 in equatorial coordinates are conveniently contracted for tabulation into the form here given; the first four figures give the hours and minutes of right ascension, and the sign and subsequent figures indicate the declination in degrees (and may be extended to minutes, if desired).

³ The distance in kiloparsecs is estimated on the assumption that the clusters are globular.

The numbers of globular clusters have been discussed by BAILLY, HINKS, BOHLIN, and Miss CLERKE, but the data on which their estimates are based lack homogeneity¹ MELLOTTE's catalogue², however, which was made from the FRANKLIN-ADAMS plates and contains eighty-three globular and one hundred and sixty-two galactic clusters, constitutes a fairly homogeneous list of all clusters with diameters greater than one minute of arc and brighter than the sixteenth or seventeenth photographic magnitude. His list of galactic clusters is revised and extended in Appendix B, which contains 249 entries. From his list of globular clusters a few objects have been dropped, others have been added, mainly as a result of HUNDELT's work and my own with the 100-inch and 60-inch reflectors at Mt. Wilson. The total number accepted for the table in Appendix A is 103,

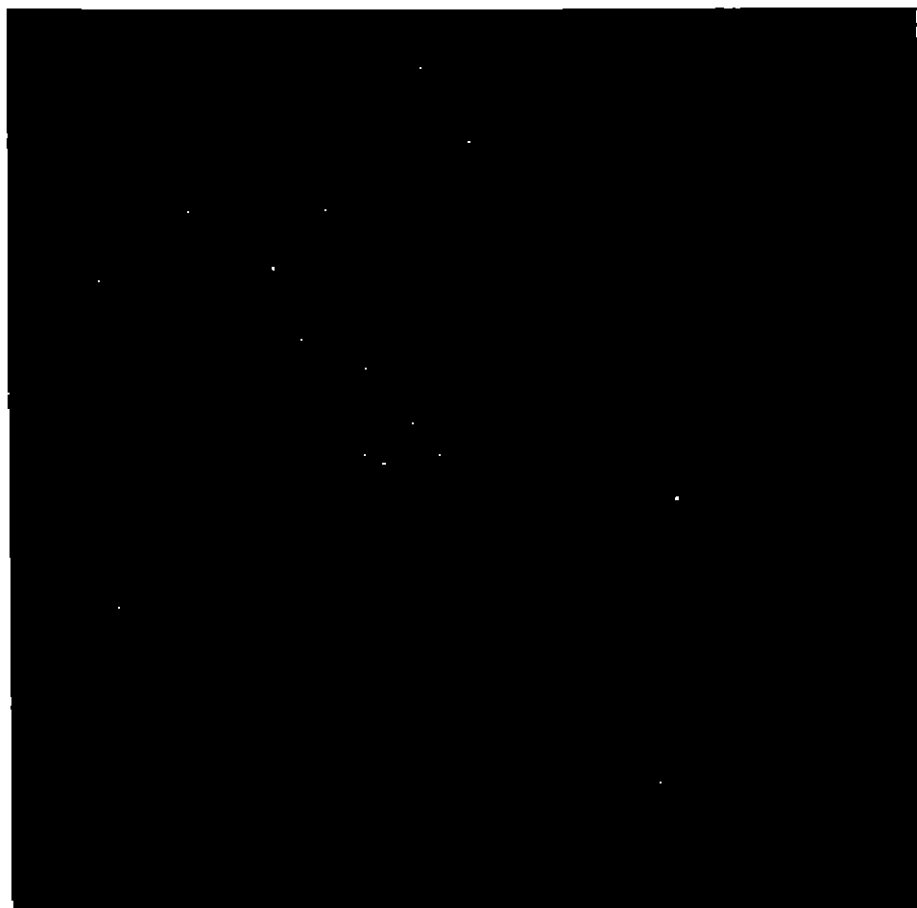


Fig. 3 Galactic cluster NGC 3552 taken with the 13-inch Boyden telescope at the Harvard Observatory

including ten globular clusters in the Magellanic Clouds³. An example of a recent addition is the observation at the Lowell Observatory, verified at Mount Wilson,

¹ BAILLY, *Harv Ann* 76, p. 43 (1915), HINKS, *M N* 71, p. 693 (1911), BOHLIN, *Svenska Vet Akad Handl* 43, No. 40 (1909), CLERKE, *Problems in Astrophysics* (London) p. 428 (1903).

² *Mem R A S* 61, p. 75 (1915).

³ See Footnote 3 on page 700.

that the object N G C 2419, described in the N G C as "pB, pI, 11E 90°, vghM, *78 267°, 4' dist", and not listed by MÉROTTE, is in fact a remote globular cluster in a part of the sky that is otherwise devoid of these systems.

Some of the faint extra-galactic nebulae, as yet unresolved, may prove to be essentially globular star clusters, perhaps with greater distances and dimensions than those now known. A comparative study of the distribution of light throughout the images can, however, give us some indication of their nature, their distribution with respect to other extra-galactic objects will probably show most of them to be sidereal systems of a higher order than globular clusters.

5. Classification of Galactic Clusters. In the studies of galactic clusters at Harvard we have for some time followed a two-dimensional classification. One parameter is related to the apparent number and concentration of the stars and may be called compactness, the other depends on the distribution of spectral classes among the cluster members.

The classification based on appearance is intended to cover the whole range of galactic clusterings, from multiple stars to globular clusters. The subdivisions are as follows:

a) Field irregularities. That there are many deviations from random stellar distribution is obvious from star counts, or even from a casual inspection of photographic plates in nearly any region of the sky. There seems to be no immediate need of attempting to unravel or catalogue such non-uniformities in stellar fields, but the assignment of a classification letter to the field irregularity is recognition of its significance in stellar distribution.

b) Star associations. In this category fall wide-spread moving clusters, such as the Ursa Major group, and the peculiar stars of high and parallel velocities. The class will be recruited largely through studies of proper motion and radial velocity. It grades imperceptibly into the next class.

c) Very loose and irregular clusters, typified by the Hyades and the Pleiades. The large cluster of bright stars around α Persei might be placed in this class, or better, perhaps, placed with the Orion Nebula cluster in class b. Class c corresponds in general with BAILEY's D3 and with MÉROTTE's IV.

d) Loose clusters. Messier 21 and Messier 34 are examples of a class equivalent to BAILEY's D2 and MÉROTTE's III.

e, f, g) Compact clusters. These three groups are equivalent to BAILEY's D1 and MÉROTTE's II. The division into three types is on the basis of richness and concentration, examples are Messier 38, Messier 37, N G C 2477. In the classification of clusters the globular systems follow immediately after class g. In fact, several of the most compact class g galactic clusters appear more nearly like globular clusters than do the loosest globular clusters classified as such by criteria other than appearance.

In practice the galactic clusters are generally taken to comprise only classes c to g. The distribution among these classes of the 249 clusters listed in Appendix B is as follows:

Class	Number
c	22
d	85
e	67
f	46
g	29

I have found it convenient to divide galactic clusters also into two principal groups on the basis of the spectra or colors of the component stars. (1) The Pleiades type, and (2) the Hyades type. Each includes members of classes c to g.

In the Pleiades type the stars, almost without exception, lie along the "main branch" of a RUSSELL diagram, with the earliest classes B or A; in the Hyades type, yellow spectral classes occur with the same apparent brightness as the predominant A stars.

More than ninety-five per cent of the galactic clusters for which spectral classes or colors have been determined fall into one or the other of these two groups, which are about equally numerous. There are a few aberrant clusters. Messier 67, for instance, appears to be a variant of the Hyades type in that blue giant stars are absent. Prominent examples of the Pleiades type are the double cluster in Perseus, Messier 36, and Messier 34; the Hyades type includes Messier 14, Messier 37, Praesepe, and the scattered cluster in Coma Berenices.

TRUMPLER has also proposed and used a classification of galactic clusters based on spectral composition¹. For clusters that he has so far observed he uses Types 1a, 1b, 2a, and 2f, with provision for other types if found. Type 1 is equivalent, in general, to my Pleiades type, and type 2 corresponds to the Hyades type.

6. Classification of Globular Clusters. Notwithstanding the general similarity of globular clusters in size, form, content, and absolute brightness, there are many deviations from the average. Clusters such as Messier 19 and ω Centauri are conspicuously elongated; Messier 62 is strikingly non-symmetrical; N.G.C. 4147 is deficient in giant stars; and nearly one third of the globular systems are so loosely organized that their inclusion in the list depends on such further criteria as high galactic latitude, the presence of cluster-type variables, and the appearance of thousands of faint stars on long exposure photographs.

Until recently no systematic attempt has been made to classify the globular clusters beyond noting that some were variable-rich, some variable-poor; some open, some compact. A detailed examination by Miss SAWYER and the writer of the globular clusters on good Bruce photographs, which are available in the Harvard collection for practically all the 103 systems now listed as globular, shows that many intermediate forms exist between the loosest and most concentrated clusters. Instead of classing the clusters, therefore, in the two or three broad and obvious categories, such as compact, medium, loose, we arrange them in finer subdivisions, in a series of grades on the basis of central concentration. For the classification of individual clusters reference may be made to Appendix A. Class I represents the highest concentration towards the center, and Class XII the least. The distribution among the various classes and the mean photographic magnitude for each class are as follows:

Class	Magnitude	Number	Class	Magnitude	Number
I	8.85	4	VII	7.90	8
II	7.80	7	VIII	7.85	10
III	6.76	7	IX	8.84	10
IV	9.01	12	X	8.88	9
V	7.88	12	XI	9.54	9
VI	8.91	11	XII	9.58	4

The present classification of globular clusters is essentially a description of apparent central concentration. It is interesting therefore to note that there is no correlation of class with integrated photographic magnitude as determined

¹ Publ. A.S.P. 37, p. 307 (1925). A more recent study of galactic clusters is presented by TRUMPLER in Lick Bull. 14, p. 154 (1930), where he gives a more complex, three-dimensional classification. The investigation also includes statistical material on distances, magnitudes, dimensions, and spectra.

from Harvard plates of small scale. The distribution of magnitude among the various classes is shown in the scatter diagram in Figure 4, where also the mean magnitude for a given class is plotted as a cross, and the average class for each interval of one magnitude is plotted as a circle.

To maintain homogeneity, the classifications of globular clusters were all made on plates with the scale of $1 \text{ mm} = 1'$. Superposed stars have occasionally interfered somewhat with the assignment of the class, especially for N.G.C. 4147, 6284, 6453, 6553, 6569, 6624. A few peculiarities were noted that are not completely taken care of by our classification based on central condensation alone. For

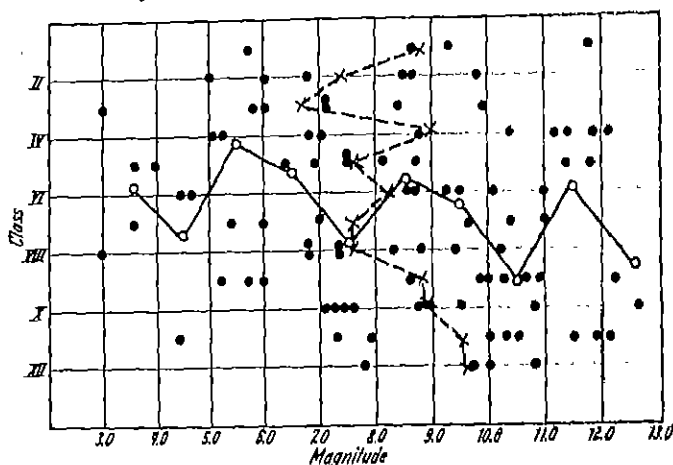


Fig. 4. The scatter diagram of classes of globular clusters (ordinates) and integrated photographic magnitudes. Circles and crosses indicate means.

instance, the bright cluster ω Centauri is peculiar in what appears to be a remarkable uniformity in the magnitudes of the brighter stars. Clusters somewhat similar to ω Centauri in this respect are N.G.C. 5272 (Messier 3), 5927, 6273, 6656 (Messier 22). These clusters also resemble each other in their moderate concentration (Classes VI to VIII), and two of them, ω Centauri and Messier 3, are the richest of all in variable stars. It should be noted, however, that the clusters with many variable stars are scattered throughout all classes.

In conclusion we observe that the classes of globular clusters are probably indicators of developmental age. They should prove increasingly useful in studies of linear diameters, motions, luminosity curves, and the deeper problems of the origin and life history of stellar clusters.

Table 1. Typical Globular Clusters of the Twelve Classes.

Class	N.G.C.	R.A. (1900)	Dec. (1900)	Pg. Mag.	Class	N.G.C.	R.A. (1900)	Dec. (1900)	Pg. Mag.
I	2808	9 ^h 10 ^m .0	-64° 27'	5.7	VII	6656	18 ^h 30 ^m .3	-23° 59'	3.6
II	7089	21 28 .3	- 1 16	5.0	VIII	6402	17 32 .4	- 3 11	7.4
III	104	0 19 .6	-72 38	3.0	IX	6218	16 42 .0	- 1 46	6.0
IV	1866	5 13 .3	-65 35	8.0	X	288	0 47 .8	-27 8	7.2
V	7099	21 34 .7	-23 38	6.4	XI	6809	19 33 .7	-31 10	4.4
VI	6752	19 2 .0	-60 8	4.6	XII	7492	23 3 .1	-16 10	10.8

7. Clusters in or near Obstructing Nebulosity. The large groups of bright B stars in Orion, Scorpio, and elsewhere are associated with important bright and dark nebulosity. The Pleiades nebulosity is well known. A number of

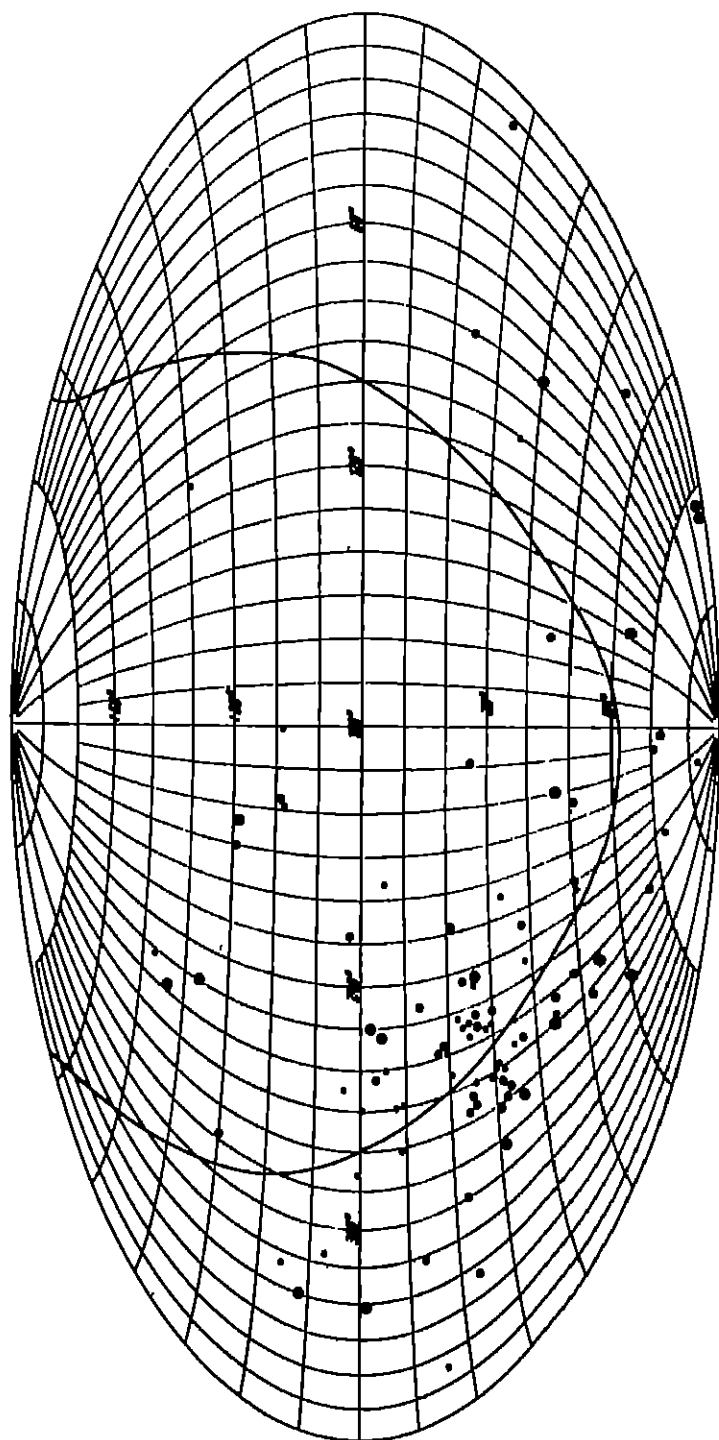


Fig. 5. Distribution of globular clusters in equatorial coordinates. Small dots indicate more distant clusters. The galactic circle is shown by a heavy line. The clusters in the Magellanic Clouds have been omitted.

nebulous galactic clusters, such as Messier 8, are on record, and clusters of this sort also appear in the Magellanic Clouds. It is doubtful, however, if many would be known of the nebosity in these galactic clusters if their distances were ten times accepted.

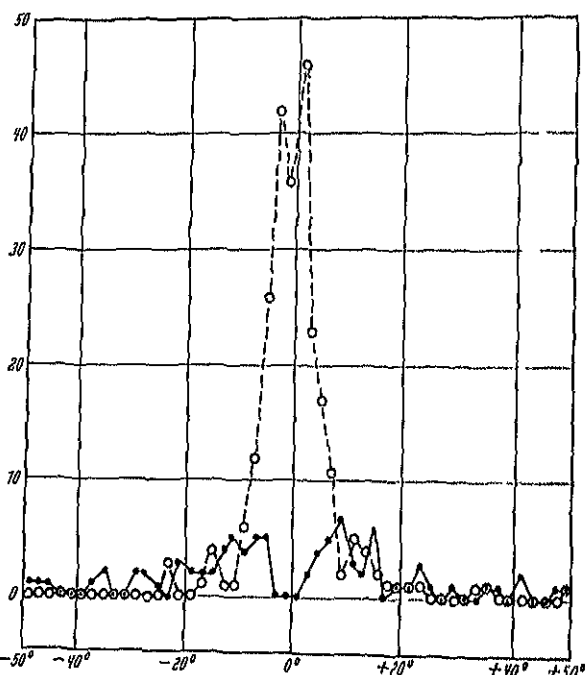


Fig 6 Numbers of galactic clusters (circles) and globular clusters (dots) for two degree intervals in galactic latitude

By implication, therefore, nebosity might be more common than appears from general appearance.

There are a few undivided globular clusters, N.G.C. 13, 2, N.G.C. 6144, and N.G.C. 6529, that are in or near recognized dark or luminous nebulae. Of these, the first appears to be dimmed by one of the long dark trunks from the Coal Sack; the second is at the edge of the heavy ρ Ophiuchi nebula; N.G.C. 6529 is in a rich star field in Sagittarius but may also be involved in wisps of obscuring nebulae.

To what extent the magnitudes and colors of galactic and globular clusters are directly affected by associated nebosity is not as yet determined. For individual nebulous stars SFARIS and HUMMER have found a color effect and presumably a corresponding deficiency in apparent brightness.

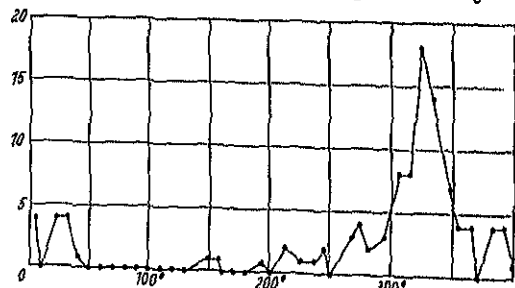


Fig 7 The frequency distribution of globular clusters in galactic longitude. Ordinates are numbers of clusters, abscissae, degrees of longitude

8. The Apparent Distribution of Globular Clusters.

In Figure 5 is shown the distribution of globular clusters; the remarkable contrast in the galactic affiliation of the galactic and globular clusters is shown in Figure 6. The equatorial and galactic coordinates of globular clusters are given in Appendix A, and a discussion of their distribution in space appears in later sections. The remoteness of these clusters suggests that obstruction by dark nebosity in the Milky Way can easily account for their observed scarcity near the galactic equator without seriously affecting at the same time the distribution of the nearer galactic clusters.

In Figure 7 is shown the distribution of globular clusters in galactic longitude. From this diagram and the preceding figure we find that the center of the system

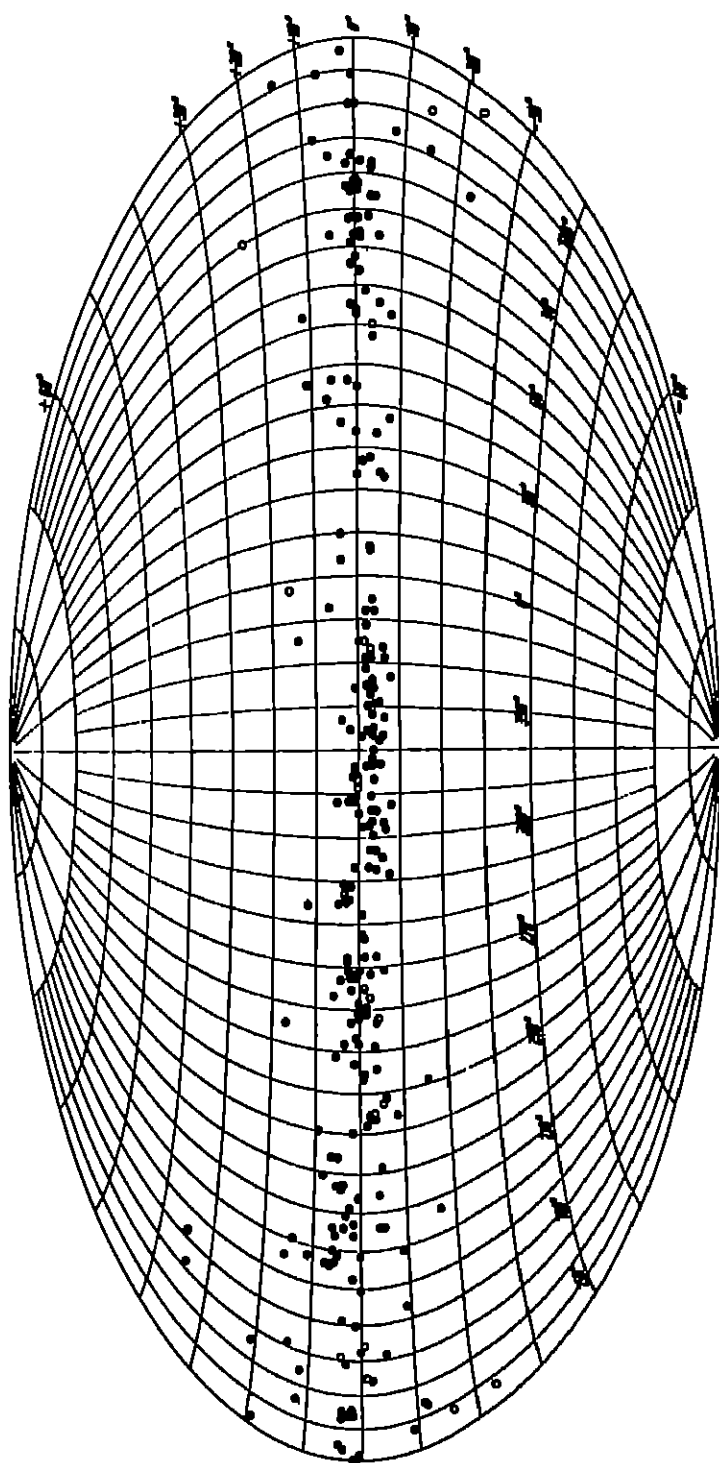


Fig. 8. Distribution of galactic clusters in galactic coordinates. Cluster classes are indicated as follows: c, o; d, \oplus , e, \odot , f, \odot , g, \bullet .

of globular clusters lies in the direction of galactic longitude 327° , galactic latitude 0° . The probable error of this determination is about one degree. The corresponding equatorial coordinates are right ascension $17^h 28^m$, declination -29° .

9. The Apparent Distribution of Galactic Clusters. The distribution of galactic clusters in galactic coordinates is shown in Figure 8. The high concentration in low latitudes is evident. The galactic clusters with latitudes greater than $\pm 15^\circ$ are given in Table 2. The high latitudes for Coma, Praesepe, the Pleiades, and the Hyades, are not remarkable, because the parallaxes are relatively large and the linear distances from the galactic plane are relatively small. The fainter galactic clusters in high latitude merit further detailed study.

Table 2. Galactic Clusters with Latitude Greater than $\pm 15^\circ$.

N.G.C.	Galactic		Remarks
	Longitude	Latitude	
188	90°	$+23^\circ$	
752	105	-23	
Melotte 22	134	-22	Pleiades
Melotte 25	147	-23	Hyades
2243	206	-16	
2281	142	$+18$	
2420	166	$+21$	
2548	196	$+17$	
2632	174	$+34$	Praesepe
2682	184	$+33$	Messier 67
Melotte 111	200	$+85$	Coma Berenices
I 4665	358	$+16$	

An interesting and significant result of the special surveys that have been made of objects once doubtfully classed is the evidence that nearly every faint little-condensed cluster in galactic latitude higher than 15° or 20° is really globular, although for many of them short exposures and visual observations had originally recorded few stars. Long exposures, however, bring out the globular nature of such clusters. Nearly all the similar faint objects along the galactic equator remain open groups, with no condensed background of faint stars appearing on long exposures.

10. Peculiarities in the Distribution of Galactic Clusters. The clusters listed in the catalogue in Appendix B do not extend deep into the galactic structure; they tell us nothing of the center or of the boundaries. There is significance, however, in certain peculiarities of their distribution. Already we have noted that in contrast with globular clusters they are rather uniformly dispersed in galactic longitude, and also that they are largely confined to the low galactic regions where globular clusters are scarce. There are two additional features of their distribution that are worth consideration: (1) the infrequency of galactic clusters in the first quadrant of galactic longitude; there are very few of these systems in the Aquila-Cygnus region of the Milky Way; (2) the narrow restriction of the clusters to low galactic latitudes in the direction of the galactic center and their wide dispersion in galactic latitude in the opposite part of the sky.

This second phenomenon might be explained as a consequence of the motions of galactic clusters in long orbits around the nucleus in Sagittarius. If their orbital inclinations differ from zero, when seen from the earth's eccentric position in the Galaxy those in the direction of the center would on the average appear to be in lower latitudes than those away from the center. It is probable that none of the galactic clusters that are now beyond the center of the Galaxy enters our catalogue.

The alternative and, I think, preferable interpretation is that galactic star clusters are associated largely with particular galactic star clouds. Irregularities of distribution and concentration in low galactic latitude are therefore merely consequences of the distribution of the nearer star clouds. If the galactic clusters are closely affiliated with various star clouds, we may find them differing systematically in spectral and structural characteristics from one part of the sky to another. We already have an indication of such diversity in the orientation of the axes of elongation, discussed in ciph 24 below. The brighter clusters of Auriga are rich and not strongly condensed (Messier 36, Messier 37, Messier 38); many of the small condensed clusters of Sagittarius are nebulous, and the groups in Carina are systematically bright.

c) On the Spectral Composition of Clusters.

11. Integrated Spectra of Globular Clusters. Integrated spectra were determined for several clusters many years ago at the Lick, Mount Wilson, and Lowell Observatories, mainly by FATH¹ and SLIPHER², who found spectra of composite character, principally classes F and G. The HENRY DRAPER Catalogue records without close classification the integrated spectra of numerous clusters.

Miss CANNON has recently examined closely all available Harvard photographs showing spectra of globular clusters³. The results are briefly summarized in Table 3, which gives the N.G.C. designation, the cluster class, and the spectrum. For some clusters, such as N.G.C. 4147 and 6624, the observed spectrum may be largely due to one or two stars, and they of course may be foreground objects.

Table 3 Spectra of Globular Clusters.

N.G.C.	Cluster Class	Spectral Class	N.G.C.	Cluster Class	Spectral Class
104	III	G5	6293	IV	G5
362	III	G5	6304	VI	K:
1261	II	G	6316	III	G5
1851	II	G0	6333	VIII	K.
1866	IV	F8	6341	IV	G5.
1904	V	F8	6356	II	K0
2808	I	K0	6388	III	K
4147	IX	A7:	6397	IX	G:
4590	X	Note	6441	III	K0
5024	V	Note	6541	III	G
5272	VI	G	6624	VI	M0
5286	V	G0	6626	IV	G5
5824	I	F8	6637	V	K2
5904	V	G.	6652	VI	K5
5986	VII	F8	6715	III	F8
6093	II	K0	6723	VII	G5:
6121	IX	F	6752	VI	G0
6205	V	G0	6864	I	G0
6229	VII	Note	6934	VIII	G0
6254	VII	Note	7078	IV	F
6266	IV	K0	7089	II	F5
6273	VIII	G5:	7099	V	F8
6284	IX	F:			

N.G.C. 4590 Dark lines are seen in the violet.

5024 Dark lines $H\delta$, H , and K faintly seen.

6229. Several dark lines are seen, apparently including H and K .

6254. Dark lines in the violet appear to be H , K , and $H\zeta$.

¹ Lick Bull 3, p. 74 (1908); Mt Wilson Contr 49 (1911).

² Pop Astr 25, p. 36 (1917), 26, p. 8 (1918)

³ Harv Bull 868 (1929).

A frequency diagram of the classes is given in Figure 9; classes F, G, and K of Table 3 are taken as F0, G0, and K0. The class of spectrum does not appear to be closely related to cluster class, apparent magnitude, or any other significant property of the clusters. We have here only an indication of the probable diversity

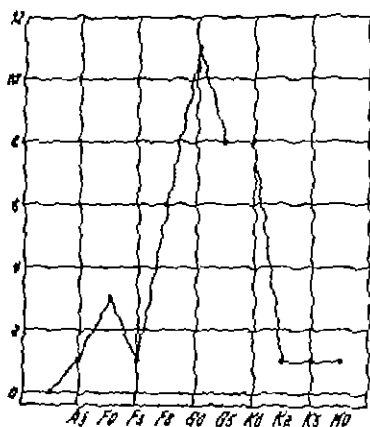


Fig. 9. Frequency curve of integrated spectra of globular clusters. Coordinates are numbers of clusters and spectral classes.

in predominant type of the stars that are effective in producing the integrated spectrum.

12. Stellar Types in Globular Clusters.

From integrated spectra and colors we pass to the types of individual stars in globular clusters, noting some similarities to the distribution of types in the Galaxy, but also some important differences.

a) Common Spectral Classes. The color indices in various globular clusters show a normal range¹ from about -0.3 to $+1.6$. This indicates, no doubt, the presence of all spectral classes from B to M; and normal spectra have in fact been directly observed from A to G. The average color index² in Messier 13 is -0.55 , corresponding to the spectrum gF4.

Seventeen per cent of the stars in Messier 13 brighter than the working limit (photovisual magnitude 15.5) have negative color indices. In Messier 3, on the other hand, there is a smaller proportion of negative color indices (4.7 per cent down to photovisual magnitude 17.00), but an excess of Class A stars of about the magnitude and color of the cluster type variables. It should be noted, however, that an error in the zero point of either photovisual or photographic magnitudes would shift the spectral frequency curve bodily. Such error may exist, and may not be inappreciable.

b) The Color-Magnitude Arrays. The distribution of color indices and photovisual magnitudes are shown for Messier 22 in Table 4. The tabulated quantities are numbers of stars³. The last tabulated line or two are near the practical fainter limit for magnitude work and may be deficient in numbers and inaccurate. The color classes, b, a, f, . . . , corresponding to the color index intervals⁴ -0.4 to 0.0 , 0.0 to $+0.4$, $+0.4$ to $+0.8$, . . . , are nearly analogous to the spectral classes B, A, F, . . . This analogy is close because the cluster stars under study are all giants; the agreement would not be so satisfactory for dwarfs.

In the array for Messier 22 the dispersion of magnitude within any one color class is conspicuously small. All stars are included which are brighter than the magnitude limit of the photovisual plates and within $5'$ of the center of the

¹ SHAPLEY, Mt Wilson Comm 44 (1917).

² SHAPLEY, Mt Wilson Contr 116 (1917); see also PRASE, Mt Wilson Ann Rep 9, p. 219 (1913); 10, p. 268 (1914); SANFORD, Mt Wilson Ann Rep 14, p. 212 (1918); Pop Astr 27, p. 99 (1919).

³ Harv Obs Mon 2 (1930); Harv Bull 874 (1930). TENBRUGGENCATE has plotted the coordinates (my magnitudes and colors) for the individual stars used in making the color-magnitude summaries for Messier 13 and Messier 3. (Die Sternhaufen, Berlin, 1927). I think there is little gain and some danger in detailed subdividing of the observational material. Experience with the photometric measures in globular clusters leads to a belief that the group values presented in my color-magnitude arrays go as far as is justifiable in subdivision.

⁴ SHAPLEY, Mt Wilson Comm 16 (1915).

Table 4¹ Color-Magnitude Array for Messier 22

Limits of Photovisual Magnitude	Color Class												> m 5	AB Colors
	< b0	b0 to b5	b5 to a0	a0 to a5	a5 to f0	f0 to f5	f5 to g0	g0 to g5	g5 to k0	k0 to k5	k5 to m0	m0 to m5		
10.20-.39	—	—	—	—	—	—	—	—	—	—	—	—	1	1
.40-.59	—	—	—	—	—	—	—	—	—	—	—	—	—	—
.60-.79	—	—	—	—	—	—	—	—	—	—	—	—	1	1
.80-.99	—	—	—	—	—	1	—	—	—	—	—	—	3	4
11.00-.19	—	—	—	—	—	—	—	—	1	—	—	3	3	7
.20-.39	—	—	—	—	—	—	—	—	—	—	3	6	—	9
.40-.59	—	—	—	—	—	—	—	—	—	2	2	1	—	5
.60-.79	—	—	—	—	—	—	—	1	1	2	1	1	—	5
.80-.99	—	—	—	—	—	—	1	2	5	1	1	—	—	9
12.00-.19	—	—	—	—	—	—	—	3	—	—	1	1	—	5
.20-.39	—	—	—	—	—	—	2	2	8	2	—	—	—	14
.40-.59	—	—	—	—	—	—	1	3	5	2	2	—	—	13
.60-.79	—	—	—	—	1	—	1	6	15	2	—	—	—	25
.80-.99	—	—	—	—	—	1	3	4	3	—	—	—	—	11
13.00-.19	—	—	—	—	—	1	1	4	3	1	—	—	—	10
.20-.39	—	—	—	—	—	1	6	9	3	1	—	—	—	20
.40-.59	—	1	—	—	1	8	6	6	1	—	—	—	—	23
.60-.79	—	—	—	—	1	12	28	16	—	—	—	—	—	57
.80-.99	—	—	1	1	4	34	59	7	—	—	—	—	—	106
14.00-.19	—	—	2	1	7	39	12	—	—	—	—	—	—	71
.20-.39	1	1	11	40	61	39	3	—	—	—	—	—	—	156
.40-.59	—	1	19	26	20	2	—	—	—	—	—	—	—	68
.60-.79	—	—	3	—	—	—	—	—	—	—	—	—	—	3
Totals . .	1	3	36	68	105	138	123	57	45	17	10	12	8	623

cluster It is of interest that more than six per cent of the stars have negative color indices, the cluster resembling² in this respect Messier 13 rather than Messier 3.

No correction has been made in the color-magnitude array for superposed stars. The cluster lies in a rich star cloud in Sagittarius, and probably ten per cent of the stars included in this discussion are not cluster members. The color-magnitude array is therefore applicable both to the cluster and to the star cloud, and the small dispersion in brightness of both together suggests that the two are associated. The color-magnitude arrays establish the fact that in the condensed clusters, as well as in some loose galactic groups, the average color is redder the higher the visual brightness. The result naturally bears on current considerations of the evolution of stars.

The general similarity of globular clusters, especially in the color-magnitude relation for giant and supergiant stars, is shown by a comparison of the brightest stars in Messier 3 and Messier 13 with the brightest stars in the faintest and most remote globular cluster known. N G.C. 7006 is five times as distant as Messier 3 and Messier 13, yet the most luminous stars in all three clusters have about the same average color and the same progression of color with magnitude. The mean results are as follows

	Mean Photographic Magnitude	Number of Stars	Mean Color Index
N.G.C. 7006	16.46	38	+1.09
Messier 3	13.17	35	+1.15
Messier 13	12.72	36	+1.02

¹ See Harv Bull 873 (1930)

² Mt Wilson Contr 155, p. 8 (1918).

A similar result is found in all globular clusters tested, though some, such as N.G.C. 4147 and N.G.C. 5053, are less populous in giant stars.

13. On the Masses of Giant Stars. The color-magnitude array can be transformed into a relation between spectral class and mass by means of the observed mass-luminosity relation for galactic stars. It is necessary to assume that we can safely replace color class by spectral class for giant stars; the uncertainties involved both in this assumption and in the temperature scale, used for reduction from photovisual to bolometric magnitude, are not negligible, but still they are not serious enough to falsify the results except for stars of extreme color. It is possible that the chief source of error lies in the mass-luminosity curve itself, which depends mainly on nearby double stars and possibly is inappropriately applied to single stars, especially in a globular cluster.

The computation of the stellar masses in terms of the sun's mass for successive intervals of magnitude and color has been carried through for Messier 22; the results are shown in Table 5. The distance modulus, $m_{pv} - M_{pv} = 14.16$,

Table 5. The Mass-Spectrum Relation for Messier 22.

Apparent Pv. Mag.	Spectrum	Absolute Pv. Mag.	Absolute Bol. Mag.	Mass
11.2	M2.5	-2.96	-4.62	29:
.4	K9.0	-2.76	-4.10	22.4:
.6	K5.8	-2.56	-3.72	17.8
.8	K3.0	-2.36	-3.13	14.1
12.0	K1.0	-2.16	-2.74	11.7
.2	G9.0	-1.96	-2.41	10.0
.4	G7.0	-1.76	-2.10	8.3
.6	G5.5	-1.56	-1.84	7.4
.8	G4.0	-1.36	-1.58	6.5
13.0	G2.5	-1.16	-1.30	5.9
.2	G1.2	-0.96	-1.16	5.4
.4	F9.8	-0.76	-0.80	4.8
.6	F7.8	-0.56	-0.58	4.5
.8	F5.8	-0.36	-0.36	4.1
14.0	F3.0	-0.16	-0.16	3.9
.2	A9.5	+0.04	+0.04	3.7
.3	A6.8	+0.14	+0.07	3.6
.4	B7.5	+0.24	+0.49	5.7

is taken from Appendix A; the reduction to bolometric magnitudes and the computation of the masses are made with the aid of tables given by EDDINGTON¹. The masses of the reddest stars would have been from ten to twenty per cent less with BRILL's scale of temperatures and corrections to bolometric magnitude². The values of photovisual magnitude and spectrum in Table 5 are read directly from the curve drawn through a plot of the colors and magnitudes of the individual stars that appear in the color-magnitude array.

Masses for the average giant stars of various spectral classes in Messier 22 are as follows:

A0	<4.8	F5	4.0	K0	10.8
A5	<3.5	G0	4.9	K5	16.5
F0	<3.6	G5	7.0	M0	24.0

It is possible to give only upper limits of average mass for classes A0, A5, and F0 because of the incompleteness of the observational material for the corresponding intervals of color index.

¹ Internal Constitution of the Stars, Chapter VII (1926).

² Babelsberg Veröff 5, p. 16 (1924).

For the rich galactic cluster Messier 37, VON ZRIPEL and LINDGREN find the mass of the giant g5 stars 2.15 times as large as the average mass of the b and a stars¹, in good agreement with the present results. They have used space distribution of the stars as a criterion and a measure of the masses of different types.

It is interesting to note the small dispersion in color for stars of a given photovisual magnitude. Accepting the mass-luminosity relation, we can only conclude that in a globular cluster such as Messier 22 the giant stars of a given mass have a very small spread in surface temperature.

14. Spectra in Individual Galactic Clusters. Numerous investigations have been made of the colors and magnitudes of galactic clusters, notably by TEN BRUGENCATE, DOIG, GRAFF, HERTZSPRUNG, PICKERING and FLEMING, RAAB, SEARES, SHAPLEY, TRUMPLER, and VON ZRIPEL and LINDGREN². The HENRY DRAPER Catalogue contains spectral data for only the brightest clusters. The Harvard material is discussed first, followed by brief accounts of a few individual clusters and the spectral classification of clusters by TRUMPLER.

a) Harvard Studies. Mrs. FLEMING³ tabulated the spectra for seven galactic clusters, the Pleiades, Praesepe, Coma Berenices, I.C. 2602, N G C. 3592, Messier 6, and Messier 7. The stars for which spectra are classified are distributed over a larger area than that actually covered by the clusters, and foreground stars of course cannot generally be differentiated and excluded. Some very faint stars, barely distinguishable on the plates, are included. The results are summarized for Class A in Table 6.

Table 6. Percentage of Class A Stars in Seven Galactic Clusters.

Cluster	Stars Classified	Stars in H.D.C.	Percent Class A
Pleiades	91	*	65
Praesepe	90	*	31
I.C. 2602	64	58	77
N G C 3592	204	135	93
Coma	117	*	15
Messier 6	91	75	75
Messier 7	346	177	78

* Limits indefinite.

Although the classification was crude, and for some stars quite uncertain, the existence is clearly shown of a different spectral distribution in Praesepe and Coma from that in the other five clusters. It is the same distinction that is now recognized in the Pleiades and Hyades types, or in TRUMPLER's types 1 and 2⁴.

The frequency of A stars in galactic clusters has led to attempts to determine spectral parallaxes on the basis of the material of the HENRY DRAPER Catalogue⁵; but because of the wide dispersion in magnitude the attempts are not always happy.

b) Spectra in the Brighter Galactic Clusters. The Pleiades⁶, the Hyades, and Coma fall under the head of "very loose and irregular clusters",

¹ Svenska Vet Akad Handl 61, No. 15, p. 126 (1921).

² See bibliography in Harv Mon No. 2 (1930).

³ R. C. PICKERING, Harv Ann 26 (1897); see also Table 6.

⁴ Publ A S P 37, p. 307 (1925). See note 1, p. 705, on his later work.

⁵ DOIG, J B A A 35, p. 201 (1925); RAAB, Lund Medd, Série II, No. 28 (1922).

⁶ HERTZSPRUNG, M N 89, p. 660 (1929). See also Harv Bull 764 (1922).

division c in the classification of galactic clusters in ciph 5. Figure 10 shows for the Pleiades the spectrum-magnitude relation as compiled by HERTZSPRUNG¹. The spectral data on η Persei, Messier 11, and two southern clusters may be summarized as follows:

1 The Double Cluster in Perseus. Sixty-six bright stars in the double cluster in Perseus, classified mainly by TRUMPLER², range in spectrum from A0 to B9, and in magnitude from 5.5 to 10.9. Two matters of exceptional interest

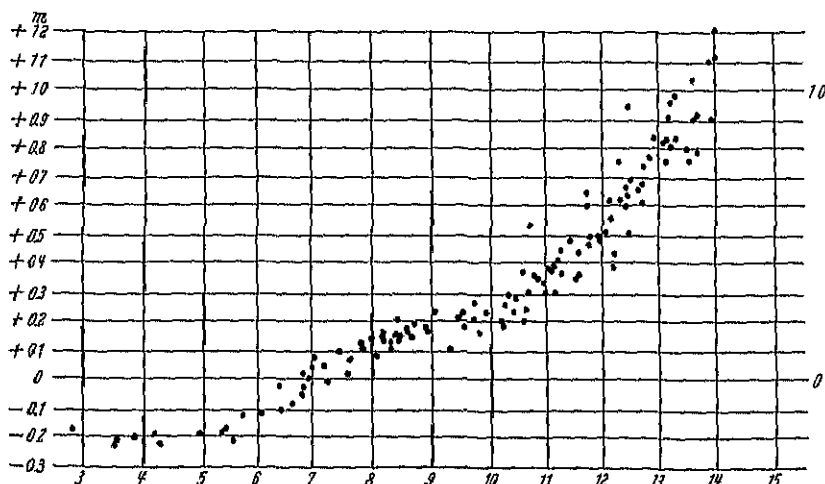


Fig 10 Relation of color to luminosity in the Pleiades. Ordinates, color indices, abscissae, photographic magnitudes. (From HERTZSPRUNG.)

in this cluster are the fact that a large number of the brighter stars show the c-character, and that the numerous bright line stars are by no means the brightest members of the cluster.

2 Messier 11. In supplementing my earlier work on the colors in Messier 11, I found³ from plates made with the 100-inch reflector at Mount Wilson that the brighter spectra are chiefly of class A. This observation was later verified by LINDBLAD on other Mount Wilson spectrograms. The spectral classes of fifty-nine stars in and around the cluster have since been given by TRUMPLER⁴.

3 NGC 3532 and NGC 3766. The distribution of spectra in two southern galactic clusters has been derived by BECKER from his own photographs made at La Paz⁵. He finds percentages as follows:

	B0-B7	B8-A1	A5-A8	K0	K4	Number of Stars
NGC 3532	3.8	86.3	1.5	8.4	—	131
NGC 3766	44.2	39.5	4.7	—	11.6	13

¹ M N 89, p 660 (1929)

² Publ A S P 38, p 350 (1926)

³ The magnitudes determined for this cluster are apparently in error, probably by a constant amount, notwithstanding the consistency of the Mount Wilson photometric plates [Mt Wilson Contr 126 (1917)]. The color indices are systematically too great, as shown by my own spectrum plates (unpublished), and subsequently by the similar work of LINDBLAD and TRUMPLER. A correction of -0.4 to the photographic magnitudes is indicated by an unpublished Harvard plate, but even then the colors and spectra are inconsistent. There is a probability of differential light absorption within the cluster.

⁴ Lick Bull 12, p 10 (1924)

⁵ A N 236, p 327 (1929)

For N G C 3532 Mrs. FLEMING recorded ninety-three per cent of the 204 stars as Class A¹

c) TRUMPLER's Investigations The kinds of spectral distribution among the stars of a galactic cluster, first recognized in the early Harvard work, and amplified by all subsequent studies, are defined in some detail in TRUMPLER's scheme of classification (ciph. 5 above), and a number of galactic clusters have now been assigned by him to the classes and their subdivisions. For fifty-two clusters the relative numbers in the various classes are as follows

Type	Number	Type	Number
1b	24	2f	1
1a	6	Others	1
2a	20		

It will be seen that the Pleiades type preponderates among the systems bright enough to classify. This may, however, be an effect of selection, as Type 1b contains far brighter stars than any of the others. The bearing of this selection on estimates of distance is considered on page 748, footnote 1.

d) Variable Stars in Star Clusters.

15. The Frequency and General Properties of Variable Stars in Clusters.

Periods have been determined for 466 variable stars discovered in forty-five globular clusters²; all but nineteen are found to be cluster type Cepheids. There is a slight correlation between frequency and galactic latitude, the rich clusters having a greater mean distance from the galactic plane than have the poor. The latter are distributed equally throughout all classes, while the rich clusters are confined to the intermediate classes. It seems unlikely that observational selection is responsible for this result; the effect, however, may be due in part to the decreased discovery chance in a very condensed cluster.

The general properties of variable stars are discussed elsewhere³. There is no evidence that the Cepheid variables in clusters, whether of short or long period, are different in their various characteristics from those in the Galaxy at large. The color changes and light curves are of the usual sort. The long period variables in 47 Tucanae are also normal in period, range, and form of light curve.

Certain features of cluster variables, however, are to be noted. The great majority are, on the average, 1.5 to 2.0 magnitudes fainter than the brightest stars in the cluster (see ciph. 34 below). There is observed, particularly in ω Centauri, Messier 3, Messier 5, and Messier 13, a definite fainter limit to the magnitudes of Cepheids, similar to that found in Miss LEAVITT's survey⁴ of the Magellanic Clouds. The negative results of the searches for faint variables, and the form of the period-luminosity curve, which flattens conspicuously for periods less than a day, suggest that dwarf Cepheids do not occur. There is likewise no convincing evidence of eclipsing binaries in any globular cluster⁵; but the faintness of such stars would preclude their discovery on most of the existing plates.

The peculiarities of variables in clusters lie in the relative numbers of different types and subtypes as compared with those in the galactic system, galactic star clouds, or the Clouds of Magellan; but it is to be noted that very serious factors of incompleteness and selection affect the comparison of clusters

¹ See Table 6 above.

² Previous to 1930.

³ LUDKENDORFF, volume VI, chapter 2.

⁴ Harv Circ 173 (1912).

⁵ But see GUTHRIE and PRAGER, *Sitzber Preuss Akad Wiss* 1925, p. 508.

with the Galaxy, and also that there appear to be just as great differences in variable star content between clusters as there is, say between ω Centauri or 47 Tucanae and the solar neighborhood

18. A Summary of Known Variables. Despite a careful search, few variable stars are definitely known to belong to galactic clusters, some that have been tentatively assigned to such systems are of unrecognized type, and probably lie in the surrounding star fields. Many have been found, however, in globular clusters, as remarked above. The history of their discovery is short. Examining some of his earlier photographs, Dr. COMMON¹ first noted the probable variability of some stars in Messier 5. Professor E. C. PICKERING² in 1889 and Mr. DAVID PACKER³ in 1890 also made some early observations of the variables in globular clusters, which were independently confirmed by BARNARD a few years later.⁴ But the whole development of this special branch of variable star astronomy is essentially due to Professor BAILEY, whose extensive research on globular clusters, begun about thirty years ago, is the basis of much of our knowledge concerning cluster variable stars. Employing mainly the photographs made at Arequipa with various telescopes, BAILEY has found the majority of cluster variables now known, and has made by far the most important investigations of light curves and periods. Aside from BAILEY's work, the discovery and study of the variables has been almost exclusively the work of Miss WOODS at Harvard, BAADJE and LARINK at Bergedorf, and the writer and his collaborators at Mt. Wilson and Harvard [see references in Harv Mon No 2 (1930)]. LARINK has made an extensive check of BAILEY's periods for cluster-type variable stars in Messier 3, finding that, after a twenty-year interval, 82 periods were unchanged and 29 probably had varied. My similar check on 54 of BAILEY's variables in Messier 5 results in periods accurate to within a tenth of a second; in this cluster nearly all the periods are constant throughout an interval of thirty years.

The data at present available concerning the variable stars in globular clusters are summarized in Table 7. Clusters examined with care but without discovery of variable stars are also included in the table. Some stars suspected of variability are omitted in the absence of numerous or decisive observations. Three of these, for instance, are in the Hercules cluster⁵, where my measures on a few plates can not be considered to furnish sufficient evidence of variability. In crowded regions and for close doubles the photographic development (EBERHARD) effect⁶ may produce spurious variability, for it varies from plate to plate under ordinary working conditions. Aside from this and similar uncertainties, which lead to the inclusion and exclusion of suspected variables, there is another element of incompleteness in these tabulated results because of the difficulty of thoroughly examining the centers of clusters, and also because of the small number of plates sometimes involved in the surveys. In general it may be said that scarcely a cluster has been examined with the accuracy and thoroughness necessary to detect ordinary eclipsing stars of short range or narrow minimum, and to exhaust the possibility of Cepheids of small range.

¹ M N 50, p 517 (1890), 51 p 226 (1891)

² A N 123, p 207 (1889), Harv Circ 2 (1895)

³ Sid Mess 6, p 381 (1890), 10, 170 (1890), Engl Mech 51, p 378 (1890).

⁴ A N 147, p 243 (1898)

⁵ SHAPLEY, Mt Wilson Contr 116, p 79 (1915)

⁶ EBERHARD, Z f Phys 13, p 288 (1912), Publ Astrophys Obs Potsdam No 84,

Table 7 Summary of Variables in Clusters.

N.G.C.	λ	β	Class	HIP- licity	Vari- ables	Period		Sus- pected	References
						<14	>14		
104	272°	-44°	III	8	7	—	3	—	1, 2
288	214	-88	X	9	2	—	—	—	3
362	268	-46	III	8	14	—	—	—	1
1851	211	-34	II	9	3	—	—	—	4, 5
1904	195	-28	V	9	5	—	—	—	1
2419	148	+23	VII	9	26	—	—	—	40
3201	244	+10	X	9	61	—	—	—	6, 7
4147	227	+78	IX	—	4	—	—	8	8, 42
4590	268	+37	X	9	28	27	1	—	9, 10
4833	271	-8	VIII	8	5	—	—	—	5
5024	307	+79	V	9	42	—	—	—	11, 12, 41
5053	310	+77	XI	8	9	8	—	—	13
5139	277	+16	VIII	8	132	95	5	—	1, 14
5272	8	+77	VI	8	166	110	1	79	1, 15, 16, 17, 18, 19
5286	280	+10	V	9, 5	—	—	—	—	20
5466	8	+70	XII	9	14	12	—	—	12
5904	333	+45	V	9	84	69	3	8	1, 21
5986	305	+13	VII	—	1	—	—	—	1
6093	320	+18	II	10	4	—	—	—	1, 39
6121	319	+15	IX	9	33	3	—	5	22
6205	26	+40	V	9, 5	7	1	2	3	1, 17, 23, 24
6229	41	+39	VII	—	1	—	—	—	8
6266	320	+7	IV	8	26	—	—	—	1
6293	325	+8	IV	9	3	—	—	—	25
6333	333	+10	VIII	9	1	—	—	—	3
6341	35	+34	IV	8	14	—	—	—	17, 26
6362	293	-17	X	8	17	—	—	—	27, 28
6397	304	-12	IX	9	2	—	—	—	1
6426	356	+15	IX	9	2	—	—	—	40
6539	348	+6	X	9	1	—	—	—	29
6541	317	-12	III	9	1	—	—	—	30
6553	333	-4	XI	9	—	—	—	2	25
6584	310	-18	VIII	9	—	—	—	—	20
6626	336	-7	IV	9	9	—	—	—	1
6656	338	-9	VII	8	21	9	2	4	1, 31, 32, 33
6712	353	-6	IX	—	1	—	—	—	8
6723	327	-18	VII	9, 5	17	16	—	—	1, 34
6752	303	-26	VI	—	1	—	—	—	1
6779	30	+7	X	8	1	—	—	2	25, 35
6809	335	-24	XI	9	2	—	—	—	1
6864	348	-28	I	9	11	—	—	5	25, 36
6981	3	-34	IX	—	29	29	—	5	8, 25, 36
7006	32	-20	I	—	11	11	—	—	25, 37
7078	33	-29	IV	8	74	60	1	—	1, 21
7089	22	-37	II	9	11	—	1	—	1, 38
7099	356	-48	V	9	3	—	—	—	1
7492	23	-65	XII	9	9	—	—	5	3

1 BAILEY, *Harv Ann* 38, p. 2 (1902) 2 BAILEY, *Harv Bull* 783 (1923). 3 Mt Wilson Observatory, unpublished. 4 BAILEY, *Harv Bull* 802 (1924). 5 Miss SWOFF, unpublished. 6 Miss WOODS, *Harv Circ* 216 (1919) 7 BAILEY, *Harv Circ* p. 234 (1922) 8 Miss DAVIS, *Publ A S P* 29, p. 260 (1917). 9 SHAPLEY, *Mt Wilson Contr* 175 (1920). 10 SHAPLEY, *Publ A S P* 31, p. 226 (1919). 11 BAADÉ, *Hamburg Mitt* 5, No. 16 (1922) 12 BAADÉ, *Hamburg Mitt* 6, No. 27 (1928). 13 BAADÉ, *Hamburg Mitt* 6, No. 29 (1928) 14 INNES, *Union Circ* 59, 201 (1923). 15 SHAPLEY, *Mt Wilson Contr* 91 (1914). 16 SHAPLEY, *Mt Wilson Contr* 176 (1920) 17 GUTHRIE and PRAGER, *Sitzber Preuss Akad Wiss* 1925, p. 508. 18 LANDAU, *Bergedorf Abhandlungen* 2, No. 6 (1921) 19 BARNARD, *A N* 172, p. 345 (1906). 20 BAILEY, *Harv Bull* 801 (1924) 21 BAILEY, *Harv Ann* 78 (1917) 22 Miss LEAVITT, *Harv Circ* 90 (1904) 23 R A J 1, p. 16 (1924) 24 SHAPLEY, *Mt Wilson Contr* 116 (1917) 25 SHAPLEY, *Mt Wilson Contr* 190 (1920) 26 Miss WOODS, *Harv Bull* 773 (1922). 27 Miss WOODS, *Harv Circ* 217 (1919). 28 Miss WOODS,

(Continued next page below.)

e) The Distribution of Stars in Globular Clusters.

17. Are Cluster Stars Arranged Spirally? In order to determine whether the frequently described spiral structure in or near the center of globular clusters could be seen on large scale photographs, I made a series of exposures on bright northern globular clusters some years ago with the Mount Wilson reflectors. The exposures varied in length. When only a few hundred stars were shown in a cluster, the spiral structure could almost invariably be traced, if the exposures were longer, the spiral arms became inconspicuous, or another set of arms, sometimes with different center and pitch, was found or imagined. The conclusion was reached that the phenomenon is wholly illusory. The significance to be attached to chance groupings and chance vacancies decreases remarkably with increasing exposure time. Nebulous obscurations that are reported to conceal the brighter stars are found, upon deeper penetration, to be ineffective for the more numerous faint stars, and therefore they cannot be real.

Spiral structure is the easiest form to visualize in centrally concentrated random groupings—especially when the number, pitch, thickness, origin, length, symmetry, and definiteness of the spiral arms are all arbitrary. Structural features other than flattening and central concentration may be present, but it is certainly inadvisable to conclude definitely, from knowledge of only a small percentage of the total number of the stars, that such structure occurs. Probably in only one globular cluster (Messier 22) have stars as faint as the sun been photographed, and in only a few of those studied for stellar distribution have stars other than giants or supergiants been thoroughly examined.

The *a priori* argument against the existence of spiral form in the images of globular clusters is, of course, simply that the clusters are three-dimensional. Cleanly traceable spiral arms would mean a most remarkable and unbelievable arrangement of stars in systems that are always nearly spherical. The discussion in ciph. 22 of the ellipticity of globular clusters will show how little they are flattened. Even the images of the much sparser galactic clusters are very rarely so elongated that we can assume them to be essentially two-dimensional.

18. On the Laws of Distribution. The first detailed numerical consideration of the space arrangement of stars in globular clusters was made by Professor E. C. PICKERING¹, who examined the distribution in ω Centauri, 47 Tucanae, and Messier 13, and proposed general empirical relations connecting surface density, γ , with the distance from the center, r , in the forms

$$\gamma = \int (1 - r^2) dz$$

and

$$\gamma = \int (1 - r)^n dz$$

Subsequently much time has been devoted to studies of the laws of the distribution of stars in globular clusters. Various formulae relating the number of stars per unit volume, N , with distance from the center of the projected image

¹ Harv Ann 26, Chap XI (1897)

unpublished, 29 HUBBLE, letter 30 Miss Woods, Harv Bull 764 (1922), see also
A N 215, p 391 (1922) 31 Harv Bull 848 (1927) 32 Zö-Sé Annals 10 (1918)
33 BAILEY, Pop Astr 28, p 518 (1920) 34 BAILEY, Harv Circ 266 (1924) 35 Mis
DAVIS, Publ A S P 29, p 210 (1917) 36 Mt Wilson Contr 195 (1920) 37 Wash Na
Ac Proc 7, p 152 (1921) 38 CHÈVREMENT, B S A F 12, pp 16, 90 (1898) 39 BAILEY
Harv Bull 798 (1924) 40 BAADÉ, letter of June 8, 1932 41 GROSSE, A N 246, p 2
(1932). 42 BAADÉ, A N 230, p 353 (1930).

r , or with ϱ , the distance from the cluster center, have been derived (or assumed) and applied to published counts of stars. We have, for instance, from VON ZEIPPEL,

$$N(\varrho) = \frac{1}{\pi} \int_0^R \sqrt{r^2 - \varrho^2} \frac{d}{dr} \left(\frac{1}{r} \frac{dn}{dr} \right) dr$$

where R is the radius of the cluster and n is the number of stars in the corresponding unit area of the projected image.

The problem of finding a law of space distribution from the law of apparent distribution in a globular star system has been solved by VON ZEIPPEL, who has been the leader in the attempt to deduce the structure of clusters from observation of stellar distribution. He was the first to utilize in this problem the principles of the theory of gases. Analogies with the kinetic theory have encouraged a number of theoretical and observational researches, but as yet no completely satisfactory representation of the observations has been found.

It seems unnecessary to treat in detail the history, methods, successes, and failures of these various investigations of distribution. No other phase of the study of globular clusters has been so frequently and thoroughly described. Special attention should be called, however, to the discussions by H. C. PLUMMER, TEN BRUGGENCAT, STRÖMGREN, EDDINGTON, JEANS, PARVULESCO, and MARTENS¹. A further important step has been made by VON ZEIPPEL and LINDGREN, who proceed, from the assumption that the stars of different masses are distributed in equilibrium in relation to surrounding stars, to the determination, from the observed distribution, of the mean masses for various color classes and absolute luminosities. They have used the method with success in the study of the rich galactic cluster Messier 37, and WALLINQUIST has further discussed their analysis and applied the method to his own study of the magnitudes in Messier 36. FREUNDLICH and HEISKANEN have provisionally applied it to the study of the distribution of stars in globular clusters, but the observational material is yet too uncertain for satisfactory results.

That the discussions of the adiabatic or isothermal distributions of stars in globular clusters have been unsatisfactory in practice is not surprising, since the data from which comparisons have been made are inherently faulty. The best chance for improvement and successful application of the theory lies in the few rich galactic clusters from which the foreground and background stars can be satisfactorily differentiated. For the globular clusters, however, the crowded centers and the attendant difficulties with BIERHARD effect and background contrast vitiate the counts, except for the outer parts. Furthermore, the available counts deal with only the few hundred or few thousand supergiant stars; tens or hundreds of thousands of fainter stars, which must play a major rôle in stellar distribution, have not yet appreciably entered the investigations. TEN BRUGGENCAT has recognized the importance of ellipticity in the distribution of stars in globular clusters, but otherwise all discussions of the problem have ignored this lack of radial symmetry.

The star counts that have been used for the study of globular clusters are almost exclusively those of BAILEY at Harvard and of PEASE and SHAPLEY at Mount Wilson. Photographs on a larger scale are needed. Special attention should be given to the brighter and more open globular clusters (ω Centauri, N.G.C. 3201, N.G.C. 6397), and also to "giant-poor" anomalous systems and those clusters like N.G.C. 2477 that are possibly intermediate between the globular

¹ See references in Harv Mon No 2 (1930). See also the later papers by HECKMANN and SCHNECKTOFF, Zf Phys 54, p. 183 (1929) and Zf Astrophys 1, p. 67 (1930).

and the galactic types. Tables and figures of the distribution of the stars in globular clusters are given for several of the brighter clusters by PICKERING, PLUMMER, VON ZEIPPEL, and HECKMANN and SIEDENFOPF.

In conclusion, we must admit that the situation is not very hopeful. The frequency is (roughly) inversely proportional to the fourth power of the distance from the center, this holds only for giant stars in the typical globular clusters. The law of distribution of fainter stars is even less definitely known. We find them more widely dispersed than the giants, but we can say nothing of their distribution within the central sphere of ten parsecs diameter, where the crowding of brighter stars "burns out" the photographs.

The distribution of brightness in a globular cluster as a function of distance from the center has been investigated by HERTZSPRUNG for Messier 3, by HOGG and by NABAKOV for Messier 13, and by SCHILT for ω Centauri.¹

19. Luminosity Curves for Stars in Clusters. Distribution in absolute brightness as well as in space can be satisfactorily studied as yet only for the giant and supergiant cluster stars. Although, as we have seen, the space distribution is not independent of the influence of dwarf stars, the fragmentary absolute luminosity curves have a meaning and a certainty that are essentially unimpaired by such forced neglect of the dwarfs. Moreover, with the use of more powerful telescopes, especially on the borders of bright southern clusters in high galactic latitude, we shall soon be able to extend both the general luminosity curves and the luminosity curves for specific color classes to stars as faint as the sun or fainter. In the near future we should therefore have for the globular clusters much more satisfactory data on the frequency of luminosities than we now have for stars of the general galactic system.

The labor of determining magnitudes and colors on a satisfactory photometric basis is so considerable that luminosity curves will come slowly, for only three globular clusters are the color and magnitude surveys at all extensive. It is necessary, therefore, to resort for the time being to general luminosity curves based on provisional magnitude scales, except for the giant stars in the three systems for which results are herewith presented.

a) **Frequency Distribution of Giant Stars.** Observations of frequency distributions in Messier 3, Messier 13, and Messier 22 are combined to give Table 8. Results are tabulated for six intervals of color class redder than f0. Stars redder than k5 are grouped together, since the data are insufficient for class m alone, for classes b and a the observational limits cut off the luminosity curves so quickly that the results are not significant. Probably the curve for class f is also affected both by the confluence of giant and dwarf series and by the magnitude limitations of the catalogues. Distance moduli used for reduction from apparent to absolute photovisual magnitudes are taken from Appendix A. The absolute photovisual magnitude limits of the catalogues are +0.4 for Messier 22, +0.5 for Messier 13, and +1.6 for Messier 3. The table is therefore of low weight for stars fainter than $M_{pv} = +0.5$. The preliminary maximum at 0.0 for interval f0 to f5 is probably related to the humps in the general luminosity curves of these three clusters (Figure 11), which are caused mainly by an abundance of blue stars and variables. The average dispersion of absolute magnitude for the various intervals of color is about half a magnitude, which is probably well in excess of the observational errors.

¹ HERTZSPRUNG, A N 207, p 89 (1918), NABAKOV, R A J 1, p 109 (1924), HOGG, Harv Bull 870 (1929), SCHILT, A J 38, p. 109 (1928), Pop Astr 36, p 296 (1928). See also HOGG's recent discussion of the luminosity distribution in six globular clusters A J 42, p 77 (1932).

Table 8. Composite Luminosity Curve of Messier 3, Messier 13, Messier 22

Absolute Photo- visual Magnitude	Color Class						All Colors
	to 15	15 to g0	g0 to g5	g5 to k0	k0 to k5	> k5	
-4.0 to -3.5	—	—	—	1	1	1	3
-3.5 to -3.0	1	—	—	1	—	11	13
-3.0 to -2.5	—	2	—	5	13	18	38
-2.5 to -2.0	1	1	5	16	11	5	39
-2.0 to -1.5	1	7	34	32	6	2	83
-1.5 to -1.0	8	24	28	32	4	1	97
-1.0 to -0.5	18	85	71	20	1	—	195
-0.5 to 0.0	103	136	73	7	1	—	320
0.0 to +0.5	91	132	44	5	1	—	273
+0.5 to +1.0	38	31	8	1	—	—	78
+1.0 to +1.5	85	31	1	—	—	—	117
Totals	346	449	264	120	38	38	1255

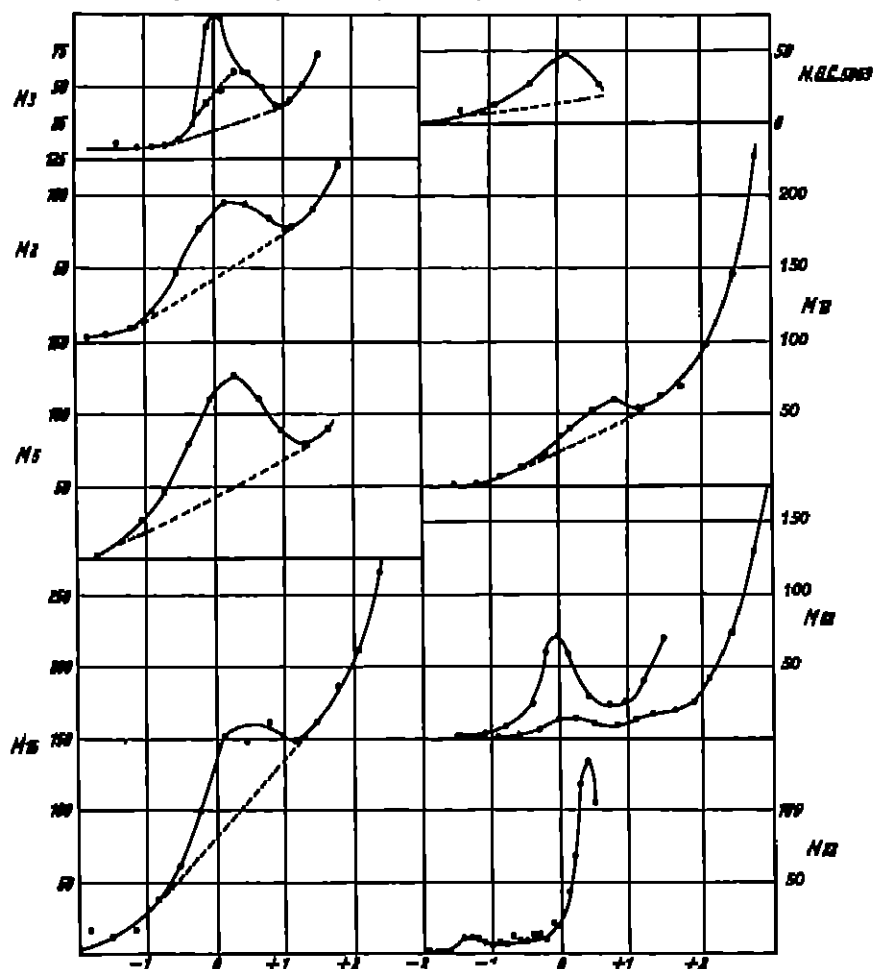


Fig. 11 Luminosity curves for eight globular clusters. Ordinates are numbers of stars, abscissae are photographic absolute magnitudes (approximate).

Until we have obtained data from other clusters, there is little point in fitting the usual exponential curves to the observations. Some of the asymmetries

may be real in the curves representing magnitudes and practically disappear in the corresponding curves showing the distribution with respect to total radiation or mass

b) **The Preliminary Maximum** General photographic luminosity curves based on provisional magnitude scales are given in Figure 11 for eight globular clusters. All the plotted material except that for N G C 5053 is derived from my work on Mount Wilson plates. The methods of estimating the magnitudes and some of the numerical data are published elsewhere¹. The curves suggest two general comments, which are followed below by a few special notes on the individual clusters

1 There is a considerable variety in form, an indication of the impropriety of using any method of parallax determinations that depends on the form of only the brightest portion of the general luminosity curve

2 Without exception, all the globular clusters show preliminary maxima, which fall within half a magnitude of the median magnitude of cluster type variables, as indicated by the two heavy vertical lines in Figure 11. We have evidence in all of these globular clusters, though it is not shown graphically for N G C 5053 and Messier 22, that the general luminosity curve rises steeply and high for stars fainter than the critical absolute luminosity near absolute magnitude zero. The bunching of stars at this particular brightness is probably of considerable significance in the economy of globular clusters. The resultant hump in the luminosity curves has possibilities in the measurement of distance

3 Details concerning Figure 11

a) The preliminary maximum for Messier 3 is partially due to the hundred and fifty known variable stars, when the cluster type variables are omitted from the diagram we have the milder and fainter hump shown by the broken line and small circles

b) For Messier 2, Messier 5, and Messier 15 the variable stars have not been excluded, but they are not sufficiently numerous, even in Messier 5, to contribute much to the very conspicuous preliminary maxima

c) The somewhat fragmentary luminosity curve for N G C 5053 is derived from data published by BAADÉ², with variables excluded

d) The preliminary maximum for Messier 13 is built up largely by stars of small or negative color index; the cluster has no definitely recognized cluster type Cepheids

e) For Messier 68 the two luminosity curves result from stars in different selected areas, measured on two plates. The curves are in fair agreement, a second preliminary maximum at $M = +1.4$ is suggested

f) The fragmentary luminosity curve for Messier 22 is based on an unpublished catalogue, prepared at Harvard from my Mount Wilson photographs. The wide displacement of the maximum from absolute magnitude zero suggests that the correct distance may be ten to twenty per cent larger than that given in Appendix A; but further work on the magnitudes of the fainter stars is necessary before anomalies of the luminosity curve can be taken seriously.

f) The Forms of Clusters.

20. Definition and Difficulties. By the ellipticity of globular clusters we may choose to refer either to the symmetrical elongation of integrated images on photographs, or to the systematically greater number of stars along one axis of the projected image than along any other, as determined by detailed star

¹ Mt Wilson Contr 155 (1917), 175 (1919)

² Hamburg Mitt 6, No 29 (1928)

counts Both of these phenomena can be explained most naturally by assuming that the clusters are oblate — that is, that the gradient of the space density of the stars differs in different directions from the center and is usually symmetrical about a polar axis and an equatorial plane. Probably the forms of the integrated photographic images are related as directly to star density as are the counts.

It is difficult, however, to determine the actual bounds of a globular cluster along various radii, or even the limits of the projected image, because of (1) the unknown and possibly peculiar density laws in different directions for a flattened stellar system, (2) the confusion with foreground stars, (3) the present lack, near the edges of individual clusters, of sufficiently long exposures made with large reflectors.

The detection of the planes of symmetry, moreover, depends on the degree, the orientation, and the nature of the ellipticity. Thus, if the ratio of minor to major axis is near unity, if the polar axis is nearly parallel to the line of sight, or if the property of concentration toward a plane is confined to the fainter unobserved stars in the cluster, the successful analysis of form is impossible.

Early studies of globular clusters, such as BAILY's star counts¹, dealt with but one or two thousand stars in each cluster, while the underlying ellipticity usually becomes evident only when large numbers of stars are considered. Consequently, nothing very definite was known of the important fact of deformation until the systematic star counts on Mount Wilson photographs were analyzed². Later it was noted that the numerous faint stars frequently make their presence known en masse as well as in detailed counts, so that the diffuse integrated images of clusters photographed with small telescopes can be used to study cluster forms, even if few or no individual stars are shown. The counts, however, are sometimes more searching. For example, in Messier 13, described below, the Harvard plates do not show, on inspection, the marked ellipticity revealed by the counts, they indicate, if anything, a slight elongation in a direction 45° from the major axis. The same is true of some other clusters. When an integrated image is clearly elliptical, the numerical ellipticity shown by star counts is very large. In a condensed cluster the LEBERHARD effect and other difficulties may interfere seriously with the determination of the frequency of stars as a function of the distance from the center, but errors arising from such sources do not affect measures of the orientation of the major axis of the cluster image.

21. The Elongation of Messier 13. Among the globular clusters whose forms were investigated by the writer, partly in collaboration with Mr. PRASE, Mrs. SHAPLEY, and Miss SAWYER, the Hercules cluster, Messier 13, best illustrates the nature of the ellipticity throughout a wide range in magnitude.

The stars in Messier 13 were counted on nine plates, and the results arranged for analysis in a framework of twelve equal radial sectors and a series of concentric rings³. The plates are of various exposure times, ranging from one minute to five hours. The counts of the total number of stars in each of the twelve equal sectors show the amount of ellipticity and its change with magnitude. The counts for each of the zones between concentric circles show how the degree and direction of ellipticity varies with distance from the center of the cluster.

In Table 9 the numbers of stars are given for six different plates for each sector separately, but with the zones not differentiated. For the two photographs of longest exposure Table 10 again gives the number of stars in different sectors, but divides the material into four zones for each plate. The central regions are too much burned out to be included in the star counts.

¹ *Harv Ann* 76, No. 4 (1915).

² PRASE and SHAPLEY, *Mt Wilson Contr* 129 (1917).

Table 9. Ellipticity for Different Exposures in Messier 13.

Duration of Exposure	Total Number of Stars	Number of Stars in Sectors											
		15°	45°	75°	105°	135°	165°	195°	225°	255°	285°	315°	345°
6 ^m	5800	163	149	211	235	214	213	154	154	174	256	235	198
15	7700	296	264	433	396	420	314	284	230	259	401	309	305
22	14150	734	672	744	859	814	638	569	583	684	825	852	738
37.5	16600	749	770	913	1008	1026	853	779	804	974	1011	963	763
94	25000	1261	1340	1475	1590	1580	1431	1338	1343	1486	1500	1580	1361
300	30000	1126	1234	1254	1416	1463	1232	1079	1085	1187	1300	1368	1258

Table 10. Ellipticity and Distance from Center in Messier 13.
(Results from two plates.)

Distance from Center	Number of Stars in Sectors											
	15°	45°	75°	105°	135°	165°	195°	225°	255°	285°	315°	345°
2' to 4'	623	668	750	762	764	728	712	683	758	778	718	670
4' to 6'	358	361	423	464	476	386	330	352	402	438	479	394
6' to 8'	168	207	212	236	226	202	188	194	214	248	249	198
8' to 10'	112	104	90	128	114	115	108	114	112	126	134	99
3' to 5'	560	640	624	684	788	642	586	597	629	658	712	662
5' to 7'	362	374	410	471	431	360	302	292	358	396	424	394
7' to 9'	204	220	220	261	244	230	191	196	200	246	232	202
9' to 11'	141	136	116	118	130	129	131	124	130	157	134	100

The ellipticity is illustrated in Figure 12, which shows the amount and position angle of the elongation at different distances from the center. The cluster is

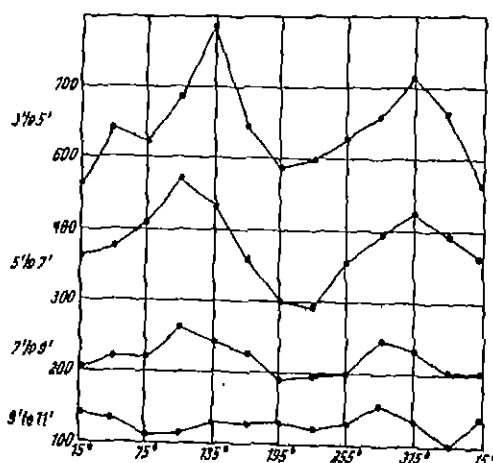


Fig. 12. Ellipticity of Messier 13 for different intervals of distance from the center. Ordinates are numbers of stars and abscissae are position angles.

seen, from these tables and from the figure, to be conspicuously elongated, showing approximately twenty-five per cent more stars in the direction of the major axis than in the direction perpendicular thereto. The ellipticity, which shows throughout the cluster from center to edge, appears in all magnitudes from the thirteenth to the twentieth and fainter, though it is relatively inconspicuous for the stars brighter than the fifteenth magnitude.

22. Ellipticity and Orientation of Globular Clusters. Over half a million stars have been counted in the course of the Mount Wilson and Harvard studies of the forms of globular clusters. By means of star counts the position angles of the major axes have been found for

twelve systems, and evidence of approximate circularity or asymmetry adduced for a few others¹. Direct estimates of the position angles for the integrated images of most of these clusters are found to agree closely with those determined from the laborious counts; hence further surveys of the forms have been made using only the direct estimates of ellipticity on small scale plates.

¹ H. SHAPLEY and MARTHA B. SHAPLEY, Mt Wilson Contr 160 (1918).

a) Orientation of Major Axes The ellipticity and orientation given in columns 13 and 14 of Appendix A are based on a Harvard investigation¹, except for starred values which are taken from the earlier Mount Wilson counts². The ellipticity is expressed as ten times the ratio of the minor to the major axis. The orientations, with respect to the galactic circle, are given only for those thirty-nine clusters in which the ellipticity is 8 or less, or if 9, only when the orientation could be certainly determined³. The orientation with respect to the galactic circle is reckoned from the "galactic east" (direction of increasing longitude) through the "galactic south"; negative angles consequently indicate reckoning from the east in the opposite direction.

b) Inclination to Galactic Circle The data bearing on the relation of the elongation to the plane of the Galaxy are collected for thirty-seven globular clusters in Table 11 (N.G.C. 1866 and N.G.C. 1978, in the Large Magellanic Cloud, are omitted from the table).

Table 11 Orientation of Globular Clusters

N G C	Class	Galactic Latitude	Distance from Galactic Plane kpc	Degree of Elongation	Inclination to Galactic Circle
104	III	-45°	- 4.8	8	-55°
362	III	-47	- 9.4	8	+65:
1851	II	-34.5	- 8.1	9	-75
1904	V	-28	- 9.6	9	+ 5
2298	VI	-15	- 6.9	8	+39
2419	VII	+23	+11.9	9	-56
2808	I	-11	- 3.1	8	+84
4833	VIII	- 8.5	- 2.2	8	-80°
5024	V	+79	+17.9	9	-79
5053	XI	+78	+17.0	8	-61
5139	VIII	+15	+ 1.8	8	+30
5272	VI	+77.5	+11.9	8	+54
5897	XI	+29	+ 8.0	8	-44:
5904	V	+46	+ 7.8	9	+16
6101	X	-16	- 5.7	8	+35
6121	IX	+15	+ 1.9	9	+72
6139	II	+ 6	+ 3.1	9	-64
6144	XI	+15	+ 4.8	8	-22.
6203	V	+40	+ 6.6	9.5	-63
6235	X	+12	+ 5.9	8	+89
6266	IV	+ 7	+ 2.3	8	+16
6273	VIII	+ 9	+ 2.6	6	-28
6341	IV	+35	+ 6.4	8	+16:
6356	II	+ 9	+ 7.8:	9	-14
6362	X	-18	- 4.7	8	+78:
6397	IX	-12.5	- 1.2	9	+73
6402	VIII	+14	+ 4.8	9	+76
6440	V	+ 2	+ 1.7:	8	+10:
6441	III	- 6.5	- 2.2	8	+40
6517	IV	+ 6	+ 5.2	8	- 4:
6626	IV	- 7	- 2.0	9	+18
6638	VI	- 7.5	- 3.9	8	-27
6652	VI:	-13	- 5.3	8	-11:
6656	VII	- 9	- 1.1	8	+18
6779	X	+ 8	+ 2.8	8	+12:
7078	IV	-28	- 6.1	8	+11
7089	II	-36	- 8.2	9	-80

¹ SHAPLEY and SAWYER, Harv Bull 852 (1928).² SHAPLEY, Mt Wilson Comm 45 (1917).³ That is, position angles without a colon in Harv Bull 852 (1927).

Although the estimates here presented are probably better than any previously made, I feel that they are not of much significance except for the few clusters for which the ellipticity is conspicuous and the orientation angle is given without a colon. The average deviation of a position angle from the values previously determined¹ from FRANKLIN-ADAMS charts is about 30° , an indication of the inherent difficulty of the estimates. Some of the clusters are definitely asymmetrical. For most of those not listed in Table 11 the deviations from circularity are small, or the clusters are too faint or too involved in a star field for useful determinations of form. Notwithstanding the difficulties and uncertainties, for all but eighteen of the ninety-three clusters in Appendix A the degree of ellipticity is estimated.

Attention should be paid in the future not so much to small and difficult objects as to closer analyses of the distinctly asymmetrical systems and of the brighter clusters in which the degrees of ellipticity can be studied with respect to colors and magnitudes. From detailed investigations, as VON ZEDEL has shown, we may hope to get information on the masses of stars of different colors and luminosities, using as criteria of mass the distribution with respect to the centers and to the hypothetical galactic planes within the clusters².

Although the estimates of orientation are admittedly uncertain, the measures show definitely that large and small values are scattered throughout all distances from the galactic plane. In order that the equatorial plane of a cluster be parallel to the plane of the Galaxy, parallelism of the major axis with the galactic circle is a necessary though not a sufficient condition. We need to know the true form, or an equivalent, and get another component of the inclination, before we can fix the plane of the cluster in space; at present there is little prospect of measuring the true oblateness³. The equatorial planes in the clusters with low inclinations of course may or may not be parallel to the galactic plane; those with high inclinations are certainly not parallel. There is no good evidence as yet that the clusters are not inclined at random in space.

23. Some Peculiar Clusters. A few globular clusters that depart considerably from a spherical form have been studied. They are of interest in connection with the possible dissolution of clusters and also in considerations of the distribution laws.

a) Messier 3 (N.G.C. 5272), Messier 5 (N.G.C. 5904), and Messier 62 (N.G.C. 6266). It is difficult to account for such pronounced and deep-seated asymmetries in globular clusters as those of Messier 3, Messier 5, and Messier 62. For Messier 3 the distance from other stellar systems is now, and probably for hundreds of millions of years has been, extremely great; the galactic latitude is $+77^\circ.5$. There is no evidence of occulting matter in the cluster or in front of it that might be responsible for a spurious appearance of irregularity. The measure of asymmetry is illustrated by the following data⁴, based on the counts of two Mount Wilson plates, the numbers of stars being given for thirty degree intervals of position angle:

Position Angle	15°	45°	75°	105°	135°	165°	195°	225°	255°	285°	315°	345°
Number of Stars	244	234	246	220	198	242	222	282	292	321	303	263

Further work should be done on this cluster, as the counts on different plates are not wholly consistent.

¹ H. SHAPLEY and MARTHA B. SHAPLEY, Mt Wilson Contr 160 (1918).

² FREUNDLICH and HEISKANEN, Z f Phys 14, p. 226 (1923).

³ See discussion by TEN BRUGGENCATE, Die Sternhaufen p. 72 (1927).

⁴ FEASE and SHAPLEY, Mt Wilson Contr 129 (1917).

For Messier 5 we have comparable data from a long exposure plate showing 15000 stars, made by PRASE and counted by Miss DAVIS¹, the star numbers referring to a region between 3' and 15' from the cluster's center.

Position Angle	15°	45°	75°	105°	135°	165°	195°	225°	255°	285°	315°	345°
Number of Stars . . .	924	1016	972	861	693	783	870	978	1037	955	907	952

The asymmetry of Messier 62 is shown numerically in the following counts based on a Mount Wilson photograph, a central burned-out area one minute in diameter being excluded

Position Angle . . .	15°	45°	75°	105°	135°	165°	195°	225°	255°	285°	315°	345°
Number of Stars . . .	67	56	67	45	35	42	49	56	68	79	72	72

When opposite sectors are combined, the position angle of the major axis appears to be about 75°, the values of the angle estimated from the integrated image² are 70° and 55° for two independent determinations.

Messier 62 is the most irregular globular cluster. Does absorbing nebulosity cause its apparent asymmetry? Or has collision or encounter deformed it?

b) Messier 19 (N.G.C. 6273). Figure 13 and the estimated ellipticities in Table 11 show that Messier 19 is the most elongated globular cluster so far studied. The circular coordinates of the diagram are position angles; the radial coordinates are relative numbers of stars in each thirty-degree sector. The position angle of the major axis of the diagram is 15°, and along this axis there are more than twice as many stars as along the minor axis. Photographs show no evidence of a double nucleus. Since the galactic latitude is +9°, and the major axis is inclined less than thirty degrees to the galactic circle, the equatorial plane of the cluster is probably nearly parallel to the galactic plane.

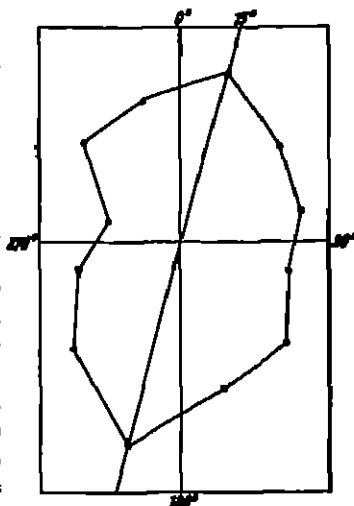


Fig 13. Diagram of star density in Messier 19

Considering this extreme example, we conclude that the flattening of a cluster is systematically of a lower order than that of spirals and the galactic system

c) Messier 22 (N.G.C. 6656). The form of globular clusters near the galactic plane may have an important bearing on the relationship of the Galaxy and galactic clusters to the globular systems. Messier 22, in galactic latitude -9° and one of the nearest globular clusters, is significantly situated for a test of deformation and of the orientation of its central plane. On a photograph which shows more than seventy thousand stars from the twelfth to the twentieth magnitude, most of which are undoubtedly members of the cluster though it is located in the direction of a rich galactic star cloud, a detailed count has been made³.

The number of stars in the direction of the major axis is nearly thirty per cent greater than the number along the minor axis. The orientation of only 18° and the high ellipticity, which suggests that we see the cluster edgewise, indicate that it may lie nearly parallel to the galactic plane.

¹ SHAPLEY and DAVIS, Publ. A.S.P. 30, p. 164 (1918)

² Mt. Wilson Contr. 160, p. 7 (1918); Harv. Bull. 852, p. 25 (1927).

³ SHAPLEY and DUNCAN, Pop. Astr. 27, p. 100 (1919)

d) ω Centauri (N G C 5139) The 128 cluster type variables in ω Centauri appear to lie preferentially along the equatorial plane of the system Table 12 and Figure 14 illustrate this remarkable distribution¹ The data are obtained

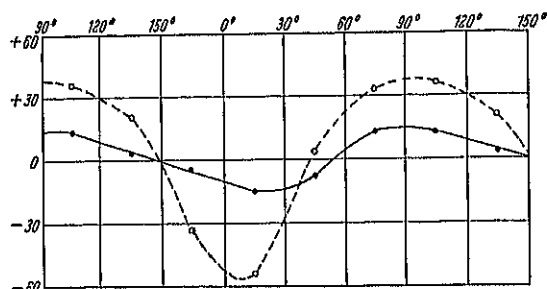


Fig 14 The distribution of stars in ω Centauri Ordinates are percentage excesses along the various radii indicated by the position angles (abscissae) The full line shows that the position angle of the major axis for all stars is about ninety degrees For the variables alone (broken line) the axis is about the same, but the relative excess is three times as great

from Harvard plates, which show the ellipticity for all distances from the center.

Table 12 Distribution of 5000 Stars in ω Centauri (Results from two plates)

Width of Zone	Sectors												Mean
	15°	45°	75°	105°	135°	165°	195°	225°	255°	285°	315°	345°	
3' to 6'	148	129	151	182	165	159	164	173	203	182	198	163	168
6 to 9	84	89	151	142	139	113	105	119	153	163	125	117	125
9 to 12	66	81	96	74	64	79	64	68	88	97	74	68	77
12 to 15	44	54	61	61	57	57	40	59	57	59	51	45	54
3 to 9	232	218	302	324	304	272	269	292	356	345	323	280	293
9 to 15	110	135	157	135	121	136	104	127	145	156	125	113	130
3 to 15	342	353	459	459	425	408	373	419	501	501	448	393	423
Variables	8	6	17	12	9	5	2	16	11	17	16	9	11

The numbers of variables in opposite sectors are combined in making the diagram. The relative amplitudes of the two curves show that towards the supposed plane of symmetry the variables are three times as condensed as the stars in general, and the latter exhibit such strong ellipticity that ω Centauri is easily seen to be elongated on all photographs

24. The Structure of Galactic Clusters. a) Orientations. Only for the comparatively rich and compact galactic clusters is it possible to estimate the orientation. The loose systems—classes a, b, and c—are generally of too indefinite size and membership to show significant boundaries Eighty-one clusters are found sufficiently condensed for examination, of these, fifty-seven show measurable orientations Taken as a whole, the clusters appear to be oriented at random, within the uncertainty of the determinations In points of detail, however, we see that the average inclination to the Galaxy differs from place to place, so that in some regions the clusters appear to be mainly aligned with the galactic circle, in others they are oriented approximately at right angles to it² Tables 13 and 14, showing the mean inclination for intervals of galactic longitude and latitude respectively, indicate that there is no correlation of orientation with either longitude or distance from the galactic plane.

¹ Mt Wilson Comm 45 (1917)

² Harv Mon 2, sec 33 (1930), see also COLLINDER, I und Circ No 2 (1931).

Table 13 Longitude and Inclination

Mean Galactic Longitude	Number of Clusters	Mean Inclination	Mean Galactic Longitude	Number of Clusters	Mean Inclination
82° 6	5	60°	242° 2	6	30
128° 0	5	55	279° 1	5	62
156° 5	5	33	302° 3	5	53
183° 5	5	42	322° 3	5	31
201° 7	5	44	337° 6	6	33
217° 9	5	50			

Table 14 Inclination and Distance from Galactic Plane

Mean Radius (in parsecs)	Number of Clusters	Mean Inclination	Mean Inclination	Number of Clusters	Mean Radius (in parsecs)
677	5	45°	80°	7	69
425	5	38	70	5	203
265	5	47	66	4	167
196	5	34	59	7	279
143	5	51	47	5	215
100	5	52	40	5	131
62	5	47	29	6	281
30	5	39	18	5	175
17	6	53	12	4	222
6	6	47	4	4	108

b) The "shoulder" effect. A peculiarity in the distribution of stars has been observed in a number of galactic clusters, and leads to the conclusion that their dimensions are much larger than at first appears. Messier 67 plainly exhibits this unusual distribution. A summary of the average star density, photovisual magnitude, and color index is given in Table 15 for 232 stars of the cluster. There is no decrease of star density, or change of average magnitude or color outside a circle of 6'.5 radius about the center of the cluster, but inside that circle the density, brightness, and redness of the stars increase towards the center.

Table 15. Average Star Density, Photovisual Magnitude, and Color Index in Messier 67

Distance from Center	No. of Stars	Area in Sq. Minutes	No. Stars per Square Minute	Av. Pv. Mag.	Average Color Index	Number of Stars	
						Background	Cluster
0'.0—2'.5	35	19.6	1.78	12.49	+1.00	6	29
2'.5—4'.5	64	44.0	1.45	12.85	+1.00	13	51
4'.5—6'.5	49	69.1	0.71	12.32	+0.91	21	28
6'.5—8'.5	30	94.3	0.32	13.03	+0.81	28	2
8'.5—10'.5	34	119.5	0.28	13.06	+0.82	36	(-2)
10'.5—11'.5	20	69.1	0.29	13.11	+0.80	21	(-1)
Total	232	—	—	—	—	123	107

If it is assumed that the constant density outside the circle of radius 6'.5 refers to the background or foreground stars, the cluster appears to be composed of about one hundred stars scattered over an area of radius 6'.5. Further study, however, indicates that the evidence is misleading. The background density of 0.3 stars per square minute is nearly ten times as large as would be expected for the galactic latitude and the photovisual magnitude concerned. This condition suggests that the cluster with radius 6'.5 is merely a well-marked nucleus of brighter and redder stars in a much larger system. Further counts made on WOLF-PALMA photographic charts of all stars within a degree of the center of the cluster show that the system extends far beyond the limits of the plates used

for the magnitude work. The real diameter may be as much as one degree. If Messier 67 is roughly spherical in form, the space occupied by the nucleus is about a hundredth of the total volume of the cluster. The total membership is approximately five hundred stars between photovisual magnitudes ten and fifteen, but only the central concentration of one hundred and fifty stars is noticeable in an ordinary survey.

The "shoulder" effect has appeared in studies of Messier 11, Messier 37, and other galactic clusters. TRUMPLER found it in Praesepe, the Pleiades, and in Perseus¹. The change of radius with magnitude (outside the nucleus) is shown for in Perseus in Figure 15, based on data accumulated by VAN MAANEN and

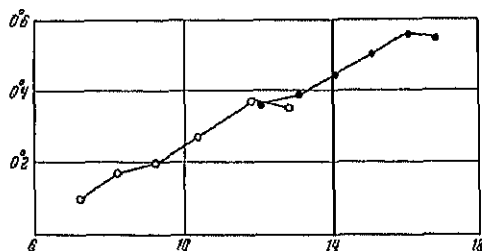


Fig 15 Relation of radius to magnitude for in Perseus. Ordinates are distances from the center in degrees, abscissae, photographic magnitudes. (From TRUMPLER)

TRUMPLER, the effect is even more pronounced for the Pleiades and Praesepe.

c) Additional Remarks on Galactic Clusters. Various other studies have been made of the structure of galactic clusters. Of especial value is the work of VON ZEIPPEL and LINDGREN on the magnitudes and distributions in Messier 37. The luminosities tabulated by them (Table 16) illustrate the double maximum for class a stars, a phenomenon that may be of some value in estimating the distances of galactic clusters. From the space distribution for different magnitudes and colors they have determined, by the ingenious method devised by VON ZEIPPEL, the approximate mean masses of the stars of various spectral classes. The method has been applied by WALLENQUIST to other galactic clusters.

Table 16 Luminosity Curves for Various Color Classes in Messier 37

Limits of Magnitude	Color Classes					
	b	a	f	g	k	m
] 11.0	0	2	0	0	0	0
11.0—11.5	0	4	1	1	0	0
11.5—12.0	0	12	0	5	0	0
12.0—12.5	7	21	0	10	0	0
12.5—13.0	8	18	0	1	0	0
13.0—13.5	20	16	3	0	1	0
13.5—14.0	5	37	2	0	0	0
14.0—14.5	3	29	7	1	0	0
14.5—15.0	1	19	16	3	1	0
[15.0	0	2	38	9	1	0

KÜSTNER and CHEVALIER have made accurate modern catalogues of positions in several galactic clusters, which will be of importance for future analyses of proper motions. Photographic and photovisual magnitudes of stars in Messier 35, Messier 36, and other northern clusters, as determined by WALLENQUIST, afford material for the discussion of bolometric magnitudes, luminosity curves, density laws, and probable mean masses, as well as star colors. The ratio of field stars to cluster stars for five thousand stars in the faint northern cluster NGC 7789 is shown in Table 17². It is well to observe from the first line that the rapidly decreasing ratio does not mean the total absence of dwarf stars from the cluster, or even their relative scarcity.

¹ Allegheny Publ 6, No 4 (1922)

² Mt Wilson Contr 190, p 7 (1920)

Table 17 Star counts for NGC 7789

Photographic Magnitude Interval	1-16	16-17	17-18	18-19	19-20	Total
Cluster Stars	347	210	155	266	126	1104
Field Stars	592	256	666	1178	1475	4167
Ratio	0.59	0.82	0.23	0.23	0.09	—

The structure of well known moving clusters and streams of stars, such as the groups in Taurus, Ursa Major, Scorpio, and Perseus, has been treated by numerous writers¹. The group motions are essentially parallel to the galactic plane, though the clusters are flattened variously with respect to the direction of motion; the flattening of the Perseus and Ursa Major clusters is at right angles to the direction of motion, while the Scorpio group is flattened parallel to the galactic plane, and the Hyades cluster is nearly spherical

g) The Transparency of Space.

25. Early Investigations of Light Scattering In all researches on the structure of the stellar universe the possibility of the loss of light in its passage through interstellar space must be recognized. If the loss of visual light due to absorption or scattering in space should be as much as a millionth of one per cent in each hundred million miles, stars thirty-five hundred light years away would appear about two magnitudes too faint. Uncertainty in the coefficient of scattering is, therefore, very serious in studies of the distances of faint stars.

The early work on light scattering indicated high absorption in space. KAPTEYN² in 1914 derived a coefficient, expressed in stellar magnitudes per parsec, of 0.0003, corresponding to a change of a tenth of a magnitude in color index for each three hundred parsecs of distance. At the beginning of the work on star clusters at Mount Wilson (1915) the following values were on record for the increase of color index with each parsec of distance³.

Observer	JONES	KAPTEYN	KING	TURNER	VAN RHIJN
Coefficient	0.00047	0.00031	0.0019	0.0030	0.00015

In all work yielding positive results the stars of small proper motion have appeared to be redder. In view of the fact that small proper motion is now recognized as characteristic of highly luminous stars, this excess of redness is to be regarded as merely a correlate of bright absolute magnitude, rather than as indicative of light scattering. The work of SEARES and others has clearly shown differences in color for giants and dwarfs.

There remains, however, some evidence of a tenuous local cloud of absorbing matter, estimated by KING⁴ as extending to a distance of thirty parsecs, reddening the stars at the rate of $d = 0.0003$ magnitudes per parsec, but affecting more distant stars only by a constant (and negligible) amount.

A more decisive test of light scattering is to be found in the study of colors of objects at much greater distances, such as those of globular clusters.

26. Blue Stars in Messier 13. After KAPTEYN's work on light scattering, and the contemporary results of KING, JONES, and VAN RHIJN, which independently confirmed it, the discovery in 1915 of stars with negative color indices in Messier 13 was unexpected⁵. A critical examination of photovisual and photographic magnitude scales failed to assign the apparent blueness of the cluster

¹ See references in Appendix D of Harv Mon No 2 (1930).

² Mt. Wilson Contr 83 (1914).

³ See references in bibliography of Harv Mon No 2 (1930)

⁴ Harv Circ 299 (1927)

⁵ Mt. Wilson Contr 116 (1915)

stars to observational error. Out of 495 stars with well determined color indices, 86 were found to be of color class b, and 63 of class a.

With a scattering coefficient of $d = 0.0003$ (KAPTEYN's last value), and an assumed distance for the cluster of as little as a thousand parsecs, practically no negative colors should appear if the stars are of usual spectral classes. With the obviously better parallax of $0''.0001$, the color index produced by KAPTEYN scattering should be $+3.0$ for stars of spectral class A, and many color indices should be greater than $+4$ in a typical distribution of spectral classes. It was found from the Mount Wilson photometric work that the range of color index

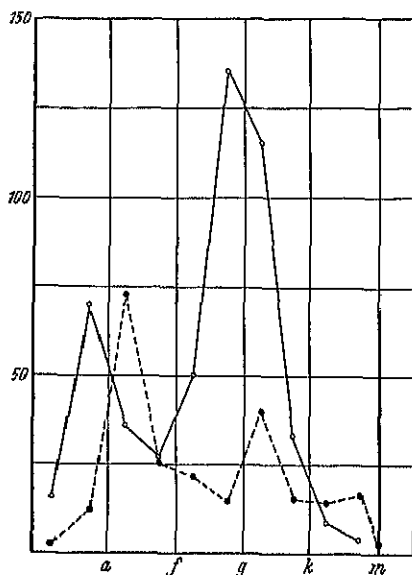


Fig 16 Frequency of color classes in Messier 13 (full line) and in the neighborhood of the sun (Yerkes Actinometry). Coordinates are relative numbers of stars and color classes.

observed in Messier 13 is the same as that found among nearby galactic stars, as illustrated in Figure 16. (The direct correspondence of color class with spectral class in this cluster has been verified by the spectrograms made by PEASE¹). There are no color indices in the cluster larger than $+2$. The largest admissible color excess appears to be about $0^m.1$, and, even if this excess is attributed entirely to light scattering, we derive $d = 0.00001$, a twentieth of the value derived by KAPTEYN, and a fifteenth of the value found by VAN RIJN from a consideration of the stars in the Yerkes Actinometry.

The foregoing upper limit of scattering is so small as to be entirely negligible in dealing with nearby stars in high galactic latitudes, but a more accurate value is desirable, and fortunately it can be found from studies of external stellar systems.

27 Faint Blue Stars in the Milky Way. The galactic latitude of Messier 13 is $+40^\circ$. That light scattering is absent in this direction is no proof that it does not occur elsewhere, especially in low galactic

latitudes where stars and diffuse nebulosity are concentrated. To make the test more comprehensive with respect to galactic latitude and longitude, the search for negative color indices has been carried out in several distant cluster systems, on the assumption that a normal range of color index and the presence of numerous blue stars are strong evidence of the transparency of space in the directions and to the distances considered. The results are in Table 18, where the observed extremes of color are shown in the fourth and fifth columns, and, in the next two columns, the mean photovisual magnitude and mean color index for a group (usually ten) of the faintest blue stars. The distances in the last column are taken from the tables in Appendices A and B.

Similar results have been obtained for faint stars in four Milky Way fields², and SEARIS has found faint blue stars in the Selected Areas that fall in low galactic latitude.

Considering the relatively large distances of the tabulated objects, and their wide distribution, we appear justified in generalizing the results of the

¹ See ciph 12

² SHAPLEY, Mt Wilson Comm 44 (1917)

Table 18 Test for Space Transparency in Various Regions

Cluster	Galactic		Color Index		Mean P _v Mag.	Mean Color Index	Distance in Kiloparsecs
	Longitude	Latitude	Largest	Smallest			
Messier 3	12°	+78°	+1.77	-0.39	15.1	-0.16	12.2
13	27	+40	+1.42	-0.52	16.54	-0.34	10.3
15	33	-28	+1.50	-0.21	16.0	-0.14	13.1
38	139	+1	+2.12	-0.45	13.5	-0.16	1.1
36	142	+1	+1.50	-0.30	12.5	-0.23	1.2
35	154	+3	+1.31	-0.15	11.5	-0.07	0.8
50	189	-1	+2.00	-0.04	12.3	-0.02	0.8
5	332	+46	+1.67	-0.11	14.6	-0.10	10.8
22	338	-9	+2.05	-0.45	14.34	-0.28	6.8
11	355	-3	+2.06	-0.16	14.32	-0.08	1.2

study of Messier 13, and in concluding that interstellar media, throughout the distances here concerned, have no serious effect on the color of light. This conclusion does not bear on obstruction of light by recognised diffuse nebulosity (dark and bright), nor on the colors of nebulous stars¹, nor on the absorption within galactic clusters which has been found lately by several investigators and sometimes interpreted, perhaps prematurely, as evidence of strong general space absorption.

28. Colors in Other Distant Objects. The magnitudes and color indices of thirty-eight supergiant red stars in N G C 7006 have been measured². Even at a distance more than five times that of Messier 13, no abnormal redness appears in this cluster, and there is no other peculiarity in its star colors, although its radiation has travelled through space for an interval of 180000 years. The mean color index of 1.10 for the brightest thirty-five stars, which is comparable with that of 1.15 for Messier 3 and 1.03 for Messier 13, shows that the reddening does not exceed a tenth of a magnitude. Therefore the absorption coefficient, expressed as change of color index for each parsec of distance, is $k < 0.000002$.

This same coefficient of space absorption was found by LUNDMARK and LINDBLAD³ in a study of the Andromeda Nebula. Investigations at Harvard of the cloud of three hundred bright extra-galactic nebulae in Coma and Virgo⁴ have resulted in the determination of the coefficient, $k < 0.00000007$.

29. Messier 5 and the Relative Speeds of Blue and Yellow Light. One significant consequence of the study of variables in Messier 5 has been a determination of the relative speeds of light of different wave lengths. Periods ranging from six to twenty hours, with an average of thirteen hours, have been found for a large number of stars; many of them are known to within a fraction of a second⁵. The steep rise to maximum brightness of a typical cluster type Cepheid variable makes the time of median magnitude on the ascending branch more accurately determinable than the times of maximum or minimum. It was found by WENDELL at Harvard and by the writer at Princeton that the time of median magnitude can be determined to within two or three minutes.

For the revision of the periods and for the test of the speed of light I made five special series of photographs of Messier 5 in 1917, using the 60-inch reflector of the Mount Wilson Observatory. The exposures of twenty to thirty minutes

¹ SHAPLEY and HUBBLE, Mt Wilson Contr 187 (1920)

² SHAPLEY, Mt Wilson Contr 165, p 5 (1918); see also SHAPLEY and MAYBERRY, Mt Wilson Comm 74 (1921).

³ Ap J 50, p. 386 (1919). Through an error the value is printed ten times too small.

⁴ SHAPLEY and AMES, Harv Circ 294 (1926)

⁵ Harv Ann 73, Part 2 (1917), Harv Bull 763 (1922), Harv Repr 5 (1923), Wash Nat Ac Proc 9, p 386 (1923); see also clph 16 above

that were necessary to record the yellow light with an isochromatic plate and yellow filter were interrupted in the middle for an exposure of one or two minutes on an ordinary plate sensitive to blue light. In this manner the variable stars were photographed in two regions of the spectrum at essentially identical times. Photographic and photovisual observations were carried on throughout several hours of the night. Each run of plates gives fragments of the light curves of all the variables, but since the average period is thirteen hours, for only a few stars in each series was the light rising from minimum through median to maximum during a given night's run on the cluster.

The measurement of the plates yielded 6300 magnitudes, from which fourteen measures of the times of median magnitude both in blue and in yellow light were obtained for eleven different variables. The results appear in Table 19. The maximum effective wave length for blue light is approximately 4500 Å, and for yellow light, 5500 Å. The observed difference in the times, t , of rise to median magnitude,

$$\Delta t = t_{pg} - t_{py}$$

is given in thousandths of a day in the fourth column. Thus a positive residual would indicate that the yellow light is measured as arriving first.

Table 19 Differences in Times of Median Magnitudes

Number of Variable	Photographic Range	Photovisual Range	Δt	Weight
1	1 ^m .2	0 ^m .7	+0 ^d .009	3
4	1.4	0.9	-0.001	2
8	1.1	0.7	-0.005	1
12	1.3	1.0	-0.012	1
18	1.5	1.05	-0.005	2
20	0.9	0.7	+0.001	1
28	1.2	0.8	0.000	2
59	1.0	0.7	+0.003	1
63	1.2	0.9	+0.006	2
64	1.0	0.7	-0.003	1
81	1.1	0.8	-0.002	3
			+0.005	1
			+0.001	3
			-0.008	2

It is seen immediately that there is no measurable difference in velocity, the values of Δt being of the order of the uncertainties of measurement, six are positive, seven are negative, and one is zero. The mean value of the difference in time required for the passage of blue and of yellow light over the distance from the cluster to the earth is

$$\text{Blue—Yellow} = -0^d.00012 \pm 0^d.0007 = -10 \text{ seconds} \pm 60 \text{ seconds.}$$

We have determined in this experiment merely an upper limit to the difference in speed. We find that since the distance to the cluster is approximately 41 000 parsecs, light of these two colors, which differ by twenty-five per cent in wave length, differs in time of arrival at the earth by no more than one minute after traversing space for more than thirty-five thousand years. In other words, the relative size of the probable error indicates that the chances are even that the speeds of blue and yellow light do not differ by more than one part in twenty thousand million; probably they do not differ at all.

From eleven determinations of the maxima for nine variables in Messier 5, a similar equality in speed was found for blue and yellow light. In this result,

also, the probable error exceeds the observed average difference, but the determination has much less weight than the one based on median magnitudes.

It is to be noted in conclusion, however, that the essential equality in speed does not necessarily indicate a perfectly transparent interstellar medium. As GROOSMULLER¹, among others, has pointed out, a large amount of dust and gas can exist in space without measurably affecting the speed of light.

h) The Distances and Dimensions of Clusters.

80. The Photographic Period-Luminosity Curve. The correlation of absolute magnitude with period for Cepheid variables is discussed in detail elsewhere². But the importance of the period-luminosity curve in obtaining the distances of globular clusters is sufficiently great to justify a brief consideration here of some outstanding features. Because of their bearing on the investigations of cluster magnitudes and distances, it is well to mention the derivation of the adopted photographic period-luminosity curve, and the determination of its zero point.

a) **The Photographic Period-Luminosity Curve.** The curve relating period to magnitude was obtained from variables in the Small Magellanic Cloud. The plot of the median apparent photographic magnitudes against logarithms of the periods for 106 variables is shown in Figure 17. Points of low weight are enclosed in circles, and the periods determined by Miss LEAVITT are indicated by crosses. A few of the stars diverging most widely from the curve may not be actual members of the system, but the fairly high galactic latitude (-33°) makes rather unlikely the occurrence of typical Cepheids except as members of the Cloud.

The deviations from the curve in Figure 17 are not larger than might be expected in view of the difficulties of observation. The average deviation in magnitude of the thirty-two variables whose periods Miss LEAVITT obtained is 0.19, for the seventy-four other stars it is 0.25, for all, 0.23. The systematic magnitude deviation from the curve is -0.063 for the LEAVITT variables and $+0.049$ for the others, showing a negligible systematic difference between the earlier and the later work.

Some of the dispersion in magnitude can be attributed to the thickness of the Cloud in the line of sight, but between the variables at the near and far edges this correction amounts to only 0.14 magnitudes. If α is the angular radius of a sensibly spherical system, the maximum dispersion in magnitude arising from the thickness is given with sufficient approximation for remote systems by

$$\Delta m = 5 \log [(1 + \sin \alpha)/(1 - \sin \alpha)]$$

The correction is thus independent of the distance and real thickness. The diameter of the Small Cloud is $3^{\circ}.6$ and the extreme correction to mean values is therefore less than a tenth of a magnitude.

Other factors contributing to residuals from the period-luminosity curve are the RUHRHARD effect and obstruction by nebulosity. To these may be added actual deviations for the periods and magnitudes from average conditions—that is, a true scattering which may arise from differences in mass, structure, or other physical properties. We should also consider errors in the periods and the observational uncertainties for individual variables, which may easily amount to two tenths of a magnitude. Errors due to the failure to resolve double stars are not likely to be serious.

¹ HEMMEL and DAMPFKING, 22, p. 153 (1924).

² LUDENDORFF, Volume VI, 2, chapter 2.

In Figure 17 only two stars with periods shorter than a day are included. There appear to be many others of this sort in the Cloud¹, but they are not considered in the present discussion because of the relative weakness of the magnitude scale fainter than 17.0. These cluster type variables will soon be studied with a large reflector, when short exposure photographs and better magnitude sequences can be used.

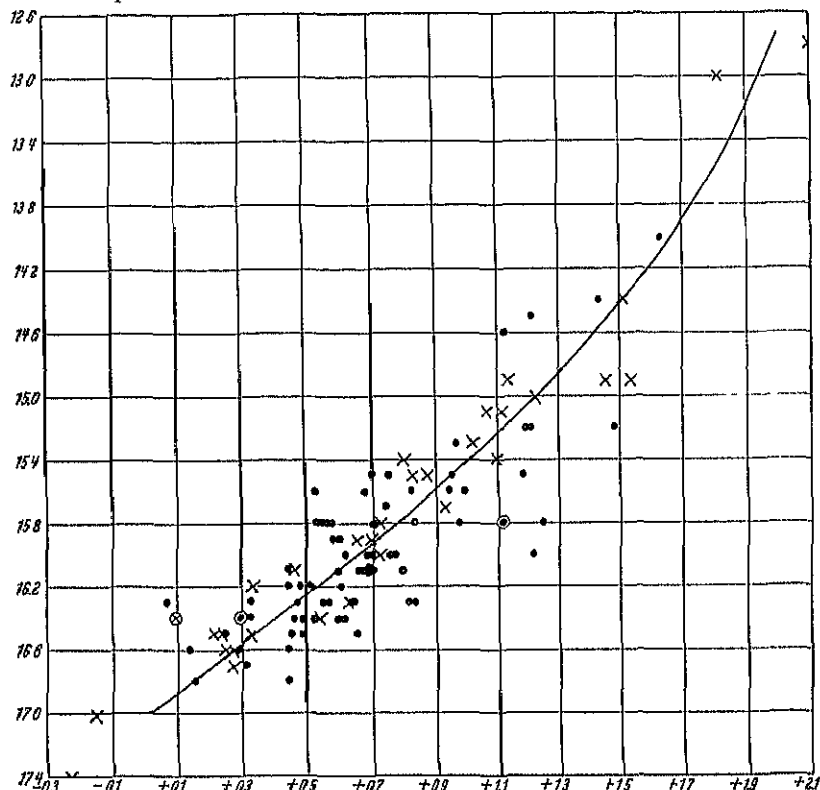


Fig. 17 Photographic period-luminosity curve. Ordinates are apparent magnitudes; abscissae are logarithms of the periods. Crosses refer to periods determined by Miss LEAVITT. Circles enclose values of low weight.

By grouping the points plotted in Figure 17, first in order of the logarithms of the period, and then in order of apparent magnitude, we get the two sets of means shown in Table 20. All magnitudes of Cepheids in this chapter are median values; that is, $(\max + \min)/2$.

Table 20 Data for the Photographic Period-Luminosity Curve

Mean $\log P$	Mean Magnitude	Number	Absolute Magnitude	Mean Magnitude	Mean $\log P$	Number	Absolute Magnitude
-0.194	17.2	2	-0.12	17.00	+0.054	4	-0.32
+0.253	16.51	17	-0.81	16.44	0.437	33	-0.88
0.610	16.08	53	-1.24	15.99	0.677	36	-1.33
0.986	15.48	21	-1.84	15.51	0.871	17	-1.81
1.357	14.93	11	-2.39	15.05	1.267	9	-2.27
1.961	12.90	2	-4.42	14.38	1.380	5	-2.94
				12.90	1.961	2	-4.42

¹ SHAPLEY, Wash Nat Ac Proc 8, p 69 (1922)

The distance modulus for the Small Magellanic Cloud (see cph 39) is 17.32, and the absolute magnitudes for variables in the Cloud are therefore given by $M = m - 17.32$. In the fourth and eighth columns of Table 20 are the absolute magnitudes corresponding to mean values of $\log P$.

A by-product of work on the period-luminosity curve is a determination of the relation between period and spectral class, shown in Figure 18. The period-spectrum curve is discussed by LUDENDORFF, in Vol VI, Chapter 2, of this Handbuch. It may be noted here that the relation holds for long-period and RV Tauri variables, as well as for the cluster types.

b) The zero point. Although the form of the period-luminosity curve and the deviations from it are now fairly well known, we remain for the time being in a state of suspense with regard to the zero point. Originally based on the parallactic motions of the few bright Cepheid variables for which accurate proper motions were available, the zero point has been the target of much discussion and suggested revision.

KAPTEYN and VAN RIJN believed that the large observed proper motions of cluster type Cepheids in the Galaxy show them to be dwarfs and necessitate an enormous shift of the zero point I had adopted¹, with consequent disaster for my measures of galactic dimensions. Later discussions of the proper motions and radial velocities of these variable stars indicated, however, that they could not be used in the manner adopted by KAPTEYN and VAN RIJN². Many of the stars of this subtype belong to the well known high velocity group, and when allowance is made for their high space velocities, the proper motion data are not in disagreement with the zero point indicated by the classical Cepheids.

The most thorough study of the zero point is that by R. E. WILSON³. He concluded that the distances that I had based on the period-luminosity relation should be decreased by twenty or thirty per cent, but in view of the now generally accepted KAPTEYN correction to BOSS' proper motions, this change in the zero point by WILSON may be, as he himself pointed out, largely effaced. In the most recent discussions of Cepheid motions OORT gets 1.06 ± 0.26 (m. s.) as the correction factor to my parallaxes, using Mount Wilson measures of radial velocity⁴.

So far as they go, the trigonometric parallaxes in the Yale Catalogue and the Mount Wilson and Upsala spectroscopic parallaxes⁵ support the system based on the period-luminosity curve. VAN MAANEN has found satisfactory agreement of his trigonometric parallaxes⁶ with the values from the period-luminosity relation.

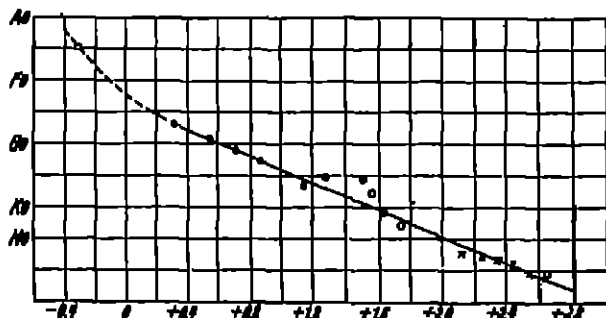


Fig 18. The relation of spectral class (ordinates) to logarithm of the period (abscissae) for variable stars. Open circles refer to RV Tauri variables, crosses to long period variables, dots to Cepheid variables, and the open square to the mean cluster type Cepheids.

¹ B A N 4, p. 37 (1922).

² Harv Circ 237 (1922); R. E. WILSON, A J 35, p. 35 (1923).

³ A J 35, p. 35 (1923).

⁴ B A N 4, p. 91 (1927).

⁵ SCHLESINGER, Catalogue of Parallaxes, Yale Univ. Obs. 1924; SHAPLEY, Harv Circ 237 (1922), LONDREAU, Ap J 59, p. 37 (1924).

⁶ Publ A S F 32, p. 62 (1924).

In view of WILSON's work, however, and of other indications that the nearer galactic Cepheids give too bright a zero point¹, I have made a provisional correction of $+0.23$ magnitudes, which reduces to 0.00 the absolute photographic magnitude of cluster type variables. The correction has been applied to the period-luminosity curves, and to all the computed distances appearing in this chapter. It amounts to a systematic decrease of eleven per cent in the distances computed from older period-luminosity curves.

Awaiting the completion in a few years of the McCormick and Mount Wilson investigations of the proper motions of a large number of galactic Cepheids, we adopt this corrected zero point and the scale of distances dependent on it.

The resulting absolute magnitudes in clusters and Magellanic Clouds are accordant with a large body of astronomical observations, and compatible with recent astrophysical theory. There seems to be no serious inconsistency in the resulting luminosities, except that the revision has made the maximum brightness of stars in globular clusters surprisingly low. I am inclined to predict that the correction to the zero point now adopted will never exceed a quarter of a magnitude, and that it may be in either direction, but this prediction should be made with caution because of the increasing evidence of peculiar drifts and of heterogeneity in the star structure in the immediate vicinity of the sun.

81. Distances of Globular Clusters Obtained from Cepheids and Bright Stars. From the period-luminosity curve distances can be determined directly for all the globular clusters in which the Cepheid variables have been studied and magnitude scales determined. In Table 21 are collected all the relevant observational data now available from my own studies², and also, for N G C 5053 and N G C 5466, the magnitudes measured by BAADÉ with the Beigedorf reflector. For the sake of homogeneity, the magnitudes measured at Bonn by KUSCHER for three globular clusters (M3, M15, and M56) were not used.

a) *The Observations.* The new material represents a considerable expansion over that in hand twelve years ago. The determination, in 1917, of the parallaxes of sixty-eight globular clusters included only seven for which the variable stars had been studied, and for two of these the preliminary data could not be used quantitatively. As variable stars in clusters are fundamental in calibrating methods of determining distances, I have given considerable attention since 1917 to the discovery and observation of variable stars in clusters. Mount Wilson plates and various series in the Harvard collection have been used for this work. I am indebted to several assistants at Mount Wilson and Harvard for aiding in this laborious research, and especially to Miss SAWYER who has taken an active part in the recent revision of cluster distances.³

There are now nineteen instead of five clusters in which variable stars have been measured sufficiently to enter the new determination of distances. Of the 730 variable stars in these nineteen clusters, 524 have been studied enough to be useful in fixing the "median magnitudes" for the clusters concerned. In 1917 the absolute magnitudes of the high luminosity stars had been measured for only twenty-eight clusters, we now have measures on the brighter stars in forty-eight systems.

b) *The Methods.* For a new determination of distances and distribution, I have followed in principle, though not in detail, the methods developed and

¹ See various papers by TEN BRUGGENCATÉ, CURTIS, DOIG, KIENLE, MAIQUIST, and STRÖMBERG. Since this chapter was written in 1930 there have been further discussions of the zero point by GERASIMOVICH [A J 41, p. 17 (1931)], NORDSTRÖM [Lund Obs Circ 2 (1931)], and others.

² From Harv Bull 869 (1929).

³ Harv Bull 869 (1929).

Table 21 Magnitudes of Variables and Bright Stars

N G.C.	Class	Photographic Magnitude				Preliminary Modulus	Notes
		Variables	25 Br	6th Star	30th Star		
104	III	—	13.09	12.4	13.4	14.33	Note 1, 47 Tucanae
288	X	—	14.80	14.5	15.1	15.87	Note 2
362	III	15.5 (4)	14.12	13.5	14.8	15.49	
1904	V	—	15.29	15.01	15.72	16.61	Member 79
2808	I	—	14.9	14.3	15.4	16.25	
3201	X	14.52 (5)	13.52	13.3	13.8	14.57	Note 3
4147	LK	16.8 (1)	16.58	16.23	16.93	16.99	GP, note 6
4590	X	15.90 (6)	14.80	14.31	15.08	15.87	Member 68
5024	V	—	15.07	14.94	15.26	16.36	Member 53
5053	XI	16.19 (8)	15.65	15.1	16.0	16.15	GP
5139	VIII	14.37 (5)	12.91	12.6	13.1	14.22	ω Centauri
5272	VI	15.30 (8)	14.23	13.92	14.45	15.48	Member 3
5466	XII	16.17 (6)	15.72	15.1	16.2	16.16	GP
5897	XI	—	15.15	14.9	15.4	16.16	
5904	V	15.26 (8)	13.97	13.74	14.27	15.26	Member 5
6093	II	—	14.88	14.72	15.09	16.24	
6121	LK	14.27 (6)	13.88	13.3	14.4	14.29	Note 4, GP, Member 4
6144	XI	—	15.76	15.2	16.3	16.22	GP
6171	X	—	15.46	15.2	15.9	16.57	
6205	V	15.20 (4)	13.75	13.45	13.92	15.10	Member 13, Note 5
6218	LK	—	13.97	13.56	14.31	15.07	Member 12
6229	VII	—	16.18	15.90	16.37	17.36	
6235	X	—	16.17	15.7	16.8	17.28	
6254	VII	—	14.06	13.35	14.38	15.17	Member 10
6266	IV	16.40 (6)	15.87	15.6	16.1	16.37	Irreg., Member 62
6333	VIII	—	15.61	15.08	15.88	16.70	Member 9
6341	IV	—	13.86	13.60	14.16	15.18	Member 92
6356	II	—	17.16	16.86	17.44	18.51	
6397	LK	—	12.61	11.9	13.1	13.67	GP
6402	VIII	—	15.44	14.85	15.86	16.56	Member 14
6535†	XI	—	15.9	15.3	16.4	16.89	
6541	III	14.42 (4)	13.35	12.7	13.8	14.53	Note 3
6626	IV	—	14.87	14.49	15.11	16.14	Member 28
6638	VI	—	16.22	15.90	16.60	17.48	
6656	VII	14.06 (5)	12.93	12.80	13.26	14.12	Member 22
6712	LK	—	16.10	15.65	16.36	17.17	
6723	VII	15.33 (6)	14.20	13.7	14.8	15.37	
6752	VI	—	13.26	12.8	13.6	14.47	
6779	X	—	15.31	14.98	15.70	16.39	Member 56
6809	XI	—	13.58	12.9	14.2	14.58	Member 55
6864	I	—	17.06	16.76	17.35	18.43	Member 75
6934	VIII	—	15.78	15.33	16.11	16.91	
6981	IX	16.80 (8)	15.86	15.53	16.20	16.86	Member 72
7006	I	18.96 (6)	17.50	16.99	17.89	18.91	
7078	IV	15.63 (7)	14.31	14.13	14.55	15.63	Member 15
7089	II	15.71 (4)	14.61	14.25	14.76	15.81	Member 2
7099	V	—	14.63	13.77	15.04	15.80	Member 30
7492	XII	—	16.82	16.3	17.1	17.22	GP

1 The long period variables in 47 Tucanae (Harv Bull 783) could not be safely used in measuring the distance. 2 The mean magnitude of the 25 brightest stars was determined at Mount Wilson to be 14.81, with a range of 14.38 to 15.04. 3 The magnitudes of N G C. 3201 and N G C. 6541 may be considerably in error due to unsatisfactory comparison sequences. They are not included in the determination of the reduction curves for apparent integrated magnitudes and diameters, though they are appropriately used in constructing Table 22. 4 For N G.C. 6121 the zero point of the magnitude scale depends on both Harvard and Mount Wilson measures of Mount Wilson plates. 5 The mean magnitude of the 25 brightest stars was determined at Harvard to be 13.76 with a range of 13.4 to 14.1. 6 BAARD has recently studied this difficult system [A N 239, p. 353 (1930)] and his better results give a modulus $16^m.52 \pm 0^m.05$. He correctly reassigns the cluster to a much earlier class (on the basis of new long exposure plates)

described in 1917. As before, the reasonable assumption is made that the median absolute magnitude of variables with periods less than a day is constant from cluster to cluster. The difference between the median magnitudes of the variables and the magnitudes of the brightest stars is again found, on the average, to be so definite a quantity that brighter star magnitudes themselves can be used as criteria for those clusters where variable stars are lacking or have not been analyzed. We go farther by taking measures of integrated apparent brightness (total magnitude) and angular diameter as criteria of relative distance, using these measures, after appropriate calibration, not only to strengthen the determination for the forty-eight clusters whose variables and bright stars have been studied in some detail (Table 21), but also for the other forty-five clusters now known in the galactic system for which we have as yet no measures of variables or of individual bright stars.

c) The Results. A few of the essential details of Table 21 should be mentioned. The classes in the second column are those described in ciph 6 and listed for all globular clusters in Appendix A. The apparent median magnitude of cluster type variables is in the third column. When a cluster contains long period Cepheids, their magnitudes are reduced to the cluster type median by means of the period-luminosity relation and are then combined with the magnitudes of the cluster type variables.

Since we have adopted zero as the absolute photographic magnitude for cluster type Cepheids, the third column actually contains a direct determination for nineteen clusters of the distance modulus, $m - M = 5 (\log d - 1)$, where d is the distance in parsecs and m is the apparent median photographic magnitude.

The parenthetical numbers in the third column are the combining weights assigned to the mean median magnitudes of the variables in each cluster. These weights depend on the number of variables, on the detail with which periods and light curves are known, and on the estimated accuracy of the magnitudes. The means of the third column are used in conjunction with the distance modulus derivable from the next three columns to determine the preliminary modulus in the seventh column.

The fourth column contains the mean magnitude of the twenty-five brightest stars (after the exclusion of five of maximum brightness in order to avoid, or at least to diminish, the effect of optical doubles and of the chance superposition of bright field stars). A weakness in using this method lies in the dependence of the area in each cluster surveyed on the compactness or distance of the cluster, or on the richness of the foreground of galactic stars. Uniformity of selection was strenuously sought, and I am convinced that for most clusters the mean of the twenty-five brightest stars, as well as the magnitude of the thirtieth star, would not be appreciably disturbed by including or excluding too much of the dense central region.

In the following columns are given the apparent magnitudes of the sixth and thirtieth stars in each cluster, the sixth star is the brightest object and the thirtieth the faintest included in the mean of the twenty-five brightest.

The difference between the median magnitudes of the cluster type variables (third column) and the magnitudes of the three succeeding columns are found to depend on the class of the cluster. Table 22 gives the readings from the smooth curves that represent the changes of the three sets of differences with class. In the earlier work a single constant value, 1.28, for the difference between the median and the twenty-five brightest, was used; the two other sets of differences were not then considered in obtaining distances. The range of variation now found for med.—25 br is from 0.92 (Class XII) to 1.34 (Class I),

The present method of using three different points in the sequence of apparent magnitudes is essentially equivalent to comparing, from one cluster to another, the general luminosity curves for giant stars. Its advantage over previous practice lies in the allowance it makes for abnormal distribution—or even small deviations from the average—in limited groups of stars. The extended method is obviously justified by the non-parallelism of the three curves representing the relation of reduction factors to class of cluster.

A comparison of the modulus from variable stars alone (third column of Table 21) with the preliminary modulus (seventh column) based on bright stars and variables together, indicates how satisfactorily the data for bright stars agree with the results from the variables. The agreement shows, in fact, to what extent one typical cluster is comparable with another inside the various classes.

d) Giant-poor Clusters. A number of the clusters of the more open classes (Classes IX—XII) were found upon examinations for star frequency to be poor in giant stars. Their luminosity curves are abnormal. Such objects are indicated by the letters GP in the last column of Table 21. They were not used in deriving differences in Table 22 for normal clusters, and the irregular cluster Messier 62 (N.G.C. 6266) was also excluded.

Table 22 Reduction to the Median Magnitude of Cluster Type Variable Stars.

Class of Cluster	Median—25 Br	Median—6th Star	Median—30th Star
I	1.34	1.77	1.04
II	1.33	1.74	1.01
III	1.32	1.71	0.98
IV	1.30	1.68	0.95
V	1.28	1.64	0.92
VI	1.24	1.60	0.89
VII	1.20	1.56	0.86
VIII	1.15	1.51	0.83
IX	1.10	1.46	0.80
X	1.05	1.40	0.77
XI	0.99	1.34	0.74
XII	0.92	1.29	0.71

The GP clusters with measured variables were used, however, to determine special reduction factors for all the "giant-poor" clusters. A study of these abnormal systems shows that the following mean values can be satisfactorily used in reducing the magnitude measures to the standard median magnitude of the cluster type variables:

Median—Mean of 25	= + 0.44
Median—6th brightest	= + 0.94
Median—30th brightest	= + 0.03

e) The System of Weighting. For the typical clusters for which bright star magnitudes have been measured (Table 21) the reductions to "median magnitude" are made directly with the aid of Table 22, and the three resulting determinations for each cluster are combined with weights 2, 1, 1, for the mean of 25, 6th, and 30th, respectively, to get the preliminary distance modulus. The modulus from variable stars, when available, was, of course, included with appropriate weight in the mean value in the seventh column of Table 21. The final weight of each preliminary modulus is therefore the weight in the third column (from the variable stars) increased by four.

32 Distances of Globular Clusters Obtained from Diameters and Integrated Magnitudes. Further steps in deriving the distances of the clusters are now obvious and need only be summarized. Plotting the values of the preliminary modulus in Table 21 first against the angular diameter and then against integrated brightness¹, we get two empirical curves that may be used for the derivation of the distance modulus of any globular cluster for which the total magnitude and angular dimensions have been measured. The coordinates of these curves are given in Tables 23 and 24.

Table 23 Modulus-Diameter Curve for Globular Clusters

Modulus	Log Diameter
14.0	1.30
14.5	1.20
15.0	1.05
15.5	0.89
16.0	0.67
16.5	0.42
17.0	0.24
17.5	0.11
18.0	0.02
18.5	9.92

Table 24 Modulus-Magnitude Curve for Typical Globular Clusters

Modulus	Integrated Magnitude
14.0	3.1
14.5	3.7
15.0	4.5
15.5	5.6
16.0	6.7
16.5	8.1
17.0	9.4
17.5	10.5
18.0	11.4
18.5	12.2

a) **Angular Diameters.** The adopted diameters, which are given for all globular clusters in Appendix A, are based on measures made at Harvard on photographs of Series A (Bruce 24-inch refractor) and of Series AX and AY, which are made with short focus cameras, double weight is assigned to the large scale plates. It should be noted that the measured angular diameter of a cluster depends on exposure time, the recorded diameters, d , are therefore not exactly proportional to the parallaxes nor related by the normal formula $d = k 10^{0.2m}$ to the integrated apparent magnitudes, m . This limitation, however, does not decrease their value as a measure of relative distances.

In general the measures of diameter refer to the nucleus or the main body of the cluster. Plates of long exposure, made with large telescopes, when carefully counted and analyzed, show that the clusters are of considerably greater extent than is recorded in these "surface" measures of angular diameter. The distribution of cluster type variables also frequently indicates the wide dispersion of cluster stars. For example, BAILEY² notes the existence of variables 19' from the center of NGC 3201, though the "working diameter" in the catalogue is 7'.7, in agreement with the value given in the NGC.

b) **Integrated Apparent Magnitudes.** The photographic magnitudes for globular clusters are on a convenient but not the conventional scale. They were measured by Miss SAWYER on plates of the AX and AY series³. The scale is much more open than in the customary Pogson system and as a result the integrated brightness listed in Appendix A ranges from the third to nearly the thirteenth magnitude. If the scale were on the usual system of stellar magnitudes, this difference of ten magnitudes would indicate a range of one hundred in the relative distances, rather than the factor of ten which is actually found.

The measures of brightness are, however, fairly accurate, since much care was taken in the selection of plates and of magnitude sequences. Photographic images of globular clusters depend on the lenses, plates, and photographic development, and for the brighter and larger clusters are necessarily uncertain.

¹ Harv Bull 852 (1927)

² Harv Circ 234 (1922)

³ Harv Bull 848 (1927)

not only because of the size and texture of the photographic image, but also because of the scarcity of suitable comparison stars and the general weakness of photographic sequences for bright magnitudes. With the warning that these new measures of brightness cannot be used for the computation of absolute magnitudes or for comparison with visual integrated magnitudes for the determinations of color index, or, as DUFAY¹ has discovered, used directly for the derivation of relative distances, we can proceed to make important indirect use of them, when properly calibrated, to get at the distances of clusters for which we have no data on individual bright stars or variables.

c) *The Distance Moduli and Their Weights.* Unit weight is assigned to each of the determinations of cluster distances based on magnitude and on angular diameter. When other values are available, as in forty-eight of the clusters, the weight four is assigned to the modulus depending on the bright stars, and the weight for the modulus from variable stars is that given in Table 21 above. For instance, the four values of the modulus for Messier 3 (N G C. 5272) are 15.50 (variable stars), 15.45 (bright stars), 15.23 (diameter), and 15.0 (integrated magnitude). The corresponding weights are 8, 4, 1, 1. The adopted mean modulus is 15.43, corresponding to a mean distance of 12.2 kiloparsecs or about 40000 light years.

For the "giant-poor" clusters the modulus from the angular diameter is derived from the curve for normal systems, but the modulus from the integrated magnitude is derived from a smoothed curve based on only the clusters that are deficient in giant stars. Loose globular clusters, such as N G C 288 and N G C 3201, may approach the deficient condition, but the variable reduction factors of Table 22 largely correct for minor systematic deviations from average conditions of magnitude frequency.

The adopted mean modulus for each cluster is given in Appendix A, followed by a letter indicating the quality of the determination. The assumed quality depends on both the final weight of the modulus and the accordance of the various determinations. The letter "a" indicates the values of highest weight, the letter "e" refers to the most uncertain determinations, which are, unfortunately, still too numerous. The distribution among the qualities is, a 13, b 25, c 23, d 17, and e 15.

For clusters in which there is good material on variable stars, the determinations based on total magnitude and diameter contribute but slightly to the finally adopted modulus. The computed distances for nearly half of the clusters, however, depend entirely on the relatively low weight determinations of the apparent brightness and diameter. Efforts will be made within the next few years to extend the work on variables and magnitudes of individual stars. As a result, alterations in the distances of individual clusters can confidently be expected, but it is practically certain that the scale of the system of clusters and of the Galaxy will not be affected thereby. The zero point correction predicted above is the only agent likely to disturb the general scale of distances.

d) *Comparison with Earlier Results.* As previously noted, we have made a systematic correction of eleven per cent to the distances of globular clusters through making a provisional alteration in the zero point of the period-luminosity curve. On comparing the individual distances now given (Appendix A) with those previously obtained through my investigations at Mount Wilson², the average difference is found to be twelve per cent (after allowing for the systematic change). The revision of the individual distances has therefore not

¹ *Lyon Bull.* 11, p. 59 (1929).

² *Mt. Wilson Contr.* 152 (1918).

been at all diastic, though in a few cases where the early material was unusually weak it has been more than thirty per cent. Because of the great increase in the basic photometric data and in the number of globular clusters whose Cepheid variable stars have been studied, the present values are much more secure than those formerly determined.

At times during the past twelve years the scale of distances has been challenged, and evidence or argument advanced to show that I had derived cluster distances and galactic dimensions that might be from five to one hundred times too large. It is inadvisable to take space to reproduce here or even to summarize these many discussions, because the general order of distances, and consequent galactic arrangement, is now very generally accepted. It should suffice to mention TEN BRUGGENCATE, CHARLIER, CROMMELIN, CURTIS, DOIG, HOPMANN, KAPILYN and VAN RIJN, LUNDMARK, VAN MAANEN, MALMQUIST, OORI, PARVULSCO, PERRINE, SCHOUFEN, SPARES, and R. E. WILSON as principal contributors on one side or the other of the discussion, and for the details refer to their papers which are listed in the general bibliography of star clusters in Harvard Observatory Monograph No. 2.

33 A Working Catalogue of Galactic Clusters (Appendix B). The discussion of the number and distribution of galactic clusters in ciph 9 was based on a new and fairly homogeneous catalogue which is given in Appendix B. Although intentionally incomplete because of the adopted restrictions which exclude poor or indefinite groups, as well as the galactic clusters in the Magellanic Clouds, the catalogue is probably the most serviceable yet compiled for the general study of galactic clusters. Miss PAYNE is responsible for the classification of the individual clusters and for the estimates of magnitudes and of numbers of stars. The classifications (sixth column of the catalogue) are on the system proposed in ciph 5. The galactic coordinates are on the Harvard system (Pole at $12^{\text{h}} 40^{\text{m}}$, $+28^{\circ}1'$). The angular diameter is from MELOTTE's catalogue, except when in heavy type, in which case the estimate was made by Miss ROPER using Harvard photographs; it is necessarily approximate and generally refers to the obvious nucleus. Detailed star counts nearly always extend the diameter.

The orientation, expressed as the position angle of the major axis of an elongated cluster with reference to the galactic equator, was estimated independently by Miss PAYNE and the writer on Harvard photographs for the more compact galactic clusters (MELOTTE's Class II), the results, which are very accordant, are discussed in ciph 24 above. The ninth column of the catalogue indicates the approximate number of stars that could be assigned to each cluster on plates whose fainter magnitude limits are as given in the tenth column. In the clusters for which this fainter limit is not given, the majority of the cluster stars are much brighter than the limit.

It is probable that many stars within the bounds of a cluster are superposed members of the intermediate galactic field, for these systems usually lie in rich regions in low galactic latitude. Obvious bright foreground stars were not considered in choosing the fifth star for each group and estimating its magnitude. It is probable, therefore, that nearly always the estimated magnitudes in the eleventh column actually refer to a star that is near the maximum luminosity in its cluster. How bright absolutely that object may be depends to some extent on whether it is a member of a Pleiades or a Hyades type of cluster, and also whether the cluster is poor or rich in stars. No claim to accuracy is made for these estimated magnitudes; they are given as rough indicators of the brighter

¹ PICKERING, *Harv Ann* 56, p. 1 (1912)

limit of apparent magnitude, and as a means of making preliminary estimates of the distances and space distribution of galactic clusters.

34. **Parallaxes of Galactic Clusters.** Direct trigonometric measures must necessarily fail to give useful information on the distances of galactic clusters, even when they are as near as the Pleiades. Measures of proper motions and fairly extensive studies of the spectral composition of some of the nearer galactic clusters have led to useful estimates of the approximate distances. For ten systems, including the Pleiades, the Hyades, Praesepe, Messier 11, Messier 37, the double cluster in Perseus, and the bright cluster in Coma Berenices, the distance in kiloparsecs has been determined through more or less detailed studies of motions, magnitudes, and spectra, and is entered between the twelfth and thirteenth columns of Appendix B. The sources are given in the notes at the end of the catalogue. The accuracy of these ten values is not high, except for the Hyades.

For other galactic clusters no equally dependable measures of the distances are yet available, though provisional photometric or spectral parallaxes have been published by various investigators. DORE¹ and RAAB² in particular have analyzed the spectral data and derived useful preliminary estimates for many of the brighter groups. My own early values for a number of the galactic clusters³ are systematically too great; the published estimates were admittedly very provisional, and gave distances that now appear on the average to be two or three times too large because of the tentative assumption that the brighter stars were of exceptionally high luminosity.

TRUMPLER's spectroscopic and photometric researches on galactic clusters, which have been in progress for some years⁴, should eventually give fairly accurate values of the distances of many of the galactic clusters; his method involves the use of luminosity curves for various spectral classes in the clusters⁵, or, what is essentially the same, the use of a RUSSELL diagram for fixing the distance modulus. The final standardization of his system of distances will probably await much serious work on the absolute luminosity dispersion for stars of Class A.

In 1931, P. COLLINDER published an exhaustive study of galactic clusters, dealing with their structural properties and distribution in space⁶.

Spectroscopic parallaxes should eventually give the distances of a number of galactic clusters which contain late type stars; and with the development of dependable spectroscopic methods for early type stars, such as those foreshadowed by Miss WILLIAMS⁷ in analyses of absorption lines in Class A spectra, the spectrum line method may turn out to be the most dependable one for measuring the distances of galactic groups. It will be a procedure much less time-consuming than the RUSSELL diagram method.

Since the accurate determination of the distances of galactic clusters is still mainly in the future, it seems worth while for the time being to tabulate direct photometric estimates. Assuming that the fifth star in order of brightness in a galactic cluster has the absolute magnitude of an average bright Class A star, $+0.5$, we derive the distances given in the twelfth column of Appendix B. In the thirteenth column are given the distances corresponding to an assumed absolute magnitude of -0.5 . Since we are dealing with objects selected on

¹ J. B. A. 35, p. 201 (1925).

² Lund Medd. Serie II, No. 28 (1922).

³ Mt. Wilson Comm. 62 (1919).

⁴ Preliminary publication in Lick Bull. 14, p. 154 (1930), after the completion of this manuscript.

⁵ Publ. A. S. P. 37, p. 307 (1925).

⁶ Lund Obs. Ann. 2 (1931).

⁷ Harv. Circ. p. 348 (1929). Miss ANGER has extended the method and applied it to various galactic clusters. [Harv. Circ. 352 (1930); Harv. Bull. 882 and 883 (1931)].

account of high luminosity, these greater distances are probably more nearly correct¹. They have therefore been used in computing, in the next two columns, the linear diameter of each cluster in parsecs and the distance of the cluster from the galactic plane. The wide range in linear diameters, reflecting in part the difficulty of estimating the bounds of a galactic cluster, is a striking feature of these computed results. The smallest objects appear to be only a few light years in diameter, and the largest more than fifty. Not much weight can be put on individual values of the distance, but it is practically certain that these values are of the right order of magnitude and can serve to give a correct idea of the distribution of galactic clusters in space. The light they throw on galactic dimensions is considered in ciph 42.

35. Radial Velocities of Globular Clusters. The measured radial velocities of globular clusters range from -350 to $+315$ km/sec. From Table 25 it can be seen that there is no clear dependence of velocity on class of cluster, galactic latitude, angular diameter, total magnitude, or distance from the sun. The only appreciable correlation appears to be that of speed with distance from the solar apex, pointed out by STRÖMBERG². The dependence is in the sense of increasing velocity with increasing distance from the solar apex.

The simplest interpretation of the relation of speed to position in the sky is based on the assumption that the apparent systematic drift of the clusters is but the reflection of the motion of the local system in the Galaxy. When corrected for this motion, the average speed of globular clusters remains high—approximately a hundred kilometers a second, but as a group, the globular clusters are essentially at rest with respect to the whole galactic system, unlike the extra-galactic nebulae, which show a large K term apparently dependent on distance.

The radial velocities of globular clusters have been measured mainly by SLIPHER at the Lowell Observatory. Except for two or three clusters, all measures refer to the integrated images and not to individual stars. The study of differential radial motions in a globular cluster is one of our important future problems. The successful measure of the proper motions in globular clusters, also, must await the photographs of the future. VAN MAANEN has shown that the proper motion of Messier 13 as a whole and its average internal proper motion are less than $0''.001$ annually, an amount to be expected from a consideration of the distance and the radial velocity³. The values of the annual proper motions are slightly larger for Messier 2 and Messier 56, but are consistent, he finds, with my estimated distances and the average radial velocities⁴.

¹ The assumption that the fifth star in the cluster is not more luminous than -0.5 implies, in general, that the star is not earlier in spectral class than B8. For a cluster of the spectral constitution and richness of the Pleiades, this assumption would therefore give too small a distance. TRUMPLER has found that about half the clusters he has classified are of the Pleiades type, but, as pointed out in ciph 14, this proportion is probably too large because of observational selection. The clusters of the Pleiades type are apparently poor in highly luminous stars of early type, for of fifteen enumerated by RAAB, not one has a fifth star of class as early as B5. The adopted method, therefore, probably does not lead to serious systematic error.

² Mt. Wilson Contr. 292, p. 5 (1925). A suggestion of a dependence of velocity (corrected for solar motion) on galactic latitude and therefore on mass of the intervening star fields is discussed by TEN BRUGGENCATE [Wash. Nat. Ac. Proc. 16, p. 111 (1930)], who seeks a trace of the red-shift, characteristic of the spectra of distant spiral nebulae. The material is as yet insufficient to establish the correlation securely, or to discriminate among its possible interpretations.

³ Mt. Wilson Contr. 284 (1925).

⁴ Mt. Wilson Contr. 338 (1927).

Table 25 Radial Velocities of Globular Clusters

N G C.	Class	β	Spectrum	Angular Diameter	Pg. Mag.	Distance (kpc.)	Radial Velocity
1851	II	-34 ⁰ .5	—	5'.3	6.0	14.3	+315 km/sec
1904	V	-28	—	3.2	8.1	20.4	+235
5024	V	+79	—	3.3	6.9	18.2	-180
5272	VI	+77.5	G	9.8	4.5	12.2	-130
5904	V	+46	G	12.7	3.6	10.8	+ 10
6093	II	+18	K0	3.3	6.8	17.5	+ 70
6205	V	+40	G0	10.0	4.0	10.3	-265
6218	IX	+25	—	9.3	6.0	11.0	+160
6229	VII	+40	—	1.2	9.7	29.8	-100
6266	IV	+ 7	K0	4.3	7.0	18.6	+ 50
6273	VIII	+ 9	G5	4.3	6.8	16.3	+ 30
6333	VIII	+10	K?	2.4	7.4	20.8	+225
6341	IV	+35	G5	8.3	5.1	11.2	-160
6626	IV	- 7	G5	4.7	6.8	16.6	0
6934	VIII	-20	G0	1.5	9.4	24.9	-350
7078	IV	-28	F	7.4	5.2	13.1	- 94
7089	II	-36	F5	8.2	5.0	13.9	- 10
7099	V	-48.5	F8	5.7	6.4	14.6	-125

86. Dimensions and Star Densities of Clusters. It is impossible to say how many stars constitute a typical globular cluster. Our photographs can reach only a little way down the main sequence towards the dwarfs. When we attempt to go further, the high density of the central stars "burns out" the photograph and conceals the information we might otherwise obtain. From available counts on our most suitable photographs of the brightest clusters we estimate¹ that in the average globular cluster there are more than twenty thousand stars brighter than absolute magnitude +5. To the same magnitude limits, the population of an average galactic cluster is less than two hundred stars.

The diameter of a globular cluster is also indeterminate. It is probable that the actual linear dimensions depend on the brightness of the stars involved, becoming greater for stars of lower luminosity and mass; the same dependence appears also in galactic clusters². From Table 23, which gives the relation of distance modulus to angular diameter for normal globular clusters, we can compute the following relation of linear diameter to distance:

Distance	Modulus $m-M$	Angular Diameter	Linear Diameter
10 kpc	15.0	11'.2	33 pc
20	16.5	2.6	16
30	17.4	1.4	13
40	18.0	1.02	12
50	18.5	0.85	12

The measured decrease of linear diameter with increasing distance is of course mainly photographic. The loss of light in space is here of minor significance. We under-measure the angular diameters of remote clusters because of the failure of outlying faint stars to rise to measurable prominence on the photographic plate. I think we can safely take the diameter of a typical globular cluster to exceed thirty-five parsecs, but the diameter of the nucleus, in which the brightest stars are concentrated, appears to be only one third as large.

The average linear diameter of the galactic clusters for which definite estimates can be made (Appendix B) is 6.24 parsecs. Few galactic clusters

¹ See, for example, Pop Astr 27, p 101 (1919)

² See Figure 15

exceed twenty parsecs in diameter. TRUMPLER has determined preliminary distances from observations of magnitudes and spectral types for fifty-two systems. He finds a range in linear diameter from 3.5 to 25 parsecs, with the great majority between 4.5 and 10 parsecs.

The number of stars per cubic parsec in a typical globular cluster cannot be computed at present, except for the supergiant stars. It is obvious, when the dwarfs are taken into consideration, that the distances separating stars at the center of a rich globular cluster are on a planetary rather than a stellar scale. It seems probable that sooner or later we should have evidence of stellar encounters in such crowded regions; but only one nova in a globular cluster is now on record—the seventh magnitude object in Messier 80, which appeared in 1860.

The space density and the distances separating individual stars can be more readily computed for galactic clusters when reliable estimates of the parallaxes become available, and when we have made sufficient allowance for superposed stars. TRUMPLER's study of one of the richest of the galactic clusters, Messier 11, provides material that illustrates the conditions in these systems. He finds that the cluster is 1250 parsecs distant¹. It lies in the rich Scutum star cloud, which has a star density nearly four times that of the average field of the galactic belt. The cluster itself is made up of about 480 stars brighter than magnitude 15.5, distributed over an area approximately a quarter of a degree in diameter. The bright stars are concentrated within a central area of less than 4' radius².

For stars brighter than absolute magnitude +4.5 the relation of density to distance in Messier 11 is found to be as follows:

Distance from Center in Parsecs	Stars per Cubic Parsec	Distance from Center in Parsecs	Stars per Cubic Parsec
0.27	83	1.68	4.9
0.60	80	2.04	2.2
0.96	33	2.40	0.5
1.32	9.5		

The central density of Messier 11 is much higher than that of the average galactic cluster. In contrast with the density of 83 stars per cubic parsec for Messier 11 is the density for Messier 37 of only eighteen stars per cubic parsec for stars brighter than absolute magnitude +4.5. The corresponding number for Messier 36 is twelve (WALLENQUIST), for the Pleiades, 2.8 (if the parallax is taken as 0''.008), and, for the vicinity of the sun, 0.014. The average separation of stars at the center of Messier 11 is one light year.

TRUMPLER points out that "an observer at the center of Messier 11 would find about forty stars with parallaxes of 2" or more and which would appear three to fifty times as brilliant as Sirius shines in our sky." It is quite probable, however, that this display would be very dull compared with the show at the center of the Hercules cluster.

i) Star Clusters in the Magellanic Clouds.

37. Types of Clusters and Nebulae. Both globular and galactic clusters appear in the Magellanic Clouds, the latter type exhibiting much variety in richness, dimensions, and nebulosity. In the New General Catalogue and the Index Catalogues 41 clusters and nebulae are listed within the limits of the

¹ Later revised to 1340 parsecs. Lick Bull 14, p. 154 (1930).

² Lick Bull 12, p. 10 (1925).

Small Cloud and 301 within the Large Cloud. The descriptions, however, are meager, and photographic plates reveal scores of clusters and nebulae that have not yet been catalogued and described. For the Small Cloud a catalogue by SHAPLEY and Miss WILSON¹ gives 237 new objects, chiefly nebulous stars and groups of stars. A manuscript catalogue of the star clusters in the Large Cloud, recently prepared from Harvard plates, contains 110 new entries—nearly doubling the number known from HERSCHEL's survey and subsequent investigations. A complete catalogue and analysis of the clusters in the Magellanic Clouds, however, must await future surveys with the reflectors, since the telescopes at present available do not permit adequate resolution of the small groups.

Among the great number of nebulae in both Clouds, none has been found which could be assigned safely to the spiral class. As would be expected from their total absolute magnitudes, mainly between -3 and -7 , they are for the most part of the diffuse and irregular types, with a meager sprinkling of planetaries. Of the many diffuse nebulae in the Large Cloud the greatest is the famous "Looped Nebula", 30 Doradus. Its absolute brightness probably exceeds magnitude -13 , and its total diameter, including the fainter wisps and loops of nebulosity, is thirty parsecs or more.

88. The Globular Star Clusters. DUNLOP, Sir JOHN HERSCHEL, and others have described many of the compact star groups in both Clouds as globular. The N.G.C. records sixteen globular clusters in the Large Cloud and two in the Small. On the basis of photographic material BAILEY, MELOTTE, and others have remarked that few if any of these objects are correctly assigned. In fact, none of them is now retained as truly globular. On the other hand, the accepted globular clusters, listed for both Clouds in Table 26, are not described as such in the N.G.C., though they all appear in that catalogue. The existence of globular systems in the Magellanic Clouds affords a valuable opportunity for the comparative study of globular and galactic types, and for the examination of the relation of globular clusters to galaxies.

The first two clusters of Table 26 belong to the Small Magellanic Cloud; the eight others to the Large Cloud. The angular diameters and integrated magnitudes are given on the same basis as in Appendix A for globular clusters in general. The diameters, therefore, are not indicators of the extreme bounds of the clusters—they are rather measures of nuclei. N.G.C. 416 in the Small Cloud is more uncertain than the others and later may be dropped.

It is seen that the globular clusters in the Large Cloud range from the compact Class II to the fairly open Class VIII. In earlier considerations of clusters in the Large Cloud² seven objects were listed as possibly globular. Of these N.G.C. 1651 has now been definitely dropped³, and N.G.C. 1835 and N.G.C. 1856 have been added to the list. Later analysis may show that some of the following N.G.C. objects are globular clusters⁴:

1711	1926	2056	2133
1789	1939	2058	2134
1852	1944	2065	2157
1872	1986	2107	2164
1903	2019	2108	
1916	2031		

¹ Harv Circ 275, 276 (1925)

² Harv Bull 775 (1922); Harv Circ 271 (1925)

³ It was included in Harv Bull 848, 849, and 852 as a doubtful object.

⁴ In 1932 (two years after the completion of the manuscript) a dozen new globular clusters were found in the vicinity of the Large Cloud (Harv Bull 889).

Table 26 Globular Clusters in the Magellanic Clouds

N G C	R A 1900	Dec 1900	Galactic		Angular Diameter	Integrated Magnitude	Class	Adopted Modulus	Quality
			Long	Lat					
416	1 ^h 5 ^m 0	-72° 53' 5	262°	-43°	0' 9	11,3	VI	18,05	c
419	1 5 ,4	-73 25 ,1	262	-42	1,4	10,2	IV	17,36	c
Mean	—	—	—	—	—	—	—	17,50	—
1783	4 58 ,8	-66 8 ,1	242	-37	1,4	10,1	VII	17,32	c
1806	5 2 ,4	-68 8 ,0	245	-36	0,9	10,6	VI	17,94	d
1831	5 5 ,8	-65 3 ,6	242	-35	1,3	10,0	V	17,38	c
1835	5 5 ,8	-69 32 ,1	247	-34	1,2	9,9	II	17,44	d
1846	5 7 ,7	-67 35 ,0	245	-34	1,2	10,4	VIII	17,56	c
1856	5 10 ,1	-69 15 ,1	247	-34	2,1	8,8	V	16,76	c
1866	5 13 ,6	-65 34 ,9	241	-34	2,2	8,0	IV	16,58	c
1978	5 28 ,1	-66 18 ,5	242	-33	1,0	10,2	VI	17,72	d
Means	—	—	—	—	1,5	9,64 ± 0,24 (m c)	—	17,25 0,11 (m c)	—

In none of the globular clusters of the Magellanic Clouds have variable stars been found, nor have the brighter stars been measured individually. The final test as to whether the doubtful objects are typical globular systems, or merely open groups involved in nebulosity, will be in future examinations for variable stars, and in the study of density and luminosity laws.

Miss CANNON has thrown doubt on the globular nature of a number of bright objects in both clouds by showing that their integrated spectra are of early class; we have already seen¹ that practically all typical clusters belong to Classes F and G. Thus she finds

N G C	Spectrum	N G C	Spectrum
294	A?	2107	A?
1872	A3	2134	A
1903	A	2157	A2
2041	A3	2164	A5

The spectrum of N G C 419, in the Small Cloud, resembles Class K in its distribution of light and in the faint appearance of the G band and of lines *H* and *K*. The spectrum of N G C 416 is too diffuse and faint to classify. The spectral class² of N G C 1866, in the Large Cloud, is F8, that of N G C 1835 is possibly G5, though for it and the other compact clusters of the Large Cloud the spectral images on the Harvard objective prism plates are too difficult for classification.

89. Distances of the Clouds. Values of the distances of the Magellanic Clouds can be based on measures of the globular clusters, but from Cepheid variable stars more accurate results are obtained, which can then be used to determine the absolute magnitudes of the clusters. In the ninth column of Table 26 the distance modulus is given for each cluster, derived from the measures of angular diameter and integrated photographic magnitude. In the use of these data we follow the principles developed in an earlier section on the distances of globular clusters of the galactic system. In getting mean values of the modulus for each cloud, weights were assigned as follows

Quality	Weight
c	4
d	2
e	1

¹ See Appendix A² Harv Bull 868 (1929)

While clusters of quality c may be accepted as almost certainly globular, some doubt still attaches to those qualified as d and o.

The mean modulus derived for the Small Magellanic Cloud is nearly identical with the value 17.55, previously derived from 107 Cepheid variable stars¹. With the adopted revision of the zero point of the period-luminosity curve² the distance modulus from the variables becomes 17.32. Accepting this value we have for the Small Magellanic Cloud:

$$\begin{aligned}\pi &= 0''.0000345 \\ \text{Distance} &= 29 \text{ kiloparsecs} \\ &= 95000 \text{ light years} \\ \text{Linear Diameter} &= 6000 \text{ light years.}\end{aligned}$$

At this distance the integrated absolute magnitude is -7.12 for N.G.C. 419, the only object that appears definitely, from the survey of existing plates, to be a globular cluster.

For the Large Magellanic Cloud the mean distance modulus from eight globular clusters is 17.25, with a mean computed error of only one tenth of a magnitude. But the Cepheid variable stars should eventually give us a much more dependable value of the modulus. The modulus derived from a recent study of the variables is 17.10. Adopting this value, we obtain the following results for the Large Magellanic Cloud.

$$\begin{aligned}\pi &= 0''.000038 \\ \text{Distance} &= 26.2 \text{ kiloparsecs} \\ &= 86000 \text{ light years} \\ \text{Linear Diameter} &= 10800 \text{ light years}\end{aligned}$$

The corresponding mean absolute photographic magnitude of a globular cluster in the Large Magellanic Cloud is -7.46 (weighted mean). The absolute values range from -9.1 to -6.5 , an indication of the degree of uncertainty involved in assuming a constant integrated absolute magnitude for globular clusters. The spread is considerably less if the cluster N.G.C. 1866 is assigned to the foreground rather than to the Magellanic Cloud, and it would be very small indeed (-7.2 to -6.5) if the newly admitted N.G.C. 1856, when analyzed with a large telescope, proved to be a nebulous open group.

40 On the Relation of the Clusters to the Magellanic Clouds. The angular diameters of the globular clusters in the Large Cloud are at most two or three minutes of arc; the angular diameter of the Cloud as a whole is slightly more than seven degrees³. Enormous and rich as we know a typical globular cluster to be, it is obviously small compared with ordinary external galaxies. The clusters of the various sorts, however, are important in the general appearance of the Clouds, and especially in the make-up of the high luminosity population.

The distribution of the open clusters throughout the Clouds is much the same as the distribution of the Cepheid variable stars and of the general stellar population, on the other hand, the accepted globular clusters in the Large Cloud are almost exclusively to the north, and N.G.C. 1866 and N.G.C. 1831 lie quite outside the main structure of the Cloud. There are, however, a half dozen variable stars, apparently of the Cepheid class, in the same region as these clusters, and long exposures on short scale plates show that the outlying clusters and variables are within the observable bounds of the Cloud.

¹ SHAPLEY, YAMAMOTO, and WILSON, *Harv Circ* 280 (1925), see also SHAPLEY, *Harv Circ* 255 (1924).

² See clph. 30.

³ SHAPLEY, *Harv Circ* 268 (1924).

The asymmetrical distribution of the globular clusters in the Large Cloud has led some to surmise that the globular clusters of the galactic system may also be eccentrially arranged with respect to the general galactic structure, and therefore that they cannot be used as I have used them, in estimating minimum values of galactic dimensions. But this one-sided distribution of the globular clusters in the Large Cloud is modified by the inclusion of N G C 1835 and N G C 1856 in the list accepted at present, and it would be quite altered if a considerable proportion of the list of suspected globular clusters prove to be typical systems. The two clusters N G C 1789 and N G C 1944, both of which are strongly suspected as globular, lie far from the center of the Cloud on the south—directly across from the outlying globular clusters of Table 26.

It is of significance that the 1400 known variable stars in the Large Cloud and the 969 in the Small Cloud¹ avoid the numerous open clusters. In this respect the Clouds are like the galactic system, where open clusters are free of variable stars of all kinds. The globular systems in the Magellanic Clouds, are, of course, too compact to have been searched as yet for variables.

Possibly the most striking fact arising from the study of globular clusters in the Magellanic Clouds is the low absolute magnitude of their brightest stars when compared with the brightest objects in the open and nebulous groups. If the new values of the distance moduli are correct, there is scarcely a star in the ten accepted globular systems of the two Clouds that exceeds -3 in absolute photographic magnitude. This result, however, is in complete agreement with the condition found in globular clusters of our own galactic system. In contrast, the individual stars in scores of the nebulous star groups in the Magellanic Clouds appear to exceed -3 in absolute photographic magnitude, and in many groups they attain the excessively high luminosities of -5 and -6 . This again is in agreement with the data on absolute magnitudes in galactic clusters, especially in those large early spectrum groups in Orion, Scorpio, and elsewhere that are associated with bright nebulosity.

It may be remarked in conclusion that, notwithstanding their remoteness, isolation, and high galactic latitudes, the Magellanic Clouds may be more closely allied to our galactic system than we have heretofore supposed². It is probable that the observed high speed recession of the Clouds should be assigned almost wholly to the motion of our local system in the Galaxy. Apparently the Clouds are not in rapid motion with respect to the sum total of the galactic system, or the system of globular clusters.

j) Dimensions of the Galaxy.

41. Membership in the Galaxy. Our galactic system, as here defined, is composed of the aggregate of stars and nebulae whose distribution appears to be organized with respect to the galactic plane. Globular clusters are therefore included, with galactic stars and galactic clusters and nebulae, but the Magellanic Clouds and the extra-galactic nebulae (spiral nebula family) are outside the organization.

A final judgment, however, of galactic membership must await more information on speeds and masses, and on the phenomena of galactic rotation. Possibly some of the remote globular clusters (e g. N G C. 7006, N G C. 4147, and Messier 75) are actually independent, being either fugitives from the Galaxy,

¹ LEAVITT, *Harv Ann* 60, No. 4 (1908). Approximately 600 new variables have been found on Harvard plates of the Large Cloud since 1930 (as yet unpublished).

² *Harv Reps* 61 (1929).

or only chancing for the moment (cosmically speaking) to be moving in this part of space. On the other hand, the Magellanic Clouds may sometime be shown to be affiliated with our Galaxy, or, at least, with a local group of galaxies including the three Andromeda nebulae, Messier 33, and some others¹.

In measuring the Galaxy we should at the start admit indefinite limits, and also striking irregularities, not only in the interior but probably also at the edges. The dimensions discussed below are therefore not to be taken too literally as marking the boundaries, or even as giving sharp limits of star density. At best we measure or estimate the distances of the remotest attainable stars, or groups of stars, which yield to present methods and which appear to be members of the galactic system.

42. The System of Galactic Clusters. Although the loose star groups contribute little to our knowledge of the dimensions of the Galaxy, their space distribution may be mentioned here as bearing on the structure of the nearer parts of the Milky Way. The catalogue of 249 galactic clusters in Appendix B contains galactic longitude, approximate distance, and $R \sin \beta$ (distance from the galactic plane). Some features to be noted in the distribution of the galactic clusters are:

1 The contrast in galactic distribution of galactic and globular clusters (see Figure 6).

2. Close confinement of galactic clusters to the neighborhood of the galactic plane

3 The relative nearness of galactic clusters to the sun, which results in a distribution essentially free from effects of the obstructing clouds that contribute much to the anomalous distribution of the globular clusters. The galactic clusters are in large part members of our local system and the circumjacent star clouds.

43. The Higher Systems of Globular Clusters. To illustrate the space distribution of the ninety-three known globular clusters of the galactic system (Appendix A), the following rectangular coordinates have been computed for all

$$X = R \cos(\lambda - 327^\circ) \cos \beta,$$

$$Y = R \sin(\lambda - 327^\circ) \cos \beta,$$

$$Z = R \sin \beta,$$

where R is the distance in kiloparsecs, β is the galactic latitude, and $(\lambda - 327^\circ)$ is the galactic longitude measured from the direction of the center of the cluster system. The latitude, longitude, distance, and $R \sin \beta$ are given in Appendix A; the computed quantities X and Y are given in Table 27.

a) **Eccentric Position of the Solar System.** A diagram of the distribution of the globular clusters in the plane of the Galaxy (XY plane) is shown in Figure 19. Crosses indicate clusters lying on the north of the galactic plane, and dots those on the south; the smaller the symbol, the more distant is the object from the plane. The equality of the division by the galactic plane of the supersystem of clusters is remarkable—forty-seven clusters are on the north, forty-six on the south.

The direction to the center of the system, derived from the apparent positions of globular clusters, is seen to agree with the direction on the basis of space coordinates; in Figure 19 there are forty-six positive values of Y and forty-six negative values, with $Y = 0$ for one cluster. (The remote system N.G.C. 7006,

¹ SHAPLEY, Harv Repr 61 (1929).

Table 27 Coordinates of Globular Clusters

NGC	$R \cos \beta \times$ $\cos(\lambda - 327^\circ)$	$R \cos \beta \times$ $\sin(\lambda - 327^\circ)$	NGC	$R \cos \beta \times$ $\cos(\lambda - 327^\circ)$	$R \cos \beta \times$ $\sin(\lambda - 327^\circ)$
104	+ 2,8	- 3,9	6581	+ 18,6	- 5,9
288	- 0,5	- 0,1	6624	+ 21,7	+ 1,2
362	+ 4,5	- 7,5	6626	+ 16,2	+ 2,3
1261	0	- 13,7	6637	+ 18,4	+ 0,6
1851	- 5,0	- 10,6	6638	+ 29,0	+ 1,3
1904	- 12,3	- 13,2	6205	+ 4,0	+ 6,8
2298	- 10,4	- 23,4	6218	+ 9,5	+ 2,9
2419	- 28,0	- 0,5	6229	+ 6,7	+ 21,8
2808	+ 3,0	- 15,6	6235	+ 28,0	0
3201	+ 1,1	- 9,0	6254	+ 10,0	+ 2,9
4147	- 0,9	- 4,5	6266	+ 18,3	+ 1,6
4372	+ 5,0	- 8,0	6273	+ 16,0	0,7
4590	+ 6,7	- 10,7	6281	+ 27,6	0,5
4833	+ 8,8	- 13,0	6287	+ 27,1	+ 0,5
5021	+ 3,2	- 1,3	6293	+ 22,8	- 0,8
5053	+ 3,5	- 1,0	6304	+ 25,0	+ 1,8
5139	+ 1,2	- 5,0	6316	+ 31,5	- 0,8
5272	+ 2,0	+ 1,7	6325	+ 46,0	+ 0,1
5286	+ 16,0	- 17,0	6333	+ 20,3	+ 2,1
5466	+ 3,8	+ 3,1	6341	+ 3,3	+ 8,6
5634	+ 19,8	- 5,8	6342	+ 39,1	+ 1,1
I 4499	+ 14,0	- 18,0	6352	+ 18,4	6,0
5824	+ 24,4	- 11,9	6356	+ 48,5	+ 6,0
5897	+ 15,0	- 4,0	6362	+ 12,0	8,0
5904	+ 7,4	+ 0,6	6366	+ 26,3	+ 9,1
5927	+ 16,8	- 11,0	6388	+ 16,6	4,2
5946	+ 27,2	- 17,0	6397	+ 5,1	- 2,1
5986	+ 15,4	- 6,2	6402	+ 17,7	+ 7,2
6093	+ 16,5	- 1,9	6652	+ 23,0	+ 0,6
6101	+ 14,7	- 13,5	6656	+ 6,3	+ 1,2
6121	+ 6,9	- 1,0	6681	+ 18,7	+ 1,0
6139	+ 27,7	- 8,5	6712	+ 23,2	+ 11,6
6144	+ 17,3	- 2,4	6715	+ 18,6	+ 1,9
6171	+ 19,4	+ 1,7	6723	+ 11,7	+ 0,2
6426	+ 31,3	+ 17,4	6752	+ 6,7	3,0
6440	+ 49,5	+ 7,0	6760	+ 23,1	+ 16,8
6441	+ 21,0	- 0,2	6779	+ 9,1	+ 17,8
6453	+ 50,0	- 0,4	6809	+ 7,9	+ 1,2
6496	+ 21,2	- 4,5	6864	+ 40,7	+ 14,8
6517	+ 47,0	+ 17,1	6934	+ 11,1	+ 18,7
6522	+ 35,8	+ 0,6	6981	+ 15,6	+ 11,4
6528	+ 44,0	+ 1,2	7006	+ 22,4	+ 48,0
6535	+ 23,0	+ 12,3	7078	+ 4,7	+ 10,6
6539	+ 35,8	+ 13,8	7089	+ 6,6	+ 9,2
6541	+ 8,6	- 1,5	7099	+ 8,6	+ 4,6
6553	+ 26,6	+ 2,6	7492	+ 6,4	+ 9,1
6569	+ 29,1	+ 0,5			

with coordinates $X = +22,4$, $Y = +48,0$, falls outside the limits of the diagram)

The origin of coordinates for Figure 19 — that is, the position of the observer — is on the border of the globular cluster system. The center of gravity of the system of clusters, indicated by an open square, has the coordinates $X = +16,4$, $Y = -0,3$ (or $Y = +0,2$ if the remote and isolated NGC 7006 is included)

Probably ten or twenty globular clusters, within the limits of space represented by the diagram, await discovery. Obscuring nebulosity possibly conceals most of these systems, of which the existence is intimated by the scarcity of

observed points in the right half of Figure 19. Of course we need not assume high regularity in distribution, or even approximate circularity in the projected array, but it is probably the observational difficulties caused by nebulosity and by the small dimensions and faint magnitudes of remote clusters, and not

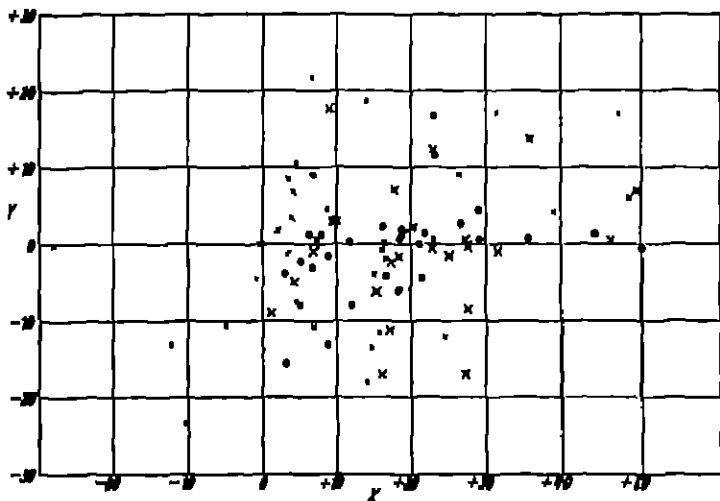


Fig 19 Distribution of globular clusters in the plane of the Galaxy. The sun is at the origin of coordinates.

inherent irregularities, that have produced the apparent deficiency for X greater than +30 kiloparsecs. On the left side of the diagram, from $X \approx 0$ to $X \approx -20$, where the survey may be considered sufficiently exhaustive, the complete absence

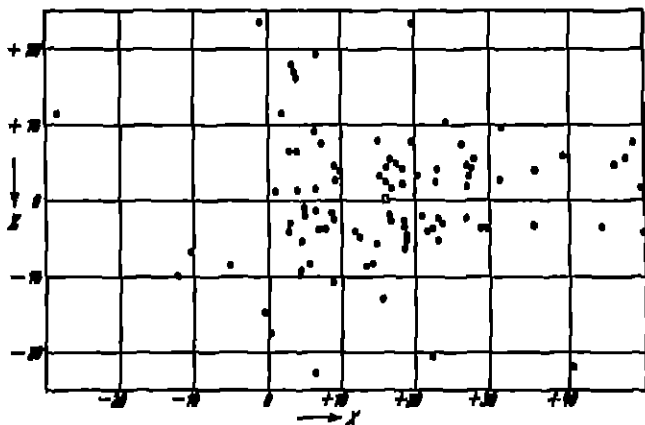


Fig 20 Distribution of globular clusters in the XZ plane.

of clusters from one quadrant is even more striking and significant structurally than the scarcity of values of X greater than +30.

The cluster at the extreme left is N G.C. 2419—an object in a region far from other clusters, found through studies of the Lowell Observatory photographs¹.

¹ Harv Bull 776 (1922)

b) The "Region of Avoidance" The same asymmetrical position of the sun with respect to the supersystem of globular clusters is shown in Figure 20, where all ninety-three systems are plotted on the XZ plane. The center of gravity, that is, the algebraic mean values of X and Z , indicated by an open square, is at $X = +16.4$, $Z = +0.4$. NGC 2419 again stands out on the extreme left.

The most interesting feature of Figure 20, which represents a section perpendicular to the galactic plane, is the "region of avoidance". The scarcity of globular clusters in low galactic latitudes is again in evidence. Here is a central section 2.5 kiloparsecs (8000 light years) in diameter, in which no globular cluster has been found. On the other hand there is only one galactic cluster out of the

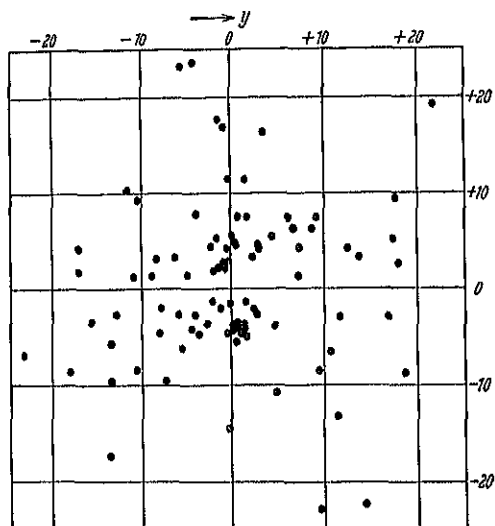


Fig 21 Distribution of globular clusters in the YZ plane

249 listed in Appendix B that does not fall well within this mid-galactic segment and that cluster, NGC 2243, is of doubtful nature and uncertain distance. Practically all known galactic stars and nebulae also fall within this "region of avoidance".

c) Projection on the YZ Plane. Figure 21 shows the distribution of globular clusters projected on the YZ plane, which is perpendicular to the line joining the sun and the center of the system at galactic longitude 327° , galactic latitude 0° . The "region of avoidance" is again clearly shown, and also the essential symmetry of the globular cluster system, for the numbers of clusters in the four quadrants are 23, 24, 22, and 24. Again NGC 7006 is outside the diagram, with coordinates $Y = +48.0$, $Z = -20.4$.

44. The Distance to the Galactic Center. It appears to be a tenable hypothesis that the supersystem of globular clusters is coextensive with the Galaxy itself. Researches on variable stars in the Milky Way¹ will eventually afford an instructive check on this hypothesis. Until we have such direct measures we can only assume that the galactic system is at least as large as the system of globular clusters. We have shown rather convincingly that the globular clusters are galactic members or associates.

¹ SHAPLEY, Harv Repr 51 (1928)

The algebraic mean of the values of $R \cos (l - 327^\circ) \cos \beta$ gives a preliminary indication of the distance to the center of the cluster system, and provisionally, therefore, of the distance to the center of the Galaxy. In so far as it depends on the globular clusters now known, the uncertainty of the distance does not exceed ten per cent. Further research on faint globular clusters, especially if now ones be found, will be more likely to extend the system than to reduce it; on the other hand, the distances of the more remote clusters are the least certainly determined and must be given low weight. We shall adopt as the distance to the center

$$R_c = 16 \text{ kiloparsecs} \\ = 52000 \text{ light years}$$

The galactic star clusters and the ordinary individual stars are too near the sun to contribute effectively to the determination of the distance to the center. But the direction to the center, as is well known, is confirmed by the counts of faint stars¹, and through the recent studies of galactic rotation by LINDBLAD, OORT, J. S. PLASKETT, SCHILT, and others; it is shown, though less definitely, by the distribution of Milky Way star clouds, planetary nebulae, Class O stars, and other objects of high luminosity. Practically all types of stars, however, with the possible exception of the novae and Cepheid variables, are too faint absolutely and too infrequent in number to contribute to the current surveys of galactic regions that are near or beyond the center of the cluster system.

Studies of the cluster type Cepheids and the long period variable stars in the southern Milky Way have led the writer and Miss SWORN to a value of the distance of the centrally located star clouds that is very much like the value given above². The variable star investigations of several observers at Harvard tend to support this suggestion that the heavy star clouds in Ophiuchus, Sagittarius, Scorpio, and neighboring constellations are parts of a massive stellar nucleus of the galactic system. The distribution of the cluster type Cepheids in these regions suggests that the nucleus extends perhaps half way from the center toward the sun. The speed of rotation about this nucleus is approximately 300 kilometers a second at the sun's distance from the center.

One important feature of the galactic central region is that the center itself lies behind heavily obscuring nebulosity. The dark clouds at the center are apparently but a part of those causing the rift in the Milky Way that extends from Cygnus southward to Centaurus; they seem to be largely responsible for the apparent avoidance of the mid-galactic regions by globular clusters.

45. On the Size and Structure of the Galaxy. An inspection of Figures 19 and 20 gives only a rough idea of the total diameter of the flattened galactic system. The most remote globular clusters are the following:

N.G.C.	Distance kpc	N.G.C.	Distance kpc
6323	46	6517	50
6342	40	6528	44.4
6356	50.	6864	48.5
6440	50:	7006	56.8
6453	50		

¹ NORT, *Recherches Ast Obs Utrecht* 8, p. 113 (1917); *SKANES*, *Mt Wilson Contr* 347 (1927).

² SNAPLEY, *Harv Rep* 52 (1928)

Some of these values are uncertain, the distances may be greater or less, but the superior distance of N G C 7006, a cluster in Vulpecula with $R = 56.8$ kpc $= 185,000$ light years, seems to be well attested by observations on its individual stars and on its cluster type Cepheids¹

The greatest distance separating two of the clusters is

$$\text{N G C 7006} - \text{N G C 2298} = 80 \text{ kiloparsecs}$$

Several other clusters are nearly as widely separated, N G C 2298 in Puppis is 71.3 kiloparsecs from N G C 6517 across the sky in Ophiuchus, and N G C 2419 in Lynx is 79 kiloparsecs from N G C 6453 in Scorpio. We may take such distances to indicate the extreme dimensions of the galactic system, for certainly most of these globular clusters, if not all, are integral parts of the Galaxy.

It does not follow from the wide dispersion of globular clusters that individual stars of the Galaxy are so widely dispersed, but it appears reasonable to maintain that the greatest diameter of the Galaxy in its plane is not less than seventy thousand parsecs, and it may be thirty per cent larger. The thickness of the system varies with distance from its center, being perhaps ten to fifteen thousand parsecs at the galactic nucleus, and one-half as much out where the solar system is located. Occasional isolated stars, however, and, of course, the globular clusters extend to twenty thousand parsecs and more from the galactic plane, lying well outside the relatively thin mid-galactic stratum.

The most remote individual stars known in the Galaxy are the novae and a few long period Cepheid variables, of faint apparent magnitude, studied by GERASIMOVIC, MISS SWOPE, MISS HARWOOD, and others, on Harvard and Nantucket plates. Some of these appear to be well beyond the galactic nucleus, with distances comparable with those of the remote globular clusters and the Magellanic Clouds. Since progress is rapid in the discovery and study of faint variables, it will be advisable to postpone the discussion of the part they play in the measurement of the extent and orientation of the galactic system. It may be twenty years or more before the detailed picture of the structure of the galactic star clouds can be drawn.

It is of significance, however, to compare the picture of the Galaxy that grew out of the earlier work on clusters and the local star system² with that resulting from the more recent studies of galactic structure³. The earlier view visualized the Galaxy as a unified discoidal stellar system, evolved from amalgamating star clouds and clusters. The local cloud was mapped out and described as one of the minor elements. The Galaxy was considered, not a single spiral nebula, but rather an organization of many half-digested star clouds and clusters, moving in an extensive stratum of stars and galactic nebulae.

It was suggested that the obvious dynamical equilibrium of a globular cluster, acquired originally at a great distance from external perturbing matter, results in a delicate adjustment that readily breaks down under stresses such as those prevailing in a large galactic system, further, that faint stars in a globular cluster, as in the galactic system, are of small mass and therefore of more than average velocity, so that in their motions in the cluster they frequently attain great distances from the center. When such globular systems approach or mingle with other clusters or the dense stellar fields in the mid-galactic segment, the dwarfs will preferentially become scattered through encounters. The massive

¹ SHAPLEY and MAYBERRY, Mt Wilson Comm 74 (1921)

² Mt Wilson Contr 157, Sect 7 (1918)

³ Harv Circ 350 (1930)

cluster stars, which are mostly of high luminosity, and which are concentrated to the center and endowed with low peculiar velocities, will retain their cluster organization longer in a disrupting neighborhood. A globular cluster thus becomes a galactic cluster which slowly dissolves into the galactic field. Flattening and distortion of galactic clusters and star clouds arise through the "encounter machinery" discussed by JEANS, and through rotation. Star streaming appears to be a complication of the various motions in and of the local system and general galactic field.

The galactic system, it appears on this interpretation, is in an advanced stage of the survival of the most massive. In size the spiral nebulae are not comparable to it, ours is a Continent Universe if the average spirals are considered Island Universes.

The relation of galactic and globular star clusters to each other, and their relation to star clouds and galactic systems, remains obscure in many respects. Yet the recent study of these structures brings increasing evidence that the above interpretation should be extended. Its modification is necessitated, in part, by difficulties such as the scarcity of clusters intermediate between globular and galactic groups, and the slowness or even impossibility of the amalgamation of clusters and star clouds with no more potent a rescaling medium available than the galactic star field with its infrequent encounters. In view of these obstacles, and others related to the distribution of dark nebulosities and the anomalous position of the Galaxy among other systems, the amended hypothesis is advanced¹ that our galactic system is neither a spiral, such as the Andromeda Nebula, nor a single unified discoidal star system, like a Magellanic Cloud on a grand scale. It is rather a super-galaxy—a flattened system of typical galaxies. It is comparable, in mass and population, with the Coma-Virgo cloud of bright galaxies, rather than with one of its members. Within the galactic system are fairly distinct galaxies, such as the local system, the Scutum star cloud, and the great star fields in Sagittarius. The dark nebulosities are associated with the local system.

Galactic star clusters, from the new point of view, are not evolved from globular systems. They are probably the results of a quite different developmental process. The test of the amended hypothesis lies in future studies of star distribution and motions, faint variable stars, and the accurate determination of the space distribution and affiliations of galactic clusters.²

Appendix A. Catalogue of Globular Clusters.

The material on which is based the catalogue of globular clusters has been described in the text. For three clusters, N.G.C. 4372, N.G.C. 6356, and N.G.C. 6864, special notes appear at the end of the catalogue³. Daggars after the N.G.C. numbers in the first column indicate questionable objects (clph. 4). Galactic coordinates are on the Harvard system (Pole $12^h 40^m$, $+28^\circ$). The values of the ellipticity and orientation are described in clph. 22. Colons in the orientation column indicate less certain values, and asterisks mark those derived from star counts on Mount Wilson plates. The magnitudes and diameters are explained in part h), and there and in part j) are described the derivation of the distances listed in the last three columns of the catalogue.

¹ Harv Circ 350 (1930)

² See Addendum on p. 773.

³ Cf. footnote on N.G.C. 4147 on page 741

Appendix A Catalogue of

NGC	Name	RA 1900	Dec 1900	Galactic		Angular Diameter	Integrat- ed Magni- tude	Class	Spec- trum	No of Variables
				Long	Lat					
104	47 Tuc	0 ^h 19 ^m 6	-72° 38'	272°	-45°	23'	3	III	G5	7
288	—	0 47 8	-27 8	157	-88	10.0	7.2	X	—	2
362	Δ 62	0 58 9	-71 23	268	-47	5.3	6.0	III	G5	14
1261	—	3 9 5	-55 36	237	-51.5	2.0	8.5	II	G	—
1851	Δ 508	5 10 8	-40 9	212	-34.5	5.3	6.0	II	—	3
1904	M79	5 20 1	-24 37	194	-28	3.2	8.1	V	—	5
2298	—	6 45 4	-35 54	213	-15	1.8	10.1	VI	—	—
2419	—	7 31 4	+39 6	148	+23	1.7	11.0	VII	—	—
2808	—	9 10 0	-64 27	249	-11	6.3	5.7	I	K0	—
3201	Δ 445	10 13 5	-45 54	244	+ 9	7.7	7.4	X	—	61
4147	—	12 5 0	+19 6	226	+79	1.7	10.3	IX	A7	5
4372 ⁿ	—	12 20 1	-72 7	269	-10	12.0	7.8	XII	—	—
4590	M68	12 34 2	-26 12	269	+36	2.9	7.6	X	—	28
4833	—	12 52 7	-70 20	271	- 8.5	4.7	6.8	VIII	—	5
5024	M53	13 8 0	+18 42	305	+79	3.3	6.9	V	—	40
5053	—	13 11 5	+18 13	309.5	+78	3.5	10.5	XI	—	9
5139	ω Cen	13 20 8	-46 47	277	+15	23	3	VIII	—	132
5272	M3	13 37 6	+28 53	8	+77.5	9.8	4.5	VI	G	160
5286	Δ 388	13 39 9	-50 52	280	+10	1.6	8.5	V	G0	0
5466	—	14 1 0	+29 0	8	+72.5	5.0	10.0	XII	—	14
5634	—	14 24 4	- 5 32	310.5	+48.5	1.3	10.4	IV	—	—
I 4499	—	14 45 0	-81 49	275	-20	3.1	11.5	XI	—	—
5824	—	14 57 8	-32 40	301	+21	1.0	9.3	I	1.8	—
5897	—	15 11 7	-20 39	312	+29	7.3	7.3	XI	—	—
5904	M5	15 13 5	+ 2 27	332	+46	12.7	3.6	V	G	84
5927	—	15 20 8	-50 19	294	+ 4	3.0	8.8	VIII	—	—
5946†	—	15 28 2	-50 19	295.5	+ 3.5	1.3	10.6	IX	—	—
5986	Δ 552	15 39 5	-37 27	305	+12	3.7	7.0	VII	1.8	1
6093	M80	16 11 1	-22 44	320.5	+18	3.3	6.8	II	K0	4
6101	—	16 14 4	-71 58	284.5	-16	3.8	9.5	X	—	—
6121	M4	16 17 5	-26 17	319	+15	14.0	5.2	IX	F	33
6139	—	16 21 0	-38 36	310	+ 6	1.3	9.8	II	—	—
6144	—	16 21 1	-25 49	319	+15	3.3	10.3	XI	—	—
6171	—	16 26 9	-12 50	332	+22	2.2	8.9	X	—	—
6205	M13	16 38 1	+36 39	27	+40	10.0	4.0	V	G0	7
6218	M12	16 42 0	- 1 46	344	+25	9.3	6.0	IX	—	—
6229	—	16 44 2	+47 42	40	+40	1.2	9.7	VII	—	1
6235	—	16 47 4	-22 0	327	+12	1.9	10.8	X	—	—
6254	M10	16 51 9	- 3 57	343	+22	8.2	5.4	VII	—	—
6266	M62	16 54 9	-29 58	322	+ 7	4.3	7.0	IV	K0	26
6273	M19	16 56 4	-26 7	324.5	+ 9	4.3	6.8	VIII	G5	—
6284	—	16 58 4	-24 37	326	+ 9	1.5	10.0	IX	F	—
6287	—	16 59 1	-22 34	328	+10	1.7	10.4	VII	—	—
6293	—	17 4 0	-26 26	325	+ 7	1.9	8.8	IV	G5	3
6304	—	17 8 2	-29 20	323	+ 5	1.6	9.2	VI	K	—
6316	—	17 10 3	-28 1	325.5	+ 5	1.1	9.9	III	G5	—
6325	—	17 11 9	-23 38	327.5	+ 6	0.7	11.9	IV	—	—
6333	M 9	17 13 3	-18 25	333	+10	2.4	7.4	VIII	K?	1
6341	M92	17 14 1	+43 15	36	+35	8.3	5.1	IV	G5	14
6342	—	17 15 3	-19 29	333	+ 8	0.5	11.4	IV	—	—
6352†	—	17 17 5	-48 22	309	- 8	2.5	7.9	XI	—	—
6356 ⁿ	—	17 17 8	-17 43	334	+ 9	1.7	8.6	II	K0	—
6362	Δ 225	17 21 5	-66 58	293	-18	6.7	7.1	X	—	17
6366	—	17 22 4	- 4 59	346	+15	4	12.1	XI	—	—
6388	—	17 29 0	-44 40	313	- 8	3.4	7.1	III	K	—
6402	M14	17 32 4	- 3 11	349	+14	3.0	7.4	VIII	—	—
6397	Δ 366	17 32 7	-53 37	304.5	-12.5	19.0	4.7	IX	G?	2
6426	—	17 39 9	+ 3 13	356	+15	1.3	12.2	IX	—	—
6440	—	17 43 0	-20 20	335	+ 2	0.7	11.4	V	—	—
6441	—	17 43 4	-37 1	321	- 6.5	2.3	8.4	III	K0	—
6453	—	17 44 7	-34 36	322.5	- 5.5	0.7	11.2	IV	—	—

Globular Clusters

NGC	R.M.P.	Orion	Photographic Magnitude				Adopted Modulus	Quality	Distance kpc	R sin β kpc	R cos β kpc
			Var	Bright	6th	30th					
104	8	-55°	—	13.09	12.4	13.4	14.17	b	6.8	-4.8	4.8
288	9	—	—	14.80	14.5	15.1	15.81	b	14.5	-14.5	0.5
362	8	+65°	15.5	14.12	13.5	14.8	15.55	b	12.9	-9.4	8.8
1261	9.5	—	—	—	—	—	16.72	c	22.0	-17.2	13.7
1851	9	-75°	—	—	—	—	15.78	c	14.3	-8.1	11.7
1904	9	+35°	—	15.29	15.01	15.72	16.54	b	20.4	-9.6	18.0
2298	8	+39°	—	—	—	—	17.12	d	26.5	-6.9	25.6
2419	9	-56°	—	—	—	—	17.41	d	30.3	+11.9	28.0
2808	8	+84°	—	14.9	14.3	15.4	16.05	b	16.3	-3.1	16.0
3201	9	—	14.52	13.52	13.3	13.8	14.81	c	9.2	+1.4	9.1
4147	—	—	16.8	16.58	16.23	16.93	16.93	b	24.2	+23.7	4.6
4372	9	—	—	—	—	—	14.91	c	9.6	-1.7	9.5
4590	9	—	15.90	14.80	14.31	15.08	15.95	a	15.5	+9.1	12.6
4833	8	-80°	—	—	—	—	16.01	c	15.9	-2.2	15.7
5024	9	-79°	—	15.07	14.94	15.26	16.30	a	18.2	+17.9	3.5
5053	8	-61°	16.19	15.65	15.1	16.0	16.20	a	17.3	+17.0	3.6
5139	8	+30°	14.37	12.91	12.6	13.1	14.15	b	6.8	+1.8	6.6
5272	8	+54°	15.50	14.23	13.92	14.45	15.43	n	12.2	+11.9	2.6
5286	9.5	—	—	—	—	—	16.89	d	23.9	+4.2	23.5
5466	9	—	16.17	15.72	15.1	16.2	16.16	b	17.0	+16.2	5.1
5634	9	—	—	—	—	—	17.49	c	31.4	+23.2	20.5
I 4499	9	—	—	—	—	—	16.91	c	24.1	-8.2	22.7
5824	—	—	—	—	—	—	17.32	c	29.1	+10.4	27.2
5897	8	-44°	—	15.15	14.9	15.4	16.07	b	16.4	+8.0	15.5
5904	9	+16°	15.26	13.97	13.74	14.27	15.17	a	10.8	+7.8	7.5
5927	9	—	—	—	—	—	16.56	d	20.5	+1.4	20.1
5946†	9	—	—	—	—	—	17.54	d	32.2	+2.0	32.1
5986	—	—	—	—	—	—	16.14	c	16.9	+3.5	16.6
6093	10	—	—	14.88	14.72	15.09	16.22	a	17.5	+5.4	16.6
6101	8	+35°	—	—	—	—	16.60	d	20.8	-5.7	20.0
6121	9	+72°	14.27	13.88	13.3	14.4	14.30	b	7.2	+1.9	7.0
6139	9	-64°	—	—	—	—	17.34	d	29.3	+3.1	29.1
6144	8	-22°	—	15.76	15.2	16.3	16.29	b	18.1	+4.8	17.5
6171	9	—	—	15.46	15.2	15.9	16.63	b	21.2	+7.9	19.6
6205	9.5	-63°	15.20	13.75	13.45	13.92	15.07	a	10.3	+6.6	7.9
6218	—	—	—	13.97	13.56	14.31	15.21	b	11.0	+4.6	9.9
6229	—	—	—	16.18	15.90	16.37	17.37	b	29.8	+19.2	2.8
6235	8	+89°	—	16.17	15.7	16.8	17.28	c	28.6	+5.9	28.0
6254	9	—	—	14.06	13.35	14.38	15.26	b	11.2	+4.2	10.4
6266	8	+16°	16.40	15.87	15.6	16.1	16.35	c	18.6	+2.3	18.4
6273	6	-28°	—	—	—	—	16.06	c	16.3	+2.6	16.1
6284	10	—	—	—	—	—	17.24	c	28.0	+4.4	27.7
6287	9	—	—	—	—	—	17.24	d	28.0	+4.9	27.5
6293	9	—	—	—	—	—	16.82	c	23.1	+2.8	22.9
6304	9.5	—	—	—	—	—	17.02	c	25.3	+2.2	25.2
6316	9	—	—	—	—	—	17.52	d	31.8	+2.8	31.6
6325	—	—	—	—	—	—	18.3	c	46°	+4.8	46°
6333	9	—	—	15.61	16.76	15.08	16.61	b	20.8	+3.6	20.5
6341	8	+16°	—	13.86	13.60	14.16	15.24	b	11.2	+6.4	9.2
6342	—	—	—	—	—	—	18.01	c	40	+5.6	39.5
6352†	9	—	—	—	—	—	16.48	d	19.7	-2.7	19.4
6356	9	-14°	—	17.16	16.86	17.44	18.51	c	50.	+7.8	49
6362	8	+78°	—	—	—	—	15.90	d	15.1	-4.7	14.4
6366	—	—	—	—	—	—	17.34	e	29	+7.5	28
6388	9.5	—	—	—	—	—	16.20	c	17.3	-2.4	17.2
6402	9	+76°	—	15.44	14.85	15.86	16.48	a	19.7	+4.8	19.1
6397	9	+73°	—	12.61	11.9	13.1	13.76	c	5.65	-1.2	5.5
6426†	9	—	—	—	—	—	17.85	c	37.1	+9.6	35.9
6440	8	+10°	—	—	—	—	18.5	c	50	+1.7	50
6441	8	+40°	—	—	—	—	16.62	c	21.1	-2.2	21.0
6453	—	—	—	—	—	—	18.51	c	50	-4.8	50

Catalogue of Globular

NGC	Name	R A 1900	Dec 1900	Galactic		Angular Diameter	Integrated Magnitude	Class	Spectrum	No of Variables
				Long	Lat					
6496	—	17 ^h 51 ^m .8	-44° 14'	315°	-10° .5	2'.2	9.7	XII	-	-
6517	—	17 56 .4	- 8 57	347	+ 6	0.4	12.1	IV	-	-
6522	—	17 57 .2	-30 2	328	- 5	0.7	11.0	VI	-	-
6528	—	17 58 .4	-30 4	328.5	- 5	0.5	11.8	V	-	-
6535†	—	17 58 .7	- 0 18	355	+ 9 .5	1.3	11.9	XI	-	-
6539†	—	17 59 .4	- 7 35	348	+ 5	1.3	12.6	X	-	1
6541	Δ 473	18 0 .8	-43 44	317	-12	6.3	5.8	III	G	1
6553	—	18 3 .2	-25 56	332.5	- 5	1.7	10.0	XI	-	0
6569	—	18 7 .2	-31 51	328	- 7 .5	1.4	10.2	VIII	-	-
6584	Δ 376	18 10 .6	-52 15	309.5	-17	2.5	8.3	VIII	-	0
6624	—	18 17 .3	-30 24	330	-10	2.0	8.6	VI	M0	-
6626	M28	18 18 .4	-24 55	335	- 7	4.7	6.8	IV	G5	9
6637	M69	18 24 .8	-32 25	329	-11	2.8	7.5	V	K2	-
6638	—	18 24 .8	-25 34	335.5	- 7 .5	1.4	9.2	VI	-	-
6652	—	18 29 .2	-33 4	328.5	-13	1.7	8.7	VI	K5	-
6656	M22	18 30 .3	-24 0	337	- 9	17.3	3.6	VII	-	21
6681	M70	18 36 .7	-32 23	330	-13 .5	2.5	7.5	V	-	-
6712	—	18 47 .6	- 8 50	353.5	- 6	2.1	9.9	IX	-	1
6715	M54	18 48 .7	-30 36	333	-15	2.1	7.1	III	F8	-
6723	Δ 573	18 52 .8	-36 46	328	-19	5.8	6.0	VII	G5?	17
6752	Δ 295	19 2 .0	-60 8	303	-26 .5	13.3	4.6	VI	G0	1
6760	—	19 6 .1	+ 0 52	3	- 5	1.9	10.9	XI	-	-
6779	M56	19 12 .7	+30 0	30	+ 8	1.8	8.8	X	-	1
6809	M55	19 33 .7	-31 10	336	-25	10.0	4.4	XI	-	2
6864m	M75	20 0 .2	-22 12	347	-27	1.9	8.6	I	G0	11
6934	—	20 29 .3	+ 7 4	20	-20	1.5	9.4	VIII	G0	-
6981	M72	20 48 .0	-12 55	3	-34	2.0	8.6	IX	-	29
7006	—	20 56 .8	+15 48	32	-21	1.1	11.8	I	-	11
7078	M15	21 25 .2	+11 44	33	-28	7.4	5.2	IV	I	74
7089	M 2	21 28 .3	- 1 16	21	-36	8.2	5.0	II	F5	10
7099	M30	21 34 .7	-23 38	355	-48 .5	5.7	6.4	V	F8	3
7492	—	23 3 .1	-16 10	22	-64	3.3	10.8	XII	-	9

Notes to Appendix A

NGC 4372 The distance depends only on the diameter measure. The cluster appears to be partially obscured by one of the streamers from the Coal Sack nebula. A special investigation of the magnitudes is being made on Harvard plates.

NGC 6356, 6864 The distance depends only on the magnitudes of the bright stars, since the integrated brightness and diameter appear to be abnormally large. There may be obscuring nebulosity in the field of NGC 6356.

Clusters. (Continued.)

N.G.C.	Ellipt.	Orient.	Photographic Magnitude				Adopted Modulus	Quality	Distance kpc	R sin β kpc	R cos β kpc
			Var	Bright	6h	30h					
6496	—	—	—	—	—	—	16,90	d	24,0	— 4,0	21,6
6517	8	—4°	—	—	—	—	18,5	o	50	+ 5,2	50
6522	—	—	—	—	—	—	17,78	o	36,0	— 3,2	35,8
6528	—	—	—	—	—	—	18,24	o	44,4	— 3,9	44,1
6535†	—	—	—	15,9	15,3	16,4	17,13	d	26,7	+ 4,4	26,3
6539†	9	—	—	—	—	—	17,94	o	38,7	+ 3,4	38,4
6541	9	—	14,42	13,35	12,7	13,8	14,76	o	8,9	— 1,8	8,7
6553	9	—	—	—	—	—	17,14	o	26,8	— 2,3	26,7
6569	9,5	—	—	—	—	—	17,35	o	29,5	— 3,8	29,2
6584	9	—	—	—	—	—	16,56	c	20,5	— 6,0	19,6
6624	10	—	—	—	—	—	16,74	c	22,2	— 3,8	21,8
6626	9	+18	—	14,87	14,49	15,11	16,10	a	16,6	— 2,0	16,4
6637	9	—	—	—	—	—	16,36	o	18,7	— 3,6	18,4
6638	8	—27	—	16,22	15,90	16,60	17,36	b	29,6	— 3,9	29,3
6652	8	—11	—	—	—	—	16,87	d	23,6	— 5,3	23,0
6656	8	+18	14,06	12,93	12,80	13,26	14,16	a	6,8	— 1,1	6,7
6681	9,5	—	—	—	—	—	16,41	o	19,2	— 4,5	18,8
6712†	—	—	—	16,10	15,65	16,36	17,10	d	26,2	— 2,7	26,0
6715	10	—	—	—	—	—	16,44	d	19,4	— 5,0	18,7
6723	9,5	—	15,33	14,20	13,7	14,8	15,44	b	12,3	— 4,1	11,7
6752	—	—	—	13,26	12,8	13,6	14,62	b	8,4	— 3,8	7,4
6760†	—	—	—	—	—	—	17,28	o	28,6	— 2,5	28,5
6779	8	+12	—	15,31	14,98	15,70	16,54	b	20,3	+ 2,8	20,0
6809	9	—	—	13,58	12,9	14,2	14,74	b	8,8	— 3,7	8,0
6864	9	—	—	17,06	16,76	17,35	18,43	d	48,5	—22,0	43,2
6934	9	—	—	15,78	15,33	16,11	16,98	b	24,9	— 8,5	23,4
6981	—	—	16,80	15,86	15,53	16,20	16,84	a	23,3	—13,0	19,3
7006	—	—	18,96	17,50	16,99	17,89	18,77	b	56,8	—20,4	53,0
7078	8	—11	15,63	14,31	14,13	14,55	15,60	a	13,1	— 6,1	11,6
7089	9	—80*	15,71	14,61	14,23	14,76	15,72	a	13,9	— 8,2	11,3
7090	9	—	—	14,63	13,77	15,04	15,82	b	14,6	—10,9	9,7
7492	9	—	—	16,82	16,3	17,1	17,01	o	25,2	—22,7	11,1

Appendix B

Catalogue of Galactic Clusters¹

NGC	R.A. 1900	Dec. 1900	Galactic		Class	Approx. Diameter	Orient	No of Stars	Approx. Mag. Lim of Plate	Mag. 5th Star	Distance		Linear Diameter $M = -0.5$	$R \sin \beta$ $M = -0.5$	Notes
			Long	Lat.							$M = +0.5$	$M = -0.5$			
103	0 ^h 19 ^m 8	+60° 47'	88°	+1° 1'	f	13'	—	35	13 ^m	12 ^m 4	2.40	3.80	14.4	—	—
129	0 24.3	+59 40	88.5	-2 3	e	11	—	50	13	11.0	1.26	2.00	6.4	—	—
133	0 25.6	+62 48	88.5	+0 8	e	7	—	50	13	11.7	1.74	2.75	5.6	—	—
146	0 27.5	+62 44	88.5	+0 8	e	6	—	50	13	10.3	0.91	1.45	2.5	—	—
188	0 35.1	+84 47	90	+22 6	c	15	Ind	50	16	14.6	6.61	10.5	45.8	—	—
436	1 9.4	+58 17	94.5	-3 5	d	4	Ind	40	12.8	9.8	0.72	1.15	1.3	—	—
457	1 12.8	+57 48	94.5	-3 9	e	10	84	100	12.8	8.6	0.42	0.66	1.9	—	—
559	1 22.8	+62 47	95	+1 5	e	7	—	60	12.8	11.7	1.74	2.75	5.6	—	—
581	1 26.6	+60 11	96	-1 3	d	5	—	60	12.8	9.8	0.72	1.15	1.7	—	—
637	1 34.9	+63 32	96.5	+2 6	d	3	—	20	12.8	10.2	0.87	1.38	1.2	—	—
654	1 37.2	+61 23	98	-0 1	d	5	—	50	12.8	9.8	0.72	1.15	1.7	—	—
659	1 37.4	+60 12	98	-1 0	d	5	—	30	12.8	10.9	1.20	1.91	2.8	—	—
663	1 39.2	+60 44	98	-0 4	e	11	81	80	12.8	9.8	0.79	1.05	2.5	—	—
752	1 51.8	+37 11	105	-22 7	d	45	Ind	70	12	9.6	0.66	1.05	15.8	—	—
869	2 12.0	+56 41	102.5	-3 1	f	36	63	—	—	9.5	2.51	—	26.3	—	—
884	2 15.4	+56 39	103	-3 1	e	36	84	—	—	—	—	—	26.3	—	—
Mel 15	2 25.2	+61 0	106.5	+1 5	d	20	—	20	12.8	18.6	<0.42	<0.66	<3.8	<18	—
957	2 26.4	+57 5	104	-2 0	e	10	—	40	12.8	11.3	1.45	2.29	6.6	—	—
1027	2 35.0	+61 7	103	+2 1	d	7	—	11	12.8	9.8	0.72	1.15	2.3	—	—
1039	2 35.6	+42 21	111.5	-14 8	d	18	—	80	12.8	18.6	<0.42	<0.66	<3.5	<168	—
H 1	3 3.3	+62 51	105.5	+5 2	e	15	—	30	12.8	10.8	1.15	1.82	7.9	—	—
1245	3 7.8	+46 52	114.5	-8 0	e	30	—	40	12.8	13	3.2	5.0	44	—	—
1342	3 25.2	+36 59	123.5	-14 3	c	15	Ind	40	—	9.1	0.52	0.83	3.6	—	—
Pleades	3 41	+23 48	134.5	-22 3	c	—	—	—	13.2	4.2	0.15	—	10	—	—
1502	3 58.6	+62 3	110.5	+8 4	e	7	—	15	12.8	9.8	0.72	1.15	2.3	—	—
1513	4 2.5	+49 15	120	-0 6	d	12	—	40	12.8	12.8	2.88	4.57	16.0	—	—
1528	4 7.6	+50 59	120	+1 2	e	25	71	80	12.8	9.2	0.55	0.87	6.3	—	—
Hyades	4 14	+15 23	147	-22 6	c	—	—	—	—	—	0.04	—	10	—	—
1647	4 40.2	+18 53	148.5	-15 2	c	40	33	30	—	9.7	0.69	1.10	12.8	—	—
1664	4 43.9	+43 31	129.5	+0 7	e	15	Ind	40	—	10.9	1.20	1.91	8.3	—	—
1746	4 57.6	+23 40	147	-9 3	e	45	71	60	12.6	9.5	0.63	1.00	13.1	—	—
1807	5 4.9	+16 24	153.5	-12 1	e	10	—	15	13	9.7	0.69	1.10	3.2	—	—
1817	5 6.5	+16 34	154	-11 7	d	15	69	10	13	11.1	1.32	2.09	9.1	—	—
1857	5 13.2	+39 14	136	-2 5	d	9	—	45	12.6	10.6	1.05	1.66	4.3	—	—

¹ Described in crph 33, above

R.G.C.	R.A. 1900	Dec. 1900	Galactic		Class	Approx. Diameter	Orient.	No. of Stars	Approx. Mag. Lim. of Field	Mag. per Star	Distances		Linear Diameter	$\frac{E \sin \beta}{M} = -0.5$	Notes
			Long.	Lat.		in arcmin					$M = +0.5$	$M = -0.5$			
1893	5 ^h 18 ^m .5	+46° 27'	130°.5	7°.4	f	2	—	20	12 ^m .6	[12 ^m .6	>2.63	>4.17	>3.6	>536	—
1893	5 19.2	+33 18	141.5	+0 2	d	12	—	20	12 ^m .6	9.0	0.50	0.79	2.8	+23	—
1907	5 21.4	+35 14	140	+1 6	f	5	Ind	40	12.6	11.4	1.32	2.09	3.0	+59	—
1912	5 22.0	+35 45	140	+2 0	e	20	Ind	100	—	9.7	0.69	1.10	6.4	+39	7
1960	5 29.5	+34 4	143	+2.4	f	12	Ind	60	—	8.7	1.16	—	4.0	+48	8
2099	5 45.8	+32 31	145	+4.5	f	20	—	150	12.6	9.7	1.48	—	8.4	+113	9
2126	5 55.2	+49 54	131	+14.4	d	5	—	—	—	—	—	—	—	—	—
2129	5 55.0	+23 18	154	+1.6	d	8	—	25	13.0	11.2	1.38	2.19	3.2	+60	—
I 2157	5 58.7	+24 2	154	+2.7	d	4	—	20	13.0	11.2	1.38	2.19	2.5	+102	—
2158	6 1.3	+24 6	154	+2.8	e	4	—	40	—	13	3.2	5.0	5.8	+226	—
2168	6 2.7	+24 21	154	+3.6	e	40	46	120	13.0	9.0	0.50	0.79	9.4	+50	10
2169	6 2.8	+13 59	163.5	-1.4	d	5	—	18	—	—	0.50	0.79	1.1	-20	—
2186	6 6.8	+5 28	171	-4.7	e	5	—	30	14	11.9	1.91	3.02	4.4	-248	—
2194	6 8.2	+12 50	165	-1.0	d	8	19	100	—	[13	>3.16	>5.01	>11.7	>-92	—
2215	6 16.0	-7 15	183.5	-8.7	d	8	—	20	14	11.2	1.38	2.19	5.1	-330	—
2236	6 24.3	+6 54	172.5	-0.4	f	5	—	50	15.5	14.1	5.25	8.32	12.1	-62	—
2243	6 25.7	-31 13	206.5	-16.5	f	4	Ind	10	—	14.3	5.76	9.12	10.6	-2585	11
2244	6 27.0	+4 56	174	-0.6	c	40	—	16	—	18.9	<0.48	<0.76	<8.8	<-0.7	12
2259	6 33.0	+10 58	169.5	+3.6	d	3	—	8	—	15.5	10.0	15.8	13.8	+993	—
2264	6 35.5	+9 59	170.5	+3.7	f	30	—	20	14	11.3	<0.48	<0.76	<6.6	+466	13
2266	6 37.0	+27 4	155.5	+11.7	f	5	13	30	13	10.6	1.45	2.29	3.3	+49	—
2281	6 42.3	+41 10	142.5	+18.4	e	15	17	50	13	8.9	1.05	1.66	7.2	+524	—
2287	6 42.7	-20 38	198.5	-9.0	e	30	0	60	14	—	<0.48	<0.76	<6.6	<-118	14
2301	6 46.6	+0 35	180	+1.5	d	15	—	60	—	8.9	0.48	0.76	3.3	+20	—
2304	6 49.2	+18 8	165	+10.4	d	4	—	100	—	—	—	—	—	—	—
2323	6 58.2	-8 12	189.5	-0.1	e	10	10	30	—	9	0.5	0.8	3.7	+1.9	15
2324	6 59.0	+1 12	181	+4.8	d	9	47	30	14	13.7	4.37	6.92	18.1	+574	—
2333	7 9.8	-10 8	192.5	+1.7	d	20	—	25	14	9.4	0.60	0.95	5.5	+28	—
2354	7 10.1	-25 34	205.5	-5.6	e	25	—	60	13.5	11.2	1.38	2.19	15.9	-216	—
2355	7 11.3	+13 57	171	+13.5	e	6	Ind	—	—	—	—	—	—	—	—
2360	7 13.2	-15 27	198.5	-0.1	d	12	Ind	50	—	9.4	0.60	0.95	3.3	+2.1	16
2362	7 14.6	-24 46	205.5	-4.4	d	6	—	40	—	9.4	0.60	0.95	1.7	-73	—
2420	7 32.5	+21 48	166	+21.1	e	7	30	20	—	12	2.0	3.2	6.5	+115	—
2421	7 31.9	-20 23	204	+1.5	f	8	64	50	13.5	9.4	0.60	0.95	2.3	+24	—
2423	7 32.0	-14 16	198.5	+4.6	d	25	—	50	10.8	9.8	0.72	1.15	8.4	+88	—
2425	7 32.5	-13 38	198.5	+4.9	d	20	—	60	13.8	10.8	1.15	1.82	10.6	+156	—

(Continued.)

(Continued)

NGC	R.A. 1900	Dec. 1900	Galactic		Class	Approx. Diameter	Orient.	No. of Stars	Approx. Mag. Lim of Plate	Mag. 5th Star	Distance		Linear Diameter	$R \sin \beta$	Notes
			Long	Lat							$M = -0.5$	$M = -0.5$			
Mel 71	7 ^h 32 ^m 9 ^s	-11° 50'	197°	+5° 8'	g	8'	64	65	13 ^m 8	10 ^m 8	1.15	1.82	4.2	+184	—
Mel 72	7 33 3	-10 27	196	+6 7	d	5	86	40	13 8	12 8	2.88	4.57	6.7	+532	—
2439	7 37 0	-31 25	214	+3 4	g	9	—	50	13 5	10 6	1.05	1.66	4.3	—98	—
2437	7 37 2	-14 55	200	+5 3	f	24	11	150	13 8	10 8	1.15	1.82	12.8	—212	17
2447	7 40 4	-23 38	207.5	+1 1	g	25	72	60	12 5	9 7	0.69	1.10	8.0	+20	18
2455	7 44 6	-21 3	206.5	+3 4	d	5	—	20	13 5	12 7	2.75	4.37	6.4	+261	—
2477	7 48 7	-38 17	221	+5 0	g	25	5	300	13 5	10 9	1.20	1.91	13.9	+165	—
2479	7 50 5	-17 27	203.5	+6 6	f	8	—	40	13 5	11 6	1.66	2.65	6.1	+300	—
2482	7 50 7	-24 2	209.5	+3 1	e	18	—	50	13 5	10 0	0.79	1.26	6.6	+68	—
H 2	7 51 7	-25 39	211	+2 2	d	7	—	20	—	10 3	0.91	1.45	3.0	+57	—
2489	7 52 2	-29 48	214	+0 2	g	7	Ind	30	13 5	11 1	1.32	2.09	4.3	+86	—
2506	7 55 2	-10 21	198	+11 5	g	10	—	50	13 8	11 3	1.45	2.29	6.6	+448	—
2509	7 56 3	-18 48	205.5	+7 0	g	4	75	40	13 8	10 2	0.87	1.38	1.6	+168	—
2516	7 56 7	-60 36	241	+15 4	g	60	—	80	—	10 1	0.83	1.32	23.0	+352	—
2539	8 6 0	-12 32	200.5	+12 4	f	21	—	150	12 8	10 8	1.15	1.82	11.2	+390	—
2547	8 7 7	-48 58	233	+7 9	d	15	—	50	13 5	9 4	0.60	0.95	4.2	+131	—
2548	8 8 8	-5 30	195.5	+16 6	f	30	—	80	13 8	9 4	0.60	0.95	3.7	+86	—
2567	8 14 6	-30 20	217.5	+4 5	f	10	16	50	13 5	10 0	0.79	1.26	3.7	+75	—
2571	8 14 9	-29 26	217.5	+4 6	c	8	—	25	13 5	9 4	0.60	0.95	2.2	+154	—
2580	8 17 4	-30 0	217.5	+4 6	c	9	—	30	13 5	10 9	1.20	1.91	5.0	+181	—
2587	8 19 3	-29 10	217.5	+5 4	c	6	—	30	13 5	10 9	1.20	1.91	3.3	+331	—
2627	8 33 1	-29 36	219.5	+7 6	f	8	69	40	13 5	11 5	1.58	2.51	5.8	+10	19
2632	8 34 3	+20 20	173.5	+34 0	d	—	—	—	—	—	0.18	—	—	+365	—
2635	8 34 5	-34 25	223.5	+4 8	d	3	—	20	13 5	12 7	2.75	4.37	3.8	+0.01	—
I 2391	8 37 5	-52 34	237.5	+6 3	c	20	—	10	—	3 5	0.04	0.06	0.5	—69	—
2659	8 39 2	-44 36	232	-1 0	d	10	—	50	13 4	12 5	2.51	3.98	11.6	—	—
2660	8 39 3	-46 51	233.5	-2 4	d	15	6	25	—	13	3.2	5.0	2.2	—211	—
2668	8 39 4	-32 18	223	+6 9	f	9	36	30	13 5	12 2	2.19	3.47	9.1	+418	—
I 2395	8 40 0	-47 49	234	-3 0	e	10	—	16	—	10 1	0.83	1.32	3.8	+68	—
2670	8 42 4	-48 25	234	-3 0	d	15	—	16	—	11 2	1.38	2.19	9.5	+116	—
2671	8 42 6	-41 51	230	+1 5	e	8	—	20	—	13	3.2	5.0	4.4	+129	—
H 3	8 45 3	-52 25	238.5	-5 5	e	7	—	35	13 4	10 4	0.95	1.51	3.1	+152	—
2682	8 45 8	+12 11	184	+33 4	f	15	57	67	12 8	10 8	1.15	1.82	7.9	+1002	20
2818	9 12 0	-36 12	230	+9 3	e	9	53	20	—	13	3.2	5.0	13	+807	21
I 2488	9 24 6	-56 32	245.5	+4 1	d	20	—	50	12 5	11 2	1.38	2.19	12.8	+156	—
2910	9 26 9	-52 28	243	-0 8	f	6	—	30	12 5	11 2	1.38	2.19	3.8	+31	—

(Continued.)

N.G.C.	R.A. 1900	Dec. 1900	Galactic		Class	Apparent Diameter in arc- minutes	Orient. °	No. of Stars	Apparent Mag. Lim. of Field	Mag. of Star	Distances		Lower Diameter $M = -0.5$ pc	R in β $M = -0.5$ pc	Notes
			Long.	Lat.							$M = +0.5$ kpc	$M = -0.5$ kpc			
2025	9 ^h 30 ^m 3	-53° 0'	243.5	0° 9	d	11'	—	30	12 ^m 5	10 ^m 7	1.10	1.74	5.6	—	—
3105	9 57 2	-54 18	247.5	-0 6	f	1.5	—	15	—	[12 5	> 2.51	> 3.98	> 1.7	—	—
3114	9 59 5	-59 38	251	-3 6	e	30	Ind	100	—	7	0.2	0.3	2.6	—	—
3208	10 17 8	-51 13	248.5	+4 6	f	30	—	12	—	10 1	0.83	1.32	41.5	+105	—
I 2581	10 23 7	-57 8	252	+0 4	f	5	—	35	12 5	11 8	1.82	2.88	4.2	+20	—
3393	10 29 6	-57 41	253	0 0	d	8	—	50	—	[7 8	< 0.46	< 1.0	< 1.0	0	—
H 4	10 35	-53 38	252	+4 0	f	8	—	25	—	10 2	0.87	1.38	3.2	+96	—
Mal 101	10 38 6	-64 34	257	-5 6	e	15	—	40	—	11 4	1.51	2.40	10.5	-238	—
I 2602	10 39 4	-63 52	257	-4 9	e	70	—	32	—	6	0.43	0.20	4.1	-17	22
3532	11 2 2	-58 8	257	+1 5	f	60	—	130	—	8 1	0.33	0.52	9.1	+13	—
3572	11 6 2	-59 42	258.5	+1 0	d	8	—	30	13	9 6	0.66	1.05	1.5	—	—
3590	11 8 7	-60 15	259	-0 2	f	3	—	25	13	9 9	0.76	1.20	4.1	+4	—
I 2714	11 13 6	-62 10	260	-1 5	e	12	—	150	13	10 7	1.10	1.74	6.1	—	—
Mal 105	11 15 2	-62 58	260	-2 5	f	4	—	50	13	11 0	1.26	2.00	2.3	-88	—
3766	11 31 5	-61 3	261.5	+0 1	g	10	—	60	13	8 1	0.33	0.52	1.5	+1	—
I 2948	11 34 1	-62 58	262.5	+1 9	e	15	—	25	13	8 6	0.42	0.66	2.9	-22	—
Mal 108	11 45 9	-55 8	262.5	+6 0	g	6	Ind	50	—	13 1	3.31	5.25	9.1	+552	—
4052	11 58 0	-62 38	265	+1 0	e	10	—	25	13	11 6	1.66	2.63	7.6	-47	—
4103	12 1 5	-60 41	265	+1 0	d	9	—	25	13	9 4	0.60	0.95	2.5	+16	—
4337	12 18 5	-57 34	267	+4 3	f	4	—	20	13 5	13 1	3.31	5.25	6.1	+395	—
4349	12 19 0	-61 20	267.5	+0 7	g	15	—	100	13 6	10 4	0.95	1.51	6.6	+18	—
Mal 111	12 20	+26 40	260	-85 4	c	—	75	—	—	—	0.1	—	—	+100	23
H 5	12 22 4	-60 12	267.5	+1 7	d	7	—	30	13 6	9 6	0.66	1.05	2.1	+32	—
4439	12 23 0	-59 32 4	268	+2 4	d	3	—	10	13 6	10 2	0.87	1.38	1.2	+58	—
4463	12 24 5	-64 14 2	268	-2 3	f	3	—	20	13 6	10 2	0.87	1.38	1.2	—	—
H 6	12 32 5	-67 53	269	-5 9	e	7	—	75	—	13 6	4.17	6.61	13.5	-679	—
H 7	12 33 4	-60 3	269	+1 9	c	18	—	200	—	14	5.0	7.9	41.4	+267	—
4609	12 36 5	-62 25	269	-0 4	e	4	—	20	13 6	9 3	0.57	0.91	1.1	-7	—
4755	12 47 7	-59 48	271	-2 2	g	10	—	50	13 6	7 6	0.2	0.3	0.9	+11	24
4815	12 51 8	-64 25	272.5	+2 4	f	4	—	40	14	13 6	4.17	6.61	7.7	-282	—
4852	12 54 1	-59 4	272	+2 8	d	10	—	40	13 6	9 9	0.76	1.20	3.5	+58	—
H 8	13 11 7	-66 33	272	-4 7	f	4	—	25	14	13 6	4.17	6.61	7.7	-546	—
5281	13 39 7	-62 24	277	-1 2	d	3	—	20	13 6	10 1	0.83	1.32	1.1	-27	—
5316	13 46 9	-61 23	278	-0 4	d	12	—	50	13 6	10 5	1.00	1.58	5.5	-11	—
5460	14 1 2	-47 50	284	+12 0	d	30	—	25	13 5	9 1	0.52	0.83	7.3	+173	—
5593	14 19 0	-54 21	284.5	+4 9	e	8	—	10	13 5	11 5	1.58	2.51	5.8	+245	—

(Continued)

N G.C.	R. A. 1900	Dec. 1900	Galactic		Class	Approx. Dia. meter	Orient.	No of Stars	Approx. Mag. Lum of Plate	Mag. in Star	Distance		Linear Diameter $M = -0.5$ pc	$R \sin \beta$ $M = -0.5$ pc	Notes
			Long	Lat							$M = +0.5$ kpc	$M = -0.5$ kpc			
5617	14 ^h 22 ^m 3	60° 16'	282° 5	0° 7	f	15'	65	50	13 ^m 6	10 ^m 8	1.15	1.82	7.9	—	23
5662	14 28 0	— 56 7	285	— 2 8	d	8	—	30	10 5	9 7	0.69	1 10	2 6	+	34
5715	14 36 1	— 57 7	285 5	— 1 4	e	6	38	30	13 6	12 4	2.40	3.80	6 6	+	94
5749	14 41 8	— 54 6	287 5	— 3 8	e	10	—	16	—	10 5	1.00	1 58	4 6	+	104
5822	14 57 9	— 53 57	289 5	— 3 8	d	40	—	120	13 6	10 8	1.15	1 82	21 2	+	89
5823	14 58 3	— 55 12	289	— 1 7	f	9	64	80	13 6	10 8	1 15	1 82	4 8	+	53
H9	15 44 3	— 53 15	293 5	— 1 1	e	3	Ind	30	—	13 6	4 17	6 61	5 8	+	126
5999	15 47 8	— 57 8	293	— 3 8	f	4	—	100	13 6	12 4	2.40	3.80	4 4	—	186
6005	15 47 8	— 57 8	293	— 3 8	f	3	50	30	—	13 6	4 17	6 61	5 8	—	145
6025	15 55 2	— 60 13	291 5	— 6 8	d	10	—	30	9 5	15 6	0.40	0.63	1 8	—	75
6067	16 5 4	— 53 57	297 5	— 3 2	f	15	46	120	13 6	10 9	1.20	1.91	8 3	—	105
6087	16 10 6	— 57 39	295 5	— 6 4	d	20	—	35	13 6	9 7	0.69	1 10	6 4	—	122
H10	16 11 9	— 54 44	297 5	— 4 5	d	30	—	30	13 5	10 6	1.05	1.66	14 5	—	130
6124	16 18 8	— 40 26	308 5	— 4 8	e	25	Ind	120	13 5	9 1	0.52	0.85	6 0	+	70
6134	16 20 3	— 48 55	302 5	— 1 2	f	9	Ind	60	12 2	11 3	1.45	2.29	6 0	—	50
6152	16 24 9	— 52 24	300 5	— 4 2	e	30	—	60	13 5	11 0	1.26	2.00	17 5	—	145
H11	16 27 9	— 49 25	303	— 2 5	d	10	—	60	13 5	10	0.8	1 3	3 8	—	56
6178	16 28 5	— 45 25	306	— 0 1	f	4	—	10	—	10 3	0.91	1 45	1 7	+	3
6192	16 33 8	— 43 10	308 5	— 1 0	f	7	75	30	13 6	9 0	0.50	0.79	1 6	+	15
6195	16 39 0	— 46 50	306 5	— 2 6	e	20	—	30	—	10 4	0.95	1 51	8 8	—	70
6204	16 41 5	— 53 38	301 5	— 6 8	f	5	—	25	—	10 6	1 05	1 66	2 4	—	63
6208	16 43 5	— 44 53	308 5	— 1 3	e	22	—	50	13 5	12 8	2.88	3 98	2 5	—	475
6222	16 47 0	— 44 38	308 5	— 0 2	d	3	—	20	—	12 8	2 88	4 57	4 0	—	105
6231	16 48 8	— 39 20	313 5	— 0 4	c	15	—	120	—	17 4	<0.24	<0.38	<1.7	<	1
6242	16 49 2	— 40 33	312 5	— 1 2	f	10	44	40	12 2	8 5	0.36	0.57	1 7	+	4
H12	16 51 2	— 52 33	303	— 7 5	c	40	—	200	12 2	17 4	<0.24	<0.38	<1.7	<	8
6253	16 53 5	— 44 31	309 5	— 2 7	f	6	45	70	—	13 4	>3.16	>5.01	>8.7	>	637
6259	16 55 2	— 39 35	314	— 0 1	e	15	49	100	12 2	11 3	1 45	2 29	10 0	—	108
6268	16 57 9	— 48 2	307	— 5 4	f	10	—	30	—	10 4	0.95	1 51	4 4	—	2
H13	16 58 0	— 37 45	316	— 0 8	d	15	—	70	13 8	13	3 2	5 0	22	—	+74
6281	17 10 8	— 39 20	316	— 2 2	d	5	39	60	12 2	11 5	1 58	2 51	3 6	—	4
6318	17 11 6	— 42 46	313	— 4 3	e	12	—	20	12 2	9 6	0.66	1 05	5 7	—	97
6322	17 16 9	— 49 50	307 5	— 9 0	e	14	—	200	13	10 3	0.91	1 45	5 9	—	79
I 4651	17 17 7	— 38 57	317	— 3 1	f	10	—	50	—	11 6	1 66	2 63	7 6	—	227
6355	17 17 8	— 26 15	327	— 4 0	g	1	—	—	—	—	—	—	—	—	82

(Continued.)

R.G.C.	R.A. 1900	Dec. 1900	Galactic		Class	Apparent Diameter	Orbital Period	No. of Stars	Apparent Mag. Lim. of Field	Mag. per Star	Distance		Linear Diameter $M = -0.5$ pc	R in β $M = -0.5$ pc	Notes
			Long.	Lat.							$M = -0.5$ kpc	$M = -0.5$ kpc			
I 1257	17 ^h 21 ^m 18	-7° 0'	345° 5	+13° 7	e	—	—	20	18 ^m	8 ^m 7	—	—	—	—	26
H 15	17 22 16	-29 26	325	+1 4	e	18	—	15	—	8 4	0.69	0.44	2.0	+ 17	—
H 16	17 24 17	-36 46	328 5	+ 3 0	e	15	—	20	—	8 4	0.60	0.38	2.6	+ 32	—
6383	17 28 2	-32 30	323 5	- 1 2	e	6	—	12	—	9 6	1.05	0.66	1.8	- 24	—
6400	17 32 17	-36 53	320	- 4 4	d	6	—	25	—	8 7	0.69	0.44	1.2	- 53	—
6404	17 33 11	-33 10.9	323	- 2 5	e	8	—	20	—	[9 6	> 0.66	> 0.66	> 0.9	> 46	—
6405	17 33 5	-32 9	324	- 2 1	e	25	—	50	12 2	8 3	0.36	0.37	4.1	- 20	27
H 17	17 33 17	-40 1	317	- 6 3	d	10	—	20	13	9 6	0.66	0.66	3.0	- 114	—
6416	17 37 8	-32 18	324 5	- 2 9	e	20	—	25	8	8 3	0.36	0.37	3.3	- 29	—
I 4665	17 41 4	+ 5 45	358	+15 6	e	60	—	13	—	7 5	0.2	0.3	5.2	+ 81	—
6451	17 44 3	-30 11	327	- 3 0	e	6	—	50	—	10 3	0.91	1.45	2.5	- 76	—
6469	17 46 9	-22 19	334	+ 0 5	e	12	—	40	—	11 8	1.82	2.88	10.1	+ 25	—
6475	17 47 3	-34 47	323 5	- 5 9	e	60	—	50	12 2	7 4	0.44	0.38	6.6	- 39	—
H 18	17 49 7	-35 16	323	- 6 6	d	18	—	80	12 2	8 7	0.24	0.24	3.0	- 79	—
6494	17 51 0	-35 0	337 5	- 1 4	e	25	—	120	12 5	10 2	0.87	1.38	10.0	- 34	—
6520	17 57 1	-27 54	331	- 3 7	e	5	—	25	11 8	9 3	0.44	0.69	1.0	- 44	—
6531	17 58 6	-22 30	335	- 2 8	d	10	—	50	—	8 7	0.57	0.91	2.6	- 30	—
6530	18 1 2	-25 1	333	- 4 8	e	1	—	25	—	9 3	0.57	0.91	2.6	- 44	—
6540	18 3 8	-31 47	327 5	- 7 4	e	1	—	—	—	[13	—	—	—	—	25
6558	18 9 8	-22 10	336 5	- 4 0	e	0.75	—	—	—	[13	—	—	—	—	25
H 19	18 11 5	-13 19	345	- 0 1	e	1.8	—	30	13 2	13 2	3.2	5.0	2.2	- 348	—
6603	18 12 6	-18 27	340 5	- 2 8	e	5	—	20	13 2	13 0	3.47	5.50	8.0	- 9	—
6611	18 13 2	-13 49	345	- 0 6	e	4	—	50	13 2	13 0	3.16	5.01	5.8	- 244	31
6613	18 14 1	-17 10	341 5	- 2 5	c	25	—	55	12 5	10 6	1.05	1.66	12.1	- 18	32
6618	18 15 0	-16 13	342 5	- 2 2	d	12	—	12	12 5	10 9	1.20	1.91	6.7	- 83	33
6633	18 22 7	+ 6 30	3 5	+ 6 8	c	—	—	35	12 5	10 6	1.05	1.66	—	- 64	34
I 4725	18 25 8	-19 19	341	- 6 0	d	20	—	65	9 6	8 0	0.32	0.50	2.9	+ 60	—
6642	18 25 8	-23 32	337	- 7 9	d	40	—	50	13 2	9 3	0.57	0.91	10.6	- 94	35
6645	18 26 8	-16 58	343 5	- 5 1	e	1	—	—	—	—	—	—	—	- 207	—
6649	18 27 9	-10 28	349	- 2 3	f	10	—	75	13 2	11 3	1.45	2.29	6.6	- 207	—
6664	18 31 1	- 8 18	352	- 2 0	d	8	—	35	13 2	12 1	2.09	3.31	7.7	- 131	—
I 4756	18 34 0	+ 5 22	4	+ 3 8	d	18	—	80	10 2	11 3	1.45	2.29	12.0	+ 79	—
6694	18 39 8	- 9 30	351 5	- 4 4	f	70	—	20	13	8	0.3	0.5	10.2	+ 33	36
6705	18 45 7	- 6 23	355	- 4 2	e	9	—	200	13	11 9	1.91	3.92	7.9	- 231	—
						10	—	—	13	12	1.25	—	3.6	- 92	37

Notes to Appendix B

- 1 Messier 103
- 2 Distance from WALLENQUIST, Upsala Medd 42 (1929)
- 3 h and z Persei, fifth star assumed of magnitude $-2^m.5$ TRUMPLER [Publ A S P 38, p 352 (1926)] gives a distance of 2.3 on the basis of the mean magnitude for Class A0.
- 4 Messier 34
- 5 Messier 45, the diameter from RUSSELL, DUGAN, and STEWART.
- 6 Distance and diameter from RUSSELL, DUGAN, and STEWART corresponds to an angular radius of nearly two degrees
- 7 Messier 38
- 8 Messier 36, distance from WALLENQUIST, Upsala Medd 32 (1927)
- 9 Messier 37, distance from VON ZEPPEL and LINDGREN, Svenska Vet Akad Handl 61, No 15 (1921).
- 10 Messier 35
- 11 Scarcely resolved
- 12 Eccentric in an elliptical diffuse nebula.
- 13 S Monocerotis in cluster.
- 14 Messier 41
- 15 Messier 50
- 16 ϵ Canis Majoris in cluster.
- 17 Messier 46, an important photographic catalogue by CHEVALIER
- 18 Messier 93
- 19 Praseope, Messier 44, distance from RUSSELL, DUGAN, and STEWART
- 20 Messier 67
- 21 Diffuse nebula in a coarse cluster
- 22 η Carinae involved
- 23 Coma Berenices, distance from RUSSELL, DUGAN, and STEWART
- 24 κ Crucis.
- 25 Not resolved, a photograph of N G.C. 6540 appears in Pop Astr Tidssk 8, p 62 (1927).
- 26 Mount Wilson plate.
- 27 Messier 6.
- 28 Messier 7
- 29 Messier 23.
- 30 Messier 21.
- 31 Messier 24
- 32 Messier 16.
- 33 Messier 18
- 34 Messier 17, nebulosity.
- 35 Messier 25
- 36 Messier 26, TRUMPLER finds a distance of 2.75 [Lick Bull 14, p 122 (1929)].
- 37 Messier 11, distance from TRUMPLER.
- 38 Messier 71.
- 39 Messier 29.
- 40 Messier 39
- 41 Messier 52, distance from WALLENQUIST, Upsala Medd 42 (1929).

Addendum Current work on problems of both our own and external systems, in progress since this section was written, contributes effectively to our view of galactic structure and indicates the necessity for gathering much more evidence before any conclusive theory can be advanced. For instance, there have been important studies at Harvard, Mount Wilson (STROMBERG), and McCormick Observatories on the integrated magnitudes and colors of globular clusters. The absorption extending out from the "region of avoidance" appears to affect the magnitudes and distances of clusters in low latitudes, making uncertain and impractical the estimate of the dimensions of the Milky Way in its own plane, but, on the other hand, the Harvard studies of faint cluster type variables in high latitudes (Wash Nat. Ac. Proc in press, 1933) indicate a total galactic extent of the order of that given above.

Chapter 6

The Nebulae.

By

Heber D. CURTIS—Ann Arbor, Mich

With 58 illustrations in the text and on a plate

a) Introduction.

1. Definition of Nebulae. In the early historical development of the field, any object that was non-stellar with the limited telescopic powers available, and that did not appertain to the solar system, was termed a nebula. The earlier lists and even the more important later catalogues have in general made no complete or satisfactory distinction as to the character of the nebulous object, and the genetic influence of such reference media as the great catalogues of DREYER have involved the subject in a number of contradictions through the inclusion of such non-nebular classes as the globular star-clusters and the spirals. These inconsistencies persist in all the modern bibliographical apparatus of the field, and doubtless can never be entirely removed. Further reference to these difficulties will be made in ciph 4 and 34.

2. Historical Notes. As in most fields of astronomy, research on the nebulae may be divided into three moderately well-marked periods.

A. The period preceding 1782, marked by visual or sporadic telescopic observation, and now of little more than historical interest. A few brighter star-clusters and the Great Spiral in Andromeda, which can be made out by the unaided eye, were noted very early. ARATUS (300? A.D.) mentions Praesepe; AL-SUFY (ca. 960 A.D.) notes Andromeda, HEVELIUS (1690), HALLEY (1715), and LA CAILLE (1755), catalogued a few of such brighter objects. MESSIER's lists of 103 bright nebulae and clusters appeared in 1771 and 1781—82. See Appendix No. 1 for the modern identification of these objects, for which MESSIER's numbers are still in frequent use.

B. From 1782 to 1898. To SIR WILLIAM HERSCHEL must be given the unchallenged rank of pioneer in the field of nebular discovery¹. For nearly a quarter of a century following 1782, with tremendous zeal, with instruments which would seem totally inadequate to the modern observer, with an acuity of vision which has perhaps never been surpassed and which is a constant source of amazement to those who review his work with the much more powerful instruments of the present day, he discovered and catalogued in eight classes (cf. Appendix No. 2) 2509 nebulae and clusters.

Second only to the work of his famous father was the continuation made by SIR JOHN HERSCHEL, who observed 2307 nebulae at Slough, and 1708 southern

¹ HERSCHEL's numerous papers in the Phil Trans and other media are now most easily accessible in: Scientific Papers of SIR WILLIAM HERSCHEL, Published by the Royal Society and the Royal Astronomical Society 2 vols, quarto London (1912).

objects on his expedition to the Cape of Good Hope, in the years from 1830 to 1847. He collected his own and his father's discoveries in his General Catalogue of Nebulae¹, containing 5079 entries, and referred to as GC in the older literature.

The impetus which had been given to the work of nebular discovery by the **HERSCHELS** brought a large number of other workers into this field in the middle third of the nineteenth century. Space prevents more than a mention of the names of **ROSSE**, **LASSALL**, **STEPHAN**, **D'ARREST**, **SWIFT**, **SCHÖNFELD**, **BOND**, and **VOGEL**. To **ROSSE** is due the first detection of the spiral form; he discovered perhaps twenty spirals with the 6-foot reflector. There were many observers in this period who concentrated solely upon the discovery of new objects, with little care for accuracy of position. Others, as **D'ARREST**², made careful determinations of position, which may conceivably serve as a point d'appui for proper motion investigations of the distant future.

C. 1898 and following. While there is no well-marked line of demarkation between the second and third chronological divisions, the year 1898 may be conveniently taken as the starting point of the modern epoch, even though the very first photographic and spectrographic results are considerably earlier in point of time³. The discovery of bright lines in the spectra of gaseous nebulae was made by **SIR WILLIAM HUGGINS** in 1864⁴, to whom also is due the first spectrogram (of the Orion Nebula) in 1882⁵. The first nebular photograph (also of the Orion Nebula) was taken by **DRAPER** in 1880⁶. The first extensive series of nebular photographs is due to **SIR ISAAC ROBERTS**, and was made in the years from 1885 to 1904. His photographs confirmed **ROSSE**'s discoveries of spirals, and increased the number of known spirals to about forty.

It now seems strange that an immediate wider application of photography did not at once follow the significant pioneer efforts of **ROBERTS**, **DRAPER**, **COMMON**, **HUGGINS**, **JANSSEN**, and others. During the two decades following 1870 a considerable amount of purely stellar photography was carried on, but the great value of the reflecting telescope was not fully appreciated until its epoch-making revivification by **KEELER**, at Lick Observatory, in 1898—1900⁷. **KEELER**'s results showed the following salient advances, which have formed the norm for much subsequent nebular research⁸:

1. Reflecting telescopes of moderately large focal ratios (1.5 to 1:6) are the most efficient instruments known for nebular research.

2. A wealth of structural detail was shown, impossible to secure visually or with refractors.

3. A predominantly spiral form was shown to exist in a large proportion of the objects recorded. About 40 objects had been previously found to be spiral.

¹ Phil Trans (1864).

² Sidarum nebulosorum observationes Havnienses (1867), 1942 entries.

³ The first stellar photograph was taken with the 15-inch equatorial of Harvard College Observatory on July 17, 1850, by **MR WHIPPLE** working under the direction of Professor **BOND**. An image of α Lyrae was obtained.

⁴ Proc R S London 13, p. 492 (1864).

⁵ C R 94, p. 94 (1882).

⁶ Amer J Sc (3) 20, p. 433 (1880).

⁷ Lick Publ 8 (1908).

⁸ Perhaps the main reason for this neglect of the reflector came from purely mechanical considerations. With scarcely an exception, reflecting telescopes from the days of the older **HERSCHELS** down were mounted and equipped most crudely, in comparison with the mechanical excellence developed in the mountings of refracting telescopes. **LASSALL**'s reflector at Malta utilized man-power for its "driving-clock", a workman gave one revolution per second to a heavy flywheel suitably geared to the telescope. There was, in this period, scarcely a single reflector possessing adequate rigidity, accurate clock-work, or convenience of manipulation.

4 Very large numbers of very small and faint objects were recorded "A conservative estimate places the number within reach of the Crossley reflector at about 120000. The number of nebulae in our catalogues is but a small fraction of this." See ciph 36

KEELER's program with the Crossley reflector was continued and completed by PERRINE (1901—1903), and extended by CURTIS (1909—1918). Later, the magnificent 60-inch and 100-inch reflectors at Mt Wilson, in the hands of RITCHIEY, HUBBLE, PEASE, DUNCAN, HUMASON, and others, have secured larger scale nebular photographs of the highest perfection. A vast amount of survey data has been accumulated by the Harvard workers and on the FRANKLIN-ADAMS star charts. All work in the radial velocities and spectrographic rotations of the spirals goes back to the extensive pioneer contributions made by SLIPHER, at Lowell Observatory. In Europe, to mention but a few, notable investigations have been carried out by WOLF, REINMUTH, WIRTZ, HOLETSCHEK, HAGEN, and others. In the still comparatively neglected southern heavens, a beginning has been made by PERRINE, at Córdoba, and by KNOX-SHAW and associates, at Helwan. More complete details of the progress which has been made since 1900 in the nebular field should be sought in the separate sections.

8. **Bibliographical Notes**¹. The culmination of a century of discovery, marked by some slight progress in delineation of form and classification, was marked in 1888 by DRYER's collection and revision of all previous results in his New General Catalogue (NGC), which, with his two supplementary Index Catalogues (I, II), contains 13223 entries. These are still the most complete catalogues of nebular objects, and the indispensable basis for all succeeding surveys.

The older nebular literature refers frequently to nebulae by the MESSIER number M, by SIR W. HERSCHEL's Classes and numbers, by the numbers in SIR J. HERSCHEL's lists (JII), or by the same author's General Catalogue number (GC). The bright spiral numbered 4303 in the New General Catalogue (NGC), may then possibly have also the designations M61, I 139, JII1202, or GC2878. This is a source of considerable confusion and loss of time in consulting references in the older literature. Appendices Nos 1, 2, 3, and 4, give finding lists for locating such references in the NGC, which is the only method that should be employed in designating such objects. Throughout this treatment, nebulae will accordingly be referred to solely in the forms 7619, I 562, II 2418 (i. e., their numbers in the NGC or in the First and Second Index Catalogues), and with the omission of the qualifying letters NGC.

While many faint nebulae have been photographed which are not given in the NGC (see Appendix No 7), to be found in various published lists, the most comprehensive and homogeneous photographic catalogue of such NGC objects as can be reached from northern latitudes is doubtless that due to REINMUTH, with 6251 entries of NGC objects, a summary of the photographic work at Königstuhl by WOLF, REINMUTH, WIRTZ, and others².

There are already many thousand small nebulae listed that are not included in the NGC, and HUBBLE has estimated that there may exist as many as $3 \cdot 10^7$ small and faint objects in the great group of the spirals (see ciph 36). The labor of observation and subsequent cataloguing adequate to a really complete

¹ J. L. E. DRYER, A New General Catalogue of Nebulae and Clusters of Stars. Mem. RAS 49 (1888), Index Catalogue of Nebulae found in the Years 1888 to 1894, *ibid.* 51 (1895), Second Index Catalogue of Nebulae and Clusters of Stars, containing Objects found in the Years 1895 to 1907, *ibid.* 59 (1908).

² Die Herschel-Nebel nach Aufnahmen der Königstuhlsternearte, Publ. Sternw. Heidelberg 9 (1926).

Durchmusterung of all such objects brighter than magnitude ca. 20 is so tremendous that it will doubtless be necessary to leave its completion to the centuries following our own. Even the systematic study and classification of the $25\,000 \pm$ objects of present lists, as suggested by the Committee on Nebulae and Star Clusters of the International Astronomical Union (1925), demands international co-operation. A new General Catalogue of Nebulae in the form of a card catalogue is being prepared by LUNDMARK at Upsala¹ and will be available for consultation by investigators. About 16000 cards have been written out, and it is expected that the complete catalogue will enumerate 35 000 objects, publication is planned within the next few years.

A card catalogue which the author has compiled of literature relating to the nebular and allied fields since 1890, with the inclusion of older works of importance but with the omission of minor notes and papers of a purely general or popular nature, contains over 2000 entries. It is manifestly impossible, therefore, to aim at completeness in the bibliographical references quoted in treating this subject. In general, only a few of the more important references can be cited, and the names of numerous investigators must perforce be omitted.

4. *Classification and Units.* A descriptive summary of the present status of the subject of the nebulae manifestly requires a less complicated and detailed system of classification than might be deemed necessary for the purposes of a catalogue. For this reason, the field is treated in this paper under its larger outlines, as follows:

The Diffuse Nebulae

1. Dark Nebulae.
2. Cosmic Clouds
3. Luminous Diffuse Nebulae

The Planetary Nebulae.

The Spirals

1. True Spirals.
2. Barred Spirals.
3. Elliptical and Globular Objects.
4. Magellanic Type Spirals

In Appendix No. 5 are collected a considerable number of systems of nebular classification which have been suggested or used by investigators of the field.

There are some elements of inconsistency in all existing systems of classification, that of this treatment included. The genetic development of the field, largely through the influence of the HERTSCHEL and the NGC, which perforce combined in one catalogue all diffuse nebulae, planetaries, clusters, and spirals, has forced us into a somewhat illogical position as regards nomenclature and classification. There has never been any difficulty as to the segregation of the clusters as a class, inasmuch as they are not nebulae at all. The spirals are likewise not nebulae, in the rigorous sense², yet these objects form the overwhelming preponderance of all existing "nebular" catalogues. We are presented with the dilemma, on the one hand, of continuing to distort somewhat the true concept of bona-fide nebulous matter by calling them "spiral nebulae", "anagalactic nebulae", "extra-galactic nebulae", "non-galactic nebulae", "außergalaktische Nebel", and the like, or, on the other hand, of abandoning entirely this lack of nomenclatural rigor forced upon us by the historical development of a field.

¹ Publ A S P 42, p. 31 (1929)

² The comparatively rare cases where emission lines have been detected in the spectra of spirals may doubtless be adequately explained as due to the inclusion of true luminous nebulosity. See diph. 48.

in which the substantiation of the non-nebular character of the spirals is less than fifteen years old

The author would personally prefer to use the term "galaxies" or "external galaxies", rather than the word "spirals" in describing these objects¹, thus avoiding the partial inconsistency that no spiral structure is discernible with present resolution in the small elliptical and globular members of the class. The name "spiral" may, however, be regarded as a more or less satisfactory compromise

A unit frequently used for the distances and dimensions of spirals in recent research literature is the parsec, which is the distance corresponding to a parallax of 1". This concept of distance is less familiar to investigators in allied fields of science, and the unit of distance employed throughout this treatment will be the light-year, abbreviated to ly, and equal to $9.46 \cdot 10^{12}$ km, or $5.87 \cdot 10^{13}$ miles. 1 parsec = 3.26 ly = $3.1 \cdot 10^{13}$ km.²

¹ E. g., H. SHAPLEY, Note on a Remote Cloud of Galaxies in Centaurus, Harv Bull 871, The Coma-Virgo Galaxies, I-VI, *ibid*, 865 to 869 and 873 (1929)

² With an error of ca. 8%, which is entirely negligible in comparison with the uncertainties of present cosmic data, the transfer from light-years to parsecs, or vice versa, may be made through the simple relations

$$D_1 \cdot 3/10 = D_{\text{parsec}}$$

$$D_{\text{parsec}} \cdot 10/3 = D_1$$

Of the equivalent methods of expressing the distance of a spiral, all of which may be found in the literature of the past decade

$$\pi = 0''.0000007$$

$$D = 1.4 \cdot 10^6 \text{ parsecs}$$

$$= 4.8 \cdot 10^6 \text{ ly}$$

$$= 4.5 \text{ A}$$

the value in light-years has some advantages on the score of easy visualization

The added "historical" element involved in the use of the light-year as a measure of galactic distances is of great interest and value. Though the light-year was not used as a formal unit in his time, attention was perhaps first called to this point by Sir WILLIAM HERSCHEL (Coll Sc Papers 2, p 213)

"a telescope with a power of penetrating into space, like my 40-foot one, has also, as it may be called, a power of penetrating into time past. It may be proved, that when we look at Sirius, the rays which enter the eye cannot have been less than 6 years and $4\frac{1}{2}$ months coming from that star to the observer. Hence it follows, that when we see an object of the calculated distance at which one of the remote nebulae may still be perceived, the rays of light which convey its image to the eye, must have been more than nineteen hundred and ten thousand, that is, almost two millions of years on their way, and that, consequently, so many years ago, this object must already have had an existence in the sidereal heavens, in order to send out those rays by which we now perceive it."

The following short table gives a number of the units which have been used in expressing the enormous distances of other galaxies

Light-year	= distance traversed by light in 1 year = $9.46 \cdot 10^{12}$ cm
Parsec	= distance for $\pi = 1'' = 3.26 \text{ ly} = 3.1 \cdot 10^{13}$ cm
Cubic parsec	= $34.65 \text{ ly}^3 = 2.9 \cdot 10^{35} \text{ cm}^3$
Kiloparsec	= 10^3 parsecs = 3260 ly
Megaparsec	= 10^6 parsecs = $3.26 \cdot 10^6 \text{ ly}$
Sternweite, Macron, Astron	= parsec
Sinometer	= 10^6 astr units = 15.8 ly
Siriusweite	= distance for $\pi = 0''.2 = 16.3 \text{ ly}$
Andromede	= distance of Great Spiral in Andromeda, supposed to be of the order of 1000 ly at the time this unit was suggested by VARY
A	= an unnamed unit used by DE SITTER in recent papers = $1.06 \cdot 10^6 \text{ ly} = 10^{21} \text{ cm}$

b) The Diffuse Nebulae.

5. Definition. The diffuse nebulae, which are rightly to be regarded as par excellence the actual nebulous elements of the cosmos, are irregular cloud-like formations (ex Lat nebula = cloud) of tremendous extent, of random and inchoate structure, of the utmost tenuity, and composed of finely divided matter or matter in the atomic or molecular state.

In apparent size, they vary from small irregular patches or detached wisps to complicated structures of enormous extent and volume. Several of HERSCHTEL's regions of diffuse nebulosity cover over 7 square degrees, while the "North America" in Cygnus (7000) has an area of about 10 square degrees. There are even larger areas of very faint diffuse nebulosity in Orion, Taurus and Perseus¹ which must cover over 100 square degrees in their extreme dimensions.

6. Number and Distribution. The diffuse nebulae are essentially and definitely galactic in distribution, and are rarely found at any considerable distance from the galactic plane. Save as possible constituents of other galaxies (see clph. 48), all are apparently within the bounds of our own galactic system. They are, moreover, nearly always more or less closely associated with stars.

While no accurate data are available as to the total number of the diffuse nebulae, it seems fairly certain that this total is not large, and that this class does not form 10% of existing nebular catalogues. One may conservatively estimate their number as roughly 1000.

CURTIS², in the Crossley Reflector program, sought to secure a photographic record of all NGC objects with the Herschellian characterization B or L; the program was otherwise at random. He photographed 56 diffuse nebulae, as against 513 spiral, from which may be deduced a total number of ca. 1000 objects in this class.

CHARLIER³ plotted the galactic coördinates of 11 475 NGC entries (reproduced as Figure 29), excluding all objects known to be planetary, annular, clusters, or of stellar type. For the zone 30° in width between galactic latitudes +15° and -15°, he found that the number of nebulae per 25 square degrees was but 1.3, and the numbers in the zones at $\pm 15^\circ$ were twice as great as those at $\pm 10^\circ$. As the diffuse nebulae are most frequently seen in low galactic latitudes, if the area of the Milky Way be taken at 10800 square degrees (probably excessive), one would expect only ca. 560 such objects, to which total would be added the numbers of any diffuse nebulae lying farther from the galactic plane.

HARDCASTLE's counts of nebulae observed on the FRANKLIN-ADAMS plates⁴ may be regarded as referring to the brighter objects of the entire sky. In this count there were tabulated:

Spiral or probably spiral	173
Elongated, spindle-shaped, oval	233
Diffuse	51
Small, just distinguishable from star images	327
Total	784

This proportion of 6.5% again points to the number of the diffuse nebulae as of the order of 1000. New objects of the class are occasionally discovered, and doubtless additions will be made in the future, but present photographic surveys of the Milky Way area are of such completeness that no large number of such accessions is to be expected.

¹ Cf. Ross, Ap J 67, p. 280, Plates VI and VII (1928)

² Lick Publ 13 (1918)

³ Lund Medd (I) No 98 (1921)

⁴ M N 74, p. 699 (1914)

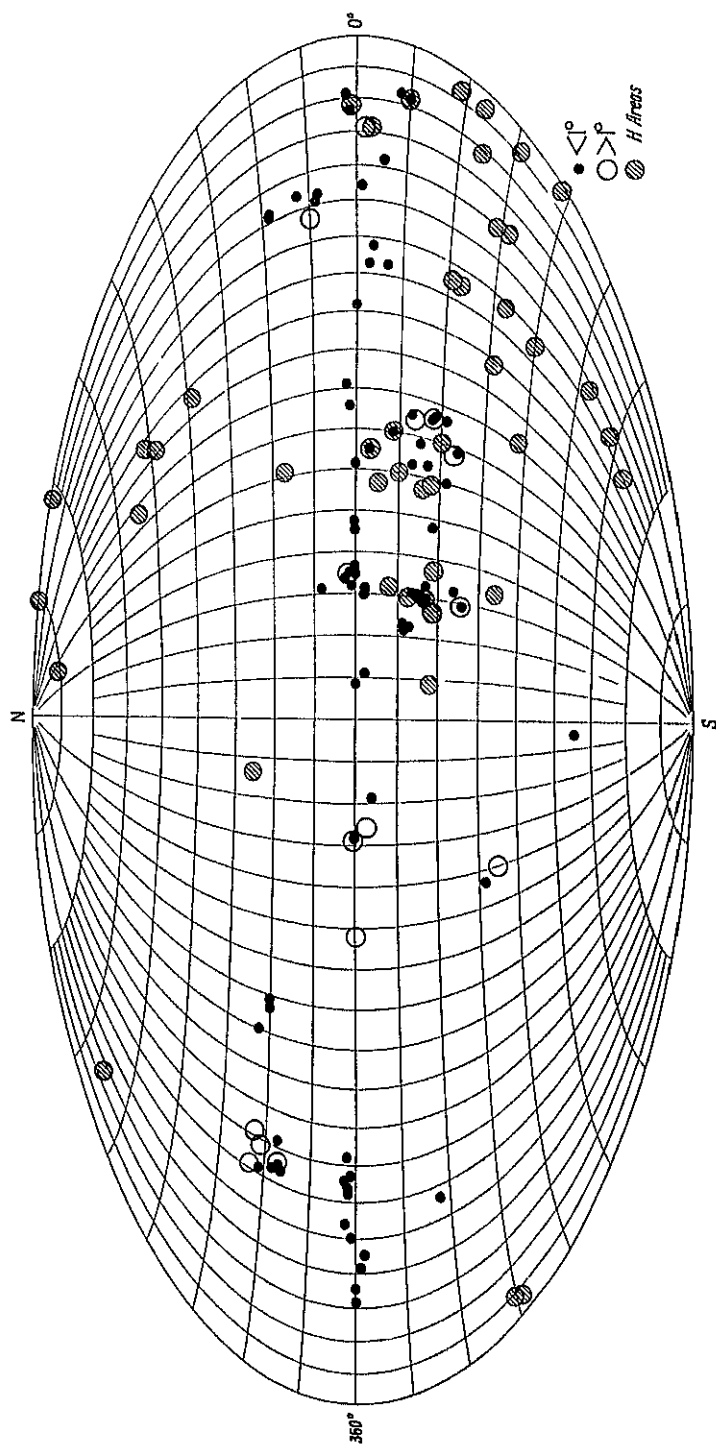


Fig 1 Galactic Distribution of Diffuse Nebulae

7. Physical Characteristics of Diffuse Nebulae. The spectral characteristics of nebulous matter will be treated later in ciph 15, 16 and 25, while reference will be made to the large body of theory based on quantum relationships as applied to the nebulosity of planetaries in ciph. 31 and 32. In the present section will be collected data referring more particularly to the mechanical attributes of such matter, even though it will occasionally be necessary to anticipate in part the conclusions of later sections.

The following subdivisions of the field seem clearly indicated

- A Dark nobulas, see ciph 8.
- B Cosmic Clouds (??), see ciph 9
- C. Luminous diffuse nebulae
 - 1 Showing emission spectra.
 - 2 Exhibiting reflection or resonance effects
 - 3 Variable in light

Not infrequently several of the sub-classes mentioned will occur in one and the same object. As to outward appearance, etc., the following characteristics may be noted:

1. Irregularity. In general, there seems to be no such thing as a regular diffuse nebulosity, or one with clear-cut and sharp periphery. The pointed ends of certain fan-shaped nebulosities (see Figure 8; I 59) approach most closely to a definite boundary. In the great majority of cases, however, no sharp and clear-cut boundary can be made out in the random and irregular formations of the diffuse nebulae.

2. An enormous variation in apparent luminosity. This range is very great; from objects like BARNARD 33 (see Figure 3), which are like a drop of ink by contrast with the brighter regions around, and which are non-luminous or, at best, very faintly luminous, to objects as bright as the Trapezium Region of the Great Nebula in Orion (see Figure 9), for which WIRTZ¹ finds an areal brightness of magn. 7.76. His corresponding value for the central part of the Great Spiral in Andromeda is but 8.82.

3. Extreme tenuity. The really significant datum for any theory of the diffuse nebulae (and doubtless for the planetaries as well) is a density almost vanishingly small (10^{-14} to 10^{-20} ?)

The intimate alliance of luminous and dark matter in numerous diffuse nebulae leads one naturally to a theory postulating similar, or at least closely allied, constitution of the two sorts. Fluorescing or resonating molecules seem a reasonable hypothesis for the luminous diffuse nebulae, and this does not require the assumption of inordinate masses. If one postulates, however, a similar atomic or molecular condition for the matter in the dark diffuse nebulae, it is found that the density necessary to produce the amount of absorption observed requires "excessive" total masses.

While most of the evidence as to the extreme tenuity of diffuse nebulosity is of an indirect nature, it is somewhat surprising that one such line of evidence may be derived from a phenomenon within the solar system. As to the possible density of a swarm of fluorescing molecules, we have no very close analogies in other phenomena, yet the work of SCHWARZSCHILD and KRON² is very suggestive. In this brilliant piece of research, these authors determined the effective density of the matter within the tail of HALLEY's Comet on two assumptions, and from photographic data secured at Tenerife with relatively small and inexpensive apparatus (two identical lenses of 2.5 cm. aperture, used extra-focally). The

¹ Lund Medd (II) No 29 (1923).

² Ap J 34, p. 342 (1911)

second of these postulates assumes that the light in the tail of this comet is given off by fluorescing molecules with a radius of the order of 10^{-8} cm. Though there is evident danger in comparing fluorescing molecules so different as may be those in a diffuse nebula and in a comet's tail, the analogy is illuminating and can not be rejected as an impossibility. For the density in the tail of HALLA's Comet, on this assumption, is $4 \cdot 10^{-21}$.

Further indirect evidence, pointing to densities vanishingly small, may be derived from mass limitations. We may assume for the distance of the Great Nebula in Orion a quantity of the order of 10^3 ly, a rough mean of the determinations of several investigators. The tremendous diffuse nebulaosity which fills most of the central portion of the constellation of Orion, of which the well known Trapezium Nebula (1976) is but a bright minor part, can scarcely contain less than 10^5 cubic ly (10^{68} cm³) if at the distance adopted. With a density of 10^{-24} , the mass of the entire structure would then be about $10 \cdot \odot$, a very moderate total. If, however, the effective density were as great as 10^{-15} , the mass involved (ca $10^{10} \cdot \odot$) would be so great as to dominate the gravitational motions of all this portion of our galaxy.

Allied with the subject of finely divided matter in a state of vanishing tenuity, the question of "stationary" or "inter-stellar" gaseous clouds should be briefly touched upon. There is manifestly a possible contradiction in any such correlation of two presumably different states of matter, even two different sorts of matter. For the inter-stellar clouds of this type are detected through the behavior of the lines of ionized calcium or sodium, whereas these have not yet been discovered in the spectra of either the diffuse or the planetary types of nebulaosity. EDDINGTON, GERASIMOVICH and STRUVE, and others¹ have postulated the existence of uniformly distributed diffuse matter in inter-stellar space, with densities of 10^{-24} (EDDINGTON), or 10^{-26} (GERASIMOVICH and STRUVE), and temperatures of 10000° to 15000° abs., as defined by the molecular speed². At such temperatures, while most of the Ca will be³ in the form Ca_{III} , there should be one part in 3000 of Ca_{II} , one part in $2 \cdot 10^6$ of Na_{I} , and one part in $2 \cdot 10^9$ of Ca_{I} . It was calculated that this amount of Ca_{II} should show absorption in a thickness of ca $3 \cdot 10^{12}$ ly. This should theoretically show in all stars, though the strength of the stellar H and K lines of Ca makes it practically impossible to detect this in stars of types later than B5, unless the star is a binary of large range, or has a peculiar velocity of the order of 100 km/sec. There should also be a correlation between the distance of the star and the intensity of the absorption.

PLASKETT and PEARCE⁴ in a series of brilliant papers, have studied the behavior of the Ca_{II} lines in a list of 261 stars of types earlier than B5, nearly all of which are close to the galactic plane and within the Milky Way structure. The results are remarkable. The speed and direction of the solar motion comes

¹ Proc R S London 111, p 424 (1926), Ap J 69, p 7 (1929), 65, p 163 (1927); 67, p 151 (1928)

² If uniformly distributed at the first density named, the total mass within a spheroidal galaxy 10000 ly thick and 60000 ly in diameter would be ca. $6 \cdot 10^{10} \odot$

³ Strictly speaking, Ca^{++} should be used for the state, and Ca_{III} for the spectrum corresponding to that state. The subject is involved in a good deal of confusion at present on the nomenclatural side, there is a tendency on the part of some physicists to abandon the use of the + sign, and it seems probable that this will eventually be abandoned entirely, though there is as yet no international agreement on the subject.

Throughout this treatment, in the interests of uniformity, ionization will be represented by the Roman numeral subscripts alone, that is, the designation for the spectrum only will be employed, and we shall write, for example, O_{II} instead of O^{++} .

⁴ Publ. Astroph. Obs. Victoria 2, p 335 (1924), M N 84, p 80 (1924), 90, p 243 (1930)

out practically the same as that determined from naked-eye stars in general, though the apex is displaced about 20° to the eastward. The K-term for these inter-stellar clouds is negligible. A rotational term, rA , of 7.9 km/sec., seems indicated. Assuming for the factor A the value 0.0052 km/sec per ly., a center of gravity is found for the inter-stellar clouds at a distance of 1400 ly and in longitude 335° . This inter-stellar matter is found to be uniformly distributed, and the mean distance of the stars treated is twice that of the clouds.

For the dark clouds in Taurus, with apparent dimensions about $9^\circ \cdot 3'$, PANNEKOEK¹ derives a distance of 450 ly, giving an actual area covered about $20 \cdot 60$ ly. From probable assumptions as to the absorptive power of a gas, he finds that a gas would have to have a density of 10^{-18} to produce an absorption of 2 magn. But with this density the total mass of the Taurus dark clouds would be $4 \cdot 10^6 \cdot \odot$, which would be expected to have a marked effect upon the motions in this portion of the galaxy. Such a gaseous absorption would also be expected to exert some selective action on the spectra of stars observed through it, all of which leads PANNEKOEK to regard a cloud of material particles as the more probable state.

C. SCHALKN² has investigated the dark nebulae in Cepheus through an analysis of the spectral types of the stars in this region. He derives three dark nebulae at different distances: 1. absorption 0.3 magn., distance 810 ly., 2. absorption 0.6 magn., distance 1920 ly.; 3. absorption 1.5 magn., distance 2600 ly.

The extended investigations of TRUMPLER³ and L. T. SLOCUM⁴ on absorptive matter in our galaxy should be mentioned here. Both authors find a coefficient of absorption amounting to 0.0001 magn. per ly.

H. N. RUSSELL⁵ has investigated the theory that the dark nebulae consist of finely divided matter, i. e., fine "dust". In a cloud composed of spherical particles of radius r and density q , distributed at random so that the average quantity per unit volume is \bar{d} , the extinction of a ray of light in passing through such a cloud will be s stellar magnitudes per unit of distance, where s is given by the equation:

$$s = 0.814 \frac{q\bar{d}}{q\bar{r}}.$$

In this equation, q is a factor introduced to take care of the variation when the particles are of dimensions comparable with the wave-length. It is nearly unity for particles larger than 2 to 3 wave-lengths, and a maximum, 2.56, when the circumference of the particle is 1.12 times the wave-length. For visual light the maximum opacity occurs when the radius of the particles is 0.086μ , and a cloud of rock particles of this size and density 2.7 will exert an absorption of 1 magn. if it contains but 0.0116 mg./cm.³ in cross-section, regardless of its thickness.

RUSSELL further suggests that this matter is repelled from the stars by radiation pressure, the giant stars being the main cause of such repulsion. The gravitational action of the cloud itself is regarded as the force which holds it together. An extinction of 10 magnitudes (quite sufficient for opacity) would be produced by particles 144μ in diameter.

On RUSSELL's highly reasonable theory, diffuse nebulae would be composed of two sorts of matter: 1. actual minute particles which would provide for the opacity of the dark nebulae without the postulation of inordinately great masses, and, 2. intermingled atomic or molecular matter which by reflection, resonance, or fluorescence produces the observed intrinsic luminosity. On this theory,

¹ Amsterdam Proc. 23, No. 5 (1920).

² Lick Bull. 14, p. 154 (1930).

³ Wash. Nat. Ac. Proc. 8, p. 115 (1922).

⁴ Ups. Medd. No. 50 (1930).

⁵ Lick Bull. 15, p. 123 (1931).

BARNARD's dark spot in Ophiuchus, if 500 ly distant, would need to have a total mass only about equal to that of the sun. See further ciph 8 and 42.

8 Dark Nebulae¹ A very considerable number of areas of dark nebosity or occulting matter have been observed in our own and in neighboring galaxies.

Such dark nebulae are of the following modes of occurrence, though it is not maintained that these are necessarily a manifestation of the same phenomenon.

1 Dark spots seen against the luminous background of large diffuse nebulae; type example 6523 (M8 Sagittarii)

2 Similar isolated spots seen against the background of the stars type example, BARNARD's Dark Nebula at $17^h 57^m$, $-27^\circ 50'$

3 Peripheral occulting matter surrounding masses of luminous diffuse nebosity, as shown by diminution of star density, type examples, 7000 (America Nebula), the dark lanes extending from the nebosity II 5146 about ϵ Ophiuchi.

4 Larger areas of occulting matter as indicated by decreased density of stellar distribution, cf the references in the preceding Section.

5 Calcium clouds in space, as evidenced by the behavior of the calcium lines in certain stellar spectra.

6 In other galaxies, the evidences of peripheral occulting matter so frequently seen in edgewise spirals, cf ciph 42.

Whether any of the numerous dark or obscuring nebulae are entirely non-luminous is an open question. It is quite possible that we have, throughout the class of the diffuse nebulae, a regular progression from objects giving no light whatever to objects of the intrinsic brightness of the Nebula in Orion, and that a division of the group into bright and dark objects is superfluous. These dark nebulae are best seen by contrast, set off and accentuated by the luminous background of the Milky Way or of bright nebosity. In some of these cases it is possible that the apparent lack of all luminosity is only subjective, rather than real. Certain it is that BARNARD has recorded the detection of exceedingly faint luminosity in most of the so-called "dark" nebulae.

In distribution, the dark nebulae, like the luminous members of the class, are definitely galactic, as may be seen from Figure 2.

It seems certain also that we have to do with essentially the same sort of material in both cases, as is evidenced by the very frequent occurrence of the two sorts, luminous and non-luminous, in the same object.

One of the most striking examples of this alliance is exhibited in the nebosity south of ζ Orionis². This remarkable region contains the bright diffuse nebulae 2023, 2024, I 431, I 432, and I 434, and the dark nebula BARNARD 33, which projects into and seems to lie nearer than I 434. The main feature of this remarkable region is the long wisp-like diffuse nebula I 434, which extends for

¹ E E BARNARD, On the Dark Markings of the Sky with a Catalogue of 182 such Objects Ap J 49, p 1, 360 (1919), Catalogue of 349 Dark Objects in the Sky. Carn Inst Publ No 247 (1928), Ap J 31, p 8 (1910), 38, p 496 (1913), Pop Astr 23, p 596 (1915), W S FRANKS, M N 65, p 160 (1905), 90, p 326 (1930), T E ESPIN, Dark Structures in the Milky Way R A S Can 6, p 225 (1912), 16, p 218 (1925), Investigation of Star Gaps with a Catalogue of 202 such Areas, M WOLF, A N 161, p 130 (1903), 249, p 109 (1923), 223, p 89 (1925), M N 64, p 838 (1904), Seeliger-Festschrift (1924), p 312; K LUNDMARK, Ups Medd 12 (1925), J G ILIAGEN, A N 224, p 421 (1925). See also references under ciph 9, II KNOX-SHAW, Obs 37, p 98 (1914).

² J C DUNCAN, Bright and Dark Nebulae near ζ Orionis Photographed with the 100-inch Hooker Telescope Ap J 53, p 392 (1924). Cf also, W II PICKERING, Harv Ann 32, p 66, and Plate III, Fig 3 (1895), I ROBERTS, Ap J 17, p 74, with Plate IV (1903), M WOLF, M N 63, p 304, Plate 11 (1903), J E KEELER, Lick Publ 8, Plate XIII (1908), E E BARNARD, Ap J 38, p 500, Plate XX, Fig 1 (1913), H D CURTIS, Lick Publ 13, p 23, and Plate II, Fig. 5 (1928).

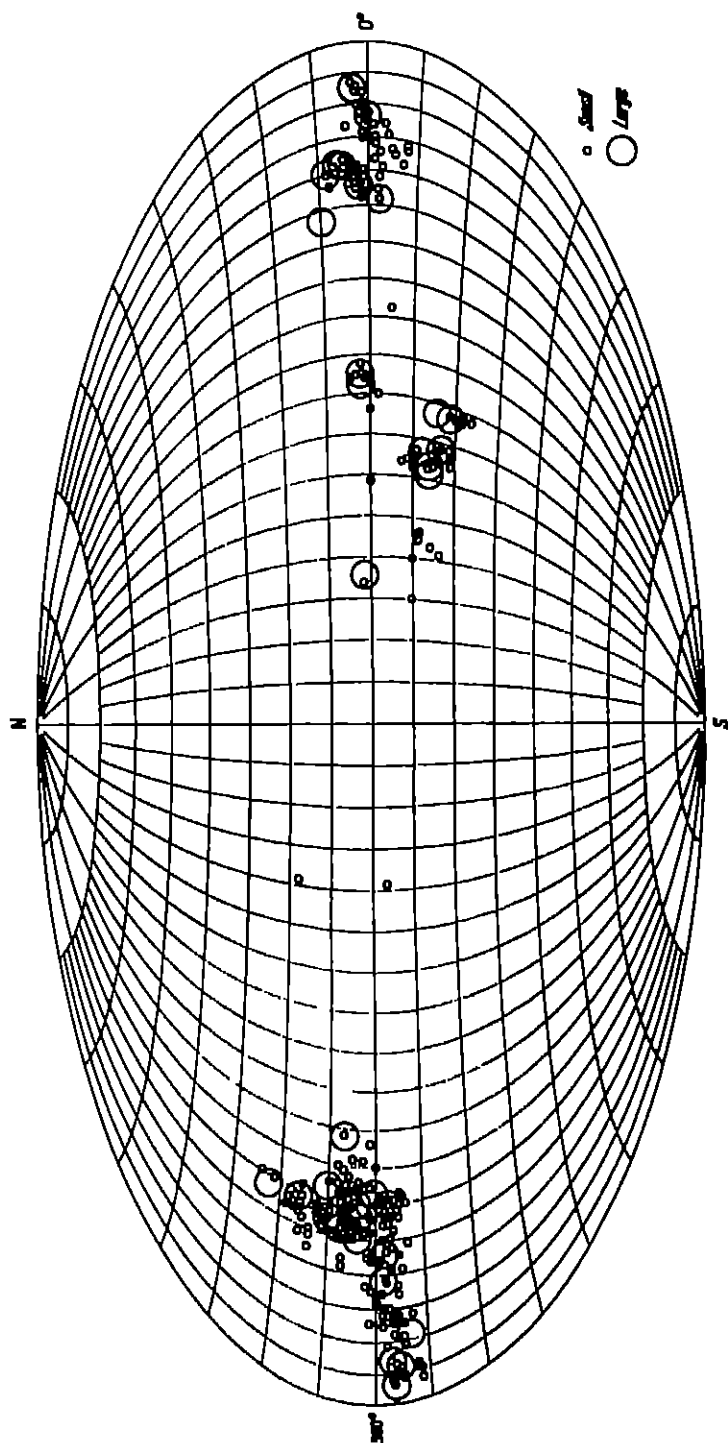


Fig 2. Galactic Distribution of BARNARD'S Dark Nebulae.

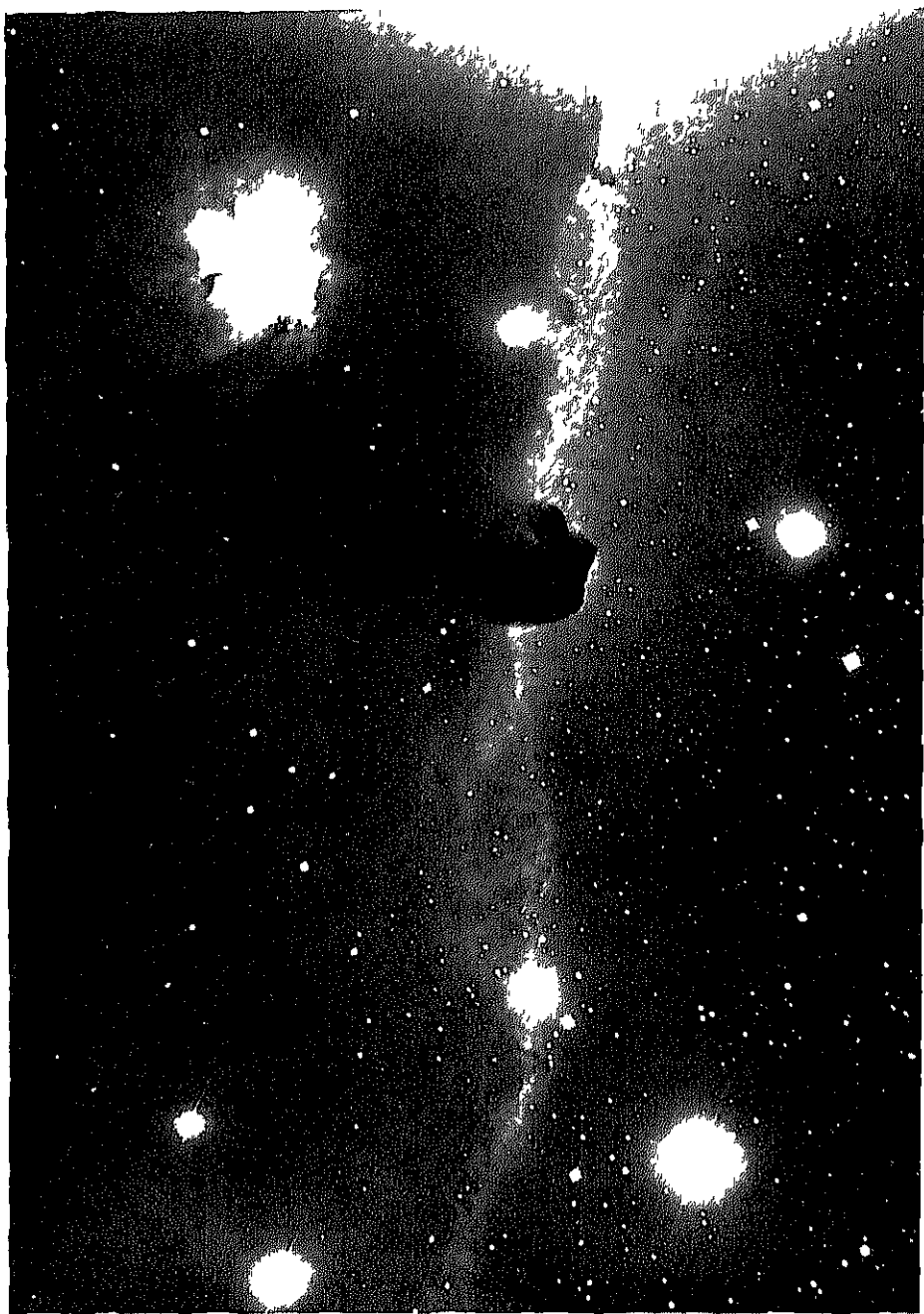


Fig 3 Dark Nebula south of Zeta Orionis (BARNARD 33, near I 434) (Mt Wilson graph)

nearly 1° to the south of ζ Orionis. To the west of this is very faint, text diffuse nebulosity and numerous faint stars, to the east lies a large area

nebulousity, with very few stars showing. From this dark area a "bay" about $4' \cdot 5'$ juts across I 434 at a point about $30'$ south of ζ , this is quite clear-cut and dark except for a small wisp in its northern portion, while the transition from dark to luminous matter is very abrupt at the western and southern edges, resembling nothing so much as a blot of ink. Even at these western and southern edges, however, the largest scale photographs show a very narrow rim of luminous nebulousity belonging to the dark "bay" rather than to I 434 beneath it.

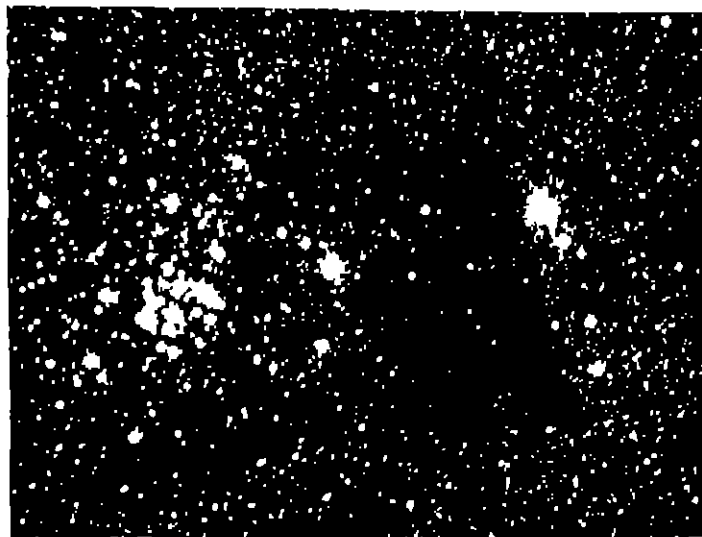


Fig. 4. The Dark Nebula BARNARD 86 ($\alpha = 17^h 57^m$, $\delta = -27^\circ 50'$) (Lick Photograph.)

DUNCAN suggests that four distinct types of diffuse nebulousity are exemplified here: 1. the rosy, branching nebulousity of I 434, 2. the more compact nebulousity of 2024; 3. the nebulous stars 2023, I 431, 432 and 435; 4. dark nebulousity, best exemplified by BARNARD 33 described above.

Numerous larger areas are known where occulting nebulousity is more or less clearly indicated. Among these may be mentioned the Northern "Coal Sack" ($20^h 56^m$, $+51^\circ 30'$); BARNARD 144, described as a large, semi-vacant region $6^\circ \cdot 3'$, the area about $3'$ in diameter southeast of θ Ophiuchi (BARNARD 78), where an exposure of two hours with the Crossley Reflector shows almost a stellar desert, or the region at $18^h 55^m$, -37° , of which KNOX-SHAW says¹, "There are as many as twenty r6seau spaces (each $5' \cdot 5'$) in which not a single star appears on a two hours' exposure with the reflector. These dark spaces are especially noteworthy as the region can not be said to be in the Milky Way, being 49° from the galactic plane and well away from the visible star clouds."

9. Cosmic Clouds. Vastly greater areas of slightly occulting dark matter or very feebly luminous nebulousity have been catalogued by HAGEN and his associates²,

¹ *Ibid* Bull No 9 (1912)

² J G HAGEN, *A N* 213, p. 351, 214, p. 449 (1921), 225, p. 383 (1925), 227, p. 391 (1926), *A N* Jub-Nr., p. 13 (1924), *M N* 81, p. 449 (1924), *Scientia* (1922), p. 185, *Mem S A It* (3) 1, p. 9 (1920), *Publ A S P* 39, p. 167 (1925), *Att Pont and Spec Vat passim* (1922 and ff.), G ARNETT, *Univars* 9, No 4 (1928), shows that the BARNARD-HAGEN idea of dark nebulae was anticipated by SACCHI in 1877, P BECKER, *A N* 223, p. 303 (1925), 225, p. 129 (1925), 224, p. 113, 235 (1925), J. HARTMANN, *ibid* 229, p. 61 (1927), J HOFMANN, *ibid* 238, p. 285 (1930), W L RIDGE, *Pop Astr* 30, p. 203 (1924), J STEIN, *V J S* 61, p. 250 (1926), C WITZ, *A N* 223, p. 123 (1925); K HAIDRICH, *ibid* 241, p. 397 (1931)

to which he has given the name cosmic clouds. These areas are often very large, 30 to 50 square degrees, and certain parts of the sky are held to be



Fig 5 The Dark Nebula BARNARD 72 (Yeikes Photograph)

almost completely covered by them. BECKER¹ gives in the final column of his General Catalogue the degrees of obscuration caused by obscure nebulae in the

¹ A Preparatory Catalogue for a Durchmusterung of Nebulae Spec Vat 13 (1925)

same field of view with the entry, on a scale of increasing density from I to VI. There are apparently none of the 4100 NGC entries in the main catalogue which are not affected in this way! This is regarded as confirming the fact that the cosmic clouds are not a galactic phenomenon. If one will refer to HAGEN's chart¹

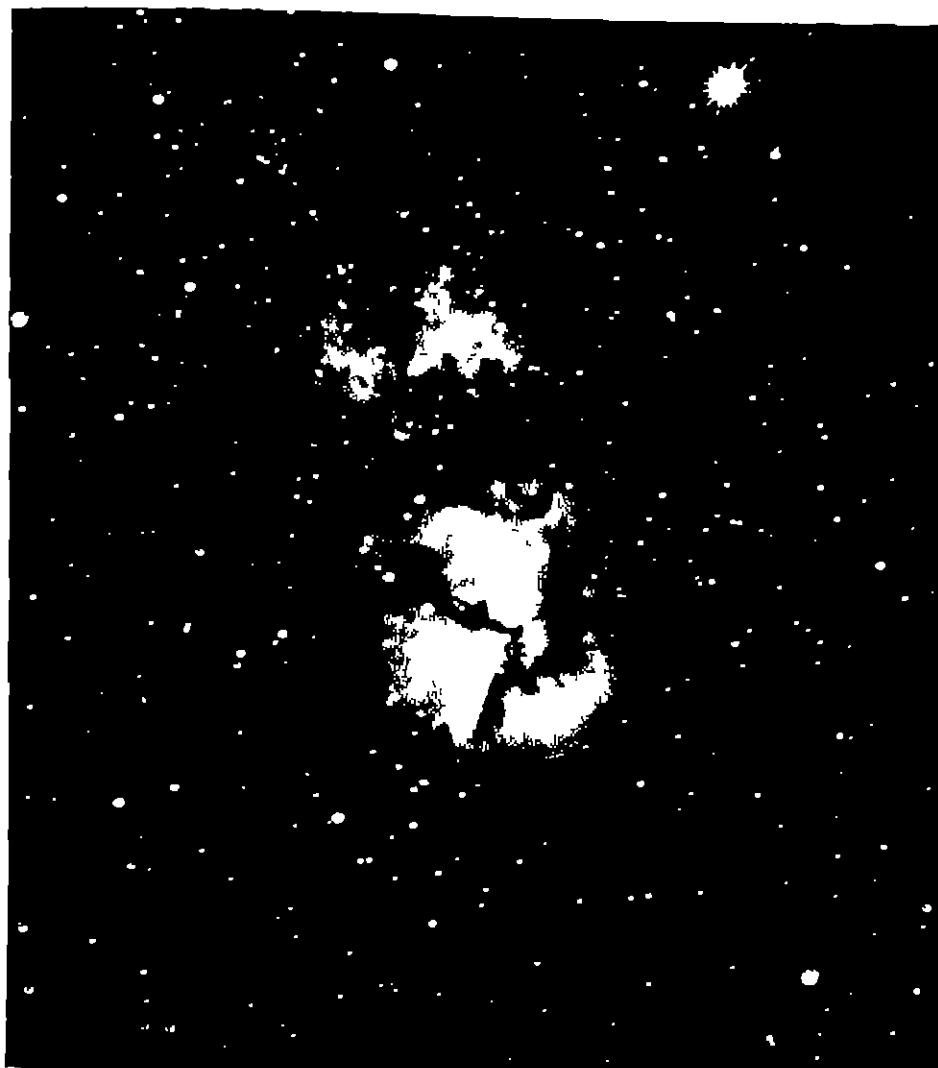


Fig. 6. The Diffuse Nebula NGC 6514 (Trifid) (Lick Photograph)

it will be found that in the portion of the lune bounded by $\delta = +45^\circ$ to $\delta = +90^\circ$, and $\alpha = 130^\circ$ to 230° , the area which HAGEN holds to be covered by cosmic clouds is at least 75%, or about 3000 square degrees. These clouds seem actually to shun the Milky Way, HAGEN locates comparatively few in the Milky Way structure (cf. in this connection the chart of distribution of BARNARD's dark nebulae, Figure 2)

¹ M N 71, p 434, Plate 9 (1924).

The status of the cosmic clouds postulated by HAGEN is still (1931) in doubt. He has pointed out that HIRSCHL's large areas of diffuse nebulosity (52 such were noted by HIRSCHL, but the number is 15, as 7 regions were counted twice coincide with certain of the cosmic clouds he has observed¹.

On the other hand, attempts to corroborate HAGEN's results by photography seem to have been uniformly unsuccessful. HORMANN has supported these appearances by analogies drawn from the photography of faint nebulae coming to the conclusion that the eye, in observing extended areas, has sensitivity about five magnitudes fainter than can be detected with a large reflector photographically.²

HARTMANN, from some indications that the cosmic clouds may be actually faintly brownish or reddish in color, has suggested the use of extremely rapid lenses plus a color-filter as a possible means of securing a photographic record. WIRIZ holds that these appearances are subjective, rather than objective, and represent in reality the contrast with the apparent brightness of the various celestial backgrounds.³ IVANOV⁴ failed to photograph the cosmic clouds noted by HAGEN and BICKER in the regions of V and W Draconis, and R and S Lani.

HADRIICH describes in detail an extended series of attempts to photograph the cosmic clouds by means of plates hypersensitized in the green. He records failure in all attempts save one, taken with an $f = 1$ 4.8 Zeiss triplet of 104 mm aperture, on which he believes he has secured a faint record. Numerous observers have felt that HAGEN's observations should be repeated by other investigators with other instruments, and in other climates.⁵ Some such corroboration seems indispensable before the cosmic clouds, of the number and extent assumed, can be regarded as completely substantiated.

The Lattu counts of about 250000 stars to phot. magn. 11.5 on the Paris Astrogaphic Charts⁶ were at first thought to give a considerable measure of support to HAGEN's results. In a belt 2° wide at $\delta = 121^\circ$ ÖRK catalogued 196 obscured regions. From these counts it was estimated that the entire sky would show some 14000 similar patches and that, were this obstructing material removed, about five times as many stars would be visible in low galactic latitude.

SHAPIRO⁷ has reinvestigated this question with plates of longer exposure on twenty-two of the Paris regions which had been employed in the Lattu counts taken with the 24-inch and 16-inch refractors, and showing stars from one to three magnitudes fainter than the Paris Charts. A real obscuring nebulosity should conceal such fainter stars much more effectively than would be the case for magn. 11.5. While JULI LUKK's counts to that magnitude were in all cases verified, and her localized vacancies and clusterings corroborated, it was found that the count to fainter stars in practically all cases obliterated such local irregularities. On the Harvard plates covering the same regions as the twenty-two selected Paris charts, seven clusterings and twenty-eight observations were surveyed, together with the surrounding unaffected areas. When faint stars alone were considered, all of the clusterings and all but four of the observations disappeared.

SHAPIRO⁸ has secured similar negative results from the Harvard star count on the region of X Cancri, reported by HAGEN⁹ to be surrounded by cosmic clouds. SHAPIRO concludes from these results, as did WIRIZ, that HAGEN

¹ M N 86, five papers (1926), 87, p. 1 (1927).

² A N 224, p. 267 etc. (1925).

³ M V B M No. 8, p. 57 (1927).

⁴ e. g., LUNDMARK, Publ. A S P 34, p. 191 (1922), HAGEN's reply, ibid., p. 321.

⁵ L. ÖRK and JULI M. LUKK, Publ. Lattu (Dorpat) 26, No. 2 (1921).

⁶ Harv. Circ. 281 (1925).

⁷ Harv. Bull. 834 (1926).

⁸ A N 225, p. 383 (1925).

cosmic clouds are apparently observable phenomena, but are merely the effects, in general, of the uneven distribution of the stars brighter than the fifteenth magnitude, and that, except in well-known nebulous regions near the Milky

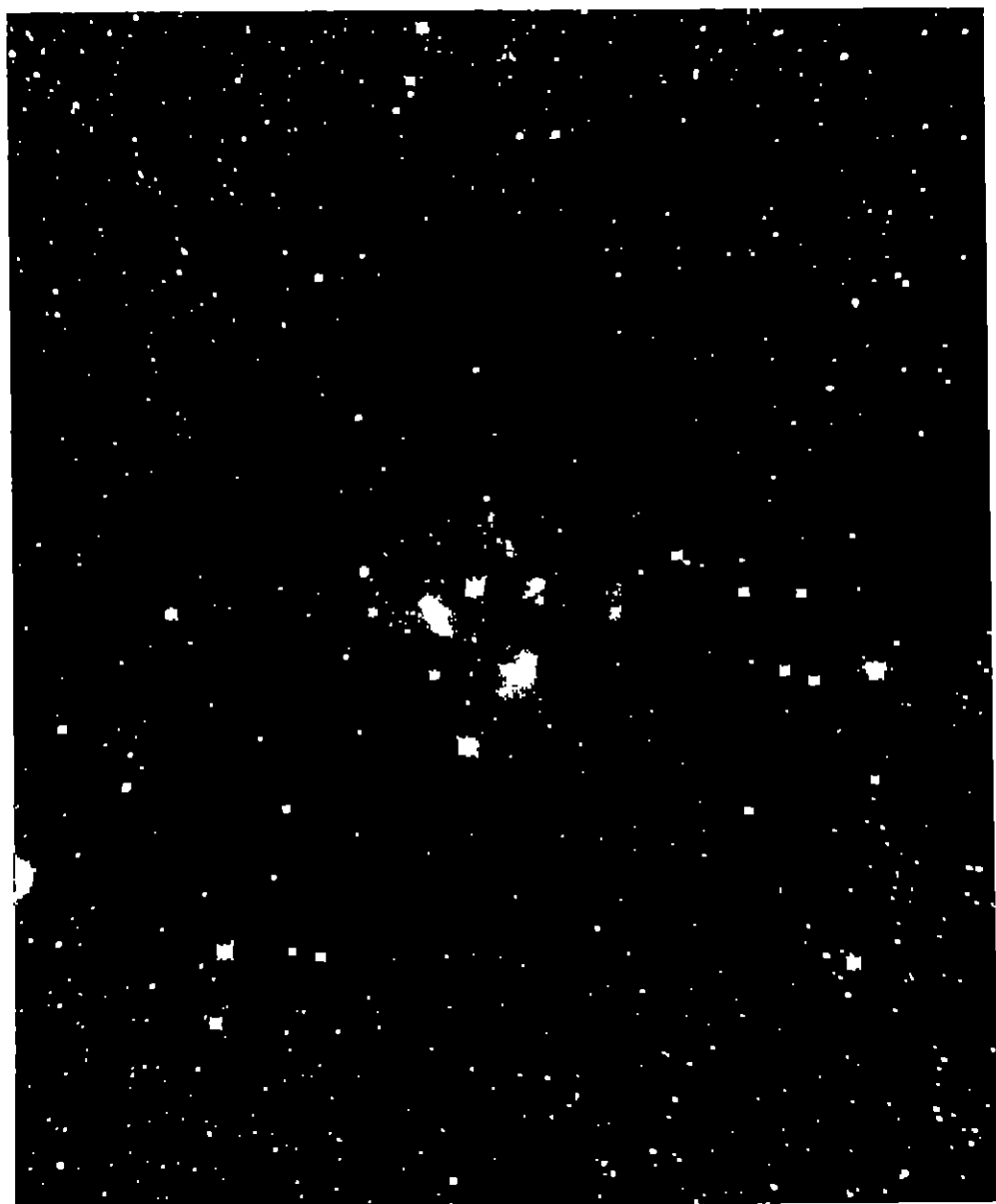


Fig 7 NGC 11 5146 This object combines luminous and non-luminous diffuse nebulosity, shown clearly in its structure and in the marked falling off in the number of stars at its periphery (Mt Wilson Photograph)

Way, the obscurations suggested by the Tartu investigations are apparent rather than real.

10 Distances and Dimensions of Diffuse Nebulae Direct determinations of the distances of the diffuse nebulae by the parallax method are manifestly impossible because of the lack of sharp definition in the configurations of the

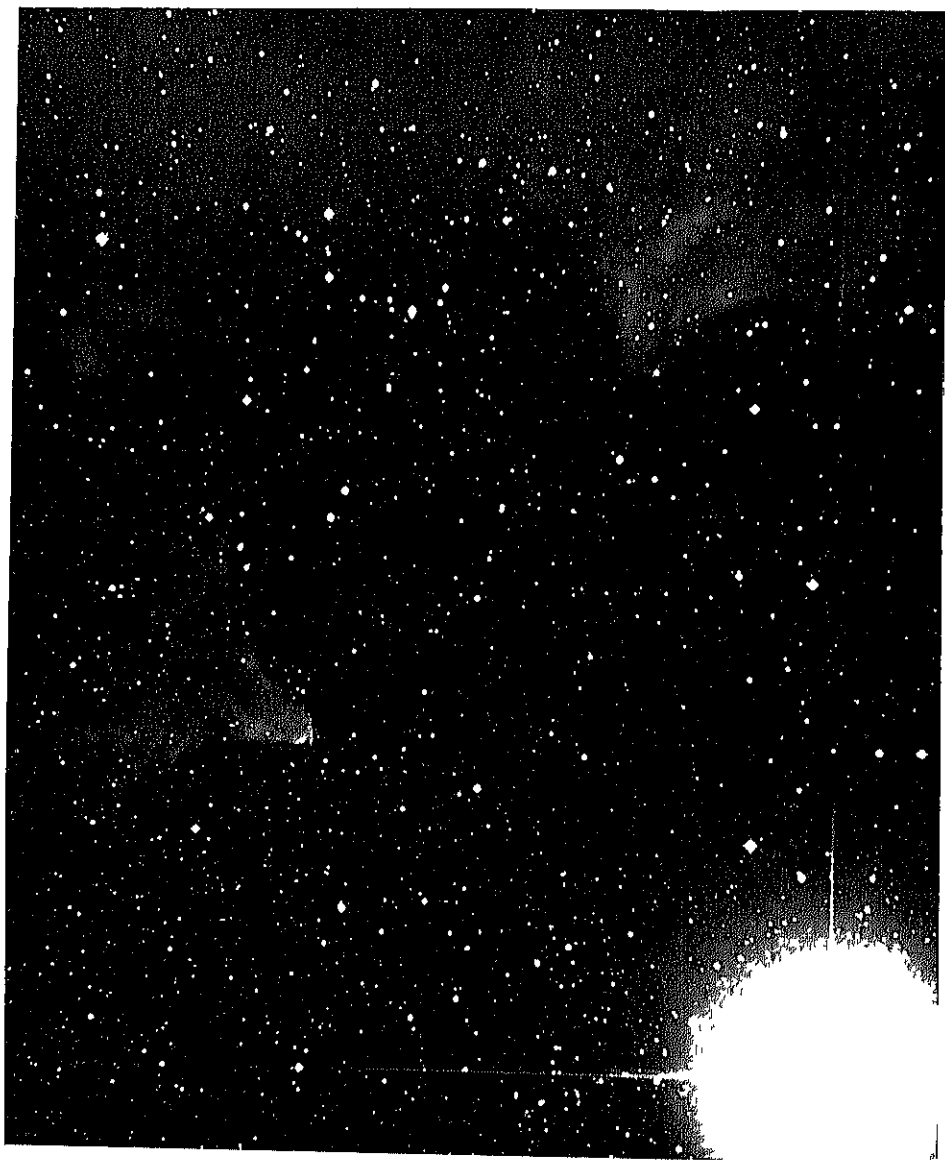


Fig 8 The Diffuse Nebula NGC 159 (Northeast of γ Cassiopeiae) (Lick Photograph)

two main classes seen, irregular and textureless clouds, or tangled masses of wisps and streamers. It is evident that the distances of these objects can only be derived by indirect methods, and on the basis of more or less probable analogies or extrapolations. As the stars involved in such nebulosities have been found to be mainly of the earlier types, reasonable assumptions as to the average

distances of such stars of the given type and magnitude furnish an approximation to the distance of the nebula. Similar indirect evidence may be secured from star counts, in the case of dark nebulae, from the radial velocities and proper motions of involved stars, when available from involved variable stars¹, etc.

Variables in Diffuse Nebulae.

NGC	Number	Magn.	Discoverer
2264	20	14 (max.)	WOLF, A N 221, p. 379 (1924)
6514	3	—	LAMPLAND, Pop Astr 27, p. 32 (1919); Publ A S P 33, p. 267 (1921)
6727	1	8.6—10.5	INNES, Union Circ 33 (1916)
7023	2	—	PERRINE, Lick Bull 1, p. 187 (1902)
I 405	1	—	Harv Bull 786 (1923)

Table 4. Distances of Diffuse Nebulae.

NGC	α		δ	Type	Distance in l. y.	Obs.
281	0 ^h 47 ^m .4		+56° 3'	Diffuse	3600	L (LUNDMARK)
I 59	0 50 .7		+60 11	Diffuse	250	L
II 1805	2 24 .5		+61 3	Diffuse	460	L
I 348	3 38 .2		+31 31	Diffuse	350	GINGRICH
—	3 41		+24	Pleiades	540	L
—	3 25		+28	Dark neb.	350	L
I 405	5 9 .7		+34 21	Star + neb.	460	L
I 410	5 16		+33 23	Neb. + cl. + lane	2300	L
I 417	5 20		+34 12	Neb. + cl.	1500	L
2070	5 39 .5		+69 5	Diffuse	3200	L
—	5 30		— 5 27	Orion	large	L
					900	L
					400	BERGSTRAND
					600	KAPTEYN
					1800	TRUMPLER
2175	6 3 .7		+20 31	Diffuse	3600	L
I 446	6 25 .3		+10 32	Neb. star	3200	L
2245	6 27 .2		+10 14	Cl. + diff. neb.	800	L
2237	6 27		+ 5 0	Cl. + neb.	1500	L
2261	6 33 .7		+ 8 49	Var. neb. + star	large	L
—	6 35 .5		+ 6 59	Br. + dark neb.	3300	L
—12° 2771	7 0 .6		—12 11	Neb. star	1100	L
—	10 41 .2		— 59 9	η Carinae	2200	L
5189	13 26 .4		—65 28	Neb. + stars	1100	L
—	16 14		—19 59	Dark neb. + star	550	L
—	16 20		—25	ρ Oph. region	460	L
6514	17 55 .7		—23 2	Trifid neb.	550	L
—	17 55 .1		—27 50	Dark neb.	4000	L
6523	17 58 .4		—24 20	Diff. M8	1600	L
—	18 11		—19 43	Dark neb. + star	3300	L
—	18 9		—18 15	Dark neb.	1600	L
6618	18 15		—16 14	Diffuse	3600	L
—	18 55		—10 52	Dark neb. + star	460	L
—	18 55		—37 6	Neb. region	400	L
—	19 14		+ 7 32	Dark neb.	650	L
—	19 35		+10 20	Dark neb.	1300	L
—	19 54		+34 30	Dark neb.	1600	L
7000	20 50		+44 0	Diff. (America)	620	L
					560	BUCH-ANDERSON
					220	DUNCAN
7023	21 0 .5		+67 46	Diff. + dark	650	L
—	21 35 .0		+67 42	Neb. star	360	L
—	21 35 .9		+57 2	Br. + dark + cl.	3600	L
—	22		+59	Cepheus, dark	810 to 2600	SCHALÉN
7635	23 16 .5		+60 39	Neb. star	4100	L

¹ LUDENDORFF, Handbuch VI, Chap. 2, p. 243.



Fig 9 The Diffuse Nebula NGC 1976 (The Great Nebula in Orion) (Iick Photograph)

The approximate distances of a number of typical diffuse nebulae, both luminous and non-luminous, are given in the preceding table. Nearly all the values have been derived by LUNDMARK¹ by various indirect methods, a few

¹ Publ A S P 34, p 40 (1922)

ave been added from other sources. The majority of the values given must be regarded as subject to very large uncertainties.

The actual dimensions of many of the larger diffuse nebulae must be measured in tens or even hundreds of light-years. On the basis of the estimated distances given in the table above, 6523 (M8) will be about 111.y. long; the America Nebula (7000) must extend over 40 ± 1 .y.; the very large faint nebula in the constellation of Orion must be over 100 l.y. in diameter, etc.

11. Luminous Diffuse Nebulae. The salient characteristics of the diffuse nebulae: indefinite and random structure; extreme tenuity; general association with stars; and galactic distribution, have been noted in the preceding sections. In proceeding from such more mechanical qualities of structure and form to the acts of their constitution as exhibited by their spectra, the peculiarity is at once met that the diffuse luminous nebulae show two sorts of spectrum; one showing emission lines, and another sort resembling the spectra of the involved stars, ascribed to reflection or to some sort of resonance effect. This will necessitate a separate treatment.

There seems, furthermore, no reason to doubt that the spectra of the planetary nebulae and those of the diffuse nebulae which show bright lines are caused by the excitation of the same sorts of matter, for the most part in similar conditions as to density and ionization. This similarity has been well put by W. H. WRIGHT¹: "The spectra of the planetary nebulae differ much more among themselves than some of them do from the spectrum of the Orion Nebula. Whether or not the spectral similarity which exists between the planetaries on the one hand and the Orion Nebula on the other indicates approximate equality of physical constitution depends upon the sensitiveness of the nebular spectrum as an index of the state of its source."

In spite of this similarity in the spectra of the two classes, however, it has been thought best, with the aim of segregating the pertinent data of each class, to treat the spectra of the diffuse nebulae and the planetaries separately. The emission spectra exhibited by certain of the diffuse nebulae will therefore be given in ciph. 15, and this matter will be repeated, with the addition of the series relationships and ionization potentials assigned by BOWEN, under the planetary nebulae in ciph. 25.

12. Proper Motions and Internal Motions (Visual). The older literature of the subject contains numerous references to researches attempting to show changes or motions in the larger diffuse nebulae². These attempts were based upon the often vague and inaccurate visual descriptions of earlier observers, and are now of value only as examples of energy and perseverance unfortunately directed.

Though the advent of the photographic process has given a far greater degree of attainable precision, the available time interval is still far too short to establish motions larger than the unavoidably gross errors of measurement of the ill-defined wisps, streamers, or other structural features of the diffuse nebulae³. Aside from apparent changes due to light variations in a few variable diffuse nebulae, there seem to be no certain evidences of structural changes detected as yet. LAMPLAND⁴ has pointed out that the intricate structure and

¹ Lick Publ 13, p. 262 (1918).

² e. g. E. S. HOLDEN, On the Proper Motion of the Trifid Nebula. Amer J Sc 34, p. 433 to 458 (1877).

³ The classification of the "Crab" Nebula, 1952, is somewhat uncertain. The changes which DUNCAN has noted in this object will be described later in ciph. 27.

⁴ Publ A S P 28, p. 192 (1916).

definite character of some of the delicate filaments in the diffuse nebula 6992 [the beautiful "Net-work Nebula" in Cygnus, cf. Lick Publ. 8, Plate 63 (1908)]

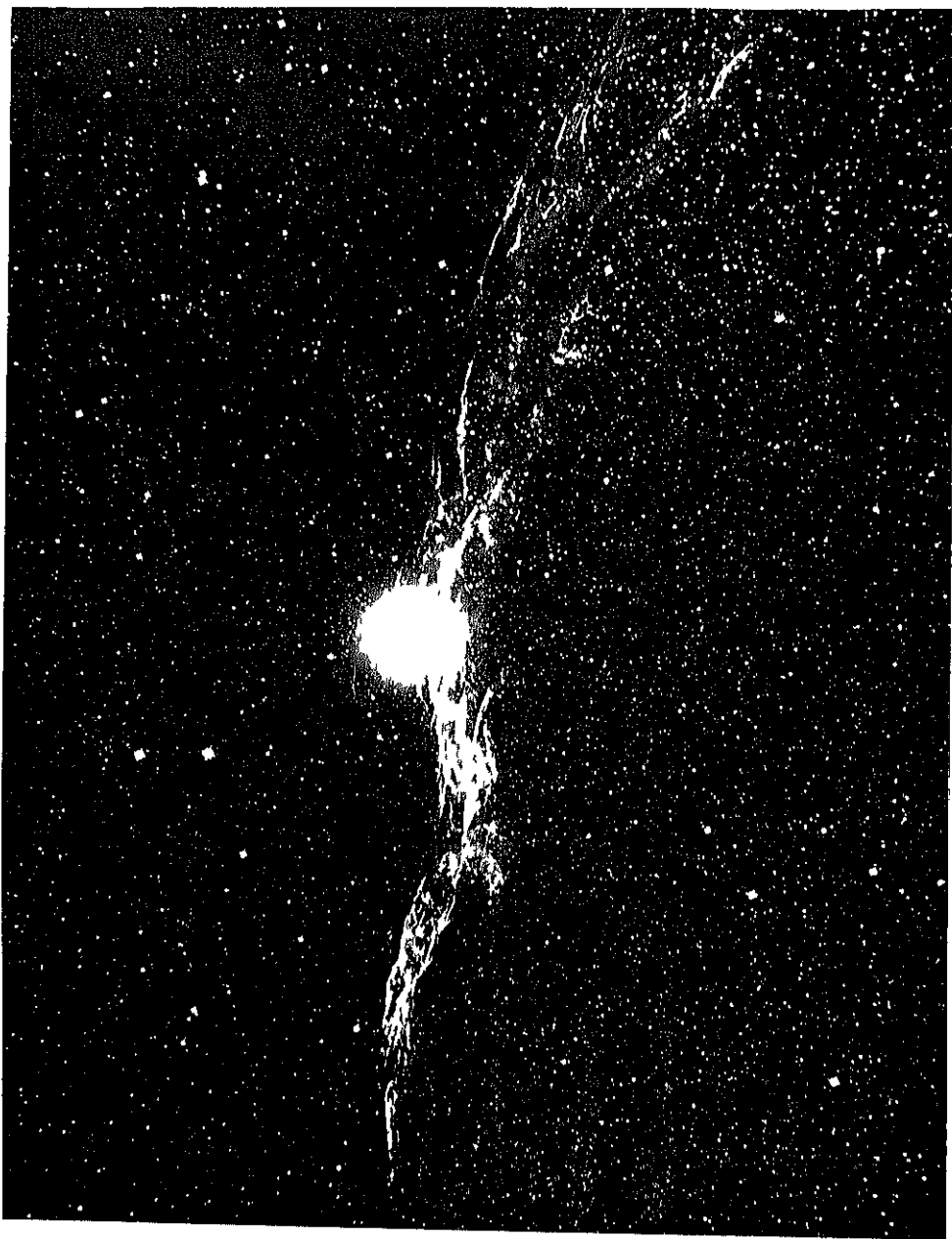


Fig. 10. The Diffuse Nebula NGC 6990 in Cygnus (Mt. Wilson Photograph) 11

should make it possible to detect comparatively small motions, and has studied two plates of this object separated by an interval of about 14 years. He states

that there are apparently slight displacements in small portions of some of the filaments in the southern part of this nebulosity DUNCAN notes several new filaments found at the northern end of the "nebulous wreath in Cygnus"¹ CURTIS² made measures of features in 10 large diffuse nebulae on Crossley plates with a time interval of about fifteen years, with the conclusion, "the most that can be said, both from the measures and from careful examination, is that there has pretty certainly been no change in the intricate formations of these enormous objects as large as one second of arc during the past fifteen years".

18 Radial Velocities of Diffuse Nebulae Such of the luminous diffuse nebulae as have an emission spectrum, with much of the light concentrated in a few bright lines, are suitable for radial velocity determinations, unless too faint, a condition which unfortunately prevails. Observing the Nebula of Orion in 1872, HUGGINS³ determined the position of the chief nebular line as 5005 Å, he attributed it to nitrogen, and ascribed its displacement as due to a recession of the Orion Nebula from the sun MAUNDER's attempts on the same nebula⁴ showed variations too large to permit any definite conclusion

It remained for KESTLER⁵ to secure the first definite radial velocity results on nebulae. He employed a grating spectrograph attached to the 36-inch refractor at Lick Observatory, using the third or fourth order. He determined the radial velocities of the Orion Nebula and of thirteen planetaries. When it is recalled that this was done visually, in the "prehistoric" days of the spectroscopic method, and that his values are in close accord with later spectrographic results, his achievements in this field must be regarded as an observational triumph (on Orion KESTLER, +17.7 km./sec., CAMPBELL and MOORE, +17.5 km./sec.)

Very few radial velocities are known for diffuse nebulae. From the descriptions, 5 nebulae in the Greater Magellanic Cloud may possibly be of the diffuse type, these have the mean velocity of the Cloud, +276 km./sec. Others are⁶

Object	V (sun's motion removed)
Orion	0.1 km./sec.
3372 η Carinae	-5
6514 (Tritid Nebula)	+21
6523 (M8 Sagittarii)	-18
6618 (Horsehoe Neb.)	+20.7

14. Turbulence Effects in Diffuse Nebulae. Although radial velocities are known for but a few diffuse nebulae, in one case we possess fairly accurate knowledge of the relative motions of different portions of the same nebula, that of Orion. KESTLER (loc cit.) had earlier considered the question of relative radial velocity in different parts of the Orion Nebula, but obtained negative results. He estimated that differential radial velocities as great as 8 km./sec. in the brighter parts of the nebula would have been detected. VOGEL and EHRHARDT⁷ found evidences of differential velocities in the Orion Nebula, indicating that the radial velocities of the material east of θ₁ Orionis was 5 or 6 km./sec. larger in the positive sense than that of the material θ₁ west of this star.

¹ Mt Wilson Year Book No. 29 (1930)

² H. D. CURTIS, Proper Motions of the Nebulae, Publ. A.S.P. 27, p. 214 (1915). In all, CURTIS made measures on 150 objects of the various classes, based on Crossley negatives with time intervals averaging about 15 years. CURTIS is since convinced that the probable errors of measurement on such vague and diffuse elements or nebulous nuclei are vastly larger than the quantities sought. He therefore now regards the numerical results derived in his paper as meaningless, and relegates them to the status of the older visual comparisons.

³ Proc. R.S. London 20, p. 383 (1872)

⁴ Greenwich Spectr. and Phot. Results (1884 and 1887)

⁵ Lick Publ. 3, p. 165 (1894)

⁶ CAMPBELL and MOORE, Lick Publ. 13, p. 77 (1918)

⁷ Ap J 15, p. 307 (1902).

Our modern results on this nebula are due to the brilliant application of the interferometric method by BUISSON, FABRY and BOURGET¹ and to the detailed and accurate spectrographic survey of the Orion Nebula by CAMPBELL and MOORE².

The French investigators, with high technical skill, made use of an interferometer with a preliminary telescopic magnification ($80\times$), so that the resulting interference rings formed a picture of the chosen region, an area about 4' square about the Trapezium. Measurement of the diameters of the interference rings will then give, first, the mean radial velocity of the nebula as a whole by using some known radiation as $H\gamma$; secondly, variations in different diameters of a given ring of known (or unknown) source give at once the relative radial velocities of the portions of the nebula covered by this ring; and, finally, certain assumed laws connecting the limiting order of interference with the atomic mass and the absolute temperature make an estimate possible as to the effective temperature of the nebular matter.

The authors measured 58 points on the interference rings, distributed in 12 directions from the Trapezium, and within a radius of about 2'; their resulting mean value for the radial velocity of the Orion Nebula was $+15.5$ km./sec.

As to the turbulence effects observed, they write: "The rings show local deformations in certain regions, indicating, in certain portions of the nebula covering a very small area, irregularities of speed which may amount to about 10 km./sec. Movements of this sort are manifested in the region to the southeast of the Trapezium in the direction of the star Bond 685. Moreover, there are great collective movements; with respect to the mean velocity, the northeast region is withdrawing at a speed of something like 5 km./sec., while the southwest region is approaching at pretty nearly the same speed. In general, the part of the nebula which we have studied has a sort of rotary movement about a line southeast-northwest, but with numerous irregularities."

15 plates were taken, with étalon separations ranging from 0.13 to 2.8 mm. The final values found for the wave-lengths of the chief violet nebular lines are:

$$\begin{aligned} &3726,100 \text{ \AA} \\ &3728,838 \text{ \AA}. \end{aligned}$$

Next, by the use of the formula,

$$N = 1,22 \cdot 10^6 \sqrt{m/T},$$

where N is the limiting order of interference, m the atomic mass, and T the absolute temperature³, and through the use of étalons of gradually increasing separation, they set the limiting orders of interference as follows:

Hydrogen	about 10000
"Nebulium"	16500

This value of the interference limit was regarded as indicating a source of atomic mass about 3 as the origin of the "nebulium" lines. Also, by the use of the same formula, a high effective temperature, in the sense of molecular motions involved, was derived, amounting to 15000° abs.

¹ Ap J 40, p. 241 (1914); cf. also *ibid.*, 33, p. 406 (1911).

² Lick Publ 13, p. 96 (1918).

³ This empirical formula should not be taken too seriously, as is indicated by its failure in this case; the atomic mass of O is 8.

The formula in question was derived by SCHÖNROCK, *Ann d Phys* (4) 20, p. 995 (1906), and later, with a slightly different constant, by RAYLEIGH, *Phil Mag* (6) 29, p. 274 (1915). It involves, in the latter case, a postulated intensity difference of $1/40$ (2.5%) as the minimum detectable in the formation of an interference ring. Though in no sense a rigorous formula, the temperatures found are probably of the right order.

The researches of CAMPBELL and MOORE confirmed the results secured by the interferometric method in most respects, but did not support the idea of a general rotation. In all, 86 spectrograms were taken, and the total of the exposures amounted to nearly 400 hours. In an area 2' square about the Trapezium they found a total velocity range of 13.5 km./sec., and interesting plates are given in the work quoted, tabulating the excess or deficiency of radial velocity at the numerous points observed in the nebula. "... a consideration of the charted velocities, especially those in the outer southwestern areas, seems to negative the suggestion of a rotation of the nebula. While the intermediate region from 1' to 4' northwest, west, and southwest of the Trapezium is a region of prevailingly low radial velocities, moderately low radial velocities are to be found also to the north-east, east, and south of the Trapezium . . . but when we consider all parts of the nebula covered by our observations, we are inclined to favor the hypothesis of great collective variations of velocity rather than a rotation as the prevailing factor." Widening of the lines in certain regions suggests that the radiations in such areas may be coming from widely different depths in the nebula, the different strata having different radial velocities. See further ciph. 16 and 28.

15. Luminosity of the Diffuse Nebulae: Gaseous Spectra. A considerable number of the diffuse nebulae exhibit an emission spectrum of the type associated with matter in a gaseous condition. The type example of this class is the Great Nebula in Orion: because of its intrinsic brightness, the spectrum of this nebula has been more studied than any other, just as it was the first diffuse nebula in which bright lines were observed visually and later photographed.

In the preceding table are given the lines observed in the Orion Nebula by WRIGHT¹. Additions to the identifications have been made from BOWEN's papers.

Table 2. Wave-lengths of Lines in the Orion Nebula (WRIGHT).

λ (Å)	Intensity	Origin
3704	2	$H\epsilon$ 3703.9; He 3705
3712.4	1	$H\gamma$ 3712.0
3722	2	$H\mu$ 3721.0
3726.16	40	O_{II} ; B., F. & B., 3726.100
3728.91	30	O_{II} ; B., F. & B., 3728.838
3734	2	$H\delta$ 3734.4
3750	3	$H\zeta$ 3750.2
3771	6	$H\eta$ 3770.6
3798	10	$H\theta$ 3797.9
3820	1	He I 3819.6
3835.5	15	$H\eta$ 3835.42
3868.74	40	Unidentified
3888.96	40	$H\zeta$ 3889.05; He 3888.64
3964.8	10	He I 3964.7
3967.51	30	Unidentified
3970.08	40	$H\epsilon$ 3970.07
4026.2	10	He II; He I 4026.2
4068.62	5	S_{II}
4076.22	2	S_{II}
4101.74	60	$H\delta$ 4101.74
4120.6	1	He I 4120.8
4144.0	1	He I 4143.7
4267.1	1	C_{II} 4267.14
4340.46	100	$H\gamma$ 4340.47
4353	1—	Unidentified
4363.21	6	O_{III}
4388.0	4	He I 4388.0
4471.54	20	He I 4471.49
4658.2	2	Unidentified
4712.6	1	He I 4713.2
4861.32	70	$H\beta$ 4861.33
4922.2	1—	He I 4921.9
4958.91	50	O_{III}
5006.84	70	O_{III}
5876	—	He I
6563	—	$H\alpha$

¹ The Wave-lengths of the Nebular Lines and General Observations of the Spectra of the Gaseous Nebulae. Lick Publ 13, p. 191—239, with many plates (1918). This monograph is the most complete collection of observational data on the gaseous nebular spectrum existing.

These lines will be found also, with the addition of numerous others found in the planetaries, and with series relationships and ionization potentials, in Table 7, Ceph. 25.

The lines at 5007 Å and 4959 Å have had a long and interesting history under their older designations, N_1 and N_2 for which the hypothetical source "nebulium" was postulated. The identification of these and other formerly unknown lines in the spectrum of the gaseous nebulae as multiply ionized O and N is due to BOWEN¹.

It will be seen from the identifications in Table 2 that the more prominent features of the emission spectrum of gaseous diffuse nebulae are H_I , He_I , O_{II} , and O_{III} . A single weak line, 4267 Å, is ascribed to C, and two are possibly S_{II} . Although $\text{H}\alpha$ is visible in Orion, the two lines of N_{II} , 6548 and 6854 Å, so prominent in many planetaries, as well as the weaker lines of N_{III} at 4634 Å and 4641 Å, are not found. The puzzle which had been presented for so many years by "nebulium" has thus been almost completely solved by BOWEN. Of the stronger lines, only the two at 3869 Å, intensity 40, and 3968 Å, intensity 30, remain unidentified.

HUBBARD² tabulates the following twenty-nine diffuse nebulae with emission spectrum, only thirteen of which were known as such before.

Table 3. Diffuse Nebulae with Emission Spectra (Hubbard)

Number	Pv magn. and spectrum of stars involved		Remarks
281	8.6	10.2	4 components of BD +55°191 3 stars Plan nebula near γ Cass
I 59	10.3	11.6	
1491			
1199	10.6		
1621	13.0	11.0	3 st., magnitudes estimated Boss 1219, 1 faint continuous Also strong continuous
I 405		5.8	
1952			
1972	5.1	7.9	Orion 4 st. in Trapezium Bond 731 Bay neb. near ϵ Orionis Also faint continuous
1982		6.8	
I 131			
2024			BD +20°1281 1 brightest st. of cluster Union Circ. No. 7 (1911) Magn. estimated
2175	7.5		
2237	7.1	8.2	
2359			Invid. 2 comp. of BD 23°338 2 brightest st. in M8 3 brightest st. in M16
3372			
5128			
6302			Enormous loop in Cygnus America neb. Cf. also Wirtz Sitzb. Heidelb. Akad., Abt. 27 (1910)
6357			
6511	7.8	8.5	
6523	6.1	6.9	
6611	8.3	9.2	
6618			
6888			
6960			
6922			
7000			
7635			

¹ J. S. BOWEN, Nature 120, p. 173 (1927), 123, p. 150 (1929), Publ. A.S.P. 39, p. 295 (1927), Ap. J. 67, p. 1 (1928).

² The Diffuse Galactic Nebulae. Ap. J. 56, p. 162 (1922), Mt. Wilson Contr. No. 241 (1922). This is the most comprehensive monograph on the diffuse nebulae which has appeared to date.

16. Emission Variations. The relative intensities of the lines in gaseous nebular spectra, whether of the diffuse or planetary types, vary in a very striking and puzzling manner, not only in different objects of the same class, but also in different portions of the same object. The Orion Nebula is the most striking example of this phenomenon among the diffuse nebulae¹.

This variation in the relative intensities of nebular emission lines is a problem which has yet received no entirely satisfactory explanation (see, however, ciph 28, 31, and 32). It is conceivably in some way connected with variations in the extremely low densities of these objects or of parts of the same object, as in Orion. Modern physics can parallel the enormous temperatures of stars (ANDERSON's exploding wires), or temperatures near the absolute zero (ca. 1° K.), it can also deal with relatively high pressures. It is unfortunate that the gases occluded from the walls of our laboratory apparatus, as well as the great length of the mean free path, limit us to rarefactions whose ultimate tenuity is perhaps of the order of 10^{-10} , and that the presumably very fertile experimental field in densities less than this by factors of the order of 10^{-10} seems forever closed to us. Our stellar and nebular laboratories will long remain our only source of ionization phenomenon in gases of densities vanishingly small.

CAMPBELL and MOORE (loc cit.), in their work on Orion, have tabulated a great variety of ratios for the intensities of the N_1 , N_2 , and $H\beta$ lines, ranging from $N_1/N_2 H\beta = 10.3/5$ for the center of the Trapezium region to 0.0/10 in the neighborhood of the detached nebulosity 1982 in the northeast quadrant, whereas the normal ratio in the planetaries is 10.3/4. CAMPBELL and MOORE, and WILSON, in the work quoted give also the values for the following five objects

NGC	N_1	N_2	$H\beta$	NGC	N_1	N_2	$H\beta$
1976	10	3	5	6523	3	1	10
3372	10	3	5	6618	10	3	5
6514	3	1	10				

HUBBARD adds data for 12 others

NGC	N_1/N_2	$H\beta$	NGC	N_1/N_2	$H\beta$
1499	1	2	6611	1	3
1423	1	1	6888	0	2
1434	0	5	6960	0	2
2024	1	3	6992		
2175	1	3	7000	0	2
2237	2	1	7635	0	5
5128	0	2			

KERRICK² took perhaps the earliest photographs of the Orion Nebula through a color screen, and found N_1 and N_2 concentrated in the Huygenian region. HARTMANN, by a similar method³, corroborated these results, and noted that 3727 Å was of much greater extent. SLIPHER⁴ worked spectrographically over a large part of the more distant nebulous regions in the constellation of Orion, in general confirmation of CAMPBELL's earlier visual observations, and found that the emission lines decreased in strength till out at NGC 2068 the spectrum was continuous. "then the variation in the spectrum may be said to begin

¹ CAMPBELL's discovery of this effect in different areas of the Orion Nebula, and SCHUMER's attempts to disprove, formed an interesting and lively tilt of the earlier days of the spectroscopic method. Cf. J. SCHUMER, V. J. 5 (1897), p. 51, Ap. J. 7 (1898), C. RUNNIG, Ibk. 8, p. 32 (1899), CAMPBELL, WRIGHT, SCHUMER, and ATKIN, Ibk. 6, p. 363 (1897), W. W. CAMPBELL, Ibk. 8, p. 317 (1899), 9, p. 312 (1899).

² Ap. J. 9, p. 133 (1899).

³ Ap. J. 21, p. 389 (1905).

⁴ Publ. A. S. P. 31, p. 212 (1919).

in the center with the usual emission type which loses strength (different substances differently) with distance outward and ends finally, in the most distant masses, with a continuous spectrum of the normal stellar absorption type." WRIGHT (1921, unpublished) using a quartz slitless spectrograph attached to the Crossley Reflector, found the relative sizes of the monochromatic images to be $3727 \text{ H}\gamma, H\beta > N_{1,2}$. The latest determination of variations of state or constitution of the Orion Nebula, made with powerful apparatus (a large objective prism), has been carried out by W. J. S. LOCKYER¹. The outstanding feature of LOCKYER's plates is the great size of the image due to 3727 \AA , next in size are $H\beta$ and $H\gamma$, following these in order of size come 5007 \AA , 4959 \AA , and 3869 \AA , which is the smallest of all. The radiation from the Huygenian region is found to be composed almost entirely of hydrogen and N_1 and N_2 , the Messianian branch contains these elements plus 3727 \AA , the outlying regions are composed almost entirely of 3727 \AA . Similar interesting variations are noted in the planetaries (see ciph 28), and have formed the basis of the quantum state theories of these objects.

17. Luminosity of the Diffuse Nebulae Reflection or Resonance Effects. A relatively large proportion of the diffuse nebulae fail to show any emission lines whatever, or show them at best very faintly upon a background of relatively strong continuous and absorption spectrum. As nebulae with an emission spectrum are more easily identified than those with a continuous spectrum, if of the same surface brightness, HUBBARD regards it as probable that diffuse nebulae with continuous spectrum are actually more numerous than those with bright lines. He catalogues 33 diffuse nebulae with continuous spectrum, of which but 8 were known earlier. See Table 4.

Table 4 Diffuse Nebulae with Continuous Spectra (HUBBARD)

Number	Position and spectrum of stars involved	Remarks
1333	10,6	B8
I 318	8,4	B6
Plades	9,8-10,6	B8-A2
		B5
—		—
—	12,5	K8
1579	12,0-12,2	A0-B5
II 2087	—	—
1788	10,0-13,0	B8
II 2118	—	—
1977	1,6	B1
2023	7,8	B2
2068	10,1-10,8	B5-B8
—	—	—

¹ M N 90, p 580 (1930)

(Continued.)

Number	Pc. magn. and spectrum of stars involved	Remarks
2183	14,0	B3
-	13,5	B1
		Bright uncatalogued "comet" neb. $\alpha = 6^h 3^m 4, \delta = +18^\circ 42'.$
I 446	11,3	B1
I 447	8,1	B1
2245	10,7	B1
2247	8,8	B2p
2261	var.	Pec.
	8,2	B1
---	3,1	B2
II 5592	4,2	B2
4601	7,1--8,4	B8--A0
4603	7,8	B2
4604	5,2--5,9	B2--B3
		Approximates a nova spectrum Cf. SLIPPER, Lowell Bull 3, p. 63 (1918). Uncatalogued neb. about BD --- 12" 1774. Nebulosity about π Scorpii. Nebulosity about ν Scorpii. 4 stars. Neb. about BD - 24" 12684. 2 components of ρ Ophiuchi. SLIPPER, Lowell Bull 2, p. 155 (1916), finds spectrum continuous and probably like that of ρ . Neb. about 22 Scorpii. Neb. about BD - 37" 13023--4. R Cor Austr; resembles T Tauri. SLIPPER, Lowell Bull 3, p. 66 (1918), finds weak emission on strong continuous. BD + 41" 3731 and 3737. PRASER, Publ A S P 27, p. 240 (1915), finds strong continuous crossed by absorption lines. SLIPPER, <i>Ibid.</i> 30, p. 63 (1918), finds H and He absorption + H emission, which is strong in H β , and apparently identical with the star imbedded in the nebula. 3 stars. BD + 46" 3474.
4605	4,9	B3
6726	7,2--9,4	B9
6727		
6729	var.	Gp
6914	9,3--9,9	B5
7023	7,2	B2p
7129	10,2--12,4	B3--B8
II 5146	10,0	B1

The positions given in Tables 3 and 4 are for 1920,0. For data and deductions summarizing the character of the stars involved, see ciph. 19.

18. Variable Diffuse Nebulae. A few diffuse nebulae are definitely known to be variable.

These comparatively rare examples of variable nebulae are of great theoretical interest, and have certain characteristics in common:

1. Nearly all are fan-shaped, with a variable or suspected variable at the tip (in T Tauri the star is slightly removed from the tip of the fan).

2. All seem to lie in dark lanes or gaps, presumably filled with non-luminous matter.

3. No certain correlation has yet been derived between the stellar and the nebular variation¹.

4. The example most thoroughly studied, HUBBLE's variable nebula, shows no actual outward or other movement of formations.

The irregular and hap-hazard character of the variations in these objects, and the lack of correlation with variations in the involved stars, seem to negative any explanation involving the lighting up of successive regions outward by light pulses from the star. The dimming of the structural features by passing clouds

¹ LAMPLAND, however, states in his last paper that 2261 is generally faint at times when the star is faintest.

Variable Diffuse Nebulae

Number	α	δ	Description
1585	ph 16 ^m , 1	10 17 ^m 1	HINDS variable nebula near the variable star ϵ Lyncis (M 41 bright line σ). Companion in 1870. The nebula has been very faint since 1900. Further observations discussed by BARNARD, M. N. 55, p. 412 (1901), 56, p. 60 (1895), 59, p. 522 (1899). Sketch and description by PRYER, Ap. J. 15, p. 89 (1917). No parallelism has been established between the variation of the star and nebula. Situated in a dark lane.
2215	6 27 .2	10 11	Bright fan-shaped mass extending to ϵ from an apparently stellar nucleus. 5' \times 5'. Little structural detail. Faint in a dark lane. Variation suspected by PRYER, M. W. L. Contr. No. 186 (1920).
2261	6 53 7	1 8 49	HUMMER'S variable nebula, a bright fan-shaped mass about 2' \times 1' extending to the n. of the variable R Monocerotis (9.5-13.2). HUMMER'S plates show no variation in the nucleus, and he found strong, continuous spectrum. Ap. J. 11, p. 100 (1917), 18, p. 351 (1917). CURRIE, Lowell Bull. 5, p. 66 (1918) with an exposure of 4 hours, found a spectrum strikingly resembling that of a nova. Cf. also Ap. J. 20, p. 198 (1909), 31, p. 26 (1911). LAMPERT, in Pop. Astr. 26, p. 219 (1918), 27, p. 51 (1919), 29, p. 632 (1921), 31, p. 621 (1926) and in his later paper (abstract) in Publ. A.S.P. 45, p. 296 (1926) gives the results of a study of several hundred plates taken with the 12 inch reflector. While all parts of the nebula are subject to variation, there is no outward movement of the parts, which evidently shine by reflected or locally engendered light. The apparent displacement and motion of parts of the structure are evidently only apparent. Veilings and obscuration prevail over the nebula and the effects produced give an impression of displacement of parts. Some of the apparent progressive displacement of boundaries of obscuration have been measured, and rates of motion as high as $1/10''$ a day have been observed. The changes cannot be described as periodic. That there are recurrence of identical forms of the entire nebula appears certain. No correlation has been found between the light variations of the nucleus and that of the nebula. Structures. Cf. also, KNOX SHAW, Helv. Bull. 1, p. 128, 152 (1926). GREGORY, ibid. p. 235 (1921). The nebula lies in a dark lane.
5572	10 11 .2	59 9	Nebulosity about η Carinae. Early description with regard to suspected variability of this object (from visual descriptions only) to be found preceding in M. N. 31, 32, 34, and 36. Not confirmed by modern photographs.
6511	17 50 .3	23 2	The Trifid Nebula. Variability suspected by LYSTER, in Pop. Astr. 29, p. 631 (1920). Dark matter involved.
6720	18 55 .2	37 6	SCHMIDT'S variable nebula discovered by him at Athens in 1861, a fan-shaped wing with the variable R Ceti. Angular at the tip, and lying in a pronounced dark region. The star varies irregularly from ca. magn. 11.5 to 14.5 (Healy Bull. 805 (1924)). SCHMIDT, Lowell Bull. 3, p. 66 (1918) in a 20 hour exposure, found spectrum of nova type. No certain correlation between variation of star and of nebulosity. Cf. also, KNOX SHAW, Helv. Bull. 1, p. 131 (1915), 1, p. 182, with plates, (1920). No. 46 (1921). IRWIN, Union Circ. No. 33, p. 260 (1916). No. 46, p. 285 (1916), LAMPERT, Pop. Astr. 25, p. 650 (1917).

of occulting matter, quite heterogeneous as to density, has been suggested, and derives some measure of support from the location of these nebulae in dark lanes or gaps.

A theory put forward with some hesitation by LAPLACE would ascribe the irregular variations in the nebular luminosity to a luminescence or fluorescence engendered by the passage of the body through clouds of non-luminous matter¹. This, also, is supported by the milieu in which such nebulae are found. There are some very strong objections to such an explanation. 2261 seems to have remained unchanged in structure during all the period through which it has been observed. The theory would then require a density in such dark clouds vastly less than that of the luminous matter itself (10^{-24} ?), else this would be changed in configuration or even swept completely away by the passage of the non-luminous matter through its structure. Further work is urgently needed on the spectrum and light variation of the involved stars, as well as on changes in the nebulosity, before a satisfactory theory can be derived for these interesting objects.

10. Evolutionary Status of the Diffuse Nebulae. No definite decision can as yet be given as to the precise evolutionary position of the diffuse nebulae. Without any precise formulation of the successive steps of the process, and by tacit analogy with early or later forms of the now discredited KANT-LAPLACE nebular hypothesis, it has long been customary to regard the diffuse nebulae as the first step in the evolutionary process which has formed the stars. Man's mind demands a logical sequence in such an evolutionary process, and it is possible that the insistence of this demand occasionally blinds us to the fact that the "logic" of the process may have been injected from our own laws of thought, or by fallacious analogy with totally unaltered developmental germs. Provided, however, that we cast aside all somewhat vague modern indications of an eternal or cyclically renewed universe, and that we assume an initial state of undifferentiated heterogeneity, it must be admitted that such a theory possesses a measure of sequential harmony, and is to that extent alluring.

In roughest outline, such a theory will run

1. An initial chaos of completely mixed or shuffled primordial elements, a tohu-wa-bohu.

2. Gradual and irregular accretions into very rare and tenuous, non-luminous clouds, the possible creation of matter by "cosmic" rays from other already existing sources of radiation, the formation of "dark" nebulae.

3. Development under contraction of higher molecular speeds and "temperatures", light emission, the luminous diffuse nebulae, containing only a few of the "earlier" forms of matter.

4. Gravitational condensation of this luminous nebulosity into the "youngest" stars, the process is nearly finished in such cases as the Pleiades nebulosity, final development within the stars of the "later" and more complex forms of matter, etc.

It is said that ROWLAND jokingly laid down the dictum to a student that if a theory could not be right, the next best thing was for it to be exactly and diametrically wrong. It is not impossible that the rather attractive theory outlined above is exactly wrong. It is at least as probable, a priori, that the nebulosity surrounding the Pleiades and other high temperature stars may be being emitted, rather than a residue of evolutionary contraction processes.

¹ Cf. F. W. BROWN, *On the Passage of a Star through a Nebula*. Ap J 53, p. 169 (1921).

Our best summary of the facts that may bear on any theory of the diffuse nebulae is due to HUBBLE (l. c.). From the average spectral types of the stars involved in nebulosities of the emission and the absorption spectrum types, he has drawn the following important conclusions (cf. Tables 3 and 4 above):

1. Stars involved in nebulae having continuous spectrum are nearly all of Class B1 or later.
2. Stars involved in nebulae having emission spectrum nearly always have spectra earlier than Class B1, rarely showing any bright lines.

HUBBLE therefore holds that all nebulae of the diffuse type are intrinsically non-luminous, and that in every case the luminosity of nebulae showing an emission spectrum is excited by an involved hot star of earlier type, while the luminosity of those displaying a continuous spectrum is due to simple reflection or to some sort of resonance phenomenon, from similarly involved stars of later type. "A casual inspection of diffuse nebular structure and configurations of involved stars suggests that the association is for the most part temporary. This may be one fundamental distinction between diffuse nebulae and planetaries, for in the latter the central stars must be permanently associated with the surrounding nebulosity; otherwise their central positions could not in general be maintained."

These significant results introduce another difficulty in the long current assumption or theory that diffuse nebulosity forms the initial stage of stellar evolution. For most modern theories hold that the typical star begins its life as a red giant, of relatively low temperature, reaching the high temperature of the B stars only much later in its life history. If the primordial state of the stellar matter was nebular, and if this process is in some cases still incomplete, the fact that practically no red stars are involved in such nebulosities becomes a very serious objection to the older theory, and one that it seems impossible at present to remove.

There are, however, several very serious exceptions, as admitted by HUBBLE, to his theory that the light of the diffuse nebulae comes in every case from involved stars. Notable among such exceptions are the America (7000) and Network (6995) Nebulae: vast structures in which no bright stars whatever seem to be physically involved. If such objects are not intrinsically luminous, one can only make the assumption, on HUBBLE's theory, that the luminosity is in some way engendered from the stars of neighboring regions of the Milky Way.

c) The Planetary Nebulae.

20. Definition of the Planetary Type. The term planetary has long been restricted to a limited class of relatively small and clearcut nebulae of emission spectrum, possessing a more or less definite spheroidal or annular symmetry with regard to a center which is nearly always stellar. Their apparent dimensions average less than $1'$, though this is greatly exceeded by some of the giants of the class (e. g., 7293 is $15' \cdot 12'$, and doubtless the largest planetary known); not a few of the genus are so small as to be apparently stellar in large telescopes. In apparent surface luminosity, they range from objects with the brightest nebular matter known (7009, 7027) to faint disks several hundred times less intense, which leave only a slight impression in an exposure of two hours (7139). While there are some exceptions to the rule, the typical planetary has a central star, whose apparent luminosities range from the 9th to the 19th magnitude, or fainter.

21. Number and Distribution of the Planetary. In distribution, the planetary nebulae are definitely galactic, with a marked concentration in the Milky Way regions from $\alpha = 18^h$ to 20^h . See Figure 11

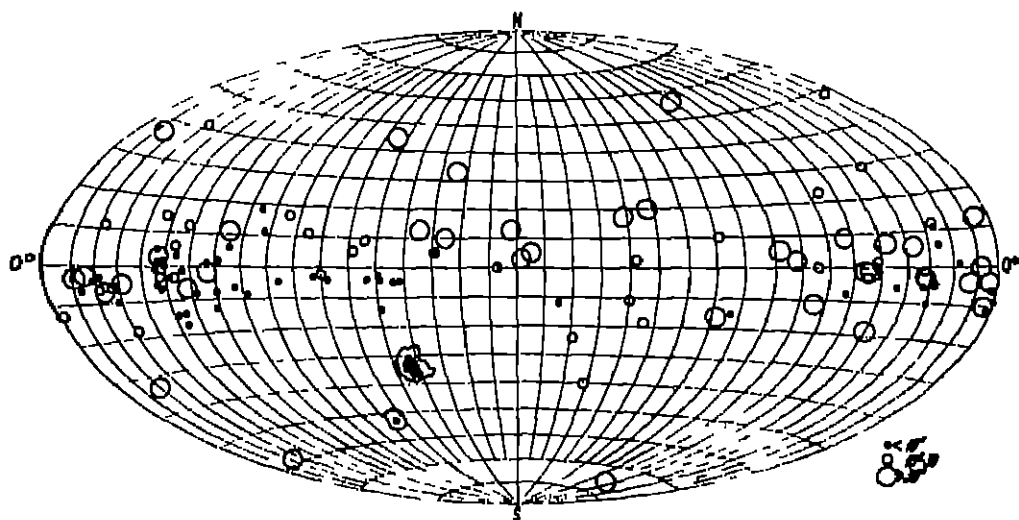
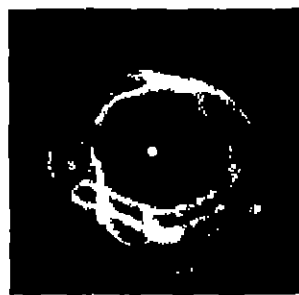


Fig 11 Galactic Distribution of the Planetary Nebulae. It will be noted that those distant from the galactic plane are in general the larger members of the group, which are presumably closer. The smaller and more distant objects are closer to the galactic plane.

Fewer than 150 objects of this class are at present known, nor does it seem probable that future surveys will add greatly to this total¹. The most complete collection of data on the planetary nebulae yet published will be found in Volume 13



a



b

Fig 12a and b The Planetary Nebula NGC 6720 (Ring Nebula in Lyra) (Lick Photograph) A photograph of the object is shown at the left, at the right is a sketch by CURTIS showing the intricate structure

¹ About 135 are noted in the NGC lists as planetary or possibly planetary. A few have since been discovered by HUMASON, HUBBLE, PEASE, INNES, JONCKHEERE, CURTIS, and others. At the time of publication of Vol 13 of the Lick Publ (1918), but 78 were known north of declination -34° . The following considerations indicate that no great increase in the number of planetaries is probable.

1 To test this point, CURTIS examined with a slitless spectroscope (Lick Publ 13, p. 73) 79 small objects within 25° of the Milky Way which have the NGC descriptions, small, very small, or stellar. But one object of planetary type was found.

2 The revision of the DRAPER Catalogue increased the number of listed stellar spectra from 9000 to 22700. But one new object with a planetary spectrum was found.

of the Publications of the Lick Observatory, 1918, to be referred to henceforth as Lick Publ 13, with the omission of the date. It contains the following monographs:

Part III. The Planetary Nebulae, by H. D. CURTIS.

Part IV. The Spectrographic Velocities of the Bright-Line Nebulae, by W. W. CANNIBELL and J. H. MOORE.

Part V. The Radial Velocity of the Greater Magellanic Cloud, by R. F. WILSON.

Part VI. The Wave-lengths of the Nebular Lines and General Observations of the Spectra of the Gaseous Nebulae, by W. H. WRIGHT.

22. Forms Assumed by the Planetary Nebulae. Of the 78 planetaries north of decl. -34° , depicted by CURTIS in Lick Publ 13, 55 have a central star, as follows:

	40	2452	6572	6891
	246	2610	6578	6894
	650	3242	6620	6905
II	4747	3587	6629	7008
I	351	4361	6720	7009
	1504	II 3568	6751	7036
	1514	6058	6772	7139
	1535	II 4593	6778	7293
J	320	6210	6781	7351
I	418	6309	6803	7662
	2022	6369	6804	
II	2149	6439	6818	
	2371	6445	6826	
	2392	6543	6853	
	2438	6563	6881	

8 very small planetaries, only $2''$ or $3''$ in diameter, may possibly possess a central star, though their small size makes it impossible to distinguish such. These are:

	6644	6807
II	4732	6833
II	4846	II 4997
	6790	II 5117

No central star can be made out in the following 13 objects:

1952	6537	6886
II 2165	6565	7027
J 900	II 4776	II 5217
2440	6744	
II 4634	6884	

4 planetaries are binuclear, trinuclear, or too irregular to classify:

1952	J 900	2440	7027
------	-------	------	------

From a consideration of the data given above, it seems evident that the typical planetary has a central star, of Class O.

The planetaries may be further classified as to apparent form:

A. Forms apparently helical.

6543	7293
------	------

B. Annular forms; main feature a circular or elliptical ring.

246	2438	6369	7662
1535	2610	6720	
I 418	3242	6804	
2022	3587	6894	
2392	4361	7009	

C. Disks showing brighter edges; elliptical rings less perfect than those under (B), fading out at the extremities of the major axis, and giving the impression of ellipsoidal shells.

II	1717	6058	6751	6854
	1501	6561	6772	7009
	1514	6565	6781	7139
II	2165	6720	6804	7354
	2452	6741	6818	7662

D. Forms like those under (C), but with a more pronounced truncated effect, as though the ends at the terminations of the major axis of the shell had been cut off, faint ansae are generally seen at these extremities

	40	6561	7026
	650	6720	
	2371	6778	
	6058	6851	
	6445	6905	

E. Objects considerably fainter along and at the ends of the major axis, this group contains some nebulae from all the first four classes

	10	6445	7009
	1501	6563	7026
	1514	6565	7139
II	2165	6720	7293
J	900	6741	7354
	2372	6772	
	2458	6778	
	2452	6818	
	6058	6853	
	6369	6905	

F. Circular or elliptical disks, fading out slightly at the periphery, and without discernible structure. Most of these are small, and the lack of structural details may be only apparent

I	141	6537	6629	6884
J	320	6572	II 4776	6886
II	3568	6567	6803	II 5217
II	4644	6578	6879	
	6439	6620	6881	

G. Stellar planetaries. These are indistinguishable from a star on the scale of the Crossley negatives, but have been shown by visual observations to have a minute disk. In all probability they differ from the objects under (F) only in size

	6544	6833
II	4732	II 4997
II	1846	II 5117
	6790	
	6807	

Mechanical and quantum theories of the forms assumed by planetaries will be treated in clph. 30, 31, and 32.

23. Proper Motions of the Planetary Nebulae. The almost stellar image presented by a planetary when observed with small apertures, as by a meridian circle, and the stellar nucleus exhibited in many of the group when higher powers are employed, have made these objects attractive subjects for position measures for over a century. The total number of measures on a few of these planetaries by filar micrometer, meridian circle, and photographic plates is quite large.

If any combination of position measures of three-quarters of a century ago with modern photographic positions has any chance of a trustworthy result in the nebular field, we should expect this from the almost stellar appearance of certain planetaries. LUNDMARK¹ has discussed all available older measures

¹ Uppsala No. 39 (1923)

(using recent plates for the final term) of six of the better determined planetaries, plotting the positions on charts and determining the proper motions graphically. Reference to the "scatter" of these significant and illuminating diagrams (the

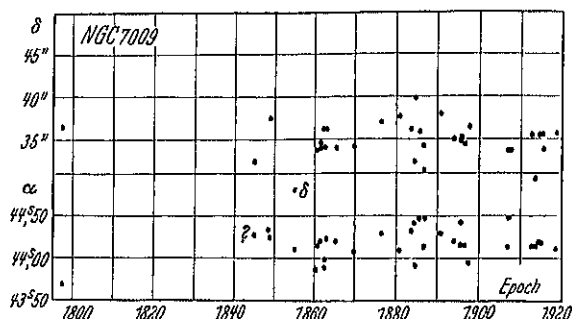


Fig. 13 Positions of the Planetary Nebula NGC 7009, 1794 - 1920 (LUNDMARK). No certain proper motion is observable.

contains VAN MAANEN's latest values¹. These values of VAN MAANEN are considerably more trustworthy, depending solely upon modern large scale photographic plates with an average time interval of 11 years. His probable errors are

0".0010 in α , and 0".0012 in δ , the mean parallax resulting from his values in combination with the rotation results of CAMPBELL and MOORE is 0".001, giving a mean mass of 180 \odot , and a mean absolute magnitude for the central stars of 13.

In Table 5 I give LUNDMARK, VAN MAANEN, W. WILSON, MA MAKENSON, N&C, NICHOLSON (revision of CURTIS), LY, LUYTEN. In each pair of values, the proper motion in α is given above, with that in declination below.

24. Distances and Dimensions of the Planetary Nebulae. While a number of investigators have discussed the parallaxes of the planetaries by various indirect methods, practically all results by the trigonometric

Fig. 14 The Planetary Nebula NGC 7293 (Ick Photo-graph). This beautiful object is the largest known planetary, and is about 15' 12". It appears to be two turns of a helix.

cal method are due to VAN MAANEN. His values, with some additions, have been collected by LUNDMARK and are given in Table 6, with the apparent and the derived absolute magnitudes of the central stars. To these values have been added

¹ Mt Wilson Contr. No. 406 (1930)

the dimensions of the planetaries and their distances, the latter are manifestly subject to large uncertainty

Table 5 Proper Motions of Planetary Nebulae

Object	Interv	Ln	W	Ma	N&C	Ly	vM (11 y)
2371	45 y	-",040 + ,041			-",016 + ,074		
2392	65 y	- ,006 - ,008	-",004 - ,010				
6058	11 y						",000 - ,000
6543	118 y	-- ,013 -- ,007	,000 - ,014				+ ,003 ,000
6572	91 y	+ ,012 - ,009	+ ,003 - ,004		- ,008 + ,024	+",006 - ,017	- ,004 + ,007
6720	11 y						+ ,004 + ,008
6804	11 y						,008 - ,002
6905	11 y						- ,006 ,000
7009	123 y	+ ,006 - ,004	+ ,009 + ,048				
7662	121 y	+ ,012 + ,011		- ,024 + ,026	- ,015 + ,020		{ + ,022 - ,004 }

Table 6 Distances and Dimensions of the Planetary Nebulae

Neb	Dimension		M _{app}	M _{abs}	Rel π	Dist. ly	Other values τ
	Arc	ly					
40	60"	0,12	11,6	+ 1,6	+",013	1000	
1501	56	,06	13,0	+ 8,7	16	200	
1514	120	,95	8,0	- 0,5	2	1600	
1952	160	,96	15,5	+ 9,2	6	600	
2022	28	,04	14,2	+ 8,1	8	400	
2371	60	,09	13,5	+ 8,3	11	300	
2392	17	,04	10,0	+ 5,5	20	160	+",006 S
3242	40	,02	12,2	+ 7,8	31	100	
II 4593	15	-	10,0	-	-	-	- ,007 S
6058	43	-	13,0	-	-- 16	--	
6210	43	-	11,7	--	- 3	-	
6543	22	,01	11,3	+ 8,4	29	100	
6572	16	,09	10,8	+ 6,8	3	1000	
6720	83	,66	14,7	+ 8,5	2	1600	+ ,015 N
6778	25	,08	14,8	+ 6,3	5	650	
6804	63	,05	13,4	+ 9,7	20	160	{ - ,002 S
30° 3639	5	,04	10,2	+ 1,7	2	1600	,010 L
6826	27	-	9,5	-	-	-	- ,006 S
6853	480	,77	13,7	+ 8,3	10	320	
6891	15	,02	12,1	+ 8,0	17	190	
6905	44	,05	14,5	+ 9,7	13	250	
7008	86	,10	12,8	+ 8,2	14	230	
7026	25	,04	15,1	+ 9,9	11	300	
7027	18	,04	10,9	+ 4,9	8	400	
7293	900	,38	13,3	+ 11,1	38	86	
7625	200	,20	8,5	+ 4,2	16	200	
7662	32	,02	12,9	+ 9,3	21	150	

S = SWARTHMORE, N = NEWKIRK, L = LARK

It seems fairly certain that the values given above are much too small as regards distances and diameters, and that these must be multiplied by some as yet unknown factor, perhaps as large as 3 or 5. The mean absolute magnitude (about $+8$) is much lower than that derived from VAN MAANEN's last determinations of proper motion ($+3$). GERASIMOVICH¹ has discussed this dilemma, deducing from VAN MAANEN's (earlier) proper motions in combination with the Lick radial velocities a mean abs. phot. magn. for the nuclei of -5.9 . By various indirect methods, using the angular galactic dip, galactic rotation, and novae at the planetary stage, he derives

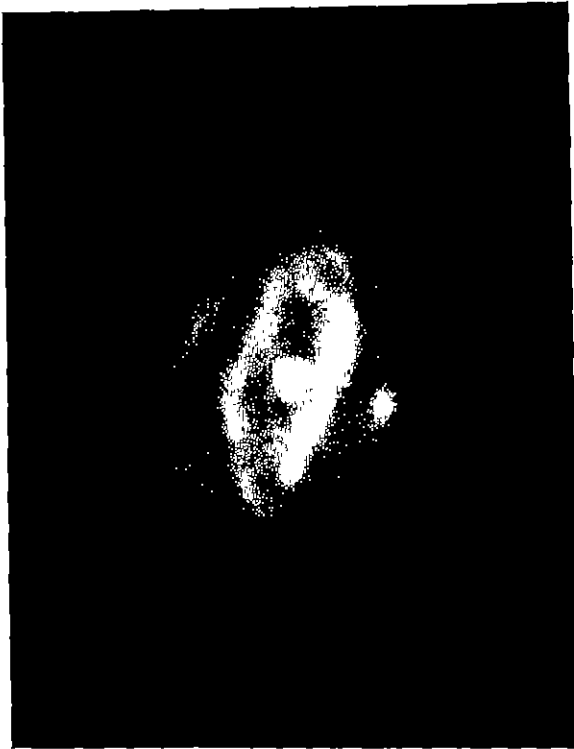


Fig. 15. The Planetary Nebula NGC 7009. (Mt. Wilson Photograph.)

$+4.9$ as the most satisfactory value of M , and points out: "None of the indirect methods used above has given so low an absolute magnitude ($+8.1$), or so large a mean absolute parallax ($0''.012$) as derived from the Mt. Wilson parallax plates. No other case is yet known for which the discrepancy between trigonometrical parallax determinations and the results of indirect methods is as great as for the peculiar group under consideration. The explanation of this paradox seems therefore to be of much importance." As a possible cause of the difference, he somewhat doubtfully assigns the existence of some sort of "sampling error" in the selection of the Mt. Wilson objects.

¹ Harv Bull No. 864 (1929).

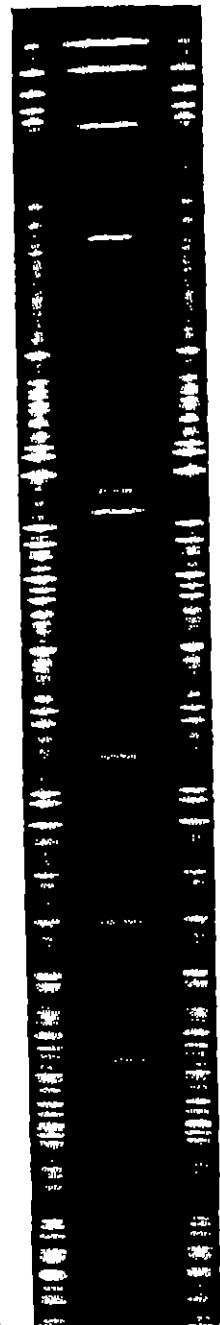


Fig. 16. Six Spectra of the Planetary Nebula NGC 7009. (Photographs by W. H. Loomis.)

25. Planetary Spectra; Spectrum of the Nebulous Matter. While the spectrum of the nebulous portions of the planetary nebulae is in most respects a duplicate of the emission spectra of the diffuse nebulae, there are a number of points of difference. In the case of the fainter lines, these differences may arise from the far greater areal luminosity of such an object as 7027 as compared with the Trapezium region of Orion. In other cases, it is possible that actual differences of state or constitution may be indicated. These differences do not seem, however, to be vital, or to indicate different sorts of component matter. There are also frequent differences among the planetaries themselves, as well as



Fig. 17. Objective Spectrogram of the Planetary NGC 7662. (Photograph by WRIGHT.)

in comparison with the diffuse nebulae, in the relative intensities of the lines, as noted for the diffuse nebulae in ciph. 16.

Table 7 is composite, in that it includes all the lines measured by WRIGHT in various planetaries; for the peculiarities of individual objects, reference should be made to his monograph in Lick Publ 43. The series relationships and ionization potentials are as given by BOWEN¹. The intensities are mainly for 7027; in a few cases these are merely estimates.

Table 7. The Spectrum of the Planetary Nebulae.

λ Å.	Source	Series designation	Excitation potential, v.	Intens.	Notes
3313	O III	3h ³ P ₁ - 3m ³ S	36,72	1	1
3342	O III	3h ³ P ₂ - 3m ³ S	36,72	—	5
3346	O IV?	3m ³ P - 3n ³ D	54,76	—	2
3420,2	N IV?	3 ³ S - 3 ³ P	47,	20	3
3445	O III	3m ³ P ₂ - 3n ³ P ₂	40,66	8	
3704	Hδ, He I	2 ³ P - 7 ³ D	13,49; 24,22	—	4
3712	Hγ	—	13,49	—	4
3722	Hβ	—	13,48	—	4
3726,16	O II	a ⁴ S - a ² D _{5/2}	3,31	50	5
3728,91	O II	a ⁴ S - a ³ D ₃	3,31	30	5
3734	Hδ	—	13,47	—	4
3750	Hγ	—	13,45	3	6
3759	O III	3h ³ P ₂ - 3m ³ D ₃	36,49	4	
3771	Hγ	—	13,43	4	
3798	Hβ	—	13,41	5	
3820	He I	3 ³ P - 6 ³ D	24,11	1	
3835,5	Hγ	—	13,38	8	
3840,2	—	—	—	5	
3868,74	—	—	—	70	7
3888,96	Hδ, He I	2 ³ S - 3 ³ P	13,33; 22,92	10	8
3935	C III?	4 ² S - 4 ² P ₂	3,14	—	
3964,8	He	2 ¹ S - 4 ¹ P	23,65	5	9
3967,51	—	—	—	70	7
3970,08	Hγ	—	13,27	30	
4009	He I	2 ¹ P - 7 ¹ D	24,22	1—	
4026,2	He II, He I	2 ³ P - 5 ³ D	53,78; 23,95	1	
4064	—	—	—	1—	
4068,62	S II	a ⁴ S - a ² P _{3/2}	—	20	10
4076,22	S II	a ⁴ S - a ¹ P ₁	—	2	10
4097,3	N III	3h ² S - 3m ² P ₂	30,35	1	
4104,74	Hδ, N III	3k ² S - 3m ² P ₁	13,17; 30,34	70	

¹ Ap J 67, p. 1 (1928).

(Continued)

λ , μ	Source	Series designation	Excitation potential, μ	Inten	Note
4120.6	He I	2^3P-5^1S	23.88	1	
4144.0	He I	2^1P-6^1D	24.12	1	
4200	He II		53.76	1	
4267.1	C II	$3n^1D-4^2I$	20.87	5	
4310.16	H γ	—	13.00	90	11
4353	—	—	—	80	
4363.21	O III	a^1D-a^1S	5.53	5	
4368.0	He I	2^1P-5^1D	23.95	1	
4416	O II'	$3k^2P_{1/2}-3m^2D_{3/2}$	26.18	8	
4471.54	He I	2^3P-1^3D	23.61	2	
4541.4	He II	—	53.54	1	
4571.5	—	—	—	2	
4634.1	N III	$3m^2P_1-3n^2D_{3/2}$	33.01	5	
4640.9	N III	$3m^2P_2-3n^2D_{5/2}$	33.01	1	11
4649.2	C III	3^1S-5^3P	30.1	2	11
4658.2	—	—	—	90	
4685.76	He II	—	50.82	10	
4711.4	—	—	—	5	
4712.6	He I	2^3P-1^1S	23.50	1	
4725.5	—	—	—	20	11
4740.2	—	—	—	80	
4861.32	H β	—	12.70	2	
4922.2	He I	2^1P-4^1D	23.61	200	
4958.91	O III	$a^3P_1-a^1D_2$	2.50	500	
5006.84	O III	$a^3P_2-a^1D_2$	2.50	1	
5017	He I	2^1S-3^1P	23.00	1	
5411.3	He II	—	53.10	1	
5655	—	—	—	1	
5737	—	—	—	1	
5754.8	—	—	—	1	
5875.7	He I	2^3P-3^3D	22.98	5	
6302	—	—	—	2	
6313	—	—	—	2	
6364	—	—	—	10	
6548.1	N II	$a^3P_1-a^1D_2$	1.89	100	
6562.79	H α	—	12.04	30	
6583.6	N II	$a^3P_2-a^1D_2$	1.89	1	
6677	He I	2^1P-3^1D	22.98	1	10
6730	S II	$a^1S-a^2D_2$	—	1	
7009	—	—	—	—	
7065	He I	2^3P-3^3S	22.63	15	
7138	—	—	—	15	
7325	O II	a^2D-a^2P	5.00	15	

Notes to the table of wave-lengths

Note 1 The electron configurations in this table are indicated by BOWEN as follows:
 Terms arising from the most stable configurations, n being the number of valence electrons remaining in the atom

(2) $2s$, ($n-2$) $2p$ electrons	a
(2) $2s$, ($n-3$) $2p$ electrons and an excited s electron	k
(2) $2s$, ($n-3$) $2p$ electrons and an excited p electron	m
(2) $2s$, ($n-3$) $2p$ electrons and an excited d electron	n

The numeral preceding these letters indicates the total quantum number of the excited electron, these letters are omitted in one- and two-valence electron systems, since for all the cases considered here the type of the term is the same as the type of the orbit of the excited electron

Notes 2, and 3 These are the lines reported by PATMLER at 3371 and 3151 $\mu\mu$

Note 4 Observed in Orion, but not in planetaries

Note 5 BUISSON, FABRY and BOURGET derived the wave-lengths 3726,100, 3728,838

Note 6 H α 3750,52

Note 7 The strong lines at 3868.74 and 3967.51 are still unidentified. Carbon has been suggested. L. BERMAN, reported in *Phys. Astr.* 39, p. 184 (1931), has studied the behavior of these lines, whose intensity ratio is constant in various planetary nebulae. He rejects the explanation of their origin as due to C_{II} , and considers the availability of P_{III} or Si_{III} .

Note 8 HC 3889,051 Ho 3884,64

Note 9 Suspected with intensity 10 in
BD +30" 3639

Note 10 Cf HOWEN, Nat 123, p 450 (1929)

Note 41 Suspected in Orion, not in planetary

Note 12 See Note 7 Lines of C at 4647.4,
4650.7, 4651.6

Note 13 MERRILL finds this line in R Aquarii and BD - 12° 5145

Note 14 Unidentifiable

Note 15. MERRILL gives 7135.6 and 7330.4

28 Planetary Spectra; Spectrum of Planetary Nuclei¹. The resemblance of the spectrum of planetary nuclei to that



Fig 18a.

of the WOLF-RAYET stars, tentatively suggested by PICKERING, has been established beyond all doubt by the extensive researches of WRIGHT.

The main characteristics of the spectrum of planetary nuclei are:

4 A marked and uniform extension of continuous spectrum into the ultra-violet

2 The occurrence of bright bands identical with those observed in the WOLF-RAYET stars (Class O). The relative strength of these bright bands with respect to the continuous spectrum varies from object to object, in some, as 7026 and 6751, they occur almost without it, while in others they are barely visible against the strong continuous background.

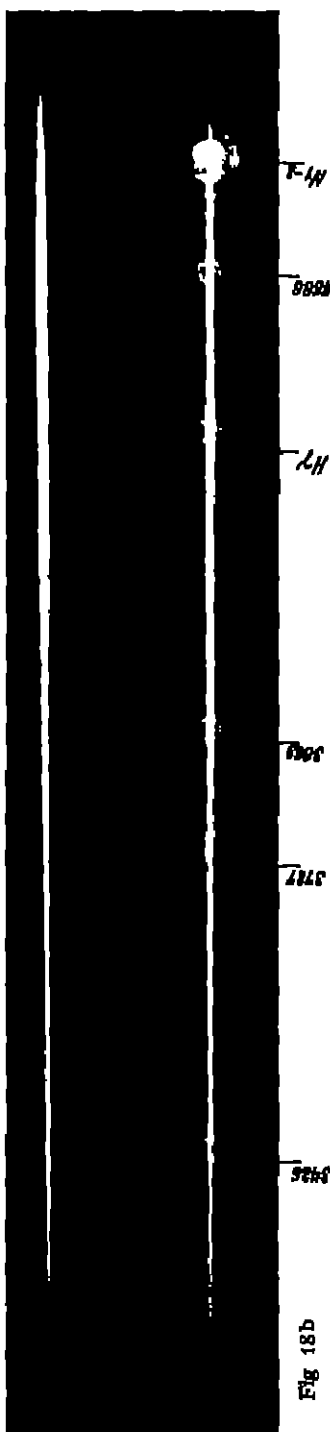


Fig 18b

Fig. 18. Objective Spectrogram of the Planetary, NGC 2392. (Photographs by WRIGHT.) The upper cut, Figure 18a, shows the planetary with a star in the same field. Below, Figure 18b, are shown the spectrum of the star and that of 2392. It will be noted that the spectrum of the star is much stronger than that of the nucleus, except in the ultra-violet region, where the two spectra are of about the same intensity. The star is probably about Class A. The plate illustrates in a striking manner the great luminosity of planetary nuclei in the violet and ultra-violet regions.

¹ R. C. PICKERING, *AN* 127, p. 1 (1891), J. E. KEELER, *Lick Publ* 3, p. 227 (1894), *Astr and Astroph* 13, p. 497 (1894), W. H. WRIGHT, *Ap J* 40, p. 466 (1914), *Lick Publ* 13 (1918).

Out of 30 planetary nuclei, WRIGHT finds that about one-half are Class O stars, and regards the evidence as unequivocal that the nuclei of all the planetary nebulae belong to the same stellar division as the Class O stars. The sequence will then be:

1. Nebulae without nuclei.
2. Nebulae with nuclei. These nuclei are in all cases stars of very high temperature, and in half the cases show the WOLF-RAYET bands.
3. Class O stars, with no (observed) nebulous surroundings. Temperature high.

The number of the WOLF-RAYET stars is about the same as that of the planetary nebulae. Miss PAYNE¹ enumerates a total of 238; of these 166 are of galactic occurrence, 39 are planetary nuclei, and 33 are in the Magellanic Clouds.

The spectral classifications of planetary nuclei have been tabulated by Miss PAYNE in tables VI, II, of the work quoted.

Table 8.

Object	Spectrum classification	Object	Spectrum classification
40	W III	6629	Cont.
246	O6	II 4776	W III
II 1747	W	6720	Cont.
I 351	W	6751	W III
II 2003	Cont.?	6790	Cont.?
1514	O8	6803	Cont.?
1535	Cont.	30" 3639	W III
I 418	O7w	6826	O6w
2022	Cont.	6833	Cont.?
II 2149	O7	6879	Cont.
2392	O8w	6891	Cont.
3242	Cont.	II 4997	Cont.?
4361	Cont.	6905	W III
II 3568	Cont.	7000	Cont.
6058	Cont.	7026	W III
II 4593	O7 + Cont.	II 5217	W III
6210	W	I 4470	O
II 4634	Cont.	7635	O7
6543	W I	7662	Cont.
6572	W I		

(The small w in the above Table indicates WOLF-RAYET lines in addition to continuous spectrum; W I has the line at 4686 Å stronger than combined lines near 4340 Å; W III has the 4686 Å line weaker.)

WRIGHT has suggested a classification of the planetaries based upon the relative intensity of characteristic lines, as follows:

Class I. 4686 Å present in the nebula

- | | |
|--|-------------|
| a) 3426 Å stronger than 3445 Å | Type object |
| b) 3445 Å stronger than 3426 Å | 7027 |
| c) 3445 Å and 3426 Å absent | 7000 |
| | 6884 |

Class II. 4686 Å absent from nebula, 3869 Å present

- | | |
|--|--------|
| a) 3869 stronger than H δ | 6572 |
| b) 3869 Å weaker than H δ | I 2419 |

Class III. 4686 Å and 3869 Å absent I 418

Further details as to the application of spectroscopic theory to the planetaries will be found under ciph. 28 and 31.

¹ The Stars of High Luminosity. Harv Monograph No. 3 (1930).

27 Radial Velocities of Planetary Nebulae; Rotation. Our knowledge of the radial velocities of the planetary nebulae north of declination -34° is very satisfactory and complete, thanks to the work of CAMPBELL and MOORE, south of this our results are due to WILSON (Lick Publ 13). Details as to the radial velocities of individual planetaries should be sought in the tabulation given on pages 168-9 of the papers quoted.

The more important results of CAMPBELL and MOORE, and WILSON may be summarized:

1. 6 planetaries show abnormally high velocities. These are:

5873	-127 km/sec	6644	+205 km/sec
6567	+133	II 4732	-134
II 4699	-117	II 4846	+165

These values are excluded from the averages which follow.

2. 17 nebulae (12 probably of planetary type) in the Greater Magellanic Cloud show an average radial velocity of $+276$ km/sec. The velocity spread is small, and there is no doubt that this represents the radial velocity of the Cloud as a whole.

3. 1 planetary in the Smaller Magellanic Cloud has a radial velocity of $+168$ km/sec. With less certainty, this may be regarded as indicating the approximate velocity of this Cloud.

4. 96 objects of planetary type yield a speed of -29.6 km/sec for the solar motion. The mean radial velocity of 34 of these with diameters less than $5''$ is 28 km/sec, while that of the 65 larger objects is 34 km/sec. These velocities are about five times the average radial velocities of the B-type stars.

5. Of 46 planetaries examined, 25 showed internal motion effects, which may be interpreted as rotations about axes approximately perpendicular to the line of sight, while 4 are not so interpretable. The most elongated planetaries show the highest rotational speeds and, in general, the speed of rotation of outer strata is less than that of strata nearer the center.

6. With some more or less probable assumptions, the mass of a planetary seems in general to exceed that of the solar system.

Physical change has been noted to date in but one object, and that is the "Crab Nebula", 1952. While it is somewhat doubtful whether it is a typical planetary, reference to its internal motions will be included at this point. Variations ascribed either to luminosity changes or to motion were first noted by LAMPARD¹ and this nebula was later subjected to careful investigation by DUNCAN². His measures are based upon Mt. Wilson plates separated by an interval of 11.5 years. For twelve selected nebular points or configurations, radial motion outward from the center was definitely indicated, amounting to $1''.54$ in the interval. This displacement, if at a velocity of 25 km/sec, would correspond to a distance of 1001 ly, and DUNCAN points out that it is necessary to assume neither an enormous distance nor an extraordinary velocity in the nebular particles in order to believe that the observed motions are real.

28. Spectroscopic Distribution Effects. The phenomenon of varying distribution of matter indicated by different spectral lines in the Nebula of Orion has already been noted under eph 16 above.

Objective prism spectrograms likewise show more remarkable and equally definite evidence of differences in ionization distribution or constitution of

¹ Publ A S P 31, p 79 (1921)

² Wash Nat Ac Proc 7, p 179 (1921), with plate

different elements in the shells of many planetaries. CAMPBELL¹ had already called attention in 1894 to the differences in the diameters of the spectroscopic images in I 418. This effect was perhaps first noted photographically by WORT² and corroborated by BURNS for the Ring Nebula in Lyra.³ WRIGHT has illustrated many cases in his monograph in Lick Publ. 13, and most of the data in the following summary are derived from his researches.

Table 9. Distribution of Planetary Materials (WRIGHT). Sizes of Rings or Formations.

NGC	Largest ———→ Smallest				Notes
40	—	—	—	—	No difference noted
I 351	—	—	—	—	Slight difference
1535	II	—	—	1686	
I 418	3727	$H\beta$	1171	N_{1-2}	
2022	—	—	—	—	Slight difference
II 2149	3727	—	—	—	
II 2165	3727	3967	1686	3426	
2392	—	—	—	—	Differences in intensity but not in size
2410	3727	N_{1-2}	4686	3126	Large differences
3242	—	—	—	—	Slight differences
II 4593	—	—	—	—	Nearly equal
6309	—	—	—	1686	
6543	3727	—	—	—	Some structural differences
II 4776	3727	—	—	—	
6720	3727	N_{1-2}	II	1686	WORT
	3727	N_{1-2}	—	—	BURNS, $H\alpha$ 3727
	3727	N_{1-2}	—	1686	WRIGHT
6741	3727	3869	1686	3126	
6751	3727	II	—	N_{1-2}	
6818	—	—	{	3426	} Structural differences
				1686	
6826	—	—	—	—	Structural differences
6881	3727	—	—	1686	
6886	3727	3869	1686	3126	
6891	3727	—	—	—	
7009	—	—	—	—	Notable structural differences
7026	3727	N_{1-2}	II	1686	
7027	—	—	—	4686?	About same size
7662	{ 3869	N_{1-2}	{	1542	} Notable structural differences
	3967	II			

It will be noted from the above compilation that the largest image in the majority of cases is given by 3727 Å, O_{III} . The smallest ring is generally either 3426 Å ($N_{IV}^?$), or 4686 Å, He_{II} . Reference should be made at this point to the far more detailed results secured by BERMAN, discussed in Ceph. 33. BERMAN determined isophotal contours for the various spectrographic images, and his diagrams show remarkable variations, not only in size, but in contour, so that the distribution due to a given state may be entirely unlike that given by another. See BERMAN's diagrams, reproduced as Figures 25 and 26, *a, b, c*.

¹ Ast. and Astroph. 13, p. 491 (1894).

² V J S. 43, p. 283 (1908), also Geschichte der Linienemission im Ringnebel. Sitzber. d. Ak., Abh. No. 27 (1911), Die Spektren zweier planetarischer Nebel, ibid., Abh. 35 (1911) Der Ringnebel und der Dumbbellnebel, ibid., Abh. 1 (1915), NGC 2448, ibid., Abh. 2 (1916).

³ Lick Bull. 6, p. 92 (1910).

29. Turbulence Effects in the Planetaries. This name is chosen to designate one of the most remarkable characteristics of the spectra of some of the planetary

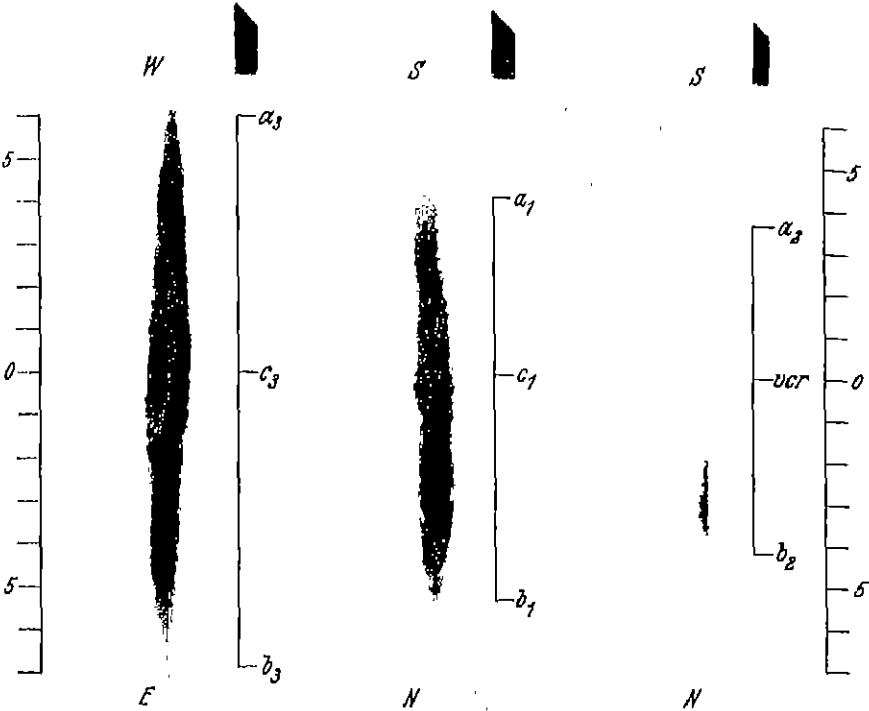


Fig. 19. Drawings of the N_1 Line in NGC 6210. a minor axis; b and c major axis. (MOORE.)

Table 10. Turbulence Effects in Planetary Nebulae.

NGC	Descriptions
40	The line N_1 is not straight, but a very flat, S.
2302	The line N_1 is single at its outer ends, with an irregularly doubled central portion.
3242	The nebular lines are tortuous, with a suspicion of doubling in the central part of N_1 .
6210	The N_1 line is tortuous and irregular, with a slight doubling in an exposure along the major axis.
6543	The N_2 line is tortuous, with several slight bends.
6572	The N_1 line is irregular and wavy.
6567	The nebular lines are S-shaped.
6720	The N_1 line is wavy, with a marked bowing toward the red in the central portion along the minor axis.
6818	The N_1 line is tortuous at the ends, and is slightly but clearly doubled, though irregularly, over the central portion of the planetary.
6891	N_1 irregular, and on some plates a very flat S.
7009	N_1 irregular; a very flat S.
7026	N_1 broad and very irregular, with marked minor effects of turbulence.
7027	N_1 shows numerous local irregularities and mottlings.
7662	N_1 is doubled in its central portion, with interesting differences between major, minor, and diagonal axis positions of the slit. On the major axis, the red component is stronger at one end of the doubling, while the violet component is the stronger at the other end. The contours of the line 4686 Å show striking differences from those displayed by the chief nebular lines ¹ . See Figure 22.

¹ WRIGHT and MOORE, Publ A S P 41, p. 307 (1929).

nebulae, a phenomenon so peculiar and so anomalous that no entirely satisfactory explanation seems as yet attainable. These phenomena differ from nebula to nebula, and the differences defy verbal description, so that reference should be made to the spectra exhibited pictorially in the papers of WRIGHT and CAMP-

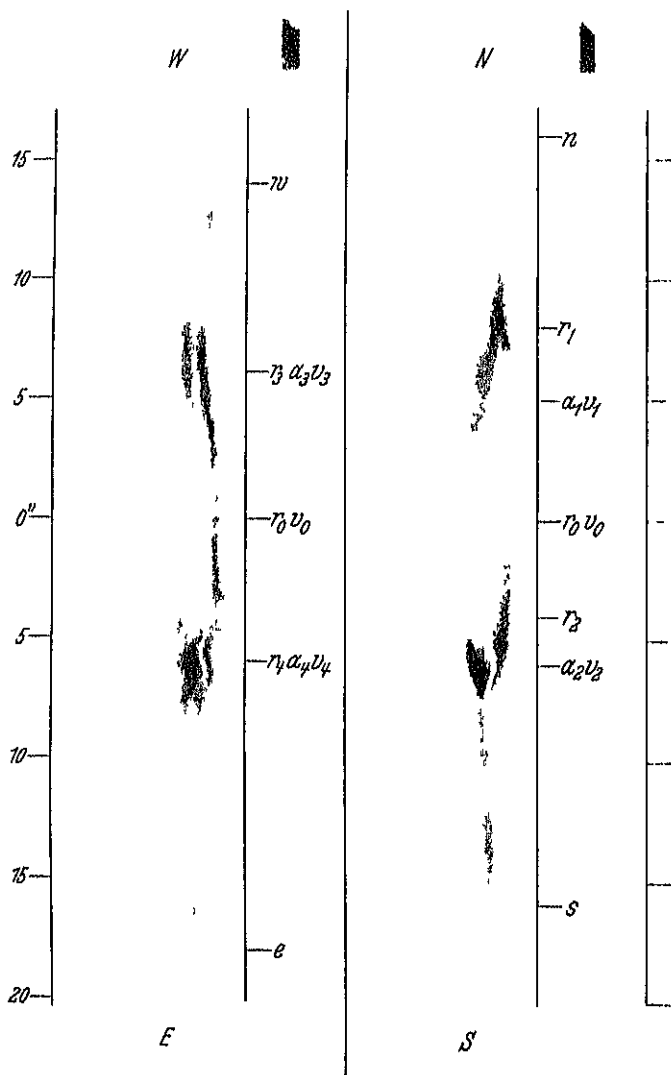


Fig. 20. Drawings of the N_1 line in NGC 2592 a minor axis, b major axis (MOORE)

BLIT and MOORE in Lick Publ. 13, and particularly in the sketches made by MOORE, three of which are reproduced here as Figures 19, 20, and 21.

While this phenomenon has some resemblance to the turbulence effects observed in the Orion Nebula, it is difficult to connect it with the distribution effects described in the preceding Section, and motions of the different elements or states of the same element seem to be involved. It is exhibited in the slit

spectrograms of a considerable proportion of the brighter planetaries, which show an astonishing complexity in the doubling, bowing, or distortion of the lines of the brighter radiations. There are, in addition, frequent minor differences between the appearances along the major and minor axes of the planetary disks.

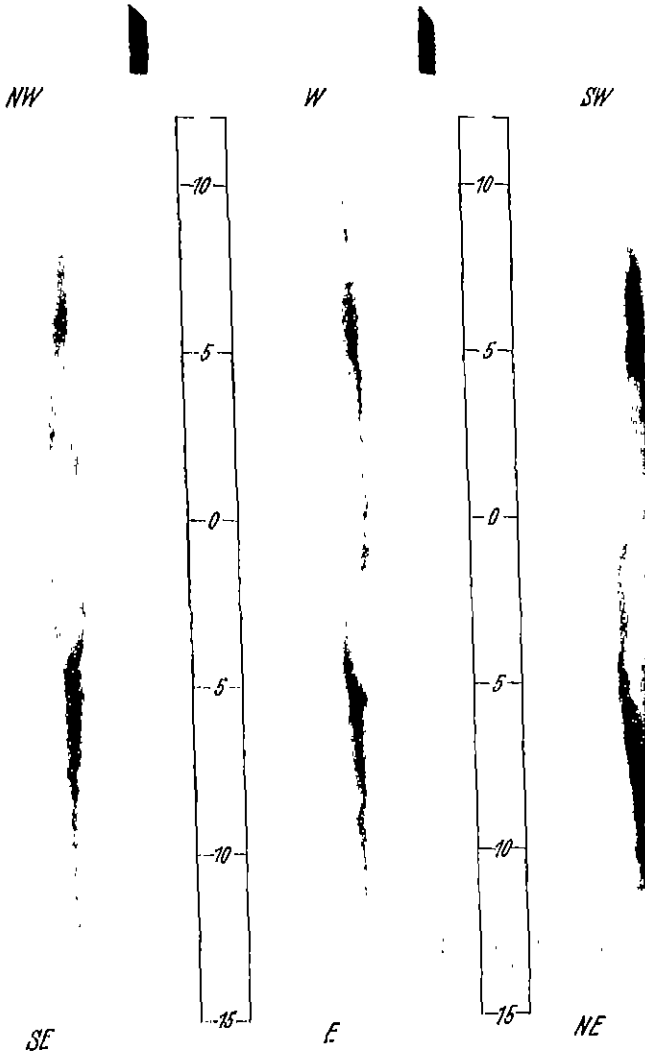


Fig. 21. Drawings of the N_1 line in NGC 7662. *a* minor axis; *b* diagonal axis; *c* major axis. (MOORE.)

The radial velocities measured at different parts of the doubled lines in 2392 vary from ± 36 to ± 130 km./sec. The local irregularities in these spectral images are so masked by the process of photographic enlargement that they are best studied in Moore's drawings. Evidence for these turbulence effects is assembled in Table 40.

Polarization tests gave no support to the ZEFMAN or STARK effects as possible causes of these irregularities and doublings, and relative radial motions seem an admissible explanation

CURTIS (Lick Publ 13, p 66ff), from his studies of planetary forms through direct photography, attempted to set up reasonable mechanical models for the production of these curious spectriographic phenomena. He found that most of the peculiarities in these bowed and doubled lines could be produced by the

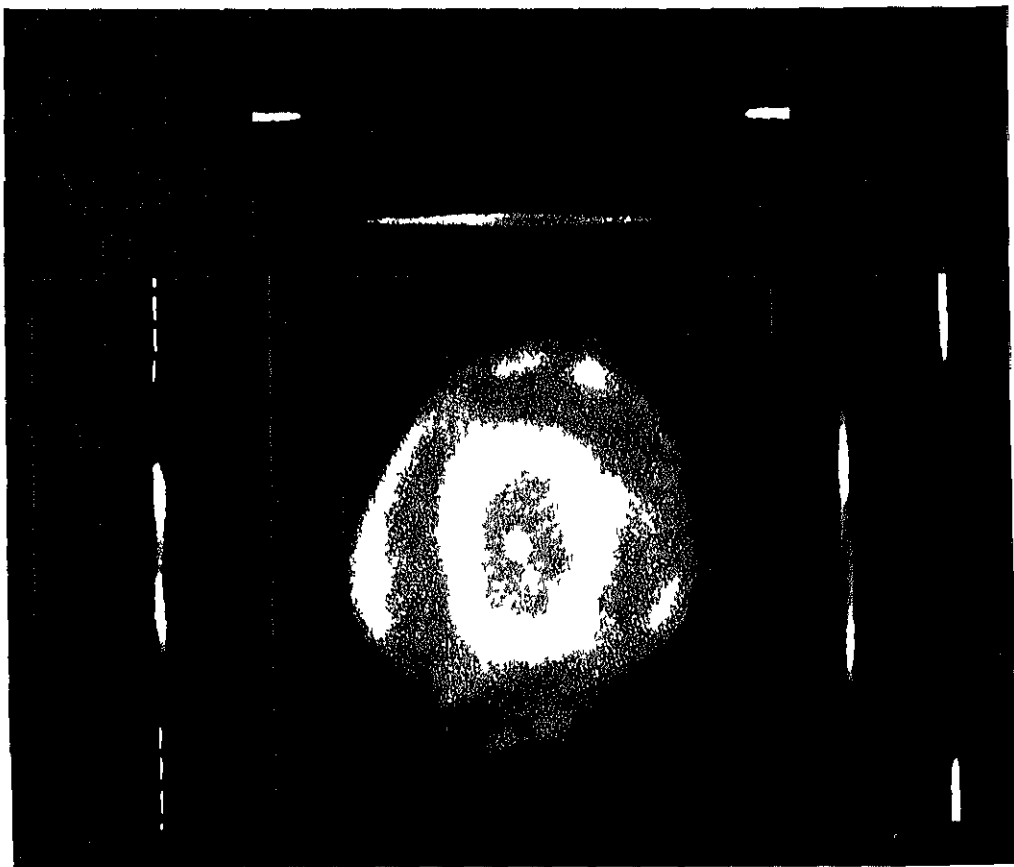


Fig 22 The Planetary Nebula NGC 7662, and Turbulence Effects (Lick Photographs) The central figure is a drawing of the planetary by CURTIS. The spectra on each side and above are by WRIGHI and MOORR. — At the left is the image of 5007 Å (N_2) with the slit along the major axis of the planetary, while the upper figure is the configuration of the same line with the slit along the minor axis. — The line at the right is that due to 4686 Å, with the slit along the major axis. It will be noted that there are striking differences in the images of 5007 Å and 4686 Å with a complete reversal of pattern. — In their bearing on theories of planetary structure and ionization state distribution, these remarkable photographs are doubtless the most significant which have been secured to date

assumption of a planetary as a homogeneous, somewhat truncated spheroidal shell of gaseous matter, a form which seems to have numerous analogues in the photographic data. Matter falling in from the polar zones of such a shell, toward the nucleus, would, at various increasing inclinations of the equatorial plane of the rotating structure to our line of sight, produce through pure radial velocity

effects, first, shallow S-shaped lines, next bifid lines, and finally, at 90° , lines which would be symmetrically doubled across the central portion of the planetary, while remaining single at the ends.

This mechanical explanation, with the assumption of some degree of turbulence and irregularity in individual portions or features, would produce essentially all the line forms and anomalies exhibited (see Lick Publ 13, Plate XXVI, fig 84). Yet it is probable that the matter is far from being so simple as this. The varying sizes of the planetary shells produced by different elements, or even by different ionizations of the same element, together with the difference in the contours of 4686 Å and 5007 Å found by WRIGHT and MOORE, indicate that the planetary is a structure whose complexity may not be a problem of the grosser laws of matter, or of the devising of mechanical models, but rather a complexity whose source lies in temperature conditions and the quantum theory. In conclusion, it would seem that no satisfactory theory of the curious phenomena of these distorted and doubled planetary spectral lines exists as yet, a vast amount of further work is indicated on these objects with instruments of greater power, and the field will inevitably prove to be a very rich one.

30. Mechanical Theories of Planetary Structure. It has been noted in the preceding Section that, of all the various mechanical models set up by way of trial, CURTIS found that the assumption of a homogeneous truncated spheroidal shell formed not only a close representation of observed profiles, but satisfied the peculiar turbulence effects as exhibited by the spectrum line distortions.

There are numerous planetaries which, in projection, give the effect of a shell of luminous matter apparently detached from the nucleus, and even with the regions between this shell and the nucleus nearly devoid of matter. CURTIS investigated this condition for available planetaries in Lick Publ 13. If the thickness of such a shell, supposed to be spherical, be expressed by d , with respect to the external radius, the brightness of the projected transparent ring should exceed that at the center of the planetary by the factor $\sqrt{2/d} - 1$, giving the following values for various assumed shell thicknesses:

Thickness of shell	Relative brightness of ring
0.001	44.7
.01	14.1
.1	4.4
.3	2.3
.5	1.7

For 35 planetaries, with a mean brightness of the projected ring equal to 2.5 times that of the central area, the mean thickness of the shell was estimated at 0.26 that of the external radius, and hence in good agreement with this conception of their structure. For ten other planetaries, however, the estimated brightness of the ring was far in excess of the value computed from the estimated thickness of the shell. The mean relative brightness of the ring was 32 times that of the central area, while the mean thickness of the shell was about 0.39, instead of the approximately 0.002 required by theory.

There is no very satisfactory explanation of such exceptional cases. That these exceptions are due to the fact that the objects are true rings, instead of shells, seems to be negatived by the fact that such rings would not be expected to be, in practically every case, arranged in space with the planes of the rings essentially perpendicular to our line of sight. This is not impossible, but almost infinitely improbable.

Also, the existence of peripheral rings of occulting matter in the equatorial planes of the planetaries, tentatively suggested by CAMPBELL and MOORE as an explanation of the frequently fainter matter along and at the ends of the major axis, seems likewise to be negatived by probability considerations. There is practically a complete lack of planetaries showing an asymmetry in brightness on the two sides of the major axis, hence, if such peripheral rings exist, the equatorial planes of the planetaries must, practically without exception, pass through our position in space.

GERASIMOVICH¹ has further considered the shell forms assumed by the planetaries. He has made a more accurate derivation of the relative optical thickness of such a shell and the central areas of a planetary through a somewhat complicated integral expression which takes account both of the direction of the emitted radiant energy and the curvature of the spherical shell. He thus derives the following values:

Optical thickness	Estimated relative thickness of shell		
	0.1	0.2	0.3-0.4
	Ratio of luminosity of ring to that of the center		
2	1.8	1.4	1.1
6	4.1	3.3	2.7
10	7.5	5.6	4.1

Using these values and CURTIS' estimates of the thickness of the rings and the relative intensities, he derives a quantity, Im , for the absorption due to the nebular matter, and finds also the photographic magnitude of the nucleus, were the nebular veil removed. The average value of the photographic magnitude thus found for the nuclei is 7.7, agreeing well with the value 6.7 found by WILSON for 83 O-type stars. GERASIMOVICH regards the mean parallax of 0''.011 as determined by VAN MAANEN for 20 planetary nuclei as about 10 times too large, and with his revised values he finds that the absolute brightness of the nucleus is inversely proportional to the square of the linear diameter of the planetary. He further derives the mass of the shell of a normal planetary as of the order of $2 \odot$, with an average density of 10^{-10} , for the temperature over the sphere of maximal density he gives the abnormally low value of 8° abs.

There have been a number of attempts to explain the mechanism of such suspended and occasionally apparently detached spheroidal shells. JANSZ² has treated the possible adequacy of radiation pressure in supporting such detached shells. MILNE, however³, after an extensive investigation of the theory of a chromospheric atmosphere, comes to the conclusion that any such detached shell of gas, e.g., Ca II atoms, is an impossibility under the action of radiation pressure, or at least until it absorbs more radiation than it emits, and is thus in an unsteady thermal state. "An atmosphere partially supported by radiation pressure is so strongly condensed toward its base that it can hardly be distinguished from the reversing layer itself, either theoretically or observationally."

31 Quantum Theory and Planetary Structure In this and the following Sections there will be reviewed certain new tendencies in the theory of the diffuse and the planetary nebulae, that may be differentiated from those of the past by the factor of atomic constitution or molecular state, for these comparatively

¹ A. N. 225, p. 89 (1925)

² M. N. 83, p. 481 (1923)

³ M. N. 85, p. 111 (1924)

recent developments, which must be regarded as still in the formative period, the name quantum theory seems most applicable, and can lead to no confusion¹

32. The Theories of ZANSTRA, BOWEN, CARROLL and BERMAN ZANSTRA² has employed HUBBLE's observational data for a theory of the luminosity of nebulous matter with involved stars. Compare also RUSSELL's original suggestion of excitation in emission nebulae by radiation from a very hot body³

HUBBLE's results are re-summarized thus

1 The light from a patch of diffuse nebulosity having a continuous spectrum is the equivalent of the starlight intercepted (stars of classes B1 and later)

2 The light from a patch of diffuse nebulosity having an emission spectrum is the equivalent of the starlight intercepted (stellar classes mainly B0 and O05)

3 The light from a patch of nebulosity in a planetary is, on the average, 4 to 5 magnitudes brighter than the equivalent of the starlight intercepted (stars of classes earlier than O05)

Assuming that the emitting star is a black body of temperature T , ZANSTRA first derives from the quantum theory the number, N_{ph} , of "photographic quanta" intercepted per second by the given patch of nebulosity.

$$N_{ph} = \Omega \frac{2\pi R^2 k^2}{c^2 h^3} T^3 \int_{\sigma_1}^{\sigma_2} \frac{x^2}{e^x - 1} dx,$$

$$\sigma_1 = \frac{h\nu_1}{kT}, \quad \sigma_2 = \frac{h\nu_2}{kT},$$

where

Ω = solid angle intercepted

$h = 6.54 \cdot 10^{-27}$

$k = 1.372 \cdot 10^{-16}$

The emitted light from the nebulosity may be due first to the mechanism of ordinary excitation, though this is regarded as too weak to cause the luminosity observed. The more important part is considered due to ionization and successive recombination. An atom in the normal state is capable of absorbing all the energy of a wave-length shorter than the head of the LYMAN series, frequency $= \nu_0 = 32,84 \cdot 10^{14}$. The number of quanta thus absorbed will be

$$N_{at} = \Omega \frac{2\pi R^2 k^2}{c^2 h^3} T^3 \int_{\sigma_0}^{\infty} \frac{x^2}{e^x - 1} dx$$

¹ Although his findings were not at all in accord with modern results based upon more accurate knowledge of wave-lengths, the detailed investigation of the problem of the nebular spectrum by J. W. NICHOLSON should be mentioned here. The more important of his papers are

The pressure of radiation on reflecting spherical particles. M. N. 70, p. 544 (1910)

The spectrum of nebulium. M. N. 72, p. 49 (1911)

The constitution of the Ring Nebula in Lyra. M. N. 72, p. 176 (1912)

On the new nebular line λ 1353. M. N. 72, p. 691 (1912)

Hydrogen and the primary constituents of nebulae. M. N. 74, p. 204 (1914)

The constitution of nebulae. M. N. 74, p. 486 (1914)

On the nebular line λ 3729. M. N. 74, p. 623 (1914)

The atomic weights of the elements in nebulae. M. N. 78, p. 349 (1918)

Atoms with nucleus $2e$ were regarded by NICHOLSON as the origin of 3869 Å, one with nucleus $3e$ produced 3187 Å, while "nebulium" was attributed to an atom with nucleus $4e$. His "protobismuth", postulated for the corona, was held not to occur in nebulae. The atomic weight of nebulium was placed at 1.31

² Ap. J. 65, p. 50 (1927)

³ Obs. 44, p. 72 (1921); Wash. Nat. Ac. Proc. 8, p. 115 (1922).

The free electrons thus "knocked out" of the atom will recombine with the nuclei by falling back to one of the different levels, emitting the continuous spectrum at the head of the LYMAN, BALMER, PASCHEN series, etc. Subsequently the electrons in the higher levels will return to the normal level either directly, under emission of the LYMAN series, or in steps, emitting the other H lines. In this way a number of continuous spectra and line spectra will be produced (see EDDINGTON'S discussion below).

After a discussion of the quanta affecting the photographic plate, ZANSTRA derives the following ratio of the number of photographic quanta emerging from a patch of nebulosity, N'_{ph} , to the number of photographic quanta in the starlight intercepted by the patch, N_{ph} :

$$\frac{N'_{ph}}{N_{ph}} = \frac{N_{ul}}{N_{ph}} = \frac{\int_{\nu_0}^{\infty} \frac{\nu^2}{e^{\nu} - 1} d\nu}{\int_{\nu_1}^{\nu_2} \frac{\nu^2}{e^{\nu} - 1} d\nu}, \quad \lambda = \frac{hc}{h\nu}$$

ν_0	32,84 · 10 ¹¹ ,
ν_1	5,95 · 10 ¹¹ ,
ν_2	9,10 · 10 ¹¹

Evaluating the integrals in this expression, the following actual ratios for different stellar temperatures are derived:

T	Ratio N'_{ph}/N_{ph}	Ratio in magnitudes	I	Ratio N'_{ph}/N_{ph}	Ratio in magnitudes
15000°	0,0075	5,51	10000	2,50	0,99
20000	,006	2,95	50000	5,1	1,55
25000	,271	1,41	100000	48	3,98
30000	72	0,36	150000	101	5,01
35000	1,41	0,37			

In this table, a unit ratio occurs at about 35000°, and the stellar temperatures, for the mechanism suggested, are

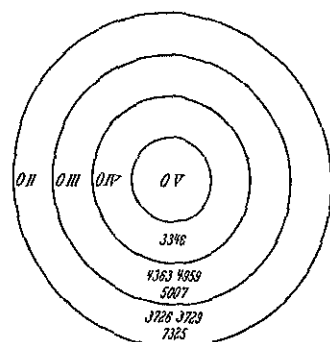


Fig. 23 BOWEN'S Ionization Theory of Planetary Structure (After BOWEN)

Type	T_{ul}
B4	21000
B0	28000
O	31000

ZANSTRA'S later values require a much higher temperature than this, because of similarity in the comparison with observation, however, his latest theory will be discussed along with BICKMAN'S below.

BOWEN¹, following certain of ZANSTRA'S conclusions, has set up an interesting and convincing mechanism for the planetary, based upon the quantum theory and postulating exceedingly high temperatures for the central star. The resulting theory shows considerable resemblance to the observed data.

As a first approximation, he assumes a central star with a surface temperature of 150000° K, surrounded by an atmosphere of oxygen of very low density. At this temperature, from the strong photo-electric absorption of light of greater frequency than the ionization frequency of the atom or ion, oxygen in the sur-

¹ Ap J 67, p. 1 (1928)

mediate neighborhood of the star could not exist in a state of ionization lower than O_V (author's O^{+1+1}). Occasionally an electron will unite with such an O_V ion, emitting the O_{IV} spectrum, to be immediately ejected by the radiation below 160 Å. After traversing a distance represented by the inner circle in Figure 23, the radiation of wave-lengths below 160 Å will have been so completely absorbed that now O_{IV} can exist in the region outside, and by a similar process there will be a region farther out where O_{III} may exist.

This mechanism gives a series of concentric shells whose diameters increase with the decrease of the ionization potentials of the ions present within them. BOWEN's theory thus furnishes a possible explanation of the relative sizes observed for the monochromatic images of the planetaries.

BOWEN regards a temperature of at least 100000° necessary for the hottest planetary nuclei.

EDDINGTON¹ and WOLTJER² have discussed the difficulty of an adequate explanation of the great strength of such "forbidden" lines in comparison with the ordinary lines of the spectrum. EDDINGTON suggests that this difficulty may be removed by a simple addition to BOWEN's original condition, namely, that the stimulating radiation must be so weak that the atom is unlikely to absorb a quantum during the full duration of the metastable state. The strengthening of the forbidden emission is then merely relative to that of the ordinary emission. He gives the following illustration of this effect:

"Let (2) be a metastable state, the forbidden transition being $2 \rightarrow 1$. Let (3) be the state next above (2), from which there is an ordinary transition to (2). The full duration of (2) is taken as 1 sec., and that of (3) 10^{-8} sec.

First let the radiation be moderately strong so that each atom . . . absorbs about once in 10^{-8} sec. Then practically all the atoms arriving by any route from state (3) will forthwith emit, only about 1 in 10^8 being arrested and jerked to some higher state by absorption. A fixed proportion will emit the line $3 \rightarrow 2$ and reach state (2). Of these, only 1 in 1000 will go on to state (1); the others are forestalled by absorption which diverts them to higher states. Accordingly the forbidden emission in $2 \rightarrow 1$ is very much less than ordinary radiation.

Next let the radiation be so weak that each atom absorbs but once in 10 seconds. As before, the atoms arriving in state (3) will forthwith emit, a fixed proportion of them traveling to state (2). But now $9/10$ of these will go on to state (1), because the chance of absorption (once in 10 seconds) is only $1/10$ of the chance of emission (once in 1 second). There will be more quanta emitted in the forbidden line $2 \rightarrow 1$ than in the ordinary line $3 \rightarrow 2$, because (2) is the end-point of other transitions besides $3 \rightarrow 2$, and $9/10$ of all of them are followed by $2 \rightarrow 1$. . .

A forbidden line starting from state (2) becomes more or less equivalent to an ordinary line starting from state (3)."

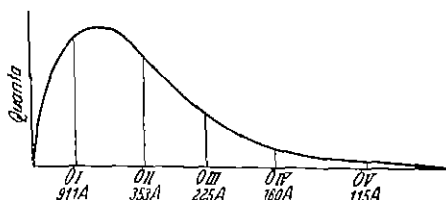


Fig. 24. Ionization Mechanism in Planetary Nebulae. (After BOWEN.) The distribution in frequency of quanta emitted by a black body at a temperature of 150000° K.

λ	Source	Size
3426 Å	N_{IV}	Smallest
3346	O_{IV}	"
4686	He_{II}	Next in size
3313	}	"
3342		
3444		
4859	O_{II}	Large
5007	O_{II}	"
3726	O_{II}	Largest

¹ M N 88, p. 134 (1927).

² B A N 4, p. 107 (1927).

A late and quite complete theory of such spectral excitation is due to CARROLL¹. His work is based largely on certain observational data of H. H. PLASKETT² with the correction of certain of his conclusions attributed to errors in the equations employed³. The existence of the so-called forbidden lines is taken, as by most previous investigators, as an indication that the density must be very low, as otherwise the atoms would be disturbed by collisions. Also, as pointed out by EDDINGTON, the stimulation by radiation is assumed to be very weak.

The processes postulated as affecting an atom of H are:

1. Capture of an electron by an ionized atom; effects small.
2. Excitation from the normal state by electron collision or by absorption of a line of the LYMAN series; effects small.
3. Ionization, photo-electric, or by electron collisions. The predominant cause.
4. The numbers of atoms, electrons, or quanta of any particular specification are assumed to be constant.

The mean density is taken as 10^{-20} , giving a mean free path which lies between $2.25 \cdot 10^{12}$ and $2.25 \cdot 10^{11}$ cm, with an average duration of free path of the order $10^7/T^{1/2}$ seconds. For all probable temperatures this is more than 10^4 seconds, while the life of excited H atoms is 10^{-8} sec., or less. Collisions (and radiation as well) are accordingly regarded as insignificant in removing atoms from excited states.

CARROLL carries out extensive probability investigations as to the relative frequency of excited atoms in the various states and under different modes of excitation, and reaches the following general conclusions:

1. The H atoms are nearly all ionized.
2. The temperature is of the order of 10000° .
3. The BALMER emission lines are generated by electron captures by ionized atoms and their subsequent transitions.
4. The dilution of the radiation is of the order of 10^{12} .
5. The density is of the order 10^{-21} .
6. While LYMAN absorption must occur, indeed not much less nor more frequently than ionization, it has little effect in producing BALMER lines.
7. The mechanism of ionization is presumably photo-electric rather than electron collision or line absorption.

A late and coherent theory of the nebular phenomena in the planetaries, based in large part upon investigations of intensity and isophotal contours of individual monochromatic images obtained with slitless spectrographs, is due to BERMAN and ZANSTRA⁴.

ZANSTRA's results are based upon slitless spectrograms taken with an ultra-violet spectrograph in the primary focus of the Victoria 72-inch reflector, while BERMAN's were obtained with a two-prism quartz spectrograph in the primary focus of the Crossley Reflector at Lick. In both cases the monochromatic images were studied with registering microphotometers. Because of the brightness of

¹ M N 90, p. 588 (1930).

² Harv Circ 335 (1928).

³ PLASKETT's answer, Obs 54, p. 49 (1931).

⁴ D. H. MENZEL, The planetary nebulae. Publ A S P 38, p. 295 (1926); The dilution of radiation in a nebula, *ibid.* 43, p. 70 (1931); Physical processes in gaseous nebulae, *ibid.* 43, p. 334 (1931); L. BERMAN, A spectrophotometric study of certain planetary nebulae. Lick Bull 15, p. 86 (1930); H. ZANSTRA, Untersuchungen über planetarische Nebel. Erster Teil. Die Leuchtprozesse planetarischer Nebel und die Temperatur der Zentralsterne. Z f Astroph 2, p. 1 (1931); Publ Astroph Obs Victoria 4, p. 209 (1930). Earlier references quoted above.

These objects, most of the results were obtained on 6543 and 6572; BERMAN gives data also for 11 4593, 6826, 7009, 7027, and 7662.

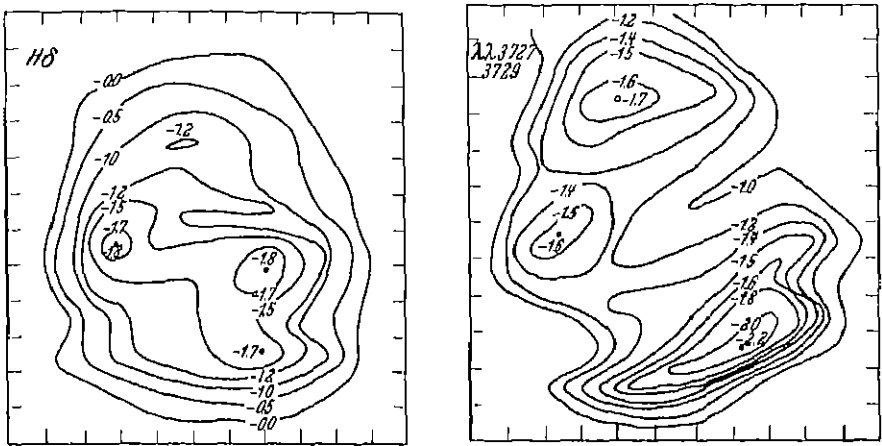


Fig. 25. Contour Diagrams of the H and O_{II} Constituents of NGC 6543. (After BERMAN.) Note that the distribution of the two sorts of material is radically different within the same planetary.

BERMAN's isophotal contours are shown below in Figures 25 and 26, as an illustration of the power of the method. They give in compact form a mass of

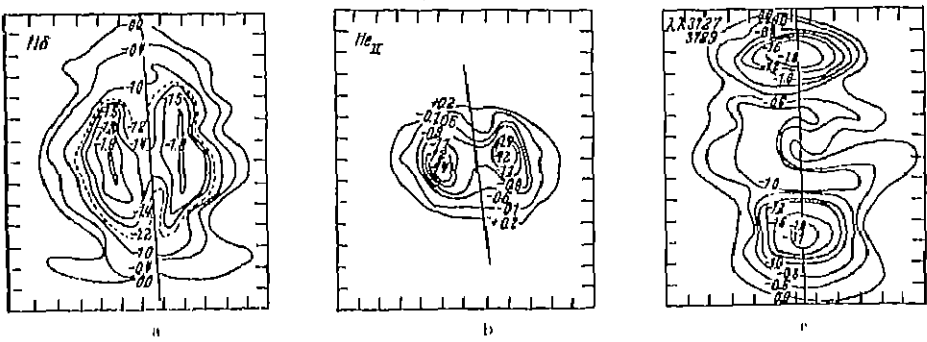


Fig. 26a, b, and c. Contour Diagrams of H, He_{II}, and O_{II} in the Planetary NGC 7009. (BERMAN.) The distribution of the three elements is entirely different; He_{II} is smallest, and O_{II} largest.

data as to the distribution of different elements or ionizations which is vastly more complete than earlier data. BERMAN's total integrated intensities of the different sources (from his Table VII) are given below in Table 44.

Taking the ratio of the intensity of O_{III} to O_{II} as a rough measure of the degree of ionization, BERMAN determines the following percentages of ionized O_{II}:

Object	O _{III} /O _{II}	Fraction of O _{II} ionized	Object	O _{III} /O _{II}	Fraction of O _{II} ionized
6543	1: 0.17	83%	7009	1: 0.02	98
6826	1: 0.13	87	7027	1: 0.02	98
6572	1: 0.08	92			

Table 11. Total Integrated Intensities of Planetary Sources (BERMAN).

Source	λ	6543	6826	6572	7009	7027
O III	5007	-1.54	-1.67	-2.09	-2.52	-2.69
O III	4959	-0.48	-0.71	-1.03	-1.44	-1.64
O III	4363	—	+1.86	+1.84	+2.14	+1.58
O III	3445	—	—	—	—	+1.47
O II	3726, 3729	+0.03	+0.20	+0.27	+1.37	+1.30
H β	4861	0.00	0.00	0.00	0.00	0.00
H γ	4340	+0.44	+0.61	+0.60	+0.57	+1.02
H δ	4102	+0.86	+0.83	+1.16	+1.06	+1.68
H ϵ	3970	(+1.27)	(+1.20)	(+1.48)	(+1.51)	(+2.09)
H ζ	3889	(+1.65)	(+1.50)	(+1.82)	(+1.98)	(+2.40)
H η	3835	+1.95	+1.71	+2.05	+2.42	+2.74
H θ	3798	+2.34	—	+2.49	—	+3.03
H i	3771	—	—	+2.61	—	+3.43
H κ	3750	—	—	+2.79	—	—
He + 3867	—	+0.72	+0.54	+0.61	+0.39	+1.04
H ζ + He I	—	+1.12	+0.96	+1.43	+1.02	+2.38
He II	4686	—	—	—	+2.18	+1.03
He II	4542	—	—	—	—	+3.60
He II	4200	—	—	—	—	+4.3
He I	4471	+2.47	+2.46	+2.61	+2.66	+3.04
He I (-He II?)	4026	+2.36	—	+2.69	—	+3.54
He I	3889	(+2.15)	(+1.97)	(+2.74)	(+1.60)	+4.0
S II	4069, 4076	—	—	—	—	+2.38
N III	4634	—	—	—	—	—
N III	4641	—	—	—	—	—
C III	4649	—	—	—	—	+2.69
?	3967	(+1.72)	(+1.40)	(+1.26)	(+0.87)	(+1.56)
?	3869	+0.07	+0.05	-0.17	-0.56	+0.04
?	4571	—	—	—	—	+4.15
?	3426	—	—	—	—	-0.09
?	3346	—	—	—	—	+0.92

ZANSTRA considers two mechanisms of the luminous process:

1. The mechanism of re-combination.

2. The mechanism of electron impact, regarded as the cause of the "neb-
ulium" lines.

Placing

$$x = \frac{h\nu}{kT},$$

he derives the following formulae for the determination of the temperatures of the central stars:

Mechanism 1,
$$\int_{x_0}^{\infty} \frac{x^2}{e^x - 1} dx = x_0 \int_{x_0}^{\infty} \frac{x^3}{e^x - 1} A_r dx,$$

where A_r is the arbitrary measure of relative intensity derived from the observations. Similarly for

Mechanism 2,
$$\int_{x_0}^{\infty} \frac{x^3}{e^x - 1} dx = x_0 \int_{x_0}^{\infty} \frac{x^4}{e^x - 1} dx = \sum \frac{x^4}{e^x - 1} A_r$$

where the original paper should be referred to for the derivation and for the measures.

A table is then derived for the temperature as a function of the difference in brightness between the nucleus and the nebular matter, and from this the temperature values are derived for 22 planetaries. These are given below in Table 12, with the addition of BERMAN's values, when available. The latter author determined the temperatures separately for H, He_I, and He_{II} on the hypothesis of ionization and electron capture, and according to the theory of impact excitation for the N_1 and N_2 images. Both authors note that the greater the difference in brightness between the nebula and the nucleus the higher should be the temperature. "Failure to observe nuclei in planetary nebulae with the above spectral characteristics may reasonably be attributed to the high temperature rather than to the non-existence of the nuclear stars (BERMAN)." The mean of BERMAN's values have in general been taken.

It will be noted from this table that there is a considerable measure of agreement in the values derived, and that the authors both attribute exceedingly high temperatures to planetary nuclei. Closely similar results as to a high average nuclear temperature have been obtained through a number of methods of analytical attack by VORONTSOV-VELYAMINOV¹.

Table 12. Approximate Temperatures of Planetary Nuclei, derived by ZANSTRA from Luminosity Differences, Nucleus-Nebulosity, with the Addition of BERMAN's Values.

Object	m_{neb}	m_{nuc}	d	Temperatures	
				ZANSTRA	BERMAN
650	16.6	9.9	6.7	85 000 ^b	
1535	11.6	8.8	2.8	38 000	
1952	15.9	8.4	7.5	100 000	
2438	16.6	9.8	6.8	85 000	
2392	10.0	8.1	1.6	31 000	
3242	11.7	7.1	4.6	55 000	
3587	11.3	9.1	4.9	55 000	
4361	12.8	10.1	2.7	37 000	
II 4593			—	—	25 000 ^b
6210	11.7	8.5	3.2	40 000	
6445	19	10.1	8.6	140 000	
6309	14.5	10.7	3.8	45 000	
6513	11.3	8.1	3.2	40 000	33 000
6572	10.5	8.4	2.1	34 000	43 000
6720	11.7	8.8	5.9	70 000	
6801	13.1	11.8	1.6	31 000	
6818	11.9	8.8	6.1	70 000	
6826	10.8	8.1	2.4	35 000	27 000
6853	13.6	7.3	6.3	75 000	
6905	14.5	10.7	3.8	45 000	
7008	12.8	12.2	0.6	28 000	
7009	11.7	7.2	4.5	50 000	40 000
7027			—	—	50 000+
7662	12.7	8.4	4.3	50 000	

33. Evolutionary Status of the Planetary Nebulae. There seems little doubt that the class of the planetary nebulae must be regarded as an exceptional, and doubtless very rare, branch of cosmical evolutionary development. We must consider them as presumably of catastrophic origin; *lusus naturae* impossible to fit in any orderly fashion within a reasonable gamut of stellar evolution.

¹ R A J S, pp. 15, 122 (1931).

The arguments for such an exceptional status are two fold:

1. Their rarity of occurrence. Fewer than 150 are at present known. It is quite probable that the nucleus of a planetary is in all cases a *Wray-Kay* star. These, too, are an exceptional class, and the number known at present, excluding the planetary nuclei and those in the Magellanic Clouds, is 160, or about that of the planetaries. Because of this rarity, the planetaries can not well be placed either at the beginning or the end of the general course of stellar evolution, except by making most improbable assumptions. There have been attempts, also, because of their small numbers, to link up the planetary class with the novae; these attempts can not be said to have been very successful and meet with many difficulties as to spectrum and frequency.

The planetaries are quite certainly fewer than 0.01% of the number of stars which may be assumed to be roughly within the apparent magnitude limit of the planetary nuclei. It thus appears impossible to postulate the planetary stage as one through which all stars pass, for it would then be necessary to assume that existence in the planetary stage can be but a negligible period in the life history of a star, and only a few thousand years in duration.

2. If the attempt is made to place the planetaries at any point in the stellar progression, their relationship with the Class B stars would seem most probable. In fact, any connection whatever with red stars seems entirely out of the question. Here we meet the almost insuperable difficulty caused by the observed fact that the average space velocity of the planetaries is five times that of the average Class B star.

JUDENDORFF, however, has assembled some data which partially remove this difficulty.¹ For known double stars of Classes Oe to B9, he assembles the values of $f = a/(1+a)^3 M \sin^3 i$, where $a = m_2/m_1$, and $M = m_2 + m_1$. So far as is known, $a/(1+a)^3$ is always less than 1, hence a large value of f will indicate a large value of M . CAMPBELL and MOORE had already derived quite large values for the masses of certain planetaries. The radial velocities of the centers of mass of the systems were then freed from the effects of the solar motion and the K-term, giving a quantity γ_0 . The available material was then grouped in the class subdivisions Oe to B5, and B8 and B9, following the values of f as follows:

Value of f	γ_0 larger than the mean value 7.5 km/sec. (Classes Oe to B5, proportion)	Classes B8 and B9, proportion
0.75	7 out of 12, 58%	2 stars 100%
0.10 to 0.75	5 out of 13, 38%	2 out of 5, 33%
0.10	0 out of 12, 0%	0 out of 5, 0%

There is thus indicated a marked increase of velocity with increasing mass, with the conclusion that the systems with largest mass possess velocities which approach those of the planetary nebulae, hence the deduction that large velocities may be expected for bodies with the masses attributed to the planetaries, and that their large velocity, on this assumption, is no bar to a connection between these objects and the O and B stars. There remain the difficulties as to the small frequency of these objects, in which respect they are still exceptional.

Certain of the recent planetary theories of the quantum type postulate nuclei of tremendous temperatures, 50000° to 100000° abs., or more. If these high values are substantiated by future observation and analysis, it will be merely one more proof of their exceptional nature.

¹ Über die Beziehungen der planetarischen Nebel zu den Heliun-Sternen. A. N. 212, p. 3 (1920) and 221, p. 357 (1921).

d) The Spirals.

84 Historical Note on the Spirals. In the cosmogenes of the eighteenth century, most nebulae were regarded as composed of stars, but too distant to be individually resolvable. Certain clusters and stellar aggregations which had appeared nebulous with lower powers had been found to be resolvable when higher powers or larger telescopes were employed. Hence by analogy, reasonable enough in the light of then existing data, all nebulous objects were believed to be similarly resolvable. HUYGENS wrote in 1682¹

"Nam craterae nebulae olim existimatae, atque ipsa Via Lactea, perspicillo inspectae nullas nebulae habere comperuntur, neque aliud esse quam plurium stellarum congeries et frequentia"

GALILEO, CASSINI and MICHELL regarded nebulae as thus resolvable; HALLBY, DEBHAM, LAMBERT, KANT, and LACAILLE maintained the existence of nebulous masses.

Such was also Sir WILLIAM HERSCHEL's earlier belief, namely, that all objects of a nebular texture could be resolved into stars if only sufficient power could be applied. Certain of his earlier papers contain references to other Milky Ways and to distances of the order of 10^{20} km, which have striking resemblances to the conclusions of the island universe theory. These beliefs were abandoned by 1791 through the conviction that there were many objects which were intrinsically nebulous in character, and impossible to resolve into stars. The cosmogonical speculations of KANT, LAMBERT, MICHELL, and others, may be dismissed as philosophical rather than observational deductions.

It is an interesting fact that the spiral nature of these objects seems completely to have escaped the HERSCHELS. It is doubtful whether a single one of their objects contains this word in its description; it certainly is not given as an abbreviation, nor does the concept occur in any of their notes or papers describing the various types of nebulae observed. The spiral nature of these celestial objects was first discovered by the Earl of ROSSE, with his 6-foot reflector. The spiral character of 5194 (M51) was first noted in 1845, and announcement was made in 1849².

VON HUMBOLDT's view at the time of the publication of his *Kosmos* (1845—50) was essentially the same as HERSCHEL's later position. Certain nebulous objects were regarded as truly gaseous, while others of different texture were thought to be composed of stars. For the latter objects VON HUMBOLDT coined the expressive phrase, "Weltinsel"³, which is perhaps the parent of the more modern "island universe".

A completely different phase was brought into the puzzling problem of the nebulae by the first spectroscopic observations. It was at once recognized that nebulae showing bright emission lines (the diffuse and planetary classes) must be truly gaseous. Here, again, an insufficiently evidenced analogy was to impede unduly the final solution of the enigma. Because of the great numerical preponderance of the objects now known as spirals, it was found that the majority of the "nebulae" showed no bright lines, but a continuous spectrum, in which much later the more prominent *FRANKLIN* lines were detected. These were frequently called "white nebulae", a name coined for them by YOUNG. It was tacitly assumed that these objects also must be gaseous, premising some as yet unknown form of spectral excitation, or reflection effects from Milky Way stars.

¹ *Opera Vtrius* (1784), p. 540.

² *Brit. Ass. Report* (1849), p. 53.

³ *Kosmos* 3, p. 187, cf. *passim*.

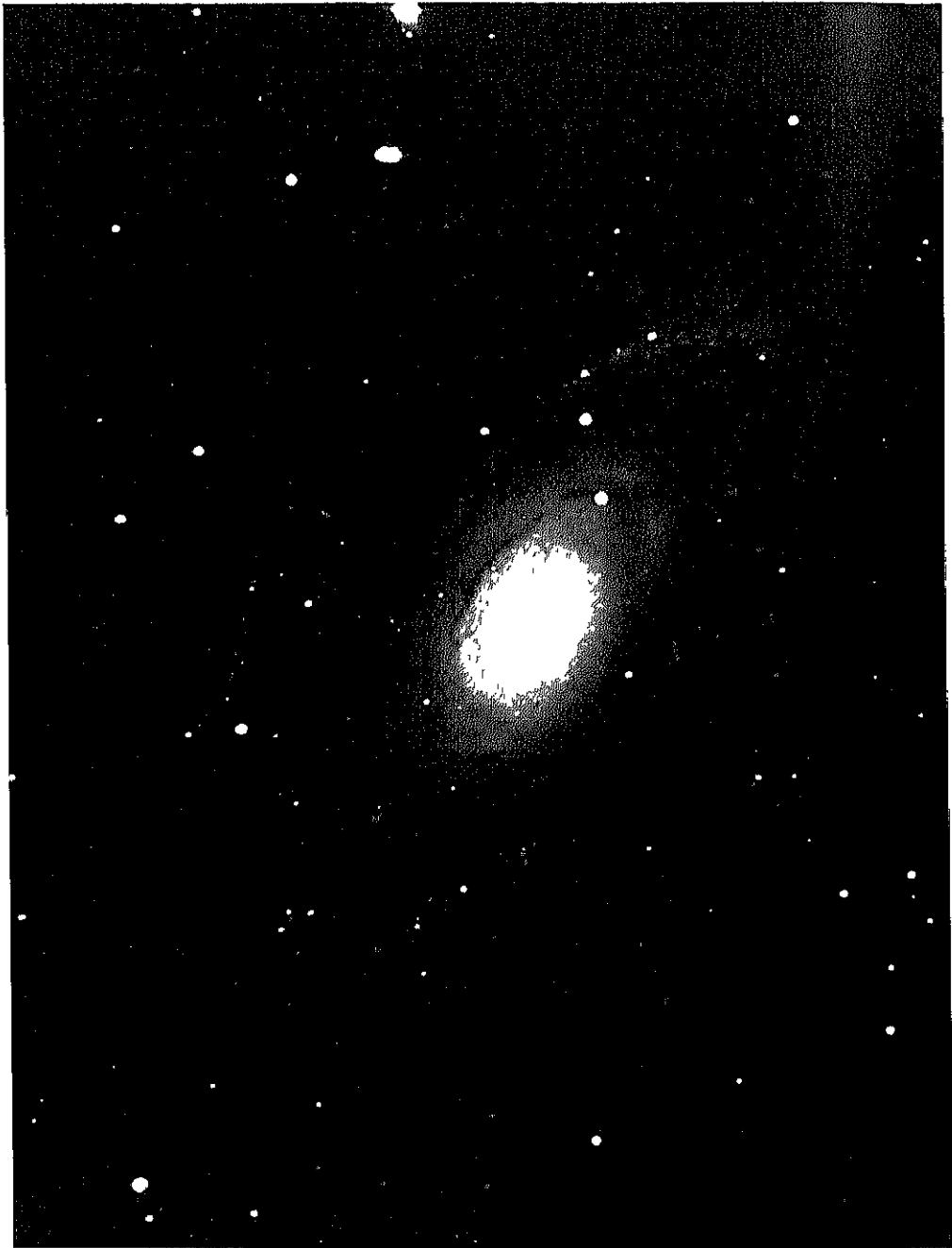


Fig 27 The Spiral NGC 3031 (M81) (Tuck Photograph)

To this latter theory, the fact that the spectra of the white nebulae were later found apparently identical with those of solar type stars gave some measure of support.

It had long been known that the "nebulae" were to be found in greatest numbers in the regions about the galactic poles, but it remained for PROCTOR¹ and WATERS², through their conclusive and convincing charts of distribution, to emphasize beyond question the radical differences between the class of nebulae as a whole and the stars as to predominant galactic arrangement (See Plate I, Figure 28, at the end of this volume, and Figure 29.)

So keen a thinker as HERBERT SPENCER, in fact, regarded this peculiar grouping of the "white nebulae" about the galactic poles as a conclusive proof of alliance with, rather than dissociation from the stars.

"In that zone of celestial space where the stars are excessively abundant, nebulae are rare, while in the two opposite celestial spaces that are farthest removed from this zone nebulae are abundant. Scarcely any nebulae lie near the galactic circle, and the great mass of them lie round the galactic poles. Can this be mere coincidence? When to the fact that the general mass of the nebulae are antithetical in position to the general mass of the stars, we add the fact that the local regions of nebulae are regions where stars are scarce, and the further fact that single nebulae are habitually found in comparatively starless spots, does not the proof of a physical connection become overwhelming?" [II SPENCER, *The Nebular Hypothesis* (1854), p. 112.]

"Have we, on the other hand, any satisfactory reasons for regarding the nebulae as external galaxies? can we indicate any argument which may be looked upon as definitely pointing to such a conclusion? I know not of one." [PROCTOR, *The Universe of Stars* (1878), p. 105.]

"The question whether nebulae are external galaxies hardly any longer needs discussion. It has been answered by the progress of research. No competent thinker, with the whole of the available evidence before him, can now, it is safe to say, maintain any single nebula to be a star system of co-ordinate rank with the Milky Way." [CREECH, *The System of the Stars* (1905), p. 119.]

"Observation and discussion of the radial velocities, internal motions, and distribution of the spiral nebulae, of the real and apparent brightness of novae, of the maximum luminosity of galactic and cluster stars, and finally of the dimensions of our galactic system, all seem definitely to oppose the 'Island Universe' hypothesis of the spiral nebulae." [II SHAPLEY, *Publ A S P* 31, p. 261 (1919).]

Here and there occasional voices were raised in protest, but in view of the prevalence of such ideas, the definite pronouncements of SCHUBINKER and others had little effect.

(Following a description of a spectrogram of $7\frac{1}{2}$ hours exposure time, which showed the spectrum of the Nebula of Andromeda to be essentially similar to that of solar-type stars.)

"Der Andromedanebel gehört zur Klasse der Spiralnebel, die sämtlich ein kontinuierliches Spektrum geben. Nachdem nun die bisherige Vermutung, daß die Spiralnebel Sternhaufen seien, zur Sicherheit erhoben ist, liegt es nahe, dieses System mit unserem Fixsternsysteme zu vergleichen und auf die große Ähnlichkeit des letzteren speziell mit dem Andromedanebel hinzuweisen." [J. SCHUBINKER, *AN* 148, p. 327 (1899).]

The discovery of novae in spirals by RITCHEY and CURTIS in 1917³ followed by a large number of similar discoveries by others (see ciph 52), gave a new impetus to the then almost discarded "island universe" hypothesis. The theory was at once strongly supported by CURTIS⁴, and others, and by assuming essential similarity between galactic and spiral novae, very great distances were derived for the spirals. STARK'S results on the color of the spirals⁵, the influence of

¹ *M N* 29, p. 337 (1869).

² *M N* 33, p. 406 (1873).

³ *Publ A S P* 29, p. 180, 210, 213, 257 (1917), *Lick Bull* 9, p. 108 (1917).

⁴ II D CURTIS, *The Nebulae*, in Adolfo Stahl Lectures (1917), *Modern Theories of the Spiral Nebulae*, lecture before Wash Acad Sci March 1918, 9, p. 218 (1919), II SHAPLEY and II D CURTIS, *The Scale of the Universe*, a debate held before the Nat Acad Sci at Washington, April 26, 1920, published in *Bull Nat Res Council* 2, part 3, No. 11 (1921). SHAPLEY'S earlier views as published in *Publ A S P* 30, p. 53 (1918); 31, p. 261 (1919), and in this debate have since been modified to strong support of the spirals as external galaxies.

⁵ *Pop Astr* 25, p. 34 (1918).

CHAMBERLIN and MOUTON's planetesimal hypothesis, which suggested the origin of the solar system from a relatively small spiral structure, and VAN MANNING's

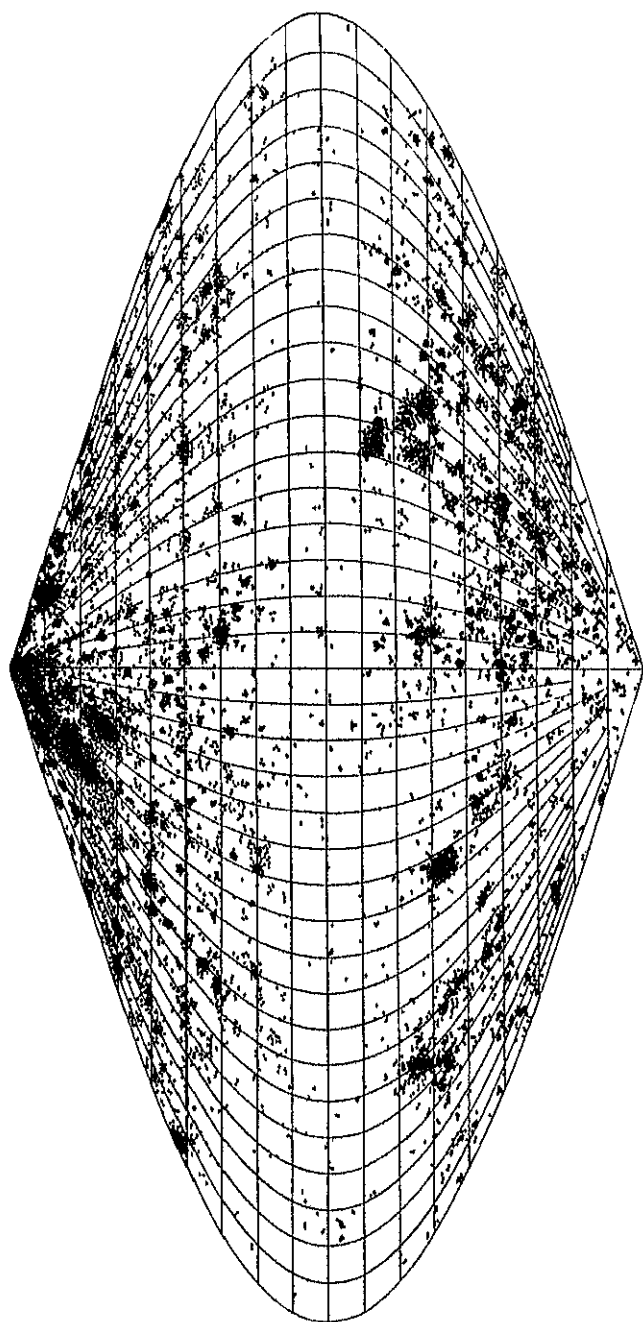


Fig. 29. Galactic Distribution of Spirals (CHARLIER). This chart contains 11,475 NGC objects. Clusters, known annular or planetary nebulae, and stellar nebulae were excluded. While the chart contains the diffuse nebulae, these are comparatively few and occur near the galactic plane. For all practical purposes, this is the most complete chart extant of spiral distribution.

values of the internal motions in the spirals, secured in 1922 and following, for a time made full acceptance of the theory difficult to many. All doubts as to

the island universe character of the spirals were finally swept away by HUBBLE's discovery of Cepheid variables in these objects in 1924

At present it may safely be said that the combination of the lines of evidence

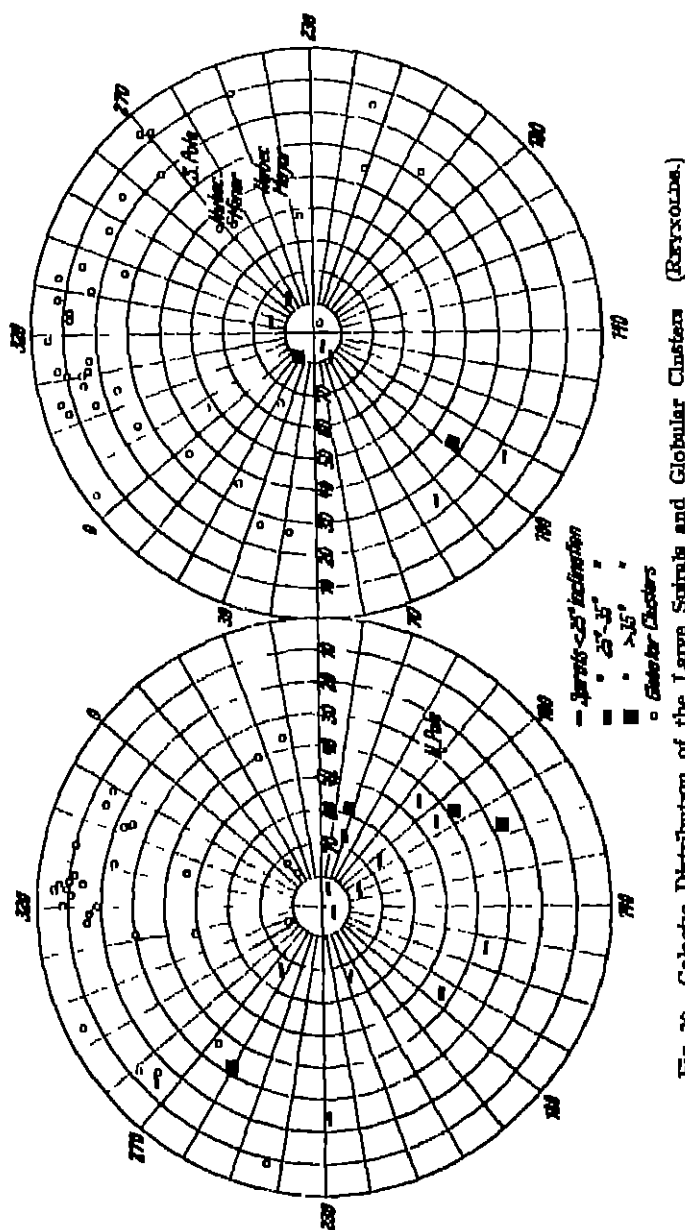


Fig. 30. Galactic Distribution of the Large Spirals and Globular Clusters (Bartelds.)

secured from the peculiar space-distribution of the spirals, their enormous radial velocities, their star-like spectrum, and the occurrence of novae and Cepheid variables within their structures, has nullified all former objections. The theory that the spirals are conglomerations of stars, comparable in many cases with

our own galaxy in size and in number of component units, is now universally accepted¹.

35 Apparent Distribution of the Spirals, Super-Galaxies². The fact that there is a marked concentration of "nebulae" about the galactic poles has long been known, and has been the subject of numerous papers. This tendency, first clearly indicated by PROCTOR and WATERS, is shown as well in all subsequent

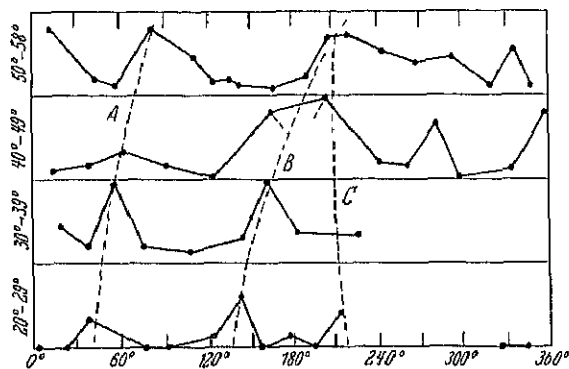


Fig 31 Variation of Nebular Distribution with Galactic Longitude (SLARIS) Distribution of nebulae in the north galactic hemisphere according to galactic longitude (abscissae) Four curves for the latitude intervals are noted in the margin A, B, C, are the more-or-less hypothetical lines of maximum frequency 1 and C correspond to the maximum in longitudes 50° and 220°

studies of the smaller spirals. All agree in showing that the concentration about the north galactic pole is greater than about the southern, and in indicating a marked falling off in numbers as the galactic plane is approached. This diminution is clearly shown in CURTIS' counts of small objects (Lick Publ 13)

Galactic latitudes	Number per square degree
+15° to +90°	34
-15° to -90°	28
+30° to +15°	24
+30° to 30°	7

Such variations in distribution have been more thoroughly studied by SLARIS,

who finds definite differences with galactic longitude. See his Figure reproduced as Figure 31.

That our own galaxy should thus be situated about midway between two tremendous groups of several million galaxies each, and be, by such unique location, still more definitely an "island universe", is, of course, not an impossibility, whatever objections may be urged against this on the score of probability. This uniqueness of location and this exceptional isolation must be accepted, however, unless one prefers to assume a reasonable degree of uniformity of distribution for the 10⁷ or so galaxies accessible to our telescopes, and to postulate, from the analogy of the phenomenon seen in so many spirals (see ciph 42), that a similar tremendous ring of occulting matter in our galactic plane and for the most part outside the Milky Way structure, cuts off from our view the spirals that would otherwise be seen in the zone between +15° and -15° galactic latitude.

A recent development of the highest interest is the substantiation by HUMASON of the arrangement of certain spirals in great groups, or "super-galaxies",

¹ This acceptance is not quite unanimous, cf ciph 58. Also "La manera de formarse de las nebulosas espirales es indudablemente la postulada por Chamberlain y Moulton para explicar el origen del sistema solar, el paso de un cuerpo a poca distancia de otro, con la expulsión de materia en forma de dos corrientes o brazos. Ahora se sabe que las espirales son sistemas mas pequeños y muy probablemente dependientes del sistema galáctico" C. D. PERRINI, Asoc. Cult. de Conf. de Rosario (Argentina) No. 2 (1930).

² R. A. PROCTOR, M.N. 29, p. 337 (1869), S. WATERS, *ibid.* 33, p. 406 (1873), 51, p. 526 (1894), J. H. RYNOIDS, *ibid.* 81, p. 129 (1921), 83, p. 147 (1923), 84, p. 76 (1924), R. F. SANFORD, Lick Bull. 9, p. 80 (1917), F. HERZSPRUNG, A.N. 192, p. 261 (1912), C. EASTON, *ibid.* 166, p. 130 (1904), C. ABBE, M.N. 27, p. 264 (1867), S. I. BAILEY, Sc.N.S. 25, p. 565 (1909), A. R. HINKS, M.N. 71, p. 588 (1911), E. A. FATH, Pop. Ast. 18, p. 544 (1910), F. SLARIS, Ap. J. 62, p. 168 (1915), P. DORG, J.B.A.A. 33, p. 238 (1923).

which possess contiguity of location and have, moreover, recently been found to possess radial velocities of nearly the same size for such of their component members as have been observed. Their special interest lies in the strong resemblance of such a structure of groups or super-galaxies to CHARTIER's theory of an infinite universe. As this characteristic grouping will be discussed in some

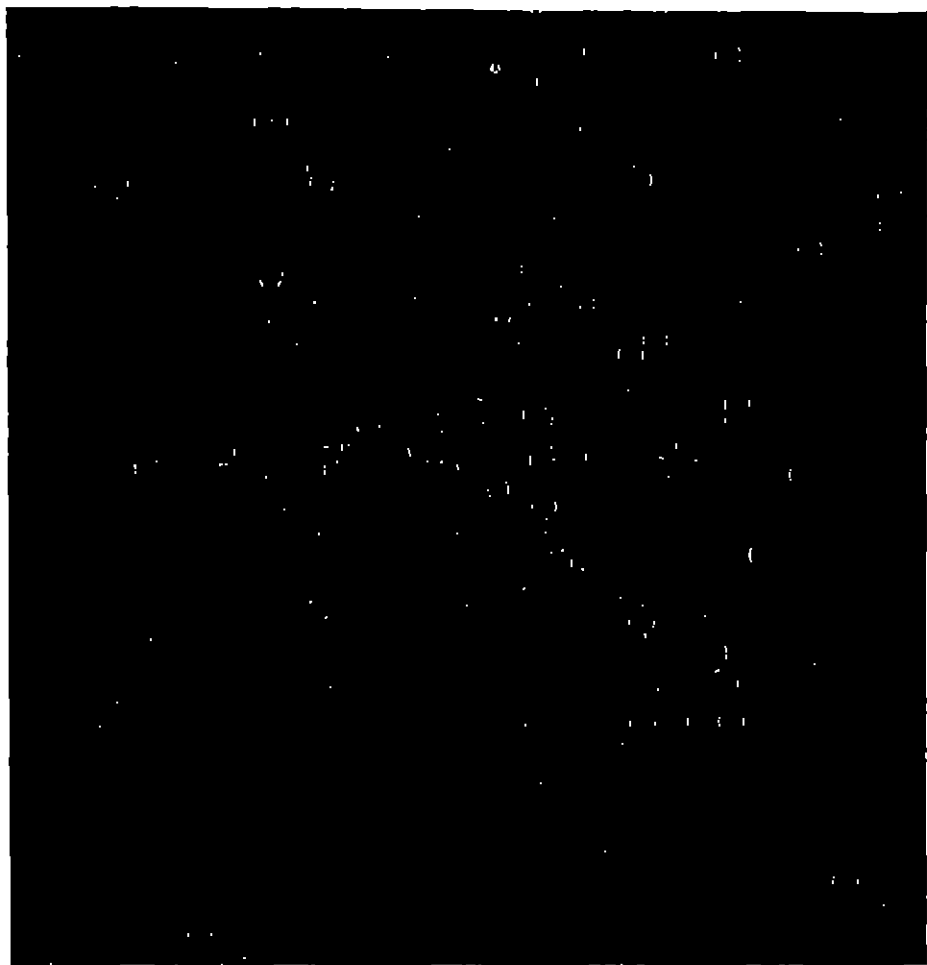


Fig. 32. Cluster of Small Spirals (Dak Photograph). This is a portion of the rich region at $12^{\text{h}} 55^{\text{m}}$, $+28^{\circ} 50'$. It is $38' \times 39'$ in size, and shows 249 small spirals and elliptical objects.

detail in clph 56, 68, and 78, the details of such super-galaxies will be left for the Sections noted.

86. The Number of the Spirals¹. Early in his program of photography with the Crossley Reflector, and when the total number of regions observed was relatively small, KKKERER discovered a very large number of very small and hitherto

¹ J. K. KKKERER, *A N* 151, p. 1 (1899), *BN* 60, p. 128 (1899), *Dak Publ* 8, Introduction (1908), *C D PERRINE*, *Ap J* 20, p. 356 (1904), *Dak Bull* 3, p. 64 (1904), *A J* 29, p. 79 (1915), H. D. CURTIS, *Publ A S P* 30, p. 159 (1913), *Proc Amer Phil Soc* 57, p. 513 (1918), *Dak Publ* 13, p. 12 ff. (1918), R. J. MATH, *A J* 28, p. 73 (1914), R. P. SANFORD, *Dak Bull* 9, p. 80 (1917), F. H. SHAW, *Ap J* 62, p. 168 (1925), R. HUNBLE, *Science*, Suppl. 73, No. 1904 (1934).

unrecorded nebulous objects in all regions well removed from the Milky Way. At that time he estimated the total number accessible in the sky with the Crossley Reflector as 120000. When it is recalled that only about 11000 nebulae had been catalogued up to 1900, the increase of roughly 1000% made by KIECKHEF stands out as a contribution to cosmogony of the highest rank.

The question has since been investigated by PERRINE, CURTIS, FATH, SANFORD, SEARES, and HUBBLE. The various estimates are given below in tabular form.

KELLER	1899	120000	
PERRINE	1904	500000	(eventually a million)
CURTIS	1913	700000	
FATH	1914	162000	
CURTIS	1918	722000	(eventually a million)
SEARES	1925	300000	
HUBBLE	1931	30000000	

There is little value in reviewing here the efforts which have been made to reconcile the smaller estimate of FATH (162000) and the larger ones of PERRINE and CURTIS ($1000000 \pm$), CURTIS' support of these larger values may be found in Lick Publ 13. The great power of the 100-inch telescope has shown clearly that the number of small objects of the spiral class is very great.

As pointed out by W W CAMPBELL, there is less difference than appears at first sight between HUBBLE's value and those secured from the Crossley surveys, when one takes into account the larger volume of space accessible to the larger instruments. HUBBLE's estimate is for the entire number of such objects existing in the spherical volume of space whose radius is the distance of the most remote objects found on the Mt Wilson plates, without regard to those occulted in the Milky Way area. As, other things being equal, the 100-inch reflector should penetrate 2.83 times as far into space as the 36-inch Crossley Reflector, the former should therefore command a volume of space about 22.6 times the volume accessible to the latter. Assuming that the distribution of these objects in space is roughly uniform, and making reasonable additions to the PERRINE-CURTIS totals for those objects which are prevented from recording their images on the negatives by obstructing materials in our Milky Way system, it will be seen that there is a very satisfactory agreement in the two sets of estimates with regard to the density of distribution of the spirals. No one can predict, naturally, whether this observed density of distribution continues indefinitely. See further ciph 77-79.

37. Conspectus of Forms Assumed For the purposes of this treatment, the spirals are considered under the following main headings:

- 1 True spirals, objects which show the spiral arms so characteristic of the class
- 2 Barred spirals, marked by a nearly straight band across the nuclear portion
- 3 Elliptical objects, with no spiral structure discernible by present resolution
- 4 Irregular and Magellanic type spirals

While the field is conveniently divided thus, there is a very wide difference in the forms assumed. The following examples, taken for the most part from the list and descriptions in Lick Publ 13, will give a partial illustration of such variation in details of structure. Edgewise or greatly elongated spirals have in general been omitted, as in such the essential features are masked by the inclination of the object to our line of sight.

There is no very large amount of agreement as to the relative proportions of the different types of spirals. The most important factor in the percentages found seems to lie, as would be expected, in the aperture of the instrument used.

HARDCASTLE's¹ counts of the brighter nebulae on the FRANKLIN-ADAMS star charts, after the exclusion of objects evidently of the diffuse type, give 173 as spiral, 233 of the elliptical type, and 327 objects so small as to resemble star



Fig. 31 The Magellanic Type Spiral NGC 4449 (Mt. Wilson Photograph)

images. SHAPLEY² finds a very small proportion of spirals in the 2829 objects catalogued in Harv Ann 85, p 413 (1924)

Spheroidal	80%
Spindle	12%
Oval	7%
Spiral	less than 1%

However, in his study of the Coma-Virgo cluster of galaxies³ he reports a slight preponderance of the bona-fide spiral type, 30 to 27, and of 167 objects in the Coma A cloud, 48% are classified as spiral and 5% as irregular. SHAPLEY and AMIS⁴ find much smaller proportions on the BRUCE plates (8% spiral and 4% irregular), but admit that "obviously the recording of spiral structure is

¹ M N 74, p 699 (1914). ³ Harv Bull 808 (1924)
² Harv Bull 838 (1926) ⁴ Harv Bull 876 (1930).

largely a matter of telescopic resolution." Doubtless the most trustworthy proportions are those found by HUBBLE in his detailed and valuable monograph, "The Extra-galactic Nebulae", in Ap J 64, p. 321 (1926), as follows:

Elliptical	23%
Normal and barred spirals	71%
Irregular	6%

It is the belief of the writer that the proportion of true spirals may be even larger because of instrumental limitations in recording the smallest objects of the spiral class, see ciph. 40.

38. True Spirals. These are the "normal" spirals of HUBBLE, and the term is self-explanatory, in these the characteristic spiral whorls are more or less clearly seen, nearly always making them start from a nuclear portion at points very closely 180° apart. They vary in size and in the distinctness with which the spiral arms are shown, from minute objects where faint traces of spiral character can just be made out, to enormous structures like 224 (Andromeda) and 598 (M33), where the spiral arms are clearly shown, and where the obtainable scale is such that many portions of the arms can be resolved into stars.

The nuclear portion shows considerable variation in both the true spirals and the barred variety.

	Nuclear portion				
	Examples				
Rather large	{ 151, 221, 221, 2903, 3501				
	{ 4011, 1736, 5218				
Small and bright	{ 29, 200, 628, 772, 3134				
	{ 3341, 3189, 3523, 3686, 3726				
	{ 3938, 1826, 5033, 5055, 5346				
Immuclear?	7752				
Quite faint	253, 3556, 1321				
No nucleus apparent	1337, 2537, 7511				

There is also a wide variation in the character of the whorls.

Delicate and very compact	188, 2775, 5055, 5806
Rather compact	278, 1068, 2811, 1736
Moderately open	221, 4826, 5191, 5
	{ 598, 628, 697, 1637, 1612
	{ 2532, 3147, 3181, 3108, 3031
	{ 3341, 3686, 3726, 3892, 3938
	{ 4321, 5326
Two branched or S-shape	{ 3625, 1051, 4236, 5217, 5191
	{ 6217, 6296, 7610
Single whorl?	7393
With satellite	(near 1612), 5191, 7753

39. Barred Spirals. The designation "barred spiral", introduced by HUBBLE is far preferable to "p-type spirals", used earlier by CURTIS. These interesting objects have as their characteristic feature a straight or nearly straight bar of matter across a nucleus which is generally rather indistinct. Sometimes the whorls will apparently start from the ends of this bar, in other cases, the whorls may form nearly a perfect ring with the bar as a diameter. See Figure 34, where four of these objects are shown.

Among the barred spirals are

Barred spirals	{ 613, 1300, 1326, 1530, 1781
	{ 2859, 3351, 3367, 3501, 3601
Barred, Saturn-shaped	{ 4340, 4391, 1725, 5921, 7179
	936, 1455

HUBBLE (1 c) lists 59 barred spirals, and it would seem that it is a by no means rare type. See ciph. 62—64 for references to its possible significance in theories of spiral structure.

40. Elliptical Spirals; the Provenance of the "Minute" Spirals. The type example of this class is 221, the bright oval companion south of the Great Spiral in Andromeda. HUBBLE lists 93 objects of this type, ranging from E0 (practically round) to E7 (considerably elongated), at which point the transition to the class of true spirals is held to occur. Strictly speaking, this class contains the overwhelming majority of the spiral class, simply because the smallest flecks are necessarily recorded without distinguishable structure.

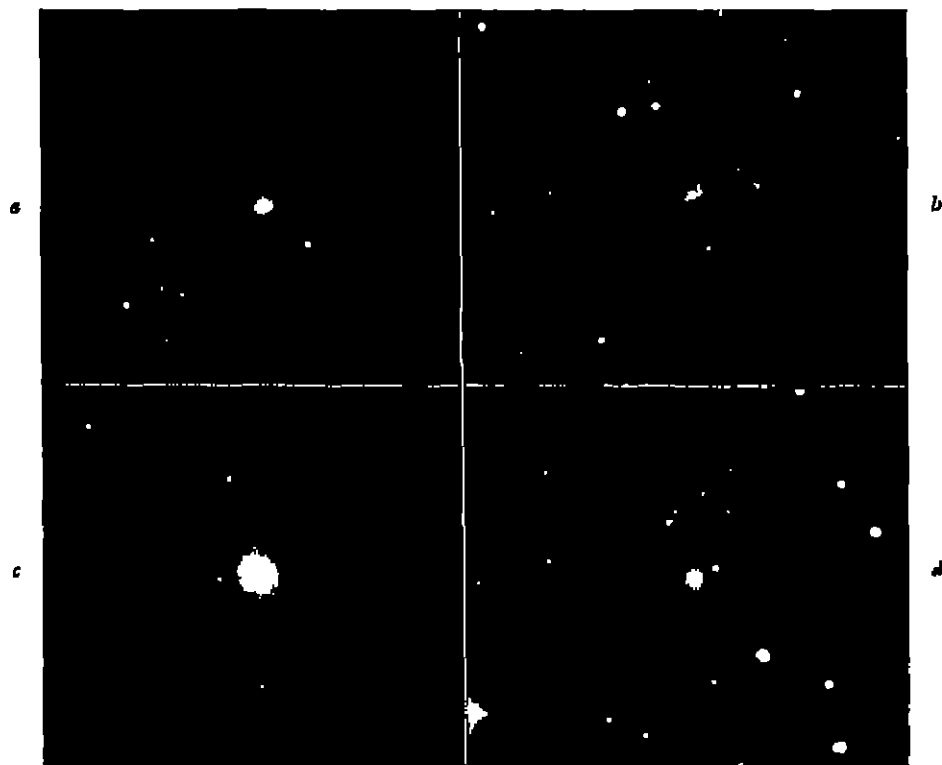


Fig. 34. Four Barred Spirals: a NGC 1300, b NGC 1530, c NGC 3351; d NGC 5921 (Lick Photographs)

Some doubts have been expressed as to the provenance of the countless very small round or elliptical objects, and their right to be classed with the genus of spirals. The writer in 1948 made the following generalization (Lick Publ. 13, p. 12).

"It is my belief that all the many thousands of nebulae not definitely to be classed as diffuse or planetary are true spirals, and that the very minute spiral nebulae appear as textureless disks or ovals solely because of their small size. Were the Great Nebula in Andromeda situated five hundred times as far away as at present, it would appear as a structureless oval about 0'.2 long, with very bright center, and not to be distinguished from the thousands of very small, round or oval nebulae found wherever the spirals are found. There is an unbroken progression from such minute objects up to the Great Nebula in Andromeda itself, I see no reason to believe that these very small nebulae are of a different type from their larger neighbors."

Though this conclusion has been objected to as a "daring extrapolation", the writer feels that all the evidence as to distribution, character, radial velocity,

etc., which has been obtained since 1918, serves only to strengthen this opinion, and were he re-writing it today, his only modifications would be minor changes in the phrasing so as to avoid the word "nebula" as far as possible. The writer finds no escape from the conclusion that all the objects of the spiral class, near or distant, 2" or 5" in diameter, with or without visible whorls, round, spindle-shaped or elongated, are stellar aggregations of structures closely similar, and presumably of the same order of actual size. He places the smallest objects seen on the Crossley plates, 3" to 5" in diameter, at a probable distance of 10^6 ly, at this distance an object 3" in diameter would have a linear diameter of 14500 ly.

There are doubtless a considerable number of objects like 221, whose projected outline is that of a slightly elongated ellipsoid, with any other exterior formations either non-existent or too faint to be recorded. As is well known, the type form of the spiral is a flat, discoidal structure, roughly circular in plan, and with thicknesses $\frac{1}{6}$ to $\frac{1}{10}$ the diameter. When seen edgewise or nearly so, such objects will appear only as narrow spindles, with all evidences of spiral structure obliterated by the high inclination to the line of sight, whereas objects like 221 will present nearly the same cross-section from any point in space. These may be regarded as, in effect, ellipsoidal star clusters of gigantic size.

That the vast majority of the small round and elliptical objects are necessarily of the same type as 221 does not follow, though their precise nature, on any assumption, requires some measure of extrapolation. The detection of spiral structure is very markedly a function of the apparent size of the object, of the aperture of the telescope and its focal length, of plate grain and exposure time. Any of the considerable number of large spirals with somewhat accentuated central condensations or nuclear regions, if removed to several hundred times their present distance, would lose all details of spiral structure through the limits of the photographic process. The relatively very much brighter central portions of such objects as 224 and 598 require no excessive exposure times at their present distances, for many of these objects an exposure of a few minutes is adequate to obtain a legible record of the nuclear condensation, while an exposure of twenty times this length will be needed to show the whorls as strongly. Assuming these objects removed to a distance 100 times as great, our present reflectors will still be able to obtain a record of the nuclear portions in an exposure of one to three hours. But, for the same object at the greater distance, any adequate record of the outlying whorls will now require an exposure of ten to twenty hours, if such were possible without undue sky blackening, even then, because of the minuteness of the structural features, these would be further obliterated by the factors of plate grain and telescopic resolution.

41. Irregular and Magellanic Type Spirals. There are a number of quite irregular objects of the spiral class, where the spiral structure is only faintly indicated, or entirely lacking, in some a looped or falcated structure made up of patches is seen. Among such objects are

1428, 1156, 2359, 2537, 2777
3034, 3077, 4214, 4401, II 2574
4618, 5144, 7309

Even more irregular are objects of the Magellanic type, of which our best examples are the Magellanic Clouds and such objects as 4449 (see Figure 33 and 35). While lacking the characteristic spiral formation, the Magellanic Clouds must be regarded as among our most "valuable" spirals because of their nearness ($0.1 \cdot 10^6$ ly) with the consequent facility of study of individual components.

42. Occulting Matter in the Spirals, and its Bearing on Observed Distribution. No description of the forms assumed by the spirals would be complete

without a reference to the occurrence of non-luminous occulting matter, the evidence of the spirals seen edgewise or nearly so proves that these are relatively



Fig. 35 The Large Magellanic Cloud. (Harvard Photograph.)

flat, round structures, and the occulting matter seems to occur in a peripheral band around the circumference. The characteristic has long been known, and was the source of some of the "bifid" and "double" objects noted by the Har-

SCHLES and ROSSE CURRIS has treated this subject in Lick Publ 13, with illustrations showing the phenomenon in 77 spirals. This occulting matter may be

1 Irregular dark patches, generally in the central portions of the spiral, as in 147, 205, and 2655

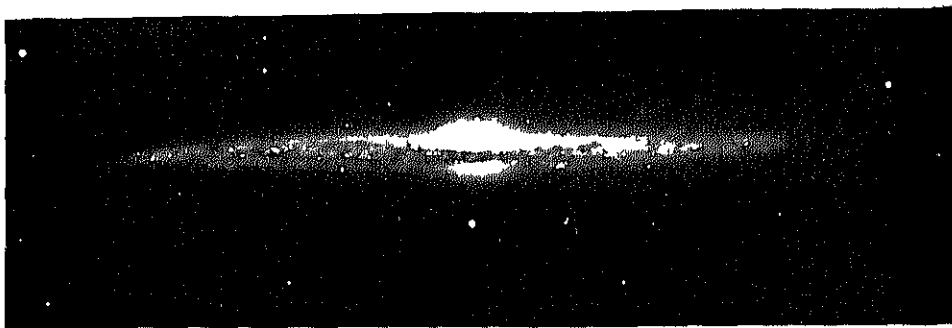


Fig 36 The Edgewise Spiral NGC 4565 (Mt Wilson Photograph)

2 As manifested in spirals whose planes make a moderate angle with the line of sight, where one side is definitely fainter than the other, or seems to extend to a smaller distance on one side of the major axis. Examples, 2683, 2841, 4192, and 5033

3 Dark lanes clearly in evidence on one side of the major axis in spirals of small inclination to the line of sight, as in 3623, 4129, and 3169



Fig 37 The Edgewise Elliptical Spiral NGC 3115 (Mt Wilson Photograph)

4 Spirals seen almost exactly edgewise, and showing indubitable evidence of a peripheral equatorial occulting ring, as in 4565 (finest example of the class), 891, 4591, and 5746

Though not observable in all edgewise spirals, the phenomenon is so frequent a one that it must be regarded as a very common characteristic of the spirals as a class. This evidence, by analogy solely, may then be regarded as lending considerable support to the hypothesis that a similar peripheral band of occulting matter in the plane of our galaxy, and in large part presumably outside its structure, serves to cut off from our view the distant spirals which lie near the projection of our galactic plane in space¹

Indirectly, also, such a theory lends support to the belief that our galaxy is but one of many similar structures, as held by ELLISON and others, and more recently supported by TRUMPLER's investigations of the amount and localization of absorption within our galaxy. Though this theory is supported only by the

¹ Cf also R T SANFORD Lick Bull 9, p 80 (1917)

significant analogy of numerous external galaxies, it offers perhaps the best explanation of the curious fact presented by the peculiar distribution of the spirals, found in greatest numbers near the galactic poles, but almost never seen within the actual Milky Way structure, a phenomenon for which no other adequate explanation exists

43. Proper Motions of the Spirals¹. Regarded as an external galaxy, a relatively close spiral at a distance of 10^{21} ly, and assumed to possess a motion of 10^4 km/sec across our line of sight, would exhibit an annual proper motion of $0''.007$. If we limit the velocity across the line of sight to but 10^3 km/sec, a quantity of the order of the radial velocities of the larger and nearer spirals observed to date, the annual proper motion will be but $0''.0007$. Bearing in mind the very difficult character, from the standpoint of measurement, of even the best spiral nuclei and knots, together with the relatively short time interval yet available (ca. 30 \pm years for photographic comparison and ca. 75 years for visual), and the minuteness of the probable proper motions of these objects, the conclusion seems certain that the definite detection of proper motion in the spirals is far beyond existing methods and obtainable observational data.

A very large amount of honest and painstaking effort has been expended on this problem, beginning with the carefully determined positions of such observers as D'ARREST three-quarters of a century ago, and extending to the photographic

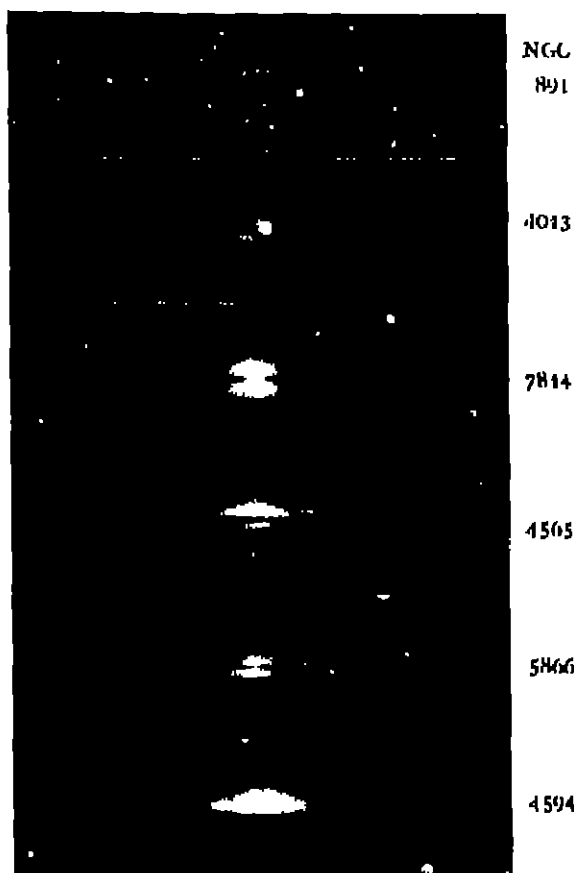


Fig. 48. Occulting Effects in Spirals. (Edg. Photographs.) Photographed by H. D. Curtis with the Cassegrain Reflector

¹ VAN MAANKEN, Mt Wilson Contr No 111 (1916), No 136 (1917), No 158 (1918), No 182 (1920), No 204 (1921), No 237 (1922), No 270 (1923), No 290 (1925), No 321 (1926), No 356 (1928), No 391 (1929), No 405 8 (1930), C. WIRTZ, *Strasbourg Ann* 4, p. 112, 304 (1912), *A N* 203, p. 197, criticized by KOHOLS and SEELIGER, p. 290 and 305 (1917), 206, p. 109, 216 (1918), S. K. KONINKSKY, *Bull Acad St Pétersb* (1916), p. 871, K. RAINMUTU, *Finsk Heltellberg* 7, p. 144 (1915), O. J. LEE, *Pop Astr* 34, p. 492 (1916), J. M. HAWKIN, *Dist Obs Publ* 3, p. 135 (1923); C. O. LAMMEND, *Pop Astr* 22, p. 631 (1914), 24, p. 658 (1916), *Lowell Bull* No 73 (1916), P. K. HANWARD, *A J* 30, p. 175 (1917), K. LUNDMARK, *Pop Astr* 30, p. 623 (1922), *Publ A S J* 14, p. 108 (1922), M. WOLF, *Finsk Heltellberg* 3, p. 109 (1909), 6, p. 31 (1913), *A N* 190, p. 229 (1912), 202, p. 147 (1916)



Fig 39 The Spiral NGC 7217 (Mt. Wilson Photograph) An excellent example of a spiral with compact and delicate whorls

measures and discussions of VAN MAANEN, LAMPLAND, LUNDMARK, and others, in recent years.

With a full appreciation of the sincere and careful investigation which has been devoted to this difficult problem, but with the conviction that any tabulation of the often contradictory results would only mislead and cause confusion, the

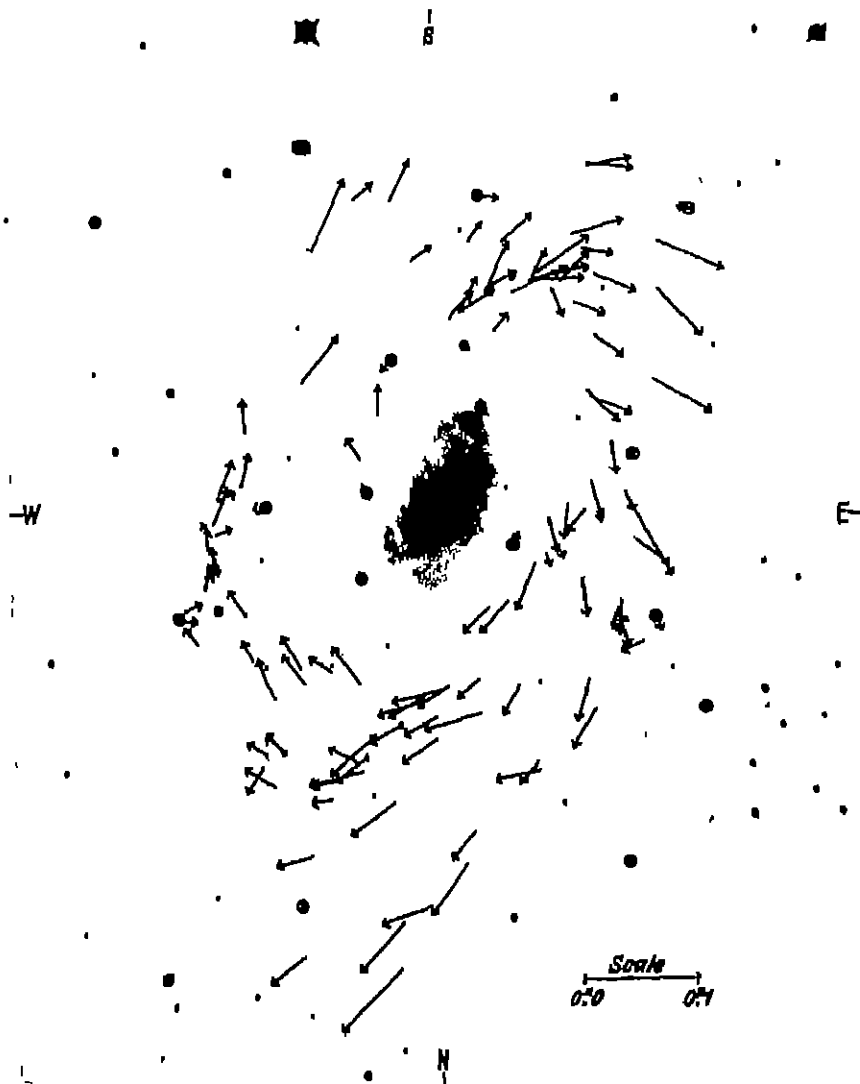


Fig. 40. Internal Motions in NGC 3031 (M81) as determined by VAN MAANEN (VAN MAANEN.) This spiral has been chosen as a typical example of VAN MAANEN's derived motions. It will be noted that the motions are prevaillingly outward along the spiral arms. The arrows indicate the magnitude and direction of the mean annual motions, and their scale (0".1) is indicated on the illustration. The comparison stars are inclosed in circles.

author prefers to omit any discussion of past proper motion results on the spirals, and to refer the reader to the references quoted, VAN MAANEN's values for several

will be found in ciph 45. We have as yet no certain knowledge of the proper motion of any spiral.

44. The Spirals as a System of Reference. There is, however, a possible interesting by-product of the apparent total lack of a motion of translation in the spirals. Their tremendous distances, and their lack of detectable proper motion, give us a large number of essentially "stationary" points of reference, which should eventually prove to be of great importance in studies of the rotation of our own galaxy. The assumption of average fixidity seems amply justified, for small motions peculiarities ought to be at random and to disappear in the mean. If then two sets of measures at a considerable time interval could be made of a large number of small and almost stellar spirals uniformly distributed in galactic longitude, preferably not more than 30° from the galactic plane, and referred to adjacent faint stars (magn $18\pm$), it is conceivable that results of great value might be secured as to the rotation of the galaxy, local irregularities, etc. Were our galaxy rotating in 10^8 years, stars in the peripheral regions would be expected to show tangential annual proper motions with reference to such points d'appui of the order of $0''.01$, which might be detectable with some certainty in 100 years.

45. Internal Motions of the Spirals, Visual Determinations¹. At a distance of 10^6 l. y., annual motions across our line of sight will correspond to actual velocities as follows:

Annual motion	$0''.0001$	$0''.001$	$0''.01$	$0''.05$
Velocity, km/sec	145	1450	14500	72500

These results indicate that, on the island universe hypothesis, internal motions in the spirals must be enormous to be detected by present methods. Such high velocities will also presuppose the existence of inordinate masses.

A vast amount of work has been done by VAN MAANEN in his investigations of spirals for internal motions. VAN MAANEN's more important results are given below in Table 13.

It will be noted from this tabulation that all eight objects agree in showing a stream motion outward along the spiral arms amounting to about $0''.02$ annually in the mean. The average distance of these spirals is $2.6 \cdot 10^6$ l. y., so that this motion would correspond to an actual velocity of 79000 km/sec. In general, VAN MAANEN's values indicate a quasi-rotation in the direction of the concave side of the spiral arms, which seems directly opposite to the spectrographic results of STIPHER (see ciph 46). In his final paper² VAN MAANEN investigates all possible sources of error in the plates or in the methods of measurement which he employed, and concludes that the values he has given represent actual motions of roughly the order found. He has accordingly derived distances for the larger spirals ranging from 10^3 to 10^4 l. y., with diameters ranging

¹ A. VAN MAANEN, See the references under preceding section, K. LUNDMARK, Internal motions of Messier 33. Ap J 63, p. 67 (1926), Mt Wilson Contr. No. 308 (1926), On the internal motions of spirals. Publ. A. S. P. 34, p. 108 (1922), J. H. JEANS, Internal motions in spiral nebulae. M. N. 84, p. 60 (1923), W. H. SMART, The motions of spiral nebulae. Ibid. 84, p. 333 (1924), W. J. A. SCHOUTEN, Probable motions in the spiral nebula Messier 51. Obs. 42, p. 441 (1919), D. PARCHEMIRNKO, Eine von den möglichen Interpretationen der inneren Bewegung in den Spiralnebeln. A. N. 222, p. 369 (1924), B. MEYERMAN, Die innere Bewegung in den Spiralnebeln. Ibid. 221, p. 239 (1924), J. JACKSON, On the influence of comparison stars on photographic proper motions. M. N. 84, p. 404 (1924), J. H. JEANS, On the internal motions in spiral nebulae. Obs. 40, p. 60 (1917) and 44, p. 352 (1921), S. KOSTINSKY, Motions in M 51 stereoscopically determined (Russian). Bull. Acad. St. Pétersb. (1916), p. 871, M. N. 77, p. 233 (1916).

² Mt Wilson Contr. No. 407 (1930).

Table 13 Internal Motion in Spirals, from VAN MAANKEN

Object	Proper motion		Annual internal motions
	α	δ	
598 (M 33)	+ 0",003	- 0",004	399 nebular points measured. Mean stream motion outward along arms, + 0",020, mean transverse, - 0",003. Periods deduced from 60000 to 240000 years. LUNDMARK's measures of same object gave mean stream motion + 0",002, mean transverse - 0",0004.
2403	+ ,002	,000	Mean rotational, 0",015, mean radial outward + 0",014, with considerable differences with distance from center. Periods deduced, 50000 to 120000 years.
3031 (M 81)	+ ,014	- ,005	Stream motion outward along arms of 0",039, combined with slight transverse motion of + 0",007. Deduced period, 58000 years.
4051	- ,003	+ ,015	Radial motion outward 0",014.
4736 (M 94)	- ,014	,000	Stream motion along arms of 0",024, plus transverse motion of 0",009.
5055	+ ,005	,015	Stream motion outward + 0",019, combined with transverse motion of + 0",004. Slight decrease with distance from center.
5195 (M 51)	- ,001	+ ,006	Mean stream outward, + 0",021, mean transverse, + 0",008.
5457 (M 101)	- ,005	- ,012	Rotation of 0",022 at 5' from center. Motions prevalently outward, with slight increase of rotation toward center. Deduced period, 85000 years.

from a few light-years to several hundred. As noted later, both JEANS and BROWN have published theories of spiral structure to fit the magnitude of the motions found by VAN MAANKEN.

LUNDMARK has pointed out that the outward motions found by VAN MAANKEN mean the comparatively rapid disintegration of the spiral, and that, with such motions, no spiral could exist longer than $3 \cdot 10^6$ years as a shining body.

The measures of VAN MAANKEN and the conception of the spirals as individual galaxies can not both be true, unless we are willing to assume velocities in the spiral arms which must occasionally amount to one-third the velocity of light. It seems impossible, moreover, to reconcile these values with the direction of the spectrographic velocity of rotation.

The intervals available for VAN MAANKEN's measures were under twenty years. There seems at present no escape from the conclusion that these carefully made measures are subject to some instrumental error as yet undetected, and that they must be rejected until confirmation is secured by other observers and with materially increased time intervals. In view of the numerous other lines of evidence which now point so unequivocally to the adequacy of the island universe theory of the spirals, no other course is open.

46. Rotation of the Spirals; Spectrographic¹. Spectrographic evidence of the rotation of a spiral was first secured by V. M. SLIPHER in 1914, and evidence

¹ V. M. SLIPHER, The detection of nebular rotation. *Lowell Bull.* 2, p. 65 (1914), Spectrographic observations of nebulae. *Pop. Astr.* 23, p. 21 (1915); Spectrographic observations of nebulae and star clusters. *Ibid.* 25, p. 36 (1917); Spectrographic observations of the rotation of spiral nebulae. *Ibid.* 29, p. 272 (1921), V. G. JEANS, The rotation and radial velocity of the spiral nebula NGC 4594. *Wash. Nat. Ac. Proc.* 2, p. 517 (1916), Mt. Wilson Comm. No. 32 (1916), *Publ. A. S. U.* 28, p. 191 (1916), The rotation and radial velocity of the central part of the Andromeda Nebula. *Wash. Nat. Ac. Proc.* 4, p. 21 (1918), Mt. Wilson Comm. No. 51 (1918).

has since been obtained by SLIPHER and by PEASE for the rotations of a number of objects of the spiral class. Rotations have been definitely established by SLIPHER for six objects, and these effects are suspected in a number of others. Those definitely determined are

- 221, the well-known elliptical companion south of the Great Spiral in Andromeda
- 224, Andromeda (M31)
- 1068, (M77)
- 2683
- 3623, (M65)
- 1591

On the assumption that the side of the spiral which shows the most prominent lanes or other occulting effects is the nearer to us, which seems a certainty, SLIPHER states that all these spirals rotate in the same direction. "The direction is that in which the arbor of a spiral spring turns when the spring is being wound up." SLIPHER found that the rotation in 224 was greater near the nucleus, the inclination of the lines of 4594 indicated a speed of 100 km/sec at 20" from the nucleus (PEASE, 330 km/sec at a distance of 2' from the nucleus).

The two papers by PEASE contain the most detailed as well as the most authoritative information yet available in this exceedingly difficult field (an exposure of 80 hours was necessary on 4594, and 79 hours on Andromeda!). For 4594 he found that the velocities, as determined by a least squares solution, followed the linear relation

$$v = -2.78 v + 1180 \text{ km/sec.}$$

and similarly he found for the Andromeda spiral (224)

$$v = -0.48 v - 316 \text{ km/sec.}$$

That is, in both spirals the angular speed of rotation is essentially the same for different distances from the nucleus. This relation gave a speed of 58 km/sec at a point 2' from the nucleus in 224. In this object also,

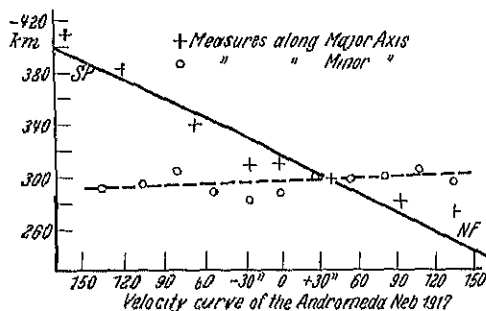


Fig. 41. Rotational Velocity Diagram of NGC 224 (Andromeda) (PEASE)

the dynamical models of every earlier theorist, in which the component elements move in orbits obeying the inverse square law. It would seem that the only theory which can satisfy these spectrographic results is one of the nature of the still uncompleted theory of BROWN (see ciph. 63), in which the particles are assumed to move in central ellipses, under a law of attraction of the form $-k^2/r$.

47. Spectra of the Spirals, Stellar Type. The great majority of objects in the spiral class show a continuous spectrum crossed, where the brightness of

a plot derived from an exposure taken with the slit along the minor axis of the spiral likewise shows a linear relation, but with a much smaller slope than that derived from the spectrogram along the major axis.

These rotational results of PEASE, in their indication of a rotation obeying a linear instead of a quadratic law with varying distances from the nucleus, are of tremendous theoretical interest. They apparently require that we abandon

the object permits the use of a sufficient scale for their detection, by the dark absorption lines characteristic of stellar spectra, and in all essential features a duplicate of the integrated spectrum of the Milky Way or of a star cluster. It is this almost invariable continuous spectrum which earlier earned for them the name "white" nebulae. The descriptions of their spectrum will almost always be of the form solar type, like a Class G star, type G0 or later, etc. Reference should be made here to the investigations of LUNDMARK and LINDBLAD¹ on the effective spectrum of celestial objects. They investigated 24 objects in all, and obtained the following mean values

Number	Class	Wave-length maximum	Equivalent stellar class
6	Planetary	4130 Å	B±
4	Cluster	4190 Å	A8
14	Spiral	4290 Å	G2

See also clph. 49, 50

48. Spectra of the Spirals; Emission Lines There are some relatively rare and for that reason very puzzling exceptions to the almost universal rule that the spectrum of a spiral is such as would be obtained from a large congeries of stars. The total number of such exceptional cases is unknown, but it is probably not large. Among these may be noted.

- 1068 Velocity ± 1100 km/sec. Continuous spectrum with absorption lines, crossed by nebular emission lines. STIMMER, Lowell Bull 3, p 59 (1917) reports that these lines are not images of the slit, but small disks. N_1 and N_2 were found strongly inclined, indicating a velocity of 300 km/sec. at 1' from the nucleus.
- 4051 Nucleus like a planetary nebula, showing bright H, 4686 Å, and O lines (HUMASON)
- 4214 Continuous spectrum crossed by some absorption lines and by nebular emission lines (STIMMER)
- 4449 This is a very irregular object of the Magellanic type, cf. Figure 33. PRAGER [Ap J 46, p 24 (1917), Plate VIII, b)] notes the presence of 230 nebulous stars or patches (with the analogy with the Large Magellanic Cloud). Noted as continuous plus possible emission lines by WOLF in *Sitzber Heidelberg Ak.*, Abt A, Nr 15 (1912). STIMMER describes an strong continuous spectrum crossed by the strong emission lines peculiar to the gaseous nebulae. He records H δ , H γ , 4686 Å, H β , 4959 and 5007 Å, and derives a radial velocity of ± 200 km/sec.

A possible explanation for such exceptions to the almost universal absorption character of the spectrum of the spirals is doubtless to be found in the assumption of a large number of masses of the type of the diffuse or planetary nebulae intermingled in the prevaillingly stellar composition of occasional spirals. 4449 contains 230 nebulous stars or patches, 278 patches of diffuse nebosity (or planetaries) have been catalogued in the Greater Magellanic Cloud, a number of such diffuse patches have been noted in 224 (Andromeda) and other large spirals. Were the Cloud removed to 100 times its present distance, it would appear as an unresolved patch not unlike 4449, and about 2.5 long.

It is probable also that, in such a case, the emission lines are vastly easier to record than the continuous spectrum of the background of stars. With the very long exposures which are necessary to secure even a faint record of the continuous spectrum of an integrated mass of stars in a cluster or spiral, and bearing in mind the advantage of concentration of the emission spectrum of such nebulous inclusions into a few bright lines, it would seem possible that such nebulous patches would easily be spectrographically recorded as emission lines overlying the continuous background.

¹ Photographish effective wave-lengths of nebulae and clusters. Ap J 46, p. 206 (1917), 50, p 176 (1920).

By way of illustration of this point using the ratio of speed between the spectrograph attached to the Lick Refractor and the quartz spectrograph of the Crossley Reflector, as given by FAHJ, = 1.25, FAHJ's instrument should have recorded easily in 30 minutes the bright lines of 6853 (the Dumb-bell Nebula), whose areal brightness is given as 10.8 by WIRIZ. FAHJ secured nothing at all of the continuous spectrum of the spiral 5194 in an exposure of 14.5 hours, although WIRIZ' value for the areal brightness of this spiral is 10.9.

49. Color Indices of the Spirals, the Results of SEARLS¹ Considerable work has been done by SEARLS, SHAPLEY, and others, on the color indices of objects or different parts of objects of the spiral class.

Taking two series of exposures, one on ordinary photographic plates and the other on isochromatic plates through a color screen which transmitted the light to the red of 4900 Å, SEARLS found notable differences in different parts of the spirals 4254, 4736, and 5194. The nuclear portions are strong on the "yellow" plates. On the other hand, the branches and especially the condensations found along the spiral arms are very blue. "the knots of nebulosity are certainly bluer than the bluest of the neighboring stars", and are described as resembling in that respect the central star of the Ring Nebula in Lyra. For elliptical nebulae, however, HUBBLE reports that plates exposed through a visual color filter show no difference between the nuclei and the outer regions².

SHAPLEY, using the HÖRSCHEK-HOPMANN visual magnitudes for comparison with the photographic, has tabulated the color indices of 43 spirals, with the mean results

	Number	Color index
All elliptical objects	12	+0.33
All spirals	28	+0.22
Irregular	3	-0.37

He points out for 7619 (not included in the tabulation) that this spiral, the faintest, fastest, and probably the most remote of those discussed, has the largest color index, $M_{ph} - M_v = 2.8$. HUBBLE and HUMASON, however, (see ciph 55) find a mean color index of +1.1 for the spirals they observed.

CARPENTER finds for 3034 (M82) no difference between the yellow and the blue images, although a photograph on a panchromatic plate shows a substantially different distribution of brightness. For 5194 (M51), however, he corroborates the results obtained by SEARLS. The nucleus appears red, and has a color index of +1.6, there is a continuous increase in blueness in passing outward along the arms from their base, the color index varying from +0.6 near the nucleus to -0.3 at about one revolution from the nucleus. He suggests that such an effect might be due to the fact that younger stars are prevailingly near the nucleus, and older stars further out, most of the light in the latter case coming from the hotter stars of the giant sequence.

¹ F. H. SEARLS, Preliminary results on the color of nebulae. Wash Nat. Ac. Proc. 2, p. 553 (1916), Mt. Wilson Comm. No. 36 (1916), Publ. A. S. P. 28, p. 191 (1916), Distribution of color in certain spiral nebulae. Pop. Ast. 25, p. 34 (1917), The surface brightness of the galactic system as seen from a distant external point, and a comparison with spiral nebulae. Ap. J. 52, p. 162 (1920), Mt. Wilson Cont. No. 191 (1920), H. SHAPLEY, Note on the velocities and magnitudes of external galaxies. Wash Nat. Ac. Proc. 15, p. 565 (1929), E. C. CARPENTER, The distribution of color in two extra-galactic nebulae (abstract). Publ. A. S. P. 43, p. 294 (1931).

² Ap. J. 71, p. 231 (1930).

50. The Radial Velocities of the Spirals¹. The first radial velocity of a spiral (plates taken in 1914), the first spectrographic evidence of rotation of a spiral (1914), and the first spiral velocities of considerable magnitude, are due to V M SRIPIPER. Very noteworthy extensions to our knowledge of the radial velocities of the spirals have been made at Mt. Wilson through the work of HUMASON, PRASKE, and others.

Very rapid progress has been recently made in this difficult field at Mt. Wilson, owing to the use of the new RAYTON lens, which very materially shortens the exposure times needed, 46 spiral velocities secured thus have recently been published.²

This lens, of very short focal length and remarkable focal ratio, is an 8-fold enlargement of a microscope objective, with an extra element added to provide for a source at an infinite distance. Its aperture is 50 mm., and its focal length is 32 mm., giving a focal ratio of 1.059, without doubt the highest ratio ever employed for such purposes. The dispersion at 4500 Å is 418 angstroms per mm. with two prisms, and about 875 angstroms per mm. with one prism, the total length of the spectrum from 3888 Å to 5045 Å is only 2.67 mm. A wide slit can be used, 0.2 to 0.6 mm. While the probable error of a spectrogram taken with this remarkable lens is estimated to be of the order of 100 km./sec., this is of little importance in comparison with the large radial velocities which are being obtained.

Radial velocities are now (January, 1932) available for 90 objects, this total includes the two Magellanic Clouds. The radial velocities of the spirals have the following salient characteristics:

- 1 They are preponderantly velocities of recession (+)
- 2 They display an enormous range, from -300 km./sec. to +19 600 km./sec.
- 3 Remarkable groupings of spirals have been discovered by HUMASON, contiguous in apparent location in the sky, and with large radial velocities nearly identical in amount.

¹ V M SRIPIPER, The radial velocity of the Andromeda nebula. Lowell Bull 2, p. 56 (1914). Spectrographic observations of nebulae. Pop Astr 23, p. 21 (1915). Two nebulae with unparallelled velocities. Lowell Circ. January (1917), A N 243, p. 47 (1917). Spectrographic observations of nebulae and star clusters. Pop Astr 23, p. 36 (1917), 30, p. 9 (1922). Nebulae. Proc Amer Phil Soc No. 5 (1917), R A S Can 42, p. 72 (1917). M. WOLF, Reports in V J S 49, p. 162 (1914), 50, p. 97 (1915). Y G. PRASKE, Radial velocities of nebulae. Publ A S P 27, p. 133 (1915). The radial velocity of M33. Ibid 28, p. 33 (1916). Radial velocities of NGC 3379 and 1700. Ibid 30, p. 235 (1918), Ap J 51, p. 276 (1920). M. L. HUMASON, Radial velocities of two nebulae. Publ A S P 39, p. 317 (1927). The large radial velocity of NGC 7619. Wash Nat Ar Ltr 15, p. 167 (1929). Radial velocity of one nebula in the cluster of faint nebulae in Ursa Major described by BLADIN [A N 233, p. 65 (1928), Ap J 71, p. 356 (1930)]. Radial velocity of two nebulae in the Perseus Cluster. Ibid 71, p. 355 (1930). Apparent velocity-shifts in the spectra of faint nebulae. Ibid 74, p. 35 (1931). R. F. SANFORD, Radial velocity of NGC 2681. Publ A S P 34, p. 222 (1922). The radial velocity of the companion to the Andromeda Nebula. Ibid 38, p. 44 (1926). G. H. TRUMAN, The motions of the spiral nebulae. Pop Astr 24, p. 111 (1916). H. N. ROBERTS, Radiation pressure and celestial motions. Ap J 33, p. 1 (1920). J. H. REYNOLDS, Radial velocities of spiral nebulae. Obs 45, p. 267 (1922). W. W. CAMPBELL and G. Y. PRASKE, The spectrum and radial velocity of the spiral nebula NGC 4151. Publ A S P 30, p. 68 (1918). K. LUNDMARK, Determination of the apices and the mean parallax of the spirals. Obs 47, p. 279 (1924). Studies of anagalactic nebulae. Nov Act R S Utm, volumen extra ordinem editum (1923). Ups Medd No. 30, Relations of the globular clusters and spiral nebulae to the stellar system. K. Sv Vet Akad Handl 60, No. 8 (1919). G. STRANDBERG, Analysis of radial velocities of globular clusters and non-galactic nebulae. Ap J 61, p. 351 (1923). L. COURVOISIER, Bestimmung der absoluten Translational der Ringe aus der säkularen Aberration. A N 241, p. 201 (1931). W. B. RAYTON, Two high-speed camera objectives for astronomical spectrographs. Ap J 72, p. 59 (1930). M. L. HUMASON, The Rayton short-focus spectrographic objective. Ibid 71, p. 331 (1930).

² Ap J 74, p. 35 (1931)

Table 14 Radial Velocities of the Spirals

NGC No	Galactic		Rad. vel km/sec	Author	Spectral class	Affiliation
	<i>l</i>	<i>b</i>				
205	63°,9	-22°,1	- 300	IHum		Local
221	64,4	-23,1	- 185	S		Local
224	64,1	-23,1	- 220	S+	G811	Local
278	66,4	-18,2	+ 650	S		Local
380	70,2	-31,1	+ 1400	IHum	G5	Pisces Cluster
383	70,2	-31,4	+ 4500	IHum	G3	Pisces Cluster
384	70,2	-31,6	+ 4500	IHum	G5	Pisces Cluster
385	70,2	-31,6	+ 4000	IHum	G5	Pisces Cluster
401	70,3	-28,1	- 25	S		Local
584	94,2	-68,9	+ 1800	S		Local?
598	77,0	-32,6	- 70	P		Local
936	110,0	-54,7	+ 1300	S		Local
1023	88,5	-20,2	+ 300	S		Local
1068	115,7	-52,2	+ 920	S+	G511	Local
1270	93,9	-14,3	+ 4800	IHum	G1	Pisces Cluster
1273	93,9	-14,3	+ 5800	IHum	G5	Pisces Cluster
1275	94,0	-14,2	+ 5200	IHum	G+1 P	Pisces Cluster
1277	94,0	-14,2	+ 5200	IHum	G3	Pisces Cluster
1700	147,5	-27,7	+ 800	P		Local
2562	145,2	+28,0	+ 5100	IHum	G4	Cancer Cluster
2563	145,2	+28,0	+ 4800	IHum	G1	Cancer Cluster
2681	110,0	+38,4	+ 700	San		Local
2683	132,9	+38,3	+ 400	S+		Local
2841	109,7	+43,0	+ 600	S		Local
2859	132,6	+44,8	+ 1500	IHum	G3	Local?
2950	98,0	+43,7	+ 1500	IHum	G4	Local?
3031	85,2	+39,8	- 30	S	KLL	Local
3034	84,3	+39,4	+ 290	S	KLL	Local
3115	190,1	+37,7	+ 600	S		Local
3193	154,7	+54,8	+ 1300	IHum	G3	Local?
3227	158,7	+55,4	+ 1150	IHum	G+1 P	Local?
(1)	170,3	+48,5	+19600	IHum	G5	Local Cluster
3368	176,3	+57,6	+ 940	S		Local
3379	175,1	+58,0	+ 810	S+		Local
3489	176,0	+61,2	+ 600	S		Local
3521	197,7	+53,5	+ 730	S		Local
3610	86,4	+53,5	+ 1850	IHum	G2	Isolated
3623	181,4	+64,7	+ 800	S		Local
3627	181,9	+64,7	+ 650	S		Local
4051	104,5	+64,6	+ 650	S		Local
(2)	83,4	+58,1	+11800	IHum	G5	Ursa Maj Cluster
4111	92,1	+71,2	+ 800	S		Local
4151	97,1	+74,1	+ 960	S+		Local
4192	207,0	+75,9	+ 1150	IHum	G2	Local? (Virgo)
4214	102,1	+77,4	+ 300	S		Local
4258	80,8	+67,8	+ 500	S		Local
4374	220,1	+74,6	+ 1050	IHum	G4	Local? (Virgo)
1382	206,2	+80,2	+ 500	S		Local? (Virgo)
4449	79,4	+71,5	+ 200	S		Local
4472	229,4	+71,0	+ 850	S		Local? (Virgo)
4486	225,9	+75,6	+ 800	S		Local? (Virgo)
4526	232,7	+70,9	+ 580	S		Local? (Virgo)
4565	166,0	+86,6	+ 1100	S		Local
4591	241,8	+52,8	+ 1140	S+		Local
4649	238,0	+75,1	+ 1090	S		Local? (Virgo)

(Continued)

NGC No.	Declination		Rad. vel. km./sec.	Author	Spectral class	Allocation
	<i>l</i>	<i>b</i>				
4736	71.1	174.7	+ 290	S	GLL	Local
4826	262.6	+85.4	+ 150	S	GLL	Local
4853	21.1	+88.1	+ 7600	Hum	G1	Coma Ber Cluster
4860	27.7	+87.6	+ 7900	Hum	G3	Coma Ber Cluster
4865	26.0	+87.9	+ 5000	Hum	G3	Coma Ber Cluster
4872	24.1	+87.7	+ 6900	Hum	G3	Coma Ber Cluster
4874	24.4	+87.7	+ 7000	Hum	G4	Coma Ber Cluster
4881	15.6	+86.6	+ 6900	Hum	G3	Coma Ber Cluster
4884	26.6	+88.2	+ 6700	Hum	G3	Coma Ber Cluster
4895	26.4	+86.5	+ 8500	Hum	G4	Coma Ber Cluster
II 4045	26.0	+86.5	+ 6600	Hum	G1	Coma Ber Cluster
5005	46.1	+78.1	+ 900	S		Local
5055	49.9	+73.1	+ 450	S		Local
5194	49.0	+67.5	+ 250	S	GLL	Local
5236	261.1	+42.9	+ 500	S		Local
5457	45.9	+59.1	+ 300	Hum	G+P	Local
5866	36.0	+51.1	+ 650	S		Local
6359	34.9	+33.7	+ 7000	Hum	G3	Isolated
6658	355.4	+14.6	+ 4100	Hum	G3	Isolated
6661	355.6	+14.6	+ 3900	Hum	G5	Isolated
6702	18.5	+18.7	+ 2250	Hum	G4	Isolated
6703	18.6	+18.6	+ 2000	Hum	G3	Isolated
6710	0.2	+11.6	+ 5100	Hum	G3	Isolated
6822	127.8	+18.3	+ 150	Hum	Pd	Local
6824	12.0	+14.6	+ 3200	Hum	G4	Isolated
7217	29.6	+20.6	+ 1050	Hum	G4	Local
7212	34.8	+17.0	+ 5000	Hum	G3	Isolated
7331	36.8	+21.7	+ 500	S		Local
7611	30.1	+48.8	+ 1400	Hum	G2	Pegasus Cluster
7616	30.1	+49.0	+ 3900	Hum	G1	Pegasus Cluster
7619	30.1	+49.2	+ 3800	Hum	G3	Pegasus Cluster
7621	30.1	+49.1	+ 3800	Hum	G2	Pegasus Cluster
7626	30.5	+49.2	+ 3700	Hum	G3	Pegasus Cluster
I. C1.	224	+32	+ 280	Wils		Local
S. C1	244	+41	+ 170	Wils		Local

Notes to Table 14.

- 1 One of the brightest spirals in COMPTON'S Cluster in Leo, $\alpha = 10^h 24^m.0$, $\delta = +10^\circ 50'$ (1930.0).
 2 Brightest object (No. 24) in HAAKE'S Ursa Major Cluster, $\alpha = 11^h 43^m.3$, $\delta = +56^\circ 8'$ (1930.0).

These values are so exceptional in the respects mentioned that there is a tendency in recent literature to refer to them as "apparent" velocities. While it is not at present possible to render any decision as to the reality of these speeds, there is reason for the belief that they represent actual velocities, at least in greater part. For this reason, and for convenience, they will be referred to in the balance of this treatment simply as radial velocities. Because of their size and their prevailing characteristics of recession, they have formed the basis of numerous speculations and have, in particular, been regarded as the subject matter for various types of "relativity universes".

So intimately have they come to be connected with such questions and with one theory of the distances of the spirals, that the pertinent data concerning the radial velocities of the spirals will be segregated, at the risk of some repetition. The values are given at this point, with spectral class where known, galactic

coordinates, and allocation into groups. They will be given again, with derived data as to dimensions and distances, in ciph. 56. See also Appendix 8.

The successive columns in Table 14 are as follows:

Column 1. The NGC number.

Columns 2 and 3. The galactic coordinates. These are taken from EMANUEL's excellent tables, where the origin of galactic longitudes is chosen so as to make the longitude of the solar apex = 0.

Column 4. The radial velocity.

Column 5. The authority for the velocity. This is not always the observer, for example, the plates of 4192, 4374, 4853, 4860, 6702, 6703, 7217, 7242, and 7626 were obtained by PLASE. In this column, Hum = HUMASON, S = SHAPIRO, S+ = SHAPIRO and others, San = SANFORD, Wil = WILSON.

Column 6. The spectral class, when known, when standing alone, the values are as assigned by HUMASON, when followed by LL, they are from LUNDMARK and LINDBLAD.

Column 7. HUMASON's allocation of objects to clusters of spirals. The term "isolated" is used for spirals of high velocity which may belong to similar clusters, not yet substantiated, while "local" is applied to objects which are presumably members of our own local system of galaxies.

51. Distances of the Spirals. Parallaxes. There have been numerous published values of direct parallaxes of the spirals in both the older and the more modern literature of the field. These give distances which are in diametrical contradiction with the values secured by other methods, and their range is wide. A tabulation of these conflicting and now almost universally discarded values could only cause confusion, and the writer prefers to omit all reference to them for this reason.

52. Distances of the Spirals from Novae. Since 1917 a very large number of novae have been discovered in several spirals, among which the Great Spiral in Andromeda (224) leads the list. These are given in Table 15.



Fig. 42. Two Novae in the Spiral NGC 4321. (Lick Photographs.) Left, taken April 19, 1901. Right, taken March 2, 1914.

The wealth of novae in the Andromeda spiral far exceeds the number of galactic novae (fewer than 40). As HUBBLE has well pointed out, aside from the uncertainty in the determination of the zero point, the mean absolute magnitudes are determined for the novae in 224 with much greater precision than for those in our galaxy.



Fig. 43 Novae and Variables in NGC 224 (Andromeda) (HUMAZU.) A Yerkes negative of the Great Spiral in Andromeda on which are marked the novae which have appeared in this spiral (indicated by crosses). A number of variable stars are also shown marked with a γ . From HUMAZU, Ap J 69, Plate II (1929). HUMAZU estimates that 30 novae appear in this spiral per year.

Table 15 Novae in Spirals

No	Number of novae	Mean magn at maximum	Notes
22†	87	17.2	Including S Andromedae, which appeared in 1885 (magn 7.2 at maximum), 87 novae have been discovered in 22† (Andromeda). Nos 2 to 22 were discovered in 1917 to 1922 by RITCHIEY, PIASEL, SHAPLEY, SANFORD, and HUMASON. Nos 23 to 86 were discovered by HUBBLE, of which he has since rejected Nos 26, 36, and 39 as possibly long period variables. Nos 87 to 90 were found by DUNCAN, Publ A S P 40, p 347 (1928). S Andromedae is not included in the maximum given. The magnitudes, coordinates, dates of observation, etc., of these novae are assembled by HUBBLE in, "A Spiral Nebula as a Stellar System, Messier 31" Ap J 69, p 103 (1929), Mt Wilson Contl No 376 (1929).
2103	1	16.5?	RITCHIEY, Publ A S P 29, p 210 (1917)
2608	1	11 ?	WOLF, A N 210, p 373 (1920)
2841	1	16	PIASEL, Publ A S P 29, p 213 (1917)
3031	1	18 ?	RITCHIEY, Publ A S P 29, p 210 (1917)
3147	1	14 ?	Mrs ROBERTS, Publ A S P 29, p 211 (1917)
4303	1	14 ?	REFINMUTH and WOLF, Harv Bull 836 (1926)
4321	2	14	CURTIS, Lick Bull 9, p 108 (1917)
4486	1	11.5	BARANOWSKI, A N 215, p 215 (1922).
4527	1	15	CURTIS, l c
5253	1	7.2	Mrs HUMMING, Harv Bull 1 (1895)
5857-8	2	18.5	RITCHIEY, l c
6946	1	14.6	RITCHIEY, l c
598	4	—	HUBBLE, l c, p 119, footnote
Total	105		

The first attempts to determine the distance of the spirals by analogy with the galactic novae, made by CURTIS¹ in 1917 were roughly of the right order, though rendered somewhat uncertain by the lack of accurate knowledge of the absolute magnitudes of galactic novae, an uncertainty which still persists. Assuming tentatively that the galactic novae were at an average distance of 10000 ly, and with an average apparent magnitude at maximum of 5, he derived a difference of about 13 magnitudes between the galactic and spiral novae, indicating that the spirals were 400 times as far distant as the galactic novae. This gave a distance of the order of $4 \cdot 10^6$ ly for the spirals. "Correlations between the novae in spirals and those in our galaxy indicate distances ranging from perhaps 500000 ly in the case of Andromeda, to 10000000 or more light-years for the more remote spirals."

A slightly greater amount of data on the galactic novae has since become available, and several similar and more accurate correlations have been made. There are few who would maintain, however, that it may not eventually be necessary to multiply or divide the distances of spirals found by the novae method, by a factor of from 2 to 5. Our knowledge of the absolute magnitude of galactic novae at maximum must be regarded as still highly uncertain. LUNDMARK has placed this at -6.1 , while HUBBLE, determining the distance of 224 from Cepheids, places the mean absolute magnitude of galactic novae at -5.7 .

There are, in addition, some other difficulties. The absolute magnitude of S Andromedae, in order to correspond with the values found for the fainter novae in that spiral, must have reached nearly -15 . This is a truly enormous

¹ Wash Nat Ac Proc 9, p 218 (1919), Lick Bull 9, p 108 (1917)

value, though as a parallel instance we have but to assume that TYCHO's nova (which reached an apparent magnitude of about -5) was in reality as distant as 3300 ly. If the smaller spirals 3147, 4321, and 4527 are at a distance of $5 \cdot 10^6$ ly (HUBBLE places 4321 at $4.6 \cdot 10^6$ ly), the absolute magnitude of the four 14th magnitude novae found in these objects must have been close to -12 , the same is true for the nova found in 5253 by Mrs FLEMING. It would seem that we must assume two classes of novae to take care of all these discrepancies,—the one of roughly abs magn -5 at maximum, and a class of comparatively rare exceptions 10000-fold brighter.

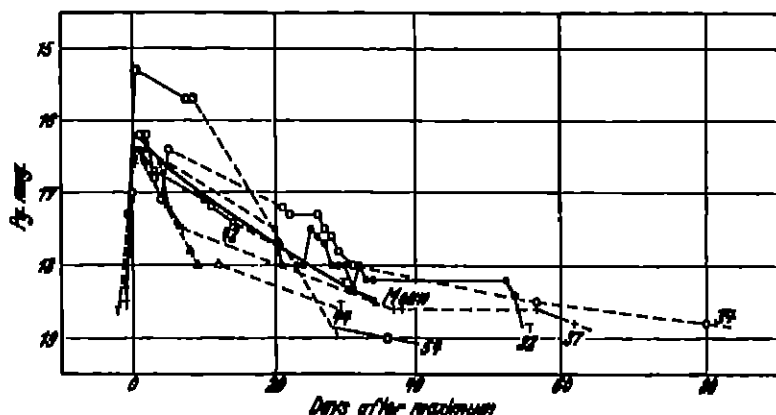


Fig 44 Light-curves of Six Novae in NGC 224 (Andromeda) (HUBBLE) Observed near maximum

There is no doubt that the majority of the objects in 224 attributed to this class are really novae. While for many of the objects the data are fragmentary, HUBBLE assembles the data for six which were observed over a longer interval (see Figure 44), and the composite light-curve of these has all the characteristics expected from novae in rapid rise, slow decline, and minor fluctuations.

58. Distances of the Spirals: from Cepheids. The derivation of the distances of the spirals through the period-luminosity relation adduced for Cepheid variables is due entirely to HUBBLE (1924). He has found 50 variables in 224, of which 40 are Cepheids, and 35 Cepheids in 598. 9 have been discovered in 6822, none have thus far been reported from other spirals. The characteristics of these, together with 105 determined by SHAPLEY in the Small Magellanic Cloud, and 6 from 6822, are shown in HUBBLE's diagrams, reproduced below as Figures 45 and 46.

Using SHAPLEY's values for the Cepheids in the Small Magellanic Cloud, for which he had derived the relation:

$$m - M = 17.55,$$

the corresponding modulus for 598 (M33) was found to be,

$$m - M = 22.1, \text{ or a distance of } 850000 \text{ ly}$$

Similarly for 224 (Andromeda), the modulus is,

$$m - M = 22.2, \text{ or a distance of } 900000 \text{ ly}.$$

HUBBLE definitely calls attention to the fact that all these values are affected by any change of the zero-point of the Cepheid period-luminosity relation, as derived by SHAPLEY.

There have been a number of revisions of SHAPLEY'S values, of which one of the latest and most authoritative is that due to ADAMS, JOY, and HUMASON¹

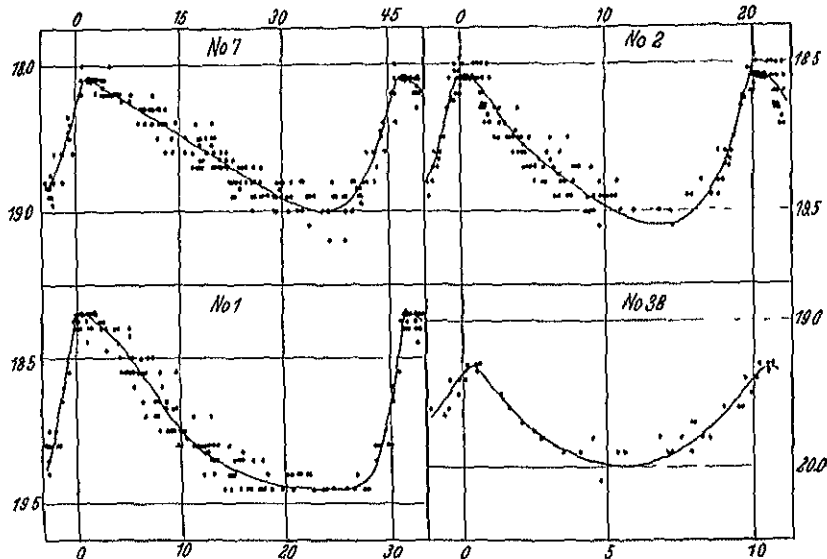


Fig 45 Light-curves of Four Cepheids in 224 (Andromeda) (HUBBLE) The ordinates are photographic magnitudes, and the abscissae, days

These authors have determined the spectroscopic absolute magnitudes of 80 Cepheids with periods between 1.6 and 45.2 days, using an extrapolation from the

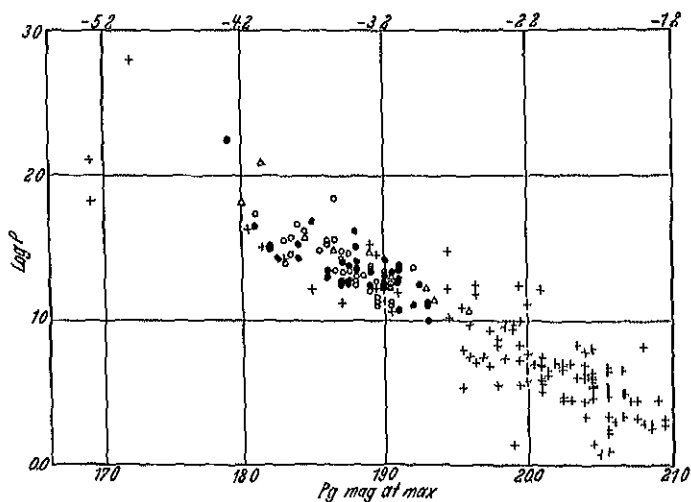


Fig 46 Period-Luminosity Relation for Cepheids in Spirals (HUBBLE) The crosses refer to 105 Cepheids observed by SHAPLEY in the Small Magellanic Cloud, the black disks, to 40 Cepheids in 224 (Andromeda), the open circles, to 35 Cepheids in 598 (M33), the triangles, to 9 Cepheids in 6822. The apparent magnitudes at maxima have been reduced to the distance of 224 by adding 4.65 to those in the Small Magellanic Cl, 0.4 to those in 598, and 0.55 to those in 6822. The absolute photographic magnitudes at the top of the diagram are based upon SHAPLEY'S zero point ($m - M = 17.55$ for the Small Magellanic Cl)

¹ Publ A S P 41, p 252 (1929, abstract)

reduction curves for ordinary giant stars, and with a comparison with trigonometric parallaxes for 16 members of the group. The derived mean of the spectroscopic absolute magnitudes is -1.74 . As compared with SHAPLEY's original value, these results show a displacement of the zero-point of about one magnitude, SHAPLEY's values being the higher. This would serve to bring objects determined by the period-luminosity relation about 37% closer. A KIRK¹ makes a somewhat similar investigation and changes SHAPLEY's zero-point by 1.1 magnitudes; he regards this as the minimum change required, this would mean a diminution of spiral distances of about 40% or more.

A more precise determination of cosmic distances by all these methods must await the accumulation of more accurate data on the maximum brightness of novae, of the brightest stars, and the Cepheid variable stars. While present values of spiral distances show a fairly satisfactory measure of agreement between the results of the different methods employed, it must be remembered that the corresponding values of the galactic data are likewise intimately interdependent.

54. Distances of the Spirals: from a Distance-Velocity Correlation². The radial velocities of the spirals have, as noted above, such magnitude and range, as well as prevailing positive character, that these features have long been noted as differentiating them most sharply from any other class of celestial body. There have been numerous attempts to determine from these velocities the speed and direction of motion of our own galaxy (see references under clph 50 above, and also clph. 77). With the later enormous values of $+3000$ to $+19600$ km/sec, there has come in certain quarters, however, the feeling that these can not be actual speeds, and attempts have been made to explain the observed speeds as due to distance, or as necessary consequences of one or another type of limited, quasi-spherical relativity universes.

The idea that there might be a correlation between the radial velocity and the distance of a spiral seems to have occurred nearly simultaneously to WIRTZ, LUNDMARK, and RUSSELL (in a suggestion made to SILVERSTEIN) in 1924. It has since been much more definitely treated, using a larger number of radial velocities, by HUMBLE, DE SITTER, and OORT.

WIRTZ shows quite clearly from the velocities of the 42 spirals available at that time, that these velocities diminish with increasing diameter, i. e., increase with increasing distance.

WIRTZ, Argument log Diameter

Log diam	Mean V	No.	Log diam	Mean V	No.
0.24	$+827$ km/sec.	9	0.88	$+555$ km/sec.	10
0.43	$+636$	7	1.07	$+334$	5
0.66	$+512$	8	1.71	-20	3

¹ A N 241, p. 249 (1931)

² C. WIRTZ, *De Sitters Kosmologie und die Radialbewegung der Spiralnebel* A N 222, p. 21 (1924), K. LUNDMARK, *The determination of the curvature of space-time in de Sitter's world*, M N 84, p. 747 (1924), R. HUMBLE, *Extra-galactic nebulae*, Ap J 64, p. 321 (1926), *A relation between the distance and radial velocity among extra-galactic nebulae* Wash Nat Ac Proc 15, p. 168 (1929), Mt Wilson Comm No 105 (1929), R. HUMBLE and M. W. HUMASON, *The velocity-distance relation among extra-galactic nebulae*, Ap J 74, p. 43 (1931), A. JONES, *Zur Statistik der nichtgalaktischen Nebel auf Grund der Königsstuhl-Nebellisten* A N 229, p. 157 (1927), H. SHAPLEY, *Note on the velocities and magnitudes of external galaxies* Wash Nat Ac Proc 15, p. 565 (1929), J. H. OORT, *Note on the velocities of extra-galactic nebulae*, BAN 5, p. 239 (1930); *Some problems concerning the distribution of luminosities and peculiar velocities of extragalactic nebulae* Ibid 6, p. 155 (1930), W. DE SITTER, *On the magnitudes, diameters, and distances of the extra-galactic nebulae, and their apparent radial velocities* Ibid. 5, p. 157 (1930), Wash Nat Ac Proc 16, p. 474 (1930), L. SILVERSTEIN, *Nat* 113, p. 602 (1924). See also references in clph 69.

From these values he derived the relation

$$V(\text{km/sec}) = 914 - 479 \log \text{diam}$$

LUNDMARK plotted the radial velocities against the distance, reproduced below as Figure 49. It will be seen from an inspection of this diagram that his scale of abscissae is greatly foreshortened by the scale he employed in lieu of

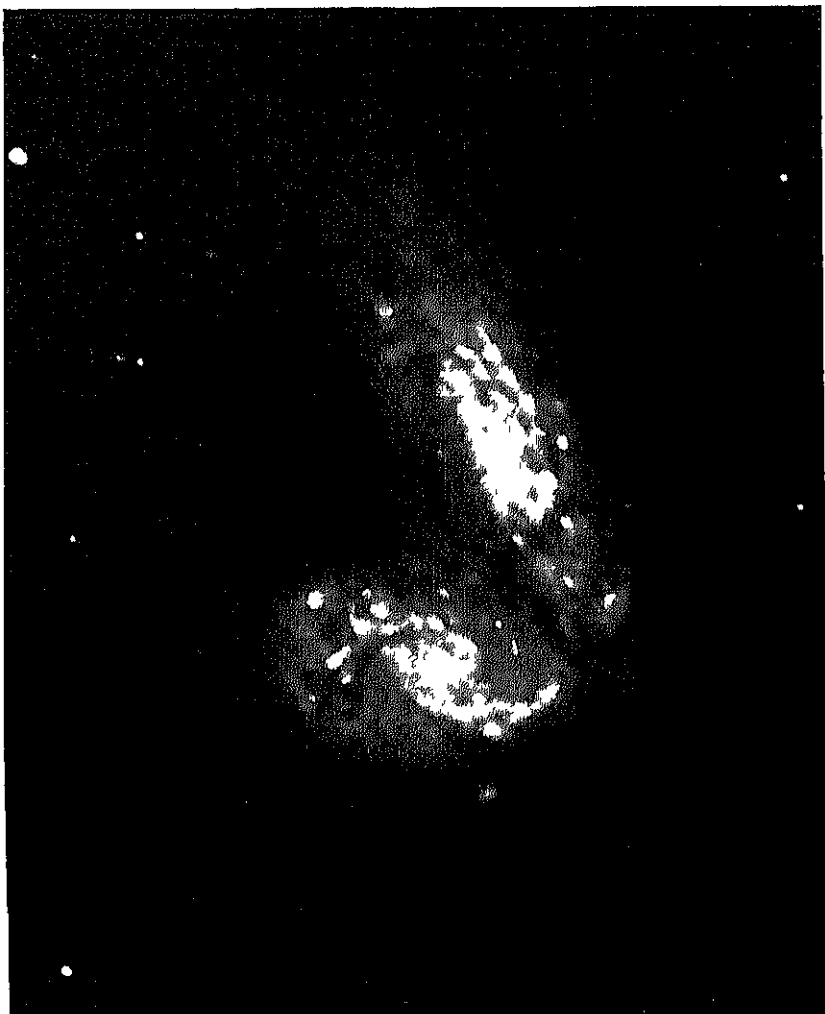


Fig 47 The Spirls NGC 1567-8 (Mt Wilson Photograph)

more accurate distances, i.e., 50, 100, 150, etc., times the assumed distance of the Andromeda spiral, and that the relation indicated might have been more apparent with an expanded horizontal scale. He states "Plotting the radial velocities against the relative distances, we find that there may be a relation between the two quantities, although not a very definite one."

The results of DOSE are based upon a statistical analysis of the Königstuhl nebulae lists, with attempts to secure correlations as to brightness, etc. Taking

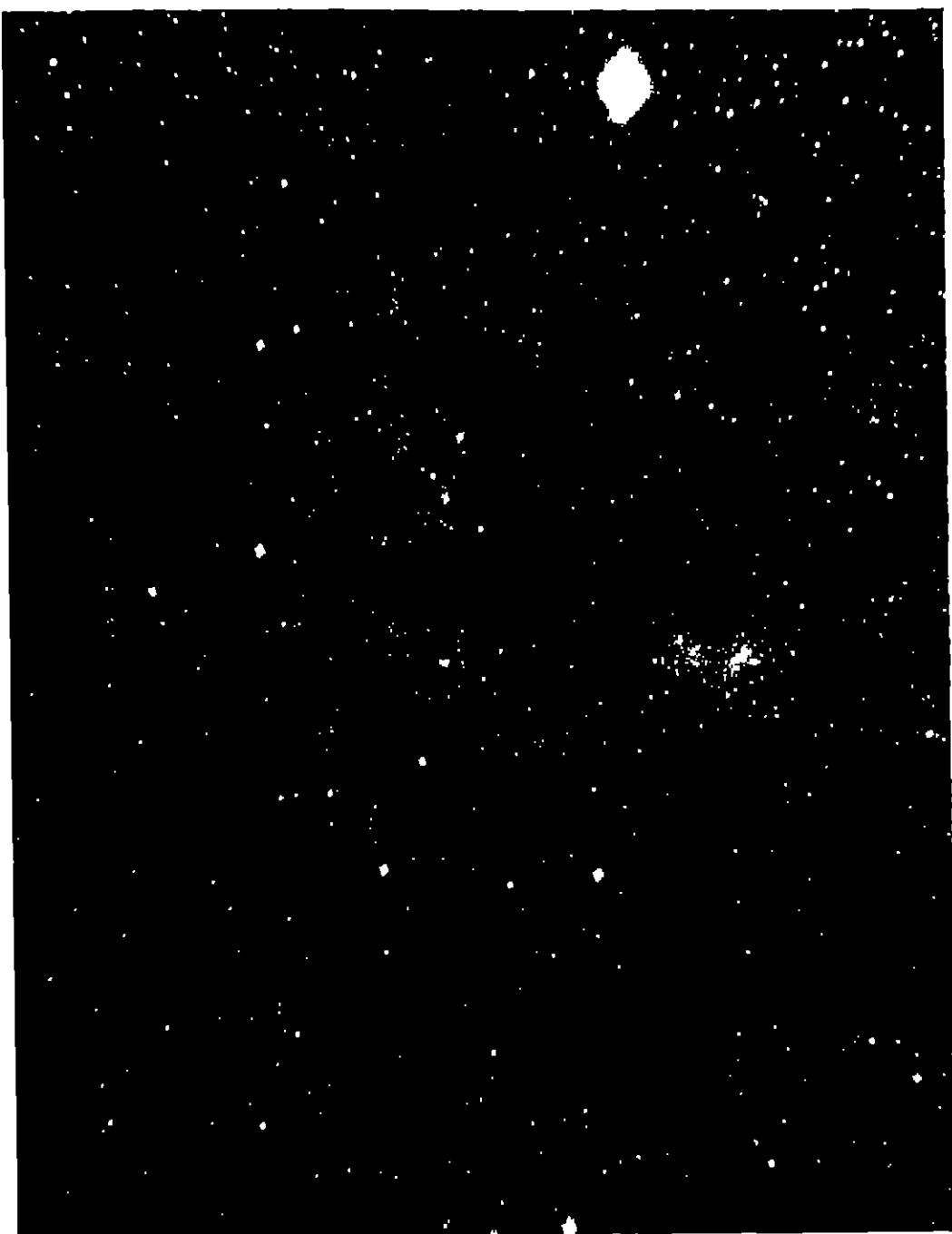


Fig 48 The Spiral NGC 224 (Andromeda) (Mt Wilson Photograph.) South preceding portion.

the radial velocities of the 44 spirals available, he first made a solution for the direction of motion and speed of our galaxy, finding

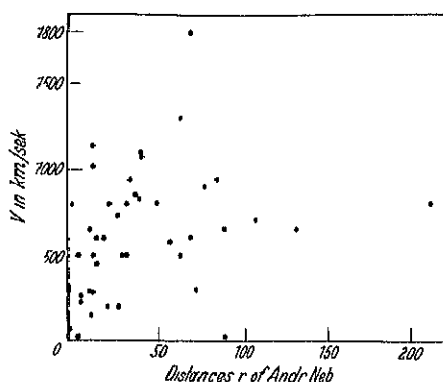


Fig. 49. Radial Velocity Distance Correlation for the Spirals (LUNDMARK). The unit of distance is that assumed for 221.

$$l = 299^{\circ} 8'$$

$$D = -167^{\circ} 32'$$

$$K = 765 \pm 110 \text{ km/sec}$$

He then found, on correcting the individual values for this motion, that there is a slight but definite correlation between distance and radial velocity. No diagram is given, but he divides the spirals employed into three groups as regards size

Group	Diameter	Radial velocity
I	120' to 6'	631 km/sec
II	6' to 3'	719 "
III	3' to 0.7	880 "

That is, the peculiar radial velocity increases inversely as the diameter of the object, or directly as the distance. Both WIRTZ and DOPPEL, as is manifest, assume that the diameters are of the same order of magnitude.

In his earlier paper, HUBBLE took the distances of 22 spirals and the two Magellanic Clouds, estimated by various methods, as the basis, and introduced into the individual equations of condition for galactic motion a K -term varying as the distance, the equations taking the form

$$rK + X \cos \alpha \cos \delta + Y \sin \alpha \cos \delta + Z \sin \delta = V$$

Two solutions were made, the first by using the 24 spirals individually, and the second by combining objects apparently contiguous as to direction and distance into 9 groups. The solutions gave

	24 spirals	9 groups
X	65 ± 50	$+3 \pm 70$
Y	$+226 \pm 95$	$+230 \pm 120$
Z	-195 ± 10	-133 ± 70
K	$+465 \pm 50$	$+513 \pm 60 \text{ km/sec per } 10^6 \text{ parsecs}$
A	286°	269°
D	$+40^{\circ}$	$+33^{\circ}$
V_0	306 km/sec	247 km/sec

As a result of a more detailed analysis, and with the employment of a larger number of velocities, HUBBLE and HUMASON in their latest paper derive a value of $558 \text{ km/sec per } 10^6 \text{ parsecs}$, which corresponds to

$$+170 \text{ km/sec per } 10^6 \text{ ly}$$

The values for this red shift with distance as determined by DE SITTER, and in OORT's earlier paper, do not differ materially from this value. OORT, however, later derives a smaller value, ca. $90 \text{ km/sec per } 10^6 \text{ ly}$.

This interesting relation, should it persist to the most remote spirals, may lead to some curious and rather bizarre consequences. If the faintest and smallest spirals at present observable are at a distance of 10^6 ly , such objects should show a radial velocity of about $+170000 \text{ km/sec}$, corresponding to a shift to

the red of ca. 1500 Å. Unless counterbalanced by radiation coming in from rich ultra-violet regions, one might even expect the most distant spirals to be invisible on account of redness.

Except for the nearer spirals, whose distances have been determined by other methods, it should be mentioned that earlier diagrams were simply plots of one variable charted in two dimensions, and that there was thus no reason why all the plotted points should not fall precisely upon the line of the correlation.

SHAPIRO, for example, criticized certain features of the velocity-distance correlation, and pointed out that the total magnitude may equally well be regarded as a vital factor. Correcting the tabular radial velocities available for a galactic motion toward the apex and using the Harvard photographic magnitudes of the objects, he plotted the resulting radial velocities against the function $10^{0.2m-2.0}$. This corresponds to a plot of velocity against distance expressed in parsecs, provided space is assumed to be transparent, and provided that the absolute magnitude of the typical spiral is placed at -15.

It will be noted from SHAPIRO's diagram reproduced as Figure 54, that the internal agreement of the plotted velocities is fully as good as that for radial velocity alone. Reference may also be made here to LUNDMARK's diagram of the relation between areal brightness and the relative parallax of the spirals¹.

The latest treatment of this relation, the brilliant paper by HUBBLE and HUMASON (l.c.), has removed, at least in part, the effect of such criticisms. They have here made use of parallel correlations through the factors of absolute

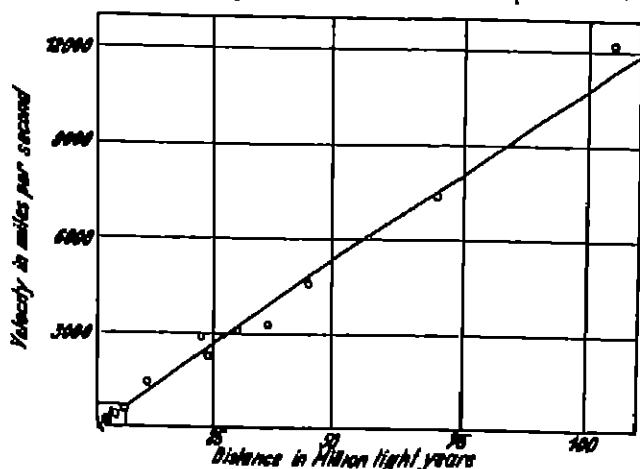


Fig. 50. Radial Velocity-Distance Correlation for the Spirals (HUBBLE and HUMASON). The small black dots in the lower left hand corner represent the only available observations up to 1928. The open circles represent recent observations.

total magnitude may equally well be regarded as a vital factor. Correcting the tabular radial velocities available for a galactic motion toward the apex $A = 277^\circ$, $D = -36^\circ$; $V = 280$ km./sec.,

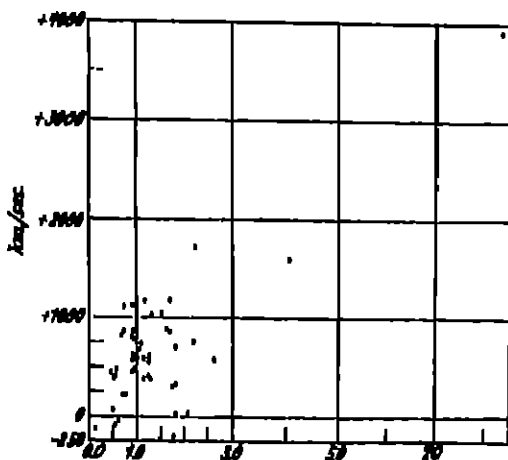


Fig. 51. Radial Velocity-Magnitude Correlation for the Spirals (SHAPIRO). This diagram shows the relation of the reduced radial velocity to the quantity $10^{0.2m-2.0}$.

¹ M N 86, p. 877, Fig. 7 (1925)

magnitude and apparent diameter, relations which may be more fittingly included with the matter of the Section following this one.

55 Distances of the Spirals. Photometric, the "Average" Galaxy¹ Under this heading will be assembled certain photometric data, and deductions as to the distances of the spirals which may be made from them. See also the last portion of ciph. 54, and Figures 50 and 51.

Two main classes of photometric data have been obtained, from which eventually statistical results of great value may be secured. These are:

1. Estimates of the total magnitude of the spiral. Knowing the distance D_1 , of selected typical objects, the mean absolute magnitude of these may be deduced through

$$M = m + 7.6 - 5 \log D_1,$$

or similar relations. Then, on the assumption that the "average" galaxy has a given absolute magnitude, the distances may be determined for other objects for which the total apparent magnitude is known. The method differs from that in which a mean diameter is assumed for the spirals in that the density of distribution within the spiral is a factor.

2. Estimates of the areal brightness, expressed in magnitudes per square second of arc, or in other luminosity units. Our data in this field are due mainly to WIRTZ.

The valuable researches of WIRTZ on the areal brightness of the spirals seem not to have received sufficient attention as yet, and certain of his numerous correlations may fittingly be repeated at this point, the comparisons are with his quantity M_g , an areal brightness of unit luminosity.

1. Diameters. There is a slight, but not very definitely established tendency, for an increase of areal brightness with diameter.

2. Galactic Latitude. If the absence of the spirals near the galactic plane is due largely to occulting matter, as suggested by CURTIS and others, a falling off in areal brightness would be expected as this plane is approached. No such tendency is noted. The mean areal brightness of 517 spirals shows but slight variation between $+80^\circ$ and -80° of galactic latitude, and as a matter of fact those nearest to the galactic plane have slightly greater areal brightness.

Galactic latitude	$+80$	± 60	± 40	$+20^\circ$	0°
M_g	11.62	11.65	11.80	11.83	11.35

¹ C. WIRTZ, Flächenhelligkeiten von 566 Nebellücken und Sternhaufen. Land. Medd. (U) No. 29 (1923). While some values were found for the diffuse and planetary types, and clusters, he uses over 500 spirals in his correlations. WIRTZ tabulates the dimensions, both visual and photographic when available, the areal brightness M_g , and the total brightness, H , expressed in magnitudes. This work forms one of the largest and most homogeneous body of data in this field. Dr. C. PICKERING, Harv. Ann. 33, p. 135 (1900). Photometric areal brightness of 11 objects, J. HORTSCHAK, Wien. Ann. 20 (1907). Total brightness of 576 objects, J. HORTMANN, Revision of HORTSCHAK's results for 88 objects, A. N. 211, p. 425 (1921), J. H. RYAN, The light curve of the Andromeda Nebula, M. N. 72, p. 132 (1913), A. MARKOV, A. N. 234, p. 329 (1929), correction *ibid.*, 235, p. 113 (1930). By methods somewhat analogous to those of WIRTZ, he derives values of the surface brightness of 172 spirals (m per square second of arc), H. SHAPLEY, Note on the velocities and magnitudes of external galaxies, Wash. Nat. Ac. Proc. 15, p. 565 (1929), J. S. PARASKEVOPOULOS, Integrated photographic magnitude of the Small Magellanic Cloud, Harv. Bull. No. 840 (1926), Dr. H. STARK, The surface brightness of the galactic system as seen from a distant external point, and a comparison with spiral nebulae, Ap. J. 52, p. 162 (1920), Mt. Wilson Contr. No. 191 (1920), Dr. BECKER, A preparatory catalogue for a Durchmusterung of nebulae, the General Catalogue, Spec. Vol. 13 (1928). For about 1100 objects the total magnitude is expressed in "grades" these may be converted into magnitudes on the scale of WIRTZ by the formula, $M = 10^m/86 + 0^m/32(N - 7)$, see his introduction, p. XII. See also the references under ciph. 54.

3 Orientation and Form 503 spirals are treated for a relationship between the ratio of the major and minor axes, A , and the areal brightness. The observed areal brightness shows no connection with this ratio, and also no



Fig 52 The Spiral NGC 4736. (Mt Wilson Photograph)

dependence upon from which side the spiral is observed. There is further no tendency to a parallelism between the planes of the spirals and the plane of the galaxy.

4 Radial Velocity. No adequate degree of correlation is found between speed and areal brightness, though the radial velocities show a slight tendency to increase with diminishing areal brightness.

5 Total Brightness and Radial Velocity. See also ciph. 51. A fairly well-marked increase of speed with diminishing total brightness is indicated.

6 Distance. If the spirals are like galaxies, it would be expected that the areal brightness should be independent of the distance in the statistical mean. Using LUNDMARK's estimates of the distances of 216 spirals (subject to error in comparison with more recent results), WIRTZ finds that there is a marked decrease of areal brightness with increasing distance, the reverse is true for the diffuse nebulae.

$D \cdot 10^{11}$	100	10	20	13	9	7	6	5	1
M_g	12.2	12.1	11.67	11.52	11.12	11.10	10.80	10.70	10.58
No.	15	23	33	12	11	6	1	7	5

The fact that areal brightness is found to diminish with increasing distance is regarded by WIRTZ as an indication of the absorption of light in space.

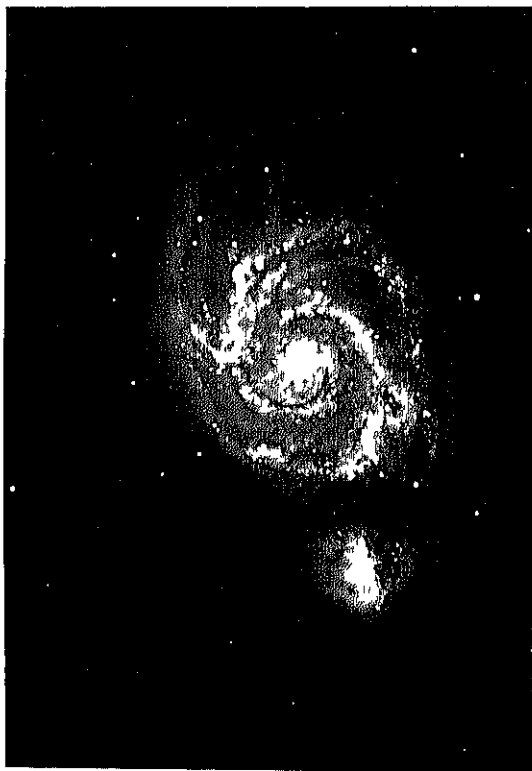


Fig. 53. The Spiral NGC 5194-5 (M51) (Mt. Wilson Photograph)

There are patent analogies between the large spirals and our own galaxy. On the more moderate assumptions of its size (60000 ly., KAPTEIN, and others), see ciph. 56. STARK's estimate of a diameter of $3 \cdot 10^5$ ly. allots our galaxy to a much more exceptional position in the group 221 (Andromeda) appears likewise to be exceptional as regards luminosity distribution. STARKS found a wide difference between the areal brightness of the spiral and that of our galaxy system as seen from a distant point in space, magnitude 23.1 per square second, as for our galaxy, as against magn. 17-18 as estimated for several spirals. MARKOWSKI, however, in the derivation of areal brightness for 172 spirals, finds that 224 is 2 magn., or 12.2 times brighter than the average spiral, and 76 times brighter than our galaxy. In other words

224 may be exceptional, and thus a portion of the lack of agreement between our galaxy and the (typical) spirals would be removed.

A recent treatment of this question from the standpoint of absolute magnitude, etc., is due to LUNDMARK¹. He now derives an abs. magn. of -5.7 for

¹ Über die Bestimmung der Entfernungen, Dimensionen, Massen und Dichtigkeit für die nächstgelegenen anagalaktischen Sternsysteme. VJS 65, p. 275 (1930).

the galactic novae, in comparison with the value -5.5 found for those in 224 on the basis of HUMPHRIS's distance of that object derived from the Cepheids. A relation is next derived for the mean abs magn of the 20 brightest objects in 8 spirals, in the form

$$-6^m.8 \pm 0^m.35 + k\sigma_{M^*} = M_{20}$$

From this relation he derives the distances, total abs magn, and abs magn of the 20 brightest objects, M_{20} , as follows

Object	Distance	Total abs magn.	M_{20}
Large Mag (1)	0.1×10^6 ly	-17.5	-6.5
Small Mag (1)	0.1	-17.4	-7.4
224 (Andromeda)	0.9	-17.2	-7.1
205	0.9	-12.0	-
598 (M 13)	1.1	-15.8	-6.5
6822	0.7	-17.2	7.2

The latest and most authoritative investigations in this aspect of the subject, made as they are with the most powerful instruments, are due to HUMPHRIS and HUMASON (references under clph 54). While the primary purpose of their paper is the consideration of the velocity-distance correlation, it may be said that they have drawn upon all methods as yet known in the derivation of the distances of the spirals, the distances of nearer spirals forming a "zero point" rest upon the phenomena of novae and Cepheids in spirals, for the more distant objects, they have combined the velocity-distance correlation with correlations based upon total absolute magnitude, the magnitude of the brightest stars visible in individual spirals, and apparent diameter-distance comparisons. Whatever changes may be made in the future in their adopted zero-point, and whether or not a velocity-distance correlation may be proved untenable, their values certainly represent the best that astronomy is able to secure from present observational data.

The basal data are derived from 10 objects, for which distances have been determined from stars of recognized types, novae, Cepheid variables, irregular variables, helium stars and P Cygni stars.

These objects, with the adopted distances, are,

Object	Distance	Total abs magn	Abs. magn brightest stars
Large Mag (1)	0.095×10^6 ly	-16.6	5.8
Small Mag (1)	0.085	-15.8	-7.4
6822	0.61	-12.0	-5.6
598 (M 13)	0.77	-14.9	-6.3
224 (Andromeda)	0.8	-17.0	5.8
221	0.8	-13.2	-
205	0.8	-12.7	-
5457 (M 101)	1.3	-13.1	-6.0
2403	(2.1)	-15.3	-6.0
3031 (M 81)	(2.4)	-16.0	-5.8

For 40 spirals investigation was made of the mean magnitude m_2 of the brightest stars, and the difference between this and the magnitude of the object. The mean of all values is $m_2 - m_0 = 8.88$ magn.

From these were derived the following important values:

Mean phot. abs. magn. brightest stars	-6.0
Mean vis. abs. magn. of spirals	-14.9
Mean phot. abs. magn. of spirals	-13.8
Mean color index	+1.1

Given m_s , the mean apparent magn. of the brightest stars in a spiral, its distance may be calculated by the formula,

$$\log D_{10} = 0,2 m_s + 2,7$$

A close correlation was found between the velocities and the most frequent or mean apparent magnitudes for the clusters of spirals and for two groups of

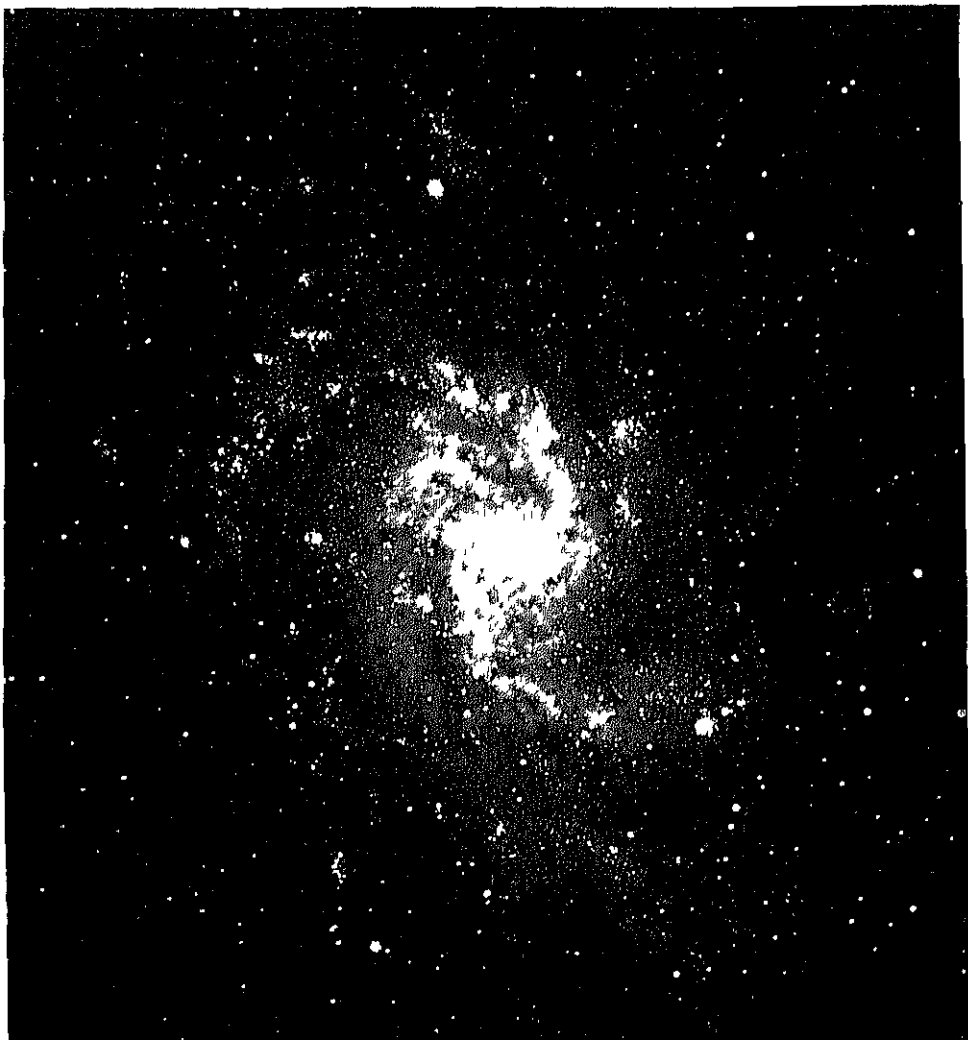


Fig. 54. The Spiral NGC 598 (M33) (Lick Photograph)

isolated spirals, and it was found that the ratio of the red-shift to distance is constant.

The distances derived by HUBBLE and HUMASON, together with data on clusters of spirals, are given in the next section.

OORT's latest treatment of the data now available finds a large spread in the values of $m - 5 \log V$, and concludes that either the luminosity curve of

isolated spirals deviates widely from the one found in clusters of spirals, or else that the galactic system is surrounded by an extensive local agglomeration, the peculiar velocities of which are much smaller than those of outside objects.

56. Distances and Dimensions of the Spirals. Given fairly reliable estimates of the distances of the spirals, and the apparent diameter, it becomes possible to determine their real dimensions, at least approximately. In Table 16 are collected the dimensions of the spirals for which radial velocities are known, and, except for the larger and closer spirals, these depend in general upon values secured through the distance-velocity correlation. If the distance-velocity correlation be accepted, the values of the diameters are still subject to some uncertainty, and it may be that those given for the smallest and most distant objects are two or three times too small, 1. because of uncertainties in this relation,

Table 16. Distances and Dimensions of Spirals: Velocity-Distance.

1 No.	2 Descr.	3 Dimens	4 Mg	5 Rad. vel. km./sec.	6 Dist. 10 ⁶ Ly.	7 Diameter Ly.	
205	Spir.	8' × 3'	11 ^m .7	---	300	0.8 H	3 500
221	Ell.	2.6 × 1.8	8 .9	-	185	0.8 II	1000?
224	Spir.	120 × 30	8 .8	-	220	0.8 III	31 000
278	Spir.	1.2 ×	-	+	650	5.0 II	1750
380	Spir.	0.3	-	+	4400	24.0 III	2400
383	Spir.?	0.3	-	+	4500	24.0 III	2400
384	Spir.	0.25	-	+	4500	24.0 III	1700
385	Spir.?	0.25	-	+	4900	24.0 III	1700
404	Ell.	1.3	11 .1	-	25	1.2 dS	450
584	Spir.?	2	10 .6	+	1800	11.4 II	6500
598	Spir.	55 × 40	12 .4	-	70	0.7 dS	11 000
936	Barr.	3 × 2	11 .1	+	1300	7.7 II	6700
1023	Spir.	6 × 1.3	10 .2	+	300	3.4 dS	5900
1068	Spir.	2.5 × 1.7	9 .8	+	920	2.3 II	2400
1270	Spir.	0.5 × 0.2	-	+	4800	36.0 III	5200
1273	Spir.?	0.5	12 .4	+	5800	36.0 III	5200
1275	Spir.?	0.5	-	+	5200	36.0 III	5200
1277	Spir.	0.4 × 0.1	-	+	5200	36.0 III	4200
1700	Spir.?	0.5 × 0.3	11 .1	+	800	5.1 dS	700
2562	Spir.	0.4 × 0.2	-	+	5400	29.5 III	3400
2563	Spir.	1.1 × 0.5	-	+	4800	29.5 III	9400
2681	Spir.	2.5 × 1.5	-	+	700	5.8 dS	4200
2683	Spir.	10 × 1	11 .4	+	400	3.2 dS	9300
2841	Spir.	6 × 1.6	-	+	600	5.1 dS	8900
2859	Spir.	1.4 × 0.7	11 .3	+	1500	8.5	4100
2950	Ell.?	1.0 × 0.4	-	+	1500	8.5	2900
3031	Spir.	16 × 10	-	-	30	2.4 III	13400
3034	Irr.	7 × 1.5	-	+	290	2.6 H	5300
3115	Spir.?	4 × 1	9 .8	+	600	3.3 II	3800
3193	Spir.	1.0 × 0.8	11 .0	+	1300	7.6	2500
3227	Spir.	3 × 1.2	-	+	1150	8.1 dS	7400
-	Spir.?	0.5?	-	+	19600	105 III	15200
3368	Spir.	7 × 3.5	10 .7	+	940	5.7 II	11400
3379	Ell.	2	10 .2	+	810	4.8 II	2800
3489	Spir.	2.5 × 1	10 .3	+	600	3.6 II	2600
3521	Spir.	4.0 × 1.0	10 .3	+	730	4.1 II	4700
3610	Spir.?	1.0 × 0.7	11 .0	+	1850	1	3500
3623	Spir.	8 × 2	10 .9	+	800	5.0 II	11600
3627	Spir.	8 × 2.5	10 .6	+	650	4.3 dS	10000
4051	Spir.	4 × 2	12 .0	+	650	5.4 dS	6200

(Continued.)

1 No.	2 Descr.	3 Dimens	4 M _g	5 Rad. vel. km./sec.	6 Dist. 10 ⁶ l.y.	7 Diameter l.y.
—	Spir.	0',5?	—	+ 11800	150 B	22000
4111	Spir.	3',8 · 0',5	10 ,3	+ 800	5,8 II	6400
4151	Spir.	2',6 · 1',6	10 ,8	+ 950	7,3 dS	5500
4192	Spir.	8 · 2	12 ,0	+ 1150	6,0 HII	13900
4214	Spir.	8 · 4	11 ,8	+ 300	2,8 dS	6500
4258	Spir.	20 · 6	—	+ 500	4,6 II	26800
4374	Ell.	2 · 1,8	10 ,5	+ 1050	6,0 HII	3500
4382	Spir.	4 · 2	10 ,4	+ 500	3,7 dS	4300
4449	Mag.	3,5 · 2	—	+ 200	2,3 dS	2300
4472	Spir.	2	10 ,2	+ 850	5,7 dS	3300
4486	Ell.	2	10 ,4	+ 800	5,5 dS	3200
4526	Spir.	5 · 1	10 ,7	+ 580	3,9 H	5600
4565	Spir.	15 · 1,1	11 ,2	+ 1100	7,6 H	31000
4594	Spir.	7 · 1,5	9 ,7	+ 1140	7,2 H	14600
4649	Ell.?	2	10 ,3	+ 1090	7,5 dS	4400
4736	Spir.	5 · 3,5	—	+ 290	3,0 dS	4400
4826	Spir.	3 · 4	11 ^m ,0	+ 150	1,3 dS	3000
4853	Ell.?	0,3	—	+ 7600	45 HII	3000
4860	Ell.?	0,5	—	+ 7900	45 HII	6500
4865	Ell.?	0,5	—	+ 5000	45 HII	6500
4872	Spir.?	1,0	—	+ 6900	45 HII	13000
4874	Spir.?	0,2	—	+ 7000	45 HII	2600
4881	Ell.?	0,3	—	+ 6900	45 HII	3900
4884	Spir.?	1,5 · 0,8	—	+ 6700	45 HII	19000
4895	Spir.?	1 · 0,3	—	+ 8500	45 HII	13000
II 4045	Ell.?	0,5?	—	+ 6600	45 HII	6300
5005	Spir.	4,5 · 1,5	10 ,9	+ 900	6,6 H	8600
5055	Spir.	8 · 3	—	+ 450	3,6 H	8300
5194	Spir.	12 · 6	10 ,9	+ 250	3,0 dS	10400
5236	Spir.	10 · 8	—	+ 500	2,9 H	8400
5457	Spir.	27	12 ,2	+ 300	3,0 dS	23400
5866	Spir.	3 · 1	10 ,9	+ 650	6,0 dS	5200
6359	Spir.?	0,2	—	+ 3000	21,6 dS	1200
6658	Spir.	0,4 · 0,2	—	+ 4100	24	3100
6661	Spir.?	0,5	—	+ 3900	23	3800
6702	Spir.?	0,2	—	+ 2000	12	750
6703	Spir.?	0,3	—	+ 2000	12	1100
6710	Spir.?	0,2	—	+ 5100	29	1600
6822	Mag.	20	—	+ 150	1,0 S	5800
6824	Spir.?	0,9 · 0,5	—	+ 3200	19	5100
7217	Spir.	2,5 · 2	11 ,4	+ 1050	6	1000
7242	Ell.?	0,5	—	+ 5000	29	4600
7331	Spir.	9,5 · 2	10 ,8	+ 500	5,2 dS	14600
7611	Spir.	0,7 · 0,3	—	+ 3400	23,5 HII	4700
7617	Ell.	0,2	—	+ 3900	23,5 HII	1400
7619	Ell.	0,8	11 ,5	+ 3800	23,5 HII	5400
7623	Ell.?	0,3	—	+ 3800	23,5 HII	2000
7626	Ell.	0,7	11 ,6	+ 3700	23,5 HII	4700
L. Cl.	Mag.	432	—	+ 280	0,09 S	11000
Sm. Cl.	Mag.	216	—	+ 170	0,1 S	6500

which has been determined from a relatively small number of moderately close objects, and, 2. because the observed diameters may not record the full extension of the spiral, for reasons noted in ciph. 40.

In the first column of the table will be found the NGC number, a brief characterization, when available, is given in column 2, in column 3 are given the apparent dimensions in minutes of arc, a single value indicating that the object is round, or nearly so, Wirtz' areal brightness, M_g , is given in column 4, column 5 contains the radial velocity, column 6 the distance, expressed in units of 10^6 ly, in column 7 are given the computed diameters, given in ly. Abbreviations used are H = HUBBLE, HH = HUBBLE and HUMASON, dS = DE SITTER, S = SHAPIRO. Where no letter follows a distance, it has been computed from the relation $D = V/170$, where D is in units of 10^6 ly.

The distances derived from the velocity-distance correlation are taken from HUBBLE and HUMASON's paper in Ap J 74, p 43 (1931), where the following data are assembled concerning super-galactic groups:

Cluster	Distance	No. in cl.	No. observ.	Mean velocity km./sec.	Mean photo. mag.	Diam. of cl.
Virgo	6.0×10^6 ly	(500)	7	+ 890	12.5	$12''$
Роговик	23.5	100	5	+ 3810	15.5	1
Риксон	24.0	20	4	+ 4630	15.4	0.5
Скапел	29.5	150	2	+ 4820	16.0	1.5
Роговик	36.0	500	4	+ 5230	16.4	2.0
Coma Berenices	45.0	800	3	+ 7500	17.0	1.7
Урна Major	72.0	300	1	+ 11800	18.0	0.7
Лео	105.0	400	1	+ 19600	19.0	0.6

We may include here SHAPIRO's results on the diameters of spirals in certain well-populated clusters of external galaxies¹

The Coma-Virgo Groups

Number of galaxies in area	2775
Distance of Cloud A	$10.5 \cdot 10^6$ ly
Diameter of Cloud A	$2 \cdot 10^6$ ly
Average diameter of component members	5500 ly
Larger members of Cloud A	
4206 edgewise spir.	15500 ly
4216 edgewise spir.	18000
4304 open spir.	18600
4321 open spir.	18900
4382 ell.	15300
4418 spir.	24000
4501 compact spir.	18000
4526 ell.	18300
4535 open spir.	19400
4569 compact spir.	16500
Distance of Cloud B	$39 \cdot 10^6$ ly
Distance of Cloud C	$139 \cdot 10^6$ ly
Distance of Cloud D	$169 \cdot 10^6$ ly
Largest members of C and D, Diameter	25000 ly

The Centaurus Group

Number of galaxies in area	1000
Distance of group	$146 \cdot 10^6$ ly
Length, $7 \cdot 10^6$ ly	
Width, $1.8 \cdot 10^6$ ly	
Diameter of largest members	45000 ly
Average diameter of members, $15''$	9700 ly

The Ursa Major Group

Distance of group (M31 group)	$100 \cdot 10^6$ ly
Mean distance apart	$6.7 \cdot 10^6$ ly
Diameter of largest members	20000 ly

¹ Harv Bull 863, 864, 874 (1929)

By way of summary, assuming only the distances and diameters which have thus far been determined for spirals and groups of spirals, there appear to be two main classes as regards size: the majority have more moderate dimensions of 2000 to 9000 ly, with a class of giant spirals whose diameters range from 15000 ly to 50000 ly, or more. See also HUBBLE's values, given in Ap J 61, p. 329 (1926).

Mention should be made here of the results derived by LUNDMARK in his extended paper, "The Relations of the Globular Clusters and Spiral Nebulae to the Stellar System" [K Svenska Vet Ak Handl 60, No. 8 (1920)]. In this paper he has derived distances for 276 spirals, taking the mean of values secured from their apparent magnitudes and their apparent diameters. These are distributed as follows:

No. of spirals	Adopted distance	Density per 10^{20} cub ly	No. of spirals	Adopted distance	Density per 10^{20} cub ly
1	0.7 10^6 ly	5.3	6	6.0 10^6 ly	0.3
1	1.3	1.1	10	7.2	0.2
4	2.2	0.5	18	9.1	0.1
2	3.4	0.5	25	13	0.07
3	3.9	0.5	62	22	0.017
6	4.1	0.5	65	41	0.003
7	5.0	0.4	63	101	0.00003

LUNDMARK's distances from diameter and magnitude relations are in general larger than those found from the distance-velocity relation, as will be seen from the tabulation below comparing such objects as are common to the two methods:

VCC No.	Distance from dist-vel corr.	LUNDMARK'S dist. from mag. and diam.	NGC No.	Distance from dist-vel corr.	LUNDMARK'S dist. from mag. and diam.
205	1.0 10^6 ly	7.5 10^6 ly	4371	6.0 10^6 ly	3.4 10^6 ly
278	5.0	45	1382	3.7	6.0
598	0.7	1.4	1419	2.3	6.5
936	7.7	28	4472	5.7	8.1
1023	3.1	11	1186	5.5	5.8
1068	2.3	1.5	1526	3.9	27
2681	5.8	23	4565	2.6	6.8
2685	3.2	10	1594	7.2	1.1
2841	5.1	7.6	4736	3.0	3.5
3031	2.9	3.0	1826	1.3	1.8
3034	2.6	7.1	5005	6.6	7.1
3115	3.3	4.6	5055	2.9	1.1
3368	5.7	5.5	5191	3.0	3.0
3521	4.1	10	5236	2.9	8.6
3623	5.0	6.3	5217	3.0	3.7
3627	4.3	5.2	5157	3.0	10
4051	5.1	20	7217	7.0	27
4192	6.0	8.2	7331	5.2	11
4214	2.8	10			
4258	4.6	5.3			

57 Masses of the Spirals In general, the estimates of the total mass of typical spirals are roughly of the same order as that derived for our galaxy. The latter is a quantity still imperfectly known, and any derivation of spiral masses requires a large measure of hypothesis and extrapolation. ÖPİK's method¹ assumes that the luminous materials of the spirals have the same coefficient of

¹ Ap J 55, p. 406 (1922)

emission as those in our own galaxy, while HUBBLE (1 c) uses the spectrographic rotation LUNDMARK assumes the mass-luminosity law effective in all such systems, and starts from the total abs magn (see the preceding Section). He points out that the total gravitational mass must be larger, and postulates large ratios of dark material. The value derived from the total abs magn is styled the luminosity-mass, while that derived from spectrographic rotation values will be a gravitational mass. LUNDMARK assembles the following values, to which have been added determinations by HUBBLE (H), and ÖPK (O)

Object	Gravitation-mass	Ratio: km dark to lum. matter	Stars per ly ³	Authority
224	$0.2 \cdot 10^{10} \odot$	20:1	0.006	L.
	$3.5 \cdot 10^9$			11
	$1.6 \cdot 10^9$			(O)
1594	$2.0 \cdot 10^9$			11
	$2.6 \cdot 10^9$			(O)
	10^{11}			Our
	$1 \cdot 10^{10}$	30:1	0.042	L.
3031	$76 \cdot 10^{10}$	100:1	0.20	L.
5194	$0.1 \cdot 10^{10}$	10:1	0.012	L.
Galaxy	$10 \cdot 10^{10}$	10:1	0.08	L.

58. TEN BRUGGENCATK's Theory of Elliptical Spirals¹. The investigations of HUBBLE, TEN BRUGGENCATK, and others may fittingly be mentioned at this point.

HUBBLE's very thorough and detailed investigation is based upon observations made with a self-registering microphotometer, and he derived isophotal curves for the following 15 elliptical objects:

221	1278	4472	1115	4482	4621
410	1281	1486	3379	4406	1749
584	4374	4552			

The isophotal contours are approximately circles for globular objects (HUBBLE's 1,0), except for the extremely elongated objects (15,7), the deviations of the contours from symmetrical ellipses are slight. An interesting investigation is made of the projected densities of different types of structure, and he gives a comparison of the density distribution in the projected images of the mean elliptical spiral, an isothermal gas sphere, and a bounded gas sphere.

REYNOLDS believed that he had detected evidences of polarization in the spiral 4826 (M64). GREEN and MEYER, however, were unable to substantiate any such effect in a number of nebulae of various types which they tested.

Somewhat in contrast to these failures to detect polarization are TEN BRUGGENCATK's recent results. He investigates the spatial distribution laws of a nebula symmetrical through rotation, and extends the theory to the case where the isophotal surfaces within the object are concentric, coaxial, and similar ellipsoids of rotation. He finds a satisfactory agreement between his values and those observed by HUBBLE (supra). Based on HUBBLE's results, TEN BRUGGENCATK concludes that all elliptical objects have the same axial ratio, about 10:3, and in support of this, the probabilities of different degrees of ellipticity are investigated. To a first approximation, the brightness within the ellipsoid diminishes

¹ 1. HUBBLE, The distribution of luminosity in elliptical nebulae. *Ap J* 71, p. 231 (1930).
 P. TEN BRUGGENCATK, Die Helligkeitsverteilung im inneren elliptischen Nebel. *Z. Astroph.*
 4, p. 275 (1930), 2, p. 83 (1931).
 J. H. REYNOLDS, Preliminary observations of spiral nebulae
 in polarized light. *M. N.* 72, p. 553 (1911).
 W. K. GREEN, An investigation of certain nebulae
 for evidence of polarized light. *Publ. A. S. P.* 29, p. 108 (1917).
 W. F. MEYER, A study of certain
 nebulae for evidence of polarization effects. *Publ. A. S. P.* 31, p. 194 (1919).

as the inverse square of the distance from the center. He therefore interprets the elliptical objects as conglomerations of particles, rather than stars.

"Die elliptischen Nebel dürften aus einem zentralen Kern bestehen, der als Lichtquelle dient, und dessen Licht in der ihn umgebenden Materie nicht merklich absorbiert und re-emittiert, sondern gleichmäßig nach allen Seiten gestreut und reflektiert wird. Die von HUBBARD empirisch gefundene Beziehung, die Identität der Intensitätsverteilungen in den Projektionen aller elliptischen Nebel ausdrückt, bildet den Schlüssel zum Verständnis des physikalischen Zustandes dieser kosmischen Objekte: daß elliptische Nebel keine durch ihre große Entfernung nicht auflösende Sternwolken sein können." (1)

The structure is postulated as transparent throughout the greater part, and the particles reflect and disperse the light from the nucleus in all directions. Taking HUBBARD's value of the radius, ca. 1000 ly, the total average mass is placed at 10^8 \odot , and the effective density is of the order of 10^{-26} . The diameter of the "nucleus" is of the order of 10^3 ly, with a mean density of about 10^{-10} , the mean free path of the particles in the outer portions is of the order of 10^3 ly.

There are a number of very serious objections to this theory of DEN BRUGGEN-CAT.

1 All existing evidence as to super-galactic groups indicates that the elliptical and the true spirals are inextricably intermingled as to arrangement and location. This theory assumes an entirely different constitution for these bodies, as contrasted with their immediate neighbors in space. This is most improbable.

2 From this contiguity in space with the spirals, and from the areal and apparent brightness of the elliptical objects, their total absolute magnitude must be of the same order as that of the spirals —15 to —17. This accordingly requires that the "nuclei" of the elliptical objects be sources of tremendous energy, equivalent to absolute magnitude —15 or higher. No such "sources" are known with certainty.

3 Furthermore, we should expect that the light from such central sources would be polarized, or that it would show selective reflection or absorption effects. None have been detected.

59. Theories of Spiral Structure: Introductory¹ The structure of the spirals, showing as it does so frequently two well-marked spiral whorls starting

¹ S. ALEXANDER, 8 papers in A J 2 (1852), E. J. WIERZYNSKI, Outlines of a theory of spiral and planetary nebulae. Ap J 4, p. 97 (1896), Dynamics of a nebula. A J 20, p. 67 (1899), F. C. CHAMBERLIN, On the possible function of disruptive approach in the formation of meteorites, comets, and nebulae. Ap J 14, p. 17 (1901), The origin of the earth. Chicago (1916), E. STRÖMGREN, Über die Bedeutung kleiner Massenänderung für die Newtonsche Zentralbewegung. A N 163, p. 130 (1903), J. H. JEANS, The stability of a spherical nebula. Proc R A S Lond 68, p. 454 (1901), Problems of cosmogony and stellar dynamics. Cambridge (1919), Astronomy and cosmogony. Cambridge (1928), M. WOLF, Length of axes and position angles of 52 oval nebulae. M N 68, p. 626 (1908), H. KNOX SNIAW, On the inclinations of the planes of some spiral nebulae to the galaxy. M N 69, p. 72 (1908), W. SUHRFRIED, Bode's law and spiral structure in nebulae. Ap J 34, p. 251 (1911), L. J. J. SELL, Evolution of the stellar systems, 2 (1910), E. v. D. PAULSEN, Über die Gestalten einiger Spiralnebel. A N 188, p. 240 (1911), L. NÖRKE, Über die Entwicklung der kosmischen Nebel. A N 188, p. 353 (1911), E. BELLOT, Expérience reproduisant les spires des nébuleuses spirales. C R 154, p. 1780 (1912), G. W. WALKER, Some problems illustrating the forms of nebulae. Proc R S Lond (A) 91, p. 410 (1915), G. F. BECKER, A possible origin for some spiral nebulae. Wash Nat Ac Proc 2, p. 1 (1918), B. IL'YASSOVITCH, Sur les mouvements tourbillonnaires dans les nébuleuses. A N 126, p. 81 (1919), K. BOTTLINGER, Zur Bildung der Spiralnebel. A N 210, p. 5 (1919), C. V. L. CHARLIER, Sur les nébuleuses spirales. C R 169, p. 430 (1919), M. VALIER, Die Gestalt der Nebelflecke, insbesondere der Spiralnebel. A N 212, p. 17 (1920), criticized by NÖRKE, *ibid*, p. 373, H. JEFFERYS, On Jeans' theory of the origin of spiral nebulae. M N 83, p. 449 (1923), Jeans' answer, *ibid*, p. 458. H. VOGEL, Beitrag zur Entstehung der Spiralnebel. A N 220, p. 97 (1923), H. GROOT, On the true shape of some spiral nebulae. M N 85, p. 535 (1924), On the spiral form of some nebulae. *ibid*, 86, p. 146.

from exactly opposite points on a nuclear portion, has long been a puzzle. No adequate, complete, and entirely satisfactory theory of the spirals as a result of classical dynamical laws has as yet (1932) been derived. A satisfactory theory of the forms assumed by the spirals must then

A. Furnish a reasonable dynamic explanation of the origin, shape, motions within, and permanence of the spiral whorls.

B. It must explain why these take their origin at points 180° apart on a nuclear portion (very difficult).

C. The component matter of the structure must be taken to be discrete stars, rather than gas, or dust particles.

The literature of the field is already very extensive, and additions are constantly being made to it.

60. Agreement of Spiral Arms with Mathematical Spirals. A number of mathematical curves show more or less close approximation to the observed forms of the whorls of the spirals. Some of these, with the law of attraction required in each case (SER, I, c.), are:

$$r^3(\psi - \psi')^2 = c, \quad P = \frac{h^2}{r^3}$$

The spiral of ARCHIMEDES,

$$r = a\theta, \quad P = \frac{h^2}{r^3} \left(1 + \frac{2a^2}{r^2}\right)$$

The logarithmic spiral,

$$r = a^u, \quad P = \frac{h^2}{r^3} (1 + \log^2 a)$$

The lituus,

$$r^2\theta = a^2, \quad P = \frac{h^2}{r^3} \left(1 + \frac{4a^2}{r^2}\right)$$

The hyperbolic spiral,

$$r\theta = a, \quad P = \frac{h^2}{r^3}.$$

The parabolic spiral,

$$(r - a)^2 = 4ca\theta, \quad P = \frac{h^2}{r^3} \left(1 + \frac{3a^2(2\theta + 1)^2}{r^2}\right).$$

Spirals of other types show even more complex functions. It will be noted that only for the gravitational, logarithmic, and hyperbolic spiral is the law of force a relatively simple one, being as the inverse cube of the distance, for the other common types of spiral the law of force depends upon the third and fifth, or third and seventh power of the distances. It is unnecessary to emphasize that no cosmic forces are known whose action varies in this way.

(1926), J. H. REYNOLDS, The condensations in the spiral nebulae, *M.N.* 85, p. 142 (1924). The form and development of the spiral nebulae, *ibid.*, 85, p. 1014 (1925). The spiral form and development of the Andromeda Nebula, *ibid.*, 87, p. 112 (1926). F. A. LINDEMANN, Note on the constitution of the spiral nebulae, *M.N.* 83, p. 334 (1923). Approved by REYNOLDS, *ibid.*, p. 382, criticized by PHILLIPS and GIFFORD, *ibid.*, p. 272, 283. E. W. BROWN, Gravitational forces in spiral nebulae, *J. Roy. Astr. Soc.* 32, p. 545 (1924), *Ap. J.* 61, p. 97 (1925). later views, *ibid.* 51, p. 277 (1928). H. LINDBLAD, Cosmogonic consequences of a theory of the stellar system, *Upps. Medd.* No. 43 (1926). On the spiral orbits in the plane of a spheroidal disk, with applications to some typical spiral nebulae, *ibid.*, No. 31 (1927). On the nature of spiral nebulae, *M.N.* 87, p. 420 (1927). H. MARIN, The formation of spiral nebulae, *Phys. Rev.* (2) 31, p. 1100 (1929). C. L'ARVIERESCO, Sur la dynamique des nébuleuses spirales, *C.R.* 181, p. 653 (1920). KORTZIM, ILLVI, and OUCHAKOFF, Sur la forme des nébuleuses spirales, *R.A.S.* 3, p. 157 (1927). J. C. SOLA, Algunas consideraciones sobre las nebulosas en espiral, *Rev. Soc. Astr. Arg.* 2, p. 149 (1929).

There is a general, though not entirely unanimous, agreement among those who have investigated the whorls of typical spirals, that, on the whole, these curves approximate most closely to those of the logarithmic (also called equiangular) spiral. In this curve, the angle between the tangent to the curve and the radius vector to the given point should be constant and equal to $\arctan (1/\log_e a)$.

EDWARD PAMMEL made careful measures of the whorls of three large spirals 598 (M33), 5194-5 (M51), and 628 (M74). He found the agreement of all three with the logarithmic spiral relatively close (there are, in all such investigations, considerable variations in the density, width, or location of salient features in the whorls which can only be explained as chance irregularities, resulting doubtless from random differences of distribution in the original mass or aggregation). The spiral of ARCADELL was tested in 598, but did not give nearly so good a measure of agreement as the logarithmic spiral. It was impossible to substantiate any similarity with WIERZINSKI's gravitational spiral (see ciph. 61).

L. BRICKER made measurements of the points in both whorls of 5194-5, with a least squares reduction. His measures result in an empirical spiral with characteristics as follows:

a) The two whorls are practically duplicates, and corresponding points stand diametrically opposite to each other, and equally far from a certain point near the middle of the central condensation.

b) Lines of length $r_p - a + b l^2$ may be drawn from the points of the real spiral to the line of sight which passes through the central point, and these lines, when displaced parallel to themselves to a point, all lie in a plane. The longitude of the node of this plane is 160° , and its inclination 42° .

The essential duplication of the whorls is taken as an indication that the motion is outwards, for it is deemed unlikely that matter coming in from outside would arrange itself in two identical whorls 180° apart. The assumption is made that the increase in the longitude of the moving particles is proportional to the time. Such a relation is found possible with a certain spheroid whose equator coincides with the plane of the spiral, in which each particle acts according to the inverse square of the distance, and with a density varying from the center outward. The law of such a required density variation is investigated, and the resulting calculated curve shows a fair agreement with the observed contour of the whorls.

II. GROOT made an extended series of measures on the following eight large spirals (nine sets are given, on 17 individual spiral arms, but one spiral was measured twice): 5194-5 (M51), 4258, 3198, 4321, 4501, 4725, 3623, and 3031. The logarithmic spiral, the spiral of ARCADELL, and the lituus were all tested. All the 17 arms investigated could be properly represented by the logarithmic spiral. Only 5 whorls (two each in 3623 and 3031, and one in 4321) could also be represented by the spiral of ARCADELL or the lituus, and it was thought that this was partially explained by the fact that the arms of these spirals could be investigated only over a very limited range. Equations were set up for each whorl investigated, and the two found for 4321 may be selected as examples:

$$\begin{array}{ll} 4321, \text{ whorl I} & \log r = 1.2041 - [8.9406] q \\ 4321, \text{ whorl II} & \log r = 1.1761 - [9.0327] q \end{array}$$

The fairly close agreement of the constants of the equations for the two whorls in this and in practically all the other spirals studied indicates essential duplication for the whorls of individual spirals, and argues for an evolution proceeding from within outward. The total range in the value of the angles

between the tangents to the whorls and the radii vectores is remarkably small (73° to 86°), the greatest range found for the two whorls of the same spiral was 4° , the mean value for all whorls measured is 79° . Some evidence was found for skewness in the arms of 3031, the structure of all the others seems to be in one plane. Six other spirals were investigated by GROOT in his second paper, with essentially the same conclusions.

REYNOLDS has measured the configurations of a number of spirals and, in general, agrees with GROOT as to their correspondence with the logarithmic spiral. The objects investigated were 5247, 2835, 4254, 4321, 1232, and 5457. He finds, however, a greater degree of irregularity in the run of the angles between the tangent and the radius vector. "The angle made by the tangent of the curve with the radius vector is usually between 50° to 70° in the earlier part of the curve, but in more advanced stages the angle may be anything between 40° and 80° . In many cases these extremes may be observed in the two arms and bifurcations of the same spiral." He regards both the filamentous and the massive spirals as in an advanced stage of development, and points out that spirals developed for less than half a revolution are rare, while spirals developed for more than two revolutions in an actual spiral form are unknown.

81. WILCZYŃSKI'S Gravitational Spiral. Most earlier theories attempting to explain spiral structure are influenced by the hypothesis of gaseous constitution. The most general assumption has been that of a rotating gaseous spheroid, though dust-clouds which have been repelled from regions near the galactic plane have also been suggested. SCHAEFERLI even proposed that the spirals were formed by matter ejected from volcanoes! Repulsive forces acting from the nucleus outward have also been a favorite method (radiation pressure, etc.) giving rise to the "Dampfstrahl" or "pin-whirl" theory of whorl formation.

The theory of the origin of the solar system from a (small) spiral in the planetesimal hypothesis of CHAMBERLIN and MOUTON is well known. This theory suggests that a spiral would be formed by the disruptive tidal action of two stars making a close approach. While this theory has been carefully and rigorously worked out by its authors, they admit that the enormous dimensions of the spirals make their origin in this way untenable (solar system: mass 1,001 \odot ; diameter, ca. 0,001 Ly.; Andromeda Nebula: mass $3,5 \cdot 10^6 \odot$, diameter ca. 31000 ly.).

Among earlier attempts to identify the class of curve assumed, mention must be made of the gravitational spiral of WILCZYŃSKI. His explanation is as suitable for a stellar composition as for other constitution. The component elements are assumed in his theory to revolve about a center of attraction under the action of gravitation, the inner components will manifestly rotate more rapidly than the components on the periphery, and initial irregularities as regards density of distribution will thus in course of time trail out into the whorls of a gravitational spiral. The number of whorl-turns will give an indication of the age of the spiral through the formula,

$$t = \frac{2\pi\pi}{\omega_1} \frac{1}{1 - (a/b)^{2/n}}.$$

Here a and b are the radii of the circles between which the structure of the spiral lies, ω_1 is the angular velocity of rotation at the inner circle, n the number of turns, and t the elapsed time or age.

WILCZYŃSKI'S theory agrees with the observational data in the following respect: it gives a direction of rotation in the same direction as is indicated by SLIPHER'S spectrographic determinations of rotation.

The theory appears to fail in the following points

a) No adequate explanation is given of the diametrical symmetry of the two sets of whorls

b) The curves of a gravitational spiral do not "fit" the great majority of the curves observed. One has only to draw a gravitational spiral on a sheet of semi-transparent paper and place it over available reproductions of spirals to establish the entire lack of agreement

In this connection one may compare the theory of G F BLACKER, where the nebular aggregation is assumed to start in the form of an extended cylinder or rod, to which the term "baculae" is applied. Such forms, if existent at all, are exceedingly rare among observed spirals, the long and narrow spindles seem always to be more reasonably interpreted as relatively thin disks seen edgewise

62 JEANS' Theory of Spiral Structure. JEANS' earlier theory is a by-product of his extensive stellar investigations collected in his *Problems of Cosmogony*¹. Through a complicated dynamical investigation, the details of which can not be given here but must be sought in the work quoted, the initial state of a spiral is assumed to be a rapidly rotating, gaseous, lenticular disk, with sharp peripheral boundary, this form is regarded as represented by numerous examples of edgewise spirals (4565, 4594, etc.). Small tidal forces due to distant objects of the same class are postulated as the cause of the ejection of matter from points 180° apart on the periphery of the lenticular disk

"Thus our conjectural interpretation of all spiral nebulae is that they are masses of gas or clouds of dust in rotation, the rotation being so rapid that no figure of statical equilibrium is possible. In the earlier stages of their evolution, they must have passed through a series of figures of equilibrium of the Pseudo spherical type discovered in Chapter VII, until a sharp edge was formed. (WATKER has criticized this feature of JEANS' development.) After this, matter was ejected along the two arms originating from the spiral edge. At first the points of origin of these arms were determined by the infinitesimal tidal forces set up by other objects in the rest of the universe, subsequently, the tidal forces from the symmetrical arms themselves would suffice to confine the emission to two antipodal points."

JEANS' theory gives no statement of the law governing the forms of the arms thus tidally ejected, nor any comparison with the spiral forms observed. His earlier calculations of the distance between condensations in the spiral whorls, mass of the nuclear portion, etc., were influenced by the attempt to satisfy VAN MAANEN's internal motions. In a later note², JEANS revised his earlier computations to take account of the character of a spiral as an island universe. The differences are naturally considerable, in view of the change in the adopted distance of 224 (Andromeda) from 5000 ly. to 900 000 ly. The revised mass of the nucleus is $5 \cdot 10^{12}$ g, or $2.5 \cdot 10^6$ O, regarded as significantly near the estimated total mass of our galaxy.

63. BROWN's Theory of Spiral Structure. Like JEANS, BROWN in his earlier work on the subject had attempted to set up a reasonable gravitational mechanism to account for the spirals and at the same time to satisfy VAN MAANEN's values of the internal motion. His second paper³ bids fair to be a very important contribution to the problem. Unfortunately, his complete analysis has not yet been published, so that comparison between theory and observation is not possible as regards the shape of the spiral arms⁴

¹ Cambridge (1928)

² M N 85, p 531 (1925)

³ Obs 51, p 277 (1928)

⁴ In the abridgements of this and other theories treated in the balance of this paper, as is permissible in a survey of progress, statements will frequently be phrased in the exact words of the author, but with the omission of quotation marks

The system of the spiral is supposed to originate in a lens-shaped aggregate of stars arranged in an ellipsoid of revolution. The distances between the component stars are very great in comparison with their diameters; the number of stars is postulated as very large. Furthermore, the number of stars in a given volume of the ellipsoid is assumed to be everywhere the same.

A field of force varying directly as the distance was chosen, this field permits circular motion, and deviations from circular motion which are symmetrical across the center, which is a vital factor in explaining the diametrical symmetry of the spiral whorls. The mathematical treatment is then made to depend upon two well-known gravitational phenomena. If such a particle or star be attracted toward a fixed center with a force $-n^2 r$, it can move in a central ellipse with a mean angular velocity, n . Uniform distribution of the stars within the ellipsoid, if the flattening be considerable, will then cause the star to move under a force $-Kr$, in an ellipse whose center coincides with that of the ellipsoid, and every particle will be moving with nearly the same angular velocity about the polar axis of the flattened disk.

The initial requirement of constant density of distribution can be waived provided the amount of matter in a cylindrical volume standing on an element of area of the equatorial plane be proportional to $(1 - r^2/a^2)^{1/2}$, where r_1 is the distance of a particle (star) from the center, and a is the external radius. It is this function which admits of an observational test by counts of stars at different distances from the center. A dominating central mass is thus abandoned in favor of the action of the entire field upon the star.

A near (but not too near) approach and passage of a similar aggregate of the same order of total mass disturbs this field by a kind of "tidal" force which has several effects which can be separately considered. Actual distortions of the figure are small, and are bound to be subject to oscillations which are soon masked by other effects. There also arise variations of density which have a maximum along one axis in the equatorial plane and a minimum along an axis perpendicular to it, a change of density also occurs along any radius of this plane, the linear rate of change being proportional to the distance from the center. This gives the appearance of a bar, nearly straight, across the plane of the object. (Compare a similar feature in LINDBLAD's theory, ciph. 64, and note the great importance of this feature as an explanation of the relatively frequent barred spirals.) The altered gravitational field will eventually cause this bar to coil into a spiral, the "coiling" being produced by the radial variation of density. During the process the "arms" become denser, and the coiling (finally) becomes so close that the evidence of structure disappears. At this stage, the aggregate has reverted substantially to its original condition, and on BROWN's theory the elliptical objects or close-packed and "compact" spirals may be "late" instead of "early".

Knots or subordinate aggregations in the arms are attributed (the least satisfactory of BROWN's postulates) to the approach of another similar aggregate which starts a new set of arms, the intersection of the two sets producing the condensations (?).

BROWN's theory may then be summarized as requiring an initial very populous aggregation of stars which by rotation has assumed the shape of a flattened ellipsoid of revolution. The start of the spiral arms requires an approach to another similar large aggregation. The postulate of this approach is the most difficult point in this or any similar theory, such approaches would seem to be of almost vanishing rarity. The theory has the following very notable points of merit:

a) It provides for the symmetry of the two whorls from the nature of the central force adopted

b) It gives a possible explanation of the frequent occurrence of barred spirals

c) Alone among existing theories, it offers a dynamical explanation of the rotational results secured by PRASE (see ciph 46) in that the spiral rotates essentially as a whole

It does not, however, give any law for the curves observed in the spiral arms

64. LINDBLAD's Theory of Spiral Structure LINDBLAD has been almost the only modern theorist to make a comparison between theory and observation as regards the shape of the spiral arms¹. His theory rests upon a certain class of spiral orbits which are asymptotic to the peripheral edge of a flattened, rotating ellipsoid. The orbit of a material particle moving in a circular orbit outside the spheroid in the equatorial plane is derived in the form

$$\left(\frac{dy}{d\theta}\right)^2 = \kappa \left[\left(2 - \frac{1}{y^2}\right) \arcsin y + \frac{1}{y} \sqrt{1 - y^2} + \frac{4}{3} \mu y \right] + c_0, \quad (1)$$

where

$$\kappa = \frac{e^4}{\arcsin e - e \sqrt{1 - e^2} + \frac{2}{3} \mu e^3},$$

and

$$c_0 = 2e^2 \frac{(1 - e)^2 \arcsin e - e \sqrt{1 - e^2} - \frac{1}{3} \mu e^3}{\arcsin e - e \sqrt{1 - e^2} + \frac{2}{3} \mu e^3}$$

In the above

r and θ are the polar coordinates in the equatorial plane,

$u = 1/r$,

$y = e/r$,

e = eccentricity of meridian section,

a = equatorial radius,

μ = ratio of mass of nucleus to mass of spheroid

For (1) there is first substituted the symbolical expression $\left(\frac{dy}{d\theta}\right)^2 = \psi(y)$, and for a slightly disturbed motion, when the disturbance does not affect the value of the areal constant, h ,

$$\left(\frac{dy}{d\theta}\right)^2 = \psi(y) + \Delta c \quad (2)$$

Since $\psi(e) = 0$ and $\psi'(e) = 0$, for a value of y slightly less than e ,

$$\left(\frac{dy}{d\theta}\right)^2 = \frac{1}{2} \psi''(e) (\delta y)^2 + \dots \Delta c \quad (3)$$

The condition for the appearance of an asymptotic spiral orbit is then,

$$\psi''(e) > 0, \quad (4)$$

and this orbit possesses the characteristic feature that $du/d\theta$, or $dy/d\theta$, has a minimum value at $y = e$ or $u = 1$, and a maximum value for some smaller value of y , corresponding to a greater distance.

¹ LINDBLAD's papers on the subject have appeared at intervals preceding 1928 in the Ark Mat Astr Fys of the K Svenska Vetensk Akad, and issued also as Ups Medd. The more important papers are Ups Medd Nos 13, 19, and 31. No 31 is Series III, Vol IV, No 7 of Handl K Svenska Vetensk Akad, and contains a summary of his preceding investigations, and diagrams showing agreement with the whorls of known spirals.

LINDBLAD then selects four values for μ : 0, $\frac{1}{2}$, 1, and 2, which give for the ratios between the central mass and the total mass the values

$$0, \frac{1}{2}, \frac{1}{2}, \text{ and } \frac{1}{2}$$

With these values of μ , and with values of ϵ equal to unity or very slightly less (e.g., for $\mu = 0$ the values $\epsilon = 1.000, 0.995, 0.980, 0.965, 0.950$, and 0.920 were successively chosen), he then performed the numerical integration of equation (1) and tabulated the resulting values of ξ and η , and from these derived the corresponding curves. Those for $\mu = 0$ were found closest to observed spiral whorls.

The equation was next integrated for $\mu = 0$ and $\epsilon = 0.995$, with the assumption of a small but finite disturbance. For this purpose the square of the area constant, h^2 , was assumed to be 10% smaller than in the first integration. The resulting curve gave better agreement and later, using $\mu = 0$ and $\epsilon = 0.965$, a quite close agreement was found for the calculated spiral and the arms of 3034 (M81). See Figure 55 and 56

The impetus necessary to cause a star to pass from its orbit on the periphery of the rotating "mother system" over into the asymptotic spiral is assigned by LINDBLAD to one of two causes:

a) It is supposed that this may result from the tidal action of exterior systems, as in BROWN's theory, producing a condensation along one axis of the system, and a corresponding rarefaction along the axis at 90° from this.

b) In the absence of sufficiently strong tidal forces, it is postulated as conceivable that the matter rotating most rapidly in the "mother system" may be ejected as a consequence of a certain type of sectorial harmonic waves analogous to that which renders the MACLAURIN ellipsoid of a homogeneous liquid "ordinarily" unstable.

While it is pointed out that either of these postulated forces need be slight enough only to cause a star to pass over the boundary into an asymptotic spiral orbit, neither cause seems entirely convincing.

Furthermore, there is a "turning point" in all of LINDBLAD's spiral orbits at a finite distance, except for the case $\mu = 0, \epsilon = 1.000$, where it is at infinity. This point marks the greatest distance from the nucleus which a star will reach in its asymptotic spiral orbit; after passing this point its distance will decrease. While there are slight inward bendings at the outer ends of the whorls of some spirals, the theory is scarcely supported by these random and infrequent irregularities, and it is legitimate to ask why this re-entrant portion of the curves is not a prominent feature of most spirals.

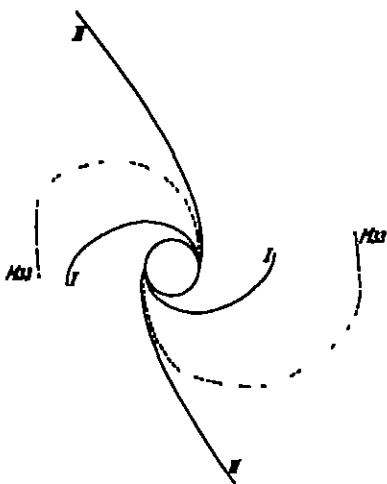


Fig 55 Theory of Spiral Structure. (LINDBLAD) Theoretical curves for $\epsilon = 0.99$, compared with the spiral arms of 598 (M33)

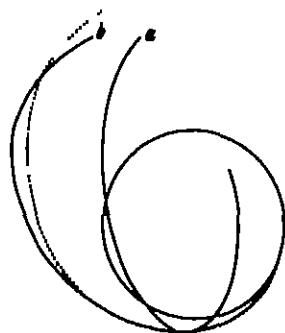


Fig. 56 LINDBLAD's Theory of Spiral Structure. The spiral arm of 3034 (M81) compared with the theoretical curve for $\epsilon = 0.97$ (dotted curve) a is the apparent arm, b, the shape of the arm in the plane of the spiral, assuming an inclination of 60°

H VOGT¹ has attempted to derive a theory which attributes the recession of the spirals and their internal mechanism to one and the same cause, a postulated "cosmic repulsion". This repulsion, from the results of HUBBLE and HUMASON, is evaluated as

$$\frac{1}{R} \frac{dR}{dt} = \alpha = 1,8 \cdot 10^{-17} \text{ sec}^{-1}$$

The equations of motion are then written in the form

$$\begin{aligned} \frac{d^2 r}{dt^2} - r \left(\frac{d\theta}{dt} \right)^2 + \frac{GM}{r^2} - \alpha^2 r &= 0, \\ \frac{d}{dt} \left(r^2 \frac{d\theta}{dt} \right) &= 0, \quad \text{or} \quad r^2 \frac{d\theta}{dt} = h, \end{aligned}$$

in which α is assumed not to vary with the time

Integration of these equations gives

$$v^2 = \frac{2GM}{r} + \alpha^2 r^2 + Ch^2,$$

while the radius of curvature is given by

$$\rho = \frac{v^3}{h \left[\frac{GM}{r^3} - \alpha^2 \right]},$$

C and h are constants of integration

When α^2 is less than GM/r^3 the orbit will be a spiral concave to the center of attraction, when α^2 is the greater, the curve will be of hyperbolic character and convex to the origin

Assembling the numerical data for 224 (Andromeda, outer portions),

$$\begin{aligned} M &= 2 \cdot 10^{12} g \\ r &= 2 \cdot 10^{22} \text{ cm} \\ G &= 6,66 \cdot 10^{-8}, \\ \alpha &= 1,8 \cdot 10^{-17}, \end{aligned}$$

he finds that $\alpha^2 (GM/r^3) = 0,02$, approximately, i. e., the spiral is here concave to the origin

VOGT's theory assumes

- 1 A "cosmic" repulsion as the "Dampfstrahl" component.
- 2 Motion outward along the spiral arms

It gives no explanation of the diametrical symmetry of the two spiral whorls. Furthermore, there should come a time when the whorls will change from a form concave to the origin to one which is convex. In the numerical example given, this will take place when r increases to a value 3,7 times its present value ($50^{1/3}$). That no spirals are found with such hyperbolic outer whorls, in fact, none with more than two or three spiral circuits, is naively attributed to the present youth of the universe

65. Theories of Spiral Structure Summary. It will be noted that the "pin-wheel" theory of the spiral arms, LINDBLAD's asymptotic spirals, JEANS' hypothesis, and all theories which postulate the ejection of matter at diametrically opposite points from a rotating spheroid, as well as VAN MAANEN's measures, seem to require motions proceeding mainly outward along the spiral arms. It is not easy to reconcile this feature of most theories with SLIPHER's direction

¹ Zur Dynamik der Spiralnebel A N 243, p 405 (1931)

of rotation of the spirals "the motion is invariably that similar to a spiral spring when it is being wound up" Equally difficult is a comparison of such theories with PRASE's rotational results. BROWN's theory of stars in a spheroidal mass, all rotating with nearly the same angular velocity, comes closest to observation in this respect.

Though the present writer does not share the philosophy of despair voiced by JEANS¹ it is perhaps fitting to close this discussion of theories of the structure of the spiral arms, none as yet entirely adequate, with a few quotations giving some of his recent views.

"It seems almost impossible to explain pure rotation dynamically in terms of known forces, and we are led to the disconcerting, but almost inevitable conjecture, that the motions in the spiral nebulae must be governed by forces unknown to us .

The only result that seems to emerge with some clearness is that the spiral arms are permanent features of the nebulae. They appear to have been formed in the process of shrinkage, two convolutions or thereabouts being formed by each nebula, and to have been perpetuated in static form ever since .

Their further interpretation forms one of the most puzzling, as well as disconcerting, problems of cosmogony

Each failure to explain the spiral arms makes it more and more difficult to resist a suspicion that the spiral nebulae are the seat of forces unknown to us, which may possibly express novel and unsuspected motrical properties of space "

66. Evolutionary Status of the Spirals. These considerations can be presented very briefly, in view of the length of the discussion to follow on the larger aspects of cosmogony raised by the spirals. There is a general agreement that the spirals are structures of a galactic nature. The larger members of the class, at least, seem to be vast congeries of suns, whose linear dimensions, masses, and total number of component stars are approximately of the same order as the similar relations in our galaxy. Our galaxy, in turn, is the most accessible spiral for study, just as our sun is the most accessible star.

Nothing is as yet definitely known as to the laws which govern the characteristic structure of the spirals, nor as to the direction of the evolutionary process exhibited in them as a class. We do not know certainly whether the process as now observed is one of formation, permanency, or disintegration. However, from the time which light takes to reach us from such enormous distances (10^6 to 10^9 or more light-years), and from the analogy of the present similar condition of that member of the class in which we are situated, the relative permanency and quasi-eternal duration of these great structures seems a certainty. It seems further self-evident that they represent the main, if not the only, course of evolution exhibited by the macroscopic cosmos as accessible to our investigation

67. Cosmogonical Deductions: Introduction. A large literature is rapidly assembling whose subject matter is the formulation of that larger cosmos of which the millions of other galaxies (the spirals) form the individual units. While the greater number of such speculations (for few would claim for these any other terminology in the present state of our knowledge) are attempts to include the spirals and their predominant characteristics of size, constitution, and tremendous velocities of recession, in some form of "relativity universæ", emphasis should here be placed upon the fact that this, at present, is not the only alternative. There are still two alternatives, and may forever be two:

1. An infinite Newtonian universe of the CHARLIER type.
2. A closed universe, infinite only in the relativity sense.

¹ Astronomy and Cosmogony, pp 351-2 (1928).

68 The CHARLIER Infinite Universe¹. There have been several vague and somewhat inchoate cosmical structures postulated by philosophers which involve the assumption of system on system (e g, LAMBERT), but these must be dismissed as hypotheses for which observational bases did not yet exist, and more or less common as a speculation among thinking men of all time

In all older astronomical treatises, and in some which are comparatively recent, we find the familiar statement that an infinite universe is an impossibility, were it infinite, the night sky should be everywhere as bright as the sun. This objection can be shown to be mathematically true, granted only that a density of stellar distribution equal to that of our galaxy be assumed to extend outward without limit. A more serious and equally cogent earlier objection to an infinite universe came from the dynamical dilemma arising from an infinite mass-total, here also it can be shown that a regularly distributed infinite universe must give rise at some point to an infinite attraction and corresponding infinite velocities

So far as is known to the writer, the first statement that these arguments against an infinite universe might be nullified by a particular and artificial arrangement of the component stars or systems is due to PROCTOR²

"But there is another way in which we may explain the darkness of the sky at night, without assuming either the extinction of light, or that occupied space is an infinitely minute speck amidst an infinity of vacant space. Assuming our system to form one of a finite number of such systems, separated from each other by distances bearing a very large ratio to the dimensions of each, and that thus a system of higher order is formed, which again forms one of a finite number of similar systems, and so on continually, the dimensions of each system of whatever order being always very small in comparison with the distance separating it from its neighbors, then there would no longer result as a necessary consequence even an appreciable illumination of the whole heavens."

OLBERS' criterion for the postulation of a uniformly luminous sky was as follows³

"So wird also nicht bloß das ganze Himmelsgewölbe von den Sternen bedeckt, sondern sie müssen noch hintereinander in unendlichen Reihen stehen, und sich untereinander wieder verdecken. Es ist klar, daß derselbe Schluß stattfindet, wenn die Fixsterne nicht gleichförmig im Raume, sondern in einzelne Systeme mit großen Zwischenräumen verteilt sind."

SEELIGER's treatment of the dilemma of infinite mass in the cosmos is contained in his paper, "Über das Newtonsche Gravitationsgesetz"⁴

"Es wird deshalb notwendigerweise zwischen den beiden Annahmen eine Wahl zu treffen sein, 1 die Gesamtmasse des Weltalls ist unermesslich groß, dann kann das NEWTONsche Gesetz nicht als mathematisch strenger Ausdruck für die herrschenden Anziehungskräfte gelten, 2 das NEWTONsche Gesetz ist absolut genau, dann muß die Gesamtmaterie des Weltalls endlich sein oder genauer ausgedrückt, es dürfen nicht unendlich große Teile des Raumes mit Masse von endlicher Dichtigkeit erfüllt sein."

¹ To call this hypothesis the LAMBERT-CHARLIER system is neither fitting nor just. The speculations of LAMBERT, KANT, and other earlier thinkers are guesses, nothing more, and too deficient in scientific character to warrant the annexing of their names. A reference to the appropriate passages in LAMBERT's *Cosmologische Briefe*, Augsburg (1761), with its assumptions of multitudes of comets, central "Regent" attracting masses, and the like, will confirm this conclusion.

E g, p 304

"Wenn die Fixsternsysteme solche Körper zu Regenten haben, ob sie nicht wieder zusammen ein größeres System ausmachen, in dessen Mittelpunkt wieder ein Regent ist, der seinen Wirkungskreis durch dieses größere System ausbreitet? Die Systeme zusammen genommen machen bereits die Milchstraße aus. Findet sich, daß jedes oder wenigstens nur eines derselben einen Regenten habe, so mag die Analogie sicher fortgehen, und die Milchstraße hat auch einen der sie ganz beherrsche und herumlenke."

² The Universe of Stars London (1878), p 67

³ BODE's Jahrb 1826

⁴ A N 137, p 122 (1895)

CHARLIER's¹ method of obviating the consequences of the criteria of OLBERS and SEELIGER may be described as a mathematical extension of the mystical speculations of early philosophers. He imagines the material elements of the cosmos arranged in a series of systems, with essential identity in the component elements of each system or stage.

Let N_1 stars, each of radius R_0 , form a galaxy, G_1 .

Let N_2 galaxies, each of radius R_1 , form a super-system of the second order, G_2 .

Let N_3 systems of the second order, of radius R_2 , form a still higher system of the third order, G_3 , etc., etc.

A distance r_i is then defined on the assumption that N_i spheres of radius r_i would be equivalent in volume to the system G_i , that is, r_i satisfies the equation

$$N_i \frac{4\pi}{3} r_i^3 = \frac{4\pi}{3} R_i^3,$$

or

$$R_i = r_i \sqrt[3]{N_i}. \quad (1)$$

Then $2r_i$ = the distance of a component in G_i to the next component.

The mass of any system will be,

$$M_i = N_i N_{i-1} N_{i-2} \dots N_1 N_0 M_0, \quad (2)$$

where M_0 is the mass of the initial element, a star.

Considering now a star G_0 which lies on the boundary of a galaxy, G_1 , and that each succeeding system in turn lies on the boundary of the next system above it, the total attraction of all such higher systems on the star G_0 will take the form:

$$\frac{M_1}{R_1^2} + \frac{M_2}{R_2^2} + \frac{M_3}{R_3^2} + \dots$$

The condition for the convergence of this series is that M_i/R_i^2 shall be less than M_{i-1}/R_{i-1}^2 , or, from equation (2):

$$\frac{R_i}{R_{i-1}} > \sqrt[3]{N_i}. \quad (3)$$

This is CHARLIER's fundamental relation, and if this inequality between the radii of the successive systems is satisfied, the total attraction of a CHARLIER universe on the given star will not be infinite, but finite. Such an arrangement will then satisfy the criterion of SEELIGER.

By a similar analysis it is further found that the criterion of OLBERS reduces to the same relation between the radii and the number of components, i.e., if this same inequality is satisfied, the total luminosity of an infinite CHARLIER universe as seen from a star thus situated will be finite in amount.

A value is next found for the total luminosity received by a star situated at the center of the lowest system, this amount is found to be greater than for any other location, and in addition the inequality satisfying the two criteria remains unchanged; hence the relative position within a system has no effect in invalidating the inequality.

If instead of the respective radii of the systems and supersystems one employs the distances between the elements of a system, $2r_i$, there results from equations (1) and (2) the following inequality which must be satisfied for both OLBERS' and SEELIGER's criteria.

$$\frac{r_i}{r_{i-1}} > N_i^{1/2} N_{i-1}^{1/6}, \quad (4)$$

¹ C. V. L. CHARLIER, How an infinite world may be built up. Ark Mat Astr Fys 16, No. 21 (1921), Lund Medd. No. 98

and this in turn will reduce to

$$\frac{r_i}{r_{i-1}} > \sqrt[N_i]{N_i}, \quad (5)$$

if the various systems are assumed to have each the same number of components

The velocity of a body at the limit of a system G_i , supposing that the velocity at infinity is zero, will be

$$v_i = \frac{h\sqrt{2\bar{M}_i}}{\sqrt{R_i}},$$

whereas the velocity at the limit of the next sub-system below will be

$$v_{i-1} = \frac{h\sqrt{2\bar{M}_{i-1}}}{\sqrt{R_{i-1}}},$$

whence

$$v_i - v_{i-1} = \sqrt[N_i]{N_i} \sqrt{\frac{R_{i-1}}{R_i}}, \quad (6)$$

resulting in the following inequality as regards the velocity necessary to satisfy the two criteria

$$v_i < v_{i-1} \sqrt[N_i]{N_i} \quad (7)$$

If a particle falls inward from the limit of a system, supposed spherical, and with initial velocity = 0, the velocity will be

$$v = \frac{h\sqrt{2\bar{M}_i}}{\sqrt{R_i}} \quad (8)$$

Now the interesting and highly significant fact in CHARLIER's theory of an infinite universe is that, so far as this is accessible at present, the arrangement of objects and systems is precisely what would be expected on such a theory. That is, we do have aggregations of 10^{10} or more stars arranged in a galaxy, while at distances relatively very great compared with the distances between the stars or the diameters of the galaxies we observe a very large number, perhaps $3 \cdot 10^7$, similar galactic structures.

It is perhaps not necessary to assume that we see more than a part of the super-system G_2 , and the existence of such higher arrangements as G_3 and G_4 must remain highly speculative. There is a natural tendency to regard the well-populated clusters of galaxies in the Coma-Virgo, Ursa Major, Centaurus groups, etc., as distinct G_2 systems. Their comparatively limited numbers (10^{12}) might be against such a deduction, and lend support to the consideration of such groups as merely local regions of greater density of population within the system G_2 . Their community of radial velocity is, however, rather a strong argument for their G_2 character, forming separate units in the super-system G_3 . See Appendix No 8.

While an effort to set up an extended CHARLIER arrangement must be regarded as merely an interesting speculation, the attempt is not without value. One needs only to be limited by approximations to the mass of a galaxy, by assumed bounds to the total number of galaxies within G_2 systems, and by permissible upper limits of velocity.

It is, of course, entirely possible to speculate upon radically different arrangements under the CHARLIER scheme, and still satisfy the inequalities which render nugatory the criteria of OLBERS and SEELIGER. As a matter of fact, the tentative scheme illustrated in Table 17, should doubtless be changed to smaller values of the number of units in a G_2 system, in view of data at hand for clusters of galaxies.

Table 17 Tentative Illustration of CHARLIER'S SYSTEM.

System	G_0	G_1	G_2	G_3
Object	Star	Spiral	Super-galaxy	Super-system
N_1	1	10^8 stars	10^6 galaxies	10^8 super-gal
M_1	$2 \cdot 10^{30}$ g	$4 \cdot 10^{40}$ g	$4 \cdot 10^{40}$ g.	$4 \cdot 10^{40}$ g
R_1	$7 \cdot 10^5$ km	$3 \cdot 10^4$ ly	10^3 ly	10^{13} Ly
Vol_1	—	$3 \cdot 10^{27}$ cm ³	$4 \cdot 10^{31}$ cm ³	$3.6 \cdot 10^{30}$ cm ³
δ_1	—	$8 \cdot 10^{-24}$	$9 \cdot 10^{-24}$	$9 \cdot 10^{-41}$
Abs. magn	+5	-15	-30?	-50?
Mean V_1	6.8 km./sec	168 km./sec.	1700 km./sec	—
Av app. magn	—	12	25	—
Av dist. apart	30 ly	10^3 ly	$3.5 \cdot 10^{13}$ ly	—
Diam at av dist.	—	$1'$	$6''$	—

Note The mass of the galaxy has been multiplied by the factor 2 to provide for non-luminous matter. The average distance apart presupposes symmetrical cubical piling. The velocity and average distances apart are for the given system in the system $\frac{1}{2} + 1$.

Using 10^8 for the number of the spirals, and 10^6 for the number of stars in a spiral, etc., CHARLIER derives the following inequality for the limiting angular diameter of a spiral.

$$\alpha < \frac{1}{N^{1/2}}$$

whence the nearest spiral to us should have an angular diameter less than $5^\circ.7$; 224 (Andromeda) is about 2° . Also, he finds that the apparent magn. of the nearest spiral should not be greater than ca. 4.5 (Andromeda, 4.6 magn.) He finds furthermore that the radius of the farthestmost spiral in the super-galaxy (with the numerical data assumed) should be smaller than $3'.4$, and it should be fainter than the 15th app. magn. His estimate of the distance of the most remote spiral, on these assumptions, is $54 \cdot 10^6$ l.y., doubtless too small, but of the order of some recent estimates. With the same initial data, he finds that the velocity of a spiral should be less than 178 times the velocity of the stars in our galaxy, giving a value less than 5300 km./sec (present maximum, +49600 km./sec)

There seems no escape from the conclusion that it is possible to arrange an infinite universe on CHARLIER'S scheme, without causing infinite luminosities or infinite velocities, and the close parallelism of his plan with the observed arrangement of the accessible visible cosmos is certainly startling. Any mean velocity for spirals or for super-galaxies composed of spirals may be provided for by the postulation of suitable values for the masses, number of units, and distances apart. It is to be noted, however, that while the CHARLIER construction can be made to provide for any mean velocity of the spirals, it must be admitted that, in its original form, it offers no explanation of the preponderance of velocities of recession. See Appendix No 8 for further treatment.

69. The Spirals and Relativity Universes: Introduction¹. The very large amount of reference material, of which the more important treatments are given below¹, on this aspect of the position of the spirals, together with the high standing

¹ A. EINSTEIN (with GROSSMANN), Entwurf einer verallgemeinerten Relativitätstheorie und einer Theorie der Gravitation. Zf Math Phys. Jan. (1914), Die formale Grundlage der allgemeinen Relativitätstheorie. Zeits. Berl (1914), p. 1030; Zur allgemeinen Relativitätstheorie, ibid. (1915), p. 778, Erklärung der Perihelbewegung des Merkur aus der allgemeinen Relativitätstheorie, ibid (1915), p. 831; Die Feldgleichungen der Gravitation, ibid (1915), p. 844; Die Grundlagen der allgemeinen Relativitätstheorie, Ann Phys 49, p. 769 (1916), also published separately by BARTH; Näherungsweise Integration der Feldgleichungen der

of the authors quoted, is a sufficient proof of the importance of this comparatively recent cosmological development, and warrants a somewhat detailed treatment

In roughest outline, the development of ideas postulating universes of the relativity type during the past thirty years has been about as follows

1 1900 SCHWARZSCHILD discusses the characteristics of non-Euclidean closed universes

2 1914-1918 EINSTEIN develops his general theory of relativity and postulates a closed cylindrical universe whose "radius" is a function of the amount of matter contained in it

Gravitation Szber Berl (1916), p 688, Kosmologische Betrachtungen zur allgemeinen Relativitätstheorie, *ibid* (1917), p 147, Kritisches zu einer von HEINRICH SITTER gegebenen Lösung der Gravitationsgleichung, *ibid* (1918), p 270, Prinzipielles zur allgemeinen Relativitätstheorie *Ann Phys* 55, p 243 (1918), The new field theory *Obs* 52, p 82 (1929), Zum kosmologischen Problem der allgemeinen Relativitätstheorie Szber Berl (1931), p 235, W DE SITTER, On the relativity of inertia *Amst Proc* 19, No 9, 10 (1917), On the curvature of space, *ibid* 20, No 2 (1918), On Einstein's theory of gravitation and its astronomical consequences *M N* 76, p 699 (1916), 77, p 155 (1916), 78, p 1 (1917), The expanding universe Discussion of Lemaitre's solution of the equations of the material field *B A N* 5, p 211 (1930), Remarks on the astronomical consequences of the theory of the expanding universe, *ibid*, 5, p 274 (1930), On the distances and radial velocities of the extra-galactic nebulae and the explanation of the latter by the relativity theory of inertia *Wash Nat Ac Proc* 16, p 474 (1930), Some further computations regarding non-static universes *B A N* 6, p 141 (1931), Do the galaxies expand with the universe? *ibid*, 6, p 146 (1931); R C TOLMAN, On the astronomical implications of the de Sitter line element for the universe *Ap J* 69, p 245 (1929), The effect of the annihilation of matter on the wave-length of light from the nebulae *Wash Nat Ac Proc* 16, p 320 (1930), On the estimation of distances in a curved universe with a non static line element, *ibid*, 16, p 409, 511 (1930), G LEMAITRE, Un univers homogène de masse constante et de rayon croissant, rendant compte de la vitesse radiale des nébuleuses extra-galactiques *Ann Soc Sc Brux* 47, p 49 (1927), translated into English in *M N* 91, p 483 (1931), On the random motion of material particles in the expanding universe Explanation of a paradox *B A N* 5, p 273 (1930), The expanding universe *M N* 91, p 490 (1931), On thermodynamic equilibrium in a non-static universe *Wash Nat Ac Proc* 17, p 153 (1931), McCREA and McVITTIE, On the contraction of the universe *M N* 91, p 128 (1930), *Proc Edinb Math Soc* (2) 2, part 3 (1931), G C McVITTIE, The problem of n bodies and the expansion of the universe *M N* 91, p 274 (1931), A S EDDINGTON, On the instability of Einstein's spherical world *M N* 90, p 668 (1930), cf *Nat* 125, p 850 (1930), On the significance of Einstein's gravitation equations in terms of the curvature of the world *Phil Mag* (6) 42, p 800 (1921), 43, p 174 (1922), K SCHWARZSCHILD, Über den zulässigen Krümmungsradius des Raumes *V J S* 35, p 337 (1900); H D ROBERTSON, On the foundations of relativistic cosmogony *Wash Nat Ac Proc* 15, p 822 (1929), A FRIEDMAN, *Z f Phys* 10, p 377 (1922), P HARZER, Über die astronomischen Ergebnisse der allgemeinen Relativitätstheorie *A N* 227, p 81 (1926), K LANZOS, Über eine stationäre Kosmologie im Sinne der Einsteinschen Gravitationstheorie *Z f Phys* 12, p 73 (1924), Über die Rotverschiebung in der de Sitterschen Welt, *ibid*, 17, p 168 (1923), V FRIEDRICHSEN u A SCHUCHTER, Notiz zur Frage nach der Berechnung der Aberration und Parallaxe in Einsteins, de Sitters und Friedmans Welten in der allgemeinen Relativitätstheorie *Z f Phys* 51, p 584 (1928), K LUNDMARK, The determination of the curvature of space-time in de Sitter's world *M N* 84, p 747 (1924), H VOGT, Die Instabilität der Welt *A N* 241, p 247 (1931), Die kosmologische Deutung der Spiralnebel, *ibid*, 242, p 181 (1931), J CRAZY, Effet Doppler-Fizeau dans l'univers de de Sitter *C R* 183, p 1093 (1926), C WIRZ, De Sitters Kosmologie und die Radialbewegungen der Spiralnebel *A N* 222, p 21 (1924), F SFLERTY, Beiträge zum kosmologischen Problem *Ann Phys* (4) 68, p 281 (1922), F ZWICKY, On the red shift of spectral lines through interstellar space *Wash Nat Ac Proc* 15, p 773 (1929), *Phys Rev* (2) 33, p 1077 (1929), L SILBERSTEIN, The determination of the curvature radius of space-time *M N* 85, p 285 (1925), cf *ibid*, 84, p 747 (1924), The curvature of de Sitter's space-time derived from the globular clusters, *ibid*, 84, p 363 (1924), New determination of the radius of space-time *Pop Astr* 38, p 92 (1930), The radial velocities of globular clusters and de Sitters cosmology *Phil Mag* (6) 47, p 907 (1924), *Nat* 113, p 350, 602, 818 (1924), 114, p 347 (1925), 125, p 850 (1930), The size of the universe, attempts at a determination of the curvature radius of space time, Oxford Press, (1930), VIII +215 pp.

3. 1917—1929. DE SITTER, FRIEDMAN, TOLMAN, and others, develop further the idea of an EINSTEIN closed, static universe, with excess of positive velocities among distant objects

4. 1927—1930 LEMAITRE finds a paradox in the static EINSTEIN universe, and shows that it must be expanding. The latest papers of DE SITTER accept the idea of an expanding universe, and it is enthusiastically adopted by EDDINGTON

"Hence the radius of the universe has expanded by one part in 2000 in the last million years. The result is impressive. It indicates that the radius of space has doubled within ordinary geological time. We conclude that the radius of space was originally about $1.2 \cdot 10^{11}$ ly. that it has since expanded considerably, but to an amount practically undeterminable, and that its present rate of expansion is 1 per cent in about 20 million years—a rate which will continue indefinitely. The universe is now doubling its radius every 1400 million years and this rate will, if anything, slightly increase in the future. In 10^{10} years the spiral nebulae will be 10 magnitudes fainter than they are now. With a time scale of billions of years, astronomers must count themselves extraordinarily fortunate that they are just in time to observe this interesting but evanescent feature of the sky" (1) [M N 9], p. 677 (1930)]

5. 1929—1930. TOLMAN discusses the DE SITTER line element with rigor, and finds that the earlier conclusions as to uniform excess of velocities of recession are less inevitable than earlier held.

"The conclusion is drawn that the DE SITTER line element does not afford a simple and unmistakably evident explanation of our present knowledge of the distribution, distances, and Doppler effects for the extra-galactic nebulae" [Ap J 69, p. 245 (1929)]

6. 1930. Basing their investigation upon the line element of a universe containing matter scattered throughout and, in addition, with a concentration of matter around the origin, two Scotchmen, MCCREA and MCVITTIE, come to the conclusion that a contraction process is as probable as one of expansion.

"It seems therefore that a condensation starting in an EINSTEIN universe would cause this universe to contract. . . We must conclude that if the actual universe started as an EDDINGTON universe and is now expanding, as the work of LEMAITRE and EDDINGTON suggests, this expansion can not have been caused by a redistribution of the matter into massive nuclei. Thus, as yet, no mechanism for setting up the expansion has been found."

SCHWARZSCHILD's initial paper on this general subject is an academic discussion of the possibility of various types of hyperspace rather than a treatment along relativity lines. By making estimates of the lowest limits of error in angular measurements now attainable, he derives the corresponding limiting dimensions for several forms of hyper-space. In the case of hyperbolic hyper-space, he shows that any radius of curvature larger than ca. 63 ly. would be difficult to detect by present methods. In elliptical hyper-space the corresponding minimum detectable radius of curvature is found to be ca. 2500 Ly., with a "distance around the world", πR , of $8 \cdot 10^{11}$ ly.

The EINSTEIN field equations are now available in many treatises (see references quoted). The general course of the historical development of these theories as relating to the excess of velocities of recession among the spirals has already been outlined. A complete study of this entire development would involve, first, a large amount of repetition in the treatment of the line element by the various investigators, combined with some measure of confusion due to occasional differences in mathematical nomenclature, and, secondly, such a treatment would in many cases, for completeness, be involved with discussions of the relativity effects adduced for the deflection of light in a gravitational field, and the shift of the FRAUNHOFER lines to the red in such fields: questions which are of interest in other fields of astronomical investigation, but in no way germane to the present problem of the spirals.

For these and other reasons, the detailed treatment of the work done by the multitude of investigators will be greatly abridged, and will be replaced with a somewhat composite treatment drawn in the main from two or three of the latest workers in this subject a method which has some elements of the illogical, but also many advantages on the score of convenience and brevity.

The investigation chosen to represent the EINSTEIN-DE SITTER universe will be that of TOLMAN¹. Several reasons have motivated this choice. TOLMAN's paper is one of the latest in point of time, and is definitely restricted to the problem set by the large positive velocities of the spirals. Furthermore, it not only possesses great clarity of treatment, but it appears to the present writer to display a commendable and judicial saneness, in that no all-embracing inspiration is claimed, but difficulties are frankly emphasized.

The subsequent theory of a necessarily expanding universe, as treated originally by LEMAITRE and FRIEDMAN, and also by TOLMAN on the theory of the annihilation of matter, will be drawn mainly from LEMAITRE's original paper on the subject, and also from recent papers of EDDINGTON and DE SITTER. Following a description of these methods of treatment, a summary will be given of the radii of various postulated relativity universes.

70. TOLMAN's Critique of the DE SITTER Relativity Universe TOLMAN employs DE SITTER's form of the line element, as derived from EINSTEIN's generalized equation

$$-8\pi T = G_{\mu\nu} - \frac{1}{2}Gg_{\mu\nu} + \lambda g_{\mu\nu},$$

and the line element itself is an expression in angular variables of an element on the surface of a four-dimensional sphere of radius R

$$ds^2 = -R^2[d\omega^2 + \sin^2\omega\{d\xi^2 + \sin^2\xi\{d\theta^2 + \sin^2\theta d\varphi^2\}\}].$$

Substituting the variables ω and ξ by

$$\cos\omega = \cos\chi\cos\iota t,$$

$$\cot\xi = \cot\chi\sin\iota t,$$

and placing further

$$\sin\chi = r/R,$$

the equation of the line element is written in the form

$$ds^2 = \frac{1}{1-r^2/R^2}dr^2 - r^2d\theta^2 - r^2\sin^2\theta d\varphi^2 + (1-r^2/R^2)dt^2. \quad (1)$$

The geodesic equations will take the following forms from the norm form (after EDDINGTON)

$$\frac{d^2x_\alpha}{ds^2} + (\mu\nu, \alpha) \frac{dx_\mu}{ds} \frac{dx_\nu}{ds} = 0, \quad (2)$$

$$\frac{d^2r}{ds^2} + \frac{1}{2} \frac{dr}{dr} \left(\frac{dr}{ds} \right)^2 - r e^{-\lambda} \left(\frac{d\varphi}{ds} \right)^2 + \frac{1}{2} e^{\nu-\lambda} \frac{dr}{dr} \left(\frac{dt}{ds} \right)^2 = 0. \quad (3)$$

This is integrated best by substitution of the values found from (5) and (6), finding the equation

$$\frac{dr}{ds} = \pm \sqrt{h^2 - 1 + \frac{r^2}{R^2} - \frac{h^2}{r^2} + \frac{h^2}{R^2}}. \quad (A)$$

¹ Ap J 69, p 245 (1929)

With $\alpha = 2$ the geodesic equation is that of a particle moving in the plane $\theta = \pi/2$, with $d\theta/ds = 0$, in accordance with the equations:

$$\frac{d\theta}{ds} = 0, \quad \frac{d^2\theta}{ds^2} = 0, \quad \theta = \frac{\pi}{2}, \quad (4, B)$$

$$\frac{d^2\varphi}{ds^2} + \frac{2}{r} \frac{dr}{ds} \frac{d\varphi}{ds} = 0, \quad (5)$$

the integral of which is:

$$\frac{d\varphi}{ds} = \frac{h}{r^2}, \quad (C)$$

$$\frac{d^2t}{ds^2} + \frac{dr}{ds} \frac{dr}{ds} \frac{dt}{ds} = 0. \quad (6)$$

The integration of (6) gives:

$$\frac{dt}{ds} = k e^{-r} = \frac{k}{1 - r^2/R^2}. \quad (D)$$

In the above, h and k are the constants of integration; h can assume positive or negative values according to the direction of motion of the particle, while k , a time-like constant, can be only positive unless time is supposed reversible. For the special case of light, both h and k become infinite.

The form of the orbit is obtained by dividing (C) by (A), with rearrangement of terms:

$$d\varphi = \frac{h dr}{r^2 \sqrt{\frac{r^2}{R^2} + \left(k^2 - 1 + \frac{h^2}{R^2}\right) - \frac{h^2}{r^2}}}. \quad (7)$$

This is the form of the relation, in Newtonian mechanics, applying to the shape of the orbit due to a central repulsive force proportional to the radius r . Hence in the DE SITTER universe the orbits of free particles are in general curved away from the origin.

Perihelion of the particle will be found by making $dr/d\varphi = 0$. Hence perihelion will be obtained by making the quantity under the radical sign in (7) equal to zero, or:

$$k^2 - 1 + \frac{r_m^2}{R^2} - \frac{h^2}{r_m^2} + \frac{h^2}{R^2} = 0. \quad (8)$$

The velocity of motion of the particle in its orbit will be:

$$\frac{dr}{dt} = \pm \frac{(1 - r^2/R^2)}{k} \sqrt{k^2 - 1 + \frac{r^2}{R^2} - \frac{h^2}{r^2} + \frac{h^2}{R^2}}. \quad (9)$$

From the equation of the original line element, putting $ds^2 = 0$, the purely radial velocity of light becomes:

$$dr/dt = \pm (1 - r^2/R^2). \quad (10)$$

In both the preceding expressions the velocity becomes zero at $r = R$. Hence all movement ceases at the radius R from the origin. Furthermore, since the integral of (10) shows that light would take an infinite time to travel over the radius R , we can never have any information of events happening at R or beyond, and hence may speak of a horizon to the universe at this distance.

TOLMAN determines the DOPPLER shift in two ways, with the origin at the observer, and with the origin at the source. In the first of these methods, the period of emission, from equation (E), will be:

$$dt_o = \frac{h}{1 - r^2/R^2} ds, \quad (11)$$

during which the source will have moved the radial distance

$$dr = \frac{d}{dt} dt = \frac{h}{r^2 K^2} \frac{d}{dt} dt, \quad (12)$$

and, by equation (10) for the velocity of light, the time taken by light to traverse the distance will be

$$dt_0 = \frac{h}{1 - r^2/K^2} \frac{d}{dt} dt.$$

Hence the period of the light arriving at the origin will be

$$dt_0 = \frac{h}{1 - r^2/K^2} \frac{d}{dt} dt \pm \left(1 - \frac{h}{r^2 K^2}\right) \frac{d}{dt} dt, \quad (13)$$

where the plus sign applies to receding objects. As the period dt_0 is proportional to the wave-length observed at the origin and dt to the emitted wave-length, equation (13) may be rewritten in the form

$$\frac{dt_0}{dt} = \frac{h}{1 - r^2/K^2} \pm \left(1 - \frac{h}{r^2 K^2}\right) \frac{d}{dt} dt = 1. \quad (14)$$

Substituting from equation (9), the Doppler shift is obtained in terms of the parameters of the orbit and the distance alone

$$\frac{dt_0}{dt} = \frac{h \pm \sqrt{h^2 - 1 + \frac{r^2}{K^2} - \frac{h^2}{K^2}}}{1 - r^2/K^2} = 1. \quad (15)$$

For the Doppler shift with the source at the origin, (14) will take the form

$$\frac{dt_0}{dt} = \frac{1 - r^2/K^2}{h \mp \sqrt{h^2 - 1 + \frac{r^2}{K^2} - \frac{h^2}{K^2}}} = 1. \quad (16)$$

By putting $dr/dt = 0$ in equation (14), the Doppler effect of the source at perihelion at the time of emission is

$$\frac{dt_0}{dt} = \frac{h}{1 - r_m^2/K^2} = 1, \quad (17)$$

where r_m is the distance from the origin to perihelion, and this equation, by the application of (8) can be rewritten in the form

$$\frac{dt_0}{dt} = \frac{\sqrt{1 - \frac{r_m^2}{K^2} + \frac{r_m^2}{K^2} - \frac{h^2}{K^2}}}{1 - r_m^2/K^2} = 1. \quad (18)$$

Since h^2 is not its negative and K^2 is larger than r_m^2 , this may be written in the inequality

$$\frac{dt_0}{dt} \geq \frac{1}{1 - r_m^2/K^2} = 1, \quad (19)$$

or, expanding and neglecting higher order terms

$$d\lambda/\lambda = r_m^2/2K^2, \quad (20)$$

whence the Doppler effect at perihelion is positive, and would ordinarily be interpreted as a velocity of recession.

However, it is not always positive, and the most valuable part of Tolman's analysis is his determination of the approximate relative durations of the positive and negative Doppler effects of the moving particle in such a universe.

The equations of motion in a DE SITTER universe are completely reversible, as was first pointed out by SILBERSTEIN, and there seems no *a priori* reason why the number of positive and negative velocities among the spirals should not be approximately equal. TOLMAN therefore next investigates the conditions for a reversed DOPPLER effect, i. e., as a particle in a DE SITTER universe, though at rest at perihelion, will give the effect of a positive velocity of recession, over what range of its orbit will this positive velocity effect be of sufficient magnitude to cancel its negative velocity as it approaches perihelion?

In order to investigate the range of such a reversed DOPPLER effect, $d\lambda/\lambda$ is set equal to zero in equation (15), giving as the condition for the radius r_1 , at which reversal takes place:

$$\frac{r_1}{R^2} - \frac{h^2}{r_1^2} = 2 - 2k,$$

while equation (8) gives as the condition for perihelion

$$\frac{r_p^2}{R^2} - \frac{h^2}{r_p^2} = 1 - k^2 - \frac{h^2}{R^2},$$

so that the reversed DOPPLER effect will be produced when an approaching source lies in the range between r_1 and r_p . Since it is found later that k is of the order unity, and h^2/R^2 of the order zero, the range of such a reversed DOPPLER effect will be small. Taking the radius r_p at which an oncoming source would come into observation as twice the distance to perihelion, which in its turn is taken as one-tenth of the distance to the horizon, which will give a DOPPLER shift at perihelion, $d\lambda/\lambda = 0.005$, the fraction of the time of approach to perihelion during which the particle would lie within the range which produces the reversed effect is only about $1/100$ (0.038).

As possible explanations of the facts observed in the spirals, TOLMAN considers in detail some four hypotheses:

A. The Hypothesis of Continuous Entry. Here the uniform concentration of spirals within our observation would be produced by the continuous arrival of new objects to take the place of those which have passed perihelion and will never return. On this hypothesis, as the range of the reversed DOPPLER effect has been shown to be so small, there should be nearly an equality of the velocities of approach and recession. Only by making some rather radical assumptions as to the numbers of spirals which make perihelion at different distances from the origin, and making the assumption that the number of spirals which make perihelion at a given radius increase very rapidly with the radius, can the excess of velocities of recession be accounted for. A linear increase of DOPPLER effect with distance is possible, but in no way inevitable. The radius of the observable universe must be at least ten times the range of distances at which spirals are now observed, as otherwise higher values would be expected than have been observed (order of 0.01). R would therefore not be less than $2 \cdot 10^6$ l.y.

B. The Hypothesis of Continuous Formation. The process of formation would be a continuing one, which will permanently maintain an approximately uniform concentration of the spirals. This idea is abandoned as having little inherent probability. R on this hypothesis would be about $2 \cdot 10^6$ l.y.

C. The Hypothesis of a Concentrating Fluctuation. This assumes that the present concentration is the result of a fluctuation from a smaller general concentration, which has occurred some time in the past. The chief demerit of this hypothesis is its appeal to some sort of special fluctuation in the concentration to account for the observed facts.

D The Hypothesis of Recent Formation, seems even more improbable than that of continuous formation, and for that reason may be abandoned at once

The conclusion which TOLMAN draws from his investigation is that the DE SITTER universe gives us no simple, adequate and, more than all, inevitable explanation of the facts exhibited by the spirals. In particular, he shows that only by rather drastic ad hoc specifications can this assemblage of data be explained at all. In detail, it can not be regarded as a satisfactory mechanism for the production of the present excess of large velocities of recession.

71 An Expanding Relativity Universe the Work of LEMAITRE, EDDINGTON, McCREA, and McVIRNIE. If the spherical universe is to be permanent and unchanging, the solutions of EINSTEIN and DE SITTER are both permissible. ROBERTSON, and others, have shown that these are the only two possible solutions under such a condition. LEMAITRE has shown, however, that these universes are intrinsically unstable. That of EINSTEIN has been described as containing "all the matter it can hold", while that of DE SITTER is empty of matter. EDDINGTON points out that there are an infinity of solutions for a spherical universe which is not in equilibrium, and that to every expanding solution there corresponds an individual contracting solution.

LEMAITRE places the pressure, p , equal to zero, while ρ is the density of the total energy. The density of the radiant energy will be 3ρ , and the density of the energy concentrated in matter, $\delta = \rho - 3\rho$. δ is identified with T , while ρ and $-p$ are identified with the components T^1_1 and $T^1_1 = T^2_2 = T^3_3$ of the tensor of material energy. The components of the contracted Riemannian tensor are calculated for the interval:

$$ds^2 = -R^2 d\sigma^2 + dt^2 \quad (1)$$

Here $d\sigma$ is the element of length in a space of radius unity, R is the radius of space, and is a function of the time. This feature is the essential advance of LEMAITRE's analysis, and has been followed in the latest papers of TOLMAN, EDDINGTON, and DE SITTER.

The equations of the gravitational field are written

$$3 \frac{1}{R^2} \left(\frac{dR}{dt} \right)^2 + \frac{1}{R^2} = \lambda + 8\pi\rho, \quad (2)$$

$$\frac{2}{R^2} \frac{d^2 R}{dt^2} + \frac{1}{R^2} \left(\frac{dR}{dt} \right)^2 + \frac{1}{R^2} = \lambda - 8\pi\rho. \quad (3)$$

In the above, λ is a cosmological constant whose precise value (or even its precise signification) is unknown, it is, however, very small. 8π is EINSTEIN'S constant, which is written κ by LEMAITRE.¹

A solution is then sought for the case where the mass of the universe remains constant while the radius increases. Calling this total mass $M = V\delta$ and placing $8\pi\delta = \alpha/R^3$, where α is a constant, and by aid of the relation $\rho = \delta + 3\rho$, the principle of the conservation of energy becomes

$$3d(pR^2) + 3\rho R^2 dR = 0. \quad (4)$$

¹ 8π is a constant in "natural" units. Some values in the natural and in the CGS system which are frequently employed in such investigations are

EINSTEIN'S constant	$8\pi = 1.87 \cdot 10^{-27} \text{ c. g. s.}$
Gravitation constant	$k = 6.675 \cdot 10^{-8}$
Unit mass	$= 4.045 \cdot 10^{33}$
Sun's radius in light-seconds	$= 2.32$
Mass of sun	$= 1.48 \text{ km.}$

Placing β as the constant of integration, this is integrated to

$$8\pi p = \frac{\beta}{R^4}, \quad (5)$$

and hence.

$$8\pi q = \frac{\alpha}{R^3} + \frac{3\beta}{R^4}. \quad (6)$$

Substituting these values in (2), he derives

$$\frac{1}{R^3} \left(\frac{dR}{dt} \right)^3 = \frac{\lambda}{3} - \frac{1}{R^3} + \frac{8\pi q}{3} = \frac{\lambda}{3} - \frac{1}{R^3} + \frac{\alpha}{3R^3} + \frac{\beta}{R^4}, \quad (7)$$

where,

$$t = \int \frac{dR}{\sqrt{\frac{\lambda R}{3} - 1 + \frac{\alpha}{3R} + \frac{\beta}{R^2}}}. \quad (8)$$

Placing α and β equal to zero and integrating, the solution of DE SITTER is found:

$$R = \sqrt{\frac{3}{\lambda}} \cosh \sqrt{\frac{\lambda}{3}} (t - t_0). \quad (9)$$

EINSTEIN's solution will be found by making $\beta = 0$ and $R = a$ constant. Since dR/dt and d^2R/dt^2 then become $= 0$ in (2) and (3), and

$$\frac{1}{R^3} = \lambda, \quad \frac{3}{R^3} = \lambda + 8\pi q; \quad q = \frac{2}{8\pi R^3},$$

whence.

$$R = 1/\sqrt{\lambda}; \quad 8\pi q = 2/R^3, \quad (10)$$

and, from (3)

$$\alpha = 8\pi q R^3 = 2/\sqrt{\lambda}. \quad (11)$$

For EINSTEIN's solution, (11) is not enough, the initial value of dR/dt must also be equated to zero. Putting

$$\lambda = 1/R_0^2, \quad (12)$$

and $\beta = 0$ and $\alpha = 2R_0$ in (8), there results:

$$t = R_0 \sqrt{3} \int \frac{dR}{R - R_0} \sqrt{\frac{R}{R + 2R_0}}. \quad (13)$$

Writing

$$8\pi q = 2/R^3, \quad (14)$$

there results from (11) and (12).

$$R^3 = R_E^3 R_0. \quad (15)$$

The value of R_E = the radius of the universe, deduced from the mean density on EINSTEIN's formula (14), has been estimated at $8.8 \cdot 10^{10}$ Ly.

In order to find the DOPPLER effect for a universe of increasing radius, the equation of a ray of light from the line element (1) takes the form.

$$\sigma_2 - \sigma_1 = \int_{t_1}^{t_2} \frac{dt}{R}, \quad (16)$$

where σ_1 and σ_2 are coordinates characterizing the position in space, σ_2 being the position of the observer and σ_1 that of the source. A slightly later ray will leave σ_1 at the time $t_1 + \delta t_1$, and arrive at σ_2 at the time $t_2 + \delta t_2$. Whence:

$$\delta t_2/R_2 - \delta t_1/R_1 = 0, \quad \text{and} \quad \delta t_2/\delta t_1 - 1 = R_2/R_1 - 1, \quad (17)$$

where R_1 and R_2 are the values of R at the times t_1 and t_2 . t is the proper time, if δt_1 is the period of the emitted light, δt_2 is the period of the light received. Thence

$$\frac{v}{c} = \frac{\delta t_2}{\delta t_1} - 1 = \frac{R_2}{R_1} - 1, \quad (18)$$

which is the measure of the apparent DOPPLER effect due to the variation in the radius of the universe. It is equal to the excess over unity of the ratio of the radii of the universe at the time when the light is emitted and the time when it is received.

When r is placed for the distance of the source the approximate relation holds

$$\frac{1}{R} \frac{dR}{dt} = \frac{v}{cr} \quad (19)$$

Utilizing the radial velocities of 42 spirals, and taking out a solar motion of 300 km/sec in the direction, $\alpha = 315^\circ$, $\delta = +62^\circ$, LEMAITRE then derives a mean distance of $3.2 \cdot 10^6$ ly, and a variable radial velocity which amounts to 190 km/sec at 10^6 ly. Using equation (19), this gives

$$\frac{625 \cdot 10^5}{10^6 \cdot 3.08 \cdot 10^{18} \cdot 3 \cdot 10^{10}} = 0.68 \cdot 10^{-27} \text{ cm}^{-1}.$$

From this, by transformation and substitution in (13), (15), and (23), LEMAITRE derives the value

$$R_0 = 9 \cdot 10^6 \text{ ly}$$

By substituting,

$$x^2 = \frac{R}{R + 2R_0},$$

the integral of (13) is transformed to

$$t = R_0 \sqrt{3} \int \frac{4x^2 dx}{(1-x^2)(3x^2-1)} = R_0 \sqrt{3} \log \frac{1+x}{1-x} + R_0 \log \frac{\sqrt{3}x-1}{\sqrt{3}x+1} + C', \quad (20)$$

and designating by σ the fraction of the radius of the universe traversed by the light in the time t , and using (16),

$$\sigma = \frac{dt}{R} = \sqrt{3} \int \frac{2dx}{3x^2-1} = \log \frac{\sqrt{3}x-1}{\sqrt{3}x+1} + C'', \quad (21)$$

from which LEMAITRE has derived the following table for σ and t as functions of R/R_0 . The constants of integration in Table 18 were chosen so that σ and t

Table 18 DOPPLER Effect in LEMAITRE'S Expanding Universe

R/R_0	t/R_0	σ in degrees	v/c
1	$-\infty$	$-\infty^\circ$	19
2	-4.31	-51	9
3	-3.42	-30	5.7
4	-2.86	-21	4
5	-2.45	-15	3
10	-1.21	-5	1
15	-0.50	-1.7	0.33
20	0	0	0
25	+0.39	1	
∞	∞	5	

should be zero for $R/R_0 = 20$. The last column of the table gives the DOPPLER effects calculated from formula (19).

The shifts are seen to be excessive for all values of R/R_0 less than 10, as LEMAITRE well expresses it, there need be no speculation as to the formation of mirror or phantom images of the spirals or suns because, entirely aside from any questions of absorption of light in space, such

images, if received, would be displaced several octaves into the infra-red!

These results of LEMAITRE, obtained in 1927, have been the norm of most work in this field since that date, and his conclusions may be summarized

1 The mass of the universe is constant, and is connected with the cosmological constant, λ , through EINSTEIN's relation.

$$\sqrt{\lambda} = \frac{2\pi^2}{8\pi M} = \frac{\pi}{4M} = \frac{1}{R_0}$$

2 The radius of the universe increases without limit from an asymptotic R_0 for $t = -\infty$.

3 The recession of the extra-galactic objects is a cosmical effect of the expansion of space, and permits the derivation of a value for R_0 .

4 The radius of the universe is of the same order as that deduced from the density by EINSTEIN's formula

$$R = R_E \sqrt[3]{\frac{R_0}{R_E}} = \frac{1}{5} R_E.$$

EDDINGTON transforms the foregoing formulae into:

$$\frac{dR}{dt} = \sqrt{\frac{R^2 \lambda}{3} - 1 + \frac{4M}{3\pi R}},$$

and points out that there are three cases which may arise 1. If $M > M_E$, the system can expand continuously from a very small to a very large radius. 2. If $M < M_E$, the right-hand side of the equation vanishes for two positive values of R , and is imaginary between these values. Hence the world will either start with a finite velocity of expansion and expand to one of these values of R , or it will start with a finite velocity of contraction, and contract to the other of these values. 3. The limiting case is when $M = M_E$. As $R \rightarrow R_E$, $dR/dt \rightarrow 0$ like $(R - R_E)$, hence the time that the radius remains in the neighborhood of R_E is logarithmically infinite.

EDDINGTON secures the spectral shift by the relation:

$$0 = \frac{\delta t}{R(t_0)} - \frac{\delta t}{R(t)},$$

where $R(t)$ is the radius of the world at the time t , hence:

$$\frac{\delta t_0}{\delta t} = \frac{R(t_0)}{R(t)}$$

Taking the red-shift of the spirals as determined by HUBBLE as 153 km./sec. per 10^6 ly, he finds that this expansion amounts to about 1/2000 of the velocity of light. Hence $\delta t_0/\delta t = 2001/2000$ for an interval $t_0 - t = 10^6$ years. From this relation, the radius of the universe is considered to have expanded by 1 part in 2000 in the last million years. EDDINGTON places the total mass of such a universe at:

$$1.1 \cdot 10^{28} \odot = 2.3 \cdot 10^{55} \text{ g}$$

$$\text{"Radius"} = 1.2 \cdot 10^6 \text{ ly.}$$

DR SITTER's values of the "initial" and "present" radii of the universe are, respectively, 0.8 and $1.6 \cdot 10^6$ ly.

That the universe is not only as likely to contract as expand (as admitted also by EDDINGTON), but that it must in fact contract if there exists a single condensation at the origin, was maintained by MCCREA and McVITTIE. If the start were made with an EINSTEIN universe, and a condensation allowed to form, they maintained in their original paper that a process of contraction would be set up, which would persist indefinitely. They have since¹ discovered an error in the analysis which led them to this theory, and now conclude that the total

¹ Obs 64, p 267 (1931)

volume of space is not altered to the first approximation by the change in the distribution of matter

In his latest paper EINSTEIN has discussed non-static relativity universes, and has expressed a preference for a solution corresponding to a value $\lambda = 0$ for the "cosmological constant" DE SITTER shows that a family of oscillating universes result, and has investigated these in his most recent paper in the B A N 6, p 141 (1931)

He makes the assumptions that the total mass of the universe, M , is constant and that the pressure is zero, from which the field equations reduce to the single form

$$\frac{1}{R^3} \left(\frac{dR}{dt} \right)^2 + \frac{1}{R} = \frac{1}{3} \lambda + \frac{R_1}{R^3},$$

where $R_1 = \alpha/3 = \kappa M/3\pi^2$ Placing

$$y = \frac{R}{R_1}, \quad t = \frac{ct}{R}, \quad \text{and} \quad \gamma = \frac{1}{3} R_1^2 \lambda,$$

the equation becomes

$$\frac{dy^2}{dt} = \frac{1}{y} - 1 + \gamma y^2$$

The solutions of this equation are investigated graphically, with the aid of the relation

$$p = 1 - y + \gamma y^3$$

If γ is greater than $4/27$, there is but one solution in which y increases from zero to infinity, i.e., an expanding universe

For $0 \leq \gamma \leq 4/27$, there are two solutions, in one of which y increases from y_2 to infinity, and oscillates between the limits 0 and y_1 , y_1 and y_2 being the two points on the curve $p = 0$ where γ has the prescribed value, and $y_1 < 1, 5 < y_2$ There are then two families of solutions, a type of expanding universes, for positive values of γ , and the oscillating universes, for values of γ smaller than $4/27$

Very significant are DE SITTER's comments on the not very successful attempts to correlate the "expansion times" of such universes and present beliefs as to the time scale of stellar evolutionary processes.

"... the time scale of the evolutionary processes can only be formally fitted into the scheme of the expanding universe by means of such a tremendous extrapolation as to deprive the theory of all real meaning This is only another way of expressing the utter impossibility, which has already been repeatedly pointed out, of reconciling the short time scale of the expanding universe with our ideas regarding the evolution of stars and stellar systems In the theory of relativity a year and a light-year are equivalent, whilst in astronomy 10^9 light-years is a very large distance, but 10^9 years is a short time"

DE SITTER also derives expressions which indicate that while there is a quasi-expansion effect within a galaxy, this is so very much slower than the expansion of the universe as a whole as to be practically entirely negligible

72. The Size of the Universe According to SILBERSTEIN Radically different conclusions as to the dimensions of the curvature of space-time have been derived by SILBERSTEIN in his book, "The Size of the Universe" (1930) In this work he has collected and revised his earlier articles in scientific periodicals, and it thus forms the most accessible summary of his views The book contains one of the clearest and best introductions to the methods of tensor manipulation and analysis as yet available in English (see also the same author's article, TENSOR, in the Encyc. Brit.). Among the faults of the book are its marked polemic tendency, the apparent total rejection of modern results as to the distances of

the spirals, and the fact that most of the largest of the spiral velocities could not be included at the time the book went to press. It contains, however, valuable criticisms as to the validity of the EINSTEIN and DE SITTER universes, the author was the first to point out that negative velocities should be as apt to occur as positive ones; furthermore, SILBERSTEIN's method of attack differs from that of all other investigators in that he has applied his formulae to galactic objects.

SILBERSTEIN's development and method of attack is set forth in part V of the work referred to, to which reference should be made. His method consists essentially in the application of statistical methods for large groups of data, involving relations connecting the distance of perihelion, the speed which the object has in passing through perihelion, and the distance of the objects from the observer.

For 20 clusters, he derives a value of the curvature radius, $R = 10^8$ ly. For 38 spirals employed, he points out that R would be from 1 to $2.3 \cdot 10^9$ ly., but is unwilling to accept. From 29 Cepheids he secures $R = 4.7 \cdot 10^8$ ly. Using 459 stars from YOUNG and HARPER's list¹, he finds $R = 6.4 \cdot 10^8$ ly. He finally adopts (p. 242, as of date of 1929) $6.27 \cdot 10^8$ ly. This is roughly one-twentieth of the distances assigned by other investigators to the Coma-Virgo and Centaurus groups of external galaxies! The present writer feels that SILBERSTEIN's values for the "dimensions" of space are inordinately small, and that they will not stand the test of comparison with modern cosmical data, even if the inevitableness of some form of closed relativity universe be granted.

73. Various Determinations of the "Radius" of Space-Time.

Table 19 Values of Radius of Curvature of Space-Time

Author	R, Ly.	Mass, g	Date
DE SITTER	$1.4 \cdot 10^7$	$1.4 \cdot 10^{58}$	1917
SILBERSTEIN,	10^8		1924
HUBBLE	$1.5 \cdot 10^{11}$	$9 \cdot 10^{58}$	1926
LEMAITRE	$9 \cdot 10^8$		1927, initial value
EDDINGTON	$1.2 \cdot 10^9$	$2.3 \cdot 10^{58}$	1930
TOLMAN, more than	$2 \cdot 10^8$		1929
DE SITTER	$0.8 \cdot 10^9$	10^{58}	1930, initial value
DE SITTER	$1.6 \cdot 10^9$		1930, present value
SILBERSTEIN,	$5.1 \cdot 10^8$		1929, O-stars
SILBERSTEIN	$4.8 \cdot 10^8$		1929, Cepheids
SILBERSTEIN	$6.4 \cdot 10^8$		1929, 459 stars

The values range from $4.8 \cdot 10^8$ ly. (SILBERSTEIN) to $1.5 \cdot 10^{11}$ ly. (HUBBLE), though most investigators have postulated values of the order of 10^9 ly. Were the present writer to accept some form of closed universe as inevitable, he would regard a radius of the order of 10^{11} ly. as the minimum admissible.

74. Summary: the Dilemma of Choice between an Expanding Relativity Universe and the Distance-Velocity Correlation. The recent history of theories of relativity universes has passed through a stage of great confidence, perhaps over-confidence, in which considerable finality was thought to have been attained. As far as certainty is in consideration, its present condition does not appear quite so satisfactory. Omitting for the present other possible theories of Newtonian character, to be discussed later, there seems a partial dilemma, as individual hypotheses, between the two theories on which most recent work has been done. It would seem necessary to combine into one system the distance-

¹ Publ. Astrophys. Obs. Victoria 3, No. 1 (1924)

velocity correlation and the expanding universe, and no treatment has yet appeared showing in just what way the two are combined

It has been customary in some quarters to consider the velocities secured under the distance-velocity relation as apparent velocities (aside from individual motus peculiaries, of course). This can not be so if the theory is to be allied with that of an expanding universe, for in such a structure the velocities must be real. If they are real, and if the present value of 170 km/sec per 10^6 ly holds indefinitely, the outer parts at a distance of $2 \cdot 10^6$ ly must be expanding with the velocity of light. Velocities nearly that of light in the region just this side of a finitely near horizon, do not appeal to the reason, this is, however, no argument against it, for in a domain beyond the scope of experience (a four-dimensional manifold in a continuum of six-fold curvature) it would be expected, perhaps, that the relations or seeming paradoxes which are the results of the basal hypotheses may also be beyond the domain of experience.

The simplest explanation of a distance-velocity relation (BURNS) is the manifest one that the objects with highest speeds would have reached greater distances from us. This presupposes, however, a universe without re-entries, and, like the theory of an expanding universe, meets with insuperable difficulties when the attempt is made to visualize the "initial" state. As a further alternative, it is perhaps reasonable to assume that the vibrations of the light-ray (not its speed) may be slowed up by minute amounts in passing through tremendous distances, were this so, the velocities of recession exhibited would be only apparent, and the most distant objects would be invisible, not from a horizon limitation, but from redness.

On the allied question of an expansion in a comparatively minute realm, one naturally recalls the K-term in stellar radial velocities. Such K-terms have been found by CAMPBELL, and others, particularly in the early type stars. They have given rise to a great deal of discussion, pro and con, of which one of the most recent and thorough investigations is that due to ROSENHAGEN¹. If existing, such effects may be regarded as giving support to a theory of expansion, as an expansion of spiral distances should be accompanied by corresponding expansion in *kleinen*. VOGT considers that the spiral arms are due to this same expansion effect. Assuming a star in our galaxy at a distance of 10^4 ly to be subject to this expansion effect of 1 part in 2000 per 10^6 years, it should have a radial velocity, in this extreme case, of but 1.5 km/sec.

75. Other Cosmogonical Deductions: an Aberration Effect Suggestions have been made that the high velocities of the spirals might produce an effect on the observed aberration. PERRINE² suggested that the aberration constant derived from a spiral of velocity 10^4 km/sec. should be $20''.18$ instead of the usual $20''.47$. BORČEV³ shows that PERRINE's deduction is erroneous. "It should be remembered, however, that aberration can only be explained on the assumption that the observer moves relative to the ether. The absence of the ether discredits, in turn, the constant velocity of light, whatever be the velocity of the source." VAN BIESBROECK has made careful position measures of the spiral in Ursa Major which has a radial velocity of $+11700$ km/sec (paper read at the September, 1931, meeting of the Amer Astr Soc), and has found no evidence whatever of a different value of the aberration constant for this object. COURVOISIER⁴ has lately carried through some investigations of great interest,

¹ A N 242, p 401 (1931) ² A N 240, p 319 (1930) ³ A N 241, p 343 (1931)

⁴ L. COURVOISIER, Zur Frage der Mitführung des Lichtäthers durch die Erde A N 243, p 281 (1931); Bestimmung der absoluten Translation der Erde aus säkularer Aberration, *ibid*, 244, p 201 (1930); G v GLEICH, Bemerkungen zur absoluten Translation unseres lokalen Fixsternsystems A N 242, p 265 (1931)

which form an excellent illustration of the manifold scientific fields which contact with the high velocities of recession shown by the spirals. He holds that the observed aberration constant should be written,

$$k = k_0 \left(1 - \frac{v}{c} \cos \varphi \right)$$

where k is the observed value, k_0 its "absolute" value, v the velocity of the source, c the velocity of light, and φ the angle between the observed object and the apex of motion. One observes then not the absolute velocity of light but a velocity which is relative because of the absolute translation of the earth. This infers that the constant of annual aberration is variable with the position of the object, it is smaller in the apex-hemisphere, and larger in the celestial hemisphere which is antipodal to the apex. The possibility of such an effect was noted first by VILLARCEAU in 1872.

COURVOISIER investigates this effect in two ways

1. From observations of zodiacal stars

2. From declination observations

He gives as his final result from all observational data considered:

$$k_0 = 20''.498 \pm .009$$

$$A = 112^\circ \pm 20^\circ$$

$$D = +47^\circ \pm 20^\circ$$

$$V = 600 \pm 305 \text{ km./sec.}$$

These results, agreeing roughly as they do with the approximate location of the apex of galactic motion found by other methods, are of high interest. He points out that further work is urgently needed on objects of widely different celestial types.

76. Further Considerations on the Apparent Recession of the Spirals. The main difficulty which impedes a solution of the puzzle presented by the large positive values of the radial velocity of the spirals is due to the exceedingly fragmentary character of our present observational data on the score of distribution. Of the 90 velocities given in Table 14, only 30 (including the two Clouds) are below the galactic plane. Only 7 indicate a velocity of approach. The algebraic mean of all is $+2470 \text{ km./sec.}$

It will be noted, both from Table 24 giving the galactic coördinates and from Figures 57 and 58 (Appendix No. 8), that the arrangement of spirals for which radial velocities have been determined is of such a nature that a definite solution, on any theory, is scarcely to be hoped for. The region about the north galactic pole is quite well represented. Only one velocity ($584; +1800 \text{ km./sec.}$) is known within 30° of the south galactic pole. Furthermore, in the stretch of about 240° of galactic longitude from $l = 150^\circ$ to $l = 30^\circ$, there are but 4 determined velocities south of the galactic plane. Because of these very serious gaps in distribution, any solution for the velocity of our system becomes highly indeterminate. Again, such a solution, with a very large K -term which seems to indicate an expansion, gives us very little information other than we already have, and leaves the puzzle of such an expansion unsolved.

It is therefore clear that the final solution of the problem may have to await the day when a considerable number of spiral velocities have been determined in the regions contiguous to the south galactic pole, and particularly in the quarter of a sphere, $180^\circ - 360^\circ$, which is now almost entirely blank. Astronomy has no more pressing observational task, nor one which would be of more service in clearing up modern cosmogonical theories. A decision between the theories treated earlier and in the following sections, must evidently await the establishment of a powerful reflector in the Southern Hemisphere!

A second uncertainty, which may eventually be turned into an advantage, rests upon the amount of random velocity, or average peculiar motion, which can be permitted a spiral or a group of galaxies. As to the variations within a group of galaxies, from the evidence of those determined at Mt. Wilson and given in Table 14, ciph 50, it would seem evident that this is 2000 km/sec, or more. If the cosmos be arranged on CHARLIER's scheme, in supergalactic groups, we may expect, also, an even higher variation in the velocities of such groups.

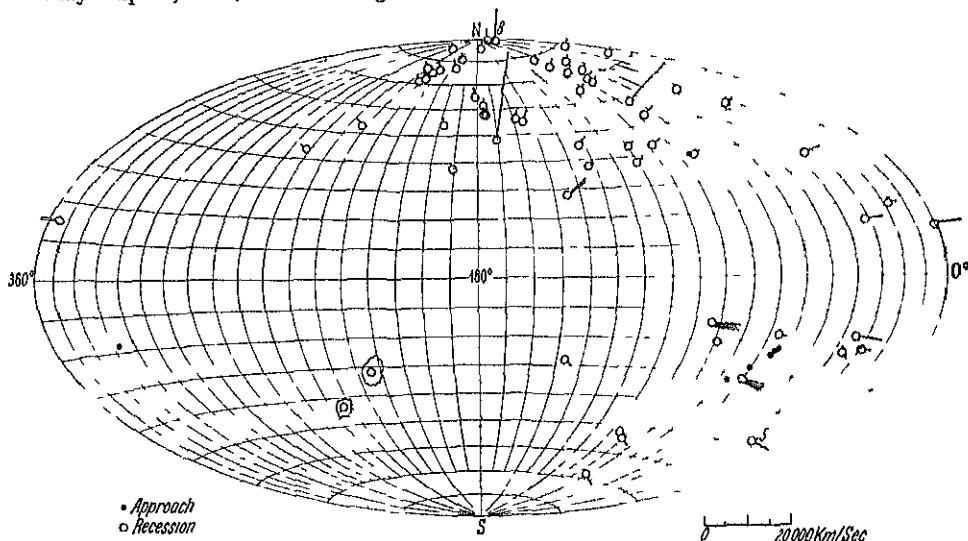


Fig 57 Galactic Distribution of Spirals of Determined Radial Velocity. Positive velocities are indicated by lines extending away from the center of the diagram, and negative velocities by lines toward the center. The scale of the lines is indicated on the figure.

77. Earlier Values of the Motion of our Galaxy in Space. A few of these values are collected in this Section, not because they are believed in any way to be a solution of the problem of the velocities of recession, but rather to indicate the past trend of research in this line. The distance-velocity values have been added. In this tabulation, A is the right ascension of the apex, D its declination, V_{gal} the galactic motion, and K the "expansion" term common to all objects treated.

Table 20 Values of the Apex and Motion of the Galaxy

Author	A	D	V_{gal} km/sec	K km/sec	Reference
TRUMAN	300°	-20°	670		Pop Ast 24, p 111 (1916)
PADDOCK	270	+30	200±	300±	Publ A S P 28, p 109 (1916)
YOUNG and HARPER	300	-12	600		R A S Can 10, p 134 (1916)
DOSE	299	+68	765		A N 229, p 157 (1927)
LUNDMARK	305	+75	651		Obs 47, p 279 (1924)
STROMBERG	310	+60	460	660	Ap J 61, p 353 (1925), mean of 7 groupings of data.
WIRTZ	195	+89	693	887	A N 215, p 349 (1922)
HUBBLE	286	+40	360	142/10 ⁰ 1 y	Wash Nat Ac Proc 15, p 168 (1929); 24 spu.
HUBBLE	269	+33	306	157/10 ⁰ 1 y	ibid, 9 groups
HUBBLE	—	—	—	170/10 ⁰ 1 y	Ap J 74, p 43 (1931)
OORT	170	-64	360	132/10 ⁰ 1 y	B A N 5, p 239 (1930)
OORT	—	—	—	90/10 ⁰ 1 y	B A N 6, p 155 (1931)
DE SITTER	—	—	—	146/10 ⁰ 1 y	B A N 5, p 157 (1930)

See further Appendix No 8

78. MOISSARD'S Modification of the DOPPLER Formula There have been several attempts to seek for other causes which might explain the recession of the spirals. RUSSELL¹ shows that neither radiation pressure, nor gravitational or electrical forces can reasonably account for the high velocities of the spirals, to say nothing of their predominant positive sign.

W. MICHELSON² pointed out that some of the assumptions in the derivation of DOPPLER's principle are necessarily arbitrary; 1 that the period of vibration of the source is not affected by its motion along the line of sight, 2 that the medium is at rest, and, 3 that its velocity is not changing.

It is not impossible that a high "absolute" motion of our galaxy or our super-system of galaxies might contribute largely to the effect, as noted by DRUDE³.

"In this case (both bodies moving) the rigorous calculation shows that the actual period T and the relative period observed at B stand to each other in the relation:

$$\frac{T}{T'} = \frac{c - u}{c \pm v},$$

(characters changed from original to conform with later nomenclature H D C.) in which u is the absolute velocity of B, v that of A in the direction of the ray, and c that of the light in the medium between A and B. . . Now we know nothing at all as to the absolute velocities of the heavenly bodies, hence in the ultimate analysis the application of the usual equation representing DOPPLER's principle to the determination of the relative motion in the line of sight of the heavenly bodies with respect to the earth might lead to errors. Attention was first called to this point by MOISSARD⁴."

The MOISSARD-DRUDE suggestion that the ordinary formula for the DOPPLER shift is not rigorously accurate has not hitherto been considered, so far as the author knows. The great interest which attaches to the puzzle exhibited by the great positive velocities of the spirals is sufficient warrant for the somewhat tentative illustration of this hypothesis given in Appendix No 8.

79. Conclusion. We must wait for many more velocities of spirals, with adequate representation near the south galactic pole and south of the galactic plane in the region from 180° to 360° galactic longitude, before any acceptable decision can be made between the various theories which have been advanced to explain the excess of velocities of recession exhibited by the spirals.

There are no theories of this very curious phenomenon which do not require the introduction of rather radical ad hoc hypotheses. In the velocity-distance correlation we need either to assume, with a considerable measure of observational support, that the vibration period of light is diminished by its passage through space, or that the universe is actually expanding, the outer parts more rapidly than the inner. If the cause is assumed a consequence of some form of expanding relativity universe, we find at once another basal assumption in the cosmological constant λ , which is inserted in the EINSTEIN form of the gravitational equation:

$$G_{\mu\nu} = \lambda g_{\mu\nu}$$

"Plintude of space depends upon a "cosmical constant" λ . Except in so far as a value may be suggested by astronomical survey of the extra-galactic universe λ is unknown (EDDINGTON)." "The constant λ , which is a measure of the inherent expanding force of the universe, is still very mysterious, and it is difficult to see what its real meaning is. It might even be one constant too many, unless we may hope that it will ultimately be found to be in some way connected with PLANCK's constant h . Evidently the dynamical solution of LEMAITRE is not

¹ Ap J 53, p 1 (1920).

² Ap J 13, p. 192 (1900)

³ Optics, English translation (1902), p 473, footnote

⁴ C R 114, p. 1471 (1892)

the last word, but it can hardly be doubted that it represents an important step towards the true interpretation of nature (DE SITTER)." As noted earlier, the most recent solutions of EINSTEIN and DE SITTER place $\lambda = 0$. There is no theory yet advanced, in other words, which is free from somewhat diastatic ad hoc hypotheses, all require a measure of extrapolation or speculation far beyond the available range of observational data¹

Whether one prefers to assume that light vibrations are slowed up by their passage through space (velocity-distance correlation, spiral velocities apparent), or to postulate a universe that is actually expanding (LEMAÎTRE's and other relativity universes, spiral velocities real), or to accept a universe of the CHARLIER type with the MOLSSARD modification (spiral velocities in part real, in part apparent), is doubtless entirely a matter of individual choice and belief. The remarkably close parallelism between the structure of the suggested CHARLIER universe and the observed arrangement of the accessible exterior universe, is too exact and detailed to be cast lightly aside. Under assumptions which seem not more ad hoc than those which have been made for other theories tested, it would appear within the bounds of possibility to remove the excess of positive velocities which have formed the main obstacle to the acceptance of a universe of the CHARLIER type (see treatment in Appendix No. 8). For this and other reasons, therefore, the writer prefers, solely as a matter of personal choice and belief, to adhere, until more evidence may be gathered, to a cosmogony based on the scheme of CHARLIER, rather than to accept one or another of those which seem as yet somewhat nebulously based upon a four-dimensional frame of reference.

It can not be too strongly emphasized, however, that many aspects of our present available observational evidence are so inadequate and so incomplete that no final decision is possible, and that the field of speculation is still open as regards any of the theories which have been advanced in explanation of the excess of velocities of recession in the spiral class.

e) Appendices.

Appendix No. 1.

Indexing List for Names frequently used in the older literature

Name	NGC	MESSIER	Description
America nebula	7000	—	Enormous diffuse neb
Andromeda nebula	224	31	Largest spiral
Crab nebula	1952	1	Planetary
Dumb-bell nebula	6853	27	Planetary
Hercules cluster	6295	13	Large globular cluster
Horse shoe nebula	6618	17	Bright diffuse nebula, cf Omega neb
Lagoon nebula	6523	8	Large diffuse nebula
Network nebula	6995	—	Very large diffuse nebula
Omega nebula	6618	17	Bright diffuse nebula, cf Horse-shoe neb
Orion nebula, Great nebula in Orion	1976	42	Very bright diffuse neb
Owl nebula	3587	97	Planetary
Præsepe	2632	44	Bright open cluster
Ring nebula (in Lya)	6720	57	Planetary
Swan nebula	6618	17	Diffuse cf Omega nebula
Trifid nebula	6514	20	Bright diffuse nebula
Whirlpool nebula	5194	51	Fine spiral

¹ Cf. JEFFREYS' interesting and suggestive book, *Scientific Inference*, Cambridge (1931).

Finding List for **MESSIER** Numbers. (Abridged from SHAPLEY and DAVIS, Publ A S P
29, p. 178 (1917))

MESSIER	NGC No.	Description	MESSIER	NGC No.	Description
1	1952	Crab Nebula	51	5194	Spiral
2	7089	Globular cluster	52	7654	Cluster
3	5272	Globular cluster	53	5024	Globular cluster
4	6121	Globular cluster	54	6715	Globular cluster
5	5904	Globular cluster	55	6809	Globular cluster
6	6405	Open cluster	56	6779	Globular cluster
7	6475	Open cluster	57	6720	Planetary (Ring neb in Lyra)
8	6523	Diffuse nebula	58	4579	Spiral
9	6333	Globular cluster	59	4621	Spiral
10	6254	Globular cluster	60	4649	Spiral (elliptical)
11	6705	Open cluster	61	4303	Spiral
12	6218	Globular cluster	62	6266	Globular cluster
13	6205	Heracles cluster	63	5055	Spiral
14	6402	Globular cluster	64	4826	Spiral
15	7078	Globular cluster	65	3623	Spiral
16	6611	Open cluster	66	3627	Spiral
17	6618	Diffuse nebula (Horse-shoe or Omega neb.)	67	2682	Open cluster
18	6613	Open cluster	68	4590	Globular cluster
19	6273	Globular cluster	69	6637	Globular cluster
20	6514	Diffuse nebula (Trifid neb.)	70	6681	Globular cluster
21	6531	Open cluster	71	6838	Open cluster
22	6656	Globular cluster	72	6981	Globular cluster
23	6494	Open cluster	73	6994	Open cluster
24	6603	Open cluster	74	628	Spiral
25	4725	Open cluster	75	6864	Globular cluster
26	6694	Open cluster	76	650	Planetary
27	6853	Planetary (Dumb-bell neb.)	77	1068	Spiral
28	6626	Globular cluster	78	2068	Diffuse nebula
29	6913	Open cluster	79	1904	Globular cluster
30	7099	Globular cluster	80	6093	Globular cluster
31	224	Spiral (Andromeda neb.)	81	3031	Spiral
32	221	Spiral (elliptical)	82	3034	Spiral
33	598	Spiral	83	5236	Spiral
34	1039	Open cluster	84	4374	Spiral (elliptical)
35	2168	Open cluster	85	4382	Spiral
36	1960	Open cluster	86	4406	Spiral (elliptical)
37	2099	Open cluster	87	4486	Spiral (elliptical)
38	1912	Open cluster	88	4501	Spiral
39	7092	Open cluster	89	4552	Spiral
40	—	Two faint stars	90	4569	Spiral
41	2287	Open cluster	91	—	Comet??
42	1976	Diffuse nebula (Great Ne- bula in Orion)	92	6341	Globular cluster
43	1982	Diffuse nebula	93	2447	Open cluster
44	2632	Open cluster (Praesepe)	94	4736	Spiral
45	—	Platades	95	3351	Spiral
46	2437	Open cluster	96	3368	Spiral
47	2478	Cluster	97	3587	Planetary (Owl nebula)
48	—	Very open cluster	98	4192	Spiral
49	4472	Compact spiral	99	4254	Spiral
50	2323	Open cluster	100	4321	Spiral
			101	5457	Spiral
			102	5866	Spiral, identification doubtful
			103	581	Open cluster

Appendix No 2

Finding Lists for SIR W HERSCHEL's Classes and Numbers.

HERSCHEL's Class I, 1-288

I 1 to I 50	I 51 to I 100	I 101 to I 150	I 151 to I 200	I 201 to I 250	I 251 to I 288
1055	6638	779	524	3877	3945
2775	7006	1022	821	3949	4041
3166	7331	6934	908	3938	4036
3169	393	7606	949	2639	4605
3655	7479	720	1453	2841	5308
5363	2903	1309	1023	4088	5322
4472	2905	1407	672	4096	1344
4698	1395	467	1600	4157	1491
4179	2784	1201	278	4220	3923
4643	1332	7723	4546	4346	2880
4153	2974	7727	4159	4800	1931
1377	701	772	4866	4460	3682
3521	1052	2830	3115	4449	4128
4632	1084	2964	3294	5474	4250
4666	4361	3021	4151	5866	3182
4753	2781	3395	4369	2787	3206
3379	3962	3396	2782	1579	3445
3384	4856	3430	3184	2419	3458
4147	4902	4560	4145	3665	3488
3666	5634	3887	5290	3549	3610
3810	5812	4030	5739	3718	3613
4371	3254	1637	3432	3729	3332
4452	4150	4378	3941	4026	4589
4596	4245	4580	4062	4085	4648
4754	4274	4586	4203	4102	4291
3345	4314	5746	4656	3631	4319
3412	4414	5813	4657	3780	4386
4438	2985	5846	4618	3898	4144
3593	3147	4699	4618	3998	4127
4365	3348	4958	5297	5422	6217
4526	3344	3672	5383	5473	613
4570	3900	2855	5713	5485	2977
4124	4494	2742	5750	3448	3183
5248	4725	4781	5728	4500	3329
4216	5012	4782	5633	5585	2976
4550	3245	4783	5195	5631	3077
4551	3486	2859	5377	5678	3735
4526	3504	5061	5689	5376	2655
4697	4251	4303	5676	5379	
4941	4278	4713	5395	5389	
4731	4448	4808	5394	3621	
4995	4559	4665	7008	2681	
4594	4793	4900	651	4814	
6401	3813	5566	3675	3619	
6316	4214	5574	4111	3642	
6355	5005	5576	4138	3683	
6712	5033	6304	4485	3690	
6356	5273	5921	4490	3894	
6522	5557	6342	3198	2742	
6624	584	6440	2683	2768	

HERSCHEL'S CLASS II, 1-350.

II 1 to II 50	II 51 to II 100	II 101 to II 150	II 151 to II 200	II 201 to II 250	II 251 to II 300	II 301 to II 350
7184	3608	3489	6106	6569	7448	4984
7507	3626	3596	3692	6847	514	2481
157	3659	3800	3822	7013	660	2554
596	3691	3872	3825	6629	1134	2316
1032	4394	4168	4417	6642	7742	3110
1055	4450	4189	4442	6979	7743	5306
1580	2872	4208	4469	7217	95	5324
1587	2874	4212	4519	7741	1232	5343
1588	3070	4222	3681	214	2577	5426
7800	4124	4262	3686	315	2916	5427
4237	4294	4298	3801	972	7137	2986
4651	4299	4302	3968	7457	1371	5068
3705	4313	4419	4193	7753	1385	5084
4119	4352	4473	4200	296	2139	5134
4578	4429	4477	4206	379	2196	2592
3462	4503	4479	4267	380	2613	2371
4235	4528	4474	4387	383	1415	2372
4470	4564	4501	4388	392	3078	2608
4610	4608	4540	4413	407	3585	2619
4612	4638	4548	4425	410	718	3106
4795	4660	4458	4431	736?	741	4136
5106	4694	4461	4436	750	742	4278
4420	4733	4476	4440	777	1070	4283
4772	4754	4478	4461	404	1153	4317
5147	4762	4639	4531	890	2967	4525
4453	5970	4654	4638	7678	4045	4676
5665	3338	4659	5600	7817	4073	5089
3226	3367	4689	5953	678	955	5127
3227	5669	5020	5954	680	1507	5623
3626	2672	5936	4454	7769	2695	5653
4592	3370	3423	4684	7771	2708	5607
3645	3455	3976	4691	7798	615	5832
3640	4152	4180	4593	7332	636	3063
4412	4328	4197	4602	7339	1035	3065
4457	4340	4215	4989	7556	1208	3403
4496	4350	4224	4775	7585	1241	3516
4527	4379	4223	4786	958	1299	3562
4636	4405	4260	4951	1003	1376	3629
4664	4421	4261	4981	1161	1888	3689
2911	4450	4264	4928	7814	1357	3798
3389	4489	4326	4933	57	1421	3826
3547	4502	4333	5861	7681	1832	3912
3162	4515	4339	5077	57	3091	4555
3190	4540	4370	5548	7711	3957	4747
3193	4710	4423	6287	234	4024	4789
3301	5962	4430	5694	877	4027	4819
3437	5996	4532	6544	7177	5247	5248
2672	3041	4612	6540	7280	4727	3727
3599	3377	4623	6517	7454	4877	3701
3607	3485	5645	6528	7625	4899	3710

HIRSCHEL's Class II, 351-700

II 351 to II 400	II 401 to II 450	II 451 to II 500	II 501 to II 550	II 551 to II 600	II 601 to II 650	II 651 to II 700
3728	5937	7444	682	3637	1123	5930
3772	6118	210	1172	3732	1129	6160
4162	3947	7393	1199	3892	1278	5129
4213	4032	7576	1209	2507	818	5951
4455	4158	1417	2811	2889	828	5980
5016	4336	1418	2907	2935	7231	5984
5637	4561	1065	3508	2718	1175	6012
3274	3897	1440	4033	4658	1193	2691
3277	4190	1452	4050	4759	252	4627
3380	4534	1161	5037	4790	661	4625
3400	4619	521	5044	4939	670	4655
3414	4711	533	5049	3715	681	4704
3418	4956	550	5054	4825	855	4963
3451	5014	1550	1620	2778	2274	5023
3510	5352	1090	1635	3381	2275	5103
3512	5440	1087	1713	5078	2435	5123
3713	5444	7562	4904	5101	691	5145
4008	5533	7785	4227	4270	695	5289
4017	5544	7284	4229	4273	1156	5320
4104	5614	1140	2765	4277	1169	5336
4134	5656	137	3611	4281	259	5362
4173	5675	255	1636	4300	428	5410
4185	5695	599	4646	4281	3955	5608
4196	5347	873	1618	5668	2990	5630
4209	5990	1200	1638	5701	4348	5697
4275	6962	7310	1653	5770	3604	5784
4283	6964	7371	1682	4600	2545	5787
4310	7311	151	1684	4701	4312	5893
4375	7541	191	2721	5560	4474	5183
4556	7537	217	4376	5638	4468	5184
4692	7600	681	4480	5636	4506	5691
4798	7721	833	4630	5690	4595	5719
4816	337	835	5300	6010	1058	5792
4827	357	838	5364	6235	2563	5865
4840	788	839	4771	5864	3660	5327
4839	881	853	4845	6445	4597	5345
4841	883	945	4999	6426	5015	5506
4869	895	1045	5740	665	5253	5301
4872	7619	932	5806	673	3158	5198
4892	7626	2770	5831	7458	3163	6155
4889	7634	2968	5839	14	3334	5448
4911	7364	3067	5838	1024	4156	5480
4921	7391	3413	5850	1400	4662	5481
4923	227	3424	5854	1442	4868	5602
4944	245	2906	5869	7183	4914	5660
4952	271	4233	2872	706	5112	5673
4957	430	4434	2874	1441	6158	5351
4961	545	4470	4129	7377	5696	5380
5958	547	4492	4818	7197	5704	5406
5910	7443	4535	3636	7640	3899	5698

HERSCHEL's Class II, 701—909

II 701 to II 750	II 751 to II 800	II 801 to II 850	II 851 to II 900	II 901 to II 910
6207	5857	5486	7773	6389
7392	5859	4149	1425	6555
259	6181	4161	29	30617
1184	5582	4271	128	3523
7354	5875	4290	132	3752
7538	5820	4335	194	5949
185	5879	5667	198	6646
2798	5905	5687	200	2650
3600	5907	5751	693	3063
5311	5908	6125	196	46467
5313	5963	6143	2320	
5326	5965	6338	2332	
5350	5894	4187	257	
5353	5982	4732	3904	
5354	5987	4987	4105	
5371	5985	5040	4106	
2998	6340	5250	4194	
3415	1569	5881	2814	
2543	2339	3571	2820	
3202	3687	2387	3259	
3205	4504	2415	3266	
3207	4626	2426	3394	
3891	4628	2693	6048	
3971	4671	3917	5928	
4020	3652	3924	6166	
2532	4487	5109	5492	
2649	4813	5430	5513	
3583	4888	2756	6824	
3614	4925	3669	3622	
3726	5085	3804	3654	
3769	4068	3838	3879	
3782	3656	3895	3225	
4013	3738	3958	3238	
2326	3756	2726	3517	
2329	3888	3043	3625	
2340	3913	3725	3674	
3811	3916	3762	3435	
3893	3921	3770	3470	
3896	3972	3796	5374	
3928	3977	3978	5491	
4047	3990	5216	5652	
4248	4172	5218	5661	
4381	4198	5370	5674	
4617	4644	5376	5679	
3320	4686	3668	5257	
5018	4695	4256	5258	
4144	5201	4332	7218	
4217	5278	4441	3107	
4389	5443	4521	5323	
4460	5475	4545	1247	

HERSCHER's Class III, 1-350

III 1 to III 50	III 51 to III 100	III 101 to III 150	III 151 to III 200	III 201 to III 250	III 251 to III 300	III 301 to III 350
1982	3020	5230	807	871	474	4495
867	3024	3833	1012	7468	488	4514
4028	3153	3876	266	7497	520	4962
2939	3299	3874	421	251	3044	4966
3342	3300	4598	420	459	3156	5004
4698	5416	4779	495	473	2555	5056
2508	5146	3356	496	794	2618	5057
2894	5463	3425	499	803	4077	5065
5208	5482	3790	507	7042	850	5074
5209	2744	5587	508	7463	863	5672
5417	2774	3535	987	7165	941	5808
5570	2802	3679	1060	7659	1239	5836
4577	2803	3915	1066	7691	1409	6011
5621	2843	4422	1240	774	2722	6091
3646	3129	5146	7186	781	755	2963
3649	3303	5885	7335	7385	731	3252
4409	3473	5076	515	7386	2076	3343
4505	4126	5079	517	7648	1781	3364
2402	4498	5111	513	6956	1993	5620
3433	4758	5605	537	7515	2089	3812
3491	5180	5597	536	7559	2283	3902
3506	5249	5595	552	7563	3052	3944
3524	6021	6267	553	171	3072	4015?
3088	6073	6278	614	907	3981	4021?
3177	3498	5396	679	2124	2763	4007?
4529	3616	5642	735	7671	2902	4101
3605	4037	5706	925	827	2992	4146
3686	4516	5709	1167	1044	2993	4670
3768	3559	5771	697	1046	4035	4673
3802	3731	5773	7316	7469	4724	3216
4344	3773	5798	7550?	7778	4756	3270
5490	4752	5635	7578	7779	5073	3475
6046	4880	5735	52	7782	5677	3615
2984	5136	5523	7506	2599	3818	3618
3848	5222	5594	7566	2628	5369	3651
3852	5221	5610	7592	2764	5468	3653
4067	5230	6372	7694	7321	5476	3670
4368	3401	5898	7701	7570	2566	3808
4390	3567	5903	7725	922	2983	3815
4482	3914	6064	7832	1979	3956	3832
4491	4246	6907	352	2073	2750	3911
4497	4296	6926	702	2815	2604	3951
4606	4297	6717	748	7436	3068	3983
4647	4343	6857	1266	216	2679	4002
5174	4341	7052	1287	1187	2783	4003
5175	4342	7720	1321	1353	2796	4979
5532	4366	23	1320	1401	2893	5559
5747	4588	108	1003	1426	2918	3196
2648	5210	233	1160	1439	4272	3265
2661	5235	604	213	470	4286	3527

HERSCHEL's Class III, 351-700.

III 351 to III 400	III 401 to III 450	III 451 to III 500	III 501 to III 550	III 551 to III 600	III 601 to III 650	III 651 to III 700
3550	4986	1393	1670	5546	3060	5157
3552	5141	7156	1678	5549	4571	5187
3714	5142	1762	1729	6070	4634	5433
4004	5149	622	4591	5775	845	4985
4080	5154	1073	5252	6548	2512	5003
4131	5199	36	5356	532	2558	5214
4132	5223	864	5203	990	2562	5730
4169	5228	7252	5729	7492	2743	5731
4174	5240	686	4599	1370	3791	5888
4175	5265	723	2110	551	4705	5900
4393	5399	24	5845	687	4720	5922
4475	5401	1094	2513	703	3952	4653
II 4051	5445	268	2914	704	4843	4668
4927	5529	762	4703	705	4890	4690
4983	5579	7432	4739	706	3304	5334
5000	5589	7794	4773	797	3930	5392
5032	5590	154	4777	834	4025	5400
5116	5533	773	3145	1308	4774	5604
5251	5616	1162	2948	1397	5107	5017
5263	5654	7526	2863	898	5243	5047
6001	5684	624	2979	910	5305	5716
3883	5312	977	3411	980	6038	5173
5768	5318	7647	4682	982	6120	5256
5913	4719	924	4700	1293	6137	5500
3805	5233	1036	4770	1294	2704?	5714
3821	7685	160	4784	7426	2755	5520
3837	7750	280	2069	477	2838	5622
3842	61	3099	2980	1207	2844	5797
3926	274	2459	3591	7707	2852	5804
3940	273	II 3115	3661	1138	2853	6154
3954	586	4356	3667	1030	3237	5303
4095	600	4415	3693	1088	3468	5361
4098	790	4464	4114	780	5093	5403
4099	991	4488	4177	1056	5966	5407
3862	7623	244	4265	1609	5992	5515
3860	7816	887	4714	1611	5993	5732
3875	7751	1354	4748	1576	6058	5754
3884	7665	2848	4794	1643	6146	6104
3937	279	4763	5094	1659	6150	6235
4049	450	1552	2719	1954	6173	5757
4070	560	4044	2955	1242	6175	5791
4069	564	4418	3074	426	5185	7171
4074	1248	4541	4688	429	5207	7180
4061	1304	4642	4765	493	5522	1343
4065	1324	4583	5019	193	5649	896
4076	1358	4737	5382	3081	6018	7139
4204	1924	3434	5386	2921	2759	4183
4685	2110	3495	4799	3509	4359	5337
4163	1114	1516	5329	2595	5025	5355
4097	1125	1779	5718	3053	5096	3319

HERSCHILL's Class III, 701 - 981

III 701 to III 750	III 751 to III 800	III 801 to III 850	III 851 to III 900	III 901 to III 950	III 951 to III 981
3374	2965	4364	4238	2388	6331
4253	2530	4547	4391	2578	1633
2389	2582	5255	3073	4034	1634
3192	4087	5526	7760	1120	163
3478	4403	5540	7805	3961	270
3595	4404	5777	7806	4693	1284
3985	4520	4549	1366	4749	6500
4117	4878	5113	7016	4857	6501
2500	4879	5372	7081	5034	1331
2541	4928	5402	7680	3188	1362
2552	4942	5821	39	3220	1377
2684	5478	6088	7223	3284	1482
2856	5618	6182	7248	3408	2938
2854	4462	4142	7250	3440	3174?
3906	4970	4707	1985	3530	3194?
3922	4993	4801	13	3102	3197?
4100	3298	4834	7797	3286	3500?
4218	3657	4932	12	3288	3500?
4231	3931	4998	125	3407	3747?
4232	3594	5009	182	3543	3901?
4741	3733	5163	173	3589	3939
4708	3737	5225	192	3671	3471
3577	3794	5238	201	5328	6068
5087	3824	3497	2322	5592	6251
4242	3829	2746	2329	5118	6252
4288	3850	2780	180	5224	5789
6239	4181	2840	2525	5599	2908
6283	4675	3885	2805	5227	3057
4392	4964	2431	4384	5331	3210
6186	4977	2474	4566	7165	3212
5536	4973	2692	3392	7230	3215
5541	4974	2800	5671	7246	2629
5598	4967	3870	6071	7251	2641
5603	5164	4511	6079	3080	7810
6241	5294	5526	5760	3734	
5878	5368	2469	5851	7076	
5902	5447	2488	5852	4972	
5989	5461	2497	6103	4363	
6015	5462	2505	6089	4572	
6140	5477	2534	6177	3890	
6434	5484	2710	6129	4159	
6742	3398	3353	6142	4331	
6781	3499	3757	6195	5909	
6814	4054	3795	5702	5912	
7423	4141	4154	5710	6324	
2347	4195	2870	5737	5295	
II 2133	4199	3740	2290	5452	
2366	4284	5007	2289	5547	
2810	4358	5342	2333	5640	
2493	4362	4210	2385	5712	

HERSCHEL'S Class IV, 1-79		HERSCHEL'S Class V, 1-52		HERSCHEL'S CLASSES VI, 1-42, VII, 1-67, VIII, 1-88				
IV 1 to IV 30	IV 31 to IV 79	V 1 to V 50	V 51 to V 52	VI 1 to VI 42	VII 1 to VII 30	VII 31 to VII 67	VIII 1 to VIII 30	VIII 31 to VIII 88
7009	6818	253	4236	2420	1662	7062	2509	2306
2261	7635	4536	3359	2304	2244	7082	2063	2413
2245	1501	4910		2269	1498	7209	2251	6507
3662	4143	4123		3055	1817	2253	1896	6561
4517	2537	4293		2194	2236	7762	2264	6596
3423	4051	5293		2355	2356	7790	2180	6910
3507	6301	3346		5053	6520	2192	1663	7024
4567	40	3628		—	6940	2479	1647	6997
4568	3658	6526		5466	6930	6866	2234	1664
3239	3310	6514		6144	2482	1513	2678	2311
6369	3992	6514		6284	2539	1528	2395	1778
6553	3982	6514		6293	2360	6756	6664	7708
6894	5204	6533		6451	2204	2627	6728	7234
6772	2440	6992		6802	2318	2567	6647	381
16	2346	6960		6678	2352	2401	6604	659
6905	2701	68		6839	2354	7142	6834	1027
1253	3963	598		2158	2362	2421	6938	7160
7662	2950	205		2309	6823		6837	2126
2170	1514	891		5897	6755		6840	7686
2185	5144	247		288	2215		6885	1582
1964	5856	2359		2266	1758		6800	2281
2467	6888	5170		2548	2254		6882	6633
936	6826	3027		6645	2489		6950	6828
2023	7023	4565		7044	2112		2169	7031
2327	7129	246		1245	2186		2232	7243
1535	6946	3003		1605	2225		2129	6991
3242	1325	2264		2301	2349		2367	7380
4038	4730	2024		2259	2423		2026	225
3456	3034	4395		7245	5998		7826	129
4861		1977		7789	6568		2627	1444
7302		1980		663	6583		2286	6793
1700		1788		7086	752		2335	6989
1999		1908		869	1857		2343	6895
2022		1990		884	1883		2353	1348
2610		—		136	2224		2374	1545
2071		206		2432	2270		2396	6874
6543		7000		2506	2262		2414	2425
2182		1909		6804	2324		2422	1342
2438		3511		2571	1907		2302	
4804		3513		6171	7128		2331	
6514		4244		6412	7296		1802	
676		4631		6939	437		1996	
1186		4258			7419		1750	
2167		2403			7510		2394	
2392		3953			436		2358	
5493		3556			654		2430	
4915		3079			1502		2428	
3104		1097			559		2260	
5507		1624			637		2240	
6229		2997			7067		2252	

Appendix No 3

Finding List for General Catalogue Numbers

GC	NGC	GC	NGC	GC	NGC
100	196	5057	7832	5100	113
200	376	58	119	5200	751
300	516	59	313	5300	1236
400	676	60	1251	5400	2487
500	812	5061	1312	5500	2943
600	1068	62	1767	5600	4031
700	1370	63	1922	5700	4893
800	1500	64	2189	5800	6041
900	1653	65	2198	5900	6579
1000	1783	66	2515	6000	7085
1100	1892	67	3123	6100	7420
1200	1997	68	3229	6200	7670
1300	2102	69	3801		
1400	2216	70	4270		
1500	2436	5071	4582		
1600	2488	72	5200		
1700	2666	73	5310		
1800	2816	74	5366		
1900	2969	75	5404		
2000	3105	76	6634		
2100	3240	77	7150		
2200	3376	78	7285		
2300	3519	79	7692		
2400	3658	80	3		
2500	3812				
2600	3911				
2700	4077				
2800	4209				
2900	4334				
3000	4444				
3100	4556				
3200	4668				
3300	4793				
3400	4961				
3500	5095				
3600	5227				
3700	5361				
3800	5492				
3900	5634				
4000	5771				
4100	5925				
4200	6152				
4300	6362				
4400	6611				
4500	6805				
4600	6960				
4700	7127				
4800	7299				
4900	7507				
5000	7727				

Appendix No. 4

Finding List for Sir J HERSCHTEL'S Numbers

J H.	NGC	J H.	NGC	J H.	NGC	J H.	NGC
1	12	1500	4864	3000	2150	4000	7713
50	224	50	5009	50	2231	4006	7764
100	477	1600	5142	3100	2452	4007	319
50	672	50	5248	50	2788	4008	322
200	835	1700	5352	3200	3053	4009	7796
50	1043	50	5475	50	3247	4010	7812
300	1343	1800	5603	3300	3447	4011	7823
50	1857	50	5696	50	3742	4012	368
400	2262	1900	5834	3400	4553	4013	7832
50	2392	50	6103	50	4903	4014	7
500	2562	2000	6572	3500	5126	4015	10
50	2742	50	6826	50	5393	4016	1905
600	2889	2100	7010	3600	5915	4017	2658
50	3032	50	7218	50	6222	4018	2973
700	3207	2200	7458	3700	6407	4019	3244
50	3370	50	7691	50	6653	4020	6404
800	3475	2300	7817	3800	6816	4021	6708
50	3614	50	264	50	7007		
900	3697	2400	461	3900	7154		
50	3819	50	754	50	7322		
1000	3930	2500	1140				
50	4036	50	1359				
1100	4123	2600	1493				
50	4221	50	1616				
1200	4299	2700	1759				
50	4387	50	1816				
1300	4484	2800	1871				
50	4555	50	1943				
1400	4635	2900	2014				
50	4727	50	2080				

Appendix No. 5

Systems of Nebular Classification.

A Classification of Sir Wm HERSCHTEL. This consisted of eight main classes,

- I Bright nebulae.
- II Faint nebulae.
- III Very faint nebulae
- IV. Planetary nebulae Stars with bars, with milky chevrons, with short rays, remarkable shapes, etc.
- V Very large nebulae.
- VI Very compressed and rich clusters of stars
- VII. Pretty much compressed clusters of large or small stars.
- VIII Coarsely scattered clusters of stars.

As an amplification of these main classes, HERSCHTEL used the abbreviations,

B Bright	v. very
F. Faint	c. considerably
L. Large	p. pretty
S. Small	e. extremely,

the combination of which gave him sixteen available subdivisions in each class. A dozen or so other easily understood abbreviations gave a further description of the object in a very compact form, as,

vBpLvmbM = "very bright, pretty large, very gradually much brighter in the middle."

B Classification of Sir J HIRSCHLIE He introduced into his father's system five categories, each with five subdivisions

Sub class	Magnitude	Brightness	Roundness	Condensation	Resolvability
1	Great	Lucid	Circular	Stellate	Discrete
2	Large	Bright	Round	Nuclear	Resolvable
3	Middle-sized	Faint	Oval	Concentrated	Granulate
4	Small	Dim	Elongate	Graduating	Mottled
5	Minute	Obscure	Linear	Discoid	Milky

The object was then described by five numerals, 32255 would indicate "Middle sized, bright, round, discoid, milky" This system, with minor modifications, was employed by SCHWARTZ, *Nov Act Reg Ups* 9 (1874) A somewhat similar system was employed by BIGOURDAN, *C R* 158, p 1949 (1914), making use of nine sub classes under each of the categories, brightness, extension, form, condensation, and resolvability

C BAILEY'S Classification The merit of this classification is that the element of spectral type was included *Harv Ann* 60 (8), p 200 (1908)

- A Vast, faint, irregular nebulosities, shown on photographs of long exposure
Examples, Nebula in Cygnus, Great Spiral about Orion
- B Gaseous nebulae Objects having gaseous spectrum
 - B1 Large, diffused, irregular
Examples Orion, η Carinae
 - B2 Planetary, ring, and other small, well-defined gaseous nebulae
Examples 3587 (Plan), 6720 (Ring neb), 6618
 - B3 Nebulous stars
Examples, 1514, 2003
- C White nebulae and globular clusters Objects having continuous spectra
 - C1 Nebulae, small, round, unresolved, of somewhat definite form, generally round or elliptical
 - C2 Spiral nebulae
Examples 224 (Andromeda), 5194
 - C3 Globular clusters
Examples 5139 (ω Centauri), 6205 (Hercules)
- D Irregular clusters
 - D1 Fairly condensed, somewhat regular, stars of comparatively uniform magnitudes
Examples 2437, 6194
 - D2 Fairly condensed, irregular, stars of different magnitudes
Examples 869 and 884 (double cluster in Perseus), 4755 (κ Crucis)
 - D3 Coarse, irregular, stars of different magnitudes
Examples: Hyades, Pleiades

D Classification suggested by H SHAPLEY [*Harv Bull* 849 (1928)]

Brightness,	Class A, brighter than 12	phg	magn
	" B,	12-14	" "
	" C,	14-16	" "
	" D,	16-18	" "
	" E,	18-20	" "
Concentration,	a, least concentrated		
	b,		
	c,		
	d,		
	e,		
	f, most concentrated		
Degree of elongation,	10 (round) to 1 (most elongated), determined from $10 \cdot b/a$, where a and b are the major and minor axes		
Spiral form,	classification preceded by s		
Irregular,	" " " "		
	Example: sAb9 = "a nearly round, bright spiral, very little concentrated"		

E WOLFF'S Classification Die Klassifizierung der kleinen Nebelflecken, mit Tafel, Heidelberg Astroph Inst 3, No 5 (1908), used also by HUMBOLDT, *Verkes Publ* 4, part II (1917), with the addition of an extra type h_0

An empirical system of classification, of 22 types indicated by the letters from *a* to *w*, with the omission of *f*, *s*, *y*, and *z*. The forms corresponding to these letters are given in a chart, to which reference must be made. See also LUNDMARK's allocation of WOLF's types under G below.

F HUMBLY's Nebular Classification. Mt Wilson Contr 324 (1926), cf also ibid. 214 (1921). In this system it is assumed that the evolution of the spirals is from an earlier, closely arranged and compact form to an older form of more open arrangement.

Character	Symbol		NGC Example
I. Galactic nebulae			
A. Planetary	P		7662
B. Diffuse	D		
1 Predominantly luminous	DL		6619
2 Predominantly obscure	DO		Barnard 92
3 Conspicuously mixed	DLO		7023
II. Extra-galactic nebulae			
A. Regular			
1 Elliptical	E _n	E0	3379
(<i>n</i> , omitting the decimal point = 1, 2, . . . , 7, indicates the ellipticity of the object)		E2	221
		E5	4621
		E7	2117
2 Spirals			
a) Normal spirals	S		
1 Early	Sa		4594
2 Intermediate	Sb		2841
3 Late	Sc		5457
b) Barred spirals	SB		
1 Early	SBa		2859
2 Intermediate	SBb		7479
3 Late	SBc		3351
B. Irregular	Irr		4449
Extra-galactic nebulae too faint to be classified	Q		

G LUNDMARK's Nebular Classification. Studies of Anagalactic Nebulae, First Paper, Ups Modd 30 (1927) is perhaps the most detailed classification which has appeared to date. It is given below with a few verbal changes, and with LUNDMARK's allocation of WOLF's types.

Character	Symbol	Example	Wolf
I. Galactic Nebulae	G		
1 Quasi-planetary nebulae	Gp		a, b, c
a) No central star	Gp0	6537	a, b,
b) Helicoidal forms	Gph	6543	a
c) Central star and different gradations in the ratio of total light to light of central star	Gp1—Gp10	40	c
2 Irregular nebulae	Gl		
a) Irregular bright nebulae	Gl b		
b) Irregular dark nebulae	Gl d		
II. Anagalactic nebulae	A		
1. Anomalous nebulae	Aa	2537 5144	
2. Globular, elliptical, elongated, ovate, or lenticular nebulae	Ao		
a) Very little compressed toward center	Aa0	4302	d, h,
b) Slightly compressed toward center	Aa1	2233	e
c) Somewhat " " " "	Aa2	1600	

Character	Symbol	Example	Wolf
d) Rather " " "	Ae3	1382	f, g, h, i, k
e) Much " " "	Ae4	1278	
f) Very much " " "	Ae5	4486	
The letter a is added if absorption is present, e g			
	Ae3a		
3 Magellanic nebulae	Am		
a) Very little if at all compressed towards center	Am0		p? q?
b) Different degrees of compression	Am1—Am5	1449	
4 Spiral nebulae	As		
a) Spiral structure barely seen	As0	4194	o
b) Different degrees of compression towards center	As1—As5		
Spiral arms continuous	As1c—As5c	3031	s, v
Spiral arms broken	As1b—As5b	598	r, u, v
c) One-branched spirals	As0	5278	t
d) Spiral arms form a bright ring	Asr	4736	
e) Doubtful connection of ring with center (Saturn-shaped)	Ass	936	
f) Barred spirals	Asp	1326	
g) Spiral arms have an appendix nebula	Asa	5194—5	

Appendix No 6.

Published Reproductions of Nebulae

Introductory Any system of classification, however detailed, has serious limitations in the representation of objects which differ so greatly from individual to individual as do the diffuse and planetary types, and the spirals. For this purpose, there is nothing quite so satisfactory as a pictorial representation. The ideal NGC of the future would have a picture of the object at each entry!

Photographs and sketches of the various classes comprised under the term "nebulae" are for the most part widely scattered in the periodical literature. The following list is intended to give, in general, the best available representations that are available up to 1931. The list does not pretend to be complete, where there are very many representations available, as for an object like the Great Nebula in Orion, only a few of the better plates are mentioned. Reproductions in articles or books of a more popular nature are omitted, unless no other example occurs.

The sketches of ROSSE and LASSELL have been included for their historical interest; these observers were the first to employ apertures adequate to recognize spiral character. Sketches will be indicated by asterisks* * It should be noted that the sketches made at Helwan and those of the planetaries made at Lick were carefully drawn from photographs and are nearly the equivalent of a photograph. The very large number of sketches in the older literature, made from visual observations, have been omitted, except as noted above.

References are given in the form: Publication, volume, page preceding plate, number of figure on the plate if more than one is given, date. Dates are omitted for Lick Publ 8 (1909), 11 (1913), 13 (1918), for BARNARD's Atlas of Selected Regions of the Milky Way, Carnegie Institution, Washington, 1927 (abbreviated to 'Atlas').

Rosse's drawings appeared originally in Phil Trans 1850 and 1861, they are now most easily accessible in his Collected Scientific Papers, 1926. The plates retain the pagination of the Phil Trans, Plates XXXVI—XXXVIII.

follow pages 112, 114, and 116 of the Collected Papers, and are from Phil Trans 1850; Plates XXV—XXXI follow page 150, and are from Phil Trans 1861. In citations of Rosse the page and date will be omitted.

LASSELL's sketches (LAS) appeared in Mem R A S 36, pp. 82ff. (1866). The plate only will be quoted, omitting the page and the date.

ROBERTS, Photographs of Stars, Star Clusters and Nebulae, London, 1893, 2 vols., will be referred to by ROB I and II. The dates given are those on which the respective plates were made, as for many objects the photographs of ROBERTS were the first taken. Other photographs published and discussed by Mrs. ISAAC ROBERTS in the M N are also headed ROB.

A large number of BARNARD's dark nebulae are best studied in the Atlas; entry is generally given for these objects only when taken individually. fr. = frontispiece; end = at end of volume, etc.

Most of the illustrations in the Ap J will be found also in Mt Wilson Contr where the paper is repeated.

Number	Class	Reference
40	plan.	Lick Publ 13, p. 58, VIII, 1a and *L*; spectrum, ibid., p. 86, XXVII, 4, 5, 15; p. 240, XLIV, 3, 4, 5; I., 3.
68	nob. st.?	*Rosse, XXV, 1*; *ROB, M N 73, VI, VII (1913)*.
131	ell.	*Helw Bull No. 9, II, 1 (1912)*.
134	spir.	*Helw Bull No. 9, II, 1 (1912)*.
150	barr. sp.?	*Helw Bull No. 9, II, 2 (1912)*.
151	spir.	Helw Bull No. 22, III (1921).
169	edgew. sp.	Lick Publ 13, p. 54, III, 20.
205	spir.	Ap J 46, p. 25, IX, a (1917).
221	ell.	Ap J 64, p. 324, XIV (1926).
224 (Andr.)	spir.	ROB II, X (1894); Yerkes Publ 2, XXIV (1903); Lick Publ 8, I; 13, p. 54, VI, 76, 77, 78; Ap J 69, p. 158, I—VI, the best direct, and also with novae and variables. Spectrum, WOLF, Szberr Heidelb Akad Abh 27 (1910), 8.
246	plan.	ROB II, XVIII (1898); *M N 74, p. 712, XX (1914)*; *Helw Bull No. 9, II (1912)*; Lick Publ 13, p. 58, VIII, 2.
247	spir.?	*Helw Bull No. 9, II, 4 (1912)*; *ROB, M N 75, p. 191, XV (1915)*.
253	spir.	Lick Publ 8, II; *LAS I, 1*.
255	spir.	Publ A S P 43, p. 352 (1931).
274—5	diff.	*Helw Bull No. 9, II, 6 (1912)*.
278	spir.	Ap J 46, p. 25, IX, b (1917); *ROB, M N 72, p. 408, III (1912)*.
281	diff.	ROB II, XXII (1896).
300	spir.	Helw Bull No. 22, I. (1921); *ibid., No. 9, II, 5 (1912)*.
578	spir.	Helw Bull No. 22, III (1921).
598	spir.	*Rosse, XXVI; XXXVI, 5*; ROB II, X (1895); Yerkes Publ 2, XXV (1903); Lick Publ 8, III.
613	barr. sp.	Helw Bull No. 9, I (1912).
628	spir.	ROB II, XI (1893); Lick Publ 8, IV.
650—1	plan.	Lick Publ 8, V; 13, p. 58, VIII, 3.
678	edgew. sp.	*Lick Publ 13, p. 54, III, 19*.
693	spindle	*Rosse, XXV, 2*.
697	spir.	Lick Publ 13, p. 54, IV, 45.
770	?	*Rosse, XXXVIII, 12*.
821	spir.	*ROB, M N 74, p. 238, X, 4 (1914)*.
828	spir.	*Lick Publ 13, p. 54, IV, 33*.
891	edgew. sp.	ROB I, VIII (1891); FRANKS, M N 65, p. 160, VIII, 1 (1904); Lick Publ 8, VI; 13, III, 1.
908	spir.	FRANKS, M N 65, p. 228, VIII (1904).
936	barr. sp.	*Helw Bull No. 9, III, 7 (1912)*.
972	spir.	*Rosse, XXV, 3*; Ap J 46, p. 25, IX, c (1917); Lick Publ 13, p. 54, V, 66.
1012	spir.?	*Rosse, XXV, 4*.
1023	spir.?	*Rosse, XXV, 5*.

Number	Class	Reference
1068	spir	*ROSSER, XXV, 6*, *LAS I, 2*, ROB I, X (1892), Lick Publ 8, VII, Ap J 46, p 25, IX, c, d (1917)
1084	spir	*JAS I, 3*
1087	spir	Helw Bull No 22, III (1921)
1097	barr sp	Helw Bull No 22, I, III (1921), M N 85, p 1018, XXI (1925)
1186	spu	Ap J 51, p 279, XIII, d (1920)
1187	barr sp	Helw Bull No 22, IV (1921), *ibid, No 9, III, 8 (1912)*
1270	spir	Spectra taken with RAYON lens and photograph of region in Ap J 71, p 354 (1930)
1273	spir	
1300	barr sp	Publ A S P 24, p 227 (1912), Lick Publ 13, p 13, I, 2, a
1309	spir	Helw Bull No 22, IV (1921)
1316	diff ?	*Helw Bull No 9, III, 9 (1912)*
1350	spir	*Helw Bull No 9, III, 10 (1912)*
1365	barr sp ?	*Helw Bull No 9, III, 11 (1912)*
1491	barr sp	Ap J 51, p 279, XIII, c (1920)
1499	diff	ROB II, XX (1897), Ap J 2, p 350, XI (1895)
1501	plan	Ap J 46, p 25, VI, a (1917), Lick Publ 13, p 58, IX, 6a, *6*
1514	plan	*ROSSER, XXV, 7*, *ROB, M N 71, p 234, VIII, 1 (1914)*, Lick Publ 13, p 58, IX, 7
1518	itr sp	Helw Bull No 22, IV (1921)
1530	barr sp	Lick Publ 13, p 43, I, 2, b
1531	ell	*Helw Bull No 9, III, 12 (1912)*
1532	edgew sp	*Helw Bull No 9, III, 12 (1912)*
1535	plan	*LAS, I, 4*, Ap J 46, p 25, VI, b (1917), M N 60, p 424 (1900), Lick Publ 13, p 58, IX, 8a and *8*
1555	var diff	*PFASE, Ap J 45, p 89, I, 1, a (1917)*
1579	diff	*ROSSER, XXV, 8*, Ap J 46, p 25, VIII, a (1917)
1714	plan	*Lick Publ 13, p 90, fig 7*
1722	plan	*Lick Publ 13, p 92, fig 9*
1743	plan ?	*Lick Publ 13, p 92, fig 10*
1763	diff	*Lick Publ 13, p 92, fig 11*
1788	diff	Helw Bull No 22, II (1921)
1792	spu	*Helw Bull No 9, IV, 13 (1912)*
1888	edgew sp	Lick Publ 13, p 54, IV, 29
1935	plan	*Lick Publ 13, p 94, fig 14*
1952	plan ?	*LAS, I, 6*, ROB I, XIV (1892), ibid, II, XXVI (1895), Lick Publ 8, IX, ibid, 13, p 58, X, 11
(Crab)	diff	ROB I, XVI (1888), ibid, II, XXVI (1896), Lick Publ 8, fi and XI, Pop Astr 31, p 376, XXV (1923), Yerkes Publ 2 (inner), XXI, (whole) XXIII (1903) Radial velocities
1976		Lick Publ 13, p 98, XXVIII, 18, 19, Spectrum, ibid, XXIV, 20, 21, 22, XLIII, 4, Great outer portions and 'loop' (II 2418), WOLR, M N 65, p 303, XI (1903), Szber
(Orion)		Heidelb Akad 1, p 23 (1902), M N 65, p 528 (1925), Ap J 65, p 136, II (1927) (best)
1977	diff	Lick Publ 8, XII, Ap J 57, p 138, VI (1923)
1980	diff	*ROSSER, XXXVIII, 16*
2022	plan	*LAS, I, 8*, Ap J 46, p 25, VI, c (1917), *Lick Publ 13, p 58, X, 12*
2024	diff	Lick Publ 8, XIII, Ap J 53, p 392, XI, XII (1921)
2029	plan ?	*Lick Publ 13, p 108, fig 23*
2068	diff	Lick Publ 8, XIV
2070	diff	*Lick Publ 13, p 108, fig 24*
2077	plan ?	*Lick Publ 13, p 109, fig 25*
2079	plan	*Lick Publ 13, p 109, fig 26*
2080	plan	*Lick Publ 13, p 109, fig 25*
2086	plan (2)	*Lick Publ 13, p 110, fig 27*
2146	edgew sp	Lick Publ 13, p 54, III, 14, Ap J 51, p 279, XIII, f (1920)
2175	diff	Atlas, IX
2237-9	diff	ROB II, XXVII (1899), Lick Publ 11, XXVI, XXVII
2245	diff	*ROSSER, XXVII, 11*
2247	diff.	Ap J 51, p 279, XIV, b (1920)

Number	Class	Reference
2261	var. diff.	*ROSSER, XXXVII, 10*; Helw Bull No. 22, VII, VIII (1921); Pop Astr 26, p. 248, XI (1918); HUBBLE, Ap J 44, p. 192 (1916); 45, p. 352, IX (1917).
2264	diff.	Lick Publ 8, XV; A N 221, p. 376 (1924).
2288		
2289		
2290	spir. (5)	Ap J 51, p. 279, XIII, a (1920).
2291		
2294		
2316	?	*ROSSER, XXVII, 12*.
2359	diff.	*LAS, II, 9*; Ap J 51, p. 279, XVI, b (1920).
2371-2	plan.	*ROSSER, XXXVII, 6*; *LAS I, 10*; Ap J 46, p. 25, VI, d (1917); Lick Publ 13, p. 58, XI, 16.
2392	plan.	*LAS I, 11*; Ap J 46, p. 25, VI, d (1917); Lick Publ 13, p. 58, XI, 17a and *17*; Spectra; ibid., 13, p. 112, XXX, 28; XXXI, 29; 240, XLIII, 1; XLVII, 1.
2403	spir.	ROB II, XI; Ap J 46, p. 25, X, c (1917); Lick Publ 8, XVII.
2438	plan.	ROB II, XVIII; Lick Publ 13, p. 58, XII, 18a, and *18*.
2440	plan.	Lick Publ 13, p. 58, XII, 19a, and *19*.
2452	plan.	*Lick Publ 13, p. 58, XII, 20*.
2537	spir.	*Lick Publ 13, p. 43, II, 6.
2610	plan.	*Lick Publ 13, p. 58, XII, 21*.
2655	barr. sp.	*ROB M N 74, p. 238, X, 5 (1914)*.
2681	spir.	Ap J 46, p. 25, IX, f (1917).
2683	spir.	Lick Publ 8, XVIII; 13, p. 54, III, 24.
2782	barr. sp.	*ROB M N 74, p. 238, X, 6 (1914)*.
2787	barr. sp.	*ROB M N 74, p. 238, X, 8 (1914)*.
2830	barr. sp.	*ROB M N 74, p. 238, X, 7 (1914)*.
2835	spir.	Helw Bull No. 22, II (1921).
2841	spir.	Lick Publ 8, XIX; 13, p. 54, IV, 40; Ap J 46, p. 25, X, a (1917); 64, p. 326, XIII (1926).
2859	spir.	Ap J 64, p. 326, XIII (1926); *ROB M N 74, p. 234, XIII, 2 (1914)*.
2880	spir.	*ROB M N 74, p. 238, X, 3 (1914)*.
2903	spir.	*ROSSER, XXXVI, 3*; *LAS, II, 12*; ROB I, XXV (1893); Lick Publ 8, XX; 13, p. 54, V, 57.
2868	spir.	Lick Publ 13, p. 54, III, 16.
2976	spir.	ROB II, XI (1895); Ap J 46, p. 25, X, b (1917).
3003	irr. sp.	Lick Publ 13, p. 54, VI, 72.
3031	spir.	ROB I, XXVI (1899); Lick Publ 8, XXI.
3034	irr. sp.	ROB I, XXVI (1899); Lick Publ 13, p. 54, V, 68; Ap J 64, p. 324, XII.
3079	irr. sp.	ROB II, XVII (1895); Lick Publ 13, p. 54, V, 67.
3115	ell.	Lick Publ 8, XXII; Ap J 46, p. 25, XI, a (1917); 57, p. 276, XX (1923); 64, p. 324, XII (1926).
3132	plan.	*LAS, III, 13*; *Lick Publ 13, p. 118, fig. 35*.
3169	spir.	Lick Publ 13, p. 54, IV, 39.
3184	spir.	*ROSSER, XXVII, 13*; ROB I, XXVII (1893).
3190	?	*ROSSER, XXVII, 14*.
3198	spir.	ROB II, XI (1898); Lick Publ 8, XXIII.
3226-7	spir.	Lick Publ 8, XXIV.
3242	plan.	*LAS, III, 14*; Lick Publ 8, XXV; *13, p. 58, XII, 22*; Spectrum, ibid., 13, p. 120, XXII, 38.
3351	barr. sp.	*ROSSER, XXXVIII, 15*; Lick Publ 13, p. 43, I, 2, c.
3367	barr. sp.	*ROB M N 76, p. 647, XIV (1916)*; Ap J 51, p. 279, XIII, c (1920).
3368	spir.	Publ A S P 25, p. 111 (1913); Lick Publ 13, p. 54, V, 52.
3372	diff.	*Lick Publ 13, p. 121, fig. 39*.
3379	ell.	Ap J 64, p. 324, XIV (1926); 51, p. 279, XV, a (1920).
3384	spir.?	Ap J 51, p. 279, XV, a (1920).
3389	spir.	Lick Publ 13, p. 54, V, 59; Ap J 51, p. 279, XV, a (1920).
3395-6	spir.	*ROSSER, XXVII, 15*; Ap J 51, p. 279, XVI, a (1920).
3404	edgew. sp.	Lick Publ 13, p. 54, V, 52.

Number	Class	Reference
3423	spir	ROB II, XII (1898)
3434	spu	*Rossr, XXXVIII, 13*
3556	spir	ROB II, XVII (1895), Lick Publ 8, XXVI, 13, p 54, III, 21
3587	plan	*Rossr, XXXVII, 11*, ROB II, XIX (1895), Lick Publ 8, XXXVII, 13, p 58, XIII, 23
(Owl)		Ap J 46, p 25, XI, b (1917)
3593	spir	*Lick Publ 13, p 54, IV, 34*
3607	spir	*Helw Bull No 9, IV, 18 (1012)*
3621	spu	*Rossr, XXXVII, 7*, *LAS, III, 15*, ROB II, XII (1898), Lick Publ 8, XXXVIII, 13, p 54, III, 23.
3623	spir	*Rossr, XXVII, 16*, ROB II, XII (1898), Lick Publ 8, XXIX
3627	spir	ROB II, XX (1894), FRANKS, M N 65, p 180, VII, 4 (1904), Lick Publ 13, p 58, III, 8
3628	edgew sp	ROB II, XII (1896)
3631	spir	Lick Publ 13, p 58, IV, 43
3675	spir	Lick Publ 13, p 58, III, 13
3718	edgew sp	ROB II, XIII (1898), Lick Publ 8, XXX
3726	spir	Ap J 51, p 279, XIII, b (1920)
3786	spir (2)	*Rossr, XXVII, 17*
3788	edgew sp ?	Lick Publ 13, p 58, III, 2
3953	edgew sp	*Rossr, XXVII, 19*, Ap J 57, p 138, VII (1923)
4013	irr	*Rossr, XXVII, 19*, ROB II, XIII (1897)
4038-9	spu	ROB II, XIII (1896)
4051	bari sp	*Rossr, XXVII, 20*
4088	?	*Rossr, XXVII, 20*
4151	spir ?	Lick Publ 13, p 58, IV, 44
4156	spir	Lick Publ 13, p 58, V, 50
4192	edgew sp	Lick Publ 13, p 58, V, 58
4206	spir	Ap J 64, p 328, XIV (1926)
4212	irr sp	Ap J 46, p 25, XI, c (1917), Lick Publ 13, p 58, IV, 41
4214	spu	Lick Publ 13, p 58, IV, 48
4216	spir	ROB II, XX (1897), Lick Publ 8, XXXI, 13, p 58, III, 12
4220	edgew sp	*Rossr, end, XXXV, 2*, *LAS, IV, 16*, ROB II, XIII (1896), Lick Publ 8, XXXII
4244	spir	Lick Publ 8, XXXIII, 13, p 58, V, 64
4254	spir	Lick Publ 13, p 58, V, 51
4258	spir	Lick Publ 13, p 58, V, 61
4266	edgew sp	*Lick Publ 13, p 58, III, 18*
4274	spu	*Rossr, XXVII, 21*
4282	edgew sp	Lick Publ 8, XXXIV
4292	spir	*Lick Publ 13, p 58, IV, 32*
4303	spir	*LAS, III, 17*, Lick Publ 8, XXXV
4312	spir	*Lick Publ 13, p 58, XIII, 24*, Helw Bull No 22, V (1921)
4321	plan	Lick Publ 13, p 58, III, 15
4361	edgew sp	*Rossr, XXVII, 22*
4388	edgew sp	Ap J 51, p 279, XV, b (1920)
4389	spir	Lick Publ 13, p 58, III, 11
4395-4401	edgew sp	Lick Publ 13, p 58, VI, 70
4402	spir	Lick Publ 13, p 58, IV, 38
4414	spir	Ap J 46, p 25, VIII, b (1917), 64, p 324, XII (1926)
4429	irr sp	*LAS, IV, 18*
4449	?	*LAS, IV, 19*
4476	?	*Rossr, XXVII, 23*
4477	spir	Ap J 56, p 166, III (1922), 57, p 276, XX (1923)
4485-90	ell	Lick Publ 13, p 58, VI, 75
4486	irr sp	*LAS, IV, 20*, Lick Publ 8, XXXVII
4490	spir	Lick Publ 13, p 58, III, 9
4501	edgew sp	Lick Publ 13, p 58, III, 7
4517	ell	Lick Publ 13, p 58, IV, 46
4526	spir	*Rossr, XXVIII, 24*, ROB II, XIV (1894), Lick Publ 8, XXXVIII, 13, p 58, V, 63
4527	spir	
4536	spir	

Number	Class	Reference
4559	spir	ROB II, XIV (1894), Lick Publ 8, XXXIX
4565	edgow sp	*LAS, V, 21*, ROB II, XX (1896), Lick Publ 8, XL, 13, p 58, III, 4, Ap J 57, p 275, XX (1923), M N 65, p 180, VII, 2 (1904)
4567-8	spir (2)	Ap J 46, p 25, XI, d (1917)
4594	edgow sp	Ap J 46, p 25, XI, o (1917) (best), *LAS, V, 22*, ROB II, XX (1897), FRANKS, M N 65, p 180, VII, 3 (1904), Lick Publ 13, p 58, III, 6, Ap J 64, p 326, XIII (1926)
4618	spir ?	*ROSSE, XXVIII, 25*
4621	oll	*LAS V, 23*, Ap J 64, p 324, XII (1926)
4631	edgow sp	*ROSSE, XXXVII, 9*, ROB II, XVIII (1894), Lick Publ 8, XLI, 13, p 58, III, 22, RAYMONDS, M N 85, p 1018, XXI (1925)
4634	edgow sp ?	*LAS V, 24*
4647	spir	Ap J 56, p. 166, III (1922).
4649	oll	Ap J 56, p. 166, III (1922)
4656-7	spir	*ROSSE, XXVIII, 26*, ROB II, XVIII (1894), Ap J 51, p. 279, XVI, 2 (1920)
4666	spir	Lick Publ 13, p. 58, IV, 47
4710	oll	*ROSSE, XXVIII, 27*, Lick Publ 13, p. 58, IV, 28
4725	spir	ROB II, XIV (1894), Lick Publ 8, XLII
4736	spir.	Ap J 46, p 25, XII (1917) (best), *LAS, V, 25*, ROB I, XXVIII (1932), Lick Publ 8, XLIV
4781	spir	Halw Bull No 22, V (1921)
4826	spir	*LAS, VI, 26*, ROB II, XV (1896), Lick Publ 8, XLV, 13, p. 58, V, 54.
4900	spir ?	ROB II, XIX (1894)
5005	spir	Lick Publ 13, p. 58, IV, 37
5033	spir	Lick Publ 13, p 58, IV, 36.
5055	spir.	ROB II, XV (1896), Lick Publ 8, XLVI, 13, p 58, V, 56
5112	spir ?	*ROSSE, XXVIII, 28*
5128	diff.	Halw Bull No 22, V (1921).
5189	plan.?	*Lick Publ 13, p. 124, fig 45*
5194-5	spir.	*LAS, VI, 27*; *ROSSE, XXXV, 1*, ROB I, XXX (1889), II, XV (1898), Yerkes Publ 2, XXIX (1903), Pop Astr 31, p. 374, XXIV (1923), Lick Publ 8, XLVII, 13, p 58, VI, 74
5236	spir	*LAS, VII, 28*; *Halw Bull No 9, IV, 17 (1912)*, RAYMONDS, M N 85, p 1018, XXI (1925), Lick Publ 13, p. 43, II, 7
5247	spir.	*LAS, VII, 29*, Halw Bull No 9, I, *IV, 19* (1912)
5257-8	spir (2)	Ap J 51, p. 279, XVII, b (1919)
5278-9	spir	Ap J 51, p. 279, XVII, a (1919)
5378	oll.?	*ROSSE, XXVIII, 30*
5383	barr sp.	Ap J 46, p 25, XIV, a, b (1917)
5394-5	spir	Lick Publ 13, p. 58, VI, 73
5427	spir	Halw Bull No 22, V (1921)
5457-8	spir	*ROSSE, XXIX*; ROB I, XXXII (1892), Ap J 14, p. 34, II, 2 (1901), Lick Publ 8, XLIX, Pop Astr 27, p 496, XLII (1919), Ap J 64, p 326, XIII (1926)
5506	spir	*Lick Publ 13, p 58, IV, 31*
5529	edgow sp	Lick Publ 13, p. 58, IV, 25
5544-5	spir. (2)	Ap J 46, p. 25, XIII, o (1917), 51, p 279, XVIII, b (1920)
5746	edgow sp	Ap J 46, p. 25, XIII, d (1917), Lick Publ 13, p 58, III, 7.
5850	barr sp	M N 85, p 1018, XXI (1925), Ap J 64, p 326, XIII (1926)
5857-9	spir	Lick Publ 8, L; *ROSSE, XXVIII, 31*
5866	edgow sp	*ROSSE, XXXVII, 8*, Lick Publ 8, LI, 13, p. 58, III, 5, Ap J 46, p. 25, XIII, o (1917).
5907	edgow sp	Lick Publ 13, p. 58, III, 10.
5921	barr. sp.	Publ A S P 24, p. 227 (1912), Lick Publ 13, p. 43, I, 2, d.
5981	edgow. sp.	Lick Publ 13, p. 58, IV, 26.
6058	plan.	*ROSSE, XXVIII, 32*; *Lick Publ 13, p 58, XIII, 26.
6070	spir	Ap J 46, p. 25, XIV, a (1917)
6205	diff.?	*ROSSE, XXVIII, 33*
6210	plan	*Lick Publ 13, p 58, XIV, 28*; Spectrum, ibid., XXXIII, 52.

Number	Class	Reference
6302	plan ?	*Helw Bull No 9, IV, 14 (1912)*
6309	plan	Ap J 46, p 25, VII, a (1917), *Lick Publ 13, p 58, XIV, 30*
6337	plan	*LAS, VII, 30*, Helw Bull No 22, VI (1921)
6369	plan	*Lick Publ 13, p 58, XIV, 31*
6439	plan	*Lick Publ 13, p 58, XIV, 32*
6445	plan	Lick Publ 13, p 58, XV, 33a, and *33?
6482	?	*LAS, VII, 31*
6503	spir	Lick Publ 13, VI, 71
6514	diff	*LAS, VIII, 32*, Lick Publ 8, LV, Pop Astu 27, p 494, XL (1919), Ap J 57, p 143, IX (1923)
(Diffid)	diff	Ap J 51, p 5, III (1920) (best), Lick Publ 8, LVI, 11, I II, 13, p 58, VII, 81, Atlas XXX
6537	plan	*Lick Publ 13, p 58, XV, 35*
6543	plan	Ap J 46, p 25, VII, b (1917) (best), Lick Publ 8, LVII, *13, p 58, XV, 34*, Spectrum, ibid, 138, XXXIV, 53, 240, XLIII, 2, XLIX, 1, 2, 3, Lick Bull 15, p 95, III, g (1930)
6555	spir	Ap J 46, p 25, XIV, b (1917)
6563	plan	*Lick Publ 13, p 58, XV, 36*
6565	plan	*Lick Publ 13, p 58, XV, 37*
6567	plan	*Lick Publ 13, p 58, XVI, 39*
6572	plan	*Lick Publ 13, p 58, XVI, 38, Spectrum, ibid, 138, XXXIV, 54; 240, XLIII, 3, XLVII, 3, Lick Bull 15, p 95, III, d, e, f (1930)
+30° 3639	plan	Lick Publ 13, p 240, XLIV, 1, 2, L, 2 (spectrum only)
6578	plan	*Lick Publ 13, p 58, XVI, 40*
6595	diff	Helw Bull No 9, I (1912)
6611	diff	ROB II, XXIII (1897), Ap J 51, p 7, IV (1920)
6618	diff	*LAS, VII, 33*, ROB I, XXXVIII (1893), Lick Publ 8, LVIII, Ap J 51, p 9, V (1920)
6620	plan	*Lick Publ 13, p 58, XVI, 41*
6629	plan	*Lick Publ 13, p 58, XVI, 42*
6644	plan	Lick Publ 13, p 58, XVII, 43
6690	spir	Lick Publ 13, p 58, IV, 35
6720	plan	ROB I, XLI (1891), II, XIX (1898), Lick Publ 8, LIX, 13, p 58, XVII, 46a, and *46*, Spectrum, ibid, 144, XXXV, 55, 146, XXXVI, 56, 240, XLII, 4, XLVIII, 2, Knox-Shaw, MN 76, p 646, XIII (1916), Helw Bull No 20, I, II, III (1920)
6729	var diff	
6741	plan	*Lick Publ 13, p 58, XVII, 47*
6751	plan	*Lick Publ 13, p 58, XVIII, 48*
6772	plan	*Lick Publ 13, p 58, XVIII, 49*
6778	plan	*Lick Publ 13, p 58, XVIII, 51*
6781	plan	*LAS, IX, 34*, *Lick Publ 13, p 58, XVIII, 52*
6790	plan	Lick Publ 13, p 58, XIX, 53
6803	plan	*Lick Publ 13, p 58, XIX, 54*
6804	plan	Lick Publ 13, p 58, XIX, 55a, and *55*
6807	plan	Lick Publ 13, p 58, XIX, 56
6818	plan	*Lick Publ 13, XIX, 57*, Spectrum, ibid, 146, XXXVI, 57, 240, XLVIII, 1, Ap J 46, p 25, VII, c (1917)
6822	Mag type	Ap J 52, p 408, XIV (1925)
6826	plan	*Lick Publ 13, p 58, XX, 58*, Spectrum, ibid, 158, XXXVII, 58, 240, L, 1
6833	plan	Lick Publ 13, p 58, XX, 59
6853	plan	*Rosse, XXXVIII, 17*, XXXI*, ROB I, XLIV (1888), Lick Publ 8, LX, 13, p 58, XX, 60
6879	plan	*Lick Publ 13, p 58, XX, 61*
6881	plan	*Lick Publ 13, p 58, XXI, 62*
6884	plan	*Lick Publ 13, p 58, XXI, 63*
6886	plan	*Lick Publ 13, p 58, XXI, 64*
6888	diff	ROB II, XXI (1897); Ap J 51, p 279, XVIII, c (1920)
6891	plan	*Lick Publ 13, p 58, XXI, 65*
6894	plan	ROB II, XIX (1897), Lick Publ 8, LXI, *13, p 58, XXI, 66*
6905	plan	*Rosse, XXVIII, 34*; *LAS, IX, 36*

Number	Class	Reference
6907	harr sp	*Helw Bull No 9, IV, 15 (1912)*
6925	spir	*Helw Bull No 9, IV, 16 (1912)*
6928	spir	Lick Publ 13, p. 54, IV, 27
6946	spir	*Rosae, XXX, 36*, ROB II, XV (1896), Lick Publ 8, LXII
6960	diff	ROB I, XLV (1891), Pop Astr 10, p 392, XIV (1902), Yerkes Publ 2, XXVII (1903), Lick Publ 11, LXXIX, LXXX, Ap J 57, p 146, XIII (1923)
6992 (Notw'k)	diff	ROB II, XXI (1896), Publ A S P, fr, 16 (1904), Yerkes Publ 2, XXVIII (1903)
6995	diff	Lick Publ 8, LXIII, 11, LXXIX, LXXX
7000	diff	Worff, Publ Haldelb 1, fr Atlas, XLVI (best for full ex- tension), ROB II, XXIV (1896), M N 63, p 32, II (1903), Lick Publ 11, LXXVII, LXXVIII, Ap J 57, p 147, XIV—XVI (1923).
7008	plan	*Rosae, XXX, 37*, ROB I, XLVI (1892), Ap J 46, p 25, VII, c (1917), Lick Publ 13, p 58, XXII, 69
7009	plan	*Rosae, XXXVIII, 15*, *LAS, X, 37*, Ap J 46, p 25, VII, c (1917), Lick Publ 8, LXIV, *13, p 58, XXII, 70*, Spectrum, ibid, 158, XXXVII, 59, 240, XLII, 3, XLVIII, 4, 5, Lick Bull 15, p 95, III, h (1930)
7023	diff	Worff, M N 68, p 30, IV, 1, 2 (1907), ROB II, XXIV (1898), Lick Publ 8, LXV
7026	plan	*Lick Publ 13, p 58, XXII, 71*, Spectrum, ibid, 158, XXXVII, 60, 61, 240, XLVII, 2
7027	plan	*Lick Publ 13, p 58, XXIII, 72*, Spectrum, ibid, 160, XXXVIII, 62, XXXIX, 63, a, b, c, 240, XLII, 1, XLVI, 1, 2
7129	diff	ROB II, IX (1895)
7139	plan	*Lick Publ 13, p 58, XXIII, 74*
7177	oil	*Rosae, XXX, 38*
7184	spir	Lick Publ 13, p. 54, V, 53
7217	spir	Lick Publ 8, LXVI, Ap J 46, p 25, XIV, c (1917)
7293	plan	Publ A S P 24, p 211 (1912), Helw Bull No 9, I (1912), Lick Publ 13, p 58, XXIV, 76
7309	spir	Helw Bull No 22, VI (1921)
7331	spir	*Rosae, XXX, 39*, Lick Publ 8, LXVII, 13, p 58, IV, 42
7354	plan	*Lick Publ 13, p 58, XXIV, 77*
7418	spir	*Helw Bull No 9, IV, 20 (1912)*
7421	spir	*Helw Bull No 9, IV, 20 (1912)*
7457	spir	Publ A S P 25, p 111 (1913)
7479	spir	*Rosae, XXXVI, 4*, ROB I, L (1892), Lick Publ 8, LXVIII, Ap J 64, p. 326, XIII (1926)
7537	spir	Lick Publ 13, p 54, V, 55
7640	spir	Lick Publ 13, p 54, V, 65
7662	plan	*Rosae, XXX, 40*, *LAS, X, 38*, Lick Publ 8, LXIX, Ap J 46, p 25, VII, f (1917), *Lick Publ 13, p 58, XXIV, 78*, Spectrum, ibid, 164, XL, 64, 240, XLII, 2, XLVI, 3, 4, 5
7678	spir	*Rosae, XXX, 41*
7814	odgaw sp	*Rosae, XXX, 42*, ROB I, LIII (1891), Lick Publ 8, LXX, 13, p 54, III, 3
7817	spir	Lick Publ 13, p 54, IV, 49
		First Index Catalogue
I 59	diff	ROB II, XXV (1895), Lick Publ 13, p 43, II, 4
I 351	plan	*Lick Publ 13, p 58, IX, 5*
I 405	diff	Knowl 26, p. 81 (1903), Sirius 38, p 288, XIII (1906)
I 418	plan	*Lick Publ 13, p 58, X, 10*, Spectrum, ibid, 240, XLIX, 4
I 434	diff + dark	I 431, 433, 434, near ϵ Orionis, ROB M N 63, p 32, I (1902), Ap J 53, p 392, XI (1921), Lick Publ 13, p. 42, II, 5, Harv Ann 32, III, 3 (1895), Ap J 38, p 500, XX, 1 (1913)
I 1029	spir	*Lick Publ 13, p 54, IV, 30*
I 1470	diff	Ap J 51, p 279, XVIII, a (1920)

Number	Class	References
Second Index Catalogue		
II 1747	plan	*Lick Publ 13, p 58 VIII 1 st
II 2116	plan	*Lick Publ 13 p 92 fig 12 th
II 2118	diff	Sec 1976 Orion
II 2149	plan	*Lick Publ 13 p 58 X 13 th
II 2165	plan	*Lick Publ 13 p 58 XI 11 th
II 2187	spn	Lick Publ 13 p 58 V 60
II 3568	plan	*Lick Publ 13, p 58, XIII, 25 th
II 4406	plan	*Lick Publ 13 p 126 fig 19 th
II 1593	plan	*Lick Publ 13, p 58 XII 27 th
II 4634	plan	*Lick Publ 13, p 58, XIV 29 th
II 4732	plan	Lick Publ 13 p 58 XVII, 11
II 4776	plan	*Lick Publ 13, p 58 XVII 15 th
II 1546	plan	Lick Publ 13 p 58, XVIII 50
II 4997	plan	Lick Publ 13, p 58, XXII 67
II 5117	plan	Lick Publ 13 p 58 XXIII 73
II 5116	diff	Lick Publ 13, p 58, VII 79 Ap J 51, p 270 XVII, c (1920)
II 5217	plan	*Lick Publ 13, p 58, XXIII 75 th

JONCKHEFLRL

320 plan

*Lick Publ 13, p 58 IX, 9th

JONCKHEFLRE

900 plan

*Lick Publ 13, p 58 XI, 15th249 galaxies at 12^h 55^m

+28° 30'

Lick Publ 13, p 13 I, 3

Cluster of galaxies in Ursa

Maj (BAUDE)

A N 233 p 71, II (1928)

CHRISTIE'S Cluster in Leo

Publ A S P 13, p 350 (1931)

Large Magellanic Cloud

Harv Ann 20, end, IV, 2 (1891), 60 p 108 II (1908), Mem

R A S 60, p 144 V (1903), Harv Bull No 881, 11 (1931)

Small Magellanic Cloud

Harv Ann 26, end, IV (1891), 60, p 108, I (1908)

The largest of the diffuse nebulae are best seen in plates taken with instruments of shorter focus. Many such, frequently combining luminous and dark nebulosity, can be found in BARNARD's Atlas, *passim*. Others are

Very large diffuse neb in

Auriga

Near I 405 WOLF, M N 63, p 506 XX (1903)

About η Carinae

Harv Ann 26, end, V, I, 2, 3, VII 2 (1891) 60 p 229, IV (1908) (best), Mem R A S 60, p 111, VI (1910)

Detached diff neb in

Cygnus

FRANKS M N 65 p 158, VI (1901)

Near γ Cygni

Lick Publ 11, I XXVI, Ap J 63, p 121, VIII, 126, IX (1926),

Atlas XLIV, ROB II, XXIII (1895)

Very large, near η Eridani

WOLF, M N 65, p 528 XV (1905)

Diff, in Monoceros

Lick Publ 8 XVI

Bright and dark neb near

 ρ Ophiuchi

Atlas, XIII, Lick Publ 11 XXXVI

Very large diffuse near

 ξ Persei

Lick Publ 11, XVI, XVII

Large diff + dark near

 α Persei

Atlas III

Pleiades diffuse neb

Lick Publ 8, IX, Yerkes Publ 2, XXVI (1903), ROB I, XI (1888), II, XXV (1897)

Outer nebulosity of Pleiades

BARNARD, M N 60 p 258 IX, X (1900), Ross, Ap J 64, p 294, VIII (1928), Lick Publ 11 XV

Very large diff near τ Scorpii

Atlas, XII

Very large diff near τ Scorpii

Atlas, XI

Several diff neb in Vela

MELOTT M N 86, p 636 XV (1926)

Preceding 7000

Ap J 63 p 122 VII (1926)

Enormous diff in Monoceros

Ross, Ap J 67, p 280, VI (1928)

Enormous diff in Taurus

and Perseus

Ross, Ap J 67, p 292, VII (1928)

'Cave' neb in Cepheus

WOLF, M N 69, p 117 VI (1908)

Dark Nebulae

Most of the dark nebulae which BARNARD has catalogued will be found noted in the descriptive matter accompanying the plates of his Atlas, without doubt the most wonderful Milky Way photographs which have ever been made. Some of the smaller spots which have been observed with instruments of greater focal length are given below.

BARNARD No	α 1875.0	δ 1875.0	Reference
13	$5^h 34^m.6$	$-2^\circ 32'$	Ap J 53, p 392, VI (1921), Lick Publ 13, p 43, II, 5
63	17 9	21 20	Ap J 49, p 10, III, a (1919)
64	17 10	-18 21	Ap J 49, p 10, IV, d (1919)
72	17 16	-23 30	Ap J 49, p 10, III, b (1919), 57, p 143, VIII (1923)
75	17 18	-21 55	Ap J 49, p 8, II, b (1918)
84	17 39	20 12	Ap J 49, p 8, II, a (1919)
86	17 55	-27 52	Lick Publ 13, p 54, VII, 80, Ap J 63, p 122, VI (1926)
92-93	18 9	-18 10	Ap J 57, p 143, X, XI (1923)
98	18 25	-26 9	Ap J 49, p 10, IV, c (1919)
127	18 55	-5 37	Ap J 49, p 10, IV, a (1919)
129	18 55	-5 29	Ap J 49, p 10, IV, a (1919)
133	19 00	-7 5	Ap J 57, p 144, XII (1923), 49, p 10, IV, b (1919)

Appendix No. 7

Abridged Nebular Bibliographical Apparatus

1. Lists of Nebulae Visual Micrometric Positions.

W HERSCHEL, Scientific Papers of, published by the Royal Society and the Royal Astronomical Society, London (1912), 2 vols. Collects his papers scattered in the Phil Trans and other media. 2500 entries. J HERSCHEL, General Catalogue of Nebulae, Phil Trans (1864) 5079 entries. ROMBER, Phil Trans (1853) and (1861), observations assembled in Trans Roy Dublin Soc 2 (1880), now most easily accessible in his Collected Scientific Papers, London (1926). JAHNELI, MARTIN's catalogue of 600 objects found at Malta, Mem RAS 36 (1866). D'ARREST, Micrum nebularum observationes Havnienses Copenhagen (1867) 4942 entries. Micrometer, RÖMNER, A N 63 to 68, Nos 1508, 1531, 1566, 1599, 1631 (1863 to 1866). Ring micrometer 135 objects. SCHÖNHEIM, Astr Beob Mannheim 1, 2 (1862-1875). Ring micrometer 489 objects. SCHULTZ, Nov Acta Reg Ups 9 (1874). Micrometer 500 objects. General catalogue of nebulae observed at Strassburg, by various observers, 1881 to 1910, Ann Sternw Strassb 4, p 79 (1911). 1257 NGC objects. Micrometer, WINNECKE, Beobacht von B BECKER, Ann Sternw Strassb 3, p 1 (1909). Micrometer 406 NGC objects. WIRTZ, Beobachtung von Nebelflecken, ausgeführt in den Jahren 1880-1902, von H KOBOLD, A WINNECKE und W SCHULZ. Micrometer 619 objects. Ann Sternw Strassb 3, JAVELLE, Catalogue des nébuleuses, Ann Née 4 (1895), 6 (1897), 11 (1908). Micrometer 1469 objects. BIGOURDAN, Ann Paris (1884ff.) 1 hour in a per volume. Since published by Gauthier-Villars. Micrometer BIGOURDAN not out to observe every NGC object visible from the latitude of Paris. STEPHAN, Many references in periodical literature, collected in the introduction to the NGC, p. 9. DREYER, A New General Catalogue of Nebulae and Clusters of Stars, being the Catalogue of the late Sir JOHN D. W HERSCHEL, revised, corrected, and enlarged. Mem RAS Lond 49, p 1 (1888). Includes all results known to the end of 1887. 7840 entries + 88 objects found by SWIFT. The introduction contains references to the work of all earlier investigators. See also WIRTZ' comparisons in Ann Sternw Strassb 4, Index Catalogue of Nebulae found in the Years 1888 to 1894, with Notes and Corrections to the New General Catalogue. Mem RAS Lond 51, p 185 (1895). 1529 entries. Second Index Catalogue of Nebulae and Clusters of Stars, containing those found in the years 1895 to 1897, etc. Mem RAS Lond 59 (1908). 3857 entries, continuing from First Index Catalogue to No 5386, here, for the first time, photography begins to overwhelm the cataloguer, of the 2800 WOLF nebulae known at that time, the 1500 in the third list are omitted. "the future great catalogue of nebulae will certainly have to be arranged in zones of one degree." AUWERK, Verzeichnis der Orte von vierzig Nebelflecken A N 58, p 369 (1862). Holometer 40 objects, RÖMNER, Beobachtungen von Zirkumpolar Nebeln

auf der Hamburger Steinwaite A N 63, p 305 (1865) 64, p 289 (1865), 66, p 81 (1866), 67, p 225 (1866) 68, p 353 (1867) 137 entries Ring micrometer, VOGEL, Beobachtungen von Nebelflecken Leipzig (1867) Micrometer 100 objects Publ Leipzig 1 p 3 (1882) Micrometer 132 nebulae ENGELMANN, Meridian-Beobachtungen von Nebelflecken A N 101, p 193 (1883) Meridian circle 12 nebulae KLEMP, Publ Astroph Potsdam 7 p 115 (1892) Micrometer 82 objects PORTER, Publ Cmc 11 (1891) Micrometer 105 nebulae D'ENNET, Observations astronomiques faites a Dieuze 3, p 96 (1895) Micrometer 90 nebulae, BRUCKER, Ann Obs Ldmb 1, p 1 (1902) 217 objects Meridian circle MONNICHMAYER, Veröff Sternw Bonn 1 (1895) Ring micrometer 236 objects SPIATZ, A N 132, p 369 (1893) Ring micrometer 136 entries, MILLER, Observations micrométriques de nébuleuses, I, Wusaw (1903) 72 objects Micrometer, HAGEN, A preparatory catalogue for a Durchmusterung of nebulae The zone catalogue Spec Vat 10 (1922-1927) 1 BRUCKER A preparatory catalogue for a Durchmusterung of nebulae The general catalogue Spec Vat 13 (1928) About 4100 entries, + 705 with designation *st* (stellar), and 700 unconfirmed objects

2 Lists of Nebulae Photographic

Wolf (and colleagues)				Königstuhl Nebel-Listen	Publ Heidelberg (Königstuhl)				
List	No	p	Year	entries	List	No	p	Year	entries
No 1	1	p 11	(1902)	151	No 9	3	p 149	(1909)	402
No 2	1	p 17	(1902)	301	No 10	6	p 1	(1909)	62
No 3	1	p 125	(1902)	1528	No 11	6	No 2	(1909)	91
No 4	2	p 57	(1904)	272	No 12	6	No 3	(1911)	279
No 5	2	p 77	(1904)	239	No 13	6	No 8	(1912)	114
No 6	2	p 89	(1905)	204	No 14	6	No 10	(1913)	511
No 7	3	p 77	(1907)	310	No 15	7	No 7	(1916)	189
No 8	3	p 87	(1908)	770	No 16	8	No 11	(1928)	678

WOLF and KAISLER, Positionsbestimmung von 124 Nebelflecken im Perseus-Nebelhaufen Publ Heidelberg 6, No 11 (1913), JORINZ, Positionsbestimmung von 178 Nebelflecken Publ Heidelberg 6, No 4 (1911) Nearly all NGC objects REINMUTH, Photographische Positionsbestimmung von Nebelflecken (Winnecke-Nebel) Publ Heidelberg 8, No 2 (1927) 321 entries, 141 photographische Nebelpositionen, ibid 7, No 8 (1916) 141 objects, mostly new, ibid 8, No 14 (1929) 351 entries, Photographische Positionsbestimmung von 356 Schultzeschen Nebelflecken ibid 7, No 6 (1916) 356 entries, all NGC, Photographische Positionsbestimmung von Nebelflecken in Virgo, ibid 8, No 7 (1927) 331 entries, ibid 8, No 11 (1928) 317 entries, mostly new Die Herschel-Nebel nach Aufnahmen der Königstuhl-Steinwaite, Heidelberg 9 (1926) This work contains 6251 NGC objects and is the largest single photographic nebular catalogue in existence It assembles all the previous Königstuhl work by WIRTZ, REINMUTH, and others It gives α , δ , L, B, the diameters along major and minor axes and brief description, PRASER, Photographs of nebulae with the 60 inch reflector, 1917-1919, Ap J 51, p 276 (1920) Descriptions of 330 objects, CURTIS, Descriptions of 762 Nebulae and Clusters photographed with the Crossley Reflector Lick Publ 13 KNOX-SHAW, Helw Bull No 9, p 69 (1912) 112 NGC and 48 new, ibid No 15, p 129 (1915) ca 195 NGC and 31 new, ibid No 30, p 71 (1924) 70 entries GRIGORY, Helw Bull No 21, p 201 (1921) 168 NGC, 177 new, ibid No 22, p 219 (1921) 183 NGC 60 new, BARRY Nebulae discovered at the Harvard College Observatory Harv Ann 60, p 147 (1908) 1238 new objects 1650 new nebulae, ibid 72, p 17 (1913), SHAPLEY, MENZELL, and CAMPBELL, Descriptions and positions of 2829 new nebulae Harv Ann 85 p 113 (1924), MINZEL, Harv Bull No 773 ca 2000 new objects, mostly south of -45° , HUBBL, Extra galactic nebulae Ap J 64, p 321 (1926) Classifies 400 objects of the spiral type, DUNCAN, Photographic studies of nebulae Ap J 51, p 4 (1920), 53 p 392 (1921) 57, p 137 (1923), KILMER, 744 nebulae (small) discovered on the plates of the Crossley program Lick Publ 8, p 31 (1908), SCHLERNAGER, Positions-messung von Nebelflecken A N 230, p 305, 441 (1927) 189 entries

References to other phenomena of the nebulae will be found in the separate sections.

Appendix No 8

A Test of the MOISSARD Modification of the DOPPLER Formula in a Universe of the CHARLIER Type

The MOISSARD hypothesis (see ciph 78) requires that we take into account the absolute velocity of the observer's system through the medium, as well as the relative motion of source and observer in the line of sight In applying this theory to the observed data, it does not seem at all essential that we hold to the word "absolute", for we know nothing

of our absolute speed in space, and apparently must remain forever ignorant of its direction and amount. We may think, however, of various frames of reference to which our motion is relative e.g., the motion of our galaxy within the frame of reference given by the totality of members of our particular cluster of galaxies. We may even continue the analysis and consider the motion of this cluster of galaxies with regard to a reference frame composed of other similar groups of galaxies. We shall accordingly use the phrase "total motion" to describe such motions through various systems of reference, and thus avoid the anathema attending the concept of absolute motion.

Relatively to such reference frames, MOERBAARD's modification of the customary DOPPLER formula, requires that the total motion of the observer be taken into account. Following MOERBAARD, we may make the postulate on classical grounds and replace $c/(c \pm v)$ in the usual formula for the DOPPLER shift by $(c - w)/(c \pm v)$, where v is the velocity of the source relative to the observer in the line of sight, and w the total motion of the observer's system through the medium. This is equivalent to the assumption that our total motion through our reference frame "speeds up" our own wave vibrations and standards, so that vibrations from far distant sources at rest, or moving more slowly within this frame at random, would seem to be slower than our own. An observer in a system moving more rapidly than the mean total motion of the other members of the system would then observe an apparent excess of positive velocities. That we happen to be situated in a system of higher velocity than the average may be assumed to be but a happy accident, similar to that by which the universe has not expanded sufficiently to render the beautiful spirals invisible. Like aberration, this effect would apparently not act in Kleinon.

The very large scatter of our velocity data on the spirals, together with the limited number of velocities known, preclude any need for rigor in the treatment. Placing X , Y , and Z as the components of such a total motion, the assumed effect of the total motion will then be two-fold:

1. It will be assumed to act with its full value as expressing the amount by which the observed radial velocity of a distant object tends to appear more positive.
2. In addition to the above effect, the component of such a motion in the line of sight will be manifested as the customary DOPPLER effect.

Then the total effect to be removed from the velocities of distant sources will be

$$X(1 + \cos \alpha \cos \delta) + Y(1 + \sin \alpha \cos \delta) + Z(1 + \sin \delta) = V,$$

where V is the observed radial velocity of the source.

The scheme of MOERBAARD, applied as above, may be regarded as of the nature of a "directed" K-term, placing discrepancies of excess upon our own galaxy, rather than upon ALL other galaxies.

The astonishing degree of similarity between the CHARLIER theory and data thus far observed has been noted above. HUMASON's brilliant work at Mt. Wilson has shown clearly the existence of clusters of galaxies, localized as to grouping, and with radial velocities nearly the same.

While such clusters of external galaxies are for the most part very definitely indicated, it is, as yet, considerably more difficult to select with certainty those spirals which may be assumed to be members of our own local cluster of galaxies. It was finally decided to segregate as members of our local cluster all objects with an observed velocity less than 2000 km/sec., while all objects with velocities 2000 km/sec. or greater were assumed to be members of other G_2 systems. This selection may have introduced some error, though approximate tests of the available material in different ways indicated that any over-precise refinement or grouping of the limited data is superfluous. This process, in particular, allocates to our local group the 7 objects assigned by HUMASON to the Virgo cluster.

The procedure employed in the application of the MOERBAARD formula was then as follows:

1. Using the formula given above, the total motion of our galaxy was first computed with reference to our assumed local reference frame, or G_2 , composed of 56 objects.
2. The 34 remaining objects, belonging to well determined clusters of spirals, or "isolated" objects of high velocity, were formed into 13 groups, on the assumption that they represented other G_2 systems in a CHARLIER universe. The effect of the total motion of our own galaxy having been first removed, a second solution was made for the total motion of our local system of galaxies within the reference frame formed by the 13 other G_2 systems. The locations of these are plotted in Figure 58.

The results of the two least square solutions are as follows:

1. Total motion of our Galaxy within its local reference frame of 56 Spirals

$$\begin{aligned} 770 \pm 100 \text{ km/sec. , toward,} \\ \alpha = 288^\circ, \quad l = 339^\circ \\ \delta = -1^\circ, \quad b = -7^\circ \end{aligned}$$

2. Total motion of G_2 cluster of 50 spirals within reference frame of 15 galactic clusters and isolated spirals of high velocity

$$5670 \pm 1500 \text{ km/sec. toward}$$

$$l = 307 \quad b = 308$$

$$d = -38 \quad b = 35$$

The residual velocities obtained from these two solutions are given in the subjoined table: these have been rounded off to tens of kilometers for the first solution and to hundreds for our local G_2 in G_1 . The column headings in this table are self-explanatory.

Residual Velocities of Spirals on a MOUSSARD-CHARNIER Scheme

1 NGC	2 Obs. vel. km/sec		3 Residual, within G_1		Allocation
			Residual within G_1	Residual, G_2 in G_1	
205	—	300	— 710		Local
221	—	500	600		Local
224	—	220	— 640		Local
275	+	650	+ 200		Local
350	+	1400	—		
383	+	4500	—	600	Pisces Cluster
354	+	4500	—		
385	+	4900	—		
404	—	25	610		
554	+	1500	+ 1260		Local
598	—	70	— 620		Local
936	+	1300	— 580		Local
1025	+	300	— 420		Local
1068	+	920	+ 150		Local
1270	+	4800	—		
1273	+	5800	—	— 2800	Pisces Cluster
1275	+	5200	—		
1277	+	5200	—		
1700	+	500	— 520		
2562	+	5100	—	— 9400	Coma Cluster
2563	+	4800	—		
2681	+	700	— 250		
2683	+	400	— 700		
2841	+	600	— 350		Local
2859	+	1500	+ 450		Local
2950	+	1500	+ 660		Local
3031	—	30	— 760		Local
3034	—	290	— 430		Local
3115	+	600	— 470		Local
3193	+	1300	+ 280		Local
3227	+	1150	+ 140		Local
—	+	19600	—	+ 9500	Leo Cluster
3368	+	940	— 30		
3379	+	810	— 170		
3480	+	600	— 330		
3521	+	730	— 300		Local
3610	—	1850	+ 1130		Local
3623	+	800	— 80		Local
3627	+	650	— 230		Local
4051	+	650	— 40		Local
—	+	11800	—	+ 2100	Ursa Major Cluster
4111	+	800	+ 110		
4151	+	960	+ 270		
4192	+	1150	+ 440		
4214	+	300	— 380		Local? (Vulgo)

(Continued)

1 NGC	2 Obs. vel km/sec.	3		Allocation
		Residual within G_2	Residual, G_2 in G_1	
4258	+ 500	- 150	-	Local
4374	+ 1050	+ 360	-	Local? (Virgo)
4382	+ 500	- 180	-	Local? (Virgo)
4449	+ 200	- 480	-	Local
4472	+ 850	+ 180	-	Local? (Virgo)
4486	+ 800	+ 130	-	Local? (Virgo)
4526	+ 580	- 80	-	Local? (Virgo)
4565	+ 1100	+ 460	-	Local
4594	+ 1140	+ 540	-	Local
4649	+ 1190	+ 460	-	Local? (Virgo)
4736	+ 290	- 300	-	Local
4826	+ 150	- 390	-	Local
4853	+ 7600	-	-	Coma Berenices Cluster
4860	+ 7900	-	-	
4865	+ 5000	-	-	
4872	+ 6900	-	-	
4874	+ 7000	-	-1200	
4881	+ 6900	-	-	
4884	+ 6700	-	-	
4895	+ 8500	-	-	
II 4045	+ 6600	-	-	Local
5005	+ 900	+ 360	-	
5055	+ 450	- 80	-	
5194	+ 250	- 240	-	
5236	+ 500	+ 50	-	Local
5457	+ 300	- 130	-	Local
5866	+ 650	+ 330	-	Local
6359	+ 3000	-	-3200	Isolated
6658	+ 4100	-	+2200	Isolated
6661	+ 3900	-	+2000	Isolated
6702	+ 2000	-	-1900	Isolated
6703	+ 2000	-	-1900	Isolated
6710	+ 5100	-	+2900	Isolated
6822	+ 150	+ 90	-	Local
6824	+ 3200	-	-1200	Isolated
7217	+ 1050	+1040	-	Local
7242	+ 5000	-	+1800	Isolated
7331	+ 500	+ 400	-	Local
7611	+ 3400	-	-	Pegasus Cluster
7617	+ 3900	-	-	
7619	+ 3800	-	+2200	
7623	+ 3800	-	-	
7626	+ 3700	-	-	
L M C	+ 280	- 390	-	Local
S M C	+ 170	- 310	-	Local

The results from both solutions may be regarded as on the whole satisfactory, and perhaps significant. Those found for the motion of our own galaxy within its G_2 are in general "reasonable". We know so little as to a possible upper limit to the speed of a cluster of galaxies that the larger residuals found for our G_2 moving in a G_2 system do not seem impossible. The total motion of our own G_2 cluster, ca. 5700 km/sec., is of the order of the larger residuals in the second solution.

A study of the residuals from the two solutions will indicate that the excess of positive velocities has been almost completely removed. It is unnecessary to reiterate that a slightly different grouping of the objects in the two classes treated, or the acquisition of a number

of velocities of spirals in the regions adjacent to the south galactic pole, would be expected to make significant changes in the magnitudes and directions of the total motions resulting

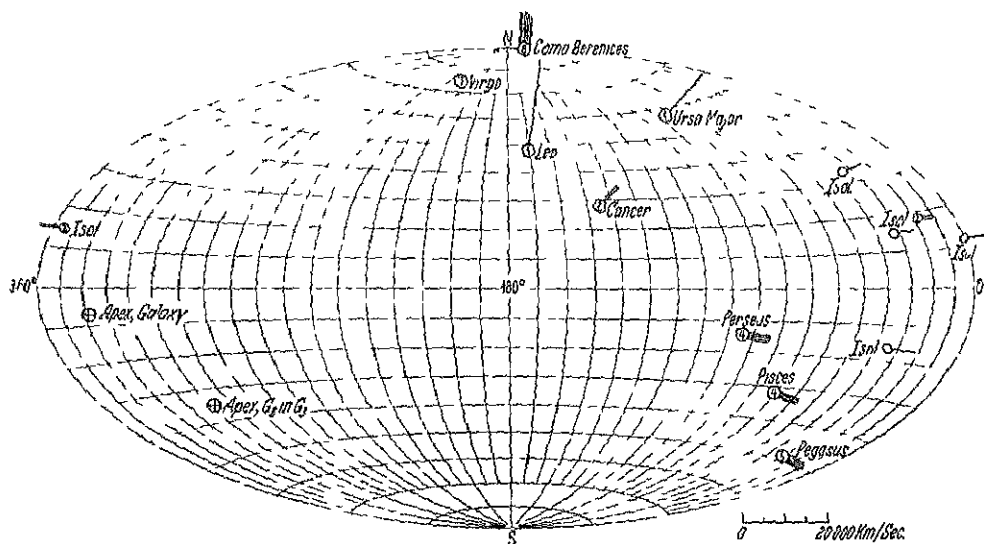


Fig. 58. Distribution of Clusters of Galaxies.

from this method of treatment. The data are manifestly too limited in amount and in distribution to warrant any further refinement in the analysis.

Kapitel 7.

Die Milchstraße.

Von

B. LINDBLAD-Stockholm.

Mit 28 Abbildungen und 1 Tafel.

a) Einleitung.

1. Die Milchstraße als Objekt der Forschung. Das schwach leuchtende, diffuse und komplizierte, aber doch in einem gewissen Sinne sehr regelmäßige Gebilde unseres Nachthimmels, das den Namen Milchstraße (*Voie lactée*, *Milky Way*, griech. *γαλαξίας*, lat. *Via lactea*) trägt, ist in seiner Gesamtheit, der scheinbaren Ausdehnung nach, das gewaltigste aller Himmelsobjekte. In der Forschung haben wir zuerst die Milchstraße als scheinbares Gebilde, das „Phänomen der Milchstraße“, zu betrachten. Es gilt hier, soweit möglich, persönliche Differenzen verschiedener Beobachter auszugleichen und ein mittleres Bild der Milchstraße, wie sie einem normalen menschlichen Auge erscheint, zu geben. Dieses Bild wird durch photometrische Schätzungen und Messungen in systematischer Weise ergänzt. Endlich greift hier auch die Photographie in bedeutungsvoller Weise ein. Doch muß immer daran erinnert werden, daß das visuelle und das photographische Milchstraßenbild in vielen Beziehungen prinzipiell streng zu unterscheiden sind.

Diese Festlegung des scheinbaren Phänomens hat aber nur einen Sinn, wenn sie für eine tiefer gehende Forschung die Grundlage bildet. Die Stellarastronomie sieht in der Milchstraße den Effekt einer Konzentration der Sterne unseres Systems gegen eine Fundamentalebene, die als Milchstraßenebene oder galaktische Ebene bezeichnet wird. Diese Konzentration gegen eine Ebene ist sogar in ihrer offenbaren Gesetzmäßigkeit das unmittelbarste Zeichen dafür, daß wirklich die uns umgebenden Sterne in ein gewaltiges System eingeordnet sind. In der Stellarastronomie wird das Wort Milchstraße bisweilen als ein Synonym für das Sternsystem verwendet. Es wird schließlich eine Aufgabe der Astronomie, die Erscheinung der Milchstraße in ihrer stellarastronomischen Bedeutung dynamisch zu erklären, welche Aufgabe es bedingt, eine statistische Mechanik des Sternsystems zu entwickeln. Die Methoden einer solchen statistischen Mechanik haben mehrere Berührungspunkte mit den statistisch-mechanischen Methoden der allgemeinen theoretischen Physik, wenn auch keineswegs die Theorien der kontinuierlichen Medien, der Gase und Flüssigkeiten, unmittelbar auf das Sternsystem angewandt werden können.

2. Übersichtliche Darstellungen und Monographien. Von Übersichtswerken über die Ergebnisse und Methoden der Milchstraßenforschung sollen hier nur einige erwähnt werden, welche, ohne neues Primärmaterial zu geben, durch selbständige zusammenfassende Gesichtspunkte gekennzeichnet sind. Unter

den älteren Werken dieser Art sind zu nennen J. G. W. STRUVE, *Etudes d'Astronomie stellaire*¹, J. HIRSCHL, *Outlines of Astronomy*², H. J. KILIN, *Der Fixsternhimmel* usw.³, R. A. PROCTOR, *The Universe and the Coming Transits*⁴. Einer späteren Zeit gehören z. B. die Übersichtswerke von MISS CERKKI⁵ und S. NIWCOMB⁶ an. F. RISINPARI gibt unter dem Wort „Universe“ in V. V. V. HINDEL'S Handbuch⁷ eine eingehende Beschreibung der damaligen Resultate der Milchstraßenbeobachtungen und der Stellarstatistik. Etwas später erscheint H. KOBOLD, *Der Bau des Fixsternsystems*⁸. Aus der Zeit der zwei letzten Jahrzehnte sind besonders zu erwähnen A. S. EDDINGTON, *Stellar Movements and the Structure of the Universe*⁹, und H. KOBOLD, *Das Sternsystem*¹⁰ und *Stellarastronomie*¹¹. K. GRAFF gibt in R. HINSPINGS „*Astronomisches Handbuch*“, herausgegeben vom Bund der Sternfreunde¹², eine Darstellung der Resultate der visuellen und photometrischen Milchstraßenbeobachtungen. J. PRYSMANN¹³ hat eine sehr verdienstvolle Monographie, „*Die Milchstraße*“ herausgegeben, die auch einen Zusatz von J. HAGN über „*Die Nebelstraße*“ enthält. A. KOPPEL gibt in MUTTER-POURCHES Lehrbuch der Physik¹⁴ eine inhaltreiche Übersicht über den Bau des Sternsystems nach den modernen Untersuchungen. Eine zusammenfassende Darstellung über den Bau des Kosmos ist von W. BLERNHARDT in *Handbuch der Physik*¹⁵ gegeben worden.

b) Das visuelle Milchstraßenbild.

3 Die Beschreibung und zeichnerische Darstellung der Milchstraße Die Milchstraße ist schon für eine flüchtige Beobachtung ein auffälliges Phänomen des gestirnten Himmels und ist doch nicht leicht durch wissenschaftliche Vermessung quantitativ zu erfassen und darzustellen. Selbst eine genaue qualitative Beschreibung der Milchstraßenstruktur in ihren Einzelheiten und eine detaillierte zeichnerische Darstellung derselben ist erst in der Mitte des vorigen Jahrhunderts erstlich angefangen worden. Hindernisse der exakten Beobachtung sind die mit der Höhe über dem Horizont wechselnde atmosphärische Absorption und auch allerlei Trübungen durch fremdes Licht, die den Eindruck des schwach leuchtenden Gebildes verfälschen können. Zu bemerken ist, daß die Milchstraße nur in geringem Kontrast gegen das allgemeine schwache Himmelslicht leuchtet. Die Schwierigkeiten sind natürlich mit der komplizierten Natur des Phänomens verbunden, mit der sanften und doch in einem Gewebe unendlich reicher Struktur vor sich gehenden Abstufung der Lichtstärke von den verhältnismäßig hellen Wolken bis zu den kaum wahrnehmbaren feinen Lichtschleiern, die dunklere Partien umgeben oder allmählich in den dunklen Himmelsgrund der außergalaktischen Regionen übergehen.

Die Schwierigkeiten, ein einheitliches Bild des ganzen Milchstraßengürtels zu schaffen, sind weiterhin eine Folge der Ausdehnung des Phänomens längs eines großen Kreises des Himmels, der um etwa 60 Grad gegen den Äquator geneigt erscheint. Nur in den Tropen kommt die ganze Milchstraße während

¹ St.-Petersbourg: Imprim. de l'Acad. Imp. des Sc. (1847)

² London: Longman, Brown etc. (1849, mit späteren Auflagen)

³ Handb. der allgemeinen Himmelsbeschreibung II. Braunschweig (1872)

⁴ London: Longmans, Green, and Co. (1874)

⁵ The System of the Stars. London: Black (1890, 2. Aufl. 1905)

⁶ The Stars. London: Murray (1902)

⁷ IV, S. 65. Leipzig: Barth (1902)

⁸ Braunschweig: Vieweg u. Sohn (1906)

⁹ London: Macmillan (1911)

¹⁰ Kultur der Gegenwart III (Astronomie) S. 511. Leipzig und Berlin: Teubner (1912)

¹¹ Encyclopädie der math. Wiss. VI 2 B, Heft 2. Leipzig: Teubner (1926)

¹² S. 183. Stuttgart: Franckhsche Verl. (1921)

¹³ Probleme der Kosmischen Physik IV. Hamburg: Grun. (1924)

¹⁴ 11. Aufl., V, 2. Hälfte, S. 429 (1928)

¹⁵ IV, S. 577 (1929)

eines Jahreslaufs über den nächtlichen Horizont. Die gegenwärtig in den Einzelheiten genauesten Darstellungen des visuellen Milchstraßenbildes sind hauptsächlich über den nördlichen Teil der Milchstraße ausgedehnt, während zur Zeit der Vollendung der Uranometria Argentina der südliche Teil der Milchstraße der durch gute Darstellung begünstigte war.

Aus dem Altertum sind zwei Beschreibungen der Milchstraße aufbewahrt worden, von ARISTOTELIS¹ und von PROKLOS². Die letztere ist ziemlich eingehend und ist wahrscheinlich erst im 19. Jahrhundert übertroffen worden. Eine deutsche Übertragung des Almagest mit der heutigen Sternbenennung gibt K. MARITIUS³. PROKLOS' Milchstraßenbeschreibung ist von EASTON⁴ nach HAIMAS Übersetzung mit Erklärungen wiedergegeben worden. Ein Bruchstück in freier Übersetzung mit Bemerkungen hat PANNEKOKK in seinem unten besprochenen Werke „Die südliche Milchstraße“ gegeben. Eine nur wenig in Einzelheiten gehende Beschreibung der Milchstraße hat THOMAS WRIGHT in seinem seltenen Werke „Theory of the Universe“ (London 1750) geliefert. Die Sternkarten des 17. und des 18. Jahrhunderts behandeln die Milchstraße nur sehr dürftig. Noch auf BOUDYs Karten⁵ ist nur eine schematische Milchstraßenkontur grob gezogen worden. J. K. HÖRNER⁶ hat als erster neben einer Milchstraßenbeschreibung eine elementare Photometrie der MAGELLANSchen Wolken und hellerer Partien der südlichen Milchstraße mit Hilfe von farbigen Gläsern verschiedener Dicke versucht. W. HERSCHEL⁷ gibt ein kurzes Verzeichnis von hellen und dunklen Partien der Milchstraße zwischen Sagittarius und Perseus. Einige Fortschritte in bildlicher Darstellung sind wohl in den Karten von W. H. WOLLASTON⁸, J. W. LUBBOCK⁹ und J. DUNLOP¹⁰ zu registrieren.

F. W. A. ARGELANDER fordert in SCHUMACHERs Jahrbuch, 1844, die Freunde der Astronomie zu Beobachtungen der Milchstraße auf. In den 40er Jahren erscheint J. HERSCHELs¹¹ verdienstvolle Zeichnung der südlichen Milchstraße mit eingehender Beschreibung. A. V. HUMBOLDT gibt im dritten Bande des „Kosmos“ hauptsächlich nach den Arbeiten von J. HERSCHEL eine Beschreibung des Zuges der Milchstraße unter den Sternen.

Ein Bruchstück einer detaillierten wörtlichen Beschreibung wurde im Jahre 1867 von H. J. KIRBY in HEIS' „Wochenschrift für Astronomie“ veröffentlicht, und einige Jahre später gab endlich E. HEIS¹² seine Zeichnungen der Milchstraße heraus. Sie gehen südlich bis zur Deklination -35° . HEIS unterscheidet fünf Lichtstufen, die als Schattierungen verschiedener Tiefe in den Zeichnungen wiedergegeben sind. Seine Darstellung steht daher mit den isophotischen Karten späterer Beobachter in Verwandtschaft. Die feineren Einzelheiten werden in dieser Weise nicht berücksichtigt, sondern in Lichtflecken einfacherer Kontur ausgeglichen. Die niedrigste Stufe bei HEIS entspricht dem schwachen Schimmer, in den die Milchstraße einem Beobachter mit scharfen Augen unter guten atmosphärischen Verhältnissen eingehüllt erscheint.

¹ Meteorologica, Lib. I, Cap. 8

² Almagest, Lib. VIII, Cap. 2

³ Leipzig Teubner (1912)

⁴ La voie lactée dans l'hémisphère boréal. Paris. Gauthier Villars (1893)

⁵ Uranographia sive astrorum descriptio. Berlin (1801)

⁶ Monatliche Correspondenz 10, S. 220 (1804)

⁷ Phil. Trans. 1817, S. 302, Coll. Scient. Papers II, S. 586.

⁸ A Portraiture of the Heavens as they appear to the Naked Eye. London (1811)

⁹ The Stars in six Maps, etc. London (1830, mit späteren Aufl.)

¹⁰ Phil. Trans. 1828, S. 152

¹¹ Results of Astronomical Observations, etc., p. 383. London. Smith, Elder (1847); Beschreibung auch in Outlines of Astronomy (5. Edition, S. 527)

¹² Atlas coelestis novus. Köln (1872)

Die südliche Milchstraße wurde in der großartigen Uranometria Argentina von B A GOULD¹ nach Zeichnungen von W M DAVIS und J M THOM in genauer Weise wiedergegeben. Die Art der Reproduktion der Zeichnungen war eine photolithographische, die Wiedergabe der Einzelheiten ist weniger durch vereinfachende Ausgleichung gebunden als in den Karten von HUIS

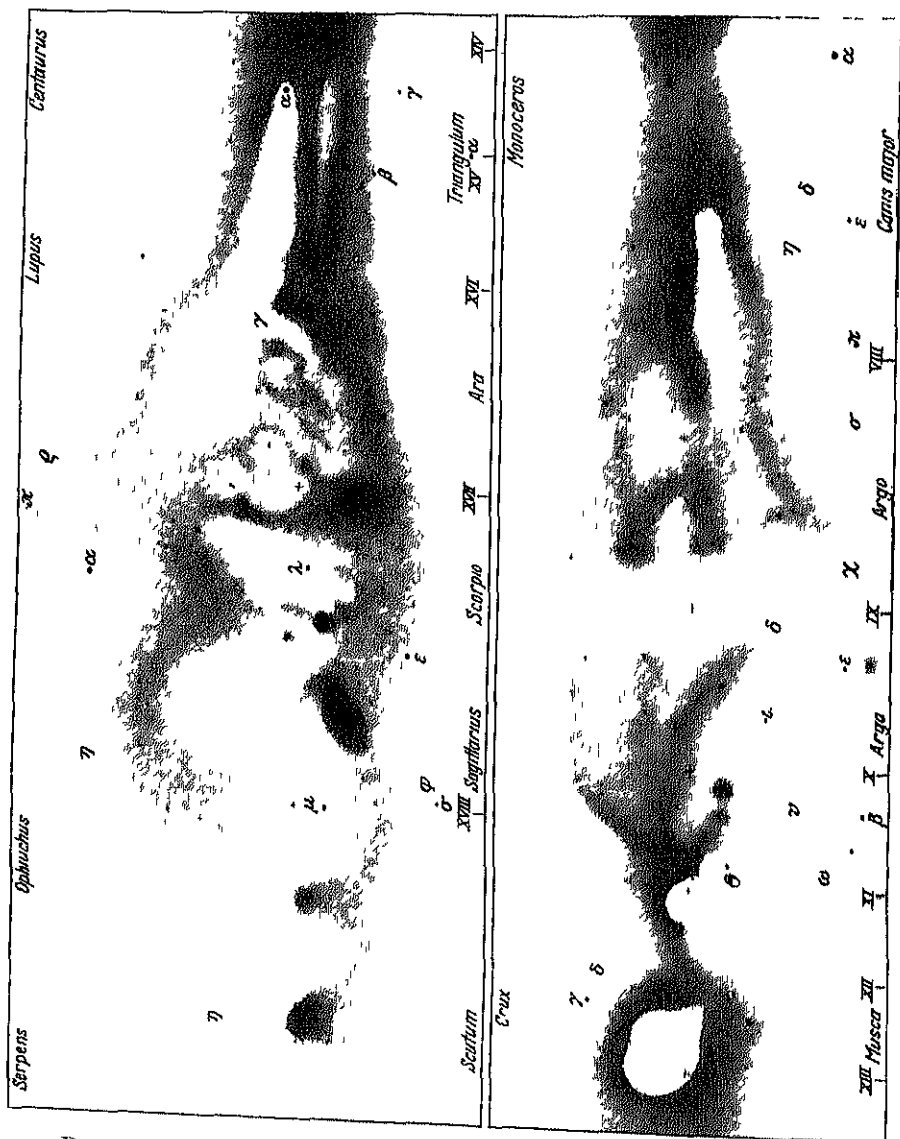


Abb 1 Reproduktion der HERSCHEL'Schen Zeichnung der südlichen Milchstraße

Durch die Arbeiten von HUIS und GOULD war somit eine eingehende und wissenschaftlich einigermaßen brauchbare Darstellung des ganzen Milchstraßengürtels geschaffen worden. Die bisweilen erheblichen Unterschiede der zwei Bilder in den gemeinsamen Teilen lassen jedoch die Subjektivität der Auffassung selbst in den zeichnerischen Arbeiten höchster Klasse deutlich erkennen.

¹ Resultados del Observatorio Nacional Argentino I (1879) Mit Atlas

Inzwischen war eine Reproduktion der ganzen Milchstraße erschienen, die zwar eine noch schematischere Darstellung als die HAUSSCHE bot, aber auf eine neue methodische Schätzung der Lichtstufen gegründet war. Dieses Werk ist in der „*Uranométrie générale*“ von J. C. HOUZEAU¹ enthalten. Die Beobachtungen wurden auf Jamaika angestellt. HOUZEAU hat einen Versuch gemacht, die Linien konstanter Lichtstärke, die Isophoten, zu zeichnen. Er ordnet die Helligkeiten verschiedener Partien in eine Skala von Größenklassen, die eine Art Anschluß an die Größenskala der Sterne dadurch gewinnt, daß man das Hervortreten oder Verschwinden der Lichtflecken in der Dämmerung oder in der Himmelsbeleuchtung durch den Mond zur selben Zeit wie das Hervortreten oder Verschwinden benachbarter Sterne einer gewissen Größe beobachtet. HOUZEAU gibt in einer Tabelle die Intensitäten für 33 Punkte maximaler Helligkeit. Um diese Maxima sind die isophotischen Linien in ziemlich schematischer Weise gezeichnet, oftmals als regelmäßig abgerundete Ovale. Durch diese schematische Regelmäßigkeit steht HOUZEAU'S Darstellung in einer Sondorklasse unter den visuellen Milchstraßenbildern. Die größten Intensitäten (Größen 4,5 und 5) notiert HOUZEAU für die Gegenden, die in Tabelle 1 zusammengestellt sind (Koordinaten für Äqu. 1880).

In schärfstem Gegensatz zu HOUZEAU'S Methode steht die Art der Milchstraßendarstellung, die von O. BORDDICKER² zu Birr Castle in Irland praktiziert wurde. Die Milchstraße ist hier in eine komplizierte Struktur von feinen Strömungen mit oftmals ziemlich scharfen Begrenzungen aufgelöst. Die Subjektivität dieser schönen und technisch vollendeten Darstellung ist offenbar. PANNIKOFF, der die Gelegenheit hatte, die Originalzeichnungen zu untersuchen und zu benutzen, macht jedoch die Bemerkung, daß diese Bilder viel mehr als die Reproduktionen sich dem wirklichen Anblick der Milchstraße nähern, und daß also der lithographische Prozeß, trotz größter Sorgfalt, viele schwache Nuancen modifiziert hat. Eine Beschreibung seiner Arbeitsmethode hat BORDDICKER selbst in einer Notiz³ gegeben.

Tabelle 1

A.R.	Decl.	Größe	Sternbild
16 ^h 4 ^m	-54° 3	5	Norma
17 46	-34 7	5	Scorpius (M7) ⁴
18 0	-28 5	5	Sagittarius
18 8	-18 7	4,5	Sagittarius
18 23	-14 4	5	Scutum
18 41	-7 0	4,5	Scutum
21 2	+45 5	5	Cygnus

Unter den Zeichnungen dieser Zeit ist auch eine Chromolithographie von L. TROUVELOT⁵ von der Milchstraße zwischen Caslopera und Scorpius zu nennen. Die Originale befinden sich nach EASTON in Meudon.

Zu den schönsten Zeichnungen der Milchstraße gehören wohl die von JULIUS SCHMIDT, die in den Jahren 1864—1867 zu Athen hergestellt worden sind und die erst kürzlich in phototypischer Reproduktion von der Sternwarte zu Leiden⁶ publiziert wurden. Die Zeichnungen erstrecken sich im Süden bis zur Deklination -45°. Besonders die südlichen Partien, von Scorpius bis Aquila, sind mit erstaunlicher Fülle von Einzelheiten mit größter Sorgfalt ausgearbeitet worden.

¹ *Annales de l'Observatoire de Bruxelles*, N S, I (1878)

² *The Milky Way from the North Pole to 10° South Declination*. London (1892)

³ Die Größe der Gegend um M7 ist in HOUZEAU'S Tabelle als 4, auf der Karte aber als 5 bezeichnet. Die letztere Zahl ist von EASTON (l. c.) aufgenommen worden.

⁴ *M N* 50, S 12 (1889)

⁵ *The Trouvelot Astronomical Drawings*. New York: Scribner (1882)

⁶ *Annales van de Sterrewacht te Leiden* XIV. Tweede Stuk (1923)



Abb 2 Reproduktion von EASTONS „carte generale der nordlichen Milchstraße

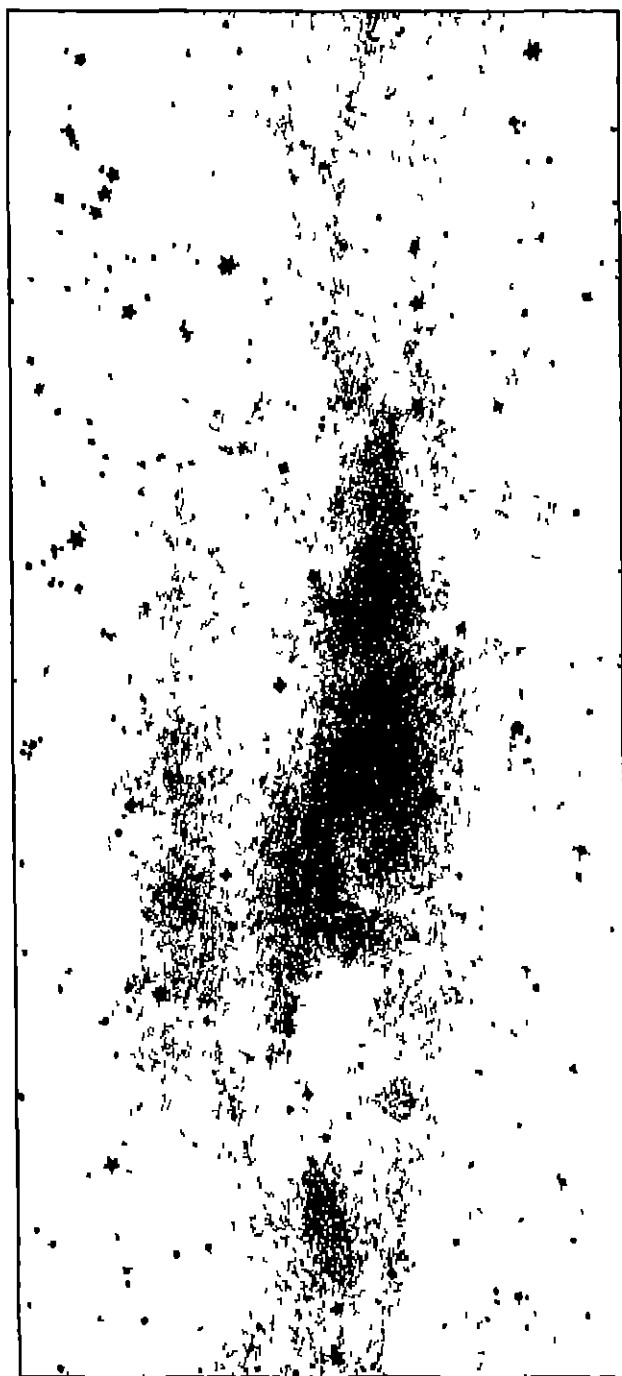


Abb 2a.

Nach J HOPMANN¹ befindet sich auf der Bonner Steinwarte im Manuskript eine Reihe von SCHMIDTS Milchstraßenbeobachtungen, Beschreibungen und Helligkeitsschätzungen, beginnend 1859 in Athen, die nur teilweise in direktem Zusammenhang mit seiner Karte stehen

Die Milchstraße nördlich der Deklination -10° ist in sehr eingehender Weise von den zwei holländischen Astronomen, C EASTON und A PANNIKOLK, behandelt worden EASTONS vorher erwähnte, 1893 erschienene Arbeit, „La voie lactée dans l'hémisphère boréal“, bildet einen sehr merkwürdigen Fortschritt in der bildlichen Darstellung der Milchstraße EASTON hat seine Karten ganz unabhängig von anderen Darstellungen gezeichnet Die Reproduktion ist auf lithographischem Wege ausgeführt worden, wobei der Zeichner selbst die zur Vorbereitung nötige Kopierarbeit sowie eine Retusche der gedruckten Karten ausgeführt hat EASTON betont besonders die großen Schwierigkeiten, durch Zeichnung ein exaktes Bild der Milchstraße, wie sie dem Auge erscheint, wiederzugeben Das Milchstraßenlicht ist so schwach und die Helligkeitsdifferenzen der verschiedenen Partien sind so sanft akzentuiert, daß die Wiedergabe immer ein wenig übertrieben werden muß EASTON gibt eine Hauptkarte (carte générale), welche die Gradation des Milchstraßenlichts und die relative Helligkeit der Milchstraßenpartien wiedergeben soll, während drei „cartes explicatives“ in etwas feiner Einzelheiten gehen Die Hauptkarte, welche ein bemerkenswertes, vorzügliches Stück Arbeit ist, wird hier in Abb 2 reproduziert Der Text enthält eine ausführliche geschichtliche Übersicht über das Problem der Milchstraßenbeschreibung Zuletzt gibt EASTON hier eine eigene, sehr eingehende Beschreibung der nördlichen Milchstraße nebst einem Katalog, der die Randkoordinaten von 164 hellen Flecken und Strömungen und von 47 dunklen Partien enthält In einer späteren Arbeit² hat EASTON auch eine Karte mit isophotischen Linien gegeben

PANNIKOLK scheint der erste zu sein, der die Mahnung ARGELANDERS in seiner „Aufforderung“, eine feste Skala relativer Helligkeiten durch wiederholte Vergleichen verschiedener Teile der Milchstraßenstruktur auszubilden, beherzigt hat In seinem Werke³ „Die nördliche Milchstraße“ gibt er die Resultate seiner umfangreichen Helligkeitsschätzungen Die Helligkeiten wurden zuerst in einer willkürlichen Skala ausgedrückt, nachher wurde eine Zahl von Normalstellen ausgesucht, diese wiederholt aneinander angeschlossen und damit alle anderen zu beobachtenden Stellen verglichen Die relativen Helligkeiten wurden nach der Stufenmethode ARGELANDERS geschätzt, und die Ausgleichen für die Normalstellen in einer zusammenhängenden Skala mit der Stufe als Einheit geschah auf dem Wege wiederholter Annäherung In dieser Skala wurden die Helligkeiten von 128 Stellen der Milchstraße ausgedrückt Der Stufenwert wurde zunächst unter Benutzung der atmosphärischen Absorption durch Vergleichung heller Flecken, wenn sie in geringer Höhe stehen, mit hochliegenden Stellen der Milchstraße und auch nach HOUZEAS Methode aus Beobachtungen in der Dämmerung bestimmt Eine bessere Bestimmung ergab sich später⁴ aus einer Vergleichung mit den Helligkeitsmessungen von VAN RIJN (Ziff 5) Der Stufenwert der Gesamthelligkeit des Himmelsgrundes („Eidlicht“ in weiterem Sinne + Milchstraßenlicht) ergibt sich hier zu 0,11 Größenklassen, was aber, wenn das „Eidlicht“ eliminiert wird, im Mittel für das Milchstraßenlicht 0,3 Größenklassen bedeutet

¹ VJS 64, S 320 (1929)

² Verh der K Akademie van Wetenschappen, Amsterdam, VIII, Nr 3 (1903)

³ Annalen van de Sterrewacht te Leiden XI Derde Stuk (1920)

⁴ AN 214, S 389 (1921)

PANNEKOEK gibt seine Resultate teils in einer sehr ausführlichen wörtlichen Beschreibung der Einzelheiten, teils als Zeichnungen, die auf den zahlenmäßigen Resultaten fußen und durch ein photographisches Reproduktionsverfahren vervielfältigt wurden, teils endlich als Karten mit isophotischen Linien, die direkt die Zahlenergebnisse zum Ausdruck bringen. Weiter folgen der sehr eingehenden Beschreibung der nördlichen Milchstraßenstruktur ausführliche Vergleichen mit anderen Darstellungen (EASTON, SCHMIDT, BOEDDICKER, KLIN, BACKHOUSE¹, Uranometria Argentina). Schließlich werden die Isophotendarstellungen von PANNEKOEK und von EASTON mit den Zeichnungen von SCHMIDT und von BOEDDICKER in ein „mittleres Milchstraßenbild“ von zahlenmäßiger Form zusammengefaßt, das auch in Isophotekarten wiedergegeben wird. Der mittlere Stufenwert wird für die Eckpunkte und für das Zentrum jedes Quadratgrades des galaktischen Gürtels gegeben. Dieses Zahlensystem sollte als „das beste Gesamtergebnis zu betrachten sein, das sich aus den bisherigen Arbeiten über die Milchstraße ableiten läßt“.

Ganz kürzlich hat PANNEKOEK² nach demselben Plan seine Arbeit auch über die südliche Milchstraße ausgedehnt. Die Beobachtungen wurden gelegentlich einer Expedition, die von der K Akademie der Wissenschaften in Amsterdam zur Beobachtung der am 14. Januar 1926 stattfindenden totalen Sonnenfinsternis nach Indien geschickt wurde, ausgeführt, und zwar sowohl auf der Bosscha-Sternwarte in Lembang auf Java, als auf dem Dampfer während der Reise. Die Witterungsverhältnisse waren durchgehend ziemlich ungünstig. Nichtsdestoweniger ist es dem unermüdeten Astronomen gelungen, sein Programm durchzuführen und die südliche Milchstraße in ihren Einzelheiten auf photometrischer Grundlage darzustellen.

Eine Anzahl Normalpunkte wurde ausgewählt und durch wiederholte Vergleichen untereinander in eine „südliche Skala“ eingeordnet, welche sowohl an der Aquilaseite als an der Monocerosseite mit der nördlichen verglichen und auf diese reduziert werden konnte. Die Helligkeiten anderer Punkte wurden mit Hilfe der Normalstellen geschätzt. PANNEKOEK gibt einen Katalog über die Beobachtungsergebnisse für 189 Stellen der südlichen Milchstraße.

Wie für die nördliche Partie der Milchstraße hat PANNEKOEK auch in dieser Arbeit auf Grund seiner Resultate Zeichnungen und Isophotekarten ausgearbeitet und gibt auch eine in die feinsten Einzelheiten gehende wörtliche Beschreibung, der er die Beschreibungen von PROCLUS und von J. HERSCHEL folgen läßt.

Der große Reichtum der südlichen Milchstraße wird besonders von PANNEKOEK hervorgehoben:

„Wer nur die Teile des Sternhimmels kennt, die in den mittleren Breiten Europas sichtbar sind, kann sich keine Vorstellung von der wundervollen Schönheit der südlichen Milchstraße machen. Gewiß gehört eine dunkle Augustnacht in Europa mit den großen hellen Lichtwolken im Schwan und dem anschließenden buchtigen Fleckenband im Adler und in der Cassiopeia zu den schönsten Natureindrücken in unserem Weltteil. Aber die Pracht des Südhimmels ist doch ganz anderer Ordnung, man möchte ihre höhere Potenz nach einer unrichtigen, aber verständlichen Gedankenassoziation mit dem üppigen Reichtum aller Tropennatur in Zusammenhang bringen. Es ist zuerst die viel größere Helligkeit, die die Milchstraße in ihrer südlichen Hälfte erreicht. Ihr Licht wächst von dem schwachen, einförmigen Schimmer des Januarhimmels bei Orion und Sirius allmählich an und erreicht in Carina, in 250° Länge, eine Helligkeit, die schon

¹ The Structure of the Universe. Publ. of West-Hendon House Observatory I, II.

² „Die südliche Milchstraße“, Annalen v. d. Bosscha-Sternwarte Lembang (Java) II, 1ste Gedr. (1929).

übertrifft weitaus alle anderen Gebilde der Milchstraße, die Eigentümlichkeit des Eindrucks wird noch gesteigert durch die Armut dieser Gegenden an für das bloße Auge sichtbaren Sternen. Bei jedem Vergleich fällt der Gegensatz auf, wie die Milchstraße im Schwan und in Lacerta mit szintillierendem Sternstaub dicht besät ist, während die hellen Schützenwolken wie mit ruhiger Leuchtfarbe auf einen sternleeren Himmelsgrund gemalt erscheinen.“

Als ein Beispiel der PANNEKORRSchen Milchstraßendarstellung wird in Abb 3 die Isophotenkarte der kontrastreichen Carina-Cruy-Centaurus-Region des Südhimmels wiedergegeben.

4. Photometrische Eichung der Isophoten. Eine wichtige Ergänzung zu dem rein visuellen Milchstraßenbild, wie es nach den Beobachtungen mit bloßem Auge erscheint, liegt in den Resultaten photometrischer Messungen des Milchstraßenlichts. In dem Universalphotometer von K. GRAFF¹ wird ein Bild der beobachteten Himmelsgegend durch ein kleines Mikroskopobjektiv in der Kontaktfläche eines LUMMER-BROUHNschen Prismas erzeugt. Von der Seite her wird das Bild einer beleuchteten Milchglasscheibe nach dem Okular zu total reflektiert, so daß man den eingestellten Teil des Himmels als einen runden Fleck inmitten eines gleichmäßig erhellten Feldes sieht, das durch einen Photometerkeil vor der Milchglasscheibe auf die Lichtstärke des Fleckes abgeschwächt wird. Als Anschlußhelligkeit für GRAFFs Messungen diente der Hintergrund in Ursa minor bei R. A. 0^h 0^m und Dekl. +85°, dem willkürlich die Größe 2^m,0 beigelegt wurde. Als zweiter Anhaltspunkt diente die Cygnuswolke zwischen γ und β Cygni, für die der Wert 1^m,30 photometrisch erhalten wurde. GRAFFs Beobachtungen verteilen sich auf 32 Stellen des Himmels, in Verbindung mit Stufenschätzungen wurden 47 Punkte der nördlichen Milchstraße von Sagittarius bis Canis major in ihrer relativen Helligkeit photometrisch festgelegt.

J. HOPMANN² hat als eine Nebenaufgabe bei der Sonnenfinsternisexpedition 1922 nach Christmas Island mit Anschluß an GRAFFs Messungen ähnliche Beobachtungen für einige Punkte der südlichen Milchstraße ausgeführt und auch eine Menge Stufenschätzungen relativer Intensitäten in dieser Gegend gemacht. Unter Benützung der PANNEKORRSchen Isophoten der nördlichen Milchstraße und Zuhilfenahme von GOULDS Darstellung der südlichen Milchstraße in der Uranometria Argentina zur Ergänzung seiner Stufenschätzungen hat HOPMANN dann eine Isophotenkarte der ganzen Milchstraße konstruiert. Für PANNEKORRS Stufenwort findet HOPMANN aus GRAFFs Messungen 0^m,138, für seinen eigenen findet er 0^m,0996. Es sollte hervorgehoben werden, daß die Stufenmethode erheblich genauer ist als die photometrischen Messungen, deren w. F. einer Beobachtung etwa 0^m,1 beträgt. Die im Photometer gemessene Fläche ist auch größer als die mit dem Auge verglichenen Gebiete. Der Vorteil des Photometers besteht also wesentlich in der Einführung einer unpersönlichen Skala.

PANNEKORR³ hat der HOPMANNschen Darstellung einige kritische Bemerkungen gewidmet. Es scheint sehr möglich, daß infolge unzulänglicher Verblindung der zwei Hälften der südlichen Milchstraße, Centaurus- und Carinaselte, in den Stufenschätzungen HOPMANNs die Gegend um 6^h R. A. (Monoceros) zu schwach, verglichen mit der Gegend um 18^h (Sagittarius), ausgefallen ist. PANNEKORR hebt auch hervor, daß infolge variablen „Erdlichts“ das Helligkeitsverhältnis zwischen Normalstelle und Milchstraßengegend veränderlich sein muß, und daß

¹ Abhandl. der Hamburger Sternw. zu Bergedorf II, Nr. 5 (1920).

² A. N. 249, S. 189 (1923).

³ B. A. N. 3, S. 44 (1925), Die südliche Milchstraße (1929).

die GRAFFSCHE Methode daher kaum geeignet ist, eine ganz zuverlässige absolute Skala zu geben. In einer eingehenden Rezension der PANNEKOLK'schen Werke über die Milchstraßenstruktur macht HOPMANN¹ auch einige Bemerkungen zu PANNEKOLK'S Kritik. Es wäre noch zu früh, mit Sicherheit über das wahre Intensitätsverhältnis zwischen den zwei Milchstraßengebieten zu urteilen. Es scheint, als ob man vielleicht bei PANNEKOLK mit einer kleinen Variation der Stufe zwischen Nord- und Südhimmel zu rechnen hat (vgl. Ziff 5).

5 Die absolute Helligkeit des Himmelsgrundes. Zur Ermittlung der wahren Intensitätsverteilung des Milchstraßenlichts oder des allgemeinen Sternenlichts aus den Resultaten der photometrischen Stufenschätzungen und Messungen ist es notwendig, die beobachteten Helligkeiten von dem Einfluß der allgemeinen zerstreuten Strahlung des Himmels, die als „Eidlicht“ im weiteren Sinne bezeichnet werden kann, zu befreien. Diese Strahlung rußt größtenteils von Nordlichtern und vom Zodiakallicht her. Die Scheidung der zwei Strahlungsarten, Sternlicht und „Eidlicht“, ist dadurch möglich, daß die Sternstrahlung für hohe galaktische Breiten aus den Sternzahlen mit genügender Approximation berechnet werden kann.

Nach Pionierarbeiten von S. NEWCOMB², C. J. BURNS³, S. D. TOWNLEY⁴ und J. C. KAPTEYN⁵ haben besonders L. YNTEMA⁶ und P. J. VAN RIJN⁷ das Problem sehr eingehend behandelt. Das benutzte Flächenphotometer besteht im Prinzip aus einer kleinen beleuchteten Scheibe, die gegen den Himmel gerichtet wird, und deren Helligkeit durch Änderung der Beleuchtung in meßbarer Weise gleich der Helligkeit des Himmels an der betrachteten Stelle gemacht werden kann. VAN RIJN findet aus seinen auf Mount Wilson angestellten Beobachtungen die totale Helligkeit der direkten Sternstrahlung äquivalent mit 1440 Sternen der Größe $1^m,0$, was in guter Übereinstimmung mit YNTEMA'S Resultat, 1350 Sternen derselben Größe, ist. Die beobachtete Sternstrahlung für mehrere galaktische Breiten liegt zwischen den aus den Sternzahlen in den Groninger Publikationen Nr. 18 und 27 berechneten Werten, ist aber in besserer Übereinstimmung mit den letzteren Daten.

VAN RIJN gibt für den mittleren Anteil der verschiedenen Strahlungsarten in der direkt gemessenen nachtlischen Strahlung folgende Werte. Die Einheit der Helligkeit ist ein Stern von der Größe 1,0 im Harvardsystem per Quadratgrad. Die Sterngröße 1,0 entspricht $0,94 \cdot 10^{-6}$ Meterkerzen (Hefner)⁸. Die benutzte Einheit der Flächenhelligkeit des Himmelsgrundes entspricht daher etwa $0,78 \cdot 10^{-6}$ der Flächenhelligkeit des Vollmondes.

Zodiakallicht	0,071
Direktes Sternenlicht	0,029
Aurora borealis	0,024
Gestreutes Erdlicht	0,032
Gestreutes Sternenlicht	0,009

C. HOFFMANN⁹ macht jedoch wahrscheinlich, daß VAN RIJN den Anteil des Zodiakallichts zu hoch geschätzt hat. Er findet überhaupt einen viel kleineren Betrag für das „Eidlicht“, nur etwa ein Fünftel von YNTEMA'S und VAN RIJN'S Wert.

² V J S 64, S. 327 (1929) ³ Ap J 14, S. 297 (1901) ⁴ Ap J 16, S. 166 (1902)

⁵ Publ. A. S. P. 15, S. 13 (1903) ⁶ Plan of Selected Areas, S. 11 (1906)

⁷ Publ. Astron. Lab. Groningen, Nr. 22 (1909)

⁸ Publ. Astron. Lab. Groningen, Nr. 31 (1921)

⁹ Vgl. RUSSELL, Ap J 43, S. 128 (1916)

¹⁰ Veröff. d. Sternw. Berlin-Babelsberg, 8, H. 2 (1930)

VAN RHIJNS Resultate wurden von PANNEKOEK zur Ermittlung seines Stufenwerts benutzt (Ziff. 3). In ähnlicher Weise hat HOPMANN¹ seine scheinbaren Flächenhelligkeiten der Milchstraße durch eine summarische Korrektur in wahre Intensitäten verwandelt. Das Resultat, die mittlere Intensität, pro Quadratgrad gerechnet, für sukzessive Areale in dem galaktischen Koordinatennetze (galaktische Länge und Breite), wird hier in Tabelle 2 wiedergegeben.

Tabelle 2 Die mittlere Verteilung des galaktischen Lichts nach HOPMANN,

l°	-30°	-25°	-15°	-5°	$+5^\circ$	$+15^\circ$	$+25^\circ$	$+30^\circ$
0°	17 ^m	49 ^m	62 ^m	55 ^m	49 ^m	40 ^m	36 ^m	
10	36	43	71	56	51	37	36	
20	36	40	76	53	49	36	36	
30	36	41	74	100	56	36	36	
40	36	46	62	77	51	36	36	
50	36	45	65	63	56	36	36	
60	36	46	74	60	46	36	36	
70	36	48	73	63	45	36	36	
80	36	45	62	62	46	36	36	
90	36	45	57	49	42	36	36	
100	36	45	51	51	39	36	36	
110	36	41	49	46	46	36	36	
120	36	43	49	45	43	36	36	
130	36	49	46	54	47	37	36	
140	36	45	47	59	51	39	36	
150	36	42	53	63	51	45	36	
160	36	49	51	62	51	45	36	
170	36	49	51	65	56	45	36	
180	36	43	56	68	68	45	36	
190	36	39	44	68	58	44	36	
200	36	42	57	83	60	48	36	
210	36	46	57	79	66	48	37	
220	36	46	71	79	73	51	40	
230	36	42	64	73	66	51	39	
240	36	37	57	80	61	48	36	
250	36	36	50	89	62	41	36	
260	36	36	44	95	51	39	36	
270	36	39	94	116	90	42	36	
280	36	45	106	117	105	49	36	
290	36	53	108	117	116	57	39	
300	36	57	104	118	113	73	46	
310	36	56	109	109	126	89	51	
320	36	56	133	125	136	83	46	
330	36	51	83	123	95	60	36	
340	39	53	76	99	54	36	36	
350	40	54	83	76	46	37	36	
360								

Die Einheit der Helligkeit ist so gewählt worden, daß ein Stern von der Größe 1,00 im visuellen Harvardsystem gleich 1000 gesetzt wird. Es ist klar, daß die Resultate nicht als endgültig angesehen werden können, sondern einer sorgfältigen Prüfung durch wiederholte Messungen und Vergleichen verschiedener Teile der Milchstraße unterworfen werden müssen. Sehr auffallend ist die relativ große Intensität des Milchstraßenlichts im Intervalle l 270°—360°, die jedoch nach PANNEKOEK (Ziff. 4) etwas übertrieben sein kann. HOPMANN gibt in einer Figur einen Vergleich der Verteilung des Milchstraßenlichts nach galaktischer Länge mit den in analoger Weise behandelten Sternzahlen für die Grenzgrößen 8^m,25 und 11^m,0 (vgl. Ziff. 16). Die Maxima der Sternzahlen sind in galak-

¹ A N 222, S 81 (1924)

tischer Länge beträchtlich gegen die Richtung zur Sagittariusregion, wo das Milchstraßenlicht sein Maximum hat, gedieht

In C. HOFFMEISTERS oben erwähnter Arbeit wurden auch die PANNEKOEKschen Normalstellen der Milchstraße mit dem Flächenphotometer, dessen Konstruktion im Prinzip mit dem von NYLMA und VAN RIJN benutzten analog ist, ausgemessen. Tabelle 3 gibt die Normalstellen mit den von HOFFMEISTER angenommenen Koordinaten. Die Tabelle enthält die Stufenschätzungen von PANNEKOEK und HOPMANN und weiter die gemessenen, auf das Zenith reduzierten

Tabelle 3

Stelle	α	δ	Sternbild	L	PANN	HOPM	J_z	J_{abs}	Größe	
η	121°	-32	Puppis	219,5	3,1	—	0,321	0,042	0,316	3 ^m ,71
—	105	-16	—	195,5	—	—	279	—	264	3,91
η'	107	-4	Monoceros	186,3	2,8	1,7	313	0,032	306	3,75
γ'	109	-15	Canis major	197,0	2,7	3,7	300	0,021	290	3,80
V	100	-5	Monoceros	183,8	1,8	—	219	0,002	189	4,20
Y	117	-31	Puppis	217,6	1,1	—	259	0,053	239	4,01
U	91	-19	Leopold	193,0	0,5	2,3	186	0,031	181	4,53
A	166	-60	Carina	257,4	6,5	7,3	868	0,026	1,000	2,16
A'	178	-62	Centaurus	263,3	5,8	—	608	0,043	0,675	2,30
C	114	-53	Vela	213,8	3,0	—	321	0,035	320	3,70
D	141	-16	Vela	237,5	1,7	6,3	233	0,051	206	4,18
D'	131	-57	Carina	212,2	1,9	3,1	196	0,018	160	4,15
E	135	-50	Vela	238,3	0,9	—	184	0,023	115	4,56
E'	160	-44	Vela	247,7	1,0	—	169	0,015	126	4,71
F	200	-63	Centaurus	271,0	1,0	—	543	0,077	591	3,02
G	219	-63	Centaurus	282,6	2,7	7,1	423	0,032	441	3,31
G'	201	-58	Centaurus	275,2	2,9	—	471	0,037	508	3,19
H	196	-51	Centaurus	273,5	1,5	7,9	208	0,014	175	4,35
K	191	-63	Cruce	269,9	0,0	7,9	233	0,009	206	4,18
ζ	232	50	Noxia	295,1	3,1	7,6	133	—	156	3,31
τ	270	-28	Sagittarius	330,3	9,8	12,2	1,367	0,060	1,624	1,93
L	280	-8	Scutum	353,0	7,2	9,5	0,845	0,104	0,971	2,42
Nordpol	—	+90	—	—	—	—	136	0,009	0,085	5,13
—	84	+7	—	—	—	—	202	0,013	168	4,40
—	175	+60	—	—	—	—	109	0,003	0,051	5,69

Intensitäten J_z , die auf den leeren Raum und auf Erdoberfläche reduzierten „absoluten“ Intensitäten J_{abs} und deren Äquivalente in Steingroßen pro Quadratgrad. Die Einheit der Intensitäten entspricht einem Stein von der Größe 2,22 pro Quadratgrad und ist also im Verhältnis 1:3,076 kleiner als die VAN RIJNSche Einheit. Die Tabelle enthält auch einige Stellen außerhalb der Milchstraßenstruktur.

Der Vollständigkeit halber werden hier in Tabelle 4 auch PANNEKOEKS Stufenwerte für die Normalstellen der nördlichen Milchstraße, wie sie in PANNEKOEKS eistem großen Werke angegeben worden sind, aufgeführt. Die galaktischen Koordinaten sind nach dem MARIUSschen Pol ($\alpha = 12^h 40^m$, $\delta = +30^\circ$, 1880) gerechnet worden.

Der Anschluß zwischen HOFFMEISTERS photometrisch bestimmten Intensitäten und PANNEKOEKS Stufenwerten in Tabelle 3 ist sehr gut und entspricht im Mittel der Gleichung

$$J_z = 0,100 + 0,086 S + 0,00045 S^2,$$

wo S PANNEKOEKS Stufenwert ist. Daß systematische Fehler bei den Stufenschätzungen auftreten müssen, ist von vornherein fast selbstverständlich (vgl. Ziff 4). Die Messungen scheinen zu zeigen, daß bei PANNEKOEK die Gegend von 200° bis 250° galaktischer Länge etwas zu hell, die Fortsetzung bis etwa 300° etwas zu schwach beobachtet ist, wobei die Angaben relativ zum mittleren

Nullpunkt jenes Teils der Milchstraße bei PANNEKOEK zu verstehen sind. Man kann dann nach HOFMANN¹ folgende Berichtigungen zu den Stufenwerten annehmen:

Gal. Länge	st	Gal. Länge	st
200°	-0,2	260°	0,0
220°	-0,3	280°	+0,8
240°	-0,3	300°	+0,6

Die systematischen Fehler bei PANNEKOEK sind also jedenfalls sehr klein und erreichen kaum den Betrag von 1 st. Eine der obigen ähnliche Relation gibt der Vergleich mit HOFMANN'S Stufenwerten. Hier sind einige größere Differenzen zu bemerken, besonders für die südlichen Normalstellen H und K, die in HOFMANN'S Arbeit auffallend hell geschätzt worden sind.

Tabelle 4.

Stelle	Bezeichnung	I	H	Stufenwert
I	3 II Scuti $\frac{1}{2}$ Aquilae	353°,0	- 3°,0	6,4
P	ζ Aquilae - 110 Hore	16°,1	+ 6°,3	2,2
M	γ Aquilae $\frac{1}{2}$ 110 Hore	16°,7	- 5°,4	4,3
Q	6 Vulpec - 113 Hore.	23°,6	+ 6°,2	1,4
N	γ Sagittae - 12 Vulpec	26°,6	- 3°,8	3,3
A	57 Cygni $\frac{1}{2}$ 60 Cygni	53°,1	+ 0°,9	5,1
B	κ Cephei - 3 Lacertae	69°,7	- 0°,3	4,5
C	γ Lacertae - 2 Cass	73°,5	- 2°,0	3,7
Z	δ Cephei $\frac{1}{2}$ ϵ Cephei	74°,2	+ 3°,7	0,4
D	β Cass - 7 Androm	79°,9	- 4°,9	2,3
E	κ Androm - ζ Cass	83°,2	-10°,8	1,5
V	$\left\{ \begin{array}{l} \beta \text{ Cass. } \frac{1}{2} \epsilon \text{ Cephei} \\ \beta \text{ Cass. } \frac{1}{2} \epsilon \text{ Cephei} \end{array} \right.$	83°,9	+ 1°,4	3,6
S	$\left\{ \begin{array}{l} 50 \text{ Cass. } \frac{1}{2} \gamma \text{ Cass.} \\ 50 \text{ Cass. } \frac{1}{2} \gamma \text{ Cass.} \end{array} \right.$	94°,8	+10°,1	1,6
T	δ Cass - η Persei	96°,3	- 7°,1	1,1
X	δ Cass. η Persei	97°,8	- 2°,3	2,6
H	β Tauri - τ Tauri - ι Aurigae	142°,4	- 6°,1	1,0
K	β Tauri κ Aurigae	148°,0	+ 3°,3	2,6
G	μ Comae - κ Comae - π Comae	158°,3	+ 8°,0	2,0

J DUFAY¹ hat in seiner eingehenden Arbeit „Recherches sur la lumière du ciel nocturne“ die Intensitäten einiger Milchstraßengegenden mit der Intensität des Himmels am Pol, wie auch mit den Intensitäten an Punkten in derselben Zenitdistanz eben außerhalb der Milchstraße verglichen. Er findet die dichtesten galaktischen Wolken etwa 2,5mal so hell wie den Himmel am Pol, während für die meisten Milchstraßengegenden das Helligkeitsverhältnis den Wert 2,0 nicht erreicht. Die Messungen wurden teils mit einem visuellen Photometer, einer für die Aufgabe geeigneten Form des Photometers von FERRY-Buisson, teils photographisch ausgeführt. DUFAY findet, daß, nachdem die Strahlung des Himmels für die Diffusion des Lichts in der Atmosphäre korrigiert worden ist, etwa $\frac{1}{10}$ der Strahlung von den schwachen Sternen herrührt. Das Zodiacallicht entspricht in einer Sonnenentfernung von 60° etwa einem Sechstel der totalen Helligkeit. Der Rest der Strahlung, von Nordlichtern abgesehen, stammt vielleicht aus einer Diffusion des Sonnenlichts durch Meteoriten außerhalb der Atmosphäre. Die Strahlung des Nachthimmels ist nur in geringem Maße polarisiert, erscheint auch nicht besonders reich an blauem Licht.

¹ Lyon Bull. 10, Nr. 9, S. 70 (1928).

c) Die Photographie der Milchstraße.

6 Die prinzipiellen Verschiedenheiten der visuellen und photographischen Beobachtungen. Während schon Sterne 7 Größe einzeln dem normalen Auge unsichtbar bleiben, wächst die Zahl schwächerer Sterne in den Milchstraßenzonen so gewaltig, daß ihr Gesamtheit über ein kleines Areal einen merklichen Reiz auf die Stäbchen der Netzhaut des Auges ausübt. In dieser Weise entsteht die optische Illusion, die wir als das Phänomen der Milchstraße wahrnehmen¹.

Der photographischen Platte gegenüber liegt die Sache merklich anders. Die Empfindung des Auges ist vom Lichteffect der pro Zeiteinheit aufgenommenen Energiemenge abhängig, während die Platte in der Expositionszeit Belichtungsenergie akkumuliert. Die Sterne sehr geringer Helligkeit drängen sich zwar auf der Platte so dicht aneinander, daß ihre Scheibchen nicht mehr als distinct anzusehen sind, aber Sterne, die noch viel schwächer als die visuelle Sichtbarkeitsgrenze (Größe etwa 6^m,5) sind, werden wesentlich unabhängig voneinander als mit der Belichtungsdauer wachsende runde Flecke abgebildet. Die Fläche eines Scheibchens wächst jedoch nicht proportional zu der totalen wirksamen Belichtungsenergie, sondern langsamer. Der Einfluß der helleren Sterne wird somit in der Photographie relativ zurückgehalten, wenn wir mit den Verhältnissen bei der visuellen Beobachtung vergleichen. PANNEKOEK², der diese Tatsachen besonders auseinanderzusetzen hat, hebt hervor, daß die visuellen Beobachtungen und die photographischen Aufnahmen zwei verschiedenartige Darstellungen der Milchstraße bieten. „Die Photographie zeigt die kleinsten Einzelheiten und Unregelmäßigkeiten, aber hauptsächlich in Sternpunkten aufgelöst, nur mitunter von einer Flächentönung ergänzt, und daher ist die richtige Gesamthelligkeit nur schwierig zu ermitteln. Das visuelle Bild erfährt sofort die Gesamthelligkeit als solche, aber es gibt nur die grobere Struktur des Milchstraßenlichts wieder, in subjektiv abgerundeten Formen.“

Eine andere Grundverschiedenheit der zwei Beobachtungsmethoden liegt in der Beweglichkeit des Auges, die es gestattet, in kurzer Zeit ein großes Areal zu überblicken und weit entfernte Punkte des Himmels unmittelbar nacheinander zu betrachten. Das bedeutet zwar in erster Linie eine Überlegenheit gegenüber der photographischen Kamera und ein notwendiges Mittel zur Überwindung der Unvollkommenheiten des Auges als optischen Instruments, aber es liegt doch in der schnellen Drehung des Auges eine Quelle zur subjektiven Umformung des wahrgenommenen diffusen Objektes. PANNEKOEK schreibt über diesen Umstand folgendes: „In ausgedehnten Gebieten mit schwachen oder gleichmäßigen Lichtfluktuationen sucht das Auge Anhaltspunkte, um überhaupt etwas zeichnen und beschreiben zu können. es sucht helle und dunkle Gebilde zu erkennen und findet sie oft in völlig zufälliger und persönlicher Weise. Ruhen schwächer Sterne 5 und 6 Größe, die bei dem irrenden Herumtasten des Blickes die vorhandenen Lichteindrücke verstärken, rufen immer wieder das Bild deutlicher Lichtstreifen hervor, wo sich vielleicht gar keine größere Lichtmasse der wirklich teleskopischen Sterne befindet. Lichtstreifen, die Reihen sichtbarer Sterne folgen, finden sich bei allen Beobachtern, ohne daß es deshalb sicher ist, daß dem etwas Reales der Milchstraße selbst entspricht.“ Die photometrischen Messungen aber, die mit einem visuellen Flächenphotometer gemacht werden, sind natürlich frei von Fehlern dieser Art. Die Vergleichung verschiedener Gegenden geschieht hier durch Anschluß an eine künstliche Lichtquelle, die in

¹ Vgl. J. PLASSMANN, Die Milchstraße als Gegenstand der Sinneswahrnehmung. Z f Psychol (I) 88, S 120 (1921).

² Die nördliche Milchstraße, S 110.

meßbarer Weise abgeschwächt oder verstärkt wird. Wir haben hier ein Mittel, ein objektives visuelles Bild der Milchstraße zu erhalten, das außerdem auf quantitativen Messungen der Helligkeit beruht. Wie vorher hervorgehoben ist, besteht jedoch noch die Schwierigkeit, den Einfluß der von Zeit zu Zeit variablen allgemeinen Himmelsbeleuchtung zu eliminieren.

Wenn wir die Gesamtleistung der visuellen Methoden betrachten, müssen wir anerkennen, daß es schwer ist, auf photographischem Wege etwas Ähnliches zu erreichen. Wir haben oben von der Tendenz der photographischen Abbildung, die Struktur in Sternscheibchen aufzulösen, gesprochen. Schon die Körnigkeit der lichtempfindlichen Substanz der Platten muß aber bewirken, daß bei genügend kleiner Fokaldistanz und also genügend kleiner Skala des Bildes die schwachen Sterne einer Milchstraßenregion in derselben Weise wie eine kontinuierlich leuchtende Fläche auf die Platte wirken. Um eine Schwärzung auf der Platte hervorzurufen, muß dann die gesammelte Intensität pro Flächeneltheit der Platte einen Minimumwert erreichen, was durch ein großes Öffnungsverhältnis des Objektivs befördert wird. Der in Winkelmaß ausgedrückte Durchmesser der Sternscheibchen, welcher bei vollkommener Abbildung dem Objektivdurchmesser umgekehrt proportional sein sollte, wächst in der Regel mit dem Öffnungsverhältnis als eine Folge der unvermeidlichen Abbildungsfehler, die wesentlich Form und Größe der einzelnen Bilder bestimmen. Eine große Objektivöffnung bei kleiner Fokaldistanz bewirkt daher auch ein vollständigeres Zusammenfließen der Sternscheibchen einer gewissen Größenklasse, so daß man den Verhältnissen einer wirklichen Flächenabbildung nahekommt. Das Gebiet kontinuierlicher Schwärzung, welches durch das Zusammenwirken der Sterne entsteht, und seine Umgebung auf der Platte sind aber immer von einer mehr oder weniger lockeren Ansammlung von einzelnen oder in kleinen Gruppen zusammenfließenden Sternscheibchen besetzt. Die Begrenzung der kontinuierlichen Schwärzung wird daher wesentlich von der Optik des Linsensystems und von der Expositionszeit abhängig. Natürlich soll das Objektiv außer einem großen Öffnungsverhältnis auch ein großes nutzbares Bildfeld haben, um gleichzeitige Abbildung eines großen Areals des Himmels auf der Platte zu geben. Die optischen Abbildungsfehler des Linsensystems und die Vignettierung für schräg gegen die Achse verlaufende Strahlenbündel, deren Einfluß mit dem Abstände vom Plattenzentrum variiert, lassen aber eine Beurteilung der relativen Intensitäten nur für ein ziemlich kleines Gebiet auf ein und derselben Platte zu.

Nichtsdostoweniger ist die Photographie für ein Studium der Einzelheiten des Milchstraßenbildes unentbehrlich. Durch das Zusammenfließen der Scheibchen an den dichten Stellen wird gegenüber den leeren eine starke Kontrastwirkung erzeugt. Wo das Auge nur strukturlose Lichtflecke wahrnimmt, enthüllt die Photographie oftmals ein reiches, unendlich kompliziertes Spiel von Sternanhäufungen, leuchtenden Nebelmassen, wirklichen oder durch absorbierende Materie hervorgerufenen scheinbaren Sternleeren. Unsere jetzige Auffassung von der Struktur des Milchstraßenphänomens beruht daher in stärkstem Grade auf den photographischen Aufnahmen.

7. Die photographischen Arbeiten einzelner Forscher. Der Beginn der photographischen Milchstraßenforschung erfolgte durch E. F. BARNARD¹ erste Versuche im Jahre 1889 mit der „Willard-Lenso“, einem Petzvalobjektiv von 15 cm Öffnung und 78 cm Fokallänge, das später nach Umschleifung von BRASHEAR am „Crocker-Teleskop“ der Licksternwarte montiert wurde. Einige der früheren von BARNARD aufgenommenen Bilder sind in den ersten Bänden der

¹ M N 50, S. 310 (1890); Publ. A S P 2, S. 240 (1890)

Zeitschriften „Astrophysical Journal“ und „Popular Astronomy“ reproduziert worden. In der letztgenannten Zeitschrift hat auch H C WILSON¹ seine frühen Milchstraßenphotographien, die hauptsächlich mit einer der BARNARDschen ähnlichen Linse aufgenommen sind, wiedergegeben. Eine größere Sammlung ausgezeichneter Reproduktionen hat BARNARD erst im Jahre 1913 als eine Publikation der Lick-Sternwarte² herausgegeben. Die Reproduktion der Negative geschah nach der „Photogelatin“-Methode. Von hervorragender Schönheit sind besonders die Aufnahmen der sternreichen Sagittarius-Ophiuchus-Scorpius-Regionen. Die Bilder sind von Erläuterungen begleitet, die auf einer Analyse der Originalnegative beruhen.

Als ein Beispiel soll die folgende sehr interessante Bemerkung zu Tafel Nr. 42, eine Partie des westlichen Astes der Milchstraße um den Stern 58 Ophiuchi (galaktische Länge 334° , Breite $+5^\circ$), mitgeteilt werden: „The very singular mass of irregular clouds that occupies the middle of the plate looks strange out of place. It is quite unique in the milky way and does not give the impression of being clouds either of stars or of nebulous matter in its general makeup. In some respects these clouds have the appearance of being quite separate from the background of small stars, as if the masses were nearer to us. One would hesitate in passing on these as to their being nebulous, and yet the appearance does not suggest star masses. If, however, we examine the two small tufts at the left of the general mass, it will be seen that they are clearly made up of small stars which spread out in a scattering manner to the southeast from both masses, almost like coarse dust.“ In seinem unten erwähnten neuen photographischen Atlas sagt BARNARD von denselben Wolkenbildungen (Tafel 23): „They are probably entirely stellar, though this does not seem altogether certain. If stellar they probably are relatively very far away, though from their brightness this does not seem to be the case. Between us and these stars is a generous sprinkling of considerably larger stars. . . they are doubtless much nearer to us than the clouds.“ Die Lage dieser Wolke in einer Gegend, die wahrscheinlich nahezu einer Richtung gegen das Zentrum des Milchstraßensystems entspricht, macht es möglich, anzunehmen, daß diese Wolke ein sehr entferntes Gebilde ist, dessen Platz im Raume vielleicht nahe am Zentrum oder vielleicht sogar in einer noch weiteren Entfernung gelegen ist.

Nach seiner Übersiedlung an die Yerkes-Sternwarte setzte BARNARD mit dem 10/11füßigen Bruce-Teleskop, das er auf einige Zeit (1905) auch nach Mount Wilson brachte, seine Milchstraßenaufnahmen fort. Seine Arbeit findet ihren Abschluß in der großartigen posthumen Publikation „A Photographic Atlas of Selected Regions of the Milky Way“, die im Jahre 1927 von der Carnegie-Institution unter Redaktion der Yerkes-Sternwarte herausgegeben wurde. Die Karten sind photographische Kopien von sekundären Negativen, die besonders hergestellt wurden, um einen größeren Kontrast oder größere Stärke als die Originalnegative zu geben. Ein zweiter Teil des Werkes dient als Schlüssel und enthält für jede Karte ein gleich großes Blatt, wo die hellen Sterne der Bonner oder Córdobaer Durchmusterung eingezeichnet und alle bemerkenswerten Objekte aufgenommen und nummeriert sind. Jedes Blatt enthält auch die Eckpunkte eines aquatorialen Koordinatennetzes.

Die Einleitung zum ersten Teil gibt eine ausführliche Bibliographie über die Arbeiten von BARNARD, die in irgendeiner Weise die Photographie von Milchstraßenobjekten berühren.

Ungefähr gleichzeitig mit BARNARDS ersten Versuchen hat H C RUSSELL auf der Sidney-Sternwarte mit einem Dallmeyerschen Objektiv von 6 Zoll

¹ Pop Astr 3, S. 58 (1895)

² Publ Lick Obs 41 (1913)

³ MN 51, S. 39 (1896)

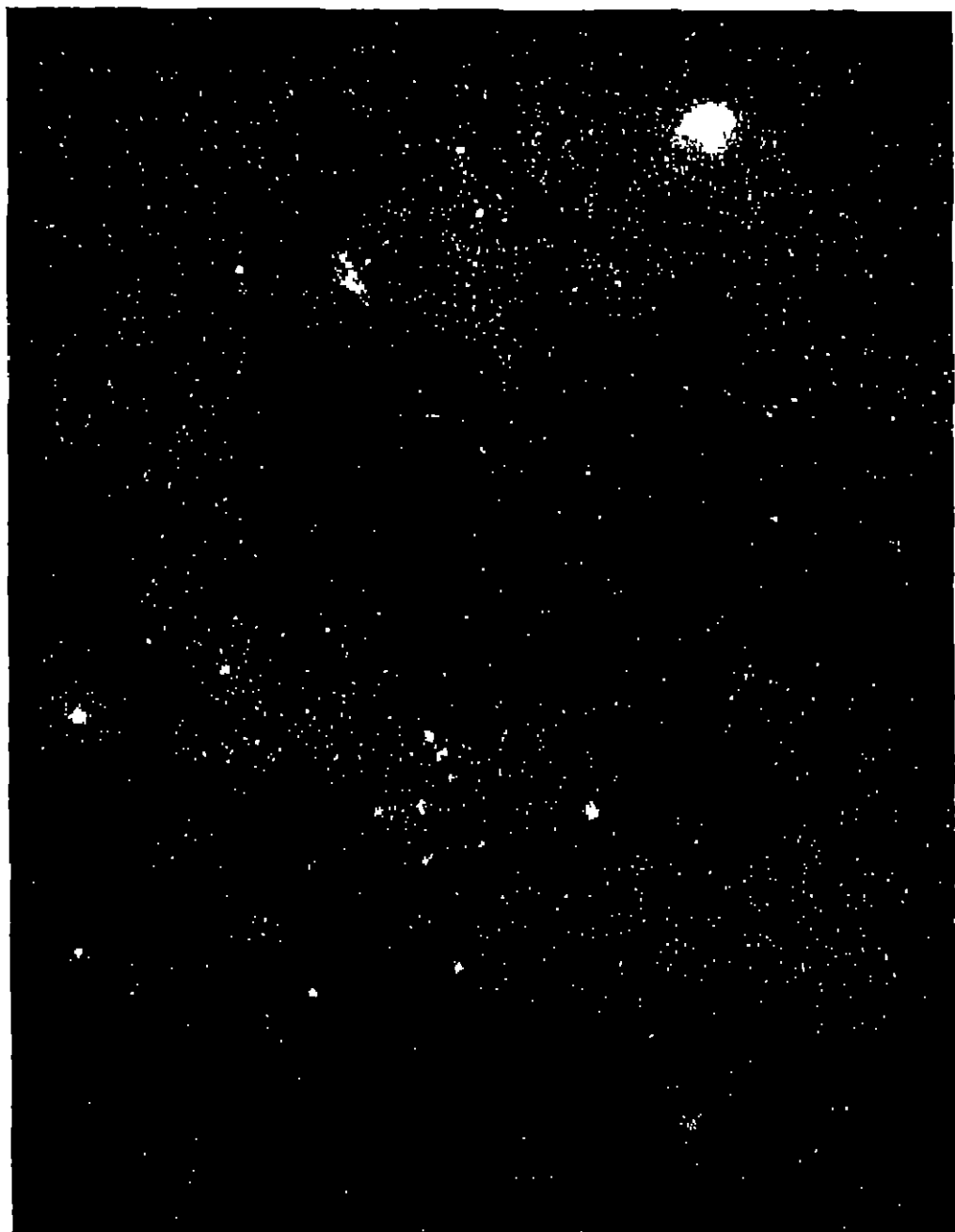


Abb 4 Milchstraße in Taurus, Auriga und Perseus. Aufnahme von M WOLF mit Zeiss-Tessar (31/145 mm) Belichtung 5 Stunden 2 Minuten

Öffnung Aufnahmen der südlichen Milchstraße und der Magellanschen Wolken gemacht. Unter den interessanten Bemerkungen, die er an seine Aufnahmen

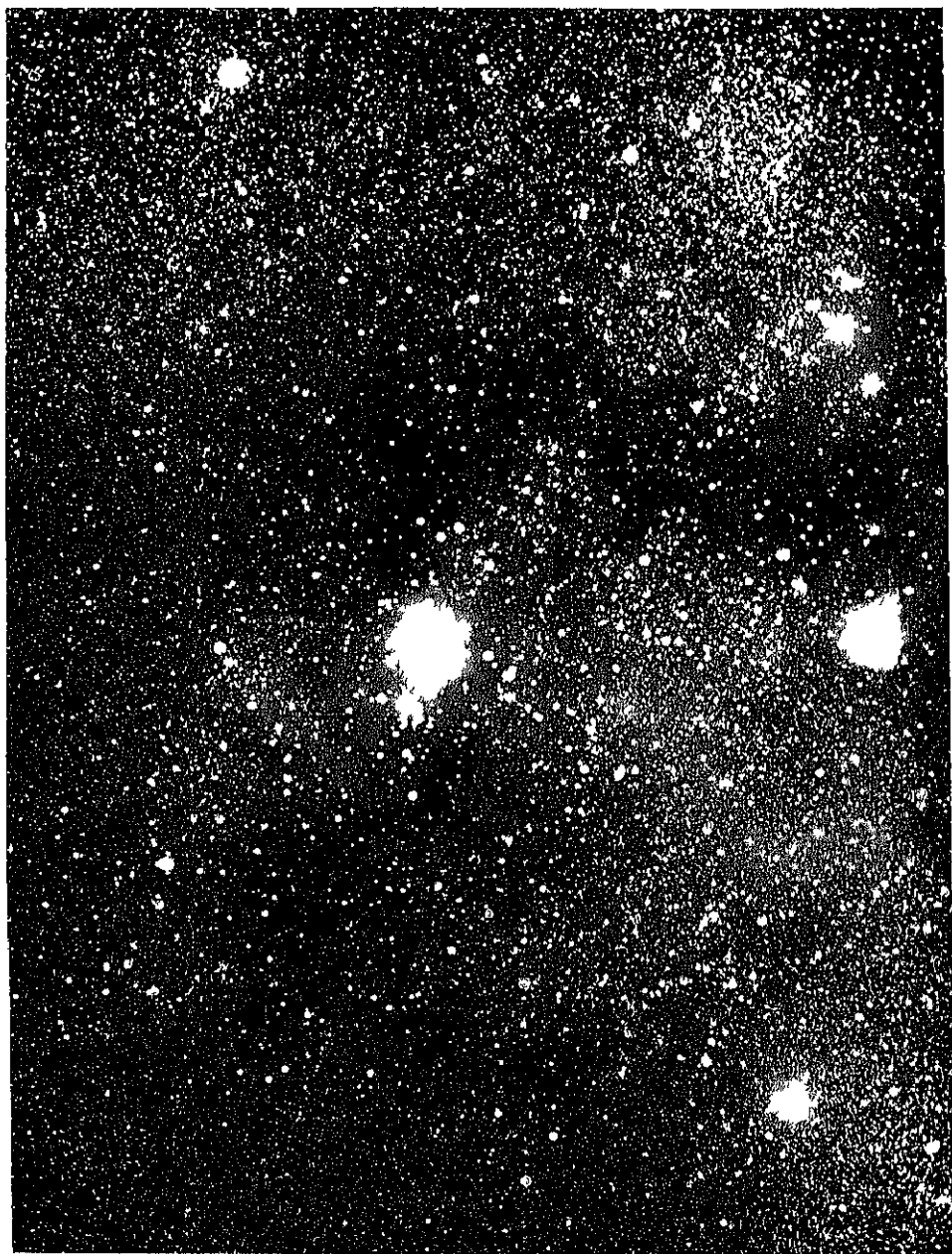


Abb. 5 Umgebung von δ Monocerotis Aufnahme von M. WOLF mit dem 16 zölligen Bruce-Refraktor (40/202 cm) Belichtung 5 Stunden 18 Minuten

knüpft, kann erwähnt werden, daß er als erster eine verwischte Spiralstruktur in der Nubecula Major zu sehen behauptet

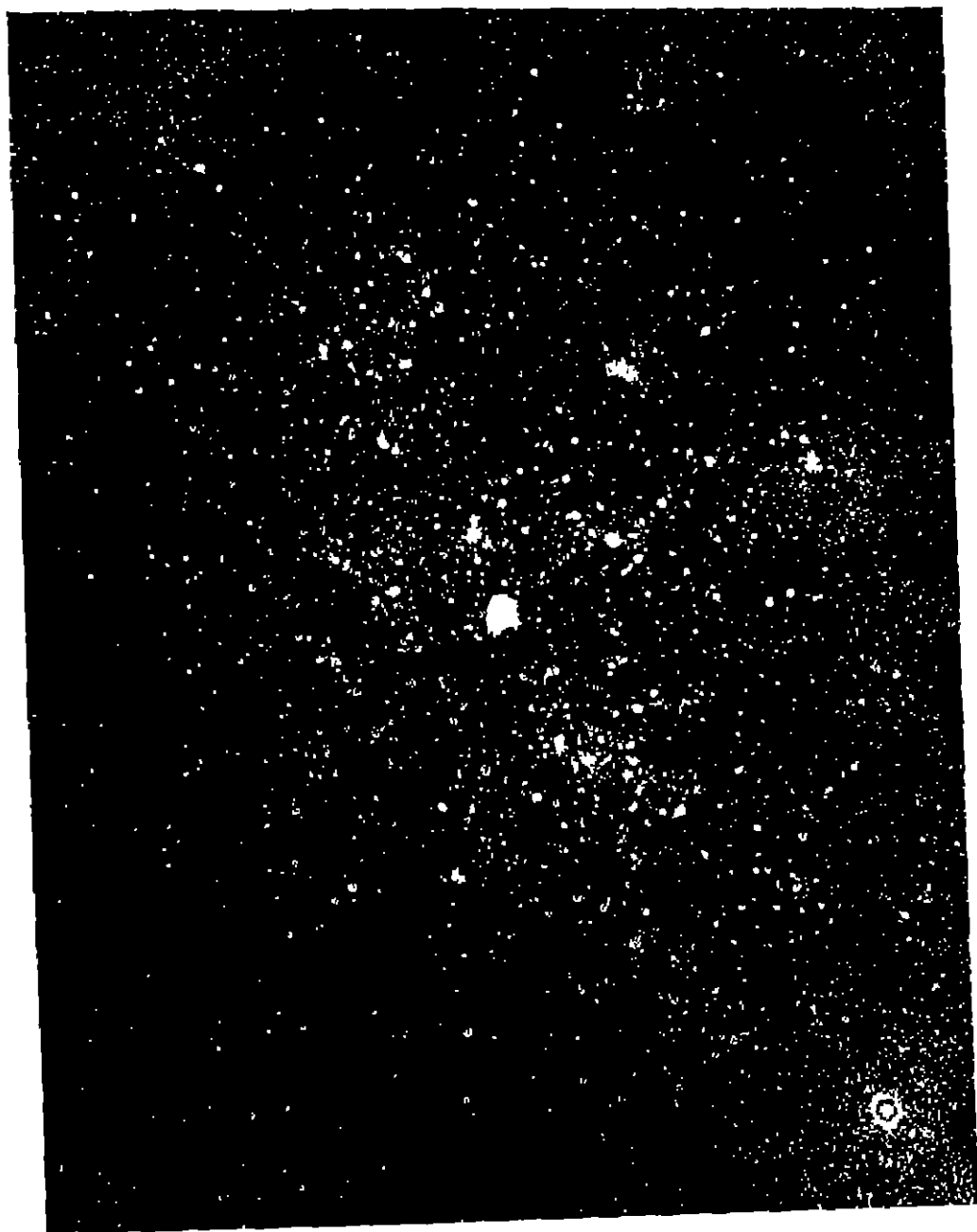


Abb 6. Umgebung von γ Cygni Aufnahme von M WOLF mit dem Bruce-Refraktor
Belichtung 6 Stunden 50 Minuten

M WOLF ist nebst BARNARD einer der erfolgreichsten auf dem Gebiete der Milchstraßenphotographie. Auf der Sternwarte Königstuhl, Heidelberg, hat WOLF mit dem 16zölligen „Bruce-Refraktor“ und auch mit kurzbreitweitigen

Objektiven (besonders zwei Zeiss-Iessaren von 31 mm Öffnung und 145 mm Brennweite) in großem Umfang verschiedene, und zwar meistens nördliche Gegenden der Milchstraße photographisch aufgenommen. Mehrere der WOLF'schen Aufnahmen sind oft in Lehrbüchern und Monographien als Illustrationsmaterial reproduziert worden. Vollständigere Sammlungen hat WOLF in den Werken „Die Milchstraße“ (Leipzig 1908) und „Die Milchstraße und die Kosmischen Nebel“ (Verlag Die Steine, Potsdam 1925) herausgegeben. Das letztere Werk enthält 16 ausgezeichnete Lichtdrucke von Milchstraßenpartien und Nebeln.

Einige Prachtstücke der WOLF'schen Aufnahmen beziehen sich auf die Milchstraße im Sternbilde Cygnus, speziell auf die große Cygnuswolke, die viele Einzelheiten von großem Interesse zeigt. Einige bemerkenswerte Erscheinungen, z. B. der „Amerikanebel“ und der „Kokonebel“, sind besonders durch WOLF's Aufnahmen in ihren Einzelheiten klargestellt worden. Im ganzen hat WOLF bewundernswürdige Aufnahmen aller Gegenden der Milchstraße von Scutum bis Monoceros gemacht. Durch Geheimrat WOLF's freundliches Entgegenkommen werden hier einige von seinen Aufnahmen in Abb 4 bis 6 reproduziert.

Die Milchstraßenzeichnung von GOOS, die nach WOLF's Aufnahmen hergestellt ist, wird unten in Ziff 8 besprochen.

Unter den wichtigsten Milchstraßenaufnahmen sind weiter die sehr schönen Photographien der südlichen Milchstraße zu nennen, die von S. I. BAILEY¹ zu Hannover in der Kapkolonie mit einem Cooke-Objektiv von 1½ Zoll Öffnung und 13 Zoll Brennweite aufgenommen worden sind. Diese Aufnahmen bilden eine wertvolle Ergänzung zu den BARNARD'schen und WOLF'schen Aufnahmen der nördlichen Gegenden. Die strukturelle Zersplitterung der Milchstraße von α Centauri aus nach wachsender galaktischer Länge hin und die große Mächtigkeit der Wolkenbildungen in den Längen 300° bis 360° treten hier in imposanter Weise hervor.

Die Arbeit wurde später in der nördlichen Milchstraße² fortgesetzt; die zur Umspannung des ganzen Milchstraßengürtels erforderlichen Photographien wurden von W. H. PICKERING auf Jamaika und von BAILEY in Cambridge, Massachusetts, hergestellt.

Ein interessanter Versuch, aus einem Material von Harvard-Platten ein photographisches Bild der Milchstraße in den Regionen zwischen Cygnus und Aquila zusammenzusetzen, ist von H. SHAPLEY gemacht worden und wird hier durch Herrn SHAPLEY's Entgegenkommen in Abb 7 reproduziert. Interessant ist ein Vergleich zwischen diesem Bild und der HERSCHEL'schen Zeichnung in Abb 1.

Von großer Bedeutung als photographische Darstellung der Milchstraße, besonders in ihrem südlichen Verlauf, ist die über den ganzen Himmel sich erstreckende FRANKLIN-ADAMS-Karte³. Die Aufnahmen wurden von J. FRANKLIN-ADAMS mit einem Taylor-Objektiv von 10 Zoll Öffnung und 45 Zoll Brennweite zu Mevel Hill, Godalming, in England in den Jahren 1905 bis 1909 und später zu Johannesburg in Südafrika gemacht. Da die Fokallänge bedeutend größer ist als bei BAILEY's Instrument, erscheinen die Sternwolken hier weit mehr aufgelöst. Viele Gegenden der südlichen Milchstraße, in Cygnus und Sagittarius, zeigen jedoch die komplizierte Struktur der ungeheuer dichten Sternwolken in außerordentlich auffälligem Kontrast gegen die benachbarten Sternleeren und gegen die gleichförmigeren sternenärmeren Gegenden höherer galaktischer

¹ Harv Ann 72, Nr. 3 (1913)

² Harv Ann 80, Nr. 4 (1917)

³ FRANKLIN-ADAMS-Chart, R. Astronomical Soc. (London 1921)

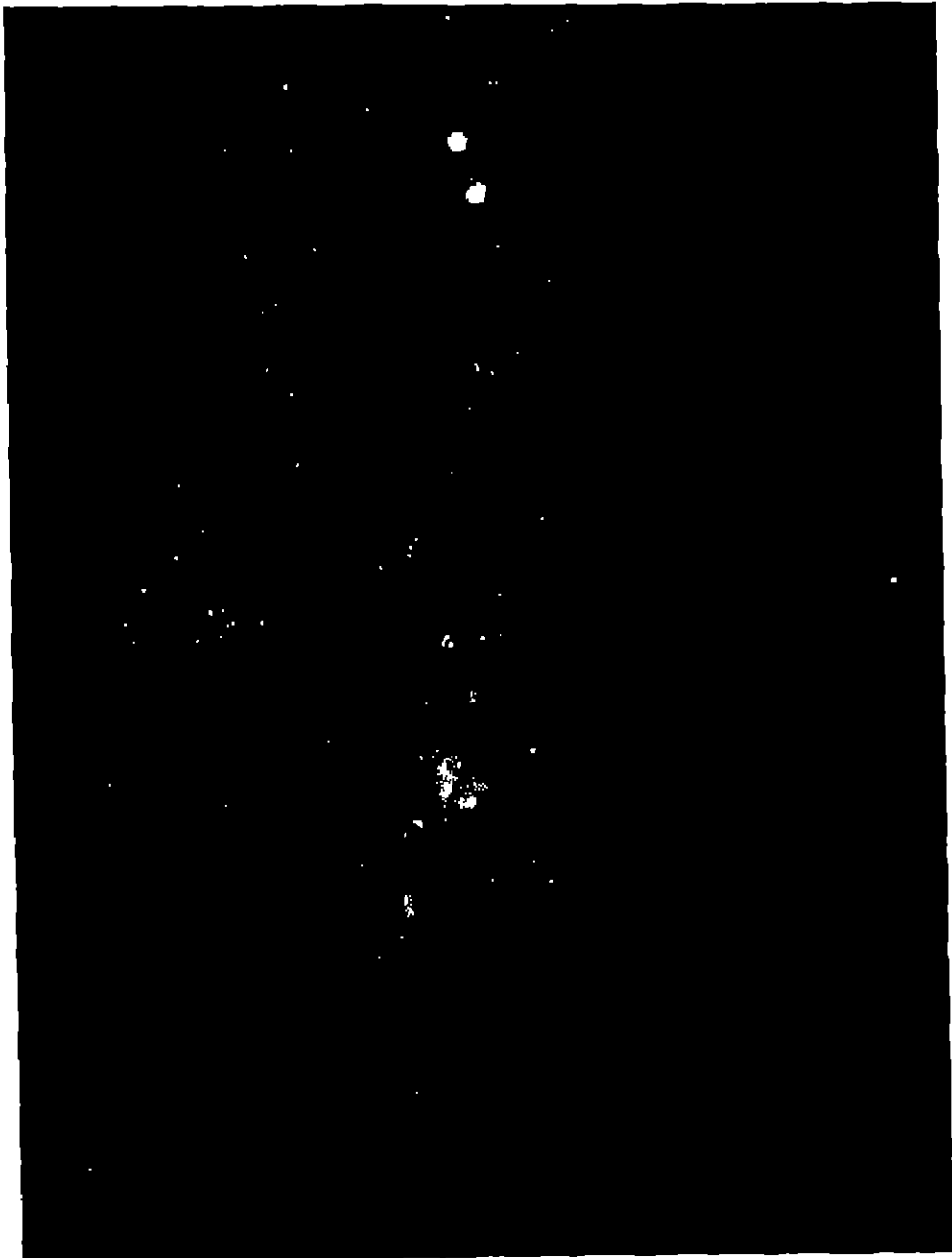


Abb 7. Zusammengesetztes Bild der zentralen Milchstraßengegend zwischen Crux und Aquila nach mit einem Ross-Tessar-Objektiv zu Arecibo aufgenommenen Platten

Breite. Die Reproduktionen (FRANKLIN-ADAMS-Karten) wie die Originalplatten selbst, die zu Greenwich aufbewahrt werden, sind schon von großer Bedeutung für mehrere Arbeiten in der Stellarastronomie gewesen.

Unter neueren Milchstraßenaufnahmen sind / B die von E H COLLINSON¹ mit einem Anastigmaten 1 3, mit 6 Zoll Brennweite, gemachten zu erwähnen.

Eine hohe Entwicklung der photographischen Technik ist aber besonders in den Aufnahmen von F E ROSS² erreicht worden. Mit einem Objektiv seiner eigenen Konstruktion (3 Zoll Öffnung, 21 Zoll Brennweite) hat er mit vielstündigen Expositionszeiten überaus schwache Nebelschleier in Orion, Monoceros, Icarus und Perseus photographiert. Bei solchen Objekten hängt der Erfolg, außer von der Empfindlichkeit der Platten, sehr stark von einer kontrastreichen Reproduktion der Originalnegative ab. In dem Reproduktionsprozeß benutzt ROSS panchromatische Platten mit Rotfilter. Er macht auch wichtige Bemerkungen über die Grenzgrößen verschiedener Instrumente, wenn es sich um die Aufnahme von Sternen handelt. Es zeigt sich, daß für schwache Sterne gewissermaßen ein langbrennwertiger Refraktor einem Reflektor gegenüber an Wirksamkeit gewinnt infolge der kleineren Dimensionen der Steinscheiben und der größeren Reduktion der Himmelselliptizität.

8 Milchstraßenzeichnungen auf Grund photographischer Aufnahmen.
Photographische Photometrie der Milchstraße. Eine Zeichnung der Milchstraße auf Grund photographischer Reproduktionen ist zuerst von EASTON³ publiziert worden. Sein Material war eine Kompilation der Aufnahmen verschiedener Milchstraßenregionen von BARNARD, WOLF, PICKERING, RUSSELL, BAILEY und anderen. Die Zeichnung gibt in einer „zirkularen“ Projektion die Milchstraße zwischen den galaktischen Breiten $+20^{\circ}$ und -20° . In einer späteren Arbeit⁴ hat er eine in äußerst feine Einzelheiten ausgearbeitete Karte der nördlichen Milchstraße gegeben.

Die Worsche Sammlung von Milchstraßenaufnahmen ist in besonders genauer Weise von F GOOS⁵ zu einer zeichnerischen Konstruktion des nördlichen Milchstraßenverlaufs benutzt worden. Die mit den Zeiss-Tessaren aufgenommenen Milchstraßenbilder wurden in ein einheitliches Kartennetz eingezeichnet. Die vielen Sternhaufen, Nebel und Kanäle wurden mit größter Sorgfalt wiedergegeben, wobei der Zeichner sich bemüht hat, alles subjektive Vorurteil auszuschalten, und nur zu zeichnen, was die photographische Platte zeigt. Die Helligkeitsverhältnisse im großen wurden durch direkte Beobachtung am Himmel und durch Anlehnung an ältere direkte Zeichnungen, besonders die von EASTON, möglichst wahrheitsgetreu wiedergegeben. So ist eine Zeichnung entstanden, mit der an Darstellung der Einzelheiten keine durch direkte Augenbeobachtung erhaltene verglichen werden kann.

Goos hat auch in verdienstvoller Weise die Zeichnungen von HELS, der Uranometria Argentina, von EASTON, BOEDDICKER und HOUZEAU in dieselbe Kartenprojektion umgezeichnet, was für die Kenntnis der zur Zeit teilweise schwer zugänglichen älteren Zeichnungen von Bedeutung ist.

Eine sehr bemerkenswerte Zeichnung der ganzen Milchstraße auf Grund von Reproduktionen der BAILEYSchen Platten und von ergänzendem photographischen Material hat kürzlich K. LUNDMARK unter technischer Mithilfe von O JAHNKE hergestellt und in Druck vervielfältigt. Durch Herrn LUNDMARKS Entgegenkommen wird diese Karte hier in einer Tafel reproduziert. Sie findet sich auch in Reproduktion in LUNDMARKS Neubearbeitung eines Werkes von ARRIENIUS⁶ und im Handbuch der Physik⁷.

¹ J B A A 37, S 132 (1927)

² Ap J 65, S 137 (1927), 67, S 281 (1928)

³ Ap J 37, S 105 (1913)

⁴ M N 89, S 207 (1928)

⁵ Die Milchstraße, mit einem Geleitwort von Professor MAX WOLF. Hamburg 1921

⁶ Världarnas utveckling. Stockholm 1929

⁷ IV (1929), Tafel

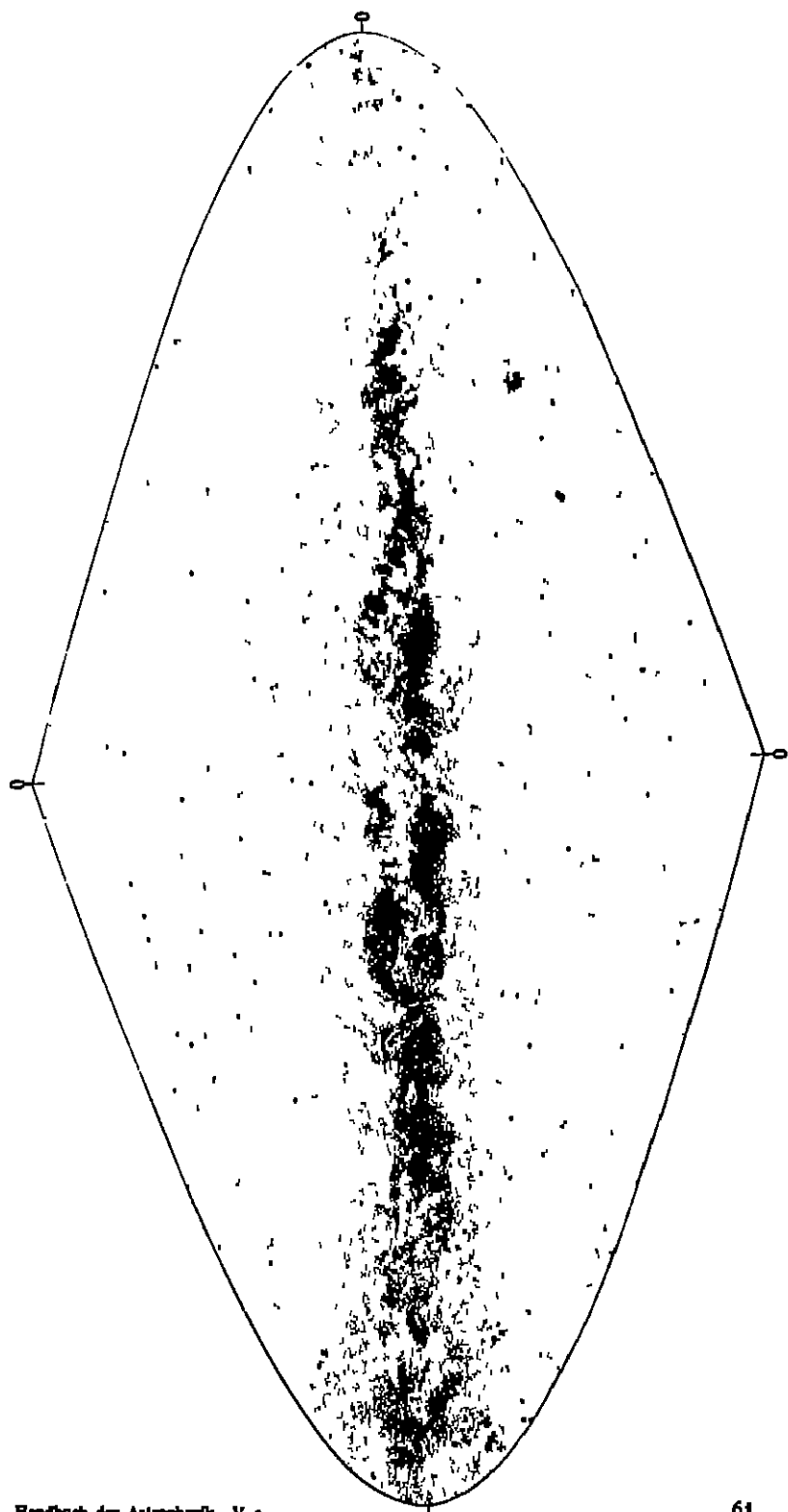


Abb. 8. Milchstraßenkarte, gemachet von F. C. LEONARD.

Auf der Stockholmer Steinwaite hat F C LLDEBOLR eine Zeichnung über den Verlauf der Milchstraße in FLAMSTEEDS Projektion nach galaktischen Koordinaten ausgeführt (Abb 8). Von dieser Karte ist auch eine kleine Auflage im Druck herausgegeben worden¹. Als Vorbild dienten zum Teil die Zeichnung von GOOS, besonders aber Reproduktionen der BAILEYSchen und anderen Harvard-Photographien, die von HEIN SHAPLEY wohlwollend zur Verfügung gestellt worden sind, weiter auch für die Benützung der relativen Intensitäten verschiedener Partien die Karten von PANNEKOK.

Unsere durch die Photographie erlangte Kenntnis der allgemeinen Lichtverteilung im Milchstraßengebilde ist bisher wesentlich nur von qualitativer Art geblieben. Eine wichtige Arbeit, in der eine quantitative photographische Photometrie der nördlichen Milchstraße beginnt, wird, hat aber PANNEKOK² ausgeführt, unter Benützung eines von M WOLF auf der Steinwaite Heidelberg angesammelten Plattenmaterials. Die Platten wurden mit einem kleinen Tessarobjektiv von 33 mm Öffnung und 145 mm Brennweite extrafokal aufgenommen, und die Ausmessung geschah mit einem HARTMANNSchen Mikrophotometer des Astronomischen Institutes zu Amsterdam. Die Gradation der Platten für schwache Intensitäten wurde aus den extrafokalen Sternscheiben dadurch ermittelt, daß die Differenz zwischen der Schwärzung eines Scheibchens und der kontinuierlichen Schwärzung der unmittelbaren Umgebung auf der Platte als Funktion der bekannten Helligkeit des Sterns angesetzt wurde, wobei Korrekturen für wechselnde Größe der Scheibchen auf der Platte, Unregelmäßigkeiten in der Lichtverteilung in den Scheibchen usw. angebracht wurden. Die photographische Himmels-helligkeit eines Punktes wurde dann aus der Differenz zwischen der Schwärzung im betreffenden Punkt auf der Platte und im unbelichteten Teil der Platte berechnet. Nach Berücksichtigung von Mittelpunktskorrektion und Nullpunktskorrektion für die einander in großem Umfange überdeckenden Platten sind endlich die Intensitäten, wie sie auf jeder der 35 Platten für die Eckpunkte eines engmaschigen Netzes gefunden worden sind, auf 35 Karten wiedergegeben. Einheit der Intensität ist die Helligkeit eines Sterns 10 Größe pro Quadratgrad. Die Karten sind auch in einem Gesamtbilde zusammengefügt worden. — Die Beseitigung der systematischen Fehlerquellen hat in der Arbeit viel Schwierigkeit gemacht, und unerklärte Differenzen zwischen einander teilweise überdeckenden Platten treten auf. Sie entstehen teils durch unberechenbare Einflüsse von Extinktion und von fremder Erhellung des Himmelsgrundes. Es ist auch nicht möglich, exakt anzugeben, für welche Größe die Sterne auf den Platten noch einzeln als Scheiben sichtbar sind. Eine ähnliche Unbestimmtheit besteht aber auch, wie wir oben gesehen haben, für visuelle Beobachtungen. — Auf der Bosscha-Sternwarte zu Leiden werden gegenwärtig extrafokale Aufnahmen der südlichen Milchstraße für eine ähnliche Arbeit gemacht.

d) Das allgemeine Bild der Milchstraße nach den visuellen und photographischen Beobachtungen.

9. Der Verlauf der Milchstraße am Himmel in großen Zügen. Als hellste Flecke der Milchstraße können zwei in Sagittarius und Scutum gelegene bezeichnet werden. Der erste und größere erstreckt sich südlich von μ Sagittarii gegen γ , δ und λ desselben Sternbildes. An diesen Fleck schließt sich im Süden eine nur wenig schwächere Masse gegen ε und η Sagittarii und gegen die charakte-

¹ Eine Reproduktion dieses Druckes findet sich in K Svenska Vetenskapsakademiens Årsbok 1930.

² Publ Astr Inst Univ Amst, Nr 3 (1932)

riatische Sterngruppe in der Schwanzspitze des Skorpions (γ , ϵ , λ Scorpii) an, sie erscheint besonders hell um den Sternhaufen M7 herum. Diese ganze Partie der Milchstraße ist als die große Sagittariuswolke wohl bekannt und bildet den hervorragendsten Teil des östlichen Milchstraßenastes oder Hauptastes. Das Intensitätsmaximum der Wolke, wenn wir vom hellen Fleck um M7 herum absehen, liegt nördlich von γ Sagittarii und südlich von dem Nebel M8 und dem Trifidnebel, die als helle Knoten am Rande des dunklen Zentralgebietes, das hier die Milchstraße in zwei gewaltige Äste teilt, erscheinen. Gegen dieses Zentralgebiet fällt die Intensität der Wolke sehr schnell und in einer sehr verwickelten Struktur ab.

Vom südlichsten Gebiet der Wolke bei M7 geht über den Sternhaufen M6 eine schwache Lichtbrücke gerade bis zum westlichen Ast hinüber, der sich hier in der weitgestreckten hellen Lichtmasse zwischen α Scorpii, ϵ Scorpii und θ Ophiuchi ausbreitet. Nördlich von dieser Masse wird der westliche Ast durch einen dunklen Kanal durchquert, der von dem ρ Ophiuchi-Nebel ausgeht und der sich über die Milchstraße nördlich und östlich von θ Ophiuchi in der Form eines gewaltigen Ankers ausbreitet. In der Nähe von θ Ophiuchi sind in dieser Formation einige sehr dunkle Partien zu finden. Auf der anderen Seite des Kanals, von θ Ophiuchi aus, finden wir einige weniger helle, aber doch mächtig erscheinende Wolken, die zum Teil ihrer „Feinkörnigkeit“ wegen sehr merkwürdig sind (vgl. BARNARD, Ziff 7), und die ihrerseits gegen Norden hin von einem mächtigen dunklen Gebiet begrenzt sind, das wie ein etwas gebogener Keil von Südwest her in die Milchstraße einsetzt, seine Spitze ungefähr in der galaktischen Länge von Altair hat und den westlichen Ast in Ophiuchus in zwei weit getrennte Partien teilt. Die Spitze des Keils bildet auch die stellenweise sehr dunkle Trennungsregion zwischen dem östlichen und dem westlichen Ast der Milchstraße in den Sternbildern Serpens und Aquila. Die Trennung ist hier weit stärker markiert als in den Regionen von Sagittarius und Scorpius, wo die Trennung der zwei Äste überhaupt sehr irregulär und oft von hellen Brücken unterbrochen erscheint.

In dem östlichen Ast ist die helle Verbindung zwischen Sagittarius- und Scutumwolke durch mehrere durchquerende dunkle Kanäle gestört, vor allem durch den zwischen δ und γ Scuti gelegenen, der an einigen Stellen sehr dunkle Gebiete aufweist. Sehr helle Flecken finden sich nördlich von μ Sagittarii, ziemlich in der Zentrallinie der Milchstraße (kleine Sagittariuswolke) und um γ Scuti herum. Die große Wolke in Scutum ist nach BARNARD „the gem of the Milky Way, the finest of the star clouds“. Der hellste Fleck befindet sich südlich von β Scuti. In östlicher Richtung verbreitert sich die Wolke und nimmt das Licht sanft ab; das schwächste Milchstraßenlicht ist hier weit in südliche galaktische Breiten zu verfolgen. Die Wolke zeigt nach BARNARD eine gleichförmigere Fläche, als die Milchstraßenwolken im allgemeinen. Eine Anzahl sehr dunkler Flecke zeichnet sich außerordentlich scharf gegen die nördliche Partie der Wolke ab, besonders unmittelbar nördlich vom Sternhaufen M41.

Nördlich von der Scutumwolke wird der östliche Ast durch das Sternbild Aquila hindurch fortgesetzt. Von der dunklen Durchquerung bei λ Aquilae an der Grenze der Scutumwolke aus geht der Lichtstrom weiter gegen Norden und bildet nach einer dunklen Durchquerung bei δ Aquilae den hellen Fleck unmittelbar westlich von γ Aquilae, der sich weiter nördlich in der hellen Partie im kleinen Sternbild Sagitta fortsetzt.

Der weniger ausgeprägte westliche Ast geht der nördlichen Seite des dunklen Gebietes in Ophiuchus entlang in nordöstlicher Richtung und bildet zwischen β Ophiuchi und ζ Aquilae eine längliche Wolke. Dann folgt wieder eine weite

dunkle Region. Schwache Verbindungsströme gehen von der eben genannten Wolke nach Sagitta und in einem Bogen gegen die südwestlichen Ausläufer der großen Cygnuswolke. Die dunkle Trennungsregion zwischen dieser westlichen Ophiuchus-Aquilawolke und der Cygnuswolke setzt in ähnlicher Weise wie das südlichere dunkle Gebiet in Ophiuchus in die Milchstraße ein. In der Form eines gebeugten Armes geht sie von den Sternbildern Lyra und Hercules gegen Sagitta, wo sie umbiegt, und von hier aus der Zentrallinie der Milchstraße entlang zwischen ϵ und γ Cygni gegen α Cygni. Die Region zwischen α , γ und λ Cygni, welche die geballte Hand des „Armes“ darstellt, ist sehr dunkel. Dieses Gebiet ist zum Teil von den mächtigen unregelmäßigen Nebeln nahe γ Cygni und α Cygni („Amerikanenebel“) begrenzt. Von hier aus geht weiter ein breiter dunkler Kanal in westlicher Richtung, der die nördliche Begrenzung der großen Cygnuswolke bildet.

Die große Cygnuswolke steht mit der Partie des östlichen Astes in Sagitta mittels einer schwachen Lichtbrücke zwischen γ Sagittae und β Cygni in Verbindung. Diese Wolke hat einen fast ellipsenförmigen Umriss, mit der größeren Achse zwischen den Sternen β und γ Cygni, und bildet unzweifelhaft mit ihrer nächsten Umgebung eine der interessantesten Partien der ganzen Milchstraße. Gegen die dunkle Trennungsregion im Osten fällt die Intensität ziemlich steil ab, während gegen das Sternbild Lyra hin die Lichtstärke in sanfter Weise abnimmt. In der Mitte der Wolke, um η Cygni herum, liegt eine dunklere Region.

Vom Sternbilde Sagitta geht als eine Fortsetzung des östlichen Astes ein schwacher Lichtstrom gegen ϵ und ζ Cygni, der nördlich von diesen Sternen an Intensität gewinnt und dann in stetiger Konvergenz gegen die zentrale Milchstraßenlinie über σ und τ Cygni durch die Sternbilder Lacerta und Cassiopeia läuft, um in der dunklen Region um γ Persei herum seinen Endpunkt zu finden. Dieser Strom kann als Hauptstrom bezeichnet werden. Am nördlichen Rande dieses Stromes erscheinen einige Wolkenbildungen, die vielleicht als eine Fortsetzung des westlichen Milchstraßenastes angesehen werden können. So erscheint östlich von α Cygni die helle und sehr konzentrierte kleine Cygnuswolke, die in einem Bogen über α , σ_1 , σ_2 und δ Cygni mit der großen Cygnuswolke in schwacher Verbindung steht. Nördlich von der kleinen Wolke liegt das tiefdunkle Gebiet, das als „nördlicher Kohlsack“ bezeichnet wird. Von diesem erstreckt sich in südöstlicher Richtung ein dunkler Kanal, der schließlich nahe den Sternen A und σ Cygni den Hauptstrom durchquert und damit die kleine Cygnuswolke von dem kleinen hellen Gebiet um π_1 , π_2 und g Cygni trennt. Ziemlich weit nach Norden hin vom Hauptstrome aus erstreckt sich die schwache Cepheuswolke zwischen α , δ und ι Cephei. Gegen Cassiopeia hin teilt sich der Hauptstrom gewissermaßen in Lichtstreifen, die von dunklen Gebieten (δ Cephei bis 4 Cassiopeiae, 1 H bis β Cassiopeiae) getrennt sind. Nördlich von einer Verbindungslinie zwischen β und κ Cassiopeiae liegt ein Lichtmaximum, das sich in südlicher Richtung über α Cassiopeiae in schwächeren Lichtmassen fortsetzt. Die Gegend bei δ Cassiopeiae vereint sich mit den Perseushaufen h und χ in einem langgestreckten hellen Fleck auf der Zentrallinie, der sich schließlich in das weitgestreckte Dunkelgebiet um γ Persei herum verliert. Eine schwache, bogenförmige Lichtbrücke über ϑ Persei vereint die erwähnte helle Partie mit einem kleinen Lichtmaximum unmittelbar südlich von α Persei. Auf der Nordseite geht ein mit der Zentrallinie paralleler Lichtstreifen über ϵ Cassiopeiae zum Dunkelgebiet in Perseus.

In der Perseus-Camelopardalis-Region ist die Milchstraße nur sehr schwach markiert, gewinnt aber in Auriga wieder an Intensität. In der Gegend um η Geminorum herum hat die Milchstraße eine eigentümliche Struktur, von hier

aus gehen nach allen Seiten helle und dunkle Streifen wie von einem Zentrum¹ BARNARD² macht die wichtige Bemerkung, daß in dieser Himmelsregion auf der nördlichen Seite der Milchstraße ein allgemeiner schwacher Lichtschimmer viel weiter zu verfolgen ist als auf der südlichen, gegen Orion hin, während in der diametral entgegengesetzten Sagittariusregion der Lichtschimmer auf der Südseite der Milchstraße weiter ausgedehnt als auf der Nordseite erscheint. Von dem genannten Punkte in Gemini weiter südlich verläuft die Milchstraße als ein ziemlich einheitliches, schwaches, aber an Intensität wachsendes Lichtband durch die Sternbilder Monoceros und Canis major hindurch, um im Sternbild Puppis eine etwas verwickeltere Natur zu zeigen. In südöstlicher Richtung von η Puppis, mit ζ Puppis nahe auf der Westseite, zieht ein langgestrecktes, von der Zentrallinie gegen Süden divergierendes dunkles Gebiet. Dieses wird von einer hellen Partie östlich von γ Velorum im wesentlichen überbrückt und geschlossen. Bei α – β Velorum zeigt diese Partie ein kleines Gebiet von beträchtlicher Helligkeit. Südlich von dieser Stelle erweitert sich aber eine dunkle Region gegen beide Seiten der Milchstraße, so daß zwischen γ und δ Velorum eine breite dunkle Durchquerung, auf die wohl zuerst J. HERSCHEL³ aufmerksam gemacht hat, zustande kommt. Von hier aus wächst die allgemeine Intensität der Milchstraße sehr schnell und verjüngt sich gleichzeitig der Lichtstrom, um in die schmale, aber sehr helle Milchstraßenpartie in Carina überzugehen.

Die Carinawolke zeigt gegen den Südpol hin einen sehr schnellen Intensitätsabfall; nach einem sehr konzentrierten Helligkeitsmaximum um η Carinae herum bildet sich gegen λ Centauri eine sehr markierte dunkle Einbuchtung in der intensiv leuchtenden Masse. In Crux wird der Strom breiter und umschließt den großen, dunklen, zentral gelegenen „Kohlensack“ östlich von ζ Crucis. Dieses birnenförmige Oval hat eine größte Länge von etwa 8° und eine größte Breite von etwa 5° . Der helle Lichtstrom wird dann immer breiter, bei α Centauri wird durch eine langgestreckte, im Sternbild Norma gegen Norden hin umgebogene dunkle Masse ein westlicher Ast abgesondert, der in wachsendem Abstand von der Zentrallinie der Milchstraße und mit abnehmender Intensität sich schließlich mit der hellen Partie des westlichen Milchstraßenastes in Scorpius vereint.

Der östliche Hauptstrom hat ein starkes Intensitätsmaximum in Norma und sondert dort noch einen Strom gegen die westliche Scorpiuspartie ab. Der hier abgesonderte Strom wird jedoch in mehreren Punkten, bei γ Normae, bei ζ Scorpii und zwischen μ und ϵ Scorpii, durch dunkle Risse durchquert. Der östliche Hauptstrom wird durch die Spaltung nach Süden gedrückt und verliert zuerst bedeutend an Intensität, gewinnt aber in Scorpius und Sagittarius wieder an Stärke und trifft endlich über die Schwanzsterne des Skorpions mit der großen Sagittariuswolke zusammen. Bei den eben erwähnten Sternen erweitert sich die Lichtmasse gegen den westlichen Ast hin, so daß hier von θ bis μ Scorpii eine weite Überbrückung zwischen den zwei Hauptästen entsteht. Zwischen dieser Lichtbrücke und der vorher erwähnten, über die Sternhaufen M7 und M6 gehenden liegt bei λ und ν Scorpii eine weite dunkle Höhle.

10. Die Magellanschen Wolken. Die zwei Gebilde des Südhimmels, die als die MAGELLANSCHEN WOLKEN (auch die Kapwolken oder die zwei Nubeculae, (N. major und N. minor) bezeichnet werden, sind oftmals als „versprengte Stücke der Milchstraße“ bezeichnet worden, wenngleich ihre vollkommene Abgeschlossenheit von der Milchstraße selbst schon von J. HERSCHEL ausdrücklich betont

¹ PANDEROSK, Die nördliche Milchstraße, S. 76.

² Photographic Atlas I, B. 10.

³ Results of Astronomical Observations, S. 384 und Pl. XIII (in Abb. 1 oben reproduziert).

wurde. Nach HERSCHEL'S Beschreibung erreicht man die kleinere Wolke an allen Seiten „durch eine Wüste“

Die größere Wolke befindet sich in der Position $\alpha = 5^h 20^m$, $\delta = -69^\circ$ (1900). Die galaktischen Koordinaten sind $L = 247^\circ$, $B = -32^\circ$. Der zentrale Teil der Wolke ist ein langgestrecktes, fast elliptisches, auf den photographischen Aufnahmen ziemlich amorph erscheinendes Gebilde, das speziell gegen Süden hin von einem weiten, schwachen Lichtschleier umgeben ist. Um und über diese zentrale Partie ist außerdem eine Menge kleinerer Gebilde von grobkörniger Struktur in unregelmäßiger Weise gestreut. In dieser Weise erstreckt sich die Wolke im ganzen über ein fast kreisförmiges Areal von ungefähr 6° Durchmesser. Die Wolke enthält zahlreiche Sternhaufen und Nebel.

Die kleinere Wolke hat die Koordinaten $\alpha = 0^h 40^m$, $\delta = -74^\circ$, $L = 270^\circ$, $B = -43^\circ$. Die Struktur dieser Wolke erscheint durchaus armer als die der größeren, wenngleich im ganzen große Ähnlichkeiten bestehen. Der größte Durchmesser des Gebildes ist etwa 3° . In einer Entfernung von nur 2° von der Wolke, aber sonst ohne irgendein Zeichen einer physischen Verbindung mit der Wolke, liegt auf der nordwestlichen Seite der schöne Kugelhauften NGC 104, ξ Tucanae.

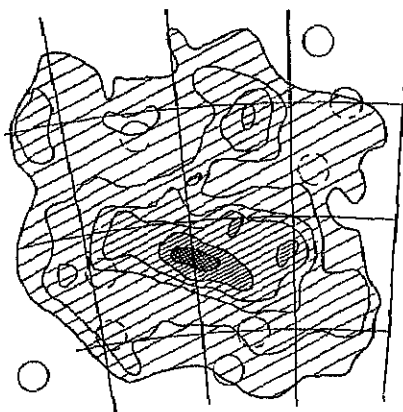


Abb 9 Die Isophoten der größeren MAGELLANSchen Wolke

Nach den Messungen von HOPMANN (Ziff 4) erreicht die Flächenhelligkeit der größeren Wolke nahe die maximale Helligkeit der großen Sagittariuswolke. Die Flächenhelligkeit der kleinen Wolke ist bedeutend geringer, aber kommt doch nach HOPMANN vielen der helleren Milchstraßenwolken gleich. Nach E. HERTZSPRUNG¹ würde, wenn die Flächenhelligkeit der kleineren Wolke über dem ganzen Himmel vorherrschen sollte, die entsprechende Strahlungsintensität an einem

Punkt der Erdoberfläche derjenigen eines Sterns im Zenit von der Größe $-6,6$ äquivalent sein. Für ein gleichmäßig helles kreisrundes Objekt vom Radius ϱ und von der integrierten Größe m bekommt man den Ausdruck für die Flächenhelligkeit durch die äquivalente Größe eines Zenitsterns im oben definierten Sinne einfach gleich $m + 5 \log \sin \varrho$.

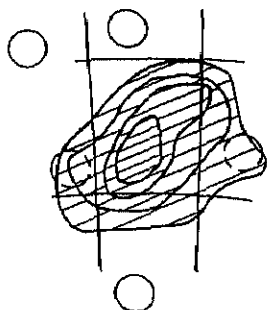


Abb 10 Die Isophoten der kleineren MAGELLANSchen Wolke

Eine photographische Photometrie der Wolken hat kürzlich G. VAN HERK² ausgeführt. Die Platten sind auf der Sternwarte zu Leimbach aufgenommen worden und die Methode, die früher von PANNEKOEK in einer Photometrie der Scutumwolke (Ziff 17) verwendet wurde, war die folgende. Die Platten werden ein wenig extrafokal exponiert und mikrophotometrisch ausgemessen. Die Schwärzungsskala wird aus den extrafokalen Scheibchen der Sterne von bekannter Größe ermittelt. Die in dieser Weise bestimmten isophotischen Linien der größeren und kleineren Wolke sind hier in Abb 9 und 10

gegeben. Die Linien sind für die Helligkeiten 20, 40, 70, 100, 140 und 200 gegeben, wo die Einheit einem Stern von 10 Größe pro Quadratgrad entspricht.

¹ BAN 2, S 209 (1925)

² BAN 6, S 61 (1930)

VAN HERR findet durch Vergleich mit PANNEKOEKS Resultaten, daß die hellste Partie der Scutumwolke erheblich heller als die hellsten Stellen der MAGELLANschen Wolken ist. Für die integrierte photographische Größe in der gewöhnlichen Skala findet er für zwei Platten

Größere Wolke	. +1 ^m ,2	+1 ^m ,2
Kleinere Wolke	. +2 ^m ,8	+2 ^m ,9

Für die kleinere Wolke hat SHAPLEY¹ eine photographische Größe zwischen +2^m und +3^m und J S PARASKEVOPOULOS² +1^m,8 angegeben. HERTZSPRUNGS oben erwähnte visuelle Flächenhelligkeit entspricht 424 Sternen der Größe 10^m pro Quadratgrad. Man muß wohl hier aber bei dem Vergleich mit VAN HERRS kleinerem Wert in Betracht ziehen, daß wir wahrscheinlich mit einem Farbenindex der Wolken von etwa +0^m,5 zu rechnen haben.

11. Die Lage der Milchstraße. Die zentrale Linie des Milchstraßengürtels folgt sehr nahe einem größten Kreis am Himmel. Für den Pol dieses Kreises sind mehrere Bestimmungen gemacht worden. W. HERSCHEL³ gibt die Koordinaten RA = 186°, Decl. = +32° für das Äquinoktium 1785. Die Werte von ARGELANDER⁴, aus BODES Darstellung der Milchstraße in seinem Atlas bestimmt, und von F. W. STRUV⁵ haben nur historisches Interesse, sind aber schon mit den heutigen Werten nahe übereinstimmend. HOUZEAU benutzte die Koordinaten seiner 33 Punkte maximaler Helligkeit und berechnete, von STRUVES Pol ausgehend, in einer Ausgleichung nach der Methode der kleinsten Quadrate den Pol des größten Kreises, der sich diesen Punkten am besten anschmiegt. Einmal rechnet er mit gleichem Gewichte für alle Punkte, ein zweites Mal mit Gewichten nach den Helligkeiten. Eine Ausgleichung desselben Materials unter Einführung der Nordpolldistanz σ des Kreises als unbekannte Größe in die Gleichungen haben RISTENPART⁶ und KOBOLD⁷ unternommen. Das Resultat von KOBOLD ist in der ersten Zeile der Tabelle 5 aufgeführt. Die Tabelle gibt auf das Äquinoktium 1900 reduzierte Werte (außer für NEWCOMB, der sein Äquinoktium nicht angibt) der zur Zeit besten Bestimmungen, die auf Zeichnungen und photometrischen Beobachtungen der Milchstraße beruhen.

HUIS⁸ hat eine Bestimmung aus seinen Milchstraßenzeichnungen im Atlas Coelestis Novus gemacht, die nicht sehr von GOULDS⁹ und NEWCOMBS¹⁰ Resultaten abweicht, die aus Bearbeitungen der Milchstraßenzeichnungen im Atlas Coelestis Novus und in der Uranometria Argentina herrühren. Besonders GOULDS Resultat ist sehr viel benutzt worden.

Eine Bestimmung auf Grund der GOOSSCHEN Darstellung der nördlichen Milchstraße ist von C. WIRTZ¹¹ gemacht worden. Diese Bestimmung behandelt aber die beiden Arme der Milchstraße getrennt (vgl. weiter unten). GRAFF¹² und HOPMANN¹³ haben weiter ihre photometrischen Messungen zur Lösung der Aufgabe benutzt.

Hinsichtlich der Daten, die man zur Bestimmung der Symmetrieebene heranziehen kann, sind in Anschluß an PANNEKOEKS Ausführungen die folgenden Typen zu unterscheiden.

¹ Harv Circ 260 (1924) ² Harv Bull 840 (1926).

³ Phil Trans 75, S. 253 (1785), Collected Scientific Papers I, S. 251.

⁴ Bonner Beobachtungen V, § 3 (1862).

⁵ Etudes d'Astronomie Stellaire, S. 62 (1847).

⁶ Untersuchungen über die Constante der Präcession, S. 63. Karlsruhe 1892.

⁷ Der Bau des Fixsternsystems, S. 184 (1906).

⁸ Vorrede zum Atlas, vgl. HAGEN, A N 217, S. 291 (1922).

⁹ Uranometria Argentina, S. 371.

¹⁰ Publications of the Carnegie Inst. of Washington, No 10 (1904).

¹¹ V J S 57, S. 22 (1922) ¹² A N 213, S. 27 (1921). ¹³ A N 222, S. 92 (1924).

a) Man kann von den Rändern ausgehen und überall die Mittellinie möglichst an die Mitte zwischen Nord- und Sudrand anschmiegen

Eine größere Sicherheit gewinnt man, wenn man die helleren Gebilde der Milchstraße als ihre Hauptobjekte ansieht und hellere isophotische Linien als Begrenzung ihres wesentlichen Teiles betrachtet. Dies führt zum entgegen gesetzten Grenzfall

b) Man sucht alle hervortretenden hellsten Stellen Zentren der Lichtwolken und Maxima der Ströme auf und legt die Mittellinie durch sie hindurch. Willkürlichkeiten in der Auswahl solcher Stellen lassen sich dann schwer vermeiden

Die Festlegung der Helligkeitsverteilung in Zahlen bietet die Möglichkeit, diese Willkürlichkeiten zu vermeiden, indem man entweder

c) für jeden Querschnitt die Lage des Lichtschwerpunktes bestimmt, also $\sum h \cdot b(N)$ gleich $\sum h \cdot b(S)$ macht, wo h Helligkeit, b Breite im Koordinatensystem der Karte ist,

d) oder es wird für jeden Querschnitt die „Lichtmitte“, also $\sum h(N) = \sum h(S)$, berechnet

In der Tabelle 5 sind die Bestimmungen nach diesem Schema klassifiziert worden. Nach HOPMANN kann man konstatieren, daß die Ansätze a) und c), die Wert auf die mittlere Helligkeitsverteilung legen, die Milchstraße als genau in einem Großkreis verlaufend hinstellen. Dagegen liegt der Zug der hellen Wolken (Ansatz b) und d)) in einem Kleinkreis, dessen Pol nordöstlich von dem der anderen Methoden liegt. NEWCOMBS Behandlungsweise muß als ein Kompromiß zwischen a) und b) bezeichnet werden, da er 42 Punkte teils auf der Mittellinie, teils an Stellen maximaler Intensität, in ziemlich gleichmäßiger Verteilung nach galaktischer Länge, benutzt hat. Das in die Tabelle aufgenommene Resultat von WIRTZ ist in ähnlicher Weise zu bezeichnen, bezieht sich aber auf den „Hauptzweig“ der Milchstraße.

Besonders großes Vertrauen verdient ohne Zweifel PANNEKÖKS Bestimmung der Mittellinie der Milchstraße und die daraus folgende Lage des Pols in seiner oben (Ziff 3) erwähnten Arbeit über die südliche Milchstraße. Für jeden Grad der galaktischen Länge am Nord- und Sudhimmel wurde die Summe der Helligkeiten in dem entsprechenden Querschnitt der Milchstraße gebildet, und die Breite der Mitte, welche die Totalhelligkeit in zwei gleiche Hälften teilt, bestimmt. Die schwachsten Helligkeiten wurden vor der Summenbildung ausgeschlossen (die gegebenen Helligkeitszahlen wurden um eine Einheit vermindert und negative Zahlen durch 0 ersetzt). Die erhaltenen Werte sind in einer Tabelle in der erwähnten Arbeit aufgeführt. PANNEKÖK hebt hervor, daß eine sich an die erhaltene Mittellinie schmiegende Ebene vielleicht noch nicht die wahre Symmetrieebene des galaktischen Systems darstellt, da die absorbierenden Nebelmassen in Taurus die Mittellinie nach Norden und in Ophiuchus nach Süden drängen und daher der Pol scheinbar in der Richtung nach 330° Länge verschoben wird, seine R.A. hierdurch zu groß und seine Deklination ein wenig zu klein wird.

Die Gesamthelligkeit als Funktion der galaktischen Länge zeigt nach PANNEKÖKS Zahlen ein hohes, scharfes Maximum in Sagittarius. Die Darstellung der Helligkeit durch eine einfache goniometrische Formel ergab

$$h = 319 + 179 \cos (L - 323^\circ)$$

Die Abweichungen gegen diese Formel zeigen noch vier Maxima bei 325° in Sagittarius, 50° in Cygnus-Lacerta, 170° in Gemini, 260° in Carina. Minima dazwischen bei 10° in Aquila, 110° in Perseus, 230° in Vela, 290° in Cygnus-Lupus.

Tabelle 5

Autorität		A		D	σ
HOUSSEAU-KOBOLD	(b)	191° 26'		+27° 56'	91° 14',5 ± 50' (m F)
GOULD	(a)	190 38		27 13	90 0 ± 6'
NEWCOMB	(a, b)	191 6		26 48	90 39
GOOS-WIRTZ ¹	(a, b)	195 8		29 8	90 31 ± 23'
GRAFF	(a)	192 16		26 48	90 0
HOPMANN	(c)	189 44		26 0	90 14,2 ± 6'
PANNERROCK	(d)	194 0		27 43	91 5

Aus den Zahlenangaben für σ ersieht man, daß die Sonne wahrscheinlich ein wenig nördlich von der zentralen Ebene der Milchstraße gelegen ist. Der Betrag der Abweichung ist jedenfalls nach diesen Resultaten sehr gering, aber noch ziemlich unsicher bestimmt.

Eine Neuberechnung des Pols der photographischen Milchstraße (GOOS-WOLF) von WIRTZ² unter Berücksichtigung von Haupt- und Nebenzweig zusammen gibt $A = 191^{\circ},9$, $D = +31^{\circ},0$ (1900), $\sigma = 87^{\circ},9$. Eine Auflösung für die photographische Milchstraße nach BARNARDS Atlas gibt $A = 194^{\circ},2$, $D = +28^{\circ},7$ (1900), $\sigma = 88^{\circ},0$. Die Sonne stünde also etwas südlich von der Hauptebene der „aktinischen“ Milchstraße. Die wahre Bedeutung dieses Phänomens ist wohl aber noch ganz unklar.

Über die zur Bestimmung des Pols benutzten mathematischen Methoden mag folgendes gesagt werden.

1. HOUSSEAU berechnet den sphärischen Radius der Milchstraßenpunkte von STRUVES Pol aus. Die Abweichung von 90° für einen Punkt wird als eine kleine Verschiebung des wahren Pols gedeutet. RISTENPART und KOBOLD geben der etwas verallgemeinerten Methode von HOUSSEAU die folgende Form. Seien α, δ die Koordinaten einzelner beobachteter Punkte (etwa Punkte größter Wichtigkeit), A, D die Koordinaten des Pols, für welche man die Näherungswerte A_0, D_0 hat. Von diesem genäherten Pol aus berechnet man den Abstand σ_0 eines beobachteten Maximums folgendermaßen.

$$\left. \begin{aligned} \cos \sigma_0 &= \sin \delta \sin D_0 + \cos \delta \cos D_0 \cos (\alpha - A_0) \\ \sin \sigma_0 \sin P &= \cos \delta \sin (\alpha - A_0) \\ \sin \sigma_0 \cos P &= \sin \delta \cos D_0 - \cos \delta \sin D_0 \cos (\alpha - A_0) \end{aligned} \right\} \quad (1)$$

Die Bedingungsgleichungen zur Bestimmung der Korrekturen dA und dD des provisorischen Pols und der Größe σ sind dann von der Form

$$\sin P \cos D_0 \cdot dA + \cos P \cdot dD + \sigma = \sigma_0. \quad (2)$$

2. Wenn wir die beobachteten Punkte des Milchstraßengürtels in einem provisorischen galaktischen System mit l, b bezeichnen und die Koordinaten des wahren Pols in demselben System mit L, B , so haben wir unmittelbar die Relation

$$\cos b \cos l \cos B \cos L + \cos b \sin l \cos B \sin L + \sin b \sin B + \cos \sigma = 0 \quad (3)$$

Da wir voraussetzen können, daß der provisorische Pol nahe dem richtigen liegt, so kann $\sin B = 1$ gesetzt werden, und wir können eine direkte Auflösung nach der Methode der kleinsten Quadrate mit den Unbekannten $\cos B \cos L$, $\cos B \sin L$, σ vornehmen. Für σ kann man $90^{\circ} + \phi$, wo ϕ die Tiefe („dip“) der Milchstraßenlinie bedeutet, einführen.

3. NEWCOMB sucht die Ebene durch unseren Beobachtungsort zu bestimmen, für welche die Summe S der Quadrate ϕ^2 ein Minimum ist, wo ϕ den Sinus

¹ Hauptzweig der Milchstraße.

² V J S 65, S 64 (1930)

der Winkeldistanz der Objekte von der Ebene bezeichnet. Wenn wir die folgenden Bezeichnungen für die Richtungskosinusse einführen

$$\begin{aligned} a &= \cos \delta \cos \alpha, & b &= \cos \delta \sin \alpha, & c &= \sin \delta, \\ x &= \cos D \cos A, & y &= \cos D \sin A, & z &= \sin D, \end{aligned}$$

so ergibt sich

$$p = ax + by + cz$$

Wir bekommen dann die Summenformel

$$S = [aa]x^2 + 2[ab]xy + [bb]y^2 + 2[ac]xz + 2[bc]yz + [cc]z^2$$

Außerdem haben wir

$$x^2 + y^2 + z^2 = 1$$

Die Differentiation dieser Ausdrücke gibt, wenn wir die Bedingung $dS = 0$ einführen, für x, y, z die Gleichungen

$$\begin{aligned} ([aa] - \lambda)x + [ab]y + [ac]z &= 0, \\ [ab]x + ([bb] - \lambda)y + [bc]z &= 0, \\ [ac]x + [bc]y + ([cc] - \lambda)z &= 0, \end{aligned}$$

wo λ also durch die folgende Gleichung bestimmt werden muß

$$\begin{vmatrix} [aa] - \lambda & [ab] & [ac] \\ [ab] & [bb] - \lambda & [bc] \\ [ac] & [bc] & [cc] - \lambda \end{vmatrix} = 0 \quad (4)$$

Die Wurzeln dieser Gleichung sind reell und positiv. Sie bestimmen die drei Hauptebenen des Systems. NEWCOMB zeigt, daß die Kondensationsebene durch die kleinste Wurzel λ definiert wird. Eine ausführliche Darstellung der NEWCOMBSchen Methode hat PHILIPPOT¹ gegeben.

Da die Milchstraße als der Kreis maximaler scheinbarer Sterndichtigkeit am Himmel definiert werden kann, so ist es klar, daß auch die Resultate der Sternzählungen zur Bestimmung der Lage dieses Kreises benutzt werden können. Die frühen Sternzählungen beruhten im wesentlichen auf dem Material der Bonner Durchmusterung und ihrer südlichen Fortsetzung. Nach den Arbeiten von RISTENPART² und PREY³ folgen die Dichtigkeitsmaxima der Sterne heller als 9^m,5 zwei etwas gegeneinander geneigten Ebenen. Die Lage der weniger ausgeprägten sekundären Ebene fällt jedoch für die beiden Autoren sehr verschieden aus.

Aus der Verteilung der Sterne bis zur photographischen Größe 11,0 (Statistik der Zählungen von H. HENIE⁴ nach der „Harvard Map“) hat H. NORI⁵ unter der Annahme $A = 491^\circ$, $D = +27^\circ$ für die Lage des Pols die Tiefe $p = +1^\circ 38' \pm 70'$ (in F) erhalten.

Die die schwachsten Sterne berücksichtigenden Bestimmungen der Symmetrieebene sind erst kurzlich von F. H. SEARES⁶ und P. J. VAN RIJN⁷ gemacht worden. SEARES Resultate wurden aus einer Statistik der Selected Areas bis zur 18 photographischen Größe, zusammen mit einigen Zonen der photographischen Himmelskarte, erhalten. Er untersucht die systematischen Ab-

¹ Annuaire de l'Observatoire Royal de Belgique, 1923, S. 195

² Unters. über die Konstante der Präzession (1892)

³ Denkschriften der math.-naturw. Klasse der K. Akad. der Wiss., Wien, Bd. 43 (1896).

⁴ Lund Medd., Serie II, Nr. 10 (1913)

⁵ Recherches astron. de l'Observatoire d'Utrecht VII, S. 115 (1917)

⁶ Mt. Wilson Contr. 347, S. 19, Ap. J. 67, S. 141 (1928)

⁷ Groningen Publications, Nr. 43 (1930)

weichungen Δ der Logarithmen der Sternzahlen von einem rotationsymmetrischen Verlauf in galaktischer Länge und bestimmt die Konstanten a , b und L' der Formel

$$\Delta = a + b \cos(L - L')$$

sowohl für verschiedene Größen als auch für verschiedene Zonen der galaktischen Breite. Die Abhängigkeit von der galaktischen Länge wird als Folge dieser Verschiebung des galaktischen Pols wie auch einer exzentrischen Lage der Sonne im System gedeutet (Ziff 18). Aus den Werten von a , b und L' für verschiedene Zonen werden also der Betrag der Polverschiebung und die Länge des Zentrums ermittelt.

VAN RHIJN Material sind für schwächere Sterne die Selected Areas (Harvard Durchmusterung und Mount Wilson-Katalog, wie oben bei SEARES). Bis zur Grenzgröße 14 verwendet er die Franklin-Adams-Karten, bis zur Größe 10 die Bonner und Córdoba Durchmusterungen und für Sterne heller als 6^m die Harvard Revised Photometry. Beide Verfasser gehen von dem GOULDSchen Pol aus und bestimmen Länge und Breite des wahren Pols für die in Frage kommenden Sterne. Die Resultate sind in Tabelle 6 zusammengefaßt worden. L und B sind die galaktischen Koordinaten des wahren Pols in GOULDS System. Die Grenzgrößen m sind photographisch. VAN RHIJN gibt auch den „dip“ ϕ des Symmetriekreises.

Tabelle 6

SEARES			VAN RHIJN			
m	L	B	m	L	B	ϕ
9	275°	81°,9	4	152°	69°,0	-0°,7
11	296	83°,2	5	166	88°,4	+2°,1
13,5	319	82°,0	6	213	87°,3	1°,2
16	357	85°,9	8	290	88°,7	1°,8
18	350	87°,3	10	293	87°,2	1°,6
			14	347	85°,0	3°,0 (FRANKLIN-ADAMS-K)
			14	354	87°,6	0°,5 (Selected Areas)
			16	359	86°,1	1°,0

Den wahrscheinlichen Fehler in B , L cos B und ϕ schätzt VAN RHIJN zu etwa 1°

Für die Sterne zwischen 9^m und 14^m zeigen die Resultate der zwei Verfasser sehr erhebliche Differenzen in der Breite B . Es ist bemerkenswert, daß nach VAN RHIJN für Sterne schwächer als 8^m praktisch dieselbe Lage des Pols für alle Klassen wiedergefunden wird. Die große Bedeutung diesbezüglicher Fragen wird in den folgenden Abschnitten ersichtlich.

Für die Größen 8 bis 16 geben VAN RHIJNS Resultate im Mittel $L = 330^\circ$, $B = 86^\circ,6$, $\phi = +1^\circ,9$, und in Äquatorialen Koordinaten für das Äquinoktium 1900.

$$A = 193^\circ 54', \quad D = +25^\circ 29', \quad \sigma = 91^\circ,9$$

Wenn wir mit diesem Pol als Grundlage galaktische Koordinaten berechnen und diese mit L_1 , B_1 bezeichnen, bekommt man nach VAN RHIJN für sukzessive Grenzgrößen die Werte in Tabelle 7.

Die Verschiebung des Pols für die hellsten Grenzgrößen ist ein Phänomen, das schon in großen Zügen von J. HERSCHEL¹ und von GOULD² beobachtet wurde. GOULD fand, daß von den 527 Sternen bis zur 4. Größe 306 auch der

Tabelle 7

m	L_1	B_1	ϕ
4	150°,2	65°,6	0°,0
5-6	167°,2	84°,7	+1°,5
7	167°,2	87°,3	+1°,5
8-16	—	90°,0	+1°,9

¹ Results of Observations, etc., p. 385

² Proc Amer Assoc for Adv Science, S. 115 (1874), Uranometria Argentina, S. 354

Milchstraße, aber 330 sich einer anderen Symmetrieebene (dem „GOUIN'schen Kreise“) innerhalb 30° anlehnen. Für den Pol seines Kreises fand GOUIN etwa $A = 171^\circ$, $D = +30^\circ$, oder im galaktischen System der Tabelle 7 $L_1 = 162^\circ$, $B_1 = 69^\circ$. Dieselbe Verschiebung erscheint auch in NEWCOMBS¹ Resultaten über die Lage des Pols für verschiedene hellere Größenklassen, verglichen mit dem Milchstraßenpol. Nach VAN RIJNS Resultaten ist das Phänomen noch bis zu 7 Größe schwach zu spüren. VAN DE LINDE² findet für Sterne heller als $6^m,25$ den Pol $A = 183^\circ$, $D = +28^\circ$. Über die Bedeutung dieser Erscheinung zu sprechen werden wir im folgenden mehrfach die Gelegenheit haben. Unter anderem wird es hervortreten, daß die Erscheinung auch besonders ausgeprägt für die Heliumsterne und die Gasnebel in unserer nächsten Umgebung ist (Ziff 13 und 19).

Zu erwähnen ist noch, daß J. BAILLAUD³ für die Zone $+22^\circ$ der photographischen Himmelskarte, Grenzgröße etwa 12,5, eine sehr erhebliche galaktische Konzentration gefunden hat, eine Lage des Pols $A = 200^\circ,5$, $D = +27^\circ,2$ (1900) und eine Tiefe von 3° . Später hat er⁴ aus SEARES' Beobachtungsmaterial, aber nach einer allgemeineren und einfacheren Methode als der von SEARES benutzten, für die Polkoordinaten $A = 193^\circ,7$, $D = +27^\circ,1$

berechnet, mit einer Unsicherheit von etwa 2° . Diese Lage des Pols stimmt sehr wohl mit dem PANNEKOEK'schen Wert in Tabelle 5 und ist auch mit VAN RIJNS oben angeführten, aus analogem Material bestimmten in leidlicher Übereinstimmung.

Von großem Interesse ist die galaktische Verteilung für Objekte von großer absoluter Leuchtkraft und daher großer mittlerer Entfernung, da wir hier beurteilen können, in welcher Weise die räumliche Anordnung dieser Objekte sich der galaktischen Ebene anschmiegt. Diesbezügliche Fragen werden in Ziff 19 und 20 näher diskutiert.

12. Galaktische Koordinaten. Die Fundamentalebene der galaktischen Koordinaten wird durch den zum Milchstraßenpol gehörigen größten Kreis festgelegt. Die galaktische Länge wird längs diesem größten Kreis, gewöhnlich vom aufsteigenden Knoten des Kreises auf dem Äquator, gezählt. Die galaktische Breite ist das Komplement der Distanz vom Nordpol der Milchstraße. Die Formeln zur Übertragung der äquatorealen Koordinaten α , δ in galaktische sind dann, wenn wir wie vorher galaktische Länge und Breite mit L und B , $R A$ und Dekl. des galaktischen Pols mit A und D bezeichnen

$$\left. \begin{aligned} \cos B \cos L &= \cos \delta \sin(\alpha - A) \\ \cos B \sin L &= \sin \delta \cos D - \cos \delta \sin D \cos(\alpha - A) \\ \sin B &= \sin \delta \sin D + \cos \delta \cos D \cos(\alpha - A) \end{aligned} \right\} \quad (5)$$

Nach der gegebenen Definition liegt die galaktische Länge 0° auf dem galaktischen größten Kreis im Sternbilde Aquila, die Länge 90° in Cassiopeia, 180° in Monoceros, 270° in Crux. Die über ein größeres Areal hellsten Partien der Milchstraße befinden sich in den galaktischen Längen 315° bis 335° , in den Sternbildern Sagittarius, Scorpius und Ophiuchus.

Andere Vorschläge zur Annahme des Anfangspunktes in galaktischer Länge sind gemacht worden. Man hat zuweilen als Nullpunkt den Sonnenapex benutzt (vgl. unten) oder einen hellen Stern mit sehr kleiner Eigenbewegung wie α Cygni⁵. Keine von diesen Zahlungen ist bisher allgemein angenommen worden.

¹ Publ. of the Carnegie Inst., No 10 (1904)

² De Verdeling der heldere Sterren, S 59. Rotterdam Wyt & Zonen 1921

³ C R 175, S 144 u 256 (1922)

⁴ C R 188, S 377 (1929).

⁵ Trans Intern Astron Union 2, S 177 (1925)

Von dieser Willkürlichkeit des Anfangspunktes der galaktischen Länge abgesehen, gibt es ebenso viele Systeme galaktischer Koordinaten wie Bestimmungen der Lage des Milchstraßenpols. Da verschiedene Bestimmungen oft ziemlich stark voneinander abweichen und es überdies nie darauf ankommt, eine galaktische Position mit äußerster Genauigkeit anzugeben, so wäre es natürlich am zweckmäßigsten, durch eine allgemeine Konvention unter Berücksichtigung der besten Bestimmungen eine gewisse Lage des Pols für allgemeine Zwecke zu fixieren. Hier herrscht gegenwärtig noch eine gewisse Verwirrung. Oft werden abgerundete Ziffern, wie z. B. $A = 190^\circ$, $D = +30^\circ$, benutzt, in anderen Fällen z. B. der GOULDSche Pol.

A. MART¹ hat zur Benutzung bei Milchstraßenbeobachtungen die galaktischen Koordinaten für die sichtbaren Sterne innerhalb des galaktischen Breiten $\pm 20^\circ$ gegeben. Für den Pol der Milchstraße wurde dabei $A = 190^\circ$, $D = +30^\circ$ (Äqu 1880) angenommen. Der MARTsche Katalog ist speziell als Hilfe für die Konstruktion einer Karte aufgestellt und ist auch in dieser Weise vielfach benutzt worden. PANNEKOEK, EASTON und PLASSMANN haben z. B. Reproduktionen solcher Karten unter Astronomen und Liebhabern verteilt, um die Praxis des Milchstraßenzeichnens allgemeinere zu verbreiten².

J. C. KAPTEYN³ hat eine Tafel für Berechnung der galaktischen Breite unter Benutzung des GOULDSchen Pols ausgearbeitet. Die Intervalle der Argumente sind 1^h in α und 1° in δ . Eine Spezialtabelle für die Umgebung des galaktischen Pols wird auch gegeben.

E. C. PICKERING⁴ gibt nach A. SEAR⁵ eine Tafel für galaktische Länge und Breite gemäß der Lage des Pols $A = 190^\circ$, $D = +28^\circ$ (1900). Die Intervalle sind 40^m in α und 10° in δ .

O. R. WALKER⁶ hat eine Tafel für die Lage des Pols $A = 12^h 47^m$, $D = +27^\circ$ und mit den Intervallen 1^h und 10° gegeben.

E. L. JOHNSON⁷ hat unter Verwendung des NEWCOMBSchen Pols, $A = 191^\circ, 1$, $D = +26^\circ, 8$, eine Tafel mit Intervallen 20^m in α und 5° in δ berechnet.

A. PANNEKOEK gibt in seinem oben referierten Werke „Die nördliche Milchstraße“ eine Tafel gemäß dem MARTschen Pol und mit denselben Intervallen wie in JOHNSONS Arbeit.

J. PLASSMANN gibt in seinem Werke „Die Milchstraße“ Tafeln mit den Argumenten $\alpha - Q$ und δ in Intervallen von 6° , wo Q die A. R. des aufsteigenden Knotens der Milchstraße ist. Ein paar Differentialtafeln lassen die Korrekturen in L und B für eine andere Deklination des Pols als die zur Konstruktion der Haupttafeln gewählte $+27^\circ 26'$ berechnen.

Eine Tafel, die nach Intervallen von 1° in α und δ fortschreitet, ist von C. V. L. CHARLIER auf der Sternwarte Lund ausgearbeitet worden. Die angenommene Lage des Pols ist hier $A = 190^\circ$, $D = +28^\circ$ (1900). Die genauesten gegenwärtig existierenden Tafeln sind später von derselben Sternwarte veröffentlicht worden. Die Arbeit geschah unter Leitung von J. OHLSSON, der auch ein Vorwort zu den Tafeln geschrieben hat. Für jeden ganzen Grad in α und δ werden L und B auf ein Hundertstel des Grades gegeben. Außerdem wird der Winkel φ zwischen Deklinationskreis und galaktischem Breitenkreis gegeben, um die Berechnung der Eigenbewegungskomponente längs der galaktischen Koordinatenkreise zu erleichtern. Die Lage des Pols ist die oben er-

¹ M. N. 33, S. 1 u. 517 (1872), 34, S. 77 (1873), 53, S. 74 u. 384 (1893)

² Vgl. PANNEKOEK, Pop. Astr. 5, S. 395, 485 u. 524 (1898)

³ Groningen Publ. Nr. 18 (1908)

⁴ Harv. Ann. 56, S. 5 (1912)

⁵ M. N. 74, S. 201 (1913)

⁶ Union Circ. 29, S. 226 (1915)

⁷ Lund Obs. Ann. 3 (1932).

wahnte, aber ausführliche Reduktionstabellen zur Erleichterung des Übergangs auf einen anderen Pol werden auch gegeben

P EMANUELLI¹ hat ausführliche Tabellen mit Angabe der Zehntelgrade in L und B gegeben. Die Tabelle schneidet nach Intervallen von 10^m in α und 1° in δ fort und ist gemäß dem NEWCOMBSchen Pol $A = 12^h 44^m$, $D = 26^\circ 8'$ (für das Jahr 1900 gültig angenommen) konstruiert worden. Die galaktische Länge wird hier vom Sonnenapex ($\alpha = 270^\circ$, $\delta = +30^\circ$) gerechnet. Der Verfasser gibt in der Einleitung eine ausführliche Bibliographie über Tabellen zur Berechnung galaktischer Koordinaten und über die verschiedenen Bestimmungen der Lage des Milchstraßenpols.

P J VAN RIJN² gibt für jede Stunde in α und jeden Grad in δ die galaktischen Koordinaten in einem System, dessen Pol mit dem Pol der schwachen Sterne ($m > 8$), $A = 194^\circ$, $D = +25^\circ 5'$ (1900), übereinstimmt. Eine Spezialtabelle gibt für die Umgebung des galaktischen Pols. Außerdem werden Differentialtabellen entsprechend Verschiebungen des Pols in Übereinstimmung mit den Resultaten für die helleren Sterne (heller als $m = 4, 5, 6, 7$ resp.) gegeben.

Graphische Verwandlungstabellen sind von H SELTIGER³, P SIROOBAN⁴, H NORT⁵, J. A. PEARCE und S. N. HILL⁶ publiziert worden. Zu diesen kommen auch ein paar Karten von O SEYDL, „Maps of the Boundaries of the Constellations in the Galactic System of Coordinates“⁷, gezeichnet werden.

R INNES⁸ und nach ihm H PHILIPPO⁹ entwickeln die Vorteile, an Stelle der „mittleren“ Orte der Gestirne die galaktischen einzuführen. INNES gibt Formeln und Tabellen zur genauen Übertragung mittlerer Orte der Jahresanfänge zwischen 1750 und 1950 in galaktische Koordinaten unter Zugrundelegung des NEWCOMBSchen Pols der Milchstraße. Die galaktischen Längen werden vom Sonnenapex $\alpha = 270^\circ$, $\delta = +30^\circ$ (1900) gezählt. Es gibt auch eine Spezialtabelle zur direkten Verwandlung der scheinbaren Orte für das Jahr 1913 in „mittlere“ galaktische. Mehrere Beispiele, unter anderem für Polaris und Polarisima, sind gerechnet worden. Eine neue Bezeichnung der Sterne schlägt INNES auch vor. Es sollten also an Stelle etwa der Benennung nach BD die helleren Sterne in den Vierecken sukzessiver Grade der galaktischen Länge und Breite nach der Länge numeriert werden. Eine Bezeichnung

$$325^\circ 8' 8'' \text{ oder } 325,8,8$$

bezeichnet also den achten Stern im Viereck zwischen Länge 325° und 326° , Breite $+8'$ und $+9'$. Negative Breiten sollten etwa durch Kursivstil ausgezeichnet werden.

Eine Konsequenz der Benutzung galaktischer Koordinaten ist naturgemäß, daß auch die Bewegungskomponenten der Sterne im galaktischen Koordinatensystem Ausdruck finden. Formeln und Tabellen zur Berechnung von galaktischen rechtwinkligen Bewegungskomponenten, wenn Parallaxe, Eigenbewegung in R.A. und Dekl. samt Geschwindigkeit im Visionsradius gegeben sind, hat kürzlich A. KOHLSCHÜTTER¹⁰ veröffentlicht. Die Lage des Pols wurde zu R.A. 190° , Dekl. $+27^\circ$ angenommen. In einer Spezialtabelle werden aber auch Verbesserungen

¹ Pubblicazioni della Specola Vaticana, N. XIV, Appendice prima (1929)

² Groningen Publ. Nr. 43 (1929)

³ Sitzber. d. K. Bayer. Akad. d. Wiss., Math.-Phys. Kl. 16, S. 220 (1886)

⁴ Annales Obs. Roy. de Belg. 11, S. 97 (1908)

⁵ Recherches astron. de l'Observatoire d'Utrecht VII (1917)

⁶ Publ. Astroph. Obs. Victoria 4, Nr. 4 (1927) ⁷ Publ. Obs. Nat. de Prague N. 5 (1928)

⁸ Union Circ. 2 (1912), 5, 6 (1913) ⁹ Annuaire de l'Obs. Roy. de Belg. 1923, S. 155

¹⁰ Veröff. Univ.-Sternw. Bonn Nr. 22 (1930)

zu den neun Übertragungskoeffizienten der Geschwindigkeitskomponente bei Übergang zu einem anderen galaktischen Pol gegeben. Eine Stern tafel enthält die Koeffizienten für alle Sterne, deren Radialgeschwindigkeit zur Zeit bekannt war.

e) Der Einfluß der diffusen Nebel auf das Milchstraßenbild.

18. Die galaktischen Nebelfelder. Die Photographie hat uns in unverkennbarer Weise gezeigt, daß der Milchstraßengürtel nicht nur eine von Sternen bevorzugte Region des Himmels ist, sondern auch reichlich leuchtende und dunkle, unregelmäßig begrenzte Nebelmassen enthält. Die Felder der leuchtenden Nebel sind in der Regel als Gebiete eigenartiger Struktur der Milchstraße ausgezeichnet. Die helle Nebelmasse selbst ist oft dicht mit Sternen, bisweilen von beträchtlicher Helligkeit, besät. Gebiete auffallend kleiner Sternanzahl erstrecken sich gewöhnlich in unregelmäßiger Weise um die hellen Partien herum. Es ist offenbar, daß man diese Reduktion der Sternfülle am einfachsten als einen Absorptionseffekt dunkler nobliger oder staubförmiger Massen auf das Licht entfernterer Sterne erklären kann, da wir andernfalls sehr langgestreckte, von uns aus radial gerichtete Lücken durch das Sternsystem hindurch in der Umgebung der hellen Nebel annehmen müßten, und das würde eine sehr unwahrscheinliche Anordnung bedeuten¹. Damit haben wir auf die Existenz mächtiger, nicht-leuchtender Massen geschlossen, die imstande sind, allgemeine Absorption oder Diffusion des Lichtes auszuüben. Solche Massen sind aber nicht notwendig nur in Verbindung mit leuchtenden Nebeln vorhanden, sondern verraten oft ihre Existenz nur durch ihre Absorptionswirkung als dunkle, an Sternen auffallend arme Gebiete, die gegen den hellen Hintergrund der Milchstraße kontrastieren.

In diesem Zusammenhang mag erwähnt werden, daß die Luminiszenz der hellen Nebelpartien wahrscheinlich von der Einstrahlung nahegelegender Sterne bedingt ist. V. M. SLIPINER² fand, daß für Merope, Maia, ρ Ophiuchi, NGC 2068 und 7023 das Spektrum der Nebelmasse wenigstens ungefähr mit den Spektren der hellsten eingestrahlten Sterne übereinstimmt. E. HERTZSPRUNG³ hat die Theorie einer partiellen Reflexion oder Streuung durch Photometrierung der Plejadennebel zu prüfen gesucht; er findet, daß die Flächenhelligkeit der Nebel an ihren hellsten Stellen um etwa 4 bis 5 Sterngrößen schwächer ist, als sie bei vollständiger Streuung des Lichtes des Zentralsterns an den betreffenden Punkten sein würde. H. N. RUSSELL⁴ hat die Reflexionstheorie für die galaktischen Nebel aufgenommen und weiter die Hypothese aufgestellt, daß auch die Nebel mit Linienspektren durch das Licht von nahegelegenden Sternen zur Strahlung erregt werden. L. HUMBLE⁵ hat diese Theorien auf Grund eines größeren Materials geprüft und im allgemeinen Durchschnitt gute Bestätigung gefunden. Er hebt hervor, daß in den hellen diffusen Nebeln fast immer Sterne zu finden sind, die mit der Nebelmasse in deutlicher Verbindung stehen. Wenn das Sternspektrum vom Typus O—B0 ist, strahlt der Nebel mit Linienspektrum, aber wenn der Spektraltypus des Sterns ein späterer ist, erscheint das Nebelspektrum kontinuierlich. HUMBLE findet auch einige interessante, aber weniger klar ausgesprochene Verschiedenheiten zwischen Nebeln mit Linienspektrum und Nebeln mit kontinuierlichem Spektrum. Die Netzwerknebel haben gewöhnlich Linienspektrum,

¹ Vgl. Ziff. 22.

² Lowell Obs. Bull. Nr. 35 (1912), Nr. 75 (1916); Publ. A. S. P. 30, S. 63 (1918); 31, S. 212 (1919).

³ A. N. 195, S. 449 (1913).

⁴ Wash. Nat. Ac. Proc. 8, S. 115 (1922), Obs. 44, S. 72 (1921).

⁵ Mt. Wilson Contr. 241 = Ap. J. 56, S. 162 (1922), 250 = Ap. J. 56, S. 400 (1922).

und die mehr regelmäßigen, wolkenartigen ein kontinuierliches. Die kontinuierlich strahlenden sind mit größerer Verdunklung verbunden, obgleich schwerwiegende Ausnahmen von dieser Regel in dem Orionnebel und in NGC 7000 (Amerikanenebel) gefunden werden. Die hellsten Nebel haben Linienspektrum, die ausgedehntesten kontinuierliches Spektrum. Die letztere Klasse hat die stärkere Tendenz zu einer Konzentration um in den Nebel eingehüllte Sterne.

Auch die allgemeine Verteilung der hellen diffusen Nebel am Himmel ist von HUBBLE diskutiert worden. Diese Verteilung ist nicht einfach eine Konzentration gegen die galaktische Ebene. Zwei verschiedene Gürtel sind zu unterscheiden, die Milchstraße und ein Gürtel, der gegen den galaktischen Kreis um ungefähr 20° geneigt ist. Die Knoten fallen ziemlich genau mit denen der hellen Heliumsterne zusammen, aber die Neigung der Nebelschicht ist erheblich größer. Die Verbindung zwischen Nebeln und Heliumsteinen wird jedoch durch diese Verteilung sehr augenscheinlich. Wir wollen im folgenden einige hervorragende Nebelfelder, die für die scheinbare Milchstraßenstruktur von Bedeutung sind, kurz erwähnen.

Ein heller Nebelschleier, der auf Milchstraßenaufnahmen der Perseusgegend (Abb 4) in markanter Weise hervortritt, ist NGC 1499. Dieser Nebel befindet sich am südlichen Rande der Milchstraße etwas nördlich vom Stern ξ Persei (Spektraltypus Oe5), der wahrscheinlich der erleuchtende Stern ist. Der Nebel liegt nahe der weitgestreckten dunklen Masse zwischen ι Tauri und ε Persei. Diese Masse ist in nördlicher Richtung durch einen feinen Kanal mit einer dunklen Höhle einige Grade westlich von α Aurigae, ziemlich auf der Zentrallinie der Milchstraße, verbunden und hat in südlicher Richtung Verbindung mit einer sehr dunklen Partie nördlich von τ Tauri, die sowohl in östlicher Richtung gegen β Tauri als in westlicher Richtung gegen die Nebelpartien um σ Persei herum schmale Kanäle aussendet. Wir sind hier schon in beträchtlich südliche galaktische Breite geföhrt. In der Nahe erscheint die in Nebel eingehüllte Plejadengruppe¹.

Eine Fortsetzung der eben genannten Nebelpartien, die augenscheinlich der gegen die Milchstraße um 20° geneigten Nebelschicht angehören, bilden die Nebel in der Oriongegend.

Ziemlich in der Zentrallinie der Milchstraße finden sich in dieser Gegend die interessanten Nebel um S Monocerotis (Abb 5) und um 12 Monocerotis herum. Der letztere Nebel erscheint am Rande einer Dunkelregion, die gegen Orion hinzieht.

Im südlichsten Verlaufe der Milchstraße ist vor allem zu erwähnen die mächtige und sehr helle Nebelmasse NGC 3372 um η Carinae herum², die nahe zentral in der Milchstraße gelegen ist, wo diese sich zu einem schmalen hellen Lichtstrom verjüngt. Die scharfe Einbuchtung der Milchstraße südöstlich von diesem Nebel ist wohl mit größter Wahrscheinlichkeit einer nebularen Absorption zuzuschreiben. Nach der FRANKLIN-ADAMS-Karte scheinen λ Centauri und naheliegende Sterne am Rande der hellen Partie in helle Nebel eingehüllt zu sein. Von dunklen Gebieten ist aber in dieser Himmelsgegend vor allem zu bemerken der „Kohlensack“ östlich von α und β Crucis. Nahe an α und im nördlichsten Teil unweit von β ist das dunkle Gebiet sehr arm an Sternen, in südwestlicher Richtung erstreckt sich vom Dunkelgebiet aus ein schmaler Kanal, der sich auf mehrere Grade hin verfolgen läßt.

In den Sternbildern Norma, Ara und Scorpius wird die sich erweiternde Milchstraße in sehr komplizierter Weise von dunklen Flecken und Kanälen

¹ Vgl. auch Aufnahmen von Ross, Ap J 67, S 281 (1928).

² Vgl. FRANKLIN ADAMS Karte oder Harv Ann 80, Pl IV (1908).

zerrissen. Es ist sehr wahrscheinlich, daß die sukzessive Abspaltung der zwei westlichen Milchstraßenäste in dieser Gegend auf Absorption durch dunkle Massen zurückzuführen ist. Von deutlichem Nebelcharakter erscheint eine komplizierte, vielfach in Kanäle aufgelöste, langgestreckte dunkle Region, die vom Schwanz des Skorpions nördlich von λ und ν Scorpi in westlicher Richtung den westlichen Milchstraßenast durchquert, um in der Gegend von η und ϕ Lupi ein ziemlich weitgestrecktes dunkles Gebiet zu bilden, an dessen südlichem Rande der Sternhaufen NGC 6124 gelegen ist. Von diesem Gebiete gehen schmale Kanäle weiter nach Westen. Im ganzen zeigt die Nebelpartie eine gewisse Ähnlichkeit mit den weiter nördlich gelegenen Nebeln, die mit dem hellen Nebel um ρ Ophiuchi in Verbindung stehen.

Die hellen Nebel in Scorpius und Ophiuchus bilden gewissermaßen ein Gegenstück zu den Nebeln in Orion, da sie in beinahe entgegengesetzter Richtung am Himmel erscheinen und also im ganzen eine erhebliche westliche Abweichung von der zentralen Milchstraßenlinie zeigen. Von außerordentlichem Interesse ist die Nebelmasse um ρ Ophiuchi und 22 Scorpi herum, die vielleicht auch in einiger Verbindung mit den Nebeln um σ und ν Scorpi herum steht. Von diesem Nebel gehen nach Osten hin mehrere dunkle Kanäle. Einer von diesen geht auf den westlichen Ast der Milchstraße in Ophiuchus zu, teilt sich dort in einen nördlichen und einen südlichen Ast, so daß das ganze Gebilde fast die Form eines gewaltigen Ankers erhält (vgl. Ziff. 9). Der südliche Ast enthält die außerordentlich dunkle Partie südöstlich von θ Ophiuchi. Der nördliche Ast spaltet einen Zweig in östlicher Richtung ab, der gegen den Sternhaufen M23 hinläuft, aber von diesem Haufen in südlicher Richtung umbiegt und sich dann in der großen dunklen Mittelpartie zwischen den Milchstraßenästen verliert.

Die dunkle Region zwischen den Milchstraßenästen in Sagittarius enthält am östlichen Rande die zwei schönen Nebel M8¹ und M20 (NGC 6523 und 6514); der letztere ist der berühmte Trifidnebel². Sie stehen an der Spitze einer Reihe von kleineren Sternwolken, die von der Scutumgegend über μ Sagittarii hinlaufen, und die von einer „grobkörnigeren“ Struktur als die umgebenden großen Wolken in Sagittarius und Ophiuchus zu sein scheinen. An die helle kleine Wolke in der Nähe von μ Sagittarii schließt sich im Süden ein dunkles Gebiet, das die Nebel NGC 6589 und 6590 enthält. Im nördlichen Teil derselben Wolke erscheinen die bekannten dunklen Nebel BARNARD 92 und 93. An die genannte Wolkenreihe schließen sich auch der Nebel M17 (NGC 6618) und der neblige Haufen M16 (NGC 6611) an, aber vor allem weiter nördlich der Nebel IC 1287 (um den Stern Boss 4687), der auf allen Seiten in weite Sternleeren übergeht, zu denen die großen, die Milchstraße durchquerenden Kanäle südlich von der Scutumwolke gehören.

Es ist wohl kaum zu bezweifeln, daß der große, in Ziff. 9 besprochene dunkle „Kanal“, der in die Milchstraße in Ophiuchus von Westen her einsetzt und die Aufspaltung der Milchstraße in Ophiuchus und Aquila bewirkt, in der Lichtabsorption dunkler Massen seinen Ursprung hat. Eine Verbindung der absorbierenden Massen mit dem ρ Ophiuchi-Nebel scheint nicht ausgeschlossen. Dieselbe Erklärung folgt dann mit großer Wahrscheinlichkeit für den dunklen „gebeugten Arm“ der Cygnusgegend, der in seinem oberen Teil den „Nordamerika-Nebel“ und die hellen Nebel um γ Cygni herum enthält.

Es liegt nahe zu bemerken, daß die zwei letztgenannten dunklen Gebiete von nördlicher galaktischer Breite her in der Richtung wachsender galaktischer Länge in die Milchstraße hineindringen, während die entsprechenden dunklen

¹ Vgl. Aufnahme von DUNCAN, Mt Wilson Contr 177 = Ap J 51, S. 4 (1920).

² DUNCAN, Mt Wilson Contr 256 = Ap J 57, S. 137 (1923).

Trennungsmassen der Milchstraßenäste in Scorpius und Norma von überwiegend nördlicher Breite gegen abnehmende Länge hinziehen. Man kann aus dieser Tatsache allein Veranlassung haben, den Schluß zu ziehen, daß die neblige Materie unserer nächsten Umgebung in größerer Häufigkeit in einer Ebene beträchtlicher Neigung gegen die Milchstraße verteilt ist, und daß diese Ebene ihre größte galaktische Breite in der Scorpius-Ophiuchus-Gegend erreicht. Es scheint, daß ein wesentlicher Teil der dunklen Nebelmassen, die die Milchstraße zwischen α Centauri und α Cygni zerkleinern, als Ausläufer einer solchen Schicht anzusehen ist, und daß besonders der westliche Ast in dieser Milchstraßengegend durch die Nähe an der Absorptionsebene in seiner mittleren Lichtstärke reduziert worden ist. Wenn wir die Knoten der Ebene in Cygnus und Cassiopeia annehmen, scheint es möglich, viele der größten verdunkelten Gebiete anderer Gegenden als zur genannten Nebelschicht gehörig anzusehen. Es ist aber auch deutlich ersichtlich, daß die Zweiteilung der Milchstraße in Scorpius, Sagittarius und Ophiuchus zum Teil auch auf in der zentralen Milchstraßenebene orientierte dunkle Massen zurückzuführen ist, und wir haben somit eine doppelte Verteilung der dunklen Massen gefunden, die der vorher besprochenen Verteilung der hellen diffusen Nebel durchaus ähnelt.

Der nördlichste Verlauf der Milchstraße ist reich an unregelmäßigen dunklen Gebilden, die bis in die Perseusgegend hauptsächlich auf der Nordseite der zentralen Milchstraßenlinie gelegen sind. So haben wir den „Kohlensack“ nördlich von der kleinen Cygnuswolke mit seinem in südlicher Richtung den „Hauptstrom“ der Milchstraße durchquerenden schmalen Kanal, den dunklen Fleck östlich von δ Cephei und das langgestreckte dunkle Gebiet westlich von β Cassiopeiae.

In der östlichen Milchstraßenpartie in Cygnus erscheinen α B die zwei wahrscheinlich zusammengehörigen Netzwerknebel NGC 6960 und 6992. Daß die Nebelschlinge 6960 auf der Außenseite, von 6992 aus gerechnet, von dunklen Nebeln begleitet ist, die eine merkliche Absorption ausüben, ist besonders auf J. C. DUNCANS¹ Aufnahme mit dem Hooker-Teleskop deutlich zu erkennen (vgl. M. WOLF, Ziff 22).

Östlich von der in unserer allgemeinen Beschreibung der Milchstraße erwähnten Durchquerung des Hauptstromes bei α Cygni haben wir eine schwächere bei π_1 und π_2 Cygni. Dieser Kanal steht mit einem eigenartigen Nebel in Verbindung. Aus einer ziemlich großen dunklen Höhle geht in südöstlicher Richtung ein ziemlich langer, kanalartiger, sternarmer Streifen hervor. In dessen östlichem Ende liegt ein heller, rundlicher Nebelfleck², der sog. „Kokon-Nebel“ (IIC 5146). Wir sehen hier in einem kleinen Maßstab, aber in sehr deutlicher Weise, eine Art Verbindung zwischen leuchtender und dunkler Nebelmaterie, die wir schon mehrmals, nur in etwas verschiedener Form, gefunden haben. Es scheint, als ob die helle Nebelpartie sich fortbewege, einen Schweif von allmählich sich weit verbreitender dunkler Materie hinterlassend. Die oben genannte Durchquerung besteht aus einem fast geradlinigen, zerhackten Zug von dunklen Stellen, der in nördlicher Richtung hinzieht und bei dem Stern 14 Cephei in einen sehr dunklen eiförmigen Fleck, BARNARD 169, ausmündet. Dieser Fleck liegt am südlichen Rande der Cepheuswolke.

Westlich vom eben genannten Fleck und südlich von μ Cephei liegt ein in ausgedehnte schwache Nebel gehüllter Sternhaufen um den Stern 13 H Cephei (Oe5) herum. Diese Gegend zeigt eine Menge schmaler, tiefdunkler Kanäle und Flecke und wird ringsum von größeren dunklen Partien umgeben (vgl. BARNARD, „A Photographic Atlas etc.“, Pl. 49).

¹ Mt. Wilson Contr. 256 = Ap J 57, S. 137 (1923)

² WOLF, Die Milchstraße und die kosmischen Nebel, Pl. III

14. Dunkle, wohl markierte Flecke im Sternstratum Manchmal sehr scharf begrenzte, tiefdunkle Flecke treten oft in außerordentlich auffälliger Weise gegen den Hintergrund einer sternreichen Gegend hervor. Schon A. SECCHI¹ hat auf tiefschwarze Höhlen in den Sternwolken in Sagittarius aufmerksam gemacht, und G. F. CHAMBERS² zählt solche Flecke auch in Scorpius auf. Eine kleine schwarze Höhle von nur 2' Durchmesser in der Sagittariuswolke (B 86) wurde von BARNARD³ im Jahre 1883 durch visuelle Beobachtung entdeckt. Diese Höhle hat den kleinen Sternhaufen NGC 6520 unmittelbar auf der östlichen Seite und erscheint daher in besonders starkem Kontrast gegen ihre Umgebung. BARNARD hat sich dann besonders einem Studium der dunklen Flecke auf photographischem Wege gewidmet und schließlich einen Katalog und eine Beschreibung für 182 Objekte dieser Art gegeben⁴. Sein photographischer Atlas der Milchstraße enthält auch reichlich Bemerkungen über diese Objekte. Es ist selbstverständlich, daß für die Erklärung dieser Flecke nur die Absorptionshypothese ernstlich in Frage kommen kann.

Ein systematisches Aufsuchen dunkler Flecke des Himmels ist kürzlich mit Hilfe der FRANKLIN-ADAMS-Platten von K. LUNDMARK und P. J. MELOTTE ausgeführt worden. Eine Karte, welche die Verteilung der 1550 gefundenen Objekte zeigt, hat LUNDMARK⁵ gegeben. Er schätzt das ganze Areal der dunklen Flecke auf ungefähr 850 Quadratgrade, was etwa 1·50 des ganzen Himmels entspricht.

Man muß bei der Deutung dieses Resultats die Bemerkungen vorausschicken, erstens, daß nicht alle Flecke notwendigerweise durch Absorption in dunklen Massen hervorgerufen sein müssen, sondern bisweilen wirklichen sternreichen Regionen im Raume entsprechen können, was auch von LUNDMARK hervorgehoben wird, zweitens aber, daß eben die größten verdunkelten Gebiete des Himmels, deren Grenzen verwaschen oder mehr unregelmäßig definiert erscheinen, z. B. das große Absorptionsgebiet in Ophiuchus, mitunter nur durch ihre dunkelsten Gebiete repräsentiert werden.

Die Verteilung der dunklen Flecke zeigt eine große Frequenz in der südlichen Milchstraße zwischen Carina und Aquila, wie auch eine große Häufigkeit in der Oriongegend (südliche galaktische Breite) und in der Cephæus-Cassiopeia-Gegend (nördliche galaktische Breite). Das Auftreten von Flecken auch in sehr beträchtlicher galaktischer Breite hat H. SHAPLEY⁶ veranlaßt, für 50 Regionen hoher galaktischer Breite die Verteilung schwacher Sterne auf Harvard-Platten zu untersuchen. Nur für eines der untersuchten Gebiete (östlich von μ und η Serpentis) wird eine Absorption durch Dunkelwolken bestätigt; die Sterne, die schwächer sind, als es der Grenzgröße der FRANKLIN-ADAMS-Platten entspricht, zeigen für andere Regionen eine wesentlich gleichförmige Verteilung. SHAPLEY hat vorher⁷ ein ähnliches Resultat für eine sternarme Region auf den Karten der Pariser Astrographischen Zone, auf die von E. ÖRTZ und M. LUKR⁸ hingewiesen worden war, gefunden.

15. HAGGERS dunkle Nebel. Auf die Existenz dunkler Nebelwolken, die wesentlich außerhalb der Milchstraße auftreten und dort ein zusammenhängendes

¹ A. N. 41, S. 238 (1855).

² Descriptive Astronomy, 3rd ed., Oxford 1877.

³ A. N. 108, S. 369 (1884).

⁴ Ap. J. 49, S. 1 (1919).

⁵ Pop. Astr. Tidnkr. 7, S. 18 (1926) = Upsala Medd. 12; Studies of Anagallactic Nebulae, N. Acta Reg. Soc. Scientiarum Upsal., Volumen extra ordinem editum (1927), Upsala Medd. 30, Pl. I.

⁶ Harv. Bull. 844 (1927).

⁷ Harv. Circ. 281 (1925).

⁸ Publ. Obs. Univ. de Tartu (Dorpat) 26, Nr. 2 (1924).

Gewebe ähnlich den Gestaltungen irdischer Wolken bilden, hat J G HAGEN¹ aus umfangreichen visuellen Beobachtungen mit dem 16zölligen Refraktor der Vatikan-Steinwarte geschlossen. Schon W HERSCHEL² hatte 52 weit ausgedehnte milchige Nebelgebilde angegeben, die in allen galaktischen Breiten auftreten, und die zusammen sicher weit mehr als 150 Quadratgrade des Himmels bedecken. In neuerer Zeit ist aber für diese Felder nur in Ausnahmefällen auf photographischem Wege die Anwesenheit von Nebelmaterie nachgewiesen worden³. HAGENS Nebel umfassen auch die HERSCHELschen. Sie haben eine graue neutrale Färbung und für die Dichte oder Trübung der Nebel hat HAGEN eine Skala von fünf Stufen eingeführt, deren Nummern mit dem Trübungsgrad wachsen. Stufe V entspricht also den dichtesten, „fast alle Sterne verdunkelnden“ Partien. In der Durchmusterung der Nebel wurde das Fernrohr auf volle Grade in R A eingestellt und in Dekl. bewegt. Das Gesichtsfeld hatte 25' Durchmesser. Die Beobachtungsmethode besteht in einem Überfahren („sweeping“) eines Streifens benachbarter Gebiete.

Das Hauptresultat der HAGENSchen Untersuchungen ist, daß die dunklen Nebel ein zusammenhängendes Netzwerk bilden, das aber von kanal- und ovalförmigen Lichtungen vielfach durchbrochen ist. Sie bevorzugen die außergalaktischen Regionen des Himmels, kommen aber auch in der Milchstraße vor. Da der geschätzte Trübungsgrad augenscheinlich auf der Sternfülle beruht, so ist es von vornherein klar, daß eine negative Korrelation zwischen Dichte des Nebels und Sternanzahl zu erwarten ist.

Die hellen Nebelflecke der außergalaktischen Regionen finden sich selten innerhalb großer Wolkenkontinente, sondern meist an deren Rande oder wo die Dichte sich schnell verändert. Große Wolkengebiete erscheinen oft von Sternketten umsäumt.

HAGEN schließt, daß unser Milchstraßensystem von einem dunklen Nebelmeer eingehüllt ist, das auch die hellen außergalaktischen Nebelflecke umfaßt. Er sucht auch in weitgehender Weise die kosmogonische Stellung der dunklen Nebel aufzuklären, nach ihm waren die dunklen Nebel der Ustoff der ursprünglich kalten und dunklen Riesensterne, die sich in dem LOCKYER-HERTZSPRUNG-RUSSELLschen Schema weiterentwickeln.

Die Resultate von HAGEN sind von F BECKER⁴ und J STEIN⁵ dargelegt und verteidigt worden. J HELLERICH⁶ und V CERULLI⁷ haben zusammenfassende Übersichten gegeben.

¹ Mem S A I t 1 (1920), M N 81, S 449 (1921), A N, Jubil.-Nr. (1921), 213, S 351 (1921), 214, S 449 (1921), Naturwiss 9, S 935 (1921), Scientia 31, S 185 (1922), Publ. A S P 34, S 320 (1922), Atti Pontif. Accad. Sci. 75, S 71 u. 83 (1922), 76, S 31, 89 u. 200 (1923), 77, S 131 (1924) (Durchmusterung und kleinere Notizen), Specola Astronomica Vaticana, Miscellanea Astronomica 1, parte 3 (1924) (Neudruck älterer Abhandlungen), A N 224, S 421 (1925), 225, S 129 u. 383 (1925), Specola Vaticana X (1922, 1925 u. 1927) (Katalog), M N 86, S 144, 146, 349, 439, 548 u. 642 (1926), A N 227, S 391 (1926), B Z 23 (1927), Atti Pontif. Accad. Sci. 80, S 51 u. 94 (1927), A N 229, S 303 (1927), 230, S 325 (1927), M N 87, S 106 (1926), Publ. A S P 39, S 167 (1927), Atti Pontif. Accad. Sci. 81, S 343 (1928), 82, S 263 (1929), B Z 16 (1929), Pop. Astr. 37, S 284 u. 395 (1929), A N 235, S 313 (1929), M N 90, S 331 (1930), außerdem „Die Nebelstraße“, Anhang zu der Monographie „Die Milchstraße“ von PLASSMANN (1924), „Das photographische Problem der Nebelwolken“, Festschrift Stella Matutina II (1931), Miscellanea Astronomica 6, No 93 (1931).

² Phil. Trans. S 269 (1811), Coll. Scientific Papers II, S 459.

³ Vgl. besonders Mrs I ROBERTS, I Roberts' Atlas of 52 Regions. A Guide to HERSCHEL'S Fields. Preface by J G HAGEN. Paris 1928.

⁴ A N 223, S 303 (1925), 224, S 113 u. 235 (1925), 225, S 129 (1925), Die Sterne, S 97 (1926), Specola Astronomica Vaticana XIII (1928), Dunkelwolken in der Umgebung von NGC-Objekten.

⁵ V J S 61, S 250 (1926). ⁶ Naturwiss 14, S 107 (1926). ⁷ Scientia 40, S 133 (1926).

Es hat aber auch nicht an Einwänden gegen HAGENS Deutung seiner Beobachtungen gefehlt. So besteht die Schwierigkeit, daß auf langexponierten Platten unter Verwendung von lichtstarken Instrumenten keine den Nebeln entsprechende Struktur hervortritt. Dieser Schluß kann aus den ausgedehnten photographischen Arbeiten, z. B. von BARNARD, WOLF und HUBBLE, gezogen werden, da diese keine diffusen Nebel in hohen galaktischen Breiten nachgewiesen haben. N. IVANOV¹ konstatierte kürzlich dasselbe Sachverhältnis für die HAGENSchen Nebelwolken bei V und UW Draconis und bei R und S Tauri. LUNDMARK² hebt unter anderem hervor, daß Fehlerquellen wie Tierkreislucht, Erdlicht, physiologische Effekte, Farbgleichung des Instrumentes einwirken können. Er schlägt vor, daß HAGENS Beobachtungen von anderen Beobachtern, in einem anderen Klima, mit Teleskopen von größerem Öffnungsverhältnis und größerem Feld wiederholt werden sollten.

Angesichts der großen Schwierigkeiten, die eine Einpassung des „Nebelmeers“ in unser Weltbild verursacht, wäre es wohl jedenfalls angemessen, eine weniger revolutionierende Erklärung des beobachteten Phänomens zu suchen. WIRTZ³ stützt in den Beobachtungen der HAGENSchen Nebel Stufenschätzungen der scheinbaren Helligkeit des Himmelsgrundes. Der negative Korrelationskoeffizient r zwischen Dunkelstufen und Sternlichtigkeit wird numerisch um so größer, je schwächer die Sterne der verglichenen Sternzählungen sind. Bei der Grenzgröße 11,0 ist $r = -0,16$, bei 14,5 ist $r = -0,64$. Es liegt also in HAGENS Resultaten ein ungemaschtes Netz grober schematischer Sternzeichnungen vor. Praktisch denselben Schluß hat auch SHAPLEY⁴ aus ähnlichen Überlegungen gezogen. HAGEN und BECKER lehnen jedoch diese Auffassung ab auf Grund von dem unmittelbaren subjektiven Eindruck, der direkt die unzweideutige Existenz der Wolken gewährleistet soll.

Es scheint jedoch wohl noch die Möglichkeit zu bestehen, daß der schwache graue „Nobelschein“, der keine Struktur auf den photographischen Platten gibt, als „Erdlicht“ im weiteren Sinne (Ziff 5) erklärt werden kann, daß er nach HAGENS Angaben mit großer Sternfülle im Felde zu verschwinden scheint, wäre als ein physiologischer Kontrasteffekt zu deuten. Es ist schon oben der Schluß gezogen worden, daß Sternanzahl und Trübungsgrad korreliert sein müssen, da offenbar die Sternleere des Feldes als Maß der Trübung benutzt wird. Auf die Gefahr einer Selbsttäuschung bei der Einordnung benachbarter Sterne im Gesichtsfelde in „Ketten“ sollte wohl auch hingewiesen werden.

Wenngleich eine „einfachere“ Erklärung dieser Art gegenwärtig vielleicht vorzuziehen wäre, verdienen doch ohne Zweifel die scharfen und kühnen Beobachtungen HAGENS mit größtem Interesse aufgenommen zu werden, was besonders durch die zahlreichen Kommentare und Erklärungsversuche, z. B. in neuester Zeit von H. ORTHOFF⁵, J. HARTMANN⁶ und J. HOPMANN⁷, bewiesen wird.

f) Die astrophysikalisch-statistischen Ergebnisse über die Natur der Milchstraße.

16. Die galaktische Konzentration der Sterne und die effektive Sterngröße des Milchstraßenlichts. Es ist seit drei Jahrhunderten eine wohlbekannte Tatsache, daß das Milchstraßenphänomen auf einem scheinbaren Zusammendrängen der Sterne gegen einen gewissen Gürtel des Himmels beruht. Durch die

¹ Bulletin of the Observing Corp. of the Soc. of Amateur Astronomers of Moscow Nr. 8, S. 57 (1927).

² Publ. A. S. P. 34, S. 191 (1922).

³ A. N. 223, S. 123 (1924); 224, S. 267 (1925), 225, S. 299 (1925).

⁴ Harv. Circ. 281 (1925).

⁵ A. N. 238, S. 233 (1930).

⁶ A. N. 239, S. 61 (1930).

⁷ A. N. 238, S. 285 (1930).

Arbeiten von HOUZEAU, SEELIGER, SCHIAPARELLI, PICKERING, STRAIKONOFF u. a. wurde es auch klargestellt, daß diese „galaktische Konzentration“ der Sterne in allen Größenklassen zu finden ist, wenn auch die Sterne der hellsten Größen sich eher gegen den GOULDSCHEN Kreis (Ziff 11), als gegen die zentrale Milchstraßenlinie konzentrieren. Jedenfalls wurden wir, wenn wir den ganzen Himmel betrachten, eine positive Korrelation zwischen Milchstraßenlicht und Sternanzahl finden, und zwar für alle Größenklassen, auch die hellsten. In diesem Sinne kann man sagen, daß das Phänomen der Milchstraße in allen Größenklassen widergespiegelt wird, wenn auch in weit höherem Maße für die sehr schwachen Größen als für die helleren.

HOUZEAU vergleicht nach der Uranométrie Générale die Sterndichtigkeit in verschiedenen galaktischen Zonen miteinander. Wenn man die Zonen -30° bis $+30^\circ$, um die Milchstraße herum, mit den übrigen bleibenden Kalotten des Himmels vergleicht, findet man nach HOUZEAU für die so definierte galaktische Konzentration den Wert 1,38 für die Größen 1 bis 3 und 1,22 für die Größen 4 bis 6.

PICKERING¹ hat aus den Milchstraßenzeichnungen von ILLIS und GOULD eine rohe Intensitätstabelle für das Milchstraßenlicht hergestellt. Er gibt in einer Skala von zehn Stufen die mittleren Intensitäten für Intervalle von 1^h in R. A. und 5° in Dekl. Wenn er die Sternzahlen, auf gleiche Fläche reduziert, in der Milchstraßenzone (10999 Quadratgrade) und in den außergalaktischen Partien (25641 Quadratgrade) vergleicht, findet er bis zur Größe 7 eine nahe konstante galaktische Konzentration vom Betrage 1,85. Die Konzentration ist sogar für die hellsten Größen ein wenig stärker.

KAPTEYN und VAN RIJN definieren die galaktische Kondensation für die Größe m als das Verhältnis zwischen der Anzahl der Sterne von den hellsten bis zur Größe m pro Quadratgrad (N_m) in der Zone 0 bis 20° und der entsprechenden Anzahl für die Zone 40° bis 90° . Nach SEARFS und VAN RIJN² ergeben sich für sukzessive photographische Größen die Werte in Tabelle 8. Die Kondensation ist nahezu konstant bis zur Größe 10,0 und steigt dann allmählich, um für die schwachsten Größen sehr erhebliche Werte anzunehmen.

Tabelle 8

m	Kond	m	Kond	m	Kond
4,0	2,5	10,0	2,6	16,0	5,8
5,0	2,5	11,0	2,9	17,0	7,1
6,0	2,5	12,0	3,1	18,0	8,5
7,0	2,5	13,0	3,5	19,0	10,7
8,0	2,5	14,0	4,1	20,0	13,2
9,0	2,5	15,0	4,8	21,0	16,2

Im Raume betrachtet sehen wir den unmittelbaren Grund des Milchstraßenphänomens und des damit verbundenen, zum Teil äquivalenten Phänomens der galaktischen Konzentration der Sterne in einem Zusammenhängen der Sterne gegen eine gewisse Ebene, die galaktische Ebene, welche durch die Zentrallinie der Milchstraße definiert wird. Wenn aber die Milchstraße etwa einer gleichförmigen Verteilung der Sterne in einem zweidimensional unendlichen Stratum entspräche und keine Absorption des Lichtes in diesem Stratum vorauszusetzen wäre, so ist es leicht einzusehen, daß die effektive Steingröße oder die Größe, welche der maximalen Gesamthelligkeit für Sterne innerhalb einer Größenklasse

¹ Harv Ann 48, S 149 (1903)² Transactions of the International Astronomical Union II, S 96 (1925)

entspricht, nach der Zentrallinie der Milchstraße hin sich gegen eine unendlich lichtschwache Größe verschieben würde, und daß gleichzeitig die Intensität gegen diese Zentrallinie anwachsen würde, so daß in der unmittelbaren Umgebung der genannten Linie selbst, wo die Sterne unendlich dicht gegeneinander gedrängt erscheinen würden, die Helligkeit sogar die photosphärische Helligkeit der Sterne erreichen sollte. Die unmittelbare Beobachtung zeigt uns, daß die genannten Annahmen nicht zutreffend sind, was auf eine Begrenzung des Sternstratums oder auf Schwankungen der räumlichen Dichte hinweisen, aber auch durch eine Absorption des Lichts im interstellaren Raume bedingt sein kann. Mit größter Wahrscheinlichkeit sind alle drei Ursachen vorhanden. Ohne Zweifel können wir jedoch a priori voraussetzen, daß die effektive Sterngröße der verschiedenen Partien der visuellen Milchstraße nicht überall dieselbe sein kann.

Wenn wir die Anzahl von Sternen zwischen den scheinbaren Größen m und $m + dm$ mit $a(m) dm$ bezeichnen, so ist offenbar $a(m) \cdot 10^{-0.4m} dm$ ein Ausdruck für die Gesamthelligkeit dieser Sterne. Wenn wir also genügend genaue Sternzählungen zur Verfügung haben, so ist es leicht, den Anteil verschiedener Größenklassen an der Gesamtlichtwirkung zu bestimmen.

Für einen Quadratgrad der großen Sagittariuswolke hat S. BAILEY¹ eine Sternzählung bis zur 19 photographischen Größe vorgenommen. Tabelle 9 gibt die Größe $f(m)$ gemäß der Formel

$$\log f(m) = \log a(m) - 0,4 m + 3$$

für sukzessive Größenklassen nach diesen Zählungen. $a(m)$ ist hier die Anzahl Sterne zwischen $m - \frac{1}{2}$ und $m + \frac{1}{2}$.

Man ersieht aus der Tabelle, daß nach BAILEYs Resultaten die in dieser Gegend wirksamsten Sterne von der Größe 15 und 16 sind, aber auch daß die Funktion $f(m)$ sich ziemlich langsam mit der Größe ändert. Der Anteil

der helleren Sterne an dem Gesamtlicht ist daher auch nicht unerheblich. Für Größen heller als 10 wird jedoch die Anzahl Sterne so klein, daß es fraglich erscheint, ob die entsprechende Lichtmenge wirklich im wahrgenommenen kontinuierlichen Milchstraßenschein mitwirkt. Die effektive Größe des Milchstraßenlichts liegt daher hier wahrscheinlich nahe der Größe 15.

PANNIKOFF² macht aber zu BAILEYs Sternzählung die Bemerkung, daß die daraus resultierende Totalhelligkeit (0,024 Sterne der Größe 0,0 pro Quadratgrad) viel kleiner ist als die aus dem Glanz der Wolke in Verbindung mit VAN RHYNs Messungen (Ziff. 5) ermittelte. Es ist daher möglich, daß BAILEYs Zahlen von der Größe 17 ab zu klein sind, wahrscheinlich infolge des Zusammendrängens der Sterne auf der Platte, oder vielleicht, daß die Größenskala nicht ganz in Ordnung ist. Nach der ersten Alternative wäre die effektive Größe noch schwächer als die oben gefundene.

Es mag in diesem Zusammenhang von Interesse sein, die am meisten effektive Sterngröße verschiedener galaktischer Zonen gemäß den über alle Längen gemittelten Sternzahlen, wie sie den Untersuchungen über das „typische System“ zugrunde liegen, zu ermitteln. In Tabelle 10 ist $f(m)$ für die galaktische Breite 0° und 90° gemäß F. H. SEARES³ Sternzahlen berechnet worden. Die effektive Sterngröße liegt offenbar nahe der Größe 13,0 für die galaktische Zone und nahe 8,5 für den galaktischen Pol.

Tabelle 9

m	$f(m)$	m	$f(m)$	m	$f(m)$
10,0	1,5	13,0	1,4	16,0	5,1
11,0	1,5	14,0	2,9	17,0	2,8
12,0	1,0	15,0	6,9	18,0	1,3

¹ Harv Circ 242 (1922).² BAN 4, S 39 (1927).³ Mt Wilson Contr 346 = Ap J 67, S. 67 (1928)

Die Beziehung der mittleren Steinnzahlen zu der beobachteten Strahlung des allgemeinen Himmelsgrundes ist schon in Ziff 5 besprochen worden

HOPMANN¹ hat aus seiner Isophotenkarte unter Heranziehung der von H HENIE² und H NORT³ ausgearbeiteten Verteilung der Sterne heller als 11^m

Tabelle 10

<i>m</i>	<i>b</i> = 0° <i>f</i> (<i>m</i>)	<i>b</i> = 90° <i>f</i> (<i>m</i>)	<i>m</i>	<i>b</i> = 0° <i>f</i> (<i>m</i>)	<i>b</i> = 90° <i>f</i> (<i>m</i>)
5	0,49	0,14	13	0,90	0,10
6	,55	,16	14	,88	,08
7	,62	,17	15	,82	,06
8	,68	,18	16	,72	,04
9	,75	,18	17	,60	,02
10	,81	,17	18	,48	,01
11	,85	,15	19	,36	,01
12	,89	,13	20	,26	,00

den Anteil am Milchstraßenlicht der Sterne heller und schwächer als 11^m für verschiedene Regionen zu bestimmen versucht Für die Sagittariuswolke stimmt sein Resultat qualitativ mit dem oben gegebenen überein Für andere Regionen ergibt sich ein relativ größerer Anteil der helleren Sterne als für die Sagittariuswolke

Ohne sehr weitgehende genaue Steinnzahlungen bis zu außerordentlich

schwachen Größenklassen für verschiedene Gegenden der Milchstraße können wir die Frage nach der effektiven Steingröße nicht streng beantworten, und genügende Zahlungen dieser Art liegen noch kaum vor Da aber die Photographie weit mehr als die direkte Beobachtung die Umrisse der Milchstraßenstruktur in isolierte Sterne auflöst, so liegt in der Milchstraßenphotographie wenigstens ein Mittel vor, eine obere Grenze der mittleren Helligkeit der Sterne in den Grenzgebieten der visuellen Milchstraße zu finden Wenn wir auf den Photographien feststellen, für welche Grenzgröße eine Struktur der Verteilung, den Umrissen der visuellen Milchstraße entsprechend, zuerst hervortritt, können wir wenigstens den Schluß ziehen, daß die effektive Steingröße nicht merklich heller als diese Grenzgröße sein kann Nach K GRAFF⁴ kann man annehmen, daß erst Sterne von der Größe 13 abwärts die klare Begrenzung der Milchstraßenwolken hervorgerufen Trotz des Umstandes, daß einige Einzelheiten der Milchstraßenstruktur schon bei helleren Größen hervortreten, können wir mit großer Sicherheit annehmen, daß die effektive Größe des Milchstraßenlichts, gemäß der oben gegebenen Definition, in den helleren Partien der eben erwähnten oder sogar einer noch schwächeren Größe entspricht

Für eine Deutung der Wolkenstruktur der Milchstraße ist es übrigens von Bedeutung, festzustellen, für welche Steingröße die scheinbare Verteilung der Sterne innerhalb der Milchstraßenzone eine deutliche Korrelation mit der Lichtverteilung der Milchstraße selbst zeigt Sehr ausführlich ist dieses Problem von EASON⁵ behandelt worden Er untersucht zuerst helle und dunklere Partien der Milchstraße in Aquila und Cygnus Für die Steinnzahlungen lieferte für hellere Sterne die BD das Material, und für schwächere Sterne wurden die Steinnzahlungen von HERSCHEL, CRIORIA, EPSTEIN und WOLF innerhalb der betreffenden Regionen benutzt Die sehr klare Korrelation zwischen Steinnzahl und Milchstraßenhelligkeit für die schwachen Sterne bleibt in geringerem Maße auch für die BD-Sterne schwächer als 9^m bestehen, während für hellere Sterne jede deutliche Korrelation verschwindet In seiner späteren Arbeit vergleicht EASON den Dichtigkeitsgrad der BD-Sterne nach der ausführlichen Bearbeitung dieser Sterne von W. STRATONOFF⁶ mit dem Helligkeitsgrad der Milchstraße und erstreckt seine Untersuchung über den ganzen nördlichen Milchstraßenverlauf.

¹ A N 222, S 86 (1924)

² Lund Medd Ser II, Nr 10 (1913)

³ Recherches astion de l'Obs d'Utrecht VII (1917)

⁴ Grundriß der Astrophysik, S 715 (1928)

⁵ A N 137, S 81 (1894), Ap J 1, S 216 (1895), A N 159, S 169 (1902), Proc Acad Amsterdam 8, Nr 3 (1903)

⁶ Publ Obs Taschkent 2 (1900)

Es stellt sich hier heraus, daß eine kleine mit steigender Helligkeit abnehmende Korrelation im ganzen auch für die helleren Klassen der ARGELANDERSchen Sterne besteht. Noch für die hellste Klasse, welche die Größen 0 bis 6,5 umfaßte, ist eine Spur davon vorhanden. Eine erheblich größere Korrelation für diese hellste Klasse ist aber von NEWCOMB¹ hergeleitet worden, was wohl auch mit J. C. VAN DE LINDERS² Resultaten übereinstimmt.

EASTON zieht aus der Übereinstimmung der Konzentrationspunkte für verschiedene Größen den Schluß, daß die schwachen Sterne der Milchstraße von uns nicht viel weiter entfernt sein können als etwa die Sterne 9. oder 10. Größe, und daß die scheinbaren Sternwolken auch wirklichen reellen Anhäufungen im Raume entsprechen. Von unserem jetzigen Standpunkt aus müssen wir aber diese Auffassung als einen Fehlschluß betrachten. Daß eine Korrelation zwischen Sternverteilung und Milchstraßenhelligkeit auch für helle Größenklassen besteht, kann auch bedeuten, daß die Ursachen der Wolkenstruktur wenigstens zum Teil in unserer Nähe liegen und wesentlich in einer Absorption des Lichts in dunklen Wolken von nebliger oder staubförmiger Materie zu suchen sind. Wir werden im folgenden sehen, daß diese Auffassung in der letzten Zeit mehr und mehr Platz greift. Es ist jedoch jedenfalls ein bleibendes Verdienst von EASTON, die Bedeutung der großen Streuung in absoluter Größe unter den Sternen für das Milchstraßenproblem erkannt zu haben.

NORT hat in seiner eben erwähnten Arbeit die Untersuchung von EASTON auf Grund der Sternzählungen bis zur 11. Größe erweitert. Unter Verwendung einer von EASTON hergestellten Isophotokarte für den Südhimmel, die auf GOULDS, HOUZEARS und BACKHOUSES Arbeiten beruht, hat er die Untersuchung auch auf die südliche Milchstraße ausgedehnt. Er gibt in Tabellen und Figuren einen Vergleich zwischen Lichtintensität und Sterndichte für Gebiete der galaktischen Zone in Intervallen von 15° in L und 4° in B . Er zieht den Schluß, daß das Phänomen der Milchstraße im ganzen noch nicht in der Verteilung der Sterne zwischen $9^m,0$ und $11^m,0$ widerspiegelt wird. Dieser Schluß ist in Übereinstimmung mit PANNIKOWSKIs Resultaten³, daß keine organische Verbindung zwischen der großen Masse der Sterne von der 9. bis vielleicht zu der 11. Größe und den Wolken, welche die Milchstraße bilden, besteht, widerspricht jedoch wohl in einem gewissen Grade den oben referierten Resultaten von HOPMANN, nach denen in vielen Fällen die Sterne heller als von der Größe 11 sogar in der Gesamtlichtwirkung dominieren sollen.

Daß eine ausgeprägte Korrelation zwischen dem Verlauf der Milchstraße und der Verteilung der Sterne bis etwa zur Größe 14 (visuell) besteht, ist z. B. aus den umfangreichen Zählungen auf der FRANKLIN-ADAMS-Karte, die von CHARLIER und seinen Mitarbeitern in Lund ausgeführt worden sind⁴, ersichtlich. Eine Tafel, welche die Resultate bildlich wiedergibt, ist in CHARLIERS „California Lectures“⁵ gegeben.

17. Das Integralspektrum der Milchstraße. Effektive Entfernung der Milchstraßensterne. Das integrierte Spektrum von einigen galaktischen Wolken wurde zuerst von E. A. FATH⁶ auf dem Mount Wilson mit Expositionszeiten von 30, 67 und 74 Stunden erhalten. Das Ergebnis war ein Spektrum approximativ vom Sonnentypus. Da nach VAN RHYNs oben (Ziff 5) besprochener Arbeit ein beträchtlicher Teil der Strahlung des Himmelgrundes auch für helle galak-

¹ The Stars, S. 273 (1902)

² De Verdoeling der heldere Sterren, S. 63. Rotterdam, Wyt & Zonen 1921.

³ Verh. Akad. Amsterdam 19, S. 243 (1910); Proc. Acad. Amsterdam 13, S. 239 (1910).

⁴ Lund Medd. Ser. II, 31 (1923)

⁵ Mem. Univ. Calif. 7 (1926).

⁶ Mt. Wilson Contr. 63 = Ap. J. 36, S. 362 (1912)

tische Regionen wahrscheinlich dem Zodiakallicht zuzuschreiben ist, so ist es möglich, daß diese Lichtquelle in dem Resultat etwas mitspielt

E A KREIKEN¹ hat für 4000 Sterne der Scutumwolke bis zur Größe 14,9 die photographisch effektiven Wellenlangen bestimmt. Das Plattenmaterial hatte E HERRZSPRUNG mit dem 60zölligen Reflektor auf dem Mount Wilson gesammelt. Im Mittel ergibt sich ein Farbentypus, der eine Spektralklasse etwas früher als G0 andeutet. Nach unseren Überlegungen in Ziff 16 ist es wahrscheinlich, daß KREIKENS Untersuchung die effektive Größe des Milchstraßenlichts erreicht, und daß also die berechnete mittlere Farbe der Sterne für dieses Gesamtlicht einigermaßen repräsentativ sein sollte. Das gewonnene Resultat ist natürlich von jedem Erdlicht oder Zodiakallicht frei und stützt daher die Gültigkeit der von FATH erhaltenen Spektralklasse.

In einer späteren Arbeit² hat KREIKEN unter Heranziehung anderer Materials die Farben der Milchstraßensterne bis zu noch schwächeren Größen studiert (vgl. Ziff 22). Im Mittel ergibt sich für die Scutumwolke bis zur Größe 17,3 ein Farbindex +0,38, während SHAPLEY³ für 310 Sterne zwischen den Größen 12 und 15 in derselben Wolke in der Umgebung des Sternhaufens M11 im Mittel +0,77 findet.

Eine direkte Bestimmung des Farbindex derselben Wolke hat PANNIKOEK⁴ vorgenommen. Die Platten wurden von WOLF mit einem kleinen Zeiss-Tessar aufgenommen und extrafokal eingestellt, so daß die helleren Sterne als isolierte Scheibchen erscheinen. Die Schwärzung auf der Platte ruht außerdem vom galaktischen Licht und vom „Erdlicht“ her, letzteres kann als über das Feld konstant angesehen werden. Die Variation der Schwärzung mit einer Variation der photographischen Helligkeit (in Sternen der Größe 0 per Quadratgrad ausgedrückt) wurde aus den Sternscheibchen heller Sterne ermittelt. Der Zusammenhang zwischen Schwärzung und visueller Helligkeit des Milchstraßenlichts in einer entsprechenden Einheit wurde aus den PANNIKOEKSchen Isophoten nach ihrer Eichung gemäß VAN RIJNS Messungen bestimmt. Aus dem Verhältnis der Koeffizienten der zwei Ausdrücke zieht PANNIKOEK den Schluß, daß die photographische Lichtstärke der Milchstraßenwolke 57/85 der visuellen beträgt. Dieses Verhältnis entspricht einem Farbindex von +0,43 und einer Spektralklasse F5.

Kürzlich haben W S ADAMS, M HUMASON und A. H. JOY⁵ mit einem kleinen Spektrographen in Verbindung mit dem 10zölligen Cooke-Reflektor auf dem Mount Wilson Spektrogramme der Milchstraßenwolken in Sagittarius und Cygnus aufgenommen. Die Expositionszeiten waren 93 und 141 Stunden. Die Spektralklassen wurden in beiden Fällen früher als vom Sonnentypus, nämlich F5 für die Sagittariuswolke und F3 für die Cygnuswolke, gefunden. Infolge der kleinen Dispersion des Spektrographen läßt sich natürlich eine genauere Bestimmung der Radialgeschwindigkeit der Wolken nicht durchführen. Von Bedeutung ist aber die Bemerkung, daß die Radialgeschwindigkeiten beider Wolken klein gefunden werden.

Wenn wir also für das Integralspektrum der Milchstraße die Klasse F5 annehmen, so ist es klar, daß wir es in diesem Falle mit einer Art von Mischspektrum zu tun haben, zu dem verschiedene Sterntypen mehr oder weniger ihren Beitrag liefern. Da aber die Klasse F5 und die diese Klasse in der Spektralliste unmittelbar umgebenden Typen unter den schwachen Sternen sehr zahlreich vertreten

¹ On the Colour of Faint Stars in the Milky Way, and the Distance of the Scutum Group. Dissert. Groningen 1923

² M N 87, S 196 (1927)

³ B A N 2, S 19 (1923)

⁴ Mt Wilson Contr 133 = Ap J 46, S 64 (1917)

⁵ Publ A S P 39, S 368 (1927)

sind, so können wir mit einiger Wahrscheinlichkeit schließen, daß wir es in der Nähe der „effektiven“ scheinbaren Größe im Durchschnitt mit Sternen dieser Spektralklasse zu tun haben, und zwar mit gewöhnlichen „Zwergsternen“, da die „Riesen“ dieser Klasse sehr selten im Raume sind und wir für die Sterne der schwachen Größenklassen keine sehr extreme Selektion nach großer absoluter Leuchtkraft voraussetzen haben. Wir können also für die mittlere absolute Größe der Sterne etwa $+3$ annehmen. Die effektive Entfernung der Milchstraßensterne können wir als die Entfernung definieren, in der die effektive absolute Größe auf die effektive scheinbare Größe des Milchstraßenlichts reduziert wird. Wenn wir für die letztere die Größe 14 fixieren, bekommen wir für die effektive Entfernung der Milchstraßensterne 1600 Parsec. Für die Sagittariuswolke beträgt die effektive Entfernung etwa 2500 Parsec. Der eingeführte Begriff der effektiven Entfernung ist natürlich ganz unabhängig von der Frage, ob die Sterne Mitglieder einer reellen Wolkenstruktur sind oder in einem sehr ausgedehnten Stratum ziemlich gleichmäßig gestreut vorkommen. Man ersieht ohne Schwierigkeit aus dem symmetrischen Verlauf von $f(m)$ um die effektive Größe herum in Tabelle 9, daß diese Entfernung approximativ so abgemessen ist, daß eine Hälfte des galaktischen Lichts aus größerer, eine Hälfte aus kürzerer Entfernung stammt.

Eine wenn auch nur sehr grobe Kontrolle dieser Schätzung der effektiven Entfernung gibt uns das Phänomen der Tiefe oder des „dip“ der Milchstraße. Nach Tabelle 5, Ziff 11, bekommen wir im Mittel für die Tiefe $p = \sigma - 90^\circ$ den Wert $26'$. Andererseits finden wir in Ziff 21, daß die Sonne wahrscheinlich etwa 34 Parsec nördlich von der mittleren galaktischen Ebene gelegen ist. Wenn wir diese zwei Daten zusammenstellen, ergibt sich für die „effektive Entfernung“ rein geometrisch etwa 4500 Parsec, was wenigstens der Größenordnung nach mit dem obigen photometrischen Resultat stimmt. Wenn wir z. B. PANNEKOKS Wert der Tiefe, $p = 65'$, angenommen hätten, wäre die Übereinstimmung viel besser.

18. Übersicht der allgemeinen statistischen Untersuchungen über die Verteilung der Sterne im Raume. Daß die Milchstraße als Phänomen durch eine Zusammenwirkung des Lichts von unzähligen Sternen, die in einer Schicht großer Sternhäufigkeit verteilt sind, entsteht, ist eine Ansicht, die im Altertum von DEMOKRIT, in der Neuzeit von KEPLER und GALILEI, und auf mehr naturphilosophischer Grundlage von SWEDENBORG, WRIGHT, KANT und LAMBERT ausgesprochen wurde. Als Begründer der Stellarastronomie als empirischer Wissenschaft ist aber W. HERSCHEL anzusehen. Die empirische Grundlage der Feststellungen HERSCHELS sind in den vielerwähnten Sternelchungen¹ enthalten. Er zählte für verschiedene Punkte des Himmels die Anzahl Sterne, die im Felde seines Reflektors sichtbar waren. Der Bearbeitung des Materials lag die Annahme einer bis zu einer gewissen Grenzfläche gleichförmigen Dichte im Sternsystem zugrunde. Die verschiedene Fülle sichtbarer Sterne in verschiedenen Gegenden des Himmels mußte dann auf eine Erschöpfung aller Sterne bis zur Grenze des Systems zurückgeführt werden, und der Abstand der Grenze in einer gewissen Richtung wurde durch eine einfache Formel direkt aus der Sternzahl berechnet. So gelangte HERSCHEL zu der wohlbekannten Darstellung des Systems in Form eines linsenförmigen Gebildes, dessen größter und kleinster Durchmesser 860 und 220 „Siriusbstände“ betragen. In seinen späteren Jahren wurden allerdings die Ansichten HERSCHELS etwas modifiziert; die Tiefe der Milchstraße erscheint ihm in gewissen Gegenden unermesslich.

¹ Phil Trans 74, S. 437 (1784), 75, S. 213 (1785), Collected Scientific Papers I, S. 157 ff., 223 ff.

Die Weiterentwicklung der Stellaistatistik im 19. Jahrhundert ist an eine Reihe von Namen geknüpft, von denen wir H. G. W. STRUVE, G. V. SCHIAPARELLI, H. GYLDÉN erwähnen können. Ihre vollständigste Entwicklung und gewissermaßen einen vorläufigen Abschluß finden die neuen Methoden in den Arbeiten H. V. SEELIGERS¹.

An Stelle der Annahme, daß die Sterne alle ungefähr dieselbe absolute Leuchtkraft besitzen, tritt die Annahme einer statistischen Verteilung der wirklichen Helligkeiten, die durch eine Luminositätsfunktion ausgedrückt wird. Die absolute Leuchtkraft ι wird als die auf die Entfernung 1 reduzierte scheinbare Helligkeit verstanden, und die Proportion der Sterne in einer Volumeneinheit, die zwischen ι und $\iota + d\iota$ liegen, wird durch den Ausdruck $\varphi(\iota) d\iota$ definiert, wo $\varphi(\iota)$ die Luminositätsfunktion darstellt. Die Anzahl aller Sterne in der Volumeneinheit für die Distanz r innerhalb der betreffenden Region des Himmels ist eine Funktion $D(r)$ von r . Wenn wir das Problem der Verteilung in aller Allgemeinheit angreifen, müssen wir die Möglichkeit offen lassen, daß $\varphi(\iota)$ von Ort zu Ort wechseln kann, in a. W. daß das Mischungsverhältnis verschiedener absoluter Größen mit der Entfernung wechseln kann. Die Leuchtkraftsfunktion sollte also $\varphi(\iota, r)$ geschrieben werden.

Die scheinbare Helligkeit h ist mit ι durch die Relation

$$\iota = \frac{h r^2}{\psi(r)} \quad (1)$$

verbunden, wo $\psi(r)$ die Einwirkung einer etwaigen Absorption des Lichtes im Raume Rechnung trägt.

Die Anzahl A aller Sterne, die auf ein Flächenstück des Himmels von der Größe ω projiziert und die heller als von der scheinbaren Lichtstärke h erscheinen, kann jetzt in der Form eines Doppelintegrals aus den Funktionen φ , D und ψ ausgedrückt werden. Wenn wir zuerst die Anzahl dA der Sterne im scheinbaren Helligkeitsbereiche zwischen h und $h + dh$ ins Auge fassen, bekommen wir fast unmittelbar die folgende Integralrelation

$$\frac{dA}{dh} = -\omega \int_0^\sigma D(r) \frac{r^2}{\psi(r)} \varphi\left(\frac{hr^2}{\psi(r)}, r\right) dr, \quad (2)$$

wo σ die obere Integrationsgrenze in r angibt. Für die mittlere Parallaxe $\pi(h)$ der in Betracht genommenen Sterne von der scheinbaren Helligkeit h oder von der scheinbaren Größe m , wo

$$m = -2,5 \log h,$$

haben wir dann auch, wenn r in Parsec ausgedrückt wird,

$$\pi(h) \frac{dA}{dh} = -\omega \int_0^\sigma D(r) \frac{r^3}{\psi(r)} \varphi\left(\frac{hr^2}{\psi(r)}, r\right) dr \quad (3)$$

Für SEELIGERS Analyse besonders charakteristisch sind die folgenden Annahmen, erstens, daß für die absolute Leuchtkraft ι eine obere Grenze ι_1 angegeben werden kann, welche allerdings vom Orte im System abhängen kann, und zweitens, daß eine Entfernung r_1 gefunden werden kann, außerhalb welcher die Sterndichtigkeit so schnell abnimmt, daß wir von einer wirklichen Begrenzung des Systems bei $r = r_1$ reden können. Diese Annahmen sind natürlich von Be-

¹ Ausführliche Bibliographie und zusammenfassende Darstellung von G. DI URSCILAND, V. J. S. 54, S. 25 (1919). Eine spätere Arbeit ist „Untersuchungen über das Sternsystem“ Sitzber. d. Bayer. Akad. d. Wiss., Math.-phys. Kl. (1920).

deutung für die obere Integrationsgrenze σ . Wenn wir Sterne von so großer scheinbarer Helligkeit in Betracht ziehen, daß auch Sterne der absoluten Leuchtkraft H noch innerhalb der Grenze r_1 stehen müssen, um der gewählten scheinbaren Helligkeit m entsprechen, ergibt sich σ aus der Relation

$$h = \frac{H(\sigma) \psi(\sigma)}{\sigma^2}$$

Wenn aber die Entfernung, in der die absolut hellsten Sterne die scheinbare Helligkeit h besitzen, die Grenze r_1 überschreitet, haben wir als obere Integrationsgrenze $\sigma = r_1$ zu setzen. In dieser Weise bekommt man zwei verschiedene Ausdrücke für die theoretischen Sternzahlen und mittleren Parallaxen für hellere und schwächere Sterngrößen.

Eine Folge dieser Aufspaltung der Formeln für die theoretischen Sternzahlen bei einer gewissen Sterngröße $m = n$, welche einen Stern der absoluten Helligkeit H an der Grenze $r = r_1$ kennzeichnen würde, ist eine Unstetigkeit in den zweiten Differenzen der Sternzahlen A . Wenn wir also in üblicher Weise die Sternzahlen A durch eine Interpolationsformel $\log A(m) = \alpha + \beta m + \gamma m^2$ darstellen wollen, so genügt diese Formel nicht in dem ganzen Bereich von Größenklassen, sondern wir müssen mit SEKLIGER annehmen

$$\log A(m) = \alpha + \beta (m - n) - \gamma (m - n)^2, \quad \text{für } m < n,$$

$$\log A(m) = \alpha + \beta (m - n) - \gamma_1 (m - n)^2, \quad \text{für } m > n$$

Um aber aus den beobachteten Sternzahlen zu einer praktischen Bestimmung der Dichte- und Luminositätsverteilung zu gelangen, müssen wir die vereinfachende Annahme einführen, daß die Luminositätsfunktion und auch die maximale Helligkeit unabhängig vom Orte sind, d. h. das Mischungsverhältnis der absoluten Helligkeiten soll überall dasselbe sein. Die Frage, ob eine Absorption im Raume vorhanden ist, kann dadurch vorläufig umgangen werden, daß wir die „scheinbare“ Entfernung q und Dichte $A(q)$ in folgender Weise einführen,

$$q^2 = \frac{r^2}{\psi(r)}, \quad A(q) = D(r) \varphi(r) \frac{dr}{dq}. \quad (4)$$

Wir bekommen dann aus (2) für die Sternzahlen verschiedener Grenzgrößen m

$$A(m) = \omega \int_0^q A(q) q^2 dq \int_{h_m}^H \varphi(x) dx, \quad (5)$$

wo

$$\sigma = \begin{cases} \sqrt{\frac{H}{h_m}}, & \text{für } m < n, \\ \sqrt{\frac{H}{h_n}}, & \text{für } m > n. \end{cases}$$

h_m und h_n sind die den Größen m und n entsprechenden Helligkeiten.

Für die mittleren Parallaxen haben wir dann die Formel

$$m(m) \frac{dA}{dh_m} = -\omega \int_0^q A(q) \frac{q^2}{\sqrt{\psi(r)}} \varphi(h_m q^2) dq, \quad (6)$$

wo also die Absorptionsfunktion $\varphi(r)$ explizit auftritt.

Die Sternzahlen der helleren Größenklassen folgen nahezu dem Gesetz

$$A = o h^{\frac{1-3}{2}}, \quad (7)$$

wo λ mit der galaktischen Breite zunimmt. SEELIGER weist nach, daß eine solche Form der Funktion A unabhängig von der Luminositätsfunktion einem Dichtegesetz

$$A = \gamma \varrho^{-\lambda} \quad (8)$$

entsprechen muß. Die Integralgleichung (5) für hellere Größenklassen gibt somit Aufschluß über die „scheinbare“ Dichteverteilung, während die entsprechende Gleichung für schwächere Klassen die Eigenschaften der Luminositätsfunktion bestimmen kann. Die Gleichung der mittleren Parallaxen kann dann zur Bestimmung der Absorptionsfunktion $\psi(r)$ benutzt werden, wodurch die wahre Dichtefunktion D aus A hergeleitet wird; praktisch muß jedoch eine solche Verwendung dieser Gleichung für eine Verbesserung der „scheinbaren“ Dichtefunktion A zurücktreten. Bei zu vernachlässigender Absorption ergibt nämlich die Dichtefunktion (8)

$$\pi(m) = c \left(\frac{h_m}{H} \right)^{\frac{1}{\lambda}} \quad (9)$$

unabhängig von der Luminositätsfunktion, eine Formel, die mit den KAPTEYN'schen mittleren Parallaxen in Widerspruch steht. Zur Erzielung einer Übereinstimmung muß die Dichtefunktion (8) modifiziert werden, da nur eine Einführung der Absorptionsfunktion nicht genügt.

Die veränderte Form des Dichtigkeitsgesetzes lautet

$$A(\varrho) = \gamma(\varrho^{-\lambda} - a\varrho^{-\lambda_1}), \quad (10)$$

wo der zweite Term in der Klammer nur für unsere nähere Umgebung von Bedeutung ist (aller nächste Umgebung, $\varrho = 0$, ist ausgeschlossen). Für die Luminositätsfunktion nimmt SEELIGER an

$$\varphi(i) = I' \{ x^{-r} e^{-h^2[(\log x)^2 + b \log x + c]} - x e^{-h^2 c} \}, \quad (11)$$

wo $x = i/H$ ist.

Bei der Konstantenbestimmung aus den empirischen Daten vereinfacht sich jedoch dieser Ausdruck praktisch auf $\varphi(i) = I' e^{-a(\log i)^2 - b \log i}$. Die maximale Leuchtkraft H wird aus den mittleren Parallaxen der hellsten scheinbaren Größen gemäß (9) bestimmt. Die Grenzentfernung r_1 ist durch einen Sprung in den Differentialquotienten $\frac{d^2 \log A}{d m^2}$ und $\frac{d \log \pi}{d m}$ bei einer gewissen Größe $m = m$ bedingt, und kann direkt durch die Beträge dieser Sprünge berechnet werden, aber auch durch die Beziehung $\varrho_1 = H^{\frac{1}{\lambda}} h_n^{-\frac{1}{\lambda}}$.

Die Beobachtungsdaten für SEELIGER'S Untersuchungen waren in den ersten Arbeiten die BD und deren stidliche Fortsetzung bis zur Dekl. -23° . Für die helleren Sterne dienten die Harvard-Photometry und die Potsdamer Durchmusterung, und für die schwächeren Größenklassen wurden die Eichungen von den beiden HERSCHEL ausgewertet. Für spätere Arbeiten spielte das in Groningen von KAPTEYN und VAN RIJN zusammengestellte Material die größte Rolle. Die Werte der mittleren Parallaxen waren die von KAPTEYN aus den parallaktischen Eigenbewegungen hergeleiteten.

Die Ermittlung der räumlichen Verteilung geschah teils für das schematische Sternsystem, bei welchem die Abhängigkeit der Sternzahlen von dem scheinbaren Ort völlig vernachlässigt wird, und teils für das typische Sternsystem, für welches die Abhängigkeit von der galaktischen Breite berücksichtigt wird. Das Phänomen der Milchstraße äußert sich in SEELIGER'S Resultaten wie in den HERSCHEL'Schen in einer beträchtlich größeren Ausdehnung des Systems in der Ebene der Milchstraße als in anderen Richtungen. Für die Grenze in der Milchstraßenzone gibt SEELIGER in seiner letzten Arbeit den Abstand 725 Sirius-

weiten (3625 Parsec) und für die Grenze in der Richtung des galaktischen Pols den Abstand 180 Sirlusweiten (900 Parsec). W. SAMETINGER¹ hat später in einer neuen Durchrechnung für die Grenzentfernung in den zwei Richtungen 2820 und 1260 Parsec gefunden.

Die Schnelligkeit, mit der die Sterndichtigkeit gegen die Grenzfläche des Systems abnimmt, und auch die Entfernung der Grenze selbst in verschiedenen Richtungen hängt natürlich von einer Schätzung der Absorption des Lichts im Raume, d. h. von der Funktion $\psi(r)$, ab. Die eben gegebenen Entfernungen der Grenze setzen voraus, daß die Absorption zu vernachlässigen ist, also daß $\psi(r) = 1$ zu setzen ist, womit Δ und D identisch werden. Wenn man mit SEKIGER vom Gesetze $\Delta(q) = \gamma q^{-2}$ ausgeht und voraussetzt, daß die wahre Sterndichtigkeit $D(r)$ nicht gegen die Grenzfläche hin wachsen darf, so bekommt man einen Höchstbetrag für die Absorption durch vorgelagerte Massen wie auch für eine allgemeine Absorption des Lichtes im Raume, der in beiden Fällen sehr klein ausfällt, und zwar so klein, daß der Einfluß auf die räumliche Ausdehnung des Systems als gering anzusehen ist. Im letzteren Falle hat man $\psi(r) = e^{-\tau}$ zu setzen und bekommt dann nach (4) die wahre Dichtigkeit durch die Formel

$$D(r) = \Delta(r e^{\frac{1}{2}\tau}) (1 + \frac{1}{2}\tau) e^{\frac{1}{2}\tau} \quad (12)$$

Für den maximalen Absorptionskoeffizienten (per Parsec gerechnet) in diesem Falle findet SEKIGER 0,0000617.

Mit dieser Überlegung ist aber sicher nicht die Frage einer merklichen Absorption des Lichtes definitiv erledigt. Das vorausgesetzte „scheinbare“ Dichtigkeitsgesetz, einschließend der scharfen Grenze bei $r = r_1$, ist für die großen Entfernungen ohne sehr schematische Annahme über die Dichtefunktion und kann keine strengere Gültigkeit beanspruchen. Es scheint schon aus diesem Grunde sehr fraglich, ob irgendeine zuverlässige Abschätzung der Absorption nach dem genannten Prinzip gemacht werden kann.

Es ist auch aus anderen Gründen ersichtlich, daß die Maschen des „typischen“ Sternsystems viel zu grob sind, um die Verteilung der Sterne für größere Entfernungen in dem dünnen galaktischen Stratum mit einiger Zuverlässigkeit zu fassen. Die Struktur der Milchstraße zeigt in mehreren Zügen unzweideutige Einflüsse einer mit dem scheinbaren Orte wechselnden Absorption durch neblige oder staubförmige Materie. Im „typischen Sternsystem“ werden Einzelheiten dieser Art, die Abhängigkeit von der galaktischen Breite innerhalb einer Zone sowie jede Abhängigkeit von der galaktischen Länge in einer allgemeinen Mittelbildung ausgeglichen. Wir wenden auf die diesbezüglichen Fragen in späteren Abschnitten zurückkommen.

Die Methode, die von J. C. KAPTEYN² und seinem Mitarbeiter und Nachfolger P. J. VAN RIJN³ befolgt wurde, um aus beobachteten Sternzahlen und statistischen Parallaxen die Dichtigkeitsfunktion und die Lichtkraftsfunktion zu bestimmen, ist nicht an mathematisch definierte Näherungsansätze gebunden, sondern besteht in einer im Prinzip voraussetzungsfreeeren tabellarischen Behandlung des empirisch gegebenen Materials. Die Anzahl $N_{m,\mu}$ der Sterne zwischen sukzessiven Intervallen in scheinbarer Größe m und Eigenbewegung μ wird unter Benutzung der empirisch bestimmten Funktionen $\pi_{m,\mu}$ (mittlere Parallaxe für gegebene Werte von m und μ) und $\chi_{\pi,m,\mu}$ (die Verteilungsfunktion der wahren Parallaxen um diesen Mittelwert herum) über sukzessive Intervalle in

¹ SEKIGER-Festschr. S. 276 (1924)

² Groningen Publ. Nr. 11 (1902); A. J. 566 (1904); Groningen Publ. Nr. 29 (1918), Nr. 30 (1920); Mt. Wilson Contr. 188 = Ap. J. 52, S. 23 (1920).

³ Groningen Publ. Nr. 34 (1923), Nr. 36 (1925), Nr. 38 (1925)

π verteilt. Aus der resultierenden Tabelle mit doppeltem Eingang nach m und π können Luminositätsfunktion und Dichtigkeitsfunktion direkt abgelesen werden, und zwar wird die erstere für sukzessive Parallaxenintervalle wiederholt bestimmt. Die Methode ist im grundlegenden Prinzip frei von einer Hypothese über die Absorption des Lichtes im Raume. Die Verschiebung der Luminositätskurve zwischen sukzessiven Parallaxenintervallen ist aber durch das Vorhandensein einer Absorption bedingt; wenn man dieselbe Luminositätsfunktion für verschiedene Distanzen postuliert, kann der Absorptionsbetrag gewissermaßen beurteilt werden. Da aber keine deutliche Spur einer Absorption vorhanden ist, kann nur ein Höchstbetrag derselben geschätzt werden. Für die Luminositätsfunktion wurde in den früheren Arbeiten sehr nahe eine normale Verteilung in absoluter Größe (der GAUSSschen Fehlerkurve analog) gefunden, was auch mit SEELIGERS Resultaten übereinstimmt. In der späteren Arbeit von VAN RIJN wird jedoch dieses Ergebnis für die schwächsten absoluten Größen erheblich modifiziert, indem die Häufigkeit der schwächsten absoluten Größen keine Abnahme zeigt, sondern einen weiteren schwachen Anstieg. Für die Herleitung der Luminositätsfunktion ist hier auch eine andere Methode, welche nur gemessene trigonometrische Parallaxen benutzt, herangezogen worden.

In Analogie mit SEELIGERS typischem Sternsystem wird in der KAPTEYNschen Statistik angenommen, daß die Dichtigkeitsverteilung Rotationssymmetrie

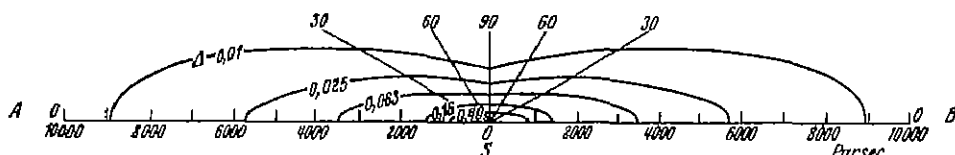


Abb. 11. Die Dichtigkeitsverteilung im typischen System nach KAPTEYN und VAN RIJN.

um eine Achse durch die Sonne senkrecht zur Milchstraße hat. Die ermittelte Dichtigkeitsverteilung ist in Abb. 11 illustriert. Die Abbildung stellt einen Schnitt durch das Sternsystem senkrecht zur Milchstraße dar. Die Kurven entsprechen Flächen konstanter Dichtigkeit und sind nur auf der einen Seite der Symmetrieebene ausgezogen worden.

Eine ausführliche Darlegung der KAPTEYNschen Methoden in einer allgemeinen Behandlung der stellarstatistischen Probleme hat W. J. A. SCHOUTEN¹ gegeben.

In SEELIGERS Theorie sind die Annahmen einer maximalen Grenze der absoluten Leuchtkraft und einer Begrenzungsfläche, außerhalb der die Stern-dichtigkeit als verschwindend klein angesehen werden kann, miteinander eng verknüpft. Die Erfahrungstatsachen, auf denen diese Annahmen beruhen, d. h. die Sprünge in den Werten gewisser Differentialquotienten, sind, wenn auch wahrscheinlich vorhanden, doch verhältnismäßig sehr geringe Effekte. Die speziellen Ansätze der eben genannten Art sind daher für eine statistische Analyse nicht als notwendig zu betrachten. Ohne irgendeine vorausgesetzte Beschränkung der absoluten Leuchtkraft i oder der oberen Integrationsgrenze in r hat SCHWARZSCHILD² eine allgemeine Lösung der zwei Integralgleichungen der Sternzahlen und mittleren Parallaxen gegeben.

Von großer praktischer Bedeutung ist eine Lösung von SCHWARZSCHILD, bei der für die Sternanzahl einer Größenklasse und für die mittleren Parallaxen

¹ On the Determination of the Principal Laws of Statistical Astronomy. Diss. Amsterdam 1918.

² A N 185, S. 81 (1910).

gewisse geeignete Näherungsausdrücke gewählt worden¹. Wir bezeichnen mit $a(m)dm$ die Anzahl der Sterne zwischen den Größen m und $m + dm$ und mit $\pi(m)$ die mittlere Parallaxe derselben Sterne. Wenn die absolute Größe

$$M = -2,5 \log i$$

eingeführt wird und die Verteilung der absoluten Größen durch eine Funktion $\varphi_1(M)$ gegeben wird, so daß

$$\varphi(i) di = -\varphi_1(M) dM,$$

und wenn die Absorptionsfunktion $\varphi(r) = 1$ gesetzt wird, so können die Integralausdrücke für $a(m)$ und $\pi(m)$ in folgender Form geschrieben werden

$$\left. \begin{aligned} a(m) &= \omega \int_0^{\infty} D(r) \varphi_1(m - 5 \log r) r^2 dr, \\ \pi(m) a(m) &= \omega \int_0^{\infty} D(r) \varphi_1(m - 5 \log r) r dr. \end{aligned} \right\} \quad (13)$$

Jetzt wird vorausgesetzt

$$\left. \begin{aligned} \log a(m) &= x_0 - x_1 m - x_2 m^2, \\ \log \pi(m) &= P_0 - P_1 m, \end{aligned} \right\} \quad (14)$$

wo x_0, x_1, x_2, P_0, P_1 Konstanten sind. Diese Annahmen führen auf die folgende Form der Funktionen $D(r)$ und $\varphi_1(M)$, wenn wir $\tau = -5 \log r$ einführen,

$$\left. \begin{aligned} \log D(r) &= a_0 - a_1 \tau - a_2 \tau^2, \\ \log \varphi_1(M) &= b_0 - b_1 M - b_2 M^2, \end{aligned} \right\} \quad (15)$$

was direkt durch Einsetzung in die Gleichungen (13) und Ausführung der Integration verifiziert werden kann.

Die Funktion $\varphi_1(M)$ ist eine GAUSSSCHE Fehlerkurve mit der Streuung

$$\sigma = \sqrt{\frac{\log e}{2 b_2}}$$

und dem Mittelwert

$$M_0 = -\frac{1}{2} \frac{b_1}{b_2}$$

Der Ansatz (14) entspricht im Durchschnitt sehr wohl den empirischen Resultaten von KAPTEYN, und die Ausdrücke (15) für D und φ_1 geben auch die analytische Form der Hauptresultate der KAPTEYNSCHEN Analyse wieder.

K SCHWARZSCHILD hat auch gezeigt, daß man unter der Annahme einer normalen Verteilung der Logarithmen der räumlichen Geschwindigkeiten der Sterne in bezug auf die Sonne die KAPTEYNSCHEN Resultate für die Funktionen $\pi_{m,\mu}$ und $\chi_{m,\mu,\mu}$ reproduzieren kann.

Wenn $\varphi_1(M)$ und $a(m)$ bekannt sind, bekommt man die Koeffizienten a_1 und a_2 von D nach den Formeln

$$\left. \begin{aligned} a_1 &= -0,6 + \frac{b_1 x_1 - b_2 x_1}{b_1 - x_1}, \\ a_2 &= \frac{b_2 x_2}{b_1 - x_2}. \end{aligned} \right\} \quad (16)$$

¹ A N 190, S. 361 (1912).

Aus den numerischen Werten von KAPTEYN und VAN RIJN¹ erhält man z. B. die folgenden Resultate, wo $a(m)$ pro Quadratgrad gerechnet wird:

$$\log a(m) = -4,542 + 0,724 m - 0,0141 m^2 \text{ (Gal. Breite } 0^\circ)$$

$$\log a(m) = -4,903 + 0,774 m - 0,0221 m^2 \text{ (Gal. Breite } 90^\circ)$$

$$\log \varphi_1(M) = -2,394 + 0,1858 M - 0,03450 M^2$$

$$\log D(r) = -2,532 + 2,478 \log r - 0,593 (\log r)^2 \text{ (Gal. Breite } 0^\circ)$$

$$\log D(r) = -6,219 + 6,120 \log r - 1,538 (\log r)^2 \text{ (Gal. Breite } 90^\circ)$$

Die Konstanten a_0 und b_0 sind hier so angepaßt, daß die Dichte in der Umgebung der Sonne als Einheit für D benutzt wird, während $\varphi_1(M)$ die Anzahl Sterne pro Kubikparsec nahe der Sonne für verschiedene absolute Größen gibt.

Die hier gegebene Funktion $\varphi_1(M)$ entspricht

$$M_0 = +2,7, \quad \sigma = 2,5.$$

Zu bemerken ist, daß die gegenwärtig am meisten gebrauchte Skala der absoluten Größen um fünf Einheiten größer ist als die oben benutzte. In dieser Skala, in der die absolute Größe als die auf die Entfernung 10 Parsec reduzierte scheinbare Größe definiert wird, ist daher $M_0 = +7,7$. Die Formel für $D(r)$ hat natürlich keine Gültigkeit in unserer unmittelbaren Umgebung, da offenbar für $r=0$ die Formel $D=0$ gibt. Es soll schließlich betont werden, daß die eben gegebenen einfachen Ausdrücke für $\varphi_1(M)$ und $D(r)$ durch neuere Untersuchungen, besonders durch VAN RIJNS Arbeit in Groningen Publ. 38, wo auch die einzelnen Spektraltypen separat behandelt werden, in mehrfacher Weise modifiziert worden sind.

Wichtige Beiträge zu der statistischen Behandlung der Dichtigkeitsverteilung sind in C. V. L. CHARLIERS² Arbeit „Studies in Stellar Statistics“ enthalten. Unter anderem wird von CHARLIER bemerkt, daß, wenn man die STELLIGERSchen Annahmen der oberen Begrenzungen in Leuchtkraft und Entfernung fallen läßt, die Gleichung

$$\frac{dA}{dh} = -w \int_0^\infty D(r) \varphi(hr^2) r^4 dr,$$

in Verbindung mit dem Sternzahlgesetz (7) der helleren Größen

$$\frac{dA}{dh} = ch^{-\alpha},$$

nicht mit Notwendigkeit auf die Lösung $D(r) = \gamma r^{-\lambda}$ und eine arbiträre Leuchtkraftsfunktion führt, sondern daß ihr auch durch den Ansatz

$$\varphi(x) = \frac{1}{x^\alpha} \quad (17)$$

bei beliebiger Dichteverteilung Genüge geleistet wird, und zwar ist es möglich, daß sogar unendlich viele Lösungen existieren.

CHARLIER nimmt für die Funktionen $a(m)$ und $\varphi_1(M)$ normale Frequenzkurven vom „Typus A“ an, wo jedoch nur die generierende Funktion selbst gebraucht wird. Die Ansätze sind also mit denen der oben besprochenen gleichzeitig publizierten Arbeit von SCHWARZSCHILD identisch. Die Dichtigkeitsfunktion $D(r)$ wird dann auch eine normale Frequenzkurve in $\log r$. Die mittleren Parallaxen werden in der Form

$$\pi(m) = K e^{-\lambda m} \quad (18)$$

¹ Mt Wilson Contr 188 = Ap J 52, S. 23 (1920).

² Lund Medd Ser II, 8 (1912).

ausgedrückt, λ wird aus den mittleren Eigenbewegungen verschiedener scheinbarer Größen bestimmt, die einem analogen Gesetz mit demselben Werte von λ gehorchen. Die Konstanten der Leuchtkrafts- und Dichtigkeitsfunktionen werden gemäß diesem Resultat ermittelt.

CHARLIER verläßt die Approximation des „typischen Systems“ und teilt den Himmel in 48 gleich große Flächen nach galaktischer Länge und Breite, innerhalb deren die Statistik unabhängig ausgeführt wird, was unzweifelhaft eine prinzipiell weit richtigere Problemstellung bedeutet. Eine ausführliche Übersicht der mathematisch-statistischen Grundlagen zur Analyse der Dichtigkeitsverteilung ist in CHARLIERS vorher (Ziff. 17) erwähnten „California Lectures“ gegeben.

Einige für die Stellarstatistik besonders wichtige Relationen sind von K. G. MALMQUIST¹ hergeleitet worden. Wenn die Leuchtkraftfunktion eines Volumens im Raume einem normalen Verteilungsgesetz gehorcht, so ist unter gewöhnlichen Bedingungen auch die scheinbare Leuchtkraftfunktion, d. h. die Verteilung der Sterne von der scheinbaren Größe m nach absoluter Größe M , sehr nahe eine normale Frequenzkurve. Wenn die wahre Leuchtkraftfunktion durch den Mittelwert M_0 und die Dispersion σ bestimmt wird und wenn wir die scheinbare Leuchtkraftfunktion durch eine Entwicklung vom Typus A ,

$$F(M) = \varphi_m(M) + A_2 \varphi_m^{III}(M) + A_4 \varphi_m^{IV}(M) + \dots, \quad (19)$$

ausdrücken, wo

$$\varphi_m(M) = \frac{1}{\sigma_m \sqrt{2\pi}} e^{-\frac{(M-M_m)^2}{2\sigma_m^2}} \quad (20)$$

die genormte Funktion und φ_m^{III} , φ_m^{IV} , die dritten und vierten Ableitungen nach M darstellen, so hat man

$$\left. \begin{aligned} M_m &= M_0 - \sigma^2 \frac{d}{dm}, \\ \sigma_m^2 &= \sigma^2 + \sigma^4 \frac{d^2}{dm^2}, \\ \left[\begin{aligned} 3 A_2 &= \sigma^2 \frac{d^3}{dm^3}, \\ 4 A_4 &= \sigma^4 \frac{d^4}{dm^4}, \end{aligned} \right. \end{aligned} \right\} \quad (21)$$

wo

$$/ (m) = \log \text{nat } a(m) \quad (22)$$

Ähnliche Beziehungen gelten auch für die Leuchtkraftfunktion der Sterne heller als eine gewisse Größe m . Wenn M_0 und σ für eine besondere Klasse von Sternen bekannt sind, kann die scheinbare Leuchtkraftfunktion, durch die Ableitungen von $\log a(m)$ in der oben gegebenen Weise gebildet, für eine Ermittlung der Dichtigkeitsverteilung der betreffenden Sterne im Raume gebraucht werden, da diese mit einfacher Rechnung durch die doppelte Verteilung der Sterne nach scheinbarer und wirklicher Größe gegeben sein muß. Von besonderer Bedeutung sind diese Relationen, wenn σ klein ist, so daß die höheren Potenzen dieser Größe vernachlässigt werden können.

Wenn aber die Dispersion der absoluten Größen für irgendeine Klasse von Sternen klein ist, können wir auch folgendermaßen vorgehen. Wenn die Dispersion Null wäre und alle Sterne dieselbe absolute Größe M_0 besäßen, so hätte

¹ Lund Medd 100 = Ark Mat Astr Fys 16, Nr. 23 (1922).

man offenbar zwischen der Dichtigkeitsfunktion $D(r)$ und der Sternzahlfunktion $a_1(m)$ die Relation

$$\omega r^2 D(r) dr = a_1(M_0 + 5 \log r) d(5 \log r),$$

also

$$D(r) = \frac{5 \log e}{\omega r^3} a_1(M_0 + 5 \log r). \quad (23)$$

Die Variation von M , der Dispersion σ entsprechend, kann jetzt als eine Abweichung von einem idealen Zustande betrachtet werden und ihr Einfluß auf $a(m)$ dem eines gleich großen Beobachtungsfehlers in m gleichgesetzt werden. Wir suchen daher die ideale Funktion $a_1(m)$ aus der beobachteten $a(m)$ zu bestimmen. Nach einer Formel von EDDINGTON¹ haben wir in der Tat

$$a_1(m) = a(m) - \frac{\sigma^2}{2} \frac{d^2 a}{dm^2} + \frac{\sigma^4}{8} \frac{d^4 a}{dm^4} - \dots \quad (24)$$

Wenn $a(m)$ tabuliert mit dem Intervalle α in m vorliegt, haben wir approximativ die zweite Differenz

$$a(m + \alpha) - a(m - \alpha) - 2a(m) = \alpha^2 \frac{d^2 a}{dm^2}, \quad (25)$$

woraus $d^2 a/dm^2$ bestimmt wird. Der Term in σ^4 wird für kleines σ vernachlässigt.

Ernster Zweifel an der Gültigkeit der Annahme einer approximativ rotations-symmetrischen Verteilung der Sterne um die Sonne herum wurde wohl zuerst durch H. SHAPLEYS² Studien über die Lagen der kugelförmigen Sternhaufen im Raume erregt. Auf die eigentümliche scheinbare Verteilung der Haufen scheint zuerst K. BOHLIN³ in einer bemerkenswerten Arbeit aufmerksam gemacht zu haben; er hat auch eine Anordnung dieser Haufen um den Zentralpunkt des Sternsystems herum für wahrscheinlich gehalten. Für diesen Punkt ergeben sich nach seinen Resultaten die Koordinaten $L = 321^\circ 34'$, $B = -2^\circ 56'$. Die scheinbare Verteilung wurde weiter von A. R. HINKS⁴ und von E. HERTZSPRUNG⁵ untersucht. Gleichzeitig mit SHAPLEY hat CHARLIER⁶ die Verteilung im Raume ermittelt auf Grund der Annahme, daß der wahre Durchmesser für alle Haufen derselbe ist. Die absolute Skala der Entfernungen wurde jedoch hier viel zu klein angenommen. In SHAPLEYS Arbeit wurde die Stellung der Haufen als trotz der gewaltigen Entfernungen zum Sternsystem gehörige Gebilde sehr wahrscheinlich gemacht. Der Zentralpunkt des Sternhaufensystems liegt nach SHAPLEY in der Richtung $L = 327^\circ$, $B = 0^\circ$, in einer Entfernung von etwa 16000 Parsec. Das „System der Haufen“ ist jedoch in Hinsicht auf die Dichtigkeitsverteilung so unregelmäßig definiert, daß die Schätzung der Entfernung des Zentralpunktes unsicher bleibt. (Über den Einfluß der Absorption vgl. Ziff. 33.)

Außer durch die regelmäßige Verteilung der Haufen in bezug auf die galaktische Ebene wird die Zugehörigkeit dieser Objekte zum Milchstraßensystem durch den Umstand gestützt, daß die allgemeine Intensität und Mächtigkeit der Milchstraßenwolken in der Gegend des scheinbaren Zentralpunktes ihr Maximum erreicht. Der Beweis, daß die Stellung der Sonne im Sternsystem in der Tat eine ausgeprägt exzentrische ist, und daß das Zentrum in einer Richtung nahe $L = 327^\circ$ zu suchen ist, wurde jedoch erst kürzlich durch die Sternzählungen schwacher Sterne in den KAPTEYNschen Selected Areas gegeben. Die Harvard-Groningen Durchmusterung wurde von KREIKEN⁷ zu einer Statistik der Dichte-

¹ M N 73, S. 359 (1913).

² Mt Wilson Contr 151–157, 160, 161, 175, 176, 190 u. 195; Ap J 48–52 (1918–1920).

³ K Svenska Vet Akad Handl 43, Nr. 10 (1909).

⁴ M N 71, S. 693 (1911).

⁵ A N 192, S. 261 (1912).

⁶ Lund Medd Ser II, 19 (1918).

⁷ M N 85, S. 499 (1925); 86, S. 665 (1926).

verteilung ausgenutzt, und endlich das vorzügliche, auf exakten photometrischen Messungen gegründete Mount Wilson-Material von SEARES¹ diskutiert. Für hellere Größen wurden auch die Kataloge der photographischen Himmelskarte benutzt. Die Abweichungen Δ der Zahlen $\log N_m$ (N_m = Zahl der Sterne pro Quadratgrad heller als die Größe m in der internationalen photographischen Skala) von einer mittleren rotationssymmetrischen Verteilung werden von SEARES versuchsweise in der Form

$$\Delta = a + b \cos(L - L') \quad (26)$$

dargestellt. Die Länge L' wurde für verschiedene Grenzgrößen zwischen $m = 9$ und $m = 18$ und für verschiedene galaktische Breiten ermittelt.

Eine etwas exzentrische Stellung der Sonne in einem sphäroidischen System von konstanter Dichtigkeit gibt als theoretischen Ausdruck für Δ

$$s + F \cos(L - L_0) \quad (27)$$

L_0 ist dann die Richtung gegen das Zentrum des Systems². Aus einer systematischen Verschiedenheit für nördliche und südliche Breiten schließt SEARES auf

eine mit der Sterngröße wechselnde Korrektur des GOULDschen Milchstraßenpols. Er führt daher in den theoretischen Ausdruck für Δ auch die Terme

$$\pm G \mp k \cos(L - L_1) \quad (28)$$

ein, wo obere und untere Vorzeichen für nördliche bzw. südliche Breiten gelten. Der wahre Pol, durch die Sterne einer gewissen Breite B ermittelt, ist um den Betrag ϕ in der Länge L_1 vom GOULDschen Pol entfernt, wo

$$\phi = \frac{k}{D}, \quad D = \frac{d \log N}{dB}. \quad (29)$$

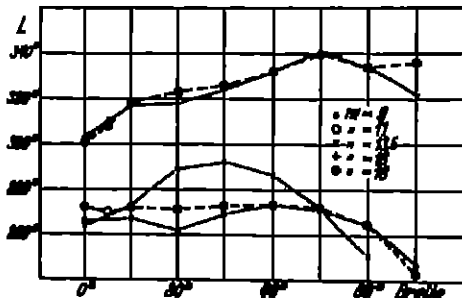


Abb. 12. Die Länge des Zentrums (Ordinate) für verschiedene galaktische Zonen (Abszisse) und verschiedene Grenzgrößen

Durch Zusammensetzung von (27) und (28) bekommt man offenbar eine Form (26), wo aber L' , a , b für nördliche und südliche Breiten verschieden ausfallen. Aus den empirischen Werten für L' , a , b für nördliche und südliche Breiten berechnet man dann leicht die wahre Länge L_0 der tiefsten Richtung im System und die wahre Amplitude der logarithmischen Sternzahlen, wie auch die Werte L_1 und ϕ . In dieser Weise bekommt SEARES die Lagen des Pols für verschiedene Grenzgrößen, die in Ziff. 11 gegeben und diskutiert worden sind, und die folgenden Werte für die Länge des Zentrums

m	9	11	13.5	16	18
L_0	267°	270°	275°	319°	319°

Die Werte $L = L_0$ für verschiedene Zonen und Grenzgrößen werden in Abb. 12 dargestellt.

SEARES findet eine markante parallele Verschiebung in L_0 , L_1 und ϕ mit der Sterngröße m . Da aber die Werte für L_1 und ϕ für hellere Größen erhebliche Differenzen gegen die in direkter Weise von VAN RHIJN ermittelten zeigen, so dürfte wohl die mehr indirekte Methode von SEARES hier nicht als ganz einwandfrei zu bezeichnen sein.

Für die schwächsten Größen $m = 16$ und 18 findet SEARES $L_0 = 319^\circ$, was sehr wohl mit SHAPLEYS Zentralpunkt für die Kugelhaupten, $L = 327^\circ$,

¹ Mt Wilson Contr. 346-347 = Ap J 67 (1928)

² L_0 bzw. L_1 sind bei SEARES mit L bzw. L_0 bezeichnet.

harmonisiert. KRIEKEN hatte für die Grenzgröße 17 in seiner Arbeit $L_0 = 314^\circ$ gefunden. Man kann diese Werte mit HOPMANNs und PANNEKOEKs Resultaten für die Verteilung des galaktischen Lichts vergleichen (Ziff. 5 und 11). HOPMANN fand ein sehr ausgeprägtes Maximum um $L = 315^\circ$ herum, während PANNEKOEK für die Länge des allgemeinen Lichtmaximums 323° herleitete.

Die Verschiebung in L_0 von 267° für $m=9$ bis 319° für die schwächsten Größen schreibt SEARES, in Übereinstimmung mit den Ansichten vieler anderer Forscher, z. B. mit HOPMANNs Ausführungen in seiner eben besprochenen Arbeit, dem Einfluß eines weit ausgedehnten „lokalen Systems“ zu, das hauptsächlich die Verteilung der helleren Sterne bestimmt, während die Verteilung der schwächsten Größen dem großen System entspricht. Die Ausdehnung des lokalen Systems in der galaktischen Ebene schätzt er auf ungefähr 6000 Parsec. Da die Verschiebung des Pols für die helleren Größen gegen den Pol der hellen Heliumsterne vor sich geht und gleichzeitig die Länge des Konzentrationspunktes gegen die Länge der größten Häufigkeit dieser Sterne verschoben erscheint, schließt er auf eine Zusammengehörigkeit, und daß also der Haufen der nahen Heliumsterne den Kern des großen lokalen Systems bildet (vgl. Ziff. 19). Nach VAN RIJNS Resultaten scheint jedoch die Verschiebung des Pols für die Größen 9 bis 13,5 sehr zweifelhaft, was die Argumentation von SEARES einigermaßen abschwächt.

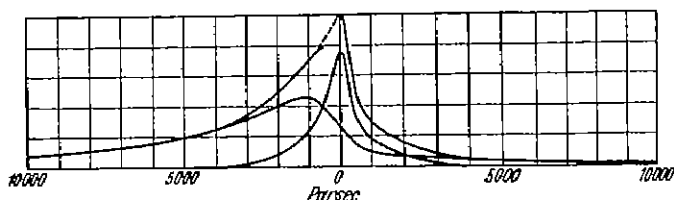


Abb. 13. Die Dichtefunktion nach SEARES (obere Kurve) in zwei Teile, dem lokalen System und dem großen System entsprechend, zerlegt.

Um die Sachlage noch mehr zu beleuchten, berechnet SEARES aus den Sternzahlen für die Längen L_0 und $180^\circ + L_0$ in der galaktischen Ebene mit Hilfe einer GAUSSschen Luminositätskurve die entsprechende Dichtigkeitsverteilung nach

der SCHWARZSCHILDschen Methode. Für die Sterndichte $D(r)$ findet er die Resultate der Tabelle 11.

Tabelle 11.

r	$D(r)$		r	$D(r)$	
	L_0	$180^\circ + L_0$		L_0	$180^\circ + L_0$
1	1,00	1,00	6310	0,15	0,03
100	0,98	0,93	7943	,11	,02
200	,95	,79	10000	,08	,014
316	,90	,63	12590	,06	,01
500	,84	,47	15850	,04	—
1000	,70	,28	19950	,03	—
2000	,49	,17	25120	,02	—
3162	,33	,08			
3981	,27	,06			
5012	,20	,04			

Die räumliche Sterndichtigkeit nimmt also viel schneller gegen das Antizentrum als gegen das Zentrum ab. Trotzdem ist ein großer Überschuß in unserer unmittelbaren Nähe ersichtlich. SEARES versucht (Abb. 13) die Frequenz in zwei Kurven zu zerlegen, von denen die eine das lokale System, die andere das große System repräsentieren soll. Den totalen Durchmesser des großen Systems schätzt SEARES zu 60 000 bis 90 000 Parsec. Daß die letztere Kurve asymmetrisch erscheint, deutet SEARES als einen Einfluß der großen Absorptionsgebiete der Milchstraße in der zentralen Himmelsgegend.

Außer diesem Hinweis auf eine mögliche Absorption des Lichtes in gewissen Gegenden des Systems hat aber SEARES die Möglichkeit der Erklärung der größeren Sterndichtigkeit in unserer Nähe durch eine allgemeine Absorption des Lichtes in den galaktischen Regionen nicht berücksichtigt. Wir werden später Gelegenheit haben, ein wenig auf diese Frage einzugehen.

Unter früheren wichtigen Arbeiten anderer in diesem Zusammenhang nicht erwähnter Autoren, die mit weniger Vollständigkeit des zur Verfügung stehenden Materials Abweichungen von einer rotationsymmetrischen Verteilung studiert haben, sind zu nennen die von H. NORT¹, H. C. PLUMMER² und H. H. TURNER³.

J. HALM⁴ stellt ornstlich in Frage, ob die gewöhnliche Annahme einer vom Orte im System unabhängigen Leuchtkraftfunktion wirklich als annähernd zutreffend anzusehen ist. Es scheint nach seiner Ansicht vielmehr, daß die Heterogenität der beobachtbaren Verteilung eher durch Schwankungen der Leuchtkraftfunktion als durch Variationen der räumlichen Dichte erklärt werden kann. Es scheint sogar möglich, daß die Sterne in der Milchstraße scheinbar zahlreicher vorkommen, nicht weil sie räumlich zusammengedrängt sind, sondern weil sie eine größere absolute Leuchtkraft besitzen.

Von großer Bedeutung ist auch die Untersuchung PANNEKOKS⁵ über die Dichtigkeitsverteilung in unserer näheren Umgebung auf Grund einer erneuten sorgfältigen Analyse der Durchmusterungskataloge. Er verläßt vollkommen die schematischen Annahmen des „typischen Systems“ und sucht in unserer Umgebung die wahren Kondensationen zu bestimmen. Er vertritt auch die Ansicht, daß ein lokales System als eine selbständige geschlossene Einheit, eine „Wolke“, nicht existiert, sondern sich in eine Menge kleinerer Gruppen, die als Individuen in das große System eingehen, auflösen läßt.

19. Die Verteilungsgesetze verschiedener Spektraltypen. Die große Streuung der allgemeinen Leuchtkraftfunktion der Sterne und die wahrscheinlich bedeutende Abweichung dieser Funktion von einer GAUSSschen Fehlerkurve für die schwachen absoluten Helligkeiten macht es sehr schwierig oder sogar unmöglich, ohne eine Aufspaltung des Materials in Klassen von kleinerer Dispersion sichere Resultate über die Dichtigkeitsverteilung im Sternsystem zu bekommen. Eine partielle Aufspaltung der genannten Art bietet schon die Klassifizierung in die Harvard-Spektraltypen und auch die in großen Zügen mit dieser Klassifizierung äquivalenten Bestimmungen der Sternfarbe. Für die „frühen“, heißen Spektraltypen bedeutet nämlich die Klassifizierung oder Farbenbestimmung eine Gruppierung nach absoluter Größe mit verhältnismäßig kleiner Streuung innerhalb der Gruppen. Da weiter die spezielleren Methoden zur spektrographischen Bestimmung absoluter Größen gegenwärtig auch für schwache Sterne, wenn auch in mehr summarischer Form, verwendbar sind, so eröffnet sich hier ein Weg zu einer genaueren Analyse der Sternverteilung in den verschiedenen Richtungen von unserem Ort im System aus. Wir sind jedoch auf diesem Gebiete noch kaum über die Pionierarbeit hinausgekommen. Wir wollen hier die Hauptergebnisse der Spektraldurchmusterungen in bezug auf die allgemeine Dichtigkeitsverteilung unserer näheren Umgebung im Sternsystem kurz erwähnen und später (Ziff. 22) die spezielleren Untersuchungen der Milchstraßenregionen behandeln.

Das gegenwärtig wichtigste statistisch ausgenutzte Material ist in dem DRAPER-Katalog der Harvard-Sternwarte enthalten. Die scheinbare Verteilung

¹ Recherches astronomiques de l'Obs d'Utrecht VII (1917)

² M N 78, S. 668 (1918).

³ M N 85, S. 610 (1925).

⁴ M N 80, S. 162 (1919).

⁵ Publ. Astr. Inst. Univ. Amsterdam Nr. 1 (1924); Nr. 2 (1929)

verschiedener Spektraltypen am Himmel ist ausführlich von G. ZAPPA¹, H. SHAPLEY², C. V. L. CHARLIER³, A. PANNEKOEK⁴ und O. SEYDL⁵ statistisch untersucht worden. SEYDL gibt im zweiten Teil seiner Arbeit für Sterne heller als 7^m,0 die scheinbare Dichtigkeitsverteilung der verschiedenen Spektraltypen in galaktischen Koordinaten in einer Serie von Karten wieder. Die zuerst von E. C. PICKERING⁶ nachgewiesene Variation der scheinbaren galaktischen Konzentration mit der Spektralklasse kommt in diesen Untersuchungen sehr schön zum Vorschein. Die viel kleinere galaktische Konzentration der Spektralklassen von F bis M, mit den Klassen B und A verglichen, wurde oft als ein im wesentlichen scheinbarer Effekt gedeutet, der als eine Folge einer mit der Spektralklasse sich ändernden mittleren absoluten Leuchtkraft der Sterne auftritt. Eine Vergrößerung der absoluten Leuchtkraft bedeutet nämlich einen Zuwachs der mittleren Entfernung für eine und dieselbe scheinbare Größe, was infolge der allgemeinen Konzentration der Sterne gegen die galaktische Ebene eine vergrößerte scheinbare Konzentration gegen die Milchstraße mit sich bringt. Wenn auch dieser Erklärungsgrund für das Intervall B—F einigermaßen zutrifft, ist es doch wegen der ziemlich großen absoluten Helligkeiten der großen Mehrzahl der K- und M-Sterne des Katalogs, die kaum der mittleren Helligkeit der A-Sterne nachstehen, durchaus klar, daß das Phänomen auch auf reelle Verschiedenheiten in der Anhäufung gegen die Milchstraßenebene zurückzuführen ist. Einen direkten Nachweis in dieser Richtung hat P. J. VAN RIJN⁷ gegeben, der eine Trennung verschiedener Spektraltypen bei Bestimmung der Leuchtkrafts- und Dichtigkeitsverteilung nach der KAPTEYN-Methode unternommen hat. Die Abnahme der absoluten Dichtigkeit der A-Sterne und der Riesensterne späterer Spektraltypen mit wachsender Entfernung von der galaktischen Ebene ist auch von B. LINDBLAD⁸ und H. PETERSSON⁹ bestimmt worden. Die kleinere Konzentration der späten Riesen tritt hier sehr deutlich hervor und wird als eine Folge der für diese Sterne größeren Dispersion der Geschwindigkeitskomponente senkrecht zur Milchstraße gedeutet (vgl. Ziff. 28).

Die Dichtigkeitsverteilung der A-Sterne in der Richtung gegen den galaktischen Pol ist von K. G. MALMQUIST¹⁰ ermittelt worden auf Grund einer Bestimmung der Farbäquivalente nach der Methode von SEARES für 3700 Sterne innerhalb 10° Distanz von dem galaktischen Pol, von denen jedoch nur eine kleine Prozentzahl A-Sterne sind.

Zu den bedeutendsten aus dem Harvard-Material der helleren Sterne gewonnenen stellarstatistischen Resultaten gehört dasjenige über die Verteilung der Sterne der Spektralklasse B, der Heliumsterne, in unserer Umgebung. Wichtige Untersuchungen sind hier von KAPTEYN¹¹, CHARLIER¹², SHAPLEY¹³, B. P. GERASIMO-

¹ Publ. R. Specola di Collurania (A) 1, S. 59 (1921). ² Harv Circ 240 (1922); 248 (1923).

³ Lund Medd Ser II, 36 = K. Svenska Vet. Akad. Handl. 4, Nr. 3 (1927).

⁴ Publ. Astr. Inst. Univ. Amsterdam Nr. 2 (1929). ⁵ Publ. Obs. Nat. Prague 6 (1929).

⁶ Harv. Ann. 26, S. 152 (1891); 56, S. 1 (1912). ⁷ Groningen Publ. 38, Tab. 27, 45 (1925).

⁸ Nova Acta Reg. Soc. Scient. Upsalensis, Volumen extra ordinem 1927 = Upsala Medd. 11; Ark. Mat. Astr. Fys. 19 B, Nr. 15 (1926) = Upsala Medd. 14.

⁹ The Distribution of Distances and Velocities of Stars in the Carrington Zone on the Basis of Spectrophotometric Analysis. Diss. Upsala 1927 = Upsala Medd. 29.

¹⁰ Lund Medd Ser II Nr. 37 und 46 (1927).

¹¹ Mt. Wilson Contr. 32 = Ap. J. 40, S. 43 (1914); Mt. Wilson Contr. 147 = Ap. J. 47, S. 104, 146 u. 255 (1918).

¹² Nova Acta Reg. Soc. Scient. Upsalensis (IV) 4, Nr. 7 (1916); Ibid., Volumen extra ordinem 1927; Lund Medd Ser II, 14 und 34.

¹³ Mt. Wilson Contr. 157 = Ap. J. 49, S. 311 (1918); Mt. Wilson Comm. 54 (1918); 64 (1919); Scientia, März 1920; A. N. Jub.-Nr. S. 25 (1921); Harv. Circ. 239 (1922); Harv. Bull. 846, S. 12 (1927).

VČ¹ und PANNEKOEK² ausgeführt worden. Die Hellumsterne zeigen eine sehr starke scheinbare Konzentration gegen die Milchstraße hin, aber wie oben (Ziff. 13) erwähnt wurde, hat die Symmetrieebene der helleren B-Sterne eine beträchtliche Neigung gegen den aus den Milchstraßenwolken ermittelten größten Kreis. CHARLIER gibt für den Pol der helleren B-Sterne seiner ersten Arbeit R.A. 183°,34, Dekl. +28°,74, was bei Annahme des GOULDSchen Milchstraßenpols den galaktischen Koordinaten $L = 165^\circ$, $B = +83^\circ,4$ entspricht und im System der Tabelle 7, Ziff. 11, $L = 158^\circ$, $B = +80^\circ,0$ gibt. Die Neigung der Symmetrieebene gegen die GOULDSche Milchstraßenlinie ist also $6^\circ,6$, mit dem aufsteigenden Knoten in $L = 255^\circ$; die Neigung gegen die mittlere Ebene der schwachen Sterne beträgt $10^\circ,0$. SHAPLEY zeigt, daß diese Neigung mit abnehmender Helligkeit abnimmt und schon zwischen den Größen 7 und 8 fast vollständig verschwindet. Dasselbe Verhältnis wiederholt sich in geringerem Maße für die A-Sterne. Die Verteilung der helleren Sterne zeigt auch hier eine gewisse Neigung der Symmetrieebene gegen die Milchstraße, welche Neigung für schwächere Größen verschwindet.³

Die scheinbare Verteilung der Hellumsterne heller als $8^m,0$ am Himmel wird nach CHARLIER in Abb. 14 illustriert. Es ist offenbar, in welchem hohen Grade diese Sterne in getrennten Flecken von beträchtlicher Konzentration auftreten, was in KAPTEJNS Arbeit eine große Rolle spielt und neuerdings von PANNEKOEK besonders hervorgehoben wird. Ein Maximum der Anhäufung findet sich in der Carinagegend, um $L = 260^\circ$ herum. Die Projektion der räumlichen Verteilung auf die Milchstraßenebene wird in Abb. 15 nach CHARLIER wiedergegeben. Die Entfernungen der individuellen Sterne sind unter der Annahme konstanter absoluter Leuchtkraft innerhalb der Untergruppen B0,

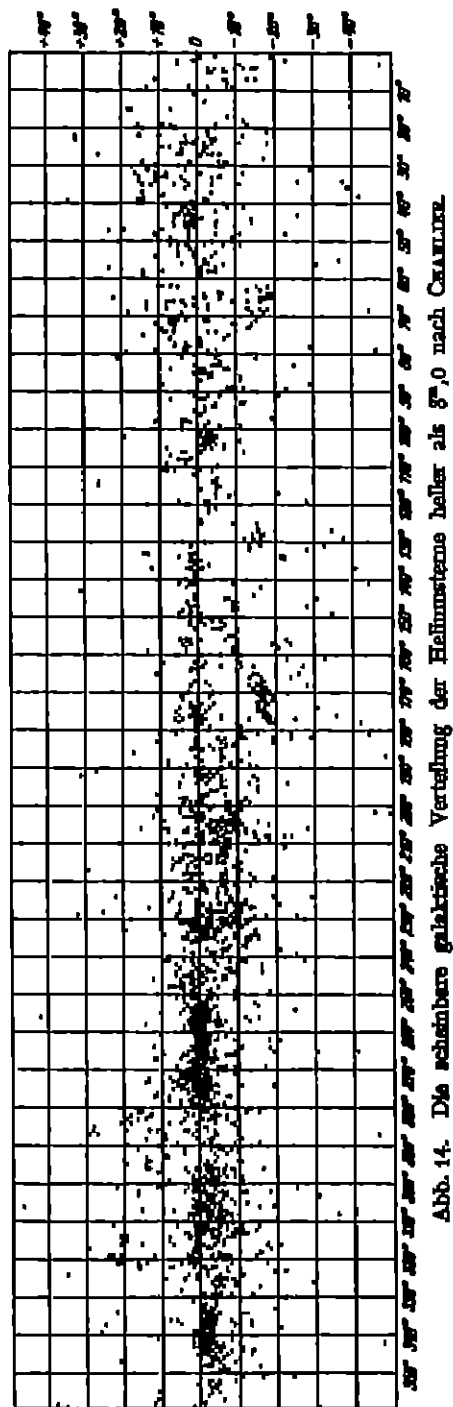


Abb. 14. Die scheinbare galaktische Verteilung der Hellumsterne heller als $8^m,0$ nach CHARLIER.

¹ V J S 61, S 219 (1926). ² L. o. ³ SHAPLEY and CANNON, Harv Circ 229 (1922).

B4 usw. ermittelt worden. Man bekommt hier den Eindruck, daß diese Sterne eine gewisse Einheit bilden. Die Aufspaltung in kleinere Gruppen, die in der scheinbaren Verteilung so deutlich hervortritt, ist aber auch hier zu spüren. Die äußere Begrenzung des Haufens ist von der Grenzgröße des Materials ($m = 8,0$) bedingt. Für das Zentrum des Haufens findet CHARLIER eine Entfernung von 63 Parsec (13 Siriometer) in der Richtung $L = 243^\circ,90$, $B = -13^\circ,80$.

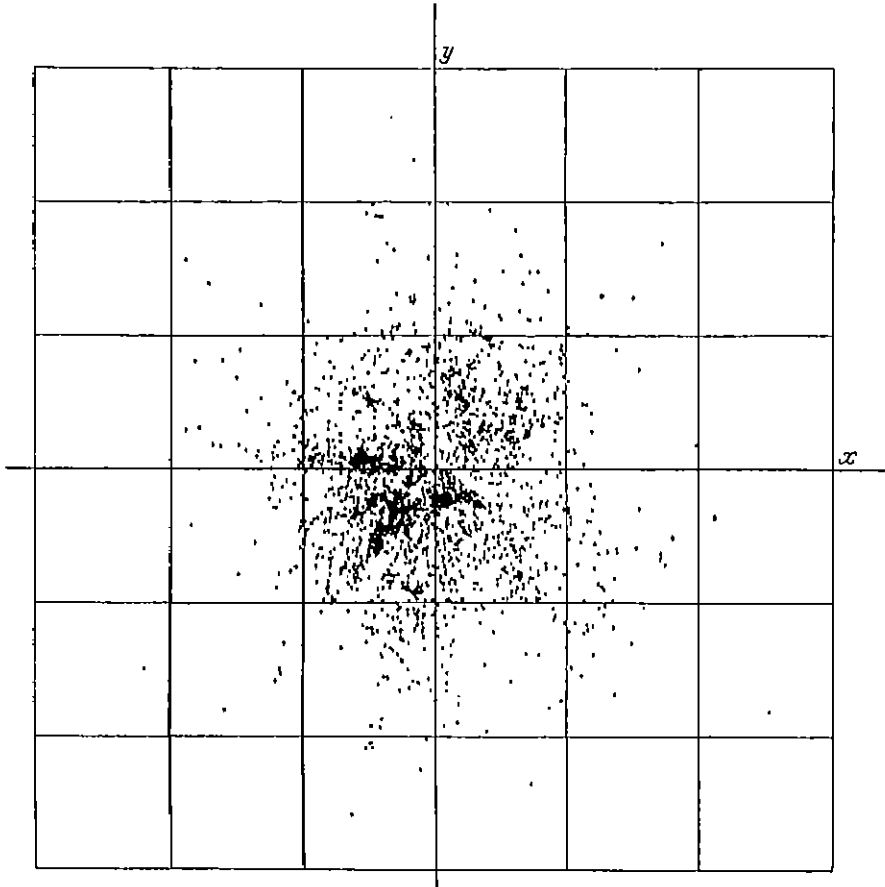


Abb. 15. Die Verteilung der Hellumsterne (BO bis B5) heller als $8^m,0$ in der galaktischen Ebene (X -Achse gegen $L = 0^\circ$ gerichtet).

GERASIMOVICH teilt die Sterne in zwei Gruppen, heller und schwächer als die Größe 6,7, und findet für das Zentrum dieser Gruppen

$$m < 6,7: L = 225^\circ,5, \quad B = -12^\circ,0, \quad R = 77 \text{ Parsec},$$

$$m > 6,7: L = 268^\circ,5, \quad B = -9^\circ,0, \quad R = 204 \text{ Parsec}.$$

Dieses Resultat stimmt mit den Ansichten SHAPLEYS überein, nach denen wir hauptsächlich in der helleren Gruppe die Mitglieder eines lokalen Haufens vor uns haben, während wir für schwächere Helligkeiten es mit einer Mischung zwischen Haufensternen und Sternen des allgemeinen Milchstraßenstratums zu tun haben. GERASIMOVICH hat auch die allgemeinen Dichtigkeitsflächen der B-Sterne ermittelt. Die Abplattung der Flächen vermindert sich je nach der

Entfernung von der Sonne. Der Halbmesser des ganzen lokalen Haufens sollte wenigstens 1000 Parsec betragen. Nach PANNEKOEK löst sich aber der „lokale Haufen“ der B-Sterne in eine Menge kleinerer, voneinander unabhängiger Haufen oder Ströme auf.

Die Kurven gleicher Dichtigkeit in der Umgebung der Sonne hat KREIKEN¹ für B- und A-Sterne zu ziehen versucht.

G. SHAJN² hat einen Versuch gemacht, die Hauptzüge der räumlichen Dichtigkeitsverteilung für B-, A-, F-, K- und M-Sterne aus dem Material des Harvard-Katalogs zu ermitteln. Die Abhängigkeit der scheinbaren galaktischen Konzentration vom Spektraltypus in der Serie O bis F wird als eine Folge der Veränderung in mittlerer absoluter Größe gedeutet; die verhältnismäßig kleine galaktische Konzentration der K-Sterne ist nach SHAJN auf eine Inhomogenität dieser Sterne in bezug auf ihre absolute Größe zurückzuführen, insbesondere auf eine Beimischung von Sternen, die intermediär zwischen „Riesen“ und „Zwergen“ sind, unter die Sterne in den schwächeren Größenklassen. Für die M-Sterne muß er aber eine reelle Abweichung der räumlichen Dichtigkeitsverteilung von ihrem gewöhnlichen Charakter annehmen. Die Schnelligkeit der Dichtigkeitsabnahme mit der Entfernung ist für fast alle Klassen beträchtlich größer als die von KAPTEYN und VAN RIJN für Sterne im allgemeinen gefunden.

Was die räumliche Dichtigkeitsverteilung in der Nähe der galaktischen Ebene bis zu größeren Entfernungen betrifft, so führen die weiteren Untersuchungen auf diesem Gebiet, angesichts der sehr erheblichen lokalen Verschiedenheiten in dem galaktischen Gürtel, mit Notwendigkeit auf detaillierte Untersuchungen der hellen und dunklen Partien der Milchstraße, die wir in Ziff. 22 näher besprechen werden.

Zur Beurteilung der allgemeineren Fragen über die galaktische Konzentration für verschiedene Spektraltypen wird in der Zukunft ein vorzügliches Material in den Spektraluntersuchungen der Selected Areas vorliegen. Ein wichtiger Beitrag liegt hier schon in F. BECKERS³ Spektraldurchmusterung der KAPTEYN-Eichfelder des Südhimmels vor. Diese Arbeit enthält auch eine vorläufige Statistik über die Verteilung der Spektralklassen nach galaktischer Breite und nach der scheinbaren Helligkeit sowie über die räumliche Verteilung der Sterne. Weitere Beiträge werden hier in der Zukunft die Sternwarten Mount Wilson und Hamburg geben, wo die Sterne der KAPTEYNschen Felder bis zu etwa der Größe 12 klassifiziert werden.

Eine auf ausgewählte Partien des Himmels sich beziehende Spektraluntersuchung, die in gewissen Gegenden bis zur Größe 11,5 bis 12 reicht, wird von MISS CANNON an der Harvard-Sternwarte in der „HENRY DRAPER-Extension“ ausgeführt⁴.

Auf der Sternwarte Stockholm ist gegenwärtig eine allgemeine Untersuchung der Spektren in gewissen Milchstraßenregionen bis zu etwa der Größe 13 begonnen worden. Es wird hier besonders eine Berücksichtigung der spektralphotometrischen Kriterien, die zur Beurteilung der absoluten Größen der Sterne dienen können, beabsichtigt.

20. Die galaktische Verteilung spezieller Objekte von großer absoluter Leuchtkraft. Die Objekte von sehr großer absoluter Helligkeit zeigen in der Regel eine außerordentlich markante scheinbare Konzentration gegen die Milch-

¹ M N 85, S. 985 (1925).

² A N 232, S. 17 (1928).

³ Publ. Astrophys. Obs. Potsdam Nr. 88, 89, 90 (1929–1931).

⁴ Über den Fortschritt dieser Arbeit s. besonders SHAPLEY, „Sidereal Explorations“. The Rice Institute Pamphlet 18, Nr. 2 = Harv. Reprint 68 (1931).

straße. Wahrscheinlich haben wir hier eine Kombination von zwei verschiedenen Ursachen, teils einen scheinbaren Effekt der größeren mittleren Entfernung, teils aber eine allgemeine Vergrößerung der absoluten galaktischen Konzentration mit steigender absoluter Helligkeit (vgl. Ziff. 19). Um zwischen diesen beiden Effekten zu unterscheiden, müssen wir aus der scheinbaren Verteilung die wahre Verteilung im Raume herleiten. Bei unserer oft mangelhaften Kenntnis der Entfernungen ist dies in vielen Fällen nur in unvollständiger Weise möglich.

Eine Folge der großen scheinbaren galaktischen Konzentration einer bestimmten Gruppe ist es zunächst, daß auch mit einer geringen Anzahl von Objekten die Feststellung der Lage der Symmetrieebene möglich wird. E. HERTZSPRUNG¹ hat (Tab. 12) eine Zusammenstellung der Lagen des Poles für verschiedene Klassen von Objekten gegeben.

Tabelle 12.

Klasse	Pol der Konzentrationsebene		Anzahl der Objekte
	A	D	
Holmsterne (Oe5 bis B9).	182°,1	+27°,9	1402
Spektraltypus N	194°,2	27°,4	228
Oa bis Oe	190°,7	26°,9	87
Bedeckungsveränderl.	188°,2	25°,8	150
δ Cephei-Sterne	195°,9	26°,8	60
c- und ac-Sterne	189°,1	26°,3	98
Gasnebel	192°,7	28°,1	130

Für 97 Sterne vom Typus Oa—Oe5 findet W. GYLLENBERG² unter der Annahme einer ellipsoidischen Verteilung für die kürzeste Achse die Richtung $A = 191^\circ,28$, $D = +27^\circ,13$.

B. P. GERASIMOVIC³ findet für 144 O-Sterne des DRAPER-Katalogs

$$A = 189^\circ 13', D = +27^\circ 22',$$

und für 78 planetarische Nebel

$$A = 192^\circ 13', D = +28^\circ 28',$$

unter Verwendung der NEWCOMBSchen Berechnungsmethode.

J. SCHILT⁴ findet für 340 c-Sterne eine sehr gute Übereinstimmung mit der galaktischen Ebene nach PICKERING (Lage des Pols $A = 190^\circ$, $D = +28^\circ$).

Es ist übrigens augenscheinlich, daß alle Klassen außer der ersten in Tabelle 12, welche die B-Sterne umfaßt, eine Lage des Pols in sehr guter Übereinstimmung mit dem allgemeinen Milchstraßenpol (Ziff. 11) ergeben.

Außer den verschiedenen Graden von galaktischer Konzentration ist es auch von großer Bedeutung, daß in vielen Fällen die galaktische Länge einen sehr merklichen Einfluß auf die scheinbare Verteilung zeigt. Allerdings muß man hier vorsichtig sein, da eine Selektion auf Grund einer mehr oder weniger intensiven Beobachtung gewisser Himmelsregionen vorliegen kann.

N. C. DUNÉR⁵ hatte auf die große galaktische Konzentration der Sterne von Secchis Typus IV (Harvard-Typus N und R) aufmerksam gemacht. Diese Erscheinung wurde von T. E. ESPIN⁶ und J. A. PARKHURST⁷ näher untersucht und bestätigt. Später hat ESPIN⁸ die galaktische Verteilung verschiedener Objekte von pekuliären Spektraltypen untersucht. Die größte Konzentration zeigen

¹ A N 192, S. 261 (1912).

² Lund Medd 75 (1917).

³ A N 226, S. 327 (1926).

⁴ B A N 2, S. 47 (1924).

⁵ Sur les étoiles à spectres de la troisième classe. IC Svenska Vet Akad Handl 21, Nr. 2, S. 126 (1883).

⁶ Ap J 10, S. 169 (1899).

⁷ Yerkes Publ 2, S. 127 (1903).

⁸ J Can R A S 7, S. 79 (1913).

nach ihm die WOLF-RAYET-Sterne (Typus O), von denen etwa 98 % zwischen galaktischer Breite 0° und $\pm 10^\circ$ liegen. Dann folgen in der Reihe abnehmender Konzentration die neuen Sterne, die Sterne mit hellen Wasserstofflinien, die Gasnebel und die N-Sterne. Auffallend ist, daß $\approx B$ die R-Sterne eine sehr viel kleinere Konzentration als die N-Sterne aufweisen. ESPIN findet auch die mittlere galaktische Breite in den einzelnen Gruppen entschieden negativ, was auf eine Lage der Sonne nördlich in bezug auf die galaktische Symmetrieebene hinweist. Er untersucht auch die Verteilung nach der galaktischen Länge. Für Gasnebel und neue Sterne findet er eine Konzentration gegen $L = 335^\circ$ bzw. 325° .

Auf die Anhäufung schwacher Novae im Sagittariusgebiet hat besonders K. LUNDMARK¹ aufmerksam gemacht. Es bestätigt sich hier, dem unmittelbaren Eindruck nach, die Vermutung, welche wir schon vorher mehrfach besprochen haben und welche wir später (Ziff. 28) auf Grund neuer Evidenz von ganz anderer Natur nochmals aufnehmen werden, daß die Partien der Milchstraße, welche die Sternbilder Sagittarius, Scorpius und Ophiuchus berühren, im wesentlichen einem gewaltigen Zentralkern unseres Sternsystems entsprechen. Ein Vergleich mit der Verteilung der Novae in der Zentralregion des großen Andromedanebels ist in vieler Hinsicht sehr bestechend. Diese Tatsachen sind aber schon ausführlich an anderer Stelle in diesem Handbuch behandelt worden.² P. DOIG³ hat die Verteilung in galaktischer Länge für verschiedene Objekte dargelegt; er zeigt besonders eine Verschiebung des Konzentrationspunktes vom Monoceros-Argo-Gebiet zum Centaurus-Sagittarius-Gebiet, wenn wir von dem B-Typus und den offenen Sternhaufen zu den O-Sternen, planetarischen Nebeln, langperiodischen Veränderlichen, Novae und Kugelsternhaufen übergehen.

GYLLENBERG⁴ gibt die räumliche Verteilung der O-Sterne gemäß der Methode, welche CHARLIER für die B-Sterne benutzt hat. Den Zentralpunkt für 97 Sterne findet er in der Entfernung 263 Parsec in der Richtung $L = 328^\circ$, $B = -4^\circ$. Eine sehr eingehende Untersuchung über die scheinbare und räumliche Verteilung der c-Sterne hat SCHILT in einer oben erwähnten Arbeit gegeben. Wenn drei spezielle Gruppen ausgeschlossen werden, findet SCHILT eine Anordnung dieser Sterne im Raume, welche der von CHARLIER für die B-Sterne gefundenen Verteilung ähnelt. Wie oben erwähnt, fällt aber die Symmetrieebene der c-Sterne mit der allgemeinen „galaktischen“ zusammen. P. DOIG⁵ untersucht die Verteilung der „Pseudo-Cepheiden“ und Übergiganten der Spektraltypen F bis M. Das Material ist jedoch für ständige Deklination sehr unvollständig. C. LUTLAU-JANSSEN und G. HAARH⁶ haben die räumliche Verteilung der N- und R-Sterne studiert und auf die oben erwähnte große Verschiedenheit der Konzentration gegen die galaktische Ebene für diese zwei Klassen hingewiesen.

Eine sehr wichtige Aufgabe für die Kenntnis unseres Systems besteht im systematischen Aufsuchen von δ Cephei-Veränderlichen, da die Relation zwischen Periode und absoluter Größe eine ziemlich genaue Ermittlung der räumlichen Verteilung erlaubt, wenn wir von Absorptionserscheinungen im interstellaren Raume absehen. HERTZSPRUNG⁷ untersucht die räumliche Verteilung der δ Cephei-Sterne und der Sterne vom Typus Oe5. SHAPLEY hat in Verbindung mit seinen Untersuchungen über die Kugelhaufen (Ziff. 18) die Verteilung der galaktischen δ Cephei-Sterne ausführlich studiert. Eine sehr eingehende Untersuchung über die galaktische Verteilung der δ Cephei-Sterne gibt M. GÜSSOW⁸. Wohlbekannt

¹ Publ. A. S. P. 33, S. 219 u. 225 (1921), Pop. Astr. Tidsskr. 4, S. 127 (1923).

² Das Handb. VI, S. 257 (1928). ³ J. B. A. A. 33, S. 238 (1923). ⁴ L. c.

⁵ J. B. A. A. 36, S. 292 (1926). ⁶ A. N. 214, S. 383 (1921). ⁷ A. N. 196, S. 201 (1913).

⁸ Kritische Zusammenstellung sämtlicher Beobachtungsergebnisse der Veränderlichen vom δ Cephei-Typus und Kritik der Eddingtonschen Pulsationstheorie, Inaug.-Diss., Berlin 1924.

ist der auffällige Unterschied in galaktischer Konzentration zwischen den langperiodischen und kurzperiodischen Sternen dieser Art¹. Die Häufigkeit der langperiodischen δ Cephei-Sterne zeigt nach M. GÜSSOW Maxima in den Längen 250° bis 260° und 330° bis 360° . J. SCHMIDT² hat die Häufigkeit der Perioden für verschiedene Milchstraßengegenden untersucht. In der Sagittarius-Aquila-Region zeigt die Häufigkeit ein Maximum für $\log P = 0,84$, während für andere Regionen das Maximum für entschieden kürzere Perioden eintritt.

Eine der großartigsten Arbeiten für die Erforschung der Milchstraßenstruktur wird gegenwärtig auf der Harvard-Sternwarte und ihrer südlichen Filiale ausgeführt, wo in mehr als 200 Feldern, welche die ganze Zentralzone der Milchstraße bis $\pm 20^\circ$ Breite bedecken, durch wiederholte Aufnahmen alle Veränderlichen systematisch aufgesucht und in ihrem Lichtwechsel verfolgt werden³. Die ersten Früchte dieses Planes sind schon erschienen in mehreren Aufsätzen von H. SHAPLEY und H. W. SWOPE unter dem Titel „Studies of the Galactic Center“.

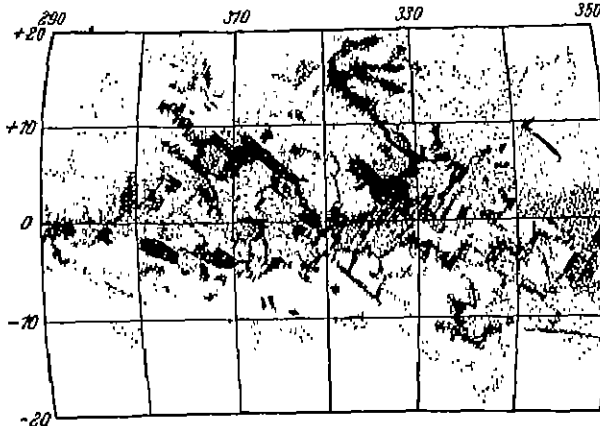


Abb. 16. Verdunklungsgebiete in der Zentralgegend der Milchstraße.

Besondere Aufmerksamkeit wird nämlich darauf verwandt, die Lage, Entfernung und Dichte des galaktischen Zentrums, welches, wie oben erwähnt, mit großer Wahrscheinlichkeit in der Sagittarius-region der Milchstraße gelegen ist, zu untersuchen. Es werden kurz- und lang-

periodische δ Cephei-Sterne, langperiodische Veränderliche, Novae und Bedeckungs-Veränderliche studiert.

In einem Feld von 70 Quadratgrad um das vermutete Zentrum herum wurden unter 450 Veränderlichen 78 kurzperiodische δ Cephei-Sterne oder „Sternhaufen-veränderliche“ gefunden. Die scheinbaren Helligkeiten dieser Sterne sind größtenteils zwischen $15^m,4$ und $16^m,2$ verteilt, mit einem Maximum bei $15^m,7$. SHAPLEY schließt, daß diese Sterne zu einer Art von System gehören, dessen mittlere Entfernung er zu 14400 Parsec schätzt. Da dieser Wert gut mit der früher von SHAPLEY gefundenen Entfernung zum Zentrum im System der Kugelhaufen übereinstimmt, so ist es sehr wahrscheinlich, daß dieses System mit dem Kern unseres Milchstraßensystems identifiziert werden kann.

Auch die Verteilung der langperiodischen δ Cephei-Veränderlichen nach scheinbarer Größe, die ein sehr starkes Maximum bei $14^m,8$ aufweist, spricht für die Existenz eines scharf ausgeprägten Kerns im galaktischen System.

Die erwähnten Studien von SHAPLEY und seinen Mitarbeitern umfassen auch eine wichtige Untersuchung der Verdunklungsgebiete in der betreffenden

¹ Vgl. LUDENDORFF, Handb. der Astrophys. VI, Kap. 2, Ziff. 63.

² Mt Wilson Contr 315 = Ap J 64, S. 149 (1926).

³ Siehe besonders „Sidereal Explorations“. The Rice Institute Pamphlet 18, Nr. 2 = Harv Repr 68 (1931).

⁴ Wash Nat Ac Proc 14, S. 825, 830 u. 958 (1928), 15, S. 174 (1929) = Harv Repr 51, 52, 53, 58.

Himmelsgegend und Erwägungen über die Durchsichtigkeitsverhältnisse des interstellaren Raumes SHAPLEY hat die auf den Photographien erkennbaren Verdunklungsgebiete der Zentralgegend in einer Zeichnung durch Schraffierung von verschiedener Stärke zu markieren versucht (Abb. 16). Das Gebiet am Himmel entspricht dem des zusammengesetzten Bildes in Abb. 7. Er hat dann auch die Verteilung der extragalaktischen Nebel in demselben Gebiet untersucht, um daraus weitere Schlüsse über die Durchsichtigkeitsverhältnisse dieser Gegend ziehen zu können (Abb. 17).

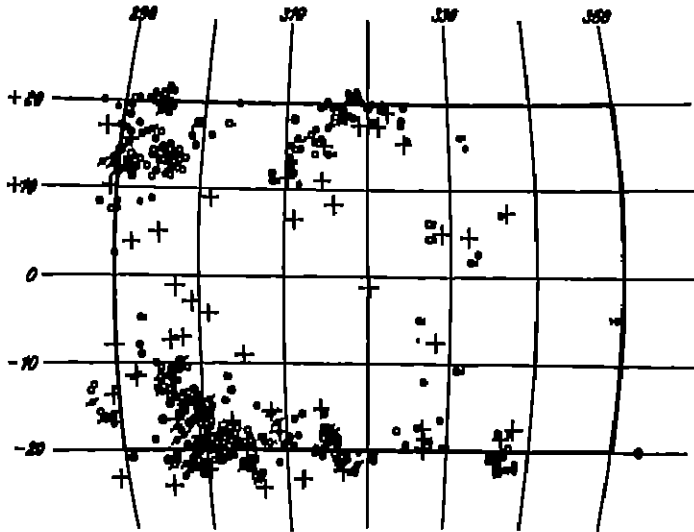


Abb. 17. Die Verteilung der extragalaktischen Nebel in der Zentralgegend. In der Abbildung repräsentieren große Punkte NGC-Objekte, kleine Punkte IC-Objekte oder Nebel in publizierten Harvard-Katalogen, die kleinen Kreise neue auf dem Harvard-Observatorium entdeckte Nebel. Die durch eine Linie gekreuzten Punkte sind deutlich spiralförmige Objekte. Die Kreuze geben die Zentren der langexponierten Platten an.

SHAPLEY zieht den Schluß, daß, wenngleich leicht festzustellendes absorbierendes Material einige galaktische Wolken in der Zentralregion und auch das Zentrum selbst verblirgt, die Milchstraße an den Grenzen dieser Dunkelnebel vollkommen durchsichtig ist und demnach die Beobachtung der entferntesten Sterne unseres Systems wie auch der äußeren, wahrscheinlich Millionen Lichtjahre von uns entfernten „Milchstraßen“ zuläßt.

P. TEN BRUGGENCATE¹ hat in Verbindung mit einer Untersuchung über die räumliche Verteilung von neu entdeckten δ Cephei-Variablen mit Perioden von mehr als einem Tage einige Bemerkungen über SHAPLEYS größeres galaktisches System gemacht. Die Veränderlichen der betreffenden Klasse kommen im Raume unter die offenen Sternhaufen gemischt vor. Es sollen also offene Sternhaufen und mehrere Kugelhaufen in den Sternwolken der Milchstraße selbst liegen.

Die Eigenschaften der Sternhaufen werden an anderem Orte in diesem Handbuch ausführlich behandelt. Hier sollen nur der Vollständigkeit wegen einige fundamentale Tatsachen betreffs der Verteilung der Haufen im Raume Erwähnung finden.

Die offenen Sternhaufen sind Objekte von außerordentlich starker galaktischer Konzentration. Versuche, ihre Verteilung im Raume zu bestimmen,

¹ BAN 4, S 195 (1928).

sind von C. V. L. CHARLIER¹, H. SHAPLEY², S. RAAB³, P. COLLINDER⁴ und R. TRÜMLER⁵ gemacht worden. Die Verteilung der zur Zeit bekannten Haufen, wie sie besonders in den zwei letztgenannten Arbeiten zutage tritt, kann folgendermaßen kurz charakterisiert werden. Die Symmetrieebene des Systems erscheint ein wenig schief gegenüber der gewöhnlich angenommenen galaktischen Ebene. TRÜMLER findet für den Pol des Haufensystems

$$A = 192^{\circ},6, D = +27^{\circ},7 \text{ (1900).}$$

Wenn wir vom GOULDSchen Pol ausgehen und die entsprechenden galaktischen Koordinaten des Haufenpols suchen, bekommen wir nach TRÜMLER

$$L = 10^{\circ}, B = +88^{\circ},3.$$

Es ist sehr bemerkenswert, daß diese Lage des Pols in derselben Richtung von GOULDS Pol abweicht wie die Lage des Pols für die schwachen Größenklassen in Tabelle 6 (Ziff. 11) gemäß den Untersuchungen von SEARES und VAN RHIJN. Die Abweichung ist jedoch für die Haufen von einem kleineren Betrag, was nach TRÜMLER andeutet, daß das System der Haufen weiter in den Raum hinausreicht als im Durchschnitt die Sterne 18. Größe. Das System der bekannten Haufen bildet eine sehr flache, nahe kreisförmige Scheibe von etwa 8000 Parsec Durchmesser und mit einem beträchtlichen Zuwachs an Dichtigkeit gegen das Zentrum hin. Dieses Zentrum befindet sich ziemlich nahe der Sonne. Wenn wir die zwei galaktischen Koordinatenachsen so ziehen, daß gleich viele Haufen auf beiden Seiten jeder Achse liegen, so bekommen wir nach TRÜMLER den Schnittpunkt in der Entfernung 350 Parsec in der galaktischen Länge 247° . Dies deutet an, daß die dichte Zentralregion des Haufensystems dem Phänomen des „lokalen Systems“ entspricht. Diese Zentralregion geht aber allmählich in die allgemeinen Milchstraßenregionen über, und wir haben oben gesehen, daß die Symmetrieebene der Haufen im ganzen gar nicht im Sinne des GOULDSchen Kreises oder der Symmetrieebene der helleren B-Sterne von der allgemeinen Milchstraßenebene abweicht, sondern in ihrer Lage mit der Tendenz der Sterne von sehr schwachen Größenklassen übereinstimmt.

Wenn wir zu den Kugelhaufen übergehen, so spricht für ihre Zugehörigkeit zum Milchstraßensystem, außer ihrer nahezu symmetrischen Anordnung in bezug auf die galaktische Ebene und ihrer größten Häufigkeit in der Gegend der hellsten Milchstraßenwolken, unter anderem der Umstand, daß es auch Objekte großer individueller Leuchtkraft gibt, die in ihrer Verteilung gewissermaßen eine Zwischenstellung zwischen den Kugelhaufen und den Klassen von großer galaktischer Konzentration einnehmen. Eine solche Klasse bilden die planetarischen Nebel, deren Verteilung von A. R. HINKS⁶, C. V. L. CHARLIER⁷ und H. D. CURTIS⁸ diskutiert worden ist. Diese Nebel kommen mit ziemlich großer Häufigkeit in der Sagittariusregion vor (besonders die Nebel von kleinem scheinbaren Durchmesser), zeigen aber sonst keine sehr ausgeprägte galaktische Konzentration.

Eine auffallend kleine galaktische Konzentration zeigen auch trotz hoher absoluter Leuchtkraft die R-Sterne und die helleren kurzperiodischen δ Cephei-Veränderlichen. Für ein Studium über die Verteilung dieser Sterne nach galaktischer Länge liegt aber kaum genügend homogenes Material in den verschiedenen Himmelsgegenden vor. SHAPLEY⁹ hat die räumliche Verteilung der letztgenannten

¹ Lund Medd Ser II, Nr. 19 (1918).

² Mt Wilson Comm 62 (1919).

³ Lund Medd Ser. II, Nr. 28 (1922).

⁴ Pop Astr Tidskr 8, S. 36 (1927); On Structural Properties of Open Galactic Clusters and their Spatial Distribution, Inaug.-Diss. Lund 1931.

⁵ Lick Bull 14, S. 154 (1930).

⁶ M N 71, S. 693 (1914).

⁷ Lund Medd Ser II, Nr. 19, Plate IV.

⁸ Publ Lick Obs 13, S. 60 (1918).

⁹ Mt Wilson Contr 153 = Ap J 48, S. 279 (1918).

Sterne aus Entfernungsbestimmungen auf Grund der Relation zwischen Periode und absoluter Größe studiert. Die kleine galaktische Konzentration wird von SHAPLEY als eine Folge der großen Streuung der räumlichen Geschwindigkeiten gedeutet. Wenn wir das oben erwähnte Vorkommen in der „zentralen“ Milchstraßengegend im Sagittarius mitrechnen, so scheint in vieler Hinsicht eine ausgeprägte Analogie zwischen der Verteilung dieser Sterne im Raume und der Verteilung der Kugelhäufen zu bestehen.

Inwieweit die hergeleitete Verteilung einer Klasse von Objekten großer absoluter Leuchtkraft das wahre Verteilungsgesetz der betreffenden Objekte im Sternsystem wiedergibt, hängt natürlich in erster Linie von der Vollständigkeit ab, mit welcher diese Objekte in unserem statistischen Material vorkommen. Eine der größten Schwierigkeiten der direkten stellarstatistischen Untersuchungsmethode liegt ohne Zweifel in der Absorption des Lichts in ausgedehnten Anhäufungen von Materie im interstellaren Raume. Eine solche Absorption beeinträchtigt nicht nur die Vollständigkeit des Materials, sondern verfälscht auch, wenn unberücksichtigt, die nach photometrischer Methode ermittelten Entfernungen und damit die aus diesen berechnete räumliche Dichtigkeit. Es wird durch beide Ursachen eine falsche „anthropozentrische“ Verteilung vorgetäuscht. Mit großer Wahrscheinlichkeit sehen wir z. B. einen Absorptionseffekt in dem scheinbaren Verminden einer zentralen Milchstraßenzone, welches die Kugelhäufen zeigen. TRÜMPLER rechnet in seiner oben erwähnten Arbeit mit einer allgemeinen Extinktion von $0^m,67$ (photographisch) per 1000 Parsec innerhalb einer dünnen Schicht um die galaktische Zentralebene herum. Inwieweit diese und andere mehr unregelmäßige Absorptionserscheinungen auf die von TRÜMPLER gefundene Verteilung der offenen Häufen in „anthropozentrischer“ Richtung einwirken, bleibt wohl noch unaufgeklärt (vgl. Ziff. 24 und 33).

21. Die Entfernung der Sonne von der Symmetrieebene der Milchstraße. In Ziff. 11 haben wir für den sphärischen Radius der zentralen Milchstraßenlinie im Mittel einen gewissen Überschuß über 90° gefunden, was als „dip“ der Milchstraße bezeichnet wird. Eine genauere Abschätzung der entsprechenden Entfernung der Sonne von der Symmetrieebene gegen den nördlichen galaktischen Pol hin kann durch eine Statistik gewisser Klassen von Objekten ermittelt werden.

CHARLIER findet in seiner ersten Arbeit über die helleren B-Sterne eine Stellung der Sonne nördlich von der Symmetrieebene um 20 Parsec (4 Strömometer) und in seiner späteren Arbeit für die B-Sterne heller als $8^m,0$ eine Entfernung von 15,5 Parsec, was sehr nahe mit einer Schätzung von SHAPLEY und CANNON¹ für die Sterne vom Typus B0 bis B5 im Größenintervall $7^m,26$ bis $8^m,25$ übereinstimmt.

GERASIMOVIC findet für B-Sterne heller als $6^m,7$ eine Distanz von 16 Parsec und für Sterne schwächer als $6^m,7$ den Wert 34 Parsec. Derselbe Verfasser² hat aus den O-Sternen eine Sonnenhöhe über die Milchstraßenebene von 31 Parsec hergeleitet.

SCHULT findet in seiner in Ziff. 20 besprochenen Arbeit für die c-Sterne mit der scheinbaren Größe ziemlich varrierende Werte, die jedoch im Mittel gut mit den Resultaten für andere Klassen übereinstimmen.

Aus den δ Cephei-Sternen fand HERTZSPRUNG³ 40 Parsec und SHAPLEY⁴ 60 Parsec, während kürzlich GERASIMOVIC und LUYTEN⁵ aus verbessertem Material 34 ± 11 Parsec gefunden haben, was mit den Resultaten für Miss

¹ Harv Circ 239 (1922) ² A N 226, S. 327 (1926).

³ A N 196, S. 207 (1913).

⁴ Mt Wilson Contr 157 = Ap J 49, S. 311 (1919)

⁵ Wash Nat Ac Proc 13, S. 387 (1927).

MAURYS c- und ac-Sterne und für die Spektralklassen O und B in bester Übereinstimmung steht. Das letztgenannte Resultat ist daher ohne Zweifel das zur Zeit zuverlässigste. Nach TRÜMLER¹ liegt die Sonne 10 Parsec nördlich von der Zentralebene der offenen Sternhaufen.

22. Spezielle Untersuchungen der Sternleeren und Sternwolken der Milchstraße. Der unmittelbare Anblick zeigt uns die Milchstraße in eine Art von Wolkenstruktur aufgelöst, die zweifellos zum großen Teil eine scheinbare, durch Absorption des Lichts in dunklen Massen hervorgerufene Zerstückelung bedeutet (vgl. Ziff. 13). Wenn wir sogar die Vermutung hegen können, daß die meisten auffälligen Risse des Milchstraßengebildes Absorptionsgebiete darstellen, so bedarf diese Behauptung doch eines direkten Nachweises, den uns in erster Linie eine statistische Analyse der Sternzahlen sukzessiver Größenklassen, soweit möglich unter Hinzufügung spektralanalytischer Daten, zu geben hat. Die Anzahl Sterne verschiedener Helligkeiten in den Dunkelgebieten wird mit den Sternzahlen benachbarter „normaler“ Gebiete verglichen. Es wird dann untersucht, ob die Abweichungen durch die Einwirkung einer Absorptionsschicht in einer gewissen anzugebenden Entfernung und mit einem gewissen Absorptionsvermögen erklärt werden können.

Es ist von vornherein klar, daß eine vollständigere Analyse, die auch die Sternbewegungen berücksichtigt, für eine Beurteilung diesbezüglicher Fragen von großer Bedeutung sein würde, da ja aus den Eigenbewegungen der Sterne des Dunkelgebiets die mittleren Entfernungen hergeleitet werden können. Unsere Kenntnis der Bewegungen ist jedoch noch viel zu mangelhaft, um im allgemeinen eine solche Analyse erfolgreich zu machen.

Schon aus einer direkten Analyse der Kurven, welche die Sternzählungen nach scheinbarer Größe wiedergeben, können wichtige Eigenschaften des Nebels, wie Entfernung und Absorptionsgrad, wenigstens grob geschätzt werden. Für genügend schwache Größen sollten die Kurven für das freie und das verdunkelte Feld einander parallel laufen, mit einer Differenz in m gleich der Absorption ϵ der verdunkelnden Nebelschicht für hinter dieser Schicht liegende Sterne.

Eine mathematisch-statistische Methode zur Abschätzung der Entfernung und der Absorption ist von A. PANNEKOEK² entwickelt worden. Für die Sternzahlen pro Größenklasse im freien und im verdunkelten Gebiet, $a(m)$ und $a_1(m)$, setzen wir $a_1(m) = \gamma_1 a(m) + \gamma_2 a(m - \epsilon)$. Wenn wir für die Dichtigkeitsfunktion die SEELIGERSche oder die SCHWARZSCHILDsche Approximation annehmen, so werden γ_1 und γ_2 durch die Konstanten dieser Funktionen und durch die Entfernung r der Nebelschicht bestimmt. Durch Variation der zwei Parameter ϵ und r wird die bestmögliche Darstellung der beobachteten Zahlen $a_1(m)$ angestrebt. W. GYLLENBERG³ hat eine ähnliche Methode entwickelt, welche aber die Unbekannten in mehr direkter Weise ergibt. Die Entfernung des Nebels kann auf drei Wegen ermittelt werden, durch die mittlere scheinbare Größe, durch die Größe maximaler Frequenz oder durch die Totalsumme der Sterne des Vordergrundes. LUNDMARK⁴ hat verschiedene Methoden zur Entfernungsbestimmung für helle und dunkle Nebel skizziert.

Wie vorher auseinandergesetzt wurde, scheint in unserer Nähe eine Nebelschicht von beträchtlicher Neigung (etwa 20°) gegen die Milchstraße zu existieren, deren ausgedehnteste Absorptionsgebiete in Taurus-Orion und in Ophiuchus zu finden sind.

Das große Dunkelgebiet in Taurus zwischen R.A. 3^h bis $5^h 30^m$ und nördl. Dekl. 20° bis 25° ist in einer detaillierten Abzählung auf den FRANKLIN-ADAMS-

¹ L. c. Ziff. 20.² Amsterdam Proc 23, Nr. 5 (1920).³ Lund Medd Ser II, Nr. 52 (1929).⁴ Publ A S P 34, S. 40 (1922).

Platten von F. W. DYSON und P. J. MELOTTE¹ behandelt worden. Die Abzählung zeigt drei Regionen starker Verdunklung im genannten Gebiet, um $3^h 20^m$, $+30^\circ$ herum (S. W. von ζ Persei und nahe α Persei), um $4^h 30^m$, $+26^\circ$ herum (zwischen den Plejaden und β Tauri) und um $5^h 20^m$, $+25^\circ$ herum (S. W. von β Tauri). Dieses Gebiet war früher von BARNARD² bemerkt worden, der auf die Existenz absorbierender Materie geschlossen hatte, was durch die Anwesenheit von hellen Nebeln um so mehr wahrscheinlich wird (Ziff 13). Es wird auf der WOLFSCHEN Aufnahme (Abb. 4) wiedergegeben. DYSON und MELOTTE schließen, daß die Entfernung der dunklen Materie nicht 300 Parsec überschreiten kann.

PANNEKOEK findet aus den Zählungen im Taurusgebiet eine Entfernung des dunklen Nebels von 140 Parsec und einen Absorptionsgrad in den dunkleren Partien von etwa zwei Größenklassen. Eine Bestätigung dieses Resultats ist kürzlich von C. SCHALÉN³ geliefert worden, der speziell die B- und A-Sterne in der betreffenden Region untersucht und diese in „Luminositätsklassen“ von wahrscheinlich sehr geringer Streuung in absoluter Größe aufgeteilt hat. Die Methode von PANNEKOEK wurde für jede einzelne Klasse befolgt. SCHALÉN findet als Mittel aus vier Luminositätsklassen, die miteinander wohl übereinstimmende Resultate geben,

$$r = 126 \text{ Parsec}, \quad s = 1^m,8$$

Aus den Zahlen der A- und K-Sterne des DRAPER-Katalogs hatte SHAPLEY⁴ als Maximalwert der Distanz 250 Parsec angegeben. Wenn die gefundene Absorption durch RAYLEIGH-Diffusion in Wasserstoff erklärt werden soll, wird die Masse des Taurusnebels nach PANNEKOEK von der Größenordnung $4 \cdot 10^6$ Sonnenmassen. Eine solche Masse in einer Entfernung von nur 126 Parsec führt indessen auf bedenkliche dynamische Konsequenzen der Sternströmung gegenüber, weshalb es nach PANNEKOEK wahrscheinlicher ist, daß wir es mit einer Diffusion durch freie Elektronen oder mit einer Absorption durch kosmischen Staub zu tun haben, in welchem Falle sehr viel kleinere Massen zur Erklärung genügen. Dann haben wir auch keine mit der Wellenlänge sich verändernde Absorption zu erwarten, was mit der bisherigen Erfahrung über die Absorption in den ausgedehnten dunklen Nebeln übereinzustimmen scheint. Dagegen ist für Sterne, die mit heller Nebulosität verbunden sind, oftmals ein großer Farbenreichtum beobachtet worden⁵.

A. EDDINGTON⁶ weist nach, daß die Annahme einer Diffusion durch freie Elektronen für den Taurusnebel eine wahrscheinlich noch zu hohe Masse gibt ($12 \cdot 10^7$ Sonnenmassen). Es scheint daher, daß nur die Hypothese einer „soliden Obstruktion“ durch kleine Partikeln stichhaltig ist.

Die Extinktion einer solchen Wolke ist bei gegebener Masse und Dichte ein Maximum, wenn der Durchmesser einer Partikel gleich der Wellenlänge des Lichtes wird. Für diese Partikelgröße geht auch der Übergang von nichtselektiver zu selektiver Extinktion vor sich. Nach H. N. RUSSELL⁷ ist es also wahrscheinlich, daß die Extinktion des Lichts im Raume hauptsächlich von festen Partikeln von einigen zehntausendsten Millimeter ausgeht.

Für die Umgebung des Orionnebels hat A. KOPFF⁸ eine umfangreiche Sternzählung auf einer Aufnahme mit dem 16zölligen Bruce-Teleskop der Sternwarte

¹ M. N. 80, S. 3 (1919).

² Ap. J. 25, S. 218 (1907).

³ K. Svenska Vetensk. Handl. (III) 6, Nr. 6 (1928) = Upsala Medd. 37.

⁴ Harv. Circ. 240 (1922).

⁵ F. H. SEARES u. E. HUMBLE, Mt. Wilson Contr. 187 = Ap. J. 52, S. 8 (1920).

⁶ The Internal Constitution of the Stars, S. 388 (1926).

⁷ Wash. Nat. Ac. Proc. 8, S. 115 (1922) = Mt. Wilson Comm. 77.

⁸ Publ. Astrophys. Obs. Königsstuhl-Heidelberg 1, S. 177 (1902).

Königstuhl, Belichtungsdauer $6^h 15^m$, durchgeführt. Die scheinbare Stern-dichtigkeit ist in einer bildlichen Darstellung durch Schraffierung verschiedener Stärke wiedergegeben worden. Es zeigt sich, daß der Nebel von einer sternarmen Region umgeben ist. Diese verbreitert sich auffallend in südöstlicher Richtung, so daß der Nebel fast an der Spitze eines langgestreckten sehr dunklen Kanals gelegen ist. Ein feiner dunkler Arm geht jedoch auch in nordwestlicher Richtung vom Nebel aus; in nordöstlicher Richtung steht die leere Region mit den Nebelmassen um ζ Orionis in Verbindung. S. ASKLÖF¹ hat eine Abzählung derselben Gegend für sukzessive Größenklassen bis zur Größe 13,0 unternommen. Für die Entfernung des dunklen Nebels erhält er im Mittel 290 Parsec, was mit den Entfernungsbestimmungen für die Heliumsterne im Orion und für Doppelsterne dieser Gegend, die wahrscheinlich mit den Heliumsternen und dem hellen Nebel verbunden sind, wohl übereinstimmt.

PANNEKOEK² hat für eine Partie der Milchstraße in Aquila Sternzählungen ausgeführt, aus welchen er schließt, daß das hier auftretende Dunkelgebiet durch

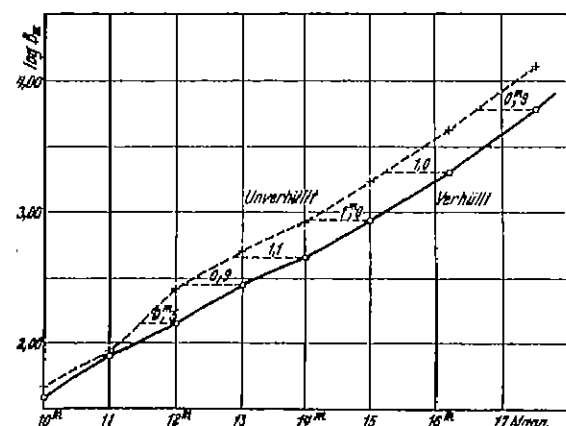


Abb. 18. Die Sternzahlen innerhalb und außerhalb des Nebels NGC 6960 nach WOLF.

eine absorbierende Nebelmasse verursacht wird, die schon für Sterne der Größen 10 und 11 sehr bemerkbar wird.

Für den großen dunklen Ophiuchusnebel gibt PANNEKOEK in seiner vorher erwähnten Arbeit über das „lokale Sternsystem“ eine Entfernung zwischen 100 und 200 Parsec, also von derselben Größenordnung wie die Entfernung des Taurusnebels. SHAPLEY³ schätzt für die dunklen Nebel der Ophiuchus-Scorpius-Region die Entfernung zu 200 bis 300 Parsec.

Eine Menge Sternzählungen für Absorptionsgebiete sind in den letzten Jahren von M. WOLF⁴ gemacht worden. Die erste unten aufgeführte Arbeit bezieht sich auf den Nebel NGC 6960, der sich in langem Bande fast genau durch den Stern 52 Cygni (R.A. $20^h 41^m$, Dekl. $+30^\circ 21'$) hindurchzieht. Der helle Nebel ist offenbar der westliche Teil einer sehr ausgedehnten Nebelmasse, die bis zu dem ebenfalls langgestreckten Netzwerknebel NGC 6992 hinüberreicht. Wir haben schon vorher (Ziff. 1 u. 13) den großen Unterschied in den Sternzahlen auf beiden Seiten des Nebels NGC 6960 besprochen. Diese Erscheinung hat WOLF durch Sternzählungen bis zur Größe 17,5 verfolgt. Das Resultat ist in Abb. 18 wiedergegeben.

Aus der Verschiebung der Sternzahlenkurve für die Absorptionsregion kann man die Extinktion des dunklen Nebels östlich von der hellen Randpartie zu einer Größenklasse schätzen. Die Entfernung schätzt WOLF zu rund 450 Parsec. Er findet keine Spur von einem Farbenexzeß im verdunkelten Teil.

¹ Nordisk Astr Tidskr 5, Nr. 1 (1924); Ark Mat Astr Fys 22 A, Nr. 14 (1930) = Upsala Medd 51. ² Versl Akad Amsterdam 27, S. 1327 (1919); Amsterdam Proc 21, Nr. 10 (1919).

³ Harv Circ 239 (1922).

⁴ A N 219, S. 109 (1923); 223, S. 89 (1924); 229, S. 1 (1926); SEELIGER-Festschr S. 312 (1924); V J S 61, S. 263 (1926).

Ähnliche Untersuchungen von WOLF beziehen sich auf den „Amerikanebel“, auf die Sternleeren bei S Monocerotis und auf die Sternleere neben der dichtesten Gegend der Scutumwolke. Bei dem Amerikanebel und der Scutumleere beträgt die Absorption 3,5 Größenklassen.

Sehr interessant ist WOLFs Vergleichung der Sternzahlen für die vier oben genannten Regionen der Milchstraße mit den Sternzahlen am galaktischen Pol. Die letztere Gegend erscheint sternärmer als die Leeren des Milchstraßengürtels. Wichtig ist auch, daß der Gang der Sternzahlen für den galaktischen Pol von der Größe 9 bis zur Größe 16,5 wenigstens keine stärkere Absorptionswirkung durch irgendeine Dunkelwolke andeutet.

Für den Amerikanebel liegen außer WOLFs oben erwähneter Arbeit mehrere Untersuchungen vor. So hat A. KOPFF¹ eine umfangreiche Sternzählung in derselben Weise wie für den großen Orionnebel ausgeführt. E. BUCH-ANDERSEN² findet aus Sternzählungen die Entfernung des Nebels gleich der mittleren Entfernung der Sterne der Größe 8,5 in der betreffenden Region. B. OKUNEV³ untersucht die Spektren von 743 Sternen zwischen R.A. $20^h 4^m$ und $21^h 13^m$ und Dekl. $+40^\circ$ bis $+47^\circ$ und findet in ziemlich guter Übereinstimmung die der Entfernung des Nebels entsprechende Sterngröße zu 9,0.

W. GYLLENBERG findet für die Parallaxe dieses Nebels nach seiner oben besprochenen Methode, aber in zwei etwas verschiedenen Durchführungen $\pi = 0'',0064$ bzw. $0'',0074$. Für den Nebel um S Monocerotis findet er $\pi = 0'',013$. K. LUNDMARK hat in seiner oben besprochenen Arbeit für diese und andere Nebel nach verschiedenen Methoden genäherte Parallaxen gegeben.

O. STRÖMVER⁴ hat in Verbindung mit seiner Arbeit über das interstellare Kalzium (Ziff 25) einen Dunkelnebel im Cepheus behandelt und aus Sternzählungen eine Entfernung von 350 Parsec erhalten.

A. UNSÖLD⁵ hat nach WOLFs Methode den südlichen „Kohlensack“ in Crux untersucht. Er findet eine Entfernung von ungefähr 150 Parsec und eine Extinktion von einer Größenklasse. Zu der UNSÖLdschen Arbeit hat E. VON DER PAHLSEN⁶ einige bestätigende theoretisch-statistische Bemerkungen hinzugefügt.

In seiner oben besprochenen Arbeit hat SCHALÉN für einige dunkle Gebiete der nördlichen Milchstraße durch eine sorgfältige Analyse der Sternzahlen der B- und A-Sterne unter Einteilung derselben in spezielle Sonderklassen, die wesentlich von der Intensität der Wasserstofflinien im Spektrum abhängen, die Entfernung und den Absorptionsgrad der Dunkelwolken bestimmt. Die Ergebnisse sind nach SCHALÉN in Tabelle 13 aufgeführt. Die Existenz des Nebels in der Cassiopejagegend ist nach ihm unsicher. In einer späteren Arbeit⁷ hat er in der Cepheusregion unter Heranziehung von Daten für andere Spektralklassen Andeutungen von zwei Nebeln in den Entfernungen 250 und 410 Parsec und mit der Absorption 0,3 bzw. 0,6 Größenklassen gefunden.

Tabelle 13

Region	Koord.		Entfernung in Parsec	Extinktion
	α	δ		
Cygnus	$20^h 25^m$	$+35^\circ$	800	2 ^m
Cepheus	21 30	+58	370	0,9
Cepheus	21 45	+57	800	1,5
Cassiopeia	1 50	+63	900	1
	1 30	+56		
Auriga-Taurus	4 45	+36	126	1,8

¹ L. c.² Ap J 38, S. 275 (1913)³ Bulletin de l'Observatoire central de Russie à Poulkovo 10, S. 594 (1927).⁴ Mt Wilson Contr 331 = Ap J 65, S. 193 (1927)⁵ Harv Bull 870 (1929)⁶ A N 238, S. 269 (1930)⁷ Ark Mat Astr Fys 22 A, Nr. 16 (1930) = Upsala Medd 50.

Wir haben oben vielfach die Sternleeren der Milchstraße als im großen ganzen durch absorbierende Dunkelwolken hervorgerufen angesehen. Diese Auffassung war jedoch nicht immer die geläufige. BARNARD und WOLF waren beide zuerst geneigt, in den dunklen kontrastierenden Gebieten wirkliche Sternleeren zu sehen; WOLF wollte z. B. früher in den Hölennenebeln eine Art Wegfegung von Sternen durch den hellen Nebel sehen, wodurch die sternleeren Kanäle entstehen sollten. Beide wurden aber später zu entschiedenen Vertretern der Absorptionshypothese bekehrt. In den meisten Fällen ist auch sicher diese Hypothese vorzuziehen, wenn auch hervorgehoben werden muß, daß nicht alle gegen ihre Umgebungen kontrastierenden dunklen Gebiete des Himmels notwendig als durch Absorption des Lichtes entstanden zu betrachten sind, wenigstens nicht in höheren galaktischen Breiten (vgl. Ziff. 14).

Trotz dieses Ergebnisses besteht noch immer die Vorstellung, daß das System der Milchstraße räumlich in eine Menge gegeneinander isolierter Wolken aufzulösen sei. Inwieweit dieser Vorstellung etwas Reales zukommt, läßt sich zwar noch kaum völlig entscheiden, doch muß nach dem Durchbruch der Absorptionshypothese für die Deutung der Dunkelgebiete der Milchstraße die ältere Auffassung betreffs der hellen Regionen jedenfalls sehr erheblich modifiziert werden.

Die Vorstellung einer Wolkenstruktur der Milchstraße wurde aber auch zum Teil aus einer Statistik der Sternzahlen hellerer Sterne abgeleitet. W. STRATONOFF¹ fand für die ARGELANDERSchen Sterne gewisse Kondensationsregionen, von denen die wichtigsten in Cygnus, Auriga, Monoceros und Argo gelegen sind. STRATONOFF hält die Sonne für ein Glied eines Haufens, dessen Mitte wir ein wenig südlich von α Cygni wahrnehmen. F. RISTENPART² suchte die räumliche Dichtigkeit für verschiedene Regionen zu ermitteln und kam zu dem Ergebnis, daß die Sonne sich in einem Sternhaufen befindet, dessen Zentrum etwa in der galaktischen Länge 290° im Sternbilde Norma liegt. Eine zweite deutlich hervortretende Wolke ist die in Cygnus. Wie vorher erwähnt, hat auch PANNEKOEK kürzlich unsere nähere Umgebung in eine Serie von Wolken aufzulösen versucht, von denen die mächtigsten in Cygnus und Monoceros liegen.

Diese Ergebnisse scheinen jedoch in einem gewissen Gegensatz zu anderen vielleicht augenblicklich allgemeiner angenommenen Ansichten zu stehen, nach denen die helleren Sterne unserer Umgebung überwiegend einem großen „lokalen System“ angehören, dessen Kern von dem „lokalen Haufen“ der Heliumsterne gebildet wird. Dieses „lokale System“ wäre aber auch als eine einheitliche Sternwolke neben anderen zu betrachten. Diese Auffassung wird vor allem durch die nach allen Seiten abnehmende Sterndichtigkeit, wie sie aus den Sternzahlen ohne Berücksichtigung einer allgemeinen Absorption ermittelt wird, gestützt. Über die Natur und Mächtigkeit dieses hypothetischen „lokalen Systems“ bestehen jedoch sehr auseinandergehende Meinungen (vgl. Ziff. 18, 19, 33). Nach einer neueren Auffassung auf Grund der differentiellen Rotationseffekte (Ziff. 30) besteht wenigstens kein beständiges, in dynamischer Hinsicht gegen andere „Wolken“ abgeschlossenes lokales System.

Nicht weniger gehen die Ansichten über die Entfernungen und Eigenschaften der äußeren galaktischen Wolken auseinander. Nach einer Arbeit von PANNEKOEK (Ziff. 16) sollte keine Verbindung zwischen den Sternen von den Größen 9 bis 11 und den wirklichen Milchstraßenwolken bestehen. Später berechnete er³ aus Sternzählungen für die Cygnuswolke und die Aquilawolke Entfernungen von 40 000 bis 60 000 Parsec. Für die Sternzahlen wurden die der BD, die Eichungen von HERSCHEL und EPSTEIN und außerdem einige Zonen der photographischen

¹ Publ Obs Taschkent Nr. 2 u. 3 (1900, 1901).

² V J S 37, S. 375 (1902).

³ M N 79, S. 500 (1919).

Himmelskarte benutzt. Der Gradient $d \log N / d m$ zeigte ein Minimum und ein Maximum, wenn wir gegen schwache Größen fortschreiten, was PANNEKOEK als einen typischen Wolkeneffekt deutete. Unter Zugrundelegung der KAPTEYNschen Luminositätskurve und mit Vernachlässigung der räumlichen Tiefe der Wolke berechnete er für verschiedene Wolkenentfernungen theoretische Sternzahlen, wobei für die Sterne des Vordergrundes die Zahlen für den galaktischen Pol angenommen wurden. Eine Konstante, die von der räumlichen Sterndichtigkeit der Wolke abhängt, wurde in Übereinstimmung mit der grob geschätzten Flächenhelligkeit der Wolke angenommen. Der schwache Punkt dieser Entfernungsbestimmung lag in der relativen Unzuverlässigkeit und in der Inhomogenität der Quellen für die Sternzahlen. Gegen PANNEKOEKS Resultate hat EASTON¹ ernste Einwände auf Grund einer neuen Ermittlung der Korrelation zwischen Sternzahlen und Milchstraßenhelligkeit erhoben. Er leitet auch die Prozentzahl der B- und A-Sterne her und berechnet die mittleren Eigenbewegungen für dunkle und helle Regionen, wobei sich zeigt, daß die Eigenbewegungen im Mittel etwas größer für die dunkleren als für die helleren Gebiete sind. EASTON schließt aus den Resultaten auf die Zugehörigkeit eines Teils der helleren Sterne zu den Wolken. Man muß jedoch hierzu die Bemerkung machen, daß EASTONS Resultate wohl eher durch die kleinen Entfernungen der Dunkelwolken, welche die hellen Milchstraßenpartien trennen, als durch kleine Entfernungen der etwaigen Sternwolken erklärt werden können (vgl. Ziff. 16).

In einem späteren Aufsatz über das Cygnusgeblot findet PANNEKOEK², daß wir hier in der Nähe von γ Cygni zuerst eine Anhäufung von Sternen in einer Entfernung von nur 200 bis 600 Parsec vor uns haben, ein Haufen, der aber nichts mit der wirklichen Cygnuswolke zu tun hat. Für die Entfernung der letzteren ergibt eine Revision der Annahmen in der oben erwähnten Arbeit 18000 Parsec. EASTON³ macht zu diesen Resultaten einige kritische Bemerkungen und veröffentlicht mit neuem Material seine Resultate für die Wolke zwischen α und π Cygni. Er lehnt auch eine weitgehende Erklärung der Milchstraßenstruktur durch Absorption in Dunkelwolken ab.

Für die Cygnuswolke liegen noch viele Untersuchungen verschiedener Autoren vor. O. BRUGSTRAND⁴ hat photographisch effektive Wellenlängen für Sterne bis zu einer photographischen Größe zwischen 13 und 14 in der Gegend R.A. $19^h 49^m$ bis 59^m , Dekl. $+35^\circ 10'$ bis $37^\circ 10'$, bestimmt. In einer plötzlichen Erhöhung des Mittelwerts der effektiven Wellenlängen für die Größe 12 sieht er die Einwirkung der Begrenzung des lokalen Systems und schätzt die Entfernung der Grenze zu 2500 Parsec. Die eigentliche, zwischen β und γ Cygni sich erstreckende Wolke liegt wahrscheinlich in einer noch größeren Entfernung.

A. KOFFE⁵ will zeigen, daß die Annahme der Gültigkeit der KAPTEYNschen Luminositätskurve für die Wolke auf einen zu hohen Wert der Flächenhelligkeit führt. Wenn man an Stelle dessen annimmt, daß die Wolkensterne hauptsächlich A- und F-Sterne sind, so wird man unter Zugrundelegung der Abzählungsergebnisse von PANNEKOEK auf eine Entfernung von nur 4000 bis 6000 Parsec geführt. PANNEKOEK⁶ selbst kommt später zu einem ähnlichen Resultat. Die gegebenen Daten sind jedoch nicht zuverlässig genug, um exakte Schlüsse auf die Luminositätsfunktion zu erlauben.

¹ M N 81, S. 215 (1921)² B A N 1, S. 157 (1922)³ A N 216, S. 325 (1922)⁴ B A N 1, S. 54 (1922).⁵ A N Jub.-Nr. (1921)⁶ B A N 2, S. 11 (1923).

H. SHAPLEY¹ hat die „Verteilung von 11000 Sternen in den Milchstraßenregionen studiert und bemerkt, daß die „relativ naheliegenden“ Wolken in Cygnus nur die Spektralklasse A zu beeinflussen scheinen, während im vorhandenen Material nur die B-Sterne den Reichtum der Carinagegend andeuten.

O. STRUVE² hat die Korrelation zwischen den O- und B-Sternen des DRAPER-Katalogs und dessen „Extension“ und der galaktischen Helligkeit studiert. Er findet eine wahrscheinliche Entfernung der Cygnuswolke von 780 Parsec. SCHALÉN hat in seiner oben erwähnten Arbeit eine Andeutung einer Verdichtung in der Entfernung 1000 Parsec gefunden, aber sonst eine ganz kontinuierlich abnehmende Dichtigkeitskurve bis zu 4000 Parsec.

Für mehrere andere Wolkenformationen liegen astrophysikalisch-statistische Resultate vor, die dazu beitragen können, die wahre Natur der Wolkenerscheinungen zu enthüllen.

SHAPLEY³ hat die Farbenindizes für 310 Sterne der Scutumwolke nahe M11 bestimmt. Er findet zwischen den Größen 12 und 15 eine Abnahme des mittleren Farbenindex von +0,98 auf +0,60. Ein analoges Phänomen sollte nach einer vorläufigen Mitteilung von SEARES⁴ auch für schwache Sterne anderer Milchstraßenregionen auftreten. Soweit eine genügend ausführliche Statistik möglich ist, besteht jedoch sicher im allgemeinen eine Zunahme der Farbe mit steigender Größe. Nach F. H. SEARES⁵ gilt für den Farbenindex C im Mittel für den ganzen Himmel bis zur Größe 17

$$C = +0,50 + 0,029 m_v,$$

$$C = -0,18 + 0,071 m_p,$$

für eine Gruppierung nach visueller bzw. photographischer Größe. Gegen die Milchstraße nimmt die mittlere Farbe schon für helle Größen merklich ab. Für die galaktische Breite $+5^\circ$ ermittelt SEARES im wesentlichen aus KREIKENS Farbenbestimmungen für schwache Milchstraßensterne (Ziff. 17)

$$C = +0,38 + 0,024 m_v,$$

$$C = -0,10 + 0,048 m_p,$$

während KREIKEN⁶ für die Milchstraße in Cepheus

$$C = -0,587 + 0,0678 m_p$$

und in Scutum-Aquila

$$C = -1,120 + 0,1051 m_p$$

herleitet.

K. GRAFF⁷ hat eine photometrische Sternfolge von 73 Sternen bis zur Größe 11,5 für eine kleine Wolke am Rande der Scutumwolke zwischen R.A. $18^h 29^m$ und $18^h 36^m$, Dekl. $-4^\circ,1$ und $-5^\circ,1$ (1855) hergestellt und auch visuell die Farben geschätzt. Er findet als bemerkenswert, daß nicht weniger als 29 Sterne die Farbenstufe 3 oder tiefer zeigen, die darauf schließen läßt, daß es sich dabei um die Spektraltypen G und K handelt. Um den Stern BD $-4^\circ 4525$ herum gruppiert sich ein ganzes Nest solcher gelber bzw. rotgelber Sterne.

S. BAILEYS Sternzählung in der großen Sagittariuswolke ist an anderem Orte (Ziff. 16) besprochen worden.

E. A. KREIKEN schätzt in seiner oben erwähnten Arbeit über die Farben schwacher Milchstraßensterne aus denjenigen Sternen der Scutumwolke, die wahrscheinlich dem Typus B angehören, nach KAPTEYS⁸ Methode die Entfernung dieser Wolke zu 1500 Parsec.

¹ Harv Circ 240 (1922).

² A N 231, S. 17 (1927).

³ Mt Wilson Contr 133 = Ap J 46, S. 64 (1917).

⁴ Mt Wilson Rep 1921.

⁵ Mt Wilson Contr 287 = Ap J 61, S. 114 (1925).

⁶ M N 87, S. 196 (1927).

⁷ A N 218, S. 109 (1923).

⁸ Mt Wilson Contr 82, S. 63 = Ap J 40, S. 103 (1914).

Dieselbe Entfernung fand H. PETERSSON¹ für die Aquilawolke westlich von γ Aquilae aus einer Bestimmung effektiver Wellenlängen von Sternen bis zur photographischen Größe 11,5. Eine etwas kleinere Entfernung wurde von C. SCHALÉN² auf Grund einer Spektralklassifizierung ermittelt.

Aus den nach ihrer Farbe wahrscheinlich zum Typus B gehörenden Sternen in der Umgebung von M37 bestimmten H. VON ZIEPEL und J. LINDGREN³ die Entfernung der Aurigawolke zu 2300 Parsec.

F. H. SEARES⁴ leitet aus den schwachen B-Sternen einiger Milchstraßengebiete (Selected Areas) in Taurus, Perseus, Scutum und Aquila vorläufig Entfernungen zwischen 7000 und 14000 Parsec ab.

P. DORG⁵ berechnet für die Milchstraße in Aquila aus langperiodischen Veränderlichen die Entfernung 3000 Parsec, aus Cepheiden 10000 Parsec.

Eine mathematisch-statistisch wohl ausgearbeitete Methode zur Bestimmung der Entfernungen und relativen Dichtigkeiten der Sternwolken ist zuerst von K. G. MALMQUIST⁶ angegeben worden. Für die Dichtigkeitsverteilung einer gewissen Klasse von Sternen innerhalb einer Sternwolke setzt MALMQUIST nach CHARLIER

$$D(r) = D_0 e^{-\frac{(r-r_0)^2}{2\sigma^2}}, \quad (30)$$

wo also die Dichtigkeit des Mittelpunktes D_0 , die mittlere Entfernung r_0 und die Dispersion σ zu bestimmen sind. Für die Leuchtkraftfunktion und die Verteilung der scheinbaren Größen werden keine bestimmten Funktionsformen eingeführt. Die erstere wird nur durch den Mittelwert M_0 und die Dispersion σ charakterisiert und die letztere durch den Mittelwert m_0 , die Dispersion α und die totale Sternanzahl N .

Für das „lokale System“ bekommt man nach CHARLIER, wenn $r_0 = 0$ gesetzt und mit N die Anzahl Sterne in dem räumlichen Winkel ω definiert wird,

$$\left. \begin{aligned} 5 \log q &= m_0 - M_0 - 0,792, \\ N_0 &= \omega \sqrt{\frac{\pi}{2}} D_0 \sigma^2. \end{aligned} \right\} \quad (31)$$

(Die absolute Größe M wird als die scheinbare Größe für die Einheit der Entfernung definiert.) MALMQUIST zeigt, daß für eine entfernte Sternwolke die Unbekannten aus den als bekannt vorausgesetzten Größen nach dem folgenden Schema berechnet werden können:

$$\left. \begin{aligned} \Phi_1\left(\frac{q}{r_0}\right) &= \sqrt{\alpha^2 - \sigma^2}, \\ 5 \log r_0 &= m_0 - M_0 - \Phi_1\left(\frac{q}{r_0}\right), \\ D_0 &= \frac{N}{\omega \sqrt{2\pi} \sigma (q^2 + r_0^2)}. \end{aligned} \right\} \quad (32)$$

Die Funktionen Φ_1 und Φ_2 sind in Tabelle 14 in Abkürzung nach MALMQUIST wiedergegeben. Für die Grenze einer Wolke kann $|r - r_0| = 3\sigma$ gewählt werden, da die Dichtigkeit für diese Entfernung vom Zentrum der Wolke nur 0,01 D_0 beträgt.

¹ Ark. Mat. Astr. Fys. 19A, Nr. 3 (1925). ² Ark. Mat. Astr. Fys. 18, Nr. 36 (1925).

³ K. Svenska Vet. Akad. Handl. 61, Nr. 15, S. 106 (1921).

⁴ Mt. Wilson Rep. (1921). ⁵ J. B. B. A. 35, S. 128 (1925).

⁶ K. Svenska Vet. Akad. Handl. (III) 4, Nr. 2 = Lund. Medd. Ser. II, 46 (1927).

Tabelle 14.

g/r_0	$\Phi_1(g/r_0)$	$\Phi_2(g/r_0)$	g/r_0	$\Phi_1(g/r_0)$	$\Phi_2(g/r_0)$
1,00	1,470	0,907	0,40	0,435	0,671
0,90	1,317	,891	,30	,264	,560
,80	1,153	,867	,20	,124	,404
,70	0,981	,836	,10	,032	,213
,60	,801	,797	,00	,000	,000
,50	,618	,745			

Für die Anwendung seiner Berechnungsmethode wählt MALMQUIST die Sterne im Farbenindexintervall 0,00 bis 0,24, was nahe der Harvard-Spektralklasse A entspricht. Die Leuchtkraftsfunktion dieser Sterne setzt sich aus zwei Frequenzfunktionen zusammen, die ein wenig voneinander verschiedene Werte von M_0 (Differenz etwa 1,6 Größenklassen) haben und von denen jede eine sehr kleine Dispersion zeigt.

Aus VON ZEIPELS und LINDGRENs Farbenbestimmungen in der Nähe von M37 findet MALMQUIST für die Aurigawolke, daß diese in einer Entfernung von ungefähr 1450 Parsec beginnt, ihre maximale Dichtigkeit bei 2900 Parsec aufweist und sich bis zu 4350 Parsec erstreckt. Für die maximale Dichtigkeit, pro Kubiksiriometer gerechnet, bekommt er

$$D_0 = 0,023 \pm 0,004.$$

Aus KREIKENS Farbenbestimmungen in der Scutumwolke findet er die entsprechenden Zahlen 1800, 3400 und 5000 Parsec und

$$D_0 = 0,055 \pm 0,011.$$

Aus eigenen Farbenbestimmungen¹ in der Umgebung des galaktischen Pols findet er für die Ausdehnung des „lokalen Systems“ in dieser Richtung 1090 ± 130 Parsec und eine Dichtigkeit der A-Sterne unserer Umgebung von

$$D_0 = 0,024 \pm 0,009.$$

Die Dichtigkeit der Wolken wäre also von derselben Größenordnung wie die Dichtigkeit des „lokalen Systems“.

KREIKEN² hat die HESS-Diagramme für die Aurigawolke und die Scutumwolke studiert. Er findet, daß die Verteilung der Sterne nach absoluter Größe und Spektraltypus dieselbe wie in der Sonnenumgebung zu sein scheint. In den absoluten Luminositätskurven der Wolken findet er ein sekundäres Maximum, das mit einem entsprechenden, von SHAPLEY gefundenen Maximum für die Kugelhaufen zusammenfällt. Die Entfernungen der Wolken ergeben sich zu $r = 2200$ bzw. 2400 Parsec, in ziemlich guter Übereinstimmung mit MALMQUISTs aus demselben Material hergeleiteten Worten.

Ein sehr brauchbares Verfahren zur Ermittlung der räumlichen Dichte für Klassen von kleiner Streuung in den absoluten Größen bedient sich der Relationen MALMQUISTs [Gl. (19) bis (22), Ziff. 18], um aus der „scheinbaren Leuchtkraftsfunktion“, nach Voraussetzung einer normalen Frequenzkurve und den beobachteten Sternzahlen in sehr direkter Weise die räumliche Verteilung numerisch zu berechnen, ohne jede Voraussetzung über die Dichtigkeitsfunktion. Die Voraussetzung einer normalen Fehlerkurve für die Leuchtkraftsfunktion scheint wegen der kleinen Streuung wenig bedenklich. Diese zuerst von MALMQUIST³ benutzte Methode ist von LINDBLAD und PETERSSON (l. c. Ziff. 19) auf A-Sterne und Riesen der späteren Spektralklassen in einigen Gebieten hoher galaktischer Breite an-

¹ Lund Medd Ser II, 37 (1927).

² B A N 5, S. 61 (1929).

³ Lund Medd 106 (1925).

gewendet worden, und auch von SCHALÉN in seiner eben behandelten Arbeit über die B- und A-Sterne in gewissen Milchstraßengebieten. Für die hellsten Milchstraßenpartien in Cygnus, Cepheus, Cassiopeia und Auriga findet SCHALÉN eine langsame kontinuierliche Abnahme der Sterndichtigkeit mit der Entfernung, im allgemeinen ohne deutlichen „Wolkeneffekt“. Dies ist besonders bemerkenswert, da die Korrelation zwischen Milchstraßenhelligkeit und der Zahl der Sterne pro Quadratgrad in SCHALÉNS Arbeit sehr ausgeprägt ist. Daß die hier gefundene scheinbare Abnahme der Sterndichtigkeit von einer Absorption im Raume verursacht sein kann, wird in Ziff 24 näher besprochen.

Ähnliche Ergebnisse, die auf eine prinzipielle Einheitlichkeit der Milchstraßenstruktur hindeuten, sind auch von A. D. MAXWELL¹ hergeleitet worden. Er hat mit einem spaltlosen Spektrographen in Verbindung mit dem Crossley-Reflektor der Licksternwarte eine Spektralklassifikation für Sterne in sechs Selected Areas in der Milchstraße bis zu einer Grenzgröße zwischen 13,5 und 14,0 ausgeführt. Dabei wurden Riesen und Zwergstern der späten Spektraltypen durch das Zyankriterium und durch die verschiedene allgemeine Intensitätsabnahme gegen kleine Wellenlängen (verschiedene Farbe) voneinander getrennt. Die Zentralpunkte der untersuchten Areale sind in Tabelle 15 aufgeführt.

Tabelle 15

Selected Area No.	R.A.	Decl.	Selected Area No.	R.A.	Decl.
64	19 ^h 58 ^m	+30° 0'	19	23 ^h 23 ^m	+60° 0'
40	20 47	+45 0	8	1 0	+60 10
18	21 24	+60 10	9	3 4	+60 20

Für die Statistik wurde auch Material aus dem DRAPER-Katalog und dessen Extension herangezogen. Die verschiedenen Spektralklassen zeigen im ganzen einander ähnliche Dichtigkeitsverteilungen. Die Dichtigkeit ist zuerst konstant bis zu Entfernungen zwischen 400 und 600 Parsec und erleidet von hier aus eine langsame Abnahme. Keine Andeutungen sekundärer Dichtigkeitsmaxima in großen Entfernungen sind vorhanden. Die Anzahl der schwachen Sterne ver trägt sich gut mit Dimensionen des galaktischen Systems von der Größenordnung 10000 Parsec. Die Frequenz der Zwergstern von spätem Typus in Vergleich mit den Riesen erscheint größer, als vorher für unsere nähere Umgebung angenommen worden ist, weshalb auch die Luminositätskurve einen stellernen Anstieg als VAN RIJNS Kurve für die absolut schwachen Größen zeigt.

Für die mittlere Farbe C als eine Funktion der photographischen Größe ergibt sich

$$C = -0,16 + 0,054 m,$$

in ziemlich guter Übereinstimmung mit den oben gegebenen Resultaten von SEARES und KREIERN.

Der Koeffizient von m stimmt auch mit dem theoretischen, von G. SHAIN² hergeleiteten Wert $+0,05$ überein. SHAIN geht von der Dichtefunktion nach KAPTEYN und VAN RIJN aus und berechnet aus der Luminositätskurve aller Sterntypen zusammen (KAPTEYN und VAN RIJN) und aus einer angenommenen Luminositätsfunktion für die B0- bis A5-Sterne separat das Verhältnis der Anzahl der B0- bis A5-Sterne zu der Anzahl der F-, G-, K-, M-Sterne für sukzessive scheinbare Größen und für verschiedene galaktische Regionen. Aus diesen Daten berechnet er für C

$$C = +0,48 + 0,05 (m - 7,0), \text{ Milchstraße, } B = 0^\circ,$$

$$C = +0,74 + 0,05 (m - 7,0), B = \pm (40^\circ \text{ bis } 90^\circ)$$

¹ Lick Bull 13, S. 68 (1927)² M.N. 86, S. 382 (1926).

Eine der MAXWELLSchen ähnliche Untersuchung hat C. J. KRIEGER¹ für die Scutumwolke ausgeführt. Die Arbeit umfaßt Sterne zwischen den Größen 5 und 18. Bis zu etwa der Größe 13 hat KRIEGER die Spektren der Sterne mit dem spaltlosen Spektrographen photographiert, und für schwächere Sterne hat er die Farbenindizes bestimmt. Es wurden in dieser Weise alle erreichbaren Sterne innerhalb gewisser kleiner Gebiete der Wolke untersucht. Wenn man die Häufig-

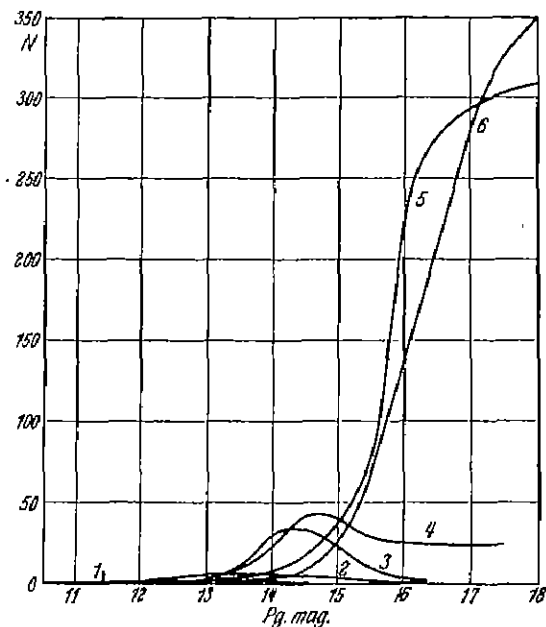


Abb. 19. Die Häufigkeit verschiedener Farbenklassen als Funktion der photographischen Größe in der Scutumwolke nach C. J. KRIEGER. Die in der Figur angegebenen Nummern haben folgende Bedeutung:

Nr.	Farbenindex	Nr.	Farbenindex
1	-0,60 bis -0,10	4	+0,40 bis +0,65
2	-0,10 „ +0,15	5	+0,65 „ +0,90
3	+0,15 „ +0,40	6	+0,90 „ +1,15

erscheinen und also jetzt gemäß den Entfernungsbestimmungen als mit der Wolke verbunden angesehen werden können. LINDBLAD² hat für M11 die Distanz 2500 Parsec gefunden und TRÜMLER³ (ohne Berücksichtigung der interstellaren Absorption) 2200 Parsec für M11 und 2750 Parsec für M26.

Wenn wir Vergleiche mit den Verhältnissen in der Umgebung der Sonne nach VAN RIJNS und MAXWELLS Resultaten anstellen, so erscheint die Scutumwolke ungefähr gleich reich an A-, F-, G-Sternen und an K-Sternen von der Riesensklasse und entschieden reicher an G-Sternen vom Zwergtypus, während die B-Sterne in der Wolke wahrscheinlich seltener als in unserer Umgebung sind. KRIEGER zieht den Schluß, daß für alle Klassen zusammen die Dichte der Wolke etwa die Hälfte der Dichte unserer Umgebung sein wird. Die Berücksichtigung

verschiedener Farbenklassen gegen die photographische Größe in einem Diagramm darstellt (Abb. 19), sieht man unmittelbar, in welchem hohem Grade die Farbe der schwächsten Sterne (Größen 15 bis 18) mit zunehmender Größe (abnehmender Leuchtkraft) wächst.

Die Dichtefunktion hat KRIEGER für verschiedene Spektralgruppen unter Berücksichtigung der Dispersion in absoluter Größe innerhalb der Gruppen gemäß der in Gleichungen (23) bis (25), Ziff. 18, skizzierten Methode bestimmt. Alle Spektralklassen geben eine ausgeprägte Trennung zwischen dem lokalen System und der Sternwolke (Abb. 20 bis 22). Für die Entfernung der Wolkenmitte von uns bekommt KRIEGER 2800 Parsec, was sich wohl mit MALMQUISTS oben zitiertem Wert von 3400 Parsec verträgt, wie auch mit KREIKENS letztem Wert von 2400 Parsec. Die Entfernung ist fast identisch mit den in ähnlicher Weise bestimmten Entfernungen der Sternhaufen M11 und M26, die am Himmel auf die Scutumwolke projiziert

¹ Lick Bull 14, S. 95 (1929).

² Mt Wilson Contr 228 = Ap J 55, S. 85 (Corr. S. 413) (1922).

³ Lick Bull 14, S. 154 (1930).

einer eventuellen Absorption des Lichts im interstellaren Raume würde aber, gleichzeitig mit einer Reduktion der Entfernungen, eine sehr erhebliche Korrektur zu jeder Schätzung der absoluten Dichte der Wolke geben

Miss L. SLOCUM¹ hat ganz kürzlich durch Farbenindexbestimmungen für 1500 Sterne zwischen den Größen 12 und 18,5 in den KAPTEJNSchen Feldern 8, 9, 18, 19, 64 die MAXWELLSche Arbeit fortgesetzt. Die Dichteverteilung im Raume wird unter Berücksichtigung einer allgemeinen Absorption im TRÜMLERSchen Sinne (Ziff. 24) hergestellt. Für die selektive Absorption ergibt sich aus 53 Sternen mit bekannten Spektrum und Farbenindizes der mit TRÜMLER nahe über-

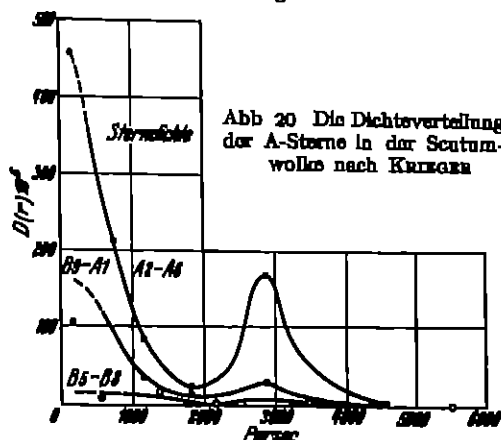


Abb. 20 Die Dichteverteilung der A-Sterne in der Scutumwolke nach KREGER

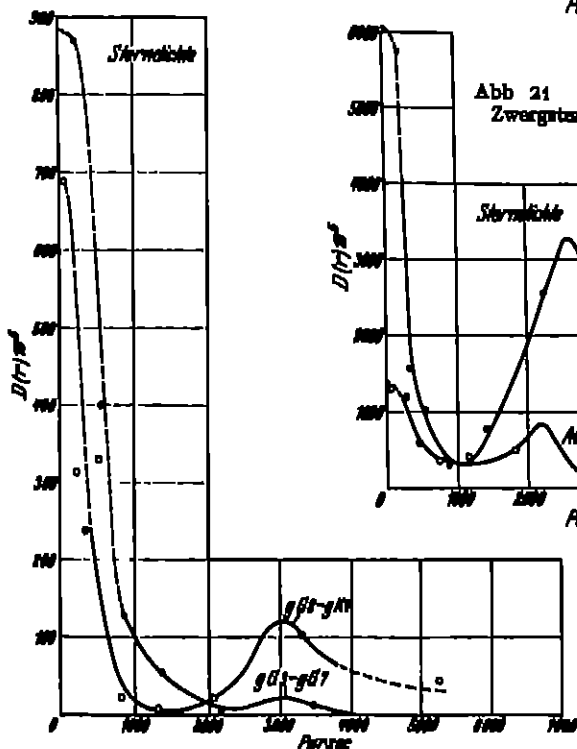


Abb. 21 Die Dichteverteilung der Zwergsterne in der Scutumwolke.

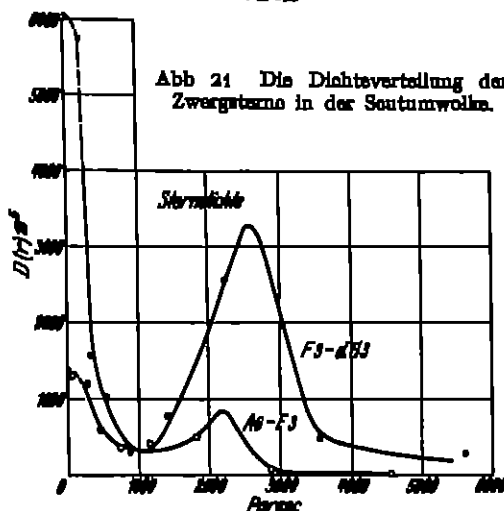


Abb. 22 Die Dichteverteilung der Riesensterne in der Scutumwolke

einstimmende Wert $+0^m,00034$ per Parsec, und es wird angenommen, daß dies etwa 0,4 der allgemeinen Absorption entspricht. Für die Dichte δ des absorbierenden Mediums wird ein Ausdruck $\delta = \delta' e^{-\mu' l}$, wo $\delta' = 2,4$, $\mu = 9000$, angesetzt; die Absorption nimmt also ziemlich schnell mit wachsender Entfernung ab. Die nach diesem Prinzip ermittelte Sterndichte nimmt mit steigender Ent-

¹ Lick Bull. 15, S. 123 (1931).

fernung ab, am schnellsten in unserer Nähe, zeigt aber eine Andeutung eines sekundären Maximums für $r = 2000$ bis 2500 Parsec, und in der Cygnusregion (Area 64) auch für $r = 6000$ Parsec. Das letztere Ergebnis stimmt mit den oben-erwähnten Entfernungsbestimmungen von KOPFF und PANNEKOEK für die Cygnuswolke überein.

28. Spezielle Untersuchungen über die Natur der MAGELLANSchen Wolken.

Wie schon in Ziff. 10 erwähnt, ist die Stellung der MAGELLANSchen Wolken eine ganz besondere. Die große Bedeutung dieser Gebilde in der gegenwärtigen Forschung können wir mit H. SHAPLEY¹ etwa folgendermaßen formulieren. Sie sind uns nahe genug gelegen, um vollständig in Millionen von Sternen aufgelöst zu werden, und doch entfernt genug, um ganz von außen her gesehen und untersucht zu werden. Sie dienen als Schlüssel zur Kenntnis entfernter Milchstraßen und eröffnen hierdurch den Weg aus lokalen Regionen in ein äußeres Universum hinaus. Die Spezialforschungen auf diesem Gebiete werden in anderen Teilen dieses Handbuchs ausführlich behandelt, und wir können hier nur in einer kurzen Übersicht die wichtigeren Punkte erwähnen.

Der große Reichtum der zwei Wolken an Nebeln und Sternhaufen wurde schon von J. HERSCHEL entdeckt, aber eine eigentliche astrophysikalische Untersuchung beginnt erst mit dem Anfang unseres Jahrhunderts durch die photographisch-photometrische Arbeit der Harvard-Sternwarte mit einem zu Arequipa aufgenommenen Plattenmaterial. Die ersten Früchte dieser Arbeit waren Miss H. LEAVITTs² Kataloge über die in den Wolken beobachteten veränderlichen Sterne, 808 in der großen, 969 in der kleinen Wolke. Die von Miss LEAVITT für 25 δ Cephei-Veränderliche in der kleinen Wolke gefundene Relation zwischen Periode und Helligkeit wurde zuerst von E. HERTZSPRUNG³ zu einer Entfernungsbestimmung dieser Wolke benutzt. SHAPLEYs Festlegung der Relation zwischen Periode und absoluter Größe für die δ Cephei-Sterne hat dann aber eine neue Bestimmung der Entfernungen der zwei Wolken herbeigeführt. Nach seiner letzten Revision der „Period-Luminosity Curve“ findet er aus 107 δ Cephei-Veränderlichen in der kleineren Wolke und 50 in der großen folgende Werte⁴:

Kleine Wolke	Große Wolke
$\pi = 0'',0000345$	$\pi = 0'',000038$
Entfernung ≈ 29 Kiloparsec	Entfernung $= 26,2$ Kiloparsec
$= 95000$ Lichtjahre	$= 86000$ Lichtjahre
Durchmesser ≈ 6000 Lichtjahre	Durchmesser $= 10800$ Lichtjahre

Die zur Zeit bekannten zehn Kugelhaufen in den Wolken haben scheinbare Durchmesser von 1 bis 2 Bogenminuten. Eine hierauf begründete Entfernungsbestimmung liefert mit den oben gegebenen sehr nahe identische Werte.

K. LUNDMARK⁵ hat für die große Wolke zur Entfernungsbestimmung außer den Kugelhaufen auch die WOLF-RAYET-Sterne und die offenen Haufen benutzt und findet im Mittel den Wert $\pi = 0'',000036$, der offenbar sehr gut mit dem oben gegebenen übereinstimmt.

Die MAGELLANSchen Wolken geben uns eine wichtige Gelegenheit, den Verlauf der Leuchtkraftfunktion im Gebiet der allerhellsten Sterne zu untersuchen, und sie geben uns auch Aufschluß über die absoluten Größen verschiedener Objekte von sehr großer Leuchtkraft, wie Nebel, Haufen und Sterne von gewissen abnormen Typen. Besonders die Untersuchungen von SHAPLEY⁶ und seinen Mitarbeitern sind hier erfolgreich gewesen. Zu erwähnen ist, daß einzelne

¹ Star Clusters, Harvard Monograph No. 2, S. 183 (1930).

² Harv Ann 60, S. 87 (1908). ³ A N 196, S. 201 (1913).

⁴ L. c. S. 189.

⁵ Obs 47, S. 276 (1924); Pop Astr Tidskr 5, S. 146 (1924).

⁶ Harv Circ 255, 260, 268, 271, 275, 276, 280, 288 (1924–1925).

Sterne die überaus hellen absoluten Größen -5 und -6 erreichen Einige rote Veränderliche der Spektralklassen K bis Mc und fünf Sterne vom P Cygni-Typus gehören zu den hellsten Sternen der großen Wolke¹. Die Nebel sind im allgemeinen von einem diffusen, irregulären Typus, unter ihnen ist der Riesennebel 30 Doradus, mit einer absoluten Größe wahrscheinlich heller als -13 und einem Durchmesser von etwa 30 Parsec, besonders auffallend LUNDMARK bemerkt, daß dieser Nebel eine Anzahl von dunklen Flecken in der Nebelfläche zeigt, in genau derselben Weise, wie wir sie in vielen von den hellen Milchstraßennebeln sehen. Überhaupt sind in der großen Wolke dunkle Risse von verwickelter Natur vorhanden, die sehr an Erscheinungen in der Milchstraßenstruktur erinnern.

Die Spektren der Gasnebel² geben für die große Wolke eine Radialgeschwindigkeit von $+276$ km/sec und für die kleine $+168$ km/sec. HERTZSPRUNG³ hat die Hypothese aufgestellt, daß gewisse Differenzen in den Radialgeschwindigkeiten für die 17 beobachteten Nebel der großen Wolke sich im wesentlichen als eine Folge einer parallelen und gleich großen Bewegung dieser Nebel im Raume erklären. Es zeigt sich dabei, daß die Radialgeschwindigkeit der kleinen Wolke sich in diese Reihe einordnen läßt, so daß die zwei Wolken in der Tat eine gemeinsame Bewegung haben können. Als Konvergenzpunkt ergibt sich $\alpha = 4^h 34^m$, $\delta = -5^\circ,5$ und für die Geschwindigkeit relativ zur Sonne 625 km/sec.

Die Rotationstheorie der Milchstraße läßt uns aber das Problem der Bewegung der Wolken aus einem anderen Gesichtspunkt betrachten. J. H. OORT⁴ bemerkt, daß mit einer Geschwindigkeit der Sonne von 286 km/sec gegen einen Punkt $L = 55^\circ$, $B = 0^\circ$ (vgl. Ziff. 30) die Residuen der Radialgeschwindigkeiten die Werte $+41$ km/sec und -9 km/sec annehmen. Es ist also recht wahrscheinlich, daß die Wolken nur kleine Geschwindigkeit relativ zum Schwerpunkt des Systems besitzen.

W. J. LUYTEN⁵ hat, wesentlich auf dem Boden der HERTZSPRUNGSchen Hypothese, die möglichen Bahnformen der Wolken relativ zum Zentrum der Milchstraße unter verschiedenen Annahmen über die Masse des Milchstraßensystems diskutiert. Das Resultat ist äußerst unsicher, zeigt aber, daß auch mit einer verhältnismäßig hohen totalen Geschwindigkeit der Wolken relativ zum erwähnten Zentrum elliptische Bahnen nicht ausgeschlossen sind.

Gegen die Annahme einer direkten Zusammengehörigkeit der zwei MAGELLANschen Wolken mit den Milchstraßenwolken hat eine andere Auffassung behauptet, daß sie eher zu den extragalaktischen Nebeln gerechnet werden sollten, also Objekte sind, die zufälligerweise in die Nähe des Milchstraßensystems gekommen sind. Die letztere Meinung ist wohl zuerst von CLEVELAND ABBE⁶ klar ausgesprochen worden. Später hat LUNDMARK⁷ die Ähnlichkeit der großen Wolke mit dem Nebel NGC 4449 nachgewiesen und dann auch die überaus wichtige Beobachtung gemacht, daß die Wolken sogar als Typen für eine gewisse Klasse von Nebeln dienen können. Zu den auffallenderen Objekten von dieser Klasse gehört der Nebel NGC 6822, der eingehend von E. HUBBLE⁸ untersucht worden ist. In der neuesten Zeit steht man zwar ganz auf dem Boden der letzteren Auffassung, ist aber geneigt anzunehmen, daß die Wolken doch etwa als „ferne Begleiter“ dem Milchstraßensystem angehören (vgl. Ziff. 34).

Zuletzt sei hier erwähnt, daß D. WATTENBERG⁹ eine eingehende Besprechung der neueren Resultate über die Natur der MAGELLANschen Wolken gegeben hat.

¹ Miss CANNON, Harv Bull 754 u. 801 (1921, 1924).

² Lick Obs Publ 13, S. 168 u. 187 (1918).

³ M N 80, S. 782 (1920); Nordisk Astr Tidsskr 1, S. 133 (1920).

⁴ B A N 4, S. 79 (1927). ⁵ Wash Nat Ac Proc 14, S. 241 (1928) = Harv Repr 44.

⁶ M N 27, S. 262 (1867). ⁷ K Svenska Vet Akad Handl 60, Nr 8 (1920).

⁸ Mt Wilson Contr 304 = Ap J 62, S. 409 (1923).

⁹ Naturwiss 18, S. 696 (1930); A N 237, S. 401 (1930).

24. Die Absorption des Lichts im interstellaren Raume. Wir haben schon oben in Ziff 18 und 20 die große Bedeutung der Frage, ob eine allgemeine Absorption im interstellaren Raume existiert, für die Erforschung der räumlichen Dichteverteilung im Milchstraßensystem hervorgehoben. SELLIGER und KAPTELYN hatten beide einen Höchstbetrag der Absorption berechnet unter der plausiblen Annahme, daß die wahre räumliche Dichte für große Entfernungen nicht erheblich anwachsen kann. KAPTELYN¹ hat λ/B aus dieser Erwägung einen Höchstbetrag von ein paar tausendstel einer Größenklasse pro Parsec angegeben, während SELLIGER nach dem in Ziff 18 erwähnten Prinzip, welches eine bestimmte Funktionsform für die „scheinbare“ Dichteverteilung einschließt, nur einen noch erheblich kleineren Absorptionskoeffizient zugeben wollte. Da eine Absorption der genannten Art sehr wahrscheinlich mit der Wellenlänge veränderlich sein wird, wurde das Interesse zunächst auf die Frage nach der Existenz einer selektiven Absorption geführt. Man hat so wiederholt versucht, eine direkte Abhängigkeit der Farbe der Sterne von ihrer Entfernung festzustellen. Anscheinend positive Resultate in dieser Hinsicht wurden von KAPTELYN, JONES, KING, VAN RIJN u a.² hergeleitet. Diese Versuche gelangten aber zu einem gewissen Abschluß dadurch, daß das Problem durch eine deutliche Abhängigkeit der Farbe von der absoluten Größe innerhalb gewisser Spektraltypen kompliziert wurde, und vor allem dadurch, daß die Evidenz aus den Farbenbestimmungen in den Kugelhaufen und für extragalaktische Nebel entschieden gegen die Existenz einer allgemeinen selektiven Absorption sprach. Eine Untersuchung von K. LUNDMARK³ über die Variation der Flächenhelligkeit der extragalaktischen Nebel mit der Entfernung und von H. SHAPLEY und A. AMES⁴ über den Zusammenhang zwischen Durchmesser, photometrischer Größe und Entfernung für Nebel im Coma-Virgo-Gebiet setzten eine ungeheuer enge obere Grenze auch für eine nichtselektive allgemeine Absorption. In derselben Richtung geht auch VAN RIJNS⁵ Resultat aus einem Studium des Zusammenhanges zwischen Durchmesser und photometrisch bestimmter Entfernung für die Kugelhaufen wie auch SHAPLEYS in Ziff 20 erwähnte Folgerung betreffs der Umgebung des zentralen Verdunklungsgebietes in Sagittarius-Ophiuchus.

Die Idee, daß die „anthropozentrische“ Anordnung der Sterne, welche die nach allen Seiten abnehmende Sterndichte unserer Umgebung anzeigt, nur scheinbar sei und den Effekt einer Absorption darstelle, eine Idee, die wohl am konsequentesten von J. HÅLM⁶ durchgeführt worden ist, ist jedoch niemals ganz aufgegeben worden. Ganz kürzlich hat C. SCHALÉN⁷ die Frage auf Grund seiner oben (Ziff 22) besprochenen Arbeit über B- und A-Sterne in ausgewählten galaktischen Regionen aufgenommen. Für die Spezialgruppen höchster Luminosität (τ und $\tau-$ genannt) hat er untersucht, welcher Absorptionskoeffizient ν für konstante räumliche Dichte in der Milchstraßenebene voranzusetzen wäre. Wenn wir die Absorption in Größenklassen pro Parsec rechnen und diesen Koeffizienten mit α bezeichnen, so hat man $\alpha = 2,5 \log e \cdot \nu = 1,09 \nu$. Für die als normal betrachteten Regionen in Cepheus und Cassiopeia findet SCHALÉN

$$\alpha = 0,0005 \text{ mag/Parsec}$$

Für die Antigaregion mag der größer gefundene Wert vielleicht auf eine wirkliche Abnahme der Dichte in der Richtung vom Zentrum des Milchstraßensystems (in

¹ A J 24, S 115 (1904)

² Für die historische Entwicklung des Problems siehe besonders H. KIENLE, Die Absorption des Lichtes im interstellaren Raume. Jahrbuch der Radioaktivität und Elektronik 20, II 1 (1922)

³ M N 85, S 865 (1925)

⁴ Harv Bull 864 (1929)

⁵ B A N 4, S 123 (1928)

⁶ M N 77, S 243 (1917), 80, S 162 (1919).

⁷ A N 236, S 249 (1929)

der galaktischen Länge 330°) zurückgeführt werden. Auch in Cygnus findet er einen größeren Wert. Wenn die letztgenannten zwei Regionen mitgerechnet werden, kann man nach SCHALÉN als obere Grenze $\alpha < 0,0020$ mag/Parsec setzen.

SCHALÉNS Resultat wurde dann in sehr bemerkenswerter Weise durch R TRÜMPLERS¹ Untersuchung über die offenen Sternhaufen (Ziff. 20) bestätigt und ergänzt. Wenn wir die photometrisch ohne Berücksichtigung der Absorption bestimmte Entfernung eines Haufens mit r' , die wahre Entfernung mit r bezeichnen, so haben wir

$$\begin{aligned} m - M &= 5 \log r' - 5 \\ &= 5 \log r + \alpha r - 5 \end{aligned}$$

Wenn weiter d der scheinbare Durchmesser in Bogenminuten, D' und D die mit r' bzw. r gerechneten linearen Durchmesser in Parsec sind, haben wir

$$\begin{aligned} \log D' &= -3,536 + \log d + \log r' \\ \log D &= -3,536 + \log d + \log r \end{aligned}$$

Wir bekommen also

$$\log D' - \log D = \frac{\alpha}{5} r,$$

und im Mittel

$$\overline{\log D'} - \overline{\log D} = \frac{\alpha}{5} \bar{r}$$

Wenn wir jetzt eine Unterabtteilung von Haufen mit kleiner Streuung in $\log D$ betrachten, so können wir $\log \bar{D} = \log D$ setzen und für die direkt aus den scheinbaren Durchmessern gebildeten Differenzen

$$v' = \log D' - \log \bar{D}'$$

bekommen wir dann direkt

$$v' = \frac{\alpha}{5} (r - \bar{r}),$$

oder

$$v' = a + br,$$

wo

$$a = \frac{\alpha}{5} \bar{r}, \quad b = \frac{\alpha}{5}$$

r wird in sukzessiven Annäherungen aus der Relation

$$\log r + br = \log r'$$

ermittelt. TRÜMPLER hat für verschiedene galaktische Längen die Werte von α , für 1000 Parsec gerechnet, zusammengestellt (Tab 16)

Es besteht offenbar eine sehr gute Übereinstimmung zwischen SCHALÉNS und TRÜMPLERS Resultaten. TRÜMPLER macht jetzt die Annahme, daß diese Absorption nur in einer verhältnismäßig dünnen Schicht um die Zentral-ebene der Milchstraße herum besteht. Vielleicht ist diese Schicht nur etwa 200 bis 300 Parsec dick, in der Milchstraßenebene selbst aber wahrscheinlich sehr weitgestreckt und geht vielleicht als eine Trennungsfläche durch das ganze System hindurch.

Tabelle 16.

Galaktische Länge	α	m, σ
$330^\circ - 45^\circ$	0 ^m ,79	$\pm 0^m,09$
$45 - 110$,59	$\pm ,08$
$110 - 195$,87	$\pm ,17$
$195 - 330$	(,37)	$\pm ,16$
Alle	,67	$\pm ,07$

¹ Lick Bull. 14, S 154 (1930).

Auch die von SHAPIREY, HFRIZSPRUNG, SEARLES und WALLENQUIST konstatierten Farbenexzesse in gewissen offenen Haufen werden von TRÜMLER als Absorptionseffekte gedeutet. Wenn wir für den Exzeß E im Farbenindex

$$E = cr$$

ansetzen, bekommt TRÜMLER für den Koeffizienten

$$c = +0^m,32 \pm 0^m,03 \text{ (per 1000 Parsec)}$$

Da auch dieser Effekt nach TRÜMLERS Annahme an die dünne absorbierende Zentralschicht gebunden ist, erklärt sich ungezwungen, warum kein Farbeffekt für Kugelhaufen und extragalaktische Nebel konstatiert worden ist.

Der Farbeffekt für den Haufen NGC 663 und für Sterne, die auf diesen Haufen projiziert erscheinen, ist nach Beobachtungen von Å. WALLENQUIST und C. SCHALÉN von letzterem¹ diskutiert worden. Er findet für den Koeffizienten c den Wert $0^m,26 \pm 0^m,03$. Die Farbeffekte für entfernte Milchstraßensterne von frühem Typus haben P. VAN DE KAMP² und Y. ÖHMAN³ behandelt. Der erstere findet ein Resultat in enger Übereinstimmung mit TRÜMLER und leitet als besten Wert ab

$$c = +0^m,331 \pm 0^m,022 \text{ (per 1000 Parsec)}$$

Er sucht auch einen Einfluß der galaktischen Breite auf die Absorption zu finden, um daraus die Dicke der absorbierenden Schicht zu bestimmen. Er findet im Mittel aus dem Absorptionseffekt für verschiedene Klassen von entfernten Objekten (Haufen, B-Sterne, Nebel) eine Dicke dieser Schicht von 175 ± 50 Parsec. Dieser Wert muß aber noch als sehr unsicher betrachtet werden.

ÖHMAN deutet den oft ausgeprägten Farbenexzeß für schwache B-Sterne als einen Entfaltungseffekt und findet aus seinem Material den Koeffizienten $0,19$ mag per 1000 Parsec für ein Farbaquivalent, welches aus dem Intensitätsverhältnis für die Wellenlängen $\lambda 3912 \text{ Å}$ und $\lambda 4415 \text{ Å}$ im Spektrum gebildet ist. Dieses Resultat läßt sich gut mit TRÜMLERS und VAN DE KAMPS Farbenkoeffizienten vereinen, welcher für die Wellenlängen $\lambda 4300 \text{ Å}$ und $\lambda 5600 \text{ Å}$ gilt. Ein mit den obigen Ergebnissen sehr nahe übereinstimmendes Resultat $c = +0^m,34 \pm 0^m,03$ hat kürzlich Miss L. SLOCUM⁴ (vgl. Ziff 22) ermittelt.

K. F. BÖTLINGER und H. SCHNELLER⁵ haben endlich auf einen anderen Effekt der absorbierenden Schicht hingewiesen. Es wird die Absorption in einer derartigen Zentralschicht zur Folge haben, daß eine Klasse von Objekten, die eine erhebliche Konzentration gegen die Milchstraßenebene zeigen, für größere Entfernungen scheinbar eine zu kleine Konzentration aufweisen wird. Denn berechnet man die Entfernungen ohne Berücksichtigung der Absorption, so daß diese für schwache Sterne zu groß ausfallen, so wird der Abstand von der Mittelebene $Z = R \sin b$ entsprechend zu groß. Je weiter also die Sterne entfernt sind, desto größer wird ihr mittlerer Abstand von der galaktischen Ebene sich errechnen. In der Tabelle 17 sind die mittleren Z -Koordinaten, erstens ohne Berücksichtigung der Absorption, zweitens (Z') mit der TRÜMLERSchen Absorption $\alpha = 0^m,67$ und zuletzt (Z'') mit einer Absorption $\alpha = 2^m$ pro 1000 Parsec gerechnet. Für diesen größeren Wert der Absorption finden BÖTLINGER und SCHNELLER einige Stütze in SCHALÉNS Resultaten für die Cygnus- und Aurigaregionen.

¹ Ark. Mat. Astr. Fys. 22A, Nr. 15 (1930) = Upsala Medd. 49

² A. J. 40, S. 145 (1930)

³ Spectrophotometric Studies of B-, A- and F-Type Stars. N. Acta Reg. Soc. Sc. Upsalensis (IV) 7, Nr. 3 (1930) = Upsala Medd. 48

⁴ Lick Bull. 15, S. 123 (1931)

⁵ Z. f. Astrophys. 1, S. 339 (1930)

Tabelle 17

Entfernungsbereich in Kiloparsec	Anzahl der Sterne	\bar{x}	$ \bar{x} $	\bar{x}^2	$ \bar{x}^2 $	\bar{x}''	$ \bar{x}'' $
0—1	38	597	71	491	59	394	48
1—2	33	1524	111	1066	77	747	54
2—3	26	2442	139	1482	85	991	55
3—4	26	3508	148	1862	79	1174	48
4—6	22	4908	144	2282	66	1386	37
6—12	10	8486	438	2975	163	1723	94
12—25	16	16385	448	4062	108	2182	57

Die stellarastronomische Bedeutung der Absorption liegt vor allem darin, daß die empirische Grundlage, auf welche die um die Sonne rotationsymmetrische Anordnung des „typischen“ Sternsystems und später des „lokalen“ Systems gegründet wurde, sich auflösen beginnt. Es wird hier mehr und mehr offenbar, daß die Verteilung der Materie in der Milchstraßenebene bis zu sehr großen Entfernungen von uns als wesentlich gleichförmig anzusehen ist, und daß wir berechtigt sind, jeder angeprägt „anthropozentrischen“ Anordnung der Materie im System mit Mißtrauen zu begegnen.

Die physikalische Erklärung der Absorption steht noch im wesentlichen offen.

25. Die Kalziumwolken in der Milchstraße. Ein Phänomen, das vielleicht mit der oben behandelten Extinktion in einer mittleren Milchstraßenschicht in Beziehung steht, haben wir in dem im Jahre 1904 von HARTMANN¹ entdeckten Absorptionseffekt der sog. „ruhenden“ Kalziumlinien. J. HARTMANN fand, daß im Spektrum des spektroskopischen Doppelsterns δ Orionis die K-Linie die periodische Verschiebung der Linien nicht zeigte und schloß daraus, daß irgendwo auf der Verbindungslinie zwischen uns und dem Stern eine Wolke existiert, die eine Absorption in der erwähnten Linie hervorruft. Er machte auch die Beobachtung, daß im Spektrum von Nova Perseus die H- und K-Linien wie auch die D-Linien als scharfe Absorptionslinien, die einer kleinen konstanten Radialgeschwindigkeit (+7 km/sec) entsprechen, vorhanden waren. Scharfe Kalziumlinien sind bald darauf von E. B. FROST und W. S. ADAMS² im spektroskopischen Doppelstern 9 Camelopardalis beobachtet worden und FROST³ machte einige Jahre später Mitteilungen über scharfe Kalziumlinien in den Spektren von 25 Sternen. Die Linien sind dann oftmals in den Spektren der spektroskopischen Doppelsterne identifiziert worden. Das Auftreten der H- und K-Linien in den Novae hat auch J. EVERAARD⁴ diskutiert. Die aus diesen Linien ermittelten Radialgeschwindigkeiten für Nova Perseus, Nova Geminorum Nr 2 und Nova Aquilae wie auch für sechs spektroskopische Doppelsterne deuten an, daß die Bewegungen dieser Sterne fast ganz der Sonnenbewegung entsprechen, und daß also das Kalzium sich sehr nahe in Ruhe relativ zum Zentroid der uns umgebenden Sterne befindet. R. H. CURRIE⁵ hat allerdings eine langsame Veränderung der Geschwindigkeit aus den H- und K-Linien für die Nova Geminorum 1912 konstatieren wollen, während für Nova Aquilae 1918 und die Nova Cygni 1920 die Linien stationär erscheinen.

Die stationären D-Linien wurden von MISS HEGGER⁶ studiert. Eine Zusammenfassung des Beobachtungsmaterials und eine eingehende Diskussion des ganzen Problems wurde zuerst von R. K. YOUNG⁷ ausgeführt. H. LUDENDORFF⁸

¹ Sitzber K Akad Wiss Berl (1904), S 527, Ap J 19, S 268 (1904)

² Ap J 19, S 350 (1904) ³ Ap J 29, S 234 (1909) ⁴ Obs 42, S 85 (1919).

⁵ Pop Astr 33, S 167 (1925) ⁶ Liek Bull 10, S 59 (1919); 10, S 141 (1921).

⁷ Publ Astrophys Obs Victoria 1, S 219 (1920), J Can R A S 14, S 389 (1920)

⁸ A N 241, S 118 (1920), 242, S 11 (1921)

hat gefunden, daß die scharfen Linien speziell für die Heliumsterne mit besonders großen Massen auftreten und betont die Schwierigkeiten der verschiedenen Erklärungs-hypothesen. Die Theorie, daß die *K*-Linie in einer zu dem betreffenden Stern gehörigen Atmosphäre entsteht, erscheint nicht befriedigend, und die Annahme einer kosmischen Wolke reicht auch nicht aus, da bei einigen Systemen die *K*-Linie Verschiebungen in derselben Periode wie die übrigen Linien zeigt, wenn auch mit kleinerer Amplitude. Einen sehr erheblichen Schritt vorwärts bedeutet dann die Untersuchung der betreffenden Linien für die O-Sterne durch J. S. PLASKETT¹. Das Vorkommen der Linien in allen Typen früher als B3 und der wahrscheinlich interstellare Ursprung der Linien wird hier besonders betont. Eine partielle Oszillation der Linien in gewissen spektroskopischen Doppelsternen vom B-Typus kann durch eine Kombination der stationären interstellaren Linien mit den schwachen Kalziumlinien der Sternatmosphären selbst erklärt werden, da nach R. H. FOWLERS und E. A. MILNES theoretischer Arbeit die *H*- und *K*-Linien erst bei dem Typus B0 oder früher vollkommen verschwinden. Unter anderen, die sich mit dem Problem beschäftigt haben, befinden sich F. HENROTEAU² und H. KIENLE³, der eine eingehende Behandlung der Geschwindigkeitsdifferenzen Stein-Wolke in ihrer Abhängigkeit vom Spektraltypus gegeben hat. Auflösungen für die Sonnenbewegung haben z. B. HENROTEAU⁴ und G. STROMBLER⁵ gegeben. J. WOLJER jr.⁶ hat der Ansicht PLASKETTS eine weitere theoretische Begründung gegeben.

Ein weiterer Fortschritt zur Deutung der stationären Linien war insbesondere A. S. EDDINGTON⁷ theoretische Behandlung des Problems. PLASKETT und WOLJER hatten den Gedanken ausgesprochen, daß die Kalziumatome vorzugsweise in der Nähe der heißeren Sterne die für das Auftreten der *Ca*⁺-Linien notwendige Ionisation erleiden. Gegen diese Ansicht hebt EDDINGTON hervor, daß die relative Konzentration der *Ca*⁺-Atome in der Nähe der heißeren Sterne als eine Folge einer zweimaligen Ionisation abnehmen muß, und er zieht den Schluß, daß die Absorption gleichmäßig langs dem Visionsradius vor sich geht. Eine außerordentlich dünne, allgemein ausgebreitete Materie aus Kalzium und anderen Elementen kann in genügend großer Menge vorkommen, ohne in meßbarer Weise die scheinbare Leuchtkraft oder die Farbe der Sterne zu ändern.

Die Temperatur der interstellaren Materie in einem gewissen Punkte ist nach EDDINGTON auf Grund der Geschwindigkeiten der durch Strahlungsionisation aus den Atomen gelösten Elektronen von derselben Größenordnung wie die Temperatur, die der spektralen Energieverteilung der Strahlung in dem betreffenden Punkte entspricht. Für diese Temperatur *T* kann aber die Temperatur der umgebenden Sterne, etwa 10000°, gesetzt werden. Wenn wir mit $I(\nu, T) d\nu$ die Strahlungsdichte bei thermodynamischem Gleichgewicht für ein Frequenzintervall zwischen ν und $\nu + d\nu$ und für die Temperatur *T* bezeichnen, so setzt EDDINGTON für die Dichte der Strahlung im interstellaren Raume

$$I(\nu, T) d\nu / \delta,$$

wo δ als „factor of dilution“ auftritt. Man hat dann die Regel, daß die Ionisationsverhältnisse der interstellaren Materie von der Dichte ρ dieselben sind wie in Materie von der Dichte $\rho\delta$ in thermodynamischem Gleichgewicht bei der Tem-

¹ Publ. Astrophys. Obs. Victoria 2, S. 335 (1924), M.N. 84, S. 80 (1924)

² J. Can. R.A.S. 15, S. 62 (1921)

³ SEELIGER-Festschr., S. 38 (1924), M.N. 84, S. 583 (1924)

⁴ J. Can. R.A.S. 14, S. 234 (1920)

⁵ Mt. Wilson Contr. 243 = Ap. J. 61, S. 372 (1925)

⁶ B.A.N. 2, S. 125 (1925)

⁷ London R.S. Proc. 111 A, S. 424 (1926), The Internal Constitution of the Stars, S. 377 Cambridge 1926

peratur T . Der Ionisationsgrad wird nämlich durch Gleichsetzung der Anzahl eingefangener Elektronen mit der Anzahl durch Ionisation ausgelöster erhalten. Die erstere Anzahl ist proportional der Elektronendichte, die letztere der Strahlungsdichte. Eine Multiplikation von beiden mit einem Faktor δ ändert das Gleichgewicht nicht. Der Faktor δ kann aus dem Gesamtbetrag des Sternenlichts berechnet werden; für ρ nimmt EDDINGTON gemäß einer isothermen Gleichgewichtstheorie für die diffusen Nebel, die als Kondensationen in der interstellaren Materie angesehen werden können, die Größenordnung 10^{-22} g/cm³. Er erhält dann nach der Ionisationstheorie für die relativen Konzentrationen der verschiedenen Ca- und Na-Atome folgende Werte

$$\frac{\text{Ca}}{\text{Ca}^+} = \frac{1}{300000}, \quad \frac{\text{Ca}^+}{\text{Ca}^{++}} = \frac{1}{400}, \quad \frac{\text{Na}}{\text{Na}^+} = \frac{1}{1000000}.$$

Für Ca wäre also der weit überwiegende Teil der Atome zweimal ionisiert und demnach zur Absorption in H und K unfähig. Ein analoges Verhältnis ergibt sich für die D -Linien des neutralen Natriums. Nur ein sehr kleiner Teil der interstellaren Materie von der angenommenen Dichte wäre also bei der Absorption in den erwähnten Linien wirksam, was auch mit den schwachen Intensitäten der Linien in den Sternspektren in Übereinstimmung steht.

In O. STRUVE¹ Arbeiten wurde das Problem auch empirisch von einer neuen Seite her angegriffen. Vorzugsweise für Sterne vom Spektraltypus O bis B₃ hat er auf Spektrogrammen die Intensität der interstellaren K -Linie geschätzt. Das Arbeitsmaterial bildeten zuerst für 321 Sterne vom Typus O bis B₃ Spaltspektrogramme, die auf den Sternwarten Mount Wilson, Victoria, Lick und Yerkes aufgenommen worden sind, dann für 1718 Sterne vom Typus O bis B₃ und für 338 Sterne von späteren Typen Objektivrismenplatten aus der großen Sammlung der Harvard-Sternwarte. Die Intensitäten wurden in einer Gedächtnisskala geschätzt, wo jede sukzessive Stufe einer eben bemerkbaren Zunahme der Intensität entspricht. Für die Spaltspektrogramme ist die Intensität der K -Linie im Spektrum der Vega auf 10 fixiert worden, später wurde der Stern η Cephei ($\alpha = 21^h 35^m, 2$, $\delta = +61^\circ 38'$, B_{2p}; 4^m, 7) als Standard mit derselben Intensität benutzt. Der wahrscheinliche Fehler einer Schätzung war 0,5 Stufen für die Platten der ersten Art und etwa 1,0 für die Harvard-Platten. Nach einer genäherten Kalibrierung der Skala entspricht jede Stufe einer Größendifferenz von etwa 0^m,1 in dem Intensitätsverhältnis zwischen Linienmitte und umgebendem kontinuierlichen Spektrum.

Mit seinem vollständigen Material hat STRUVE ausführlich die Relation zwischen Intensität, Spektraltypus und scheinbarer Größe untersucht. Tabelle 18 zeigt das Resultat für die Spektraltypen O bis B₃. Für die späteren Unterabteilungen des B-Typus übt schon die Absorption des Kalziums in der Sternatmosphäre einen merklichen Einfluß auf die Intensität der K -Linie aus.

Man sieht aus der Tabelle unmittelbar, daß für alle Untertypen die Intensität in derselben Weise mit abnehmender scheinbarer Helligkeit wächst, und auch daß für eine und dieselbe scheinbare Größe die früheren Typen in der Regel die größere Intensität aufweisen. Diese Erscheinungen können am einfachsten dadurch erklärt werden, daß die Intensität einfach eine Funktion der Entfernung der Sterne ist. Daß der Gang mit der scheinbaren Größe nicht auf irgendeinen systematischen Fehler zurückzuführen ist, beweist STRUVE durch Schätzungen der Linie $\lambda 3924$ (Si⁺⁺). Die mittlere Intensität dieser Linie zeigt keine Abhängigkeit von der scheinbaren Größe.

¹ Pop. Astr. 33, S. 639 (1925), 34, S. 158 (1926), A. N. 227, S. 377 (1926), Publ. A. S. P. 38, S. 211 (1926); Mt. Wilson Contr. 331 = Ap. J. 65, S. 163 (1927), Ap. J. 67, S. 353 (1928).

Tabelle 18

Scheib- Größe	O		B0		B1		B2		B3	
	n	I	n	I	n	I	n	I	n	I
0-1	0	—	0	—	1	1,0	0	—	0	—
1-2	0	—	2	2,0	4	0,7	3	0,9	1	0,4
2-3	3	0,9	6	1,2	5	1,8	7	1,4	11	1,4
3-4	1	5,1	2	2,6	5	1,4	10	1,7	24	1,8
4-5	6	3,9	9	2,6	11	3,0	18	3,0	97	2,1
5-6	12	4,1	21	4,2	8	4,0	23	3,3	141	2,5
6-7	17	4,2	45	3,4	11	4,2	42	3,2	201	2,0
7-8	24	5,0	66	3,8	17	3,8	85	3,9	197	3,2
8-9	19	4,8	94	3,9	4	3,0	87	3,9	168	3,1
9-10	9	3,8	55	3,7	0	—	44	4,3	74	4,0
10-11	3	3,7	2	4,8	0	—	7	4,4	15	4,6
11-12	1	11,0	0	—	0	—	0	—	0	—
Allg	95	4,40	302	3,71	66	3,13	326	3,65	929	2,97

Die mittleren Intensitäten für verschiedene Milchstraßenregionen werden nach STRUVE in Abb 23 dargestellt

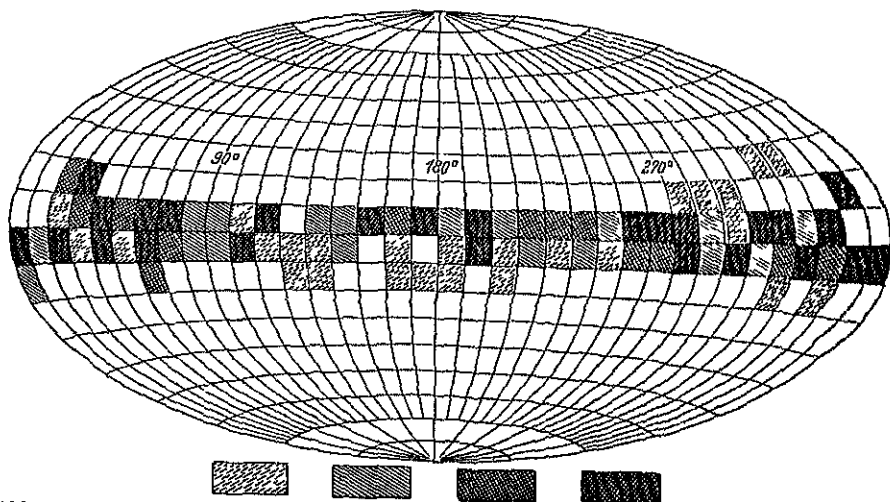


Abb 23 Galaktische Verteilung der Kalziumintensitäten. Die vier Schattierungen entsprechen der Reihe nach $I < 2,8$; $2,8 \leq I < 3,2$; $3,2 \leq I < 3,7$; $3,7 \leq I$. Die galaktischen Koordinaten der wichtigeren Regionen sind

Perseus	$L = 100^\circ - 120^\circ$	$B = -10^\circ$ bis $+10^\circ$	(sehr stark)
Orion	$160 - 180$	-10	(sehr schwach)
Monoceros	$170 - 180$	0	(sehr stark)
Carina	$250 - 260$	-10	(stark)
Cruce	$260 - 280$	$+10$	(sehr stark)
Scorpius	$300 - 320$	-10	(stark)
Sagittarius	$330 - 340$	$+10$	(stark)
Cygnus	$30 - 50$	0	(stark)
Cepheus	$60 - 80$	-10	(sehr stark)
		$+10$	(sehr stark)

Es besteht eine Andeutung, daß im Intervall zwischen den galaktischen Längen 80° und 250° die Intensitäten durchschnittlich schwächer sind als in der gegenüberliegenden Hemisphäre

STRUVE bemerkt, daß bei zusammengehörenden Doppelsternkomponenten die Linien mit derselben Intensität auftreten, und auch daß die Variation mit

der scheinbaren Größe innerhalb physisch zusammengehörender Sterngruppen, die ja bei dem B-Typus allgemein sind, aufhört. Für eine Milchstraßenregion in Cepheus wurde die Beziehung der Kalziumabsorption zu einer absorbierenden Dunkelwolke, deren Entfernung STRUVE auf Grund von Sternzählungen zu 350 Parsec schätzt, untersucht. Es stellt sich heraus, daß keine Spur einer direkten Verbindung zwischen den zwei Erscheinungen besteht, wenngleich die „Kalziumwolken“ und die Dunkelwolken vielleicht teilweise einander räumlich berühren und durchdringen.

Das eben beschriebene empirische Material haben B. P. GERASIMOVIČ und O. STRUVE¹ von theoretischem Gesichtspunkte aus eingehend behandelt. Mit dem von GERASIMOVIČ (vgl. Ziff 19) angegebenen mittleren Parallaxen der Untertypen der Hüllmaterie und unter plausiblen Annahmen über die Streuung in $\log \pi$ für Sterne von derselben scheinbaren Größe berechnen die Vorfasser den Absorptionskoeffizienten der interstellaren K-Linie. Im Falle der B3-Sterne wird für die wahrscheinliche Abweichung r in $\log \pi$, vom wahrscheinlichsten Wert $\log \pi_0$ gerechnet, nach GERASIMOVIČ der Wert 0,094 angenommen, während im Falle B0 bis B2 für r alternativ mit den zwei Werten 0,32 und 0,16 gerechnet wird. Für den Absorptionskoeffizienten β , per Parsec gerechnet, ergeben sich somit die Werte in Tabelle 19. Die Tabelle zeigt eine sehr gute Übereinstimmung

Tabelle 19 Mittlerer Absorptionskoeffizient für die interstellare K-Linie per Parsec.

Mittlere scheinbare Größe	B0 - B2		B3
	$r = 0,32$	$r = 0,16$	$r = 0,094$
2,5	1,1 $\cdot 10^{-4}$	2,8 $\cdot 10^{-4}$	1,3 $\cdot 10^{-4}$
3,5	1,1	2,8	3,0
4,5	1,7	4,2	3,6
5,5	2,0	5,0	4,2
6,5	1,6	4,0	4,4
7,5	1,6	4,0	4,1
8,5	1,4	3,5	3,6
9,5	1,3	3,2	2,9
10,5	1,3 $\cdot 10^{-4}$	3,2 $\cdot 10^{-4}$	3,7 $\cdot 10^{-4}$
Mittel	1,4 $\cdot 10^{-4}$	3,6 $\cdot 10^{-4}$	3,4 $\cdot 10^{-4}$

der β -Werte für die verschiedenen scheinbaren Größen einerseits und für die B0- bis B2-Sterne ($r = 0,16$) und die B3-Sterne andererseits. Man schließt aus diesen Resultaten, daß β bis zur Grenze der Beobachtungen konstant ist. Im Mittel ergibt sich $\beta = 3,4 \cdot 10^{-4}$ oder per cm gerechnet,

$$\beta = 1,1 \cdot 10^{-12}.$$

Die Theorie für die Absorption in der K-Linie gibt, wenn der EINSTEINsche Koeffizient A_{21} nach MILNEs Resultat für die Kalziumchromosphäre angenommen wird, die Anzahl N^+ der einmal ionisierten Kalziumatome per cm^3 in ihrer Beziehung zur totalen Absorption in der Linie. Für die letztere Größe wird gesetzt $\beta \Delta \lambda$, wo $\Delta \lambda$ die Breite der Linie, etwa 0,9 Å, ist. Wenn die Masse des Kalziumatoms in Rechnung gezogen wird, ergibt sich dann für die Dichte des einmal ionisierten Kalziums der Wert

$$Q_{0+} = 3,6 \cdot 10^{-12}.$$

Mit einer Strahlungstemperatur $T = 15300^\circ$ und einem „factor of dilution“ $W = 2,2 \cdot 10^{-17}$ ergibt die Ionisationstheorie, daß der weit überwiegende Teil

¹ Ap J 69, S 7 (1929)

der Kalziumatome im zweifach ionisierten Zustande (Ca^{++}) sein muß. Die totale Dichte des interstellaren Mediums ist natürlich außerdem dadurch bestimmt, in welcher Proportion das Kalzium überhaupt im Medium vorhanden ist. GERASIMOVIČ und STRUVE rechnen hier mit zwei alternativen Annahmen. Erstens wird die partielle Konzentration p der Kalziumatome gleich 1, zweitens gleich dem entsprechenden Wert für die Erdkruste, $1,5 \cdot 10^{-2}$, angenommen. In den zwei Fällen ergibt sich für die Totaldichte

$$5 \cdot 10^{-27} \text{ bzw. } 1 \cdot 10^{-26},$$

Werte, die sicher als extreme angesehen werden können. Da die interstellaren Wolken wahrscheinlich durch einen ständigen Ausfluß von Atomen aus den Sternatmosphären durch die Wirkung eines selektiven Strahlungsdruckes bedingt sind, so ist die Konzentration des Kalziums wahrscheinlich größer als in der Erdrinde.

Da nur der Bruchteil 10^{-11} von den Kalziumatomen im neutralen Zustande ist, so können wir gewiß nicht ein merkbares Auftreten der Linien des neutralen Kalziums in den Sternspektren erwarten. Außer den Linien H und K des Ca^+ -Atoms sollte aber auch die infrarote Doppellinie sichtbar sein. Von besonderem Interesse sind die Prinzipallinien vom Typus $1s-1d$, die vom Korrespondenzprinzip „verboten“ sind. Diese Übergänge sollten die zwei Linien im Rot $\lambda 7293,43 \text{ \AA}$ und $\lambda 7325,91 \text{ \AA}$ geben.

Y. ÖHMAN¹ hat die Möglichkeit für das Auftreten der Ca^+ -Linien in Emission im Spektrum des Nachthimmels diskutiert. Er kommt zu dem Schluß, daß die H - und K -Linien kaum zu erwarten sind, daß aber gewisse Möglichkeiten für die eben erwähnten „verbotenen“ Linien bestehen. Er betont, daß uns eventuelle Emissionslinien des interstellaren Kalziums Auskunft über die Dichte des Stratus und über die Dimensionen des Milchstraßensystems geben könnten.

GERASIMOVIČ und STRUVE diskutieren auch das interstellare Natrium, für welches jedoch gegenwärtig weit weniger Beobachtungsmaterial vorliegt. Sie gehen schließlich zu einer Diskussion der mittleren Radialgeschwindigkeiten des Kalziums für sukzessive Intervalle in galaktischer Länge über. Die Doppelwelle der OORTschen differentiellen Rotation der zentralen Milchstraßenschicht ist hier besonders deutlich ausgeprägt. Eine Auflösung nach der Formel

$$K + rA \sin 2(L - 325^\circ) = \bar{q},$$

wo \bar{q} die mittlere Radialgeschwindigkeit für die Länge L ist, gibt

$$rA = +5,3 \text{ km/sec} \pm 1,0 \text{ (w. F.)},$$

$$K = -0,6 \text{ km/sec} \pm 0,7 \text{ (w. F.)}$$

Eine weitere Diskussion der diesbezüglichen Fragen wird in Ziff 31 folgen.

Zuletzt sei hier noch erwähnt, daß O. STRUVE² im Verdunkelungsveränderlichen U Ophiuchi vom Typus B8 (nach STRUVE etwa B5) nahe dem Zeitpunkt der maximalen Trennung der stellaren K -Linien zwischen diesen Linien die interstellare K -Linie beobachtet hat. Der Stern zeigt auch interstellare Natriumlinien. Diese geben in guter Übereinstimmung mit der erwähnten K -Linie eine Radialgeschwindigkeit von -21 km/sec . Nach Abzug der parallaktischen Bewegung gibt dies für die Restgeschwindigkeit der interstellaren Linien $-3,5 \text{ km/sec}$. Die Erklärung des Verschwindens der interstellaren K -Linie für Typen später als B3 durch ein Überdecken der interstellaren Linie durch die stellare oder wenigstens durch eine in gewöhnlichen Fällen zu nahe Nachbarschaft der be-

¹ Nature, Aug 3 (1929)

² Ap J 72, S 199 (1930)

treffenden Linien im Spektrum gewinnt durch STRUVES Beobachtung sehr an Wahrscheinlichkeit.

Nach GERASIMOVIČ und STRUVE ist das interstellare Gas in seiner Gesamtmasse von nur geringer dynamischer Bedeutung. Die Totalmasse kann kaum $\frac{1}{100}$ der totalen Masse der Sterne betragen, und der Widerstandseffekt auf die Bewegungen der Sterne in ihren Bahnen muß verschwindend sein.

Andererseits ergibt sich die interstellare Materie als mögliche Quelle der harten kosmischen Strahlung. Wenn diese nach MILLIKANS Hypothese aus einer Transmutation von H in He herrührt, wäre mit der gegebenen Energiedichte der kosmischen Strahlung, $4 \cdot 10^{-16}$ erg/cm³, eine Transmutation eines gewissen Atomes einmal während 10^{20} Jahren zu erwarten. Das interstellare Gas ist aber als für die kosmische Strahlung fast vollkommen durchsichtig zu betrachten. Die monochromatische Absorption und eine Absorption für kurze Wellenlängen außerhalb der Seriengrenze ausgenommen, besteht die Durchsichtigkeit für alle Wellenlängen. Ein eventueller Zusammenhang mit dem absorbierenden Medium in der zentralen Milchstraßenzone kann daher wenigstens kein direkter sein.

g) Die Dynamik der Milchstraße.

26. Milchstraße und Gastheorie. Rotation der Milchstraße. Lord KELVIN und H. POINCARÉ¹ haben auf die Analogie zwischen den Sternen in der Milchstraße und den Molekeln eines Gases hingewiesen. Wenn wir das Gesamtsystem der Milchstraße ins Auge fassen, können wir die Sterne als eine große Menge materieller Punkte betrachten, die einander nach dem NEWTONschen Gesetze anziehen und die gegeneinander in jedem Augenblicke translatorische Bewegungen in allerlei Richtungen haben. Bei starken Annäherungen zwischen zwei Sternen werden die Bahnen nach den Gesetzen der hyperbolischen Bewegung geknickt. Die Repulsionskraft zwischen Gasmolekeln, die sehr schnell mit dem Abstände zwischen den Molekeln abnimmt, wird also hier durch eine NEWTONsche Attraktion ersetzt, die für ein einzelnes Sternpaar mit wachsender Entfernung unmerkbar wird. Wir haben also eine ziemlich bestechende Analogie. Das „Sterngas“ der Milchstraße muß aber als extrem verdünnt angesehen werden. Wenn wir den Aktionsradius eines Sterns so groß annehmen, daß ein Vortübergang eines anderen Sternes in dieser Entfernung eine Ablenkung der Bahnen von nur einem Bruchteil eines Grades verursacht, werden wir doch auf eine freie Weglänge geführt, die die wahrscheinlichen Dimensionen des Systems weit übertrifft.

Eine naheliegende Erklärung der augenscheinlich großen Abplattung des Sternsystems wäre, was wohl zuerst von J. HERSCHEL ausgesprochen wurde, die, daß das System als Ganzes eine allgemeine Rotationsbewegung besitzt und daß die Abplattung aus dem Gleichgewicht der Zentrifugalkraft mit der NEWTONschen Attraktionskraft folgt. POINCARÉ² hat gezeigt, daß für ein kontinuierliches Medium der Dichte ρ eine obere Grenze der Winkelgeschwindigkeit ω durch die Relation

$$\frac{\omega^2}{2\pi G \rho} < 1$$

gegeben ist, wo G die Gravitationskonstante bedeutet. Da im Sternsystem ρ sehr klein ist, wird ω auch sehr klein, und die minimale Rotationszeit T lang, von der Größenordnung 10^7 Jahre. (Diese Schätzung nach einem neueren Wert von ρ ergibt eine beträchtlich kleinere Grenze von T als POINCARÉs Wert von $5 \cdot 10^8$ Jahren.)

¹ Leçons sur les hypothèses cosmogoniques, S. 257. Paris 1911.

² B A 2, S. 109 (1885).

Da das astronomische Koordinatensystem ein Inertialsystem ist und die Lagebestimmungen, wie C V L CHARLIER hervorhebt, auf die invariable Ebene des Planetensystems übergeführt werden können, so wäre es möglich, in den Eigenbewegungen der Sterne einen solchen Rotationseffekt zu finden. Unter den ersten Versuchen, in den Eigenbewegungen einen Rotationseffekt aufzuspüren, ist vor allem derjenige von H GYLDÉN in einer unten (Ziff 31) näher besprochenen Arbeit aus dem Jahre 1871 zu nennen. Andere Untersuchungen rühren von E SCHONFELD¹, F BOLTE² und F RANCKEN³ her. I. SIRUVI⁴ führte Rotationsterme in die Gleichungen zur Bestimmung der Präzessionskonstante ein. CHARLIER scheint der erste zu sein, der einen ziemlich zuverlässigen Wert hergeleitet hat. Die letzte von ihm ausgeführte Bestimmung⁵ gibt eine mittlere Eigenbewegung in galaktischer Länge von $-0''.0024$, pro Jahr gezeichnet. CHARLIER macht die Bemerkung, daß eine retrograde Präzession der invariablen Ebene infolge einer dynamischen Einwirkung des umgebenden Sternsystems auf unser Planetensystem diesen Wert bedeutend erhöhen kann. Wir werden unten auf andere Bestimmungen eingehen und dabei auch bemerken, daß die mittlere Bewegung in galaktischer Länge (mit B bezeichnet) durch einen anderen Rotationseffekt, der auf einer in der Milchstraßenebene mit dem Abstände vom Zentrum varrierenden Winkelgeschwindigkeit beruht, wahrscheinlich vermindert wird und also nicht unmittelbar der Winkelgeschwindigkeit ω entspricht.

Eine Rotationsbewegung wurde weiter mit negativem Zeichen in die durch Anschluß an umgebende Sterne bestimmten Eigenbewegungen der „anagalaktischen“ Nebel eingehen, wenn diese, was gegenwärtig als gesichert angesehen werden kann, außerhalb des Sternsystems gelegen sind. Diesen Weg hat kürzlich K LUNDMARK⁶ eingeschlagen. Die Resultate geben wenigstens eine Andeutung von einem Effekt der oben genannten Art, aber das Material ist noch nicht für eine sichere Bestimmung hinreichend. Es gilt aber auch hier, daß nicht unmittelbar die Winkelgeschwindigkeit ω , sondern die Größe B gemessen wird.

27. Allgemeine statistische Mechanik des Sternsystems. Anstatt auf Grund der Analogie zwischen Sternodynamik und Gastheorie aus der letzteren Konsequenzen für die erstere zu ziehen, können wir von vornherein die Eigenschaften der Sterne als Massenpunkte einführen und eine statistische Mechanik auf Grund des NEWTONschen Gesetzes aufbauen. Wir begegnen hier sogleich einer großen Verschiedenheit zwischen Stern- und Gasdynamik. In dem Sternsystem ist nämlich die das System zusammenhaltende „reguläre“ Kraft nur eine Summe derjenigen Kräfte, die auch als Passage- oder Stoßkräfte auftreten, wenn die Sterne einander paarweise gegenübergestellt werden. Es läßt sich also nicht ohne weiteres um einen Stern ein Stoßbereich, der klein ist gegen die mittlere Distanz zwischen den Sternen und außerhalb dessen die Passagekräfte ignoriert werden können, absondern. Mit wachsender Entfernung vom betrachteten Stern aus haben wir es aber mit einem mehr und mehr komplizierten Zustand vielfacher Passagen zu tun, und die Passagekräfte gehen allmählich durch Summierung in die regulären Kräfte über. Wir können daher mehr oder weniger willkürlich eine obere Grenze für die Distanz der Passagen fixieren und nur den Einfluß der individuellen Vorübergänge innerhalb einer gewissen Sphäre in Rechnung

¹ V J S 17, S 255 (1882) ² Diss Bonn (1883)

³ A N 104, S 149 (1883), auch Diss Helsingfors

⁴ Mémoires de l'Académie Impériale de St Pétersbourg (VII) 35, Nr 3 (1887)

⁵ The Motion and the Distribution of the Stars. Mem Univ Calif 7, S 32 (1926)

⁶ Studies of Anagalactic Nebulae, S 38. Nova Acta Reg Soc Sc Upsala, Volumen extraordinarium (1927), Upsala Medd 30

ziehen. Die Kräfte der außerhalb dieser Sphäre gelegenen Massen werden dann in eine reguläre Kräfte-resultante zusammengesetzt.

J. H. JEANS¹ hat besonders den Einfluß der nahen Passagen auf die reguläre Bahn eines Sterns untersucht. Wenn wir mit σ den kleinsten Abstand zwischen zwei Sternen von den Massen M und M' bei einem Vorübergang, dem eine kleine Deflektion ψ der relativen Bahn entspricht, bezeichnen, so haben wir

$$\sigma = \frac{2G(M+M')}{\psi v^2},$$

wo v die relative Geschwindigkeit ist. Nehmen wir $\psi = 1^\circ$ und mit JEANS $M + M' = 6,8 \cdot 10^{33} \text{ g}$ ($= 3,4$ Sonnenmassen), $v = 4 \cdot 10^6 \text{ cm/sec}$ (40 km/sec), so finden wir $\sigma = 3,2 \cdot 10^{18} \text{ cm}$, einen Wert, der ungefähr siebenmal größer als der Durchmesser der Neptunbahn ist. Die mittlere Zeit t zwischen Passagen in Distanzen $\leq \sigma$ kann aus der guthooretischen Formel $t = \frac{1}{\pi \tau \sigma^2 v}$ berechnet werden, wo τ die Anzahl Sterne pro Volumeneinheit ist. Die mittlere Zeit zwischen den Passagen wird von der Größenordnung 10^{11} Jahre. Für Kollisionen innerhalb einer Distanz gleich dem Radius der Neptunbahn ergibt sich die mittlere Zwischenzeit zu $4 \cdot 10^{18}$ Jahre. Während sehr langer Zeiten können wir daher die sehr nahen Passagen ignorieren.

Für den kumulativen Effekt der Passagen zwischen den Distanzen σ_1 und σ_2 während der Zeit t leitet JEANS die Formel ab

$$v_n^2 = t \cdot \frac{6\pi\tau G^2 M'^2}{\sigma} \log \frac{\sigma_2}{\sigma_1}, \quad (1)$$

wo v_n die gegen die ursprüngliche Bewegungsrichtung senkrechte Geschwindigkeitskomponente eines Sterns ist. Wenn wir für σ_1 den obigen Wert von σ für $\psi = 1^\circ$ annehmen und nur die Passagen ziemlich naheliegender Sterne, innerhalb 20 Parsec, berücksichtigen, bekommen wir

$$v_n = \frac{1}{2} \sqrt{t}, \quad (2)$$

also eine transversale Geschwindigkeitserhöhung von $\frac{1}{2}$ cm/sec in einem Jahre und 1 km/sec nach 40000 Millionen Jahre. In dieser Weise hat JEANS bewiesen, daß der Einfluß der Passagen naheliegender Sterne in der ersten Approximation zu vernachlässigen ist, und daß die Sterndynamik in erster Linie das Problem der Bewegung unter den regulären Kräften des Systems enthält.

CHARLIER² hat nach dem Vorbild der kinetischen Gastheorie eine statistische Mechanik auf Grund des NEWTONschen Gesetzes entwickelt. Die Anzahl Sterne innerhalb des Volumenelementes $dx dy dz$ um den Punkt x, y, z herum, welche Geschwindigkeitskomponenten innerhalb $du dv dw$ um den Punkt u, v, w im Geschwindigkeitsraume herum haben, sei mit $f(x, y, z, u, v, w, t)$ bezeichnet. Die fundamentale Differentialgleichung der Verteilungsfunktion kann man in der BOLTZMANNschen Form

$$\frac{\partial f}{\partial t} + u \frac{\partial f}{\partial x} + v \frac{\partial f}{\partial y} + w \frac{\partial f}{\partial z} + X \frac{\partial f}{\partial u} + Y \frac{\partial f}{\partial v} + Z \frac{\partial f}{\partial w} = P(f) + Q(f) \quad (3)$$

ausdrücken, wo X, Y, Z die Komponenten der regulären Kraft im Punkte x, y, z sind. $P(f)$ ist die „Passagesfunktion“ und $Q(f)$ die „Kollisionsfunktion“. $P(f)$ wird wie in der kinetischen Gastheorie gemäß der Dynamik der Passagen als ein mehrfaches Integral ausgedrückt. Die Funktion $Q(f)$, die wirklichen Zusammenstößen der Sterne Rechnung trägt, wird im Hauptteil der CHARLIERSchen Arbeit

¹ Problems of Cosmogony and Stellar Dynamics, S. 224. Cambridge 1919

² Lund Medd Ser II, 16 (1917).

weggelassen, da sie während absehbarer Zeitraume keine Rolle spielt. CHARLIER entwickelt die Funktion f in eine Frequenzfunktion vom Typus A und leitet aus der BOLZMANNschen Gleichung für die Koeffizienten Differentialgleichungen ab. Für die obere Grenze der Distanz, innerhalb welcher eine Passage gerechnet wird, nimmt CHARLIER die halbe mittlere Entfernung zwischen den Sternen unserer Umgebung an.

Aus den Differentialgleichungen der Koeffizienten zweiter Ordnung leitet CHARLIER ab, daß eine ursprünglich ellipsoidische Verteilung der Geschwindigkeiten u, v, w mit der Zeit nach Gleichheit der Dispersion in verschiedenen Richtungen strebt. Die Zeit, in der ein Überschuß des Quadrates der Dispersion in einer Richtung auf $1/e$ seines Betrages reduziert wird, die „Relaxationszeit“, wird von CHARLIER zu $3,6 \cdot 10^{16}$ Jahren geschätzt. Die Langsamkeit der Wirkung der Sternpassagen ist also hier bestätigt worden.

C F LUNDAHL¹ hat CHARLIERS Auseinandersetzungen unter spezieller Berücksichtigung der Kollisionsfunktion fortgesetzt.

Da offenbar $\Gamma(f)$ und $\square(f)$ nur eine sehr langsame Veränderung der Frequenzfunktion f herbeiführen können, müssen wir zuerst in der BOLZMANNschen Gleichung Passagiefunktion und Kollisionsfunktion außer acht lassen und den Bewegungs- und Zustand des Systems unter der alleinigen Wirkung der regulären Systemkräfte X, Y, Z studieren. Wir haben also

$$\frac{\partial f}{\partial t} + u \frac{\partial f}{\partial x} + v \frac{\partial f}{\partial y} + w \frac{\partial f}{\partial z} + X \frac{\partial f}{\partial u} + Y \frac{\partial f}{\partial v} + Z \frac{\partial f}{\partial w} = 0 \quad (4)$$

zu setzen, wo

$$X = \frac{du}{dt}, \quad Y = \frac{dv}{dt}, \quad Z = \frac{dw}{dt} \quad (5)$$

Wir wollen jetzt die Lagen der einzelnen Partikeln (Steine) im generalisierten sechsdimensionalen Raume mit den Koordinatachsen x, y, z, u, v, w , betrachten. Als Ursprung für die Raumkoordinaten x, y, z können wir z. B. unseren eigenen Ort im System wählen, während wir für die Geschwindigkeitskomponenten $u = 0, v = 0, w = 0$ für den Schwerpunkt des Systems annehmen. Die Dichtigkeit ρ im gewöhnlichen dreidimensionalen x, y, z -Raume wird, wenn m eine mittlere Masse der Partikeln innerhalb einer Zelle $dx dy dz du dv dw$ ist,

$$\rho = \iiint_{-\infty}^{+\infty} m / du dv dw. \quad (6)$$

Diffuse gasförmige Materie im Raume denken wir uns über die Partikeln verteilt und in m eingerechnet. Wenn wir die Verteilung von ρ nach x, y, z für einen gewissen Augenblick festhalten, so können wir gemäß dieser Dichtigkeitsverteilung und gemäß den augenblicklichen Lagen und Geschwindigkeiten der Partikeln ihre Bahnen im sechsdimensionalen Raume berechnen. Das Gravitationspotential V wird nach POISSONS Gleichung bestimmt

$$\frac{\partial^2 V}{\partial x^2} + \frac{\partial^2 V}{\partial y^2} + \frac{\partial^2 V}{\partial z^2} = -4\pi G \rho \quad (7)$$

In der wirklichen Bewegung wird aber im allgemeinen Falle die Dichtefunktion ρ stetig modifiziert, wir wollen sagen durch eine Funktion $\Delta \rho$, welche von den Koordinaten x, y, z und der Zeit t abhängt. Wenn wir eine kontinuierliche Variation der Dichtigkeit ρ und der mittleren Geschwindigkeiten u, v, w mit x, y, z voraussetzen, so kann gemäß der Kontinuitätsgleichung

$$\frac{\partial \rho}{\partial t} + \frac{\partial (\rho \bar{u})}{\partial x} + \frac{\partial (\rho \bar{v})}{\partial y} + \frac{\partial (\rho \bar{w})}{\partial z} = 0 \quad (8)$$

¹ Lund Medd. Ser II, 45 (1926)

$\partial \rho / \partial t$ nie ins Unendliche wachsen. Wenn wir demgemäß während des Zeitelements Δt erster Ordnung das Integral $\iiint |\Delta \rho| dx dy dz$, über das ganze System erstreckt, als eine kleine Größe von der ersten oder von höherer Ordnung betrachten, so erscheinen „Störungskräfte“ erster oder höherer Ordnung mit Komponenten von der Form $\iiint \frac{\Delta \rho}{r^3} x dx dy dz$, wo r die Distanz von dem betrachteten Ort (Origo) bis zum Punkte x, y, z ist. In der Bewegung einer Partikel während des Zeitelements Δt erleiden daher die Geschwindigkeitskomponenten u, v, w „Störungen“ $\Delta u, \Delta v, \Delta w$ zweiter oder höherer Ordnung, während jedoch die entsprechenden $\Delta x, \Delta y, \Delta z$ von höherer Ordnung als der zweiten sind. Für die Berechnung der Dichtigkeitsverteilung nach einem kleinen Zeitintervall Δt von dem betrachteten Zeitpunkt an können wir daher bis auf Größen höherer Ordnung als der zweiten die wahre Bewegung der Partikeln durch die Bewegung in den augenblicklichen sechsdimensionalen Bahnen ersetzen. Wir können diese Bahnen auch als Stromlinien in der sechsdimensionalen Mannigfaltigkeit bezeichnen.

Wenn wir aber auf die Verhältnisse für längere Zeiten Rücksicht nehmen, werden infolge der Veränderungen des Kraftfeldes die Partikeln längs einer gewissen augenblicklichen Bahn über eine Serie verschiedener, mehr oder weniger benachbarter Bahnen eines späteren Zeitmoments gestreut. Dieser Umstand, wie auch die verschiedenen angulären Geschwindigkeiten in den Bahnen um den Schwerpunkt herum bewirken eine fortschreitende Mischung der Materie des Systems und eine stetige Ausgleichung der Frequenz zwischen einander benachbarten sechsdimensionalen Bahnen.

Wir nehmen jetzt an, daß eine weitgehende Mischung und Ausgleichung in der Materie des Systems stattgefunden hat. Wir teilen die Materie in eine Unzahl von augenblicklichen, sechsdimensionalen Bahnen, jede Bahn mit einer gewissen mittleren Dichtigkeit f , auf und setzen infolge der Mischung eine im wesentlichen regellose Verteilung der Partikeln längs einer Bahn voraus. Da die räumliche Dichtigkeit ρ aus einer Integration in u, v, w bestimmt wird, also aus einer Summierung über unendlich viele Bahnen, die den betrachteten Punkt durchkreuzen, so ist sie also, von kleinen Schwankungen abgesehen, als wahrscheinlich von der Zeit unabhängig zu betrachten. Die sechsdimensionalen Partikelbahnen werden dann stationär, und da wir die Verteilung in diesen Bahnen als regellos betrachten, so ist die a priori zu erwartende Frequenz f in einer solchen Bahn als von der Zeit unabhängig anzusehen, was mit der Gleichung

$$\frac{\partial f}{\partial t} = 0, \quad (9)$$

oder der daraus gemäß der Gleichung (4) folgenden

$$\frac{\partial f}{\partial w} dx + \frac{\partial f}{\partial y} dy + \frac{\partial f}{\partial z} dz + \frac{\partial f}{\partial u} du + \frac{\partial f}{\partial v} dv + \frac{\partial f}{\partial w} dw = 0 \quad (10)$$

äquivalent ist. Dieses Resultat stimmt mit einem Satz von POINCARÉ¹ überein, nach welchem in einem stationären Zustande die Dichtigkeit der Partikeln im generalisierten Raume der kanonischen Variablen $q_1, q_2, \dots, q_n, p_1, p_2, \dots, p_n$ längs der Bahn einer Partikel in diesem Raume konstant ist. Wenn die Bewegungsgleichungen k erste Integrale

$$I_1 = \text{konst.}, \quad I_2 = \text{konst.}, \quad \dots, \quad I_k = \text{konst.} \quad (11)$$

haben, so kann die Verteilungsfunktion

$$f(I_1, I_2, \dots, I_k) \quad (12)$$

¹ Leçons sur les hypothèses cosmogoniques, S. 100 (1911).

geschrieben werden, vorausgesetzt, daß die Bahn einer Partikel das Gebiet von $2n - k$ Dimensionen, welches durch die Gleichungen (11) definiert wird, ausfüllt.

Im aktuellen Falle betrachten wir jetzt sowohl die Lagen als die Geschwindigkeiten in bezug auf den Schwerpunkt des Systems. Für eine allgemeine Dichtungsverteilung haben wir nun ein erstes Integral, das Energieintegral

$$I_1 = u^2 + v^2 + w^2 - 2V = \text{konst} \quad (13)$$

Eine Verteilung $f(I_1)$ wird aber ein endliches Rotationsmoment der Masse ausschließen

Für einen stationären Zustand bei endlichem Rotationsmoment muß daher eine rotationsymmetrische Verteilung um eine gegen die fundamentale Rotationsachse senkrechte Achse vorausgesetzt werden. Die Frequenzfunktion kann dann geschrieben werden

$$f(I_1, I_2), \quad (14)$$

wo

$$I_2 = vx - uy, \quad (15)$$

wenn die xy -Ebene die Ebene maximaler Flächengeschwindigkeit des Systems ist. In dieser Form ist POINCARÉ'S Theorem speziell von JEANS¹ und von CHARLIER² aufgenommen und diskutiert worden. Die Existenz eines Gleichgewichtszustandes, welcher durch eine gewählte Funktion $f(I_1, I_2)$ bestimmt wird, unterliegt natürlich der Bedingung, daß POISSON'S Gleichung Genüge geleistet wird, d. h. daß V gemäß einer aus (14), (6) und (7) resultierenden Gleichung $\Delta V = \Psi(V, R)$ bestimmt werden kann, wo $R^2 = x^2 + y^2$.

In dem eben zitierten Werke hat POINCARÉ auch das wichtige Theorem von JACOBI, welches im Virialtheorem von CLAUSIUS enthalten ist, in die theoretische Behandlung der astrophysischen Partikelsysteme eingeführt. Eine Anwendung dieses Theorems auf den Bewegungszustand in Sternhaufen ist später von EDDINGTON³ gemacht worden. Wenn J das Trägheitsmoment in bezug auf den Koordinatenanfangspunkt, T die kinetische und W die potentielle Energie ($W = 0$ für unendliche Verdünnung des Systems) ist, so haben wir

$$\frac{1}{2} \frac{d^2 J}{dt^2} = 2T + W \quad (16)$$

Im stationären Zustande ist also

$$2T + W = 0 \quad (17)$$

JEANS⁴ hat dieses Theorem auf die Frage nach dem Ursprung des galaktischen Systems angewandt. Können wir uns z. B. denken, daß unser System aus einem Zusammenfließen von einzelnen kleineren Sternhaufen entstanden ist? Wenn T_1 und W_1 die kinetische und die potentielle Energie eines einzelnen Haufens vor dem Zusammenstoß mit anderen Haufen, U_1 die Translationsenergie des Haufens in bezug auf den gemeinsamen Schwerpunkt aller Haufen, T_0 und W_0 die kinetische und die potentielle Energie des resultierenden Systems sind, so gilt

$$T_0 + W_0 = \sum (T_1 + W_1 + U_1)$$

Wenn jeder Haufen vor dem Zusammenstoß in einem stationären Zustand sich befunden hat, so haben wir außerdem

$$2T_1 + W_1 = 0$$

und auch, sobald das große System stationär wird,

$$2T_0 + W_0 = 0$$

¹ M N 76, S 70 (1915)

² Lund Medd Ser I, 82 (1917)

³ M N 76, S 525 (1916)

⁴ M N 82, S 138 (1922), Astronomy and Cosmogony, S 377 (1929)

Man bekommt nach diesen Voraussetzungen sofort

$$W_0 = \sum W_1 + 2 \sum U_1 \quad (18)$$

Die Translationsenergie der Haufen wird also in potentielle Energie verwandelt, und in der Regel muß also eine gewaltige Expansion auf ein Zusammenfließen von der genannten Art folgen. Die große Ausdehnung des galaktischen Systems steht also durchaus nicht in Widerspruch zu einem eventuellen Ursprung in einer Kombination einer Anzahl viel kleinerer Systeme, die sich allmählich durch gegenseitige Einwirkungen auflösen.

Eine ausführliche geschichtliche Übersicht der hier behandelten Probleme und eine Weiterführung der Theorie des stationären Zustandes hat J. OHLSSON¹ gegeben. In Analogie mit einem Resultat der OHLSSONschen Arbeit beweist U. WEGNER² durch eine exakte Lösung der BOLTZMANNschen Gleichung für den Fall einer zweidimensionalen achsensymmetrischen Verteilungsfunktion von CHARLIERS Typus A, daß diese Funktion sich notwendig auf die MAXWELLSche Form $C \cdot e^{-\frac{1}{2}v^2 - \frac{1}{2}w^2}$ reduziert.

28. Theorie der Sternströmung im typischen Sternsystem. Die kapitale Entdeckung von KAPTEYN, daß die pekuliären Bewegungen der Sterne nicht regellos verteilt sind, sondern eine gewisse Richtung im Raume bevorzugen, die sehr nahe in der Milchstraßenebene gelegen ist, weckte die Hoffnung, dieses Phänomen als eine Eigenschaft eines stationären Zustandes deuten zu können, um damit über den Aufbau des Milchstraßensystems wichtige Schlüsse zu ziehen. Die erste Deutung des Phänomens im Sinne der KAPTEYNschen Zweistromtheorie sagt ja schon etwas in der Richtung einer dynamischen Erklärung aus, aber nichts zu der Frage, ob diese Bewegungsart eine stationäre Erscheinung an unserem Orte im System sein kann. H. H. TURNER³ stellte die Hypothese auf, daß die Sternströmung der ein- und ausgehenden Bewegung in Bahnen, die mit großer Exzentrizität um den Schwerpunkt des Systems verlaufen, entsprechen könne. Da der Vortex der Sternströmung ungefähr in der galaktischen Länge 340° liegt, also in der Gegend der hellsten Milchstraßenwolken, hatte diese Hypothese an sich eine nicht unerhebliche Wahrscheinlichkeit, würde aber eine sehr erhebliche zentrale Kondensation der Materie voraussetzen. Nach einer strengen Theorie gemäß den oben (Ziff. 27) gegebenen Auseinandersetzungen ist weiter in einem abgeplatteten System nur eine gegen den Radiusvector transversale Sternströmung möglich (vgl. unten JEANS) und kann eine radiale stationäre Sternströmung nur in Systemen von sphärischer Massenverteilung vorkommen.

Daß bei sphärischer Symmetrie eine radiale, überall ellipsoidische Sternströmung möglich ist, wurde zuerst von EDDINGTON⁴ nachgewiesen. Die außerdem einzige Möglichkeit einer überall streng ellipsoidischen Geschwindigkeitsverteilung (und zwar in einer nahe radialen Richtung) besteht nach EDDINGTON⁵ für ein abgeplattetes System, wenn das System ein Untersystem ist und die Gravitationskraft von einer vorherrschenden sphärischen Masse konstanter Dichte bestimmt wird.

Die Hypothese einer radialen Sternströmung wurde später praktisch außerhalb der Diskussion gelassen. JEANS suchte die Frequenzfunktion im stationären rotationsymmetrischen Zustande auf die Behandlung des Problems anzuwenden. In diesem Falle ist die Frequenzfunktion in der Form $f(I_1, I_2)$ zu schreiben, wo I_1 das Energieintegral und I_2 das Flächenintegral für die Symmetrieebene ist. JEANS führt zylindrische Koordinaten R, θ, z ein, wobei die entsprechenden

¹ Lund Medd Ser II, Nr 48 (1927). ² Zf Phys 45, S 539 (1927).

³ M N 72, S 387 (1912). ⁴ M N 75, S. 366 (1915).

⁵ M N 76, S. 37 (1915); Obs 41, S. 132 (1918).

linearen Geschwindigkeiten mit Π , Θ , Z bezeichnet werden. Das Flächenintegral ist dann $R\Theta$, und die Frequenzfunktion schreibt sich

$$f(\Pi^2 + \Theta^2 + Z^2 - 2V, R\Theta) \quad (19)$$

Die Geschwindigkeitsverteilung ist somit symmetrisch in Π und Z , eine preferentielle Strömung ist nur in Θ möglich, also in der Richtung senkrecht zum Radiusvector. Aus diesem Umstand schloß JEANS zuerst, daß die Sternströmung nicht als eine stetige Bewegung im Sternsystem gedeutet werden kann.

CHARLIER wies aber auf die Tatsache hin, daß die Heliumsterne in unserer Nähe um ein Zentrum in der galaktischen Länge 240° herum verteilt sind und daß die Richtung gegen dieses Zentrum nahezu senkrecht gegen die Verteilung der Sternströmung ist. Da weiter die stellastatistisch gefundenen Geschwindigkeitsellipsoide nahezu eine verlängerte, rotationssymmetrische Form haben, wird auch sehr nahe die Bedingung erfüllt, daß im stationären Zustande die Verteilung in den Komponenten Π und Z rotationssymmetrisch um die Θ -Komponente sein soll, wenn wir eine stationäre Bewegung um den Zentralspunkt der Heliumsterne annehmen. Diese Theorie kann mit der Anschauung eng verbunden werden, nach der die Heliumsterne den Kern eines „lokalen Systems“, einer Sternwolke innerhalb des größeren Milchstraßensystems, bilden. Eine obenerwähnte Arbeit von EDDINGTON zeigt jedoch, daß die Geschwindigkeitsverteilung bei transversaler Sternströmung nicht überall im System streng ellipsoidisch sein kann.

Auf einem ganz anderen Wege hat KARPEYN¹ einen großartigen Versuch gemacht, eine Dynamik des Sternsystems zu begründen. Er ging dabei von der empirisch gegebenen Sternverteilung im typischen Sternsystem aus, berechnete unter einigen vereinfachenden Annahmen die Gravitationskraft (zunächst in einer willkürlichen Einheit) in verschiedenen Punkten des Systems und suchte dann die empirischen Ergebnisse der Geschwindigkeitsverteilung in diesen Rahmen hineinzupassen. Für die Abhängigkeit der Dichte von der Höhe über der galaktischen Ebene wird die barometrische Gleichung angewandt; es ergibt sich dabei, daß die mittlere Masse der Sterne, die den Absolutwert der Gravitationskraft bestimmt, von 2,2 Sonnenmassen in unserer Nähe auf 1,4 für die äußerste berücksichtigte Dichteschale abnimmt. Für das Gleichgewicht in der galaktischen Ebene ist eine Rotationsbewegung notwendig, die für größere Distanzen nahezu konstant und gleich 19,5 km/sec wird. Die Sternströmung wird durch zwei einander entgegengesetzte Rotationsbewegungen erklärt, die also eine relative Geschwindigkeit von rund 40 km/sec, in Übereinstimmung mit dem empirisch gefundenen Wert, gibt. Das Zentrum soll in einer gegen die Sternströmung senkrechten Richtung, in einem Abstände von ca. 650 Parsec, gesucht werden.

Die KARPEYNSchen Resultate veranlaßten JEANS² zu einer mathematisch sehr eleganten Behandlung des Problems. Von der oben gegebenen Form der Frequenzfunktion im rotationssymmetrischen Falle ausgehend, bildet JEANS die quadratischen Momente der Geschwindigkeitskomponenten, d. h. die Mittelwerte $\overline{\Pi\Theta}$ usw. Wenn ν die Anzahl Sterne pro Volumeneinheit bedeutet, erhält man

$$\nu \overline{\Pi\Theta} = 0, \quad \nu \overline{\Pi Z} = 0, \quad \nu \overline{\Theta Z} = 0, \quad \nu \overline{\Pi^2} = \nu \overline{Z^2},$$

JEANS schreibt

$$\nu \overline{\Pi^2} = \nu \overline{Z^2} = p, \quad \nu \overline{\Theta^2} = q \quad (20)$$

¹ Mt Wilson Contr. 230 = Ap J 55, S. 302 (1922)

² M N 82, S. 122 (1922)

und zieht dann zur weiteren Behandlung des Problems die Gleichungen der Massenbewegung in einem System materieller Punkte heran, die unter Verwendung rechtwinkliger Koordinaten von der folgenden Form sind

$$\frac{d}{dt}(\nu \bar{u}) + \frac{\partial}{\partial x}(\nu \bar{u}^2) + \frac{\partial}{\partial y}(\nu \bar{u}v) + \frac{\partial}{\partial z}(\nu \bar{u}w) = \nu \frac{\partial V}{\partial x}. \quad (21)$$

Im stationären Zustande verschwindet der erste Term. Wichtig ist zu bemerken, daß in diesem Falle die Erfüllung der „Druckgleichungen“ (21) die Folge einer Frequenzfunktion vom Typus (19) ist, wovon man sich durch Berechnung der linken Seite in (21) unter Voraussetzung einer Frequenz nach (19) überzeugt. Wir bekommen nach Einführung zylindrischer Koordinaten

$$\left. \begin{aligned} \frac{\partial p}{\partial x} &= \nu \frac{\partial V}{\partial x}, \\ \frac{\partial p}{\partial R} + \frac{p-q}{R} &= \nu \frac{\partial V}{\partial R}. \end{aligned} \right\} \quad (22)$$

Diese Gleichungen gelten für jeden einzelnen physikalisch definierten Sternstypus für sich, nur ist V immer das Gravitationspotential, das von allen Sternen und aller dunklen Materie zusammengenommen herrührt.

Wenn ν und dann V , in einer von der mittleren Masse der Sterne abhängigen Einheit, als bekannte Größen angenommen werden, kann p für einen Punkt des Systems aus

$$p = - \int \nu \frac{\partial V}{\partial x} dx \quad (23)$$

berechnet werden, wo die Integration vom betrachteten Punkt sich der x -Achse parallel bis in eine Region, wo ν zu vernachlässigen ist, erstreckt. $\frac{p}{\nu} = \bar{U}^2 = \bar{Z}^2$ kann in dieser Weise für jeden Punkt des Systems in einer später zu bestimmenden Einheit berechnet werden. Dann ergibt sich aus der Gleichung die Größe $\frac{p-q}{R}$, woraus $\frac{q-p}{\nu}$ für jeden Punkt erhalten werden kann.

Wenn h_1, h_2 die Halbachsen des Geschwindigkeitsellipsoids sind, haben wir

$$\frac{h_1}{h_2} = \frac{\sum \bar{U}^2}{\sum \bar{Z}^2} = \frac{q}{p}. \quad (24)$$

In der Nähe der Sonne nimmt JEANS $h_1/h_2 = 0,577$ an, und daraus folgt

$$\frac{q-p}{\nu} = 2,00 \cdot \frac{p}{\nu}. \quad (25)$$

Aus dieser Bedingung kann die Distanz R der Sonne von der Rotationsachse mit Hilfe einer berechneten Tabelle zusammengehöriger Werte von $\frac{q-p}{\nu}$ und $\frac{p}{\nu}$ bestimmt werden. JEANS findet $R = 1090$ Parsec. Der Wert von $\frac{q-p}{\nu}$ in der angenommenen willkürlichen Einheit wird dementsprechend aus der Tabelle entnommen. Die Absolutwerte von q/ν und p/ν sind aber durch die gegebenen Werte von h_1 und h_2 bestimmt, oder man hat, wenn man nach der Zweistromtheorie die Strömungsgeschwindigkeiten U' und U'' annimmt, wie leicht zu ersehen ist,

$$\frac{q-p}{\nu} = U' U''. \quad (26)$$

Durch Vergleich der zwei Werte von $\frac{q-p}{\nu}$ erhält man den Wert der früher unbestimmten Einheit des Potentials V , und daraus die mittlere Sternmasse.

Diese ergibt sich zu $6,34 \cdot 10^{38}$ g oder 3,2 Sonnenmassen. Dieser Wert ist aber als derjenige Mittelwert der Masse anzusehen, der erhalten wird, wenn die ganze Masse des Systems auf die leuchtenden Sterne verteilt wird. Die dunkle und neblige Materie ist also in diesem Mittelwert eingerechnet.

Da KAPTEYNS typisches System Rotationssymmetrie um die Sonne besitzt, die Sternströmungstheorie nach den soeben angewendeten Prinzipien aber eine exzentrische Stellung der Sonne fordert, muß dem KAPTEYNSchen System eine gewisse Retusche gegeben werden, damit die obigen Auseinandersetzungen logisch miteinander vereinbar sind. Diese Retusche spielt dann eine gewisse Rolle für die Schätzung des Abstandes der Sonne von der Rotationsachse und auch für die Schätzung der mittleren Sternmasse. JEANS erhält in dieser Weise zuletzt

$$R = 700 \text{ Parsec}, M = 2,4 \text{ Sonnenmassen},$$

in offenkundiger Übereinstimmung mit KAPTEYNS Werten.

Sehr interessant ist JEANS' Anwendung der Methode auf CHARLIERS System der Heliumsterne. Er zeigt hier, daß die beobachtete Verteilung der Heliumsterne im Raume als notwendige Bedingung sehr kleine Geschwindigkeiten dieser Sterne voraussetzt. Die theoretischen Geschwindigkeiten Z und II im Zentrum sind von der Größenordnung 4 km/sec und die Sternströmung für eine Distanz von 90 Parsec (die Entfernung der Sonne) vom Zentrum ist nur 2,2 km/sec.

Es ist aber klar, daß die Ansichten von CHARLIER und von KAPTEYN und JEANS, wenn auch miteinander verwandt, doch nicht zusammenfallen. Die oben geforderte Distanz von 700 Parsec vom Zentrum ist nicht mit dem Abstände des Zentrums im System der Heliumsterne vereinbar. JEANS nimmt daher an, daß CHARLIERS System der B-Sterne den Charakter eines „moving cluster“ hat.

Man kann aber wohl die Frage stellen, ob wirklich dem KAPTEYNSchen typischen System eine dynamische Realität zukommt. Die Zeugnisse der letzten Zeit deuten auf sehr erhebliche Abweichungen von der Rotationssymmetrie um die Sonne, die es sehr fraglich erscheinen lassen, ob dem typischen System eine wirkliche Annäherung an die wahre Sternverteilung im Raume zuzuschreiben ist. Besonders aber sind wir auf dem Gebiete der Sternengeschwindigkeiten auf neue Phänomene gekommen, die innerhalb des typischen Systems nicht genügend Raum finden. Man kann sich jetzt fragen, ob es möglich sei, die genannten Züge der Sternverteilung im Raume und der Geschwindigkeitsverteilung in irgendeine Theorie zusammenzufassen, die aber auch den vorher besprochenen empirischen Resultaten Genüge leistet.

29. Einheitliche Theorie des Milchstraßensystems. Wir haben schon vorher (Ziff. 26) hervorgehoben, daß die große Abplattung des Milchstraßengebildes als Ganzes wahrscheinlich auf eine Rotationsbewegung des großen Systems zurückgeführt werden kann. In der Theorie des typischen Systems wird aber die Abplattung des Systems nicht als Folge einer einheitlichen Rotationsbewegung, sondern durch eine in beiden Richtungen um das Zentrum herum vor sich gehende Bewegung oder Strömung erklärt. Da aber das typische Sternsystem offenbar nicht die ganze Struktur des Sternsystems darstellen kann, so könnte man sich einen Kompromiß derart denken, daß das typische Sternsystem wesentlich die Rolle eines lokalen Systems spielt, während das große System als ein System von Wolken oder lokalen Systemen einheitlich rotiert.

Man kann aber, wie oben gesagt, ernstlich in Frage stellen, ob wirklich dem typischen System irgendeine geschlossene Einheit, wenn auch nur als lokales System, zukommt. Zwei Phänomene, denen auf dieser Grundlage eine genügende Erklärung zu geben aussichtslos erscheint, sind die asymmetrische Verschiebung der Geschwindigkeitsellipsoide verschiedener Sterngruppen mit steigender Streu-

ung der Geschwindigkeiten (Bd. VI, Chap. 1, Ziff. 18) und die unten (Ziff. 30) besprochenen „differentiellen“ Rotationseffekte in den mittleren Sternbewegungen. Die Tatsache, daß Gruppen von großer Streuung und großer asymmetrischer Verschiebung des Geschwindigkeitsmittelpunktes, welche offenbar nicht in einem lokalen System gebunden sein können, eine ellipsoidische Verteilung von ungefähr demselben Charakter wie für Gruppen kleinerer Streuung aufweisen, deutet auch an, daß der Grund der ellipsoidischen Verteilung oder der KAPTEYNschen Sternströmung nicht im lokalen System, sondern in den Eigenschaften des großen Systems selbst zu suchen ist. Von diesen Ausgangspunkten aus haben B. LINDBLAD¹ und J. H. OORT² das Problem behandelt.

Es wird in LINDBLADS Arbeit zunächst einem Zusammenhang zwischen dem Phänomen der Asymmetrie der Geschwindigkeiten, wie sie besonders in G. STRÖMBERGS³ Arbeit hervortritt, und allgemein anerkannten Tatsachen betreffs der räumlichen Verteilung der Materie im Sternsystem nachgeforscht. Wir können hier besonders die folgenden hauptsächlichlichen Gesichtspunkte in Betracht ziehen.

1. Wenn auch die auffallenden Unterschiede in scheinbarer galaktischer Konzentration zwischen verschiedenen Arten von Objekten gewissermaßen auf verschiedene mittlere Entfernung der Individuen der betreffenden Gruppen zurückgeführt werden können, so ist es doch in vielen Fällen offenbar, daß es für verschiedene Gruppen von Objekten auch eine wirkliche Variation in der „absoluten“ räumlichen Konzentration gegen die Milchstraßenebene gibt. So besteht wahrscheinlich eine wirkliche Verschiedenheit in galaktischer Konzentration zwischen den A-Sternen und den Riesensternen von späterem Spektraltypus. Wir können auch extreme Gruppen wie O-Sterne und langperiodische δ Cephei-Sterne auf der einen Seite mit planetarischen Nebeln, kurzperiodischen δ Cephei-Sternen, Kugelhaufen auf der anderen Seite einander gegenüberstellen.

2. Es werden diese Verschiedenheiten in der wahren galaktischen Konzentration von einer Variation der inneren Streuung in den Geschwindigkeiten relativ zum Zentroid begleitet und zwar in direktester Weise von dieser Variation aus erklärt. Zunolge einer größeren allgemeinen Streuung der zentroidalen Geschwindigkeiten wird die Bindung der betreffenden Objekte an die Milchstraßenebene weniger stark, die Amplituden in der Bewegung senkrecht zu dieser Ebene im Durchschnitt größer und die galaktische Konzentration weniger ausgeprägt.

3. Die fundamentale Einstellung zum Problem hängt jetzt wesentlich davon ab, daß wir zur Erklärung des Phänomens der „asymmetrischen Geschwindigkeitsverteilung“ die Hypothese einführen, daß die Streuung der Geschwindigkeiten relativ zum Zentroid klein ist gegen die systematische Bewegung des Zentroides selbst relativ zum Schwerpunkt des Systems als Ganzem. Wir werden gleich unten diese systematische Bewegung mit einer allgemeinen Rotationsbewegung identifizieren.

4. Gemäß unsren Resultaten über die allgemeine Verteilung des Milchstraßenlichts (Ziff. 9, 11), über die räumliche Verteilung der Kugelhaufen, der schwachen Sterne (Ziff. 18) und der Objekte hoher absoluter Leuchtkraft (Ziff. 20) suchen wir den Schwerpunkt des Systems in der Sagittariusgegend, etwa in den galaktischen Längen 325° — 330° .

5. Wir führen hier weiter die Annahme ein, daß das System sich wenigstens in groben Zügen in einen dynamisch stationären Zustand angeordnet hat. Eine

¹ Ark Mat Astr Fys 19A, Nr. 21, 27 u. 35; 19B, Nr. 7; 20A, Nr. 17; 21A, Nr. 3 u. 15 (1925—1929); A N 236, S. 181 (1929); M N 87, S. 553 (1927); 90, S. 503 (1930); Upsala Medd 3, 4, 6, 13, 24, 26, Stockholm Medd 1, 2, 4, 5.

² B A N 3, S. 275 (1927); 4, S. 79 und S. 91 (1927); 4, S. 269 (1928).

³ Mt Wilson Contr 275 = Ap J 59, S. 228 (1924); Mt Wilson Contr 293 = Ap J 61, S. 363 (1925).

ziemlich weitgehende Mischung der Materie von verschiedenen Bahnkom im System wird in der Tat schon nach wenigen Umläufen in der Rotbewegung erfolgen, und wir müssen von vornherein nicht mehr in den des stationären Zustandes hineinlegen (vgl. Ziff. 27).

6. Um hier noch einen Schritt weiter tun zu können, ziehen wir zu eine Erfahrungstatsache den Umstand heran, daß für die Objektgruppe kleinster Streuung in den Geschwindigkeiten (z. B. die Gruppen der langperiodischen δ Cephei-Sterne) wir in der galaktischen Ebene wenigstens keine auffallenden systematischen Veränderungen in der räumlichen Dichteverteilung und auch nicht in der Geschwindigkeitsstreuung, beobachtet haben, wenn hier oftmals die beobachteten Objekte wegen ihrer großen absoluten Leuchtheit innerhalb eines ziemlich weiten Kreises um uns herum gestreut vorkommen. Wenn wir dann auf das System als Ganzes eine Theorie analog derjenigen vorigen Ziffer, Gleichungen (19) bis (22), anwenden und die entsprechenden Bezeichnungen einführen (die Richtung gegen den Schwerpunkt aber ξ den obigen Auseinandersetzungen in einer anderen Himmelsgegend annehmen) so folgt für eine solche Gruppe aus der Kleinheit von $\overline{II^2}$ und $\partial \overline{II^2}/\partial R$ (vgl. Zi und aus der Endlichkeit von $\partial r/\partial R$

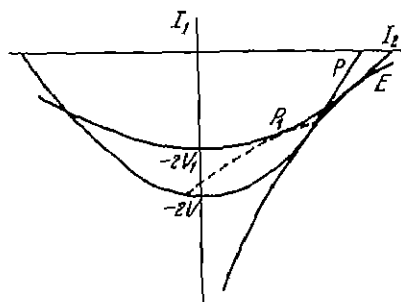


Abb. 24. Diagramm zur Erklärung der Eigenschaften einer Frequenzfunktion $f(I_1, I_2)$.

$$\frac{\partial p}{\partial R} = 0,$$

und demnach aus der zweiten Gleichung wenn wir p an der Seite von q verlässigen,

$$\frac{q}{v} = -R \frac{\partial V}{\partial R}$$

oder

$$\overline{\Theta^2} = -R \frac{\partial V}{\partial R}.$$

Wir können hier $\overline{\Theta^2}$ mit Θ_0^2 vertauschen; Θ_0 die mittlere Geschwindigkeit in der galaktischen Ebene senkrecht zur Richtung ξ den Schwerpunkt des Systems bezeichnend.

Dies zeigt uns, daß Θ_0 mit der Geschwindigkeit der zirkularen Bewegung um den Schwerpunkt herum identisch ist. Mit verschwindender Streuung der Bewegungen innerhalb einer Gruppe von Objekten geht also die Bewegungsart in eine Kreisbewegung um den Schwerpunkt herum über, während gleichzeitig die galaktische Konzentration der betreffenden Objekte außerordentlich stark ausgeprägt wird. Für diesen Satz werden wir unten (Ziff. 31) Anschluß an eine Diskussion des interstellaren Kalziums eine wichtige Stelle finden.

Wir wenden uns aber zunächst zur unmittelbaren theoretischen Bedeutung und Begründung des Satzes. Wenn wir einen stationären Zustand gemäß POINCARÉ'S Theorem annehmen wollen, so scheint zwar die einzige Möglichkeit der zuerst von JEANS und CHARLIER angegebene Spezialfall zu sein, wo die Frequenzfunktion von den zwei Integralen, Energieintegral und Flächenintegral abhängt, was eine rotationssymmetrische Anordnung des Systems im Raum einschließt (Ziff. 27). Wir haben dann für die Frequenzfunktion einen Ausdruck

$$f(I_1, I_2),$$

wo

$$I_1 = II^2 + \Theta^2 + Z^2 - 2V, \quad I_2 = R\Theta.$$

R ist wie vorher die Projektion des Radiusvektors vom Schwerpunkt auf die Milchstraßenebene, II die entsprechende Geschwindigkeit, Θ die Geschwindigkeit

in der galaktischen Ebene senkrecht zu R , Z die Geschwindigkeit senkrecht zur galaktischen Ebene. V ist das Gravitationspotential. — Wir können jetzt die Funktion $f(I_1, I_2)$ in der Weise studieren, daß wir in ein Diagramm (Abb. 24) I_2 als Abszisse und I_1 als Ordinate eintragen und das Flächenelement $dI_1 dI_2$ das sechsdimensionale Element $R dR d\theta d\varphi dI_1 dI_2$ formal repräsentieren lassen.

Die Grenzggeschwindigkeit im stationären Zustande an irgendeinem Punkte des Systems wird durch die Bedingung

$$I_1 < 0 \quad (30)$$

ausgedrückt. Man muß nämlich erwarten, daß ein Stern mit größerer Geschwindigkeit in seiner weiteren Bahn definitiv aus dem System entweicht. Wir können also eine endliche Frequenz f nur unterhalb der Achse $I_1 = 0$ haben. Eine weitere Grenzlinie im Diagramm ergibt sich aus der selbstverständlichen Bedingung

$$I_2 \leq R^2(I_1 + 2V), \quad (31)$$

welche für einen Punkt R, s im System gilt. Die Parabellinie $I_2 = R^2(I_1 + 2V)$ nennen wir die charakteristische Parabel des betreffenden Punktes. Auf dieser Parabel ist offenbar

$$H = Z = 0$$

Da für ein und denselben Radius R das Potential V mit der Entfernung s von der galaktischen Symmetrieebene abnehmen muß, wir also für einen gegebenen Wert von V umgekehrt $R = \max$ für $s = 0$ haben, so entspricht die Linie $s = 0$ auf der Potentialfläche $V = \text{konst.}$ einem maximalen Parameter $\frac{1}{2}R^2$ der charakteristischen Parabel mit beibehaltenem Vortoxpunkt ($I_2 = 0, I_1 = -2V$) im Diagramm. Das Gebiet des Diagramms, welches für das System als Ganzes in Frage kommen kann, wird also von der Enveloppe (E) der charakteristischen Parabel für Punkte in der galaktischen Ebene ($s = 0$) begrenzt. Wie man sich leicht überzeugt, wird diese Enveloppe durch die Relation

$$I_2 = -R^2 \frac{\partial V}{\partial R} \quad (32)$$

charakterisiert, woraus folgt

$$G^2 = -R \frac{\partial V}{\partial R}.$$

Da außerdem $H = Z = 0$, so bedeutet diese Bewegung eine zirkuläre Bewegung um das Zentrum herum. Umgekehrt bedeutet also eine Konzentration gegen zirkuläre Bewegungen in der galaktischen Ebene eine Konzentration der Frequenz f gegen die betrachtete Grenzlinie E im Diagramm. Da wir aber eine allgemeine Rotationsbewegung nur in einer Richtung voraussetzen, wird nur der eine von den zwei Enveloppenzweigen von Bedeutung.

Die Sache liegt demnach so, daß wir für einen gegebenen Punkt (R, s) im System mögliche Kombinationen von I_1 und I_2 im Diagramm nur zwischen der Achse $I_1 = 0$ und der dem Punkt entsprechenden charakteristischen Parabel haben, während für das System als Ganzes das in Frage kommende Gebiet zwischen der Achse $I_1 = 0$ und der Enveloppe (E), welche zirkulären Bewegungen in der galaktischen Ebene entspricht, liegt.

Die individuellen Partikeln, deren I_1, I_2 -Punkte im Diagramm innerhalb einer gewissen charakteristischen Parabel liegen, können wir aber als Partikeln die in dem betreffenden Punkte (R, s) des Systems gegeneinander stoßen, betrachten. Mit dem Begriff „Stoß“ meinen wir dann natürlich eine nahe Passage von zwei oder mehreren Partikeln in ihren Bahnen. Es ist unzweifelhaft, daß

in diesem Vorgang wenigstens eine Tendenz zu einer Gleichverteilung der Energie der Partikeln vorhanden sein muß. Wenn wir nur das Gebiet einer und derselben charakteristischen Parabel in Betracht ziehen, so würden wir, wenn die Masse einer Partikel mit m und die Geschwindigkeitsdispersion für Partikeln der Masse 1 mit σ bezeichnet wird, eine Frequenzfunktion

$$f = C e^{-\frac{m}{2\sigma^2}(I_1 - 2\omega I_2)} \quad (33)$$

erwarten. ω ist die mittlere Winkelgeschwindigkeit der Rotationsbewegung. Die Linien konstanter Frequenz in dem I_1, I_2 -Diagramm wären somit gerade Linien mit einem Winkelkoeffizienten gleich 2ω . Wenn wir aber in Betracht ziehen, daß alle Punkte des betrachteten Gebietes im Diagramm, außer den Punkten auf der Enveloppe (E) selbst, gleichzeitig verschiedenen charakteristischen Parabeln angehören, so müssen wir doch für die Frequenzlinien Kurven von allgemeinerer Natur voraussetzen. Der Prozeß der Gleichverteilung ist so langsam, daß wir eine vollkommene Ausgleichung als einen niemals erreichten Grenzfall betrachten können.

Es ist durchaus möglich, daß in der Nähe der Enveloppe die für eine kurze Strecke als die Geraden

$$I_1 - 2\omega I_2 = \text{konst.} \quad (34)$$

angenommenen Frequenzlinien mit der Tangente der charakteristischen Parabel in ihrem Kontaktpunkte mit der Enveloppe (E) parallel werden. Dies bedeutet, daß die mittlere Winkelgeschwindigkeit ω mit der Winkelgeschwindigkeit der zirkularen Bahn identisch wird. In diesem Falle werden wir eine starke Konzentration gegen die Enveloppe (E) im Diagramm und, räumlich interpretiert, gegen die zirkularen Bewegungen in der Ebene zu erwarten haben. Es ist bemerkenswert, daß (34) das JACOBISCHE Integral für die Bewegung um eine lokale Kondensation, welche einer zirkularen Bewegung mit der Winkelgeschwindigkeit ω folgt, darstellt. Es ist in der Tat möglich, daß in dem allgemeinen Ausgleichungsprozeß auch höhere Einheiten als einzelne Sterne, d. h. mehr oder weniger lockere Anhäufungen von Sternen, mitspielen, was besonders für die Ausgleichung der Frequenz nahe der Enveloppe von Bedeutung sein wird, da die Sterne sich hier mit kleinen relativen Geschwindigkeiten bewegen.

Nach den obigen Auseinandersetzungen ist also die charakteristische Verteilung der Geschwindigkeiten in unserem Punkte des Systems wie auch die räumliche Konzentration gegen eine gewisse Ebene (Milchstraßenphänomen) durch eine Konzentration gegen die Enveloppe der charakteristischen Parabel und gleichzeitig durch eine gegen $I_1 = 0$ kontinuierlich gegen Null abnehmende Frequenz bedingt.

HALM¹, CHARLIER² und SEARES³ haben die Gleichverteilung der Energie für Sterne verschiedener Massen in unserer näheren Umgebung diskutiert. Zweifellos ist in den Geschwindigkeiten relativ zum Zentroid eine deutliche Tendenz zu einer Gleichverteilung vorhanden. Es ist aber offenbar, wenn wir das System als Ganzes betrachten, daß wichtige Ausnahmen verzeichnet werden müssen. Eine Erklärung dieser Verhältnisse muß offenbar eng mit einer Kosmogonie des Systems zusammenhängen.

Wir haben oben stillschweigend vorausgesetzt, daß ein stationärer Zustand mit einer Frequenzfunktion vom Typus $f(I_1, I_2)$ wirklich existiert, d. h. daß man mit einer solchen Funktion der POISSONSCHE Gleichung Genüge leisten kann (vgl. Ziff. 27). Die Existenz des stationären Zustandes für spezielle ana-

¹ M N 71, S. 610 (1911).

² Lund Medd Nr. 76 und 81 (1917).

³ Mt Wilson Contr 226 = Ap J 55, S. 165 (1922).

lytisch definierte Funktionen $f(I_1, I_2)$ wird in den oben zitierten Arbeiten von ÖHLSSON und WIGNER behandelt. Wir können aber hier besonders auf die Existenz des Grenzfalles hinweisen, wo eine endliche Frequenz f nur an der Enveloppe E im I_1, I_2 -Diagramm vorhanden ist, was offenbar bedeutet, daß die Materie des Systems in zirkularen Bahnen in der Ebene um den Schwerpunkt schwingt, in Analogie mit den Bewegungen im Sonnensystem. Nach der hier behandelten Theorie wird das System, als Ganzes betrachtet, sich nicht sehr viel von diesem Zustand unterscheiden, und es scheint offenbar, daß auch in der Nähe vom „Sonnensystemtypus“ Lösungen existieren müssen.

Die „Druckgleichungen“ (21), deren zwei letzte Terme auf der linken Seite wir gewissermaßen als „Viskositätsterme“ bezeichnen können, sind, wie schon oben in Ziff. 28 bemerkt worden ist, bei der hier angenommenen Frequenzfunktion $f(I_1, I_2)$ von selbst erfüllt. Wenn wir den Effekt der nahen Passagen in Betracht ziehen, würde zwar die lange freie Weglänge einer Partikel außerdem einen großen Viskositätskoeffizienten, nach abstrakter Analogie mit der Gastheorie gerechnet, herbeiführen. Die unmittelbare Analogie mit den Gasen versagt aber offenbar, da der Weg eines Sterns zwischen den Stößen gar nicht als geradlinig vorauszusetzen ist, sondern die ganze gekrümmte Bahnbewegung einer Partikel im System innerhalb der freien Weglänge fällt (vgl. Ziff. 27). Wenn wir im System eine geschlossene Rotationsfläche mit dem Schwerpunkt als Mittelpunkt betrachten, so werden die Sterne, die etwa in einem gewissen Augenblicke über diese Fläche nach außen ziehen, im allgemeinen zwischen zwei Passagen in ihrer Bahnbewegung mehrmals über diese Fläche hin und her ziehen. Der Bereich um die Fläche herum, innerhalb der die betrachteten Sterne einen Austausch von Moment vermitteln können, wird im allgemeinen wegen der Bahnbewegung ziemlich eng begrenzt. Der wirkliche Transport von Moment über die Fläche infolge der Passagen wird daher sehr langsam.

Es soll außerdem hier betont werden, daß es durchaus nicht notwendig ist, einen stationären Zustand in dem vollen abstrakten Sinne dieses Wortes anzunehmen. Was vorausgesetzt wird, ist, daß eine ziemlich vollständige Mischung der Materie des Systems, wie in Ziff. 27 auseinandergesetzt, stattgefunden hat. Es kann vorkommen, daß gewisse Eigenschaften eines stationären Systems nur so langsam eintreten, daß sie in der tatsächlichen Entwicklung des Systems noch nicht erreicht worden sind. Da das System offenbar gegen eine Symmetrieebene sehr abgeplattet ist, und die Bewegung in der Nähe dieser Ebene von nahe zweidimensionaler Natur ist, so besteht z. B. eine sehr schwache statistische Verbindung zwischen der Bewegung parallel zur Ebene und der Bewegung senkrecht dazu. Da die Kraftkomponente in der s -Richtung sich nur langsam mit R ändern wird, so können wir in der Tat die Abhängigkeit der vertikalen Kraftkomponente von s als eine konstante Funktion längs der ganzen Bahn eines Sterns ansehen, wodurch die Bewegung in s unabhängig von der Bewegung parallel zur galaktischen Ebene wird. Um diesen Verhältnissen Rechnung zu tragen, schreiben wir das Energiintegral

$$I_1 = \Pi^2 + \Theta^2 + Z_0^2 - 2V_0(R), \quad Z_0^2 = Z^2 - 2(V(R, s) - V_0(R)), \quad (35)$$

wo V_0 die in der Ebene herrschende Potentialfunktion ist, Z_0 der Z -Wert für $s = 0$, und wo vorausgesetzt wird, daß die Differenz $V(R, s) - V_0(R)$ sich nur langsam mit R ändert. Diese Differenz kann gewissermaßen als ein Mittel für die Potentialdifferenzen zwischen den Höhen s und 0 in verschiedenen, sich in der Höhe s mit demselben Wert von Z kreuzenden Bahnen betrachtet werden. Z_0 wird dann als eine Konstante in der Bewegung eines einzelnen Sterns vorausgesetzt. In der unmittelbaren Umgebung der galaktischen Ebene haben wir

dann nach (28) für jedes Intervall dZ_0 die zweidimensionale Verteilung

$$dZ_0 \cdot \varphi_0(R, II, \Theta, Z_0) R dR dz dII d\Theta,$$

wo

$$\varphi_0(R, II, \Theta, Z_0) = j(I_1, I_2), \quad (36)$$

und wo I_1 gemäß (35) ausgedrückt wird. Eine allgemeinere stationäre Verteilung für beliebige Entfernung z von der galaktischen Ebene können wir dann folgendermaßen definieren

$$\varphi(R, z, II, \Theta, Z) R dR dz dII d\Theta dZ = \varphi_0(R, II, \Theta, Z_0) R dR dz dII d\Theta \cdot F(Z_0^2) dZ_0,$$

wo $F(Z_0^2)$ eine a priori unbekannte, beliebige Funktion ist. Wir haben auf der rechten Seite dZ_0 durch dZ ersetzt, weil in der Bewegung $dz dZ$ invariant ist. Es ergibt sich also

$$\varphi = \varphi_0 \cdot F(Z_0^2), \quad (37)$$

wo der Ausdruck für Z_0 gemäß (35) eingesetzt wird. Für $z = 0$, $Z = Z_0 = 0$, ist $\varphi = \varphi_0$, also gilt

$$F(0) = 1. \quad (38)$$

Was sonst die Funktion F angeht, so ist es jedenfalls sehr wahrscheinlich, daß für jeden Wert von R die Streuungen in den Komponenten II und Z in enger Beziehung zueinander stehen. Es ist aber nicht notwendig, daß sie gleich sind, wie man unter strenger Rechnung nach (28) fordern müßte. In unserer Umgebung gilt, daß \bar{Z}^2 etwas kleiner als \bar{II}^2 ausfällt. Wenn wir im folgenden der Einfachheit wegen mit (28) rechnen, setzen wir voraus, daß für Fragen, die mit der Verteilung senkrecht zur Milchstraßenebene von Bedeutung sind, eine Transformation zu machen ist, wobei die allgemeinere Verteilungsfunktion φ gemäß (37) zu bilden ist. $F(Z_0^2)$ ist gemäß dem empirisch ermittelten Geschwindigkeitskörper zu wählen, unter Beachtung der Relation (38).

30. Die asymmetrische Geschwindigkeitsverteilung in ihrer Beziehung zur Rotation. Wir wollen eine gewisse Klasse von Objekten ins Auge fassen und im I_1, I_2 -Diagramm (Abb. 24) eine Linie konstanter Frequenz

$$j(I_1, I_2) = \text{konst.},$$

für diese Klasse ziehen. Der innerhalb einer charakteristischen Parabel eingeschlossene Teil der Frequenzlinie entspricht einer geschlossenen Fläche im Geschwindigkeitsraume. Nehmen wir an, daß die Frequenzlinie (gestrichelte Linie in der Abbildung) durch eine Parabelinie

$$I_1 + \frac{1}{2p}(I_2 - M)^2 = N \quad (39)$$

approximiert werden kann, wo M, N, p zur Verfügung stehende Konstanten sind. Die Differenz ΔI_1 in den Ordinaten zwischen einem Punkte auf der Frequenzlinie und der charakteristischen Parabel

$$I_2^2 = R^2(I_1 + 2V) \quad (40)$$

ist gleich $II^2 + Z^2$, da auf der letzteren Kurve $II = Z = 0$ ist, während die tangentielle Geschwindigkeitskomponente durch die Relation $\Theta = \frac{1}{R} I_2$ gegeben ist. Man findet dann nach einigen einfachen Reduktionen für die Geschwindigkeitsfläche, welche der Frequenzlinie (39) entspricht, folgenden Ausdruck:

$$\frac{II^2 + Z^2}{a^2} + \frac{(\Theta - \Theta_0)^2}{b^2} = 1, \quad (41)$$

$$\text{wo} \quad \Theta_0 = \frac{MR}{R^2 + 2p}, \quad a^2 = 2V + N - \frac{M^2}{R^2 + 2p}, \quad \frac{b^2}{a^2} = \frac{2p}{R^2 + 2p} \quad (42)$$

Die Geschwindigkeitsfläche ist also für $p > 0$ ein in der Θ -Richtung abgeplattetes Sphäroid. Bezeichnen wir mit α und β die Halbachsen des sog. Geschwindigkeitsellipsoids für einen gegebenen Ort, so haben wir also gemäß der obigen Approximation (39)

$$f = f_0 \frac{1}{2} \left(\frac{R^2 + 2p}{a^2} + \frac{(a - a_0)^2}{p} \right), \quad (43)$$

$$\text{wo} \quad \alpha^2 = \frac{a^2}{m}, \quad \frac{\beta^2}{\alpha^2} = \frac{2p}{R^2 + 2p}. \quad (44)$$

Soweit eine ellipsoidische Approximation gilt, ist also α konstant für verschiedene Punkte des Systems, während β mit R (aber nicht mit s) variiert. Da offenbar $\alpha^2 = \overline{II^2}$, so kann man also auf Grundlage der Theorie eines stationären Zustandes wenigstens keine schnelle Variation von $\overline{II^2}$ mit der Lage (R, s) des betrachteten Punktes im System voraussetzen. Dies ist in Übereinstimmung mit unserer oben für die Sterne mit kleinem $\overline{II^2}$ getroffenen Annahme der Kleinheit von $\partial \overline{II^2} / \partial R$.

Die beobachtete Asymmetrie der Geschwindigkeitsverteilung müssen wir von unserem Standpunkte aus als eine Variation der mittleren Rotationsgeschwindigkeit Θ_0 mit der Streuung der individuellen Geschwindigkeiten deuten. Die Richtung der asymmetrischen Verschiebung der Geschwindigkeitsmittelpunkte soll dann offenbar senkrecht zur Richtung gegen das Zentrum des Systems stehen. Nach STRÖMBERG'S Arbeit über die Asymmetrie ist dies auch sehr nahe erfüllt. Wir erhalten nach seinen Resultaten für die galaktische Länge des Zentrums $331^\circ 5' \pm 5'$, was sehr wohl mit SHAPLEY'S aus der Verteilung der Kugelhaufen hergeleiteten Wert 327° übereinstimmt.

Wir wollen jetzt eine gewisse Klasse von Sternen auswählen, die wir auch mit dem Wort „Untersystem“ kennzeichnen können. Wir führen für ein solches Untersystem den Begriff „effektive Grenzfläche“ ein, deren Radius in der galaktischen Ebene wir mit R_1 bezeichnen. Wir definieren die „effektive“ Begrenzungsfläche ziemlich willkürlich derart, daß an dieser Fläche der Frequenzfaktor f_0 der Gleichung (43) im Verhältnis $1/s$, mit dem Werte an unserem Orte im Raume verglichen, abgenommen haben soll. Die Bedeutung des eingeführten Begriffs folgt aus der folgenden Überlegung. Betrachten wir im Geschwindigkeitsraume unseres Ortes eine ellipsoidische Schale (42), wo $a^2 = 2\alpha^2$, $b^2 = 2\beta^2$. An dieser Schale wird offenbar gemäß (43) die Frequenz $\frac{1}{s} f_0$ herrschen. Die Geschwindigkeitschale entspricht einer gewissen Frequenzlinie im I_1, I_2 -Diagramm, und es ist klar, daß wir einen neuen Ort ($R_1, 0$) so wählen können, daß die charakteristische Parabel für diesen Punkt die genannte Frequenzlinie tangiert. Wir haben dann für diesen Ort eine Frequenz $\frac{1}{s} f_0$ für $II = Z = \Theta - \Theta_0 = 0$. Der Wert von a^2 für $R = R_1$ muß daher verschwinden. Wir haben also gemäß (42) zu setzen, den zwei betrachteten Orten im System entsprechend,

$$\left. \begin{aligned} 2\alpha^2 &= 2V + N - \frac{M^2}{R^2 + 2p}, \\ 0 &= 2V_1 + N - \frac{M^2}{R_1^2 + 2p}. \end{aligned} \right\} \quad (45)$$

Wenn wir aus diesen Relationen und den Gleichungen (42, 44) die Parameter M, N und p eliminieren, bekommen wir

$$\Theta_0^2 + 2\alpha^2 \left(\frac{R_1^2}{R_1^2 - R^2} - \frac{\beta^2}{\alpha^2} \right) = 2(V - V_1) \left(\frac{R_1^2}{R_1^2 - R^2} - \frac{\beta^2}{\alpha^2} \right). \quad (46)$$

Für β/α ist nahe 0,7 zu setzen. Wenn wir aber annehmen, daß $R_1 - R$ klein gegenüber R selbst ist, die Sonne also sehr exzentrisch im System liegt, so vereinfacht sich diese Gleichung mit sehr guter Approximation auf die folgende:

$$\Theta_0^2 + \alpha^2 \frac{R_1}{R_1 - R} = -R \frac{\partial V}{\partial R}. \quad (47)$$

Wir können jetzt auch, wenn wir verschiedene Untersysteme betrachten, annehmen, daß $R_1 - R$ nicht gleichzeitig mit α verschwindet, und dies ist damit gleichbedeutend, daß mit verschwindender Streuung α die mittlere tangentielle Bewegung Θ_0 einer Gruppe sich der zirkularen Bewegung Θ_c um das Zentrum herum nähert. Wir haben somit $\Theta_0 = \max. = \Theta_c$ für $\alpha = 0$, und demnach

$$(\Theta_0)_{\max}^2 = \Theta_c^2 = -R \frac{\partial V}{\partial R}. \quad (48)$$

Die asymmetrische Geschwindigkeitsverschiebung wird als

$$S = \Theta_c - \Theta_0 \quad (49)$$

definiert. Wir haben jetzt dieses Verschiebungsgesetz mit der von STRÖMBERG¹ durch ein Studium der Radialgeschwindigkeiten hergeleiteten Relation zwischen Geschwindigkeitsstreuung und „asymmetrical drift“ zu vergleichen. STRÖMBERG leitet eine parabolische Relation ab, die aber auch eine langgestreckte elliptische sein kann, der Gleichung (46) entsprechend, wenn wir in diese $R_1 = \text{konst.}$ einsetzen.

Wenn wir annehmen, daß das Untersystem der Kugelsternhaufen im Mittel keine merkliche Rotationsbewegung besitzt, können wir eine rohe Abschätzung von Θ_c machen. Nach LUNDMARKS² und STRÖMBERGS³ Resultaten für die Sonnengeschwindigkeit in bezug auf die Haufen ergibt sich Θ_c zu rund 300 km/sec. Wir nehmen hier nach STRÖMBERG (vgl. Tabelle 20, Kugelhaufen) $\Theta_c = 275$ km/sec

Tabelle 20.

Klasse	H	α	S	$\frac{R_1 - R}{R_1}$	Klasse	H	α	S	$\frac{R_1 - R}{R_1}$
Mo-M9	$\leq -2,0$	19,4	+ 2,1	0,33	F0-F9	$\leq -2,0$	19,7	+ 5,4	0,13
„	-1,9 bis + 3,0	39,0	+14,6	0,19	„	-1,9 bis 0,0	24,0	+ 7,2	0,15
K4-K9	$\leq -2,0$	20,4	+ 7,4	0,10	„	+0,1 „ + 3,0	28,9	+ 1,7	0,90
„	-1,9 bis + 3,0	29,6	+15,5	0,11	„	+3,1 „ + 5,0	48,4	+ 6,8	0,63
„	$\leq +3,1$	52,2	+ 3,7	(1,35)	„	+5,1 „ +14,0	122	+ 95,0	0,34
G9-K3	$\leq -3,0$	16,7	+ 6,7	0,08	B6-A9	-2,9 „ + 2,7	16,4	+ 0,9	0,54
„	-2,9 bis - 2,0	19,6	+ 1,9	0,37	B0-B5	$\leq -4,0$	8,1	+ 8,5	0,01
„	-1,9 „ - 1,0	23,2	+ 2,5	0,39	„	-3,9 bis + 0,1	7,4	+ 9,4	0,01
„	-0,9 „ 0,0	26,0	+10,9	0,12	δ Cephei-Sterne:				
„	+0,1 „ + 1,0	28,9	+ 8,2	0,19	Per. > 2,0 d.	—	17,3	— 1,0	—
„	+1,1 „ + 3,0	41,9	+25,2	0,13	Per. < 0,7 d.	—	74	+ 97	0,12
„	+3,1 „ +12,0	33,7	+14,5	0,15	O5-O9	—	19,6	+ 23,5	0,03
Go-G8	$\leq -2,0$	17,6	+ 3,4	0,17	c-Sterne	—	12,9	+ 9,4	0,33
„	-1,9 bis + 1,0	25,8	+ 6,9	0,18	P	—	64,7	+ 15,6	0,50
„	+1,1 „ + 5,0	44,0	+ 9,7	0,37	M1e-M6e	—	52	+ 50,5	0,11
„	+5,1 „ +10,0	46,2	+21,2	0,19	M2e-M5e	—	88	+151	0,13
					Kugelhaufen	—	117	+275	0,18

¹ L. c. ² Publ A S P 35, S. 318 (1923).

³ Mit Wilson Contr 292 = Ap J 61, S. 353 (1925).

an. Die Entfernung der Sonne von der effektiven Grenze des Systems, wenn wir als Einheit den Radius selbst nahmen, berechnen wir aus

$$\frac{R_1 - R}{R_1} = \frac{\alpha^2}{S(2\Theta_0 - S)}. \quad (50)$$

Tabelle 20 gibt α , S und $\frac{R_1 - R}{R_1}$ für die verschiedenen Gruppen in STRÖMBERGS Arbeit S wird vom „limiting center“, d. h. dem Vertex der Parabel, längs deren Achse, gerechnet, α ist mit der größeren Achse des Geschwindigkeits-ellipsoids in der galaktischen Ebene identisch genommen. H ist die Quantität $m + 5 \log \mu$

Es ist aus der Tabelle ersichtlich, daß die meisten Gruppen eine bemerkenswerte Übereinstimmung zeigen. Wenn wir einige extreme Werte ausschließen (zwei extrem große und die sehr kleinen Werte der frühen B-Sterne), so bekommen wir im Mittel für 27 Gruppen

$$\frac{R_1 - R}{R_1} = 0,23 \pm 0,03 \text{ (m. F.)}.$$

Die Sonne ist also um 23 % des Radius innerhalb der „effektiven“ Grenze des Systems, also sehr exzentrisch, gelegen.

Für die räumliche Dichtigkeit ν eines Untersystems ergibt sich durch Integration von (43) $\nu = (2\pi)^{3/2} \alpha^3 \beta / \sigma$. Man bekommt dann gemäß (44) und nach der Definition der „effektiven Grenze“ für die Dichtigkeit ν_1 an dieser Grenze

$$\frac{\nu_1}{\nu} = \frac{\beta_1}{\beta} \cdot \frac{1}{\sigma},$$

und weiter gemäß (39)

$$\left(\frac{\beta_1}{\beta}\right)^3 = \frac{R^3 + 2p}{R_1^3 + 2p}, \quad \left(\frac{\beta}{\alpha}\right)^3 = \frac{2p}{R^3 + 2p}.$$

Nach Elimination von p ergibt sich

$$\frac{\nu_1}{\nu} = \left(\frac{\alpha^3 R^3}{\beta^3 R^3 + (\alpha^3 - \beta^3) R_1^3} \right)^{1/3} \cdot \frac{1}{\sigma}. \quad (51)$$

Numerisch erhält man gemäß den oben für β/α und R/R_1 gegebenen Worten $\nu_1/\nu = 0,32$. Die räumliche Dichtigkeit an der „Grenze“ ist also 0,32 der Dichtigkeit in unserer Umgebung.

Die allgemeine Dichtigkeitsverteilung in der galaktischen Ebene gemäß der ellipsoidischen Approximation ergibt sich aus (43) und dem Diagramm Abb. 24 unter Benutzung einer Methode, welche zu Gleichungen, die mit (45) und (46) analog sind, führt. Wir bezeichnen jetzt mit R_0 , ν_0 und V_0 für unseren Punkt im System geltende Werte, und mit R die laufende Koordinate. Wenn die Geschwindigkeitsverteilung an unserem Punkte wie vorher durch Θ_0 , α , β charakterisiert ist, so haben wir für das betreffende Untersystem

$$\log \frac{\nu}{\nu_0} = \frac{1}{2} \log \frac{\alpha^3 R_0^3}{\beta^3 R_0^3 + (\alpha^3 - \beta^3) R^3} + \frac{1}{\alpha^3} \left(V - V_0 + \frac{1}{2} \Theta_0^3 \frac{\alpha^3 (R^3 - R_0^3)}{\beta^3 R_0^3 + (\alpha^3 - \beta^3) R^3} \right) \log e. \quad (52)$$

Der erste Term auf der rechten Seite ist klein. Wir können mittels dieser Gleichung den Radiusvektor R für beliebige Werte von ν/ν_0 berechnen, sobald wir in genügender Weise die Kraftfunktion für sukzessive Werte von R , woraus $V - V_0$ berechnet wird, kennen. Durch Differentiation der Gleichung können wir $\partial \log \nu / \partial R$ in Relation zu Θ_0 , α und $\partial V / \partial R$ bringen, woraus, wie wir unten sehen werden, eine alternative, aber im Prinzip mit dem obigen identische Behandlung des Phänomens der Asymmetrie sich ergibt.

Eine Erklärung der approximativen Konstanz von R_1 kann uns eine Betrachtung der Abb. 24 geben. Mit wachsendem R nähert sich die charakteristische Parabel des betrachteten Systempunktes mehr und mehr der I_2 -Achse, um im Limes mit dieser Achse zusammenzufallen. Wenn wir annehmen, daß die Geschwindigkeit der zirkularen Bewegung an unserem Orte nicht sehr weit von der Grenzgeschwindigkeit, welche $I_1 = 0$ entspricht, liegt, so ist der Berührungspunkt zwischen der charakteristischen Parabel und der Enveloppe nicht weit von der I_2 -Achse entfernt, und die charakteristische Parabel unseres Ortes verläuft in der Nähe dieser Achse. Da für alle Untersysteme die Frequenz $f(I_1, I_2)$ gegen die Achse $I_1 = 0$ sukzessiv gegen Null abnimmt, so ist es a priori

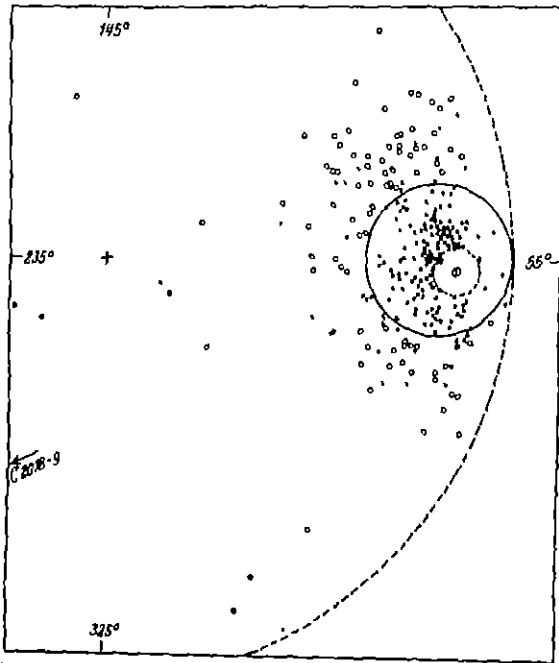


Abb. 25. Die Verteilung in der galaktischen Ebene für große Geschwindigkeiten relativ zur Sonne (nach Oort). Die schwarzen Punkte entsprechen einem homogenen Material für Geschwindigkeitsdifferenzen gegen die Sonne größer als 19,5 km/sec. Der größere (voll gezogene) Kreis entspricht Geschwindigkeiten von 65 km/sec relativ zum Zentroid. Das Kreuz soll die Schwerpunktgeschwindigkeit des Systems repräsentieren, und der große (unterbrochene) Kreis mit dem Kreuz als Zentrum hat einen Radius von 365 km/sec.

einer Richtung, welche eine gerade Fortsetzung des Geschwindigkeitsvektors Θ_0 bildet. Dieses Phänomen wird sehr gut durch ein Diagramm von J. H. Oort² veranschaulicht (Abb. 25), wo die absoluten Geschwindigkeiten für Sterne, welche große zentroidale Bewegungen zeigen, innerhalb eines Geschwindigkeitskreises vom Radius 365 km/sec gelegen erscheinen.

Oort hat eine in der Form beträchtlich verschiedene, aber der obigen, prinzipiell ähnliche Behandlung des Phänomens der Asymmetrie ausgeführt,

wahrscheinlich, wenigstens für die Gruppen von großer Asymmetrie, daß in der Figur eine einzige charakteristische Parabel, welche approximativ der effektiven Grenze $R \approx R_1$ verschiedener Untersysteme entspricht, gezogen werden kann. Die Abnahme der räumlichen Dichtigkeit gegen eine „effektive Grenzfläche“, wie auch das ganze Phänomen der Asymmetrie der Geschwindigkeitsverteilung erscheint also als eine Folge der Bedingung, daß die Partikeln des Systems der Relation $I_1 < 0$ genügen müssen, mit einer kontinuierlichen Abnahme der Frequenz gegen diese Grenze im I_1, I_2 -Diagramm.

Daß die zirkulare Geschwindigkeit an unserem Orte in der Tat nicht sehr weit von der „velocity of escape“ entfernt ist, wird angedeutet¹ durch die vollkommene Abwesenheit von großen Geschwindigkeiten relativ zum Zentroid.

¹ LINDBLAD, V J S 61, S. 265 (1926).

² B A N 4, S. 269 (1928).

Die Behandlung des stationären Zustandes in der Umgebung der Sonne ist rein analytisch, wobei eine ellipsoidische Verteilung der Geschwindigkeiten für jede Untergruppe vorausgesetzt wird. Obgleich die OORTsche Methode durch diese Annahme im ganzen etwas weniger generell als die oben gegebene wird, ist sie für unsere Umgebung gerechtfertigt, wo wir wissen, daß die ellipsoidische Verteilung als Approximation im ganzen zulässig ist, von welchem Sachverhältnis wir auch oben Gebrauch gemacht haben. Die Gleichung, welche (46) und (47) oben entspricht, ergibt sich aus (52) und schreibt sich nach OORT

$$\Theta_0^2 = -R \frac{\partial V}{\partial R} + \alpha^2 \left(\frac{R}{v} \frac{\partial v}{\partial R} + 1 - \frac{\beta^2}{\alpha^2} \right), \quad (53)$$

woraus, wenn wir mit OORT $\Theta_0/R = 0,043$ km/sec Parsec annehmen, für die asymmetrische Drift $S = \Theta_c - \Theta_0$ gilt

$$S = -11,6 \alpha^2 \left(\frac{1}{\text{Mod.}} \frac{\partial \log v}{\partial R} + \frac{1}{R} \left(1 - \frac{\beta^2}{\alpha^2} \right) \right). \quad (54)$$

Der Gradient $\partial \log v / \partial R$ ergibt sich als von derselben Größenordnung für verschiedene Gruppen und entspricht etwa einem Faktor 2 in der Dichtigkeit für eine Distanz von 1000 Parsec. Für die gewöhnlichen Spektraltypen in STRÖMBERGS Tabelle ergibt sich im Mittel

$$\partial \log v / \partial R = -0,00019 \pm 0,00005 \quad (\text{m. F.}).$$

Im vereinfachten Falle einer ebenen Bewegung der Sterne um ein Massenzentrum können wir mit K. F. BORTLINGER¹ die Abhängigkeit der Asymmetrie von der parabolischen Grenzgeschwindigkeit und von der Konzentration der Sterne gegen das Zentrum hin anschaulich machen. Die Bahnen durch unseren Ort im System können, wie Abb. 26 zeigt, nach Exzentrizität und Halbachsenlänge klassifiziert werden, was offenbar einer Aufteilung nach I_1 und I_2 entspricht, da I_1 die Halbachsenlänge a , und die Flächen- geschwindigkeit I_2 bei gegebenem a die Exzentrizität e bestimmt. Eine Linie von O nach einem beliebigen Punkt in der Abbildung entspricht einer Geschwindigkeit in bezug auf den Schwerpunkt des Systems, und man kann sogleich die entsprechenden Werte von a und e ablesen. Der Punkt P markiert die Kreisbewegung, S die Sonnenbewegung. Die Asymmetrie der Geschwindigkeitsverteilung, von P oder S aus gerechnet, wird um so größer, je stärker die inneren Bahnen, $a < 1$, im Vergleich mit den äußeren, $a > 1$, besetzt sind. Von diesem Gesichtspunkte aus

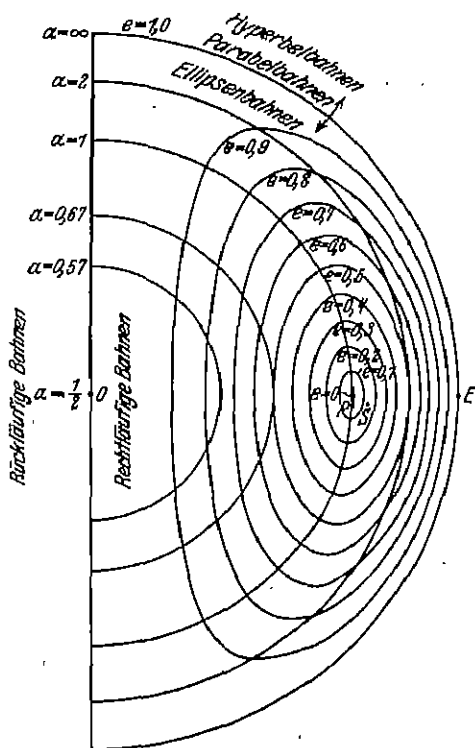


Abb. 26. Geschwindigkeitsstreuung der Bahnen durch einen gewissen Ort des Systems im Falle ebener Bewegung um ein Massenzentrum.

¹ Naturwiss 19, S. 297 (1931); Berlin-Babelsberg Veröffentl 8, H. 5 (1931).

wären also die Sterne mit großer asymmetrischer Bewegung solche, die vorzugsweise in den inneren Partien des Systems vorkommen.

Es ist wohlbekannt, daß die Geschwindigkeitsellipsoide in den meisten Fällen nicht sphäroidisch mit der kürzesten Achse in der galaktischen Ebene, sondern beträchtlich gegen die galaktische Ebene abgeplattet gefunden werden. Wie oben (Ziff. 29) erwähnt, hängt dies damit zusammen, daß die Bewegung in der Ebene von zweidimensionaler Natur ist, und daß eine Ausgleichung zwischen dieser Bewegung und der allgemeineren dreidimensionalen nur sehr langsam vor sich geht. Eine starke Korrelation zwischen den Streuungen in Π und Z müssen wir jedenfalls voraussetzen, was auch der empirischen Erfahrung entspricht. Es ist dann aber klar, daß Gruppen von verschiedener Rotationsgeschwindigkeit und verschiedener Streuung, also verschiedene Untersysteme, auch verschiedene Konzentration gegen die galaktische Ebene zeigen müssen. Wenn wir einen Meridionalschnitt durch die „effektiven Begrenzungsflächen“ ziehen, so bekommen wir also die schematische Darstellung der Untersysteme, welche in Abb. 27 gegeben ist.

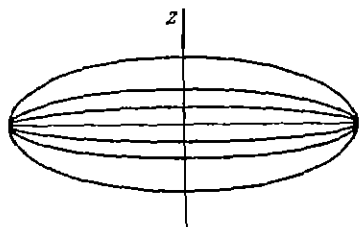


Abb. 27. Schematischer Meridionalschnitt durch das Sternsystem. Die Grenzflächen repräsentieren verschiedene Untersysteme.

Wir können jedenfalls auf die Bewegung in z senkrecht zur Milchstraßenebene das Massenbewegungsgesetz

$$\frac{\partial(\nu \bar{Z}^2)}{\partial z} = \nu \frac{\partial V}{\partial z} \quad (55)$$

anwenden. Eine unmittelbare Verwendung kann diese Formel für die A-Sterne erhalten, da diese praktisch in einem so dünnen Stratum enthalten sind, daß wir annehmen können

$$\frac{\partial V}{\partial z} = -4\pi G \varrho z, \quad (56)$$

wo ϱ die Dichtigkeit des zentralen galaktischen Stratums ist. Wenn ν_0, z_0, Z_0 die für die A-Sterne nahe unserem Punkte im System geltenden Werte der Dichtigkeit, Distanz von der Symmetrieebene und Geschwindigkeitsstreuung in Z sind, so haben wir

$$Z_0^2 = - \int_{z_0}^{\infty} \frac{\nu}{\nu_0} \frac{\partial V}{\partial z} dz = 4\pi G \varrho \int_{z_0}^{\infty} \frac{\nu}{\nu_0} z dz. \quad (57)$$

Wir können für z_0 den Wert 30 Parsec annehmen und für ν/ν_0 z. B. die von PETERSSON und LINDBLAD (Ziff. 19) hergeleitete Veränderung der Dichtigkeit mit der Entfernung von der Milchstraßenebene. Für Z_0 hat STRÖMBERG 9,1 km/sec gefunden. Nach Ausführung einer numerischen Integration finden wir dann für ϱ , in Sonnenmassen per Kubikparsec ausgedrückt, den Wert

$$\varrho = 0,11,$$

was mit anderen Schätzungen der Dichtigkeit in unserer Umgebung ziemlich übereinstimmt.

Eine ähnliche Untersuchung hat BOTTLINGER¹ für die Sterne von großer absoluter Leuchtkraft ausgeführt. Aus dem durchschnittlichen Abstand der hellen Sterne von der Milchstraßenebene (etwa 40 Parsec) läßt sich mit Hilfe der Masse und der Dimensionen des großen Systems (vgl. Ziff. 33) eine Geschwindigkeitsstreuung von 3,6 km/sec berechnen. Eine sorgfältige Diskussion der Radialgeschwindigkeiten ergibt das Resultat, daß die Streuung der O- und

¹ L. c.

B-Sterne im Rahmen dessen liegt, was man nach der Rotationstheorie erwarten muß.

Eine sehr ausführliche Arbeit über diesbezügliche Fragen ist ganz kürzlich von OORT¹ veröffentlicht worden. Wenn wir die senkrecht zur Milchstraßenebene wirkende Kraftkomponente $\partial V/\partial z$ mit $K(z)$ bezeichnen und diese als im wesentlichen in der Bewegung eines Sterns von R unabhängig betrachten, so haben wir für die Bewegung in Z , gemäß dem zweiten Teil unserer Gleichung (35) oben,

$$Z_0^2 = Z^2 - 2 \int_0^z K(z) dz, \quad (58)$$

und es ist leicht einzusehen, z. B. durch unsere Gleichung (37) oben, daß im Falle einer stationären Verteilungsfunktion $\varphi(z, Z)$ diese einfach eine Funktion von Z_0 sein wird. Im Falle einer GAUSSschen Verteilung der Geschwindigkeiten für $z = 0$ haben wir

$$\varphi(0, Z) = \nu_0 \frac{l}{\sqrt{\pi}} e^{-l^2 Z^2}, \quad (59)$$

und also für beliebige z -Werte

$$\varphi(z, Z) = \nu_0 e^{2l \int_0^z K(s) ds} \cdot \frac{l}{\sqrt{\pi}} e^{-l^2 Z^2}, \quad (60)$$

woraus wir ableiten

$$\nu(z) = \nu_0 e^{2l \int_0^z K(s) ds}. \quad (61)$$

Diese Formel ist identisch mit der von KAPTEYN für einen analogen Zweck benutzten (Ziff. 28). Wenn wir die empirische Geschwindigkeitsverteilung als eine Summe von GAUSSschen Verteilungen approximieren, welche je die Bruchteile $\theta_1, \theta_2, \dots$, der Sterne in unserer Nähe umfassen, so bekommen wir

$$\nu(z) = \nu_0 \left\{ \theta_1 e^{2l \int_0^z K(s) ds} + \theta_2 e^{2l \int_0^z K(s) ds} + \dots \right\}. \quad (62)$$

Durch die statistisch ermittelten $\nu(z)$ und gegebene Werte der θ und l können wir die Funktion $K(z)$ in sukzessiver Approximation ermitteln.

OORT bestimmt aus den Radialgeschwindigkeiten für verschiedene Sterntypen die Streuung in den vertikalen Geschwindigkeitskomponenten Z , woraus die Werte von l sich ergeben. Hauptsächlich unter Benutzung der VAN RHIJNSchen Resultate für die Dichtefunktion in hohen galaktischen Breiten (für A-Sterne und Riesensterne von spätem Typus werden auch die oben erwähnten Resultate von LINDBLAD und PETERSSON zum Vergleich herangezogen) berechnet OORT die Funktion $K(z)$ für z zwischen 0 und 600 Parsec. Das Hauptresultat wird in Tabelle 21 wiedergegeben, wo K in cm/sec^2 ausgedrückt ist. Der numerische Wert von $K(z)$ wächst linear bis ungefähr in der Höhe von 200 Parsec, der Gang mit z wird dann beträchtlich langsamer. Wenn umgekehrt für die Dichtefunktion der Ausdruck (62) angenommen wird, kann man aus ihm und aus der als bekannt vorausgesetzten Leuchtkraftfunktion die Sternzahlen für verschiedene scheinbare Größen berechnen, und als Kontrolle werden von OORT weitläufige Rechnungen dieser Art ausgeführt. Da eine Berechnung der Sternzahlen der schwächsten Größen Kenntnis von $K(z)$ bis zu etwa 5000 Parsec voraussetzt, so kann

Tabelle 21.

z	$K(z) \cdot 10^4$
50	-0,77
100	1,55
150	2,59
200	3,52
250	3,78
300	3,86
400	3,68
600	4,44

¹ B A N 6, S. 249 (1932).

man aus diesen Sternzahlen eine grobe Kontrolle etwaiger Extrapolationen von $K(z)$ für große Höhen bekommen, eine Möglichkeit, die auch von OORT ausgenutzt wird, doch vorläufig ohne definitive Resultate. Den Verlauf der Sternzahlen mit galaktischer Länge nach SEARES benutzt OORT, um den Gradienten $\partial \log r / \partial R$ zu berechnen, welchen Wert er im Mittel zu $-0,0003$, in guter Übereinstimmung mit dem oben besprochenen Resultat aus der asymmetrischen Drift, berechnet. Ein Schnitt der Dichtigkeitsflächen senkrecht zur Milchstraße in der Richtung $L = 320^\circ$ gibt für hohe galaktische Breiten Kurven, die sehr wohl als Ellipsen mit Zentrum in der Milchstraßenebene in der Entfernung 10000 Parsec angesehen werden können. Die Ellipse, bei der die Dichte des photographischen Lichts $\frac{1}{35}$ der entsprechenden Dichte in der Nähe der Sonne ist, hat die Achsen $a = 12200$, $b = 1310$, und die Ellipse für die Dichte $\frac{1}{100}$ die Achsen $a = 14300$, $b = 2240$, in Parsec ausgedrückt. OORT berechnet aus $K(z)$ unter verschiedenen schematischen Annahmen über die Massenverteilung im System die Totaldichte ρ der Materie in der Umgebung der Sonne. Er findet Werte zwischen 0,079 und 0,108 Sonnenmassen per Kubikparsec, womit offenbar LINDBLADS oben gegebener Wert gut übereinstimmt. KAPTEYN hatte den Wert 0,099 gefunden, JEANS aus der Sternströmungstheorie (Ziff. 28) 0,143. Durch Vergleich mit der wahrscheinlichen Anzahl von Sternen per Volumeneinheit zieht OORT den Schluß, daß Nebel und Meteore zusammen zu der Totalmasse weniger als die Sterne beitragen, möglicherweise sogar viel weniger.

31. Differentielle Rotationseffekte in den beobachteten Geschwindigkeiten. Nach der eben besprochenen Theorie liegt die Richtung der asymmetrischen Verschiebung der Geschwindigkeitsmittelpunkte senkrecht zur Richtung von uns nach dem Zentrum des Systems. Die asymmetrische Verschiebung ist eine differentielle Rotation verschiedener Gruppen von Objekten relativ gegeneinander. Vom Nordpol der Milchstraße gesehen, geht die Rotation in retrograder Richtung, von links nach rechts.

Es ist aber J. H. OORT¹ gelungen, auf anderem Wege eine Bestimmung der Lage des dynamischen Zentrums zu gewinnen. Die mittleren Geschwindigkeiten Θ_0 sind überall senkrecht zum Radiusvektor gerichtet, werden ja aber nicht unmittelbar beobachtet. Was in der Beobachtung gemessen wird, ist die vektorielle Differenz zwischen Θ_0 und der Geschwindigkeit der Sonne. Wir betrachten jetzt Sterne in der galaktischen Ebene in der Entfernung r von uns. Die eben erwähnte vektorielle Differenz zerlegen wir in ihre Komponente längs r , die Radialgeschwindigkeit, und ihre Komponente senkrecht zu r , die transversale Geschwindigkeit. Durch Abziehen der Komponenten der Sonnenbewegung in bezug auf die umgebenden Sterne der betreffenden Klasse bekommen wir Residuen, welche die vektorielle Differenz zwischen den ringsherum im Abstände r geltenden Θ_0 -Werten und dem Θ_0 -Wert des Sonnenorts darstellen. Wenn r gegen R klein ist, bekommen wir dann für die Radialgeschwindigkeiten eine Abhängigkeit von der galaktischen Länge der beobachteten Objekte von der Form

$$rA \sin 2(L - L_0), \quad (63)$$

wo L_0 die galaktische Länge des Zentrums ist, und für die transversalen Geschwindigkeiten

$$rA \cos 2(L - L_0) + rB, \quad (64)$$

wo

$$A = \frac{1}{2} \left(\frac{\Theta_0}{R} - \frac{\partial \Theta_0}{\partial R} \right), \quad B = \frac{1}{2} \left(-\frac{\Theta_0}{R} - \frac{\partial \Theta_0}{\partial R} \right). \quad (65)$$

¹ B A N 3, S. 275; 4, S. 79 u. S. 91 (1927).

Wir haben also $B = A - \omega$, wo $\omega = \frac{1}{R} \Theta_0$ die Winkelgeschwindigkeit der Rotationsbewegung ist. In dem speziellen Falle, wo Θ_0 die Geschwindigkeit der zirkularen Bewegung ist, also wenn die Dispersion α sehr klein ist, haben wir

$$A = \frac{1}{4} \left(\omega + \frac{1}{\omega} \frac{\partial^2 V}{\partial R^2} \right). \quad (66)$$

In Übereinstimmung mit den Ergebnissen aus dem Phänomen der Asymmetrie setzen wir voraus, daß ω eine retrograde Bewegung ist, also eine Rotation von links nach rechts, wenn sie von einem Punkte nördlich von der galaktischen Ebene betrachtet wird. Die transversale Geschwindigkeit wird im Sinne wachsender galaktischer Länge gezählt. Für die mittleren Eigenbewegungen in galaktischer Länge bekommen wir, wenn A und B in Kilometern per Sekunde für die Entfernung von einem Parsec und die Eigenbewegungen in Bogensekunden ausgedrückt werden,

$$4,74 \mu_L = A \cos 2(L - L_0) + B. \quad (67)$$

Die oben gemachten Ansätze haben viel gemeinsam mit den Gedanken, welche zuerst GYLDÉN¹ in einer Arbeit entwickelte, in der die Sternbewegungen mit den geozentrischen Bewegungen der kleinen Planeten verglichen wurden. GYLDÉN entwickelt die mittleren Eigenbewegungen in Rektaszension (α) für verschiedene α innerhalb einer Deklinationszone in eine FOURIERSche Reihe, deren einzelne Glieder von den \sin und \cos für sukzessive Vielfache von α abhängig sind. Als Terme von reeller Bedeutung behandelt er besonders den konstanten Term und die Terme in α und 2α . Die Terme in α geben den Reflex der Sonnenbewegung in bezug auf die betrachteten Sterne (sind aber zum Teil auch von galaktischen Rotationseffekten oben beschriebener Art bedingt); für den Apex findet GYLDÉN hieraus $\alpha = 270^\circ$. Die übrigen Terme deuten aber nach ihm auf eine allgemeine Umlaufbewegung der Sterne um ein gemeinsames Zentrum hin. Zwar bekommt GYLDÉN aus seinem Material, speziell nach einer Korrektur der Präzession von NYRÉN, einen konstanten Term, der einer direkten Rotationsbewegung entspricht. Aus der qualitativen Übereinstimmung der Koeffizienten der Entwicklung mit denen der geozentrischen Bewegungen der kleinen Planeten am 21. März 1868 zieht er weiter den Schluß, daß das Zentrum des Sternsystems in einer Richtung liegt, deren R.A. mit der R.A. der Sonne in der späteren Hälfte des März zusammenfällt, also in der Himmelsregion zwischen Auriga und Cygnus. Wenn man aber eine retrograde Bewegung voraussetzt, bekommt man aus GYLDÉNS Koeffizienten für $\cos 2\alpha$ und $\sin 2\alpha$ die Werte $-1'',21$ und $-0'',40$ pro 100 Jahre und für das Zentrum zwei um 180° verschiedene alternative Werte, von denen der eine einer galaktischen Länge des Zentrums von 359° entspricht, was in ziemlich guter Übereinstimmung mit unseren jetzigen Ansichten steht.

In besonders interessanter Weise hat S. OPPENHEIM² die GYLDÉNSchen Ideen weiter zu entwickeln gesucht und für die spezielle Klasse der B-Sterne die harmonische Analyse auch auf die Radialgeschwindigkeiten ausgedehnt. Sein Ziel war zuerst, unter Voraussetzung einer Analogie mit den kleinen Planeten, die Bahnebene der Bewegungen zu ermitteln und durch harmonische Analyse der Bewegungen parallel dieser Ebene die Lage des Bewegungszentrums zu finden. Er führt später, im Anschluß an die BRÜSEL-KOBOLDSche Methode zur Apexbestimmung in HARZERS Ausführung, ein „Momentenellipsoid“ ein (das

¹ Övers K Vetenskapsakad Förhandl 28, S. 956 (1871).

² A N 188, S. 137 (1911); Wien Denkschr Math Nat Kl 87, S. 297 (1912); Astron Kal 1913, S. 126; Wien Denkschr Math Nat Kl 92; A N 201, S. 241 u. 417 (1915); Wien Denkschr Math Nat Kl 93; A N 202, S. 89 (1916); 204, S. 417 (1917); SIEGLER-Festschr S. 131 (1924);

von dem Momentenellipsoide in CHARLIER-WICKSELLS statistischer Theorie der zentroidalen Bewegungen zu unterscheiden ist) von der Form

$$Ax^2 + By^2 + Cz^2 + 2Dyz + 2Exz + 2Fxy = 1, \quad (68)$$

wo

$$\left. \begin{aligned} A &= \Sigma(l\bar{l}), & C &= \Sigma(n\bar{n}), & E &= \Sigma(n\bar{l}), \\ B &= \Sigma(m\bar{m}), & D &= \Sigma(m\bar{n}), & F &= \Sigma(l\bar{m}), \\ l &= \sin i \sin \Omega, & m &= -\sin i \cos \Omega, & n &= \cos i. \end{aligned} \right\} \quad (69)$$

Ω und i sind die R.A. des aufsteigenden Knotens und die Neigung des Bewegungskreises eines Sterns. Die größte Achse dieses Ellipsoids soll gegen den Apex der Sonnenbewegung, die mittlere Achse gegen das Zentrum der Bewegung und die kleinste Achse gegen den Pol der Bewegungsebene zeigen. Aus den Eigenbewegungen der Sterne ergeben sich aber zwei Bestimmungen dieses Ellipsoids, da die Werte von Ω (nach einer einheitlichen Regel bestimmt) zwei voneinander sehr verschiedene Gruppen andeuten, die auch räumlich voneinander getrennt sind. Nach Vertauschung der zwei kleineren Achsen in dem sekundären Ellipsoid, das sonst keine verständliche Beziehung zur Milchstraßenebene zeigt, werden die Achsenrichtungen jedoch fast identisch und ein Mittel kann gebildet werden. Die Theorie ergibt, auf die Bewegungen der kleinen Planeten und der Kometen angewandt, sehr interessante und zum Teil leicht interpretierbare Resultate.

Für die Sterne des BOSS-Kataloges findet OPPENHEIM als Mittel für die Hauptrichtungen der zwei Ellipsoide in der oben gegebenen Ordnung

$$\left. \begin{aligned} \alpha_1 &= 271^\circ,5 \\ \delta_1 &= +32^\circ,3 \end{aligned} \right\}, \quad \left. \begin{aligned} \alpha_2 &= 31^\circ,4 \\ \delta_2 &= +38^\circ,1 \end{aligned} \right\}, \quad \left. \begin{aligned} \alpha_3 &= 155^\circ,1 \\ \delta_3 &= +35^\circ,2 \end{aligned} \right\}.$$

Die erste Richtung ist in guter Übereinstimmung mit dem allgemein angenommenen Apexwert, die letzte zeigt gegen eine hohe galaktische Breite ($+60^\circ$). Die der zweiten Richtung gerade entgegengesetzte am Himmel, die ebensogut die Richtung gegen das Zentrum andeuten kann, entspricht den galaktischen Koordinaten $L = 288^\circ$, $B = +21^\circ$, also einem Punkte, der nicht allzu weit von SHAPLEYS Anhäufungspunkt der Kugelhaufen entfernt ist.

OORT hat in erster Linie die Radialgeschwindigkeiten für Objekte von großer Entfernung in niedrigen galaktischen Breiten untersucht, um die Existenz des Rotationstermes (63) nachzuweisen. Es stellte sich bei dieser Untersuchung heraus, daß entfernte Objekte von verschiedener physikalischer Natur im ganzen miteinander wohl übereinstimmende Werte von L_0 und A ergaben. Für die

Tabelle 22.

Gruppe	L_0	m.F.
B3-B5	322°	$\pm 5^\circ$
A-G $\left\{ \begin{array}{l} \mu < 0'',020 \\ 4,0 < m \leq 5,8 \end{array} \right\}$	345	± 9
B0-B2	322	± 5
c-Sterne $m < 5,0$	330	± 8
A-G $\left\{ \begin{array}{l} \mu < 0'',020 \\ m > 5,8 \end{array} \right\}$	337	± 8
Oe5	308	± 7
c-Sterne $m \geq 5,0$	321	± 4
Planet, Nebel	333	± 10

auch mit der Länge des Zentrums, wie sie aus der Asymmetrie der Geschwindigkeitsverteilung (Ziff. 30) hervorgeht, gut verträgt.

Für den Koeffizienten A ergab sich im Mittel $+0,019 \text{ km/sec per Parsec} \pm 0,003$ (m.F.). Da A die Abweichung von einer gleichförmigen angularen Rotations-

Länge des Attraktionszentrums erhielt OORT die Werte in Tabelle 22, wo die Gruppen grob nach mittlerer Entfernung (von 300 bis etwa 1200 Parsec) angeordnet worden sind. Das unter Berücksichtigung der Gewichte berechnete Mittel für L_0 wird $324^\circ \pm 2^\circ$ (m.F.), was offenbar sehr gut mit SHAPLEYS Konzentrationsspunkt für die Kugelhaufen übereinstimmt und sich

geschwindigkeit mißt, so ist also gemäß diesen Resultaten die vektorielle Differenz der Rotation im oben angegebenen Sinne oder die „differentielle Rotation“, innerhalb unserer Umgebung des Sternstratus nachweisbar. Es deutet dies an, daß das Gravitationsfeld an unserem Ort im System nicht etwa dem Felde eines homogenen Rotationsellipsoids in seiner Äquatorebene entspricht, sondern, mit diesem Fall verglichen, auf eine merkliche Verdichtung der Materie gegen die zentralen Regionen des Systems schließen läßt.

Um aber eine entscheidende Evidenz für die Realität der differentiellen Rotation zu bekommen, müssen auch die Effekte (67) in den Eigenbewegungen untersucht werden. Oort hat die Eigenbewegungen des Preliminary General Catalogue von Boss behandelt. Korrekturen für die Bewegung des Frühlingspunktes und für die Präzessionskonstante wurden aus den Bewegungskomponenten in galaktischer Breite bestimmt. Als Korrekturen der NEWCOMBSchen Werte für die zwei erwähnten Größen findet Oort $+0''.0137 \pm 0''.0020$ (m.F.) bzw. $+0''.0113 \pm 0''.0020$ (m.F.). Als Wert der Lunisolarpräzession ergibt sich also $50''.3821$ (1900). Die korrigierten Eigenbewegungen in galaktischer Länge wurden zur Bestimmung von L_0 , A und B benutzt. Die Werte von L_0 stimmen gut mit den oben gegebenen, aus den Radialgeschwindigkeiten ermittelten überein, während A nicht unerheblich kleiner als der oben gegebene Wert ausfällt, was aber nach Oort sehr wohl durch Fehler in den Eigenbewegungen, speziell für Sterne in der südlichen Milchstraße, verursacht sein kann. Für die mittlere Bewegung $B/4,74$ längs der Milchstraße gibt Oort, gemäß den Resultaten für drei Gruppen von sehr entfernten Sternen, als wahrscheinlich besten Wert $-0''.0050$ oder $B = -0,024$ km/sec per Parsec $\pm 0,005$ (m.F.) (vgl. Ziff. 26 und 32).

Zur weiteren Beleuchtung des überaus wichtigen Effektes der differentiellen Rotation in den Radialbewegungen konnte J. S. PLASKETT¹ ein vorzügliches neues Material von Geschwindigkeiten für WOLF-RAYET- und Helium-Sterne ausnutzen, die auf dem Observatorium in Victoria gemessen worden sind. Für die Rotationsgrößen L_0 und A und den K -Term hat er die in Tabelle 23 aufgeführten Werte mit den angegebenen wahrscheinlichen Fehlern gefunden. Im Mittel bekommt PLASKETT hier $L_0 = 324^\circ,5 \pm 1^\circ,8$, $A = +0,0155 \pm 0,0007$ km/sec per Parsec.

Tabelle 23

Klasse und Größe	n	\bar{n}	L_0	K km/sec	\bar{A} km/sec
B0-B2 <6,21 . . .	66	5,00	$322^\circ,7 \pm 9,8$	$+3,2 \pm 1,0$	$+5,9 \pm 0,9$
B0-B2 >6,20 . . .	66	6,94	$328,5 \pm 3,0$	$-0,4 \pm 0,9$	$+16,7 \pm 1,1$
B3-B5 <6,21 . . .	181	5,16	$308,5 \pm 2,6$	$+0,9 \pm 0,3$	$+4,8 \pm 0,5$
B3-B5 >6,20 . . .	175	6,79	$325,0 \pm 2,1$	$-1,2 \pm 0,3$	$+5,9 \pm 0,3$
O	65	6,43	$322,3 \pm 7,2$	$+5,8 \pm 2,9$	$+17,1 \pm 4,0$

Eine sehr große Bedeutung hat gegenwärtig die Theorie der differentiellen Rotation für die Erscheinung der „stationären“ Kalziumlinien (Ziff. 25) gewonnen. Oort berechnete den Rotationskoeffizient für 40 Ca^+ -Geschwindigkeiten zu $+5,6$ km/sec $\pm 2,2$ (m.F.). GERASIMOVIC² und O. STRUVE³ haben dann die galaktische Rotation des interstellaren Kalziums aus den Ca^+ -Geschwindigkeiten für 103 Sterne vom Typus O-B2 studiert. Der Koeffizient \bar{A} für die „Wolken“ ergibt sich zu $+5,3$ km, während für die Sterne selbst $+12,0$ km aus PLASKETTS obenerwähnten Werten berechnet wurde. Das Verhältnis 1:2,3 zwischen den mittleren Entfernungen wurde als Zeugnis für eine approximativ gleichförmige Verteilung des Kalziums gemäß EDDINGTONS Hypothese betrachtet.

¹ M. N. 88, S. 395 (1928)² Ap. J. 69, S. 9 (1929)

Einen ungemein großen Fortschritt zur Aufklärung der diesbezüglichen Verhältnisse bedeutet aber vor allem die Arbeit von J. S. PLASKETT und J. A. PEARCE¹, die im wesentlichen auf dem umfangreichen Material von Geschwindigkeiten für B0–B5-Sterne heller als 7^m,5 visuell und nördlich von der Dekl. -11° beruht, welches in den letzten Jahren auf dem Observatorium in Victoria gesammelt worden ist. Für 261 Sterne, deren galaktische Verteilung in Abb. 28 dargestellt wird, sind Ca^+ -Geschwindigkeiten vorhanden. Mit einer angenommenen Sonnengeschwindigkeit von $+20,0$ km gegen den Apex $L = 21^\circ,8$, $B = +20^\circ$ ergaben sich für den K -Term und die Rotationsgrößen die Resultate $K = -0,61 \pm 0,57$ km, $\bar{r}A = +7,90 \pm 0,79$ km, $L_0 = 331^\circ,7 \pm 5^\circ,7$. Der Rotationskoeffizient kommt also hier mit einem Werte heraus, der zehnmal größer als sein wahrscheinlicher Fehler ist. Die Länge L_0 erscheint fast exakt um 90° gegen STRÖMBERGS Asymmetrielinie gedreht.

Die 235 Sterne, für welche sowohl „stellare“ als „interstellare“ Geschwindigkeiten vorliegen, wurden zuerst in Gruppen nach scheinbarer Größe geteilt und

Tabelle 24. Gruppierung nach Größe.

Größe	n	$\bar{r}A$		K	
		Sterne	Wolken	Sterne	Wolken
4,41	37	$+1,81 \pm 2,83$	$+3,85 \pm 1,22$	$+7,12 \pm 1,42$	$+0,02 \pm 0,61$
5,60	45	$+10,26 \pm 2,12$	$+5,02 \pm 1,24$	$+3,99 \pm 0,96$	$+0,97 \pm 0,56$
6,03	79	$+13,86 \pm 1,75$	$+7,66 \pm 0,90$	$+1,67 \pm 0,77$	$+0,09 \pm 0,40$
7,08	119	$+16,58 \pm 2,20$	$+8,31 \pm 1,36$	$+1,39 \pm 1,46$	$-0,69 \pm 0,90$
7,34	69	$+20,49 \pm 2,32$	$+10,08 \pm 1,57$	$+2,34 \pm 0,86$	$+0,23 \pm 0,56$

innerhalb jeder Gruppe ist dann der Rotationskoeffizient $\bar{r}A$ und der K -Term sowohl für Sterne als für Wolken bestimmt worden. Für L_0 wurde hier immer der Wert 325° angenommen. Die Resultate sind in Tabelle 24 aufgeführt.

Für die vier letzten Gruppen, in mittleren Entfernungen von etwa 600, 800, 1000 und 1200 Parsec, ist das Verhältnis der Rotationskoeffizienten $\bar{r}A$ für Sterne und Wolken der Reihe nach 2,04, 1,81, 1,99, 2,03 oder im Mittel 1,97. Die EDDINGTONSche Hypothese, daß die interstellare Materie gleichförmig verteilt ist, wird also hier in außerordentlich deutlicher Weise bestätigt.

Ähnliche Resultate gibt eine Einteilung des Materials nach der Intensität der interstellaren K -Linie, wie Tabelle 25 zeigt. Die erste Kolumne gibt die benutzten Intervalle in Intensität in einer konventionellen Skala.

Tabelle 25. Gruppierung nach Intensität der interstellaren Linien.

Intensität		$\bar{r}A$		K	
Intervall	Mittel	Sterne	Wolken	Sterne	Wolken
0–5,9	4,72	$+3,64 \pm 3,25$	$+4,97 \pm 0,77$	$+6,12 \pm 2,14$	$+1,15 \pm 0,50$
6,0–6,9	6,50	$+12,12 \pm 1,88$	$+4,93 \pm 0,92$	$+4,66 \pm 1,27$	$+0,10 \pm 0,62$
4,4–6,9	6,08	$+10,22 \pm 1,72$	$+5,03 \pm 0,85$	$+5,24 \pm 1,17$	$+0,10 \pm 0,58$
7,0–7,9	7,46	$+14,53 \pm 2,93$	$+6,91 \pm 1,06$	$-0,14 \pm 1,95$	$-0,21 \pm 0,70$
8,0–9,5	8,42	$+27,52 \pm 2,46$	$+13,72 \pm 1,16$	$+3,18 \pm 1,74$	$-1,17 \pm 0,82$

Es stellt sich heraus, daß die Intensität der interstellaren Linie ein besseres Entfernungskriterium als die scheinbare Größe ist. Aus den Werten von $\bar{r}A$ für die letzte Gruppe der Tabelle kann man die mittlere Entfernung – zu etwa 1600 Parsec berechnen. In wie hohem Maße der Rotationsterm $\bar{r}A \sin 2(L - 325^\circ)$ die Geschwindigkeiten innerhalb der einzelnen Längengruppen wiedergibt, zeigt

¹ M N 90, S. 243 (1930).

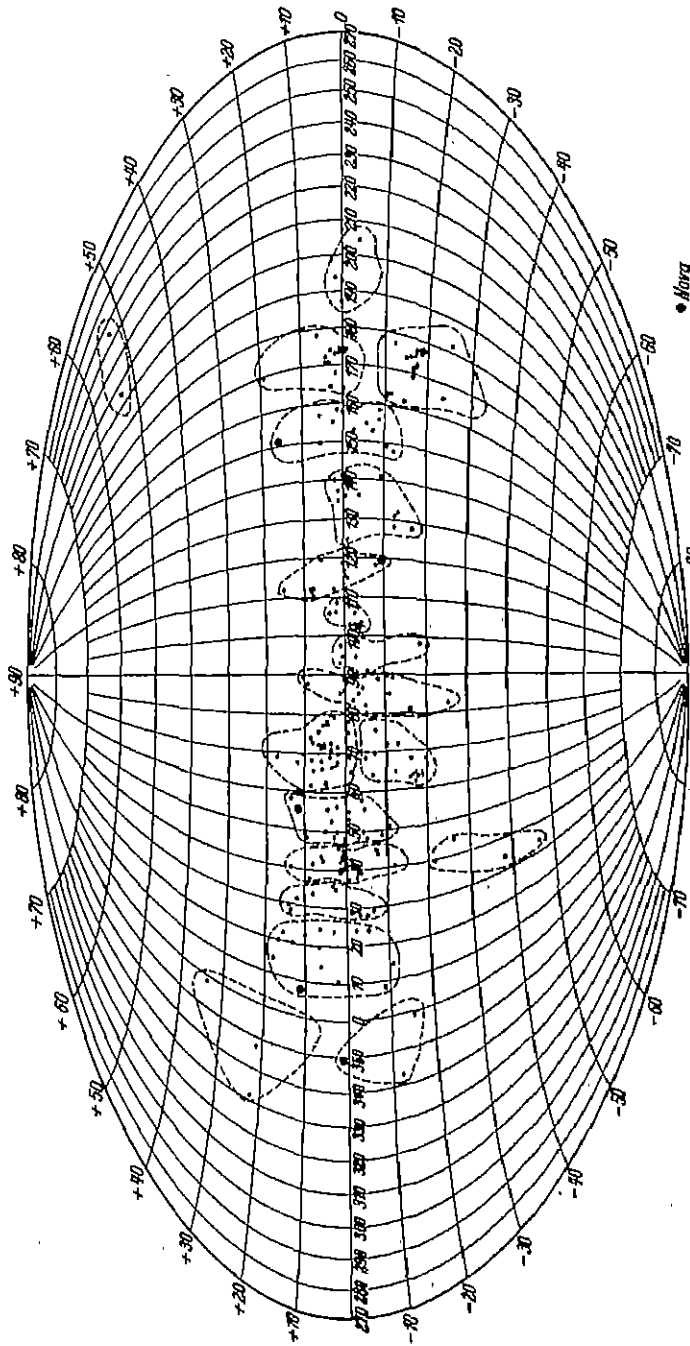


Abb. 28. Die galaktische Verteilung der Kalziumwolken mit bekannten Radialgeschwindigkeiten.

uns die Tabelle 26, wo für die letzte Intensitätsgruppe die beobachteten und die berechneten Geschwindigkeiten relativ zum Zentroid für verschiedene galaktische Längen gegeben worden sind.

Tabelle 26.

Mittlere Länge	n	Sterne		Wolken	
		Beob.	Bor.	Beob.	Bor.
358°	2	+35,7	+24,3	+ 8,2	+ 9,4
17	2	+12,2	+29,5	+ 6,1	+11,9
34	6	+21,5	+21,3	+ 7,5	+ 7,9
47	2	+11,8	+10,4	+ 6,6	+ 2,4
70	12	- 3,4	-10,4	- 5,4	- 8,0
97	4	-26,8	-23,4	-15,5	-14,3
107	9	-28,4	-23,5	-17,7	-14,5
141	4	- 4,1	- 0,9	+ 1,2	- 3,2
169	2	+13,6	+16,0	+ 1,9	+ 5,3

OORT¹ hat eine Auflösung für diese Gruppe allein mit L_0 , $\bar{r}A$ und K als Unbekannten gemacht, wobei die Bestimmung von L_0 beträchtliches Gewicht hat. Er bekommt als Resultat die folgenden Werte:

Sterne		Wolken	
$L_0 = 330^\circ,1 \pm 2^\circ,6$ (w.F.)		$L_0 = 329^\circ,3 \pm 4^\circ,3$ (w.F.)	
$\bar{r}A = 26,0 \pm 2,2$ km/sec		$\bar{r}A = 12,4 \pm 1,7$ km/sec	
$K = +0,9 \pm 1,6$ „		$K = -2,2 \pm 1,2$ „	

Es ist ohne weiteres augenscheinlich, in welchem hohen Grade die Resultate von PLASKETT und PEARCE unsere Vorstellungen über die allgemeinen Eigenschaften des rotierenden Sternsystems stützen, erstens durch die Bestätigung des Rotationseffektes selbst und zweitens durch den Schluß auf eine gleichförmige Verteilung der interstellaren Materie in der galaktischen Ebene innerhalb eines sehr weiten Kreises um uns herum. Keines von diesen Ergebnissen läßt sich wohl mit der Existenz eines lokalen Systems vereinigen, wenn mit diesem Ausdruck irgendeine dynamisch abgeschlossene Einheit gemeint wird.

EDDINGTON² hat auch hervorgehoben, daß die Existenz einer derartigen Schicht von dünnem Gase, die sich gegen das Zentroid der in ihr eingelagerten Sterne in Ruhe befindet, die beste Stütze dafür ist, daß die Bewegung des Zentroids relativ zum Schwerpunkt des Systems eine Kreisbahn beschreibt. Denn da das interstellare Gas zu gleichförmig verteilt erscheint, um wesentlich von irgendeinem hydrodynamischen Druckgradienten gegen die Attraktion des Systems getragen zu sein, so muß das Gleichgewicht durch die Zentrifugalkraft allein bewirkt werden und demnach die mittlere Bewegung innerhalb eines Elementarvolumens des Gases mit der Kreisbewegung übereinstimmen. In dieser Weise können wir mit EDDINGTON behaupten, daß schon die Existenz der kosmischen Wolken ein Beweis für die Existenz der Rotation ist. Der Beweis für die Kreisbewegung ist übrigens analog mit unserem oben (Ziff. 29) für die Sterne von kleiner Geschwindigkeitsdispersion gegebenen.

Es ist aber an sich sehr bemerkenswert, wie EDDINGTON und OORT hervorheben, daß die Bewegung der Wolken so exakt mit dem Zentroide der Sternbewegungen zusammenfällt (nach OORT innerhalb 1 km/sec), wenn wir bedenken, daß die Rotationsgeschwindigkeit auf ungefähr 300 km/sec zu schätzen ist.

In den oben referierten Arbeiten von OORT und von PLASKETT und PEARCE sind besonders Gruppen von Objekten mit großer mittlerer Entfernung und mit kleiner Streuung in den zentroidalen Geschwindigkeiten behandelt worden. Es sind aber auch Versuche gemacht worden, die Rotationsgrößen für ein mehr normales Material zu bestimmen. Es ist klar, daß die Schwierigkeiten, ein zu-

¹ B A N 5, S. 192 (1930).

² The Rotation of the Galaxy. Halley Lecture. Oxford: Clarendon Press (1930).

verlässiges Resultat zu bekommen, mit abnehmender mittlerer Entfernung (welche direkt auf die Amplitude $\bar{r}A$ einwirkt) und mit einer steigenden Streuung der Geschwindigkeiten (welche den Ausgleich der partikularen Bewegungen herabsetzt) erheblich wachsen. Im Falle der Eigenbewegungen bleibt zwar die Rotationsgröße dieselbe, wird aber mit abnehmender Entfernung immer kleiner im Verhältnis zur mittleren Eigenbewegung der Sterne. Eine Tatsache betreffs der Rotationseffekte für die gewöhnlichen Riesensterne der Spektralklassen A bis K scheint jedoch ziemlich wohl begründet. Es stellt sich heraus, daß die Länge L_0 des Rotationszentrums ein wenig höhere Werte als für die entfernteren Objekte von kleinerer Streuung in den Geschwindigkeiten annimmt. Dieses Phänomen ist schon durch OORTS Resultate in Tabelle 22 angedeutet worden, wo für die A bis G-Sterne $L_0 = 345^\circ$ bzw. 337° gefunden wurde. LINDBLAD¹ findet für die Sterne vom Typus F bis K und $\mu < 0''.040$ den Wert $L_0 = 346^\circ$. REDMAN² findet für 425 K-Sterne im Größenintervall 7,0 bis 7,5 und größtenteils innerhalb $\pm 10^\circ$ galaktischer Breite, deren Radialgeschwindigkeiten von ihm selbst in Victoria bestimmt worden sind, die differentielle Rotation $\bar{r}A = 1,9 \pm 1,3$ km/sec, $L_0 = 17^\circ \pm 18^\circ$ (w. F.). Die Sterne in diesem Material zeigen aber eine ziemlich große Streuung in den Geschwindigkeiten, und nach gewissen Eigenschaften der Frequenzkurve der Geschwindigkeiten in verschiedenen Gegenden des Himmels scheint es sehr wohl möglich, daß spezielle Strömungen unter den Sternen auf das Resultat ungünstig eingewirkt haben. H. NORDSTRÖM³ hat deshalb, anstatt das arithmetische Mittel der Geschwindigkeiten verschiedener Gegenden zu benutzen, in einem Ausgleichungsverfahren die Geschwindigkeit maximaler Frequenz für jedes Areal bestimmt und in die Gleichungen für die differentielle Rotation eingesetzt. Er findet dann aus REDMAN'S Material im Mittel $\bar{r}A = 3,0$, $L_0 = 333^\circ$, was als ganz normal anzusehen ist und auch sehr wohl mit seinen Resultaten für K- und M-Sterne heller als 6^m,0 übereinstimmt.

Es ist von großem Interesse, die eben erwähnten Resultate mit den aus einer Behandlung der Eigenbewegungen gewonnenen zu vergleichen. Für eine gesammelte Gruppe von B-, c-, O-, N- und δ Cephei-Sternen (also sehr entfernten Objekten) hat OORT gefunden $A = +0''.0024 \pm 0''.0016$ (m F.), $B = -0''.0050 \pm 0''.0011$ (m F.), $L_0 = 326^\circ \pm 17^\circ$ (m F.), während DYSON⁴ für B0- bis A0-Sterne die fast identischen Werte $A = +0''.0025$, $B = -0''.0046$, $L_0 = 326^\circ$ erhält. J. SCHILT⁵, der speziell die Eigenbewegungen verschiedener AG-Zonen auf die diesbezüglichen Effekte hin analysiert hat, findet aber folgende Werte

Katalog	A	L
GYLLENBERG (35°–40° nördl. Dekl.)	$+0''.0106$	340°
PRAGER (31°–40° nördl. Dekl.)	$+0''.0081$	337°
BOSS PGC	$+0''.0080 \pm 28$ (m F.)	$351^\circ \pm 9$ (m F.)

J. E. MERRILL⁶ findet aus dem Yale-Katalog für nördl. Dekl. 50° bis 55° , $A = +0''.0073$, $L_0 = 0^\circ$.

Da unter den von SCHILT und MERRILL untersuchten Zonensternen die Mehrheit normale Riesensterne vom Typus A bis K sein werden, so können die eben gegebenen Resultate an die Seite der aus den Radialgeschwindigkeiten für diese Typen hergeleiteten gestellt werden. Es ergibt sich also ein höherer Wert der galaktischen Länge des Zentrums L_0 ; außerdem geben offenbar die

¹ M N 90, S. 503 (1930) = Stockholm Medd. 5.

² M N 90, S. 690 (1930), 92, S. 107 (1931), Publ. Astrophys. Obs. Victoria (IV) Nr. 20 (1930).

³ Lund Medd. 131 (1933).

⁴ M N 90, S. 239 (1930).

⁵ Wash. Nat. Ac. Proc. 13, S. 642 (1927), A J 38, S. 149 (1928); 39, S. 17 (1928).

⁶ A J 39, S. 90 (1929).

Daten aus den Eigenbewegungen der Zonensterne einen ziemlich hohen Wert für den Amplitudenfaktor A . Zum Vergleich mag erwähnt werden, daß der Wert $A = +0,0155$ km/sec per Parsec aus den Radialgeschwindigkeiten, durch Division mit 4,74, dem Werte $A = +0'',0033$ im Eigenbewegungseffekt entspricht. Es liegt nahe zu bemerken, daß die Länge L_0 für die normalen Riesensterne besser mit dem beobachteten Vertex des Geschwindigkeitsellipsoids als mit der Länge L_0 für die entfernten Sterngruppen übereinstimmt.

Es sind schon verschiedene Erklärungen für das oben geschilderte Phänomen vorgeschlagen worden. H. MINEUR¹ macht darauf aufmerksam, daß wir die Länge L_0 um 90° ändern können, wenn wir gleichzeitig das Vorzeichen von A ändern. Er sucht dann das Material in zwei Gruppen zu trennen, eine Klasse von sehr entfernten Objekten, die sich um ein Zentrum in der Länge 325° bewegen und eine Klasse von nahen Sternen, die sich um ein lokales Zentrum etwa in der Länge 240° drehen; die letztere Länge stimmt mit dem Zentrum des lokalen Haufens nach CHARLIER und SHAPLEY überein. Es können jedoch wohl ernste Einwände gegen MINEURS Auffassung erhoben werden. Vor allem ist die Entfernung zum Zentrum des „lokalen Haufens“ zu klein, um die Theorie der differentiellen Rotation in der OORTschen Form hier anzuwenden. Es scheint auch, daß der spezielle Rotationseffekt in MINEURS Analyse, den er zur Scheldung zwischen den zwei Rotationsarten heranzieht, von grundsätzlich anderem Charakter als der oben diskutierte Effekt ist (Ziff. 34).

S. S. HOUGH und J. HALM² haben schon in ihren wichtigen Arbeiten über die Sternbewegungen die harmonischen Terme von zweiter Ordnung in den Radialgeschwindigkeiten und in den Eigenbewegungen gefunden und studiert. Sie sehen aber die Ursache der Erscheinung in einem verschiedenen Mischungsverhältnis der drei großen Sterntriften (KAPTEYNS Triften I, II und HALMS O-Trift) in verschiedenen Gegenden des Himmels. In neuerer Zeit ist auch J. SCHILT³ geneigt, die Theorie der differentiellen Rotation zur Erklärung der harmonischen Terme zweiter Ordnung in den Sternbewegungen ganz aufzugeben. Er bildet eine Größe U , welche die Form der Frequenzkurve für die Eigenbewegungen repräsentiert und zeigt, daß ähnliche harmonische Terme in dieser Größe auftreten. Er zieht hieraus den Schluß, daß die harmonischen Terme zweiter Ordnung einem verschiedenen Mischungsverhältnis von Sternströmen in verschiedenen Gegenden des Himmels zuzuschreiben sind. Daß die erwähnte Verschiebung in L_0 wahrscheinlich im Phänomen der Sternströmung ihren Grund hat, wird auch von REDMAN und LINDBLAD behauptet. Es ist aber nicht notwendig, deshalb die Rotationstheorie aufzugeben, was besonders nach den Ergebnissen von OORT, PLASKETT und PEARCE kaum möglich ist. Ein enger Zusammenhang zwischen dem Geschwindigkeitsellipsoid oder der Sternströmung überhaupt und der differentiellen Rotation ist übrigens durchaus in Einklang mit der Theorie, wie wir im folgenden in Ziff. 32 näher auseinandersetzen werden. Nach der Rotationstheorie hängen nämlich sowohl der Effekt der differentiellen Rotation wie die Richtung und das Größenverhältnis der Achsen des Geschwindigkeitsellipsoids in der Milchstraßenebene unmittelbar von dem Scherungseffekt einer gegenseitigen Translation der Geschwindigkeitsmittelpunkte für einander benachbarte Örter im System ab. Diese Translation soll der Richtung der Kreisbewegung folgen und ihre Größe nur auf der Differenz der Entfernung vom Zentrum zwischen den betreffenden Örtern beruhen. Es ist aber durchaus nicht

¹ C R 188, S. 236, 1086 u. 1378 (1929); 190, S. 1050 (1930); B A 5, S. 505 (1929); M N 20, S. 516 (1930).

² M N 20, S. 85 und 568 (1909, 1910); 71, S. 610 (1911).

³ A J 39, S. 143 (1929).

befremdend, daß eine Abweichung der Vertexrichtung oder andere Anomalien der allgemeinen Sternströmung, die etwa in einzelnen ausgeprägten Sternströmen ihren Grund haben, von entsprechenden Effekten in den ermittelten Rotationsquantitäten begleitet sein können.

32. Die Beziehung zwischen dem Geschwindigkeitsellipsoid und der Rotation. Nach der abstrakten Theorie sollte das Geschwindigkeitsellipsoid ein Sphäroid sein, dessen Äquatorebene auf der galaktischen Ebene senkrecht steht und mit der Ebene, welche die Rotationsachse des Systems enthält, zusammenfällt. Das Verhältnis der Achsen α und β soll aber auch in einer gewissen Beziehung zu der Größe A und zu der Winkelgeschwindigkeit ω der Rotation stehen. Wir haben gemäß den Gleichungen (65), (42), (44)

$$A = \frac{1}{2} \left(\frac{\partial \theta_0}{R} - \frac{\partial \theta_0}{\partial R} \right), \quad \theta_0 = \frac{MR}{R^2 + 2p}, \quad \left(\frac{\beta}{\alpha} \right)^2 = \frac{2p}{R^2 + 2p}$$

und bekommen dann die Relation

$$A = \omega \left[1 - \left(\frac{\beta}{\alpha} \right)^2 \right]. \tag{70}$$

ω wird positiv in retrograder Richtung gerechnet. α ist die Achse, welche in der Milchstraßenebene gegen das Zentrum des Systems zeigt. In Ziff. 30 haben wir weiter aus der Theorie ermittelt, daß, wenn die ellipsoidische Approximation streng wäre, die Achse α für alle Punkte des Systems konstant sein sollte, während β mit R (aber nicht mit z) variiert.

Die Bedeutung der Gleichung (70) ist eine zweifache: Erstens, da es sehr wohl möglich ist, daß A und β/α für verschiedene Gruppen von Sternen verschiedene Werte annehmen, können wir hoffen, durch Koordination der gemessenen Werte von A und β/α im Vergleich mit der Gleichung eine wertvolle Kontrolle der Theorie selbst zu bekommen. Zweitens können wir in dieser Weise die Größe ω bestimmen, was sonst durch direkte Analyse der Eigenbewegungen geschehen muß. Die mittlere Eigenbewegung B in galaktischer Länge ist mit A und ω durch die Relation $B = A - \omega$ verbunden. Der Wert von B aus den Eigenbewegungen muß mit dem aus dieser Relation ermittelten verglichen werden.

Gemäß den obigen Auseinandersetzungen und unserer Deutung der empirischen Daten in der vorigen Ziff. 31 betrachten wir A und ω als positive Größen. Die Achse α soll also die größere sein und die Vertexlinie der Sternströmung soll gegen das Zentrum hin zeigen.

Eine quantitative Vergleichung zwischen differentieller Rotation und Geschwindigkeitsellipsoid hat B. LINDBLAD¹ unter Benutzung des zur Zeit zugänglichen Materials von Radialgeschwindigkeiten für gewöhnliche Spektraltypen versucht. Die Resultate sind in Tabelle 27 aufgeführt. Für die Typen A bis K sind die Sterne in Gruppen nach Eigenbewegung aufgeteilt worden. Die Bestimmung von A und L_0 ist nur für die entfernteste Gruppe möglich gewesen.

Tabelle 27.

Gruppe	A	L_0	Vertex	α km/sec	β km/sec	γ km/sec	n
B0-B7	+0,006	324°	289°	10,9	9,8	4,5	445
B8-B9	+ ,013	334	275	12,4	10,8	11,4	250
A, $\mu < 0'',040$	+ ,033	319	24	18,6	12,4	3,9	304
F-K, $\mu < 0'',040$	+ ,021	346	335	17,5	13,6	16,5	714
A, $0'',040 < \mu < 0'',160$	—	—	356	19,1	8,4	10,0	391
F-K, $0'',040 < \mu < 0'',160$	—	—	342	27,7	19,4	16,9	857
F-K, $\mu > 0'',160$	—	—	349	36,3	21,4	25,5	825

¹ M N 90, S. 503 (1930) = Stockholm Medd 5.

Die Sterne vom Typus B zeigen nur geringe Spuren einer Vorzugsrichtung der relativen Bewegungen in der Milchstraßenebene, was wohl in der kleinen Streuung der Geschwindigkeiten und dem Zusammengehen dieser Sterne in mehr oder weniger losen Haufen seinen Grund hat. Im A-Typus setzt der Ursa Major-Strom ein, und dies führt eine sehr merkliche Distorsion der Geschwindigkeitsfläche mit sich. Die späteren Typen zeigen ziemlich hohe Werte von L_0 und der Länge des Vertex, ein Phänomen, das wir schon in der vorigen Ziff. 31 besprochen haben. Im ganzen scheint es sehr wohl möglich, daß die Abweichungen des Ellipsoids von den idealen Verhältnissen der Theorie wenigstens größtenteils auf den Einfluß irregulärer Strömungen in unserer näheren Umgebung zurückgeführt werden können.

Zur Erklärung des Umstandes, daß die dritte Achse gewöhnlich viel kleiner als die größte Achse in der Vertexrichtung herauskommt, haben wir schon in Ziff. 29 und 30 angeführt, daß die Bewegung parallel zur Milchstraßenebene in der unmittelbaren Nachbarschaft von dieser Ebene von nahe zweidimensionaler Natur ist, und daß demnach die statistische Ausgleichung zwischen den galaktischen Bewegungskomponenten und der dritten Bewegungskomponente senkrecht zur Milchstraßenebene eine außerordentlich langsame sein muß. Spezielle Strömungen in der Milchstraßenebene werden daher auch nur sehr langsam auf die Streuung in Z einwirken.

Nur für die erste Gruppe F bis K in Tabelle 27 ist ein direkter Vergleich zwischen dem Ellipsoid und den Größen der differentiellen Rotation möglich. Der Wert von A ist jedoch hier mit einem ziemlich großen mittleren Fehler behaftet. Wenn wir an Stelle dessen PLASKETTS Wert $A = 0,0155$ annehmen und für β/α als normalen Wert 0,78, so bekommen wir aus der Formel

$$\omega = +0,040, B = -0,024.$$

Durch Division mit dem Faktor 4,74 ergibt sich

$$\omega = +0'',0084, B = -0'',0051,$$

ein Resultat, das sich im ganzen wohl mit den direkt aus den Eigenbewegungen ermittelten Werten verträgt (vgl. Ziff. 34).

H. RAYMOND und R. E. WILSON¹ haben in einer Untersuchung über die Raumgeschwindigkeiten von 4233 Sternen die diesbezüglichen Fragen einer eingehenden Besprechung unterzogen. Die beiden Verfasser haben nach neuen Methoden eine Analyse der Asymmetrie der Geschwindigkeitsverteilung ausgeführt, welche für die Asymmetrierichtung $L = 62^\circ$, $B = +6^\circ$ gibt, in wesentlicher Übereinstimmung mit STRÖMBERGS Resultaten, und sie haben die offenbare Verbindung zwischen dieser Asymmetrie und den nahe senkrecht dazu vor sich gehenden allgemeinen Vertexbewegungen untersucht. Zuletzt haben sie sehr ausführlich die Relation zwischen den Rotationsgrößen und den Eigenschaften der Geschwindigkeitsellipsoide diskutiert. Als mittleren Wert für das Achsenverhältnis β/α erhalten sie 0,72, woraus für $A = +0,015$

$$\omega = +0,031, B = -0,016$$

folgt, oder in Bogensekunden

$$\omega = +0'',0065, B = -0'',0034.$$

Unser oben hergeleiteter Wert $B = -0'',0051$ stimmt mit dem von OORT aus den Eigenbewegungen sehr entfernter Sterne bestimmten überein. Nach RAYMOND und WILSON steht jedoch der kleinere Wert $B = -0'',0034$ in besserer Übereinstimmung mit der mittleren Eigenbewegung in galaktischer Länge für

¹ A J 40, S. 121 (1930).

die Sterne im allgemeinen. Die Verfasser haben auch aus ihrem Material die Konstanten der differentiellen Rotation sowohl für Radialgeschwindigkeiten wie für Eigenbewegungen bestimmt. Die ersteren, in zwei Gruppen nach der mittleren Parallaxe der Sterne geordnet, gaben folgendes Resultat:

$\bar{\pi}$	L_0	$\bar{r}A$	A
0,0121	329°	$+1,29 \pm 0,34$	$+0,0155$
0,0046	355	$+3,05 \pm 0,40$	$+0,0140$

Die Resultate sind in guter Übereinstimmung mit den in der vorigen Ziff. 31 referierten. Der hohe Wert von L_0 für die zweite Gruppe ist auffallend.

In den Eigenbewegungen wird ein Term vom Typus $C \cos 3(L - L_1)$ eingeführt, dessen Koeffizient $C = +0'',0022 \pm 0,0003$ gefunden wird, und wo sich für L_1 der Wert $+10^\circ$ ergibt. F. W. DYSON hatte einen ähnlichen Term für die B-Sterne eingeführt. Wahrscheinlich liegt der Grund dieses Termes in speziellen Strombewegungen, möglicherweise sogar im Ursa Major-Strom und im Taurus-Strom. Der erstere geht nahe gegen die Länge 0° , wo $\cos 3L$ und $\cos L$ Maxima haben, während der letztere gegen $L = 150^\circ$ zeigt, wo $\sin 3L$ ein Maximum hat. Für A und B ergeben sich die sehr kleinen Werte

$$A = +0'',0013, B = -0'',0005.$$

Der Übersicht wegen stellen wir in Tabelle 28 einige repräsentative Bestimmungen der wichtigen Konstanten B zusammen. Die als theoretisch bezeichneten Werte sind die aus dem Achsenverhältnis des Geschwindigkeitsellipsoids berechneten.

Tabelle 28.

B	Autortät
$-0'',0024$	CHARLIER ¹
$-0,0015$	FOTHERINGHAM ²
$-0,0023$	OORT
$-0,0005$	RAYMOND und WILSON
$-0,0050$ B-, c-, O-, N-, δ Ceph.-Sterne	OORT
$-0,0051$ Theoretisch	LINDBLAD
$-0,0034$ „	RAYMOND und WILSON

Ein einfaches Mittel aus diesen Werten gibt $B = -0'',0029$, und dieser Wert kann vorläufig als der beste für diese Größe gelten.

88. Die Dimensionen, die Masse und die Rotationszeit der Milchstraße. Wenn wir gemäß Tabelle 28 für die Konstante B im Mittel $-0'',0029$ annehmen und für A den Wert $+0'',0033$, so gibt uns die Relation $\omega = A - B$ für die Winkelgeschwindigkeit der Rotation $\omega = 0'',0062$. Nachdem wir den Wert von ω bestimmt haben, gibt uns eine Ermittlung der linearen Rotationsgeschwindigkeit Θ_0 unmittelbar unsere Entfernung R vom Zentrum des Systems. Aus den Apexbestimmungen für die Kugelhaufen haben wir oben Θ_0 für Gruppen kleiner Geschwindigkeitsstreuung zu 275 km/sec angenommen. Der entsprechende Wert der Zentrumsentfernung ist

$$R = 9400 \text{ Parsec.}$$

Die Rotationsdauer an unserem Orte wird etwa

$$P = 200 \text{ Millionen Jahre.}$$

Für die Zentralkraft an unserem Orte haben wir offenbar, da für kleine Geschwindigkeitsstreuung Θ_0 die Geschwindigkeit der Kreisbewegung ist,

$$\frac{\partial V}{\partial R} = -\frac{1}{R} \Theta_0^2 = -R \omega^2. \quad (71)$$

¹ Mem Univ Calif 7 (1926).² M N 86, S. 424 (1926).

Wir können eine „effektive Masse“ des Systems in der Weise ermitteln, daß wir diese Kraft als durch ein schematisches System erzeugt denken, welches aus einer sphärischen Zentralmasse M_1 und einer sehr abgeplatteten, homogenen, sphäroidischen Verteilung von der Gesamtmasse M_2 mit dem galaktischen Radius R_1 besteht. Das Verhältnis zwischen M_1 und M_2 soll so angepaßt werden, daß es für zirkuläre Bewegungen einen differentiellen Rotationseffekt A gibt. Wir haben dann also gemäß (71)

$$\frac{\partial V}{\partial R} = -G \left(\frac{M_1}{R^2} + \frac{3\pi}{4R_1^3} R M_2 \right) = -R\omega^2 \quad (72)$$

Wir können weiter schreiben

$$A = \frac{1}{4\omega} \left(-\frac{1}{R} \frac{\partial V}{\partial R} + \frac{\partial^2 V}{\partial R^2} \right) = \frac{3}{4} G \frac{M_1}{\omega R^3}, \quad (73)$$

und bekommen dann nach einigen Reduktionen

$$M_1 = \frac{4R^3}{3G} \omega A, \quad M_2 = \frac{4R_1^3}{3\pi G} \omega \left(\omega - \frac{4}{3} A \right) \quad (74)$$

Wenn wir R in Parsec und Θ_0 in km/sec ausdrücken, bekommen wir nach Ausrechnung des Zahlenfaktors

$$M_1 = 0,617 \cdot 10^{36} \frac{A}{\omega} R \Theta_0^3 g, \quad (75)$$

$$\frac{M_2}{M_1} = \frac{1}{\pi} \left(\frac{R_1}{R} \right)^3 \left(\frac{\omega}{A} - \frac{4}{3} \right). \quad (76)$$

Mit den obigen Werten von A , ω und R bekommen wir, wenn wir übrigens R_1 mit dem „effektiven Radius“ in Ziff 30 identifizieren,

$$M_1 = 233 \cdot 10^{12} g, \quad M_2 = 89 \cdot 10^{12} g$$

und also für die Totalmasse

$$M_1 + M_2 = 322 \cdot 10^{12} g = 16 \cdot 10^{10} \text{ Sonnenmassen}$$

Die Masse des Systems ergibt sich also von der Größenordnung 10^{11} Sonnenmassen. Die anderen hier gewonnenen Resultate können verschieden interpretiert werden. Trotz des Umstandes, daß die galaktische Länge des Zentrums gemäß dem Phänomen der differentiellen Rotation in die Gegend der hellsten Milchstraßenwolken fällt, zeigt PANNEKOEK¹, daß die Lichtstärke der Wolken keine Ansammlung von Steinen, die einer Masse von der Größenordnung von M_1 entspricht, zuläßt, auch wenn wir mit ziemlich erheblichen Absorptionseffekten rechnen. Er weist darauf hin, daß die gasförmige interstellare Materie möglicherweise ausreichend ist, um eine gegen das Zentrum konzentrierte Masse von der angeführten Größe zu geben. Andererseits ist in SHAPLEY's oben erwähnten Resultaten die Anwesenheit einer wirklichen zentralen Kondensation angedeutet. Der große Wert von M_1/M_2 in unserem schematischen System ist ja doch nur von der Natur des Kraftfeldes in unserer Umgebung bedingt und kann nach OORT² sowohl auf eine wirkliche zentrale Kondensation wie auf einen ziemlich schnellen Zuwachs der Dichtigkeit gegen das Zentrum hin in unserer unmittelbaren Umgebung zurückgeführt werden.

Zwischen der oben angenommenen Zentrumsdistanz von 9400 Parsec und den aus der Verteilung von Kugelhaufen (SHAPLEY, Ziff 18) und von Veränderlichen in einem Milchstraßenfelde (SHAPLEY und SWOPE, Ziff 20) ermittelten Werten, 16400 bzw. 14400 Parsec, besteht offenbar eine Inkongruität. Die neuen Resultate, die auf die mögliche Existenz eines absorbierenden Stratum

¹ BAN 4, S 39 (1927)

² BAN 4, S 92 (1927)

nahe der Milchstraßenebene hindeuten (Ziff. 24), stellen aber eine Revision der aus den photometrischen Daten berechneten Entfernungen in Aussicht. VAN DE KAMP¹ hat kürzlich dieses Problem zur Behandlung aufgenommen. Nach dieser Untersuchung stellt sich gegenwärtig die Sache so, wie Tabelle 29 angibt. VAN DE KAMP hat sowohl mit TRÜMPLEERS Absorptionskoeffizienten wie mit dem von BOTTLINGER und SCHNELLER, unter Annahme einer Dicke der absorbierenden Schicht von 175 Parsec, die Entfernungen der betreffenden Objekte neu ausgerechnet.

Tabelle 29

Materiel	Keine Absorption	Absorption	
		0 ^m ,67 per 1000 Parsec	2 ^m per 1000 Parsec
Geometrisches Zentrum des Systems der Kugelhaufen	16 700 Parsec	13 700 Parsec	9700 Parsec
Veränderliche in Harvard Milky Way Field 185 [Pol nach PICKERING (a) bzw. VAN RIJN (b)]	14 400	(a) 11 600 (b) 12 500	(a) 7400 (b) 9400
Galaktische Rotation		7000—11 000 Parsec	

Es scheint nach diesen Resultaten nicht ausgeschlossen, daß die Werte der verschiedenen Methoden sich in dieser Weise miteinander in leidlichen Einklang bringen lassen.

34. Übersicht verschiedener Anschauungen über die Natur des Milchstraßensystems. Wenngleich die eben besprochene Theorie eine beträchtliche innere Einheitlichkeit besitzt und in der Tat auf einem Minimum von Hypothesen beruht, so treten neben ihr andere, mehr oder weniger grundverschiedene Auffassungen hervor. Wir haben schon vorher mehrfach die Theorie erwähnt, die ein im wesentlichen dynamisch geschlossenes „lokales System“ voraussetzt. Die dynamischen Eigenschaften dieses Systems werden wohl im allgemeinen im Sinne des KAPTEYN-JEANSschen Systems in Ziff. 28 angenommen. Von diesem Gesichtspunkte aus erscheint sogar die Existenz eines allgemeinen, alle als galaktisch erkannten Objekte zusammenhaltenden Kraftfeldes fraglich. So hat früher G. STRÖMBERG² in dem Phänomen der Asymmetrie der Geschwindigkeitsverteilung den direkten Einfluß der Eigenschaft eines fundamentalen Raumes, die Größe der in ihm gemessenen Geschwindigkeiten zu beschränken, in Verbindung mit einer Tendenz der Materie in unserer Umgebung zu einem lokalen Zusammengehen gesucht.

Eine Theorie, welche in vielen Zügen Berührungspunkte mit der oben referierten Rotationstheorie hat, in anderen aber eine grundverschiedene Einstellung nimmt, haben kürzlich E. VON DER PAHLIN und E. F. FREUNDLICH³ vorgelagt. Diese Verfasser gehen von dem K-Effekt der Radialgeschwindigkeiten der Hellumsterne und dessen Variation mit der galaktischen Länge aus. Hier aber wird der ganze K-Effekt als ein Dilatationseffekt der uns umgebenden Gruppe von B-Sternen infolge einer Bahnbewegung dieser Gruppe im großen System erklärt. Die Bewegung kann als ein „Fallen“ der Sterngruppe im Gravitationsfelde des großen Systems beschrieben werden. Unter der Annahme, daß wir uns mit der Sterngruppe dem Zentrum nähern, beobachten wir, daß die uns in der Bahn voraneilenden Sterne sich relativ zu uns entfernen, da sie bereits dem Zentrum näher sind, während in der entgegengesetzten Richtung

¹ A J 41, S. 81 (1931).

² L. c. Siehe auch „Conference on Michelson-Morley-Experiment“. Mit Wilson Contr 373, S. 61 = Ap J 68, S. 401 (1928)

³ Publ Astrophys Obs Potsd 26, H. 3, Nr. 86 (1928).

die Sterne mit kleinerer Geschwindigkeit zurückbleiben. Die Richtung, in der die Bewegung vor sich geht, wird aus den galaktischen Längen der Maxima des K -Effektes zu etwa $L = 10^\circ$ gefunden, eine Richtung, welche einen Winkel von etwa 45° mit der Richtung gegen das SHAPLEYSche Zentrum einschließt. Aus den folgenden Daten: Maximalbetrag des Effektes, Ausdehnung des betrachteten Haufens von B-Steinen in der galaktischen Ebene, Entfernung vom Zentrum des großen Systems, werden die Elemente der Bahnbewegung bestimmt, unter der Voraussetzung, daß das Gravitationsfeld als von einer Punktmasse im eben genannten Zentrum beruhend angesehen werden kann.

Unter Berücksichtigung der Radialgeschwindigkeiten der Kugelhaufen wird die Geschwindigkeit in der Bahn zu 70 km/sec geschätzt. Wenn die Entfernung vom Zentrum zu 12000 Parsec geschätzt wird, ergibt sich eine Masse im Zentrum von der Größenordnung 10^{12} Sonnenmassen und eine Umlaufzeit von 10^8 Jahren. Die Eigenschaften der schnellbewegten Sterne und die KAPTEJNSchen Sternströme werden dann diskutiert. Als Zusammenfassung gilt nach dieser Ansicht, daß die Sterne im Raumgebiet um unseren Punkt im System herum in ihrer überwiegenden Mehrzahl sehr langgestreckte elliptische Bahnen im Gravitationsfeld der großen Masse im zentralen Teil des von den Kugelsternhaufen definierten galaktischen Systems, an dessen Rande sich unser lokales Sternsystem befindet, beschreiben. Die Sterne dieses lokalen Systems zerfallen im wesentlichen in zwei Wolken, die zwar sehr ähnliche, jedoch schon merklich verschiedene Bahnen beschreiben, wobei die Gruppen der helleren B-Sterne der einen Wolke, die Sonne aber der zweiten Wolke mit etwas kleinerer Exzentrizität (etwa 0,90) und augenblicklich größerer Bahngeschwindigkeit (etwa 90 bis 100 km/sec) angehören. Der Unterschied der Bahnen und der augenblicklichen Geschwindigkeiten bedingt das Phänomen der beiden Sternströme. Das Sternsystem befindet sich also noch sehr weit von einem stationären Zustande, und die erhaltenen Bahnen sind nur „momentane“. Wie ein derartiges momentanes Zusammenballen von Sternen in der Wolke des „lokalen Systems“, dessen eigene Gravitationskraft keinen merklichen störenden Einfluß auf die Bewegungen im System, insbesondere keine merkliche zusammenhaltende Kraft auf seine eigenen Mitglieder ausüben soll, zustande kommt, bleibt wohl aber gänzlich unerklärt. Die Streuung in den relativen Geschwindigkeiten innerhalb des lokalen Systems ist ja in der Tat viel größer als die Amplitude des K -Effektes, auf den die Eigengravitation des lokalen Systems keine merkliche Einwirkung haben soll. Das lokale System gemäß dieser Theorie könnte also nicht etwa durch allmähliche Auflockerung eines ursprünglich geschlossenen Systems entwickelt worden sein und kann überhaupt nicht mit dem lokalen System der geläufigen Vorstellung identifiziert werden.

J. ROSENHAGEN¹ hat eine allgemeine Untersuchung über den K -Effekt für die normalen Spektraltypen unter Ausnutzung des gesamten Materials der zur Zeit bestimmten Radialgeschwindigkeiten ausgeführt. Er untersucht den Gang des K -Termes mit einer Längenkoordinate sowohl in der Milchstraßenebene wie in zwei senkrecht zu ihr und zueinander stehenden „orthogalaktischen“ Ebenen und findet auch für die letzteren eine ausgeprägte Variation, die durch eine zweigipfelige Sinuskurve approximiert werden kann. Die Maxima erscheinen ziemlich nahe an den Polen der Milchstraße gelegen. Er sucht seine Ergebnisse sowohl nach der Theorie von VON DER PAHLEN und FREUNDLICH wie nach einer Erweiterung der OORTschen Ansätze zu deuten, ohne ein entscheidendes Argument für diese oder jene zu bekommen. Im letzteren Falle muß er zur

¹ A N 242, S. 401 (1931)

Deutung der „orthogalaktischen“ Kurven eine Variation der Geschwindigkeitsmittelpunkte in unserer Umgebung nicht nur mit der Zentrumsentfernung R , sondern auch mit der x -Koordinate annehmen. Die Rotationsgeschwindigkeit Θ_0 soll also $\Theta_0(R, x)$ geschrieben werden. Die nördlichen Schichten der Milchstraße sollten eine höhere Rotationsgeschwindigkeit als die südlichen haben. Der K -Effekt in der Milchstraße gibt in Übereinstimmung mit den oben in Ziff. 32 diskutierten Resultaten für die gewöhnlichen Spektraltypen eine Zentrallänge $L_0 = 350^\circ$. Eine Variation der Geschwindigkeitsmittelpunkte mit der x -Koordinate ist früher von H. MINOUR¹ eingeführt worden, der eine allgemeine Analyse des K -Effektes nach Kugelfunktionen entwickelt hat. MINOUR findet einen Effekt, aus dem er eine Rotation um ein lokales Zentrum in der galaktischen Länge 240° herleitet. Die anguläre Geschwindigkeit dieser Rotation soll nur wenig von der Entfernung zum Rotationszentrum abhängen, dagegen aber mit der Höhe über der galaktischen Ebene beträchtlich veränderlich sein. Der genannte Effekt läßt sich folgendermaßen beschreiben. Wenn wir die Achsen x, y, z im Raume in die folgenden Richtungen legen

$$x \begin{cases} L = 232^\circ \\ B = 0^\circ \end{cases} \quad y \begin{cases} L = 322^\circ \\ B = -10^\circ \end{cases} \quad z \begin{cases} L = 320^\circ \\ B = +80^\circ \end{cases}$$

so existiert ein Term φ in den Radialgeschwindigkeiten von der Form

$$\varphi = -0,058 yz$$

Es scheint, daß dieser Effekt auch quantitativ mit ROSENHAGENS K -Variation in einer mit der yz -Ebene nahe zusammenfallenden orthogalaktischen Ebene (G'' -Ebene genannt) ziemlich übereinstimmt.

Es ist wohl nach den geschilderten Verhältnissen klar, daß, wenn wir auf dem Boden der Rotationstheorie bleiben, wir sichere Auskunft über die Rotationsbewegungen im großen System am besten aus den sehr entfernten Objekten in der Milchstraßenebene, in der Weise, wie es besonders OORT sowie PLASKITT und PRARCE gemacht haben, bekommen, daß aber, wenn wir zur großen Masse der uns verhältnismäßig naheliegenden Sterne mit größerer Geschwindigkeitsdispersion übergangen, der differentielle Rotationseffekt teilweise durch Störungen überlagert wird, über deren wahre Natur wir noch in Unklarheit sind. Es ist jedenfalls von Interesse, zu konstatieren, daß diese Störungen den Vertexpunkt des Geschwindigkeitsellipsoids und die Länge L_0 um denselben Betrag verschieben.

Von größter Bedeutung für die kosmologischen Ideen während der letzten zwei Jahrhunderte ist die Frage nach einer möglichen Analogie zwischen unserem Milchstraßensystem und den „außergalaktischen“ oder „anagalaktischen“ Nebelflecken gewesen. Die „Weltinseltheorie“ wurde wohl zuerst in HERSCHELs Arbeit „On the Construction of the Heavens“ (1785) ausgebildet², doch macht HERSCHEL hier noch keinen prinzipiellen Unterschied zwischen wirklichen und scheinbaren Nebeln, sondern nimmt an, daß die Nebel überhaupt von der letzteren Art sind und demnach nichts anderes als entfernte Sternansammlungen darstellen. In seinen späteren Arbeiten hat er die zwei Nebelarten erkannt, neigte aber allmählich mehr und mehr zu der Ansicht, daß die Milchstraße in ihrer eigenen Ebene eine ungeheure Ausdehnung besitze, und daß sie wahrscheinlich in ihrem System alle für uns wahrnehmbaren Objekte einschleße. Bis in die letzten Jahre haben in der Tat die Ansichten über die wahre Natur der Milchstraße zwischen

¹ B A 5, S. 505 (1929).

² Vgl. geschichtliche Übersicht von K. LUNDMARK, Studies of Anagalactic Nebulae, Nova Acta Reg Soc Sc Upsal, Volumen extra ordinem 1927

den beiden Extremen der Weltinseltheorie einerseits und der Theorie eines praktisch allumfassenden Milchstraßensystems andererseits geschwankt.

Nach Lord ROSSES Entdeckung der Spiralförmigkeit einiger Nebel (1845) ist die Weltinseltheorie in interessanter Weise von STEPHEN ALEXANDER¹ und von CLEVELAND ABBE² entwickelt worden. Der erstere kann, wie LUNDMARK bemerkt, durch seine Theorie über die Nebel als sternproduzierende Mechanismen als ein Vorgänger von JEANS betrachtet werden.

Die spektroskopische und spektrographische Scheidung der galaktischen Gasnebel von den Nebeln mit typischem Absorptionsspektrum hat dann in besonderer Weise die Diskussion gefördert. Da im letzteren Falle Spektren von angenähertem Sonnentypus sich ergeben, hat man hier gleich eine schwerwiegende Bestätigung der Weltinseltheorie gesehen.

Unter den Verfassern, die sich in neuerer Zeit mit den diesbezüglichen Fragen beschäftigt haben, ist besonders EASTON³ zu nennen, der auf Grund seiner eigenen Forschungen aus dem verwickelten Verlauf der Milchstraße am Himmel die Gestalt eines gewaltigen Spiralnebels mit dem Kern in der Cygnus-region herauszulesen versuchte.

Nach SHAPLEYS grundlegenden Untersuchungen über das größere galaktische System, die eine unerwartete Erweiterung unserer Vorstellungen über den Umfang des Milchstraßensystems als Ganzem mit sich führten, neigte die Auffassung wohl zugunsten der Theorie einer praktisch allumfassenden Milchstraße, um so mehr, da die VAN MAANENSCHEN direkt gemessenen Rotationsgeschwindigkeiten der Spiralnebel gegen genügend große, der Weltinseltheorie entsprechende Entfernungen für diese Objekte sprachen. Besonders durch die Studien von CURTIS, LUNDMARK, HUBBLE u. a. über die Natur der außergalaktischen Nebel hat aber die Weltinseltheorie ihre alte Stellung als bevorzugte Theorie wiedererobert. Die gegenwärtigen Grundlagen der Entfernungsbestimmungen für die Spiralnebel und die verwandten Objekte haben schon einen bemerkenswerten Grad von Zuverlässigkeit gewonnen, und die Distanzen kommen genügend groß heraus, um in genereller Weise der Weltinseltheorie zu entsprechen.

Mit dieser wahrscheinlich endgültigen Entscheidung einer alten Streitfrage sind aber keineswegs die Fragen über die Natur und Stellung des Milchstraßensystems erledigt worden. Es scheint zwar an sich wahrscheinlich, daß unter den verschiedenen Typen von Nebeln ein „Modell“ zu unserem eigenen System gefunden werden könnte, jedoch ist von vornherein klar, daß das Material für eine rein morphologische Klassifizierung unseres Milchstraßensystems noch nicht vorliegt, und daß hier besonders große Schwierigkeiten, vor allem die mehr oder weniger regelmäßigen Absorptionserscheinungen, zu überwinden sind. SEARES⁴ hat der Lösung der Frage auf dem Wege der Flächenhelligkeiten näherzukommen versucht. Er berechnet aus KAPTEYNs und VAN RHYNs Dichtefunktion die Flächenhelligkeit des von einem sehr entfernten Punkt in der Richtung des galaktischen Pols aus gesehenen galaktischen Systems. Er findet, daß diese Helligkeit etwa der visuellen Größe 23 per Bogensekundenquadrat entspricht, etwa 100mal kleiner als die Flächenhelligkeit der helleren Partien in typischen Spiralnebeln. Daß wir so verhältnismäßig leicht die galaktischen Wolken wahrnehmen, beruht nach SEARES einfach auf dem großen Areal dieser Gebilde am Himmel. Dieses Resultat, das auf eine vom galaktischen System verschiedene Konstitution der Spiralnebel deutet, verliert wohl aber erheblich an Beweiskraft, wenn wir nicht länger das Zentrum des galaktischen Systems in unserer unmittelbaren Nachbarschaft suchen. In einer späteren, oben in

¹ A J 2 (1852). ² MN 27, S. 262 (1867). ³ Ap J 12, S. 136 (1900).

⁴ Mt Wilson Contr 191 = Ap J 52, S. 162 (1920).

in den äußeren Teilen unseres Systems nach der eben erwähnten Theorie wohl möglich, wenngleich die wahrscheinlich erhebliche zentrale Kondensation der Materie im System eine sehr mächtige Entwicklung der Spiralstruktur verhindern mag. Es soll aber hier zuletzt erwähnt werden, daß H. Vogt¹ die Bedeutung der neuen Ergebnisse über die Expansion der Welt zur Erklärung der Spiralform herangezogen hat, und es ist möglich, daß dieses Phänomen auch für unser eigenes System wichtige Konsequenzen mit sich geführt haben kann.

Von den oben referierten Gesichtspunkten wesentlich verschiedene, aber namentlich verwandte Hypothesen über die Natur des Milchstraßensystems haben gleichzeitig LUNDMARK², SHAPLEY³ und TRÜMPLER⁴ aufgestellt. Nach den Ansichten der zwei ersteren Verfasser ist das Milchstraßensystem kein einheitliches Objekt, das mit irgendeinem einzigen außergalaktischen Nebel verglichen werden kann. SHAPLEY sieht eher in den Nebelhaufen, z. B. in der Coma-Virgo-Gruppe oder noch mehr in der dichteren Centaurusgruppe, unserem Milchstraßensystem ähnliche Formationen. Die einzelnen Glieder unseres Systems, die mit den Nebeln einer Gruppe vergleichbar wären, sind die Sternwolken der Milchstraße, unter die ein lokales System gerechnet wird, ferner die MAGELLANSchen Wolken und die Kugelhaufen. LUNDMARK teilt die eigentliche Milchstraße in wesentlich zwei Teilsysteme, das lokale System und das zum großen Teil durch Absorption in Dunkelnebeln verborgene Sagittariussystem. Er betont besonders eine mögliche Verwandtschaft zwischen den Kugelhaufen und den elliptischen außergalaktischen Nebeln. TRÜMPLER deutet sein System von offenen Sternhaufen, das ziemlich Rotationssymmetrie um die Sonne besitzt, als gewissermaßen einen Grundriß zur eigentlichen Milchstraßenstruktur. Dieses um die Sonne zentrierte System wird dann in der Tat die Hauptmasse des Systems enthalten, und die Existenz des verborgenen Sagittariussystems scheint in Frage gestellt. TRÜMPLER deutet das System als einen Spiralnebel mit gegen rechts gewundenen Armen, vom Nordpol der Milchstraße aus gesehen. Die Kugelhaufen sind nicht organisch in dieses System eingegliedert. Es mag erwähnt werden, daß TRÜMPLERS System sich nicht mit dem SHAPLEYschen lokalen System oder lokalen Haufen deckt, sondern ein viel weiter gestrecktes Gebilde darstellt. Der lokale Haufen nach SHAPLEY könnte aber als die Zentralregion des Milchstraßennebels aufgefaßt werden.

Wenigstens gegen weit getriebene Hypothesen in der Richtung einer Aufteilung des Milchstraßensystems in isolierte Teilsysteme kann wohl mit Recht hervorgehoben werden, daß es als ein merkwürdiger Zufall zu bezeichnen wäre, daß die Teilsysteme, die nach dieser Annahme die eigentliche Milchstraße aufbauen, alle so nahe in einer und derselben Ebene orientiert liegen. Man darf auch sagen, daß die Anwesenheit der Kugelhaufen, welches ihr Ursprung auch sein mag, keineswegs an und für sich unserem Milchstraßensystem die Würde einer Organisation von höherer Ordnung als die gewöhnlichen Nebel verleihen kann. Ähnliche Phänomene treten wahrscheinlich auch bei Systemen von verhältnismäßig bescheidener Größe auf. Objekte, die als Kugelhaufen zu bezeichnen sind, sind ja z. B. in der unmittelbaren Umgebung der großen MAGELLANSchen Wolke vorhanden, in der Weise, daß sie offenbar mit der Wolke in Verbindung stehen. Die Angliederung der MAGELLANSchen Wolken als „ferne Begleiter“ unseres Systems erinnert ja auch an die zwei elliptischen Nebel NGC 205 und 221 bei M31. Wenn wir diese zwei Satellitennebel zum System des Andromeda-

¹ A N 242, S. 181 (1931), 245, S. 281 (1932).

² Publ. A. S. P. 42, S. 23 (1930), Pop. Astr. Tidsskr. 11, S. 85 (1930).

³ Harv. Circ. 350 (1930).

⁴ Lick Bull. 14, S. 154 (1930).

nebels rechnen wollen, so bekommen wir zwar ein mehrfaches System, der Hauptkörper selbst erscheint jedoch vollkommen einheitlich

Gegen TRÜMPLERS Auffassung seines Laufensystemes macht BORTLINGER¹ den Einwurf, daß jener die Einwirkung der Absorption des Lichtes im System nicht genügend berücksichtigt hat. TRÜMPLER ist nicht darauf gekommen, daß die von ihm gefundene Absorption in einer engen Milchstraßenschicht vielleicht die Ursache sei, die uns eine Dichteabnahme langs der Milchstraßenebene vortausche. Es ist in der Tat sehr wohl möglich, daß die Extinktion in gewissen Richtungen, z. B. gegen das Zentrum des Systems in Sagittarius, so intensiv sein kann, daß sie die Vollständigkeit des Laufensmaterials in sehr hohem Grade herabsetzt. Die Neigung des Laufensystemes gegen die Milchstraßenebene mag durch eine etwas nördliche Absorptionszone in der Sagittariusrichtung erklärt werden. TRÜMPLERS Laufensystem stellt dann einen schrägen Schnitt durch das System dar.

Die Existenz eines „lokalen Systems“ in dem gelaufenen Sinne dieses Wortes ist nach der Rotationstheorie nicht möglich, da die Materie in unserer Umgebung durch die beobachteten Effekte der differentiellen Rotation stetig zerghedert werden muß. Es wären also, wenn das örtliche System etwas Geschlossenes und Beständiges ist, diese Effekte in anderer Weise zu deuten. Bei der inneren Einheitlichkeit der erwähnten Theorie, die quantitativ eine Reihe Phänomene miteinander verknüpft, die sonst als isolierte Tatsachen auftrieten und besonders nach der Bestätigung der differentiellen Rotation für die Sterne mit interstellaren Ca-Linien durch die Arbeit von PASKETT und PEARCE, muß man wohl doch von anderen Theorien fordern, daß sie in ebenso direkter Weise und ohne komplizierte Hilfshypothesen etwas Ähnliches leisten. Es fehlt ja auch nicht an Tatsachen, die auf eine weitgehende Heterogenität des „lokalen Systems“ deuten. Es ist in der Tat wohl möglich, daß der beobachtete Überschuß an Dichtigkeit in unserer Nähe, soweit er sich nicht durch Absorption des Lichts in der Milchstraßenebene erklärt, eine Folge der mächtigen Strömungen ist, die sich hier zufälligerweise räumlich übereinanderlagern. Wir können unter solchen Strömungen den Taurus-Strom, den Ursa major-Strom und die großen Triften der Heliumsterne nennen. Das Phänomen des „lokalen Systems“ wäre dann mit den beobachteten kleineren Abweichungen von regulären Verhältnissen in der Geschwindigkeitsverteilung in Verbindung zu setzen (vgl. Ziff 31 u. 32), hätte aber an sich nichts, was mit den großen Linien der einheitlichen Theorie in Widerspruch steht. Es mag hier der Klarheit wegen bemerkt werden, daß nach dieser Theorie die Bahnen der erwähnten großen Strömungen nur wenig von der zirkulären Bewegung um das Zentrum herum abweichen. Was wir unmittelbar beobachten, sind natürlich nur ihre relativen Geschwindigkeiten.

Wenn wir auf dem Boden der Rotationstheorie etwa nach dem Ursprung der beobachteten Sedimentation verschiedener Gruppen von Objekten in „Untersysteme“ von verschiedenen dynamischen Eigenschaften fragen, so ist es möglich, wie in Ziff. 29 auseinandergesetzt, daß Effekte einer langsamen Gleichverteilung der Energie durch „Passage“ hier mitspielen können, wenn wir nur eine genügend lange, nach der Formation des Systems verflossene Zeit voraussetzen dürfen. Andere Gesichtspunkte lassen sich auch finden. So ist es vielleicht möglich, daß im Untersystem von größter Rotationsgeschwindigkeit, wo die Materie sich in nahe relativer Ruhe bewegt, sich vorzugsweise Sterne mit großer Masse und verhältnismäßig großer Dichte gebildet haben², was die große relative Häufigkeit der Sterne von frühem Spektraltypus in diesem Untersysteme erklären

¹ Berlin-Babelsberg Veröff. 8, II 5 (1931)

² LINDBLAD, Ark. Mat. Astr. Fys. 21 A, Nr. 3 = Stockholm Medd. 1, S. 24 (1928)

könnte. Die Häufigkeit gewisser Arten von Veränderlichen, wie kurzperiodische δ -Cepheiden und Me-Sterne, in den Untersystemen von großen relativen Geschwindigkeiten und von geringer Abplattung gegen die Milchstraßenebene kann vielleicht damit in Verbindung gebracht werden, daß die Mitglieder dieser Untersysteme individuell genommen in radialer Richtung sehr langgestreckte Bahnen beschreiben, welche die betreffenden Sterne ziemlich oft in die dichten Gegenden des Zentrums führen. Es besteht wenigstens die Möglichkeit, daß ein Auftreten gewisser singulärer Typen von Sternen in diesen Gegenden leichter vor sich gehen wird als in anderen. Welcher Wert derartigen Gedanken zukommt, läßt sich allerdings gegenwärtig kaum entscheiden. Ohne Zweifel kann man jedoch sagen, daß überhaupt die allgemeinen Fragen über die Entwicklung der Sterntypen wichtige Berührungspunkte mit den Fragen nach der Struktur und der Entwicklungsgeschichte des Sternsystems haben.

Es ist jedoch ohne weiteres klar, daß man bei dem jetzigen Stande der Milchstraßenforschung jeden Schluß nur mit der größten Vorsicht zu ziehen hat. Für die direkten Untersuchungen der Dichteverteilung im System scheint gegenwärtig das Problem der Absorption des Lichtes in der Milchstraßenschicht das wichtigste zu sein. Erst wenn wir einen zuverlässigen Weg zur Beseitigung der aus diesem Phänomen herkommenden Schwierigkeiten gefunden haben, können wir eine volle Einigung der rein empirischen Morphologie des Systems mit irgendeiner dynamischen Theorie erwarten.

Luminosities, Colours, Diameters, Densities, Masses of the Stars.

By

KNUT LUNDMARK-Lund

(Continued)

I. Catalogue of Stars Brighter than 5^m.00.

Contents Col 1 contains the number in the PGC by L. Boss (upper line) and the RIIP number (lower line). This number also corresponds to the number in SCHLESINGER's work, "Catalogue of Bright Stars", New Haven 1930. The catalogue of SCHLESINGER was not accessible to me when I compiled the present catalogue but it has been used for check work during the proof-reading of this chapter.

Col 2 contains the name of the stars in the usual nomenclature together with the BD number, when in italics this refers to the nearest whole degree according to the wellknown rules concerning the course of the precession.

Col 3 and 4 contain the α and δ for 1900.0

Col 5 contains the spectral type

Col 6 contains the colour in OSWALD's scale and the estimates according to FRANKS (Specula Astronomica Vaticana VIII, IX and XV.) Only in a few cases the estimates of the present writer have been added. These estimates are given in the OSWALD Scale.

Col. 7 contains the apparent magnitudes according to RIIP and to ZINNEL's work, "Helligkeitsverzeichnis von 2373 Sternen bis zur Größe 5,50". The latter magnitudes are based upon an extensive discussion of practically all available determinations of stellar magnitude and they follow very closely the scale defined by PD. (See ciph 40.)

Col. 8 and 9 contain on the upper line the total proper motion (unit is 0".001), or the quantity $\mu = [(\mu_{\alpha} \cos \delta)^2 + \mu_{\delta}^2]^{\frac{1}{2}}$ and the direction ψ of the proper motion (unit is 1°), counted in the same way as the position angles and defined as $\tan \psi = \mu_{\alpha} \cos \delta / \mu_{\delta}$, and on the lower line the τ - and ν -components, which according to KAPTEYN's definition are $\tau = \mu \sin(\chi - \psi)$ and $\nu = \mu \cos(\chi - \psi)$, where χ is the angle of the great circle through the Apex with the declination circle, counted in the same way as the position angles. The quantities μ , ψ , τ , and ν , given in columns 8 and 9 have in most cases been taken over from an unpublished determination carried out under the supervision of KAPTEYN by Dutch prisoners. The results of this extensive work of computation has been distributed earlier in typewritten manuscript to several observatories. I am under much obligation to KAPTEYN's family as well as to P. J. VAN RIJN, Director of the KAPTEYN Laboratory for kind permission to include the mentioned data in the present catalogue.

Col 10 gives the radial velocity of the star, expressed in kilometers per second. The work of J. H. MOORE, "A General Catalogue of the Radial Velocities of Stars, Nebulae and Clusters", was not accessible to me, when the present catalogue was compiled but has been used for a general check when reading the proofs. When a velocity is indicated by "Var." there are no conclusive evidences as to the nature of variation of the radial velocity. When the velocity is indicated by "Var." and a number, this number in most cases refers to the velocity of the system, derived from the variation in radial velocities interpreted as caused by orbital motion in binary systems.

Col. 11 contains on the upper line the arithmetic mean of existing parallax determinations (trigonometric or spectrographic, or in a few cases theoretic values), on the lower line the geometric mean of the same determinations, provided that they are positive. In both cases the unit is $0''.001$.

Col. 12 gives the number of parallax determinations used when forming the mean values in col. 11. When in column 12, instead of a number, an (a) is given, the parallax value in the preceding column has been inserted from additional sources, being available since the catalogue was compiled in 1927 to 1928.

Col. 13 contains on the upper line the absolute magnitude M in the RHP system and on the lower the absolute proper motion magnitude $H = m + 5 + 5 \log \mu$. In cases of variable stars the M - and H -values correspond to the magnitude at maximum.

Col. 14 and 15 contain the galactic longitude and latitude computed with aid of the tables computed at the Observatory in Lund and distributed in mimeograph form. When more accurate values for these coordinates are needed the extensive tables, "Lund Observatory Tables for the Conversion of Equatorial Coordinates into Galactic Coordinates" (Ann. Obs. Lund No. 3), should be consulted.

A few remarks as to binaries, variable stars etc. have been added to the table. In these remarks ADS refers to R. G. ARTHURS work, "New General Catalogue of Double Stars within 120° of the North Pole I—II" [Wash. Carnegie Inst. Publ. No. 417 (1932)].

04.

1	2	3	4	5	6	7	8	9	10	11	12	13	14
1	33 Pictoris	0 ^m .2	- 6°16'	K0	5 ^s .7	4 ^m .68	92	348 ^s	- 6.3	23	(2)	1.5	67 ^s
3	6357				Y ¹ .4	4.85	+ 67	- 63		23		4.5	
10	α Andromedae	3.2	+28 32	A0p	1 ^s .7	2.15	213	139 ^s	-13.0	48	(5)	0.5	81
15	4				W	2.39	- 77	+ 198		47		3.8	
12	β Cameloiae	3.8	+58 36	F5	3 ^s .1	2.42	559	109 ^s	+11.8	71	(4)	1.7	83
21	3				Y ¹ .1	2.56	- 11	+ 559		71		6.2	
16	ϵ Phoenicis	4.3	-46 18	K0		3.94	219	148 ^s	- 9.2	25	(2)	0.9	290
25	16					4.04	- 131	+ 175		25		5.6	
27	γ Pegasi	8.1	+14 38	B2	2 ^s .2	2.87	13	180 ^s	+ 4.9	6	(4)	-3.2	79
39	14				W	3.16	- 11	+ 6		6		-1.6	
31	ζ Pegasi	9.4	+19 39	Ma	7 ^s .3	4.94	94	97 ^s	-45.3	5	(4)	-1.2	80
45	27				Y ¹ .3	4.94	+ 37	+ 86		6		4.8	
33	γ Ceti	9.6	-19 30	Ma	7 ^s .0	4.68	68	201 ^s	-22.7	13	(3)	0.2	52
48	21				OY ¹ .1	4.64	- 67	+ 10		13		3.8	
43	δ Andromedae	11.9	+38 8	A2	3 ^s .0	4.44	52	247 ^s	+ 4.7	23	(4)	1.1	84
63	34				Y ¹ .1	4.65	- 40	- 33		22		3.0	
50	α Andromedae	13.1	+36 14	A2	2 ^s .9	4.51	81	237 ^s	Var.	15	(4)	0.2	84
68	44				Y ¹ .1	4.70	- 70	- 40	- 1	15		4.0	
53	ϵ Ceti	14.3	- 9 23	K0	5 ^s .9	3.75	37	209 ^s	+18.2	20	(3)	0.1	71
74	48				Y ¹ .1	3.76	- 37	+ 1		19		1.6	
55	ζ Tucanae	14.9	-65 28	F8		4.34	2058	56 ^s	+ 9.3	146	(1)	5.1	274
77	13					4.46	+1419	+1481		146		10.9	
92	B Cameloiae	19.2	+63 36	Mb? Nova	Var	-5.0 to 13.87	-	-	-	1	(1)	-15.7	88
95	47 Tucanae	19.6	-72 39	G5		[4.5]	-	-	-	0.2	(1)	-8.8	272
74	β Hydri	20.5	-77 49	G0	4 ^s .7	2.90	2240	83 ^s	+23.0	160	(2)	3.9	271
98	16					3.02	+ 381	+2195		160		9.6	
78	α Phoenicis	21.3	-42 51	K0	5 ^s .7	2.44	445	154 ^s	+74.2	60	(3)	1.3	284
99	116					2.57	- 307	+ 320		60		5.7	
77	η Phoenicis	21.3	-44 14	A3		3.90	107	74 ^s	+ 9	12	(4)	-0.7	283
100	101					4.25	+ 63	+ 87		12		4.1	

HR 92. Nova B Cameloiae of 1971. Parallax from the spectral properties of the 13^m.8 star presumed to be the Nova. — HR 95. Q16 Cluster NGC 104. Parallax from the brightest stars in the cluster.

0^h.

1	2	3	4	5	6	7	8	9	10	11	12	13	14	15
83	η Sculptoris	22 ^m .9	-33° 34'	Mb		4 ^m .96	56	210°	+11.2				298°	-82°
105	152					4.96	55	6				3.7		
97	γ Cassiopeiae	26.2	+53 59	B8	1 ^o .9	4.88	48	105°	-10	7	(a)	-0.9	88	-8
123	82				Y ¹	5.02	8	48				3.3		
99	λ^1 Phoenicis	26.6	-49 22	A2		4.88	128	83°	Var	25	(1)	1.9	275	-69
125	115					4.97	52	116	-5	25		5.4		
100	β^1 Tucanae	27.0	-63 31	B9		4.52	103	122°	+10	34	(a)	1.2	272	-54
126	50					4.61	40	95				4.6		
101	β^2 Tucanae	27.0	-63 31	A2		4.48	108	125°	+9.9	34	(a)	1.1	272	-54
127	50					4.59	48	97				4.6		
103	κ Cassiopeiae	27.3	+62 23	B0	3 ^o .5	4.21	11	85°	-4	3	(3)	-3.4	89	± 0
130	102				Y ¹	4.41	5	10		3		-0.6		
122	ζ Cassiopeiae	31.4	+53 21	B3	2 ^o .6	3.72	23	113°	+2.0	0	(4)	-3.3	89	-9
153	105				YG ¹	3.98	1	23		4		0.5		
123	π Andromedae	31.5	+33 10	B3	2 ^o .5	4.44	23	113°	+8.8	3	(3)	-2.6	88	-29
154	101				W	4.58	3	23		4		1.3		
130	ϵ Andromedae	33.3	+28 46	G5	4 ^o .7	4.52	336	222°	-83.4	30	(4)	1.8	88	-33
163	103				Y ²	4.60	329	64		28		7.2		
132	δ Andromedae	34.0	-1 30 19	K2	6 ^o .0	3.49	162	122°	-7.2	29	(4)	0.9	88	-32
165	91				Y ³	3.49	3	102		30		4.5		
135	α Cassiopeiae	34.8	+55 59	K0	5 ^o .0	2.47	60	121°	-4.1	21	(4)	-0.9	89	-6
168	139				OY ²	2.53	6	59		21		1.4		
141	ξ Cassiopeiae	36.5	+49 58	B3	2 ^o .7	4.85	21	109°	-9.4	6	(2)	-1.3	89	-12
179	164				Y ¹	5.07	3	21		6		1.5		
142	μ Phoenicis	36.6	-46 38	K0		4.65	38	227°	+16.5	14	(2)	0.4	272	-71
180	180					4.73	33	19		14		2.6		
182	33 Andromedae	37.2	+40 43	G4	3 ^o .2	[4.90]			-300	0.003	(3)	-18.	89	-21
147	β Ceti	38.6	-18 32	K0	5 ^o .8	2.21	230	80°	+13.3	41	(2)	0.3	90	-81
188	115				Y ⁰	2.30	143	182		41		4.0		
148	η Phoenicis	38.8	-58 1	A0		4.53	10	315°	+10				270	-60
191	42					4.62	6	8				-0.5		
152	σ Cassiopeiae	39.2	+47 44	B2	3 ^o .0	4.70	22	103°	-7.5	5	(2)	-1.8	90	-14
193	183				Y ¹	4.88	6	21		5		1.4		
151	η^1 Ceti	39.2	-11 9	K0	5 ^o .2	4.93	110	183°	+0.6	15	(1)	0.8	90	-73
194	128				Y ²	4.94	99	48		15		5.1		
164	ζ Andromedae	42.0	+23 43	K0	5 ^o .5	4.30	129	231°	Var	25	(4)	1.2	91	-38
215	106				Y ³	4.31	123	43	-25.9	24		4.8		
168	η Cassiopeiae	43.0	+57 17	F8	4 ^o .5	3.64	1242	115°	+9.9	148	(9)	4.4	91	-5
219	150				Y ³	3.74	25	1242		145		9.1		
173	δ Piscium	43.5	+7 2	K5	6 ^o .9	4.55	93	118°	+34.9	16	(4)	0.4	92	-55
224	107				O ²	4.59	7	93		15		4.4		
175	ν Andromedae	44.3	+40 32	B3	2 ^o .2	4.42	28	138°	Var	7	(3)	-1.3	91	-21
226	171				W	4.71	8	27	-24.0	7		1.7		
182	λ Hydri	45.1	-75 28	K5		4.96	134	98°	-9.4				270	-43
236	64					5.08	21	133				5.6		
189	Cassiopeiae	47.1	+60 34	F8	4 ^o .5	4.93	188	338°	+21.3	56	(4)	3.7	91	-2
244	124				Y ²	5.04	126	-139		56		6.3		
191	20 Ceti	47.9	-1 41	K0	6 ^o .5	4.92	17	200°	+15.5	12	(4)	0.1	94	-64
248	114				Y ³	4.88	17	3		11		1.1		
193	ν^1 Cassiopeiae	49.1	+58 26	K0	6 ^o .0	4.95	53	214°	-23.1	15	(3)	0.8	91	-4
253	134				Y ²	4.94	52	6		15		3.6		
199	γ Cassiopeiae	50.7	+60 11	B0p	2 ^o .1	2.25	30	94°	Var	17	(3)	-2.2	92	-2
264	144				W	2.48	12	28	-6.8	13		-0.4		
200	ν^2 Cassiopeiae	50.7	+58 38	K0	5 ^o .4	4.83	100	245°	-47.0	29	(5)	1.7	92	-3
265	138				Y ³	4.82	79	62		24		4.8		

33 Andr. The Great Andromeda Nebula. The parallax of 0".000003 is determined on basis of 1 Cepheid stars, 2 Novae, 3 Non variable stars observed in this object

0^h to 1^h.

1	2	3	4	5	6	7	8	9	10	11	12	13	14	15
203 269	μ Andromedae 175	51 ^m .2	+37° 57'	A2	2 ^s .6 W	3 ^m .94 4.08	+153 +103	80° +113	+8	33 32	(4)	1.5 4.9	93°	-24°
206 271	η Andromedae 153	51.9	+22 52	G5	5 ^s .0 Y ^a	4.62 4.63	-60 -59	225° 13	-10	12 12	(5)	-0.2 3.5	94	-39
212 280	α Sculptoris 287	53.8	-29 54	B5		4.39 4.55	7 +	82° +	+10.5 6			-1.3	216	-85
218 285	Cephei 19	55.0	+85 43	K0	6 ^s .2 OY ^a	4.52 4.46	86 +	93° +	+8.5 83	15 15	(3)	0.4 4.2	90	+24
226 294	ε Piscium 153	57.8	+7 21	K0	5 ^s .4 Y ^a	4.45 4.51	85 -	289° -	+6.9 82	19 19	(5)	0.8 4.1	98	-55
235 310	ψ^1 Piscium 156	0.4	+20 56	A2	2 ^s .0 Y ¹	5.55 5.69	58 +	108° +	-3.1 56			1.0 4.4	96	-41
236 311	ψ^1 Piscium 157	0.4	+20 56	A0	1 ^s .9 W	5.82 5.95	47 +	120° +	-4 47	12	(a)	1.2 4.2	96	-41
245 322	β Phoenixis 324	1.6	-47 15	K0	4 ^s .3	3.35 3.57	45 -	252° -	-1.3 39	24 24	(4)	0.3 1.6	258	-70
255 334	η Ceti 240	3.6	-10 43	K0	6 ^s .0 Y ^a	3.60 3.62	246 -	123° +	+11.3 246	33 33	(2)	1.2 5.5	109	-72
257 335	φ Andromedae 275	3.7	+46 42	B8	3 ^s .0 Y ¹	4.28 4.45	10 -	135° +	-2 10	10 10	(5)	-0.7 -0.7	94	-15
259 337	β Andromedae 198	4.1	+35 5	Ma	6 ^s .2 OY ^a	2.37 2.27	216 +	122° +	+0.5 216	41 41	(5)	0.4 4.0	96	-27
260 338	ζ Phoenixis 241	4.2	-55 47	B8		4.13 4.27	27 +	15° +	Var. 4			1.3	263	-61
264 343	θ Cassiopeiae 236	5.0	+54 37	A5	3 ^s .7 Y ¹	4.52 4.63	230 +	95° +	+11 207	24 26	(4)	0.8 6.3	93	-7
270 351	χ Piscium 172	6.1	+20 30	K0	5 ^s .6 Y ^a	4.89 4.79	21 +	73° +	+15.7 13	12 12	(4)	0.3 1.5	98	-42
271 352	τ Piscium 190	6.2	+29 34	K0	5 ^s .7 Y ^a	4.70 4.64	81 +	118° +	+30.5 80	16 16	(4)	0.7 4.2	96	-32
281 360	φ Piscium 158	8.3	+24 3	K0	5 ^s .5 OY ^a	4.64 4.73	47 -	152° +	+5.1 42	12 10	(6)	-0.4 3.0	98	-38
288 370	ν Phoenixis 346	10.6	-46 4	G0		4.88 5.17	687 +	74° +	+11.5 611			9.0	252	-71
294 377	κ^A Tucanae 45	12.4	-69 24	F8		4.96 5.09	413 +	74° +	+9.2 405	160 160	(1)	6.0 8.0	266	-49
300 383	ν Piscium 220	14.0	+26 44	A2	2 ^s .1 Y ¹	4.67 4.92	26 +	118° +	Var. +5	21 19	(3)	1.1 1.8	100	-34
304 390	ξ Andromedae 287	16.4	+45 0	K0	5 ^s .4 Y ^a	4.99 4.99	41 +	84° +	-11.7 31	17 17	(3)	1.1 3.0	97	-17
310 399	ψ Cassiopeiae 123	18.9	+67 36	K0	6 ^s .4 OY ^a	4.96 4.94	86 +	67° -	-12.0 52	13 13	(4)	0.5 4.6	94	+6
313 402	θ Ceti 244	19.0	-8 42	K0	5 ^s .6 Y ^a	3.83 3.82	228 -	201° +	+17.5 36	27 26	(4)	0.9 5.6	119	-69
314 403	δ Cassiopeiae 248	19.3	+59 43	A5	3 ^s .0 Y ¹	2.80 2.99	306 +	99° +	+9 278	55 47	(5)	1.2 5.2	95	-2
321 417	ω Andromedae 307	21.7	+44 53	F5	4 ^s .1 Y ¹	4.96 5.05	356 +	106° +	+10 335	34 33	(4)	2.5 7.7	98	-16
325 424	α Ursae Minor 8	22.6	+88 46	F8	3 ^s .8 Y ^{1.6}	2.12 2.21	44 +	89° +	Var. -17.4	12 12	(5)	-2.5 2.9	90	+27
329 429	γ Phoenixis 449	24.0	-43 50	K5	6 ^s .7	3.40 3.49	221 -	188° +	Var. +25.7	24 24	(2)	0.3 5.1	243	-71
335 437	η Piscium 231	26.1	+14 50	G5	5 ^s .4 Y ^a	3.72 3.91	31 +	109° +	+15.3 30	15 14	(4)	-0.6 1.2	106	-46
336 440	δ Phoenixis 425	27.0	-49 35	K0		3.96 4.10	194 +	40° +	-6.5 109	31 30	(2)	1.4 5.4	251	-66

Boss 218. Also 2 Urs. Min. — Boss 314. Is variable with an amplitude of 0m.1. — Boss 325. ADS 1477. Cepheid variable; 2m.3—2m.4; period 4 days; has a companion P0, 8m.79, 18", 3.217°. The radial velocity varies in two periods viz. 4.0 days and 30 years. The range in magnitude is only 0.08 according to photoelectric measurements.

1^h

1	2	3	4	5	6	7	8	9	10	11	12	13	14	15
338 442	/ Cassiopeiae 260	27 ^m ,4	+ 58° 44'	K0	1 ^s ,9 Y ^a	4 ^m ,88 4,83	38 33	245° 19	+ 6,8 13	14 13	(5)	0,4 2,8	96°	- 2°
350 458	v Andromedae 332	30,9	+40 54	G0	1 ^s ,4 Y ^a	4,18 4,28	418 410	205° 88	-28,6 +	79 78	(4)	3,6 7,3	100	-20
357 464	51 Andromedae 467	31,9	+ 18 7	K0	6 ^s ,0 Y ^a	3,77 3,78	127 52	151° 116	-15,9 +	21 24	(4)	0,7 4,3	99	-13
363 472	α Eridani 334	34,0	-57 45	B5	2 ^s ,9 0,89	0,60 0,89	94 32	108° 88	-19 +	45 45	(2)	-1,1 0,5	257	-58
369 477	τ Andromedae 378	34,7	+40 4	B8	2 ^s ,3 W	4,90 5,15	29 11	151° 27	-15 +	8 8	(1)	-0,6 4,2	101	-21
378 489	v Piscium 293	36,2	+ 4 59	K0	6 ^s ,6 Y ^a	4,68 4,66	21 11	273° 18	+ 0,1 +	21 20	(4)	1,2 1,3	111	-54
384 496	φ Persei 444	37,1	+50 11	B0p	2 ^s ,7 W	4,19 1,34	33 +	123° 33	Var ? +	14 13	(2)	-0,6 1,8	99	-11
391 509	τ Ceti 295	39,4	-16 28	K0	5 ^s ,5 Y ^a	3,65 3,68	1922 38	296° 1922	-16,1 +	312 310	(5)	6,1 10,0	142	-71
393 510	σ Piscium 273	40,1	+ 8 39	K0	5 ^s ,3 Y ^a	1,50 4,49	85 82	53° 25	+13,8 +	14 15	(4)	0,1 4,2	114	-50
411 531	γ Ceti 352	44,7	-11 11	F0	4 ^s ,0 Y ^a	4,77 4,89	178 148	243° 100	- 0,9 -	35 35	(1)	2,5 5,8	134	-67
416 539	ξ Ceti 359	46,5	-10 50	K0	6 ^s ,2 Y ^a	3,92 3,91	49 9	131° 48	+ 7 +	39 32	(2)	1,5 2,4	135	-67
419 542	ε Cassiopeiae 320	47,2	+63 11	B3	2 ^s ,7 W	3,44 3,63	43 9	114° 42	- 7,9 +	11 12	(5)	1,2 1,6	98	+ 2
421 544	α Tilianguli 312	47,4	+29 6	1 ^s ,5	4 ^s ,1 Y ^a	3,58 3,66	233 168	176° 161	Var -12,6	40 40	(4)	1,6 5,4	107	-31
422 545	γ Arietis N 243	48,0	+18 48	A0p	2 ^s ,2 W	4,83 4,99	138 43	147° 131	- 5 +	16 16	(2)	0,8 5,4	111	-40
423 546	γ Arietis S 243	48,0	+18 49		2 ^s ,2 W	4,75 4,91	135 32	143° 131	- 1 +	14 14	(1)	0,3 5,4	111	-40
426 549	ξ Piscium 290	48,4	+ 2 42		5 ^s ,8 Y ^a	4,84 4,85	33 +	41° 3	+30 +	18 18	(4)	1,1 2,4	121	-55
428 553	β Arietis 306	49,1	+20 19	A5	2 ^s ,6 W	2,72 2,96	147 25	139° 144	Var ? - 0,6	65 66	(5)	1,6 3,6	111	-39
429 555	ψ Phoenicis 552	49,6	-46 48	Mb		4,41 4,40	131 98	225° 86	+ 6,8 -				239	-66
433 558	φ Phoenicis 583	50,2	-43 0	B9		5,00 5,20	52 42	229° 31	Var +12				230	-69
438 566	γ Eridani 241	52,0	-52 7	G5		3,73 3,87	727 269	67° 676	- 6,2 +	78 78	(2)	3,2 8,0	247	-61
441 569	λ Arietis 288	52,4	+23 7	A5	3 ^s ,5 Y ^a	4,83 5,03	96 75	259° 60	+ 1 -	26 26	(4)	1,9 4,7	111	-36
442 570	η ^a Ilydri 101	52,4	-68 9	K0		4,72 4,83	111 74	33° 82	-16,2 +	30 28	(2)	2,0 4,9	261	-49
445 574	Phoenicis 597	53,2	-47 53	G5		4,74 4,86	104 12	85° 104	+11,9 +	36 36	(1)	2,5 4,8	240	-65
446 575	A Cassiopeiae 153	53,8	+70 25	A3	3 ^s ,6 Y ^a	4,61 4,77	61 32	276° 52	- 1 -	31 30	(7)	2,0 3,5	96	+ 9
449 580	50 Cassiopeiae 117	54,9	+71 56	A2	3 ^s ,1 W	4,06 4,18	45 4	301° 45	Var ? -12,5	25 24	(4)	1,0 2,3	96	+11
453 585	v Ceti 358	55,3	- 21 34	Ma	7 ^s ,2 O ^a	4,18 4,17	130 31	99° 126	+17,9 +	16 16	(3)	0,2 4,8	165	-71
459 590	g Persei 430	55,6	+54 1	B8	2 ^s ,9 YG ¹	4,99 5,21	41 28	86° 30	Var - 1,9	10 10	(3)	0,0 3,0	101	- 6
458 591	α Hydri 162	55,6	-62 3	10	4 ^s ,1	3,02 3,16	254 5	79° 254	+ 7 +	67	(a)	2,1 5,1	255	-54

1^a to 2^a.

1	2	3	4	5	6	7	8	9	10	11	12	13	14	15
463	α Pictum	56 ^m .9	+ 2° 17'	A2p	2 ^m .4 R'	5 ^m .23			Var. + 9.9				124°	-55°
595	317													
463	α Pictum	56 .9	+ 2 17	A2p	3 ^m .1 W	4 .33 4 .12	+ 42	98 ^m + 37	Var. + 9.3	20	(3)	0.4 2.0	124	-55
596	317													
467	γ Phœnix	57 .7	-45 12	K0		4 .96 5 .05	- 56 - 48	215 ^m - 20	-30.6				232	-67
602	659											3.6		
468	γ Andromedæ	57 .8	+41 51	K0	5 ^m .4 Y ^a	2 .28 2 .40	- 70 - 7	138 ^m + 69	-11.1	30	(7)	-0.6 1.5	105	-18
603	395													
469	γ Andromedæ	57 .8	+41 51	A0	3 ^m BG ^a	5 .08 5 .20	- 72 - 10	140 ^m + 71	-12.1			-0.6 1.0	105	-18
604	395													
474	γ Fornacis	0 .0	-29 47	A0p		4 .74 4 .90	+ 12 + 5	80 ^m + 11	+18			0.1	191	-72
612	706													
477	α Arietis	1 .5	+22 59	K2	5 ^m .4 Y ^a	2 .23 2 .12	+ 239 + 17	127 ^m + 239	-14.1	53	(6)	0.8 4.1	113	-35
617	306													
480	58 Andromedæ	2 .5	+37 23	A2	2 ^m .8 W	4 .77 4 .95	+ 157 + 71	105 ^m + 140	Var	24	(3)	1.7 5.7	107	-22
620	486													
482	β Trianguli	3 .6	+34 31	A5	3 ^m .3 Y ¹	3 .08 3 .29	+ 160 + 70	106 ^m + 144	+10.4	39	(6)	0.9 4.1	109	-24
622	381													
499	b Andromedæ	6 .9	+43 45	K0p	6 ^m .9 O ^a	5 .08 5 .00	- 17 - 16	245 ^m - 6	-44.0	9	(2)	-0.2 1.3	106	-15
643	447													
505	ξ Ceti	7 .7	+ 8 23	G5	5 ^m .5 Y ^a	4 .54 4 .64	- 26 - 21	254 ^m - 15	Var	7	(2)	-1.2 1.6	124	-48
649	345													
517	γ Trianguli	11 .4	+33 23	A0	2 ^m .7 Y ¹	4 .07 4 .26	- 66 - 8	141 ^m + 65	+ 6	21	(2)	0.7 3.2	111	-25
664	397													
524	ϕ Eridani	12 .9	-51 59	B8		3 .78 3 .92	- 81 - 36	111 ^m + 73	+10	15	(1)	-0.3 3.3	241	-60
674	886													
530	σ Ceti	14 .3	- 3 26	Mdp	7 ^m .0 O ^a	2 .00 2 .00	- 237 - 199	181 ^m + 128	+62.2	13	(1)	-2.4 3.9	136	-56
681	353													
545	65 Andromedæ	18 .9	+49 50	K5	5 ^m .9 O ^a	4 .86 4 .82	+ 31 + 7	122 ^m + 30	- 4.6	9	(4)	-0.9 2.3	106	- 9
699	656													
548	δ Hydri	20 .0	-69 7	A2		4 .26 4 .37	+ 56 + 31	282 ^m - 46	+11.1	44	(1)	3.0	257	-46
705	113													
550	ϵ Cassiopeiæ	20 .8	+66 57	A5p	3 ^m .9 Y ¹	4 .59 4 .77	+ 15 + 8	344 ^m + 13	Var	27	(4)	1.8 0.5	100	+ 7
707	213													
551	ρ Ceti	21 .1	-12 44	A0	2 ^m .6 W	4 .90 5 .08	- 27 - 20	250 ^m - 18	- 11	14	(2)	0.6 2.1	152	-62
708	451													
560	δ Ceti	22 .8	+ 8 1	A0	2 ^m .5 W	4 .34 4 .49	+ 39 + 22	96 ^m + 32	Var. + 7	16	(3)	0.5 2.3	129	-46
718	388													
563	π Eridani	23 .3	-48 9	B5		4 .44 4 .53	- 18 - 14	137 ^m + 12	Var. + 29			0.7	232	-61
721	637													
575	σ Ceti	27 .3	-15 41	F5	3 ^m .5 Y ¹	4 .82 4 .91	- 141 - 140	215 ^m - 20	-29.4	34	(2)	2.5 5.6	160	-62
740	449													
580	α Fornacis	29 .5	-28 40	B9		4 .95 5 .12	- 28 - 23	230 ^m - 16	Var + 10			2.2	189	-66
749	819													
604	δ Ceti	34 .4	- 0 6	B2	2 ^m .4 W	4 .04 4 .21	+ 10 + 7	84 ^m + 7	+12	4	(2)	-3.0 -1.0	139	-51
779	406													
610	12 Pictis	35 .9	+39 46	G0	4 ^m .5 Y ^a	4 .99 5 .15	- 191 - 138	184 ^m + 132	Var. - 23	29	(1)	2.3 6.4	113	-17
788	610													
611	π Eridani	36 .0	-43 20	A2		4 .53 4 .67	- 90 - 38	115 ^m + 82	+20.			4.3	220	-62
789	814													
614	ϵ Eridani	36 .7	-40 17	K0		4 .06 4 .12	- 124 - 21	104 ^m + 122	- 9.2	31	(2)	1.5 4.5	215	-63
794	689													
617	θ Pictis	37 .4	+48 48	F8	4 ^m .0 Y ^a	4 .22 4 .32	+ 351 + 197	105 ^m + 291	+25.1	85	(7)	3.8 6.9	109	- 9
799	746													
620	35 Arietis	37 .6	+27 17	B3	2 ^m .1 Y ¹	4 .58 4 .85	- 14 - 6	163 ^m + 13	+23	5	(1)	-1.9 0.3	119	-28
801	424													

Box 463. Binary ADS 1615: 2^m.7, 307°. Each component is a spectroscopic binary. No orbit determined for either pair. — Box 468. Binary ADS 1630: period 35 years. — Box 530. Variable: 1^m.7 to 9^m.6 in 328 days. Prototype for the Mira class; has a 10^m companion O^m.75, 128° (1926) evidently physically connected with σ Ceti.

2^h to 3^h.

1	2	3	4	5	6	7	8	9	10	11	12	13	14	15
622 804	γ Ceti 422	38 ^m .1	+ 2° 49	A2	2°.9 Y ²	3 ^m .58 3.79	210 — 210	224° — 19	— 5	36 36	(5)	1.4 5.2	137°	— 48°
621 806	ϵ Hydri 161	38 .1	— 68 42	B9		4.26 4.36	92 — 27	80° + 88	+ 6			4.1	256	— 45
627 811	π Ceti 519	39 .4	— 14 17	B5	2°.7 W	4.39 4.55	16 — 16	207° + 0	+ 15.0	11 11	(1)	— 0.4 0.4	160	— 59
629 813	μ Ceti 359	39 .5	+ 9 42	F0	4°.0 Y ¹	4.36 4.45	282 + 169	95° + 226	+ 29.7	32 32	(2)	1.9 6.6	132	— 42
631 818	τ^1 Eridani 518	40 .5	— 19 0	F5	4°.5 Y ²	4.61 4.70	327 + 177	82° + 275	+ 26.2	57 57	(1)	3.4 7.2	169	— 61
634 824	39 Arietis 462	42 .0	+ 28 50	K0	6°.4 Y ³	4.62 4.65	196 — 27	130° + 191	— 15.8	19 18	(5)	0.9 6.1	119	— 26
639 834	η Persei 714	43 .4	+ 55 29	K0	6°.8 O ⁸	3.93 3.92	30 + 9	123° + 29	— 1.8	10 13	(6)	— 1.8 1.3	107	— 3
642 837	ζ Hydrae 169	44 .0	— 68 3	A2		4.90 4.99	76 + 20	47° + 74	+ 4	9 9	(1)	4.3	254	— 46
643 838	41 Arietis 471	44 .1	+ 26 51	B8	2°.6 W	3.68 3.75	132 — 28	150° + 129	Var 0	22 21	(3)	0.3 4.3	121	— 27
644 840	16 Persei 646	44 .2	+ 37 55	F0	3°.8 Y ¹	4.27 4.45	213 + 72	119° + 199	+ 14	32 30	(4)	1.7 5.9	115	— 18
645 841	β Poinacis 1025	44 .9	— 32 50	K0		4.50 4.52	190 + 177	32° + 68	+ 17.2	27 27	(2)	1.7 5.9	198	— 63
646 843	17 Persei 527	45 .4	+ 34 39	K5	7°.1 O ³	4.67 4.64	77 — 34	165° + 69	+ 13.9	13 12	(5)	0.1 4.1	117	— 20
650 850	τ^2 Eridani 509	46 .5	— 21 25	K0	5° Y ³	4.81 4.80	53 — 31	257° — 43	— 8.6	16 16	(4)	0.8 6.2	173	— 61
653 854	τ Persei 641	47 .2	+ 52 21	G0 } A5 }	4°.9 Y ²	4.06 4.13	8 — 0	140° + 8	Var	20 17	(5)	0.2 1.4	109	— 5
— 868	R Iliol 860	50 .6	— 50 18	Md		4.0—10.2			+ 60				232	— 58
663 872	ν Hydri 204	51 .1	— 75 29	K2		4.70 4.82	62 + 37	271° — 50	+ 4.7	15 15	(2)	0.6 3.6	259	— 40
665 874	η Eridani 553	51 .5	— 9 18	K0	5°.8 Y ²	4.05 4.05	229 — 137	160° + 183	— 20.4	27 27	(2)	1.2 5.8	155	— 53
668 879	π Persei 681	52 .4	+ 39 16	A2	2°.5 W	4.62 4.85	63 — 2	143° + 63	+ 18	19 19	(2)	1.0 3.6	116	— 16
670 882	24 Persei 550	52 .9	+ 34 47	K0	6°.1 OY ²	4.97 5.02	63 — 40	281° — 49	— 36.0	12 12	(2)	0.4 4.0	119	— 20
674 887-888	ϵ Arietis 484	53 .5	+ 20 56	A2	3°.2 W, Y ¹	4.64 4.80	17 — 16	242° — 4	— 8 } — 6 }	13 13	(2)	0.2 — 0.2	127	— 32
679 896	λ Ceti 455	54 .1	+ 8 31	B5	2°.5 W	4.69 4.91	11 + 2	124° + 11	+ 11	9 9	(2)	— 0.5 — 0.1	136	— 42
680 897	θ^1 Eridani 771	54 .5	— 40 42	A2	3°.8	3.42 3.63	67 + 35	301° — 58	Var + 11.9	22 22	(a)	0.1 2.6	215	— 60
681 898	θ^2 Eridani 771	54 .5	— 40 42	A2	3°.8	4.42 4.63	77 + 20	285° — 75	+ 19			3.8	215	— 60
691 911	α Ceti 419	57 .1	+ 3 42	Ma	6°.7 O ³	2.82 2.85	78 — 66	190° + 41	— 25.3	24 22	(5)	— 0.5 2.3	141	— 44
694 915	γ Persei 064	57 .6	+ 53 7	F5 } A3 }	4°.5 Y ²	3.08 3.19	10 — 2	156° + 10	+ 0.6	23 21	(4)	— 0.3 — 1.9	110	— 4
697 918	κ Persei 767	58 .0	+ 56 19	K0	5°.5 Y ²	5.08 4.98	71 + 40	357° — 58	— 44.8	20 19	(2)	1.6 4.3	108	— 1
696 919	τ^3 Eridani 1387	58 .0	— 24 1	A3	4° Y ¹	4.16 4.33	150 — 90	253° — 120	— 12	28 28	(1)	1.4 5.0	181	— 59
698 921	ρ Persei 630	58 .8	+ 38 27	Mb	6°.6 O ³	3.4—4.2 3.67	173 + 42	128° + 169	+ 28.2	18 17	(4)	— 0.3 4.6	118	— 16

Boss 674 The components of this binary, ADS 2251, are in the RR1₂ system 5.55 and 5.25 — Boss 698 Irregular variable

8^a.

1	2	3	4	5	6	7	8	9	10	11	12	13	14	15
705	Camelopais	1 ^m .0	+74° 1'	A2	2 ^d .4	4 ^m .89	88	161 ^a	+24	15	(2)	0.8	99 ^a	+15°
932	168				Y ¹	5.10	— 32	+ 82		15		4.6		
708	β Persei	1.7	+40 34	B8	1 ^d .9	2.1	9	125 ^a	Var	34	(3)	-0.3	116	-14
936	673				W	2.47	— 5	+ 7	+ 5.7	33		3.1		
710	γ Persei	1.8	+49 14	G0	4 ^d .1	4.17	1269	94 ^a	+50.3	104	(4)	4.2	112	- 7
937	857				Y ²	4.25	+ 952	+ 838		101		9.7		
713	η Persei	2.7	+44 29	K0	5 ^d .8	4.00	240	130 ^a	+29	23	(6)	0.7	116	-11
941	631				Y ³	3.99	+ 53	+ 233		21		5.9		
717	ω Persei	4.8	+39 14	K0	5 ^d .4	4.82	22	278 ^a	+ 6.1	13	(4)	0.2	118	-15
947	724				Y ⁴	4.75	— 16	— 16		12		1.5		
718	δ Arietis	5.9	+19 21	K0	5 ^d .9	4.53	152	92 ^a	+24.6	22	(5)	0.9	131	-31
951	477				Y ⁵	4.56	+ 111	+ 103		19		5.4		
723	α Fornacis	7.8	-29 23	F8	5 ^d .6	3.95	726	26 ^a	-20.7	82	(3)	3.5	191	-57
963	1177				Y ⁶	4.04	+ 711	+ 152		82		8.3		
730	ζ Arietis	9.2	+20 40	A0	2 ^d .6	4.95	79	198 ^a	+15	15	(5)	0.8	130	-29
972	527				W	5.13	— 66	+ 43		15		4.4		
739	ζ Eridani	11.0	- 9 11	A3	3 ^d .8	4.90	45	355 ^a	Var				159	-49
984	624				Y ¹	5.08	+ 35	— 29				3.2		
741	Camelopardalis	11.2	+65 17	B3p	2 ^d .3	4.76	12	115 ^a	Var.	8	(1)	-0.7	105	+ 8
985	340				W	5.00	+ 6	+ 10	+ 2.2	8		0.2		
746	Persei	12.5	+33 51	K0	7 ^d .2	4.92	13	157 ^a	+ 1.7	10	(4)	-0.1	123	-18
991	619				Y ²	4.91	— 3	+ 13		10		0.5		
752	η Ceti	14.1	+ 3 0	G5	5 ^d .0	4.96	282	70 ^a	+19.3	106	(3)	5.0	146	-42
996	818				Y ¹	5.08	+ 254	+ 124		105		7.2		
753	Arietis	14.3	+28 41	K5	6 ^d .6	4.72	27	186 ^a	- 2.1	13	(3)	0.3	126	-22
999	576				OY ¹	4.61	— 18	+ 20		13		1.9		
757	ι Persei	14.7	+42 58	A2	2 ^d .9	4.98	58	260 ^a	Var	15	(2)	0.9	118	-10
1002	750				W	5.19	— 53	— 24	- 6.6	15		3.8		
759	τ Eridani	15.1	-22 7	Mb	6 ^d .9	3.95	65	50 ^a	+42.4	13	(3)	-0.5	179	-54
1003	584				O ²	3.94	+ 57	+ 31		13		3.0		
764	σ Eridani	15.9	-43 27	G5		4.30	3168	76 ^a	+86.8	219	(1)	6.0	216	-55
1008	1028					4.38	+ 317	+3136		219		11.8		
772	α Persei	17.2	+49 30	F5	3 ^d .4	1.90	39	136 ^a	- 2.1	23	(4)	-1.4	114	- 5
1017	917				Y ¹	2.08	+ 7	+ 38		22		-0.1		
778	σ Tauri	19.4	+ 8 41	G5	4 ^d .9	3.80	103	221 ^a	Var	17	(5)	-0.3	142	-36
1030	511				Y ²	3.85	— 102	+ 10	-20	15		3.9		
780	Persei	20.9	+48 43	B5	2 ^d .1	4.94	32	129 ^a	Var	8	(5)	-0.5	115	- 5
1034	920				W	5.18	+ 10	+ 30	+11	8		2.5		
781	Camelopardalis	21.0	+59 36	B9p	3 ^d .8	4.42	4	104 ^a	- 6.6	8	(2)	-1.4	109	+ 4
1035	660				Y ¹	4.54	+ 3	+ 3		7		-2.6		
784	ξ Tauri	21.7	+ 9 23	B8	2 ^d .3	3.75	72	125 ^a	Var	17	(1)	-0.1	143	-36
1038	439				YG ¹	3.95	+ 16	+ 70		17		3.0		
786	Camelopardalis	21.9	+58 32	A0p	4 ^d .5	4.76	11	90 ^a	Var	2	(1)	-3.7	110	+ 3
1040	607				Y ²	4.86	+ 9	+ 6	- 8.4	2		0.0		
790	34 Persei	22.2	+49 10	B5	2 ^d .0	4.67	44	139 ^a	0.	9	(6)	-0.6	116	- 5
1044	945				Y ¹	4.89	+ 6	+ 44		9		2.9		
791	Camelopardalis	22.4	+55 7	A2	2 ^d .1	4.98	33	266 ^a	+ 4	14	(4)	0.7	112	0
1046	684				W	5.21	— 29	— 16		14		2.6		
795	σ Persei	23.5	+47 39	K0	6 ^d .4	4.55	23	15 ^a	+14.9	13	(4)	0.1	116	- 6
1052	843				O ³	4.51	+ 17	— 15		13		1.4		
1057	Persei	24.4	+43 34	F ^a Novn	Var	0.0-13.	16	195 ^a	+ 6	7	(3)	-5.8	119	- 9
804	ι Tauri	25.4	+12 36	K0	5 ^d .3	4.28	18	103 ^a	+14	19	(3)	0.6	140	-33
1066	486				Y ²	4.33	+ 11	+ 14		18		0.6		
806	17 Eridani	25.6	- 5 25	B9	2 ^d .4	4.80	13	42 ^a	+ 9	10	(a)		157	-45
1070	674				W	4.95	+ 13	0				0.4		

Bos 708. Aigel or Aigel. A triple spectroscopic system with periods of 29 days and 1.87 years, respectively

3^h.

3	i	5	6	7	8	9	10	11	12	13	14	15
27 ^m ,6	-63° 18'	F5		4 ^m ,80 4 ,93	+ 519 + 88	44° + 509	+12,0					214° -46°
28 ,2	- 9 48	K0	5° ,8 Y ^a	3 ,81 3 ,81	972 - 573	271° - 787	+16,0	290 290	(5)	8,3 6,1 8,8	164	-47
29 ,4	+47 51	B5p	2° ,8 YG ¹	4 ,26 4 ,52	44 + 16	127° + 41	+ 3	10 9	(3)	-1,0 2,5	117	- 5
29 ,4	-21 58	B8	3° ,6 W	4 ,32 4 ,49	44 - 3	117° + 44	+15,0	13 13	(1)	-0,1 2,5	181	-51
31 ,8	+ 0 5	G5	4° ,4 Y ^a	4 ,40 4 ,43	536 - 509	206° + 177	+28,3	71 73	(4)	3,7 8,0	153	-40
33 ,5	-40 36	K0		4 ,58 4 ,61	44 - 42	191° - 14	+ 9,9	18 18	(2)	0,9 2,8	212	-53
35 ,8	+47 28	B5	2° ,5 W	3 ,10 3 ,31	46 + 11	136° + 45	+13	14 13	(6)	-1,3 1,4	118	- 5
37 ,3	+63 2	B5, A0	4° ,5 Y ^a	4 ,96 5 ,00	11 - 3	163° + 14	Var	12 12	(2)	0,4 0,7	109	+ 7
38 ,0	+31 58	B1	2° ,7 YG ¹	3 ,94 3 ,99	26 - 4	157° + 26	Var	8 8	(3)	-1,5 1,0	128	-17
38 ,3	-32 15	B5		4 ,93 5 ,11	9 + 7	324° - 6	Var				197	-52
38 ,4	+42 16	F5	3° ,8 Y ¹	3 ,93 4 ,02	9 - 7	276° - 5	+13,1	19 19	(4)	0,3 -1,3	122	- 9
38 ,5	-10 6	K0	5° ,7 Y ^a	3 ,72 3 ,71	749 + 532	353° - 532	- 6,1	110 110	(4)	3,9 -0,7	166	-45
39 ,0	+23 48	B5p	3° ,0 W	3 ,81 4 ,01	53 - 11	159° + 52	+11	15 14	(6)	-0,5 2,4	134	-22
39 ,1	-37 38	K2		4 ,64 4 ,65	113 - 75	226° - 85	+ 9,9	16 15	(2)	0,5 4,8	207	-51
39 ,3	+24 10	B5	2° ,9 W	4 ,37 4 ,59	49 - 17	167° + 16	+ 6	12 11	(5)	-0,4 2,8	134	-22
39 ,8	+71 1	A0	2° ,6 W	4 ,67 4 ,84	46 + 7	141° + 46	- 9	19 19	(1)	1,1 3,0	104	+14
39 ,9	+24 4	B5	2° ,9 W	4 ,02 4 ,16	51 0	147° + 54	+10	12 12	(5)	-0,6 2,7	134	-22
40 ,4	+65 13	Ma	7° ,1 O ^a	4 ,71 4 ,58	4 - 3	284° - 3	- 3,2	9 9	(3)	-0,5 -2,3	108	+ 9
40 ,4	+23 39	B5	2° ,9 W	4 ,25 4 ,42	59 - 10	157° + 58	+ 1	12 11	(4)	-0,5 3,1	134	-22
41 ,1	-12 25	Ma	7° ,5 OY ²	4 ,64 4 ,60	69 + 68	30° - 7	+45,7	12 12	(1)	0,0 3,8	168	-45
41 ,5	+23 48	B5p	2° ,9 G ¹	2 ,96 3 ,13	52 - 10	158° + 51	+ 5	20 17	(6)	-0,9 1,5	134	-22
42 ,5	-23 33	B8	5 Y ¹	4 ,33 4 ,42	548 - 548	197° + 38	+ 7,1	61 60	(3)	3,2 8,0	185	-49
42 ,9	-65 7	K0		3 ,80 3 ,96	307 - 144	76° + 270	Var	24 24	(2)	0,7 6,3	245	-43
43 ,2	+23 45	B8	3° ,1 YG ¹	3 ,80 3 ,96	53 - 10	159° + 52	+ 3	4 7	(4)	-2,0 2,4	135	-22
44 ,9	-37 55	A0		5 ,42 5 ,56	79 - 20	79° + 77	+15,9	25	(a)	1,4 4,9	207	-50
44 ,9	-37 55	B8		4 ,86 5 ,00	82 - 24	103° + 79	+16				207	-50
45 ,7	-36 30	K0		4 ,24 4 ,27	71 - 48	226° - 53	+ 2,9	16 16	(1)	0,3 3,5	205	-50
47 ,8	+31 35	B1	2° ,8 Y ¹	2 ,91 3 ,12	21 + 3	143° + 21	+19,2	3 3	(3)	-4,7 -0,5	130	-15

Boss 856 Faygeta — Boss 860 Main — Boss 869 Aleyone — Boss 877 Aths A difficult binary 0° 43, 39°, 4
881, 885 Doubtless a physical pair.

8^h to 4^h.

1	2	3	4	5	6	7	8	9	10	11	12	13	14	15
896 1204	Camelopardalis 628	48 ^m .6	+62° 47'	B9	2 ^s .5 Y ¹	4 ^m .87 5.12	5 +	68° 1	+ 6:	13 13	(3)	0.4 -1.6	110° 256	+ 8° -38
899 1208	7 Hydri 276	48 .8	-74 33	Ma	6 ^s .0	3.17 3.36	124 +	21° 118	+15.7	17 17	(1)	-0.7 2.7	256 159	-38 -39
901 1211	32 Eridani 631	49 .2	- 3 14	A	3 G ²	6.33 4.73	160 +	145° 158				-0.6 5.7	159 159	-39 -39
901 1212	32 Eridani 631	49 .2	- 3 14	G5	6 ^s .0 Y ³	4.95 4.73	34 +	83° 20	+26.9	12 9	(5)	0.4 2.5	159 187	-39 -48
902 1213	1 st Eridani 1945	49 .5	-24 55	B5	4 Y ¹	4.76 4.91	34 -	121° 33	Var +23			2.5	187	-48
910 1220	5 Persei 895	51 .1	+39 43	B1	2 ^s .2 W	2.96 3.14	39 +	138° 38	Var - 6	5 6	(6)	-3.2 0.9	125	- 9
913 1228	8 Persei 775	52 .5	+35 30	Oe5	5 ^s .2 Y ¹	4.05 4.26	20 +	142° 20	Var. +67.4	1 2	(2)	-4.4 0.3	129	-12
915 1231	7 Eridani 781	53 .4	-13 48	K5	7 ^s .0 Y ³	3.19 3.25	130 -	151° 117	+61.5	23 23	(4)	0.0 3.8	173	-43
920 1239	1 Tauri 539	55 .1	+12 12	B3	2 ^s .3 W	3.4-4.2 3.7-4.2	15 -	203° 8	Var. 13.0	2 3	(2)		147	-28
923 1240	1 st Eridani 2022	55 .7	-24 18	A0p	2 W	4.69 4.85	9 +	63° 6	Var +23.2	12 (a)		0.1 -0.4	187	-46
930 1247	8 Retiuli 290	57 .2	-61 41	Ma		4.41 4.53	20 -	165° 9	- 0.8			0.9	241	-43
932 1251	1 st Tauri 581	57 .8	+ 5 43	A0	3 ^s .0 YG ¹	3.94 4.15	7 -	172° 6	- 6	23 22	(4)	0.6 -1.8	152	-32
936 1256	A ¹ Tauri 585	58 .8	+21 49	K0	5 ^s .4 Y ³	4.50 4.48	113 +	125° 103	+ 9.9	19 18	(4)	-0.5 4.8	140	-21
938 1261	1 Persei 1101	59 .1	+50 5	A0	3 ^s .0 W	4.33 4.52	37 -	185° 32	+ 5.	16 16	(2)	0.4 2.2	120	0
940 1264	7 Retiuli 312	59 .5	-62 27	Mb		4.46 4.58	22 +	355° 14	- 5.9			1.2	240	-43
941 1266	1 Retiuli 293	59 .7	-61 22	K5		4.81 4.92	110 +	28° 104	+60.5			5.0	239	-43
947 1273	c Persei 939	1 .4	+47 27	B3p	2 ^s .8 YG ¹	4.03 4.26	44 +	133° 41	Var + 4	12 11	(4)	-0.8 2.2	122	- 3
963 1298	o ¹ Eridani 764	7 .0	- 7 6	F2	4 ^s .3 Y ¹	4.14 4.24	81 +	6° 52	+14	22 21	(3)	0.8 3.7	167	-37
966 1302	8 Horologii 1400	7 .4	-42 15	F0		4.85 4.98	203 +	71° 203	+37.1			6.4	223	-45
967 1303	μ Persei 1063	7 .6	+48 9	G0	5 ^s .5 Y ¹	4.28 4.33	30 +	154° 30	Var. + 7.8	16 13	(3)	-0.2 1.7	122	- 1
970 1306	f Persei 912	8 .1	+40 14	G0	6 ^s .1 Y ³	4.89 4.89	31 +	148° 31	Var. + 3	4 3	(2)	-2.7 2.4	127	- 7
972 1311	47 Tauri 668	8 .5	+ 9 1	G5	5 ^s .9 Y ³	4.98 5.02	36 -	196° 24	- 6.4	10 10	(2)	0.0 2.8	151	-28
981 1320	μ Tauri 657	10 .1	+ 8 38	B3	2 ^s .6 Y ¹	4.32 4.52	34 +	126° 32	+17	10 10	(4)	-0.7 2.0	151	-28
986 1324	b Persei 1160	10 .7	+50 3	A2	3 ^s .0 W	4.57 4.80	76 +	135° 71	Var.	16 16	(3)	0.6 4.0	121	+ 1
984 1325	o ¹ Eridani 780	10 .7	- 7 49	G5	5 ^s .7 Y ¹	4.48 4.52	4085 -	213° 899	-42.1	214 207	(6)	6.1 12.5	167	-37
985 1326	α Horologii 1423	10 .7	-42 32	K0		3.83 3.91	219 -	169° 31	+21.4	35 35	(2)	1.6 5.5	214	-45
989 1329	ω Tauri 724	11 .4	+20 20	A3	2 ^s .9 W	4.80 5.08	66 -	207° 38	+16	28 28	(2)	2.0 3.9	143	-20
994 1336	α Retiuli 332	13 .1	-62 43	G5	4 ^s .4	3.36 3.51	70 +	32° 69	+35.5	22 22	(2)	0.1 2.6	241	-41

Star 901 AD 8 1939. 6^m.98, 347° 2 (1922.8). The dynamic parallax is 0^m.002. Probably a physical system although the proper motions differ considerably - Ross 920. Resolving binary. Period 3,913 days.

4^h.

1	2	3	4	5	6	7	8	9	10	11	12	13	14	15
995 1338	γ Doradus 1066	13 ^m .4	-51° 44'	F5		4 ^m .36 4.48	202 + 89	27° + 182	+27				227°	-44°
1000	γ Tauri	14 .1	+15 23	K0	5 ^e .1 Y ^a	3.86 3.90	120 + 92	102° + 77	+38.5	25 25	(7)	5.9 0.9 4.3	147	-23
1346	612													
1001	ν^4 Eridani	14 .1	-34 3	B9		3.59 3.77	58 - 4	93° + 58	Var +17.6				202	-44
1347	1614											2.4		
1003	δ Persei	14 .3	+46 16	B3	2 ^e .8 W	4.89 5.07	45 + 8	148° + 44	+ 1	7 7	(4)	-0.9 3.2	124	- 2
1350	872											1.7	237	-42
1005	ϵ Reticuli	14 .7	-59 32	K2		4.12 4.54	177 - 65	201° + 165	+28.8	31 29	(2)	5.7		
1355	324											0.9	146	-21
1017	δ^1 or δ Tauri	17 .2	+17 18	K0	5 ^e .5 Y ^a	3.93 1.00	115 + 83	107° + 79	+38.5	25 25	(7)	4.2		
1373	712											1.7	146	-21
1022	δ^2 or δ^4 Tauri	18 .4	+17 13	A5	2 ^e .5 YG ¹	4.84 5.09	124 + 86	109° + 89	Var +36.6	25 24	(5)	5.3		
1380	714											1.4	143	-17
1026	κ^1 Tauri	19 .4	+22 4	A3	3 ^e .1 YG ¹	4.36 4.57	112 + 71	116° + 87	+41	26 26	(5)	4.6		
1387	642											2.1	143	-17
1027	κ^2 or δ^7 Tauri	19 .5	+21 58	F0	2 ^e .9 Y ¹	5.42	132 + 79	118° + 106	+16	22 22	(1)	6.0		
1388	643											1.5	146	-20
1029	δ^3 or δ^8 Tauri	19 .7	+17 42	A2	2 ^e .4 YG ¹	4.24 4.48	109 + 84	103° + 70	+36.3	29 28	(5)	4.4		
1389	719											1.4	142	-16
1033	ν^1 or δ^9 Tauri	20 .3	+22 35	A5	3 ^e .6 Y ^{1.5}	4.40 4.56	123 + 77	116° + 96	Var +33	25 25	(4)	4.8		
1392	696											-0.1	202	-43
1032	δ Eridani	20 .3	-34 15	K5		4.06 4.11	79 + 53	45° + 58	+23.3	15 15	(1)	3.6		
1393	1664											0.5	148	-21
1034	η^1 Tauri	20 .6	+15 23	A5	3 ^e .0 Y ¹	4.60 4.89	118 + 92	102° + 74	Var + 3	20 15	(6)	5.0		
1394	625											-0.1	148	-21
1036	π Tauri	20 .9	+11 29	K0	5 ^e .3 Y ^a	4.91 4.95	35 - 16	180° + 31	+31.8	10 10	(1)	2.7		
1396	697											1.1	146	-18
1044	ϵ Tauri	22 .8	+18 58	K0	5 ^e .4 Y ^a	3.63 3.73	120 + 89	107° + 80	+39.1	32 31	(5)	4.0		
1409	640											1.4	148	-20
1045	θ^1 Tauri	22 .8	+15 44	K0	5 ^e .6 OY ^a	4.04 3.99	108 + 81	104° + 71	+37.7	28 29	(6)	4.2		
1411	631											1.2	148	-20
1046	θ^2 Tauri	22 .9	+15 39	F0	2 ^e .9 W	3.62 3.73	107 + 80	104° + 71	Var +42.6	33 33	(6)	3.8		
1412	632											1.9	148	-20
1054	τ Tauri	24 .8	+15 59	A5	3 ^e .0 Y ¹	4.84	116 + 87	105° + 77	Var +37.7	27 26	(7)	5.2		
1427	637											163	-29	
1063	ζ^5 Eridani	26 .8	- 0 16	K0	5 ^e .3 OY ^a	4.97 4.97	3 - 2	180° + 3	+16.2			-2.6		
1437	713											1.6	150	-20
1067	ρ Tauri	28 .2	+14 38	A5	3 ^e .3 Y ¹	4.75 4.92	104 + 80	104° + 67	Var.	24 23	(5)	4.8		
1444	720											2.4	197	-41
1073	ν^1 Eridani	29 .6	-29 57	K0	4 ^e .4	4.59 4.59	292 - 283	201° - 64	+20.1	36 36	(1)	6.9		
1453	1883											-1.7	129	- 3
1074	σ Persei	29 .7	+41 4	K0	6 ^e .2 OY ^a	4.46 4.41	25 - 14	194° + 21	Var.	9 6	(5)	1.4		
1454	1000			A3								0.5	149	-19
1077	α Tauri	30 .2	+16 19	K5	6 ^e .3 OY ^a	1.06 1.08	203 - 18	160° + 203	+54.9	76 76	(4)	2.6		
1457	629											0.9	154	-23
1076	δ Tauri	30 .2	+ 9 57	A3	3 ^e .2 Y ¹	4.38 4.51	66 + 17	138° + 64	Var. +28.4	21 20	(2)	3.5		
1458	607											-2.4	168	-30
1079	ν Eridani	31 .3	- 3 33	B2	2 ^e .7 W	4.12 4.28	2 - 1	180° + 2	Var +15.4	5 5	(3)	4.4		
1463	834											0.2	198	-40
1080	ν^2 Eridani	31 .7	-30 46	K0	5 ^e .7	3.88 3.93	59 - 10	266° - 58	- 3.8	18 18	(1)	2.7		
1464	1901											230	-41	
1081	α Doradus	31 .8	-55 15	A0p	3 ^e .8	3.47	52	92°	+25.6			2.1		
1465	663											1.8	153	-21
1087	ϵ Tauri	32 .6	+12 19	A3	2 ^e .9 W	4.30 4.56	104 + 88	96° + 55	Var +54	31 31	(5)	4.4		
1473	618													

Boss 1026, 1027 Probably a physical pair Also member of the Taurus cluster — Boss 1076 Ellipsing binary

4b.

1	2	3	4	5	6	7	8	9	10	11	12	13	14	15
1090	α^2 Tauri	33 ^m .5	+15° 43'	A3	2 ^s .9	4 ^m .85	84	104°	Var	24	(4)	1,7	149°	-19°
1479	666				Y ¹	5,00	+ 66	+ 52	+22	23		4,5		
1091	γ Eridani	33 .6	-14 30	K0	5 ^s .6	3,98	179	205°	Var	36	(2)	1,8	179	-35
1481	933				OY ²	4,01	- 170	+ 205	+41,8	36		5,2		
1101	β Doradus	35 .6	-62 16	M0		Var	125	226°	+26,1				239	-39
1492	372					4,8-6,8	+ 28	- 121				5,3-7,3		
1105	54 Eridani	36 .1	-19 52	Mn	6 ^s .8	4,54	94	165°	-33,5	13	(2)	0,1	185	-36
1496	988				O ²	4,53	- 62	+ 70		13		4,4		
1107	ϵ Tauri	36 .2	+22 46	B5	2 ^s .3	4,33	23	165°	+ 9,6	9	(4)	-0,9	144	-14
1497	739				W	4,50	- 2	+ 23		9		1,1		
1110	α Cassi	37 .3	-42 3	F2		4,52	169	238°	Var.	27	(1)		213	-41
1502	1587					4,63	- 12	- 169	- 1,3	27		5,7		
1123	μ Eridani	40 .5	- 3 26	B5	2 ^s .5	4,18	22	117°	Var.	10	(4)	-0,8	168	-28
1520	876				W	4,34	+ 11	+ 19	+16	10		0,9		
1139	α Camelopard	44 .1	+66 10	B0	3 ^s .0	4,38	9	55°	Var	-6	(3)	-4,1	112	+15
1542	358				W	4,56	+ 9	- 3	+ 6,0	2		-0,8		
1140	π^4 Orionis	44 .4	+ 6 47	F8	4 ^s .0	3,31	471	87°	+25,0	125	(4)	3,7	159	-21
1543	762				Y ¹	3,45	+ 438	+ 170		123		6,7		
1141	π^4 Orionis	45 .1	+ 8 44	A0	3 ^s .0	4,35	33	191°	Var	22	(1)	1,1	157	-20
1544	777				W	4,60	- 19	+ 27		22		2,0		
1148	2 Aurigae	45 .9	+36 33	K2	6 ^s .6	5,04	26	211°	-16,7	14	(1)	-0,8	134	- 3
1551	952				O ²	4,96	- 19	+ 17		14		2,1		
1147	π^4 Orionis	45 .9	+ 5 26	B3	2 ^s .5	3,78	7	214°	Var.	4	(5)	-3,2	161	-23
1552	745				W	3,98	- 0	+ 4	+23,3	4		-2,0		
1149	α^1 Orionis	46 .9	+14 5	Mn	7 ^s .6	5,19	59	180°	- 7,1	10	(a)	0,2	153	-17
1556	777				O ²	4,98	- 21	+ 55				4,1		
1153	α Eridani	48 .0	- 5 37	F0	4 ^s .6	4,43	27	315°	- 8	30	(1)	1,8	172	-27
1560	1068				Y ¹	4,59	- 6	- 26		30		1,7		
1159	π^4 Orionis	49 .0	+ 2 17	B3	2 ^s .1	3,87	4	225°	Var	5	(6)	-2,6	164	-23
1567	810				W	4,04	- 4	+ 1	+23,4	5		-3,1		
1161	7 Camelopard	49 .3	+53 35	A2	2 ^s .7	4,44	12	305°	Var	21	(2)	1,1	122	+ 8
1568	829				Y ¹	4,66	- 8	- 9	- 7,9	21		-0,2		
1163	π^1 Orionis	49 .4	+10 0	A0	3 ^s .2	4,74	145	158°	+ 4,1	17	(3)	0,9	157	-19
1570	683					4,94	0	+ 145		17		5,6		
1167	ϵ Aurigae	50 .5	+33 0	K2	6 ^s .1	2,90	28	162°	+17,5	25	(5)	-0,7	138	- 5
1577	886				Y ²	2,89	+ 1	+ 28		25		0,1		
1169	α^1 Orionis	50 .7	+13 21	K0	5 ^s .9	4,28	102	233°	+ 1,1	19	(3)	0,7	155	-16
1580	740				Y ²	4,25	- 98	+ 30		19		4,3		
1178	4 Aurigae	52 .3	+37 44	A0	2 ^s .5	4,99	115	154°	Var	32	(1)	2,5	135	- 1
1592	1005				W	5,16	+ 22	+ 113	+ 6	32		5,3		
1181	π^4 Orionis	53 .4	+ 1 33	K0	7 ^s .0	4,73	6	211°	+14,0	15	(3)	0,6	165	-23
1601	872				O ²	4,66	- 5	+ 3		15		-1,4		
1185	β Camelopard.	54 .5	+60 18	G0p	5 ^s .1	4,22	13	171°	- 1,6	5	(5)	-2,3	117	+12
1603	856				Y ²	4,24	- 1	+ 13		5		-0,2		
1187	ϵ Aurigae	54 .8	+43 41	F5p	4 ^s .3	3,31-4,08	14	159°	Var	7	(3)		132	+ 2
1605	1166				Y ²	-	+ 2	+ 14	- 1,0	7				
1189	S Eridani	55 .3	-12 41	F0	4 ^s	4,85	107	155°	-15	22	(1)	1,6	180	-29
1611	1047				Y ¹	4,99	- 22	+ 105		22		5,0		
1190	ζ Aurigae	55 .5	+40 56	K0,B1	6 ^s .6	3,94	32	160°	Var	24	(3)	-0,9	133	+ 1
1612	1142				O ²	3,90	+ 3	+ 32	+11,0	11		1,5		
1192	ψ Eridani	56 .6	- 7 20	B8	2 ^s .9	4,81	10	0°	+26,1	5	(3)	-1,7	174	-26
1617	948				W	4,98	+ 5	- 9		5		-0,2		
1194	ϵ Tauri	57 .1	+21 27	A5	3 ^s .1	4,70	82	125°	+46	16	(5)	0,4	149	-11
1620	751				W	4,90	+ 52	+ 64		14		4,3		
1193	Leporis	57 .1	-20 12	B9	2 ^s .4	4,99	41	112°	+24				187	-32
1621	990					5,16	+ 14	+ 39				3,1		

Boes 1101. Long period variable, period 345 days. — Boes 1187. Long period eclipsing binary, period 27,1 years. — Boes 1189. Probably not a variable.

4^h to 5^h.

1	2	3	4	5	6	7	8	9	10	11	12	13	14	15
198	Leporis	58 ^m .1	-26° 25'	K0	6 ^e	5 ^m .01	122	131°	+27.8				194°	-34°
628	1975				O ^a	5.00	-41	+113				5.4		
202	9 Aurigae	58.8	+51 29	I0	3 ^e .9	4.99	178	185°	-1.4	47	(3)	3.2	125	+8
637	1024				Y ¹	5.15	-55	+169		44		6.2		
203	11 Orionis	58.9	+15 16	B9	2 ^e .3	4.65	41	152°	Var	14	(1)	0.4	154	-14
638	732				W	4.95	+8	+40	+15.8	14		2.7		
204	η Aurigae	59.5	+41 6	B3	1 ^e .8	3.28	81	158°	+2	14	(5)	1.0	133	+2
641	1058				B ¹	3.48	+13	+80		14		2.8		
208	γ Caeli	0.8	-35 37	K0	6 ^e .0	4.62	128	114°	+11.0	18	(2)	0.9	206	-35
652	2089					4.64	-82	+99		18		5.1		
211	ε Leporis	1.2	-22 30	K5	6 ^e .2	3.29	72	159°	+0.9	28	(4)	0.5	191	-32
654	1000				OY ²	3.34	-39	+60		28		2.6		
218	η ² Pictoris	2.3	-49 13	K5		4.92	35	78°	+36.0	4	(a)	-2.1	223	-36
663	1662					5.02	-24	+26				2.6		
220	β Iridani	2.9	-5 13	A3	3 ^e .2	2.92	118	228°	-11	46	(6)	1.2	173	-23
666	1162				Y ¹	3.12	-113	+33		45		3.3		
225	ζ Doradus	3.8	-57 37	I8		4.76	113	337°	-2.2				233	-36
671	735					4.89	+84	+76				5.0		
227	15 Orionis	4.0	+15 28	I0	4 ^e .1	4.86	11	158°	+31.4	13	(1)	0.1	155	-13
676	752				Y ^{1.5}	5.08	+1	+11		13		0.1		
231	γ Iridani	1.4	-8 53	B2	2 ^e .6	4.31	9	160°	Var	7	(3)	-1.4	177	-25
679	1040				YG ¹	1.54	-1	+9	+3	7		-0.7		
236	μ Aurigae	6.6	+38 22	A3	3 ^e .0	4.78	76	191°	Var	40	(3)	2.5	136	+1
689	1063				Y ¹	4.99	33	+68	+26	35		4.2		
239	ι Leporis	7.7	-11 59	B8	2 ^e .7	4.54	32	116°	+25	10	(2)	-0.5	180	-20
696	1095				W	4.69	+17	+27		10		3.1		
240	ρ Orionis	8.1	+2 45	K0	6 ^e .3	4.64	15	188°	Var	19	(2)	1.0	166	-19
698	888				OY ³	4.61	-7	+13	+38.8	19		0.5		
241	μ Leporis	8.4	-16 19	A0p	3 ^e .0	3.30	49	125°	+27.7	26	(1)	0.4	184	-27
702	1072				W	3.48	+16	+47		26		1.8		
242	κ Leporis S	8.7	13 3	B8	2 ^e .8	4.46	22	236°	+27	6	(2)	-1.7	181	-26
705	1092				W	4.60	-22	+1		6		1.2		
246	α Aurigae	9.3	+45 54	G0	3 ^e .3	0.21	437	168°	+30.2	87	(4)	-0.1	130	+6
708	1077				Y ²	0.33	+9	+437		85		3.4		
250	β Orionis	9.7	-8 19	B8p	1 ^e .2	0.34	1	135°	Var	6	(2)	-5.8	176	-24
713	1063				W	0.62	0	+1	+23.6	6		-9.7		
258	16 Aurigae	11.6	+33 17	K0	6 ^e .3	4.81	189	159°	Var	20	(3)	1.2	141	-1
726	1000				O ^a	4.68	+32	+185	-29.4	19		6.2		
259	λ Aurigae	12.1	+40 4	G0	4 ^e .6	4.85	843	141°	+66.6	74	(6)	4.1	135	+3
729	1248				Y ²	4.90	+396	+742		70		9.5		
262	τ Orionis	12.8	-6 57	B5	3 ^e .1	3.68	17	246°	+18	10	(3)	-1.3	176	-23
735	1028				W	3.84	-17	0		10		-0.2		
270	ο Columbae	13.9	-35 0	K0	6 ^e .5	1.91	355	167°	+21.2	32	(2)	2.4	206	-33
743	2244					4.92	-351	-57		32		7.7		
269	φ Doradus	13.9	-67 18	K0		4.78	48	353°	Var	13	(2)	0.4	244	-34
744	401					4.90	+19	+44	+10.5	13		3.2		
277	λ Leporis	15.0	-13 17	B1	2 ^e .6	4.29	3	0°	+20.0	5	(2)	-2.2	182	-24
756	1127				W	4.45	+1	-3		5		-3.2		
281	Leporis	16.2	-21 20	A0	2 ^e .8	4.73	20	45°	+30	12	(1)	0.1	190	-28
762	1135					4.90	+20	0		12		1.2		
284	ο Orionis	16.7	-0 29	B3	2 ^e .5	4.65	5	233°	+27.9	5	(5)	-1.9	170	-18
765	930				W	4.81	-5	+2		5		-1.8		
289	m Orionis	17.6	+3 27	B3	2 ^e .5	4.99	7	180°	+18	5	(2)	-1.5	167	-17
770	871				Y ¹	5.20	-2	+7		5		-0.2		
299	ο Orionis	19.1	-7 53	K0	6 ^e .3	4.21	42	207°	-18.4	20	(1)	0.7	178	-21
784	1064				Y ³	4.24	-31	+29		20		23		

Boss 1220 Member of Ursa Major Cluster? — Boss 1216 Capella Interferometer measurements as compared with the determination of orbit on basis of variable radial velocity lead to a parallax of 0".0632 which probably is the most accurate parallax value so far determined any star

1	2	3	4	5	6	7	8	9	10	11	12	13	14	15
1301 1788	η Orionis 1235	19 ^m .4	- 2° 29'	B1	2 ^s .3 W	3 ^m .44 3.64	6 + 6	80° + 1	Var +19.5	10 9	(5)	-1.8 -2.7	172	- 1 st
1302 1789	25 Orionis 1005	19.6	+ 1 45	B3p	2 ^s .6 W	4.73 5.04	21 -14	209° + 15	+18.9	8 8	(2)	-0.7 1.3	169	- 17
1303 1790	γ Orionis 919	19.8	+ 6 16	B2	1 ^s .7 W	1.70 2.01	20 -11	200° + 17	+18.7	14 13	(6)	-0.2 -1.8	165	- 15
1304 1791	β Tauri 795	20.0	+28 31	B8	1 ^s .6 W	1.78 1.98	180 + 4	169° +180	+11	33 32	(4)	-0.7 -3.1	145	2
1315 1810	σ Tauri 847	21.6	+21 51	B3	1 ^s .8 W	4.83 5.05	17 + 8	140° + 15	+15.8	7 6	(4)	-1.3 1.0	151	- "
1314 1811	η Orionis 888	21.6	+ 3 0	B2	2 ^s .2 Y ¹	4.66 4.87	14 + 7	197° + 12	Var +12.0	4 5	(7)	-1.0 0.4	168	1 st
1323 1829	β Leporis 1096	24.0	-20 50	G0	6 ^s Y ¹	2.96 3.07	94 -50	176° + 80	-13.8	14 11	(3)	-1.8 2.8	191	2 nd
1327 1834	31 Orionis 913	24.7	- 1 11	K5	7 ^s .2 O ¹	4.97 4.93	28 + 3	159° + 28	+ 7.9			2.2	172	17
1331 1839	A Orionis 939	25.4	+ 5 52	B3	2 ^s .7 W	4.32 4.50	38 + 4	169° + 38	+15	14 14	(4)	0.1 2.2	165	- 14
1841	T Aurigae 923m	25.6	+30 2	Pec Nova	Var	4.4-14.7	3.4 - 2	209° + 2	-218 ^h	0.5	(1)	-7.1 -3.0	145	- 1
1333 1843	χ Aurigae 1024	26.2	+32 7	B1	3 ^s .5 Y ¹	4.88 5.01	17 + 4	160° 17	Var - 0.2	3 3	(2)	-2.7 1.0	143	- "
1335 1845	119 Tauri 875	26.3	+18 32	Mn	7 ^s .8 O ¹	4.73 4.63	13 + 8	132° 10	+22.3	3 3	(3)	-2.9 0.3	154	- 7
1339 1852	δ Orionis 983	26.9	- 0 22	B0	1 ^s .9	2.48 2.66	4 + 1	146° 4	Var +19.9	7 6	(7)	-3.6 -4.5	171	- 16
1340 1855	ν Orionis 1106	27.1	- 7 23	B3	2 ^s .1 W	4.64 4.81	12 - 1	166° + 12	+16.6	5 5	(4)	-1.9 0.0	178	- 19
1344 1862	ϵ Columbae 2348	27.7	-35 33	K0		3.92 3.96	56 -55	151° - 6	Var - 3.8	17 17	(2)	0.1 2.7	208	- 30
1347 1865	α Leporis 1166	28.3	-17 54	F0	3 ^s .0 Y ¹	2.69 2.87	3 + 2	18° - 2	+24.5	17 17	(4)	-1.2 -4.8	189	- 24
1353 1876	ϕ ¹ Orionis 877	29.3	+ 9 25	B0	2 ^s .5 YG	4.53 4.70	- 8 + 2	187° + 8	Var +33.2	5 4	(5)	-2.5 -1.0	163	- 11
1357 1879	λ ¹ Orionis 879	29.6	+ 9 52	Oo5	2 ^s .6 W	3.66 3.69	12 + 2	161° + 12	+33	7 7	(5)	-3.3 -1.1	162	- 11
1357 1880	λ ¹ Orionis 879	29.6	+ 9 52		2 ^s Y ¹	5.56			+35			-1.4	162	- 11
1361 1886	Orionis 1233	30.1	- 6 5	B1	2 ^s .5 B ¹	5.58	4 + 2	14° - 3	+29			-1.4	177	- 19
1362 1887	Orionis 1234	30.1	- 6 5	B1	2 ^s .3 YG ¹	4.67 4.87	7 + 5	27° - 5	+28			-9.3	177	- 19
1364 1892	ϵ ¹ Orionis 1185	30.4	- 4 54	B3	2 ^s .8 W	4.65 4.80	2 + 0	153° + 2	Var +28	5 5	(3)	-1.9 -3.9	176	- 18
1363 1893	θ ¹ Orionis 1315	30.4	- 5 27	Oo5	3 ^s .0 OR ¹	6.84	7 + 7	56° - 2	+32	3 3	(1)	-1.9	176	- 18
1363 1894	θ ¹ Orionis 1315	30.4	- 5 27		2 ^s .8 Y ¹	7.93			Var -24			-0.8	176	- 18
1363 1895	θ ¹ Orionis 1315	30.4	- 5 27			5.36			Var +23			-3.4	176	- 18
1363 1896	θ ¹ Orionis 1315	30.4	- 5 27			6.85			Var +27			-2.0	176	- 18
1366 1899	ι Orionis 794	30.5	- 5 59	Oo5	2 ^s .8 W	2.87 3.09	7 - 7	124° + 2	+21.3	5 5	(2)	-3.6 -3.6	177	- 18

Bess 1304. Also named γ Aurigae. — Bess 1327. Variable star — GJ Orionis. — Bess 1339. Has a companion 51" dist. 6m. 37" —
 Bess 1337. Leading star in an open cluster. — Bess 1361, 1362. No doubt a physical pair. — Bess 1363. The Trapezium. A multiple system
 or rather part of an open stellar cluster. Best value for the parallax seems to be 0".0018. Bess 1363 makes the total magnitude 4.96 which
 corresponds to the total magnitude of 5.18 according to Harvard determinations. The total magnitude of the actuals is 2m. 9.

5^h.

1	2	3	4	5	6	7	8	9	10	11	12	13	14	15
1370 1903	ϵ Orionis 969	31 ^m .1	- 1° 16'	B0	1 ^o .6 W	1 ^h .75 2 .03	2 - 0	180 ^o + 2	+25.4	9 8	(5)	-3.7 -6.7	173 ^o	-15 ^o
1373 1907	ϕ^* Orionis 898	31 .4	+ 9 15	K0	6 ^o .0 Y ^a	4 .39 4 .30	321 + 45	163 ^o + 318	+99.3	28 28	(4)	1.6 6.9	164	-10
1375 1910	ζ Tauri 908	31 .7	+21 5	B3p	1 ^o .9 W	3 .00 3 .24	28 - 1	174 ^o + 28	Var. +16.4	10 7	(4)	-2.8 0.2	153	- 4
1384 1922	β Doradus 487	32 .8	-62 33	F5p	6 ^o .3	3 .81 3 .94	16 + 10	330 ^o + 12	+ 7.4			-0.2	239	-32
1388 1928	125 Tauri 902	33 .5	+25 50	B3	1 ^o .5 W	5 .00 5 .33	44 + 28	135 ^o + 34	Var. +14.8	5 5	(3)	1.5 3.2	149	- 1
1389 1931	σ Orionis 1326	33 .7	- 2 39	B0	2 ^o .7 W	3 .78 3 .97	1 + 0	0 ^o - 1	Var. +28.4	3 4	(6)	-3.2 -6.2	175	-16
1391 1934	ω Orionis 1002	33 .9	+ 4 4	B3p	2 ^o .8 W	4 .54 4 .74	6 + 6	72 ^o - 1	Var. +22.0	5 5	(3)	-2.0 -1.6	168	-12
1392 1937	δ Orionis 1142	34 .0	- 7 16	A3	3 ^o .7 Y ¹	4 .88 5 .04	50 - 26	199 ^o + 42	Var.	17 17	(2)	1.0 3.4	178	-18
1396 1946	126 Tauri 841	35 .5	+16 29	B3	2 ^o .1 W	4 .87 5 .09	31 + 10	155 ^o + 29	+28:	8 7	(5)	-0.9 2.3	158	- 6
1398 1948	ζ Orionis 1338	35 .7	- 2 0	B0	1 ^o .6 W	2 .05 2 .14	11 + 7	131 ^o + 9	+19	5 6	(7)	-4.1 -2.9	174	-15
1398 1949	ζ Orionis 1338	35 .7	- 2 0		Y G ¹	4 .21			+13			-1.3 -0.6	174	-15
1399 1952	Orionis 1004	35 .8	- 1 11	B3	1 ^o .8 W	5 .00 5 .17	14 - 13	236 ^o + 5	+26.1	6 6	(3)	-1.1 0.7	173	-15
1401 1956	α Columbae 2375	36 .0	-34 8	B5p	3 ^o .5	2 .75 2 .96	35 - 32	173 ^o - 15	+39	25 24	(2)	-0.4 0.5	206	-28
1419 1982	γ Leporis 1210	40 .3	-22 27	G5	6 ^o .2 O ^a	6 .41	451 -365	218 ^o +275	- 9.2				195	-23
1420 1983	γ Leporis 1211	40 .3	-22 29	F8	4 ^o .6 Y ^a	3 .80 3 .90	468 -412	216 ^o +220	- 9.2	118 115	(3)	4.1 7.2	195	-23
1429 1995	τ Aurigae 1418	42 .3	+39 9	K0	5 ^o .0 Y ^a	4 .64 4 .64	35 - 26	223 ^o + 24	-19.5	14 14	(5)	0.4 -2.4	139	+ 7
1432 1998	ζ Leporis 1232	42 .4	-14 52	A2	3 ^o .4 Y G ¹	3 .67 3 .84	17 - 16	277 ^o - 6	+13	46 46	(1)	2.0 -0.1	187	-20
1434 2002	132 Tauri 970	42 .9	+24 32	K0	6 ^o .0 Y ^a	5 .02 5 .00	36 + 1	174 ^o + 36	+15.0	27 26	(3)	2.1 2.8	152	0
1435 2004	κ Orionis 1235	43 .0	- 9 42	B0	2 ^o .5 W	2 .20 2 .44	6 + 2	149 ^o + 6	+21.7	12 10	(5)	-2.8 -3.8	182	-17
1438 2010	134 Tauri 912	43 .9	+12 37	B9	2 ^o .3 Y ¹	4 .92 5 .11	29 - 15	207 ^o + 25	+22.0	10 10	(2)	-0.1 2.2	162	- 6
1439 2011	ν Aurigae 1336	44 .2	+37 16	Ma	6 ^o .9 O Y ⁰	4 .99 4 .90	52 + 33	137 ^o + 40	+37.9	10 10	(3)	0.0 3.6	141	+ 6
1442 2012	π Aurigae 1429	44 .6	+39 7	K0	5 ^o .0 Y ^a	4 .18 4 .18	8 - 5	320 ^o - 6	+ 9.9	18 17	(6)	0.3 -1.3	139	+ 7
1443 2015	δ Doradus 496	44 .6	-65 46	A5		4 .52 4 .62	39 + 38	285 ^o + 7	- 3:			2.5	243	-31
1446 2020	β Pictoris 1620	44 .9	-51 6	A3		3 .94 4 .07	90 + 6	4 ^o + 90	+28:	58	(a)	2.7 3.7	225	-30
1453 2029	ξ Aurigae 1027	46 .5	+55 41	A2	2 ^o .9 W	4 .92 5 .14	14 - 7	326 ^o - 12	-12	10 9	(4)	-0.3 0.7	124	+16
1457 2034	136 Tauri 899	47 .0	+27 35	A0	2 ^o .3 Y ¹	4 .54 4 .76	22 + 11	146 ^o + 19	Var. -16.1	14 14	(2)	0.3 1.3	149	+ 2
1456 2035	δ Leporis 1211	47 .0	-20 53	K0	6 ^o Y ^a	3 .90 3 .92	696 + 63	160 ^o +696	+99.6	66 55	(7)	2.6 8.1	193	-21
1458 2037	56 Orionis 1151	47 .3	+ 1 50	K0	6 ^o .2 Y ^a	5 .01 4 .99	11 - 1	180 ^o + 11	+10.3	6 6	(1)	-1.0 0.2	172	-10

Boss 1384. Cepheid variable 4^m.2 to 5^m.6; period 9.8 days. — Boss 1398; H.R. 1948, 1949. A visual binary, 2^o.5. — Boss 1419, 1420. A wide pair 95", 350".

B¹.

1	2	3	4	5	6	7	8	9	10	11	12	13	14	15
1459 2040	β Columbae 2546	47 ^m .4	-35° 48'	K0	4 ^s .3	3 ^m .22 3.30	397 +131	7° +377	+89.1	29 29	(3)	0.5 6.2	209°	-26°
1460 2042	γ Pictoris 946	48.0	-56 12	K0		4.38 4.50	96 -75	135° -60	+17.0	17 17	(2)	0.5 4.3	231	-30
1461 2047	z^1 Orionis 1162	48.5	+20 16	F8	5 ^s .0 Y ^a	4.62 4.69	208 -189	243° +85	-14.1	87 89	(5)	4.2 6.2	156	-1
1462 2049	Pictoris 794	48.7	-52 8	K0		4.98 5.08	90 -11	179° -89	+1.2			4.8	227	-29
1467 2056	λ Columbae 2599	49.5	-33 50	B5		4.89 5.04	28 +15	2° +24	+30	14 14	(1)	0.6 2.1	207	-25
1468 2061	α Orionis 1055	49.8	+7 23	Ma	6 ^s .5 O ^b	0.92 1.00	29 +28	74° -6	+20.8	12 12	(5)	-3.7 -1.8	168	-8
1472 2077	δ Aurigae 970	51.3	+54 17	K0	5 ^s .5 Y ^a	3.88 3.91	153 +83	145° +129	+7.7	25 23	(4)	0.7 4.8	127	+16
1475 2084	139 Tauri 1052	51.8	+25 57	B2	2 ^s .8 Y ¹	4.90 5.07	4 -2	194° +3	+8.5	3 3	(5)	-2.7 -2.1	152	+2
1476 2085	η Leporis 1286	51.9	-14 11	F0	4 ^s .0 Y ¹	3.77 3.90	138 -29	343° -135	-1.6	49 48	(3)	2.2 4.5	187	-17
1478 2088	β Aurigae 1328	52.2	+44 56	A0p	1 ^s .9 W	2.07 2.26	47 -47	264° +4	-18.7	41 38	(6)	0.0 0.4	135	+12
1479 2091	α Aurigae 1217	52.5	+45 56	Ma	7 ^s .1 O ^b	4.59 4.47	11 +8	135° +8	+0.9	6 6	(3)	-1.5 -0.2	134	-12
1482 2095	ϕ Aurigae 1380	52.9	+37 12	A0p	1 ^s .9 W	2.71 2.90	105 +52	149° +91	+29	34 32	(6)	0.2 2.8	142	+8
1486 2102	Doradus 498	53.4	-63 8	K0		4.53 4.64	562 -118	14° +551	+24.7	21 21	(1)	1.1 8.3	239	-30
1490 2106	γ Columbae 2612	54.0	-35 18	B3		4.36 4.51	4 +4	297° +1	+24.2	7 7	(1)	1.4 -2.6	208	-25
1494 2113	Orionis 1256	55.1	-3 5	K0	5 ^s .5 Y ^a	4.68 4.67	84 +13	169° +83	+25.9	27 28	(2)	1.9 4.3	177	-11
1497 2120	η Columbae 2266	56.1	-42 49	K0		4.03 4.08	33 -23	140° -23	+17.9	13 13	(2)	-0.4 1.6	217	-26
1501 2124	μ Orionis 1064	56.9	+9 39	A2	3 ^s .6 W	4.19 4.37	34 +18	148° +29	+42	33 32	(3)	1.7 1.8	166	-5
1503 2128	3 Monocerotis 1349	57.1	-10 36	B8	2 ^s .1 W	4.97 5.14	6 +1	9° -6	Var +39	6 6	(2)	-1.1 -1.0	185	-15
1508 2134	ι Geminorum 1170	58.0	+23 16	G5	5 ^s .4 Y ^a	4.30 4.35	108 -8	184° +108	Var +20	32 31	(5)	1.8 4.5	155	+2
1507 2135	z^2 Orionis 1233	58.0	+20 8	B2p	4 ^s .3 Y ¹	4.71 4.86	15 +8	148° +13	Var +18	6 6	(3)	-1.4 0.6	157	0
1522 2155	ϕ Leporis 1331	1.6	-14 56	A0	2 ^s .6 Y ¹	4.67 4.84	24 -8	343° -23	+32	19 19	(1)	1.1 1.6	189	-15
1525 2159	ν Orionis 1152	1.9	+14 47	B2	2 ^s .5 W	4.40 4.60	37 +10	166° +36	Var. +22.1	7 7	(3)	-1.4 2.2	163	-1
1550 2198	π^1 Orionis 1035	6.2	+16 9	B3	2 ^s .4 W	4.92 5.15	24 +7	165° +23	Var. +28	8 8	(2)	-0.6 1.8	162	0
1548 2199	ξ Orionis 1187	6.3	+14 14	B3	2 ^s .5 W	4.35 4.56	35 +10	165° +34	+24.1	9 9	(3)	-0.9 2.1	163	-1
1556 2209	Camelopardalis 371	7.8	+69 21	A0	2 ^s .5 Y ¹	4.73 4.94	109 +15	174° +108	Var.	13 13	(1)	0.3 4.9	113	+23
1558 2212	δ Pictoris 980	8.4	-54 56	B1		4.84 4.94	24 +23	250° -6	Var.			1.7	230	-27
1561 2216	η Geminorum 1241	8.8	+22 32	Ma	6 ^s .9 OY ^a	Var 3.3-4.2	63 -62	255° +21	+19.4	13 12	(4)	-1.1 2.4	156	+4
1565 2219	κ Aurigae 1154	9.0	+29 33	K0	5 ^s .5 Y ^a	4.45 4.47	274 -58	194° +269	+20.5	18 18	(5)	0.7 6.6	150	+7

Boes 1468. Betelgeuse. Variable; 0m.00-0m.80. The variations in the light seem to be correlated with the variations in the diameter as derived on basis of interferometer measurements. On basis of that assumption a pulsation parallax of 0".007 has been derived. — Boes 1478. Member of Ursa Major Cluster. Halfpacing binary — Boes 1561. Long period variable. Period 231.4 days.

6^h.

1	2	3	4	5	6	7	8	9	10	11	12	13	14	15
1570	γ Monocerotis	10 ^m .0	- 6° 1'	K0	6 ^s .5 Y ^a	4 ^m .09 4 .14	21 - 2 + 21	191° - 21	- 5.2	16 16	(2)	0.1 0.7	182°	-10°
2227	1469													
1575	2 Lynx	10 .8	+59 3	A0	2 ^s .1 W	4 .42 4 .63	22 - 6 - 21	347° - 21	- 4	24 21	(4)	1.3 1.1	123	+20
2238	959													
1580	Canis maj	11 .1	-13 41	B9	2 ^s .1 W	4 .99 5 15	7 + 7 - 0	98° - 0	+33			-0.7	189	-13
2244	1411													
1579	η^a Doradus	11 .1	-65 34	Mb		4 .88	112	316°	+34.5	6	(a)	-1.0	243	-28
2245	561					1 .99	+ 18	111°				5.1		
1587	κ Columbae	13 .0	-35 6	K0		4 .51	76	353°	+24.5	13	(2)	0.1	210	-21
2256	2800					4 .53	- 36	66		13		5.1		
1601	ζ Canis maj	16 .5	- 30 1	B3	3 ^s .0 W	3 .10 3 .30	8 + 11 - 8	83° - 8	+34	6	(1)	-3.0	205	-18
2282	3038									6		-2.4		
1604	μ Gemmorum	16 .9	+22 34	Ma	6 ^s .6 Y ^a	3 .19 3 .13	128 + 72	151° +106	+54.4	16 16	(5)	-0.8 3.7	157	+ 6
2286	1304													
1609	β Canis maj	18 .3	-17 51	B1	2 ^s .1 W	1 .99 2 .21	7 - 7 + 2	270° - 2	Var	10	(5)	-3.0 -3.6	193	-13
2294	1467									10		-3.6		
1610	δ Columbae	18 .4	-33 23	G5		3 .98	65	216°	- 2.4	22	(1)	0.7 8.1	208	-19
2296	2927					4 .05	+ 61	6		22				
1611	8 Monocerotis	18 .5	+ 4 39		4 ^s .0 Y ¹	4 .48	12	256°	+16.6	19	(2)	0.9	173	- 3
2298	1236			A5		4 .54	- 11	+ 4		19		-0.1		
1611	8 Monocerotis	18 .5	+ 4 39		Y ¹	6 .54			+15.8				173	- 3
2299	1236													
	BL Orionis	19 .8	+14 17	N6		4.7-6.6	20	120°					164	- 3
2308	1283						+ 18	8						
1622	α Canis maj	21 .7	-52 38	F0		-0 .86	18	56°	+20.7	21	(2)	-5.1	229	-25
2326	914					-0 .67	17	+ 6		14		-2.8		
1629	RI Aurigae	22 .1	+30 33	G0		Var	24	195°	+21.4	3	(1)		150	+10
2332	1238					5.24-5.97	- 4	21		3				
1635	ν Gemmorum	23 .0	+20 17	B5	2 ^s .9 W	4 .06 4 .32	22 - 6	201° - 21	+38.4	10 10	(3)	-0.9 0.8	160	+ 6
2343	1441													
1634	10 Monocerotis	23 .0	- 4 42	B3	2 ^s .3 W	4 .98 5 .18	14 - 5	348° - 13	+21	5 5	(2)	-1.5 0.7	183	- 6
2344	1526											0.1	184	- 7
1639	11 ¹ Monocerotis	24 .0	- 6 58		3 ^s .0 Y ¹	4 .73	37 - 36	270° + 8	+20	12 12	(2)	0.1 2.5	184	- 7
2356	1574			B2p		5 .22	37	273°	+20			0.6	184	- 7
1640	11 ^a Monocerotis	24 .0	- 6 58		W		- 36	+ 6				3.0		
2357	1574											1.0	184	- 7
1640	11 ^a Monocerotis	24 .0	- 6 58		W	5 .60			+23			3.4		
2358	1574													
1641	λ Canis maj	24 .5	-32 31	B5		4 .48	32	300°	+40	13	(1)	0.1	209	-18
2361	3066					4 .64	8	31		13		2.0		
1657	13 Monocerotis	27 .5	+ 7 24	A0p	3 ^s .1 W	4 .50	10	163°	+11.6	13	(1)	0.1	172	+ 1
2385	1337					4 .70	+ 4	9		13		-0.5		
1660	ξ^1 Canis maj	27 .0	-23 21	B1	3 Y ¹	4 .35 4 .51	8 + 6	83° - 6	Var	6 6	(1)	-1.8 -1.2	199	-13
2387	3991													
1682	ξ^2 Canis maj	30 .9	-22 53	A0	2 Y ¹	4 .54 4 .70	14 - 4	25° - 13	+35	25 25	(1)	0.2	200	-12
2414	1458													
1690	γ Gemmorum	31 .9	+16 29	A0	1 ^s .9 W	1 .93 2 .25	65 + 52	136° +39	-11.3	54 54	(4)	0.6 1.0	165	+ 6
2421	1223													
1695	ν^2 Canis maj	32 .3	-19 10	K0	5 ^s .4 Y ^a	4 .14 4 .16	97 + 94	136° + 23	+ 2.5	59	(a)	3.0 1.1	196	-10
2429	1502													
1696	N Carinae	32 .8	-52 53	A0		4 .44	17	237°	+23			0.5	229	-23
2435	953					4 .55	+ 16	- 4						
1698	ν^3 Canis maj	33 .5	-18 9	K0	5 ^s .1 OY ^a	4 .65 4 .63	16 - 9	243° + 13	- 1.5			0.6	195	-10
2443	1492											-0.7		
	Pictoris	34 .2	-62 33	Nova	Var	1.0-12.75	45	245		2	(1)	-7.5	240	-25
1703	Canis maj	34 .7	-14 3	K0	6 ^s .5 OY ^a	4 .97 4 .96	11 + 6	175° + 10	+29.1	-21	(a)	-	192	- 7
2450	1525											0.2		

Boss 1611 Probably binary. — Boss 1629 Has been included because its maximum magnitude may fall very close to the limit 5.0 —
 Boss 1639—40 A triple system, the total magnitude of which is 3^m.91 in the Harvard system and 3^m.14 in Zinner's system

64.

1	2	3	4	5	6	7	8	9	10	11	12	13	14	15
1702 2451	* Puppis 2576	34 ^m .7	-43° 6'	B8		3 ^m .18 3.39	+ 20 + 10	177° 17	+28	25 25	(1)	0.2 -0.3	219° + 4	-19°
1706 2456	S Monocerotis 1880	35 .5	+ 9 59	Oe 5	2 ^m .5 (¹)	4.68 4.87	+ 9 + 7	138° 6	+28.8	6 4	(5)	-2.3 -0.8	171 + 4	
1711 2462	Puppis 2417	36 .0	-48 8	K0		5.00 5.10	+ 14 + 7	304° 12	+27.7			0.7	224	-21
1716 2470	12 Lynceis 1015	37 .4	+59 33	A2	2 ^m .5 W	4.89 5.05	- 15 + 1	274° 1	+ 7	24 24	(2)	1.8 1.8	123 +24	
2472	Gemlnorum —	37 .8	+30 2	Pec Nova	Var	5.0-16.3	- 7 + 2	240° 2				-0.8	153	+13
1717 2473	* Gemlnorum 1406	37 .8	+25 14	G5	5 ^m .9 Y ⁸	3.18 3.22	+ 20 + 3	180° 20	+ 9.6	10 10	(4)	-1.8 -0.3	157 +11	
1721 2478	30 Gemlnorum 1390	38 .1	+33 20	K0	6 ^m .1 Y ⁸	4.65 4.59	+ 76 + 18	178° 74	+13.0	19 19	(1)	1.1 4.0	168 + 5	
1725 2484	5 Gemlnorum 1396	39 .7	+13 0	F5	3 ^m .9 Y ¹	3.40 3.57	- 231 + 72	210° 219	+ 24	49 48	(5)	1.8 5.2	168 + 6	
1732 2491	* Canis maj 1591	40 .7	-16 35	A0	0 ^m .7 W	-1.58 -1.30	+1316 +184	204° 1303	- 7.5	375 355	(7)	1.1 7.2	195 - 8	
1737 2503	17 Monocerotis 1496	41 .9	+ 8 9	K0		5.00	- 20 + 15	232° 13	+47	12	(a)	0.4 1.5	173 + 3	
1740 2506	18 Monocerotis 1397	42 .6	+ 2 31	K0	6 ^m .1 Y ⁸	4.70 4.65	+ 26 + 2	193° 26	+11	15 15	(4)	0.6 1.8	178 + 2	
1758 2527	Camelopard 266	45 .5	+77 6	K5	6 ^m .4 OY ⁰	4.75 4.72	+ 85 + 85	100° 0	-29.4	15 15	(2)	0.6 4.4	105 +27	
1761 2538	* Canis maj 3404	46 .1	-32 23	B2p		3.78 3.95	+ 10 + 0	276° 10	+14	7 7	(1)	-2.0 -1.2	209 -14	
1763 2540	8 Gemlnorum 1481	46 .2	+34 5	A2	2 ^m .5 W	3.64 3.83	+ 54 + 16	174° 52	+14	24 24	(3)	0.5 2.3	150 +16	
1769 2550	* Pictoris 720	47 .2	-61 50	A5	4 ^m .0	3.30 3.44	- 272 - 14	343° 272	+21			5.5	239	-24
1772 2553	* Puppis 2415	47 .5	-50 30	K0		2.83 3.04	+ 90 + 22	164° 87	+36	31 31	(3)	0.3 2.6	228 -20	
1773 2554	A Caninae 1168	47 .6	-53 31	G5		4.38 4.50	+ 25 - 13	5° 21	+26.0	15 15	(1)	0.3 1.4	231 -21	
	Gemlnorum	48 .4	+32 16	Pec Nova	Var	3.7-14.5	- 21 + 12	225° 18				0.3	150	+13
1776 2560	15 Lynceis 982	48 .6	+58 33	G0	5 ^m .4 Y ⁸	4.54 4.58	+ 134 + 29	178° 130	+ 8.6	15 14	(5)	0.3 5.2	124 +25	
1778 2564	0 Gemlnorum 1462	49 .0	+13 18	F0	4 ^m .0 Y ^{1.5}	4.70 4.81	+ 112 + 93	139° 63	+21	40 38	(6)	2.6 4.9	169 + 8	
1781 2571	15 Canis maj 1616	49 .2	-20 6	B1	3 ^m W	4.66 4.73	- 8 - 3	23° 8	+30	5 5	(2)	-1.9 -0.8	199 - 8	
1783 2574	8 Canis maj 1681	49 .5	-11 55	K2	6 ^m .6 OY ⁸	4.25 4.22	- 138 - 112	264° 81	+96.5	21 21	(3)	0.9 5.0	192 - 4	
1785 2580	0 ¹ Canis maj 4567	49 .9	-24 4	K2p	6 ^m .7 OY ⁸	4.12 4.11	- 14 - 13	306° 5	+36.8	2 2	(a)	-3.9 -0.1	202 - 9	
1786 2585	ψ ¹⁰ Aurigae 1367	50 .4	+45 14	A2	2 ^m .4 W	4.80 5.07	- 25 - 24	265° 7	-22	22 22	(1)	1.5 1.8	139 +21	
1789 2590	* Canis maj 1610	51 .3	-20 1	F5	4 ^m Y ¹⁰	4.62 4.71	+ 67 + 14	57° 66	+ 8			3.8	199	- 7
1793 2596	* Canis maj 1661	51 .7	-16 55	B5	2 ^m .8 Y ¹	4.39 4.58	- 11 - 7	355° 8	+40.6	7 7	(1)	-1.4 -0.4	196 - 5	
1800 2608	Puppis 2601	53 .6	-48 35	Ma		4.88 4.99	+ 9 + 4	297° 8	+22.1			-0.3	226	-19
1804 2618	* Canis maj 3666	54 .7	-28 50	B1	2 ^m .3 G ¹	1.63 1.91	+ 1 + 1	135° 1	+28.3	8 8	(3)	-3.9 -8.4	208 -10	
1810 2646	* Canis maj 3544	57 .7	-27 47	K5	7 ^m OR ⁸	3.68 3.73	- 11 + 4	275° 10	+21.8	11 10	(2)	-1.3 -1.1	207 -10	
1812 2648	19 Monocerotis 1788	57 .9	- 4 6	B3	2 ^m .3 W	4.89 5.11	- 8 - 4	353° 7	+23	5 5	(2)	-1.6 -0.6	185 + 2	

From 1705. Uncertain if variable. Leading star in an open cluster — From 1786. Also named 16 Lynceis.

6^h to 7^h.

1	2	3	4	5	6	7	8	9	10	11	12	13	14	15
1815 2650	ζ Gemmorum 1687	58 ^m .2	1 20° 43'	Crp	4 ^o .6 Y ²	3 ^m .6 - 4 ^m .5 3.7 - 4.3	15 0	196° + 15	+ 6.7	4 3	(2)		163°	+ 13°
1817 2653	α^2 Canis maj 4797	58 .8	- 23 11	B5p	3 ^o YCr ¹	3 .12 3 .31	9 + 1	229° + 9	+ 48.4	6 6	(2)	- 9.0 - 2.1	204	- 7
1819 2657	γ Canis maj 1625	59 .2	- 15 29	B5	2 ^o .8 W	4 .07 4 .23	14 + 8	184° + 11	+ 27.6	8 8	(2)	- 1.4 - 0.2	196	- 3
1839 2693	δ Canis maj 3916	4 .3	- 26 14	B8p	5 ^o Y ²	1 .98 2 .11	5 - 3	292° + 4	+ 31.5	10 10	(2)	- 3.0 - 4.5	206	- 7
1841 2696	β Aurigae 1882	4 .8	1 39 29	K2	6 ^o .6 O ²	5 .07 4 .98	48 + 47	94° - 9	- 27.0	15 15	(1)	1.0 3.1	146	+ 22
1840 2697	τ Gemmorum 1439	4 .8	+ 30 25	K0	6 ^o .3 Y ¹	4 .48 4 .50	53 - 11	208° + 52	+ 22.1	18 18	(3)	+ 0.8 3.1	155	+ 18
1844 2701	20 Monocerotis 1810	5 .2	- 4 5	K0	5 ^o .0 Y ²	5 .02 4 .96	217 - 102	0° - 191	+ 78.5			5.7	186	+ 3
1845 2702	Λ Puppis 3105	5 .5	39 29	B3		4 .85 5 .01	13 + 3	283° + 13	+ 19.5	22 22	(1)	1.6 0.1	218	- 13
1853 2714	δ Monocerotis 1636	6 .8	- 0 20	A0	3 ^o .0 W	1 .09 4 .25	11 - 2	15° - 11	+ 14	19 19	(2)	0.5 - 0.7	184	+ 6
1866 2735	γ^1 Volantis 600	9 .6	- 70 20	G0		5 .81 5 .98	90 - 30	15° - 85	Var - 3			3.3 5.8	248	- 24
1867 2736	γ^2 Volantis 600	9 .6	- 70 20	K0		3 .87 4 .01	97 - 61	15° + 76	+ 2.7	31 31	(2)	+ 1.3 3.8	248	- 24
1869 2740	ι Puppis 2977	9 .7	46 35	B0		4 .47 4 .62	172 + 29	302° + 169	- 14			5.7	225	- 16
1872 2745	27 Canis maj 4057	10 .2	26 10	B5p	2 ^o W	4 .66 4 .82	9 - 8	311° + 11	Var + 25	8 8	(1)	- 0.9 - 0.5	206	- 6°
1875 2748	ι^2 Puppis 3227	10 .5	- 44 29	Md		Var 3.3 - 5.2	332 - 159	18° + 293	+ 53.0			5.9	223	- 14
1877 2749	ω Canis maj 4073	10 .7	26 35	B3p	3 ^o W	3 .83 4 .01	9 + 6	207° + 7	+ 29	5 5	(1)	2.7 - 1.4	208	- 6
1879 2751	ι Lynx 1612	10 .9	149 38	A2	1 ^o .8 W	4 .80 5 .09	9 - 3	212° + 9	- 8	11 11	(1)	0.0 - 0.4	135	+ 26
1884 2762	ι Puppis 2807	11 .9	- 48 6	B8		4 .88 4 .98	16 - 16	38° + 2	+ 14			0.9	227	- 15
1886 2763	ζ Gemmorum 1443	12 .3	+ 16 43	A2	3 ^o .0 YCr ¹	3 .65 3 .81	68 - 29	225° + 62	Var 13.8	37 37	(4)	1.5 2.8	168	+ 15
1888 2764	Canis maj 5189	12 .4	- 23 8	K5		4 .82 4 .77	61 - 59	314° + 18	+ 27.9	4 4	(a)	- 2.2 3.8	201	- 4
1889 2766	Canis maj 3852	12 .6	- 27 42	Mb	7 ^o O ¹	1 .77 4 .76	45 - 44	333° + 9	+ 10.6	10 10	(1)	0.2 3.0	208	- 6
1896 2773	π Puppis 3489	13 .6	36 55	K5	6 ^o .3	2 .74 2 .85	8 + 4	256° + 7	+ 15.5	17 14	(2)	- 1.5 - 2.8	216	- 11
1898 2777	δ Gemmorum 1615	14 .2	+ 22 10	F0	3 ^o .7 Y ¹	3 .51 3 .67	25 + 11	227° + 22	Var - 2	49 48	(5)	1.9 0.5	164	+ 18
1899 2781	29 Canis maj 5173	14 .5	- 24 23	Oe	2 ^o Y ²	4 .90 5 .08	12 - 7	213° + 9	- 12.1	5 5	(2)	- 1.6 0.3	205	- 5
1901 2782	τ Canis maj 5176	14 .5	- 24 47	Oe5	3 ^o Y ¹	4 .40 4 .58	8 - 6	330° + 6	Var + 40.4	8 8	(1)	- 1.1 - 1.1	206	- 5
1907 2787	ν^1 Puppis 3512	14 .8	- 36 33	B3		4 .68 4 .83	15 + 15	208° + 4	+ 19	11 11	(1)	- 0.1 0.6	217	- 10
1917 2803	δ Volantis 730	16 .9	- 67 46	F5		4 .02 4 .15	21 + 21	253° + 4	+ 22.6			0.6	246	- 23
1924 2812	Canis maj 1806	17 .8	- 18 50	B8		4 .87 5 .07	8 - 1	210° + 8	+ 26	7 7	(2)	- 0.9 - 0.6	201	- 1
1928 2818	21 Lynx 1623	19 .2	+ 49 25	A0	2 ^o .6 W	4 .45 4 .71	49 + 8	187° + 48	+ 25.9	18 18	(3)	0.7 2.9	137	+ 27

Boss 1815 Cepheid variable 3^m.7 to 4^m.3, period 10.2 days. This star has often been considered as prototype for a certain class of Cepheids but there seems to be few if any reasons nowadays to divide the Cepheids according to the shape of their light curve. — Boss 1839 A complex system

7b.

1	2	3	4	5	6	7	8	9	10	11	12	13	14	15
1931 2821	ϵ Geminorum 1385	19 ^m ,5	+28° 0'	K0	5 ^s ,3 Y ²	3 ^m ,89 3,93	145 - 77	232 ^a + 123	+ 8,0	23 23	(3)	0,7 4,7	158 ^a	+21 ^a
1934 2827	η Canis maj 4328	20,1	-29 6	B5p	4 ^s Y ¹	2,43 2,65	10 - 6	294 ^a + 8	+39	7 7	(1)	-3,3 -2,6	210	- 5
1944 2845	β Canis min 1774	21,7	+ 8 29	B8	2 ^s ,2 W	3,09 3,25	66 - 26	229 ^a + 61	Var +23	24 24	(4)	0,0 2,2	178	+13
1952 2852	α Geminorum 1802	22,7	+31 59	F0	3 ^s ,7 Y ¹	4,18 4,36	236 + 78	39 ^a - 224	- 4	40 39	(6)	2,1 6,0	155	+23
1953 2854	γ Canis min 1660	22,8	+ 9 8	K0	6 ^s ,6 O ¹	4,60 4,44	65 - 62	277 ^a + 21	Var +47	12 11	(2)	-0,2 3,7	177	+14
1962 2864	δ Canis min 1567	24,2	+12 13	K0	6 ^s ,2 Y ²	4,85 4,79	19 + 11	171 ^a + 16	-15,4	13 13	(4)	0,4 1,2	174	+15
1968 2874	Puppla 1897	25,6	-22 49	A3		4,80 4,96	11 + 3	80 ^a - 10	+36,9	28 28	(1)	2,0 0,0	205	- 2
1972 2878	σ Puppla 3260	26,1	-43 6	K5		3,27 3,38	191 - 130	139 ^a + 139	+87,3	23 22	(3)	0,0 4,7	223	-11
1973 2881	Puppla 4620	26,9	-30 45	G0		4,77 4,87	35 - 7	277 ^a + 34	+14,4				213	- 5
1979 2890	α Geminorum 1581	28,2	+32 6	A0	5 ^s G ¹	2,85 3,08	203 - 120	237 ^a + 164	- 1,2	79 78	(3)	2,3 3,1	155	+24
1979 2890	α Geminorum 1581	28,2	+32 6		1 ^s ,9 W	1,99 1,81	203 - 120	237 ^a + 164	+ 6,0	107 100	(3)	2,0 3,1	155	+24
1987 2905	τ Geminorum 1424	29,8	+27 7	K5	6 ^s ,5 O ¹	4,22 4,19	119 + 20	192 ^a + 117	-20,9	16 14	(5)	-0,1 4,6	160	+22
1988 2906	Puppla 2607	29,8	-22 5	F8		4,52 4,61	81 - 71	304 ^a + 38	+60,9				205	± 0
1994 2922	p Puppla 4566	31,4	-28 9	B8	4 ^s YG ¹	4,55 4,71	74 + 10	249 ^a + 73	+13				211	- 2
2001 2930	σ Geminorum 1649	32,6	+34 49	F0	3 ^s ,4 Y ¹	4,92 5,08	125 + 20	192 ^a + 124	+ 8	20 20	(5)	1,4 5,4	152	+26
2003 2934	Q Carinae 1231	33,2	-52 19	K5		4,92 5,03	25 + 7	148 ^a - 24	+61,1				232	-14
2004 2937	f Puppla 3755	33,6	-34 44	B8		4,62 4,77	39 - 11	291 ^a + 37	+24	13 13	(2)	0,2 2,6	217	- 6
2008 2943	α Canis min 1739	34,1	+ 5 29	F5	2 ^s ,7 Y ¹	0,48 0,64	1242 - 62	214 ^a + 1242	- 3	317 320	(5)	3,0 5,9	182	+14
2009 2944	m Puppla 4828	34,1	-25 8	B8	4 ^s -3 ^s Y ¹	4,64 4,80	16 + 3	240 ^a + 16	+41	6 6	(1)	-1,5 0,6	208	- 1
2010 2946	24 Lyncei 1103	34,5	+58 57	A2	2 ^s ,7 W	4,96 5,17	68 - 6	206 ^a + 68	+ 5	16 16	(2)	1,0 4,1	125	+30
2011 2948	n ¹ Puppla 4707	34,7	-26 34	B8	- Y ¹	4,50 4,71	26 - 26	335 ^a + 4	+23,6	10 10	(2)	-0,5 1,6	210	- 1
2012 2949	n ² Puppla 4707	34,7	-26 34	B3	- Y	4,62 4,83	32 - 22	296 ^a + 23	+33	12 12	(2)	0,0 2,1	210	- 1
2017 2961	d ¹ Puppla 3531	36,0	-38 4	B3		4,91 5,08	23 + 11	255 ^a + 20	+26	22 22	(1)	1,6 1,7	220	- 7
2021 2970	α Monocerotis 2172	36,5	- 9 19	K0	6 ^s ,2 Y ²	4,07 4,10	79 - 38	252 ^a + 69	+11,3	17 17	(2)	0,2 3,6	195	+ 8
2023 2973	σ Geminorum 1590	37,0	+29 7	K0	6 ^s ,1 OY ¹	4,26 4,32	247 + 156	164 ^a + 193	Var +45,8	33 32	(4)	1,8 6,2	159	+24
2029 2985	π Geminorum 1759	38,4	+24 38	G5	4 ^s ,7 Y ¹	3,68 3,74	66 + 6	206 ^a + 26	+20,4	25 25	(7)	0,5 2,8	163	+23
2031 2990	β Geminorum 1463	39,2	+28 16	K0	4 ^s ,4 Y ²	1,21 1,34	625 - 544	264 ^a + 312	+ 3,6	123 120	(5)	1,6 5,2	160	+25
2032 2997	i Puppla 4767	39,5	-28 10	K5	7 ^s OR ¹	4,10 4,16	14 - 13	330 ^a + 4	+31,7				212	- 1

1979. Complex system consisting of at least six members. The bright stars α^1 and α^2 are spectroscopic binaries of periods 2,9 and 2,0 days respectively. Component C is a star of 9^m at 73" distance which shares the p.m. of the bright stars and which itself is a spectroscopic binary. Furthermore a seventh member of the system close to H.R. 2890 has been suspected from perturbations in the visual orbit. — Binary 10", 318^a

7^h to 8^h.

1	2	3	4	5	6	7	8	9	10	11	12	13	14	15
2035	1 ^a Puppis	39 ^m .8	-28° 43'	A2p	4 ^c	1 ^m .10	10	197°	Var				212°	- 2°
2996	4774				Y ¹	4.26	+ 9	+ 5	+23.6			- 0.9		
2040	g Geminorum	40.3	+18 45	K2	6 ^o .5	5.02	97	225°	Var	11	(1)	0.2	169	+22
3003	1733				O ²	4.99	- 30	+ 92	+80.4	11		5.0		
	Puppis	41.5	-37 39	B3		6.45			+21.0				220	- 6
3016	3861													
2052	c Puppis	41.7	-37 44	K5		3.72	26	252°	+18.3				220	- 6
3017	3863					3.80	+ 12	+ 23				0.8		
2056	ζ Volantis	43.0	-72 22	K0		3.89	9	78°	+48.7	32	(2)	1.4	251	-22
3024	627					4.04	- 8	- 3		32		- 1.3		
2061	o Puppis	43.9	-25 42	B2	5°	1.59	11	240°	only	6	(1)	-1.5	210	+ 1
3034	5081				X G ¹	4.78	+ 3	+ 11	E lines	6		5.1		
2065	ξ Puppis	45.1	-24 37	G0p	6 ^o .7	3.47	7	278°	+ 3.9	3	(2)	-4.1	209	+ 1
3045	6030				Y ³	3.57	- 3	6		3		-2.2		
2067	Q Puppis	45.3	-46 50	K0		4.64	128	228°	- 0.5	20	(1)	1.1	228	-10
3046	3451					4.80	+ 122	+ 42		20		5.2		
2070	P Puppis	46.2	-16 8	B0		4.25	11	231°	+24.0	8	(1)	-1.2	227	-10
3055	3458					4.30	+ 13	+ 6		8		0.0		
2078	η Geminorum	47.4	+27 1	A2	2 ^o .5	4.99	47	218°	Var	17	(2)	1.1	162	+26
3067	1499				Y ¹	5.21	- 10	+ 46	+ 3	17		3.3		
2087	a Puppis	48.8	-40 19	G5		3.76	- 20	216°	Var	21	(1)	0.4	223	- 6
3080	3579					3.86	+ 13	+ 16	+24.5	21		0.3		
2089	b Puppis	49.1	-38 36	B3		4.53	16	210°	Var	9	(1)	-0.7	222y	- 5
3084	3769					4.62	+ 15	+ 5		9		0.5		
2094	Puppis	50.2	-49 21	B3		4.83	15	293°	+ 8	14	(1)	0.6	230	-11
3089	3137					4.92	+ 2	+ 15		14		0.7		
2095	J Puppis	50.3	-47 51	B1		4.32	18	186°	+41				230	-10
3090	3396					4.43	+ 17	- 7				0.6		
2099	o or J Puppis	52.6	-22 37	F8	5°-6°	4.35	41	281°	+14.3	28	(1)		209	+ 4
3102	2087				Y ²	4.45	- 39	+ 12		28		2.4		
2108	Puppis	53.7	-30 4	A2	3°	4.85	13	309°	+28.4	24	(a)	1.7	215	+ 1
3113	5236				Y ¹	5.01	- 10	+ 9				0.5		
2111	χ Carinae	54.2	-52 43	B3		3.60	38	297°	+19.1	30	(1)	1.0	234	-12
3117	1343					3.74	+ 5	+ 38		30		1.5		
2119	V Puppis	55.3	-48 58	B1p		4.50	30	258°	Var	21	(1)	1.1	231	-10
3129	3349					4.86	+ 20	+ 22		21		1.9		
2120	Puppis	55.4	-18 7	A2	2 ^o .8	4.64	46	191°	-13	17	(1)	0.8	205	+ 7
3131	2118				Y ¹	4.83	+ 34	+ 31		17		2.9		
2126	28 Monocerotis	56.2	- 1 7	K0	6 ^o .1	4.88	97	145°	+26.7	14	(1)	0.6	190	+16
3141	1882				OY ²	4.84	+ 94	+ 25		14		4.8		
2130	13 Canis min	57.1	+ 2 36	K0	6 ^o .3	4.52	106	338°	+71.2	19	(4)	0.9	186	+18
3145	1854				Y ¹	4.55	- 92	- 53		19		4.6		
2136	15 Carinae	59.1	-63 17	B3		4.96	20	319°	+21.4	12	(1)	0.4	244	-16
3159	866					5.04	- 1	+ 20		12		1.5		
2141	ζ Puppis	0.1	-39 43	Od	3°.0	2.27	32	284°	- 20	27	(1)	-0.6	224	- 4
3165	3939					2.53	- 5	+ 32		27		-0.2		
2145	27 Lynceis	0.9	+51 48	A2	2 ^o .7	4.87	55	262°	+ 4	5	(3)	- 0.9	131	+34
3173	1391				W	5.05	- 46	+ 31		7		3.6		
2153	ε Puppis	3.3	-24 1	F5	5°	2.88	100	297°	+45.9	17	(3)	-1.1	211	+ 6
3185	6828				Y ²	2.97	- 74	+ 67		16		2.9		
2154	Velorum	3.5	-44 58	K0		5.02	14	214°	+25.3				228	- 6
3187	4051					4.99	+ 14	+ 4				0.7		
2155	ξ Monocerotis	3.6	- 2 41	G0	5 ^o .7	4.41	25	253°	+29.5	11	(3)	-1.7	193	+17
3188	2450				Y ³	4.51	- 13	+ 32		6		1.4		
2158	16 Puppis	4.5	-18 57	B3	2°	4.34	16	240°	+23	7	(2)	-1.4	207	+ 8
3192	2190				W	4.50	0	+ 16		7		0.3		

Boss 2119 Eclipsing binary Relative velocity is 610 km/sec Varies from 4m.1 to 4m.8 in 1.5 days

8^h.

1	2	3	4	5	6	7	8	9	10	11	12	13	14	15
2166 3206	γ^1 Velorum 3846	6.4	-47° 3'	B3		4 ^m .79 5.03	17 + 17	205° + 1	Var			0.7 1.0	230°	- 7°
2167 3207	γ^2 Velorum 3847	6.5	-47 3	Oa.p	3 ^s .5	2.22 2.09	2 0	180° - 2	+35	15 15	(2)	-1.9	230	- 7
2168 2169 3208 to 3210	ζ^1 Cancri ζ^2 Cancri 1887	6.5	+17 57	G0	4 ^s .9 3 ^s .0 Y ^s YG ¹	5.56 6.26 6.02	155 +132	155° + 82	-10.6 - 5.6	44 44	(1)	2.9 5.7	173	+20
2170 3211	19 Puppis 2385	6.6	-12 37	K0	5 ^s .4 Y ^s	4.68 4.66	27 - 23	294° + 13	+36.3	36	(a)	2.5 1.9	202	+12
2177 3220	B Carinae 1074	7.3	-60 59	F5		4.80 4.91	326 +319	208° - 68	+25.0	53	(a)	3.4 7.4	242	-13
2179 3223	s Volantis 736	7.6	-68 19	B5		4.46 4.56	28 - 3	321° + 28	+ 9.6			1.7	249	-18
2180 3225	h ¹ Puppis 4084	7.8	-39 19	K5		4.43 4.46	20 + 20	180° - 2	Var +15.9			0.9	224	- 2
2181 3226	Puppis 3979	8.0	-42 41	A3		4.87 5.02	5 +	191° - 0	+19.2	2	(a)	-3.6 -1.6	227	- 5
2187 3237	r Puppis 4349	9.7	-35 35	B3p		4.77 4.92	13 + 13	180° 0	+34	5 5	(1)	-1.7 0.4	221	- 1
2188 3240	Puppis 4558	10.2	-36 1	B3		5.12 5.27	9 +	125° - 7	+18			0.0	221	- 1
2189 3241	Puppis 4560	10.2	-36 2	B8		5.95 -	23 - 18	135° - 15				2.7	221	- 1
2192 3243	h ² Puppis 4188	10.5	-40 2	K0		4.43 4.46	88 + 61	143° - 63	Var	15 15	(2)	0.3 4.2	225	- 3
2195 3249	β Cancri 1917	11.1	+ 9 30	K2	6 ^s .3 OY ^s	3.76 3.74	75 - 9	224° + 74	+22.4 +16.9	13 9	(4)	-1.5 3.1	182	+25
2207 3270	q Puppis 4449	14.8	-36 21	A5		4.43 4.60	144 - 85	307° +117	+ 5	42	(a)	5.2	222	+ 1
2208 3275	31 Lynce 1815	16.0	+43 31	K5	7 ^s .0 OY ^s	4.43 4.33	107 + 44	185° + 97	+24.3	16 16	(4)	0.5 4.6	144	+36
2214 3280	Volantis 907	17.2	-65 18	K0		4.98 5.09	31 - 29	21° + 11	0.0			0.7	246	-16
2216 3282	w Puppis 5185	17.5	-32 44	K0		4.94 4.95	11 +	248° + 11	+33.2			0.1	220	+ 3
2226 3294	B Velorum 3734	19.5	-48 10	B2		4.90 4.99	17 +	263° + 15	+26	11 11	(1)	0.1 1.1	233	- 6
2233 3307	s Carinae 1032	20.5	-59 11	K0	6 ^s .4	1.74 2.03	32 +	296° + 32	+11.9	10 10	(1)	-3.3 -0.8	242	-12
2237 3314	30 Monocerotis 2339	20.7	- 3 35	A0	3 ^s .0 W	3.95 4.11	71 - 26	249° + 66	+ 7	19 18	(4)	0.2 3.2	196	+20
2244 3318	α Chamaeleont. 507	21.1	-76 36	F5		4.08 4.21	146 -143	38° + 25	-13.7			4.9	257	-22
2247 3323	o Ursae maj 1054	22.0	+61 3	G0	4 ^s .6 Y ^s	3.47 3.54	166 - 46	226° +152	+19.2	6 4	(2)	-3.5 4.6	123	+36
2255 3340	β Chamaeleont. 383	23.6	-77 10	K0		4.26 4.39	151 + 95	279° +118	+22.4	17 17	(2)	0.4 5.2	257	-22
2258 3347	β Volantis 933	24.6	-65 48	K0		3.65 3.82	171 +154	193° - 75	+27.0	25 25	(1)	0.6 4.8	248	-16
2290 3403	π Ursae maj 698	31.5	+64 40	K0	6 ^s .1 Y ^s	4.76 4.73	52 - 51	293° + 9	+14.7	17 17	(4)	0.9 3.3	118	+37
2291 3407	C Velorum 3646	31.7	-49 36	K0		4.87 4.98	3 -	315° + 3	+ 4.4			-2.6	235	- 5
2293 3410	δ Hydrae 2001	32.4	+ 6 3	A0	2 ^s .5 YG ¹	4.18 4.37	74 - 46	261° + 58	Var +10.3	20 20	(2)	0.7 3.5	188	+20

Box 2166, 2167 Probably a physical pair 41", 220" — Box 2168, 2169. The total magnitude of ζ Cancri is 4^m.71 and 4^m.80 in 1 two systems used here

8^h

1	2	3	4	5	6	7	8	9	10	11	12	13	14	15	
2299 3414	e ² Carinae 1591	33 ^m ,0	-57° 40'	K0		4 ^m ,80 4 ,91	31 22	71° 22	+23,6				241°	-10°	
2302 3418	σ Hydræ 2026	33 ,5	+3 42	K0	6°,5 Y ²	1,54 4 ,55	27 1	222° 27	+25,9	14 15	(6)	0,1 1,7	190	+26	
2307 3426	e Velorum 4451	34 ,2	-42 38	A5		4 ,13 4 ,29	15 1	247° 13	+20,0	17	(4)	0,2 0,0	230	-1	
2318 3438	β Pyxidis 5128	36 ,2	-34 57	G5		4 ,04 4 ,11	20 1	165° 4	-14,8	11 14	(1)	-0,2 0,5	224	+5	
2321 3441	9 Hydræ 2551	37 ,1	15 35	K0	5°,3 Y ²	4 ,98 4 ,97	99 1	182° 83	-1,8	31 32	(2)	-2,5 5,0	209	+16	
2324 3445	b Velorum 4438	37 ,3	-46 18	F5p		4 ,06 3 ,88	15 1	208° 4	Var				233	-2	
2325 3447	o Velorum 1583	37 ,4	-52 34	B3		3 ,68 3 ,82	20 6	307° 19	+17	12 12	(1)	-0,9 0,2	238	-7	
2327 3449	γ Cancri 1895	37 ,5	+21 50	A0	2°,3 W	4 ,73 4 ,91	113 1	243° 102	Var	12 11	(3)	-0,1 5,0	172	+35	
2329 3452	n Velorum 4448	37 ,9	-46 57	A3		4 ,85 4 ,94	29 1	262° 17	Var				234	-2	
2330 3454	η Hydræ 2039	38 ,0	+3 46	B3	2°,0 W	4 ,32 4 ,53	22 1	265° 17	Var	7 7	(3)	-1,4 1,0	191	+27	
2331 3457	d Carinae 1080	38 ,5	-59 24	B2		1 ,42 1 ,50	25 1	256° 18	+12,9	11 11	(1)	-0,4 1,1	213	-10	
2335 3459	31 Monocerotis 2708	38 ,7	-6 52	G0	6°,4 Y ²	1 ,70 4 ,79	7 6	117° 3	+31,6	5 5	(1)	1,8 1,0	202	+22	
2336 3461	δ Cancri 2027	39 ,0	+18 31	K0	5°,5 Y ²	4 ,17 4 ,10	210 1	181° 199	+17,1	18 18	(6)	-0,5 6,1	175	+35	
2342 3468	α Pyxidis 5651	39 ,6	32 50	B2		3 ,70 3 ,88	13 8	299° 10	+16,5	6 6	(1)	-2,4 -0,8	223	+7	
2348 3474	ε Cancri 1824	40 ,6	+29 8	A5	-0°,1 B ⁰	6 ,61							2,2	164	+38
2348 3474	ε Cancri 1821	40 ,6	+29 8	G5	5°,4 Y ²	4 ,20 4 ,14	54 1	202° 52	+15,2	15 13	(5)	-0,3 2,9	164	+38	
2349 3477	d Velorum 4569	40 ,8	-42 17	G5		4 ,12 4 ,20	18 1	341° 8	-1,9	11 14	(1)	-0,2 9,4	230	+1	
2354 3482	ε Hydræ 2036	41 ,5	+6 17	F8	5°,3 Y ²	3 ,48 3 ,58	196 1	254° 171	+36,8	36 32	(7)	1,0 4,9	189	+30	
2355 3484	12 Hydræ 2673	41 ,7	-13 11	G5	6°,0 Y ¹	4 ,44 4 ,50	31 1	127° 11	Var	4 3	(2)	3,2 2,0	207	+20	
2356 3485	δ Velorum 1788	41 ,9	-54 21	A0	4°,1	2 ,01 2 ,25	96 1	166° 58	+2	30	(4)		240	-6	
2358 3487	α Velorum 4517	42 ,6	-45 40	A0		4 ,09 4 ,11	21 1	231° 14	+23,6				233	-1	
2361 3492	g Hydræ 2040	43 ,1	+6 13	A0	2°,4 W	4 ,42 4 ,63	40 1	108° 37	+33,4	11 9	(3)	-0,8 2,1	190	+30	
2363 3498	f Carinae 1865	44 ,1	-56 25	B3		4 ,63 4 ,72	5 1	259° 4	+27				241	-8	
2375 3518	γ Pyxidis 5986	46 ,3	27 21	K2	6° Y ²	4 ,19 4 ,19	159 1	301° 108	+24,7	17 17	(1)	0,3 2,8	220	+12	
2382 3527	f Velorum 4661	47 ,2	-46 10	B0		4 ,89 5 ,27	23 1	211° 8	Var				231	-1	
2393 3547	ξ Hydræ 2060	50 ,1	+6 20	K0	5°,5 Y ¹	3 ,30 3 ,34	104 1	276° 66	+22,7	18 17	(4)	-0,8 3,4	190	+31	
2399 3556	δ Pyxidis 6072	51 ,3	-27 18	A2	2°-3° Y ¹	4 ,87 5 ,04	127 1	150° 30	+4,6				220	+12	
2404 3569	ι Ursae maj 1707	52 ,4	+48 26	A5	3°,4 Y ¹	3 ,12 3 ,36	502 1	240° 457	+13	62 59	(8)	2,0 6,6	139	+42	

Boss 2318 A binary, the total magnitude of which is 1m,20 (RIIP)

8^h to 9^h.

1	2	3	4	5	6	7	8	9	10	11	12	13	14	15
2406	ϵ Carinae	52 ^m ,8	-60° 16'	B8		3 ^m ,98	62	336 ^m	+24,9	22	(1)	0,7	245 ^m	-10 ^m
3571	1243					4,10	-40	48		22		2,9		
2407	α Cancri	53,0	+12 15	A3	3 ^m ,3	4,27	54	137 ^m	-13,6	30	(3)	1,7	185	+35
3572	1948				W	4,50	+54	4		30		2,9		
2408	H Velorum	53,3	-52 21	B5		4,77	11	195 ^m	Var	3	(1)	-2,8	239	-4
3574	1788					4,86	+11	0	+22,2	3		0,0		
2411	ρ Ursae maj	53,5	+68 1	Ma	7 ^m ,1	4,99	21	315 ^m	+4,8	9	(4)	-0,2	113	+38
3576	551				OY ^a	4,93	-21	3		9		1,6		
2413	10 Ursae maj	54,2	+42 11	F5	4 ^m ,1	4,09	504	239 ^m	+27,1	69	(4)	3,3	147	+42
3579	1956				Y ^{1,2}	4,22	-186	469		69		7,6		
2421	w Velorum	56,3	-40 52	F8		4,42	68	299 ^m	Var	28	(a)	1,6	231	+4
3591	4810					4,54	-32	60	-65			3,6		
2424	κ Ursae maj	56,8	+47 33	A0	2 ^m ,9	3,68	73	204 ^m	+5	23	(2)	0,5	139	+43
3594	1633				YG ¹	3,87	+16	71		23		3,0		
2437	Ursae maj	0,2	+38 51	G5	5 ^m ,9	4,71	43	234 ^m	+17,4	5	(4)	-1,8	151	+43
3612	2800				Y ¹	4,76	-12	41		5		2,9		
2438	c Velorum	0,7	-46 42	K0		3,69	74	251 ^m	+24,2	22	(1)	0,4	236	\pm 0
3614	4883					3,83	+33	66		22		3,0		
2440	α Volantis	0,9	-66 0	A5		4,18	103	188 ^m	+7,7	27	(2)	1,3	250	-13
3615	1086					4,29	+96	37		27		4,2		
2441	σ^1 Ursae maj	1,6	+67 32	F8	4 ^m ,2	4,87	70	184 ^m	-1,8	53	(4)	3,5	113	+39
3616	577				Y ¹	5,00	+40	57		52		4,1		
2443	f Ursae maj	1,9	+52 0	A3p	3 ^m ,9	4,54	132	253 ^m	-1,0	19	(2)	-1,6	133	+43
3619	1365				Y ¹	4,71	-84	102		6		5,2		
2446	τ Ursae maj	2,7	+63 55	F5	4 ^m ,2	4,74	122	125 ^m	-6,5	19	(2)	1,1	118	+40
3624	788			A5	Y ¹	4,83	+122	9		19		5,2		
2450	κ Pyxidis	3,7	-25 27	K5	6 ^m -7 ^m	4,82	40	102 ^m	-44,7	13	(2)	0,2	220	+16
3628	6895			O ^a		4,80	+21	34		12		2,8		
2452	l Velorum	4,3	-43 2	K5	7 ^m ,3	2,22	26	281 ^m	+18,5	19	(2)	-1,5	234	+3
3634	4090					2,37	-4	26		18		-0,7		
2457	B Carinae	4,8	-70 8	B3p		4,86	8	310 ^m	+35				253	-15
3642	861					4,95	-1	8				-0,6		
2458	G Carinae	4,9	-72 12	F5		4,50	26	252 ^m	+21,3				255	-17
3643	779					4,63	+20	17				1,6		
2467	Velorum	7,4	-44 27	B5		4,96	14	270 ^m	+35,4	7	(1)	-0,8	235	+3
3654	5206					5,11	+1	14		7		0,7		
2473	α Carinae	8,4	-58 33	B3		3,56	41	263 ^m	+23,1	20	(2)	0,2	246	-7
3659	1419					3,70	+18	37		21		1,6		
2476	σ Ursae maj	9,0	+54 26	A5	3 ^m ,5	4,89	86	45 ^m	Var	19	(3)	1,3	130	+44
3662	1285				Y ¹	5,05	+9	85	-16,9	19		4,6		
2477	l Carinae	9,0	-61 54	B3		4,18	47	276 ^m	+16,6	25	(2)	1,1	248	-10
3663	1201					4,29	+14	45		24		2,5		
2479	δ Hydrae	9,2	+2 44	A0	2 ^m ,9	3,84	338	157 ^m	Var.	22	(4)	0,6	196	+34
3665	2167				Y ¹	4,12	+324	98		22		6,5		
2489	l Velorum	11,7	-38 9	K0		4,98	78	269 ^m	+1,8	14	(1)	0,7	231	+8
3682	5408					4,99	-4	78		14		4,4		
2491	k Velorum	11,8	-37 0	F5		4,70	23	95 ^m	+12				230	+9
3684	8808					4,78	+4	23				1,5		
2493	β Carinae	12,1	-69 18	A0	4 ^m ,1	1,80	193	301 ^m	-5				253	-14
3685	1023					2,07	-6	193				3,2		
2495	38 Lynce	12,6	+37 14	A2	2 ^m ,9	3,82	137	191 ^m	+4	29	(6)	1,0	154	+40
3690	1965				Y ¹	4,00	+68	119		27		4,5		
2500	g Carinae	13,4	-57 7	K5		4,18	36	233 ^m	-4,7	13	(1)	-0,3	245	-0
3696	1961					4,31	+29	21		13		2,0		
2503	i Carinae	14,4	-58 51	B0	4 ^m ,1	2,25	26	266 ^m	+13,2				246	-
3699	1465					2,43	+10	24				-0,6		

9^h

1	2	3	4	5	6	7	8	9	10	11	12	13	14	15
2506 3706	26 Hydiae 2609	15 ^m .0	-11° 33'	G5	5 ^s .8 Y ⁸	4 ^m .91 4.98	21 -14	281° +16	-0.9	10 10	(1)	-0.1 1.5	212°	+26°
2507 3705	40 Lynx 1979	15.0	+34 49	K5	6 ^s .5 OY ³	3.30 3.34	216 -171	273° +131	+3.9	24 16	(4)	-0.7 5.0	157	+46
2511 3709	27 Hydiae 2613	15.6	-9 8	G5	5 ^s .4 Y ³	4.97 5.01	33 +10	220° +32	+25.5	15 15	(1)	0.9 2.6	209	+28
2516 3718	θ Pyxidis 7114	17.1	-25 32	Ma	7 ^s O ³	4.93 4.91	22 +2	216° +22	+20.0	14 14	(2)	0.7 1.6	223	+17
2521 3728	k Carinae 1242	18.5	-61 58	K0		4.86 4.97	16 +16	202° 0	+50.8				218	-9
2524 3731	Leonis 1939	18.8	+26 37	K0	6 ^s .1 Y ³	4.61 1.61	61 +13	210° +59	+27.7	15 11	(5)	-0.2 3.6	169	+46
2525 3733	λ Pyxidis 7196	18.9	-28 24	K0	5 ^s Y ²	1.90 4.81	156 -64	278° +142	+10.2	39 39	(1)		225	+16
2526 3734	ν Velorum 2219	19.0	-54 35	B3	3 ^s .1	2.63 2.84	21 +9	256° +19	+21.7	12 12	(3)	-2.0 -0.8	244	-3
2533 3748	α Hydiae 2680	22.7	-8 14	K2	6 ^s .1 O ²	2.16 2.24	35 -35	333° +4	-3.9	28 23	(4)	-1.0 -0.1	210	+31
2534 3749	γ Hydiae 2802	22.7	-21 54	K0		4.91 4.89	251 +221	130° +118	28.7	17 17	(1)	1.1 6.9	221	+21
2536 3751	Draconis 302	22.9	+81 46	K2	6 ^s .6 Y ³	4.58 4.49	27 +13	200° +24	-5.9	13 13	(3)	0.2 1.7	97	+33
2540 3757	h Ursae maj 845	23.7	+63 30	K0	3 ^s .8 Y ¹	3.75 3.87	117 +67	78° -96	-8	36 35	(4)	1.5 4.1	117	+42
2541 3759	τ ¹ Hydiae 2901	24.1	-2 19	F5	4 ^s .2 Y ^{1.5}	1.78 4.89	126 -91	99° -91	+9.8	48 48	(1)	3.2 5.3	204	+34
2544 3765	ε Antliae 5724	25.1	-35 30	K2		4.61 4.65	33 +15	235° +30	+24.0	12 12	(1)	0.0 2.2	232	+11
2549 3771	d Ursae maj 565	25.6	+70 16	G0	5 ^s .0 Y ^{1.5}	4.57 4.72	90 -89	321° -9	-27.5	46 45	(5)	2.8 4.3	110	+40
2550 3773	λ Leonis 2107	26.1	+23 25	K5	6 ^s .9 O ²	4.48 4.48	56 +21	203° +52	+25.9	15 15	(4)	0.4 3.2	175	+46
2552 3775	θ Ursae maj 1401	26.2	+52 8	F8p	3 ^s .8 Y ²	3.26 3.43	1092 -339	240° +1037	+15.5	73 73	(4)	2.6 8.5	133	+46
2558 3786	ψ Velorum 6680	26.8	-40 2	F5		3.64 3.76	200 -78	289° +184	+12	65 65	(1)	2.7 5.1	235	+9
2559 3787	τ ⁴ Hydiae 2211	26.9	-0 44	A3	2 ^s .8 Y ¹	4.50 4.69	26 +4	223° +25	+7	26 26	(2)	1.6 1.6	204	+36
2565 3799	26 Ursae maj 1402	28.0	+52 30	A0	2 ^s .5 Y ¹	4.65 4.82	73 -12	233° +72	+20	18 18	(3)	0.9 4.0	131	+47
2566 3800	10 Leonis min 2004	28.1	+36 51	G5	5 ^s .3 OY ²	4.62 4.71	30 +28	154° +11	-11.4	19 19	(3)	1.0 2.0	155	+49
2567 3803	N Velorum 2270	28.2	-56 36	K5	6 ^s .3	3.04 3.23	40 +5	276° +40	-13.9	39 39	(1)	1.0 1.0	246	-4
2570 3809	Lynx 2224	28.8	+40 4	K0	5 ^s .3 Y ²	4.99 4.96	31 -23	270° +21	-11.9	17 17	(2)	1.0 2.4	150	+49
2574 3816	R Carinae 1253	29.7	-62 21	Md		Var 4.4-10.0	44 -29	293° +33	+28				249	-8
2581 3825	h Carinae 1576	31.5	-58 47	B5		4.20 4.31	18 -7	308° +16	+22.1	8 8	(1)	-1.3 0.5	248	-5
2589 3834	2 Sextantis 2207	33.2	+5 6	K0	6 ^s .3 Y ²	4.78 4.81	176 -55	249° +167	+44.9	19 20	(3)	1.3 6.0	198	+40
2590 3836	M Velorum 4836	33.3	-48 55	A5		4.49 4.59	125 -15	281° +124	+21				241	+2

9^h to 10^h

1	2	3	4	5	6	7	8	9	10	11	12	13	14	15
2595 3845	ϵ Hydrae 2231	34 ^m .7	— 0° 41'	K0	6 ^s .2 OY ^b	4 ^m .10 4.10	+ 85 + 85	148° + 6	+24.3	23 23	(2)	0.9 3.8	205° +37°	
2600 3849	κ Hydrae 2917	35.5	— 13 53	B3	2 ^s .3 W	4.96 5.22	+ 31 + 2	238° + 31	+17	9 9	(3)	-0.3 2.5	217 +29	
2602 3852	σ Leonis 2044	35.8	+10 21	F5 A3	4 ^s .0 Y ¹	3.76 3.87	150 — 66	255° + 135	+27.0	18 17	(4)	-0.1 4.6	194 +43	
2604 3856	m Carinae 1477	36.6	— 60 53	B9		4.67 4.79	39 — 10	299° + 38	+24	17 17	(1)	0.8 2.6	249 — 6	
2605 3858	ι Hydrae 2884	36.7	— 23 8	B2p		4.74 4.95	17 — 12	295° + 12	+26			0.9	224 +22	
2615 3871	ϕ Antliae 6881	39.7	— 27 19	F5p	5 ^s Y ^a	4.98 5.05	64 — 40	291° + 50	+24.0	51	(a)	3.5 4.0	228 +20	
2618 3873	ϵ Leonis 2129	40.2	+24 14	G0p	4 ^s .5 Y ^a	3.12 3.22	48 — 10	239° + 47	+ 4.5	18 9	(5)	-2.1 1.5	175 +49	
2627 3882	R Leonis 2080	42.2	+11 54	Md	7 ^s .9 OR ^b	Var 5.0—10.2	33 + 22	187° + 24	+10	2	(a)	-3.5 2.6	192 +45	
2628 3884	ι Carinae 1888	42.5	— 62 3	G0		Var 3.6—5.0	31 — 15	314° + 27	+ 4.0	1	(a)	-4.4 1.1	250 — 7	
2632 3888	ν Ursae maj 1268	43.9	+59 31	F0	3 ^s .8 YG ¹	3.89 4.02	330 — 79	241° + 320	+32	35 33	(4)	1.5 6.5	120 +46	
2635 3890	ν Carinae 1084	44.6	— 64 36	F0		3.15 3.23	21 — 0	287° + 21	+13.8			-0.2	253 — 9	
2635 3891	ν Carinae 1084	44.6	— 64 36			6.03 —						2.6	253 — 9	
2637 3894	ϕ Ursae maj. 1331	45.4	+54 32	A2	2 ^s .8 Y ¹	4.54 4.72	9 — 6	0° — 6	-12.7	15 15	(6)	0.4 -0.7	127 +48	
2645 3903	ν Hydrae 2963	46.7	— 14 23	K0	5 ^s .8 Y ^a	4.29 4.25	30 + 30	154° + 1	-14.5	11 11	(1)	-0.5 1.7	220 +31	
2648 3905	μ Leonis 2019	47.1	+26 29	K0	5 ^s .9 Y ^a	4.10 4.08	227 — 102	254° + 202	+14.3	22 21	(6)	0.7 5.9	173 +52	
2651 3912	m Velorum 5808	47.9	— 46 5	G5		4.56 4.70	39 + 26	226° + 29	Var +10.8			2.5	242 + 6	
2657 3919	Hydrae 7585	49.6	— 25 28	K0		5.00 4.99	212 — 121	285° + 174	+51.9	13 13	(1)	0.6 6.6	228 +23	
2674 3940	ϕ Velorum 8076	53.4	— 54 6	B5		3.70 3.85	23 + 8	255° + 22	+14.1	10 10	(2)	-1.3 0.5	247 0	
2680 3950	κ Leonis 2301	54.9	+ 8 31	Md	7 ^s .3 O ^a	4.89 4.82	43 + 1	231° + 43	+23.2	8 8	(4)	-0.6 3.1	198 +47	
2690 3970	ν ¹ Hydrae 3073	0.3	— 12 35	B8	3 ^s .8 YG ¹	4.72 4.89	38 — 28	280° + 25	+24	13 13	(1)	0.3 2.6	221 +34	
2692 3974	α Leonis min 2110	1.6	+35 44	A5	2 ^s .9 W	4.47 4.68	54 + 40	96° — 36	-12	26 26	(5)	1.6 3.1	156 +55	
2694 3975	η Leonis 2171	1.9	+17 15	A0p	2 ^s .2 YG ¹	3.58 3.80	12 + 9	185° + 8	+ 2.1	8 8	(1)	-1.9 -1.0	188 +52	
2696 3980	λ Leonis 2112	2.6	+10 30	K2	6 ^s .9 O ^a	4.58 4.53	117 — 4	234° + 117	+40.2	15 15	(2)	0.5 4.9	197 +50	
2697 3981	ι 5 Sextantis 2615	2.9	+ 0 7	A0	2 ^s .5 W	4.50 4.69	30 — 6	247° + 29	+ 9.8	14 14	(2)	0.2 1.9	210 +43	
2698 3982	α Leonis 2149	3.0	+12 27	B8	1 ^s .5 W	1.34 1.61	247 — 148	269° + 198	+ 7.	64 63	(3)	0.3 3.3	196 +50	
2706 3994	λ Hydrae 2820	5.7	— 11 52	K0	5 ^s .5 Y ^a	3.83 3.87	221 — 15	245° + 221	+19.9	18 17	(3)	0.0 5.5	220 +36	
2723 4023	q Velorum 5713	10.5	— 41 38	A2		4.09 4.23	160 — 54	281° + 150	+ 8	36 36	(1)	1.8 5.1	242 +12	

Boes 2627. Long period variable 50.0 to 100.2 in 310 days. — Boes 2628. Cepheid variable; period 35.5 days. — Boes 2635. A binary 5^h, 128^o — Boes 2637. ADB 7545. A well observed visual binary with a period of 113 years.

10^h.

1	2	3	4	5	6	7	8	9	10	11	12	13	14	15
2730 4031	ζ Leonis 2209	11 ^m .1	+23° 55'	F0	3 ^m .1 Y ^a	3 ^m .65 3.71	27 26	125° 8	-11	23 20	(6)	0.1 0.8	178°	+56°
2729 4033	γ Ursae maj 2005	11 .1	+43 25	A2	2 ^m .3 W	3.52 3.70	168 71	255 153	+18	18 12	(4)	-1.1 4.6	143	+56
2733 4037	ω Umicac 1178	11 .4	-69 32	B8		3.56 3.70	28 8	266° 27	1	11 11	(2)	-1.2 0.8	258	-12
2739 4050	η Carinae 1817	13 .7	-60 50	K5		3.44 3.62	16 11	261° 45	+8.1	12 12	(1)	-1.2 1.7	253	-4
2741 4054	δ Leonis 2166	14 .3	+19 59	F5	4 ^m .4 Y ¹	1.97 5.08	329 39	225° 326	+5.8	47 47	(4)	3.3 7.6	185	+55
2742 4057	γ^1 Leonis 2167	14 .5	+20 21		5 ^m .2 Y ^a	2.30 2.70	338 308	117° 142	-36.0	30 25	(8)	-0.3 5.1	185	+55
2743 4058	γ^2 Leonis 2467	14 .5	+20 21	K0	Y ¹ .2	3.80 3.89	353 328	121° 127	-36.0			1.2 6.6	185	+55
2747 4063	V Velorum 3474	15 .8	-54 32	K0		1.58 4.70	22 18	214° 12	+13.0	11 11	(1)	-0.2 1.3	250	+1
2751 4069	μ Ursae maj 2415	16 .4	+42 0	K5	6 ^m .8 O ¹	3.21 3.25	84 67	284° 50	Var	33 32	(4)	0.7 4.7	145	+57
2754 4072	Ursae maj 664	16 .9	+66 1	A0	2 ^m .3 Y ¹	4.92 5.15	25 12	206° 22	+1.4	15 15	(3)	0.8 1.9	110	+46
2755 4074	J Velorum 3286	17 .2	-55 33	B5p		4.65 4.74	18 0	270° 18	+10			1.0 3.9	251	+1
2758 4080	i Velorum 5809	18 .1	-41 9	K5		1.99 5.02	62 58	328° 22	+20.9	6	(n)	-1.0 3.9	243	+13
2768 4090	30 Leonis min 2128	20 .2	+34 18	F0	3 ^m .5 Y ¹	4.83 4.95	107 26	217° 104	+13.7	31 32	(3)	2.4 5.0	160	+59
2771 4094	μ Hydiae 3052	21 .3	-16 20	K5	6 ^m .3 O ²	4.06 4.09	153 18	236° 151	+39.7	23 23	(2)	0.9 5.0	228	+34
2776 4100	β Leonis min 2080	22 .1	+37 13	K0	5 ^m .3 Y ²	4.41 4.36	161 14	227° 161	+6.8	21 20	(5)	0.9 5.4	154	+60
2778 4102	i Carinae 733	22 .4	-73 32	F5		4.08 4.21	28 25	221° 13	+1.3			1.3	261	-15
2779 4104	α Anthiae 8465	22 .6	-30 34	K5		4.42 4.44	68 22	270° 65	+15.2	10 10	(1)	-0.6 3.6	239	+22
2783 4110	Carinae 3256	23 .7	-57 8	F5p		4.94 5.06	7 7	196° 2	+1.2			-0.8	252	+0
2785 4112	36 Ursae maj 1459	24 .2	+56 30	F5	4 ^m .5 Y ^a	4.84 5.01	182 75	258° 166	+9.60	70 69	(4)	2.4 6.1	120	+52
2784 4114	s Carinae 2227	24 .2	-58 14	F0		4.08 1.20	18 8	243° 16	+10.0			0.4	253	-1
2792 4119	30 Sextantis 2663	25 .2	0 8	B5	1 ^m .9 W	4.95 5.22	54 1	238° 54	+11	8 8	(3)	-0.5 3.6	215	+48
2802 4132	Ursae maj 2101	27 .5	+40 57	A5	3 ^m .5 W	4.84 5.04	141 80	267° 116	+15	25 25	(4)	1.8 5.6	145	+60
2804 4133	η Leonis 2166	27 .5	+9 49	B0p	2 ^m .0 W	3.85 4.03	9 1	229° 9	+37.6	11 7	(4)	-1.9 -1.4	204	+54
2809 4138	k Carinae 1034	27 .8	-71 29	A2		4.94 5.03	39 28	148° 27	+7.6			2.9	260	-12
2811 4140	p Carinae 1704	28 .5	-61 11	B5p		3.58 3.72	26 6	286° 25	+26			0.7	254	-3
2812 4142	Carinae 981	28 .7	-72 43	K5		4.90 5.01	9 9	207° 2	+11.2	10 10	(2)	-0.1 -0.3	261	-13
2823 4159	i Carinae 3544	31 .8	-57 3	K5		4.54 4.66	24 13	237° 20	+9.8	10 10	(1)	-0.5 1.4	253	+1
2827 4163	U Hydiae 3218	32 .6	-12 52	Nb		Var	40 32	110° 24	+18.8				229	+39

10^h to 11^h.

1	2	3	4	5	6	7	8	9	10	11	12	13	14	15
2829 4166	37 Leonis min 2061	33 ^m .1	+32° 30'	G0	5 ^s .3 Y ^a	4 ^m .77 4.87	7 +	117° - 3	- 6.9	13 12	(3)	0.2 -1.0	162° 249	+ 62° + 9
2830 4167	p Velorum 6042	33 .1	-47 42	F2 A3		4.06 4.19	167 +	259° +167	+19.2	26 26	(1)	1.1 5.2	249	+ 9
2837 4174	γ Chamaeleont 882	34 .3	-78 6	Ma		4.10 4.23	45 -	291° + 45	-22.8	7	(a)	-1.7 2.4	263	-18
2840 4177	t ^a Carinae 2460	34 .9	-58 40	K5 A		4.73 4.84	14 +	159° - 5	+11.0	14	(a)	0.4 0.4	255	- 1
2842 4180	z Velorum 3916	35 .3	-55 5	G0		4.37 4.49	28 +	226° + 21	+20.7			1.6	253	+ 3
2862 4199	θ Carinae 1599	39 .4	-63 52	B0	3 ^s .8	3.03 3.20	24 -	293° + 22	Var +24.0	7 7	(3)	-2.7 -0.1	257	- 5
2863 4200	w Carinae 882	39 .7	-60 3	K5		4.49 4.60	38 +	259° + 37	+12.2	16	(a)	0.5 2.4	256	- 1
2871 4210	η Carinae 2620	41 .2	-59 10	Pec Nova		Var -1.0 to 8.5	7 -	47° - 6	-25.0	2	(1)	-9.5 -6.8	255	+ 0
2875 4216	μ Velorum 5913	42 .5	-48 54	G5	5 ^s .5	2.84 3.01	78 +	139° - 41	+ 7.3	30 30	(2)	0.2 2.3	251	+ 9
2888 4232	ν Hydrae 3138	44 .7	-15 40	K0	5 ^s .8 Y ^a	3.32 3.31	214 -	26° -171	- 1.2	33 33	(3)	0.9 5.0	234	+38
2889 4234	δ Chamaeleont. 658	44 .8	-80 1	B3		4.62 4.72	48 +	265° + 46	+21.7			3.0	265	-19
2899 4247	46 Leonis min 2172	47 .7	+34 45	K0	4 ^s .9 Y ^a	3.92 3.92	304 +	163° + 94	+16.2	37 35	(7)	1.6 6.3	157	+65
2900 4248	ω Urae maj 2058	48 .2	+43 43	A0	2 ^s .4 Y ¹	4.84 4.96	57 +	128° + 18	-18.4	12 12	(3)	0.2 3.6	137	+62
2908 4257	u Carinae 2834	49 .4	-59 19	K0		3.88	63 -	70° - 62	+ 8.4	30 30	(1)	1.3 2.9	256	+ 1
2909 4259	54 Leonis 2314	50 .2	+25 17	A0	2 ^s .9 W	4.51 4.49	77 -	257° - 72	+ 6	20 20	(3)	1.0 3.9	180	+64
2909 4260	54 Leonis 2314	50 .2	+25 17		0 ^s Y ¹	6.30 -						2.8 5.7	180	+64
2919 4273	ι Antilae 6808	52 .1	-36 36	K0		4.70 4.71	164 +	148° - 39	- 0.2	14 14	(1)	0.4 5.8	247	+21
2925 4287	α Crateris 3273	54 .9	-17 46	K0	5 ^s .3 OY ^a	4.20 4.23	481 -	284° +361	+47.6	15 15	(2)	0.1 7.6	239	+38
2929 4293	l Velorum 6276	55 .5	-41 41	A2		4.56 4.71	25 +	107° - 21	- 5.1			1.6	250	+16
2930 4295	β Urae maj. 1808	55 .8	+56 55	A0	1 ^s .9 W	2.44 2.67	89 +	71° - 87	-11.4	45 44	(7)	0.7 2.2	115	+55
2931 4299	p ^a Leonis 2471	56 .8	- 1 57	Ma	7 ^s .3 O ^a	4.97 4.93	41 +	154° + 4	-13	9 8	(3)	-0.5 3.0	226	+51
2932 4300	b Leonis 2547	57 .0	+20 43	A0	2 ^s .7 W	4.42 4.62	28 -	328° - 1	-10.6	15 14	(4)	0.2 1.7	191	+65
2933 4301	α Urae maj. 1161	57 .6	+62 17	K0	5 ^s .0 Y ^a	1.95 2.07	139 +	237° +139	- 9	55 54	(4)	0.6 2.7	110	+52
2942 4310	z Leonis 8488	59 .9	+ 7 53	F0	3 ^s .9 Y ¹	4.66 4.83	350 -	262° +318	+ 6.1	13 13	(4)	0.2 7.4	216	+59
2952 4325	z Carinae 2067	2 .4	-61 53	K0		4.76 4.87	23 -	280° + 18	- 2.0	13 13	(1)	0.3 1.6	259	- 2
2958 4335	ψ Urae maj. 1897	4 .0	+45 2	K0	5 ^s .1 Y ^a	3.15 3.21	69 +	237° + 69	- 4.2	44 44	(4)	1.4 2.3	132	+64
2960 4337	x Carinae 3189	4 .4	-58 26	F8p		4.02 4.15	19 -	264° + 19	Var. + 7.3			0.4	258	+ 2
964 441	β Crateris 3095	6 .7	-22 17	A2	4 W	4.52 4.69	101 +	179° + 41	Var + 6.4			4.5	243	+35

*2909. Henry: ADS 7979. 0^s.3, 108°A (1921,6). Dynamo parallel 0^s.225.

11^h.

1	2	3	4	5	6	7	8	9	10	11	12	13	14	15
2966	γ Carinae	8 ^m ,3	-59° 46'	F5p		4 ^m ,73	11	117°	-8,4				259°	0°
4352	3190					4,85	+	6	-9			-0,1		
2972	δ Leonis	8,8	+21 4	A3	2 ^s ,8	2,58	207	135°	-23,2	66	(7)	1,6	194	+68
4357	2298				Y ¹	2,84	+	203	-43	64		4,2		
2974	θ Leonis	9,0	+15 59	A0	2 ^s ,5	3,41	106	216°	+7,2	26	(6)	0,5	204	+65
4359	2234				W	3,59	+	38	+99	26		3,5		
2976	η Leonis	9,9	+23 39	Ma	6 ^s ,8	4,87	18	236°	+15,8	8	(3)	-0,6	185	+68
4362	2322				O ⁸	4,78	+	0	+18	8		1,2		
2982	η Leonis	11,6	-3 6	A5	3 ^s ,5	4,58	120	248°	-7	29	(1)	1,9	232	+52
4368	3316				Y ¹	4,77	-	19	+119	29		5,0		
2984	ξ Ursae maj	12,9	+32 6	G0	4 ^s	4,87	732	215°	-15,5	124	(7)	5,4	163	+70
4374	2132				Y ²	4,96	+	285	+673	123		9,2		
2984	ξ Ursae maj	12,9	+32 6	G0	4 ^s ,0	4,41	732	215°	Var.			4,9	163	+73
4375	2132				Y ²	4,50	+	285	+673	-15,9		8,7		
2985	ν Ursae maj	13,1	+33 38	K0	5 ^s ,9	3,71	27	304°	-9,1	16	(3)	-0,6	157	+70
4377	2098				OY ⁸	3,67	-	1	-27	14		0,9		
2987	55 Ursae maj	13,7	+38 44	A2	2 ^s ,8	4,78	102	214°	Var	14	(5)	0,5	143	+68
4380	2225				W	4,96	+	43	+93	-3		4,8		
2989	δ Crateris	14,3	-14 14	K0	5 ^s ,4	3,82	230	328°	-5,1	20	(4)	0,1	240	+43
4382	3346				Y ⁸	3,81	-	230	+16	18		5,6		
2990	σ Leonis	16,0	+6 35	A0	2 ^s ,8	4,13	95	261°	Var	16	(4)	0,2	222	+61
4386	2437				YG ¹	4,34	-	37	+87	-5,3		4,0		
2992	π Centauri	16,4	-53 56	B5		4,26	39	243°	+16,	14	(2)	0,0	258	+6
4390	4498					4,38	+	10	+38	14		2,2		
2999	ϵ Leonis	18,7	+11 5	F5	3 ^s ,7	4,03	176	119°	-10,0	51	(3)	2,6	218	+65
4399	2348				Y ¹	4,16	+	153	-84	51		5,3		
3005	γ Crateris	19,9	-17 8	A5	4 ^s ,0	4,14	107	268°	+4	31	(2)	1,6	244	+41
4405	3244				W	4,33	-	47	+96	31		4,3		
3031	λ Draconis	25,5	+69 53	Ma	6 ^s ,9	4,06	45	238°	+7,0	15	(5)	-0,1	99	+47
4434	666				O ⁸	3,98	+	10	+44	15		2,3		
3035	α^1 Centauri	27,1	-58 53	F8p		4,96	18	174°	-20			261	+2	
4441	3692					5,09	+	18	+2			1,3		
3036	α^2 Centauri	27,1	-58 58	A2p		5,26	29	232°	-16,8			261	+2	
4442	3693					5,33	+	13	+26			2,6		
3042	ξ Ilydrae	28,1	-31 18	G5		3,72	210	256°	-4,3	16	(1)	-0,3	252	+29
4450	9083					3,80	-	36	+206	16		5,3		
3048	A Centauri	30,0	-53 42	B8		4,82	65	267°	+4	22	(2)	1,5	260	+7
4460	4637					4,91	-	12	+64	22		3,9		
3054	λ Centauri	31,2	-62 28	B9		3,34	48	242°	+8	18	(3)	-0,4	262	-1
4467	2127					3,51	+	15	+46	18		1,7		
3055	θ Crateris	31,6	-9 15	B9	2 ^s ,4	4,81	61	271°	-1	14	(4)	0,5	244	+50
4468	3202				W	4,98	-	32	+52	14		3,7		
3058	ν Leonis	31,8	-0 16	K0	5 ^s ,4	4,47	35	0°	+1,2	18	(4)	0,6	237	+58
4471	2458				Y ²	4,47	-	30	-18	17		2,2		
3073	α Ilydrae	35,2	-34 11	B8		4,88	30	272°	+6	8	(1)	-0,6	255	+26
4494	7610					4,98	-	13	+27	8		2,3		
3076	Centauri	36,2	-61 32	G0		4,88	5	68°	Var			263	-1	
4499	2514					5,01	-	1	+14,2			-1,6		
3087	ζ Crateris	39,7	-17 48	G5	4 ^s ,8	4,90	52	139°	-4,6	17	(1)	1,1	251	+42
4514	3460				OY ²	4,93	+	50	-11	17		3,5		
3089	ν Virginis	40,7	+7 5	Ma	6 ^s ,7	4,20	188	185°	+50,6	13	(5)	-0,2	233	+64
4517	2479				O ⁸	4,18	+	152	+111	13		5,6		
3090	χ Ursae maj	40,8	+48 20	K0	5 ^s ,5	3,85	137	276°	-8,7	26	(5)	0,8	116	+66
4518	1966				OY ⁸	3,85	-	69	+119	24		4,5		
3092	λ Muscae	40,9	-66 10	A5		3,80	102	286°	+16			264	-5	
4520	1640					3,94	-	43	+93			3,8		

Boss 2984 Wellknown visual binary. Period 60 years.

11^h to 12^h.

1	2	3	4	5	6	7	8	9	10	11	12	13	14	15
3094	Contauri	41 ^m .7	-60 ^m 37 ^s	G0		4 ^m .22	19	22 ^m	1.5	41	(4)	2.1	263 ^m	-0 ^s
4522	1325					4 ^m .34	22	12		40		2.0		
3098	93 Lacus	42 ^m .8	-1 20 40	F8	4 ^m .4	155	262 ^m	Var	18	(a)	2.3	207	-1 75	
4527	2183				Y ¹	4 ^m .68	57	141	0.0			5.5		
3099	// Muscena	43 ^m .4	-66 15	K5		4 ^m .71	30	168 ^m	1 17.4			2.1		-5 ^s
4530	1649					4 ^m .82	30	1						
3101	// Lacus	44 ^m .0	+15 8	A2	2 ^m .5	2 21	511	250 ^m	0	85	(a)	1.0	222	-71 ^s
4534	2183				Y ¹	2 52	148	1401		84		5.8		
3103	j Contauri	44 ^m .8	-63 14	B5		4 ^m .52	20	235 ^m	1 17					-2 ^s
4537	1988					4 ^m .63	1 11	17				1.0		
3104	Musca	45 ^m .2	-60 40	G5		4 ^m .80	11	205 ^m	1 18.2	4	(1)	2.1	265	-9 ^s
4538	1595					5 ^m .01	1	11		4		0.1		
3105	// Virginia	45 ^m .5	+1 2 20	F8	4 ^m .2	1 80	291	111 ^m	1 4.0	94	(4)	4.7	241	+60 ^s
4540	2489				Y ¹	1 89	1 626	492		94		8.4		
3109	B Contauri	46 ^m .1	-44 37	K0		4 ^m .71	98	270 ^m	1 2.2			2.0		+16 ^s
4546	7614					4 ^m .68	-15	91				4.7		
3115	// Hydrus	47 ^m .8	-73 21	B9		4 ^m .40	56	264	1	14	(1)	0.1	248	+28 ^s
4552	8018					4 ^m .55	18	51		14		1.2		
3117	γ Ursae maj.	48 ^m .6	+54 15	A0	1 ^m .9	2 54	94	88 ^m	11	18	(r)	0.1	107	+62 ^s
4554	1475				W	2 72	1 31	89		60		4.4		
3139	α Virginia	53 ^m .7	+1 7 10	A3	2 ^m .5	4 57	33	187 ^m	Var	22	(4)	1.4	241	+66 ^s
4589	2302				Y ¹	4 ^m .80	1 26	20	24.0	22		3.2		
3146	δ Crucis	58 ^m .1	-62 45	A5		4 ^m .48	146	267 ^m	-2.5	19	(a)	10.9	265	-1 ^s
4599	2543					4 ^m .58	31	143				5.3		
3151	δ Crucis	59 ^m .2	-62 36	B1		4 ^m .08	6	288 ^m	1 16.4			2.05		-1 ^s
4603	2501					5 ^m .06	-3	5				1.0		
3153	χ Chamaeleont.	59 ^m .6	-75 57	K5		5 ^m .01	91	298 ^m	2.4			2.68		-14 ^s
4605	777					5 ^m .10	54	74				4.8		
3155	α Virginia	0 ^m .1	+9 18	G5	5 ^m .1	4 24	231	280 ^m	29.0	21	(4)	0.6	241	+69 ^s
4608	2583				Y ¹	4 28	-141	170		19		6.0		
3160	γ Crucis	1 ^m .7	-64 3	F0		4 ^m .90	46	180 ^m	1 9.4			2.6		-2 ^s
4616	2148					4 ^m .42	-1 45	12						
3162	Contauri	2 ^m .9	-50 6	B5		4 ^m .81	30	261 ^m	1 16	8	(1)	0.7	264	+12 ^s
4618	2813					4 ^m .90	-6	29		8		2.2		
3165	δ Contauri	3 ^m .2	-50 10	B3p	4 ^m .0	2 88	43	240 ^m	Var	15	(1)	-1.2	264	+12 ^s
4621	6697					3 ^m .07	1	43	1 9	15		1.1		
3166	α Corvi	3 ^m .3	-24 10	F2	5 ^m	4 18	93	122 ^m	+4.6	42	(2)	2.3	260	+37 ^s
4623	10174				Y ¹	4 28	+81	-45		42		4.0		
3172	γ Corvi	5 ^m .0	-22 4	K0	5 ^m .9	3 21	65	276 ^m	4.4	28	(6)	0.5	259	+39 ^s
4630	3187				Y ¹	3 26	-37	51		28		2.3		
3176	ρ Centauri	6 ^m .4	-51 48	B3		4 20	49	243 ^m	+21	13	(2)	0.1	264	+10 ^s
4638	6455					4 32	+5	+49		15		2.7		
3187	δ Crucis	9 ^m .8	-58 12	B3	3 ^m .0	3 08	48	246 ^m	+26	13	(2)	1.0	266	+4 ^s
4656	4189					3 25	+3	+48		15		1.5		
3190	δ Ursae maj.	10 ^m .5	+57 35	A2	2 ^m .7	3 44	110	89 ^m	-12	41	(6)	1.5	99	+59 ^s
4660	1363				Y ¹	3 58	-26	-107		40		3.7		
3191	γ Corvi	10 ^m .7	-16 59	B8	3 ^m .0	2 78	160	274 ^m	Var	42	(1)	0.9	261	+44 ^s
4662	3424				W	2 08	-90	+133	-4.2	42		3.8		
3197	ρ Muscae	12 ^m .1	-67 24	Mb		4 16	237	259 ^m	+7.2	44	(m)	2.3	267	-5 ^s
4674	1931					4 29	-21	+237				6.0		
3199	χ Chamaeleont.	12 ^m .5	-78 45	B5		4 38	49	284 ^m	+23	16	(1)	0.4	269	-17 ^s
4674	741					4 49	-20	+45		16		2.8		
3200	ζ Crucis	13 ^m .0	-63 26	B3		4 26	50	247 ^m	+19	16	(2)	0.3	267	-1 ^s
4679	2235					4 37	+4	+50		16		2.8		
3203	θ Centauri	13 ^m .6	-54 35	Ma		4 58	94	241 ^m	-6.9					+7 ^s
4682	5113					5 00	+11	+93				4.9		

Note 3162, 3165. Probably a wide double.

12^h.

1	2	3	4	5	6	7	8	9	10	11	12	13	14	15
3210 4689	η Virginis 2926	14 ^m .8	— 0° 7'	A0	3 ^o .0 W	4 ^m .00 4.21	67 — 11	248° + 66	Var + 7	25 24	(2)	0.9 3.1	257°	+61°
3216 4697	11 Comae Ber 2592	15.6	+18 21	K0	5 ^o .5 Y ^a	4.91 4.87	139 —122	303° + 65	+42.4	15 14	(4)	0.6 5.6	242	+78
3218 4700	ϵ Crucis 4188	15.9	—59 51	K2	7.0	3.57 3.73	199 —133	292° +147	— 4.8				267	+ 2
3224 4707	12 Comae Ber 2337	17.5	+26 24	F5	4 ^o .1 Y ^a	4.78 4.92	13 + 8	205° + 11	Var + 1.9	36 36	(1)	2.6 0.8	200	+84
3230 4716	5 Canum Ven 1626	19.2	+52 7	K0	4 ^o .3 Y ^a	4.97 4.96	11 — 4	52° — 10	—13.4	11 11	(3)	0.2 0.2	97	+65
3237 4730	α^1 Crucis 2745	21.0	—62 33	B1		1.58 1.86	47 + 17	228° + 44	Var ? —12.2	18 17	(5)	—2.1 —0.1	268	— 1
3238 4731	α^2 Crucis 2745	21.1	—62 32	B1	2 ^o .3	2.09 2.37	49 — 1	251° + 49	Var ? + 0.3			—1.6 +0.5	268	— 1
3242 4737	γ Comae Ber 2288	22.0	+28 49	K0	5 ^o .2 Y ^a	4.56 4.52	122 + 40	225° +116	+ 4.0	13 10	(6)	—0.4 5.0	163	+85
3245 4743	σ Centauri 7115	22.6	—49 40	B3		4.16 4.27	47 + 10	233° + 46	+12	14 14	(2)	—0.1 2.5	267	+12
3256 4757	δ or δ^2 Corvi 3482	24.7	—15 58	A0	3 ^o .5 YG ¹	3.11 3.31	251 + 18	235° +251	— 4.	22 18	(2)	—0.6 5.1	264	+46
3263 4763	γ Crucis 5272	25.6	—56 33	Mb	6 ^o .9	1.61 1.90	273 +259	176° + 90	+21.4			3.8	268	+ 5
3263 4764	γ Crucis 5272	25.6	—56 33	A2		6.68 6.84							268	+ 5
3269 4773	γ Muscae 1336	26.5	—71 35	B5		4.04 4.14	46 0	253° + 46	+14	15 15	(2)	—0.1 2.3	269	—10
3272 4775	η Corvi 3489	26.9	—15 38	F0	5 ^o .2 Y ¹	4.42 4.54	444 —164	261° +413	— 5	45 45	(3)	2.7 7.7	266	+46
3279 4785	β Canum Ven 2321	29.0	+41 54	G0	5 ^o .0 Y ¹	4.32 4.43	758 —508	292° +561	+ 6.1	109 110	(4)	4.5 8.7	99	+75
3280 4786	β Corvi 3401	29.1	—22 51	G5	4 ^o .8 Y ^a	2.84 2.93	61 + 52	180° + 32	— 7.1	26 26	(3)	—0.1 1.8	266	+39
3281 4787	κ Draconis 703	29.2	+70 20	B5p	2 ^o .2 W	3.88 4.08	60 — 10	276° + 59	Var. —11.4	7 6	(4)	—2.2 2.8	92	+48
3283 4789	23 Comae Ber. 2475	29.9	+23 11	A0	2 ^o .7 W	4.78 5.03	72 — 39	276° + 60	—23.	12 12	(5)	0.2 4.1	244	+83
3284 4794	24 ¹ Comae Ber. 2684	30.1	+18 56	A3	—1° BV ^a	6.72 —	19 — 19	325° + 2		9 9	(2)	—0.3 1.4	257	+80
3285 4792	24 ² Comae Ber. 2684	30.1	+18 56	K0	5 ^o .9 O ²	5.18 4.98	16 — 12	14° — 11	+ 3.7	11 11	(1)	0.4 1.2	257	+80
3289 4798	α Muscae 1702	31.2	—68 35	B3	2 ^o .8	2.94 3.13	42 + 8	240° + 41	+18	13 13	(4)	—1.5 1.0	269	— 7
3292 4802	τ Centauri 7745	32.3	—47 59	A2		4.02 4.15	27 + 7	228° + 26	+ 5.	9 9	(1)	—1.2 1.2	269	+14
3298 4813	χ Virginis 3452	34.1	— 7 27	K0	6 ^o .0 Y ^a	4.78 4.74	85 — 8	244° + 84	—19.7	14 14	(2)	0.5 4.4	267	+55
3300 4817	1 Centauri 7748	34.4	—39 26	B8		4.79 4.94	63 + 14	227° + 61	+15				268	+23
3302 4819	γ Centauri 7597	36.0	—48 25	A0	3 ^o .8	2.38 2.59	200 — 82	266° +182	— 8	17 17	(2)	—1.5 0.9	269	+14
3307 4825	γ Virginis 2601	36.6	— 0 54	F0	3 ^o .6 Y ¹	3.65 3.92	564 —299	271° +479	—19.8			2.8 7.4	268	+61
3307 4826	γ Virginis 2601	36.6	— 0 54	F0	3 ^o .3 Y ^a	3.68 3.95	564 —299	271° +479	—20.0	67 65	(8)	1.8 7.8	268	+61
3309 4828	ϵ Virginis 2486	36.8	+10 47	A0	2 ^o .5 W	4.95 5.14	135 +132	138° — 28	0:	13 13	(5)	0.5 5.6	267	+73

Boss 3263 Binary? — Boss 3284, 3285 A binary included on basis of its total magnitude 4.95 (RHP) — Boss 3307 Visual binary with a period of about 180 years

12^h to 18^h.

1	2	3	4	5	6	7	8	9	10	11	12	13	14	15
3311	w Centauri	37 ^m .1	-48° 16'	K0		4 ^m .05	129	238 ^m	11.7	13	(1)	0.2 269	+14 ^m	
4831	7608					4.76	11	128		11		5.2		
3319	Centauri	39.7	-60 26	K0		4.68	128	129 ^m	8.9	21	(1)	1.0 270	+2	
4842	4273					4.79	111	58		24		1.2		
3320	μ Muscae	40.1	-67 34	B1		3.26	11	234	4.2	13	(5)	1.7 270	0	
4844	2004					3.44	10	38		10		1.3		
3322	Y Canum Ven	40.4	+45 59	Nb		1.0 to 1.05	8	55 ^m	1.4	0		1.0	+72	
4846	1817			Vm										
3324	Centauri	40.6	-55 50	B3		4.86	55	223 ^m	116.7	16	(2)	0.9 270	+6	
4848	5215					4.95	19	52		16		3.6		
3328	μ Centauri	41.9	-59 9	B1	2.7	1.50	56	210 ^m	120.0	13	(5)	2.3 271	+1	
4853	1451					1.77	5	56		11		0.4		
3351	α Centauri	47.5	-48 24	K2		4.35	103	253 ^m	0.2	18	(1)	0.9 271	+14	
4888	7753					4.48	22	101		18		3.4		
3352	α Centauri	47.9	-39 18	A5		4.14	77	120 ^m	2			2.2	+22	
4889	7801					4.50	67	37				1.8		
3357	λ Crucis	48.7	-58 36	B3		4.84	51	219 ^m	110	15	(2)	0.9 271	+3	
4897	4584					4.94	21	46		15		3.4		
3358	μ Crucis	48.8	-56 38	B3		4.26	46	248 ^m	111.9	11	(2)	0.8 271	+5	
4898	5487					4.37	4	16		11		2.1		
3359	μ Crucis	48.8	-56 37	B3p		5.46	27	231 ^m	119			0.8 271	+5	
4899	5487						5	26				2.6		
3362	γ Virginis	49.2	-9 0	Mb	7.1	4.91	32	279 ^m	172.0	9	(3)	0.4 271	+53	
4902	3449					13	4.92	12		9		2.4		
3363	α Ursae maj	49.6	+56 30	A0p	17.9	1.68	115	98 ^m	8.0	51	(7)	0.1 28	+61	
4905	1627					2.03	25	112		49		2.0		
3367	δ Virginis	50.6	+3 56	M4	07.6	3.66	479	262 ^m	17.9	18	(3)	0.2 277	+65	
4910	8660					7.65	187	441		17		7.1		
3370	α Canum Ven	51.4	+38 52	A0p	37	5.39	236	282 ^m	18			0.2 78	+78	
4914	8680				O1		118	204				4.7		
3371	α Canum Ven	51.4	+38 52	A0p	27.9	2.90	237	281 ^m	18	31	(5)	0.2 78	+78	
4915	8680				Y1	3.05	114	200		29		4.7		
3374	36 Comae Ber	54.9	+17 57	M4	67.7	4.96	36	62 ^m	1.7	11	(4)	0.2 286	+79	
4920	8688				O1	4.87	31	10		11		2.7		
3377	λ Muscae	55.4	-71 1	K2		3.63	264	97 ^m	136.1	26	(1)	0.1 271	-9	
4923	1848					7.79	137	227		20		5.8		
3382	78 Ursae maj.	56.5	+56 55	F0	3.4	4.89	101	103 ^m	9	35	(7)	2.6 83	+61	
4931	1408				OY1	5.08	14	95		35		4.9		
3383	γ Virginis	57.2	+11 30	K0	57.0	2.95	273	273 ^m	11.5	29	(4)	0.2 284	+73	
4932	2529				Y1	1.02	145	212		28		5.1		
3390	1 Centauri	0.4	-47 56	B3		4.96	59	221 ^m	19	16	(2)	1.0 273	+14	
4940	8048					5.04	17	57		16		3.8		
3393	γ Centauri	1.0	-49 22	B3		4.40	42	235 ^m	Var.	13	(2)	0.0 273	+13	
4942	7644					4.52	3	42	14.3	13		2.5		
3401	41 Comae Ber.	2.4	+28 10	K5	67.4	4.90	89	164 ^m	16.3	12	(3)	0.3 3	+86	
4954	2185				OY1	4.91	88	9		12		4.7		
3409	δ Virginis	4.8	-5 0	A0	27.7	4.44	37	223 ^m	0	17	(5)	0.3 281	+56	
4963	3430				W	4.60	14	55		15		3.2		
3412	α Comae Ber.	5.1	+18 4			5.22	450	286 ^m	17.5			4.6 298	+78	
4968	2697			P5	47.0	5.30	302	333		77	(1)	4.5		
3412	α Comae Ber.	5.1	+18 4		Y1	5.22				77		4.6 298	+78	
4969	2697					5.30						8.5		
3419	Centauri	6.0	-59 23	B8		4.76	61	236 ^m	Var.	18	(2)	1.0 273	+3	
4975	4815					4.85	4	61		18		3.7		
3421	Centauri	6.5	-37 16	O5		4.89	390	274 ^m	15.8	24	(1)	4.8 275	+23	
4979	8437					4.94	242	308		24		7.8		

Don 3358, 3359. A binary: 36^m, 17^m = Don 3370, 3371. A binary: 20^m, 20^m = Don 3412. Wolfswarte binary with a period of 83.9 years, its total magnitude is 4^m.47 (RMP).

18^h.

1	2	3	4	5	6	7	8	9	10	11	12	13	14	15
24	β Comae Ber	7 ^m .2	+28° 23'	G0	3 ^s .9	4 ^m .32	1184	317°	+ 5.4	112	(4)	4.5	3° +84°	
83	2193				YG ¹	4.44	-1101	+ 126		109		9.7		
29	η Muscae	8.5	-67 22	B8		4.95	32	234°	Var	9	(2)	-0.3	273 - 5	
93	2224					5.04	+ 4	+ 32	+ 5	9		2.5		
37	Muscae	10.5	-66 15	K0		4.78	35	193°	-10.3				273 - 4	
102	2142					4.90	+ 26	+ 23				2.5		
46	σ Virginis	12.6	+ 6 0	Ma	6 ^s .9	5.01	16	305°	-26.7	5	(1)	-1.7	291 +66	
115	2722				OY ⁸	4.93	- 15	+ 7		5		1.0		
47	20 Canum Ven	13.1	+41 6	F0	3 ^s .5	4.66	125	272°	+ 8.7	10	(4)	-0.6	66 +75	
117	2780				Y ¹	4.87	- 35	+ 120		9		5.1		
148	δ Virginis	13.2	-17 45	G5	4 ^s .6	4.80	1529	225°	- 8.0	125	(4)	5.2	280 +43	
119	3813				Y ²	4.84	+ 260	+ 1498		122		10.7		
149	γ Hydrae	13.5	-22 39	G5	5 ^s .0	3.33	83	128°	- 5.6	28	(5)	0.1	280 +38	
120	3554				OY ²	3.41	+ 80	- 24		26		2.9		
152	ϵ Centauri	15.0	-36 11	A2	4 ^s .5	2.91	+ 353	255°	0				278 +25	
128	8497					3.13	- 127	+ 328				5.7		
156	Centauri	16.1	-60 27	B3		6.51	26	233°	- 7				274 + 2	
134	4627					6.81	- 2	+ 26				3.6		
157	ζ Centauri	16.2	-60 28	B5		4.62	39	241°	+26	11	(2)	0.5	274 + 2	
135	4627					4.72	- 2	+ 39		11		2.3		
164	η Centauri	17.2	-64 1	G0		4.50	50	142°	+12.1				274 - 2	
141	2732					4.62	+ 50	- 6				3.0		
463	ϵ Muscae	17.2	-74 22	K0		4.96	203	222°	+28.8	14	(a)	0.7	273 -12	
142	1057					5.06	+ 73	+ 189				6.5		
474	ζ Ursae maj	19.9	+55 27	A0p	1 ^s .9	2.40	130	103°	Var	44	(12)	0.6	77 +62	
1054	1598				W	2.64	+ 36	- 125	- 9.9	44		3.0		
475	ζ Ursae maj	19.9	+55 26	A0	G ²	3.96	136	105°	-11			2.2	77 +62	
1055	1598					4.20	+ 42	- 129				4.6		
476	α Virginis	19.9	-10 38	B2	1 ^s .6	1.21	55	229°	Var	23	(4)	-2.2	285 +50	
1056	3672				W	1.52	+ 6	+ 54	+ 1.6	21		-0.8		
	ω Centauri	20.8	-46 47	-	3 ^s .5	4.4	-	-		0.14	(1)	-9.9	277 +15	
480	η Ursae maj	21.2	+55 30	A5	3 ^s .2	4.02	123	102°	-12	37	(7)	1.8	78 +61	
1062	1603				OY ¹	4.19	+ 32	- 119		36		4.5		
1482	69 Virginis	22.1	-15 27	K0	5 ^s .6	4.89	127	276°	-13.7			2.7	285 +46	
1068	3668				Y ²	4.85	- 85	+ 94				5.4		
1491	R Hydrae	24.2	-22 46	Md	7 ^s .6	Var	73	273°	- 4.0				283 +38	
1080	3601				OR ⁸	3.9	-10.1	- 47	+ 56					
1496	δ Centauri	25.2	-38 54	K0		3.96	29	211°	- 3.1				279 +22	
1089	8592					4.01	+ 71	+ 27				1.3		
1499	ι Virginis	26.8	- 5 45	Ma	7 ^s .3	4.83	112	243°	+18.5	11	(4)	0.0	291 +54	
1095	3714				O ²	4.79	- 13	+ 111		11		5.1		
1506	ν Virginis	29.1	+ 4 10	A2p	2 ^s .4	4.93	52	127°	- 8.0	18	(7)	1.1	298 +63	
1505	2764				W	5.14	+ 48	- 19		17		3.5		
1508	ζ Virginis	29.6	- 0 5	A2	3 ^s .4	3.44	288	277°	-13	36	(3)	1.2	295 +60	
1507	3076				W	3.62	- 184	+ 222		36		5.7		
1511	Canum ven	30.3	+37 42	F0	3 ^s .7	4.96	850	103°	Var	33	(3)	2.5	46 +75	
1510	2426				Y ¹	5.11	+ 38	- 76	+62	32		4.6		
1512	Canum ven	30.4	+49 32	A3	3 ^s .3	4.63	118	277°	-18	17	(4)	0.8	71 +66	
1518	2227				W	4.88	- 26	+ 114		17		5.0		
1527	24 Canum ven	33.0	+36 48	F0	3 ^s .4	4.92	104	278°	Var	27	(6)	1.8	41 +75	
1521	2433				Y ¹	5.05	- 41	+ 96	- 6	24		5.0		
1521	ϵ Centauri	33.5	-52 57	B1	2 ^s .8	2.56	41	229°	+ 6	11	(4)	-2.2	278 + 8	
15132	6655					2.77	+ 3	+ 41		11		0.6		
1536	83 Ursae maj	36.9	+55 12	Ma	7 ^s .0	4.75	28	242°	-16.9	10	(3)	-0.3	73 +61	
15154	1625				O ²	4.68	+ 13	+ 25		10		2.0		
15444	ι Centauri	40.0	-32 33	F5		4.36	489	252°	-23	61	(1)		284 +27	
15168	9603					4.47	- 176	+ 455		61		7.8		

Boss 3456, 3457 Binary: 60'', 343° — Boss 3474, 3175 Binary: 14'', 150°, member of Ursa Major Cluster — Boss 3191 Long period variable, period 114 days

18^h to 14^h.

1	2	3	4	5	6	7	8	9	10	11	12	13	14	15
547 172	M Centauri 8017	40 ^m .4	-50° 56'	K0		4 ^m .68 4 .79	32 + 27	176° + 18	Var. - 5.8	14 14	(1)	0.4 2.2	280° +10°	
558 185	τ Bootis 2782	42 .5	+17 57	F5	3 ^s .8 Y ¹	4 .51 4 .65	487 -229	273° +429	-15.7	71 67	(6)	3.7 7.9	328 +73	
564 190	ν Centauri 8171	43 .5	-41 11	B2		3 .53 3 .71	42 - 3	234° + 42	+ 8.8	9 8	(4)	-1.9 1.6	283 +19	
566 191	η Urae maj. 8087	43 .6	+49 49	B3	1 ^s .3 W	1 .91 2 .21	119 - 57	260° +104	-16	16 10	(4)	-3.1 2.3	66 +65	
567 192	g Centauri 9358	43 .6	-33 58	Mb		4 .40 4 .43	72 + 12	220° + 71	+40.8	54	(a)	3.1 3.7	285 +26	
565 193	μ Centauri 8172	43 .6	-41 59	B2p		3 .32 3 .51	28 0	230° + 28	+12.6	7 7	(1)	-2.5 0.5	282 +18	
572 200	ν Bootis 2564	44 .6	+16 17	K5	6 ^s .4 OY ²	4 .28 4 .18	106 - 73	288° + 76	- 6.3	46 31	(3)	1.7 4.4	324 +70	
577 210	k Centauri 9676	46 .0	-32 30	B5		4 .72 4 .86	66 - 0	230° + 60	+13.8	15 15	(2)	0.3 3.5	285 +27	
578 211	k Centauri 9676	46 .0	-32 30			6 .17 6 .31	17 + 4	80° - 16	+ 1.2			0.3 0.6	285 +27	
584 219	Canum Ven 8488	47 .4	+34 57	Ma	6 ^s .9 O ³	4 .96 4 .91	44 + 30	212° + 32	-43.6	10 10	(4)	0.0 3.2	29 +73	
586 221	h Centauri 10729	47 .5	-31 26	B5		4 .76 4 .91	28 + 4	221° + 28	+ 5.2			2.0	287 +29	
589 226	l Draconis 963	48 .5	+63 13	Ma	7 ^s .2 OY ²	4 .77 4 .74	4 + 2	135° - 3	-10.7	8 8	(6)	-0.7 -2.2	78 +51	
593 231	ε Centauri 8949	49 .3	-46 48	B2p	3 ^s .2	3 .06 3 .01	82 0	230° + 82	Var	16 15	(4)	-0.5 2.6	282 +13	
596 235	η Bootis 1788	49 .9	+18 54	G0	3 ^s .8 Y ^{1,2}	2 .80 3 .00	373 +306	190° +213	Var. - 0.2	105 100	(4)	2.8 5.7	334 +72	
599 241	Centauri 3070	50 .4	-63 11	K0		4 .68 4 .79	63 + 18	215° + 60	+22.2	15 15	(1)	0.6 3.7	278 - 2	
602 248	φ Centauri 8329	52 .2	-41 36	B3		4 .05 4 .21	34 - 2	233° + 34	+ 7.4	9 9	(1)	-1.2 1.7	284 +18	
603 249	ν ¹ Centauri 9010	52 .5	-44 19	B3		4 .17 4 .18	46 + 2	226° + 46	+ 7	12 12	(2)	-0.4 2.5	283 +16	
610 260	ν ² Centauri 8040	53 .4	-45 7	F5		4 .39 4 .57	41 + 21	198° + 35	Var - 1:			2.5	283 +14	
612 264	τ Virginis 2761	56 .6	+ 2 2	A2	3 ^s .0 Y ¹	4 .34 4 .51	32 + 32	141° - 3	- 5	20 18	(5)	0.6 1.9	308 +58	
615 267	β Centauri 5365	56 .8	-59 53	B1	2 ^s .6	0 .86 1 .14	41 + 8	219° + 40	Var -12	18 16	(5)	-3.1 -1.1	279 + 1	
621 285	χ Centauri 8405	59 .9	-40 42	B3		4 .54 4 .69	38 + 13	208° + 36	+12.1	9 9	(2)	-0.7 2.4	286 +19	
622 287	π Hydrae 10095	0 .7	-26 12	K0	6 ^s Y ²	3 .48 3 .54	166 +149	165° + 73	+27.1	38 37	(3)	1.3 3.6	291 +33	
623 288	θ Centauri 9260	0 .8	-35 53	K0	6 ^s .5	2 .26 2 .32	750 + 38	225° + 750	+ 1.8	59 59	(4)	2.3 6.6	288 +23	
626 291	α Draconis 878	1 .7	+64 51	A0p	2 ^s .1 W	3 .64 3 .84	54 - 3	286° + 54	Var -16.0	22 22	(3)	0.4 2.3	76 +51	
628 297	Centauri 7028	3 .3	-52 57	K0		4 .78 4 .90	189 - 23	235° +187	-17.0	18 18	(1)	1.1 6.2	283 + 7	
633 303	η Apodis 706	5 .7	-80 32	A2p		4 .97 5 .06	88 + 39	208° + 79	Var - 9			4.7	273 -20	
635 304	δ Bootis 2737	5 .8	+25 33	F5	3 ^s .8 Y ¹	4 .82 5 .00	76 + 60	198° + 47	Var + 9.8	27 27	(3)	2.0 4.2	359 +70	
639 313	Virginis 2887	7 .2	+ 2 53	A0p	2 ^s .4 W	4 .90 5 .18	60 - 3	239° + 60	Var + 3	12 12	(2)	0.3 3.8	314 +57	

14^h.

1	2	3	4	5	6	7	8	9	10	11	12	13	14	15
3642	α Virginis	7 ^m ,6	- 9° 48'	K0	6 ^o ,5	4 ^m ,31	130	3°	- 4,0	35	(4)	1,8	302°	+46°
5315	3878				Y ⁸	4 30	- 96	87		31		4,9		
3649	4 Ursae min	9,2	+78 1	K0	6 ^o ,3	5,00	38	313°	+10	17	(4)	1,0	84	+39
5321	478				OY ²	4,95	- 11	+ 36		16		2,9		
3652	α^1 Bootis	9,9	+52 16			6,61	67	140°	-23,2			3,7	62	+61
5328	1782				3 ^o ,5	6,82	+ 43	52				5,7		
3654	α^2 Bootis	9,9	+52 16	A5	R ¹	4,60	69	103°	-14,9	26	(6)	1,5	62	+61
5329	1782				YG ¹	4,81	+ 11	66		26		3,6		
3660	ϵ Virginis	10,8	- 5 31	F5	4 ^o ,3	4,16	427	183°	+11,5	37	(3)	1,9	307	+49
5338	3843				YG ²	4,26	- 320	+ 282		36		4,6		
3661	δ Octantis	10,9	-83 13	K2		4,14	93	262°	+ 5,0	19	(1)	0,5	273	-22
5339	557					4,28	- 44	+ 82		19		4,0		
3662	α Bootis	11,1	+19 42	K0	4 ^o ,7	0,24	2282	209°	- 5,4	138	(5)	0,5	344	+68
5340	2777				OY ³	0,14	+1369	+1826		115		7,0		
3667	ϵ Bootis	12,6	+51 50	A5	3 ^o ,9	4,78	169	300°	-17	26	(1)	1,9	61	+60
5350	1784				Y ¹	4,98	- 74	+ 152		26		5,9		
3666	λ Bootis	12,6	+46 33	A0	2 ^o ,6	4,26	238	309°	- 5	31		1,5	52	+63
5351	1949				W	4,43	- 152	+ 183		29	(4)	6,1		
3668	ϵ Lupi	13,0	-45 36	B3		4,10	12	228°	+22	3	(1)	-3,5	286	+13
5354	9084					3,99	- 1	+ 12		3		-0,5		
3670	ν Centauri	13,3	-55 56	B5		4,41	32	229°	+ 4,6	8	(2)	-1,1	283	+ 4
5358	5984					4,54	- 2	+ 32		8		4,0		
3672	λ Virginis	13,7	-12 55	A2	3 ^o ,2	4,60	32	316°	Var	18	(1)	0,9	302	+43
5359	4018				W	4,75	- 32	+ 2	- 7,2	18		2,1		
3673	A Bootis	13,8	+35 58	K0	5 ^o ,5	4,83	16	256°	Var.	24	(3)	1,6	28	+68
5361	2408				Y ^{1,3}	4,87	+ 1	+ 16	-25,6	23		0,9		
3680	ψ Centauri	14,5	-37 26	A0		4,17	72	257°	- 4				290	+22
5367	9336					4,34	- 38	+ 61				3,5		
3681	20 Bootis	15,0	+16 46	K0	6 ^o ,0	4,97	155	289°	- 7,3	18	(2)	1,3	339	+65
5370	2637				Y ²	4,99	- 110	+ 110		18		5,9		
3682	Centauri	15,5	-58 0	G0		5,06	50	277°	+18,4				282	+ 2
5371	6619					5,08	- 39	+ 32				3,4		
3688	α Centauri	16,8	-39 3	B5		4,55	49	215°	+ 8,7				290	+19
5378	9320					4,70	+ 8	+ 48				3,0		
3689	κ Hydrae	17,4	-27 18	K2	6 ^o -7°	4,93	231	238°	+19,9	13	(3)	0,5	295	+30
5381	9803				Y ³	4,91	- 49	+ 226		13		6,7		
3692	Bootis	18,5	+ 8 54			6,64	72	250°	Var	13	(2)	2,4	324	+60
5385	2882				2 ^o ,3	6,82	- 14	+ 71		13		6,1		
3692	Bootis	18,5	+ 8 54	A0	W	5,11						0,7	324	+60
5386	2882					5,29						5,8		
3699	τ^1 Lupi	19,7	-44 46	B3		4,65	30	197°	-17,7				288	+14
5395	9322					4,77	+ 14	+ 26				1,9		
3700	τ^2 Lupi	19,8	-44 56	F8		4,49	20	171°	- 1,2	7	(1)	-1,3	288	+14
5396	9323					4,64	+ 16	+ 12		7		1,0		
3704	θ Bootis	21,8	+52 19	F8	4 ^o ,4	4,06	471	210°	-11,2	68	(6)	3,3	59	+59
5404	1804				Y ¹	4,25	+ 433	+ 184		68		7,4		
3707	ι Hydrae	22,4	-29 3	B8	2°	5,00	42	217°	+ 6	11	(2)	0,2	295	+28
5407	10712				W	5,18	+ 6	+ 42		11		3,1		
3710	ϕ Virginis	23,0	- 1 47	K0	5 ^o ,0	4,97	134	266°	- 9,4	36	(1)	2,8	314	+51
5409	2957				Y ²	4,98	- 72	+ 143		36		5,6		
3716	σ Lupi	25,9	-50 1	B2		4,60	54	256°	- 2	12	(1)	0,0	287	+ 9
5425	8831					4,69	+ 18	+ 50		12		3,3		
3717	ρ Bootis	27,5	+30 49	K0	5 ^o ,4	3,78	149	318°	-13,8	26	(4)	0,8	14	+66
5429	2628				Y ²	3,77	- 131	+ 70		25		4,6		
3718	5 Ursae min	27,7	+76 8	K2	6 ^o ,4	4,37	21	35°	+10,5	18	(2)	0,7	82	+40
5430	527				Y ²	4,36	- 21	- 2		18		1,0		
3722	γ Bootis	28,1	+38 45	F0	2 ^o ,9	3,00	182	323°	-35	63	(4)	1,9	34	+65
5435	2565				YG ¹	3,23	- 158	+ 91		60		4,3		

Boss 3652, 3654 Is doubtless a physical system (ADS 9173) The dynamic parallax is 0'',021 - Boss 3692 Binary, ADS 9247 6'',4, 190° (1925). The fainter star is itself a binary. 0'',2, 283° (1926). The close pair has a period of 40,5 years

144.

1	2	3	4	5	6	7	8	9	10	11	12	13	14	15
3724	η Centauri	29 ^m .2	- 41° 43'	H3p	3 ^s .4	2 ^m .05	49	224 ⁿ	0	14	(1)	1.6	201	16 ⁿ
5410	8917			A2p		2.85	1	10		14		1.1		
3720	α Ikwella	30.1	+ 30 11	I-0	1 ^s .0	4.48	228	58 ⁿ	0.2	41	(4)	2.5	12	160
5417	2536				Y ¹	1.66	71	217		40		0.4		
3732	ρ Lupi	31.2	- 49 0	H5		4.14	51	221 ⁿ	1.14	13	(2)	0.4	288	9
5453	9198					4.25	0	51		13		2.7		
3735	α^1 Centauri	32.8	- 60 25	I-0		0.11	1680	281 ⁿ		773	(6)	4.5	284	1
5459	5483					0.21	1138	1050		780		8.1		
3733	α^2 Centauri	32.8	- 60 25	K5	5 ^s .0	1.70	1680	281 ⁿ	- 22.2			0.2	284	1
5460	5483					1.61	1138	1050				0.6		
3739	α Circini	34.4	- 64 12	I-0		1.41	217	185 ⁿ	1	7.1	(6)	2.1	282	6
5463	2977					1.56	1	18 ⁿ		60		5.4		
3745	α Lupi	35.3	46 58	H2	3 ^s .5	2.80	15	417 ⁿ	1	7	(4)	2.1	290	11
5469	9501					2.76	1	15		9		0.6		
3746	α Aquarii	35.4	- 78 17	K5		1.81	33	215 ⁿ	1	0.2	(1)	0.0	276	- 18
5470	803					1.97	1	12		17		1.4		
3747	η Centauri	35.7	- 37 21	H3		4.09	44	204 ⁿ	1	9	(2)	0.7	294	20
5471	9618					4.26	1	42		11		2.1		
3749	α^1 Bootis	36.0	+ 16 51	A0	2 ^s .4	4.94	16	81 ⁿ	- 3	16	(4)	0.8	344	61
5475	8768				W	5.08	1	15		15		1.0		
3750	α^2 Bootis	36.0	+ 16 51	A0	1 ^s	5.81						1.7	344	61
5476	8768				R ¹	5.95								
3752	ζ Bootis	36.4	+ 14 9			4.84	61	116 ⁿ	- 3.	20	(7)	1.2	339	50
5477	2770			A2	2 ^s .5		1	35		19		1.8		
3752	ζ Bootis	36.4	+ 14 9		Y ¹	4.43						0.8	339	59
5478	2770													
3757	α^1 Centauri	37.5	- 34 44	K0		4.11	207	201 ⁿ	- 38.7			296	21	
5485	9668					4.16	1	191				5.7		
3758	μ Virginis	37.8	- 5 13	F5	4 ^s .0	3.95	139	162 ⁿ	- 1	4	(4)	2.2	315	47
5487	3936				Y ¹	4.05	1	115		44		0.6		
3759	α^2 Centauri	38.8	- 34 46	A0		5.08	16	161 ⁿ	- 5			297	21	
5489	9888					5.15	+	16				1.0		
3761	β Bootis	39.0	+ 26 57	M4	6 ^s .6	4.93	20	191 ⁿ	+	5.2	(3)	- 0.8	5	+ 63
5490	8413				O ¹	4.91	+	11		7		1.8		
3770	α Bootis	40.5	+ 17 23	K0	5 ^s .6	4.69	83	221 ⁿ	- 9.6	17	(2)	0.8	345	+ 60
5502	2780				OY ¹	4.75	+	30		17		4.3		
3771	α Bootis	40.6	+ 27 30	A0		5.12			- 18.8			1.8	7	+ 63
5505	2417				4 ^s .3									
3771	α Bootis	40.6	+ 27 30	K0	B ¹	2.70	49	280 ⁿ	- 16.4	23	(6)	- 0.6	7	+ 63
5506	2417				OY ¹	2.65	-	22		22		1.1		
3772	109 Virginis	41.2	+ 2 19	A0	2 ^s .7	3.76	120	252 ⁿ	- 9	24	(3)	0.6	323	+ 51
5511	2862				W	3.98	-	40		23		4.2		
3781	β Hydrae	44.5	- 27 32	K2	7 ^s	4.63	230	254 ⁿ	- 9.9	28	(2)	2.2	301	+ 27
5526	10073				O ¹	4.62	-	112		33		6.6		
3783	ρ Lupi	45.1	- 43 9	D5		4.49	50	225 ⁿ	+	7.0	(3)	0.1	293	+ 14
5528	9391					4.64	-	4		13		3.0		
3784	α^1 Librae	45.2	- 15 35	I-5	3 ^s	5.33	131	235 ⁿ	- 24.1	100	(1)	5.3	308	+ 37
5530	3965				R ¹	5.42	-	22		100		3.9		
3787	α^2 Librae	45.3	- 15 38	A3	3 ^s .0	2.90	128	231 ⁿ	Var	47	(1)	1.3	308	+ 37
5531	3966				Y ¹	3.10	-	18		47		3.4		
3798	ζ Bootis	46.8	+ 19 31	G5	5 ^s .3	4.80	168	129 ⁿ	+	4.2	(8)	4.5	352	+ 60
5544	2870				OY ¹	4.72	+	151		104		5.7		
3809	β Ursae min.	51.0	+ 74 34	K5	6 ^s .1	2.24	30	286 ⁿ	+	16.9	(4)	0.3	79	+ 40
5563	595				OY ¹	2.30	+	12		29		- 0.4		
3814	δ Librae	52.0	- 3 56	F0	3 ^s .5	4.59	192	211 ⁿ	+	24	(3)	2.1	320	+ 45
5570	3696				Y ¹	4.74	+	56		32		6.0		

Boes 3749, 3750. This pair (ADS 9338) is probably a physical one. μ^1 , 105^1 (1933). Dynamic parallax is $0''.015-0''.023$. — Boes 3752. Winkler's binary ADS 9343. Dynamic parallax $0''.019$. Period 120 years. Eccentricity of the orbit greater than that of any other double star for which the elements have been derived. — Boes 3752. Zinnman gives the total magnitude of this pair as 4^m.05. — Boes 3764. Boes not to be a variable. — Boes 3771. Henry (ADS 9378) α^1 , β^1 , γ^1 (1938). The Dynamic parallax is $0''.008-0''.019$. The total magnitude is 3.19 (RHP). — Boes 3784, 3787. May be a wide physical pair although the parallaxes differ considerably.

14^h to 15^h.

1	2	3	4	5	6	7	8	9	10	11	12	13	14	15
3815	β Lupi	52 ^m .0	-42° 44'	B2p		2 ^m .81	69	223°	0	14	(4)	-1.5	294°	+13°
5571	9853					3.02	-5	+69		14		2.0		
3818	α Centauri	52.7	-41 42	B3	4 ^s .5	3.35	36	208°	+9.1	9	(4)	-1.9	295	+14
5576	9342					3.55	7	+35		9		1.2		
3825	δ Librae	55.6	-8 7	A0	2 ^s .7	4.84	69	261°	Var	14	(1)	0.6	317	+41
5586	3938				W	5.1-6.3	-39	+57	-45.0	11		4.0		
3827	Uisae min	56.0	+66 20	Mb	7 ^s .1	4.86	82	293°	Var	8	(4)	-0.6	70	+46
5589	878				O ²	4.79	+8	+81	+6.8	8		4.4		
3834	ω Bootis	57.7	+25 24	K5	6 ^s .4	4.93	58	187°	+13.5	13	(1)	0.5	3	+59
5600	2861				OY ³	5.09	+52	+26		13		3.8		
3835	110 Virginis	57.9	+2 28	K0	5 ^s .8	4.62	50	268°	-16.7	16	(1)	0.6	327	+48
5601	2905				Y ^{2.5}	4.64	-30	+40		16		3.1		
3836	β Bootis	58.2	+40 47	G5	4 ^s .9	3.63	63	227°	-19.9	21	(4)	0.1	34	+59
5602	2840				Y ²	3.68	+43	+46		20		2.6		
3837	α Librae	58.2	-24 53	Mb	7 ^s	3.41	94	234°	-4.0	25	(2)	0.3	305	+28
5603	11834				O ⁰	3.50	-23	+91		24		3.3		
3838	τ Lupi	58.3	-46 40	B5		4.72	40	215°	+16			-0.3	293	+9
5605	9773					4.85	-1	+40				2.7		
3838	π Lupi	58.3	-46 40	K0		4.82	19	118°	-3.1	10	(2)	-0.2	293	+9
5606	9773					4.95	+19	-3		10		1.2		
3842	η Bootis	0.2	+27 20	K0	5 ^s .9	4.67	178	264°	-26.2	16	(3)	0.7	7	+59
5616	2447				Y ^{2.5}	4.63	-30	+174		16		5.9		
3847	ι Bootis	0.5	+48 3	G0	5 ^s .1	4.86	387	274°	-25.6	76	(6)	4.2	46	+56
5618	2259				Y ²	4.96	+39	+383		75		7.9		
3852	γ Lupi	2.1	-44 54	B3		4.39	31	230°	+18	7	(2)	-1.4	294	+10
5626	9889					4.45	-7	+30		7		1.8		
3862	κ^1 Lupi	5.0	-48 21	B9		4.14	121	237°	+3	29	(1)	1.5	293	+7
5646	9704					4.25	-44	+113		29		4.5		
3863	κ^2 Lupi	5.0	-48 22	A0		6.04	116	245°	0			293	+7	
5647	9705						-58	+100				6.3		
3864	ζ Lupi	5.1	-51 43	K0		3.50	127	237°	-9.8	17	(1)	-0.4	291	+4
5649	8830					3.66	-46	+118		17		4.0		
3865	ϵ Lupi	6.1	-44 8	B3		4.92	51	230°	Var.			296	+11	
5651	9932					5.06	-12	+49	+11			3.5		
3866	ι Librae	6.5	-19 25	A0p	2 ^s -3 ^s	4.66	61	217°	-14	13	(3)	0.2	311	+31
5652	4047				YG ¹	4.82	+3	+61		13		3.6		
3871	ι Lupi	8.5	-31 9	F0		4.95	18	167°	-22.8			304	+21	
5660	11813					5.07	+14	+12				1.3		
3876	ϵ Circini	9.2	-63 15	K0		4.84	9	186°	-4.6			286	-6	
5666	3544					4.95	+4	+8				-0.4		
3880	β Circini	9.6	-58 26	A3		4.16	178	214°	+9			289	-1	
5670	5875					4.28	+5	+178				5.4		
3879	γ Liang Aust	9.6	-68 19	A0	4 ^s .3	3.06	67	249°	0			283	-10	
5671	2383					3.23	-36	+56				2.2		
3887	δ Bootis	11.5	+33 41	K0	4 ^s .6	3.54	155	144°	-12.6	25	(4)	0.4	20	+57
5681	2561				Y ²	3.60	+136	-73		24		4.5		
3888	μ Lupi	11.5	-47 31	B8		4.36	59	212°	+15	15	(2)	0.2	295	+7
5683	9860					4.46	+3	+59		15		3.2		
3890	β Librae	11.6	-9 1	B8	2 ^s .4	2.74	103	253°	Var	26	(1)	-0.2	320	+38
5685	3936				G ¹	2.96	-49	+90	-37	26		2.8		
3891	ι Lupi	11.7	-29 47	K0	6 ^s	4.43	27	228	-3.3	11	(3)	-0.4	305	+22
5686	11630				OY ²	4.46	-5	+26		11		1.6		
3896	δ Lupi	14.8	-40 17	B2	3 ^s .5	3.43	33	192°	+2	9	(2)	-1.8	300	+13
5695	9538					3.61	+13	+30		9		1.0		
3901	γ Circini	15.4	-58 58	B5-F8		4.54	43	193°	-17	11	(2)	-0.3	289	-3
5704	5908					4.64	+15	+40		11		2.7		
3903	η^1 Lupi	15.5	-35 54	K5		3.59	138	226°	-29.8	25	(1)	0.6	302	+16
5705	10236					3.65	-26	+135		25		4.3		

Boss 3838 Doubtful if a physical pair — Boss 3847 Visual binary (ADS 9491), period 205 years The companion 6^m.1, 3^s.38, 245° 3 (1926) is Boss 3846 and has very near the same p m as the principal The dynamic parallax is 0^s.082

15h.

1	2	3	4	5	6	7	8	9	10	11	12	13	14	15
3905	π Lupi	15 ^m 9	-44 ^o 20'	B3	3 ^s 5	1 ^m 74	28	215 ^s	Var	8	(1)	1.7 209'	1 10 ^s	
5708	10066					1 76	1	28	1 45	8		0.9		
3910	ϕ^1 Lupi	16 8	-36 30	B3		4 09	38	215 ^s	1	9	(2)	0.5 101	1 15	
5712	10103					4 85	0	18		9		2.0		
3921	κ Lupi	18 8	-38 22	A0		4 08	61	251 ^s	1			0.1	1 14	
5724	10289					4 81	37	1 49				1.0		
3926	μ^1 Librae	20 7	1 37 44	F0	3 ^s 0	4 47	169	197 ^s	- 8.0	10	(4)	2.2 47	1 55	
5733	2636				Y ¹	4 06	70	1 50		10		8.6		
3927	μ^1 Librae	20 7	1 37 42	K0	3 ^s	6 06	172	104 ^s	0 1			4.4 27	1 55	
5734	2637				VR ¹	6 85	180	1 14 1				7.8		
3928	γ Ursae min	20 9	1 72 11	A2	2 ^s 2	1 14	17	115 ^s	Var	41	(1)	1.1 75	4 41	
5735	679				W	1 44	0	17	3.9	41		0.7		
3936	ϵ Draconis	22 7	1 59 19	K0	5 ^s 5	1 47	10	111 ^s	10.9	11	(4)	0.9 59	1 48	
5744	1654				Y ¹	1 47	7	7		10		1.5		
3940	β Coronae Bor.	23 7	+29 27	F0p	7 ^s 1	1 72	190	204 ^s	23	12	(6)	0.8 12	4 54	
5747	2670				Y(G) ¹	1 88	112	1 54		20		5.1		
3947	α Fraug. Aust	27 6	-65 59	K0		4 11	75	164 ^s	14.4	27	(1)	1.1 206	- 9	
5771	3102					4 24	50	1 50		27		6.5		
3949	μ^1 Librae	28 2	1 41 14	A2	2 ^s 5	4 08	27	236 ^s	24	20	(2)	1.4 12	1 51	
5774	2611				Y(G) ¹	5 20	18	1 20		19		2.1		
3950	γ Lupi	28 5	-40 50	B3	4 ^s 5	2 95	39	204 ^s	1 0	15	(3)	-1.5 301	+ 11	
5776	9760					3 13	1	5	1 39	11		0.9		
3952	37 Librae	28 7	- 9 43	K0	5 ^s 7	4 83	180	110 ^s	+48.5	42	(1)	1.0 123	+ 34	
5777	4171				Y ¹	4 81	1 389	0		42		7.8		
3953	δ Coronae Bor	28 9	+31 42	B3	2 ^s 7	4 17	37	225 ^s	-16	12	(1)	0.4 17	+ 53	
5778	2750				W	4 40	1 22	1 30		12		2.0		
3954	δ Lupi	29 0	-44 37	B3		4 84	39	189 ^s	1 8	9	(1)	0.4 299	+ 8	
5781	10239					4 87	1 15	1 36		0		2.8		
3959	γ Librae	29 9	- 14 27	K0	5 ^s 7	4 02	65	91 ^s	-27.0	20	(2)	0.5 120	+ 32	
5787	4237				UY ¹	4 03	+ 52	- 91		20		6.1		
3960	δ Berpentia N	30 0	1 10 53	F0	6 ^s	5 16	48	255 ^s	- 14			2.2 145	+ 47	
5788	5881				Y(G) ¹	5 46						4.0		
3960	δ Berpentia N	30 0	1 10 53	F0	3 ^s 4	4 21	66	262 ^s	-38	29	(12)	1.3 145	+ 47	
5789	5881				W	4 43	- 46	1 50		26		3.1		
3961	α Coronae Bor	30 5	+27 3	A0	2 ^s 1	2 31	138	130 ^s	+ 0.4	47	(9)	0.7 9	+ 31	
5793	2512				W	2 53	+ 131	- 88		47		1.3		
3962	μ Librae	30 9	-27 48	K2	7 ^s	3 78	10	241 ^s	-24.7	14	(2)	0.7 310	+ 20	
5794	10464				OY ¹	3 80	- 4	1 9		24		1.2		
3964	μ Lupi	31 3	-42 14	K3		4 37	171	391 ^s	- 4.4	21	(1)	1.1 301	+ 10	
5797	10601					4 35	-168	+ 32		21		5.5		
3973	ϵ Librae	32 6	-29 27	B3	3 ^s	3 80	41	216 ^s	Var	10	(2)	1.2 309	+ 20	
5812	11817				W	3 99	- 2	1 41	0 1	10		1.9		
3978	μ Lupi	33 5	-34 5	K0		4 63	15	127 ^s	-21.8	18	(1)	0.9 306	+ 16	
5820	10831					4 64	1 15	1		18		0.5		
3980	μ Lupi	34 3	-44 20	F5		4 69	124	215 ^s	- 7			3.00	+ 8	
5825	10310					4 75	- 29	+ 324				7.2		
3988	ϵ^1 Coronae Bor	35 6	+36 58		1 ^s	6 00	26	149 ^s	-23	9	(1)	0.8 25	+ 52	
5833	8668				B ¹	6 18	+ 21	- 15		9		3.1		
3988	ϵ^1 Coronae Bor.	35 6	+36 58	B8	2 ^s 4	5 07			-28.6			-0.2 25	+ 52	
5834	8668				W	5 23								
3990	μ Librae	36 2	-19 21	K3	7 ^s 0	4 96	459	318 ^s	Var.	10	(2)	0.0 317	+ 27	
5838	4188				OY ¹	4 94	- 55	+ 454	- 4.9	10		8.3		
3991	μ^1 Lupi	36 3	-34 23	B3		4 82	49	221 ^s	Var.	12	(1)	0.2 307	+ 15	
5839	10494					4 95	- 8	+ 48	+ 8.5	12		3.3		
3994	ϵ Berpentia	37 1	+20 0	A2	2 ^s 4	4 49	91	232 ^s	Var.	13	(3)	0.1 359	+ 49	
5842	3138				W	4 75	+ 19	+ 89	-17.4	13		4.3		

3922 A wide physical pair (ADM 9622). The fainter star is itself a binary $\delta_{1,2}$ 1^m 41, 41^s 1 (1931.6). Period 221 years. The dynamic parallax of 1N. is 1^m 022. — 3960 — ADM 9701 Dynamic parallax 0^m 036 — 0^m 041 — 3961 — Betelgeuse binary. Period 1.236 days.

15^h.

1	2	3	4	5	6	7	8	9	10	11	12	13	14	15
998	γ Coronae Bori	38 ^m ,5	+26° 37'	A0	2 ^s ,6	3 ^m ,93	105	287°	Var	22	(6)	0,6	9°	+51°
849	2722				YG ¹	4,05	—	59	+87	—10,4	22	4,0		
1001	α Serpentis	39,3	+6 44	K0	5 ^s ,3	2,75	—	46	252°	+3,0	49	(5)	1,2	342 +42
854	3088				Y ⁸	2,84	—	12	+45		49	1,0		
1009	β Serpentis	41,6	+15 44	A2	2 ^s ,6	3,74	—	91	127°	—7	25	(6)	0,7	354 +47
867	2911				Y ¹	3,89	+	86	—30		25	0,3		
1010	γ Serpentis	41,6	+7 40	G0	4 ^s ,4	4,42	—	244	129°	—66,1	97	(4)	3,6	344 +43
868	3023				Y ^{1,5}	4,57	—	100	+222		98	6,4		
1015	κ Serpentis	44,2	+18 27	K5	6 ^s ,7	4,19	—	110	204°	—39,3	14	(4)	0,0	357 +47
879	3074				O ⁸	4,19	+	68	+87		14	4,5		
1016	μ Serpentis	44,4	—3 7	A0	2 ^s ,8	3,63	—	92	252°	—11	29	(3)	0,9	333 +36
881	4052				W	3,80	—	48	+79		29	3,4		
1018	χ Lupi	44,6	—33 19	B9		4,11	—	29	198°	Var	7	(1)	—1,7	309 +15
883	10754					4,27	+	6	+28		7	1,4		
1019	b Scorpii	45,0	—25 27	B3	2 ^s	4,77	—	42	213°	—10	10	(3)	—0,2	314 +21
5885	11131				W	4,93	—	3	+42		10	2,9		
1024	δ Coronae Bori	45,4	+26 23	G5	5 ^s ,0	4,73	—	110	222°	—19,3	25	(4)	1,5	8 +49
889	2737				Y ²	4,77	+	57	+95		23	4,9		
1026	ϵ Serpentis	45,8	+4 47	A2	3 ^s ,2	3,75	—	136	66°	—9,8	37	(4)	1,6	341 +41
892	3069				W	3,95	+	46	—128		37	4,4		
1030	β Triang. Aust.	46,3	—63 7	F0	5 ^s ,1	3,01	—	538	210°	+1	90	(1)	2,8	289 —8
5897	3723					3,18	—	0	+538		90	6,7		
1031	η Serpentis	46,9	+21 17	K5	6 ^s ,6	4,88	—	49	270°	—62,6	13	(3)	0,5	1 +47
5899	2829				OY ⁸	4,87	—	21	+45		13	3,3		
1032	κ Coronae Bori	47,5	+35 59	K0	5 ^s ,9	4,77	—	364	182°	—25,0	28	(5)	1,9	24 +49
5901	2052				OY ^{1,5}	4,88	+	364	+7		27	7,6		
1035	ζ Ursa min	47,6	+78 6	A2	2 ^s ,4	4,34	—	25	97°	Var	25	(2)	1,3	79 +36
5903	527				W	4,53	—	18	—17		25	1,3		
1034	A Scorpii	47,6	—25 2	B3	3 ^s	4,66	—	34	200°	—12	9	(2)	—0,6	315 +20
5904	12352				Y ¹	4,83	+	6	+33		9	2,3		
1039	θ Librae	48,1	—16 27	K0	5 ^s ,2	4,34	—	156	40°	+3,4			3,3	322 +27
5908	4174				Y ⁸	4,32	+	16	—154			5,3		
1042	χ Herculis	49,2	+42 44	G0	4 ^s ,4	4,61	—	760	35°	—55,8	77	(5)	4,0	34 +49
5914	2648				Y ²	4,76	—	707	—274		76	9,0		
1049	ξ ¹ Lupi	50,5	—33 40	A0		5,37	—	56	157°	—10		2,2	309 +14	
5925	10826					5,52	+	44	+35			4,1		
1050	ξ ² Lupi	50,5	—33 40	A0		5,73	—	56	145°	—12	24	(a)	2,6	309 +14
5926	10826					5,88	+	50	+25			4,5		
1052	η Scorpii	50,7	—28 55	B3	4 ^s	4,02	—	33	203°	+2,8	9	(3)	—1,2	313 +17
5928	11714				Y ¹	4,19	+	4	+33		9	1,6		
1055	γ Serpentis	51,8	+15 59	F5	4 ^s ,4	3,86	—	1332	167°	+6,9	99	(5)	3,8	355 +44
5933	2849				Y ²	3,99	+	1207	+829		96	9,5		
1059	48 Librae	52,6	—13 59	B3p		4,68	—	34	206°	—14	9	(1)	—0,6	324 +27
5941	4302					4,88	+	5	+34		9	2,3		
1062	π Scorpii	52,8	—25 50	B2	2 ^s —3 ^s	3,00	—	39	203°	Var.	11	(4)	—1,8	315 +19
5944	11228				YG ¹	3,20	+	5	+39	—3,0	11	1,0		
1063	ϵ Coronae Bori	53,4	+27 10	K0	5 ^s ,6	4,22	—	109	231°	—31,8	23	(3)	1,0	10 +48
5947	2558				OY ⁸	4,23	+	45	+99		23	4,4		
1064	η Lupi	53,4	—38 6	B3		3,61	—	44	203°	+7	11	(2)	—1,2	307 +10
5948	10797					3,80	+	1	+44		11	1,8		
1066	δ Scorpii	54,4	—22 20	B0	2 ^s —3 ^s	2,54	—	41	198°	—19,2	11	(3)	—2,3	318 +22
5953	4068				G ¹	2,77	+	9	+40		11	0,6		
	F Coronae Bori	55,3	+26 13	Mb Nova		2,0	—	13	32°	—5	1,5	(3)	—7,1	10 +47
	2765					10,3	—	7	—10			—2,4		
4072	Draconis	55,4	+55 2	A5	3 ^s ,3	4,96	—	193	304°	Var.	28	(2)	2,1	52 +46
5960	1793				Y ¹	5,18	+	4	+193	—5,7	27	6,4		

15^h to 16^h.

1	2	3	4	5	6	7	8	9	10	11	12	13	14	15
4071	ϵ^1 Normae	55 ^m .4	-57° 29'	A2		4 ^m .87	147	229°	-18:				294	-1
5961	7500					4.96	-57	-135					5.7	
4073	η Normae	55.8	-48 57	G5		4.74	30	106°	-0.3	16	(1)	0.8	300	+1
5962	10512					4.86	-29	5		16		2.1		
4076	Lupi	56.8	-38 19	B5		4.97	44	217°	0:	11	(2)	0.2	307	+10
5967	10832					5.13	-7	43		11		3.2		
4080	ϵ Coronae Bor.	57.4	+30 7	A0	2 ^m .3	4.91	45	238°	Var.	14	(4)	0.6	15	+47
5971	2738				W	5.20	-17	42		14		3.2		
4081	π Serpentis	57.9	+23 4	A2	2 ^m .4	4.82	17	25°	Var.	18	(3)	1.1	5	+46
5972	2886					5.06	-12	12	-30.1	18		1.0		
4082	ξ^1 Scorpii	58.9	-11 6		4 ^m - 5"	5.07						3.2	328	+28
5977	4237			F8	Y ^a	5.16								
4083	ξ^2 Scorpii	58.9	-11 6		5 ^m .0	4.77	71	241°	-33.6	42	(5)	2.0	328	+28
5978	4237				Y ^a	4.86	-32	63		42		4.0		
4084	δ Normae	59.5	-44 54	A3p		4.84	17	3°	-15.5	14	(4)	0.6	303	+4
5980	10625					4.98	-7	16				0.9		
4089	ν Herculis	59.6	+46 19	B9	2 ^m .3	4.64	89	140°	+5.5	11	(2)	-0.2	39	+47
5982	2142				W	4.91	-40	79		11		4.4		
4086	β^1 Scorpii	59.6	-19 32		1 ^m - 2"	2.90	31	201°	Var.	8	(4)	-2.6	321	+22
5984	4307			B1	G ¹	3.13	-1	31	-4.3	8		0.3		
4087	β^2 Scorpii	59.6	-19 32		1 ^m	5.06	34	223°	-4.3			-0.4	321	+22
5985	4307				V ^a	5.29	-7	33				2.7		
4090	ψ Draconis	0.0	+58 50	F8	4 ^m .3	4.11	458	318°	-8.5	77	(4)	3.5	57	+44
5986	1608				Y ^{1a}	4.22	-72	452		75		7.4		
4091	θ Lupi	0.0	-36 32	B3		4.33	41	211°	+15	10	(2)	-0.7	308	+10
5987	10642					4.48	-4	41		10		2.4		
4093	ω^1 Scorpii	1.0	-20 24	B2	2 ^m .8	4.13	34	192°	-8	9	(2)	-1.1	321	+22
5993	4405				YG ¹	4.29	+11	32		9		1.8		
4095	ω^2 Scorpii	1.6	-20 36	G0	5 ^m .1	4.58	70	143°	-5.2	12	(1)	0.0	320	+21
5997	4408				Y ^a	4.67	+64	27		12		3.8		
4108	ϵ Coronae Bor.	5.3	+36 45	K0	5 ^m .4	4.94	325	349°	-17.0	43	(6)	2.7	26	+46
6018	2699				Y ^a	4.93	-312	94		36		7.5		
4109	δ^1 Apodis	5.4	-78 27	Mb		4.78	42	207°	-12.0				280	-20
6020	1092					4.90	-1	42				2.9		
4110	δ^2 Apodis	5.5	-78 25	K5		5.22	32	175°	-10.2				280	-20
6021	1093					5.32	+16	27				2.7		
4112	φ Herculis	5.6	+45 12	B9p	2 ^m .5	4.26	32	221°	-15.4	16	(3)	0.3	37	+46
6023	2376				W	4.46	-48	165		15		1.8		
4116	ν^1 Scorpii	6.2	-19 12	A	3 ^m	6.49	-12	189°				1.7	322	+22
6026	4332				BV ^a	6.67	-1	12				1.0		
4117	ν^2 Scorpii	6.2	-19 12	B3	3 ^m	4.29	34	200°	Var.	12	(3)	-0.5	322	+22
6027	4333				Y ¹	4.34	+5	34	-6.5	11		1.9		
4115	ϵ^2 Scorpii	6.1	-27 40	B3	3 ^m	4.70	47	216°	+9:	10	(3)	-0.3	315	+16
6028	10841				W	4.85	-8	47		10		3.1		
4118	δ Triang. Aust.	6.4	-63 26	G0		4.03	18	171°	-5.1				291	-10
6030	3854					4.16	+10	15				0.3		
4119	ν Scorpii	6.6	-9 48	A2	2 ^m .8	4.91	27	189°	-7.9	18	(1)	1.2	330	+27
6031	4324				W	5.11	+11	25		18		2.1		
4134	δ Ophiuchi	9.1	-3 26	Ma	6 ^m .9	3.03	161	198°	-19.9	31	(5)	0.5	337	+31
6056	3903				O ^a	3.05	+47	155		31		4.1		
4135	γ^1 Normae	9.6	-49 49	F8p		5.00	7	236°	-18.5	-1	(1)		300	-1
6058	10474					5.12	-4	6				0.7		
4143	δ Scorpii	12.1	-28 22	A0	3 ^m	4.87	114	197°	-12.4				317	+14
6070	12037				W	5.08	+16	113				5.2		
4145	γ^2 Normae	12.4	-49 55	K0		4.14	182	253°	-28.8				301	-1
6072	10536					4.27	-140	116				5.4		

Boes 4082, ADS 9909. Well observed binary with a period of 45 years. Dynamic parallax 0".045. — Boes 4086, 4087. Doubtless a physical system. ADS 9913. — Boes 4093, 4095. Forms possibly a physical pair in spite of the differences in p. m., rad. vel. and parallax. — Boes 4109, 4110. Very likely a physical system. — Boes 4116, 4117. Probably a physical system (ADS 9951) 2".08, 49°.6 (1925.0). Dynamic parallax 0".007.

16^h

1	2	3	4	5	6	7	8	9	10	11	12	13	14	15
147	ϵ Ophiuchi	13 ^m ,0	- 4° 27'	K0	5 ^h ,1	3 ^m ,34	86	68°	- 9,8	31	(3)	0,7	337°	+30°
175	4086				Y ¹	3,39	+ 48	- 71		30		3,0		
155	σ Scorpi	14,6	-23 56	A3	6 ^h	4,76	42	199°	- 8,5	16	(2)	0,6	320	+16
3081	12849				OY ¹	4,92	+ 5	+ 42		15		2,9		
158	σ Scorpi	15,1	-25 21	B1	3 ^h	3,08	34	200°	Var	9	(4)	-2,2	320	+16
3084	11485				W	3,28	+ 3	+ 34	- 3,2	9		0,7		
162	τ Herculis	16,7	+46 33	B5	2 ^h ,4	3,91	32	338°	-13,8	13	(1)	-0,5	40	+44
3092	2169				W	4,13	- 20	+ 25		13		1,4		
163	σ Serpentis	17,0	+ 1 16	F0	3 ^h ,7	4,80	172	285°	-46	29	(5)	2,1	342	+32
3093	3215				Y ¹	4,96	-159	+ 64		29		6,0		
165	γ Herculis	17,5	+19 23	F0	3 ^h ,7	3,79	62	309°	-43	29	(5)	1,0	2	+40
3095	3086				Y ¹	3,95	- 59	+ 20		28		2,8		
166	ζ Triang. Aust.	17,6	-69 52	G0		4,93	228	63°	Var				287	-15
3098	2558					5,05	+150	-171	+ 8,5			6,7		
168	γ Apodis	18,1	-78 40	K0		3,90	141	237°	+ 5,1	20	(1)	0,4	280	-21
3102	1103					4,05	- 79	+117		20		4,7		
169	ξ Coronae Bor.	18,2	+31 7	K0	5 ^h ,4	4,72	132	314°	-29,7	17	(5)	0,9	18	+43
3103	2845				Y ²	4,84	-102	+ 84		17		5,3		
170	ψ Ophiuchi	18,3	-19 49	K0	5 ^h ,4	4,59	66	196°	+ 0,2	13	(1)	0,2	323	+19
3104	4365				Y ²	4,58	+ 11	+ 65		13		3,7		
173	ν^1 Coronae Bor.	18,6	+34 2	Ma	7 ^h ,1	5,36	49	174°	-13,6	11	(1)	0,6	22	+43
3107	2773				OY ³	5,35	+ 49	- 6		11		3,8		
175	ν^2 Coronae Bor.	18,7	+33 56	K5	7 ^h ,0	5,28	55	4°	-39,8	12	(1)	0,7	22	+43
3108	2771				OY ³	5,39	- 55	- 3		12		4,1		
180	ϵ Normae	19,8	-47 20	B5		4,71	10	217°	Var	2	(1)	-3,8	304	\pm 0
3115	10765					4,80	- 3	+ 10	-12	2		-0,3		
182	ω Herculis	20,8	+14 16	A0p	2 ^h ,9	4,53	79	146°	- 7	20	(3)	1,0	357	+37
3117	3049				W	4,76	+ 78	+ 9		20		4,0		
183	χ Ophiuchi	21,2	-18 14	B3p	3 ^h	4,85	31	188°	Var	8	(3)	-0,6	326	+20
3118	4282				W	5,01	+ 10	+ 29	- 8,1	8		2,4		
189	ν Ophiuchi	22,4	- 8 9	A2	2 ^h ,8	4,68	84	276°	-30,8	23	(1)	1,5	334	+26
3129	4243				W	4,84	- 76	+ 34		23		4,3		
192	η Draconis	22,6	+61 44	G5	5 ^h ,1	2,89	62	343°	-14,2	40	(5)	0,9	59	+40
3132	1591				Y ²	2,96	- 22	+ 58		39		1,8		
193	α Scorpi	23,3	-26 13	Ma	7 ^h ,2	1,22	34	192°	Var	15	(5)	-3,1	320	+14
3134	11359			A3	OR ³	1,35	+ 6	+ 33	- 3,0	14		-1,1		
198	22 Scorpi	24,1	-24 54	B3	2 ^h	4,87	28	188°	- 5	7	(3)	-0,9	321	+14
3141	12695				W	5,02	+ 7	+ 27		7		2,1		
4200	N Scorpi	24,8	-34 29	B3		4,33	26	200°	Var	6	(2)	-1,8	314	+ 8
3143	11044					4,49	+ 1	+ 26	+ 0,4	6		1,4		
4201	g Herculis	25,4	+42 6	Mb	7 ^h ,4	5,02	28	130°	+ 3,3	5	(1)	-1,7	33	+43
3146	2714				O ³	4,7-5,5	+ 8	- 27		5		2,2		
4202	φ Ophiuchi	25,4	-16 23	K0	5 ^h ,1	4,40	66	236°	-34,4	12	(3)	-0,2	328	+20
3147	4298				Y ²	4,42	- 34	+ 57		12		3,5		
4204	β Herculis	25,9	+21 42	K0	5 ^h ,1	2,81	107	257°	-25,8	27	(4)	-0,2	7	+39
3148	2934				Y ³	2,92	- 31	+103		25		3,0		
4203	λ Ophiuchi	25,9	+ 2 12	A0	2 ^h ,6	3,85	97	210°	Var	20	(5)	-0,3	344	+31
3149	3118				W	4,02	+ 9	+ 97	-15,9	15		3,8		
4206	ω Ophiuchi	26,2	-21 15	F0	2 ^h	4,57	33	39°	+ 2,5	24	(3)	1,5	324	+17
3153	4381				Y ¹	4,69	+ 9	- 32		24		2,2		
4212	h Herculis	27,9	+11 42	K5	6 ^h ,9	4,92	204	245°	+ 3,1	7	(4)	-0,9	355	+35
3159	3008				O ³	4,91	- 75	+190		7		6,5		
4213	A Draconis	28,2	+68 59	B8p	2 ^h ,4	4,98	42	325°	Var	11	(4)	0,2	68	+37
3161	860				Y ¹	5,20	+ 3	+ 42	- 9,1	11		3,1		
4215	β Apodis	28,8	-77 18	K0		4,16	451	220°	-28,9				282	-20
3163	1221					4,29	-153	+424				7,5		

Boss 4173, 4175. Seem not to form a physical pair. Have been included on basis of equally large parallaxes — Boss 4193 Antares radial velocity undergoes slight changes which seem to be real. No variations in the light of this star have been discovered so far — Boss 4203 Well known binary = ADS 10087. The period seems to be around 150 years. The dynamic parallax is 0",022-0",038

10^h to 17^h.

1	2	3	4	5	6	7	8	9	10	11	12	13	14	15
4218 u165	r Scorpii 17016	29 ^m .7	--28 ^m 4'	110	2 ^h 1 ^m W	2 ^m .91 1.11	39 4	107" 50	1.1	10	(1)	2.1	119	12 ^m
4219 6166	H Scorpii 17119	29 .8	--35 3	Mn		4 .80 4 .33	41 40	120" 7	1.2	10	(1)	0.7	114	7
4220 6168	o Hercules 2724	30 .9	+42 39	A0	2 ^m .6 W	1.25 4.45	37 27	343" 25	0			2.1	11	41
4225 6175	l Ophiuchi 4350	31 .7	-10 22	110	2 ^m .8 W	2.70 2.91	21 3	15" 21	20	8	(2)	2.4	114	22
4246 6212	z Hercules 2884	37 .5	+31 47	G0	4 ^m .4 Y ¹	3.00 3.13	604 388	310" 463	71	91	(6)	2.7	20	39
4250 6217	α Triang. Aust. 2822	38 .1	-68 51	K2	6 ^m .8	1.88 2.16	42 24	148" 21	3.4	30	(2)	0.7	280	--16
4255 6220	η Hercules 3029	39 .5	+39 7	K0	5 ^m .1 Y ¹	3.61 3.66	101 76	100" 67	1.8, 0	30	(4)	1.0	29	+40
4259 6223	g Draconis 1145	40 .2	-1 64 47	K0	6 ^m .0 Y ¹	5.00 4.93	17 5	167" 16	1 0.3	21	(1)	1.6	62	+38
4265 6229	η Aras 6906	41 .1	-58 52	K5	3 ^m .68 Y ¹	3.68 3.84	57 46	143" 34	1 9.7	29	(1)	1.0	297	-10
4270 6237	Draconis 1708	43 .4	+56 58	F0	4 ^m .0 Y ¹	4.88 5.04	62 54	26" 10	0	11	(2)	2.5	52	+39
4272 6241	ε Scorpii 11285	43 .7	-34 7	K0	5 ^m .9	2.30 2.47	667 520	248" 420	2.3	46	(2)	0.7	117	+5
4273 6243	20 Ophiuchi 4394	44 .3	-10 36	F5	4 ^m .0 Y ¹	4.73 4.81	133 116	141" 61	0.5	41	(2)	2.8	335	+19
4277 6247	μ ¹ Scorpii 11033	45 .1	-37 51	B1p	2 ^m .0	3.09 3.46	31 2	191" 31	Var.	9	(4)	2.1	114	+3
4281 6252	μ ² Scorpii 11037	45 .6	-37 51	B2		3.61 3.92	34 40	214" 11	1.2	7	(4)	2.1	114	+3
4284 6254	52 Hercules 2220	46 .3	+46 10	A2p	2 ^m .8 W	4.86 5.05	76 41	163" 64	1 0.8	21	(3)	0.6	38	+39
4287 6262	ζ ¹ Scorpii 11633	47 .0	-42 12	B1p		4.88 5.02	20 11	163" 17	26			3.1	0	
4292 6271	ζ ² Scorpii 11646	47 .6	-42 12	K5		3.75 3.82	206 51	207" 261	--18.8	17	(1)	-0.1	311	0
4302 6281	τ Ophiuchi 3092	49 .3	+10 20	B8	2 ^m .1 W	4.29 4.51	73 19	231" 71	Var.	19	(3)	0.6	356	+29
4304 6285	ζ Aras 7766	50 .3	-55 50	K5	7 ^m .5	3.06 3.25	47 11	209" 40	-6.1	21	(2)	-0.3	300	-9
4313 6295	ε ¹ Aras 10878	51 .6	-53 0	K2		4.15 4.28	4 4	284" 0	+24.4	19	(1)	0.3	303	-8
4315 6299	α Ophiuchi 3298	52 .9	+9 32	K0	5 ^m .7 Y ¹	5.42 5.41	295 -236	267" 177	--56.2	39	(3)	1.3	356	+28
4322 6315	η Draconis 1157	55 .4	+65 17	F5	5 ^m .7 Y ¹	4.82 4.96	252 -244	70" 55	Var.	64	(4)	3.9	62	+36
4323 6318	30 Ophiuchi 4215	55 .8	-4 4	K0	6 ^m .7 Y ¹	5.00 4.08	103 16	211" 102	-0.7	14	(3)	0.7	343	+21
4327 6322	α Urane min. 498	56 .2	+82 12	G5	5 ^m .6 Y ¹	4.40 4.41	15 14	94" 0	Var.	7	(2)	1.4	82	+31
4328 6324	α Hercules 2947	56 .5	+31 4	A0	2 ^m .7 W	3.92 4.14	51 24	295" 45	Var.	24	(3)	0.8	20	+35
4334 6334	κ Scorpii 11706	58 .2	-33 59	B1p		4.87 5.03	7 7	82" 3	+10			3.16	+3	
4346 6355	60 Hercules 3142	0 .7	+12 53	A3	2 ^m .6 YG ¹	4.91 5.09	56 54	108" 16	-3.2	19	(3)	1.3	0	+28
4360 6378	η Ophiuchi 4467	4 .6	-15 36	A2	3 ^m .3 W	2.63 2.86	93 13	23" 92	-1.2	30	(3)	-0.1	334	+12

Does 4246. Well-known binary — Does 4277, 4281. Certainly a physical pair — Does 4287, 4293. Does not seem to be a physical pair. — Does 4315. Variable 4m, 1—3m, 0 photographs.

17^h.

1	2	3	4	5	6	7	8	9	10	11	12	13	14	15
4361	η Scorpii	5 ^m .0	-43° 6'	F2		3 ^m .44	295	175°	-28.4				312°	-3°
6380	11485					3.56	+ 86	+ 283				5.8		
4368	ζ Diaconis	8.5	+65 50	B5	2 ^s .2	3.22	21	327°	-14.5	18	(4)	-0.8	63	+35
6396	1170				W	3.45	+ 6	+ 23		16		0.1		
4370	36 Ophiuchi	9.2	-26 27		6'	5.33	1235	202°	-0.2	158	(1)	6.3	326	+6
6401	12026				Y ³	5.32	- 198	+ 1223				10.8		
4371	36 Ophiuchi	9.2	-26 27	K0	6'	5.29	1224	203°	-0.6	158		6.3	326	+6
6402	12026				Y ³	5.28	- 208	+ 1200				10.7		
4373	α^1 Herculis	10.1	+14 30	Mb	7 ^s .0	3.32	30	336°	-32.6	9	(7)	-2.5	3	+27
6406	3207				O ³	3.52	- 25	- 17		7		0.7		
4374	α^2 Herculis	10.1	+14 30	G	5 ^s	5.39	32	349°	-38.0			-0.1	3	+27
6407	3207				BG ²	5.43	- 22	- 23				2.8		
4376	δ Herculis	10.9	+24 57	A2	2 ^s .5	3.16	165	188°	Var	38	(5)	1.1	14	+30
6410	3221				G ¹	3.41	+ 127	+ 106	-39	38		4.3		
4379	41 Ophiuchi	11.5	-0 20	K5	5 ^s .7	4.82	65	204°	Var	17	(4)	1.0	348	+19
6415	3255				Y ³	4.82	- 6	+ 65	-2.6	17		3.9		
4380	ζ Apodis	11.5	-67 40	K2		4.74	38	290°	+12.6				291	-18
6417	3310					4.85	- 37	- 6				2.6		
4381	τ Herculis	11.6	+36 55	K5	6 ^s .0	3.36	25	265°	-25.7	22	(4)	0.1	28	+33
6418	2844				Y ³	3.32	+ 14	+ 21		22		0.3		
4388	68 u Herculis	13.6	+33 12	B3	1 ^s .9	Var	24	237°	Var	5	(a)		23	+32
6431	2864				W	5.01-5.5	+ 17	- 17	-21.2					
4391	ϵ Herculis	14.2	+37 24	A2	2 ^s .2	4.80	66	323°	-10	19	(2)	1.2	28	+33
6436	2864				G ¹	4.89	- 22	+ 62		19		3.9		
4394	ξ Ophiuchi	15.0	-21 1	F5	4 ^s	4.46	315	131°	-9.2	65	(a)		331	+7
6445	4731				Y ¹	4.55	+ 274	+ 151				7.0		
4395	ι Serpentis	15.2	-12 45	A0	3 ^s .7	4.35	36	87°	+7	21	(2)	1.0	338	+12
6446	4722				YG ¹	4.51	+ 35	- 10		21		2.2		
4399	θ Ophiuchi	15.9	-24 54	B3	2 ^s	3.37	31	182°	-1	7	(3)	-2.4	328	+5
6453	13292				W	3.57	+ 5	+ 31		7		0.9		
4406	β Aiao	17.0	-55 26	K2	7 ^s .0	2.80	36	204°	-0.8	17	(2)	-1.1	303	-12
6461	8100					3.01	- 9	+ 35		17		0.6		
4405	γ Aiae	17.0	-56 17	B1	2 ^s .5	3.51	13	189°	-4	4	(2)	-3.5	302	-12
6462	8225					3.67	0	+ 13		4		-0.9		
4419	ρ Herculis	20.2	+37 14		3 ^s	5.47	34	273°	-20			0.0	28	+31
6484	2878				R ¹		+ 8	+ 33				3.1		
4419	ρ Herculis	20.2	+37 14	A0	2 ^s .2	4.52	+ 38	264°	-21	12	(4)	-1.0	28	+31
6485	2878				G ¹		+ 15	+ 35		8		2.4		
4420	b Ophiuchi	20.3	-24 5	F0	3 ^s	4.28	132	183°	-37.2	33	(2)	1.9	330	+5
6486	13337				Y ¹	4.41	+ 16	+ 131		33		4.9		
4421	d Ophiuchi	21.0	-29 47	F5	4 ^s	4.37	157	173°	+37.8				324	+2
6492	13557				Y ¹	4.47	+ 44	+ 151				5.4		
4423	Ophiuchi	21.3	-5 0	F0	4 ^s .0	4.61	104	242°	Var	21	(3)	1.0	346	+15
6493	4275				Y ^{1,6}	4.73	- 77	+ 70	+0.4	19		4.7		
4425	σ Ophiuchi	21.6	+4 14	K0	6 ^s .4	4.44	4	45°	-27.3	16	(2)	0.5	354	+19
6498	3422				Y ³	4.40	+ 2	- 4		16		-2.6		
4426	δ Arae	22.1	-60 36	B8		3.79	102	213°	+12	27	(1)	1.0	298	-16
6500	6842					3.94	- 43	+ 93		27		3.8		
4429	ν Scorpii	24.0	-37 13	B3	2 ^s .3	2.80	42	183°	Var.	10	(3)	-2.2	319	-3
6508	11638					3.01	+ 4	+ 42	+18	10		0.9		
4431	α Aiao	24.1	-49 48	B3p	3 ^s .7	2.97	90	201°	Var.	21	(3)	-0.5	308	-10
6510	11511					3.16	- 22	+ 87	-2.2	20		2.7		
	Nov Ophiuchi	24.6	-21 24	Nov		-4 to 15?							333	+6
6595														
4434	ϵ^2 Ophiuchi	25.3	-23 53	A0	3 ^s	4.89	38	178°	-12	38	(a)		339	+4
6519	13412				W	5.04	+ 7	+ 37				2.8		

Boss 4370, 4371. Certainly a binary system with a very long period of revolution. Dynamic parallax 0".054 — Boss 4373, 4371. α Herculis is probably an irregular variable between 3^m.1 and 3^m.9. The dynamic parallax is 0".006-0".022 — Boss 4388. A visual binary — ADS 10449. The principal is an eclipsing binary — Boss 4419. Zinner has derived a combined magnitude of 4^m.33 for this pair. The RHP value is 4^m.14. For p.m. see the Appendix of the PGC.

17^h.

1	2	3	4	5	6	7	8	9	10	11	12	13	14	15
4438	2 Hercules	26 ^m .7	+ 26 ^m 11'	K0	6 ^s .3	4 ^m .48	21	45°	- 26.8	21	(5)	1.1	17°	+ 27°
6526	3034				0 ^h	4.51	- 4	21		21		1.1		
4439	2 Scorpil	26 .8	- 37 2	B2	3 ^s .0	1.71	36	180°	Var	12	(4)	2.9	420	- 1
6527	11673					1.99	1	16	0	12		0.5		
4443	2 Draconis	28 .2	+ 52 23	G0	5 ^s .0	2.99	16	297°	- 20.9	8	(1)	3.8	46	+ 32
6536	2063				Y ¹	3.08	12	11		7		1.0		
4445	0 Aras	28 .3	- 46 26	A0		4.61	56	226°	4				112	9
6537	11661					4.72	15	14				3.4		
4450	3 Scorpil	29 .6	- 38 34	K0		4.74	210	185°	49.2	20	(1)	0.8	118	4
6546	12044					4.77	6	216		20		6.0		
4457	2 Scorpil	30 .1	- 42 56	F0	4 ^s .7	2.04	12	160°	1.4				114	7
6553	12312					2.23	5	11				2.0		
4458	2 ¹ Draconis	30 .2	+ 55 15	A5	2 ^s .9	4.98	158	73°	14.2	10	(5)	1.2	50	+ 13
6554	1944				Y ¹	5.18	158	1		28		6.0		
4460	2 ² Draconis	30 .3	+ 55 14	A5	2 ^s .9	4.95	165	73°	Var			2.2	50	+ 33
6555	1945				Y ¹	5.16	- 165	5	17			6.1		
4459	α Ophiuch	30 .3	+ 12 38	A5	2 ^s .5	2.14	262	151°	Var	53	(4)	0.8	4	+ 22
6556	3252				W	2.45	+ 189	181	- 15	53		4.2		
4462	2 ³ Scorpion	31 .5	- 15 20	A5	4 ^s .0	3.64	84	212°	- 42.8	50	(1)	2.1	339	+ 7
6561	4621				Y ¹	3.83	- 34	76		50		3.1		
4465	μ Ophiuch	32 .4	- 8 3	B8	3 ^s .6	4.05	25	189°	- 18	9	(2)	0.6	345	+ 11
6567	4472				W	4.81	0	25		9		1.7		
4466	λ Aras	32 .6	- 49 21	F5		4.84	200	149°	+ 3.7				310	- 11
6569	11616					4.96	+ 123	169				6.4		
4474	ν Scorpil	33 .6	- 38 59	B2	2 ^s .5	2.51	28	201°	Var.	8	(2)	- 3.3	319	- 6
6580	12137					2.76	- 8	27	- 10	7		- 0.3		
4475	α Scorpion	33 .8	- 12 40	A2	3 ^s .2	4.39	91	231°	- 30	20	(1)	0.9	341	+ 8
6581	4808				Y ¹	4.55	- 62	65		20		4.2		
4476	γ Iuvencia	33 .9	- 64 41	K0		3.58	50	188°	- 8.1	18	(1)	- 0.1	295	- 19
6582	3662					3.77	- 51	46		18		2.3		
4479	1 Hercules	36 .6	+ 46 4	B3	2 ^s .1	3.79	8	250°	- 18.6	7	(3)	- 3.8	39	+ 30
6588	2349				W	4.02	1	8		7		- 1.7		
4481	58 Ophiuch	37 .4	- 21 38	F5	3 ^s	4.89	104	239°	+ 11.0				333	+ 3
6595	4712				Y ¹	4.98	- 83	62				5.0		
4483	ω Draconis	37 .5	+ 68 48	F5	4 ^s .4	4.87	327	2°	Var	36	(4)	2.7	66	+ 32
6596	949				Y ¹	4.90	- 52	324	- 14.0	36		7.4		
4487	2 Ophiuch	38 .5	+ 4 37	K0	5 ^s .5	2.94	158	344°	- 12.2	33	(4)	0.5	357	+ 16
6603	3489				Y ¹	3.01	- 69	137		32		3.0		
4492	2 Scorpil	40 .6	- 40 5	F3p	4 ^s .4	3.14	4	56°	- 26.7	7	(1)	- 2.6	318	- 7
6615	11838					3.27	+ 3	2		7		- 3.9		
4493	X Sagittari	41 .3	- 27 48	F8	3 ^s	Var.	23	193°	- 13.5	6	(1)		328	- 1
6616	11930				Y ¹	4.4	- 5.0	- 3	+ 23	6				
4497	μ Hercules	42 .5	+ 27 47	G5	4 ^s .1	3.48	817	203°	- 16.1	102	(5)	3.5	20	+ 25
6623	2888				Y ¹	3.59	- 90	211		100		8.0		
4498	Scorpil	42 .7	- 31 40	B8		4.83	24	173°	- 13	6	(1)	- 1.3	325	- 4
6628	14609					4.98	+ 5	24		6		1.7		
4500	γ Ophiuch	42 .9	+ 2 45	A0	2 ^s .2	3.74	83	199°	Var.	17	(3)	- 0.7	356	+ 14
6629	3403				W	4.00	- 18	81		13		3.3		
4501	6 Scorpil	43 .0	- 37 1	K2	6 ^s .3	3.25	68	73°	+ 24.6	28	(2)	0.5	321	- 6
6630	11907					3.34	+ 64	- 23		28		2.4		
4503	2 ¹ Scorpil	43 .1	- 40 4	A2p		4.88	15	160°					319	- 8
6631	11886					5.03	+ 6	14				0.8		
4504	ψ Draconis	43 .7	+ 72 12			4.90	267	176°	- 10.2	39	(6)	2.9	70	+ 31
6636	804				4 ^s .1	4.96	+ 8	- 267		39		7.0		
4505	ψ Draconis	43 .7	+ 72 12	F5		6.07	275	163°	- 10.3			4.0	70	+ 31
6637	805				Y ¹	6.13	- 5	- 274				8.3		

Item 4493. Cepheid variable; period 7.0 days.

17^h to 18^h.

1	2	3	4	5	6	7	8	9	10	11	12	13	14	15
4519	Scorpi	49 ^m .5	-44° 19'	K0		4 ^m .98	28	232°	+44.9				315°	-11°
6675	12201					5.02	-22	18				2.2		
4525	Scorpi	50.7	-41 42	Ma		4.89	33	211°	+4.4				318	-10
6682	12231					4.93	-16	29				2.5		
4531	ε Draconis	51.8	+56 53	K0	5'.9	3.90	123	52°	-25.2	29	(5)	0.9	52	+29
6688	2033				Y ^a	3.93	-101	70		29		4.3		
1535	θ Herculis	52.8	+37 16	K0	5".6	3.99	6	45°	-28.1	11	(7)	1.5	30	+25
6695	2982				Y ^a	3.97	-5	4		8		-2.1		
1536	ι Ophiuchi	53.5	-9 46	K0	5'.1	3.50	118	186°	+12.7	22	(3)	0.2	345	+6
6698	1632				Y ²	3.52	-8	118		20		3.9		
4537	4 Sagittarii	53.7	-23 48	A0	2'	4.76	58	179°	-22	8	(a)	-0.7	333	-1
6700	13731				Y ¹	4.90	1	58				3.6		
4538	ε Herculis	53.9	+29 16	K0	5".4	3.82	90	107°	-1.8	26	(5)	0.7	22	+23
6703	3156				Y ^a	3.86	1	89	-14	26		3.6		
1541	γ Draconis	54.3	+51 30	K5	6'.5	2.42	27	197°	-27.2	33	(3)	0.2	47	+29
6705	2282				OY ^a	2.47	+	9	-26	30		-0.4		
4542	ν Herculis	54.7	+30 11	F0	3'.8	4.48	6	51°	-22.1	12	(3)	-4.0	23	+22
6707	3093				Y ¹	4.67	-3	5		9		-2.5		
1544	ζ Serpentis	55.2	-3 41	F0	3'.9	4.60	153	111°	-43	31	(2)	2.1	351	+8
6710	1217				Y ¹	4.72	+	144	52	31		5.5		
4545	66 Ophiuchi	55.3	+4 23	B3	2'.5	4.81	19	205°	Var	8	(3)	-0.7	358	+12
6712	3570				Y ^a	4.97	-7	17		8		1.2		
4547	93 Herculis	55.6	+16 46	K0	5".9	4.71	12	215°	-23.0	11	(4)	-0.1	10	+17
6713	3335				W	4.69	-6	10		11		0.1		
4548	67 Ophiuchi	55.6	+2 56	B5p	2".9	3.92	14	172°	-4.4	5	(4)	-3.1	357	+11
6714	3458				W	4.14	+	2	14	4		-0.4		
4552	68 Ophiuchi	56.7	+1 19	A2	3".3	4.44	26	162°	Var	20	(3)	0.9	356	+10
6723	3560				W	4.60	+	9	25	20		1.5		
4556	95 Herculis	57.3	+21 36	G5	3'.9	5.21	30	27°	-30.9	8	(1)	-0.3	15	+19
6729	3280				R ¹	5.28	+	11	-48	8		2.6		
4557	95 Herculis	57.2	+21 36	A3	G ¹	5.13	30	27°	-27	14	(a)	0.8	15	+19
6730	3280					5.20	+	11	-48			2.5		
4559	τ Ophiuchi	57.6	-8 11		4".3	6.04	45	152°	Var	18	(1)	2.3	348	+6
6733	4549			F0	Y ¹	6.19	+	21	40	18		4.3		
4559	τ Ophiuchi	57.6	-8 11		4".2	5.34						1.6	348	+6
6734	4549				Y ¹	5.49								
4564	W Sagittarii	58.6	-29 35	F8p	5"	Var	15	143°	-25.0				329	-6
6742	14447				Y ^a	4.3	-5.1	9	12					
4565	θ Aiac	58.8	-50 6	B1p		3.90	30	203°	+3	8	(2)	-1.6	311	-15
6743	11720					4.04	-12	28		8		1.3		
4566	π Pavonis	58.9	-63 40	A5		4.44	192	175°	-14.9	29	(a)	1.7	297	-21
6745	4292					4.54	+	17	192			5.9		
4568	γ Sagittarii	59.4	-30 26	K0	5".3	3.07	203	197°	+21.5	34	(3)	0.6	329	-6
6746	15215					3.31	59	195		32		4.6		
4571	70 Ophiuchi	0.4	+2 31	K0	5".3	4.07	1131	167°	-7.2	136	(8)	4.0	358	+10
6752	3482				6"-7"									
4577	Sagittarii	1.8	-28 28	K0	Y ^a	4.10	+	238	+1118	96		9.9		
6766	14174				6"	4.66	37	153°	-4.5			4.6	331	-6
4580	71 Ophiuchi	2.5	+8 43	G5	OY ^a	4.64	+	16	33			2.5		
6770	3582				5".6	4.73	25	0°	-3.5	12	(2)	0.1	4	+12
4581	72 Ophiuchi	2.6	+9 33	A3	Y ^a	4.78	0	25		12		1.7		
6771	3564				2".8	3.73	103	323°	-25	43	(3)	1.9	5	+13
4584	ο Herculis	3.6	+28 45	A0	Y ¹	3.95	-58	85		43		3.8		
6779	2925				2".2	3.83	4	56°	-27	24	(2)	0.7	23	+20
4588	ε Telescopii	3.8	-45 58	K0	W	4.05	+	4	1	24		-3.2		
6783	12251					4.60	41	205°	-26.5	11	(1)	-0.2	315	-14
						4.71	-18	37		11		2.7		

Boss 4559, ADS 11005 Wellknown visual binary the period of which is around 224 years The dynamic parallax is 0".028 - Boss 4564, Cepheid variable, period 7.6 days - Boss 4571 The components are 4^m.28 and 5^m.98 - Boss 4581 Light possibly variable

18^h.

1	2	3	4	5	6	7	8	9	10	11	12	13	14	15
4590 6787	102 Herculis 3674	4 ^m ,4	+20° 48'	B3	2 ^o ,0 W	4 ^m ,32 4,56	17 - 3	183° + 17	-13,5 5	(1)	-2,2 0,5	15°	+17°	
4591 6789	δ Ursae min. 269	4,5	+86 37	A0	2 ^o ,3 W	4,44 4,66	52 - 19	22° + 48	- 8; 17	(2)	0,6 3,0	87	+28	
4604 6812	μ Sagittarii 4908	7,8	-21 5	B8p	3 ^o ,7 Y ¹	4,01 4,20	6 + 4	141° + 5	Var. + 9,2	(a)	-0,6 -2,0	338	- 3	
4617 6832	η Sagittarii 12423	10,9	-36 47	Mb	5 ^o ,2	3,16 3,24	216 -145	219° +160	+ 0,1 20	(2)	-0,7 4,8	324	-11	
4619 6842	σ Sagittarii 12684	11,8	-27 5	K5	8 ^o O ⁸	4,69 4,66	10 + 8	53° - 5	-16,9 11	(1)	-0,1 -0,3	333	- 7	
4625 6855	ξ Pavonis 6140	14,0	-61 33	K2		4,25 4,38	11 - 7	319° - 9	Var. 23	(1)	1,1 -0,5	300	-21	
4628 6859	δ Sagittarii 14834	14,6	-29 52	K0	6 ^o -7 ^o OY ⁸	2,84 2,94	51 + 34	135° + 38	-20,0 28	(3)	0,1 1,4	331	- 9	
4635 6866	74 Ophiuchi 3680	15,8	+ 3 20	G5	5 ^o ,4 Y ²	4,92 4,90	15 - 15	259° + 1	+ 5,1 9	(2)	-0,3 0,8	0	+ 7	
4636 6868	106 Herculis 3390	16,1	+21 55	K5	6 ^o ,1 Y ¹	4,98 4,97	62 - 15	171° + 60	-32,0 11	(3)	0,2 3,9	17	+15	
4638 6869	η Serpentis 4599	16,1	- 2 55	K0	5 ^o ,6 Y ²	3,42 3,52	898 -647	219° +620	+ 8,9 56	(5)	2,2 8,2	355	+ 4	
4639 6872	κ Lyrae 3094	16,4	+36 1	K0	5 ^o ,7 Y ^{1,5}	4,34 4,41	38 + 36	325° + 12	-22,7 17	(4)	0,4 2,2	31	+20	
4645 6879	ε Sagittarii 12784	17,5	-34 26	A0	4 ^o ,5	1,95 2,20	139 - 51	198° +129	-11			327	-11	
4650 6884	ζ Scuti 4712	18,2	- 8 59	G5	5 ^o ,4 Y ²	4,83 4,89	62 + 47	44° - 40	Var. - 4,7	(4)	0,9 3,8	349	+ 1	
4656 6895	109 Herculis 3411	19,4	+21 43	K0	5 ^o ,4 Y ²	3,92 3,98	324 + 55	144° +318	-58,2 35	(5)	1,4 6,5	18	+14	
4655 6896	21 Sagittarii 5134	19,4	-20 35	K0 A0	6 ^o ,2 OY ²	4,96 4,92	23 + 7	158° + 22	-11,5 10	(a)	0,0 1,8	339	- 6	
4657 6897	α Telescopii 12379	19,6	-46 1	B3		3,76 3,88	53 - 15	191° + 51	- 0,8 12	(3)	-1,0 2,4	316	-17	
4662 6905	ζ Telescopii 12153	21,1	-49 7	K0		4,14 4,28	294 +121	151° +268	-30,5 22	(1)	0,9 6,5	313	-18	
4665 6913	λ Sagittarii 13149	21,8	-25 29	K0	6 ^o Y ²	2,94 3,02	197 - 67	194° +185	-43,2 58	(5)	0,4 4,4	335	- 7	
4666 6916	ν Pavonis 5879	22,6	-62 20	B8		4,81 4,90	34 - 10	192° + 33	+59			300	-22	
4670 6920	φ Draconis 889	22,2	+71 17	A0p	2 ^o ,2 W	4,24 4,46	32 + 8	353° + 31	Var. -16,8	(3)	-0,8 1,8	68	+28	
4671 6923	b Draconis 1809	22,5	+58 45	A2	2 ^o ,7 W	4,85 5,14	64 + 43	329° + 47	Var. -12	(3)	1,8 3,9	55	+26	
4672 6927	χ Draconis 839	22,9	+72 41	F8	4 ^o ,7 Y ²	3,69 3,77	638 -568	125° +287	+32,1 121	(4)	4,1 7,7	71	+28	
4674 6930	γ Scuti 5071	23,5	-14 38	A3	2 ^o ,7 Y ¹	4,73 4,92	9 + 2	160° + 9	-51 19	(1)	1,1 -0,5	345	- 4	
4686 6945	42 Draconis 1271	25,7	+65 30	K0	5 ^o ,6 Y ²	4,99 4,96	104 -104	105° - 9	+33,2 18	(3)	1,3 5,1	63	+27	
4689 6951	θ Coronae Aust. 13378	26,4	-42 23	G5		4,69 4,76	47 + 36	125° + 30	-0,5 8	(1)	-0,8 3,0	320	-16	
4705 6973	α Scuti 4638	29,8	- 8 19	K0	6 ^o ,1 Y ²	4,06 4,03	318 - 83	184° +308	+35,6 21	(4)	0,7 6,6	352	- 1	
4707 6978	d Draconis 2113	30,9	+56 58	F8p	4 ^o ,8 Y ^{1,6}	4,95 5,03	11 + 1	202° - 11	-11,3 3	(1)	-2,7 0,2	53	+24	
4709 6982	ζ Pavonis 2553	31,4	-71 31	K0		4,10 4,24	155 - 29	184° +152	-16,9 35	(1)	1,8 5,1	290	-26	

18^h.

1	2	3	4	5	6	7	8	9	10	11	12	13	14	15
4722	α Lyrae	33 ^m ,6	+38° 41'	A0	1 ^o ,3	0 ^m ,14	346	36°	-14,2	115	(4)	0,4	35°	+19°
7001	3238				B1	0,31	+48	+343		111		2,8		
4725	ρ Pavonis	35,7	-64 58	A2		4,90	114	182°	+5				298	-25
7012	3948					4,98	-24	+141				5,7		
4731	δ Scuti	36,8	-9 9	F0	4 ^o ,0	4,74	14	107°	Var	14	(2)	0,4	352	-3
7020	4796				Y1	4,83	+12	+7	-47,9	12		0,4		
4734	σ Sagittarii	37,6	-35 45	B3		4,82	53	180°	+2,8	14	(1)	0,6	327	-15
7029	12876					4,98	-8	+52		14		3,4		
4739	φ Sagittarii	39,4	-27 6	B8	3'	3,30	48	91°	Var	16	(1)	-0,7	336	-12
7039	13170				YG1	3,52	+47	+12	+21,5	16		1,7		
4747	ϵ^1 Lyrae	41,0	+39 34			5,06	52	10°	-31,2			1,3	37	+18
7051	3509				2 ^o ,8	5,30	+32	+41		18	(1)	3,6		
1748	ϵ^1 Lyrae	41,0	+39 34	A3	Y2	6,02	57	1°	-33,5	18		2,3	37	+18
7052	3509				OR1	6,26	+42	+39				4,8		
4749	ϵ^2 Lyrae	41,1	+39 30			5,14			-15				37	+18
7053	3510				2 ^o ,9	5,46								
4749	ϵ^2 Lyrae	41,1	+39 30	A5	Y1	5,37	64	14°	-16				37	+18
7054	3510				Y1	5,69	+36	53				4,4		
4752	ζ^1 Lyrae	41,3	+37 30	A3	3 ^o ,6	4,29	31	56°	Var	30	(6)	1,7	35	+17
7056	3222				Y1		0	+31		30		1,8		
4752	ζ^2 Lyrae	41,3	+37 30	A3	3 ^o ,0	5,87	31	56°				3,3	35	+17
7057	3223				Y1		0	+31				3,3		
4753	110 Herculis	41,4	+20 27	F5	4 ^o ,0	4,26	345	183°	+22,2	65	(4)	3,3	18	+9
7061	3926				Y1 ^o	4,40	-238	+248		65		6,9		
4756	β Scuti	41,9	-4 51	G0	5 ^o ,9	4,47	25	205°	Var	10	(3)	-0,8	356	-2
7063	4582				Y2	4,56	-16	+19	-20,9	9		1,5		
4758	Lyrae	42,0	+26 34	K0	5 ^o ,7	4,92	29	27°	-16,9	19	(2)	1,3	25	+11
7064	3349				Y2	5,11	+29	+1		19		2,2		
4759	R Scuti	42,2	-5 49	K0p	7 ^o ,3	Var	72	243°	Var	-3	(a)		356	-3
7066	4760				O2	4,7-8,0	-70	+15	-38,3			4,0		
4761	111 Herculis	42,6	+18 4	A3	2 ^o ,7	4,37	123	31°	Var	38	(5)	2,2	16	+7
7069	3823				Y1	4,50	+113	-48	-46,7	36		4,8		
4762	λ Pavonis	43,0	-62 18	B2		4,42	19	235°	+20				301	-25
7074	5983					4,53	-17	+8				0,8		
	Aquiliae	43,8	+0 28	A5	Var	-0,2 to	18	194°	-13	3,1	(3)	-8,3	0	-1
				Nova		10,9	-9	+16				-3,9		
4776	β^1 Lyrae	46,4	+33 15	B8p	3 ^o ,1	Var	8	152°		8	(1)		30	+14
7106	3223			B2p	Y1 ^o	3,4-4,1	-8	+3		8				
4778	κ Pavonis	46,6	-67 21	F5p		Var	17	335°	+36,3	3	(a)		296	-26
7107	3603					3,8-5,2	-4	-16						
4781	μ^1 Sagittarii	48,1	-22 52	G5	5 ^o ,6	4,96	18	158°	-14,6	8	(a)	-0,5	340	-12
7116	4907				OY2	4,99	+3	+18				1,3		
4784	σ Sagittarii	49,1	-26 25	B3	1 ^o -2 ^o	2,14	66	173°	-10,7	16	(2)	-1,8	337	-13
7121	13595				W	2,39	-7	+65		16		1,2		
4790	α Diaconis	49,7	+59 16	K0	6 ^o ,1	4,78	86	74°	Var	12	(5)	0,2	56	+23
7125	1925				Y2	4,75	-68	+53	+19,5	12		4,4		
4797	113 Herculis	50,5	+22 32	G0	4,9	4,56	5	325°	-23,8	18	(5)	0,3	21	+9
7133	3524			A3	Y2	4,69	+2	-5		14		-1,9		
4799	Diaconis	50,7	+50 35	G5	4 ^o ,9	4,97	33	178°	+8,2	10	(1)	0,0	48	+20
7137	2686				Y2	5,08	-16	-29		10		2,6		
4800	δ^2 Lyrae	51,0	+36 47	Mb	7 ^o ,0	4,52	10	307°	-26,6	7	(3)	-1,3	35	+14
7139	3319				O2	4,44	+9	-4		7		-0,5		
4802	θ^1 Serpentis	51,2	+4 4	A5	3 ^o ,0	4,50	53	59°	-41	22	(2)	1,2	5	-1
7141	3916				Y1	4,89	+52	-7		22		3,1		
4803	θ^2 Serpentis	51,2	+4 4	A5	3 ^o ,0	5,37	48	68°	-42			2,1	5	-1
7142	3917				Y1	5,32	+48	+1				3,8		

Boss 4722 Has a variable radial velocity and might also vary in light Photoelectric methods have revealed a slight variation in the light (GUTHRIE) — Boss 4752 ZINNAR gives the combined magnitude 10,60 for this pair — Boss 4759 Irregular variable 4m,5 to 9m — Boss 4778 Cepheid variable, period 9,1 days

18^h to 19^h.

1	2	3	4	5	6	7	8	9	10	11	12	13	14	15
4808	η Scuti 4070	51 ^u ,7	— 5° 58'	K0	5 ^u ,9 Y ^u	5 ^u ,04 5,00	71 + 50	117° + 50	-93,1				356°	- 5°
4809	ζ^h Sagittarii 5201	51,8	-21 14	K0	5 ^u ,7 Y ^u	3,61 3,60	37 + 27	120° + 26	-20,1	23 24	(4)	4,3 0,5 1,5	342	-12
4810	α Coronae Aust. 13001	52,0	-37 14	F5		4,87 5,04	161 -148	235° + 63	+53				327	-19
4814	κ Lyrae 3117	52,3	+43 49	Mb	6 ^u ,6 OY ^u	4,32 4,2-4,9	77 + 32	21° + 70	-27	8 8	(5)	5,9 -1,2 3,8	41	+17
4823	ϵ Aquilae 3736	55,1	+14 56	K0	5 ^u ,6 Y ^u	4,21 4,22	100 - 97	220° + 22	-51,6	21 21	(5)	0,8 4,2 -0,5	15	+40
4824	γ Lyrae 3286	55,2	+32 33	A0p	2 ^u ,9 W	3,30 3,51	8 - 7	203° - 4	Var. -20	18 17	(5)	-2,2 0,5 4,0	31	+12
4825	ν Draconis 915	55,6	+71 10	K0	6 ^u ,1 Y ^u	4,91 4,94	66 - 37	33° + 55	Var. - 7,2	13 13	(1)	0,5 4,0	69	+25
4830	ζ Coronae Aust. 13855	56,1	-42 14	A0		4,85 5,00	82 + 44	134° + 69	- 7				323	-21
7189	Sagittarii	56,2	-13 18	Pec. Nova		4,7-15?						4,4	350	-10
4834	ι Aquilae 4840	56,3	- 5 53	K0	5 ^u ,9 OY ^u	4,15 4,12	48 - 41	220° + 25	-44,3	28 28	(5)	1,4 2,6	357	- 6
4832	ζ Sagittarii 16575	56,3	-30 1	A2	3 ^u ,9	2,71 2,94	21 - 18	270° - 5	+22	43 40	(2)	0,7 -0,7	334	-17
4847	σ Sagittarii 5237	58,7	-21 53	K0	4 ^u ,7 Y ^u	3,90 3,86	98 + 51	133° + 84	+25,8	29 28	(3)	1,1 3,8	342	-14
4851	γ Coronae Aust. 13048	59,7	-37 12	F8	4 ^u ,0	4,26 4,37	301 + 27	161° +301	-51,0	65 65	(a)	3,3 6,7	328	-20
4857	ϵ Sagittarii 13564	0,7	-27 49	K0	6 ^u OY ^u	3,42 3,47	267 -125	193° +235	Var. -45,7	40 39	(3)	1,4 5,6	337	-17
4858	ζ Aquilae 3899	0,8	+13 43	A0	2 ^u ,7 YG ¹	3,02 3,26	102 - 69	186° + 74	Var. -26	35 35	(5)	0,7 3,1	15	+ 2
4859	λ Aquilae 4876	0,9	- 5 2	B9	2 ^u ,8 W	3,55 3,72	93 - 55	195° + 75	-13	28 27	(2)	0,7 3,4	358	- 7
4862	δ Coronae Aust. 13061	1,3	-40 39	K0		4,66 4,69	49 + 24	136° + 43	+21,7			3,1	324	-21
4868	α Coronae Aust. 13350	2,7	-38 4	A2		4,12 4,35	136 + 56	141° +124	-18	19 19	(1)	0,5 4,8	327	-21
4871	β Coronae Aust. 13146	3,1	-39 30	G5		4,16 4,29	36 - 15	184° + 33	+ 2,9	9 9	(1)	-1,1 2,0	325	-22
4874	α Sagittarii 5275	3,8	-21 11	F2	(4 ^u ,6) Y ^u	3,02 3,14	40 - 18	189° + 36	-10,2	17 17	(3)	-0,8 1,0	344	-15
4891	ψ Sagittarii 13866	9,4	-25 26	F5	3 ^u Y ¹	4,93 5,00	53 + 28	151° + 46	Var. -33,7			3,5	340	-17
4897	η Lyrae 3490	10,4	+38 58	B3	2 ^u ,1 W	4,46 4,67	3 - 3	180° - 1	- 8,7	5 5	(3)	-2,1 -3,2	38	+12
4906	ι Vulpeculae 3713	11,9	+21 13	B5	2 ^u ,1 W	4,60 4,89	4 - 3	180° + 2	-17,4	8 8	(2)	-0,3 -2,4	22	+ 3
4909	δ Draconis 1129	12,5	+67 29	K0	5 ^u ,1 Y ^u	3,24 3,29	133 - 49	48° +124	+25,9	35 35	(4)	0,9 3,9	65	+23
4912	δ Lyrae 3398	12,9	+37 57	K0	6 ^u ,0 Y ^u	4,46 4,48	10 + 0	253° - 10	-30,5	9 8	(6)	-1,0 -0,5	37	+11
4923	κ Cygni 2216	14,8	+53 11	K0	5 ^u ,2 Y ^u	3,98 3,96	133 + 23	30° +130	-29,2	29 28	(5)	1,2 4,6	52	+17
4929	β^1 Sagittarii 13277	15,4	-44 39	B8		4,24 4,30	19 - 6	183° + 18	- 8	4 4	(1)	-2,8 0,6	321	-25
4932	ϵ Sagittarii 5322	15,9	-18 2	A5	3 ^u ,3 YG ¹	3,95 4,14	31 - 15	310° - 27	+ 2	43 43	(4)	2,1 1,4	348	-16
4934	ν Sagittarii 5283	16,0	-16 8	B8p F2p	3 ^u ,3 YG ¹	4,58 4,77	5 - 4	217° + 3	+11,9				350	-15

Stars 4814, Variable 4m,0 to 4m,3 in the RHP-system - Stars 4851 Binary, the components of which are each 5^u,01 in the RHP-system. The period is 110 years.

19^b.

1	2	3	4	5	6	7	8	9	10	11	12	13	14	15
4933	β^2 Sagittarii	16 ^m .0	-44° 59'	F0		1 ^m .51	125	121°	-22	28	(a)	1.7	321°	-25°
7343	Id 171					4.52	+ 84	+ 92				5.0		
4936	α Sagittarii	17 .0	-40 48	B8		1.11	129	168°	-1	26	(2)	1.1	325	-24
7348	13215					4.27	- 13	+ 128		25		4.7		
4940	γ Draconis	17 .5	+73 10	K0	6 ^m .0	4.63	176	309°	Var	16	(2)	0.7	72	+24
7352	857				OY ²	4.53	+ 171	+ 42	-30.1	16		5.8		
4942	3 Vulpeculae	18 .7	+26 1	B5	2 ^m .1	4.92	15	191°	-13.2	8	(3)	-0.6	27	+ 4
7358	3811				W	5.23	- 15	+ 2		8		0.8		
4948	α Draconis	20 .2	+65 31	A2	2 ^m .7	4.63	45	25°	-27.7	19	(3)	1.0	65	+21
7371	1345				W	4.82	+ 4	+ 45		19		2.9		
4949	2 Cygni	20 .2	+29 26	B3	1 ^m .9	4.86	13	42°	-23	4	(1)	-2.1	30	+ 5
1372	3584				W	5.08	+ 11	+ 7		4		0.4		
4953	δ Aquilae	20 .5	+ 2 55	F0	3 ^m .9	3.44	265	73°	-25	59	(6)	2.3	7	- 7
7377	3879				Y ^{1.5}	3.65	+ 254	+ 74		58		5.6		
4962	γ Aquilae	21 .4	+ 0 9	F0	4 ^m .4	4.86	11	297°	-0.4	32	(1)	2.4	5	- 9
7387	4206				Y ²	4.93	- 6	- 9		32		0.1		
4976	α Vulpeculae	24 .5	+24 28	Ma	6 ^m .9	4.36	170	227°	-85.5	13	(5)	-0.2	27	+ 3
7405	3759				OY ²	4.52	- 155	- 70		13		5.5		
4986	β^1 Cygni	26 .7	+27 45	K0	5 ^m .4	3.24	9	198°	-24.0	20	(5)	-1.0	30	+ 3
7417	3440				A0	OY ²	3.19	- 9	0	14		-2.0		
4987	β^2 Cygni	26 .7	+27 45	B9	1 ^m .4	5.36	- 14	234°	-23			+1.1	30	+ 3
7418	3411				B ³	5.65	- 11	- 9				+1.1		
4988	ϵ Cygni	27 .2	+51 31	A2	3 ^m .0	3.94	126	9°	-18	24	(4)	0.3	52	+15
7420	2605				YG ¹	4.07	+ 78	+ 100		19		4.4		
4992	8 Cygni	28 .1	+34 14	B3	2 ^m .4	4.85	4	214°	-21.8	6	(2)	-1.3	35	+ 6
7426	3590				W	4.97	- 3	- 2		6		-2.1		
4995	μ Aquilae	29 .2	+ 7 10	K0	6 ^m .3	4.65	262	126°	-22.9	22	(5)	1.3	12	- 7
7429	4132				Y ²	4.59	+ 68	+ 254		22		6.7		
4998	9 Vulpeculae	30 .2	+19 33	B8	2 ^m .0	4.88	4	117°	4	11	(2)	0.1	23	- 1
7437	4063					5.14	+ 0	- 4		12		-2.1		
4999	h^2 Sagittarii	30 .6	-25 6	B9	4 ^m	4.66	76	109°	-19				342	-22
7440	14184				W	4.82	+ 56	+ 51				4.1		
5004	ϵ Aquilae	31 .6	- 1 31	B5	3 ^m .1	4.28	17	193°	-20	8	(2)	-1.2	4	-12
7447	3782				Y ¹	4.59	- 12	+ 12		8		-0.4		
5009	α Draconis	32 .6	+69 29	K0	5 ^m .2	4.78	1840	162°	+26.6	163	(5)	5.8	68	+22
7462	1053				Y ²	4.79	-1380	-1214		163		11.1		
5014	θ Cygni	33 .8	+49 59	F5	3 ^m .9	4.64	249	353°	-27.9	61	(4)	3.5	50	+13
7469	3062				Y ^{1.5}	4.68	+ 214	+ 129		61		6.6		
5021	η Cygni	35 .5	+29 56	K0	5 ^m .3	4.79	35	355°	+ 5.2	15	(4)	0.7	33	+ 3
7478	3684				Y ²	4.76	+ 34	- 8		15		2.5		
5023	α Sagittae	35 .6	+17 47	G0	5 ^m .1	4.37	36	153°	+ 1.6	8	(4)	-1.7	22	- 3
7479	4012				Y ²	4.49	- 17	+ 32		6		2.1		
5027	β Sagittae	36 .6	+17 15	K0	5 ^m .7	4.45	38	178°	-22.4	15	(5)	0.2	22	- 4
7488	4048				Y ²	4.49	- 30	+ 24		15		2.3		
5047	γ Aquilae	41 .5	+10 22	K2	6 ^m .2	2.80	14	107°	-2.4	28	(5)	0.0	16	- 8
7525	4043				OY ²	2.97	+ 6	+ 12		27		-1.5		
5048	δ Cygni	41 .9	+44 53	A0	2 ^m .4	2.97	65	55°	-19.1	37	(2)	0.8	46	+10
7528	3234				Y ¹	3.18	+ 10	+ 64		37		4.0		
5052	δ Sagittae	42 .9	+18 17	Ma	6 ^m .7	3.78	9	6°	Var	12	(5)	-1.2	23	- 5
7536	4240			A0	O ²	3.83	+ 8	- 4		10		-1.4		
7539	11 Vulpeculae	43 .5	+27 4	Nova		3.0-12?							31	0
5058	ζ Sagittae	44 .5	+18 53	A2	2 ^m .3	4.95	31	36°	-17	24	(3)	1.9	24	- 4
7546	4254				YG ¹	5.19	+ 31	+ 3		24		2.4		
5062	α Aquilae	45 .9	+ 8 36	A5	2 ^m .4	0.89	655	54°	-26.1	166	(4)	2.0	16	-10
7557	4236				Y ¹	1.13	+ 648	+ 92		163		5.0		

Boss 5048 Visual binary ADS 12880 Has a period of some 500 years The dynamic parallax is 0^m.026-0^m.036.

19^h to 20^h.

1	2	3	4	5	6	7	8	9	10	11	12	13	14	15
5067	χ Cygni	46 ^m .7	+32° 40'	Md	7 ^s .5	Var. 4 ^m .2 to 13 ^m .2	91	233°	— 0.5				37°	+ 2°
7564	3593				OR ^a		67	62				4.0		
5068	12 Vulpeculae	46 .8	+22 21	B3	1 ^s .5	4 .91	29	131	—28:	7	(2)	—0.9	27	— 4
7565	3833				W	5 .12	8	28		5		2.2		
5071	η Aquilae	47 .4	+ 0 45	Gop	5 ^s .1	3.5—4.7	12	138°	—14.8	7	(3)		9	—14
7570	4337				Y ³	3.8—4.5	1	12		5				
5078	ϵ Sagittarii	48 .4	—42 8	KO		4 .21	53	10°	+36.2	20	(a)	0.7	325	—30
7581	14 549					4 .26	30	44				2.8		
5079	ϵ Draconis	48 .5	+70 1	KO	5 ^s .1	3 .99	87	69°	+ 3.1	18	(5)	—0.3	70	+21
7582	1070				Y ³	3 .99	47	73		14		3.7		
5084	ϵ Pavonis	49 .0	—73 10	AO		4 .10	149	152°	0:				289	—32
7590	2086					4 .22	10	149				5.0		
5086	13 Vulpeculae	49 .2	+23 50	AO	2 ^s .6	4 .50	40	46°	—33	15	(2)	0.4	29	— 3
7592	3820				Y ¹	4 .73	36	16		15		2.5		
5089	ξ Aquilae	49 .4	+ 8 12	KO	5 ^s .5	4 .86	126	131°	—41.9	20	(5)	0.9	15	—11
7595	4261				OY ³	4 .83	9	126		21		5.4		
5091	ω Sagittarii	49 .7	—26 34	G5	3 ^s	4 .81	225	68°	—21.3	40	(1)	2.8	342	—26
7597	14637				OY ²	4 .84	225	20		40		6.6		
5093	β Aquilae	50 .4	+ 6 9	KO	5 ^s .1	3 .90	484	176°	—40.0	81	(5)	3.4	14	—12
7602	4357				OY ²	3 .86	305	378		80		7.3		
5095	b Sagittarii	50 .8	—27 26	K2	6 ^s	4 .62	19	164°	Var.	12	(2)	0.0	342	—27
7604	14 399				OY ²	4 .61	4	19	—16.2	12		1.0		
5102	22 Cygni	52 .3	+38 13	B3	1 ^s .8	4 .87	12	211°	—36.3	6	(4)	—1.2	41	+ 4
7613	3817				W	5 .11	9	8		6		0.3		
5103	η Cygni	52 .6	+34 49	KO	5 ^s .1	4 .03	52	221°	—26.3	33	(5)	1.4	39	+ 3
7615	3798				Y ³	4 .03	38	35		30		2.6		
5104	A Sagittarii	52 .8	—26 28	G5	5 ^s	4 .95	38	40°	Var.	8	(1)	—0.5	343	—27
7618	14682				OY ²	4 .99	35	14	—48.6	8		2.8		
5105	ψ Cygni	53 .0	+52 10	A3	2 ^s .5	4 .80	51	232°	—17:	13	(5)	0.2	53	+12
7619	2572				W	5 .06	3	51		12		3.3		
5108	θ Sagittarii	53 .2	—35 33	B3		4 .39	47	160°	+ 0.9	12	(1)	—0.2	332	—30
7623	13831					4 .55	5	47		12		2.7		
5118	γ Sagittae	54 .3	+19 13	K5	6 ^s .5	3 .71	62	75°	—34.1	20	(5)	0.1	25	— 6
7635	4229				OY ²	3 .75	44	44		19		2.7		
	Cygni	55 .9	+53 21	Nova	Var.	1.5 to 16.5?			—17				55	+12
5129	c Sagittarii	56 .5	—27 59	Mb	6 ^s .7	4 .60	37	74°	+11.5	13	(2)	0.2	341	—28
7650	10356				OY ²	4 .59	36	7		13		2.4		
5131	Sagittarii	56 .9	—38 13	K5		4 .79	119	140°	—38.3	14	(1)	0.5	330	—31
7652	13828					4 .80	29	115		14		5.2		
5132	15 Vulpeculae	57 .0	+27 29	A5	3 ^s .2	4 .74	52	83°	—22.5	26	(3)	1.8	33	— 2
7653	3587				Y ¹	4 .92	19	48		26		3.3		
5138	δ Pavonis	58 .9	—66 26	G5	7 ^s .0	3 .64	1625	135°	—21.5	60	(3)	1.8	297	—33
7665	3474					3 .79	536	1544		43		9.7		
5147	ξ Telescopii	59 .7	—53 10	Ma		4 .86	24	268°	+36.9				313	—34
7673	9794					4 .97	22	10				1.8		
5153	ϵ Draconis	2 .3	+67 35	KO	6 ^s .5	4 .66	51	19°	— 9.4	18	(2)	1.1	68	+18
7685	1222				O ³	4 .66	20	47		18		3.2		
5170	b ¹ Cygni	5 .7	+36 33	B2p	2 ^s .4	4 .82	10	331°	Var.	6	(2)	1.3	42	+ 2
7708	3907				Y ¹	5 .13	9	4	—13.6	6		—0.2		
5171	θ Aquilae	6 .1	— 1 7	AO	2 ^s .8	3 .37	32	85°	Var.	17	(3)	—0.5	370	—18
7710	3911				W	3 .59	26	19	—28.6	17		0.9		
5182	ϵ Aquilae	9 .7	+14 54	AO	2 ^s .8	4 .96	73	46°	Var.	19	(2)	1.3	24	—11
7724	4227				W	5 .15	72	15	—24.5	19		4.3		
5186	α^1 Cygni	10 .2	+46 31	A2	2 ^s .5	4 .96	17	123°	—22:	15	(4)	0.7	50	+ 6
7730	2881				YG ²	5 .07	14	10		14		1.1		

Boss 5071. Cepheid variable; period 7.2 days.

20^h.

1	2	3	4	5	6	7	8	9	10	11	12	13	14	15
5187	α^2 Cygni	10 ^m .5	+46° 26'	KO	6° 5	3 ^m .95	2	63°	Var	8	(4)	-2.6	50°	+ 6°
7735	2882			B8	O ²	3 .93	0	+ 2	- 3.0	5		-4.6		
5188	β^2 Cygni	10 .8	+36 30	A0	2° 7	4 .98	94	44°	-22	16	(4)	0.9	43	0
7736	3955				Y ¹	5 .17	+ 65	+ 68		15		4.8		
5190	Vulpeculae	11 .0	+25 17	B3	1° 9	4 .82	4	236°	Var	6	(2)	-1.3	33	- 6
7739	4165				W	5 .04	- 3	- 2	- 1	6		-2.2		
5191	33 Cygni	11 .1	+56 16	A3	3° 3	4 .32	102	37°	-28.6	32	(1)	1.9	58	+11
7740	2376				Y ¹	4 .52	+ 34	+ 97		32		4.4		
5195	23 Vulpeculae	11 .7	+27 30	K5	6° 5	4 .73	43	278°	+ 2.6	12	(1)	0.1	35	- 5
7744	3666				Y ²	4 .69	- 34	- 27		12		2.9		
5197	α^1 Capricorni	12 .1	-12 49	G0p	5° 6	4 .55	15	67°	-25.9	-3	(3)	-5.4	359	-26
7747	5683				Y ²	4 .65	+ 15	+ 4		1		0.5		
5199	α Cephei	12 .3	+77 25	B9	2° 4	4 .40	29	25°	-22.6	14	(3)	0.1	77	+22
7750	764				Y ¹	4 .61	+ 6	+ 28		14		1.7		
5200	α^2 Cygni	12 .3	+47 24	K0	6° 9	4 .16	5	68°	Var	3	(2)	-1.3	51	+ 6
7751	3059			A3	O ²	4 .15	0	+ 5		8		-2.3		
5202	α^2 Capricorni	12 .5	-12 51	G5	5° 5	3 .77	58	85°	+ 0.1	25	(6)	-0.1	359	-26
7754	5685				Y ²	3 .85	+ 50	+ 30		17		2.6		
5208	ρ Cygni	14 .1	+37 43	B1p	4° 1	4 .88	16	227°	- 7.9	-9	(2)	-5.1	44	+ 1
7763	3871			Nova	Y ²	5 .07	- 10	- 12		1		0.9		
5214	γ Capricorni	15 .1	-13 4	A0	2° 5	4 .84	18	158°	- 2.8	18	(1)	1.1	359	-27
7773	5642				W	5 .00	- 4	+ 17		18		1.1		
5215	β^1 Capricorni	15 .2	-15 6	B9	-1°	6 .16	45	87°		17	(a)	2.3	357	-28
7775	5626				B2		+ 36	+ 22				4.4		
5216	β^2 Capricorni	15 .4	-15 6	G0	5° 5	3 .25	35	88°	Var	20	(3)	-0.7	357	-28
7776	5629			A0	Y ²	3 .37	+ 29	+ 19	-19.0	16		1.0		
5223	α Pavonis	17 .7	-57 3	B3	1° 8	2 .12	86	177°	+ 1.8	13	(2)	-2.3	308	-36
7790	9674					2 .35	- 38	+ 77		13		1.8		
5229	γ Cygni	18 .6	+39 56	F8p	4° 5	2 .32	3	162°	- 5.4	6	(4)	-4.2	46	+ 1
7796	4159				Y ²	2 .44	- 3	+ 1		5		2.0		
5235	39 Cygni	19 .9	+31 52	K2	6° 1	4 .60	41	93°	-13.9	15	(4)	0.5	40	- 4
7806	4062				Y ²	4 .60	+ 3	+ 41		15		2.7		
5244	ρ Capricorni	23 .2	-18 9	F0	3°	4 .96	26	213°	+ 19	20	(4)	1.2	355	-34
7822	5689				Y ¹	5 .09	- 24	+ 9		18		2.1		
5255	41 Cygni	25 .3	+30 2	F5	4° 2	4 .09	10	114°	-18.6	2	(4)	-2.4	39	- 6
7834	4057				Y ¹	4 .24	- 2	+ 10		5		-0.9		
5265	ω^2 Cygni	27 .0	+48 37	B3	1° 8	4 .89	10	66°	-14.	5	(2)	-1.6	318	-38
7844	3142				W	5 .10	+ 1	+ 10		5		-0.1		
5268	ρ Pavonis	27 .3	-60 55	F0	4° 8	4 .84	176	163°	-19				303	-37
7848	6402					4 .95	- 46	+ 171				6.1		
5270	θ Cephei	27 .9	+62 39	A5	3° 3	4 .28	49	112°	Var	26	(2)	1.4	65	+14
7850	1821				W	4 .42	- 42	+ 26	- 4.9	26		2.7		
5272	ϵ Delphini	28 .4	+10 58	B5	2° 5	3 .98	28	161°	-18	7	(3)	-2.5	24	-18
7852	4321				W	4 .25	- 16	+ 23		5		1.2		
5279	47 Cygni	30 .0	+34 54	K5	6° 8	4 .85	14	188°	- 4.4	4	(2)	-2.1	43	- 4
7866	4079			A3	O ²	4 .81	- 14	- 1		4		0.6		
5281	α Indi	30 .5	-47 38	K0	4° 3	3 .21	72	33°	- 1.8	31	(2)	0.6	319	-38
7869	13477					3 .40	+ 66	- 30		30		2.5		
5282	ζ Delphini	30 .6	+14 20	A2	3° 0	4 .69	38	84°	-24	21	(4)	1.2	27	-17
7871	4353				W	4 .83	+ 24	+ 30		20		2.6		
5291	β Delphini	32 .9	+14 15	F5	4° 0	3 .72	113	109°	Var	41	(6)	1.7	27	-17
7882	4369				Y ²	3 .93	+ 25	+ 110	-22.9	39		4.0		
5294	1 Aquilae	33 .2	- 1 27	K0	5° 1	4 .51	28	154°	Var	11	(3)	-0.5	373	-25
7884	4016				Y ²	4 .50	- 10	+ 26	- 5.8	10		1.8		
5301	29 Vulpeculae	34 .1	+20 51	A0	2° 4	4 .78	58	91°	-16	12	(4)	-0.7	32	-13
7891	4658				W	5 .01	+ 24	+ 53		8		3.6		

Bosa 5215, 5216 A wide pair. The bright star is a spectroscopic binary

20^h to 21^h.

1	2	3	4	5	6	7	8	9	10	11	12	13	14	15
5310 7906	α Delphin 4222	35 ^m .0	+15° 34'	B8	3 ^s .3 Y ¹	3 ^m .86 4.10	65 + 25	97 ^s + 60	- 9 17	17 (3)	0.0 2.9	29°	-16°	
5315 7913	β Pavonis 3501	36.0	-66 34	A5	4 ^s .9	3.60 3.75	49 - 31	286 ^s + 38	+ 9.8 29	(a)	0.9 2.1	295	-37	
5318 7920	η Indi 11752	36.7	-52 17	F0		4.70 4.78	148 + 92	109° + 117	- 2 17	34 (a)	2.4 5.6	314	-40	
5320 7924	α Cygni 3541	38.0	+44 55	A2p	2 ^s .1 Y ¹	1.33 1.55	1 - 1	180° 0	Var - 4	8 (2)	-4.1 -8.7	52	+ 2	
5323 7928	δ Delphin 4403	38.8	+14 43	A5	4 ^s .0 Y ¹	4.53 4.63	56 - 55	204 ^s + 7	+ 8.3 18	20 (2)	0.8 3.3	28	-18	
5328 7936	ψ Capricorni 15018	40.2	-25 38	F8	4 ^s Y ¹	4.26 4.35	169 -142	200 ^s + 91	+26.0 50	50 (1)	2.8 5.4	347	-37	
5331 7942	δ Cygni 4167	41.6	+30 21	K0	5 ^s .6 Y ²	4.34 4.40	27 + 20	329 ^s - 18	- 1.0 24	24 (6)	1.1 1.5	41	- 8	
5334 7947	γ Delphin 4255	42.0	+15 46	G5	3 ^s .5 BG ²	5.47 5.84			- 7.4			30	-18	
5335 7948	γ Delphin 4255	42.0	+15 46	G5	5 ^s .4 OY ²	4.49 4.86	207 -193	189° + 75	- 6.5 36	36 (5)	2.3 6.1	30	-18	
5336 7949	ϵ Cygni 4018	42.2	+33 36	K0	5 ^s .5 Y ²	2.64 2.69	483 +362	48 ^s +319	-10 46	47 (6)	0.9 6.1	44	- 7	
5337 7950	ϵ Aquarii 8800	42.3	- 9 52	A0	3 ^s .0 Y ¹	3.83 4.01	44 - 3	141 ^s + 44	-15 28	28 (4)	1.1 3.0	6	-32	
5338 7951	κ Aquarii 5378	42.5	- 3 24	Ma	7 ^s .1 O ²	4.60 4.60	39 - 32	189° + 23	-22.0 15	15 (2)	0.5 2.6	11	-29	
5340 7952	ζ Indi 13718	42.6	-46 36	K5		4.90 5.02	41 + 39	73° + 13	- 5.2			321	-41	
5344 7955	ϵ Cephei 2240	42.9	+57 13	G0	5 ^s .0 Y ²	4.63 4.71	241 -178	196° -161	-32.3 57	57 (4)	3.4 6.5	62	+ 8	
5346 7957	η Cephei 2050	43.3	+61 27	K0	5 ^s .3 Y ²	3.59 3.58	826 +653	7° +512	-87.0 85	87 (4)	3.2 8.2	65	+11	
5350 7963	ζ Cygni 4867	43.5	+36 7	B5	2 ^s .4 W	4.47 4.77	12 - 11	160° + 5	Var -25	19 (4)	0.8 -0.1	46	- 5	
5352 7965	α Microscopii 14660	43.8	-34 9	K0		5.00 5.01	39 - 21	177° + 33	-14.5 11	11 (1)	0.2 3.0	337	-40	
5361 7977	δ Cygni 3291	45.5	+45 45	B2	3 ^s .0 Y ¹	4.89 5.03	5 - 4	143° + 2	- 3.9 3	3 (2)	-2.7 -1.6	53	+ 1	
5363 7980	ω Capricorni 15082	45.9	-27 18	Ma	7 ^s OY ²	4.24 4.22	17 - 16	213° + 6	+11.4 13	13 (1)	-0.2 0.4	346	-38	
5367 7986	β Indi 7788	47.0	-58 50	K0		3.72 3.88	29 - 5	155° + 28	- 4.7 18	18 (1)	0.0 1.0	305	-40	
5371 7990	μ Aquarii 5598	47.3	- 9 22	A3	4 ^s .2 Y ²	4.80 4.97	51 + 4	133° + 51	- 9 28	28 (2)	2.0 3.4	7	-32	
5373 7995	β Vulpeculae 4017	47.8	+26 43	G5	5 ^s .4 Y ²	4.76 4.79	103 - 90	227° - 52	- 0.5 11	13 (4)	0.0 4.8	40	-12	
5375 8001	δ Cygni 8768	49.7	+44 0	B3	1 ^s .9 W	4.68 4.91	18 + 3	71° + 18	Var. -16.2	8 (2)	-0.8 1.0	52	0	
5393 8028	ν Cygni 4364	53.4	+40 47	A0	2 ^s .8 YG ¹	4.04 4.17	25 - 24	168° + 4	-30 8	12 (2)	-1.4 1.0	51	- 3	
5402 8039	γ Microscopii 16353	55.2	-32 39	G5		4.71 4.75	9 + 9	63° + 2	+17.6 10	10 (1)	-0.3 -0.5	339	-42	
5410 8047	η Cygni 8138	56.4	+47 8	B0p	1 ^s .7 W	4.86 5.01	8 + 2	67° + 8	Var + 1	4 (2)	-2.1 -0.6	56	0	
5417 8060	η Capricorni 6115	58.7	-20 15	A3	3 ^s .4 W	4.93 5.10	60 - 60	224° + 5	+24 21	21 (2)	1.5 3.8	356	-40	
5427 8075	δ Capricorni 6174	0.3	-17 38	A0	2 ^s .0 W	4.19 4.34	105 + 15	129° +104	-10 21	21 (1)	0.8 4.3	359	-39	

Boss 5320, Donab. As the radial velocity is variable in a way suggesting pulsations this star should be tested for an eventual variability in its light. — Boss 5334, 5335. ADS 14279. Doubtless a physical pair. The dynamic parallax is 0^h.042.

21^h

1	2	3	4	5	6	7	8	9	10	11	12	13	14	15
5431	ϵ Cygni	1 ^m .3	+43° 32'	K5	6 ^s .6	3 ^m .92	7	117°	Var	6	(3)	-2.2	51°	-2°
8079	3800				O ^d	3.88	-4	+6	-19.9	6		-1.9		
5130	Δ Capricorni	1.3	-25 24	Ma	6 ^s -7 ^s	4.60	59	210°	+32.4	14	(2)	0.3	50	-41
8080	15235				O ^a	4.56	-56	+19		14		3.5		
5436	δ^2 Cygni	3.2	+47 15	K5	6 ^s .3	4.88	14	126°	-26.5	9	(3)	-0.4	57	-1
8089	3292				Y ³	4.75	-10	+10		9		0.6		
5441	ν Aquarii	4.1	-11 47	K0	5 ^s .8	4.52	94	98°	-11.8	29	(2)	1.9	6	-37
8093	5538				Y ^d	4.50	+56	+75		30		4.4		
5443	γ Equulei	5.5	+9 44	F0p	3 ^s .4	4.76	169	162°	-17.1	21	(6)	1.0	28	-25
8097	4732				Y ¹	4.77	-106	+132		18		5.9		
5452	ζ Cygni	8.7	+29 49	K0	5 ^s .1	3.40	59	183°	+17.0	17	(4)	-0.4	45	-13
8115	4348				Y ^d	3.13	-58	+11		17		0.6		
5455	δ Equulei	9.6	+9 36	F5	4 ^s .5	4.61	306	172°	-15.4	62	(7)	3.6	29	-26
8123	4746				Y ²	4.69	-230	+202		62		7.0		
5460	τ Cygni	10.8	+37 37	F0	4 ^s .0	3.82	455	20°	Var	48	(6)	2.2	51	-8
8130	4210				Y ²	3.93	+441	+118	-22.0	48		7.1		
5461	α Equulei	10.8	+4 50	F8	4 ^s .6	4.11	104	117°	Var	31	(5)	1.6	25	-30
8131	4635			A3	Y ¹	4.18	-37	+97	-15.9	31		4.2		
5464	μ Microscopi	11.9	-32 35	A0		4.79	66	121°	-1				340	-45
8135	16498					4.92	+120	+63				3.9		
5467	θ Indi	12.7	-53 52	A5		4.60	136	123°	-14				310	-44
8140	10037					4.69	+39	+131				5.3		
5469	σ Cygni	13.5	+38 59	A0p	3 ^s .1	4.28	8	220°	Var	-1	(1)	4.3	52	-7
8143	4431				Y ¹	4.47	-6	-5	-3.8	0		-1.2		
5471	ν Cygni	13.8	+34 29	B3p	2 ^s .5	4.42	29	136°	+6	12	(2)	-0.2	48	-11
8146	4371				W	4.61	-17	+23		12		1.7		
5473	θ Microscopi	14.4	-41 14	A2p		4.92	85	90°	+2				329	-46
8151	14475					5.06	+64	+56				4.6		
5480	α Cephei	16.2	+62 10	A5	2 ^s .8	2.60	160	72°	-8	73	(5)	-1.9	68	+9
8162	2111				YG ¹	2.81	-11	+160		73		3.6		
5484	ϵ Capricorni	16.7	-17 16	K0	5 ^s .4	4.30	32	79°	+11.2	16	(1)	0.3	2	-42
8167	6245				Y ²	4.29	+27	+18		16		6.3		
5489	λ Pegasi	17.5	+19 23	K0	5 ^s .9	4.24	118	60°	-76.3	28	(5)	1.5	38	-22
8173	4691				Y ²	4.23	+96	+70		28		4.6		
5493	γ Pavonis	18.2	-65 49	F8		4.30	815	6°	-30.1	129	(1)		295	-41
8181	3918					4.43	+603	-546		129		8.9		
5507	ζ Capricorni	21.0	-22 51	G5p	5°	3.86	23	0°	+2	4	(2)	-3.1	354	-45
8204	412				Y ^{2.5}	3.92	+16	-17		4		0.7		
5513	δ Capricorni	23.0	-22 15	G5	5°	4.59	132	93°	-22.0	18	(2)	0.9	356	-45
8213	5692				Y ^{2.5}	4.61	+88	+98		18		5.2		
5522	2 Pegasi	25.5	+23 12	K5	7 ^s .1	4.76	17	103°	-18.9	12	(5)	0.3	42	-20
8225	4325				OY ³	4.68	+2	+17		12		0.9		
5527	β Aquarii	26.3	-6 1	G0	4 ^s .6	3.07	17	115°	+6.8	5	(4)	-3.4	16	-39
8232	5770				Y ²	3.20	+4	+16		5		-0.7		
5532	β Cephei	27.4	+70 7	B1	2 ^s .4	3.32	12	65°	Var	6	(5)	-2.8	75	+14
8238	1173				W	3.53	0	+12	-7.2	6		-1.3		
5543	ρ Cygni	30.2	+45 9	K0	5 ^s .1	4.22	99	196°	+6.9	23	(4)	0.7	58	-5
8252	3866				Y ²	4.20	+95	-28		20		4.2		
5544	ν Octantis	30.4	-77 50	K0		3.74	234	169°	Var	31	(1)	1.2	281	-36
8254	1510					3.91	-140	+187	+32.1	31		5.6		
5546	72 Cygni	30.7	+38 5	K0	6 ^s .0	4.98	148	52°	-66.5	14	(5)	0.7	54	-11
8255	4369				Y ²	4.97	+105	+105		14		5.8		
5549	μ Capricorni	31.5	-19 54	B5p	2-3°	4.72	8	104°	-25	7	(2)	-1.0	0	-47
8260	6251				Y ¹	4.89	+4	+7		7		-0.8		
5551	ξ Aquarii	32.4	-8 18	A5	3 ^s .2	4.78	114	102°	-20	24	(1)	1.7	15	-41
8264	5701				W	4.93	+54	+100		24		5.1		

Boss 5460 Wellknown binary = ADS 11787 The period is 49.2 years The bright star is a very short-period spectroscopic binary

21^h to 22^h.

1	2	3	4	5	6	7	8	9	10	11	12	13	14	15
5562 8278	γ Capricorni 6340	34 ^m ,6	-17° 7'	F0p	3 ^m ,9 YG ¹	3 ^m ,80 3,93	188 + 111	96° + 152	Var -31,2	15 15	(2)	-0,9 5,2	4° 5,2	-46
5563 8279	η Cephei 2169	35,2	+61 38	B2p	3 ^m ,7 Y ¹	4,87 5,07	5 0	68° + 5	-14,7 3	3 3	(3)	-4,7 -1,6	70° -1,6	+ 7
5570 8288	κ Capricorni 6152	37,1	-19 19	G5	5 ^m ,6 OY ¹	4,82 4,86	142 + 91	93° + 109	- 3,1 6	6 6	(2)	-1,3 5,6	2 5,6	-47
8296	ζ Cygni	37,8	+42 23	Pec. Nova		3,0-15,4	4 + 3	45° + 2	-			-4,0	57	- 8
5580 8301	π^1 Cygni 3410	38,6	+50 44	B3	2 ^m ,2 W	4,78 4,96	6 - 2	100° + 6	Var.	5 5	(3)	-1,7 -1,3	64	- 2
5582 8305	ι Picula Aust. 15734	39,0	-33 29	A0		4,35 4,50	93 - 34	157° + 86	+ 2			4,2	341	-51
5584 8308	ϵ Pegasus 4891	39,3	+ 9 25	K0	6 ^m ,1 Y ¹	2,54 2,68	25 + 12	92° + 22	+ 4,7	21 15	(5)	-1,6 -0,5	34	-33
5587 8309	μ^1 Cygni 4169	39,6	+28 18	F5	4 ^m ,1 Y ¹	4,73 4,91	350 - 12	132° + 333	+18,5	58 59	(5)	3,6 7,4	49	-19
5588 8310	μ^2 Cygni 4169	39,6	+28 18		6 ^m ,08 6,26	325 - 10	130° + 309	+16,3				4,9 8,6	49	-19
5590 8313	η Pegasus 4582	39,8	+16 54	G5	5 ^m ,8 Y ¹	4,52 4,49	29 - 13	143° + 26	-22,3	11 11	(3)	-0,3 1,8	40	-27
5592 8315	κ Pegasus 4483	40,1	+25 11	F5	4 ^m ,0 Y ¹	4,27 4,32	33 + 14	86° + 30	-10,3	42 38	(8)	2,2 1,9	46	-22
5593 8316	μ Cephei 2316	40,4	+58 19	Ma	7 ^m ,9 OR ¹	3,92-4,53 3,7-4,7	2 - 2	207° + 1	Var +20,5	2 2	(1)		68	+ 4
5594 8317	η Cephei 1193	40,5	+70 51	K0	5 ^m ,8 Y ¹	4,85 4,76	153 + 43	51 + 147	-37,3	13 13	(5)	0,4 5,8	76	+14
5600 8322	δ Capricorni 5943	41,5	-16 35	A5	3 ^m ,7 Y ¹	2,98 3,18	392 - 55	139° + 388	Var. - 6,4	78 76	(4)	2,4 6,0	5	-47
5608 8334	ν Cephei 2288	42,6	+60 40	A2p	4 ^m ,1 Y ¹	4,46 4,58	2 + 0	270° - 2	-23,7	12 11	(2)	-0,3 4,0	70	+ 6
5609 8335	π^2 Cygni 3504	43,1	+48 51	B3	2 ^m ,3 W	4,26 4,44	5 - 3	127° + 4	-19,5	5 5	(3)	-2,2 2,2	63	- 4
5617 8343	η Pegasus 4525	45,4	+29 43	A0	2 ^m ,6 W	5,00 5,30	39 - 18	134° + 34	-22	10 9	(3)	-0,2 3,0	51	-18
5624 8353	γ Grus 14536	47,9	-37 50	B8	3 ^m ,7	3,16 3,37	111 + 65	98° + 90	- 2	18	(a)	-0,5 3,4	333	-53
5635 8368	δ Indi 9733	51,1	-55 28	F0	4,56 4,63	59 + 19	59 + 56	114° + 56	+15			3,4	306	-49
5650 8383	VV Cephei 8007	53,8	+63 9	Map		4,9 to 5,6	9 + 7	311° - 6	Var.	5	(a)		73	+ 7
5654 8387	ϵ Indi 10015	55,7	-57 12	K5		4,74 4,85	4696 + 657	123° + 4649	-40,4	267 265	(2)	6,8 13,0	303	-49
5663 8402	σ Aquarii 5681	58,1	- 2 38	B5p	2 ^m ,5 W	4,66 4,86	18 - 1	128° + 18	+16,1	13 13	(1)	0,2 0,9	25	-43
5672 8411	λ Grus 14639	0,1	-40 2	K2		4,60 4,62	124 - 110	195° + 56	+40,0	17 17	(1)	0,7 5,1	329	-55
5674 8413	ν Pegasus 4800	0,6	+ 4 34	K5	7 ^m ,0 OY ¹	4,90 4,97	144 + 138	50° + 42	-17,2	13 13	(4)	0,5 5,7	34	-39
5676 8414	α Aquarii 4846	0,6	- 0 48	G0	4 ^m ,8 Y ¹	3,19 3,32	15 + 3	113° + 15	+ 7,6	8 8	(3)	-2,3 -0,9	28	-43
5677 8417	ϵ^1 Cephei 1808	0,9	+64 8	G	5 ^m ,0 Y ¹	6,47	225	66°				4,8 8,2	73	+ 7
5679 8417	ϵ^2 Cephei 1808	0,9	+64 8	A3	3 ^m ,9 V ¹	4,57	226 + 43	68° + 221	- 6,0	53 47	(5)	2,9 6,3	73	+ 7
5680 8418	ι Aquarii 6209	1,0	-14 21	B8	3 ^m ,0 W	4,35 4,54	70 - 24	149° + 66	Var.	15 15	(1)	0,2 3,6	12	-50
5684 8425	α Grus 14063	1,9	-47 27	B5	2 ^m ,4	2,16 2,22	200 - 48	145° + 194	+12	31 30	(2)	-0,5 3,7	318	-53

Stars 5677, 5679. Doubtless a physical pair. The dynamical parallax is 0",041. The combined magnitude is 4m,40 (RHP), 4m,4 (Zinner).

22^h.

1	2	3	4	5	6	7	8	9	10	11	12	13	14	15
5688	<i>ε</i> Pegasi	2 ^m .4	+21° 51'	F5	3 ^s .9	3 ^m .96	299	86°	— 4.3	78	(5)	3.1	51°	—25°
8430	4533				Y ²	4.03	—126	—272		78		6.3		
5689	<i>μ</i> Piscis Aust	2.5	—33 29	A2		4.62	82	119°	+12				342	—56
8431	15922					4.78	+17	+80				4.2		
5703	<i>θ</i> Pegasi	5.2	+5 42	A2	2 ^s .7	3.70	276	83°	Var	26	(3)	0.7	36	—39
8450	4961				W	3.96	—174	+215	—7	25		5.9		
5709	<i>π</i> Pegasi	5.5	+32 41	F5	4 ^s .1	4.38	26	209°	+2	22	(5)	0.5	56	—19
8454	4352				Y ²	4.48	—25	—6		17		1.5		
5714	<i>ζ</i> Cophes	7.4	+57 42	K0	6 ^s .0	3.62	12	55°	—18.2	21	(1)	0.2	71	+2
8465	2475				O ²	3.61	+6	+10		21		—1.0		
5716	24 Cophes	7.9	+71 51	G5	5 ^s .5	4.99	28	82°	—15.0	9	(3)	—1.5	79	+13
8468	1111				Y ²	4.99	—4	+28		5		2.2		
5732	<i>ι</i> acetiae	9.6	+39 13	K2	6 ^s .2	4.64	49	84°	—10.8	11	(2)	—0.1	60	—14
8485	1711				Y ³	4.58	+14	+47		11		3.1		
5733	<i>μ</i> ¹ Gius	9.6	—41 51	G0		4.86	57	57°	—7.2	6	(a)	—1.2	325	—56
8486	14810					4.97	+55	+17				3.7		
5742	<i>ε</i> Cophes	11.3	+56 33	F0	3 ^s .6	4.23	452	84°	—1	56	(5)	2.7	71	+1
8494	2711				Y ^{1.5}	4.37	+23	+452		50		7.5		
5746	<i>ι</i> I acetiae	11.6	+37 15	K0	6 ^s .0	4.22	20	101°	—8.5	12	(5)	—0.8	60	—16
8498	4526				Y ³	4.26	+1	+20		10		0.7		
5744	<i>θ</i> Aquarii	11.6	—8 17	K0	5 ^s .5	4.32	112	100°	—14.7	14	(3)	—0.1	23	—50
8499	5845				Y ²	4.33	+49	+101		13		4.6		
5747	<i>α</i> Lucanac	11.7	—60 45	K2	5 ^s .4	2.91	87	249°	+45	36	(1)	0.7	297	—49
8502	7561					3.12	—75	—45		36		2.6		
5761	<i>γ</i> Aquarii	16.5	—1 53	A0	2 ^s .6	3.97	123	86°	Var	43	(2)	1.9	31	—47
8518	5741				W	4.12	+76	+97	—21	38		4.4		
5762	31 Pegasi	16.6	+11 42	B3p	2 ^s .2	4.93	6	67°	+8	7	(a)	—0.9	44	—37
8520	4784				W	5.15	+6	+1				—1.2		
5763	32 Pegasi	16.7	+27 50	B8	2 ^s .8	4.88	5	112°	+7	8	(1)	—0.6	55	—24
8522	4299				W	5.06	0	+5		8		—1.6		
5764	2 Lacetiae	16.9	+46 2	B5	2 ^s .1	4.66	20	90°	Var	18	(3)	0.4	66	—9
8523	3894				W	4.79	+2	+20	—9.0	14		1.2		
5776	<i>β</i> Lacetiae	19.6	+51 44	K0	5 ^s .6	4.58	190	184°	—10.6	24	(5)	1.5	69	—4
8538	3358				Y ³	4.56	—190	—6		24		6.0		
5777	<i>π</i> Aquarii	20.2	+0 52	B1p	2 ^s .9	4.64	13	85°	+4.4	6	(1)	—1.5	35	—46
8539	4872				W	4.74	+10	+10		6		—0.4		
5778	<i>δ</i> Tucanae	20.2	—65 28	B9		4.80	67	81°	+12				291	—47
8540	4044					4.89	+46	+48				3.9		
5779	4 Lacetiae	20.4	+48 58	B8p	3 ^s .1	4.64	14	216°	—26.7				68	—7
8541	3715				W	4.80	—12	—7				0.4		
5790	35 Pegasi	22.8	+4 12	K0	5 ^s .0	4.93	325	167°	+54.0	25	(4)	1.9	39	—44
8551	4710				Y ³	4.90	—23	+231		25		7.5		
5791	<i>δ</i> ¹ Gius	23.3	—44 0	G5		4.02	26	88°	+5.0	12	(1)	—0.6	320	—58
8556	14931					4.19	+17	+20		12		1.1		
5793	<i>ζ</i> ¹ Aquarii	23.7	—0 32		4 ^s .5	4.59	173	85°	+28.9	35	(6)	2.0	34	—48
8558	4365				Y ²	4.70	+107	+137		31		5.8		
5794	<i>ζ</i> ² Aquarii	23.7	—0 32	F2	Y ²	4.42	212	79°	+24.5			1.9	34	—48
8559	4365					4.53	+151	+151				6.0		
5795	<i>δ</i> ² Gius	23.8	—44 15	Mb		4.31	18	280°	+3.0				320	—58
8560	14935					4.42	—8	—16				—0.6		
5807	<i>δ</i> Cophes	25.4	+57 54	G0	4 ^s .7	Var	14	86°	—16.4	5	(3)	—2.9	73	+1
8571	2548				Y ^{2.5}	3.6—4.3	+1	+14		4		—0.7		
5804	5 Lacetiae	25.4	+47 11	K0	7 ^s .2	4.61	21	239°	—11.9	4	(5)	—2.4	67	—9
8572	3719			A0	O ³	4.54	—13	—17		4		1.2		
5803	<i>σ</i> Aquarii	25.4	—11 11	A0	2 ^s .7	4.89	30	180°	+14	15	(2)	0.6	21	—54
8573	5850				W	5.06	—24	+18		14		2.3		

Boss 5807 The prototype of the Cepheids, period 5.4 days Has also a companion 7^m.5, 11", 192°, which shares its p m

22^b.

1	2	3	4	5	6	7	8	9	10	11	12	13	14	15
5808	β Pictis Aust	25 ^m .9	-32° 52'	A0		4 ^m .36	61	109°	+ 6.3				342°	-60°
8576	17126					4.51	+ 22	+ 57				3.3		
5810	δ Lacertae	26.1	+42 36	B3	2 ^s .5	4.54	13	261°	Var	6	(3)	-1.6	65	-12
8579	4120				W	4.73	- 4	- 12	-10.5	6		0.1		
5811	τ Tucanae	26.2	-62 29	Mb		4.92	39	151°	- 3.4				294	-49
8582	6348					5.03	- 18	+ 33				2.9		
5813	α Lacertae	27.2	+49 46	A0	2 ^s .9	3.85	142	85°	-14	36	(3)	1.6	69	- 7
8585	3875				Y ¹	3.99	+ 24	+139		35		4.6		
5824	η Aquarii	30.2	- 0 38	B8	2 ^s .6	4.13	105	121°	- 8	17	(1)	0.3	35	-48
8597	4384				W	4.33	+ 3	+105		17		4.2		
	Lacertae	31.7	+52 12	Pec Nova		4.5 to 14.5	+ 1	0°					71	- 5
5837	η Lacertae	33.2	+51 1	A5	3 ^s .4	4.83	116	210°	+19	25	(1)	1.8	70	- 6
8613	3770				Y ¹	4.97	-106	- 49		25		5.2		
5844	δ Lacertae	34.8	+38 32	Oe5	2 ^s .0	4.91	11	165°	Var				65	-17
8622	4826				W	5.10	- 7	+ 8	- 9			0.3		
5849	ϵ Pictis Aust.	35.1	-27 34	B8	1 ^s -2 ^s	4.22	24	94°	+ 3				352	-62
8628	16010				Y ¹	4.41	+ 13	+ 20				1.1		
5850	β Octantis	35.8	-81 54	F0		4.34	63	275°	+25				275	-35
8630	889					4.47	- 21	- 59				3.3		
5852	η Lacertae	36.1	+43 46	K0	6 ^s .4	4.64	97	85°	-10.7	17	(4)	0.8	68	-13
8632	4266				O ¹	4.59	+ 27	+ 93		17		4.6		
5853	ζ Pegasi	36.5	+10 19	B8	2 ^s .7	3.61	78	99°	+ 4	12	(3)	-2.2	47	-42
8634	4797				W	3.79	+ 27	+ 73		7		3.1		
5854	β Crula	36.7	-47 24	Mb	6 ^s .8	2.24	130	99°	+ 1.0	15	(1)	-1.9	314	-59
8636	14308					2.43	+ 57	+117		15		2.8		
5858	σ Pegasi	37.1	+28 47	A0	2 ^s .4	4.85	36	191°	+ 7.9	17	(3)	1.0	60	-26
8641	4436				YG ¹	5.04	- 35	+ 6		17		2.6		
5860	ρ Crula	37.7	-41 56	K0		4.89	84	183°	+30.4	14	(1)	0.6	323	-61
8644	18049					4.92	- 71	+ 45		14		4.5		
5864	η Aquarii	38.2	-19 21	K5	5 ^s .3	4.88	35	215°	+21.6	11	(1)	0.1	11	-60
8649	6324				O ¹	4.84	- 35	+ 1		11		2.6		
5865	η Pegasi	38.3	+29 42	G0	5 ^s .0	3.10	36	164°	+ 4.4	24	(3)	-0.2	61	-25
8650	4741				Y ¹	3.22	- 29	+ 21		22		0.9		
5867	η Crula	39.5	-54 1	K0		4.86	25	48°	+27°	24	(1)	1.8	302	-56
8655	10123					4.97	+ 24	+ 6		24		1.9		
5874	ζ Pegasi	41.6	+11 40	F5	4 ^s .8	4.31	545	155°	- 4.5	59	(5)	3.1	50	-41
8665	4875				Y ¹	4.32	-322	+441		58		8.0		
5875	λ Pegasi	41.7	+23 2	K0	5 ^s .1	4.14	60	104°	- 3.8	21	(4)	0.4	57	-31
8667	4708				Y ¹	4.15	+ 10	+ 59		18		3.0		
5880	ϵ Crula	42.5	-51 51	A2		3.69	120	122°	0				304	-58
8675	13389					3.83	+ 2	+120				4.1		
5884	τ Aquarii	44.3	-14 7	K5	7 ^s .0	4.21	39	204°	+ 1.2	20	(4)	0.6	21	-59
8679	6354				O ¹	4.13	- 38	+ 7		19		2.2		
5885	μ Pegasi	45.2	+24 4	K0	5 ^s .3	3.67	154	107°	+13.8	31	(4)	1.1	59	-31
8684	4618				Y ¹	3.75	+ 18	+152		31		4.6		
5891	ϵ Cephei	46.1	+65 40	K0	5 ^s .1	3.68	139	209°	-12.3	34	(6)	1.3	79	+ 7
8694	1814				Y ¹	3.66	-118	- 74		34		4.4		
5893	γ Pictis Aust	47.0	-33 24	A0		4.52	44	223°	+16	7	(a)		341	-65
8695	16270					4.68	- 44	- 6				2.7		
5895	λ Aquarii	47.4	- 8 7	Ma	6 ^s .9	3.84	36	6°	- 9.5	18	(3)	0.1	32	-57
8698	5968				OY ¹	3.87	+ 32	- 17		18		1.6		
5899	Cephei	47.9	+82 37	K0	6 ^s .4	4.97	64	32°	-31.1	19	(3)	1.4	86	+22
8702	703				OY ¹	4.88	+ 45	+ 45		19		4.0		
5904	δ Aquarii	49.3	-16 21	A2	2 ^s .8	3.51	52	246°	+20	39	(2)	1.5	19	-61
8709	6173				Y ¹	3.68	- 44	- 28		39		2.1		
5910	ρ Pegasi	50.2	+ 8 17	A0	2 ^s .8	4.95	72	79°	-12	12	(4)	-0.3	49	-50
8717	4961				W	5.12	+ 48	+ 54		9		4.2		

22^h to 23^h.

1	2	3	4	5	6	7	8	9	10	11	12	13	14	15
5911	δ Piscis Aust	50 ^m .4	-33° 4'	K0		4 ^m .33	36	39°	-11.9	23	(1)	1.1	311°	-65°
8720	16303					4.35	+36	+3		23		2.1		
5916	α Piscis Aust	52.1	-30 9	A3	2 ^s .6	1.29	365	117°	+6.5	112	(2)	1.5	348	-66
8728	19370					1.57	-51	+361		111		4.1		
5926	ϵ Gaur	55.0	-53 17	G5		4.18	66	266°	Var	17	(1)	0.3	300	-58
8747	10382					4.30	-38	-51	-3	17		3.3		
5927	36 Cephei	55.2	+83 49	K5		4.96	106	73°	+2.9	13	(2)	0.5	87	+23
8718	610					4.86	+7	+106		13		5.1		
5933	α Andromedae	57.3	+11 47	B5	2 ^s .3	3.63	32	131°	-15	11	(4)	-1.6	70	-16
8762	4664			A2p	W	3.91	-13	-29		9		1.2		
5939	β Piscium	58.6	+3 17	B5p	2 ^s .4	4.58	13	129°	+2	10	(1)	-0.4	48	-51
8773	4818			W	W	4.75	-2	+13		10		0.2		
5910	β Pegasi	58.9	+27 32	Ma	6 ^s .8	2.61	234	55°	+8.7	23	(5)	-0.7	65	-29
8775	4180			OY ²	OY ²	2.66	+199	+124		22		4.6		
5942	3 Andromedae	59.7	+19 30	K0	5 ^s .9	1.91	230	46°	-31.8	14	(5)	0.1	74	-9
8780	4028			Y ³	Y ³	1.84	+189	+131		11		6.7		
5911	α Pegasi	59.8	+14 40	A0	1 ^s .8	2.57	71	128°	Var	32	(4)	0.1	57	-41
8781	4926			X(G ¹)	X(G ¹)	2.96	-13	+73	-4	32		1.9		
5919	θ Gaur	1.2	-11 1	F5		1.35	57	233°	+9.6	10	(4)	-0.6	315	-64
8787	15149					4.56	-53	-21				3.2		
5950	ϵ^1 Aquarii	1.3	-21 17	G5	5 ^s -6 ^s	1.77	68	90°	+15.2	13	(1)	-0.7	4	-67
8789	17197			OY ²	OY ²	4.81	138	+56		8		3.9		
5952	55 Pegasi	2.0	+8 52	Ma	6 ^s .8	1.69	16	153°	-5.7	9	(5)	-1.1	53	-46
8795	4997			O ²	O ²	4.61	-8	+14		7		0.7		
5954	56 Pegasi	2.2	+24 56	K0	6 ^s .4	4.98	38	180°	-26.9	16	(4)	0.7	63	-32
8796	4716			Y ¹	Y ¹	1.95	-35	+16		14		2.9		
5955	1 Cassiopeiae	2.4	+58 53	B1	2 ^s .6	1.93	12	59°	Var	3	(3)	-2.7	77	-1
8797	2515			Y ¹	Y ¹	5.07	17	+10	+8.5	3		0.3		
5960	ϵ^2 Aquarii	4.1	-21 43	K0	5 ^s -6 ^s	3.80	59	51°	+24.1	23	(3)	0.6	10	-67
8812	6168			Y ²	Y ²	3.79	+56	+18		23		2.7		
5963	ϵ^3 Aquarii	4.5	-23 0	G0	2 ^s	4.94	13	108°	-4.8	9	(2)	-0.3	7	-67
8817	17771			A2	Y ¹	5.02	+3	+13		9		0.5		
5966	π Cephei	4.7	+71 51	G5	5 ^s .2	4.56	28	154°	Var	17	(7)	0.0	84	+14
8819	1006			Y ¹	Y ¹	4.57	-26	+10	-19.3	12		1.8		
5965	ϵ Gaur	4.7	-15 47	K0		1.10	145	106°	Var	17	(1)	0.3	310	-63
8820	11947					4.19	+38	+141	-4.4	17		4.9		
5975	7 Andromedae	8.0	+48 51	F0	3 ^s .8	4.62	134	44°	+13	42	(4)	2.7	75	-10
8830	3964			Y ¹	Y ¹	4.73	+115	+70		41		5.3		
5978	ϕ Aquarii	9.1	-6 35	Ma	7 ^s .0	4.40	193	172°	-0.4	14	(4)	0.0	40	-59
8834	6170			OY ³	OY ³	4.39	-149	+124		13		5.8		
5981	ψ^1 Aquarii	10.7	-9 38	K0	5 ^s .9	4.46	367	92°	-27.0	21	(3)	1.1	37	-62
8841	6156			Y ³	Y ³	4.44	+191	+316		21		7.3		
5985	γ Lucanac	11.6	-58 47	F2		4.10	89	336°	+18				290	-55
8848	8062					4.23	+57	-69				3.8		
5988	γ Piscium	12.0	+2 44	K0	5 ^s .6	3.85	753	88°	-14.0	25	(4)	0.8	52	-52
8852	4648			Y ³	Y ³	3.97	+407	+633		25		8.2		
5992	ψ^2 Aquarii	12.7	-9 44	B5	2 ^s .6	4.56	13	103°	-3	10	(1)	-0.4	37	-62
8858	6160			YG ¹	YG ¹	4.73	+4	+12		10		0.2		
5993	8 Andromedae	13.1	+48 28	Ma	7 ^s .1	4.99	38	81°	-8.3	10	(4)	0.0	75	-11
8860	3991			O ³	O ³	4.95	+15	+35		10		2.9		
5995	γ Sculptoris	13.4	-33 5	K0		4.51	71	159°	+16.7	15	(1)	0.4	337	-70
8863	16476					4.53	-43	+57		15		7.0		
6000	α Cephei	14.5	+67 34	G5		4.90	66	75°	-17.8	22	(7)	1.5	82	+7
8872	1514					4.92	+20	+63		21		4.0		
6005	π Pegasi	15.7	+23 12	A5	2 ^s .8	4.65	35	127°	+17	28	(2)	1.8	66	-35
8880	4810			Y ¹	Y ¹	4.75	-7	+34		27		2.4		
6012	b ¹ Aquarii	17.7	-20 39	K0	5 ^s -6 ^s	4.20	153	233°	-5.6	27	(3)	1.4	15	-69
8892	6587			Y ²	Y ²	4.27	-142	-55		27		5.1		
6024	ν Pegasi	20.4	+22 51	G0	4 ^s .7	4.57	191	82°	-13	21	(4)	1.2	67	-35
8905	4833			Y ²	Y ²	4.69	+107	+159		21		6.0		

28^b.

1	2	3	4	5	6	7	8	9	10	11	12	13	14	15
6026 8906	b ^a Aquarii 6420	20 ^a , 8	-21° 12'	K5	6 ^a , 3 Y ^a	4 ^a , 52 4, 53	83 - 81	226° - 20	+15, 4	24 24	(1)	1, 4 4, 1	16° -70°	
6031 8911	π Piscium 4998	21, 8	+ 0 42	A2p	2 ^a , 6 W	4, 94 5, 17	24 - 32	136° + 120	- 4, 9	22 21	(5)	1, 0 1, 8	55 -56	
6037 8916	δ Piscium 5173	22, 9	+ 5 50	G5	5 ^a , 3 Y ^a	4, 45 4, 48	138 -102	252° - 92	+ 6, 1	9 7	(3)	-1, 3 5, 2	59 -51	
6040 8923	η Pegasi 6008	24, 1	+12 13	K0	5 ^a , 4 Y ^a	4, 67 4, 65	62 + 51	64° + 35	-15, 0	10 8	(4)	-0, 8 3, 0	63 -46	
6046 8926	Camelopardis 8748	25, 4	+58 0	B3	2 ^a , 5, 2 ^a W, V ¹	4, 89 5, 11	28 + 18	62° + 22	Var -14, 8	6 6	(3)	-1, 2 2, 1	80 - 3	
6054 8937	β Sculptoris 15527	27, 6	-38 22	B9		4, 46 4, 60	92 + 54	83° + 75	+ 2			4, 3	322 -71	
6057 8939	b ^a Aquarii 6437	28, 0	-21 28	A0	1 ^a W	4, 76 4, 92	18 + 11	338° - 15	+15			1, 1	20 -72	
6062 8949	ε Phoenicis 15420	29, 7	-43 10	A2p		4, 80 4, 94	27 - 1	110° + 27	+19			2, 0	309 -69	
6068 8959	Phoenicis 14720	32, 5	-46 3	A2		4, 86 5, 04	68 + 7	111° + 67	+10			4, 0	303 -67	
6071 8961	ι Andromedae 4283	32, 7	+45 55	K0	5 ^a , 5 Y ^a	4, 00 3, 98	449 -350	159° -283	+ 6, 7	45 45	(4)	2, 3 7, 3	78 -14	
6073 8965	ε Andromedae 4720	33, 2	+42 43	B8	2 ^a , 9 W	4, 28 4, 47	26 + 6	97° + 25	0, 0	13 13	(1)	-0, 2 1, 4	77 -17	
6077 8969	ε Piscium 6088	34, 8	+ 5 5	F8	3 ^a , 9 Y ^a	4, 28 4, 34	574 -195	140° +540	+ 5, 6	70 69	(4)	3, 5 8, 1	62 -54	
6078 8974	γ Cephei 928	35, 2	+77 4	K0	5 ^a , 4 Y ^a	3, 42 3, 45	169 +157	340° - 63	-43, 2	69 68	(4)	2, 6 4, 6	86 +15	
6080 8976	π Andromedae 4522	35, 5	+43 47	A0	2 ^a , 6 W	4, 33 4, 49	83 + 4	107° + 83	- 9,	14 13	(2)	-0, 1 3, 9	78 -17	
6083 8982	A ^a Aquarii 6358	36, 6	-18 23	G0	4 ^a , 9 Y ^a	4, 95 5, 05	18 + 14	68° + 11	+ 4, 8	2 2	(1)	-3, 6 1, 3	31 -72	
6084 8984	ι Piscium 6087	36, 9	+ 1 14	A5	3 ^a , 3 Y ¹	4, 61 4, 79	199 -195	223° - 42	+ 8	36 33	(6)	2, 2 6, 1	59 -57	
6087 8988	ω ^a Aquarii 6476	37, 5	-15 6	A0	2 ^a , 8 W	4, 62 4, 78	106 - 7	125° +106	- 3	16 16	(1)	0, 6 4, 7	39 -70	
6094 8997	78 Pegasi 4627	39, 0	+28 49	K0	5 ^a , 9 Y ^a	4, 98 4, 99	80 - 2	117° + 80	- 6, 8	16 16	(5)	1, 0 4, 5	75 -31	
6110 9016	δ Sculptoris 18353	43, 7	-28 41	A0	3 ^a Y ¹	4, 64 4, 81	146 - 35	133° +142	+14,	36 36	(a)	2, 4 5, 4	351 -77	
6135 9045	ε Camelopardis 3111	49, 4	+56 57	F8p	6 ^a , 7 Y ^a	4, 85 4, 94	7 + 3	315° - 6	-42, 5	8 4	(5)	-2, 1 -0, 9	83 - 4	
6150 9064	π Pegasi 4865	52, 7	+24 35	Ma	7 ^a , 3 OY ^a	4, 75 4, 74	56 - 53	228° - 19	- 4, 4	12 12	(3)	-0, 1 3, 5	77 -36	
6155 9071	σ Camelopardis 3088	53, 9	+55 12	B2	2 ^a , 8 W	4, 93 5, 14	12 - 1	115° + 12	- 6, 1	4 4	(3)	-2, 1 0, 3	83 - 6	
6156 9072	ω Piscium 5227	54, 2	+ 6 19	F5	4 ^a , 1 Y ^a	4, 03 4, 23	186 - 17	126° +186	- 2	31 33	(4)	0, 5 5, 4	70 -54	
6160 9076	ε Tucanae 3819	54, 7	-66 8	B9		4, 71 4, 80	48 - 14	121° + 46	+11			3, 1	277 -50	
6165 9084	δ Octantis 1596	56, 4	-77 37	K0		4, 73 4, 84	171 -164	204° - 48	+23, 7			5, 9	273 -40	
6171 9089	30 Piscium 6345	56, 8	- 6 35	Mb	7 ^a , 0 O ^a	4, 66 4, 65	53 - 8	130° + 52	-11, 8	11 11	(3)	-0, 1 3, 3	61 -66	
6173 9091	ζ Sculptoris 19790	57, 2	-30 16	B5		4, 99 5, 15	26 + 10	94° + 24	Var + 0, 3			2, 1	345 -80	
6179 9098	2 Ceti 6417	58, 6	-17 54	A0	3 ^a Y ¹	4, 62 4, 77	21 + 3	113° + 21	- 5	16 16	(1)	0, 6 1, 2	43 -76	

From 6046, Eclipsing binary — AR Cass. Period 6,066 days. — From 6135, Variable star 4m, 4 to 5m, 1

In the preceding table have been included the two globulars NGC 104 and 5139 as occurring in several Uransometries. To the objects brighter than 5m, 00 should also be added several globular clusters and open clusters and also the two Magellanic Clouds. The last mentioned objects have, according to the photographic estimates of the present writer, a total magnitude of 0m, 8 and 2m, 0, respectively.

II. Catalogue of Stellar Diameters

Explanations to the catalogue Col 1 gives the Boss number For further details as to the objects the preceding catalogue should be consulted

Col 2 gives the name of the star

Col 3 gives the hypothetical apparent radius according to HERTZSPRUNG's determination in *Annalen van de Sterrewacht te Leiden* XIV, part 1 (1922)

Col 4 the quantity $107,5 \times$ radius (unit $0''.001$)

Col 5, 6 and 7 contain the mean trigonometric parallax, the mean spectrographic parallax, and the spectral proper motion parallax, respectively (unit $0''.001$) By compiling this catalogue the available parallax material up to the beginning of 1929 was used Later on have been added a number of new determinations of trigonometric parallaxes In a very few cases the dynamic parallax has also been included in the value of π_1 The parallax values have been reduced to absolute values and corrected for systematic errors according to VAN MAANLINS tables

Col 8, 9 and 10 contain the linear radii computed by the aid of the three different parallax values π_1 , π_2 , and π_3 respectively

Col 11 the visual Harvard magnitude (RIIP)

Col 12 the Harvard spectral class according to the IHD Catalogue

Col 13 the quantity $H = m + 5 + 5 \log \mu$ computed on basis of Boss's proper motions

When the radius is within parenthesis this indicates that the value is considered to be rather inaccurate In a few cases the radii have not been computed on basis of π_3 , because of the fact that the parallax value falls outside the domain within which a fair value of π_3 can be derived

No Boss PGC	Name	Hypothetical radius (unit is $0''.0001$)	$107,5$ \times radius	Trig parallax π_1	Spectro- graphic parallax π_2	Spectral proper motion parallax π_3	Semi diameters			m_{vis} (Har- vard)	Spectral Class (Harvard)	H
							$\frac{d_1}{2}$	$\frac{d_2}{2}$	$\frac{d_3}{2}$			
10	α Andromedae	7	75,2	16	52	59	4,7	1,4	1,3	2,15	A0p	3,8
12	β Cassiopeiae	12	129,0	71	71	131	1,8	1,8	0,9	2,42	F5	6,2
27	γ Pegasi	4	43,0	— 3	7	8	—	6,1	5,4	2,87	B2	—1,6
31	χ Pegasi	32	344,0	— 9	11	13	—	31,3	26,5	4,94	Ma	4,8
43	ψ Andromedae	4	43,0	— 2	26	23	—	1,7	1,9	4,44	A2	3,0
50	σ Andromedae	2	21,5	14	21	23	1,5	1,0	1,3	4,51	A2	4,0
97	λ Cassiopeiae	1	10,8	9	17	17	1,2	—	0,3	4,88	B8	3,3
103	κ Cassiopeiae	5	53,8	—	4	3	—	13,4	17,9	4,24	B0	—0,6
122	ζ Cassiopeiae	3	32,2	—21	5	8	—	6,4	4,0	3,72	B3	0,5
123	π Andromedae	2	21,5	— 8	8	5	—	2,7	4,3	4,44	B3	1,3
130	κ Andromedae	8	86,0	40	27	28	2,1	3,2	3,0	4,52	G5	7,2
132	δ Andromedae	32	344,0	26	30	26	13,2	11,5	13,2	3,49	K2	4,5
135	α Cassiopeiae	35	376,3	16	23	33	23,5	16,4	11,4	2,47	K0	1,4
141	ϵ Cassiopeiae	2	21,5	—	5	4	—	4,3	5,4	4,85	B3	1,5
152	ϕ Cassiopeiae	3	32,2	—	—	3	—	—	10,7	4,70	B2	1,4
164	ζ Andromedae	17	182,8	34	22	19	5,4	8,3	9,6	4,30	K0	4,8
168	η Cassiopeiae	11	118,3	182	141	130	0,7	0,8	0,9	3,64	F8	9,1
173	δ Piscium	34	365,5	14	16	16	26,1	22,8	22,8	4,55	K5	4,4
175	ν Andromedae	2	21,5	—	7	5	—	3,1	4,3	4,42	B3	1,7
189	Cassiopeiae	6	64,5	65	56	52	1,0	1,2	1,2	4,93	F8	6,3
191	20 Ceti	22	236,5	—	12	11	—	19,7	21,5	4,92	K0	1,1
193	ν^1 Cassiopeiae	15	161,3	—	13	13	—	12,4	12,4	4,95	K0	3,6
199	γ Cassiopeiae	7	75,3	36	—	129	2,1	—	0,6	2,25	B0p	—0,4
200	ν^2 Cassiopeiae	14	150,5	39	16	15	3,9	9,4	10,0	4,83	K0	4,8
203	μ Andromedae	4	43,0	33	—	34	1,3	—	1,3	3,94	A2	4,9
206	η Andromedae	10	107,5	8	15	15	13,4	7,2	7,2	4,62	G5	3,5
218	2 Ursae minoris	24	258,0	—	15	16	—	17,2	16,1	4,52	K0	4,2
226	ϵ Piscium	13	139,8	25	15	17	5,6	9,3	8,2	4,45	K0	4,1
257	ϕ Andromedae	3	32,3	10	11	13	—	2,9	2,5	4,28	B8	—0,7
259	β Andromedae	81	870,7	45	40	39	19,3	21,8	22,3	2,37	Ma	4,0

No. Bonn FGC	Name	Hypothet- ical radius (unit in 0".0001)	107.5 x radius	Trig parallax " π_1	Spectro- graphic parallax " π_2	Spectral- proper motion parallax " π_3	Semi-diameters			m_{vis} (Har- vard)	Spectral class (Harvard)	H
							d_1 2	d_2 2	d_3 2			
264	θ Cassiopeiae . .	4	43.0	9	30	34	4.6	1.4	1.3	4.52	A5	6.3
270	χ Piscium . .	9	96.7	10	13	12	9.7	7.4	8.1	4.89	K0	1.5
271	τ Piscium . .	13	139.7	38	17	15		8.2	9.3	4.70	K0	4.2
281	φ Piscium . .	12	129.0	-8	16	14		8.1	9.2	4.64	K0	3.0
300	ν Piscium . . .	2	21.5	13		16	1.7		1.3	4.67	A2	1.8
304	ξ Andromedae . .	10	107.5		17	12		6.3	9.0	4.99	K0	3.0
310	ψ Cassiopeiae . .	16	172.0		14	13		12.3	13.2	4.96	K0	4.6
314	δ Cassiopeiae . .	8	86.0		68	48		1.3	1.8	2.80	A3	4.2
321	ω Andromedae . .	5	53.7	24	38	51	2.2	1.4	1.1	4.96	F5	7.7
325	α Ursae minoris	20	215.0	20	11	33	10.7	19.5	6.5	2.12	F8	-0.3
335	η Piscium . . .	19	204.2	9	17	16	22.7	12.0	12.8	3.72	G5	1.2
338	χ Cassiopeiae . .	9	96.7	17	12	12	5.7	8.1	8.1	4.88	K0	2.8
350	ν Andromedae . .	8	86.0	61	84	96	1.4	1.0	0.9	4.18	G0	7.3
357	ν Persel . . .	31	333.2	17	27	23	19.6	12.3	14.5	3.77	K0	4.3
369	τ Andromedae . .	2	21.5			11			2.0	4.90	B8	2.2
378	φ Piscium . . .	24	258.0	52	15	12	5.0	17.2	21.5	4.68	K0	1.3
384	φ Persel . . .	3	32.2	20		12	1.6		2.5	4.19	B0p	1.8
393	σ Piscium . . .	11	118.2	14	15	17	8.4	7.9	7.0	4.50	K0	4.2
419	ϵ Cassiopeiae . .	4	43.0	12	13	8	3.4	3.3	5.4	3.44	B3	1.6
421	α Trianguli . .	9	96.7	51	37	67	1.9	2.6	1.4	3.58	F5	5.4
422	γ Arietis . . .	2	21.5	7		20	3.1		(1.1)	4.04	A0p	4.7
426	ξ Piscium . . .	10	107.5		19	12		5.7	9.0	4.84	K0	2.4
428	β Arietis . . .	8	86.0	64	82	57	1.3	1.0	1.5	2.72	A5	3.6
441	λ Arietis . . .	3	32.2	25	25	25	1.3	1.3	1.3	4.83	A5	4.7
446	Δ Cassiopeiae . .	4	43.0	23	37	22	1.9	1.2	1.9	4.61	A3	3.5
449	ζ Cassiopeiae . .	4	43.0		25	22		1.7	1.9	4.06	A2	2.3
459	η Persel . . .	2	21.5	28	10	15	0.8	2.2	1.4	4.99	B8	3.0
463	α^1 Piscium . . .	4	43.0		22	17		1.9	2.5	3.94	A2p	2.1
468	γ^1 Andromedae . .	72	774.0	13	38	38	59.5	20.4	20.4	2.28	K0	1.5
477	α Arietis . . .	50	537.5	33	57	45	16.3	9.4	11.9	2.23	K2	4.1
480	δ Andromedae . .	2	21.5			27			0.8	4.77	A2	5.7
482	β Trianguli . .	7	75.3	14	49	50	5.4	1.5	1.5	3.08	A5	4.1
505	ϵ^1 Ceti . . .	11	118.2	34	7	12	3.5	16.9	9.8	4.54	G5	1.6
517	γ Trianguli . .	3	32.2	20		23	1.6		1.4	4.07	A0	3.2
545	δ Andromedae . .	37	397.7	4	12	10	99.4	33.1	39.8	4.86	K5	2.1
550	ι Cassiopeiae . .	4	43.0	24	21	33	1.8	2.0	1.3	4.59	A5p	0.5
560	ξ Ceti . . .	2	21.5	21		17	1.0		1.3	4.34	A0	2.3
604	δ Ceti . . .	2	21.5		3	6		7.2	3.6	4.04	B2	-1.0
610	η Persel . . .	5	53.8	20		12	2.7		4.5	4.99	G0	6.4
617	θ Persel . . .	7	75.3	80	94	75	0.9	0.8	1.0	4.22	F8	6.9
620	ζ Arietis . . .	1	10.8		5	22		2.2	0.5	4.58	B3	0.3
622	γ Ceti . . .	6	64.5	38	36	42	1.7	1.8	1.5	3.58	A2	5.2
629	μ Ceti . . .	6	64.5	32		42	2.0		1.5	4.36	F0	6.6
634	θ Arietis . . .	22	236.5	26	17	19	9.1	13.9	12.4	4.62	K0	6.1
639	η Persel . . .	61	655.7	-1	15	17	-	43.7	38.6	3.93	K0	1.1
643	λ Arietis . . .	4	43.0	33	21	29	1.3	2.0	1.5	3.68	B8	4.1
644	ν Persel . . .	6	64.5	21	35	38	3.1	1.8	1.7	4.27	F0	5.1
646	η Persel . . .	38	408.5	9	14	15	45.4	29.2	27.2	4.67	K5	4.1
653	τ Persel . . .	12	129.0	19	26		6.8	5.0		4.06	G0, A5	-1.1
668	α Persel . . .	2	21.5			21			1.0	4.62	A2	3.5
670	ν Persel . . .	14	150.5		10	13		15.1	11.6	4.97	K0	4.1
674	ϵ Arietis . . .	3	32.2	10	13	15	3.2	2.5	2.1	4.64	A2	+0.1
679	λ Ceti . . .	2	21.5		10	7		2.1	3.1	4.69	B5	-0.1
691	α Ceti . . .	71	763.2	11	26	22	69.4	29.4	34.7	2.82	Ma	2.1
694	γ Persel . . .	16	172.0	12	26	15	14.3	6.6	11.5	3.08	F5, A3	-1.1

325. Polaris. The parallax according to the period luminosity relation for Cepheids is 0".018, which gives a radius of 120.

H	No Boss PGC	Name	Hypothetical radius (unit is 0",0001)	107,5 radius	Trig parallax π_1	Spectro- graphic parallax π_2	Spectral proper motion parallax π_3	Semi diameters			μ_{vis} (Har- vard)	Spectral Class (Harvard)	H
								$\frac{d_1}{2}$	$\frac{d_2}{2}$	$\frac{d_3}{2}$			
6,3 1,5 4,2 3,0 1,8 3,0 4,6 4,2 7,7 -0,3 1,2 2,8 7,3 4,3 2,2 1,3 1,8 4,2 1,6 5,4 4,7 2,4 3,6 4,7 3,5 2,3 3,0 2,1 1,5 4,1 5,7 4,1 1,6 3,2 2,3 0,5 2,3 -1,0 6,4 6,9 0,3 5,2 6,6 6,1 1,3 4,3 5,9 4,1 -1,4 3,6 4,0 +0,8 -0,1 2,3	698 705 708 710 713 717 718 730 741 746 752 755 757 772 778 780 781 784 786 790 791 795 804 817 825 838 842 844 847 852 856 858 860 861 865 869 877 894 896 901 910 913 920 932 936 938 947 967 970 972	ρ Persei Cassiopeiae β Persei ϵ Persei κ Persei ω Persei δ Arietis ζ Arietis Camelopardalis Persei κ Ceti Arietis ι Persei α Persei σ Lami Persei Camelopardalis ξ Lami Camelopardalis β Persei Camelopardalis σ Persei ι Lami η Persei θ Lami δ Persei Camelopardalis σ Persei ν Persei λ Lami η Lami β Lami ζ Persei Camelopardalis ω Lami ϵ Persei ξ Persei λ Lami ν Lami A ¹ Lami λ Persei σ Persei μ Persei ι Persei f ¹ Lami	62 2 9 8 21 11 16 2 2 31 7 26 2 20 16 33 5 3 6 2 2 27 15 4 7 5 9 4 4 9 3 2 2 3 45 3 5 4 7 9 5 4 5 4 12 3 4 16 16 17 12 4 12 4 12	666,5 21,5 96,7 86,0 225,7 118,2 172,0 21,5 21,5 333,2 75,3 279,5 21,5 215,0 172,0 354,7 53,8 32,2 64,5 21,5 21,5 290,2 161,2 43,0 75,3 53,8 96,7 43,0 96,7 32,2 21,5 21,5 32,2 483,7 32,2 53,8 43,0 53,8 43,0 43,0 53,8 43,0 129,0 32,2 43,0 172,0 182,7 129,0	38 29 27 92 29 23 47 16 7 116 13 16 27 5 7 12 13 19 15 13 54 76 20 17 12 9 6 3,3 8 22 18 13 9 15 7 28 22 10 3 11 5 7 11 3 15 28 8	11 14 45 108 26 15 16 12 18 10 61 13 16 27 20 7 12 26 10 12 18 19 15 13 76 20 17 12 9 6 5 6 7 13 9 11 5 7 29 20 16 11 9 10	24 21 3,6 0,9 7,8 5,1 3,7 1,3 1,8 3,1 30,3 0,6 21,5 1,3 1,1 14,3 8,6 23 21 10 26 10 12 18 16 15 13 96 17 12 9 6 3,3 8,6 14 12 16 14 9 14 14 28 22 7 8 9 11 5 6 11 5 6 14 11 11 9 14	17,5 0,7 3,6 0,9 7,8 5,1 3,7 1,3 1,8 3,1 30,3 0,6 21,5 1,3 1,1 14,3 8,6 23 21 10 26 10 12 18 16 15 13 96 17 12 9 6 3,3 8,6 14 12 16 14 9 14 14 28 22 7 8 9 11 5 6 11 5 6 14 11 11 9 14	60,6 1,5 2,1 0,8 8,7 7,9 10,8 1,8 1,2 1,0 33,3 0,8 27,9 1,3 1,1 8,0 7,5 8,7 50,7 4,5 5,4 1,7 3,1 1,5 22,3 8,5 3,3 1,0 0,8 2,7 8,1 10,8 7,2 4,8 1,8 1,7 1,1 2,3 2,3 48,4 53,7 2,3 1,9 2,0 10,8 2,5 6,4 7,7 8,6 7,7 1,5 6,5 2,0 3,9 6,1 20,3 12,9	(27,8) 1,0 4,00 9,8 9,4 9,8 9,6 1,2 1,0 33,3 1,2 27,9 1,1 1,1 6,5 3,80 16,9 5,4 1,2 1,8 1,2 4,98 4,5 5,4 1,2 6,5 4,67 3,2 3,2 18,1 10,7 3,3 0,8 3,2 10,8 10,8 7,2 4,4 2,3 1,8 1,3 2,3 4,02 4,71 4,25 2,8 2,8 2,9 2,9 15,6 4,89 4,98	3,4 to 4,2 4,89 2,2 to 3,7 4,17 4,00 4,82 4,53 4,95 4,76 4,92 4,96 4,72 4,98 1,90 3,80 4,94 4,42 3,75 4,76 4,67 4,98 4,55 4,28 4,26 4,40 3,10 4,96 3,94 3,93 3,81 4,37 4,67 4,02 4,71 4,25 2,96 3,80 2,91 4,87 4,68 2,96 4,05 3,4 to 4,2 3,94 4,50 4,33 4,03 4,28 4,89 4,98	Mb A2 B8 G0 K0 K0 A0 B3p K0 G5 K5 A2 F5 G5 B5 B9p B8 A0p B5 A2 K0 K0 B5p G5 B5 F5, A B1 F5 B5p B5 B5 A0 B5 Ma B5 B5p B8 B1 B9 A, G5 B1 Oe5 B3 A0 K0 A0 B3p G0 G0, A5 G5	4,6 4,6 -3,1 9,7 5,9 1,5 5,4 4,4 0,2 0,5 7,2 1,9 3,8 -0,1 3,9 2,5 -2,6 3,0 0,0 2,9 2,6 1,4 0,6 2,5 8,0 1,4 0,7 1,0 -1,3 2,4 2,8 3,0 2,7 -2,3 3,1 1,5 2,4 -0,5 -1,6 2,3 0,9 0,3 -0,8 -1,8 4,8 2,2 2,2 1,7 2,4 2,8

No. Boss PGC	Name	Hypothetical radius (unit is 0",0001)	107,5 x radius	Trig parallax π_1	Spectro- graphic parallax π_2	Spectral- proper motion parallax π_3	Semi-diameters			m_{vis} (Har- vard)	Spectral Class (Harvard)	H
							$\frac{d_1}{2}$	$\frac{d_2}{2}$	$\frac{d_3}{2}$			
981	μ Tauri	2	21,5		9	10		2,4	2,2	4,32	B3	2,0
986	b ¹ Persci	3	32,2			22			1,5	4,57	A2	4,0
989	ω Tauri	4	43,0		28	20		1,5	2,2	4,80	A3	3,9
1000	γ Tauri	16	172,0	29	23	22	5,9	7,5	7,8	3,86	K0	4,3
1003	d Persci	2	21,5		5	10		4,3	2,2	4,89	B3	3,2
1017	δ^1 Tauri	19	204,2	17	26	21	12,0	7,8	9,7	3,93	K0	4,2
1022	δ^2 Tauri	2	21,5	28	34	26	0,8	0,6	0,8	4,84	A5	5,3
1026	κ^1 Tauri	4	43,0	24	30	29	1,8	1,4	1,5	4,36	A3	4,6
1029	δ^2 Tauri	3	32,2	25	28	28	1,3	1,2	1,1	4,24	A2	4,4
1033	ν^1 Tauri	5	53,8	26	30	30	2,1	1,8	1,8	4,40	A5	4,8
1034	η^1 Tauri	3	32,2	24	29	27	1,3	1,1	1,2	4,60	A5	5,0
1036	π Tauri	9	96,7			12			8,0	4,94	K0	2,7
1044	ϵ Tauri	22	236,5	31	34	24	7,6	6,9	9,8	3,63	K0	4,0
1045	θ^1 Tauri	20	215,0	37	28	21	5,8	7,7	10,2	4,04	K0	4,2
1046	θ^2 Tauri	4	43,0	28	42	25	1,5	1,0	1,7	3,62	F0	3,8
1054	Tauri	3	32,2	28	25	26	1,2	1,3	1,2	4,84	A5	5,2
1063	λ^5 Eridani	13	139,7			10			14,0	4,97	K0	-2,6
1067	η Tauri	4	43,0	23	28	26	1,9	1,5	1,7	4,75	A5	4,8
1074	ϵ Persei	25	268,7	28	4	13	9,6	67,2	20,7	4,46	K0, A3	1,4
1077	α Tauri	176	1892,0	57	83	60	33,2	22,8	31,5	1,06	K5	2,6
1076	d Tauri	4	43,0		19	24		2,3	1,8	4,38	A3	3,5
1079	ν Eridani	2	21,5		4	(2)		5,4	(10,8)	4,12	B2	-4,4
1087	ϵ^1 Tauri	3	32,2	27	36	29	1,2	0,9	1,1	4,30	A3	4,4
1090	α^2 Tauri	2	21,5	22	28	21	1,0	0,8	1,0	4,85	A3	4,5
1107	ν Tauri	2	21,5	8	9	9	2,7	2,4	2,4	4,33	B5	1,1
1123	μ Eridani	2	21,5		9	10		2,4	2,2	4,18	B5	0,9
1139	γ Camelopardalis	3	32,2	-25	4	3	-	8,1	10,7	4,38	B0	-0,8
1140	π^2 Orionis	10	107,5	136	122	115	0,8	0,9	0,9	3,31	F8	6,7
1141	π^2 Orionis	3	32,2			16			2,0	4,35	A0	2,0
1147	π^2 Orionis	3	32,2	2	4	7	16,1	8,0	4,6	3,78	B3	-2,0
1159	π^2 Orionis	2	21,5	3	7	6	7,1	3,1	3,6	3,87	B3	-3,1
1161	γ Camelopardalis	3	32,2		20	14		1,6	2,3	4,44	A2	-0,2
1163	π^1 Orionis	3	32,2		18	24		1,8	1,3	4,74	A0	5,6
1167	ι Aurigae	60	645,0	18	27	20	35,8	23,9	32,2	2,90	K2	0,1
1169	α^2 Orionis	23	247,2	20	19	18	12,3	13,0	13,7	4,28	K0	4,3
1178	λ Aurigae	2	21,5	27		20	0,8		1,1	4,99	A0	5,3
1181	π^2 Orionis	28	301,0		15	10		20,1	30,1	4,73	K0	-1,4
1185	β Camelopardalis	13	139,7	16	4	24	8,6	34,9	5,8	4,22	G0p	-0,2
1187	ϵ Aurigae	13	139,7	2	7	11	(69,6)	20,0	12,5	(3,18)	F5p	-1,1
1190	ζ Aurigae	41	440,8	-3	38	12	-	11,6	36,7	3,94	K0, B1	-1,5
1194	ϵ Tauri	3	32,2	-19	30	25	-	1,1	1,3	4,70	A5	4,3
1202	γ Aurigae	5	53,8		34	30		1,6	1,8	4,99	F0	6,2
1203	λ^1 Orionis	2	21,5	16		17	1,4		1,3	4,65	B9	2,7
1204	η Aurigae	3	32,2	14	10	19	2,3	3,2	1,7	3,28	B3	2,8
1227	λ^1 Orionis	4	43,0	-25		14	-		3,1	4,86	F0	0,1
1236	μ Aurigae	3	32,2	68		22	0,5		1,5	4,78	A3	4,2
1240	α Orionis	20	215,0	5	22	12	(43,0)	9,8	17,9	4,64	K0	0,5
1246	α Aurigae	56	602,0	75	91	91	8,0	6,6	6,6	0,21	G0	3,4
1258	λ^1 Aurigae	20	215,0	13	13	17	16,5	16,5	12,6	4,81	K0	6,2
1259	λ Aurigae	7	75,3	68	83	85	1,1	0,9	0,9	4,85	G0	9,5

No. Boss PGC	Name	Hypothet- ical radius (unit is 0",0001)	107,5 x radius	Trig parallax π_1	Spectro- graphic parallax π_2	Spectral- proper motion parallax π_3	Semi-diameters			m_{101} (Har- vard)	Spectral Class (Harvard)	H
							$\frac{d_1}{2}$	$\frac{d_2}{2}$	$\frac{d_3}{2}$			
1284	α Orionis . . .	2	21,5		4	6		5,4	3,6	4,65	B3	-0,4
1289	m Orionis . . .	1	10,8		5	5		2,2	2,2	4,99	B3	-0,8
1301	η Orionis . . .	3	32,2	12	7	5	2,7	4,6	6,4	3,44	B1	-2,7
1302	ψ^1 Orionis . . .	2	21,5		7	7			3,1	4,73	B3p	1,3
1303	γ Orionis . . .	7	75,3	19	16	16	4,0	4,7	4,7	1,70	B2	-1,8
1304	β Tauri . . .	8	86,0	24	37	67	3,6	2,3	1,3	1,78	B8	3,1
1315	α Tauri . . .	2	21,5			7			3,1	4,83	B3	1,0
1314	ψ Orionis . . .	1	10,8	-12	5	5	—	2,2	2,2	4,66	B2	0,4
1327	31 Orionis . . .	35	376,2		9	9			41,8	4,97	K5	2,2
1331	Λ Orionis . . .	2	21,5	15	11	10	1,4	2,0	2,1	4,32	B3	2,2
1333	χ Aurigae . . .	3	32,2			4			8,1	4,88	B4	1,0
1335	149 Tauri . . .	66	709,5		3	8		236,5	88,7	4,73	Ma	0,3
1339	δ Orionis . . .	5	53,8	9	7	5	6,0	7,7	10,8	2,48	B0	-4,5
1353	η^1 Orionis . . .	2	21,5	2	6	3	10,7	3,6	7,2	4,53	B0	-1,0
1357	λ Orionis . . .	3	32,2	6	4	4	5,4	8,1	8,1	3,49	Oe5	-1,3
1364	ϵ^1 Orionis . . .	2	21,5	17	6	4		3,6	5,4	4,65	B3	-3,9
1370	ϵ Orionis . . .	7	75,3	5	12	7	15,1	6,3	10,8	1,75	B0	-6,7
1373	η^3 Orionis . . .	18	193,5	27	28	24	7,2	6,9	8,1	4,39	K0	6,9
1375	ζ Tauri . . .	4	43,0	-1	15	13	—	2,9	3,3	3,00	B3p	0,2
1389	σ Orionis . . .	3	32,2	-9	4	3	—	8,1	10,7	3,78	B0	-6,2
1391	ω Orionis . . .	2	21,5		4	5		5,4	4,3	4,54	B3p	-1,6
1396	126 Tauri . . .	2	21,5	7	5	8	3,1	4,3	2,7	4,87	B3	2,3
1398	ζ Orionis . . .	6	64,5	-19	8	7	—	8,1	9,2	2,05	B0	-2,9
						3			21,5	4,21		
1399	Orionis . . .	2	21,5		7	5		3,1	4,3	5,00	B3	0,7
1429	τ Aurigae . . .	10	107,5	2	15	14	53,8	7,2	7,7	4,64	K0	2,4
1438	134 Tauri . . .	2	21,5			14			1,5	4,92	B9	2,2
1439	ν Aurigae . . .	33	354,7		10	10		35,5	35,5	4,99	Ma	3,6
1442	ν Aurigae . . .	19	204,2	19	18	13	10,7	11,3	15,7	4,18	K0	-1,3
1453	ξ Aurigae . . .	2	21,5	-14	20	12		1,1	1,8	4,92	A2	0,7
1457	136 Tauri . . .	3	32,2	16	15	13	2,0	2,1	2,5	4,54	A0	1,3
1461	χ Orionis . . .	8	86,0	104	94	57	0,8	0,9	1,5	4,62	F8	6,2
1468	α Orionis . . .	211	2268,2	11	10	39	206,2	226,8	58,2	(0,34)	Ma	-1,8
1472	δ Aurigae . . .	18	193,5	18	28	23	10,7	6,9	8,4	3,88	K0	4,8
1475	139 Tauri . . .	2	21,5		4	3		5,4	7,1	4,90	B2	-2,1
1478	β Aurigae . . .	8	86,0	34	63	38	2,5	1,4	2,3	2,07	A0p	0,4
1479	π Aurigae . . .	39	419,2		6	8		69,9	52,4	4,59	Ma	-0,2
1482	θ Aurigae . . .	6	64,5	16	34	40	4,0	1,9	1,6	2,71	A0p	2,8
1494	Orionis . . .	14	150,5		30	15		5,0	10,0	4,68	K0	4,3
1501	μ Orionis . . .	5	53,8	43	27	19	1,3	2,0	2,8	4,19	A2	1,8
1508	1 Geminorum . .	14	150,5	28	37	20	5,4	4,1	7,5	4,30	G5	4,5
1507	χ^2 Orionis . . .	5	53,8		4	5		13,4	10,8	4,71	B2p	0,6
1525	ν Orionis . . .	2	21,5	-31	4	9	—	5,4	2,4	4,40	B2	2,2
1550	Γ^1 Orionis . . .	2	21,5			7			3,1	4,92	B3	1,8
1548	ξ Orionis . . .	2	21,5		7	9		3,1	2,4	4,35	B3	2,1
1556	Camelopardalis .	2	21,5	12	13	21	1,8	1,7	1,0	4,73	A0	4,9
1561	η Geminorum . .	82	881,5	14	12		63,0	73,4	67,8	(3,2)	Ma	2,3
1565	κ Aurigae . . .	13	139,7	14	19	22	10,0	7,4	6,3	4,45	K0	6,6
1575	2 Lynce . . .	2	21,5	34	24	14	0,6	0,9	1,5	4,42	A0	1,1
1604	μ Geminorum . .	66	709,5	16	15	23	44,4	47,3	30,8	3,19	Ma	3,7
1611	8 Monocerotis . .	4	43,0	16			2,8			4,33	A5	-0,3

1468. α Orionis. This is the only star for which actual variations in the diameter have been measured by the interferometer methods. For details about these measurements consult the text. The diameter as computed from the π_1 's ranges from 116,4 \odot (maximum) to 174,4 \odot (minimum). The interferometer measures show also that the diameter is largest at minimum light.

No. Boss PGC	Name	Hypo- thetical radius (unit is 0",0001)	107,5 × radius	Trig parallax π_1	Spectro- graphic parallax π_2	Spectral- proper motion parallax π_3	Semi-diameters			m_{vis} (Har- vard)	Spectral Class (Harvard)	H
							d_1 2	d_2 2	d_3 2			
1635	ν Geminorum . .	3	32,2	19	10	9	1,7	3,2	3,6	4,06	B5	0,8
1657	13 Monocerotis . .	3	32,2	-18	13	11	—	2,5	2,9	4,50	A0p	-0,5
1690	γ Geminorum . .	9	96,7	4,3	63	41	2,2	1,5	2,4	1,93	A0	1,0
1706	S Monocerotis . .	2	21,5	8	4	(3)	2,7	5,4	(7,1)	4,68	Oe5	-0,8
1716	12 Lyncis	2	21,5	20	14	14	1,1	1,5	1,5	4,89	A2	1,8
1717	α Geminorum . .	45	483,7	7	11	18	69,1	44,0	26,9	3,18	G5	-0,3
1721	30 Geminorum . .	19	204,2	-14	19	15	—	10,7	13,6	4,65	K0	4,0
1725	ξ Geminorum . .	10	107,5	48	49	72	2,2	2,2	1,5	3,40	F5	5,2
1740	18 Monocerotis . .	15	161,2	19	14	12	8,5	11,5	13,4	4,70	K0	1,8
1758	Camelopardalis	23	247,2	13	13	15	19,0	19,0	16,5	4,75	K5	4,4
1763	θ Geminorum . .	4	43,0	19		21	2,3		2,0	3,64	A2	2,3
1776	15 Lyncis	11	118,2	6	19	17	19,7	6,2	7,0	4,54	G0	5,2
1778	ϵ Geminorum . .	4	43,0	44	34	27	1,0	1,3	1,6	4,70	F0	4,9
1786	ψ^{10} Aurigae . .	2	21,5			15			1,4	4,80	A2	1,8
1812	19 Monocerotis . .	2	21,5		6	4		3,6	5,4	4,89	B3	-0,6
1815	ζ Geminorum . .	14	150,5	5	3	4	30,1	50,2	37,6	3,6 to 4,5	G0p	-1,5
1840	τ Geminorum . .	24	258,0	5	18	15	51,6	14,3	17,2	4,48	K0	3,1
1853	δ Monocerotis . .	3	32,2	20		13	1,6		2,5	4,09	A0	-0,7
1879	Lyncis	3	32,2			6			5,4	4,80	A2	-0,4
1886	λ Geminorum . .	5	53,8	38	38	12	1,4	1,4	4,5	3,65	A2	2,8
1898	δ Geminorum . .	8	86,0	60	44	27	1,4	2,0	3,2	3,51	F0	0,5
1928	21 Lyncis	2	21,5			18			1,2	4,45	A0	2,9
1931	ϵ Geminorum . .	18	193,5	25	25	23	7,7	7,7	8,4	3,89	K0	4,1
1944	β Canis minoris .	4	43,0	20	30	32	2,1	1,4	1,3	3,09	B8	2,2
1952	ϱ Geminorum . .	6	64,5	52	37	42	1,2	1,7	1,5	4,18	F0	6,0
1953	γ Canis minoris .	33	354,7	5	9	15	71,0	39,4	23,6	4,60	K0	3,1
1962	δ Canis minoris .	20	215,0	19	12	11	11,3	17,9	19,5	4,85	K0	1,1
1979	α Geminorum . .	11	118,2	77	66	39	1,5	1,8	3,0	2,85	A0	3,1
						58			2,0	1,99		
1987	ν Geminorum . .	39	419,2	11	18	20	38,1	23,3	21,0	4,22	K5	4,1
2001	σ Geminorum . .	4	43,0	25	19	27	1,7	2,3	1,6	4,92	F0	5,1
2008	α Canis minoris .	31	333,2	312	331	305	1,1	1,0	1,1	0,48	F5	5,1
2010	24 Lyncis	3	32,2		19	19		1,7	1,7	4,96	A2	4,1
2023	σ Geminorum . .	20	215,0	20	40	22	10,7	5,4	9,8	4,26	K0	6,0
2029	κ Geminorum . .	17	182,7	22	25	9	8,3	7,3	20,3	3,68	G5	2,1
2031	β Geminorum . .	64	688,0	101	129	83	6,8	5,3	8,3	1,21	K0	5,1
2078	φ Geminorum . .	2	21,5		16	17		1,3	1,3	4,99	A2	3,1
2126	28 Monocerotis . .	16	172,0			15			11,5	4,88	K0	4,1
2130	13 Canis minoris .	24	258,0	19	19	17	13,6	13,6	15,2	4,52	K0	4,1
2145	27 Lyncis	2	21,5	-17	16	18	—	1,3	1,2	4,87	A2	3,1
2155	ζ Monocerotis . .	14	150,5	-7	4	10	—	37,6	15,1	4,41	G0	1,1
2168	ζ Cancri	7	75,3	48	44	25	1,6	1,7	3,0	4,71	G0	5,1
2195	β Cancri	38	408,5	-2	18	20	—	22,7	20,4	3,76	K2	3,1
2208	31 Lyncis	42	451,5	20	16	18	22,6	28,2	25,1	4,43	K5	4,1
2237	ϵ Hydrae	4	43,0	8	24	24	5,4	1,8	1,8	3,95	A0	3,1
2247	σ Ursae majoris .	19	204,2	-4	15	24	—	13,6	8,5	3,47	G0	4,1
2290	π^A Ursae majoris .	17	182,7	13	19	13	14,1	9,6	14,1	4,76	K0	3,1
2295	δ Hydrae	3	32,2		20	22		1,6	1,5	4,18	A0	3,1
2302	σ Hydrae	24	258,0	14	14	14	18,4	18,4	18,4	4,54	K0	1,1
2327	γ Cancri	2	21,5	6		22	3,6		1,0	4,73	A0	5,1
2330	η Hydrae	2	21,5		7	10		3,1	2,2	4,32	B3	1,1

1815. Cepheid variable. The parallax value derived on basis of the period-luminosity relation is 0",004.

No Boss PGC	Name	Hypothe- tical radius (unit is 0",0001)	107,5 radius	Trig parallax π_1	Spectro- graphic parallax π_2	Spectral proper motion parallax π_3	Semi diameters			m_{15} (Har- vard)	Spectral Class (Harvard)	11
							d_1 2	d_2 2	d_3 2			
2336	δ Cancri	18	193,5	16	19	23	12,1	10,2	8,4	4,17	K0	6,1
2348	ϵ Cancri	19	204,2	21	10	16	9,7	20,4	12,8	4,20	G5	2,9
2351	ϵ Hydrie	16	172,0	15	54	84	11,5	3,2	2,0	3,48	I 8	4,9
2361	θ Hydrie	2	21,5	4	13	16	(5,4)	1,6	1,3	4,42	A0	2,4
2393	ζ Hydrie	25	268,8	14	19	26	19,2	11,1	10,3	3,30	K0	3,4
2404	ϵ Ursae majoris	8	86,0	70	66	69	1,2	1,3	1,2	3,12	A5	6,6
2407	α Cancri	3	32,2	30	30	22	1,1	1,0	1,5	1,27	A3	2,9
2411	β Ursae majoris	27	290,2		9	8		32,2	36,3	4,99	Ma	1,6
2413	10 Ursae majoris	6	64,5	70	69	72	0,9	0,9	0,9	4,09	I 5	7,6
2424	κ Ursae majoris	4	43,0	17	26	25	2,5	1,7	1,7	3,68	A0	3,0
2437	Ursae majoris	15	161,2		1	12		40,3	13,4	4,71	G5	2,9
2441	α^2 Ursae majoris	4	43,0	43	54	40	1,0	0,8	1,1	4,87	F8	4,1
2443	ϵ Ursae majoris	5	53,8	— 2	41	28	—	1,3	1,9	4,54	A3p	5,2
2446	τ Ursae majoris	5	53,8		23	39		2,3	1,4	4,74	I 5, A5	5,2
2476	ϵ Ursae majoris	3	32,2		18	24		1,8	1,3	4,89	A5	4,6
2479	θ Hydrie	3	32,3	17	25	41	1,9	1,3	0,9	3,84	A0	6,5
2495	38 Lynxis	4	43,0	32	21	33	1,3	2,0	1,3	3,82	A2	4,5
2507	40 Lynxis	61	655,7	2	31	33	327,8	21,2	19,9	3,30	K5	5,0
2524	κ Leonis	21	225,7	— 7	20	15	—	11,3	15,0	4,61	K0	3,6
2536	Diaconis	20	215,0		15	11		14,3	19,5	4,58	K2	1,7
2540	ϵ Ursae majoris	7	75,3	29	43	20	2,6	1,8	3,8	3,75	F0	4,1
2541	τ^1 Hydrie	5	53,8	77		37	0,7		1,5	4,78	F5	5,3
2549	δ Ursae majoris	9	96,7	43	42	14	2,2	2,3	6,9	4,57	G0	4,3
2550	λ Leonis	39	419,2	21	14	14	20,0	29,9	29,9	4,48	K5	3,2
2552	θ Ursae majoris	10	107,5	56	79	147	1,9	1,4	0,7	3,26	F8p	8,5
2559	τ^2 Hydrie	3	32,2			17			1,9	4,50	A3	1,6
2565	26 Ursae majoris	2	21,5		16	20		1,3	1,1	4,65	A0	4,0
2566	10 Leonis minoris	11	118,2		20	12		5,9	9,8	4,62	G5	2,0
2570	Lynxis	11	118,2			28			4,2	4,99	K0	2,4
2589	2 Sextantis	21	225,7		20	18		11,3	12,5	4,78	K0	6,0
2595	ϵ Hydrie	28	301,0	19	22	19	15,8	13,7	15,8	4,10	K0	3,8
2602	ϵ Leonis	8	86,0	26	12	56	3,3	7,2	1,5	3,76	F5, A3	4,6
2618	ϵ Leonis	18	193,5	— 1	16	18	—	12,1	10,8	3,12	G0p	1,5
2632	ν Ursae majoris	7	75,3		38	53		2,0	1,4	3,89	F0	6,5
2637	φ Ursae majoris	3	32,2	7	15	12	4,7	2,1	2,7	4,54	A2	—0,7
2648	μ Leonis	24	258,0	19	24	23	13,6	10,7	11,2	4,10	K0	5,9
2680	τ Leonis	42	451,5		7	10		64,5	45,2	4,89	Ma	3,1
2692	21 Leonis minoris	3	32,2		28	26		1,2	1,2	4,47	A5	3,1
2694	η Leonis	3	32,3			10			3,2	3,58	A0p	—1,0
2696	A Leonis	37	397,8		14	17		28,4	23,4	4,58	K2	4,9
2697	15 Sextantis	2	21,5			9			2,4	4,50	A0	1,9
2698	α Leonis	10	107,5	58	66	81	1,9	1,6	1,3	1,34	F8	3,3
2730	ζ Leonis	6	64,5	9	29	28	7,2	2,2	2,3	3,67	F0	0,8
2729	λ Ursae majoris	4	43,0	—10			—			3,52	A2	4,6
2741	40 Leonis	6	64,5	50	46	50	1,3	1,4	1,3	4,97	I 5	7,6
2742	γ^1 and γ^2 Leonis	43	462,2	4	43	43 } 29 }	(115,5)	10,7	10,7 } 15,9 }	2,61 } 3,80 }	K0	5,3 } 6,5 }
2751	μ Ursae majoris	71	763,2	34	32	24	22,4	23,9	31,8	3,21	K5	3,8
2754	Ursae majoris	2	21,5		14	12		1,5	1,8	4,92	A0	1,9
2768	30 Leonis minoris	3	32,2		32	26		1,0	1,2	4,83	F0	5,0
2776	31 Leonis minoris	12	129,0	11	26	20	11,7	5,0	6,4	4,41	K0	5,4

No. Bonn PGC	Name	Hypothet- ical radius (unit is 0",0001)	107,5 x radius	Trig parallax π_1	Spectro- graphic parallax π_2	Spectral proper motion parallax π_3	Semi-diameters			M _v (Har- vard)	Spectral Class (Harvard)	H
							$\frac{d_1}{2}$	$\frac{d_2}{2}$	$\frac{d_3}{2}$			
2785	36 Ursa majoris	7	75,3	80	67	43	0,9	1,1	1,8	4,84	F5	6,1
2792	30 Sextantis	1	10,8		8	12		1,3	0,9	4,95	B5	3,6
2802	Ursae majoris	3	32,2	26	30	27	1,2	1,1	1,2	4,84	A5	5,6
2804	9 Leonis	2	21,5	29	5	4	0,7	4,4	5,4	3,85	B0p	-1,4
2829	37 Leonis minoris	10	107,5	21	8	6	5,1	13,4	17,9	4,77	G0	-1,0
2899	46 Leonis minoris	16	172,0	31	33	27	5,5	5,2	6,4	3,92	K0	6,3
2900	40 Ursa majoris	2	21,5			16			1,3	4,84	A0	3,6
2909	54 Leonis	2	21,5		18	21		1,2	1,0	4,32	A0	3,8
2930	8 Ursa majoris	7	75,3	47	54	41	1,6	1,4	1,8	2,44	A0	2,2
2931	p ^a Leonis	46	494,5	25	12	9	19,8	41,2	54,9	4,97	Ma	3,0
2932	b Leonis	3	32,2	10		9	3,2		3,6	4,42	A0	1,7
2933	α Ursa majoris	47	505,2	21	54	49	24,0	9,4	10,3	1,95	K0	2,7
2942	γ Leonis	5	53,8	10	14	44	5,4	3,8	1,2	4,66	F0	7,4
2958	ψ Ursa majoris	29	311,7		44	27		7,1	11,5	3,15	K0	2,3
2972	δ Leonis	8	86,0	78	58	60	1,1	1,5	1,4	2,58	A3	4,2
2974	θ Leonis	4	43,0	19	32	31	2,3	1,3	1,4	3,41	A0	3,5
2976	72 Leonis	27	290,2		8	8		36,3	36,3	4,87	Ma	1,2
2982	φ Leonis	3	32,2		27	27			1,2	4,58	A5	5,0
2984	ξ Ursa majoris	8	86,0	146	126	60	0,6	0,7	1,4	4,87	G0	8,2
2985	ζ Ursa majoris	33	354,7	7	21	19	50,7	16,9	18,7	3,71	K0	0,9
2987	55 Ursa majoris	2	21,5	13	16	22	1,7	1,3	1,0	4,78	A2	4,8
2990	σ Leonis	3	32,2		15	25		2,1	1,3	4,13	A0	4,0
2999	ι Leonis	7	73,3	58	51	54	1,3	1,5	1,4	4,03	F5	5,3
3031	λ Draconis	44	473,0	22	14	13	21,5	33,8	36,4	4,06	Ma	2,3
3038	ν Leonis	11	118,3	12	21	15	9,9	5,6	7,9	4,47	K0	2,2
3089	ζ Virginis	40	430,0	7	15	20	61,4	28,7	21,5	4,20	Ma	5,6
3090	η Ursa majoris	22	236,5	12	29	22	19,7	8,2	10,8	3,85	K0	4,5
3098	93 Leonis	6	64,5	29	45	54	2,2	1,4	1,2	4,54	F8	5,5
3101	θ Leonis	9	96,7	101	73	86	1,0	1,3	1,1	2,23	A2	5,8
3105	ρ Virginis	9	96,7	101	90	110	1,0	1,1	0,9	3,80	F8	8,3
3117	γ Ursa majoris	6	64,5	4	48	39	(16,1)	1,3	1,7	2,54	A0	2,4
3139	α Virginis	3	32,2		22	18		1,5	1,8	4,57	A3	2,2
3155	σ Virginis	13	139,7	38	15	25	3,7	9,3	5,6	4,24	G5	6,0
3190	δ Ursa majoris	4	43,0	45	32	36	1,0	1,3	1,2	3,44	A2	3,7
3210	η Virginis	3	32,2			23			1,4	4,00	A0	3,1
3216	11 ComaeBerenices	10	107,5		20	16		5,4	6,7	4,91	K0	5,6
3224	12 ComaeBerenices	6	64,5		36	21		1,8	3,1	4,78	F5	0,8
3230	5 Can Venati- orum	8	86,0		11	10		7,8	8,6	4,97	K0	0,2
3242	γ ComaeBerenices	14	150,5	1	18	18	(150,5)	8,4	8,4	4,56	K0	5,0
3279	β Can. Venati- orum	10	107,5	107	110	96	1,0	1,0	1,1	4,32	G0	8,7
3281	α Draconis	2	21,5	- 3	13	17	-	1,7	1,3	3,88	B5p	2,8
3283	23 ComaeBerenices	2	21,5	- 1	14	18	-	1,5	1,2	4,78	A0	4,1
3284	24 ComaeBerenices	11	118,2		10			11,8		4,95	K0	1,4
3302	γ Virginis	10	107,5	73	64	59	1,5	1,7	1,8	3,65	F0	6,2
3309	9 Virginis	2	21,5		13	22		1,6	1,0	4,95	A0	5,6

No. Bosa PGC	Name	Hypo- thetical radius (unit is 0",0001)	107,5 × radius	Trig parallax π_1	Spectro- graphic parallax π_2	Spectral- proper motion parallax π_3	Semi-diameters			M_{vis} (Har- vard)	Spectral Class (Harvard)	II
							d_1 2	d_2 2	d_3 2			
3770	α Bootis	12	129,0	45		15	2,9		8,6	4,69	K0	4,3
3771	ϵ Bootis	23	247,2	16	25	31	15,5	9,9	8,0	2,59	K0, A0	1,1
3772	109 Virginis	4	43,0			22			2,0	3,76	A0	4,2
3798	ξ Bootis	10	107,5	168	149	20	0,6	0,7	5,4	4,64	G5	5,2
3809	β Ursae minoris . .	82	881,5	11	41	21	80,1	21,5	42,0	2,24	K5	-0,4
3814	16 Librae	3	32,2		32	35		1,0	0,9	4,59	F0	6,0
3827	Ursae majoris . . .	33	354,7		7	12		50,7	29,6	4,86	Mb	1,4
3834	ω Bootis	21	225,7			13			17,4	4,93	K5	3,8
3835	110 Virginis	13	139,7	22	39	14	6,3	3,6	10,0	4,62	K0	3,1
3836	β Bootis	17	182,7	23	19	20	7,9	9,6	9,1	3,63	G5	2,6
3842	ψ Bootis	15	161,2		16	19		10,1	8,5	4,67	K0	5,9
3847	i Bootis	7	75,2	76	77	68	1,0	1,0	1,1	4,86	G0	7,9
3887	δ Bootis	17	182,7	24	25	26	7,6	7,3	7,0	3,54	K0	4,5
3926	μ Bootis	4	43,0	34	36	33	1,3	1,2	1,3	4,33	F0, K0	5,5
3928	γ Ursae minoris . .	5	53,8		42	24		1,3	2,2	3,14	A2	-0,7
3936	ι Draconis	30	322,5	34	30	17	9,5	10,8	19,0	3,47	K0	-1,5
3940	β Coronae borealis	5	53,8		33	45		1,6	1,2	3,72	F0p	5,1
3949	ι^2 Bootis	2	21,5			8			2,7	4,98	A2	2,1
3953	θ Coronae borealis	3	32,2			12			2,7	4,17	B5	2,0
3960	δ Serpentis	5	53,8	16	30	28	3,4	1,8	1,9	3,85	F0	3,4
3961	α Coronae borealis	6	64,5	53	51	50	1,2	1,3	1,3	2,31	A0	3,3
3988	ζ^2 Coronae borealis	2	21,5	18	9	7	1,2	2,4	3,1	4,69	B8	0,4
3994	ι Serpentis	2	21,5	7	20	24	3,1	1,1	0,9	4,49	A2	4,3
3998	γ Coronae borealis	4	43,0	22	23	27	2,0	1,9	1,6	3,93	A0	4,0
4001	α Serpentis	37	397,8	46	44	35	8,6	9,0	11,4	2,75	K0	3,5
4009	β Serpentis	4	43,0	32	30	27	1,3	1,4	1,6	3,74	A2	3,5
4010	λ Serpentis	8	86,0	87	101	60	1,0	0,9	1,4	4,42	G0	6,4
4015	κ Serpentis	45	483,7		14	19		34,6	25,5	4,28	K5	4,5
4016	μ Serpentis	4	43,0	19	22	28	2,3	2,0	1,5	3,63	A0	3,4
4024	δ Coronae borealis	9	96,7	14	28	16	6,9	3,5	6,0	4,73	G5	4,9
4026	ϵ Serpentis	4	43,0	36	42	34	1,2	1,0	1,3	3,75	A2	4,4
4031	ϵ Serpentis	25	268,7		13	12		20,7	22,4	4,88	K5	3,3
4032	κ Coronae borealis	16	172,0	31	28	23	5,5	6,1	7,5	4,77	K0	7,6
4035	ζ Ursae minoris . .	2	21,5		22	17		1,0	1,3	4,34	A2	1,3
4042	χ Herculis	8	86,0	69	85	72	1,2	1,0	1,2	4,61	G0	9,0
4055	γ Serpentis	8	86,0	78	118	102	1,1	0,7	0,7	3,86	F5	9,5
4063	ϵ Coronae borealis	21	225,7		23	19		9,8	11,9	4,22	K0	4,4
4072	Draconis	4	43,0		32	28		1,3	1,5	4,96	A5	6,4
4080	ι Coronae borealis	2	21,5		15	15		1,4	1,4	4,91	A0	3,2
4081	π Serpentis	2	21,5			13			1,7	4,82	A2	1,0
4089	ν Herculis	2	21,5			12			1,8	4,64	B9	4,4
4090	θ Draconis	8	86,0		63	87		1,4	1,0	4,11	F8	7,4
4108	τ Coronae borealis	12	129,0	30	34	21	4,3	3,8	6,1	4,94	K0	7,5
4112	ϕ Herculis	2	21,5	14		18	1,5		1,2	4,26	B9p	1,8
4134	δ Ophiuchi	67	720,2	40	30	26	18,0	24,0	27,7	3,03	Ma	4,1
4147	ϵ Ophiuchi	22	236,5	46	23	26	5,1	10,3	9,1	3,34	K0	3,0
4162	τ Herculis	3	32,2		13	11		2,5	2,9	3,91	B5	1,4
4163	σ Serpentis	4	43,0	32	28	31	1,3	1,5	1,4	4,80	F0	6,0
4165	γ Herculis	7	75,3	18	31	32	4,2	2,4	2,4	3,79	F0	2,8
4169	ξ Coronae borealis	12	129,0	15	17	16	8,6	7,6	8,1	4,72	K0	5,3

No. Boss PGC	Name	Hypothet- ical radius (unit is 0",0001)	107,5 × radius	Trig parallax π_1	Spectro- graphic parallax π_2	Spectral- proper motion parallax π_3	Semi-diameters			μ_{1015} (Har- vard)	Spectral Class (Harvard)	H
							$\frac{d_1}{2}$	$\frac{d_2}{2}$	$\frac{d_3}{2}$			
4182	ω Herculis . . .	2	21,5		19	20		1,1	1,1	4,53	A0p	4,0
4192	η Draconis . . .	25	268,7	42	42	25	6,4	6,4	10,7	2,89	G5	1,8
4204	β Herculis . . .	26	279,5	30	26	34	9,3	10,7	8,2	2,81	K0	3,0
4203	λ Ophiuchi . . .	3	32,2	0	29	27	—	1,1	1,2	3,85	A0	3,8
4212	h Herculis . . .	30	322,5	-11	13	19	—	24,8	17,0	4,92	K5	6,5
4213	Δ Draconis . . .	2	21,5	31	14	15	0,7	1,6	1,4	4,98	B8p	3,1
4220	σ Herculis . . .	3	32,2			18			1,8	4,25	A0	2,1
4246	ζ Herculis . . .	15	161,2	111	96	132	1,5	1,7	1,2	3,00	G0	6,9
4255	η Herculis . . .	18	193,5	53	31	24	3,7	6,2	8,1	3,61	K0	3,6
4259	g Draconis . . .	14	150,5	19	21	10	7,9	7,2	15,1	5,00	K0	1,1
4270	Draconis . . .	5	53,8		33	22		1,5	2,4	4,88	F0	3,8
4284	52 Herculis . . .	2	21,5	3		20	7,2		1,1	4,86	A2p	4,3
4302	ι Ophiuchi . . .	2	21,5		16	23		1,3	0,9	4,29	B8	3,6
4315	κ Ophiuchi . . .	29	311,7		39	31		8,0	10,1	3,42	K0	5,8
4322	h Draconis . . .	4	43,0	61	70	36	0,7	0,6	1,2	4,82	F5	6,8
4323	30 Ophiuchi . . .	19	204,2		11	14		18,6	14,6	5,00	K0	5,1
4327	ϵ Ursae minoris .	12	129,0	13	7	10	9,9	18,4	12,9	4,40	G5	0,3
4328	ϵ Herculis . . .	3	32,2	23	25	21	1,4	1,3	1,5	3,92	A0	2,5
4346	60 Herculis . . .	2	21,5		17	18		1,3	1,2	4,91	A3	3,6
4368	ζ Draconis . . .	4	43,0	19	15	11	2,3	2,9	3,9	3,22	B5	0,1
4373	α Herculis . . .	64	688,0	-2	6	8	—	114,8	86,0	3,48	Mb	0,7
4376	δ Herculis . . .	6	64,5	29	42	44	2,2	1,5	1,5	3,16	A2	4,3
4379	41 Ophiuchi . . .	15	161,2		16	14		10,1	11,5	4,82	K0	3,9
4381	π Herculis . . .	39	419,2	19	24	13	22,1	17,5	32,2	3,36	K5	0,3
4388	68u Herculis . . .	1	10,8	-21	5	9	—	2,2	1,2	4,6 to 5,4	B3	1,5
4391	ϵ Herculis . . .	2	21,5		17	19		1,3	1,1	4,80	A2	3,9
4419	ϱ Herculis . . .	2	21,5	-2	14	12	—	1,5	1,6	4,14	A0	2,0
4423	Ophiuchi . . .	4	43,0		19	27		2,3	1,6	4,61	F0	4,7
4425	σ Ophiuchi . . .	29	311,7		18	15		17,3	20,8	4,44	K0	-2,6
4438	λ Herculis . . .	26	279,5	19	21	13	14,7	13,3	21,5	4,48	K0	1,1
4443	β Draconis . . .	22	236,5	4	7	14	59,1	33,8	16,9	2,99	G0	-1,0
4458	ν^1 Draconis . . .	3	32,2	23	34	27	1,4	0,9	1,2	4,98	A5	6,0
4460	ν^2 Draconis . . .	3	32,2		40	27		0,8	1,2	4,95	A5	6,1
4459	α Ophiuchi . . .	10	107,5	49	52	78	2,2	2,1	1,4	2,14	A5	4,2
4479	ι Herculis . . .	3	32,2	-3	6	6	—	5,4	5,4	3,79	B3	-1,7
4483	ω Draconis . . .	6	64,5	34	36	48	1,9	1,8	1,3	4,87	F5	7,4
4487	β Ophiuchi . . .	35	376,2	24	41	34	15,7	9,2	11,1	2,94	K0	3,9
4497	μ Herculis . . .	8	86,0	111	105	139	0,8	8,2	0,6	3,48	G5	8,0
4500	γ Ophiuchi . . .	3	32,2	8	21	27	4,0	1,5	1,2	3,74	A0	3,3
4504	ψ Draconis . . .	5	53,8	45	40	45	1,2	1,3	1,2	4,58	F5	6,7
4531	ξ Draconis . . .	25	268,7	28	29	22	9,6	9,3	12,2	3,90	K0	4,3
4535	θ Herculis . . .	22	236,5	0	16	13	—	14,8	18,2	3,90	K0	-2,1
4538	ξ Herculis . . .	17	182,7	20	28	22	9,1	6,5	8,3	3,82	K0	3,6
4541	γ Draconis . . .	90	967,5	17	41	20	56,9	23,6	48,4	2,42	K5	-0,4
4542	ν Herculis . . .	5	53,8	3	18	12	17,9	3,0	4,5	4,48	F0	-2,5
4544	ζ Serpentis . . .	5	53,8	56	31	31	1,0	1,7	1,7	4,60	F0	5,5
4545	66 Ophiuchi . . .	2	21,5		8	7		2,7	3,1	4,81	B3	1,2
4547	93 Herculis . . .	17	182,7	4	12	11	45,6	15,2	16,6	4,71	K0	0,1
4548	67 Ophiuchi . . .	3	32,2	2	6	8	16,1	5,4	4,0	3,92	B5p	-0,4
4552	68 Ophiuchi . . .	3	32,2	16	17	17	2,0	1,9	1,9	4,44	A2	1,5

No Boss PGC	Name	Hypothet- ical radius (unit is 0",0001)	107,5 × radius	Irig parallax π_1	Spectro- graphic parallax π_2	Spectral proper motion parallax π_3	Semi diameters			m_v in (Har- vard)	Spectral Class (Harvard)	H
							$\frac{d_1}{2}$	$\frac{d_2}{2}$	$\frac{d_3}{2}$			
4556	95 Hercules	5	53,8	15	8	10	3,6	6,7	5,4	4,42	G 5, A 3	1,8
4571	70 Ophiuchi	13	139,7	192	190	251	0,7	0,7	0,6	4,07	K 0	9,3
4580	71 Ophiuchi	12	129,0		12	11		10,8	11,8	4,73	G 5	1,7
4581	72 Ophiuchi	5	53,8	40	42	33	1,3	1,3	1,6	3,73	A 3	3,8
4584	o Hercules	4	43,0	3		7	(14,3)		6,1	3,83	A 0	-3,2
4590	102 Hercules	2	21,5			9			2,4	4,32	B 3	0,5
4591	δ Ursae minoris	2	21,5	16	18	18	1,3	1,2	1,2	4,44	A 0	3,0
4635	74 Ophiuchi	10	107,5		8	9		13,4	11,9	4,92	G 5	0,8
4636	106 Hercules	16	172,0		11	13		15,6	13,2	4,98	K 5	3,9
4638	η Serpentis	23	247,2	65	54	50	3,8	4,6	4,9	3,42	K 0	8,2
4639	κ Lyrae	17	182,8	12	41	16	15,2	4,5	11,4	4,34	K 0	2,2
4656	109 Hercules	20	215,0	12	40	27	17,9	5,4	8,0	3,92	K 0	6,5
4670	ϕ Draconis	2	21,5	7	19	16	3,1	1,1	1,3	4,24	A 0p	1,8
4671	b Draconis	2	21,5	36		31	0,6		0,7	4,85	A 2	3,9
4672	λ Draconis	10	107,5	118	123	105	0,9	0,9	1,2	3,69	F 8	7,7
4686	42 Draconis	12	129,0	24	18	14	5,3	7,2	9,2	4,99	K 0	5,1
4707	d Draconis	7	75,3	6		11	12,5		6,8	4,95	F 8p	0,2
4722	α Lyrae	19	204,2	124	123	129	1,6	1,7	1,6	0,14	A 0	2,8
4747	ϵ^1 Lyrae	2	21,5	— 1		16	—		1,4	4,68	A 3	3,7
4749	ϵ^2 Lyrae	3	32,2			17			1,9	4,50	A 5	3,5
4752	ζ^1 Lyrae	6	64,5	28	32	20	2,3	2,0	3,2	4,06	A 3, A 3	1,5
4753	110 Hercules	6	64,5	54	69	61	1,2	0,9	1,1	4,26	F 5	6,9
4756	β Scuti	12	129,0	18	9	10	7,2	14,3	12,9	4,47	G 0	1,5
4758	γ Lyrae	11	118,2	19	12	12		6,2	9,8	4,92	K 0	2,2
4761	111 Hercules	3	32,2	54	33	28	0,6	1,0	1,1	4,37	A 3	4,8
4776	β^1 Lyrae	6	64,5	— 14			—			4,96	B 2p	— 2,1
4790	o Draconis	17	182,7	11	13	15	16,6	14,1	12,2	4,78	K 0	4,4
4797	113 Hercules	9	96,7	20	22	6	4,8	4,4	0,6	4,56	G 5, A 3	— 1,9
4799	γ Draconis	11	118,2			11			10,7	4,97	G 5	2,6
4800	δ^2 Lyrae	35	376,2		7	8		53,8	47,0	4,52	Mb	— 0,5
4802	θ Serpentis	4	43,0	24	22	21	1,8	1,9	2,0	4,10	A 5, A 5	3,1
4814	R Lyrae	25	268,7	6	7	14	44,8	38,4	19,2	4,32	Mb	3,8
4823	ϵ Aquilae	18	193,5	21	20	19	9,2	9,7	10,2	4,21	K 0	4,2
4824	γ Lyrae	5	53,8	11	21	17	4,9	2,6	3,2	3,30	A 0p	— 2,2
4825	ν Draconis	16	172,0	— 20		14	—		12,3	4,91	K 0	4,0
4858	ζ Aquilae	6	64,5	40	34	36	1,6	1,9	1,8	3,02	A 0	3,1
4859	λ Aquilae	4	43,0	38		31	1,1		1,4	3,55	B 9	3,4
4897	η Lyrae	2	21,5		5	4		4,3	5,4	4,46	B 3	— 3,2
4906	1 Vulpeculae	2	21,5		7	4		3,1	5,4	4,60	B 5	— 2,4
4909	δ Draconis	23	247,2	38	34	28	6,5	7,3	8,8	3,24	K 0	3,9
4912	ϕ Lyrae	23	247,2	— 7	11	12	—	22,5	20,6	4,46	K 0	— 0,5
4923	κ Cygni	17	182,7	35	27	22	5,2	6,8	8,3	3,98	K 0	4,6
4940	τ Draconis	18	193,5	12	16	48	16,1	12,1	4,0	4,63	K 0	8,0
4942	3 Vulpeculae	2	21,5		9	6		2,4	3,6	4,92	B 5	0,8
4948	π Draconis	2	21,5	16	22	18	1,3	1,0	1,2	4,63	A 2	2,9
4949	2 Cygni	1	10,8		4	5		2,7	2,2	4,86	B 3	0,4
4953	δ Aquilae	8	86,0		56	54	1,5	1,5	1,6	3,44	F 0	5,6
4962	ν Aquilae	6	64,5	— 12	32	13	—	2,0	5,0	4,86	F 0	0,1
4976	6 Vulpeculae	29	311,7	13	12	17	24,0	26,0	18,3	4,63	Ma	5,8
4986	β Cygni	43	462,2	3	29	19	(154,1)	15,9	24,3	3,24	K 0	— 2,0
						17			27,2		A 0	

No. Boss PGC	Name	Hypothet- ical radius (unit is 0",0001)	107,5 x radius	Trig parallax π_1	Spectro- graphic parallax π_2	Spectral proper motion parallax π_3	Semi diameters			μ_{vis} (Har- vard)	Spectral Class (Harvard)	H
							d_1 2	d_2 2	d_3 2			
4988	α Cygni	5	53,8	5	28	28	10,8	1,9	1,9	3,94	A2	4,4
4992	δ Cygni	1	10,8		5	4		2,2	2,7	4,85	B3	-2,1
4995	μ Aquilae	19	204,2	24	21	21	8,5	9,7	9,7	4,65	K0	6,7
4998	η Vulpeculae	2	21,5		12	4		1,8	5,4	4,88	B8	-2,1
5004	ϵ Aquilae	3	32,2		9	10		3,6	3,2	4,28	B5	0,4
5009	α Draconis	10	107,5	181	158	201	0,6	0,7	0,5	4,78	K0	11,1
5014	δ Cygni	4	43,0	70	37	49	0,6	0,8	0,9	4,64	F5	6,6
5021	φ Cygni	11	118,2	14	15	13	8,4	7,9	9,1	4,79	K0	2,5
5023	α Sagittae	10	107,5	0	11	16	—	9,8	6,7	4,37	G0	2,1
5027	β Sagittae	14	150,5	12	15	15	12,6	10,0	10,0	4,45	K0	2,3
5047	γ Aquilae	63	677,2	18	30	17	37,6	22,6	39,8	2,80	K2	-1,5
5048	δ Cygni	6	64,5	28	42	22	2,3	1,5	2,9	2,97	A0	2,0
5052	δ Sagittae	46	494,5	3	16	10	(164,8)	30,9	49,4	3,78	Mn, A0	-1,4
5058	ζ Sagittae	2	21,5	24	13	15	0,9	1,7	1,4	4,95	A2	2,4
5062	α Aquilae	20	215,0	204	145	152	1,1	1,5	1,4	0,89	A5	5,0
5068	12 Vulpeculae	2	21,5		6	8		3,6	2,7	4,91	B3	2,2
5071	η Aquilae	14	150,5	6	5	5	25,1	30,0	30,0	3,5 to 4,7	G0p	-0,9
5079	ϵ Draconis	14	150,5	14	26	20	10,7	5,9	7,5	3,99	K0	3,7
5086	13 Vulpeculae	2	21,5	9	16	17	2,4	1,3	1,3	4,50	A0	2,5
5089	ξ Aquilae	12	129,0	38	16	15	3,4	8,1	8,6	4,86	K0	5,4
5093	β Aquilae	14	150,5	78	90	115	1,9	1,7	1,3	3,90	K0	7,3
5102	22 Cygni	1	10,8		6	7		1,8	1,5	4,87	B3	0,3
5103	η Cygni	16	172,0	16	42	19	10,7	4,1	9,0	4,03	K0	2,6
5105	φ Cygni	2	21,5	5	17	19	4,3	1,3	1,2	4,80	A3	3,3
5118	γ Sagittae	46	494,5	10	23	18	49,4	19,8	27,5	3,71	K5	2,7
5132	15 Vulpeculae	3	32,2	30	20	11	1,1	1,6	2,9	4,74	A5	3,3
5153	η Draconis	26	279,5	-8	16	15	—	17,5	18,6	4,66	K0	3,2
5170	δ Cygni	2	21,5		28				0,8	4,82	B2p	-0,2
5171	θ Aquilae	4	43,0	15	19	13	2,9	2,3	3,3	3,37	A0	0,9
5182	η Aquilae	2	21,5		22	17		1,0	1,3	4,96	A0	4,3
5186	α^1 Cygni	2	21,5	9	15	7	2,4	1,4	3,1	4,96	A2	1,1
5187	α^2 Cygni	32	344,0	-2	8	11	—	43,0	31,3	3,95	K0, B8	-4,6
5188	δ^1 Cygni	2	21,5		18	18		1,2	1,2	4,98	A0	4,8
5190	Vulpeculae	1	10,8			4			2,7	4,82	B3	-2,2
5191	33 Cygni	4	43,0	42	6	28	1,0	7,2	1,5	4,32	A3	4,4
5195	23 Vulpeculae	30	322,5	15	15	12	21,5		26,9	4,73	K5	2,9
5199	κ Cephei	2	21,5	11	16	16	2,0	1,3	1,3	4,40	B9	1,7
5200	32 Cygni	33	354,7	-2	8		—	44,3		4,16	K0, A3	-2,3
5208	P Cygni	5	53,8	-21	6	4	—	9,0	13,5	4,88	B1p	0,9
5229	γ Cygni	23	247,2	-2	8		—	30,9		2,32	F8p	-5,3
5235	39 Cygni	26	279,5	16	15	13	17,5	18,6	21,5	4,60	K2	2,7
5253	41 Cygni	6	64,5	-19	9	11	—	7,2	5,9	4,09	F5p	-0,9
5265	ω Cygni	1	10,8		6	5		1,8	2,1	4,89	B3	-0,1
5270	θ Cephei	5	53,8		30	24		1,8	2,2	4,28	A5	2,7
5272	ϵ Delphini	3	32,2	1	10	11	(32,2)	3,2	2,9	3,98	B5	1,2
5279	47 Cygni	45	483,7	6	5	8	(80,6)	96,7	60,5	4,85	K5, A3	-0,6
5282	ζ Delphini	3	32,2	15	23	16	2,1	1,4	2,0	4,69	A2	2,6
5291	β Delphini	8	86,0	24	45	52	3,6	1,9	1,7	3,72	F5	4,0
5294	η Aquilae	10	107,5	4	17	14	(26,9)	6,3	7,7	4,51	K0	1,8
5301	29 Vulpeculae	2	21,5	1	15	17	(21,5)	1,4	1,3	4,78	A0	3,6

5071 Cepheid variable. The parallax value from the period-luminosity relation is 0",003.

No Boss PGC	Name	Hypothetical radius (unit is 0''.0001)	107.5 × radius	Trig parallax π_1	Spectro- graphic parallax π_2	Spectral proper motion parallax π_3	Semi diameters			m_v (Harvard)	Spectral Class (Harvard)	II
							d_1 2	d_2 2	d_3 2			
5310	α Delphin	4	43.0	21	21	24	2.0	2.0	1.8	3.86	B8	2.9
5320	α Cygni	13	139.7	5			27.9			1.33	A2p	-8.7
5323	δ Delphin	5	53.8	11	29	24	4.9	1.9	2.2	4.53	A5	3.3
5334	52 Cygni	17	182.7	13	25	15	11.1	7.3	12.2	4.34	K0	1.5
5334	γ^1 Delphin	13	139.7	31	32	26	4.5	4.4	5.4	4.12	G5	5.6
5336	ϵ Cygni	32	344.0	41	51	47	8.4	6.7	7.3	2.64	K0	6.1
5344	ϵ Cephei	8	86.0	41	62	57	2.1	1.4	1.5	4.63	G0	6.5
5346	η Cephei	21	225.7	71	92	158	3.2	2.5	1.4	3.59	K0	8.2
5350	ζ Cygni	2	21.5	27	12	6	0.8	1.8	3.6	4.47	B5	-0.1
5361	55 Cygni	7	75.3	18	4	3	4.2	18.8	25.1	4.89	B2	-1.6
5373	31 Vulpeculae	11	118.2	27	9	16	4.4	13.1	7.4	4.76	G5	4.8
5375	57 Cygni	2	21.5		8	7		2.7	3.1	4.68	B3	1.0
5393	ν Cygni	3	32.2	7	17	10	4.6	1.9	2.0	4.04	A0	1.0
5410	η^1 Cygni	3	32.2		3	3		10.7	10.7	4.86	B0p	-0.6
5431	ξ Cygni	51	548.2	6	6	8	91.4	91.4	68.5	3.92	K5	-1.9
5436	η^2 Cygni	26	279.5	13	8	7	21.5	34.9	39.9	4.88	K5	0.6
5443	γ Equulei	4	43.0	23	19	32	1.9	2.3	1.3	4.76	F0p	5.9
5452	ζ Cygni	19	204.2	24	15	9	8.5	13.6	22.7	3.40	K0	-3.2
5455	δ Equulei	6	64.5	60	59	52	1.1	1.1	1.2	4.61	F5	7.0
5460	τ Cygni	8	86.0	50	46	63	1.7	1.9	1.4	3.82	F0	7.1
5461	α Equulei	8	86.0	35	30	22	2.5	2.9	3.9	4.14	F8, A3	4.2
5469	σ Cygni	4	43.0	1		7			6.1	4.28	A0p	-1.2
5471	ν Cygni	2	21.5	16		9	1.3		2.4	4.42	B3p	1.7
5480	α Cephei	8	86.0	83	61	60	1.0	1.4	1.4	2.60	A5	3.6
5489	1 Pegasi	20	215.0	25	30	20	8.6	7.2	10.7	4.24	K0	4.6
5522	2 Pegasi	34	365.5	10	13	8	36.6	28.1	45.7	4.76	K5	0.9
5532	β Cephei	3	32.2	7	6	6	4.6	5.4	5.4	3.32	B1	-1.3
5543	θ Cygni	12	129.0	6	29	19	21.5	4.4	6.8	4.22	K0	4.2
5546	72 Cygni	19	204.2	12	15	15	17.0	13.6	13.6	4.98	K0	5.8
5563	η Cephei	4	43.0		4	3		10.7	14.3	4.87	B2	-1.6
5580	π^1 Cygni	1	10.8			4			2.7	4.78	B3	-1.3
5584	ϵ Pegasi	64	688.0	2	26	29	(344.0)	26.5	23.7	2.54	K0	-0.5
5587	μ^1 Cygni	6	64.5	45	57	54	1.4	1.1	1.2	4.45	F6	7.1
5590	9 Pegasi	17	182.7	10	11	12	18.3	16.6	15.2	4.52	K0	1.8
5592	κ Pegasi	7	75.3	26	34	32	2.9	2.2	2.4	4.27	F5	1.9
5593	μ Cephei	73	784.7	11	7	5	71.3	112.1	156.8	3.92-4.53	Ma	-4.0
5594	11 Cephei	13	139.7	17	15	16	8.2	9.3	8.7	4.85	K0	5.8
5608	ν Cephei	6	64.5		19			3.4		4.46	A2p	-4.0
5609	π^2 Cygni	2	21.5	-11	5	3		4.3	7.1	4.26	B3	-2.2
5617	14 Pegasi	2	21.5	4	12	14	5.4	1.8	1.5	5.00	A0	3.0
5663	σ Aquarii	2	21.5			7			3.1	4.66	B5p	0.9
5674	ν Pegasi	32	344.0	15	12	17	22.9	28.7	20.2	4.90	K5	5.7
5676	α Aquarii	18	193.5	9	8	13	21.5	24.2	14.9	3.19	G0	-0.9
5677	ξ^1 Cephei	6	64.5	39	30	35	1.7	2.1	1.8	4.40	A3, G	6.2
5688	ϵ Pegasi	7	75.3	79	77	68	1.0	1.0	1.1	3.96	F5	6.3
5703	θ Pegasi	4	43.0	20	35	43	2.1	1.2	1.0	3.70	A2	5.9
5709	π Pegasi	6	64.5	5	26	28	(12.9)	2.5	2.3	4.38	F5	1.5
5714	ζ Cephei	35	376.2	26	17	12	14.5	22.1	31.3	3.62	K0	-1.0
5716	24 Cephei	9	96.7		8	10		12.1	9.7	4.99	G5	2.2
5732	Lacertae	24	258.0		14	13		18.4	19.8	4.64	K2	3.1

5532 Cepheid variable The parallax value from the period luminosity curve is 0''.022 This attributes an astonishing small diameter (2.9 \odot) to the star

No. from PGC	Name	Hypo- thetical radius (unit in 0".0001)	107.3 × radius	Trig parallax π ₁	Spectro- graphic parallax π _s	Spectral- proper motion parallax π _p	Semi-diameters			μ vs (Har- vard)	Spectral Class (Harvard)	H
							$\frac{d_1}{2}$	$\frac{d_2}{2}$	$\frac{d_3}{2}$			
5742	ε Cephei .	5	53.8	46	37	55	1.2	1.5	1.0	4.23	F0	7.5
5746	1 Lacertae	29	311.7	2	15	15	155.8	20.8	20.8	4.22	K0	0.7
5761	γ Aquarii	3	32.2	64	28	28	0.5		1.1	3.97	A0	4.4
5762	31 Pegasi	1	10.8		4	4			2.7	4.93	B3, p	-1.2
5763	32 Pegasi	2	21.5		9	9			2.4	4.88	B8	-1.6
5764	2 Lacertae	2	21.5	37	11	8	0.6	2.0	2.7	4.66	B5	1.2
5776	β Lacertae	14	150.5	17	26	19	8.9	5.8	7.9	4.58	K0	6.0
5777	α Aquarii	3	32.2		3	3			10.7	4.64	B1 p	-0.4
5779	4 Lacertae	3	32.2		12	12			2.7	4.64	B8 p	0.4
5790	35 Pegasi	10	107.5	33	23	21	3.3	4.7	5.1	4.93	K0	7.5
5793	ζ ¹ Aquarii	9	96.7	13	28	26	7.4	3.5	3.7	4.59	F2	5.8
5805	δ Cephei	13	139.7						(3.7)	4.61	F5, G0	-0.9
5804	5 Lacertae	44	473.0	5	3	13	94.6	157.6	36.4	4.61	K0, A	1.2
5810	6 Lacertae	2	21.5		7	6		3.0	3.6	4.54	B3	0.1
5813	7 Lacertae	4	43.0	34	31	31	1.3		1.4	3.85	A0	4.6
5824	η Aquarii	2	21.5		27	27			0.8	4.13	B8	4.2
5837	9 Lacertae	3	32.2	20	26	26	1.6		1.2	4.83	A5	5.2
5844	10 Lacertae	1	10.8		3	3			3.6	4.91	Oe5	-0.3
5852	11 Lacertae	24	258.0		17	16		15.2	16.1	4.64	K0	4.6
5853	ζ Pegasi . .	4	43.0	- 2	20	28	-	2.1	1.5	3.61	B8	3.1
5858	σ Pegasi	2	21.5		19	16		1.1	1.3	4.85	A0	2.6
5865	η Pegasi . . .	21	225.7	- 1	23	17	-	9.8	13.3	3.10	G0	0.9
5874	ξ Pegasi	7	75.3	51	61	69	1.5	1.2	1.1	4.31	F5	8.0
5875	λ Pegasi . .	15	161.2	37	15	18	4.4	10.7	9.0	4.14	K0	3.0
5885	μ Pegasi . .	18	193.5	31	32	24	6.2	6.0	8.1	3.67	K0	4.6
5891	ι Cephei . .	18	193.5	40	34	24	4.8	5.7	8.1	3.68	K0	4.4
5899	Cephei . . .	19	204.2		19	13		10.7	15.7	4.97	K0	4.0
5910	ρ Pegasi . .	2	21.5	2	14	17	(10.7)	1.6	1.3	4.95	A0	4.2
5927	Cephei . . .	22	236.5		13	15		18.2	15.8	4.96	K5	5.1
5933	σ Andromedae .	4	43.0	3	16	12	(14.3)	2.7	3.6	3.63	B5, A2p	1.2
5939	β Pisium	2	21.5		6	6			3.6	4.58	B5 p	0.2
5940	β Pegasi . . .	90	967.5	16	25	34	60.5	38.7	28.5	2.61	Ma	4.6
5942	3 Andromedae .	12	129.0	- 4	19	18	-	6.8	7.2	4.91	K0	6.7
5944	α Pegasi . . .	6	64.5	38	37	36	1.7	1.7	1.8	2.57	A0	1.9
5952	55 Pegasi . . .	36	387.0	- 3	12	8	-	32.2	48.4	4.69	Ma	0.7
5954	56 Pegasi . . .	17	182.7	- 5	16	12	-	11.4	15.2	4.98	K0	2.9
5955	1 Cassiopeiae .	2	21.5		3	4		7.2	5.4	4.93	B1	0.3
5966	π Cephei . . .	11	118.2	0	19	12	-	6.2	9.8	4.56	G5	1.8
5975	7 Andromedae .	4	43.0	48	40	33	0.9	1.1	1.3	4.62	F0	6.3
5988	γ Pisium . . .	17	182.7	28	24	41	6.5	7.6	4.5	3.85	K0	8.2
5993	8 Andromedae	28	301.0		10	9		30.1	33.4	4.99	Ma	2.9
6000	σ Cephei	9	96.7	26	16	14	3.7	6.0	6.9	4.90	G5	4.0
6005	τ Pegasi	2	21.5	34	10	10	0.6		2.2	4.65	A5	2.4
6024	ν Pegasi	8	86.0	25	20	20	3.4	4.3	4.3	4.57	G0	6.0
6031	π Pisium . . .	2	21.5	41	16	29	0.5	1.3	0.7	4.94	A2 p	5.4
6037	θ Pisium	12	129.0	- 2	16	20	-	8.1	6.5	4.45	G5	5.2
6040	η Pegasi	13	139.7	- 8	16	15	-	8.7	9.3	4.67	K0	3.6
6046	Cassiopeiae . .	2	21.5		5	8		4.3	2.7	4.89	B3	2.1
6071	λ Andromedae .	17	182.7	39	47	32	4.7	3.9	5.7	4.00	K0	7.3
6073	ι Andromedae .	3	32.2		16	16			4.28	B8	1.4	

5805. Cephei variable. The period luminosity relation attributes a parallax value of 0".006 to this star.

No Boss PGC	Name	Hypothet- ical radius (unit is 0",00001)	107,5 × radius	Trig parallax π_1	Spectro- graphic parallax π_2	Spectral proper motion parallax π_3	Semi diameters			m_{vis} (Har- vard)	Spectral Class (Harvard)	H
							$\frac{d_1}{2}$	$\frac{d_2}{2}$	$\frac{d_3}{2}$			
6077	ϵ Piscium	6	64,5	73	70	87	0,9	0,9	0,7	4,28	F8	8,1
6078	γ Cephei	26	279,5	69	69	27	4,1	4,3	10,4	3,42	K0	4,6
6080	κ Andromedae	2	21,5	8		21	2,7		1,0	4,33	A0	3,9
6084	λ Piscium	3	32,2	30	32	34	1,1	1,0	0,9	4,61	A5	6,1
6094	η Pegasi	13	139,7	18	17	13	7,7	8,2	10,7	4,98	K0	4,5
6135	ϱ Cassiopejae	18	193,5	29	2	10	6,7	96,7	19,3	4,85	F8p	-0,9
6150	ψ Pegasi	36	387,0		12	11		32,3	35,2	4,75	Ma	3,5
6155	σ Cassiopejae	2	21,5	12	4	5	1,8	5,4	4,3	4,93	B2	0,3
6156	ω Piscium	8	86,0	11	37	57	7,8	2,3	1,5	4,03	F5	5,4

When a scrutiny is made as to the average size and distribution of linear diameters in the preceding table it will be noted that the mean values for the diameters computed with aid of the trigonometric, spectrographic and spectral-proper motion parallaxes respectively, will on an average agree very well. This is to be expected because the two latter parallax methods are founded upon the trigonometric method and possibly existing systematic errors in π_1 are to a certain extent taken over by the series π_2 and π_3 . But what is remarkable as to the linear diameters is the good agreement in individual cases. Any justified discussion of the material will show that our knowledge of parallaxes evidently has advanced in such a way, that we now can compute the linear diameters of the stars with a high, nay, unexpected degree of accuracy. It also seems that the material as to π_1 added since 1929 has in the majority of cases increased the agreement between the three series of linear stellar diameters.

A recent investigation by JESSE GREENSTEIN [Harv Bull 876, p 32 (1930)] reveals the existence of systematic errors in HERTZSPRUNG's colour equivalent c_2/l . GREENSTEIN computes the quantity $c_2/T - c_2/\bar{T}_s$, where \bar{T}_s is the mean temperature for a certain spectral class S . These quantities show a seasonal variation, which indicates a reddening of the winter stars, probably due to climatological phenomena. Errors of that kind affect the diameter values to a certain extent and it seems that a revision of the derivation of the stellar diameters is warranted. On that account an extensive statistical treatment of the data in the preceding catalogue is postponed until such a revision has been undertaken. During the mean time the preceding table will represent a summary of our present knowledge as to the distribution of the stellar diameters.

Sachverzeichnis.

- Absorption des Lichtes im interstellaren Raum 1024ff.
 of light in space 555ff
 Accuracy attainable with photographic methods 355
 Astrometry, Yerkes 311, 396.
 Aktinometrie, Göttinger 314f
 Areas, selected 317ff.
 Astorium 22.
 Astron 430, 778
- Binaries, angular moments of visual 695
 mass-ratio, statistical investigation 683f.
 origin of 695
 relation between mass and form of orbits of 690.
 spectroscopic, dwarf nature of 658.
 masses of 653ff
 visual, masses of 612ff
 Brightness 212
- Candle, international 212.
 power 212.
 Carte du Ciel 300ff
 Catalogues, photometric, influence of multiplicity and incompleteness on 336f
 of the Pleiades 312, 316
 of stellar spectra 106.
 Changes in the colour of Sirius 386f.
 secular, in the light of the stars 356ff
 Classification of stellar spectra 3ff
 CANNON's 34, 50ff.
 DRAPER Catalogue 27f
 additions and modifications 58ff.
 description, tabular 49ff
 descriptions, verbal 44ff.
 development of the — from 1901—1924 35ff
 LOOKYER's 19.
 MAURY's 31ff.
 SECCHI's 5ff
 VOGLER's 15ff.
 by blue intensity ratios 53.
 by measurements of effective wave length 100ff.
 by measures of colour index and heat index 104f
 comparison of the principal 57f
 Clouds of calcium 784.
 cosmic, HAOEN's 787ff.
 interstellar 782.
 star-, distance of the 543ff.
 stationary 782.
- Clusters, galactic, classification 704f
 compact 704.
 field irregularities 704.
 loose and irregular 704.
 star associations 704.
 distribution, apparent, of the 710
 parallaxes 747
 spectra in individual 715ff
 structure of the 730f
 orientation 730f
 shoulder effect 731f
 system of 755
 Clusters, globular, classes of SHAPLEY and SAWYER 705f
 classification 705.
 dimensions and star densities 749f
 distance modulus 742, 745
 distance to the galactic centre 758.
 distances from Cepheids and bright stars 740ff
 from diameters and integrated magnitudes 744ff
 from angular diameters 744.
 from integrated apparent magnitude 744
 distribution, apparent 708f
 of stars in the 720ff.
 forms of the 724ff.
 definition 724.
 ellipticity 726.
 orientation of major axes 727
 inclination to the galactic circle 727
 elongation of Messier 13 725f.
 higher systems of 755ff.
 integrated spectra 711
 in Magellanic clouds 751
 peculiar 728f
 period-luminosity curve 737f.
 zero point 739.
 radial velocities 748f
 relation of the — — to the Magellanic clouds 753
 space distribution of the 755ff.
 stellar types in the 712.
 colour-magnitude arrays 712f.
 common spectral classes 712.
 super systems 758
 variables in the 717ff.
 frequency and general properties 717
 summary of known 718f
 Clusters, stellar, catalogues of galactic 746.
 definition 698.
 galactic and globular 698
 historical notes on 698f.

- Clusters, stellar, number of 700
 variable stars in the 717f
 frequency and general properties 717
 summary of known 718f
 Colour-catalogues, index catalogue 371
 KRÜGER 370f
 LAU 375f
 MALMQUIST 397
 MÖLLER 379
 Colour, changes, of Sirius 386f
 in the — of the stars 375f
 direct estimates of 363f
 sources of error in the 371ff
 equation of catalogues 214, 427ff
 equivalents 389f
 index 215
 as a function of m 400
 from photoelectric measurements 545ff
 indices, absolute 392
 existence of preferential 424f
 from the Göttinger Aktinometrie 391f
 -mass density relation 641
 nuance 363
 saturation 364
 scale of ARGELANDER 366
 of FRANKS 366
 of HAGEN 369
 of OSTROFF 367.
 of Potsdam 369
 of SCHMIDT 360
 of H. C. VOGEL 365
 linear 366
 relation between the — of HAGEN and
 the scales of other observers 367
 two dimensional 366
 shade 363
 tone 363
 tone scale 364
 Colours of bright stars 548
 of double stars, BELL's study 380
 reduction of the — to a standard system
 421ff
 stellar 363ff
 Convergence of the sum of stellar light 361f
 Cosmogonic time-scale of EDDINGTON 662ff
 of JEANS and SMART 672
 Criterion of OLBERS 888
 of SEELIGER 888f

 Dazzle tints 381
 Densities of the stars 600ff
 binary stars 600f
 eclipsing binaries 604f
 ratio of the — in double stars 603
 Density or back-ground effect 335f
 Development, stellar, RUSSELL's investigations 442ff
 Diameter, equivalent 578
 laws 296ff
 of Sirius B 596ff
 Diameters of the stars 575ff
 equivalent 578
 from c_2/T 584
 from interferometer measurements 587ff.
 from radiometric measurements 585f

 Diameters, from scintillation observations
 599
 historical 575f
 method of DANJON 596
 of HAMV 591ff
 of POKROWSKY 599
 of RUSSELL 582
 of WILSON 578
 varying 590
 Dichtigkeit, Verteilungsfunktion der 992
 Distance method of OTTO STRUV 489ff
 modulus 712, 745
 Distribution of Iclum stars, CHARLIER's
 determinations 509ff
 GERASIMOVICH's investigations 512
 ROBB's determination 513
 Distribution, relative, of $N(m)$ 351f
 DOPPLER's formula, MOUSSARD's modification
 907ff
 DRAPER Catalogue, classes, tabular description
 49ff
 classification, verbal descriptions 44ff
 additions and modifications 58ff
 distribution of the stars in the 537ff
 DRAPER-Katalog, statistische Auswertung
 des 111
 Durchmusterung, Bonner 259ff
 Cape photographic 299f, 306ff
 Córdoba 265ff
 Potsdam, photometric 279ff, 285ff
 Dynamik der Milchstraße 1033f

 Eclipsing binaries, masses and luminosities
 686f
 parallaxes and absolute magnitudes 606
 statistics 607
 Effective wave lengths, determinations at
 Greenwich 409f
 by KREIKEN 412f
 discussion of the methods 415ff
 VON KLÜBER's modification 411
 of faint Milky Way stars 408
 of the Pleiades 407
 minimum 406
 standardization of the 415
 visual 401f
 Emissionsvermögen 146
 Energiekurve 129
 Equipartition of energy 617f
 Erdlicht 948, 981
 Exposure-ratio method 393f, 398f
 Extinction 565f
 Eye, as a photometric instrument 215ff

 Farbenindex 171
 absoluter 172, 176
 Farbtemperatur der Sonne 184f
 spektrophotometrische 165f
 der Sterne aus der Farbe oder einem
 Farbenäquivalent 168ff
 aus der Gestalt der Energiekurve 148ff
 und Strahlungstemperatur, Beziehung
 zwischen der 143
 Farbtönung 171

Fehlerquellen, systematische, bei der Bestimmung der Temperatur aus der Energielkurve 194ff.
 Fixsternntemperatur 130.
 Foot-candle 211

Galaktische Ebene 937
 Koordinaten 972
 Tafeln zur Berechnung der 973f
 Galaxy, average 868ff
 dimensions of the 754ff.
 distance to the galactic centre 758f
 higher systems of globular clusters 755
 eccentric position of the solar system 755f.
 region of avoidance 758.
 motion of our — in space 906
 size and structure of the 759ff
 supergalaxies 838.
 system of galactic clusters 755
 value of the motion of our — in space 906.
 GALLISSEOT phenomenon 290, 292f.
 Gas, interstellares 1033
 als Quelle der kosmischen Strahlung 1033.
 Temperatur 1028.
 Totalmasse des 1033
 Geschwindigkeitsellipsoid u. Rotation 1065f.
 Geschwindigkeitsverteilung, asymmetrische, in ihrer Beziehung zur Rotation, nach LINDBLAD 1048ff.
 nach OORT 1052f.
 Giants and dwarfs 437ff.
 Giant stars, masses of 714
 Gouldscher Kreis 972.
 Gradationstemperatur u. schwarze Temperatur, Beziehung zwischen der 144f
 Greenwich catalogues 313f

HAGENS dunkle Nebel 979ff.
 Helligkeit, schenbare, der einzelnen Spektralklassen 111
 Helligkeitsverteilung, wahre, der Spektralklassen 120.
 HERSCHEL (unit of distance) 430.
 Himmelsintergrund, absolute Helligkeit des 948ff.

Illumination 211
 Index, spectral 397f.
 Intensity, luminous 212.
 physiological 580.

K-Effekt der Radialgeschwindigkeiten 1069f.
 Kalkminimien, stationäre 1059ff
 Kalkminwolken 1027f.
 galaktische Verteilung der Intensitäten der 1030.
 mittlerer Absorptionskoeffizient per Parsec 1031.
 Verteilung der, mit bekannten Radialgeschwindigkeiten 1061.
 KAPTEYN's method 353.
 phenomenon 380, 390.
 universum 991f.

KIRCHHOFF's Funktion 128
 Gesetz 128
 Kollisionsfunktion 1035.

LAHBERT 212.
 mill- 212.
 Leiden catalogue 320.
 Leuchtkraftsfunktion 988.
 Light, units, definition of the 211ff
 -year 430, 778
 Lilliputian stars 585
 Limiting magnitude of star catalogues 342f.
 Limits of unaided vision 354
 Line intensity ratios for classification purposes 55f
 LOCKYER, definitions of stellar genera 22f.
 Lumen 211
 Luminositätsfunktion 988.
 Luminosity curve from differences in magnitude of double stars 504ff.
 for individual spectral classes 530f
 of different spectral classes 441
 Luminous flux 211.

Macron 778.
 Magellanic clouds 750ff
 distances of 752.
 globular clusters in the 751
 relation of clusters to the 753f.
 type of clusters and nebulae 750.
 Magallanische Wolken 965f.
 Natur der 1022ff
 Magnitude, absolute, differential determinations 537
 general distribution 498ff.
 relation between — and colour 541f.
 and proper motion 514ff
 and radial velocity 509.
 and spectral class, 493ff
 bolometric 554.
 limiting, of star catalogues 342f.
 of the stars 212.
 total, of star agglomerations 359.
 Mass-function 619f.
 Mass-luminosity law, EDDINGTON's 662ff.
 BRILL's theory 673f
 discrepancies between SEAR'S and EDDINGTON's results 666
 JAMES's theory 667ff.
 RABE's theory 678ff.
 Voer's extension of EDDINGTON's theory 682f.
 relation 658ff.
 Mass of Orion nebulae 691
 of planetary nebulae 692.
 of the stellar system 693.
 Mass-ratios in binaries, statistical investigations 683f.
 theoretical derivation of the 684.
 of stellar systems 694.
 Mass-reduction by annihilation of protons and electrons 676ff.
 Mass, stellar, relation between — and form of orbits of binaries 690.
 and proper motion 689f.

- Masses, determination, Sproul, of 626
 equipartition of energy 617f
 frequency of — for different spectral
 classes 622ff
 methods of deriving 608ff
 of FREUNDLICH and HEISKANEN 645f
 of LUDENDORFF 619ff
 of MARTENS 646ff
 of PITMAN 627f
 of SCHLESINGER and BAKER 619
 of SEARES 631ff
 of VON ZEIPPEL 641ff
 preferential values of 656ff
 real and apparent 630
 of F—K stars 638ff
 of spectroscopic binaries 653ff
 of visual binaries 612ff
 from spectrographic parallaxes 637f
 statistics of accurately determined 629f
 of stellar systems 694
 upper limit for the stellar 687
 Messungen, radiometrische und thermo-
 elektrische 164
 spektrophotometrische differentielle
 154ff
 Metron 430
 Milchstraße, Anschauungen über die Natur
 des Systems der 1069ff
 Beschreibung und zeichnerische Darstel-
 lung 938ff
 Definition der 937
 Dimensionen, Masse, Rotationsdauer der
 1067f
 dip (Tiefe) 969
 Ebene der 937
 effektive Entfernung der Sterne der 985ff
 effektive Sterngröße des Lichtes der 984ff
 Farben der Sterne der 986f
 Helligkeitsschätzungen 944f
 photometrische Eichung der Isophoten
 947
 Integralspektrum der 985ff
 Kalziumwolken in der 1027ff
 Lage der 967ff
 Phänomen der 937, 1046
 Photographie der 952ff
 Photometrie, photographische der 960
 Pol der 969
 aus der maximalen scheinbaren Stern-
 dichtigkeit 970ff
 Bestimmungsmethoden 969f
 Rotation der 1056ff
 Sternleeren und Sternwolken in der 1010ff
 Tiefe (dip) der 969
 Verlauf der — am Himmel 962ff
 Zeichnungen der — auf Grund photo-
 graphischer Aufnahmen 960ff
 Milky Way, siehe Milchstraße
 Nebelfelder, galaktische, Einfluß auf das
 Milchstraßenbild 975ff
 Verteilung gegen die galaktische Ebene
 976
 Nebelleuchten, Theorie des 205ff
 Nebulae, anagalactic 777
 Nebulae, classification 777f
 systems of classification 919ff
 dark 784ff
 distance of the 534ff
 types of the 784
 diffuse, definition 779
 distances and dimensions 792
 emission variations in the 801
 evolutionary status 805f
 gaseous spectra 799f
 internal motion 795f
 luminosity 799ff
 reflection or resonance effects 802f
 number and distribution 779
 physical characteristics 781ff
 irregularity 781
 tenacity 781ff
 variation in apparent luminosity 781
 proper motions 795
 radial velocities 797
 reflection or resonance effects 802f
 spectra, continuous 802,
 gaseous 799f
 turbulence effect in the 797f
 variable 803
 extragalactic 777
 nongalactic 777
 planetary, classification of the 816
 definition 806
 distance and dimensions 810ff
 distribution 807
 evolutionary status 831f
 forms of 808
 number 807
 parallaxes 810ff
 proper motions 809
 radial velocities 817
 rotation 817
 spectra of nebulous matter 813f
 of nuclei 815
 spectroscopic distribution effects in the
 817
 temperatures 831
 theories, mechanical 823f
 theory, quantum- 824ff
 turbulence effects in the 819ff
 reproductions of 922ff
 white 833
 OLBER's criterion 888
 Parallax methods 430ff
 BRILL's — for binaries 673ff
 dynamical 431
 moving cluster 432
 spectral-proper motion 433, 488
 spectrographic 434, 454ff
 spectroscopic 434
 trigonometric 431, 434ff
 Parallaxes, photometric 219
 radiation-energy 675f
 spectrographic, distribution of — with
 regard to m and spectral class 508
 systematic errors in the 436
 Parsec 430, 778

Parsec, cublo- 778
 kilo- 778
 mega- 778
 Passagiefunktion 1035
 Period-luminosity curve, photographic 737ff
 zero point 739f
 Phot 211
 Photometry, Harvard, Revised 276ff
 photoelectric 558
 Yorks — of Selected Areas 401
 Plancks Strahlungsgesetz 131
 Poisson's constant 213
 ratio 261
 Protometals 22.
 Radiation temperature 674.
 Radiometric measurements 559ff
 Reflecting effect in colliding variables 339
 Riesen- und Zwergsterne, Temperatur der 197ff
 Verteilung der 119.
 Rotation, differentiale, der Milchstraße,
 Theorie nach GYLDFEN 1057
 nach OORT 1056, 1058.
 nach OPPENHEIM 1057
 nach PLANKET und PRANCE 1059ff
 Rotationseffekte, differentielle, in den Ge-
 schwindigkeiten 1056ff
 Schwarzer Körper 128
 SEELIGER's Criterion 888f.
 Sequence, Mount Wilson — and Internatio-
 nal scale 326ff
 Polar 323ff.
 Shadows cast by starlight 354
 Sirlometer 430, 778
 Sirius, colour change 386f.
 Sirius B 596ff.
 Sirluswelt 430, 778.
 Solar system, eccentric position in the system
 of globular clusters 755f
 Sonne, Entfernung der — von der Sym-
 metrieebene der Milchstraße 1009
 exzentrische Stellung im System 997
 Gradationstemperatur der 165ff
 schwarze oder Strahlungstemperatur der 185ff
 spektralphotometrische Farbtemperatur
 der 165ff
 Space penetrating power 350
 Spectra of stars of class
 P 36, 64f.
 O 67ff.
 B 73ff
 A 76ff.
 F, G, K 80ff.
 M 36, 89ff.
 R 37, 94f.
 N 38, 94f.
 S 38, 92f.
 Q 62f.
 Spectral criteria, variation curves of 53f.
 photometry 549ff.
 Spectrum analysis, stellar, history of the,
 CANNON 34.
 CARPENTER 5.

Spectrum analysis, stellar, history of the,
 D'ARREST 15
 DONATI 3
 DUNER 19
 FLEMING 28
 FRAUNHOFER 1.
 HUGGINS 18
 LOCKYER 19f
 MAURY 29
 McCLEAN 25
 PICKERING 27f
 RUTHERFORD 4
 SECCHI 5ff.
 VOGEL 15f
 Spektralanalyse der schwächeren Sterne 117f.
 Spirals, colour indices 854
 cosmogonical deductions 887ff.
 direction of rotation of the 852.
 distance-velocity relation 863ff
 distances and dimensions 873ff
 from Cepheids 861
 from distance-velocity correlation 863ff.
 from novae 858ff
 from parallaxes 858.
 from photometric observations 868ff
 distribution, apparent 838
 evolutionary status 887
 forms of 840f.
 barred 842.
 elliptical 843.
 irregular 844.
 Magellanic type 844.
 groups of 838
 historical note 833ff
 internal motions 850.
 isolated 858
 local 858.
 masses of the 876
 mathematical 879
 WILCZYNSKI's gravitational 881.
 minor 843f
 number of 839.
 occulting matter in the 844ff.
 proper motions 847ff.
 recession, apparent of the 905f
 rotation 851f.
 spectra of the, stellar type 852
 emission lines 853
 theories of spiral structure 878ff.
 of BROWN 882f.
 of JEANS 882.
 of LINDBLAD 884f
 true 842.
 velocities, radial, of the 853f.
 Spirals and relativity universes 891ff.
 Star clusters, also clusters.
 colours, old observations of 383f.
 relation between — and spectra 382.
 light, total amount 340f
 Stars, illiputian 585
 number of — within certain limits of
 magnitude 347ff
 variable, in star clusters, frequency and
 general properties of 717
 summary of known 718f

- STEFANSches Strahlungsgesetz 132
 Stellar system, mass of the 693
 Sterne, galaktische Konzentration der 982ff
 Sternfarbe 168
 Sternhaufen siehe clusters
 System der 996
 Zentralpunkt des 996
 Sternleeren und Sternwolken in der Milchstraße 1010f
 Steinstratum, dunkle Flecke im 979
 Sternströmung im typischen System 1039f
 nach JEANS 1040
 nach KAPTEYN 1039f
 Sternsystem, Dynamik des, nach JEANS 1040
 nach KAPTEYN 1039f
 das große, nach LINDBLAD 1042ff
 das größere, nach SHAPLEY 1006f
 das lokale 998, 999, 1008, 1012, 1014, 1017, 1018, 1027, 1040, 1042, 1064, 1069, 1070, 1073, 1074, 1075
 Mechanik, statistische des 1034ff
 nach CHARLIER 1035
 nach JEANS 1035
 nach LUNDAHL 1036
 schematisches 990
 typisches 990
 nach KAPTEYN 1042
 Theorie der Sternströmung im typischen 1039f
 Sternweite 778
 Strahler, grauer 129
 schwarzer 128
 Strahlungskonstanten, numerische Werte der 133f
 Strahlungstemperatur der Sonne 185ff
 der Sterne 188ff
 aus der Strahlungsintensität begrenzten Spektralbezirke 185ff
 Supergalactic groups 875
 Supergalaxy 761, 838
 Symbols of W IERSCHL 245ff
 System, galactic 754
 galaktisches, Ursprung des 1038f
 of galactic clusters 755
 isophoter Wellenlängen 174
 der B-Sterne 125f
 stellar —, mass of the 693
 Temperatur, Bestimmung der, aus der Form der Spektralkurve, Fehlerquellen 194ff
 effektive 131
 Farb- 142.
 spektralphotometrische 141
 Gradations- 141
 im interstellaren Raum 1028
 schwarze 142
 -skala der Fixsterne 191ff
 der Sterne, photosphärische 204
 spektralphotometrische Farb 204
 Strahlungs- 204
 Strahlungs- 142
 Temperature radiation 674
 Temperature, stellar, determination of 549ff.
 Transparency of space 733ff
 early investigations 733
 from blue stars in Messier 13 733f
 from colours in distant objects 735
 light scattering 733
 relative speeds of blue and yellow light 735f
 Units of distance 430, 778
 Universe, CHARLIER's infinite 888ff
 continent- 761
 expanding relativity 898ff
 island- 833, 835, 837, 838
 relativity- 891ff
 of DE SITTER 893
 of LDDINGTON, FRIEDMAN, LILMAIRE, MCCREA and McVITIE 898ff
 of EINSTEIN 892
 of SILBERSTEIN 902
 Untersysteme 1049, 1075
 Uianometria Argentina 254f
 Nova 251f
 Oxoniensis 275f
 Veränderliche Sterne, Temperatur der 201ff
 Verteilung, galaktische, der Kugelhaufen 1008
 von Objekten großer absoluter Leuchtkraft 1003ff
 der Spektralklassen 112f
 B-Sterne 114
 A-Sterne 115
 F-Sterne 115
 K- und M-Sterne 116
 O-, P-, N-, R-Sterne 117
 der offenen Sternhaufen 1007
 räumliche, der verschiedenen Spektralklassen 122f
 der Sterne im Raume, statistische Untersuchungen 987
 nach CHARLIER 994f
 nach KAPTEYN 991f
 nach MALMQUIST 995
 nach SCHWARZSCHILD 992f
 nach SEELIGER 988ff
 Verteilungsgesetze der Spektraltypen 999ff
 der Sterne der Spektralklasse B 1000ff
 Wärmeindex 181ff
 Wassorzellenabsorption 181ff
 Wellenlänge, effektive 170, 175
 isophote 174f
 fundamentale 174
 minimale 170
 Weltinsel 833, 1071f
 WIENSches Strahlungsgesetz 132
 Verschiebungsgesetz 133
 Zero-point of the photographic scale 311, 324.
 of photometric measures 344f